

IODINE CHEMISTRY AND APPLICATIONS



53

I

126.9



Edited by **TATSUO KAIHO**

WILEY

IODINE CHEMISTRY AND APPLICATIONS

IODINE CHEMISTRY AND APPLICATIONS

Edited by

TATSUO KAIHO

WILEY

Copyright © 2015 by John Wiley & Sons, Inc. All rights reserved

Published by John Wiley & Sons, Inc., Hoboken, New Jersey

Published simultaneously in Canada

No part of this publication may be reproduced, stored in a retrieval system, or transmitted in any form or by any means, electronic, mechanical, photocopying, recording, scanning, or otherwise, except as permitted under Section 107 or 108 of the 1976 United States Copyright Act, without either the prior written permission of the Publisher, or authorization through payment of the appropriate per-copy fee to the Copyright Clearance Center, Inc., 222 Rosewood Drive, Danvers, MA 01923, (978) 750-8400, fax (978) 750-4470, or on the web at www.copyright.com. Requests to the Publisher for permission should be addressed to the Permissions Department, John Wiley & Sons, Inc., 111 River Street, Hoboken, NJ 07030, (201) 748-6011, fax (201) 748-6008, or online at <http://www.wiley.com/go/permission>.

Limit of Liability/Disclaimer of Warranty: While the publisher and author have used their best efforts in preparing this book, they make no representations or warranties with respect to the accuracy or completeness of the contents of this book and specifically disclaim any implied warranties of merchantability or fitness for a particular purpose. No warranty may be created or extended by sales representatives or written sales materials. The advice and strategies contained herein may not be suitable for your situation. You should consult with a professional where appropriate. Neither the publisher nor author shall be liable for any loss of profit or any other commercial damages, including but not limited to special, incidental, consequential, or other damages.

For general information on our other products and services or for technical support, please contact our Customer Care Department within the United States at (800) 762-2974, outside the United States at (317) 572-3993 or fax (317) 572-4002.

Wiley also publishes its books in a variety of electronic formats. Some content that appears in print may not be available in electronic formats. For more information about Wiley products, visit our web site at www.wiley.com.

Library of Congress Cataloging-in-Publication Data:

Kaiho, Tatsuo.

Iodine chemistry and applications / edited by Dr. Tatsuo Kaiho, Kanto Natural Gas Development Co., Ltd., Brine Resources R&D Division, Chiba, Japan.

pages cm

Includes index.

ISBN 978-1-118-46629-2 (cloth)

1. Iodine. 2. Iodine—Industrial applications. 3. Iodine—Therapeutic use. I. Title.

TP245.I6K35 2014

661'.1—dc23

2014017643

Cover Image: Courtesy of Tatsuo Kaiho

Printed in the United States of America

10 9 8 7 6 5 4 3 2 1

CONTENTS

LIST OF CONTRIBUTORS	ix
PREFACE	xiii
1 Overview <i>Tatsuo Kaiho</i>	1
PART I CHARACTERISTICS, ELEMENTAL OF IODINE	7
2 Physical Properties of Iodine <i>Tatsuo Kaiho</i>	9
3 Analytical Methods for Iodine and Iodides <i>Hirofumi Kanoh and Takehisa Konishi</i>	15
4 Ion Chromatography <i>Anna Błażewicz</i>	25
5 Inorganic Iodides <i>Tatsuo Kaiho</i>	55
6 Organic Iodides <i>Tsugio Kitamura</i>	75

7 Hypervalent Iodine	103
<i>Toshifumi Dohi and Yasuyuki Kita</i>	
8 Iodine and Halogen Bonding	159
<i>Giancarlo Terraneo, Giuseppe Resnati, and Pierangelo Metrangolo</i>	
PART II PRODUCTION OF IODINE	195
9 History of Iodine	197
<i>James L. Marshall and Virginia R. Marshall</i>	
10 Production Process in the Past	207
<i>Tatsuo Kaiho</i>	
11 Iodine Production from Caliche	213
<i>Armin Lauterbach</i>	
12 Iodine Production from Oilfield Brine	221
<i>Stanley T. Krukowski</i>	
13 Iodine Production from Natural Gas Brine	231
<i>Nobuyuki Kaneko and Tatsuo Kaiho</i>	
14 Recycling of Iodine	243
<i>Tatsuo Kaiho</i>	
PART III SYNTHESIS OF IODINE COMPOUNDS	249
15 Iodinating Reagents	251
<i>Haruhiko Taguchi</i>	
16 Oxidizing Agents	277
<i>Toshifumi Dohi and Yasuyuki Kita</i>	
17 Reaction of Iodo Compounds	303
<i>Toshifumi Dohi and Yasuyuki Kita</i>	
18 Metal Iodides–Mediated Reaction	329
<i>Makoto Shimizu, Iwao Hachiya, and Junji Inanaga</i>	

PART IV BIOLOGICAL APPLICATION OF IODINE	353
19 Iodinated X-Ray Contrast Agents	355
<i>Werner Krause</i>	
20 Iodine as Disinfectant	375
<i>Waldemar Gottardi</i>	
21 Synthetic Thyroid Hormone	411
<i>Steven E. Rokita</i>	
22 Iodine Deficiency Disorders and Their Correction Using Iodized Salt and/or Iodine Supplements	421
<i>Michael B. Zimmermann</i>	
23 Pharmaceuticals: Therapeutic Agents	433
<i>Tatsuo Kaiho</i>	
24 Agrochemicals and Anthelmintics	439
<i>Peter Jeschke and Tatsuo Kaiho</i>	
PART V INDUSTRIAL APPLICATION OF IODINE	457
25 Diaryliodonium Salt Photoacid Generators	459
<i>James V. Crivello</i>	
26 Polarizing Films	479
<i>Bart Kahr and Kevin M. Knowles</i>	
27 Iodine in Polymer Synthesis: An Important Element for Precision Polymerizations	489
<i>Mitsuo Sawamoto</i>	
28 Iodine in Dye-Sensitized Solar Cells	501
<i>Lars Kloo</i>	
29 Fluorinated Repellents	513
<i>Toyomichi Shimada</i>	
30 Etching Gas	523
<i>Seiji Samukawa</i>	
31 Other Industrial Applications	547
<i>Tatsuo Kaiho</i>	

PART VI BIOINORGANIC CHEMISTRY AND ENVIRONMENTAL CHEMISTRY OF IODINE	555
32 Iodine Bioinorganic Chemistry: Physiology, Structures, and Mechanisms	557
<i>Frithjof C. Küpper and Peter M.H. Kroneck</i>	
33 Atmospheric Chemistry of Iodine	591
<i>Lucy J. Carpenter</i>	
PART VII RADIOISOTOPE OF IODINE	603
34 Radioactive Iodine	605
<i>Yoshifumi Shirakami</i>	
INDEX	625

LIST OF CONTRIBUTORS

Anna Błażewicz Department of Analytical Chemistry, Medical University of Lublin, Lublin, Poland

Lucy J. Carpenter Wolfson Atmospheric Chemistry Laboratories, University of York, Heslington, York, UK

James V. Crivello Department of Chemistry and Chemical Biology, Rensselaer Polytechnic Institute, Troy, New York, NY, USA

Toshifumi Dohi College of Pharmaceutial Sciences, Ritsumeikan University, Kusatsu, Shiga, Japan

Waldemar Gottardi Department of Hygiene, Microbiology and Social Medicine, Division of Hygiene and Medical Microbiology, Innsbruck Medical University, Innsbruck, Austria

Iwao Hachiya Department of Chemistry for Materials, Mie University, Tsu, Mie, Japan

Junji Inanaga Institute for Molecular Chemistry and Engineering, Kyushu University, Fukuoka, Japan

Peter Jeschke Bayer CropScience AG, Monheim am Rhein, Germany

Bart Kahr Department of Chemistry and Molecular Design Institute, New York University, New York, NY, USA

Tatsuo Kaiho Nihon Tennen Gas Co., Ltd., Chiba, Japan

- Nobuyuki Kaneko** Institute for Geo-Resources and Environment, Geological Survey of Japan, AIST, Tsukuba, Ibaraki, Japan
- Hirofumi Kanoh** Chiba University, Chiba, Japan
- Yasuyuki Kita** Emeritus Professor of Osaka University, Ritsumeikan University, Kusatsu, Shiga, Japan
- Tsugio Kitamura** Department of Chemistry and Applied Chemistry, Graduate School of Science and Engineering, Saga University, Saga, Japan
- Lars Kloo** KTH Royal Institute of Technology, Stockholm, Sweden
- Kevin M. Knowles** Department of Materials Science and Metallurgy, University of Cambridge, Cambridge, UK
- Takehisa Konishi** Chiba University, Chiba, Japan
- Werner Krause** Bayer Healthcare Pharmaceuticals, Berlin, Germany
- Peter M.H. Kroneck** Department of Biology, University of Konstanz, Konstanz, Germany
- Stanley T. Krukowski** Oklahoma Geological Survey, Mewbourne College of Earth and Energy, The University of Oklahoma, Norman, OK, USA
- Frithjof C. Küpper** Oceanlab, University of Aberdeen, Newburgh, UK
- Armin Lauterbach** SQM, Santiago, Chile
- James L. Marshall** Department of Chemistry, University of North Texas, Denton, TX, USA
- Virginia R. Marshall** Department of Chemistry, University of North Texas, Denton, TX, USA
- Pierangelo Metrangolo** Laboratory of Nanostructured Fluorinated Materials (NFMLab), Department of Chemistry, Materials, and Chemical Engineering “Giulio Natta”, Politecnico di Milano, Milan, Italy
- Giuseppe Resnati** Laboratory of Nanostructured Fluorinated Materials (NFMLab), Department of Chemistry, Materials, and Chemical Engineering “Giulio Natta”, Politecnico di Milano, Milan, Italy
- Steven E. Rokita** Department of Chemistry, Johns Hopkins University, Baltimore, MD, USA
- Seiji Samukawa** Tohoku University, Sendai, Japan
- Mitsuo Sawamoto** Department of Polymer Chemistry, Graduate School of Engineering, Kyoto University, Kyoto, Japan
- Toyomichi Shimada** Asahi Glass Co., Ltd., Tokyo, Japan

Makoto Shimizu Department of Chemistry for Materials, Mie University, Tsu, Mie, Japan

Yoshifumi Shirakami Research Centre Nihon Medi-Physics, Co., Ltd., Sodegaura, Chiba, Japan

Haruhiko Taguchi Tokyo Chemical Industry Co., Ltd., Tokyo, Japan

Giancarlo Terraneo Laboratory of Nanostructured Fluorinated Materials (NFMLab), Department of Chemistry, Materials, and Chemical Engineering “Giulio Natta”, Politecnico di Milano, Milan, Italy

Michael B. Zimmermann Laboratory for Human Nutrition, Department of Health Science and Technology, Swiss Federal Institute of Technology (ETH) Zürich, Zurich, Switzerland

PREFACE

A member of the halogen group on the periodic table, iodine is found in seaweeds, the brine extracted along with natural gas, and Chilean caliche deposits. Iodine is a micronutrient element that is fundamental to a living body and is essential for the subsistence and growth of humans and animals. The goiter-preventing effects of iodine in seaweeds were known to the legendary Chinese emperor Shen-Nung as early as around 3000 BC, and the knowledge of this treatment was available in Greece by the time of Hippocrates. Nevertheless, iodine was not isolated and recognized as an element until the early nineteenth century. In 1811, Barnard Courtois of France found that violet vapor with a strong smell was generated while producing niter from seaweed ashes, and that when the vapor was cooled down, it turned into purplish-black flake-like crystalline material having a metallic luster. His friend, who was entrusted with the research of this unknown material, announced his results on December 9, 1813. In the following year, 1814, based on the results obtained from Joseph Louis Gay-Lussac's research, it was clarified that this material was a chemical element similar to chlorine. This was the beginning of iodine, named from "iodes" in Greek. Industrial production began in the same year, and in 1816, iodine was used as a medical sterilizing agent. Today it is used in many areas. Iodine use is closely linked to our daily lives. Products include medicated gargle, X-ray contrast media, and antimicrobial agents. In addition, iodine is useful as an industrial catalyst and has many applications in the field of agriculture. Recently, iodine has found a wide range of applications in innovative materials, such as liquid-crystal display (LCD) polarizing film and electrolytes of dye-sensitized solar panels.

About 90% of iodine in the world is produced in Chile (50–60%) and Japan (30–40%). In Japan, iodine is positioned as one of the most valuable resources because Japan is scarce in nonbiological resources. Chiba is the richest prefecture for

iodine resources in Japan and, thus, the Forum of Iodine Utilization (FIU) was organized on June 1, 1998, at Chiba University for further development on iodine utilization in academic and industrial fields under the cooperation of volunteers from industry, academia, and government. On July 1, 2007, the FIU was progressively reorganized to the Society of Iodine Science (SIS) based on its successful activities. In 2011, the Commemorative Symposium of Iodine Science was held at Chiba University in Japan on the occasion of the bicentennial anniversary of iodine discovery by Bernard Courtois. The special review article entitled “Commemorating Two Centuries of Iodine Research: An Interdisciplinary Overview of Current Research” was also issued in the *Angewandte Chemie International Edition* on December 2, 2011. Since iodine was officially recognized as a novel element in 1813 by Bernard Courtois and his friends, it is worth publishing a comprehensive book about iodine in 2013 to celebrate the bicentennial anniversary of this event.

Chiba, Japan
December 2013

TATSUO KAIHO

1

OVERVIEW

TATSUO KAIHO

Nihon Tennen Gas Co., Ltd., Chiba, Japan

1.1 INTRODUCTION

To the best of our knowledge, there was no book that focused on iodine chemistry and application.¹ This book will cover all of the areas related to iodine in their entirety. Therefore, it is expected to be a useful guide for both academic and industrial chemists who want to synthesize complex compounds or develop new materials by using iodine reagents or intermediates. The book consists of the following parts.

Part 1: Characteristics, elemental of iodine

Part 2: Production of iodine

Part 3: Synthesis of iodine compounds

Part 4: Biological application of iodine

Part 5: Industrial application of iodine

Part 6: Bioinorganic chemistry and environmental chemistry of iodine

Part 7: Radioisotope of iodine

¹ The books dealing with the biological activity of iodine [1] and the development of new reactions using variously hypervalent iodine as catalysts [2, 3] partially involve iodine chemistry and applications, while none of them cover the whole area of iodine chemistry.

1.2 DISCOVERY AND NAMING

In 1811, French chemist Barnard Courtois found that violet vapor with a strong smell was generated while producing niter from seaweed ashes and that when the vapor was cooled down it turned into a purplish black flake-like crystalline material having a metallic luster. His friend, who was entrusted with the research of this unknown material, announced his results in the journal *Annales de Chimie* on December 9, 1813. In the following year, 1814, based on the results of Joseph Louis Gay-Lussac's research, it was clarified that this material was a chemical element similar to chlorine. Iodine was named after “*iodes*,” which means violet or purple in Greek. Industrial production began in the same year, and in 1816 iodine was used as a medical sterilizing agent.

1.3 PHYSICOCHEMICAL PROPERTIES

Iodine is a nonmetallic element of the halogen family (fluorine, chlorine, bromine, iodine, and astatine) and appears in group 17 of the periodic table. Iodine under standard conditions is a purplish-black solid and has a glittering crystalline appearance. It has a moderate vapor pressure at room temperature and in an open vessel slowly sublimates to a deep violet vapor. If heated under the proper conditions, iodine can be made to melt at 113.7°C and to boil at 184°C. The density of iodine is 4.98 g/cm³. Because of its high electronegativity, it forms iodides with almost all elements, with iodine possessing the formal oxidation state -1 . Iodine is known in compounds with formal oxidation states ranging from -1 , $+1$, $+3$, $+5$, and $+7$. Iodine also reacts with other halogens, fluorine, chlorine, and bromine, and forms interhalogens such as IF₅, ICl, and IBr. These compounds are used for halogenation reactions. Iodine dissolves easily in most organic solvents such as hexane, benzene, carbon tetrachloride, and chloroform owing to its lack of polarity, but is only slightly soluble in water. However, the solubility of elemental iodine in water can be increased by the addition of sodium or potassium iodide.

1.4 PRODUCTION

The concentration of iodine in brown seaweeds is so high that these marine algae have been used as the raw material for iodine production since the first half of the nineteenth century. Today, iodine production is conducted in areas where brines from natural gas (Japan) and oil fields (United States) contain high iodine concentrations, as well as from Chilean caliche deposits. About 2/3 of the total iodine production in the world originates from Chile and 1/3 from Japan, together accounting for nearly 90% of the iodine globally. Two methods are employed for the production of iodine in Japan: (1) the “blowing out” method, which takes advantage of the high vapor pressure of molecular iodine and is ideal for large-scale production,

including the processing of brine at high temperature; and (2) the “ion-exchange resin” method, which uses a resin that adsorbs iodide and is suitable for both small and large production plants. In contrast, iodine production in Chile is based on the mining and leaching of nitrate ores (caliches). Caliches contain lautarite ($\text{Ca}(\text{IO}_3)_2$) and dietzeit ($\text{Ca}(\text{IO}_3)_2 \cdot 8\text{CaCrO}_4$). The solutions from the leaching of caliches carry iodine in the iodate form. Part of the iodate in solution is subsequently reduced to iodide by using sulfur dioxide obtained by the combustion of sulfur. The resulting iodide is combined with the remainder of the untreated iodate solution to generate elemental iodine.

1.5 SYNTHESIS

Generally, organic iodides can be divided into two classes of alkyl iodides and aryl iodides. Since alkyl iodides show the highest reactivity among alkyl halides, typical reactions of alkyl iodides include nucleophilic substitution, elimination, reduction, and the formation of organometallics. On the other hand, aryl halides do not undergo direct displacement by nucleophiles as observed in the case of alkyl halides, because of their low reactivity toward nucleophilic substitution. Therefore, aryl iodides undergo nucleophilic substitutions, iodine–metal exchange for organometallic compounds, and coupling reactions. The development of new reactions for the synthesis of aromatic compounds is one of the hot research fields in organic chemistry. As such, the hypervalent iodine-mediated cross-coupling reactions have been studied extensively. The new concept of halogen bonding has recently been introduced in the life sciences to develop novel drugs and in the material sciences to develop liquid crystals and organic conductors.

1.6 INDUSTRIAL APPLICATION

The industrial process for the production of acetic acid is currently dominated by the carbonylation of methanol. The three-step process involves iodomethane as an intermediate and requires a catalyst, usually a metal complex, such as rhodium iodide (Monsanto process) or iridium iodide (Cativa process). Nylon is an industrially important and useful material with multiple applications, including as an engineering resin and fiber. Thermoplastic forms of nylon are stabilized with copper iodide. Nylon fiber producers use potassium iodide for tire and airbag cord nylon. The potassium iodide reacts in situ with cupric acetate to form cupric iodide, which acts as a heat stabilizer. A polarizer with the function of transmitting and blocking light is a basic component of liquid-crystal displays (LCDs), along with the liquid crystal that functions as a switch for light. LCDs are used in a wide range of instruments, including computer and TV screens, navigation systems for automobiles, and instrument displays. The most common materials used in polarizing films are stretched polyvinyl alcohol films treated with absorbing iodine.

1.7 RECYCLE

Recovery of expensive iodine from used iodine-containing materials or iodine compounds, and, further, the manufacturing step of iodine-containing materials such as X-ray contrast agents and liquid crystal films, is very beneficial from the viewpoint of economy, natural environmental conservation, and conservation of natural resources. Many iodine manufacturers have recently focused on collecting and recycling iodine from waste streams in view of their sustainability.

1.8 BIOLOGICAL ACTIVITY

Iodine is an essential component of hormones produced by the thyroid gland. Thyroid hormones, and therefore iodine, are essential for mammalian life. The optimal dietary iodine intake for healthy adults is 150–250 µg/day. In regions where iodine in soils and drinking water is low, humans and animals may become iodine-deficient. Iodine deficiency has multiple adverse effects on humans due to inadequate thyroid hormone production that are termed the iodine deficiency disorders. Iodine deficiency during pregnancy and infancy may impair growth and neurodevelopment of the offspring and increase infant mortality. Deficiency during childhood reduces somatic growth and cognitive and motor function. In most countries, the best strategy to control iodine deficiency in populations is iodization of salt, one of the most cost-effective ways to contribute to economic and social development.

1.9 PHARMACEUTICALS

Halogens have played an important role in the development of pharmaceuticals for several decades. The effectiveness of many complex molecules is significantly enhanced by the presence of halogen atoms. The majority of halogenated drugs contain fluorine, followed by chlorine, while those with bromine are rare. Only a few iodine-containing drugs are known, such as the thyroid hormone thyroxine, an anti-herpesvirus, the antiviral drug idoxuridine, and amiodaron, a class III antiarrhythmic agent. Since C–I bonds are highly polarizable, the iodinated compounds are relatively unstable.

On the other hand, iodinated contrast media for X-rays categorized as diagnostic drugs are very stable compared to the iodinated therapeutic agents. X-ray contrast media (XRCMs) are substances that enable the visualization of soft tissues in X-ray examination. The iodine atoms function as the X-ray absorbers, and their utility can be attributed to their high atomic weight. The nonionic XRCMs, developed in the 1980s, including iopamidol, iohexol, and iopromide, offer a significant margin of safety, have fewer side effects, and provide a high level of comfort to the patients, compared to ionic compounds.

The widely used iodine tincture is an alcohol solution of iodine and potassium iodide. Iodophores are iodine complexes with surfactants that act as iodine carriers.

These are water-soluble and less irritating to the skin and other tissues than the tincture. Iodine and iodophores have a wide range of antimicrobial action against Gram-positive and -negative bacteria, tubercle bacilli, fungi, and viruses. The most popular iodophore for surgical scrub and gargle is povidone iodine.

1.10 AGROCHEMICALS

In the past three decades a significant increase of halogenated active ingredients in the field of modern crop protection research and development was observed. Interestingly, there has been a remarkable rise in the number of commercial products containing “mixed” halogens, for example, one or more further halogen atoms. Generally, iodine-containing compounds are in the minority, and some of them are “mixed” with other halogens like bromine or chlorine. A selection of three modern iodine-containing agrochemicals is as follows: iodosulfuron–methyl–sodium (herbicide), proquinazid (fungicide), and flubendiamide (insecticide). The iodo-containing compounds can reflect (i) a moderate chemical and biological stability, (ii) a good hydrophobicity or lipophilicity, which increases biological membrane permeability, (iii) a high bulkiness, and (iv) halogen bonding interactions.

1.11 ISOTOPES

In the past, with major nuclear power plant accidents occurring in Three Mile Island in the United States in 1979, Chernobyl in Ukraine (the former Soviet Union) in 1986, and recently with the Fukushima disaster, the world is once again reminded of the real dangers of contamination with radioactive materials, including radioactive iodine. Radioactive iodine is associated with such risks but can also be of great benefit when used for medical purposes. Radioactive iodine has been used in the field of medicine (nuclear medicine), as diagnostic and therapeutic radiopharmaceuticals and therapeutic medical devices, throughout the world. The isotopes iodine-123 [^{123}I] and iodine-125 [^{125}I] are used as radiopharmaceuticals to diagnose a patient's condition based on abnormalities in the internal distribution of radioactivity. Therapeutic radiopharmaceuticals include compounds labeled with radioactive iodine isotopes such as iodine-125 [^{125}I] and iodine-131 [^{131}I]. Therapeutic radiopharmaceuticals are administered orally or intravenously to the body to treat lesions with internal radiation.

REFERENCES

- [1] Preedy VR, Burrow GN, Watson RR. *Comprehensive Handbook of Iodine: Nutritional, Biochemical, Pathological and Therapeutic Aspects*. Burlington: Academic Press; 2009.
- [2] Vavoglis A. *Hypervalent Iodine in Organic Synthesis*. London: Academic Press; 1997.
- [3] Zhdankin VV. *Hypervalent Iodine Chemistry: Preparation, Structure, and Synthetic Applications of Polyvalent Iodine Compounds*. New York: John Wiley & Sons; 2013.

PART I

CHARACTERISTICS, ELEMENTAL OF IODINE

2

PHYSICAL PROPERTIES OF IODINE

TATSUO KAIHO

Nihon Tennen Gas Co., Ltd., Chiba, Japan

Iodine, I, atomic mass 129.9044, atomic number 53, is a nonmetallic element of the halogen family (fluorine, chlorine, bromine, iodine, and astatine) and appears in group 17 of the periodic table. The electronic configuration of iodine atom is [Kr] 4d¹⁰5s²5p⁵. The relative atomic mass of its only stable isotope is 127. There are 22 artificial isotopes with masses between 117 and 139 [1] (Chapter 34).

Iodine under standard conditions is a bluish-black solid and has a glittering crystalline appearance. It has a moderate vapor pressure at room temperature and in an open vessel slowly sublimates to a deep violet vapor that is irritating to the eyes, nose, and throat.

The molecular lattice contains discrete diatomic molecules that are also present in the molten and the gaseous state. Iodine melts at the relatively low temperature of 113.7°C and turns dark brown although the liquid is often obscured by a dense violet vapor of gaseous iodine [2, 3].

Physical properties of iodine are provided in Tables 2.1, 2.2, and 2.3.

Iodine dissolves easily in most organic solvents such as hexane, benzene, carbon tetrachloride, and chloroform owing to its lack of polarity, but it is only slightly soluble in water [4]. However, the solubility of elemental iodine in water can be increased by the addition of sodium or potassium iodide [5] (Tables 2.4, 2.5, and 2.6).

Molecular iodine reacts reversibly with the negative ion, generating the triiodide anion I₃[−] in equilibrium, which is soluble in water [6, 7].

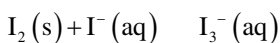


TABLE 2.1 Physical properties of iodine

Element category	Halogen
Group, period, block	17 (halogens), 5, p
Standard atomic weight	126.90447
Electron configuration	[Kr] 4d ¹⁰ 5s ² 5p ⁵
	2, 8, 18, 18, 7
Atomic radius	140 pm
Covalent radius	139 ± 3 pm
Ionic radius	220 pm
Electronegativity	2.66 (Pauling scale)
Electron affinity	301 kJ mol ⁻¹
Ionization enthalpy	1015 kJ mol ⁻¹
Ionization energies	1st: 1015 kJ mol ⁻¹
	2nd: 1852 kJ mol ⁻¹
	3rd: 3200 kJ mol ⁻¹

TABLE 2.2 Physical properties of iodine in the solid phase

Solid phase						
Density (298 K)	4.94 g cm ⁻³					
Density (333 K)	4.866 g cm ⁻³					
Refractive index	nD20 3.34					
Melting point	387 K, 114°C, 236.66°F					
Boiling point	457 K, 184°C, 363.7°F					
Triple point	386.65 K (113°C), 12.1 kPa					
Critical point	819 K, 11.7 MPa					
Heat of fusion (I ₂) at melting point	7.9 kJ mol ⁻¹ 62.17 J g ⁻¹					
Heat of vaporization (I ₂) at boiling point	41.57 kJ mol ⁻¹					
at 298 K	23.0 kJ mol ⁻¹					
Molar heat capacity (I ₂)	53.3 J mol ⁻¹ K ⁻¹					
Vapor pressure (rhombic)	1	10	100	1k	10k	100k (Pa)
	260	282	309	342	381	457 (K)
Vapor pressure	0.031 kPa (25°C) 9.17 kPa (113.6°C)					
Van der Waals radius	198 ppm					
Electrical resistivity	1.3 × 10 ⁷ Ω m (0°C) 5.85 × 10 ⁶ Ω m (25°C) 8.33 × 10 ⁵ Ω m (110°C)					
Thermal conductivity	0.45 W m ⁻¹ K ⁻¹					

When iodine is dissolved in polar solvents that are strong donor solvents such as ketones, ethers, pyridine, the formation of charge-transfer complexes leads to modification of the energy gap between the two molecular orbitals, and thus different wavelengths of light are absorbed. Iodine accepts electrons from the solvent

TABLE 2.3 Physical properties of iodine in the liquid and gas phases

<i>Liquid phase</i>	
Boiling point	184°C
Critical temperature	546°C
Critical pressure	11.7 MPa
Critical compressibility factor	0.268
<i>Density</i>	
d^{120}	3.96 g cm ⁻³
d^{180}	3.736 g cm ⁻³
Electrical resistivity at 140°C	
Kinematic viscosity at 116°C	0.5727 mm ² s ⁻¹ (=cSt)
at 184°C	0.3785 mm ² s ⁻¹ (=cSt)
Dynamic viscosity at 116°C	2.268 m Pa·s
at 184°C	1.414 m Pa·s
Dielectric constant at 118°C	11.08
Heat vaporization at boiling point	164.46 J g ⁻¹
Specific heat at 113.6–184°C	0.3163 J g ⁻¹ K ⁻¹
<i>Gaseous phase</i>	
Vapor density at 101.3 MPa 185°C	6.75 g l ⁻¹
Entropy at 298.2 K	260.63 J K ⁻¹ mol ⁻¹
Specific heat 25–1200°C	0.1464 J g ⁻¹ K ⁻¹

TABLE 2.4 Solubility of iodine in various solvents at 25°C

Solvent	Solubility (g kg ⁻¹)	Color
Benzene	164	Red
Butan-2-ol	97	Brown
Carbon disulfide	197	Red
Carbon tetrachloride	19.2	Violet
Chloroform	49.7	Violet
Ether	337.3	Brown
Ethanol	271.7	Brown
Ethyl acetate	157	Brown
Hexane	13.2	Violet
Toluene	182.5	Red
Water	0.34	Brown

molecule into its lowest unoccupied molecular orbital (LUMO). This lowers the energy of the transition from the highest occupied molecular orbital (HOMO) of the iodine atom to its LUMO, thereby changing the color from the characteristic violet to brown and other colors. Depending on the electron-donating ability of the solvent, absorption bands are observed from 520 to 540 nm in hydrocarbon and chlorocarbon solvents, from 490 to 510 nm in aromatic solvents, and from 450 to 480 nm in alcohols and amines [8, 9].

TABLE 2.5 Solubility of iodine in water

Temperature (°C)	Solubility (g l ⁻¹)
0	0.162
20	0.293
25	0.34
30	0.399
40	0.549
50	0.769
60	1.06
70	1.51
80	2.17
90	3.12
100	4.48
110	6.65

TABLE 2.6 Solubility of iodine in an aqueous solution of sodium iodide

Temperature (°C)	Solubility in NaI (aq) (10 g/100 ml)
10	8.9
20	9.6
30	10.3
40	10.9
50	11.7
60	13.6

The physical properties of the first four halogens are summarized in Table 2.7.

Bond dissociation energies of chlorine, bromine, and iodine decrease down the halogen group as the size of the atom increases. The bond energy of fluorine is, however, lower than that of chlorine, and bromine and only slightly larger than iodine because of interelectronic repulsions present in the small atom of fluorine. As a member of the halogen family, iodine shares many of the typical characteristics of the other elements in group 17, such as high electronegativity (2.66 according to the Pauling scale). The electronegativity decreases on descending the group as the size of the halogen atom increases.

Due to increase in the number of electron shells in group 17 from fluorine to iodine (because of which the effective nuclear charge decreases and the electron cloud expands), both atomic and ionic radii increase. The ionic radius of the halide anion is greater than that of the halogen atom. Further, as the atomic size increases from fluorine to iodine, the ionization energy decreases on going down the group.

The melting and boiling points increase down the group because the size of the molecules increases down the group, leading to an increase in the strength of the van der Waals forces:

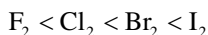


TABLE 2.7 A comparison of some physical properties of fluorine, chlorine, bromine, and iodine

	Fluorine	Chlorine	Bromine	Iodine
	9F	17Cl	35Br	53I
Electron configuration	[He]2s ² 2p ⁵	[Ne]3s ² 3p ⁵	[Ar]3d ¹⁰ 4s ² 4p ⁵	[Kr]4d ¹⁰ 5s ² 5p ⁵
First ionization energy(kJ mol ⁻¹)	1687	1257	1146	1015
Electron affinity (kJ mol ⁻¹)	334	355	331	301
Electronegativity (Allred–Rochow)	4.1	2.83	2.74	2.21
Pauling	3.98	3.16	2.96	2.66
Ionic radius (X ⁻¹ ,pm)	133	181	196	220
Covalent radius (<i>r</i> (X ₂)/2, pm)	71	99	114	133
van der Waals radius (pm)	147	175	181	198
Melting point (K)	40	172.16	265.9	387
Melting point (°C)	-220	-101	-7	114
Boiling point (K)	85	239.1	332	457
Boiling point (°C)	-188	-34	59	184
Density (g cm ⁻³ at 25°C)	0.0017	0.0032	3.1028	4.933
Bond dissociation energy (X ₂ , kJ·mol ⁻¹)	159	242	193	151
Hydration energy (X ⁻¹ , kJ·mol ⁻¹)	485	350	320	280
Reduction potential <i>E</i> ⁰ (V) ½ X ₂ (aq) + e ⁻ = X ⁻¹	2.89	1.40	1.10	0.62

These physical properties make iodine highly reactive and prone to radical reactions. As a consequence of its high electronegativity, it forms iodides with most elements, with iodine possessing the formal oxidation state -1 (Table 5.6). Iodine is known in compounds with formal oxidation states -1, +1, +3, +5, and +7. The high formal positive oxidation states are mainly found in compounds with the very electronegative elements oxygen and fluorine (IO⁻, IO₃⁻, IO₄⁻, IF₃, IF₅, IF₇) (Chapter 5). However, since the polarizability of iodine is high, chemical bonds are also formed with the more electropositive elements in the periodic table, and these tend to contain a fair degree of covalency.

Due to ns², np⁵ configuration, halogens have a strong tendency to accept an additional electron and convert to a noble gas configuration. Hence they have large negative electron gain enthalpies. In a halogen group from top to bottom, the electron gain enthalpy become less negative due to increasing size from fluorine to iodine (Table 2.7).

Since all halogens have a strong tendency to accept electrons, they act as good oxidizing agents. The oxidizing power of the halogens decreases from fluorine to iodine. Hence iodide ions are oxidized to iodine with either chlorine or bromine [10] (Table 2.8).

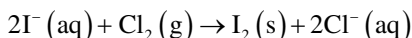


TABLE 2.8 Reactions of the halogens with ions of other halogens

	Cl_2 (aq)	Br_2 (aq)	I_2 (aq)
Cl^- (aq)		Stays yellow solution (no reaction)	Stays brown solution (no reaction)
Br^- (aq)	Orange solution forms $\text{Cl}_2 + 2\text{Br}^- \rightarrow 2\text{Cl}^- + \text{Br}_2$		Stays brown solution (no reaction)
I^- (aq)	Red solution forms $\text{Cl}_2 + 2\text{I}^- \rightarrow 2\text{Cl}^- + \text{I}_2$	Red solution forms $\text{Br}_2 + 2\text{I}^- \rightarrow 2\text{Br}^- + \text{I}_2$	

On the contrary, halide ions behave as reducing agents. Iodide has the most powerful reducing ability in the four halogens.

Least powerful $\text{F}^- < \text{Cl}^- < \text{Br}^- < \text{I}^-$ most powerful.

REFERENCES

- [1] Lyday PA. *Iodine and Iodine Compounds*, Ullmann's Encyclopedia of Industrial Chemistry. Weinheim: Wiley-VCH; 2005.
- [2] Greenwood NN, Earnshaw A. *Chemistry of the Elements*. 2nd ed. Oxford: Butterworth-Heinemann; 1997. p 807.
- [3] O'Neil MJ ed. *The Merck Index: An Encyclopedia of Chemicals, Drugs, and Biologicals*. 14th ed. New Jersey: Merck, 2006, 5014.
- [4] Kirk RE, Othmer DF. *Encyclopedia of Chemical Technology*. Volume 7, New York: Wiley; 1993. p 946.
- [5] Seidel A, editor. *Solubilities of Inorganic and Organic Compounds*. Volume 1, New York: D. van Nostrand Co., Inc.; 1911.
- [6] Wells AF. *Structural Inorganic Chemistry*. Oxford: Clarendon Press; 1984.
- [7] Cotton FA, Wilkinson G. *Advanced Inorganic Chemistry*. 5th ed. New York: John Wiley & Sons; 1988.
- [8] Housecroft CE, Sharpe AG. *Inorganic Chemistry*. 3rd ed. New York: Prentice Hall; 2008. p 541.
- [9] Küpper FC, Feiters MC, Olofsson B, Kaiho T, Yanagida S, Zimmermann MB, Carpenter LJ, Luther III GW, Lu Z, Jonsson M, Kloo L. Commemorating Two Centuries of Iodine Research: An Interdisciplinary Overview of Current Research. *Angew. Int. Ed.* 2011, 50, 11598.
- [10] Pauling L. *General Chemistry*. New York: Dover Publications; 1988.

3

ANALYTICAL METHODS FOR IODINE AND IODIDES

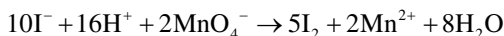
HIROFUMI KANOH AND TAKEHISA KONISHI

Chiba University, Chiba, Japan

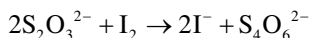
3.1 DETERMINATION OF CONCENTRATION OF IODINE OR IODIDES IN SOLUTION

3.1.1 Introduction

Iodine is one of the essential elements for human nutrition. It is estimated that more than two billion people have insufficient iodine intake and are at risk of developing iodine deficiency [1]. Methods are required to affordably and accurately quantify iodine in soil, plants, and various foods and in physiological samples, notably milk, serum, and urine, to properly assess iodine nutrition. Conventionally, iodine contents of salt samples are measured using the iodometric titration method. Addition of an oxidizing agent such as KMnO_4 or Br_2 with acid liberates free iodine from iodide in the salt sample:

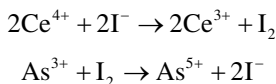


Free iodine can be titrated with a reducing agent such as thiosulfate:



However, iodine measurement in biological samples is carried out almost exclusively by one of two methods: One is a kinetic spectrophotometric method called the

Sandell–Kolthoff reaction based on the reduction of yellow Ce(IV) by As(III) to colorless Ce(III) [2], which is normally very slow. This reaction is catalyzed by trace amounts of iodide. The reaction is as follows:



The rate of disappearance of the yellow color in a Ce(IV)–As(III) mixture is monitored as a measure of iodine content. Although Ce(III) is fluorescent (λ_{ex} 254 nm, λ_{em} 350 nm) [2], the reaction is rarely used because of variable amounts of ultraviolet (UV)-absorbing species that may be present. Since many organic substances can potentially interfere by chelating Ce(IV) or Ce(III) [2, 3], complete mineralization of the sample is necessary to digest the organics. As this digestion step typically involves perchloric acid, special hoods and precautions are required because of explosion hazards. Consequently, other methods, for example, inductively coupled plasma mass spectrometry (ICP-MS), are used. ICP-MS permits excellent sensitivity and, in some cases, direct sample analysis after dilution. However, it is still necessary to use an internal standard to account for matrix effects [4].

More detailed descriptions for these analytical methods can be seen in the following sections.

3.1.2 The Sandell–Kolthoff Reaction

The Sandell–Kolthoff (S–K) reaction is likely to be the most widely used among the techniques for quantifying iodine. The decrease in absorbance due to Ce(IV) is typically measured at 405–420 nm, although the maximum sensitivity can be achieved at 310–317 nm [5, 6]. A higher concentration of thiocyanate interferes with the reaction. Traces of metal ions such as silver or mercury also interfere by binding iodide. Substances that readily undergo oxidation, notably nitrite, ascorbic acid, and ferrous iron, also interfere [2, 3].

Determination of iodide using the S–K method can be carried out in two different ways: (i) record the complete absorbance profile with time, (ii) measure the sample absorbance after some preset time interval following mixing of all components. Most often (ii) is used for higher throughput. The iodine concentration can be determined directly from the difference in absorbance between a blank and the sample at any time following the reaction [5].

The S–K method is an effective way to measure iodine in complex samples, but it is apparent that the sample preparation methods are onerous [7], leading to a major bottleneck when a large number of samples are to be analyzed. In some of the digestion methods, if digestion is conducted with multiple samples in a closed system, some iodine escapes into the gas phase from high-concentration samples and is reabsorbed by other samples [8].

A very current adaptation of the S–K method is on microtiter plates with multi-channel plate readers. These can provide high sample throughput and reduce the

amount of waste per sample [9–11], although the Technicon Autoanalyzer and equivalent segmented flow analyzers are still in use [7].

The S–K reaction was successfully applied to the analysis of protein-bound and total inorganic serum iodine, urinary iodide, plant material, food, tissue, feces, amniotic fluid, and coal. The sensitivity of the S–K assay is excellent; therefore iodine instead of radionuclides was used to tag antibodies [12].

3.1.3 Inductively Coupled Plasma Mass Spectrometry

ICP-MS is a type of mass spectrometry that can detect metals and several nonmetals at concentrations as low as 1 part in 10^{12} . This is achieved by ionizing the sample with inductively coupled plasma and then using a mass spectrometer to separate and quantify those ions. In a typical ICP-MS, microwave or radio frequency power is applied through an induction coil to generate high-temperature argon plasmas of 4,500–8,000 K, with an electron temperature of 8,000–10,000 K. The plasma atomizes the sample and strips the atoms of one or more valence electrons. The resulting positive ions then enter a single quadrupole mass analyzer for sorting out ions of different m/z and are then detected [13]. Iodine has a relatively high first ionization potential (IP to form I^+) of 10 eV [14]. Thus, the iodine present is only partially ionized (~25%). While this does not make iodine the most sensitive among elements to be measured by ICP-MS, the sensitivity for iodine in ICP-MS is superior compared to other techniques for iodine measurement. In addition, a very large linear dynamic range can be attained. Accordingly, some dilution is needed to minimize the very high salt/dissolved solids contents. It is essential to correct for matrix effects, which are best compensated for by using isotope dilution mass spectrometry with ^{129}I as an isotopic tracer [4, 14].

An ICP-MS can be used as an element specific detector, although it cannot itself distinguish between different species of a particular element. It is invaluable as a detector when used in conjunction with liquid or ion chromatography [15–19] or capillary electrophoresis [20] for speciation studies.

3.1.4 Electrochemical and Potentiometric Probes

Ion-selective electrodes (ISEs) are commercially available for iodide and have been applied for the determination of iodide [21, 22]. A direct measurement of iodine in milk and similar beverages by ISEs was compared with that by the S–K method. The S–K method produced poorer results, which the authors attributed to losses during digestion [21]. The response of the ISEs was found to be nonlinear below $20\mu M$ but was linear up to 1 mM. It takes 5–10 min to stabilize.

Commercial iodide ISEs are based on insoluble silver salt membranes and respond to high levels of other anions that form insoluble silver salts, notably other halides and pseudohalides. In recent years, much effort has been devoted to synthesizing iodide-selective ionophores that have greater selectivity than silver salt-based ISEs; these efforts were covered in a review [23]. Electrochemical detection in general and amperometric detection in particular are popular for iodine determination because of the fast response time and sensitivity for the analyte of interest.

3.2 RAMAN SPECTROSCOPIC ANALYSIS OF POLYIODIDES

Although solid iodine has a Raman-active mode at 180 cm^{-1} , no spectral features are seen in the infrared (IR) spectra as a result of the symmetry selection rules [24–26]. The ν_1 symmetric mode for molten and gaseous iodine are at 194 and 213 cm^{-1} , respectively [27, 28]. Spectral features for molten iodine indicating the presence of I_3^- and $(\text{I}_2)_n$ cluster formation have also been detected [27]. As I_2 becomes coordinated to a donor, the force constant is reduced and the ν_1 mode shifts to lower wavenumbers [29, 30]. This is due to electron density donation into the σ^* antibonding orbital of iodine. Usually, coordination to the donor species also lowers the symmetry of iodine. As a result the ν_1 mode becomes IR-active. Classical examples of this type of donor–acceptor interaction are solutions of iodine in different organic solvents [31].

Iodine molecule (I_2) and the Lewis base donors I^- and I_3^- can be regarded as the main building blocks of polyiodides [24, 30b, 32]. Polyiodides do not exist as discrete entities but are always a combination of I_2 molecules and I^- and/or I_3^- anion chains [24, 25]. They can be described by the following formula: $m\text{I}_2 + n\text{I}^- \rightarrow \text{I}_{(2m+n)}^{n-}$, leading to several possible structures. For instance, I_3^- might be a three-body system ($\text{I}-\text{I}-\text{I}$, I_3^- entity) or asymmetric anions consisting of I_2 molecules weakly interacting with I^- ions [24, 25, 30b, 32–35]. In the same way, an I_5^- anion can be described as an I_3^- entity associated to an I_2 molecule ($\text{I}_3^-\cdot\text{I}_2$) or as two I_2 molecules in interaction with an I^- ion ($2\text{I}_2\cdot\text{I}^-$). The Raman spectra of $[\text{H}_3\text{O}(\text{dibenzo-18-crown-6})][\text{I}_3]$, $[\text{H}_3\text{O}(\text{dibenzo-18-crown-6})][\text{I}_5]$, and $[\text{H}_3\text{O}(\text{dibenzo-18-crown-6})][\text{I}_7]$ are shown in Figure 3.1 [36]. In addition, polyiodides can display several shapes such as linear, V or L shape. Also, a large variety of polyiodides can be synthesized [24]. Table 1 reports the Raman mode frequencies for the main short I_n^{m-} chains reported in the literature [24, 25, 30b, 32–35], as summarized in Table 3.1.

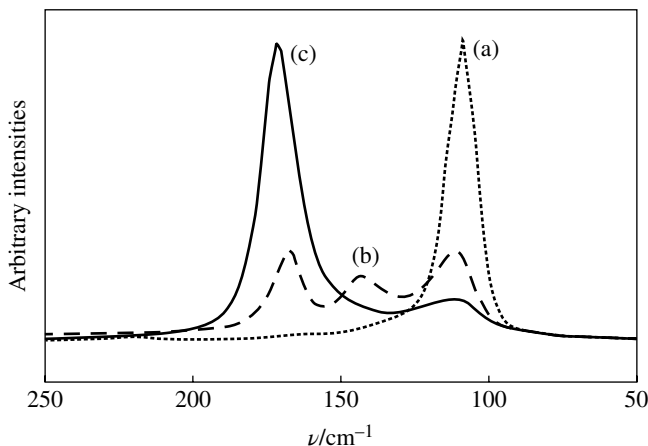


FIGURE 3.1 Raman spectra of (a) $[\text{H}_3\text{O}(\text{dibenzo-18-crown-6})][\text{I}_3]$, (b) $[\text{H}_3\text{O}(\text{dibenzo-18-crown-6})][\text{I}_5]$, and (c) $[\text{H}_3\text{O}(\text{dibenzo-18-crown-6})][\text{I}_7]$. Reproduced with permission from Ref. [36] © 2000, The Royal Society of Chemistry.

TABLE 3.1 Raman frequencies for main polyiodides reported in literature

Iodine species	Raman frequency (cm ⁻¹)	References
I ₂	174 s	[24, 30b, 32–34]
Symmetric I ₃ ⁻ (I–I–I) ⁻	110 s	[24, 30b, 32–35]
Asymmetric I ₃ ⁻ (I ₂ ·I ⁻)	167 s, 143 w, 114 w	[30b, 32–34]
I ₃ ⁻ linear (I ₂ ·I ⁻ ·I ₂)	160 s, 104 w	[30b, 32–34]
I ₃ ⁻ V shaped (I ₂ ·I ⁻ ·I ₂)	167 s, 131 m, 114 w	[30b]
I ₃ ⁻ L shaped (I ₃ ⁻ ·I ₂)	164 s, 135 m, 106 w	[32]

m, medium; s, strong; w, weak

3.3 X-RAY ABSORPTION SPECTROSCOPIC ANALYSIS OF IODINE AND IODIDES

Photoabsorption in the X-ray range, which involves electronic transition from core levels to bound unfilled valence molecular/atomic orbitals or to the unbound continuum states, can be used to obtain element-specific information about local geometric and electronic structure around the X-ray-absorbing atom. Depending on the excess energy above the core excitation threshold, the fine structure in the X-ray absorption coefficient is called XANES (X-ray absorption near-edge fine structure) or EXAFS (extended X-ray absorption fine structure). XANES usually refers to the fine structure in the X-ray absorption coefficient in the X-ray photon energy range of approximately 50 eV above the threshold and provides information about unoccupied valence electronic states as well as local coordination environment of the X-ray-absorbing atom. EXAFS refers to the oscillatory fine structure farther above the XANES energy range. Local structural information such as interatomic distances, coordination numbers, and Debye–Waller parameters, which are complementary to the vibration frequencies obtained by IR and Raman spectroscopy, can be obtained by analyzing the EXAFS part of the X-ray absorption spectra [37]. In case of iodine, the core levels whose binding energies lie in the hard X-ray range are 1s (K edge, 33,169 eV), 2s (L_I edge, 5,188 eV), 2p_{1/2} (L_{II} edge, 4,852 eV), and 2p_{3/2} (L_{III} edge, 4,557 eV) [38]. Corresponding X-ray absorption edges can be routinely measured using the conventional setup, which is widely available at hard X-ray beamlines in synchrotron facilities. For EXAFS analysis, the iodine K edge is more advantageous than iodine L edges where the intervals between the absorption thresholds are smaller. L edges are advantageous in XANES because the corehole lifetime broadening is smaller than the K edge and higher spectral resolution is possible. Nevertheless, the L_{III} edge can still be useful for EXAFS analysis when the information contained in the photoelectron wavenumber $k < 8.8 \text{ \AA}^{-1}$ (corresponding to the L_{III}–L_{II} energy interval) is sufficient. This is often the case when the neighboring atoms are light elements (such as C or O) or considerable structural disorder is present, which in any case suppress the EXAFS signal at higher k . Although the method of EXAFS analysis is in principle independent of the element under investigation, there are a few points that are to some extent specific to iodine that are worth mentioning. One is that

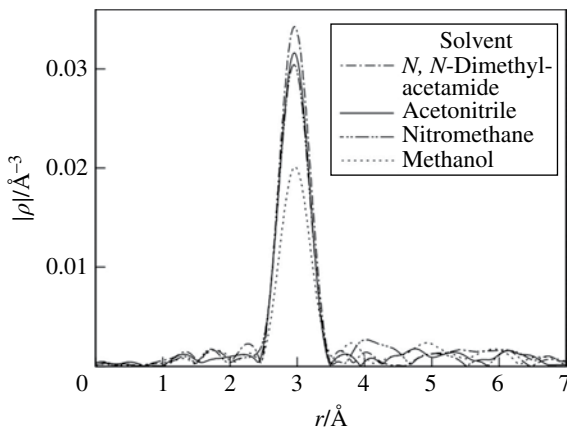


FIGURE 3.2 Iodine K-edge EXAFS Fourier transforms for I_3^- solutions of some organic solvents. Reproduced with permission from Ref. [41] © 2001, International Union of Crystallography.

there are noticeable contributions from multielectron excitations in the iodine K-edge X-ray absorption spectrum, which require special care in extracting EXAFS oscillation from raw data [39]. Another is a minimum in the backscattering amplitude, which is common in the heavier elements. This causes a minimum in the envelope function of the EXAFS oscillation, which should not be confused with the beat node that appears when two different interatomic distances are present [37].

Iodine EXAFS data of samples that contain iodine molecule or polyiodide ions where the nearest neighbor atom of X-ray-absorbing iodine atom is iodine are dominated by the I–I backscattering signal. From this, it is possible to determine the I–I interatomic distance and the amplitude of the molecular vibration of iodine molecule I_2 in various environments [40] or polyiodide I_3^- in various solvents (Fig. 3.2) [41]. In favorable cases it is possible to quantify the iodine and polyiodide species (quantify the content of I_2 , I_3^- , and I_5^-) that are present in the sample [42]. EXAFS has also been useful in determining the hydration structure of iodide or iodate ions [43–45]. EXAFS is also useful in studying the local structure of crystalline materials: it has been used in studying the thermal motion of ions in superionic conductor AgI [46–48].

The XANES part of the spectra can be used as a fingerprint for the determination of iodine/iodide species in unknown samples [49, 50]. In particular, in iodine molecules or polyiodide ions where the $5p\sigma^*$ molecular orbital is not completely filled, iodine L_{I} -edge X-ray absorption spectra shows a sharp peak at the absorption threshold, which corresponds to iodine $2s \rightarrow 5p\sigma^*$ transition, and the intensity of this peak can be a quantitative measure of the valency of the iodine/iodide species in the sample under study [51]. It is also possible to determine the three-dimensional local structure around the X-ray-absorbing iodine atom as well as the electronic structure by performing multiple-scattering XANES calculation from structural models and comparing the calculated spectra with the experiment [52–54].

REFERENCES

- [1] Zimmermann MB. Iodine deficiency. *Endocr Rev* 2009;30:376.
- [2] Sandell EB, Kolthoff IM. Micro determination of iodide by a catalytic method. *Mikrochim Acta* 1937;1:9.
- [3] May W, Wu D, Eastman C, Bourdoux P, Maberly G. Evaluation of automated urinary iodine methods: problems of interfering substances identified. *Clin Chem* 1990;36:865.
- [4] Dyke JV, Dasgupta PK, Kirk AB. Trace iodine quantitation in biological samples by mass spectrometric methods: the optimum internal standard. *Talanta* 2009;79:235.
- [5] Ke PJ, Thibert RJ, Walton RJ, Soules DK. Catalytic determination of iodine in serum at nanogram levels using the As(III)-Ce(IV) reaction. *Mikrochim Acta* 1973:569.
- [6] Sanz MC, Brechbuhler T, Green IJ. The ultramicro-determination of total and protein-bound iodine. *Clin Chim Acta* 1956;1:570.
- [7] Shelor CP, Dasgupta PK. Review of analytical methods for the quantification of iodine in complex matrices. *Anal Chim Acta* 2011;702:16.
- [8] Grossmann A, Grossmann GF. Rapid test for detection of certain iodine-containing contaminants in serum. *Clin Chem* 1958;4:296.
- [9] Wuethrich A, Jaeggi-Groisman SE, Gerber H. Comparison of two methods for the detection of urinary iodine used in epidemiological studies. *Clin Chem Lab Med* 2000;38:1027.
- [10] Houze P, Corvisier M, Toubert ME, Gourmel B, Bousquet B. Colorimetric micromethod for serum iodine determination. *Ann Biol Clin –Paris* 2004;62:222.
- [11] Hussain H, Nazaimoon W, Mohamud W. A cost-effective modified micro method for measuring urinary iodine. *Trop Biomed* 2006;23:109.
- [12] Okennedy R, Keating P. The optimization of a novel iodide microassay and its application in an immunoassay for human-antibody levels in serum. *J Immunol Methods* 1993;163:225.
- [13] Thomas R. Practical Guide to ICP-MS. New York: Marcel-Dekker; 2004.
- [14] Haldimann M, Zimmerli B, Als C, Gerber H. Direct determination of urinary iodine by inductively coupled plasma mass spectrometry using isotope dilution with iodine-129. *Clin Chem* 1998;44:817.
- [15] Buchberger W, Czizsek B, Hann S, Stingeder G. Preliminary comparison of inductively coupled plasma mass spectrometry and electrospray mass spectrometry hyphenated with ion chromatography for trace analysis of iodide. *J Anal At Spectrom* 2003;18:512.
- [16] Wuilloud RG, Selar N, Kannamkumarath SS, Caruso JA. Highly determination of 2,3,6-trinitrophenol and its metabolites in human urine by fast anion-exchange chromatography –ICP-MS. *J Anal At Spectrom* 2004;19:1442.
- [17] Stark HJ, Mattusch J, Wennrich R, Mroczek A. Investigation of the IC-ICP-MS determination of iodine species with reference to sample digestion procedures. *Fresenius J Anal Chem* 1997;359:371.
- [18] Leiterer M, Truckenbrodt D, Franke K. Determination of iodine species in milk using ion chromatographic separation and ICP-MS detection. *Eur Food Res Technol* 2001;213:150.
- [19] Sanchez LF, Szpunar J. Speciation analysis for iodine in milk by size-exclusion chromatography with inductively coupled plasma mass spectrometric detection (SEC-ICP MS). *J Anal At Spectrom* 1999;14:1697.
- [20] Michalke B, Schramel P. Iodine speciation in biological samples by capillary electrophoresis-inductively coupled plasma mass spectrometry. *Electrophoresis* 1999;20:2547.

- [21] Miles P. Determination of iodide in nutritional beverage products using an ion selective electrode. *J Assoc Off Anal Chem* 1978;61:1366.
- [22] Gushurst CA, Mueller JA, Green JA, Sedor F. Breast milk iodide: reassessment in the 1980s. *Pediatrics* 1984;73:354.
- [23] Zhang W, Mnatsakanov A, Hower R, Cantor H, Wang YZ. Urinary iodine assays and ionophore based potentiometric iodide sensors. *Front Biosci* 2005;10:88.
- [24] Svensson P, Kloo L. Synthesis, structure, and bonding in polyiodide and metal iodide-iodine systems. *Chem Rev* 2003;103:1649.
- [25] Alvarez L, Bantignies J-L, Le Parc R, Aznar R, Sauvajol J-L, Merlen A, Machon D, San Miguel A. High-pressure behavior of polyiodides confined into single-walled carbon nanotubes: a Raman study. *Phys Rev B* 2010;82:205403.
- [26] Andersson A, Sun TS. Raman spectra of molecular crystals I. Chlorine, bromine, and iodine. *Chem Phys Lett* 1970;6:611.
- [27] Magana RJ, Jannin JS. Observation of clustered molecules and ions in liquid iodine. *Phys Rev B* 1985;32:3819.
- [28] Shanabrook BV, Lannin JS. Phonon spectra of crystalline iodine. *Solid State Commun* 1981;38:49.
- [29] Blake AJ, Devilliano FA, Gould RO, Li W-S, Lippolis V, Parsons S, Radek C, Schröder M. Template self-assembly of polyiodide networks. *Chem Soc Rev* 1998;27:195.
- [30] (a) Milne J. A Raman spectroscopic study of the effect of ion-pairing on the structure of the triiodide and tribromide ions. *Spectrochim Acta A* 1992;48:533. (b) Deplano P, Devillanova FA, Ferraro JA, Isaia F, Lippolis V, Mercuri ML. On the use of Raman spectroscopy in the characterization of iodine in charge-transfer complexes. *Appl Spectrosc* 1992;46:1625. (c) Zambounis JS, Kamitsos EI, Patsis AP, Papavassiliou GC. Resonance Raman and far-infrared studies of $n\text{-Bu}_4\text{NI}_3$ and $n\text{-Bu}_4\text{NBr}_3$. *J Raman Spectrosc* 1992;23:81. (d) Bengtsson L, Füllbier H, Holmberg B, Stegemann H. The structure of room temperature molten polyiodides. *Mol Phys* 1991;73:283.
- [31] (a) Besnard M, Del Campo N. Molecular relaxation processes in liquid mixtures containing iodine complexes. *J Mol Liq* 1991;48:183. (b) Shen YR, Rosen H, Stenman F. Frequency shift of the stretching vibration of I_2 in liquid mixtures. *Chem Phys Lett* 1968;1:671. (c) Klaboe P. The Raman spectra of some Iodine, Bromine, and Iodine Monochloride charge-transfer complexes in solution. *J Am Chem Soc* 1967;89:3667.
- [32] Deplano P, Ferraro J, Mercuri ML, Trogu E. Structural and Raman spectroscopic studies as complementary tools in elucidating the nature of the bonding in polyiodides and in donor- I_2 adducts. *Coord Chem Rev* 1999;188:71.
- [33] Deplano P, Devillanova F, Ferraro J, Mercuri ML, Lippolis V, Trogu E. FT-Raman study on charge-transfer polyiodide complexes and comparison with resonance Raman results. *Appl Spectrosc* 1994;48:1236.
- [34] Teitelbaum RC, Ruby SL, Marks TJ. Charge transfer and partial oxidation in the conductive hydrocarbon-iodine complex “2Perilene- 3I_2 ”. *J Am Chem Soc* 1979;101:7568.
- [35] Hsu S, Signorelli A, Pez G, Baughman R. Highly conducting iodine derivatives of polyacetylene: Raman, XPS and x-ray diffraction studies. *J Chem Phys* 1978;69:106.
- [36] Kloo L, Svensson PH, Taylor MJ. Investigations of the polyiodides H_2OI_x ($x = 3, 5$ or 7) as dibenzo-18-crown-6 complexes. *J Chem Soc Dalton Trans* 2000:1061.
- [37] Lee PA, Citrin PH, Eisenberger P, Kincaid BM. Extended X-ray absorption fine structure—its strengths and limitations as a structural tool. *Rev Mod Phys* 1981;53:769.

- [38] Thompson C, Vaughan D, editors. *X-ray Data Booklet*. Berkeley: Lawrence Berkeley National Laboratory; 2001.
- [39] D'Angelo P, Zitolo A, Migliorati V, Pavel NV. X-ray multielectron photoexcitations at the I- K-edge. *Phys Rev B* 2008;78:144105.
- [40] Buotempo U, DiCicco A, Filliponi A, Nardone M, Postorino P. Determination of the I₂ bond-length distribution in liquid, solid and solution, by extended X-ray absorption fine structure spectroscopy. *J Chem Phys* 1997;107:5720.
- [41] Sakane H, Mitsui T, Tanida H, Watanabe I. XAFS analysis of triiodide ion in solutions. *J Synchrotron Rad* 2001;8:674.
- [42] Yokoyama T, Kaneyuki K, Sato H, Hamamatsu H, Ohta T. Structure, composition and vibrational property of Iodine-doped polyvinyl alcohol studied by temperature-dependent I K-edge extended X-ray absorption fine structure. *Bull Chem Soc Jpn* 1995;68:469.
- [43] Kaneko T, Ueda M, Nagamatsu S, Konishi T, Fujikawa T, Mizumaki M. Structure, composition and vibrational property of Iodine-doped polyvinyl alcohol studied by temperature-dependent I K-edge extended X-ray absorption fine structure. *J Phys Conf Ser* 2009;190:012062.
- [44] Fulton JL, Schenter GK, Baer MD, Mundy CJ, Dang LX, Balasubramanian M. Probing the hydration structure of polarizable halides: a multi-edge XAFS and molecular dynamics study of the iodide anion. *J Phys Chem B* 2010;114:12926.
- [45] Baer MD, Pham V-T, Fulton JL, Schenter GK, Balasubramanian M, Mundy CJ. Is iodate a strongly hydrated cation? *J Phys Chem Lett*. 2011;2:2650.
- [46] Boyce JB, Hayes TM, Mikkelsen JC. Extended-X-ray-absorption-fine-structure investigation of mobile-ion density in superionic AgI, CuI, CuBr, and CuCl. *Phys Rev B* 1981;23:2876.
- [47] Dalba G, Fornasini P, Rocca F, Mobilio S. Correlation effects in the extended X-ray-absorption fine-structure Debye-Waller factors of AgI. *Phys Rev B* 1990;41:9668.
- [48] Dalba G, Fornasini P, Rocca F. Cumulant analysis of the extended X-ray-absorption fine structure of β -AgI. *Phys Rev B* 1993;47:8502.
- [49] Schlegel ML, Reiller P, Mercier-Bion F, Barre N, Moulin V. Molecular environment of iodine in naturally iodinated humic substances: Insight from X-ray absorption spectroscopy. *Geochim Cosmochim Acta* 2006;70:5536.
- [50] Kodama S, Takahashi Y, Okumura K, Uruga T. Speciation of iodine in solid environmental samples by iodine K-edge XANES: application to soils and ferromanganese oxides. *Sci Total Environ* 2006;363:275.
- [51] Konishi T, Tanaka W, Kawai T, Fujikawa T. Iodine L-edge XAFS study of linear polyiodide chains in amylose and alpha-cyclodextrin. *J Synchrotron Rad* 2001;8:737.
- [52] Fujikawa T, Oizumi H, Oyanagi H, Tokumoto M, Kuroda H. Short-range order full multiple scattering approach to the polarized L1-edge XANES of iodine doped in trans-polyacetylene. *J Phys Soc Jpn* 1986;55:4074.
- [53] Fujikawa T, Tashiro K, Krone W, Kaindl G. Short range order multiple scattering approach to the polarized iodine L1-edge XANES of IBr-doped in trans-polyacetylene. *J Phys Soc Jpn* 1988;57:320.
- [54] Tanida H, Kato K, Watanabe I. Hydrogen atom position in hydrated iodide anion from X-ray absorption near edge structure. *Bull Chem Soc Jpn* 2003;76:1735.

4

ION CHROMATOGRAPHY

ANNA BŁAŻEWICZ

Department of Analytical Chemistry, Medical University of Lublin, Lublin, Poland

4.1 GENERAL PRINCIPLES AND INSTRUMENTATION

Since its development by Small and coworkers in 1975 [1], ion chromatography (IC) has become a widely used analytical technique for the separation of charged species. The original method made use of two columns packed with ion-exchange resins for separating ions and suppressing the conductance of the eluant. The exchange equilibrium of the analyte ions in a solution between the stationary phase and the eluent is the basis of the separation process. Most of the stationary phases employed in IC have functional groups with charged or chargeable moieties. Retention depends on the affinity of the analyte ions for the ion-exchange sites on the stationary phase. Having a high affinity for the ion-exchange sites, the analyte ions retain on the stationary phase longer than the analyte ions of a lower affinity. The choice of the separation mode, whether through ion exchange, ion exclusion, ion pair, partitioning, adsorption, or zwitterionic interaction, depends on the properties of the analyzed samples.

IC has made a rapid progress and considerable advance. At present, it is regarded as a very useful analytical technique that is not limited only to simple ions. More and more frequently, IC is applied in routine analyses, especially for environmental samples. A number of reviews, detailed studies, and textbooks concerning fundamentals of the technique, its developments, and wide applications have been published on the subject of IC so far [2–8].

4.2 STATIONARY PHASES USED FOR IC OF IODINE SPECIES

Ion exchangers can be classified as strong or weak anion exchangers or strong or weak cation exchangers. Strong ion exchangers retain their charge over the entire pH range, whereas weak ion exchangers are ionized over a narrow pH range. Generally, weak anion exchangers are formed through the addition of a primary amine on the stationary-phase matrix, and strong anion-exchange resins contain quaternary ammonium groups. The influence of the internal structure of the resin beads, that is, whether microporous (gel-type) or macroporous particle size or type of support (usually silica or copolymer of styrene with divinylbenzene (PS/DVB)) on the separation process of ions is discussed elsewhere [4, 5].

Iodide is a very polarizable anion with a relatively high lipophilic character. It is strongly retained on the PS/DVB support material due to secondary, nonionic interactions with Π -electrons. Possible problems with peak tailing can be solved by the use of a latex anion exchanger with lipophobic quaternary ammonium functions [9].

Many studies concerning modification of silica or polymeric supports for separation of iodine species have already been published. In one of them, polyethylene glycol (PEG) permanently coated on a hydrophobic surface was applied for the separation of ultraviolet (UV)-absorbing anions (iodate, nitrate, iodide, and thiocyanate). IC determination was achieved on a conventional-size C30 (triacontyl-functionalized silica) column permanently coated with PEG (Develosil C30-UG-5 column, 150 \times 4.6 mm i.d. with 5% PEG-20000). High-concentration eluents were used for the separation of anions in the partition mode. The applied chromatographic conditions enabled analyzing seawater samples without any disturbance due to complex matrix (high concentration of chlorides) [10].

IC also utilizes crown ethers as eluent additives or as bonded to the stationary phase. The ability of crown ethers to selectively complex ions was used for separation of anions, including iodide. Anions can be retained via electrostatic interaction with the eluent cation trapped on the crown ether. Cyclic polyoxyethylene (POE) added to an eluent together with a hydrophobic stationary phase were applied for the separation of iodine species by Lim et al. [11]. Iodate, bromate, nitrite, bromide, nitrate, iodide, and thiocyanate were determined in saliva samples on a Methyl-12OE-bonded stationary phase [12]. Anions were detected at 220 nm. The authors suggested that although POE does not possess ion-exchange sites, there are ion-dipole interactions between multiple POE chains (chemically bonded POE stationary phase) and eluent cations (working as the anion-exchange sites when trapped among POE chains). Thus, the retention mode of iodide was through ion exchange. Recently, iodide was well-separated from other anions on a chemically bonded 18-crown-6 ether (18C6E) stationary phase in capillary ion chromatography (CIC or CapIC) [13]. The capillary format provides the advantage of significantly reduced eluent consumption, so operating costs are reduced. In the cited study the 18C6E groups (interacting with eluent cations) were chemically bonded on a silica gel by reacting with 3-glycidyloxypropyltrimethoxysilane, followed by reaction with 2-aminomethyl-18C6E. The eluent cation and eluent anion as well as the eluent

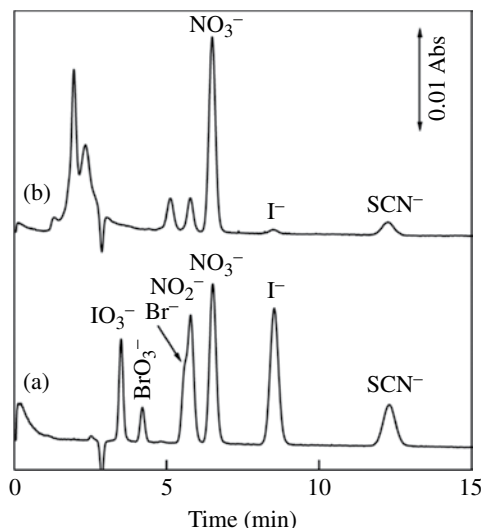


FIGURE 4.1 Ion chromatograms of a mixture of UV-absorbing anions (a) and saliva sample (b) achieved on an 18C6E column. Reproduced with permission from Ref. [13] © The Japan Society for Analytical Chemistry.

concentration affected the retention of the analyte anions. A different selectivity was achieved by using an acetonitrile-rich eluent. UV detection was used for determination of iodide in saliva samples.

Figure 4.1 shows the ion chromatograms of authentic mixture of seven UV-absorbing anions (IO_3^- , BrO_3^- , Br^- , NO_2^- , NO_3^- , I^- , SCN^-) and UV-absorbing species contained in a saliva sample achieved on 18C6E column, 100×0.53 mm i.d. at 210 nm (flow rate: $8.0 \mu\text{l min}^{-1}$, eluent: 100 mM KCl).

C30 dynamically modified with 18C6E stationary phase was prepared by the authors of the previous study [14]. Free and cation-trapped crown ether molecules in the eluent were adsorbed on a similar hydrophobic stationary phase. The size of the crown ether, the size of the salt cation, and concentrations of acetonitrile and crown ether as well as eluent anion affected the retention of analyte anions.

Generally, three types of columns have been used in CIC, that is, packed, open tubular, and monolithic columns. CIC separation of iodide from other anions was achieved on a laboratory-made capillary column (100×0.32 mm i.d.) packed with triacontyl-functionalized silica, followed by a modification with hexadimethrine bromide (HDMB). Also, 1 mM sodium chloride–acetonitrile (95 : 5, v/v) was used as the eluent and UV-absorbing analyte anions were detected at 225 nm. Iodide was determined within 7 min. The effects of the eluent composition on the retention behavior of inorganic anions were investigated. The addition of a small amount of an organic substance in an eluent, such as acetonitrile, increased the retention of iodide, while the addition of methanol decreased its retention. The method was successfully applied for rapid and direct determination of iodide in seawater without any preconcentration procedure [15].

A pyridine stationary phase commercially available for hydrophilic interaction chromatography (HILIC) was used for the ion-exchange separation and determination in saliva samples of inorganic anions (including iodate and iodide) under acidic eluent conditions [16]. The cetyltrimethylammonium (CTA⁺)-coated Octadecylsilane (ODS) column with a high anion-exchange capacity effectively separated iodide ions from deep seawater. Iodides were concentrated on the column and eluted by perchlorate ions [17].

Introduction of monolithic separation columns resulted in tremendous progress in expanding application areas of CIC. Monoliths have several important advantages over particle-based columns improving separation of ions, for example, better efficiency (limiting band broadening) or significantly higher speed of separation. It has been reported that separation of ions by IC on polymer-based monoliths is less effective than on silica monoliths (the surface area available for modification with the desired functional groups is reduced for polymer-based columns). While pH stability is definitely better for organic polymeric monoliths (pH 1–12), separation efficiency is undoubtedly better for silica monoliths [18]. Both polymer- and silica-based monolithic stationary phases can be modified to suit a variety of applications in the iodine research field.

Iodide, iodate, or both species of inorganic iodine can be separated from other anions on monolithic ion exchangers, such as C18 silica, dynamically or semipermanently coated with suitable charged surfactants; for example, commercially available Chromolith Speed ROD C18 silica monolith with UV or conductivity detection was applied for I⁻ determination [19]. The same monolithic support coated with didodecyldimethylammonium bromide (DDAB) and suppressed conductivity was used for IO₃⁻ determination [20], while Chromolith Flash C18 silica coated with DDAB with direct conductivity was used for I⁻ determination [21]. Chromolith guard cartridges C18 silica monolith coated with DDAB with suppressed conductivity detection were useful for IO₃⁻ determination [22].

Rapid separation of a mixture of inorganic anions, including I⁻ and IO₃⁻, on short monolithic columns (Chromolith C18 silica monolith) permanently coated with a long-chained zwitterionic carboxybetaine-type surfactant (*N*-dodecyl-*N,N*-(dimethylammonio) undecanoate (DDMAU)) was reported by Ó. Ríordáin et al. [23].

Both monolithic and particle-packed reversed phase (RP) columns dynamically coated with other zwitterionic surfactant–(dodecyldimethyl-amino) acetic acid (DDMAA) were applied in the separation of simple anions [24]. The retention time of iodide for the monolithic-type column was reduced almost four times comparing with the particle-packed column. The flow and pH gradients were applied in order to control selectivity of the separation.

A bare silica monolith can be converted to an anion exchanger by coating, for instance, with cetyltrimethylammonium chloride (CTAC) [25]. IO₃⁻ can be determined in less than 1 min on such a stationary phase [26]. The same anion was separated on a latex-coated monolithic polymeric stationary phase that was prepared by the *in situ* polymerization of butyl methacrylate, ethylene dimethacrylate (EDMA), and 2-acrylamido-2-methyl-1-propanesulfonic acid within fused-silica capillaries of varying internal diameters (micro-IC). Introduction of ion-exchange sites was achieved by

coating the anionic polymeric monolith with either Dionex AS10 or Dionex AS18 quaternary ammonium functionalized latex particles [27]. An extensive review on the recent development of monolithic stationary phases with the emphasis on micro-scale chromatographic separation can be found in the literature [28]. The latex-coated silica monolith enables fast separation (within 2.5 min) of CH_3COO^- , HCOO^- , NO_3^- , BrO_3^- , SCN^- , and I^- . Mixed mode retention of the mentioned ions has been reported [29]. Takahashi et al. [30] described separation of IO_3^- , NO_2^- , Br^- , NO_3^- , and I^- using a methacrylate-based anion-exchange monolithic column prepared by low-temperature UV photopolymerization. Fast gradient elution at a flow rate of 32 mm s^{-1} resulted in rapid and precise separation of the mentioned anions within 20 s. Glenn et al. [31] compared a reversed-phase silica monolith, converted into an anion-exchange column by coating with the cationic surfactant (DDAB), with a silica monolith column (Merck Chromolith, $100 \times 4.6 \text{ mm}$) coated with Dionex AS9-SC latex nanoparticles. Separations of common inorganic anions were carried out using 7.5 or 5.0 mM 4-hydroxybenzoic acid at pH 7.0 along with suppressed conductivity detection. The findings indicate that the latex-coated column was on average 50% more efficient than the DDAB-coated column. However, iodide was eluted faster from the DDAB-coated column ($\sim 7 \text{ min}$) than from the latex-coated column ($\sim 12 \text{ min}$). In both cases, no problems with resolution of peaks were observed.

Other studies describe preparation of the SiO_2 monolith column modified through in situ covalent attachment of lysine (2,6-diaminohexanoic acid) groups [32]. The stationary phase of zwitterionic nature enabled fast (within $\sim 100 \text{ s}$) separation of nitrite, bromate, bromide, nitrate, iodide, and thiocyanate. At pH 3.0 the lysine column exhibited the best retention and resolution of the anion mixture (Fig. 4.2).

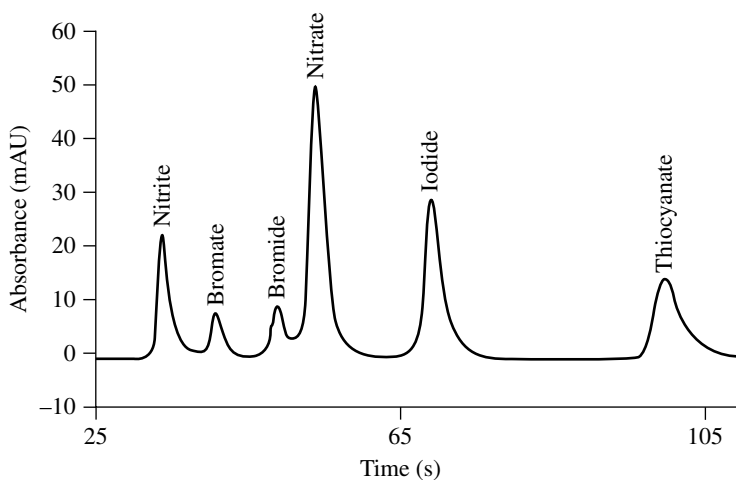


FIGURE 4.2 Separation of selected anions using a lysine-modified silica monolith. Separation conditions: Eluent: 50 mM phosphate buffer, detection: UV detection at 214 nm and flow rate: 4.9 ml min^{-1} . Reproduced with permission from Ref. [32] © Elsevier.

The AS18-coated GMA-co-EDMA (glycidyl methacrylate/ethylene dimethacrylate) monolith, sulfonated with the use of a solution of sodium sulfate and coated with the latex nanoparticles, has been reported as a suitable anion-exchange capillary column (143 mm \times 250 μ m i.d.) for iodide determination among nitrite, bromate, nitrate, bromide, and benzenesulfonate [3]. The previous studies referred to the analysis of the same anions on the same type of stationary phase (348 mm \times 250 μ m i.d.); however, the stationary phase was prepared by ring opening of the epoxy groups through reaction with thiobenzoic acid in the presence of triethylamine in acetonitrile at 60°C and followed by flushing with methanol. The generated thiol groups were oxidized using tert-butyl hydroperoxide before coating with the latex nanoparticles [7]. The Onyx C18 capillary silica monolith with DDMAU has been reported as a column for separation of IO_3^- , BrO_3^- , NO_2^- , Br^- , NO_3^- , I^- , SO_4^{2-} , SCN^- , and ClO_4^- [33]. ProSwift™ SAX-1S, a commercially available polymethacrylate-based monolithic strong anion-exchange column, enabled fast (<0.5 min) determination of IO_3^- and other anions (F^- , Br^- , PO_4^{3-} , NO_3^- , SO_4^{2-} , BrO_3^-) in the presence of a seawater sample matrix [34].

There are many chromatographic columns for the iodine species analysis available on the market, mainly manufactured by Dionex (Thermo Scientific) (USA) and Metrohm (CH) companies. Among them IonPac AS 20, IonPac AS 16, IonPac AS 11 (from Dionex), and Metrosep A Supp 4, Metrosep A Supp 5, Metrosep A Supp 7, METROSEP Anion Dual (from Metrohm) are the most frequently applied, both in environmental and in biomedical analyses of samples containing iodine species. General description and main applications of the commercially available columns are presented in Table 4.1.

4.3 MOBILE PHASES

It is obvious that the choice of eluent used in a particular separation must be compatible with the mode of detection employed in the system. Generally, for ion-exchange columns available for iodine determination, organic solvents are not necessary; however, since most of the columns are 100% high-performance liquid chromatography (HPLC) solvent compatible, they can be used to modify ion-exchange selectivity. In the case of IonPac AS11 the addition of methanol or acetonitrile to the mobile phase decreases retention and increases efficiency of the iodide peak. Figure 4.3 shows the effect of different concentrations of methanol on IC separation of a mixture of nine anions including iodide.

Organic solvents can be added to the ionic eluents used with IonPac AS16 columns in order to modify the ion-exchange process or improve sample solubility, although the optimal separation of nine anions including iodide does not require the use of an organic solvent in the mobile phase. About 22 mM NaOH is the optimum for the separation of anions including iodide [49]. The Ion Pac AS20 can withstand common HPLC solvents in a concentration range of 0–100%. Twenty-three anions, including iodide, were separated to the baseline in less than 30 min applying gradient elution with KOH solution (from 5 to 55 mM) [50]. When hydrophilic stationary phases are used for determination of iodide, usually a carbonate eluent is applied with addition

TABLE 4.1 Presentation of selected columns available on the market for the determination of iodine species by the use of IC

Chromatographic column	Description	Application	References
IonPac AS 20 (Dionex)	A high capacity: 310 $\mu\text{M Cl}^-$ per column. (4 \times 250 mm), 7.5- μm particle size, stable in 0–14 pH range; mobile-phase compatibility 0–100% organic solvent	Designed for separation of polarizable anions; enables selective separation of hydrophobic anions in samples with high ionic strength (e.g., saline, seawater, iodized table salt)	[35]
IonPac AS 16 (Dionex)	A high capacity: 170 $\mu\text{M Cl}^-$ per column (4 \times 250 mm), 9- μm particle size, stable in 0–14 pH range; mobile-phase compatibility 0–100% organic solvent. A strong anion-exchange resin quaternary amine bonded on latex particles attached to the core of 9- μm macroporous particles having a pore size of 2000 Å.	The IonPac AS16 is designed to perform analyses of large numbers of anions of varying valencies through gradient elution	[36]
IonPac AS 11 (Dionex)	Low-capacity (45 $\mu\text{M Cl}^-$) ion exchanger with a highly crosslinked core (ethylvinylbenzene crosslinked with 55% divinylbenzene) and a MicroBead® anion-exchange layer attached to the surface a 13- μm -diameter microporous resin bead. The anion-exchange layer is functionalized with quaternary ammonium groups. Very hydrophilic, pellicular resin; stable in the 0–14 pH range	Iodide in complex matrixes (urine, blood, tissues)	[37]
Metrosep A Supp 4 (Metrohm)	Polyvinyl ion-exchange resin stable in 3–12 pH range, 9- μm particle size, 71 ion-exchange capacity ($\mu\text{M/Cl}^-$)	Iodide among thiosulfate, thiocyanate, fluoride, chloride, nitrite, bromide, nitrate, phosphate, and sulfate	[38]

(Continued)

TABLE 4.1 (Cont'd)

Chromatographic column	Description	Application	References
Metrosep A Supp 5 (Metrohm)	Polyvinyl ion exchange resin stable in 3–12 pH range, 5- μ m particle size, 107 ion-exchange capacity (μ M/ Cl^-)	Iodide among bromide, sulfate, chloride in NaCl, matrix (ratio of concentration 0.5 : 1000 mg l^{-1} Cl^-/l^-)	[39]
		Iodide among thiosulfate, thiocyanate in different wastewater samples	[40]
		Iodide among fluoride, chloride, sulfate in healthcare products (multitrace 7 and multimineral)	[41]
		Iodide in table salt	[42]
		Iodide and iodate in electroplating baths	[43]
Metrosep A Supp 7 (Metrohm)	Polyvinyl ion-exchange resin stable in 3–12 pH range, 5- μ m particle size, 108 ion-exchange capacity (μ M/ Cl^-)	Iodide in human urine	[44]
		Iodide and other anions in brine samples	[45]
		Iodide among other 15 anions	[46]
		Iodide in glacial acetic acid	[47]
Metrosep Anion Dual	Polymethacrylate ion-exchange resin	Iodide in soil extract sample	

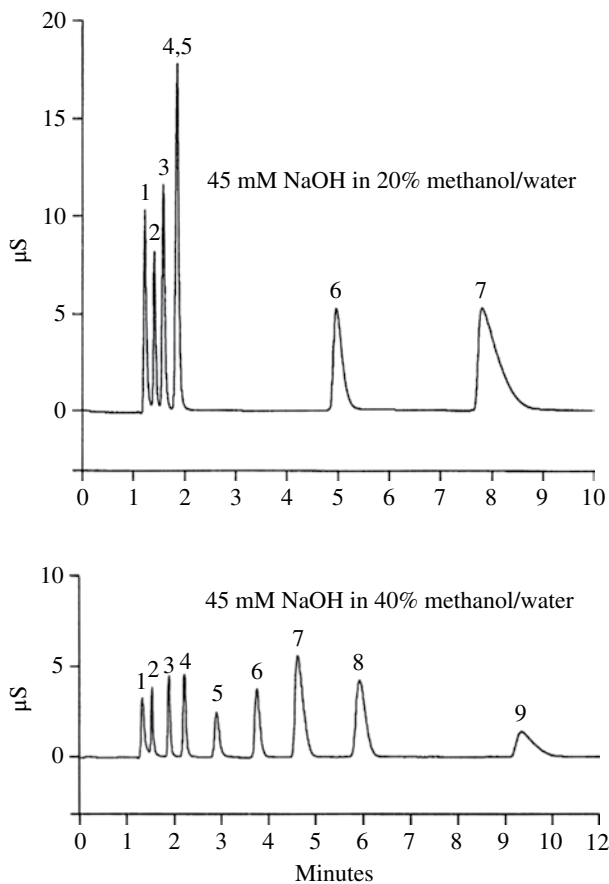


FIGURE 4.3 Effect of solvent on highly retained inorganic anions including iodide, thiocyanate, and perchlorate achieved on IonPac AS11 (1=fluoride, 2=chloride, 3=nitrate, 4=sulfate, 5=phosphate, 6=iodide, 7=thiocyanate, 8=thiosulfate, 9=perchlorate. Adapted from Ref. [48] © Dionex.

of NaHCO_3 to stabilize pH. Due to the increase of conductivity, amperometric detection (AD) is favored. Helium is recommended to purge and degas ionic eluents containing organic solvents, since nitrogen is soluble in solvent-containing eluents.

4.4 DETECTION OF IODINE SPECIES IN IC

In order to determine iodine species, numerous methods have been developed to combine highly selective IC columns with highly sensitive detection. At present, there are two main types of IC: suppressed IC and nonsuppressed IC. Conductivity detection is considered a universal detector in IC as all ions are electrically conducting.

The main advances made in nonsuppressed IC were due to the use of ion-exchange resins with low capacity since such resins require a lower concentration of eluent and thus low background conductance is maintained in a chromatographic system. Applications of coupling of nonsuppressed IC with other techniques for iodine speciation analysis are discussed in the section entitled "Speciation analysis involving IC."

Although adding some extra hardware increases the overall dead volume of a chromatographic system, suppressors made anions' determinations more sensitive, reproducible, and with improved linearity of the detector response. Haddad et al. [51] reported a comprehensive review of various types of suppressors, including packed bed suppressors, hollow fiber membrane suppressors, and micromembrane suppressors. Electrolytic suppressors that minimize the dead volume, being adapted by CIC systems (e.g., ICS 5000, Dionex), are commercially available.

The use of conductivity detection at capillary scale has been possible by capacitively coupled, contactless conductivity detection (C4D). The detailed description of C4D systems applied in IC can be found in an article by Dasgupta et al. [52]. The use of such detection eliminates the extracolumn broadening effects that are primarily related to the construction of the detector flow cell or suppressor volume for suppressed conductivity detection. Ó Ríordáin et al. [33] demonstrated the possibility of using on-column C4D in CIC with modified silica monolithic capillary columns for the first time.

The IC method coupled with electrochemical detection allows for selective and sensitive determination of iodide in complex matrices. Kolb et al. [53]. have applied AD for I^- determination using a carbon paste working electrode. The analysis of iodide can be accomplished by AD. This detection is preferable because of the electrode stability and sensitivity. Gold [54–57], platinum [57], and glassy carbon [58] electrodes have found application in amperometric or pulsed amperometric detection (PAD). Several papers have been published on the use of IC with AD on a silver electrode [59, 60]. Although iodide can be detected by direct current (DC) amperometry on a silver working electrode, a pulsed amperometric waveform is used to improve the reproducibility of the analysis [61]. When an amperometric detector with a silver working electrode is used, iodide from the sample combines with the silver of the working electrode surface to form silver iodide precipitate, oxidizing silver in the process. PAD allows for detection in the low $mg\ l^{-1}$ to $ng\ l^{-1}$ range and has high specificity for the iodide ion (the other halides are detected in the same way, but with less efficiency) [62, 63]. The findings of Liang et al. [64] showed that a disposable working electrode manifested equal or better results than the conventionally working electrode and could be used for iodide analysis. The authors compared the performance of two kinds of silver working electrode in an electrochemical detector, that is, the disposable and conventional electrode for the determination of iodide, using high-performance anion-exchange chromatography (HPAEC) hyphenated with PAD. The comparisons were carried out with regard to the time of equilibration, long- and short-term reproducibility, limits of detection, and linearity of calibration. Besides, the disposable electrode was able to work for consecutive 2660 min (about 44 h, 10 min needed for each run) with no degradation. The disposable electrode was applied for the determination of iodide in the soil and seawater samples with the detection limit of $0.5\ \mu g\ l^{-1}$ ($10\ \mu l$ injection).

The same analytical method ion chromatography-pulsed amperometric detection (IC-PAD) was used for the analysis of dissolved iodide in the surface water and in absorption solutions obtained from absorbable organic iodide (AOI) determination [60]. The proposed method enabled highly sensitive determination (limit of detection (LOD) of $0.02 \mu\text{g l}^{-1}$) of iodide from the samples that had undergone only microfiltration. The silver electrode was applied because of its high selectivity and the very low detection potential needed. Cataldi et al. [56] compared detection of iodide on gold, silver, and platinum electrodes under similar experimental conditions in terms of electrode sensitivity, selectivity, and stability. The comparison showed that the best results in terms of signal stability, peak shape, and analytical response were obtained with a modified Pt electrode, which allowed to achieve a LOD of $0.5 \mu\text{g l}^{-1}$ ($S/N=3$). PAD, using a modified Pt electrode ($E(\text{app})=+0.85 \text{ V}$ versus Ag|AgCl), was successfully applied to determine low contents of iodide in the human urine with a solid-phase extraction as the pretreatment procedure.

As for the UV detection, iodide and iodate are UV-absorbing anions and they can be detected using UV detection with a wavelength between 190 and 220 nm [4]. Ó Ríordáin used UV detection at 214 nm for the detection of iodide together with nitrate, nitrite, bromide, and thiocyanate [24]. Brandao et al. [65] used a postcolumn derivatization with *N*-chlorosuccinimide followed by a spectrometric detection at the wavelength of 605 nm for determination of I^- in saline waters. It has been reported that iodide can be determined with IC and direct UV-visible detection after preconcentration of the sample [66]. In a different study, iodide was determined as IBr_2^- at 249 nm, whereas iodate as I_3^- at 288 nm. The described advantages of the proposed method are due to lack of sample pretreatment and possibility to be run completely automatically. The reported LOD for iodide and iodate were $0.1 \mu\text{g l}^{-1}$. The methods have been successfully applied to determine iodide and iodate in several mineral waters and in drinking water as well as for the determination of iodide in table salt [67]. The UV detection exhibits some drawbacks with regard to a baseline disturbance. Hydroxide eluents can absorb in the UV and contribute to a high background, preventing detection of iodide. Therefore, it is recommended that a suppressor should be used, although conductometric detection is not applied [35].

4.5 STRONG AND WEAK POINTS OF IC DETERMINATIONS OF IODINE SPECIES

IC is a well-established analytical method for the determination of ionic species in a solution, with detection limits down to picograms per gram [68]. It has advantages over spectroscopic techniques for ion analysis because it allows for speciation analysis (described in next section) as well as simultaneous determination of many ions (both organic and inorganic) during a single chromatographic run. Other advantages include short time of analysis, high sensitivity (with preconcentration techniques, the detection limit could be lowered to the ng l^{-1} range), high selectivity in samples with complex matrixes (high ionic strength samples or samples with very small amounts of analyte in the presence of very large amounts of others ions), small sample volume

needed for the analysis, usage of safe and environmentally friendly chemicals (green chemistry), and ease of use. Because IC typically utilizes dilute acids, bases, or salt solutions as the mobile phases, costly and hazardous organic solvents are generally avoided. There is a large selection of columns (in terms of type and format), and many detection methods can be used. Various types of suppressors improve the dynamic range of the method. A small column format generates less waste and uses less eluent. The most popular applications of IC are the determination of common anions and cations in water and wastewater [4, 5, 69]; however, it is also a suitable method for analyses of clinical samples [63, 70]. IC is also an attractive procedure for the laboratories that need to define numerous ions in several thousand samples. This technique is easily automated and adapted to a high sample throughput.

One of the advantages of IC, when it comes to the practical application of this technique, is the simplicity of sample preparation. Sample preparation procedures are well-established and are being continuously improved; for example, matrix elimination procedures are a good example showing that simple dilution and/or filtration bring the analytes of interest into the working range of the method [71]. IC can also be interfaced mass spectrometry, inductively coupled plasma mass spectrometry (ICP-MS), or electrospray ionization tandem mass spectrometry (ESI-MS), which makes it a very suitable technique for speciation analysis [72–74].

Like any chromatographic technique, IC also has some limitations. The problems associated with the use of IC for iodine analysis usually concern inadequate sample preparation, a high background of an eluent, irregular baseline (e.g., some mobile phases, such as NaOH solutions, can absorb ambient CO₂ resulting in composition change and baseline artifacts), shortening of the retention times of the analyzed ions, or changes in the characteristics of analytical columns within analyses. As for detection, very sensitive electrochemical detection requires careful selection and handling of electrodes. However, current technology has dramatically changed for the better in the recent years and currently the problems with reproducibility of the results are reduced by the repeated cleaning and detecting process called pulsed amperometric detection (PAD). The pulsing waveform ensures that the surface of the electrode is always clean and the results are reproducible. The ways to solve the earlier-mentioned problems can be found elsewhere [5, 8].

4.6 SPECIATION ANALYSIS INVOLVING IC

It is known that the bioavailability and toxicity of iodine, as in the case of other essential elements, is species-dependent. Iodide and iodate are less toxic than molecular iodine and some organically bound forms of the element. Similarly, the bioavailability of organically bound iodine is also lower than that of mineral iodine [74].

According to the International Union of Pure and Applied Chemistry (IUPAC) [75], the definition of a *speciation analysis in chemistry* is as follows: *analytical activities of identifying and/or measuring the quantities of one or more individual chemical species in a sample*. Distribution of an element amongst defined chemical species

in a system is related to *speciation of an element*. Detailed principles of elemental speciation of various elements have been reviewed elsewhere [76].

IC has been described in the literature as a convenient separation method that enables sensitive and relatively fast determination of iodine species present in various matrices [76–78]. This specific advantage of IC is widely applied in environmental analysis, especially for speciation of iodine in water samples of various origin (see Table 4.2). Ocean and seawater samples represent quite complex matrices since I^- and IO_3^- are present there at a trace level together with high concentrations of Cl^- and Br^- . The prevalence of one over the other depends on redox chemistry: iodate is dominant under oxidizing conditions, iodide under reducing conditions. Table 4.2 includes the overview of detection systems, chromatographic columns, eluents, and selected applications of IC in the analysis of iodine species in various matrices over the past 20 years.

Unfortunately, the samples of high ionic strength, such as seawater, cannot be injected directly into the separation column. In order to avoid adverse effects (e.g., peak broadening caused by self-elution by the sample matrix itself), on-column matrix elimination techniques are used [65]. This involves adding the matrix ion to the eluent, usually in a higher concentration than the sample matrix. For this reason, optimization of the composition and concentration of the mobile-phase components is of paramount importance. There are several ways to analyze such samples for iodine speciation using IC. Older methods for speciation of iodine in saline waters by the use of IC involved, for example, removing interfering ions. In one study a matrix elimination procedure was reinforced by a postcolumn reaction detection that was both selective and sensitive to iodide and was based on the reaction of iodide with 4,4'-bis(dimethylamino) diphenylmethane in the presence of *N*-chlorosuccinimide. Detection was carried out at 605 nm [65]. Another method required conversion of iodate (reduction by $NaHSO_3$) and organic iodine species (measured as the difference of total iodide after organic decomposition by dehydrohalogenation and reduction by $NaHSO_3$ and total inorganic iodide) into iodide form and direct determination of I^- by IC with UV detection [92]. However, this method includes quite rigorous and labor-intensive pretreatment of the sample that may bring incorrect speciation information [93].

Coupling various analytical techniques with IC is also beneficial for speciation analysis of iodine. The online coupling of IC and ICP-MS has been widely described in the literature. Combining IC with ESI-MS or ICP-MS solves even complex separation problems, while outstanding sensitivity and selectivity are achieved at the same time. Such coupled techniques are less prone to matrix influences than IC with conductivity detection. Chen et al. [77] used a nonsuppressed IC with ICP-MS for simultaneous determination of trace iodate and iodide in seawater. The described method was performed without sample pretreatment with the exception of dilution. The other advantage of the method is relatively short time of separation (~13 min) achieved on an anion-exchange column (G3154A/101, provided by Agilent) with an eluent containing 20 mM NH_4NO_3 . LODs were as follows: $1.5 \mu g\ l^{-1}$ for iodate and $2.0 \mu g\ l^{-1}$ for iodide.

The online coupling of IC and ICP-MS has also been used for the determination of iodine species in drinking water [9]. The LODs calculated with several quantification methods were in the typical range of 0.05 – $3.5 \mu g\ l^{-1}$ reported in the literature for IC with ICP-MS detection [77].

TABLE 4.2 The overview of detection systems, chromatographic columns, eluents and selected applications of IC in the determination of iodine species in various matrices

Species (and matrix)	Method	Chromatographic columns, eluents, and detectors	LOD	References
I ⁻ (urine)	Ion pair RP HPLC	Stationary phase: Resolve tm C 18 (Waters) column; Mobile phase: 10 mM Na ₂ HPO ₄ × 12H ₂ O, 1 mM Titmplex III, 10 mM ion-pairing reagent tetrabutylammonium phosphate (TBAP), 6 mM di-n-butylamine in HPLC-grade water; pH 7 Detection: electrochemical detection with Ag/AgCl reference electrode, and a silver working electrode	5 µg/l	[79]
I ⁻ and total inorganic iodine (seawater)	IC	Stationary phase: a high-capacity anion-exchange resin with polystyrene-divinylbenzene matrix-TSK gel SAX Mobile phase: 0.35 M NaClO ₄ + 0.01 M phosphate buffer; pH 6.1 Detection: UV absorbance at 226 nm	0.2 µg/l	[66]
I ⁻ and IO ₃ ⁻ (aqueous solutions, untreated urine)	IC-ICP-MS	Stationary phase: for acidic samples AS7 (Dionex), for basic samples AS4A-SC (Dionex) Mobile phase: for acidic samples 20 mM HNO ₃ and 50 mM NaNO ₃ , pH 1.7; for basic: 5 mM Na ₂ CO ₃ , 40 mM NaOH, 8% CH ₃ OH, pH 12.5 Detection: ICP-MS	No data	[80]
I ⁻ (urine and serum)	IC	Stationary phase: C18 (Waters Nova-Pak) RP column coated with <i>N</i> -cetylpyridinium chloride (as an analytical column) and with hexadecyltrimethylammonium bromide as a concentrator pre-column; Mobile phase: 0.1 M KNO ₃ Detection: a laboratory-made iodide ion-selective electrode with tubular configuration and based on a crystalline membrane (AgI/Ag ₂ S)	1.47 µg/l	[81]
I ⁻ (ground waters and soil)	IC	Stationary phase: IonPac AS11 (Dionex) Mobile phase: 0.027 M NaOH in 2% aqueous CH ₃ OH Detection: conductivity	0.3 mg/l	[82]

I ⁻ (soil and water)	IC	Stationary phase: PRP-X100 Hamilton Mobile phase: CH ₃ OH-NaCl 0.1 M (55:45 v/v) Detection: UV at 230 nm	0.8 µg/ml	[83]
I ⁻ and IO ₃ ⁻ (mineral and drinking waters)	IC	Stationary phase: IonPac AS11 (Dionex) Mobile phase: NaBr, NaOH (for I ⁻) B(OH), NaOH (for IO ₃ ⁻) Detection: UV, I ⁻ determined as IBr ₂ ⁻ at 249 nm, IO ₃ ⁻ determined as I ₃ ⁻ at 288 nm	0.1 µg/l I ⁻ and IO ₃ ⁻	[64]
I ⁻ and IO ₃ ⁻ (diluted fresh milk and dissolved powder milk)	IC-ICP-MS	Stationary phase: IonPac AS14 (Dionex) Mobile phase: 3.5 mM Na ₂ CO ₃ + 1 mM NaHCO ₃ Detection: ICP-MS	0.6 µg/l I ⁻ , 1.1 µg/l IO ₃ ⁻ (100 µl) ^a	[84]
I ⁻ (urine)	IC	Stationary phase: IonPac AS11 (Dionex) Mobile phase: 25 mM HNO ₃ + 50 mM NaNO ₃ Detection: <i>electrochemical detection</i> of I ⁻ at <i>gold, silver and platinum electrodes</i>	3.5 µg/l (50 µL) ^a with Ag, 0.5 µg/l with Pt electrode	[55]
I ⁻ and IO ₃ ⁻ (Seawater)	IC-ICP-MS	Stationary phase: Agilent G3154A/101 Mobile phase: 20 mM NH ₄ NO ₃ , pH 5.6 Detection: ICP-MS	1.5 µg/l IO ₃ ⁻ , 2.0 µg/l I ⁻	[77]
I ⁻ (urine)	IC-MS/MS	Stationary phase: AS20 (Dionex) Mobile phase: 50 mM KOH Detection: MS	0.33 µg/l	[85]
I ⁻ (seawater)	IC	Stationary phase: a laboratory-made C30 packed column modified with polyoxyethylene oleyl ether, Mobile phase: 300 mM NaCl Detection: UV at 220 nm	19 µg/L	[86]
I ⁻ and IO ₃ ⁻ (whole milk, powder and seaweed)	IC-DRC-ICP-MS ^b	Stationary phase: Hamilton PRP-X100 Mobile phase: gradient: A: 15 mM NH ₄ NO ₃ , pH 10, B: 100 mM NH ₄ NO ₃ , pH 10 Detection: ICP-MS	0.001 µg/l IO ₃ ⁻ , 0.002 µg/l I ⁻	[28]

(Continued)

TABLE 4.2 (Cont'd)

Species (and matrix)	Method	Chromatographic columns, eluents, and detectors	LOD	References
I ⁻ (table salts, sea products, milk powder, and iodide bound drug compounds)	IC	Stationary phase: Chromsep anion-exchange LC-Varian® column (Varian NV/SA) Mobile phase: 0.5mM EDTA; acetate buffer, pH 4.9 Detection: amperometric, silver electrode as a working electrode an Ag/AgCl reference electrode	0.47 µg/l (20 µL)	[87]
I ⁻ (tap water)	IC-MS/MS	Stationary phase: AS20 column (Dionex) Mobile phase : 50mM KOH Detection: MS	0.2 µg/l	[88]
I ⁻ (human thyroid glands)	IC-PAD	Stationary phase: IonPac AS11 (Dionex) Mobile phase: 50 mM HNO ₃ Detection: pulsed amperometric (PAD)	0.17 µg/l	[63]
I ⁻ (food)	IC	Stationary phase: TSKgel- SAX Mobile phase: 0.1 M NaClO ₄ , 1.43 M NaCl, 1.5 mM Na ₂ HPO ₄ , 3.1 mM Na ₂ HPO ₄ × 2H ₂ O Detection: UV at 226 nm	0.01 µg/g	[89]
I ⁻ (seawater)	IC	Stationary phase: two dilauryldimethylammonium bromide (DDAB)-coated monolithic ODS columns Mobile phase: aqueous NaCl (0.5M; 5 mM/l phosphate buffer , pH 5) Detection: UV at 225 nm	1.6 µg/l I ⁻ (200 µL)	[90]
I ⁻ and IO ₃ ⁻ (Antarctic ice core samples)	HPLC-IC-ICP-MS	Stationary phase: IonPac® AS16 (Dionex) Mobile phase: 35 mM NaOH Detection: ICP-MS	5 pg/g I ⁻ ; 7 pg/g IO ₃ ⁻	[91]
I ⁻ (seawater)	IC ^c	Stationary phase: a laboratory-made capillary column packed with triacontyl-functionalized silica, followed by a modification with hexadimethrine bromide Mobile phase: 1 mM NaCl-ACN (95:5, v/v) Detection: UV at 225 nm	6.4 µg/l	[15]

^aInjection volume.

^bIon Chromatography/Dynamic Reaction Cell Inductively Coupled Plasma Mass Spectrometry.

^cCapillary IC.

Recently, a new approach to the simultaneous detection of iodide and iodate in a single chromatographic run has appeared. Huang et al. [78] developed a simple IC method in which columns packed with homemade functionalized PS/DVB with controllable amounts of quaternary ammonium group resins and column-switching technique were applied. The low-capacity anion-exchange column (for strongly retained iodide) and high-capacity anion-exchange column (for iodate with weak retention) were prepared. With this method, iodide and iodate in a povidone iodine solution were simultaneously detected in a short time. Iodide did not pass through the high-capacity column. The detection limits (LODs) for iodide and iodate obtained by injecting 100 μl of sample were 5.66 and 14.83 $\mu\text{g l}^{-1}$ ($S/N=3$), respectively.

Figure 4.4 shows the chromatographic instrument configuration for this column-switching system. (a) Separating anions with weak retention from strong retention (0–1.5 min); (b) analyzing the target anions and washing analytical column II. At present speciation analysis is not limited only to iodides and iodates, it also applies to organic forms of iodine (e.g., 3-iodotyrosine–MIT, and 3,5-diiodotyrosine–DIT).

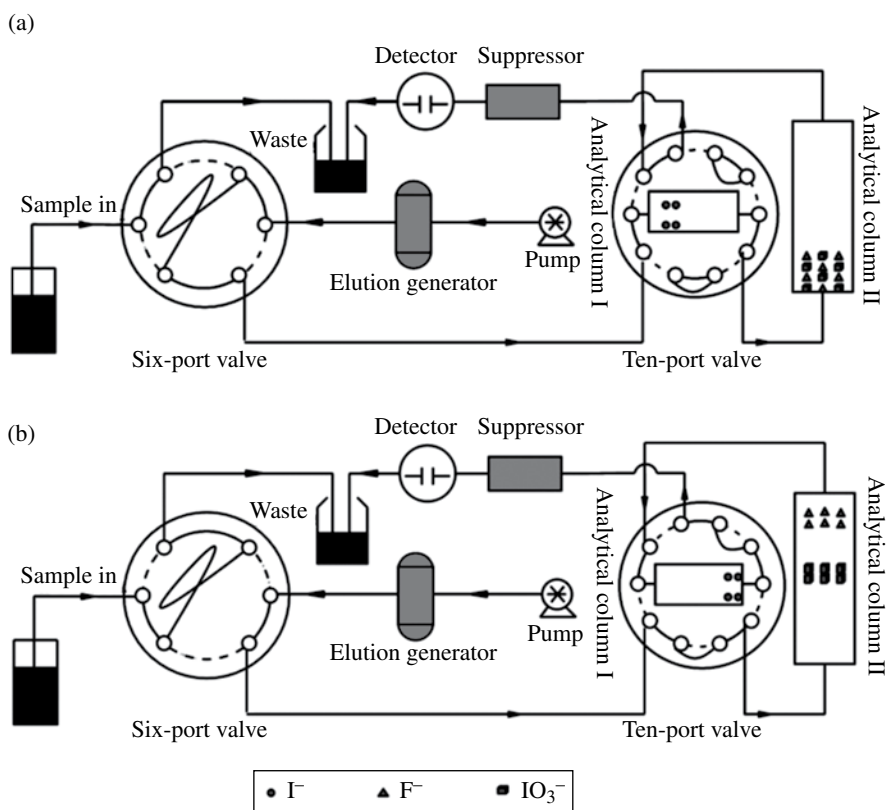


FIGURE 4.4 Chromatographic instrument configuration for a column-switching system. (a) Separating anions with weak retention from strong retention (0–1.5 min); (b) analyzing the target anions and washing analytical column II. Reproduced with permission from Ref. [78] © Elsevier.

Romarís-Hortas et al. [92] developed an anion-exchange HPLC hyphenated with ICP-MS for speciation of bioavailable iodine and bromine from edible seaweed. They applied IonPac AS7 column (Dionex) as a stationary phase and gradient elution with 175 mM NH_4NO_3 plus 15% (v/v) CH_3OH (pH 3.8) as a mobile phase. The method enabled to assess inorganic and organic (MIT and DIT) iodine species and inorganic bromine speciation analysis (bromide and bromate). The combination of reversed-phase high-performance liquid chromatography (RP-HPLC) with ICP-MS was used for the determination of MIT and DIT in the dialyzates from edible seaweed. Zorbax Eclipse double endcapped C8 (XDB-C8) phase (Agilent) with gradient elution (0.2% (m/m) CH_3COOH , and 0.2% (m/m) CH_3COOH in CH_3OH) at constant flow rate of 0.75 ml min^{-1} was used to confirm the presence of organic iodine species. Iodide and MIT were the main bioavailable species quantified. The developed method has been verified by (RP-HPLC-MS) measurement. The cited work was the first to present the determination of bioavailable iodine and bromine species from different seaweeds.

Little is known about the natural iodine cycle in the terrestrial environment; thus speciation studies involving the IC technique are currently more common. Such studies can bring an answer to important questions: What is the behavior of organically bound iodine? Which forms of iodine are more sorbed by soils? What is an iodine uptake by algae or bacteria in waters? Gilfedder et al. [94] applied IC-ICP-MS to study iodine cycling in terrestrial freshwaters and temporal changes in speciation of iodine. Dissolved iodine species (iodide, iodate, and organically bound iodine) were analyzed by coupling IC with ICP-MS. Soluble organically bound iodine (SOI) was calculated as total iodine minus the sum of the inorganic species (i.e., $\text{SOI} = \text{total I}^- (\text{I}^- + \text{IO}_3^-)$). Iodine species were quantified using IonPac AS16 column (Dionex) and 35 mmol NaOH eluent.

Applicability of several chromatographic techniques, including IC coupled to ICP-MS to iodine speciation in seaweed, has also been demonstrated by Shah et al. [95]. The use of hyphenated techniques for iodine speciation in seaweed extracts allowed obtaining important information on the association of iodine to the various matrix components of seaweed. The ability of IC to quantify different species of iodine or both inorganic and organic species is of great benefit in determining the fate, transport, and bioavailability in living organisms and their environment.

4.7 SELECTED PROBLEMS ASSOCIATED WITH PREANALYTICAL FACTORS INFLUENCING IC OF IODINE SPECIES

Sample preparation is a relevant stage of any analytical process. The interpretation of research findings can sometimes be hindered by laboratory contamination of samples and inadequate sample pretreatment procedures. High volatility of halogens in acidic solutions causes undesirable memory effects. The most common sample preparation procedures involve applying dilution or dispersion in an alkaline solution, alkaline fusion [96], combustion in bombs [97], microwave-induced combustion (MIC) [98, 99], and pyrohydrolysis [100]. These procedures are common before many analytical

methods, so IC is not an exception here. It should be noted that the simplicity of the sample preparation stage is vital.

4.8 STORAGE AND PRESERVATION

Before applying the appropriate method for a particular application, many factors have to be considered and some of them are discussed here. Samples collected for analysis by IC should ideally be collected in plastic containers, such as polypropylene. Before use, the containers should be thoroughly rinsed with reagent-grade water (18 MΩ deionized).

When it comes to quantitative evaluations of iodine concentrations (in all chemical forms) in biological samples, proper storage of samples is of paramount importance. For instance, tissues must be preserved in such a way that a potential loss of iodine is minimized. The choice of the tissue-fixing agents is quite wide. Formalin is a routinely used tissue-fixing agent after surgical procedures. Other recommended agents for tissue preservation include, for example, a mixture of 50% glutaraldehyde, 16% paraformaldehyde, and 0.2 M sodium phosphate buffer solutions (i.e., original composition of Karnovsky fixative) or its modification. Another possibility to preserve the tissues is sample freezing. It is recommended that a fresh/frozen material be used whenever possible.

Hansson et al. [101] used X-ray fluorescence analysis (XRF) and secondary ion mass spectrometry (SIMS) for evaluation of a freezing technique for preserving samples (XRF analysis) and for evaluation of the efficacy of the use of aldehyde fixatives for sample preparation (SIMS analysis). There were no significant changes in the iodine content due to freezing. Freezing for 4 weeks produced no more than a 10% change in the iodine content. For all the samples fixed in an aldehyde, there was a loss of iodine. The decrease in iodine content from baseline was significant for the samples fixed in an aldehyde ($p < 0.05$). Karnovsky fixative was the best in this regard, yielding a mean 14% loss compared to 20 and 30% for glutaraldehyde and formaldehyde, respectively. For the SIMS method, Fragu et al. [102] recommended a chemical fixation with a mixture of the Karnovsky fixative, followed by embedding in methacrylate. This method, which was evaluated for iodine loss by Rognoni et al. [103], has proven suitable for preservation of substances bound to macromolecules (e.g., iodine bound to thyroglobulin [Tg]).

The effect of sample preservation on determination of I^- in healthy and pathological human thyroids has also been studied [63]. It was pointed out that the way for tissue preservation (either in formalin or by freezing) had no significant effect on the iodine determination result by IC-PAD.

4.8.1 Stability of Analytes

Stability problems in relation to the storage medium were analyzed by Bing et al. [104]. Pure water, the mobile phase, 0.01, and 0.1% KOH were tested. According to the study, iodide was unstable and lost in pure water and the mobile-phase medium

when the stock solution was diluted or kept for a long time. Dilution factors from 10 to 10,000 and storage from 1 to 5 days were tested. However, iodide was found to be stable in 0.01 and 0.1% KOH. The authors did not observe problems with iodate in different media. In order to minimize any potential high-matrix effects, 0.01% KOH was selected as the storage medium for field sampling. The tests were performed before IC-ICP-MS of various groundwater samples [105].

4.8.2 Sample Decomposition

Generally, all reported methods have a digestion or ashing step prior to the final determination of iodine. The procedure usually requires the use of alkaline media and a high temperature [106]. A catalytic spectrophotometric method based on the Sandell-Kolthoff reaction together with many modifications and improvements of this method is a low-cost assay of iodine; however, it is not free of possible interferences (especially for foodstuffs with low range of iodine levels). Most iodine in biological media is covalently bonded and there are some substances that interfere with the determination reaction (e.g., SCN^- , NO_3^- , or Fe^{2+}). A high lipid content in the sample (e.g., milk) can cause problems in detection, so a mineralization step is absolutely necessary before analysis.

With regard to biological (clinical) samples, typically, the volume of the test sample acquired from the patient is not large. Sample decomposition is a critical step in this analysis. The decision whether to dilute or digest the samples (e.g., of body fluids) depends on various factors (e.g., concentration ranges of analytes, volume, limit of quantitation, required accuracy and precision, coexisting ions that could interfere in analysis, sample throughput). Biological fluids and tissues are usually diluted with NH_3aq , Triton-X-100, HNO_3 , or tetramethylammonium hydroxide (TMAH) solutions. The dilution procedures are identical as in the case of sample preparation for ICP-MS analysis [107].

When preparing a sample for analysis, it is necessary to take into consideration the loss of analyte due to erroneous application of decomposition procedures. Some of them, for example, "Schoeniger combustion," require a highly homogenous sample, which is sometimes difficult to obtain [108]. There are many options for biological sample preparations, among which alkaline digestion using TMAH is the most common before the analysis of I^- [109, 110]. Alkaline conditions during the extraction procedure have some advantages in comparison with acidic media, where I^- may be oxidized into volatile forms (I_2 or HI). Destruction of the organic matrix when a typical digestion reagent, like HNO_3 , is being used, is not possible because of the losses due to volatile iodine formation (therefore, no stable sample solution can be achieved). However, acid digestion procedures (by the use of mainly H_2SO_4 , HNO_3 , and HClO_4) have also been applied [111]. What is more, despite its obvious weak point (loss of analyte), the U.S. Food and Drug Administration (FDA, 2009) still recommends these procedures.

Błażewicz et al. [63] used the alkaline digestion with 25% TMAH water solution for the preparation of thyroid glands before the IC method of analysis. A diluted TMAH solution was used by Schramel and Hasse [109] in order to determine iodine in the serum, milk, plants, and tissues by means of the ICP-MS method.

Unfortunately, despite the earlier-mentioned advantages, the use of TMAH solution for the digestion of samples has some disadvantages. Since for all modern sample pretreatment methods time is a very important factor, the long procedure time remains a huge problem. As reported in the literature, digestion of biological materials with TMAH usually requires up to 6 h [112]. However, the assistance of microwaves significantly shortens the time of the sample preparation step (<20 min). Such microwave-assisted alkaline digestion has been developed by Błażewicz et al. before the IC analysis of the thyroid samples [63]. It is important to monitor all the conditions of the digestion procedure, especially temperature, in order to avoid decomposition of TMAH and bursting of the closed vessels (therefore a temperature lower than 100°C is recommended). Each time the vessels must be thoroughly cleaned with a digestion mixture in order to avoid memory effects (adsorption by the walls of containers) and consequently the loss of analyte [70].

The association of analytical communities (AOAC) expert review panel (ERP) approved ICP-MS as a First Action Official MethodSM for determination of iodine. Two procedures of sample preparation are listed, the first (AOAC Official Method 2012.14) involves using digestion in nitric acid in a closed-vessel microwave oven system. In order to prevent a loss of iodine, NH_4OH water solution should be added to the samples immediately after digestion. The second method (AOAC Official Method 2012.15) involves a unique sample digestion with a KOH solution in an oven or using an open - vessel microwave system. After digestion a stabilizer must be added. The solution is taken to volume, then filtered and analyzed either directly or after dilution [112].

Obviously, the sample pretreatment method must be chosen according to the sample type. A method blank has to be prepared before starting the analysis of target ions. Table 4.3 includes selected precautions in relation to sample pretreatment procedures prior the determination of iodine in environmental and clinical samples by IC.

4.8.3 Certified Reference Materials

A possible source of misinterpretation in research findings may arise from insufficient validity of iodine determinations at low concentration levels. The use and availability of certified reference materials (CRMs) is evident. Various CRMs are present on the market and are used for quality control studies in order to document an acceptable analysis and to check standards preparation by comparing recovered concentrations with the certified values [117].

There are several available CRMs approved by the Community Bureau of Reference (BCR) for assessing (verifying) the analytical accuracy of IC measurements, for example, skim milk CRM No. 150 with $1.29 \pm 0.09 \mu\text{g I}^- \text{g}^{-1}$ milk or skim milk CRM No. 151 with $5.35 \pm 0.14 \mu\text{g I}^- \text{g}^{-1}$ milk [118].

Iodide standard ($1000 \text{ mg I}^- \text{I}^-$ in H_2O) for IC TraceCERT® is produced and certified in accordance with ISO/IEC 17025 and ISO Guide 34 [118]. The National Institute of Standards & Technology (NIST) distributes standard reference materials (SRMs), for example, 1549 (low-fat milk powder), 1548a (typical diet), 1566a

TABLE 4.3 Selected sample pretreatment procedures in combination with detection modes for the IC analysis of samples with various matrices

Detection	Matrix	Sample pretreatment and specific precautions	References
UV at: λ =223 nm (iodide)	saline, natural and simulated seawater, iodized table salt	No sample pretreatment; Analysis within max 24 h to prevent loss of iodide by oxidation, a flush volume of min 1 mL recommended between samples, presence of suppressor maintaining an acceptable baseline (hydroxide eluent absorbs in the UV)	[35]
λ =220 nm (iodide)	mineral waters		[46]
	seawater	untreated	[86]
λ =225 nm (iodide)	glacial acetic acid	acetic acid must be diluted with ultra pure water to ionize iodide	[42]
λ =226 nm (iodide)	seawater	untreated	[113, 114]
	electroplating baths	Medium capacity preconcentration column should be used	[42]
λ =215 (iodate), 230 nm (iodide)	saline	untreated	[115]
λ =210 nm (iodide)	saline	untreated	[116]
λ =605 nm (iodide)	saline	untreated	[65]
Conductivity	saline, natural and simulated seawater, iodized table salt, mineral waters	As above	[35]
	waste water samples	Serial dilution with ultra pure water, sonicated and filtrated sample souldtions were injected into the column	[40]
	healthcare products		[41]
	brine samples		[44]
	soil extract samples	Dilution and flitration through 0.45 μ m membrane filter paper	[47]
	milk powder	Inline sample preparation by dialysis	[117]
Pulsed Amperometry* (PAD)	Urine,	Removal of urine components	[37]
	soy- and milk-based infant formulas	(>10 000 daltons); dilution; use of RP-cartridges (OnGuard™ – RP); temperature control of the electrochemical cell; on-line degassing; cleaning working electrode; replacing a reference electrode (every 6 months for Ag/AgCl)	[62]
	thyroid tissues	Microwave digestion in open or closed vessels (usually applying HNO ₃ , HClO ₄ , or tetramethyl ammonium hydroxide (TMAH)); oxygen combustion; extraction; ultracentrifugation; precipitation	[63]

*I⁻ can be detected by direct current amperometry (DC), however, using PAD reproducibility is improved [37].

(oyster tissue), 1575a (pine needles), and 1570 (spinach) for use in calibrating instrumentation and evaluating the reliability of analytical methods for the determination of constituents in milk, milk powders, and other biological matrices.

4.9 TRENDS AND FUTURE DIRECTIONS OF IODINE DETERMINATIONS BY IC

At present faster and more efficient separations, enhanced sensitivity of detection through the coupling techniques, and further steps toward miniaturization are the most apparent trends in IC. As was mentioned earlier, monolithic and capillary scale columns allow for potentially faster and more efficient separations. Monolith technology, multiple gradients are applied for a variety of sample matrices including food, beverage, and chemical samples.

Areas of applications of anions determinations by IC increase constantly due to multicolumn and multidimensional analyses utilizing multimode phases. In order to expand IC capabilities for complex applications, new chromatographic systems are designed for dual-performance analysis. Dual IC involves many applications (e.g., two-dimensional IC (2D IC), as well as dual analysis, using simultaneous or sequential injection). Multiple analyses of cations and anions can be performed with one injection. Determinations of inorganic anions among organic compounds are possible with dual-parallel conductivity and electrochemical detection.

With more and more sophisticated instrumentation the sample preparation procedures are simplified and a problem of the loss of analyte is reduced (e.g., dilution is eliminated by simultaneous injection to a large and small loop) [119].

Recently, 2D IC has been developed for the determination of iodide, thiocyanate, and perchlorate ions in environmental samples (waters) [120]. Thiocyanate is a competitive inhibitor of the sodium iodide transporter and worsens iodine deficiency by inhibition of thyroïdal iodide accumulation and by inhibition of iodide transport into breast milk [121]. Perchlorate is known to inhibit the thyroid's ability to take up iodide [122]. Therefore, also from the economical point of view, it is extremely important to assess the content of the mentioned ions together with iodide/iodate determinations. Lin et al. [120] demonstrated 2D IC in the following configuration: iodide, thiocyanate, and perchlorate ions were separated from interfering ions by a IonPac AS16 column (250×4 mm). In the next stage, ions were enriched with an enrichment column (MAC-200, 80×0.75 mm); in 2D chromatography, ions were separated on a capillary column (IonPac AS20 Capillary, 250×0.4 mm). Reported LODs were in the range 0.02–0.05 pg l⁻¹.

There are many expectations regarding iodine determination in clinical samples; among them the availability of CRMs and further simplification and reduction in the time for sample preparation seem to be urgent. In the light of the currently used hi-tech equipment and the advantages of IC presented in this chapter it seems only a matter of time before this technique is more widely used in routine clinical analyses.

REFERENCES

- [1] Small H, Stevens T, Bauman W. Novel ion exchange chromatographic method using conductometric detection. *Anal Chem* 1975;47:1801–1809.
- [2] Fritz JS. Early milestones in the development of ion-exchange chromatography: a personal account. *J Chromatogr A* 2004;1039:3–12.
- [3] Haddad PR, Nesterenko PN, Buchberger W. Recent developments and emerging directions in ion chromatography. *J Chromatogr A* 2008;1184:456–473.
- [4] Haddad PR, Jackson PE. *Ion Chromatography: Principles and Applications*. Amsterdam: Elsevier; 1990.
- [5] Weiss J. *Handbook of Ion Chromatography*. Weinheim: Wiley-VCH Verlag GmbH & Co. KGaA; 2004.
- [6] Nordborg A, Hilder EF. Recent advances in polymer monoliths for ion-exchange chromatography. *Anal Bioanal Chem* 2009;394 (1):71–84.
- [7] Paull B, Nesterenko PN. New Possibilities in ion chromatography using porous monolithic stationary-phase media. *Trends Anal Chem* 2005;24 (4):295–303.
- [8] Michalski R. Ion chromatography as a reference method for the determination of inorganic ions in water and wastewater. *Crit Rev Anal Chem* 2006;36 (2):107–127.
- [9] Eickhorst T, Seubert A. Germanium dioxide as internal standard for simplified trace determination of bromate, bromide, iodate and iodide by on-line coupling ion chromatography-inductively coupled plasma mass spectrometry. *J Chromatogr A* 2004;1050:103–109.
- [10] Rong L, Lim LW, Takeuchi T. Determination of iodide and thiocyanate in seawater by liquid chromatography with poly (ethylene glycol) stationary phase. *Chromatographia* 2005;61:371–374.
- [11] Lim LW, Rong L, Takeuchi T. Polyoxyethylene as the stationary phase in ion chromatography. *Anal Sci* 2012;28:205–213.
- [12] Takeuchi T, Lim LW. Multifunctional separation mechanism on poly(oxyethylene) stationary phases in capillary liquid chromatography. *Anal Sci* 2010;26 (9):937–941.
- [13] Takeuchi T, Tokunaga K, Lim LW. Separation of inorganic anions on a chemically bonded 18-crown-6 ether stationary phase in capillary ion chromatography. *Anal Sci* 2013;29:423–427.
- [14] Takeuchi T, Lim LW. Separation of inorganic anions by liquid chromatography with crown ether as eluent additive. *Anal Sci* 2011;27:1019–1023.
- [15] Rong L, Lim LW, Takeuchi T. Determination of iodide in seawater by capillary ion chromatography using hexadimethrine bromide modified C30 stationary phases. *Anal Sci* 2013;29 (1):31–34.
- [16] Takeuchi T, Kawasaki T, Lim LW. Separation of inorganic anions on a pyridine stationary phase in ion chromatography. *Anal Sci* 2010;26:511–514.
- [17] Ito K, Hiriokawa T. Enhanced detection of iodide in seawater by ion chromatography using an ODS column coated with cetyltrimethylammonium. *Anal Sci* 2011;17:579–581.
- [18] Cabrera K. 2012. New Generation of Silica-Based Monoliths HPLC Columns with Improved Performance, Advanstar Communications Inc. Available at <http://www.chromatographyonline.com/lcgc/article/articleDetail.jsp?id=772076>. Accessed on June 24, 2014.
- [19] Hatis P, Lucy CA. Ultra-fast HPLC separation of common anions using a monolithic stationary phase. *Analyst* 2002;127:451–454.

- [20] Hatis P, Lucy CA. Improved sensitivity and characterization of high-speed ion chromatography of inorganic anions. *Anal Chem* 2003;75:995–1001.
- [21] Connolly D, Victory D, Paull B. Rapid, low pressure, and simultaneous ion chromatography of common inorganic anions and cations on short permanently coated monolithic columns. *J Sep Sci* 2004;27:912–920.
- [22] Pelletier S, Lucy CA. Achieving rapid low-pressure ion chromatography separations on short silica-based monolithic columns. *J Chromatogr A* 2006;1118:12–18.
- [23] Ríordáin CÓ, Barron L, Nesterenko E, Nesterenko PN, Paull B. Double gradient ion chromatography using short monolithic columns modified with a long chained zwitterionic carboxybetaine surfactant. *J Chromatogr A* 2006;1109:111–119.
- [24] Ríordáin CÓ, Nesterenko P, Paull B. Zwitterionic ion chromatography with carboxybetaine surfactant-coated particle packed and monolithic type columns. *J Chromatogr A* 2005;1070:71–78.
- [25] Unger KK, Tanaka N, Machtejevas E, editors. *Monolithic Silicas in Separation Science: Concepts, Syntheses, Characterization, Modeling and Applications*. Weinheim: John Wiley & Sons; 2011.
- [26] Suzuki A, Lim LW, Hiroi T, Takeuchi T. Rapid determination of bromide in seawater samples by capillary ion chromatography using monolithic silica columns modified with cetyltrimethylammonium ion. *Talanta* 2006;70:190–193.
- [27] Zakaria P, Hutchinson JP, Avdalovic N, Liu Y, Haddad PR. Latex-coated polymeric monolithic ion-exchange stationary phases. 2. Micro-ion chromatography. *Anal Chem* 2005;77 (2):417–423.
- [28] Wu R, Hu L, Wang F, Ye M, Zou H. Recent development of monolithic stationary phases with emphasis on microscale chromatographic separation. *J Chromatogr A* 2008;1184:369–392.
- [29] Ibrahim MEA, Lucy CA. Mixed mode HILIC/anion exchange separations on latex coated silica monoliths. *Talanta* 2012;100:313–319.
- [30] Takahashi M, Hirano T, Kitagawa S, Ohtani H. Separation of small inorganic anions using methacrylate-based anion-exchange monolithic column prepared by low temperature UV photo-polymerization. *J Chromatogr A* 2012;1232:123–127.
- [31] Glenn KM, Lucy CA, Haddad PR. Ion chromatography on a latex-coated silica monolith column. *J Chromatogr A* 2007;1155:8–14.
- [32] Sugrue E, Nesterenko PN, Paull B. Fast ion chromatography of inorganic anions and cations on a lysine bonded porous silica monolith. *J Chromatogr A* 2005;1075 (1–2):167–175.
- [33] Ríordáin CÓ, Gillespie E, Connolly D, Nesterenko PN, Paull B. Capillary ion chromatography of inorganic anions on octadecyl silica monolith modified with an amphoteric surfactant. *J Chromatogr A* 2007;1142:185–193.
- [34] Evenhuis CJ, Buchberger W, Hilder EF, Flook KJ, Pohl CA, Nesterenko PN, Haddad PR. Separation of inorganic anions on a high capacity porous polymeric monolithic column and application to direct determination of anions in seawater. *J Sep Sci* 2008;31 (14): 2598–2604.
- [35] Dionex. Determination of iodide in seawater and other saline matrices using a reagent-free ion chromatography system with suppressed conductivity and UV detection. Application note 239; Dionex Corporation; 2009.
- [36] Dionex. Determination of thiosulfate in refinery and other wastewaters. Application Note 138; Dionex Corporation; 2001.

- [37] Dionex. The determination of iodide in urine. Application Update 140; Dionex Corporation; 1999.
- [38] Metrohm. Iodide, thiosulfate and thiocyanate in the presence of the standard anions. IC Application Note No. S-140. Metrohm AG Company. Available at http://www.metrohm.com/com/Applications/literature/Application_Notes.html?identifier=AN-S-140&language=en&name=AN-S-140. Accessed on June 24, 2014.
- [39] Metrohm. Bromide, sulfate, iodide, and chloride in sodium chloride matrix. IC Application Work AW CH6-0708-092001; Metrohm AG Company; 2001.
- [40] Metrohm. Iodide among thiosulfate, thiocyanate in different waste water samples. IC Application Work AW BE6-0010-042002; Metrohm AG Company; 2002
- [41] Metrohm. Determination of anions in healthcare products. IC Application Work AW UK6-0128-032002; Metrohm AG Company; 2002.
- [42] Metrohm. Metrohm determination of iodate and iodide in electroplating baths. IC Application Work AW IC DE8-0802-052012; Metrohm AG Company; 2012.
- [43] Metrohm. Iodide in human urine. IC Application Note No. S-194. Metrohm AG Company. Available at http://www.metrohm.com/com/Applications/literature/Application_Notes.html?identifier=AN-S-194&language=en&name=AN-S-194. Accessed on June 24, 2014.
- [44] Metrohm. Determination of anions in brine sample. IC Application Work AW IC IN6-1264-092012; Metrohm AG Company; 2012.
- [45] Metrohm. Sixteen anions separated on Metrosep A Supp 7-250 applying gradient elution. IC Application Note No. S-255. Metrohm AG Company. Available at http://www.metrohm.com/com/Applications/literature/Application_Notes.html?identifier=AN-S-255&language=en&name=AN-S-255. Accessed on June 24, 2014.
- [46] Metrohm. Iodide in acetic acid. IC Application Work AW CN6-0001-042006; Metrohm AG Company; 2006.
- [47] Metrohm. Iodide in soil extract sample. IC Application Work AW IN6-0275-122005; Metrohm AG Company; 2005.
- [48] Dionex. IonPac AS11 manual. Document No. 034791-09; Dionex Corporation; 2006. p 31.
- [49] Dionex. IonPac AS11 manual. Document No. 031475-06; Dionex Corporation; 2008. p 31.
- [50] Thermo Fisher Scientific. Product manual for IonPac AS20. Document No. 065044; Thermo Fisher Scientific; 2012.
- [51] Haddad PR, Jackson PE, Shaw MJ. Developments in suppressor technology for inorganic ion analysis by ion chromatography using conductivity detection. *J Chromatogr A* 2003;1000 (1–2):725–742.
- [52] Dasgupta P, Liao H, Shelor CP. Ion chromatography yesterday and today: detection. *LC GC* 2013;31:23–26.
- [53] Kolb T, Bogenschuetz G, Schaefer J. Amperometrische detektion anorganischer anionen. *LaborPraxis* 1998;22:66–72.
- [54] Below H, Kahlert H. Determination of iodide in urine by ion-pair chromatography with electrochemical detection. *Fresenius J Anal Chem* 2001;371:431–436.
- [55] Cataldi TRI, Rubino A, Laviola MC, Ciriello R. Comparison of silver, gold and modified platinum electrodes for the electrochemical detection of iodide in urine samples following ion chromatography. *J Chromatogr B* 2005;827:224–231.
- [56] Cataldi TRI, Rubino A, Ciriello R. Sensitive quantification of iodide by ion-exchange chromatography with electrochemical detection at a modified platinum electrode. *Anal Bioanal Chem* 2005;382:134–141.

- [57] Chen Z, Hibbert DB. Simultaneous amperometric and potentiometric detection of inorganic anions in flow systems using platinum and silver/silver chloride electrodes. *Anal Chim Acta* 1997;350:1–6.
- [58] Jakmunee J, Grudpan K. Flow injection amperometry for the determination of iodate in iodized table salt. *Anal Chim Acta* 2001;438:299–304.
- [59] Nguyen VTP, Piersoel V, El Mahi T. Urine iodide determination by ion-pair reversed-phase high performance liquid chromatography and pulsed amperometric detection. *Talanta* 2012;99:532–537.
- [60] Bruggink C, van Rossum WJM, Spijkerman E, van Beelen ES. Iodide analysis by anion exchange chromatography and pulsed amperometric detection in surface water and adsorbable organic iodide. *J Chromatogr A* 2007;1144:170–174.
- [61] Rocklin RD, Johnson EL. Determination of cyanide, sulfide, iodide, and bromide by ion chromatography with electrochemical detection. *Anal Chem* 1983;55:4–7.
- [62] Dionex Corporation. The determination of iodide in milk products. Application Note 37; Sunnyvale, CA: Dionex Corporation; 2003.
- [63] Błażewicz A, Orlicz-Szczęśna G, Szczyński P, Prystupa A, Grzywa-Celińska A, Trojnar M. A comparative analytical assessment of iodides in healthy and pathological human thyroids based on IC-PAD method preceded by microwave digestion. *J Chromatogr B Analyt Technol Biomed Life Sci* 2011;879 (9–10):573–578.
- [64] Liang L, Cai Y, Mou S, Cheng J. Comparisons of disposable and conventional silver working electrode for the determination of iodide using high-performance anion-exchange chromatography with pulsed amperometric detection. *J Chromatogr A* 2005;1085 (1):37–41.
- [65] Brandao ACM, Buchberger WW, Butler ECV, Fagan PA, Haddad PR. Matrix-elimination ion chromatography with postcolumn reaction detection for the determination of iodide in saline waters. *J Chromatogr A* 1995;706:271–275.
- [66] Ito K. Determination of iodide in seawater by ion chromatography. *Anal Chem* 1997;69:3628–3632.
- [67] Bichsel Y, von Gunten U. Determination of iodide and iodate by ion chromatography with postcolumn reaction and UV/visible detection. *Anal Chem* 1999;71:34–38.
- [68] Brennan RG, Butler TA, Winchester MR. Achieving 0.2% relative expanded uncertainty in ion chromatography analysis using a high-performance methodology. *Anal Chem* 2011;83:3801–3807.
- [69] Pfaff JD. *Method 300.0: Determination of Inorganic Anions by Ion Chromatography*. Cincinnati: USEPA; 1993.
- [70] Błażewicz A. A review of spectrophotometric and chromatographic methods and sample preparation procedures for determination of iodine in miscellaneous matrices. In: Uddin J, editor. *Macro to Nano Spectroscopy*. InTech; 2012, Ch. 18. p 371–379.
- [71] Villaseñor SR. Matrix elimination in ion chromatography by heart-cut column switching techniques. *J Chromatogr* 1992;602:155–161.
- [72] Gürleyük H, Gerads R. Routine arsenic speciation analysis by IC-ICP-MS? are we there yet? invited talk at the national environmental monitoring conference. Washington, DC: U.S. Environmental Protection Agency; 2006.
- [73] Hou XL, Chai CF, Qian QF, Yan X, Fan X. Determination of chemical species of iodine in some seaweeds. *Sci Total Environ* 1997;204:215–221.
- [74] Shah M, Wuilloud RG, Kannamkumarath SS, Caruso JA. Iodine speciation studies in commercially available seaweed by coupling different chromatographic techniques with UV and ICP-MS detection. *J Anal At Spectrom* 2005;20:176–182.

- [75] PAC, 2004, 76, 1033 (Glossary of terms used in toxicokinetics (IUPAC Recommendations 2003), p. 1070. Available at <http://goldbook.iupac.org/ST06848.html>. Accessed on June 24, 2014
- [76] Cornelis R, Caruso JA, Crews H, Heumann HG, editors. *Handbook of Elemental Speciation II—Species in the Environment, Food, Medicine and Occupational Health*. Chichester: John Wiley & Sons, Ltd; 2005.
- [77] Chen Z, Megharaj M, Naidu R. Speciation of iodate and iodide in seawater by non-suppressed ion chromatography with inductively coupled plasma mass spectrometry. *Talanta* 2007;72 (5):1842–1846.
- [78] Huang Z, Zhu Z, Subhani Q, Yan W, Guo W, Zhu Y. Simultaneous determination of iodide and iodate in povidone iodine solution by ion chromatography with homemade and exchange capacity controllable columns and column-switching technique. *J Chromatogr A* 2012;1251:154–159.
- [79] Rendl J, Seybold S, Boerner W. Urinary iodide determined by paired-ion reversed-phase HPLC with electrochemical detection. *Clin Chem* 1994;40 (6):908–913.
- [80] Stärk J-J, Mattusch J, Wennrich R, Mroczek A. Investigation of the IC-ICP-MS determination of iodine species with reference to sample digestion procedures. *Fresenius J Anal Chem* 1997;359 (4–5):371–374.
- [81] Almeida AA, Jun X, Lima JLFC. Ion chromatographic determination of iodide in urine and serum using a tubular ion-selective electrode based on a homogeneous crystalline membrane. *Microchim Acta* 1997;127 (1–2):55–60.
- [82] Tucker HL, Flack RW. Determination of iodide in ground water and soil by ion chromatography. *J Chromatogr A* 1998;804:131–135.
- [83] Papadoyannis IN, Samanidou VF, Moutsis KV. Determination of silver-iodide by high-pressure ion chromatography in soil and water matrices after solid-phase extraction. *J Liq Chrom Relat Technol* 1998;21 (3):361–379.
- [84] Leiterer M, Truckenbrodt D, Franke K. Determination of iodine species in milk using ion chromatographic separation and ICP-MS detection. *Eur Food Res Technol* 2001;213 (2):150–153.
- [85] Valentín-Blasini L, Blount BC, Delinsky A. Quantification of iodide and sodium-iodide symporter inhibitors in human urine using ion chromatography tandem mass spectrometry. *J Chromatogr A* 2007;1155 (1):40–46.
- [86] Rong L, Lim LW, Takeuchi T. Determination of iodide in seawater using C30 column modified with polyoxyethylene oleyl ether in ion chromatography. *Talanta* 2007;72 (5):1625–1629.
- [87] Malongo TK, Patris S, Macours P, Cotton F, Nsangu J, Kauffmann JM. Highly sensitive determination of iodide by ion chromatography with amperometric detection at a silver-based carbon paste electrode. *Talanta* 2008;76:540–547.
- [88] Blount BC, Alwis KU, Jain RB, Solomon BL, Morrow JC, Jackson WA. Perchlorate, nitrate, and iodide intake through tap water. *Environ Sci Technol* 2010;44 (24):9564–9570.
- [89] Shinoda T, Miyamoto N, Kuromoto T, Ito PK, Morikawa H, Okamoto Y, Fujiwara T, Hirokawa T. Pyrohydrolysis coupled to ion chromatography for sensitive determination of iodine in food-related materials. *Anal Lett* 2012;45 (8):862–871.
- [90] Ito K, Nomura R, Fujii T, Tanaka M, Tsumura T, Shibata H, Hirokawa T. Determination of nitrite, nitrate, bromide, and iodide in seawater by ion chromatography with UV detection using dilauryldimethylammonium-coated monolithic ODS columns and sodium chloride as an eluent. *Anal Bioanal Chem* 2012;404 (8):2513–2517.

- [91] Spolaor A, Vallelonga P, Gabrieli J, Kehrwald N, Turetta C, Cozzi G, Poto L, Plane JM, Boutron C, Barbante C. Speciation analysis of iodine and bromine at picogram-per-gram levels in polar ice. *Anal Bioanal Chem* 2013;405 (2–3):647–654.
- [92] Romarís-Hortas V, Bermejo-Barrera P, Moreda-Piñeiro A. Development of anion-exchange/reversed-phase high performance liquid chromatography-inductively coupled plasma-mass spectrometry methods for the speciation of bio-available iodine and bromine from edible seaweed. *J Chromatogr A* 2012;1236:164–176.
- [93] Schwehr KA, Santschi PH. Sensitive determination of iodine species, including organo-iodine, for freshwater and seawater samples using high performance liquid chromatography and spectrophotometric detection. *Anal Chim Acta* 2003;482:59–71.
- [94] Gilfedder BS, Petri M, Biester H. Iodine speciation and cycling in fresh waters: a case study from a humic rich headwater lake (Mummelsee). *J Limnol* 2009;68. Available at <http://www.jlimnol.it/index.php/jlimnol/article/view/jlimnol.2009.396>. Accessed on June 24, 2014.
- [95] Shah M, Wuilloud RG, Kannamkumath SS, Caruso JA. Iodine speciation studies in commercially available seaweed by coupling different chromatographic techniques with UV and ICP-MS detection. *J Anal At Spectrom* 2005;20:176–182.
- [96] Anazawa K, Tomiyasu T, Sakamoto H. Simultaneous determination of fluorine and chlorine in rocks by ion chromatography in combination with alkali fusion and cation-exchange pretreatment. *Anal Sci* 2001;17:217–219.
- [97] Souza GB, Carrilho ENVM, Oliveira CV, Nogueira ARA, Nóbrega JA. Oxygen bomb of biological samples for inductively coupled plasma optical emission spectrometry. *Spectrochim Acta B At Spectroscopy* 2002;57:2195–2201.
- [98] Pereira JSF, Diehl LO, Duarte FA, Santos MF, Guimarães RC, Dressler VL, Flores EM. Chloride determination by ion chromatography in petroleum coke after digestion by microwave-induced combustion. *J Chromatogr A* 2008;1213:249–252.
- [99] Antes FG, Duarte FA, Mesko MF, Nunes MA, Pereira VA, Müller EI, Dressler VL, Flores EM. Determination of toxic elements in coal by ICP-MS after digestion using microwave-induced combustion. *Talanta* 2010;83:364–369.
- [100] Antes FG, Duarte FA, Paniz JNG, Santos MFP. Chlorine Determination in Petroleum Coke Using Pyrohydrolysis and DRC-ICP-MS. *At Spectrosc* 2008;29:157–164.
- [101] Hansson M, Isaksson M, Berg G. Sample preparation for in vitro analysis of iodine in thyroid tissue using x-ray fluorescence. *Cancer Inform* 2008;6:51–57.
- [102] Fragu P, Briançon C, Fourré C, Clerc J, Casiraghi O, Jeusset J, Omri F, Halpern S. SIMS microscopy in the biomedical field. *Biol Cell* 1992;74:5–18.
- [103] Rognoni J, Simon C. Critical analysis of the glutaraldehyde fixation of the thyroid gland: a double-labelling experiment. *J Microsc* 1974;21:119–128.
- [104] Bing L, Wei L, Hong-xia Y, et al. Determination of iodine species using IC-ICP-MS. In: *Handbook of Hyphenated ICP-MS Applications*. Agilent Technologies, Inc; 2007. p 36.
- [105] Moxon RE, Dixon EJ. Semi-automatic method for the determination of total iodine in food. *Analyst* 1980;105:344–352.
- [106] Bárány E, Bergdahl IA, Schüätz A, Skerfving S, Oskarsson A. ICP-MS for direct multi-element analysis of diluted human blood and serum. *J Anal At Spectrom* 1999;12: 1005–1009.
- [107] Knapp G, Maichin B, Fecher P, Hasse S, Schramel P. Iodine determination in biological materials options for sample preparation and final determination. *Fresenius J Anal Chem* 1998;362:508–513.

- [108] Fecher PA, Goldman I, Nagengast A. Determination of iodine in food samples by inductively coupled plasma mass spectrometry after alkaline extraction. *J Anal At Spectrom* 1998;13:977–982.
- [109] Schramel P, Hasse S. Iodine determination in biological materials by ICP-MS. *Microchim Acta* 1994;116:4205–209.
- [110] Fischer PWF, Labbe MR, Giroux A. Colorimetric determination of total iodine in foods by iodide-catalyzed reduction of Ce+4. *J Assoc Off Anal Chem* 1986;69:687–689.
- [111] Gamallo-Lorenzo D, Barciela-Alonso MC, Moreda-Pineiro A, Bermejo-Barrera A, Bermejo-Barrera P. Microwave-assisted alkaline digestion combined with microwave-assisted distillation for the determination of iodide and total iodine in edible seaweed by catalytic spectrophotometry. *Anal Chim Acta* 2005;542:287–295.
- [112] Sullivan D. AOAC expert review panel approves Official MethodsSm for iodine, pantothenic acid, carnitine, fatty acids, vitamins c and e, and choline and additional methods for vitamins a and d and inositol. *J AOAC Int* 2013;96 (3):481–484.
- [113] Chandramouleeswaran S, Vijayalakshmi B, Kartihkeyan S, Rao TP, Iyer CSP. Ion-chromatographic determination of iodide in sea water with UV detection. *Mikrochim Acta* 1998;128:75–77.
- [114] Ito K. Semi-micro ion chromatography of iodide in seawater. *J Chromatogr A* 1999; 830:211–217.
- [115] Hu WZ, Yang PJ, Hasebe K, Haddad PR, Tanaka K. Rapid and direct determination of iodide in seawater by electrostatic ion chromatography. *J Chromatogr A* 2002;956: 103–107.
- [116] Hu WZ, Haddad PR, Hasebe K, Tanaka K, Tong P, Khoo C. Direct determination of bromide, nitrate, and iodide in saline matrixes using electrostatic ion chromatography with an electrolyte as eluent. *Anal Chem* 1999;71:1617–1620.
- [117] Metrohm. Iodide in milk powder. IC Application Note No. S-162; 2013.
- [118] EPA Method 300, Iodide Anion by Ion Chromatography. 2012. SOP: WPCL-AA-041 CDPR Title: Iodide by Ion Chromatography, 1–11. Available at http://www.cdpr.ca.gov/docs/emon/pubs/anl_methds/iodide_by_ion_chromatography.pdf. Accessed on June 24, 2014.
- [119] Shao B, Bahten K, Madden J, Christison T, Pang F, Hoefler F. Automatic resampling using Chromeleon autodilution, two injection loops, and the Dionex AS-DV autosampler. Technical Note 111, Thermo Fisher Scientific Inc; (2011).
- [120] Lin L, Wang H, Shi Y. Determination of iodide, thiocyanate and perchlorate ions in environmental water by two-dimensional ion chromatography. *Se pu* 2013;31:281–285.
- [121] Laurberg P, Andersen S, Pedersen IB, Carle A, Knudsen N, Rasmussen LB, Karmisholt J. The relationship between thiocyanate and iodine. In: Preedy VR, Burrow GN, Watson RR, editors. *Comprehensive Handbook of Iodine: Nutritional, Biochemical, Pathological and Therapeutic Aspects*. Amsterdam: Elsevier, Ch. 28. 2012; p 275–281.
- [122] Snyder SA, Vanderford BJ, Rosario-Ortiz FL. Iodate and perchlorate in bottled water: methods for discovery and impact on humans. In: Preedy VR, Burrow GN, Watson RR, editors. *Comprehensive Handbook of Iodine: Nutritional, Biochemical, Pathological and Therapeutic Aspects*. Amsterdam: Elsevier, Ch. 30. 2012; p 287–294.

5

INORGANIC IODIDES

TATSUO KAIHO

Nihon Tennen Gas Co., Ltd., Chiba, Japan

5.1 INTRODUCTION

Compounds with iodine in the formal oxidation state -1 are called iodides. Iodine forms iodide compounds with almost all of the elements except inert elements, as shown in Table 5.6. Iodide is one of the largest monoatomic anions whose radius is around 220 pm (see Chapter 2). Iodide is one of the largest monoatomic anions and it is less hydrophilic or more hydrophobic than the smaller halogen anions: bromide (196 pm), chloride (181 pm), and fluoride (133 pm). Iodides range the whole spectrum of bonding from completely ionic to covalent structures; for example, sodium iodide can be regarded as ionic and titanium iodide is predominantly covalent. The low solubility of silver iodide and lead iodide in water and other polar solvents reflects the covalent character of these metal iodides (see Table 5.7). A test for the presence of iodide ions is the formation of yellow precipitates of these compounds upon treatment of a solution of silver(I) nitrate or lead(II) nitrate [1].

Commercially available inorganic iodides are the most important class of iodine compounds [2]. They are used in various fields in our life as follows. Iodized salt, which is commonly supplied in European countries and many other countries in order to prevent iodine deficiency disorders, contains 0.01% amount of potassium iodide, KI, or sodium iodide, NaI (see Chapter 22). Lugol's iodine is a solution of elemental iodine, I_2 , and potassium iodide, KI, in water and is often used as an antiseptic and disinfectant (see Chapter 20). Polarizing films are prepared by dyeing the polyvinyl alcohol film in an aqueous solution containing iodine, I_2 , and potassium iodide, KI (see Chapter 26). Copper(I) iodide, CuI, is used as heat-stabilizing agents in manufacturing of Polyamide

6 and Polyamide 66 (see Chapter 31). It is also used for animal feed additives. Cloud seeding is the technique of inducing rain from a cloud. Silver iodide, AgI, is used as a nuclei because its structure is very similar to ice crystals, which thus lowers the activation barrier of freezing in supercooled water droplets. Inorganic iodides, such as MgI_2 , TiI_4 , CuI , PdI_2 , InI , and SmI_2 , are playing an important role in recent developments in organic synthesis (see Chapter 18). Iodine also reacts with other halogens, fluorine, chlorine, and bromine, and forms interhalogens [3], IF , IF_3 , IF_5 , IF_7 , ICl , ICl_3 , IBr , and IBr_3 . These compounds are used for halogenation reactions. Physicochemical properties and preparation methods of some representative inorganic iodides and iodo compounds are summarized in this chapter.

It should also be noted that because of the relatively high electronegativity of iodine (2.66 in the Pauling scale, as compared to 2.96 for bromine and 3.16 for chlorine) many elements form iodides corresponding to their valency, such as NaI , MgI_2 , AlI_3 , and SiI_4 . However, the high polarizability of iodine combined with the reducing power of the iodide ion makes iodide compounds corresponding to low valencies common, such as SnI_2 , Hg_2I_2 , AuI , or BiI (the latter actually corresponding to Bi_4I_4). The compounds included in Table 5.7 may thus conceal a more extensive chemistry than that of, for instance, chlorine. The low-valency compounds of iodides are often denoted as subvalent [4], referring to oxidation states of the noniodine element being lower than expected in an aqueous environment.

5.2 HYDROGEN IODIDE

Hydrogen iodide, HI, MW 127.91 g mol⁻¹, is a colorless gas that fumes in moist air. It is the least stable of the common hydrogen halides and the best reducing agent. It reacts with oxygen to give water and iodine. With moist air, HI gives a mist (or fumes) of hydroiodic acid. It is exceptionally soluble in water, 234 g 100 g⁻¹ water at 10°C, giving hydroiodic acid [5]. The industrial preparation of HI involves the reaction of I_2 with hydrazine, which also yields nitrogen gas: Equation 5.1 [5, 6]. An alternative method for producing HI is the reaction of iodine with hydrogen sulfide: Equation 5.2 [5]. I_2 reacts with phosphorus to give phosphorus triiodide, which then reacts with water to form HI and phosphorous acid: Equation 5.3 [7]. Additionally, HI can be prepared by simply combining H_2 and I_2 gas in the presence of a platinum catalyst. This method is usually employed to generate high-purity samples: Equation 5.4 [8]. High-purity HI can also be obtained by reducing iodine with tetrahydronaphthalene. Crude HI obtained by reducing iodine with tetrahydronaphthalene is contacted with a zeolite in the gaseous phase to produce high-purity HI: Equation 5.5 [9].

5.3 HYDRIODIC ACID

Hydriodic acid is the colorless solution formed when HI gas is dissolved in water. Commercial 57% hydriodic acid is a transparent, colorless to slightly yellow liquid, which may take on a brownish color because of the formation of iodine, combining

with iodide ions to form triiodide ions. The solution forms an azeotrope boiling point at 127°C with 57% HI and 43% water [10]. Hydriodic acid is used in the preparation of iodides and is an important reagent in organic chemistry. Diluted hydriodic acid reacts with many metals (including aluminum, zinc, calcium, magnesium, iron, tin, and all of the alkali metals) to generate flammable hydrogen gas, and it reacts with their hydroxide, carbonates, and salts to yield metal iodides.

5.4 SODIUM IODIDE

Sodium iodide, NaI, MW 149.92 g mol⁻¹, forms colorless cubic crystals that are soluble in polar solvents, such as water, ethanol, acetone, and glycerol. Sodium iodide is produced by the addition of sodium hydroxide or sodium carbonate to hydriodic acid: Equation 5.6 and 5.7. The anhydrous product is obtained from the solution by evaporation [11, 12].

5.5 POTASSIUM IODIDE

Potassium iodide, KI, MW 166.02 g mol⁻¹, forms colorless or white cubic crystals or granules and becomes yellowish when exposed to bright light due to photochemical decomposition, liberating traces of free iodine. It is soluble in polar solvents, such as water, ethanol, methanol, and acetone, but it is insoluble in ether. It is less hygroscopic than sodium iodide, making it easier to work with. Aged and impure samples are yellow because of aerial oxidation of iodide to elemental iodine: $4 \text{ KI} + 2 \text{ CO}_2 + \text{O}_2 \rightarrow 2 \text{ K}_2\text{CO}_3 + 2 \text{ I}_2$ [1]. Potassium iodide is produced industrially by treating KOH with iodine [13]. Potassium iodate, which is formed as a secondary product, is reduced by activated carbon: Equation 5.8. The product is purified by crystallization from water. Alternatively, iron (II) iodide, prepared by using iron powder and iodine, can be treated with potassium carbonate to obtain potassium iodide: Equation 5.9 [14]. High-purity potassium iodide can be prepared by the reaction of a potassium bicarbonate with hydriodic acid: Equation 5.10 [15].

5.6 COPPER (I) IODIDE

Copper (I) iodide (CuI), MW 190.45 g mol⁻¹, can be prepared by heating iodine and copper in concentrated hydriodic acid, HI. Another preparation route involves the precipitation of the salt by mixing aqueous solutions of potassium or sodium iodide with copper sulfate or any soluble copper(II) salt: Equation 5.11. The unstable CuI₂ compound immediately decomposes into iodine and sparingly soluble CuI, releasing I₂: Equation 5.11 [16–18]. CuI is poorly soluble in water (0.00042 g l⁻¹ at 25°C), but it dissolves in the presence of NaI or KI to give the linear complex anion [CuI₂]⁻. Dilution of such solutions with water reprecipitates CuI. In many aspects, copper(I) iodide may be regarded as a subvalent iodide of copper (vide supra).

5.7 SILVER IODIDE

Silver iodide, AgI, is prepared by the reaction of a sodium or potassium iodide solution with a hot solution of silver nitrate: Equation 5.12. A yellowish solid quickly precipitates. The precipitate can be washed with boiling water to give a pure product [19]. The preparation is made in the dark or under ruby-red light because of the sensitivity of AgI to light. The solid is a mixture of two principal phases. Dissolution of the AgI in hydroiodic acid followed by dilution with water precipitates β -AgI. Alternatively, dissolution of AgI in a solution of concentrated silver nitrate followed by dilution affords α -AgI. If the preparation is not conducted in the absence of light, the solid rapidly darkens, the light causing a reduction of ionic silver to the metal state. The photosensitivity varies with sample purity [20] and is analogous to old-type photography based on the analogous AgBr substance (Tables 5.1 and 5.2).

TABLE 5.1 Preparation of iodides

Iodide	Eq. No.	Reaction
HI	5.1	$2 \text{I}_2 + \text{N}_2\text{H}_4 \rightarrow 4 \text{HI} + \text{N}_2$
	5.2	$\text{I}_2 + \text{H}_2\text{S} \rightarrow 2 \text{HI} + \text{S}$
	5.3	$3 \text{I}_2 + 2 \text{P} + 6 \text{H}_2\text{O} \rightarrow 2 \text{PI}_3 + 6 \text{H}_2\text{O} \rightarrow 6 \text{HI} + 2 \text{H}_3\text{PO}_3$
	5.4	$\text{H}_2 + \text{I}_2 \rightarrow 2 \text{HI}$
	5.5	Tetrahydronaphthalene + $2 \text{I}_2 \rightarrow$ Naphthalene + 4HI
NaI	5.6	$\text{NaOH(aq)} + \text{HI(aq)} \rightarrow \text{NaI} + \text{H}_2\text{O}$
	5.7	$\text{Na}_2\text{CO}_3 + 2 \text{HI} \rightarrow 2 \text{NaI} + \text{CO}_2 + \text{H}_2\text{O}$
KI	5.8	$6 \text{KOH(aq)} + 3 \text{I}_2(\text{s}) \rightarrow 5 \text{KI(aq)} + \text{KIO}_3 + 3 \text{H}_2\text{O}$
		$2 \text{KIO}_3(\text{aq}) + 3 \text{C(s)} \rightarrow 2 \text{KI(aq)} + 3 \text{CO}_2$
	5.9	$\text{Fe} + \text{I}_2 \rightarrow \text{FeI}_2$
		$3 \text{FeI}_2 + \text{I}_2 \rightarrow \text{Fe}_3\text{I}_8$
CuI	5.10	$\text{Fe}_3\text{I}_8 + 4 \text{K}_2\text{CO}_3 \rightarrow 8 \text{KI} + 4 \text{CO}_2 + \text{Fe}_3\text{O}_4$
		$\text{HI} + \text{KHCO}_3 \rightarrow \text{KI} + \text{H}_2\text{O} + \text{CO}_2$
	5.11	$\text{CuSO}_4 + 2 \text{KI} \rightarrow \text{CuI}_2 + \text{K}_2\text{SO}_4$
AgI		$2 \text{CuI}_2 \rightarrow 2 \text{CuI} + \text{I}_2$
	5.12	$\text{KI} + \text{AgNO}_3 \rightarrow \text{AgI} + \text{KNO}_3$

TABLE 5.2 Thermochemical properties of iodides

	HI	NaI	KI	CuI	AgI
Melting point ($^{\circ}\text{C}$)	-50.8	662	681	606	558
Boiling point ($^{\circ}\text{C}$)	-35.55	1304	1330	~1290	1506
$\Delta_f H^{\circ}$ kcal mol $^{-1}$	6.33	-68.79	-78.37	-16.20	-14.8
$\Delta_f G^{\circ}$ kcal mol $^{-1}$	0.406	-68.38	-77.65	-16.61	-15.8
S° cal deg $^{-1}$ mol $^{-1}$	49.38	23.54	25.4	23.11	27.6
C_p cal deg $^{-1}$ mol $^{-1}$	6.98	12.45	12.65	12.93	13.6

5.8 NITROGEN TRIIODIDE

Nitrogen iodide (NI_3) was first prepared by B. Courtois in 1813. The reaction of iodine with aqueous ammonia yields an explosive brown solid claimed to be nitrogen triiodide [21]. This simple reaction, however, does not render NI_3 . Instead, either $[\text{NI}_3 \cdot \text{NH}_3]$ or $[\text{NI}_3 \cdot (\text{NH}_3)_3]$ is formed; both are complexes of ammonia. The reaction of iodine crystals with aqueous ammonia can be represented by $3\text{I}_2(\text{s}) + 5\text{NH}_3(\text{aq}) \rightarrow \text{NI}_3 \cdot \text{NH}_3(\text{s}) + 3\text{NH}_4\text{I}(\text{aq})$. Deep-red, adduct-free NI_3 can be isolated from the reaction of boron nitride with iodine monofluoride in trichlorofluoromethane (CCl_3F) at -30°C by sublimation at low temperature: $\text{BN} + 3\text{IF} \rightarrow \text{NI}_3 + \text{BF}_3$ [22]. NI_3 is an extremely sensitive contact explosive: small quantities explode with a loud, sharp snap when touched even lightly, releasing a purple cloud of iodine vapor. The detonation of NI_3 can be represented by $2\text{NI}_3(\text{s}) \rightarrow \text{N}_2(\text{g}) + 3\text{I}_2(\text{g})$.

5.9 IODINE PENTOXIDE

Iodine pentoxide, I_2O_5 , MW 333.81 g mol $^{-1}$, mp 275°C (dec.), is an iodic anhydride and can be derived from the periodate by dehydration: $2\text{HIO}_3 \rightarrow \text{I}_2\text{O}_5 + \text{H}_2\text{O}$. It forms white needle-like crystals, which are easily dissolved in water to generate the periodate. Iodine pentoxide is not readily soluble in polar solvents, such as ethanol, ethyl ether, chloroform, and carbon disulfide. It is used as an oxidant and for the detection of carbon monoxide gas [23, 24].

5.10 INTERHALOGEN COMPOUND OF IODINE

The interhalogens of the form XY_n have physical properties intermediate between those of the two parent halogens. The covalent bond between the two atoms has some ionic character, the less electronegative element, X, can be regarded as oxidized, thus possessing a partial positive charge. The compounds of one halogen bound to another are called interhalogens or interhalogen compounds. The main reason for their formation is the large electronegativity and the size differences between the different halogens. All combinations of F, Cl, Br, and I, which have the earlier-mentioned general formula, are known, but not all are stable. Iodine combines exothermically with other halogens to form interhalogen iodines: IF , IF_3 , IF_5 , IF_7 , ICl , ICl_3 , IBr , and IBr_3 . In terms of molecular structure, it can be noted that the more electronegative (thus lighter) halogen takes on the terminal positions, and when iodine is present it can be regarded as a coordination center. They are divided into the following four types and the least electronegative halogen, iodine, is always written first [3].

A special case of interhalogen compounds are those containing iodine only: so-called polyiodides. The triiodide ion can be regarded as the most simple polyiodide ion. Polyiodides are formed with a wide range of cations and with varying ratios between iodide and iodine. The vast majority of polyiodides can be rationalized

in terms of the composition $mI^- nI_2$, making up pentaiodides, heptaoidides, and so on, often forming interesting and low-dimensional crystalline compounds [25]. The bonding in polyiodides is complex involving contributions from long-range covalent interaction, as well as induction, ion-quadrupole, and dispersion interactions [26].

5.10.1 Iodine Monochloride

Iodine monochloride, ICl, exists in two modifications: stable black needles, known as the alpha form, and a labile, metastable beta modification consisting of black platelets. The alpha form melts at 27.3°C and the beta form melts at 13.9°C. Liquid ICl has bromine-like, reddish-brown color; its density is 3.10 g ml⁻¹ at 29°C; and it decomposes at around 100°C [27]. ICl is produced by simply combining iodine and chlorine in a 1 : 1 molar ratio, according to Equation 5.21. Aqueous solutions of ICl are prepared by passing chlorine gas through a suspension of iodine in moderately strong hydrochloric acid: Equation 5.22 [28, 29]. Because of the difference in electronegativity of iodine and chlorine, ICl is highly polar and is used as a source of electrophilic iodine (I⁺) in the synthesis of certain aromatic iodides, such as 5-amino-2,4,6-triiodobenzene-1,3-dioic acid (see Chapter 19). It also cleaves C–Si bonds. ICl also adds to the double bond in alkenes to give chloro-iodo alkanes: $RCH=CHR' + ICl \rightarrow RCH(I)-CH(Cl)R'$.

5.10.2 Iodine Pentafluoride

Iodine pentafluoride, IF₅, is a colorless to yellowish liquid with a pungent odor; it fumes in air, its density being 3.19 g ml⁻¹, freezes at 9.43°C, and boils at 100.5°C. It hydrolyzes spontaneously forming hydrogen fluoride and iodic acid. IF₅ is best obtained by passing fluorine gas over iodine under cooling: Equation 5.16 [30]. Also, it may be prepared by the reaction of fluorine with iodine trifluoride or the heating of potassium iodide with stoichiometric amounts of fluorine: Equations 5.17 and 5.18. IF₅ is used as a fluorinating agent in organic synthesis, but in comparison to BrF₃ or

TABLE 5.3 Interhalogen iodine compounds

Type	XY	XY ₃	XY ₅	XY ₇
Structure	Linear	Distorted trigonal bipyramidal (dsp ³ hybridization)	Distorted octahedral (d ² sp ³ hybridization)	Pentagonal bipyramidal (d ³ sp ³ hybridization)
Fluoride	Iodine monofluoride (IF)	Iodine trifluoride (IF ₃)	Iodine pentafluoride (IF ₅)	Iodine heptafluoride (IF ₇)
Chloride	Iodine monochloride (ICl)	Iodine trichloride (ICl ₃)		
Bromide	Iodine monobromide (IBr)	Iodine tribromide (IBr ₃)		

X, iodine; Y, fluoride, chloride, bromide.

ClF, it is less reactive. In addition, at room temperature there is no reaction between IF₅ and chlorine or bromine; with increased temperature, oxidation of chlorine and bromine occurs, though. Iodine is soluble in IF₅ but does not react with it [31–33]. The main application of IF₅ is in the production of alkyl iodides containing fluorine. These are valuable intermediates in the synthesis of perfluoralkylated organic compounds: $5\text{CF}_2=\text{CF}_2 + 2\text{I}_2 + \text{IF}_5 \rightarrow 5\text{C}_2\text{F}_5\text{I}$ (see Chapter 29). IF₅ is also used for etching in the manufacture of semiconductors and is used in incendiaries (Tables 5.3, 5.4, 5.5, 5.6, and 5.7).

TABLE 5.4 Physical properties of interhalogen iodine compounds

Molecular formula	IF	IF ₃	IF ₅	IF ₇	ICl	ICl ₃	IBr
Molar mass, g mol ⁻¹	145.903	183.9	221.89	259.90	162.35	233.26	206.904
Appearance	Unstable brown solid	Yellow solid	Colorless or pale yellow liquid	Colorless gas	Red to brown liquid, black crystals	Yellow solid	Dark-red solid
Density g cm ⁻³			3.19	2.8 (6°C)	3.10	3.203	
Melting point	−45°C	Dec. above −28°C	9.43°C	4.5°C (tp)	27.2°C (α), 13.9 °C (β)	~33°C	42°C
Boiling point			100.5°C	4.8°C (subl. 1 atm)	97°C		116°C
Solubility in water			Reacts	Soluble	Hydrolysis		

TABLE 5.5 Preparation of interhalogen compounds

Interhalogen	Eq. No.	Preparation
IF	5.13	$\text{I}_2 + \text{F}_2 \rightarrow 2\text{IF} (-45^\circ\text{C})$
	5.14	$\text{I}_2 + \text{AgF} \rightarrow \text{IF} + \text{AgI}$
IF ₃	5.15	$\text{IF} + \text{F}_2 \rightarrow \text{IF}_3$
IF ₅	5.16	$\text{I}_2 + 5\text{F}_2 \rightarrow 2\text{IF}_5$
	5.17	$\text{IF}_3 + \text{F}_2 \rightarrow \text{IF}_5$
	5.18	$5\text{AgF} + 3\text{I}_2 \rightarrow \text{IF}_5 + 5\text{AgI}$
IF ₇	5.19	$\text{IF}_5 + \text{F}_2 \rightarrow \text{IF}_7$
	5.20	$\text{PdI}_2 + 8\text{F}_2 \rightarrow 2\text{IF}_7 + \text{PdF}_2$
ICl	5.21	$\text{I}_2 + \text{Cl}_2 \rightarrow 2\text{ICl}$
	5.22	$5\text{I}_2 + 4\text{HCl} + 3\text{Cl}_2 \rightarrow 10\text{ICl} + 2\text{H}_2$
ICl ₃	5.23	$\text{I}_2 + 3\text{Cl}_2 \rightarrow 2\text{ICl}_3 (-80^\circ\text{C})$
	5.24	$\text{I}_2\text{O}_5 + 10\text{HCl} \rightarrow 2\text{ICl}_3 + 5\text{H}_2\text{O} + 2\text{Cl}_2$
IBr	5.25	$\text{I}_2 + \text{Br}_2 \rightarrow 2\text{IBr} (60^\circ\text{C})$

HI								Iodide	Formula									He
Hydrogen								Element	Name									Helium
10034-85-2								CAS NO										
-50.8								Mp	°C									
LiI	BeI ₂												BI ₃	Cl ₄	NI ₃	I ₂ O ₅	IF ₅	Ne
Lithium	Beryllium												Boron	Carbon	Nitrogen	Oxygen	Fluorine	Neon
10377-51-2	7787-53-3												13517-10-7	507-25-3	13444-85-4	12029-98-0	7783-66-6	
469	480												49.7	168	—	275	9.43	
NaI	MgI ₂												AlI ₃	SiI ₄	PI ₃	SI	ICl	Ar
Sodium	Magnesium												Aluminum	Silicon	Phosphorus	Sulfur	Chlorine	Argon
7681-82-5	10377-58-9												7784-23-8	13465-84-4	13455-01-1	1312-15-8	7790-99-0	
661	634												118.28	120.5	61.2		27.2(a) 13.9(b)	
KI	CaI ₂	ScI ₃	TiI ₄	VI ₃	CrI ₂	MnI ₂	FeI ₂	CoI ₂	NI ₂	CuI	ZnI ₂	GaI ₃	GeI ₂	AsI ₃	SeI ₂	IBr		Kr
Potassium	Calcium	Scandium	Titanium	Vanadium	Chromium	Manganese	Iron	Cobalt	Nickel	Copper	Zinc	Gallium	Germanium	Arsenic	Selenium	Bromine		Krypton
7681-11-0	10102-68-8	14074-33-0	7720-83-4	15513-94-7	13478-28-9	7790-33-2	7783-86-0	15238-00-3	13462-90-3	7681-65-4	10139-47-6	13450-91-4	13573-08-5	7784-45-4	81256-76-0	7789-33-5		
681	763	953	155	304dec	867	638	594	520	800	591	450	212	428	141		42		
RbI	SrI ₂	YI ₃	ZrI ₄	NbI ₅	MoI ₃	Te	RuI ₃	RhI ₃	PdI ₂	AgI	CdI ₂	IndI ₃	SnI ₄	SbI ₃	TeI ₄	I ₂		Xe
Rubidium	Strontium	Yttrium	Zirconium	Niobium	Molybdenum		Ruthenium	Rhodium	Palladium	Silver	Cadmium	Indium	Tin	Antimony	Tellurium	Iodine		Xenon
7790-29-6	10476-86-5	13470-38-7	13986-26-0	13779-92-5	14055-75-5		13896-65-6	15492-38-3	7790-38-7	7783-96-2	7790-80-9	13510-35-5	7790-47-8	7790-44-5	7790-48-9	7553-56-2		
656	538	997	500	327	927		300dec	360dec	558	388	207	143		171	280	113.7		
Cd	BaI ₂	LaI ₃	HfI ₄	TaI ₅	WI ₂	ReI ₃	OsI ₂	IrI ₃	PtI ₂	AuI	HgI ₂	TlI	PbI ₂	BiI ₃	PoI ₄	AtI ₃		Rn
Cesium	Barium	Lanthanum	Hafnium	Tantalum	Tungsten	Rhenium	Osmium	Iridium	Platinum	Gold	Mercury	Thallium	Lead	Bismuth	Polonium	Astatine		Radon
7789-17-5	13718-50-8	13813-22-4	13777-23-6	14693-81-3	13470-17-2	15622-42-1	59201-58-0	7790-41-2	7790-39-8	10294-31-2	7774-29-0	7790-30-9	10101-63-0	7787-64-6	61716-27-6	7784-45-4		
632	711	778	440tp	406	800dec			325dec	120dec	256	442	410		408.6	>200	141		
Fr	RaI ₂ 6H ₂ O	AcI ₃	Rf	Db	Sg	Bh	Hs	Mt	Ds	Rg	Cn	Uut	Fl	Uup	Lv	Uus		Uuo
Francium	Radium	Actinium	Rutherfordium	Dubnium	Seaborgium	Bohrium	Hassium	Meitnerium	Darmstadtium	Roentgenium	Copernicium	Ununtrium	Flerovium	Ununpentium	Livermorium	Ununseptium		Ununoctium
	20610-52-0	33689-82-6																

CeI ₂	PtI ₂	NdI ₃	PmI ₃	SmI ₂	EuI ₂	GdI ₃	TbI ₃	DyI ₃	HolI ₃	ErI ₃	TmI ₃	YbI ₃	LuI ₃
Cerium	Praseodymium	Neodymium	Promethium	Samarium	Europium	Gadolinium	Terbium	Dysprosium	Holmium	Erbium	Thulium	Ytterbium	Lutetium
19139-47-0	13813-23-5	13813-24-6	13818-73-0	32248-43-4	22015-35-6	13572-98-0	13813-40-6	15474-63-2	13813-41-7	13813-42-8	13813-43-9	13813-44-0	13813-45-1
808	738	787	695	520	580	930	955	978	994	1014	1021	700	1050
ThI ₄	PaI ₃	UI ₃	NpI ₃	PuI ₃	AmI ₃	CmI ₃	BkI ₃	CH ₃	EdI ₃	Fm	Md	No	Lr
Thorium	Protactinium	Uranium	Neptunium	Plutonium	Americium	Curium	Berkelium	Californium	Einsteinium	Fermium	Mendelevium	Nobelium	Lawrencium
7790-49-0	19415-71-5	13775-18-3	37501-52-3	13813-46-2	13813-47-3	14696-85-6	23171-53-1	20758-81-0	99644-28-7				
556		766		777		990							

TABLE 5.6 Table of inorganic iodides

TABLE 5.7 Physical constants of inorganic compounds [34]

No.	Name	Formula	CAS Reg. No.	Mol. weight	Physical for m	mp, °C	bp, °C	Density, g cm ⁻³	Solubility, g/100 g H ₂ O	Qualitative solubility
1.	Actinium iodide	AcI ₃	33689-82-6	608	Wh cry					s H ₂ O
2.	Aluminum iodide	AlI ₃	7784-23-8	407.695	Wh leaflets	188.28	382	3.98		reac H ₂ O
3.	Aluminum iodide hexahydrate	AlI ₃ ·6H ₂ O	10090-53-6	515.786	Yel hyg cry powder					vs H ₂ O; s EtOH, eth
4.	Americium(III) iodide	AmI ₃	13813-47-3	624	Yel ortho cry	≈950		6.9		
5.	Antimony(III) iodide	SbI ₃	7790-44-5	502.473	Red rhomb cry	171	400	4.92		reac H ₂ O; s EtOH, ace; i ctc
6.	Arsenic diiodide	AsI ₂	13770-56-4	657.461	Red cry	137				reac H ₂ O; s os
7.	Arsenic(III) iodide	AsI ₃	7784-45-4	455.635	Red hex cry	141	424	4.73		sl H ₂ O, EtOH, eth; sbz. tol
8.	Barium iodide	BaI ₂	13718-50-8	391.136	Wh orth cry	711		5.15	221	
9.	Barium iodide dihydrate	BaI ₂ ·2H ₂ O	7787-33-9	427.167	Col cry	740 dec		5.0	221	s EtOH, ace
10.	Beryllium iodide	BeI ₂	7787-53-3	262.821	Hyg needles	480	590	4.32		reac H ₂ O; s EtOH
11.	Bismuth triiodide	BiI ₃	7787-64-6	589.693	Blk-brn hex cry	408.6	542	5.778	0.00078	s EtOH
12.	Boron triiodide	BI ₃	13517-10-7	391.524	Wh needles	49.7	209.5	3.35		i H ₂ O
13.	Cadmium iodide	CdI ₂	7790-80-9	366.220	Col hex flakes	388	744	5.64	86.2	vs H ₂ O; s EtOH, eth, ace
14.	Calcium iodide	CaI ₂	10102-68-8	293.887	Hyg hex cry	783	1100	3.96	215	s MeOH, EtOH, ace; i eth
15.	Calcium iodide hexahydrate	CaI ₂ ·6H ₂ O	71626-98-7	401.978	Wh hex needles or powder	42 dec		2.55	215	vs EtOH
16.	Cerium(II) iodide	CeI ₂	19139-47-0	393.925	Bronze cry	808				

(Continued)

TABLE 5.7 (Cont'd)

No.	Name	Formula	CAS Reg. No.	Mol. weight	Physical for m	mp, °C	bp, °C	Density, g cm ⁻³	Solubility, g/100 g H ₂ O	Qualitative solubility
17.	Cerium(III) iodide	CeI ₃	7790-87-6	520.829	Yel orth cry; hyg	760				s H ₂ O
18.	Cerium(III) iodide nonahydrate	CeI ₃ • 9H ₂ O	7790-87-6	682.967	Wh-red cry					vs H ₂ O; s EtOH
19.	Cesium iodide	CsI	7789-17-5	259.809	Col cub cry; hyg	632	≈1280	4.51	84.8	s EtOH, MeOH, ace
20.	Chromium(II) iodide	CrI ₂	13478-28-9	305.805	red-brn cry; hyg	867		5.1		s H ₂ O
21.	Chromium(III) iodide	CrI ₃	13569-75-0	432.709	dark gm hex cry	500 dec		5.32		sl H ₂ O
22.	Cobalt(II) iodide	CoI ₂	15238-00-3	312.742	blk hex cry; hyg	520		5.60	203	
23.	Cobalt(II) iodide dihydrate	CoI ₂ • 2H ₂ O	13455-29-3	348.773	hyg gm cry	100 dec				
24.	Cobalt(II) iodide hexahydrate	CoI ₂ • 6H ₂ O	15238-00-3	420.833	red hex prisms	130 dec		2.90	203	s EtOH, eth, ace
25.	Copper(I) iodide	CuI	7681-65-4	190.450	wh cub cry	591	≈1290	5.67	0.000020	i dil acid
26.	Dysprosium(II) iodide	DyI ₂	36377-94-3	416.309	purp cry	659				reac H ₂ O
27.	Dysprosium(III) iodide	DyI ₃	15474-63-2	543.213	gm cry	978				
28.	Erbium iodide	ErI ₃	13813-42-8	547.972	viol hex cry; hyg	1014		≈5.5		s H ₂ O
29.	Europium(II) iodide	EuI ₂	22015-35-6	405.773	gm cry	580				s H ₂ O
30.	Europium(III) iodide	EuI ₃	13759-90-5	532.677	col cry; unstab	≈875				

31.	Gadolinium(II) iodide	GdI ₂	13814-72-7	411.06	bronze cry	831			
32.	Gadolinium(III) iodide	GdI ₃	13572-98-0	537.96	yel cry	930			
33.	Gallium(III) iodide	GaI ₃	13450-91-4	450.436	monocl cry	212	340	4.5	reac H ₂ O
34.	Germanium(II) iodide	GeI ₂	13573-08-5	326.45	oran-yel hex cry	428	550	5.4	
35.	Germanium(IV) iodide	GeI ₄	13450-95-8	580.26	red-oran cub	146	348	4.322	reac H ₂ O
36.	Gold(I) iodide	AuI	10294-31-2	323.871	cry				i H ₂ O; s CN soln
37.	Gold(III) iodide	AuI ₃	31032-13-0	577.680	yel-gm powder; tetr unstab gm powder	120 dec		8.25	
38.	Hafnium(III) iodide	HfI ₃	13779-73-2	559.20	blk cry dec	20 dec			
39.	Hafnium(IV) iodide	HfI ₄	13777-23-6	686.11	yel-oran cub	449 tp	394 sp	5.6	reac H ₂ O
40.	Holmium iodide	HoI ₃	13813-41-7	545.643	yel hex cry	994		5.4	
41.	Hydrogen iodide	HI	10034-85-2	127.912	col or yel gas	-50.76	-35.55	5.228	vs H ₂ O; s os
42.	Indium(I) iodide	InI	13966-94-4	241.722	orth cry	364.4	712	5.32	
43.	Indium(III) iodide	InI ₃	13510-35-5	495.531	yel-red monocle	207		4.69	1308
44.	Iridium(III) iodide	IrI ₃	7790-41-2	572.930	cry; hyg dark bm			≈7.4	i H ₂ O, acid, bz, chl; s alk
45.	Iron(II) iodide	FeI ₂	7783-86-0	309.654	monocle cry red-viol hex cry; hyg	594		5.3	s H ₂ O, EtOH, eth

(Continued)

TABLE 5.7 (Cont'd)

No.	Name	Formula	CAS Reg. No.	Mol. weight	Physical for m	mp, °C	bp, °C	Density, g cm ⁻³	Solubility, g/100 g H ₂ O	Qualitative solubility
46.	Iron(II) iodide tetrahydrate	FeI ₂ ·4H ₂ O	7783-86-0	381.716	blk hyg leaflets	90 dec		2.87		s H ₂ O, EtOH
47.	Lanthanum iodide	LaI ₃	13813-22-4	519.619	wh orth cry; hyg	778		5.6		s H ₂ O
48.	Lead(II) iodide	PbI ₂	10101-63-0	461.0	yel hex cry or powder	410	872 dec	6.16	0.076	i EtOH
49.	Lithium iodide	LiI	10377-51-2	133.845	wh cub cry; hyg	469	1171	4.06	165	
50.	Lithium iodide trihydrate	LiI·3H ₂ O	7790-22-9	187.891	wh hyg cry	73		2.38	165	vs EtOH, ace
51.	Lutetium iodide	LuI ₃	13813-45-1	555.680	brn hex cry; hyg	1050		≈5.6		vs H ₂ O
52.	Magnesium iodide	MgI ₂	10377-58-9	278.114	wh hex cry; hyg	634		4.43	146	
53.	Magnesium iodide hexahydrate	MgI ₂ ·6H ₂ O	66778-21-0	386.205	wh monocl cry			2.35		
54.	Magnesium iodide octahydrate	MgI ₂ ·8H ₂ O	7790-31-0	422.236	wh orth cry; hyg	41 dec		2.10	146	s EtOH
55.	Manganese(II) iodide	MnI ₂	7790-33-2	308.747	wh hex cry; hyg	638		5.04		s H ₂ O, EtOH
56.	Manganese(II) iodide tetrahydrate	MnI ₂ ·4H ₂ O	7790-33-2	380.809	red cry					vs H ₂ O; s EtOH
57.	Mercury(I) iodide	Hg ₂ I ₂	15385-57-6	654.99	yel amorp powder	290		7.70		i H ₂ O, EtOH, eth
58.	Mercury(II) iodide (yellow)	HgI ₂	7774-29-0	454.40	yel tetr cry or powder	256	351	6.28	0.0055	sl EtOH, ace, eth

59.	Mercury(II) iodide (red)	HgI ₂	7774-29-0	454.40	red pow	trans to yel 127	0.006 ²⁵	sl EtOH, ace, eth, chl
60.	Molybdenum(II) iodide	MoI ₂	14055-74-4	349.75	blk hyg cry	700	5.28	i H ₂ O
61.	Molybdenum(III) iodide	MoI ₃	14055-75-5	476.65	blk solid	927		i H ₂ O
62.	Molybdenum(IV) iodide	MoI ₄	14055-76-6	603.56	blk cry	100dec		i H ₂ O
63.	Neodymium(III) iodide	NdI ₃	13813-24-6	524.955	grn orth cry; hyg	787	5.85	s H ₂ O
64.	Nickel(II) iodide	NiI ₂	13462-90-3	312.502	blk hex cry; hyg	800	5.22	154
65.	Nickel(II) iodide hexahydrate	NiI ₂ ·6H ₂ O	7790-34-3	420.593	grm monocl cry; hyg	510 dec		154 vs EtOH
66.	Niobium(III) iodide	NbI ₃	13870-20-7	473.619	blk solid			
67.	Niobium(IV) iodide	NbI ₄	13870-21-8	600.524	gray orth cry	503	5.6	reac H ₂ O
68.	Niobium(V) iodide	NbI ₅	13779-92-5	727.428	yel-blk monocl cry	327	5.32	reac H ₂ O
69.	Nitrogen triiodide	NI ₃	13444-85-4	394.720	unstab blk cry; exp			
70.	Palladium(II) iodide	PdI ₂	7790-38-7	360.23	blk cry	360 dec	6.0	i H ₂ O, EtOH, eth
71.	Diphosphorus tetraiodide	P ₂ I ₄	13455-00-0	569.566	red tricl needles	125.5	dec	3.89
72.	Phosphorus(III) iodide	PI ₃	13455-01-1	411.687	red-oran hex cry; hyg	61.2	227	4.18 reac H ₂ O; s EtOH
73.	Platinum(II) iodide	PtI ₂	7790-39-8	448.893	blk powder	325 dec	6.4	i H ₂ O

(Continued)

TABLE 5.7 (Cont'd)

No.	Name	Formula	CAS Reg. No.	Mol. weight	Physical for m	mp, °C	bp, °C	Density, g cm ⁻³	Solubility, g/100 g H ₂ O	Qualitative solubility
74.	Platinum(IV) iodide	PtI ₄	7790-46-7	702.702	brn-blk powder	130 dec				s H ₂ O
75.	Plutonium(III) iodide	PuI ₃	13813-46-2	625	grn orth cry; hyg	777		6.92		s H ₂ O
76.	Potassium iodide	KI	7681-11-0	166.003	col cub cry	681	1323	3.12	148	sl EtOH
77.	Praseodymium(II) iodide	PrI ₂	65530-47-4	394.717	bronze solid	758				
78.	Praseodymium(III) iodide	PrI ₃	13813-23-5	521.621	orth hyg cry	738		≈5.8		s H ₂ O
79.	Promethium(III) iodide	PmI ₃	13818-73-0	526	red solid	695				
80.	Rhenium(III) iodide	ReI ₃	15622-42-1	566.920	blk solid	dec				
81.	Rhodium(III) iodide	RhI ₃	15492-38-3	483.619	blk monoel cry; hyg			6.4		
82.	Rubidium iodide	RbI	7790-29-6	212.372	wh cub cry	656	1300	3.55	165	s EtOH
83.	Ruthenium(III) iodide	RuI ₃	13896-65-6	481.78	blk hex cry	300dec		6.0		sl H ₂ O
84.	Samarium(II) iodide	SmI ₂	32248-43-4	404.17	grn cry	520				reac H ₂ O
85.	Samarium(III) iodide	SmI ₃	13813-25-7	531.07	oran cry	850				reac H ₂ O
86.	Scandium iodide	ScI	14474-33-0	425.669	hyg yel cry	953	subl			s H ₂ O, EtOH, CCD
87.	Silver(I) iodide	AgI	7783-96-2	234.772	yel powder; hex	558	1506	5.68	0.000003	i acid
88.	Sodium iodide	NaI	7681-82-5	149.894	wh cub cry; hyg	661	1304	3.67	184	s EtOH, ace

89.	Sodium iodide dihydrate	NaI 2H ₂ O	13517-06-1	185.925	hyg col monocle cry	69 dec	2.45	318	vs H ₂ O
90.	Strontium iodide	SrI ₂	10476-86-5	341.43	wh hyg cry	538	1773 dec	177	
91.	Strontium iodide hexahydrate	SrI ₂ 6H ₂ O	73796-25-5	449.52	wh-yel hex cry; hyg	120 dec	4.4	177	s EtOH
92.	Tantalum(IV) iodide	TaI ₄	14693-80-2	688.566	gray-blk solid	400 dec			reac H ₂ O
93.	Tantalum(V) iodide	TaI ₅	14693-81-3	815.470	blk hex cry; hyg	496	543	5.80	reac H ₂ O
94.	Tellurium tetraiodide	TeI ₄	7790-48-9	635.22	blk orth cry	280		5.05	reac H ₂ O; sl ace
95.	Terbium(III) iodide	TbI ₃	13813-40-6	539.638	hex cry; hyg	955		≈5.2	s H ₂ O
96.	Thallium(I) iodide	TlI	7790-30-9	331.287	yel cry powder	441.7	824	7.1	i EtOH
97.	Thorium(IV) iodide	ThI ₄	7790-49-0	739.656	wh-yel monocl cry	566	837		
98.	Thulium(II) iodide	TmI ₂	60864-26-8	422.743	blk hyg solid	756			reac H ₂ O
99.	Thulium(III) iodide	TmI ₃	13813-43-9	549.647	yel hyg cry	1021			
100.	Tin(II) iodide	SnI ₂	10294-70-9	372.519	red-oran powder	320	714	5.28	s bz, chl, CS ₂
101.	Tin(IV) iodide	SnI ₄	7790-47-8	626.328	yel-brn cub cry	143	364.35	4.46	reac H ₂ O; s EtOH, bz, chl, eth reac H ₂ O
102.	Titanium(II) iodide	TiI ₂	13783-07-8	301.676	blk hex cry	400dec		5.02	
103.	Titanium(III) iodide	TiI ₃	13783-08-9	428.580	viol cry	350dec			
104.	Titanium(IV) iodide	TiI ₄	7720-83-4	555.485	red hyg powder	155	377	4.3	reac H ₂ O
105.	Tungsten(II) iodide	WI ₂	13470-17-2	437.65	oran-brn cry	800dec		6.79	i H ₂ O
106.	Tungsten(III) iodide	WI ₃	15513-69-6	564.55	blk solid	dec r.t.			i H ₂ O; s ace; sl EtOH, chl

(Continued)

TABLE 5.7 (Cont'd)

No.	Name	Formula	CAS Reg. No.	Mol. weight	Physical for m	mp, °C	bp, °C	Density, g cm ⁻³	Solubility, g/100 g H ₂ O	Qualitative solubility
107.	Tungsten(IV) iodide	WI ₄	14055-84-6	691.46	blk cry	dec				reac H ₂ O; s EtOH; I eth chl
108.	Uranium(III) iodide	UI ₃	13775-18-3	618.742	blk hyg cry	766				s H ₂ O
109.	Uranium(IV) iodide	UI ₄	13470-22-9	745.647	blk hyg cry	506				s H ₂ O, EtOH
110.	Vanadium(II) iodide	VI ₂	15513-84-5	304.751	red-viol hex cry		subl 800	5.44		reac H ₂ O
111.	Vanadium(III) iodide	VI ₃	15513-94-7	431.655	brn-blk rhomb cry; hyg	300dec		5.21		reac H ₂ O
112.	Ytterbium(II) iodide	YbI ₂	19357-86-9	426.85	blk cry	772				reac H ₂ O
113.	Ytterbium(III) iodide	YbI ₃	13813-44-0	553.75	yel cry dec	700				s H ₂ O
114.	Yttrium iodide	YI ₃	13470-38-7	469.619	hyg wh-yel cry	997				s H ₂ O, ace, EtOH
115.	Zinc iodide	ZnI ₂	10139-47-6	319.218	wh-yel hyg cry	450	625	4.74	438	vs H ₂ O; s EtOH, eth
116.	Zirconium(II) iodide	ZrI ₂	15513-85-6	345.033	blk cry	827				
117.	Zirconium(III) iodide	ZrI ₃	13779-87-8	471.937	dark blue cry	727				
118.	Zirconium(IV) iodide	ZrI ₄	13986-26-0	598.842	yel-oran cub cry	500	431 sp	4.85		vs H ₂ O

Name: Systematic name for the substance. The valence state of a metallic element is indicated by a roman numeral, for example, copper in the +I state is written as copper(I) rather than cuprous, iron in the +3 state is iron(III) rather than ferric.

Formula: The simplest descriptive formula is given, but this does not necessarily specify the actual structure of the compound. For example, Gallium(III) iodide is the chemical compound with the formula Ga₂I₆. It reversibly forms GaI₃.

CAS Registry Number: Chemical Abstracts Service Registry Number. An asterisk* following the CAS RN for a hydrate indicates that the number refers to the anhydrous compound. In most cases the generic CAS RN for the compound is given rather than the number for a specific crystalline form or mineral.

Mol. Weight: Molecular weight (relative molar mass) as calculated with the 2005 IUPAC Recommended Atomic Weights.

Physical Form: The crystal system is given, when available, for compounds that are solid at room temperature, together with color and other descriptive features. Abbreviations are listed here:

mp: Normal melting point in degree centigrade. The notation tp indicates the temperature where solid, liquid, and gas are in equilibrium at a pressure greater than 1 atm (i.e., the normal melting point does not exist). When available, the triple point pressure is listed.

bp: Normal boiling point in degree centigrade (referred to 101.325kPa or 760mmHg pressure). The notation sp following the number indicates the temperature where the pressure of the vapor in equilibrium with the solid reaches 101.325kPa. See Reference 8, p. 23, for further discussion on sublimation points and triple points. A notation "sublimes" without a temperature being given indicates that there is a perceptible sublimation pressure above the solid at ambient temperatures.

Density: Density values for solids and liquids are always in units of grams per cubic centimeter and can be assumed to refer to temperatures near room temperature unless otherwise stated. Values for gases are the calculated ideal gas densities in grams per liter at 25°C and 101.325kPa; the unit is always specified for a gas value.

Aqueous Solubility: Solubility is expressed as the number of grams of the compound (excluding any water of hydration) that will dissolve in 100 g of water. The temperature in degree centigrade is given as a superscript. Solubility at other temperatures can be found for many compounds in the table.

Qualitative Solubility: Qualitative information on the solubility in other solvents (and in water, if quantitative data are unavailable) is given here. The abbreviations are as follows: I, insoluble; sl, slightly soluble; s, soluble; vs, very soluble; reac, reacts with the solvent.

Data were taken from a wide variety of reliable sources, including monographs, treatises, review articles, evaluated compilations and databases, and in many cases the primary literature. Some of the most useful references for the properties covered here are listed here:

ace, acetone; acid, acid solutions; alk, alkaline solutions; amorp, amorphous; blk, black; brn, brown; bz, benzene; chl, chloroform; col, colorless; cry, crystals, crystalline; cub, cubic; dec, decomposes; dil, dilute; eth, ethyl ether; EtOH, ethanol; exp, explosives; grn, green; hex, hexagonal, hexane; hyg, hygroscopic; i, insoluble in; MeOH, methanol; monoclinic, oran, orange; orth, orthorhombic; os, organic solvents; pow, powder; pur, purple; reac, reacts with; refrac, refractory; rhom, rhombohedral; r.t., room temperature; s, soluble in; sl, slightly soluble in; soln, solution; sp, sublimation point; subl, sublimes; tetr, tetragonal; tol, toluene; tp, triple point; trans, transition, transformation; tricl, triclinic; unstab, unstable; viol, violet; vs, very soluble in; wh, white; yel, yellow.

REFERENCES

- [1] Greenwood NN, Earnshaw A. *Chemistry of the Elements*. 2nd ed. Oxford: Butterworth-Heinemann; 1997.
- [2] Lyday PA. *Iodine and Iodine Compounds, Ullmann's Encyclopedia of Industrial Chemistry*. Weinheim: Wiley-VCH; 2005.
- [3] Saxena PB. *Chemistry of Interhalogen Compounds*. New Delhi: Discovery Publishing House; 2007.
- [4] Brothers PJ. Subvalent compounds. *Encyclop Inorg Chem* 2006.
- [5] Patnaik P. *Handbook of Inorganic Chemicals*. New York: McGraw-Hill Ed; 2002. p 370.
- [6] Greenwood NN, Earnshaw A. *The Chemistry of the Elements*. 2nd ed. Oxford: Butterworth-Heinemann; 1997. p 809–815.
- [7] Mellor JW. *Mellors Comprehensive Treatise on Inorganic and Theoretical Chemistry, Supplement 2, Part I*. London: Longmans Co., Ltd.; 1960. p 170.
- [8] Booth HS. Hydriodic acid by catalytic union of the elements. *Inorg Synth* 1939;1:159.
- [9] Omura M, Sasaki K, Tanaka Y, Tomoshige N, Utsunomiya A. Production process for refined hydrogen iodide. US Patent 5,693,306. Nov. 15, 1995. Mitsui Toatsu Chem. Inc., Tokyo.
- [10] O'Neil MJ, ed. *The Merck Index: An Encyclopedia of Chemicals, Drugs, and Biologicals*, 14th ed. New Jersey: Merck, 2006, 4776.
- [11] King FE, Partington JR. The solubility of sodium iodide in ethyl alcohol. *J Chem Soc* 1926;129:20–22.
- [12] (a) Richards TW, Jones G. The compressibilities of the chlorides, bromides, and iodides of sodium, potassium, silver and thallium. *J Am Chem Soc* 1909;31:158–191, (b) Richards TW, Jones G. *Z Physik Chem* 1910;71:157.
- [13] Patnaik P. *Handbook of Inorganic Chemicals*. New York: McGraw-Hill Ed; 2002. p 761.
- [14] Vanino L. *Handbuch der Preparativen Chemie* Bd. II, S. 376.
- [15] Lingane JJ, Kolthoff IM. Potassium iodide for use as a primary standard. *Inorg Synth* 1939;1:163.
- [16] Kaufman PG, Pinnell RP. Copper(I) iodide. *Inorg Syn* 1960;6:3.
- [17] Brauer G. *Handbook of Preparative Inorganic Chemistry*. 2 ed. Volume 2, New York: Academic Press; 1965. p 1007.
- [18] Patnaik P. *Handbook of Inorganic Chemicals*. New York: McGraw-Hill Ed; 2002. p 268.
- [19] Kolkmeijer NH, van Hengel JWA. Cubic and hexagonal silver iodide. *Z Kristallogr* 1934;88:317–322.
- [20] Patnaik P. *Handbook of Inorganic Chemicals*. New York: McGraw-Hill Ed; 2002. p 841.
- [21] Brauer G. *Handbuch, Paep Anorganic Chemistry*. 3rd ed. Volume 1, Stuttgart: Ferdinand Enke Verlag; 1936. p 480.
- [22] Torniepoorth-Oetting I, Klapötke T. Nitrogen triiodide. *Angew Chem* 1990;29(6):677–679.
- [23] Lamb AB, Bray WC, Walter J, Geldard WJ. The preparation of iodic acid and its anhydride. *J Am Chem Soc* 1920;42:1644.
- [24] Patnaik P. *Handbook of Inorganic Chemicals*. New York: McGraw-Hill; 2002. p 407.
- [25] Svensson PH, Kloos L. Synthesis, structure, and bonding in polyiodide and metal iodide-iodine systems. *Chem Rev* 2003;103:1649–1684.

- [26] Kloo L. Catenated compounds—group 17—polyhalides. In: Reedijk J, Poeppelmeier K, editors. *Comprehensive Inorganic Chemistry II*. Volume 1, Oxford: Elsevier; 2013. p 233–249.
- [27] Patnaik P. *Handbook of Inorganic Chemicals*. New York: McGraw-Hill Ed; 2002. p 403.
- [28] Cornog J, Karges RA, Test LA. Iodine Monochloride. *Iodine Monochloride*. 2007;1: 165–167.
- [29] Buckles RE, Bader JM. Iodine(I) chloride. *Inorg Syn* 1967;9:130.
- [30] Gore G. *Philos Mag* 1871;41 (4):309.
- [31] Moissan MH. Nouvelles Recherches sur le Fluor. *Ann Chim Phys* 1891;6 (24): 224–282.
- [32] Ruff O, Keim R. Z. The fluorination of carbon compounds (benzene and tetrachloromethane with iodine pentafluoride and tetrachloromethane with fluorine). *Anorg Allgem Chem* 1931;201 (1):245–258.
- [33] Patnaik P. *Handbook of Inorganic Chemicals*. New York: McGraw-Hill Ed; 2002. p 405.
- [34] Lide DR. *Handbook of Chemistry and Physics*. 88th ed, Boca Raton: CRC Press; 2007.

6

ORGANIC IODIDES

TSUGIO KITAMURA

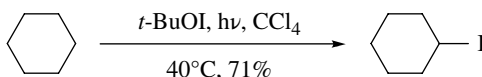
Department of Chemistry and Applied Chemistry, Graduate School of Science and Engineering, Saga University, Saga, Japan

6.1 INTRODUCTION

Generally organic iodides can be divided into two classes of alkyl iodides and aryl iodides. These iodides are applied for synthesis of various types of organic compounds. Since alkyl halides react mainly by heterolytic cleavage of the carbon–halogen bond, alkyl iodides bearing the polar C–I bond show the highest reactivity among them. Typical reactions of alkyl iodides include nucleophilic substitution, elimination, reduction, and the formation of organometallics. On the other hand, aryl halides are compounds containing halogen attached directly to an aromatic ring. Aryl halides do not undergo direct displacement by nucleophiles observed in the case of alkyl halides, that is, S_N2 -type reactions, because of their low reactivity toward nucleophilic substitution. Accordingly, aryl iodides undergo nucleophilic substitution only when substrates are activated or benzyne intermediates are involved. Therefore, aryl iodides undergo nucleophilic substitutions, iodine–metal exchange for organometallic compounds, and coupling reactions. Since the organic iodides are widely used in organic synthesis, this chapter deals with typical reactions for synthesis of alkyl and aryl iodides.

6.2 IODINATION OF ALIPHATIC HYDROCARBONS

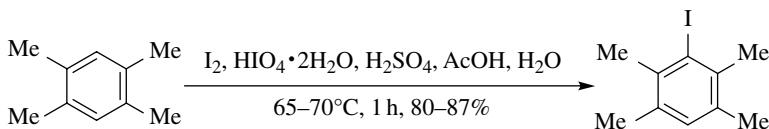
Generally, halogenation is an important method for functionalization of hydrocarbons. The process proceeds with a radical chain mechanism, which is initiated by a radical initiator or photolysis. The hydrogen atom abstraction step is rate-limiting. However, it is difficult for the iodination of hydrocarbons to occur directly because the abstraction of hydrogen from hydrocarbons by iodine is endothermic. Accordingly, the scope for iodination is narrow. The representative iodination is photoreaction of hydrocarbons with *t*-BuOI (Scheme 6.1) [1], ICl_3 [2], or lead tetraacetate and iodine [3].



SCHEME 6.1

6.3 IODINATION OF AROMATIC HYDROCARBONS

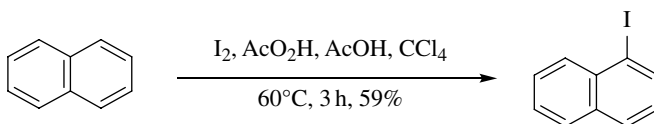
Halogenation of aromatic hydrocarbons is a very important reaction via an electrophilic aromatic substitution. The reactivity of the halogens increases in the order $\text{I}_2 < \text{Br}_2 < \text{Cl}_2$. Molecular iodine is not a very powerful halogenating agent and only reactive aromatics such as anilines or phenolate anions are reactive toward iodine. Other aromatics are iodinated with iodine together with an activator such as oxidants. General iodinating agents for aromatic hydrocarbons are iodine–periodic acid (Scheme 6.2) [4], benzyltrimethylammonium dichloriodate (BTMA ICl_2)– ZnCl_2 [5], iodine–ceric ammonium nitrate (CAN) (Scheme 6.3) [6], iodine–peracetic acid (Scheme 6.4) [7], iodine monochloride– ZnCl_2 (Scheme 6.5) [8], and iodine– CuCl_2 (Scheme 6.6) [9]. Iodine–periodic acid is suitable for iodination of polyalkylbenzenes, fused aromatics, or moderately activated heteroaromatics.



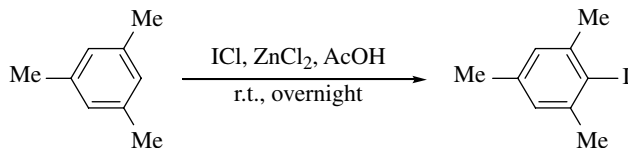
SCHEME 6.2



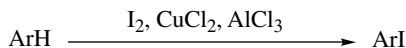
SCHEME 6.3



SCHEME 6.4

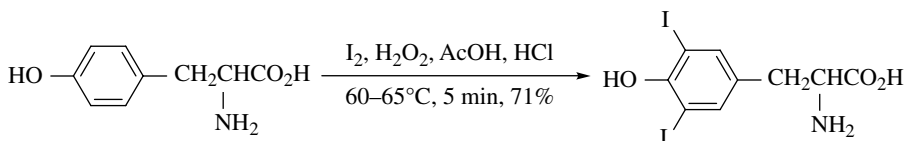


SCHEME 6.5



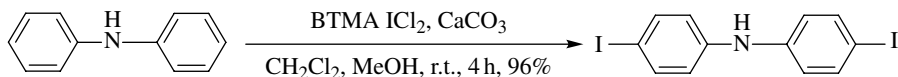
SCHEME 6.6

Iodine-fuming sulfuric acid is used for iodination of aromatics bearing deactivating groups such as carboxy and nitro groups [10–12]. Iodination of phenols is conducted by iodine–potassium iodide [13], the iodine–morpholine complex [14], iodine–hydrogen peroxide (Scheme 6.7) [15], and BTMA ICl_2 [16]. For iodination of less reactive nitrophenols and hydroxybenzoic acids, BTMA ICl_2 [16] and iodine monochloride [17, 18] are used.



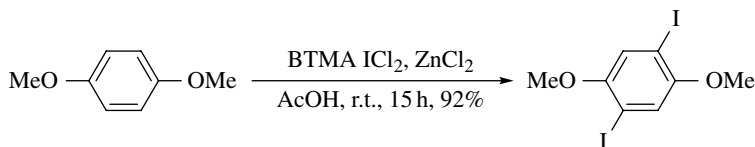
SCHEME 6.7

Aromatic amines are efficiently iodinated by BTMA ICl_2 –calcium carbonate (Scheme 6.8) [19]. Aniline reacts with iodine in the presence of sodium hydrogen carbonate to give 4-iodoaniline in high yield [20]. Aminobenzoic acids [21] and nitroanilines [22] are iodinated by iodine monochloride. Acetoanilides are iodinated by BTMA ICl_2 [23] or iodine monochloride [24].



SCHEME 6.8

Effective iodination of aromatic ethers is performed by BTMA ICl_2 – ZnCl_2 (Scheme 6.9) [25], tetrabutylammonium iodide–CAN [6], or iodine–silver trifluoroacetate [26].



SCHEME 6.9

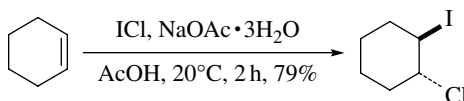
Recently, it was reported that iodination of aromatic hydrocarbons is promoted by a hypervalent iodine reagent. The iodination was conducted using the following reagents: iodine—[bis(trifluoroacetoxy)iodo]benzene and iodine—(diacetoxyiodo)benzene [27]. Similarly, other [bis(acyloxy)iodo]arenes are employed for iodination of aromatics [28]. In addition, heteroaromatic compounds are effectively iodinated by iodine—[bis(trifluoroacetoxy)iodo]benzene [29, 30]. Bis(pyridine)iodine(I) tetrafluoroborate $[I(py)_2BF_4]$ [31] or bis(2,4,6-trimethylpyridine)iodine(I) hexafluorophosphate $[I(2,4,6-Me_3py)_2PF_6]$ [32] is a powerful reagent for iodination of aromatics.

6.4 IODINATION OF ALKENES

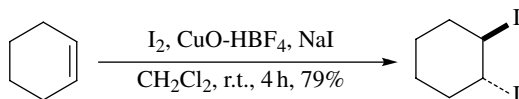
6.4.1 Addition of Iodine or Iodine–Interhalogen Compounds

Most alkenes are easily halogenated with bromine, chlorine, or interhalogen compounds. Iodination has also been accomplished, but the reaction is slower. Since *vic*-diiodoalkanes are generally unstable and tend to revert to iodine and the alkene, direct iodination has not been utilized frequently [33, 34].

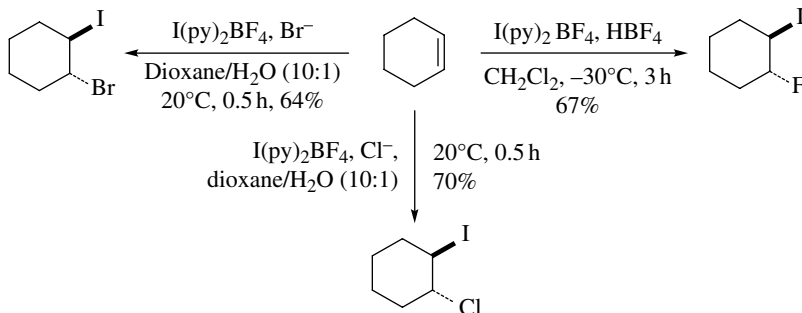
Iodine monochloride and iodine monobromide are more reactive than iodine and readily react with alkenes to give the corresponding *vic*-chloroiodo- or bromoiodoalkanes (Scheme 6.10) [35–37]. The same products are also obtained by reaction with CuX_2 –iodine (Scheme 6.11) [38]. Iodine monofluoride is more reactive than iodine monochloride and undergoes regio- and stereoselective addition to alkenes to give *vic*-fluoroiodoalkanes [39]. Similarly, *vic*-haloiodoalkanes can be prepared by using $I(py)_2BF_4-BF_4^-$, $I(py)_2BF_4-Cl^-$, or $I(py)_2BF_4-Br^-$ (Scheme 6.12) [31].



SCHEME 6.10

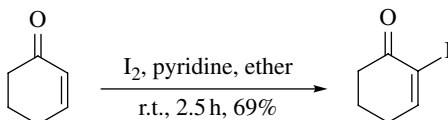


SCHEME 6.11



SCHEME 6.12

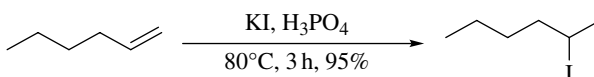
Iodination of cyclic enones is furnished by iodine–pyridine to give α -iodoalkenes (Scheme 6.13) [40]. This reaction proceeds with nucleophilic addition of pyridine followed by trapping the resulting enolate with iodine and the subsequent elimination of pyridine.



SCHEME 6.13

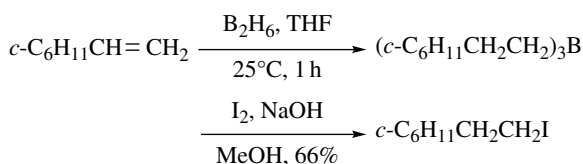
6.4.2 Addition of Hydrogen Iodide

In the addition of hydrogen halides to alkenes, it is generally found that the halogen atom becomes attached to the more substituted carbon atom (Markovnikov's rule). The order of reactivity of the hydrogen halides is $\text{HI} > \text{HBr} > \text{HCl}$. The addition of hydrogen iodide to alkenes gives iodoalkanes [41]. In the addition of hydrogen iodide, the reaction with KI–phosphoric acid on heating gives a better result than the direct reaction with hydrogen iodide (Scheme 6.14) [42].



SCHEME 6.14

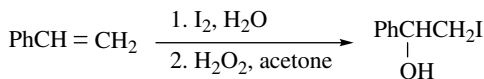
Synthesis of the *anti*-Markovnikov addition product with HI is accomplished by hydroboration of alkenes followed by reaction with iodine–sodium hydroxide (Scheme 6.15) [43], iodine–sodium methoxide [44], iodine monochloride–sodium acetate [45], and or sodium iodide–chloramine T [46]. Hydroalumination of alkenes followed by iodination also affords the *anti*-Markovnikov type of iodoalkanes [47].



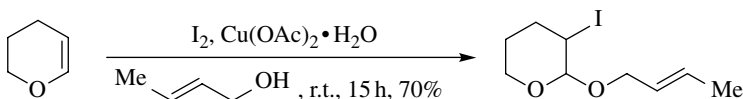
SCHEME 6.15

6.4.3 Addition of Hypoiodous Acid or the Related Compounds

Hypoiodous acid (HOI) generated from periodic acid–sodium hydrogen sulfite [48], iodine–iodic acid [49], and iodine–hydrogen peroxide (Scheme 6.16) [50] add alkenes to give iodohydrins. The same addition reaction also occurs with $\text{I}(\text{py})_2\text{BF}_4\text{-H}_2\text{O}$ [31]. In the presence of alcohols, alkenes are converted to *vic*-alkoxyiodoalkanes by the reaction with iodine– $\text{Cu}(\text{OAc})_2$ (Scheme 6.17) [51], BTMA ICl_2 [52],

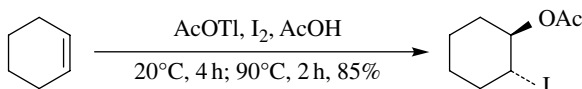


SCHEME 6.16



SCHEME 6.17

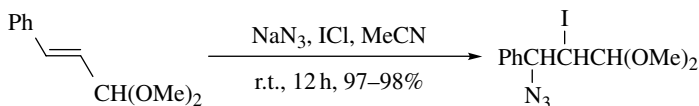
N-iodosuccinimide (NIS) [53], $\text{I}(\text{py})_2\text{BF}_4$ [31], or iodine monochloride [54]. Acetyl hypoiodite (AcOI) in situ generated from iodine–thallium(I) acetate undergoes *trans* addition toward alkenes to afford *vic*-acetyliodoalkanes (Scheme 6.18) [55]. Similarly, iodohydrin esters are obtained by reaction of alkenes with iodine–silver carboxylates [56], or with NIS [57] or $\text{I}(\text{py})_2\text{BF}_4$ [31] in the presence of carboxylic acid.



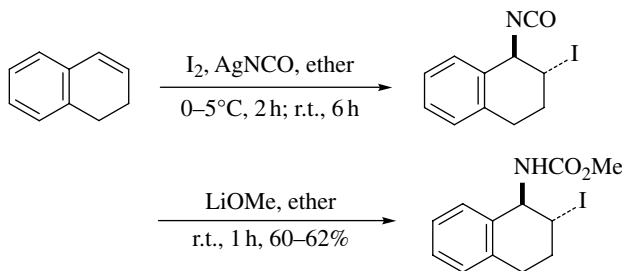
SCHEME 6.18

6.4.4 Addition of Other Iodine Compounds

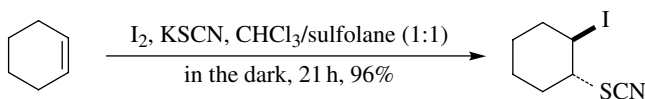
Iodine azide in situ prepared from iodine monochloride and sodium azide (Scheme 6.19) [58, 59], iodine isocyanate generated from iodine and silver isocyanate (Scheme 6.20) [60], and iodine thiocyanate generated from iodine–potassium thiocyanate or iodine–thiocyanogen (Scheme 6.21) [61, 62] undergo stereospecific *trans* addition to alkenes to give *vic*-azidoiodoalkanes, β -iodoisocyanates, and β -iodothiocyanates, respectively. Reaction of alkenes with dinitrogen tetroxide in the presence of iodine affords *vic*-nitroiodoalkenes by addition of in situ generated iodine nitrite (Scheme 6.22) [63]. On the other hand, iodoalkyl nitrates are obtained by addition of iodine nitrate generated by iodine–dinitrogen tetroxide or by adding iodine–silver nitrate [64]. Treatment of alkenes with $\text{I}(\text{py})_2\text{BF}_4$ in the presence of acetonitrile or aromatic compounds gives β -acetylamino- or aryl-substituted iodoalkanes, respectively (Scheme 6.23) [31].



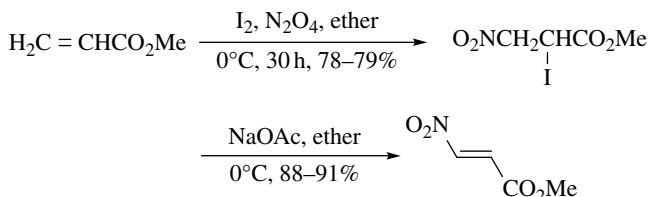
SCHEME 6.19



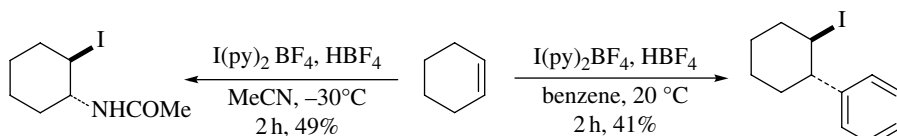
SCHEME 6.20



SCHEME 6.21



SCHEME 6.22

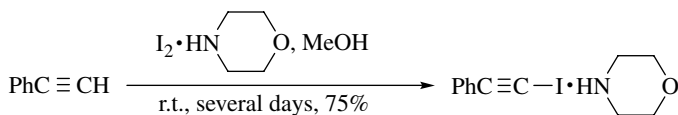


SCHEME 6.23

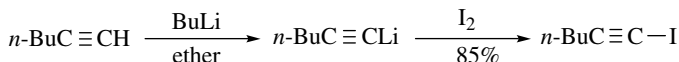
6.5 IODINATION OF ALKYNES

6.5.1 Iodination of Terminal Alkynes

Iodination of 1-alkynes gives 1-iodoalkynes in which the terminal hydrogen is replaced by iodine. The iodination of 1-alkynes is furnished by direct reaction with iodine–liquid ammonia [65] and the iodine–morpholine complex (Scheme 6.24) [66], or by reaction of lithium acetylides with iodine (Scheme 6.25) [67] and heptafluoro-1-iodopropane [68].



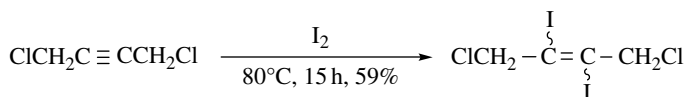
SCHEME 6.24



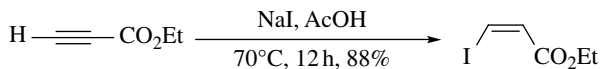
SCHEME 6.25

6.5.2 Addition of Iodine to Alkynes

Addition of iodine to alkynes occurs easily compared with alkenes. However, 1,2-diiodoalkenes thus formed readily undergo *cis-trans* isomerization in the presence of a small amount of iodine (Scheme 6.26) [69]. In the case of alkynes bearing an electron-withdrawing group such as ester, iodoalkenes are obtained by nucleophilic addition of sodium iodide (Scheme 6.27) [70]. Addition of hydrogen iodide to alkynes proceeds according to the Markovnikov rule but is not influenced by the presence of peroxides [71]. Addition of iodine monochloride to alkynes takes place regio- and stereoselectively to give (*E*)-*vic*-chloriodoalkenes [72].

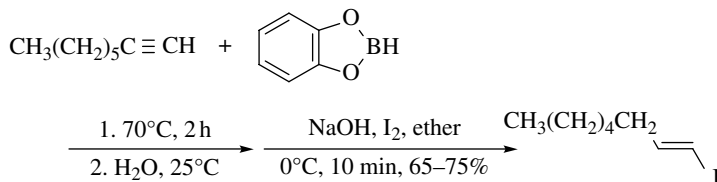


SCHEME 6.26



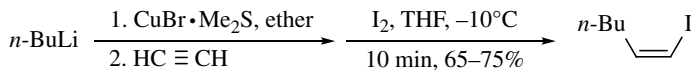
SCHEME 6.27

Hydroboration of terminal alkynes with catecholborane (Scheme 6.28) [73] or the dibromoborane–dimethyl sulfide complex [74] followed by hydrolysis gives (*E*)-1-vinylboronic acids stereospecifically, which are converted to (*E*)-iodoalkenes by iodinolysis with iodine in the presence of NaOH. Hydroalumination of terminal alkynes followed by iodination are also useful for synthesis of (*E*)-iodoalkenes [75].



SCHEME 6.28

On the other hand, (*Z*)-1-iodoalkenes can be prepared by hydroboration of 1-iodoalkynes with dicyclohexylborane and then protonolysis with acetic acid [76], or by iodination of (*Z*)-alkenylcuprates generated by treatment of alkynes with lithium dialkylcuprates (Scheme 6.29) [77].

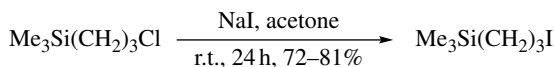


SCHEME 6.29

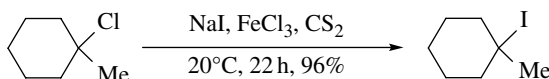
6.6 HALOGEN-IODINE EXCHANGE OF HALO COMPOUNDS

6.6.1 Substitution of Alkyl Halides by Iodine

Preparation of alkyl iodides from alkyl halides is conducted by treating alkyl chlorides or bromides with NaI or KI in organic solvents such as acetone, 2-butanone, *N,N*-dimethylformamide (DMF), and hexamethylphosphoramide (HMPA) (Scheme 6.30). This method is easy to operate and has a wide scope of the reaction [78–82]. Tertiary alkyl iodides are prepared by treating tertiary alkyl chlorides with NaI in the presence of FeCl_3 or ZnCl_2 as catalyst (Scheme 6.31) [83]. Alkyl fluorides or chlorides can be converted to alkyl iodides by using iodotrimethylsilane [84].



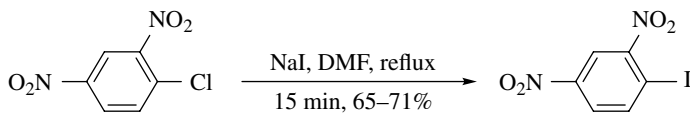
SCHEME 6.30



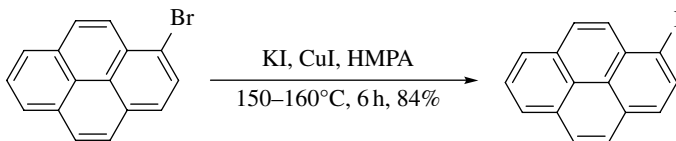
SCHEME 6.31

6.6.2 Substitution of Aryl Halides by Iodine

Aryl chlorides and bromides are activated by electron-withdrawing groups such as the nitro group and are converted to the corresponding iodides by substitution with sodium iodides (Scheme 6.32) [85, 86]. Preparation of aryl iodides from aryl bromides without activated groups is conducted by potassium iodide–copper(I) iodide (Scheme 6.33) [87] or potassium iodide–nickel catalysts [88].



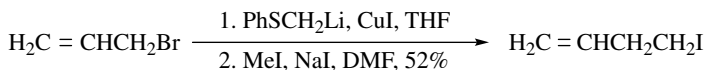
SCHEME 6.32



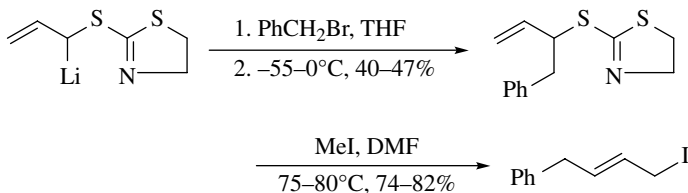
SCHEME 6.33

6.6.3 Iodomethylation of Alkyl Halides

Iodomethylation of primary alkyl halides (Scheme 6.34) [89, 90] and *trans* iodopropylation of primary and secondary alkyl halides are developed (Scheme 6.35) [90]. Similarly, iodomethylation of tellurium derivatives is also reported [91].

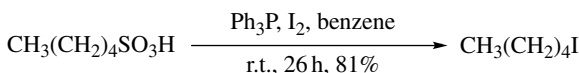


SCHEME 6.34

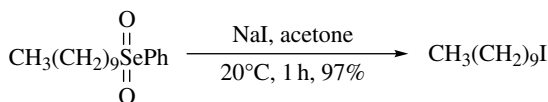


SCHEME 6.35

Sulfur functionality including alkylsulfonic acids, sulfinic acids, thiols, sulfonates, disulfides can be replaced by iodine quantitatively using triphenylphosphine–iodine (Scheme 6.36) [92]. Organoselenium dioxides easily react with sodium iodide to give the corresponding alkyl iodides (Scheme 6.37) [93].



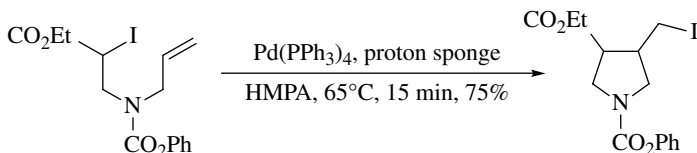
SCHEME 6.36



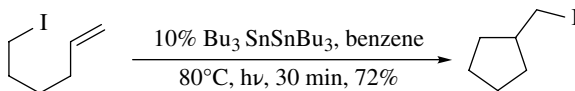
SCHEME 6.37

6.6.4 Cyclization–Rearrangement of Organoiodine Compounds

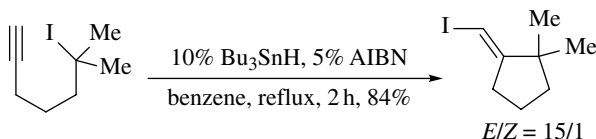
Organoiodine compounds bearing double or triple bonds provide cyclic iodine compounds by reaction in the presence of a Pd catalyst (Scheme 6.38) [94–96] or a catalytic tin compound (Schemes 6.39 and 6.40) [97–99]. Such cyclization reactions are observed efficiently in the cases of 6-iodoalkenes or alkynes.



SCHEME 6.38



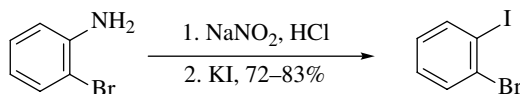
SCHEME 6.39



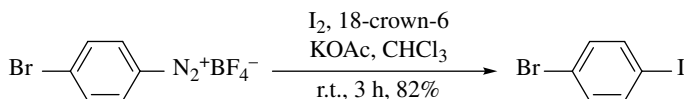
SCHEME 6.40

6.7 IODINATION OF ORGANONITROGEN COMPOUNDS

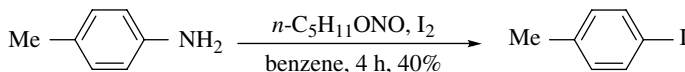
A typical method for synthesis of aromatic iodides is diazotization of primary aromatic amines followed by treatment of potassium iodide (Scheme 6.41) [100–104]. When stable arenediazonium tetrafluoroborates are isolated and then react with iodine under phase-transfer conditions, aryl iodides are obtained in high yields at room temperature for a short time (Scheme 6.42) [105]. Aromatic amines can be converted to aryl iodides in nonaqueous solutions by diazotizing with organic nitrites such as amyl nitrite and the subsequent decomposition in the presence of iodine (Scheme 6.43) [106] or iodotrimethylsilane [107]. Especially, use of *t*-butylthionitrite gives a higher yield of iodides than that of alkyl nitrites (Scheme 6.44) [108].



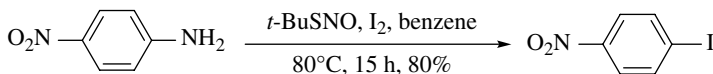
SCHEME 6.41



SCHEME 6.42

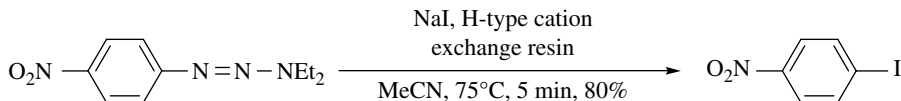


SCHEME 6.43



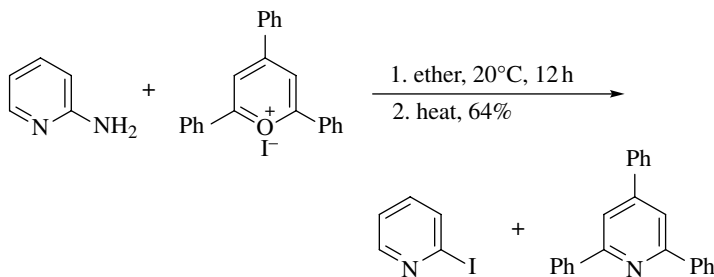
SCHEME 6.44

Triazenes are obtained by treating an aqueous solution of arenediazonium salts with diethylamine [109] or pyrrolidine [110] and act as stable equivalents of diazonium salts. Treatment of these triazenes with iodotrimethylsilane [109], KI [110], or NaI–cationic–exchange resin (Scheme 6.45) [111] affords aryl iodides in high yields. Specially, the latter method is applied to synthesis of aryl iodides containing the radioactive isotope of iodine. As the related methods for synthesis of iodides, decomposition of hydrazines [112] and hydrazones [113] and radical decomposition of azo compounds [114] are known.



SCHEME 6.45

2,4,6-Triphenylpyrriium iodide reacts with a series of alkyl, benzyl, and pridylamines to give pyridinium iodides, which undergo thermal decomposition to yield iodides easily (Scheme 6.46) [115]. Similarly, thermal decomposition of pyridinium salts derived from benzylamines and 4,6-diphenylpyran-2-thione affords benzyliodides [116]. Tertiary nitro- and nitrosoalkanes are converted to iodoalkanes by reaction with iodotrimethylsilane [117].



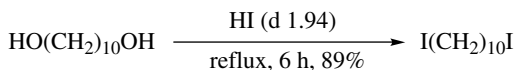
SCHEME 6.46

6.8 IODINATION OF ALCOHOLS

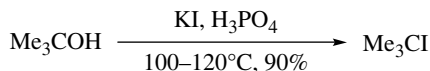
6.8.1 Reaction with Hydrogen Iodide

Aliphatic alcohols are converted to alkyl iodides by treating with HI. The reactivity of the alcohol increases in the order: primary < secondary < tertiary. Iodination of α,ω -diols (Scheme 6.47) [118] or benzyl alcohols [119] also gives the corresponding iodides in high yields. However, there are drawbacks in that secondary and tertiary alcohols bearing aryl groups at the α -position are not applied due to reduction by HI and branched alcohols cause isomerization. Iodination with KI–phosphoric acid reduces the side reactions and is applied to a wide variety of alcohols such as aliphatic and alicyclic alcohols to give the corresponding iodides in high yields

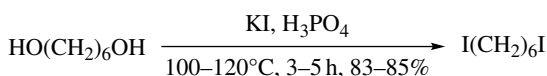
(Schemes 6.48 and 6.49) [120]. Iodination with KI–HF·pyridine is also applicable to a wide variety of alcohols and is an excellent method without isomerization and racemization [121].



SCHEME 6.47



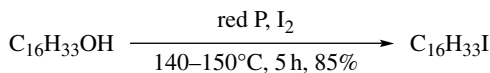
SCHEME 6.48



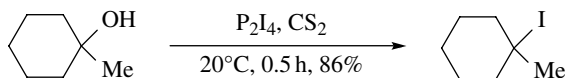
SCHEME 6.49

6.8.2 Reaction with Phosphorous Triiodide

Phosphorous triiodide (PI_3) formed from red phosphorous–iodine reacts with alcohols to give alkyl iodides. For the reaction of secondary and tertiary alcohols, it is required to conduct at a low temperature to prevent the formation of alkenes (Scheme 6.50) [122, 123]. Diphosphorous tetraiodide reacts with primary, secondary, and tertiary alcohols and α,ω -diols under milder conditions to give the corresponding alkyl iodides in high yields (Scheme 6.51) [124].



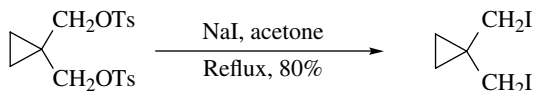
SCHEME 6.50



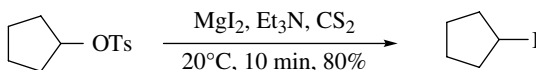
SCHEME 6.51

6.8.3 Reaction with Sulfonic Acid Esters

Alcohols are converted to alkyl iodides via sulfonic acid esters. After converting alcohols to *p*-toluenesulfonic acid esters or methanesulfonic esters, the reaction of the sulfonates with NaI or KI in acetone or DMF (Scheme 6.52) [125, 126] or with MgI_2 in ether [127] gives alkyl iodides in high yields. Specially, the iodination with MgI_2 is suitable for the conversion of cyclic alcohols, which needs severe conditions by the method of NaI (Scheme 6.53) [127]. In addition, this method can be applied to synthesis of alkenyl iodides from alkenyl triflates [128].



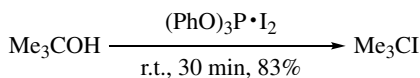
SCHEME 6.52



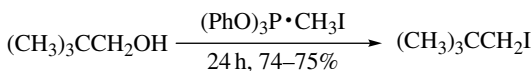
SCHEME 6.53

6.8.4 Reaction with Phosphorous Compounds

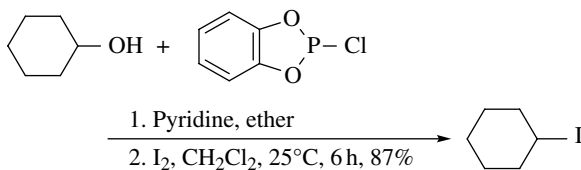
Triphenyl phosphate–iodine adduct (Scheme 6.54) [129] and $(\text{PhO})_3\text{P}(\text{Me})\text{I}$ (Scheme 6.55) [130] react with a wide range of alcohols under mild conditions to give the corresponding iodides in high yields. The method using the reaction of alcohols with *o*-phenylenephosphorochloridite in the presence of iodine is suitable for the substrates causing elimination reactions (Scheme 6.56) [131]. Tributylldiiodophosphorane and triphenyldiiodophosphorane generated in situ from the corresponding phosphines and iodine react with primary and secondary alcohols in the presence of HMPA to give the corresponding alkyl iodides [132].



SCHEME 6.54



SCHEME 6.55

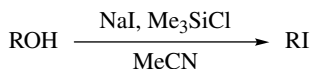


SCHEME 6.56

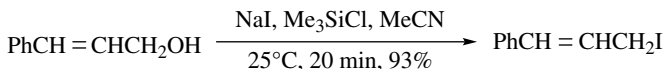
Treatment of alcohols with oxidation–reduction system of diazodicarboxylic acid diethyl ester and triphenylphosphine [133] leads to the formation of alkoxyphosphonium salts, which are subject to $\text{S}_{\text{N}}2$ replacement by iodide ion to give alkyl iodides with inversion of the stereochemistry [134]. The same reaction is observed in the case of 4-methyl-1,2,4-triazolidine-3,5-dione instead of diazodicarboxylic acid diethyl ester [135].

6.8.5 Reaction with Iodotrimethylsilane

Reaction of alcohols with two equivalents of iodotrimethylsilane gives the corresponding alkyl iodides in high yields [136]. As a convenient method, iodotrimethylsilane generated in situ from chlorotrimethylsilane and NaI in MeCN is applied for the iodination of alcohols (Scheme 6.57). This method is cheap and the reaction gets over within a short time (Scheme 6.58) [137a, 138]. The method generating iodotrimethylsilane from hexamethyldisilane and iodine enables the use of solvents other than acetonitrile [137b]. In addition, hexamethyldisiloxane–polyphosphoric acid trimethylsilyl ester is an excellent iodinating agent for primary, secondary, and benzyl alcohols [139].



SCHEME 6.57

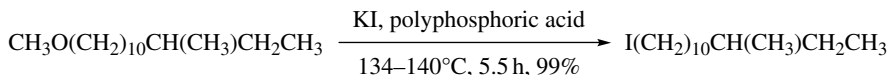


SCHEME 6.58

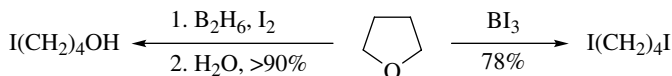
6.9 IODINATION OF OTHER COMPOUNDS

6.9.1 Cleavage–Iodination of Ethers

Although cleavage of the ether bonds by HI takes place, the method using KI–phosphoric acid can be applied to a wide range of ethers (Scheme 6.59) [140, 141]. Most of the ethers undergo cleavage by diborane–iodine readily to afford iodoalkyl-esters of boronic acids, and the subsequent hydrolysis gives alkyl iodides (Scheme 6.60) [142]. Boron triiodide is also used for synthesis of iodides from ethers [143]. Chlorotrimethylsilane–NaI reagent is good for the iodination [137a].

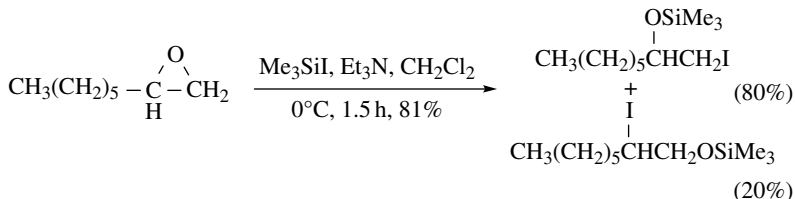


SCHEME 6.59



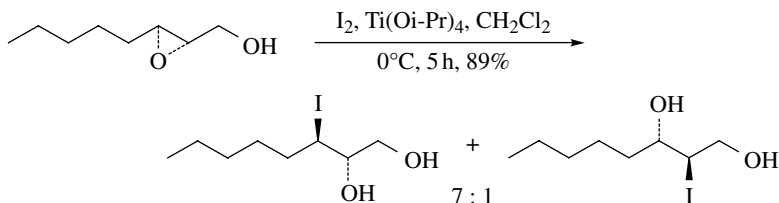
SCHEME 6.60

Oxiranes are converted to β -siloxyalkyl iodides by iodotrimethylsilane–triethylamine (Scheme 6.61) [144, 145]. In addition, reaction of oxiranes with iodotrimethylsilane in the presence of a reducing agent affords alkyl iodides directly [146].

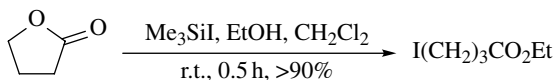


SCHEME 6.61

Reaction of α,β -epoxyesters with MgI_2 gives iodohydrins [147]. Allyl- and homoallyl-epoxyalcohols react with titanium isopropoxide–iodine to give hydroxyiodohydrins (Scheme 6.62) [148]. Lactones are converted to iodocarboxylic acids and iodoesters by HI [149] and iodotrimethylsilane–iodine (Scheme 6.63) [150], respectively.



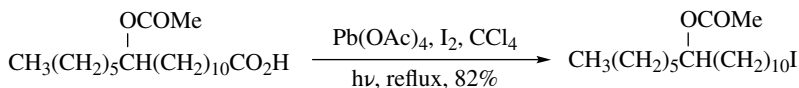
SCHEME 6.62



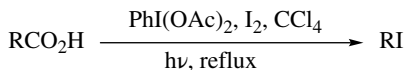
SCHEME 6.63

6.9.2 Decarboxylative Iodination of Carboxylic Acids

Decarboxylation of hypiodates generated from silver caboxylates and iodine gives iodides (Hunsdiecker reaction) [151]. The Cristol–Firth method [152] is suitable for iodination of benzoic acids and pyridinecarboxylic acids [153]. Irradiation of carboxylic acids in the presence of lead tetraacetate and iodine causes decarboxylative iodination to give alkyl iodides (Barton reaction) (Scheme 6.64) [154]. A general procedure for synthesis of alkyl iodides from primary, secondary, and tertiary alcohols is the method using *t*-butyl hypiodite generated in situ from potassium *t*-butoxide and iodine [155]. Irradiation of carboxylic acids in the presence of (diacetoxyiodo)benzene and iodine on heating affords alkyl iodides (Scheme 6.65) [156]. This method can be applied to decarboxylative iodination of aromatic carboxylic acids [157] and caged carboxylic acids [158]. This method has the advantage that it does not need heavy metals such as Hg and Pb and the workup is simple.



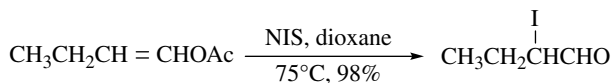
SCHEME 6.64



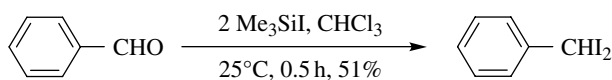
SCHEME 6.65

6.9.3 Iodination of Carbonyl and Related Compounds

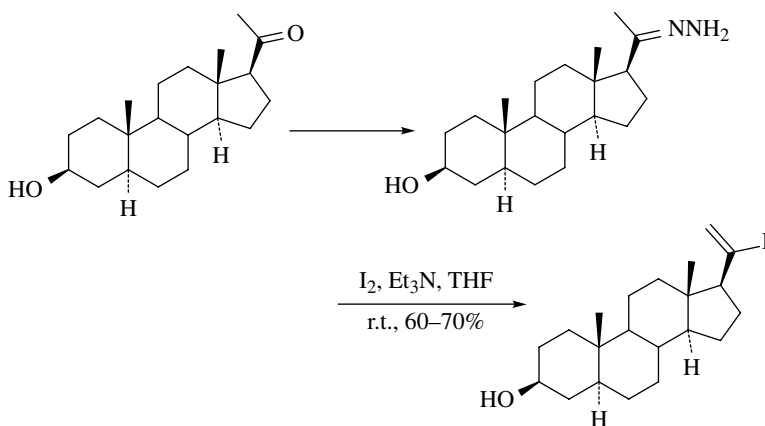
Although α -iodocarbonyl compounds can be prepared by iodination of carbonyl compounds under basic conditions [159], it is difficult to obtain highly pure α -iodocarbonyl compounds by direct iodination due to the instability. Accordingly, they are prepared by reacting enol acetates of ketones with NIS (Scheme 6.66) [160], 1,3-diiodo-5,5-dimethylhydantoin (DIH) [161], or thallium acetate–iodine [162]. Treatment of enol silyl ethers with silver acetate–iodine followed by reaction with triethylammonium fluoride affords α -iodocarbonyl compounds [163]. Benzaldehyde is converted to α,α -diiodotoluene by reaction with two equivalents of iodotrimethylsilane (Scheme 6.67) [164]. The reaction with hydrazine and iodine also provides α,α -diiodo compounds [165, 166]. However, this reaction in the case of the substrates with α -hydrogen gives alkenyl iodides and is utilized for the synthesis of alkenyl iodides (Schemes 6.68 and 6.69) [165, 167, 168]. Direct α -iodination of carboxylic acids is conducted using iodine and copper salts to give the corresponding α -iodo carboxylic acids [169].



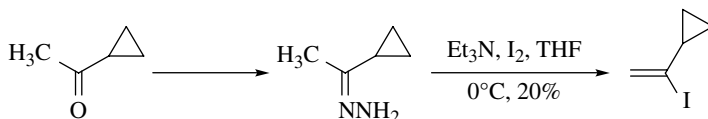
SCHEME 6.66



SCHEME 6.67



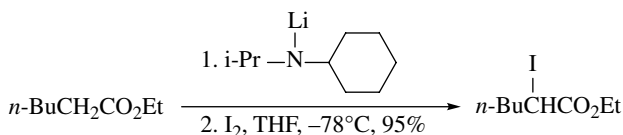
SCHEME 6.68



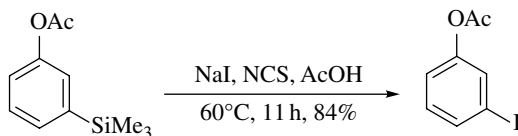
SCHEME 6.69

6.9.4 Reaction with Organometallics

When organometallics containing Li, Na, Mg, Si, B, Tl, Hg, Zn, Cu, and so on, are treated with iodine, they are converted to the corresponding iodides. This method is used for direct introduction of iodine to the desired position, transformation of other halogens to iodine, and synthesis of polyfunctionalized iodo compounds. It is convenient to use the lithium compounds in order to iodinate the α -position of carbonyl compounds (Scheme 6.70) [170] and transform aryl bromides to aryl iodides [171]. Treatment of methylsilylated aromatic compounds with ICl [172] or NaI–NCS (*N*-chlorosuccinimide) (Scheme 6.71) [173] gives aryl iodides.



SCHEME 6.70



SCHEME 6.71

REFERENCES

- [1] Tanner DD, Gidler GC. Free-radical iodination. A novel synthetic method. *J Am Chem Soc* 1968;90:808.
- [2] Hess WW, Huyser ES, Kleinberg J. The light-induced reactions of iodine trichloride with cyclohexane. *J Org Chem* 1964;29:1106.
- [3] Roller P, Djerassi C. Terpenoids. Part LXVI. Simultaneous functionalization of the angular 10- and 13-methyl groups in 11 β -hydroxylanostan-3 β -yl acetate by oxidation with lead tetra-acetate–iodine. *J Chem Soc C* 1970:1089.
- [4] Suzuki H. Direct iodination of polyalkylbenzenes: iododurene. *Org Synth Coll* 1988;VI:700.
- [5] Kajigaeshi S, Kakinami T, Moriwaki M, Tanaka T, Fujisaki S, Okamoto T. Halogenation using quaternary ammonium polyhalides. XIV. Aromatic bromination and iodination of arenes by use of benzyltrimethylammonium polyhalides–zinc chloride system. *Bull Chem Soc Jpn* 1989;62:439.

- [6] Sugiyama T. A mild and convenient procedure for conversion of aromatic compounds into their iodides using ammonium hexanitratocerate(IV). *Bull Chem Soc Jpn* 1981;54:2847.
- [7] (a) Ogata Y, Aoki K. Iodination of aromatic compounds with a mixture of iodine and peracetic acid. III. Autocatalysis and relative rates. *J Am Chem Soc* 1978;90:6187. (b) Ogata Y, Aoki K, Nakajima K. Studies on the iodination of aromatic compounds by a mixture of peroxyacetic acid and iodine. *Tetrahedron* 1964;20:2751.
- [8] (a) Keefer RM, Andrews LJ. Iodination of aromatic compounds with a mixture of iodine and peracetic acid. III. Autocatalysis and relative rates. *J Am Chem Soc* 1956;78:5623. (b) Keefer RM, Andrews LJ. The reaction of alkylbenzenes with iodine monochloride in carbon tetrachloride and in trifluoroacetic acid. *J Am Chem Soc* 1957;79:1412.
- [9] Sugita T, Idei M, Ishibashi Y, Takegami Y. Aromatic iodination with aluminum and copper(II) chlorides and iodine. *Chem Lett* 1982:1481.
- [10] Fletcher TL, Namkung MJ, Wetzel WH, Pan H-L. Derivatives of fluorene. X. Fluorofluorenes. III. *J Org Chem* 1960;25:1342.
- [11] Arotsky J, Butler R, Darby AC. Iodination and iodo-compounds. Part III. Iodination of some aromatic nitro-compounds with iodine in 20% oleum. *J Chem Soc C* 1970:1480.
- [12] Allen CFH, Cressman HWJ, Johnson HB. Tetraiodophthalic anhydride. *Org Synth Coll* 1955;III:796.
- [13] Barnes JH, Borrows ET, Elks J, Hems BA, Long AG. The synthesis of thyroxine and related substances. Part VII. The preparation of diphenyl ethers from 2: 6-di-iodophenols. *J Chem Soc* 1952:2824.
- [14] Giza CA, Hinman RL. New thyroxine analogs. Halogen derivatives of 3-carbethoxy-5-hydroxy-2-methylbenzofuran. *J Org Chem* 1964;29:1453.
- [15] Jurd L. The iodination of tyrosine and its derivatives. *J Am Chem Soc* 1955;77:5747.
- [16] Kajigaeshi S, Kakinami T, Yamasaki H, Fujisaki S, Kondo M, Okamoto T. Halogenation using quaternary ammonium polyhalides. V. Iodination of phenols by use of benzyltrimethylammonium dichloriodate(1-). *Chem Lett* 1987:2109.
- [17] Jones B, Richardson EN. Chloramines as a source of iodine chloride. The preparation of iodo-phenols, -naphthols, and -aromatic ethers by means of a chloramine and an iodide. *J Chem Soc* 1953:713.
- [18] Woollett GH, Johnson WW. 2-Hydroxy-3,5-diiodobenzoic acid. *Org Synth* 1943;II:343.
- [19] Kajigaeshi S, Kakinami T, Inoue K, Kondo M, Nakamura H, Fujisawa M, Okamoto T. Halogenation using quaternary ammonium polyhalides. VI. Bromination of aromatic amines by use of benzyltrimethylammonium tribromide. *Bull Chem Soc Jpn* 1988;61:597.
- [20] Brewster RQ. p-Iodoaniline. *Org Synth Coll* 1943;II:347.
- [21] Walllingford VH, Krueger PA. 5-Iodoanthranilic acid. *Org Synth Coll* 1943;II:349.
- [22] Sandin RB, Frakke WV, Leger F. 2,6-Diiodo-p-nitroaniline. *Org Synth Coll* 1943;II:196.
- [23] Kajigaeshi S, Kakinami T, Watanabe F, Okamoto T. Halogenation using quaternary ammonium polyhalides. XVII. Iodination of acetanilide derivatives with benzyltrimethylammonium dichloriodate and zinc chloride. *Bull Chem Soc Jpn* 1989;62:1349.
- [24] Bradfield AE, Orton KJP, Roberts IC. CV.—Chloroamines as halogenating agents. Iodination by a chloroamine and an iodide. *J Chem Soc* 1928:782.
- [25] Kajigaeshi S, Kakinami T, Moriwaki M, Watanabe M, Fujisaki S, Okamoto T. Halogenation using quaternary ammonium polyhalides. XII. Iodination of aromatic ethers by use of benzyltrimethylammonium dichloriodate and zinc chloride. *Chem Lett* 1988:795.

- [26] Janssen DE, Wilson CV. 4-Iodoveratrole. *Org Synth Coll* 1963;IV:547.
- [27] (a) Merkushev EB, Simakhina ND, Koveshnikova GM. A new, convenient iodination method of aromatic compounds. *Synthesis*, 1980:486. (b) Merkushev EB. Advances in the synthesis of iodoaromatic compounds. *Synthesis* 1988:923.
- [28] (a) Togo H, Nabana T, Yamaguchi K. Preparation and reactivities of novel (diacetoxy-iodo)arenes bearing heteroaromatics. *J Org Chem* 2000;65:8391. (b) Togo H, Nogami G, Yokoyama M. Synthetic application of poly[styrene(iodoso diacetate)]. *Synlett* 1998:534. (c) Togo H, Abe S, Nogami G, Yokoyama M. Synthetic use of poly[4-(diacetoxyiodo)styrene] for organic reactions. *Bull Chem Soc Jpn* 1999;72:2351.
- [29] (a) Auria MD, Mauriello G. Bis-(trifluoroacetoxy)iodobenzene—iodine system: an efficient and selective reagent for iodination of thiophene derivatives. *Tetrahedron Lett* 1995;36:4883. (b) Boyle RW, Johnson CK, Dolphin D. Iodination and Heck alkynylation of 5,15-diphenylporphyrin. A convenient entry to asymmetrically meso-substituted porphyrins. *J Chem Soc Chem Commun* 1995:527.
- [30] Benhida R, Blanchard P, Fourrey J-L. A mild and effective iodination method using iodine in the presence of bis-(trifluoroacetoxy)iodobenzene. *Tetrahedron Lett* 1998;39:6849.
- [31] Barluenga J, Gonzalez JM, Campos PJ, Asensio G. I(py)2BF₄, a new reagent: general methods for the 1,2-iodo functionalization of olefins. *Angew Chem Int Ed Engl* 1985;24:319.
- [32] (a) Rousseau G, Robbin S. Halogenation of pyridinols using bis(sym-collidine)iodine(I) and bis(sym-collidine)bromine(I) hexafluorophosphate. *Tetrahedron Lett* 1997;38:2467. (b) Brunel Y, Rousseau G. An easy preparation of iodoacetylenes. *Tetrahedron Lett* 1995;36:2619. (c) Homsí F, Robbin S, Rousseau G. Preparation of bis(2,4,6-trimethylpyridine)iodine(I) hexafluorophosphate and bis(2,4,6-trimethylpyridine)bromine(I) hexafluorophosphate. *Org Synth* 2001;77:206.
- [33] Barluenga J, Rodriguez MA, Campos PJ, Asensio G. A general and useful copper(II)-promoted iodofunctionalization of unsaturated systems. *J Chem Soc Chem Commun* 1987:1491.
- [34] Zanger M, Rabinowitz JL. Nuclear magnetic resonance investigation of the iodination of 1,2-disubstituted ethylenes. Evidence for a trans addition-cis elimination. *J Org Chem* 1975;40:248.
- [35] White EP, Robertson PW. The kinetics of chlorine, iodine chloride, and bromine chloride addition to olefinic compounds. *J Chem Soc* 1939:1509.
- [36] Uemura S, Fukuzaki S, Okano M, Sawada S. The chloriodination of deactivated olefins with antimony(V) chloride-iodine and iodine monochloride. *Bull Chem Soc Jpn* 1982;104:6465.
- [37] Cambie RC, Noall WI, Potter GJ, Rutledge PS, Woodgate PD. Reactions of alkenes with electrophilic iodine in tetramethylene sulphone–chloroform. *J Chem Soc Perkin Trans 1* 1977:226.
- [38] Baird WC Jr, Surridge JH, Buza M. Halogenation with copper(II) halides. Halogenation of olefins with complexed copper(II) halides. *J Org Chem* 1971;36:3324.
- [39] Rozen S, Brannnd M. A novel method for preparation of vicinal fluoro-iodo compounds using elemental fluorine. *Tetrahedron Lett* 1980;21:4543.
- [40] Ruel FS, Braun MP, Johnson CR. 2-(4-methoxyphenyl)-2-cyclohexen-1-one: preparation of 2-iodo-2-cyclohexen-1-one and suzuki coupling with 4-methoxyphenylboronic acid. *Org Synth* 1997;75:69.

- [41] (a) Clark KJ. *J Chem Soc* 1957;463. (b) Landini D, Rolla F. Addition of hydrohalogenic acids to alkenes in aqueous-organic, two-phase systems in the presence of catalytic amounts of onium salts. *J Org Chem* 1980;45:3527.
- [42] Stone H, Shechter H. Iodocyclohexane. *Org Synth Coll* 1963;IV:543.
- [43] Brown HC, Rathke MW, Rogic MM. A fast reaction of organoboranes with iodine under the influence of base. A convenient procedure for the conversion of terminal olefins into primary iodides via hydroboration-iodination. *J Am Chem Soc* 1968;90:5038.
- [44] (a) De Lue NR, Brown HC. An improved procedure for the conversion of organoboranes into alkyl iodides. *Synthesis* 1976;114. (b) Brown HC, De Lue NR, Kabalka GW, Hedgecock Jr, HC. Consistent inversion in the base-induced reaction of iodine with organoboranes. A convenient procedure for the synthesis of optically active iodides. *J Am Chem Soc* 1976;98:1290.
- [45] Kabalka GW, Gooch EG. A mild and convenient procedure for conversion of alkenes into alkyl iodides via reaction of iodine monochloride with organoboranes. *J Org Chem* 1980;45:3578.
- [46] Kabalka GW, Gooch EE. Syntheses of organic iodides via reaction of organoboranes with sodium iodide. *J Org Chem* 1981;46:2582.
- [47] Maruoka K, Sano H, Shinoda K, Nakai S, Yamamoto H. Organoborane-catalyzed hydroalumination of olefins. *J Am Chem Soc* 1986;108:6036.
- [48] Ohta H, Sakata Y, Takeuchi T, Ishii Y. Iodohydrin synthesis from simple and functionalized olefins on treatment with periodic acid and sodium bisulfate. *Chem Lett* 1990:733.
- [49] Comforth JW, Green DT. Iodohydrins and epoxides from olefins. *J Chem Soc C* 1970:846.
- [50] Sumrell S, Wyman BM, Howell RG, Harvey MC. Reaction of lower olefins and iodine in a liquid phase: novel preparation of alkene iodohydrins. *Can J Chem* 1964;42:2710.
- [51] Georgoulis C, Valery JM. A convenient procedure for the preparation of vicinal alkoxy-iodoalkanes from alkenes by means of copper(II) acetate and iodine. *Synthesis* 1978:402.
- [52] Kajigaeshi S, Moriwaki M, Fujisaki S, Kakinami T, Okamoto T. Halogenation using quaternary ammonium polyhalides XXVII.1 chloroiodination of alkenes with benzyltrimethyl-ammonium dichloroiodate. *Bull Chem Soc Jpn* 1990;63:3033.
- [53] Danishefsky SJ, Selnick HG, Armistead DM, Wincott FE. The total synthesis of avermectin A1a. New protocols for the synthesis of novel 2-deoxypyranose systems and their axial glycosides. *J Am Chem Soc* 1987;109:8119.
- [54] Jackson EL, Pasiut L. The synthesis of certain iodo-alkoxy acids and the mechanism of the reactions by which they are formed. *J Am Chem Soc* 1928;50:2249.
- [55] Cambie RC, Rutledge PS. Stereoselective hydroxylation with thallium(I) acetate and iodine: trans- and cis-1,2-cyclohexanediols. *Org Synth Coll* 1988;VI:348.
- [56] Birckenbach L, Goubeau J, Berninger E. Pseudohalogens. XXI. The reaction of silver salts of monobasic acids with iodine in the presence of cyclohexene. *Ber* 1932;65:1339.
- [57] Adinolfi M, Parrilli M, Barone G, Laonigro G, Mangoni L. Iodohydrins and iodohydrin esters. VI. A general procedure for the preparation of trans-1,2-iodocarboxylates. *Tetrahedron Lett* 1976:3661.
- [58] Padwa A, Blacklock T, Tremper A. 3-Phenyl-2H-azirine-2-carboxaldehyde. *Org Synth Coll* 1988;VI:893.
- [59] Hassner A, Fowler FW. General synthesis of vinyl azides from olefins. Stereochemistry of elimination from β -iodo azides. *J Org Chem* 1968;33:2686.

- [60] Heathcock CH, Hassner A. Methyl (trans-2-iodo-1-tetralin)carbamate. *Org Synth Coll* 1988;VI:795.
- [61] Hinshaw JC. Addition of iodine thiocyanate to olefins a new synthesis of episulfides. *Tetrahedron Lett* 1972:3567.
- [62] (a) Woodgate PD, Lee HH, Lutledge PS, Cambie RC. Reaction of alkenes with iodine(I) thiocyanate. *Tetrahedron Lett* 1976:1531. (b) Woodgate PD, Lee HH, Rutledge PS, Cambie RC. Synthesis of vicinal iodothiocyanates, iodoisothiocyanates, and iodoazides using phase-transfer reagents. *Synthesis* 1977:462.
- [63] McMurry JE, Musser JH, Fleming I, Fortunak J, Nübling C. Methyl (E)-3-nitroacrylate. *Org Synth Coll* 1988;6:799.
- [64] Kropp JE, Hassner A, Kent GJ. Addition of iodine nitrate to olefins. *J Chem Soc Chem Commun* 1968:906.
- [65] (a) Vaughn TH, Nieuwland JA. Iodination in liquid ammonia. *J Am Chem Soc* 1932;54:787. (b) Vaughn TH, Nieuwland JA. The direct iodination of monosubstituted acetylenes. *J Am Chem Soc* 1933;55:2150. (c) Vaughn TH, Nieuwland JA. Further studies of iodination in liquid ammonia. *J Am Chem Soc* 1934;56:1207. (d) Vaughn TH, Nieuwland JA. The synthesis and properties of 2-iodo-1-vinylacetylene. *J Chem Soc* 1933:741.
- [66] Southwick PL, Kirchner JR. The morpholine-iodophenylacetylene adduct or charge-transfer complex. Formation and conversion to N-styrylmorpholine. *J Org Chem* 1962;27:3305.
- [67] (a) Brandsma L. *Preparative Acetylenic Chemistry*. Amsterdam: Elsevier; 1971. p. 99. (b) Kloster-Jensen E. The preparation of monochloro-, monobromo- and monoiodo-di-acetylene. *Tetrahedron* 1966;22:965. (c) Chauhan YS, Chandraratna RAS, Miller DA, Kondrat RW, Reisel W, Okamura WH. On a tandem 1,2-elimination/[1,7]-sigmatropic shift: synthesis of double bond shifted isomers of vitamin A. *J Am Chem Soc* 1985;107:1028. (d) Boutin RH, Rapoport H. ∞ -Amino acid derivatives as chiral educts for asymmetric products. Synthesis of sphingosine from ∞' -amino- ∞,β -ynones. *J Org Chem* 1986;51:5320.
- [68] Burgess C, Cooley G, Feather P, Petrow V. Modified steroid hormones—XLVIII: a new route to 17 α -bromoethynyl- and 17 α -iodoethynyl-17 β -hydroxy steroids. *Tetrahedron* 1967;23:4111.
- [69] Wille F, Dirr K, Kerber H. Preparation and properties of 1,4-diiodobutynes; an example of 1,4-addition in butatriene. *Ann Chem* 1955;591:177.
- [70] Marek I, Meyer C, Normant J-F. A simple and convenient method for the preparation of (Z)- β -iodoacrolein and of (Z)- or (E)- γ -iodo allylic alcohols: (Z)- and (E)-1-iodohept-1-en-3-ol. *Org Synth* 1996;74:194.
- [71] Haszeldine RN. Fluoro-olefins. Part I. The synthesis of hexafluorobuta1: 3-diene. *J Chem Soc* 1952:4390.
- [72] Uemura S, Okazaki H, Onoe A, Okano M. Chlorination and interhalogenation of alkyl-phenylacetylenes with antimony pentachloride. *J Chem Soc Perkin Trans 1* 1979:548.
- [73] Brown HC, Hamaoka T, Ravindran N. Reaction of alkenylboronic acids with iodine under the influence of base. Simple procedure for the stereospecific conversion of terminal alkynes into trans-1-alkenyl iodides via hydroboration. *J Am Chem Soc* 1973;95:5786.
- [74] Brown HC, Campbell JB Jr. Hydroboration. 55. Hydroboration of alkynes with dibromoborane-dimethyl sulfide. Convenient preparation of alkenyldibromoboranes. *J Org Chem* 1980;45:389.

- [75] Zweifel G, Whitney CC. Novel method for the synthesis of isomerically pure vinyl halides from alkynes via the hydroalumination reaction. *J Am Chem Soc* 1967;89:2753.
- [76] Zweifel G, Arzoumanian H. α -Halovinylboranes. Their preparation and conversion into α -Halovinylboranes. Their preparation and conversion into cis-vinyl halides, trans-olefins, ketones, and transvinylboranes. *J Am Chem Soc* 1967;89:5086.
- [77] Alexakis A, Cahiez G, Normant J-F. Z-1-Iodoheptene. *Org Synth Coll* 1990;VII:290.
- [78] Schurink HB. Pentaerythrityl bromide and iodide. *Org Synth Coll* 1943;II:476.
- [79] Ford-Moore AH. Benzoylcholine iodide and chloride. *Org Synth Coll* 1963;IV:84.
- [80] Kulstad S, Malmsten LA. Diazacrown ethers. I. Alkali ion promoted formation of diazacrown ethers and syntheses of some N,N'-disubstituted derivatives. *Acta Chim Scand* 1979;B33:469.
- [81] Kuwajima I, Urabe H. Cyclopentanones from carboxylic acids via intramolecular acylation of alkylsilanes: 2-Methyl-2-vinylcyclopentanone. *Org Synth* 1987;66:87.
- [82] Daub GH, Castle RN. The synthesis of some substituted benzyl iodides. *J Org Chem* 1954;19:1571.
- [83] (a) Miller JA, Nunn MJ. Synthesis of alkyl iodides. *J Chem Soc, Perkin Trans 1* 1976:416. (b) Albano EL, Horton D. Synthesis of methyl 2,3,6-trideoxy- α -D-erythrohexopyranoside (methyl α -amicetoside). *J Org Chem* 1969;34:3519.
- [84] Olah GA, Narang SC, Field LD. Synthetic methods and reactions. 103. Preparation of alkyl iodides from alkyl fluorides and chlorides with iodotrimethylsilane or its in situ analogs. *J Org Chem* 1981;46:3727.
- [85] Bunnett JF, Conner RM. 2,4-Dinitroiodobenzene. *Org Synth Coll* 1973;V:478.
- [86] (a) Bunnett JF, Conner RM. Improved Preparation of 1-Iodo-2,4-dinitrobenzene. *J Org Chem* 1958;23:305. (b) Coad P, Coad RA, Clough S, Hyepock J, Salisbury L, Wilkins C. Nucleophilic substitution at the pyridazine ring carbons. I. Synthesis of iodopyridazines. *J Org Chem* 1963;28:218.
- [87] (a) Suzuki H, Kondo A, Ogawa T. Preparation of aromatic iodides from bromides via the reverse halogen exchange. *Chem Lett* 1985;411. (b) Suzuki H, Kondo A, Inoue M, Ogawa T. An alternative synthetic method for polycyclic aromatic iodides. *Synthesis* 1986:121.
- [88] (a) Takagi K, Hayama N, Okamoto T. Nucleophilic displacement catalyzed by transition metals. Part IV. Synthesis of aryl iodides from aryl halides and potassium iodide by means of a nickel catalyst. *Chem Lett* 1978:191. (b) Diercks R, Vollhardt KPJ. Tris(benzocyclobutadieno)benzene, the triangular [4]phenylene with a completely bond-fixed cyclohexatriene ring: cobalt-catalyzed synthesis from hexaethynylbenzene and thermal ring opening to 1,2:5,6:9,10-tribenzo-3,4,7,8,11,12-hexadehydro[12]annulene. *J Am Chem Soc* 1986;108:3150.
- [89] Corey EJ, Lantelat M. A synthetic method for the homologation of primary halides. *Tetrahedron Lett* 1968:5787.
- [90] (a) Hirai K, Kishida Y. Chemistry of 2-substituted thiothiazoline. IV. A new synthetic method for iodo-methylation and iodo-propenylation ($\text{ICH}_2\text{C}=\text{C}-$). *Tetrahedron Lett* 1972:2743. (b) Hirai K, Kishida Y. trans-Iodopropylation of alkyl halides: (E)-1-iodo-4-phenyl-2-butene. *Org Synth Coll* 1988;VI:704.
- [91] Chikamatsu K, Otsubo T, Ogura F, Yamaguchi H. Organotelluriums. III. Preparation of alkyl halides via organotelluriums. *Chem Lett* 1982:1081.

- [92] Oae S, Togo H. Facile conversions of aliphatic sulfonic acids, sulfinic acids, thiols, sulfonates, thiolsulfonates, and disulfides to the corresponding alkyl iodides by triphenylphosphine/iodine. *Synthesis* 1981:371.
- [93] Krief A, Dumont W, Denis J-N. Novel functional group transformations involving alkyl phenyl selenones. *J Chem Soc Chem Commun* 1985:571.
- [94] Mori M, Oda I, Ban Y. Cyclization of α -haloamide with internal double bond by use of the low-valent metal complex. *Tetrahedron Lett* 1982;23:5315.
- [95] Mori M, Kubo Y, Ban Y. Reaction of α -haloester having internal double bond with the low-valent metal complex. *Tetrahedron Lett* 1985;26:1519.
- [96] Mori M, Kanda N, Oda I, Ban Y. New synthesis of heterocycles by use of palladium catalyzed cyclization of α -haloamide with internal double bond. *Tetrahedron* 1985;41:5465.
- [97] Curran DP, Kim D. Atom transfer cyclization of simple hexenyl iodides. A caution on the use of alkenyl iodides as probes for the detection of single electron transfer processes. *Tetrahedron Lett* 1986;27:5821.
- [98] Curran DP, Chang C-T. Atom transfer cyclization reactions of α -iodo carbonyls. *Tetrahedron Lett* 1987;28:2477.
- [99] Curran DP, Chen M-H, Kim D. Atom-transfer cyclization. A novel isomerization of hex-5-ynyl iodides to iodomethylene cyclopentanes. *J Am Chem Soc* 1986;108:2489.
- [100] Sandin RB, Cairns TL. 1,2,3-Triiodo-5-nitrobenzene. *Org Synth Coll* 1943;II:604.
- [101] Dains FB, Eberly F. p-Iodophenol. *Org Synth Coll* 1943;II:355.
- [102] Heaney H, Millar IT. Triphenylene. *Org Synth Coll* 1973;V:1120.
- [103] Lucas HJ, Kennedy ER. Iodobenzene. *Org Synth Coll* 1943;II:351.
- [104] Hauptschein H, Nodiff EA, Saggiomo AJ. Trifluoromethyl derivatives of hydroxybenzoic acids and related compounds. *J Am Chem Soc* 1954;76:1051.
- [105] Korzeniowski SH, Gokel GW. Crown-cation complex effects. IX. A phase transfer catalytic synthesis of bromo- and iodoarenes. *Tetrahedron Lett* 1977:3519.
- [106] Friedman L, Chlebowski JF. Aprotic diazotization of aniline in the presence of iodine. *J Org Chem* 1968;33:1636.
- [107] Nair V, Chamberlain SD. Novel photoinduced functionalized C-alkylations in purine systems. *J Org Chem* 1985;50:5069.
- [108] Oae S, Shinham K, Kim YH. Direct conversion of arylamines to the corresponding halides, biphenyls and sulfides with tert-butyl thionitrate. *Chem Lett* 1979:939.
- [109] Ku H, Barrio JR. Convenient synthesis of aryl halides from arylamines via treatment of 1-aryl-3,3-dialkyltriazenes with trimethylsilyl halides. *J Org Chem* 1981;46:5239.
- [110] Foster NI, Heindel ND, Burns HD, Muhr M. Aryl iodides from anilines via triazene intermediates. *Synthesis* 1980:572.
- [111] Satyamurthy N, Barrio JR. Cation exchange resin (hydrogen form) assisted decomposition of 1-aryl-3,3-dialkyltriazenes. A mild and efficient method for the synthesis of aryl iodides. *J Org Chem* 1983;48:4394.
- [112] Brown DM, Jones GH. New syntheses of halogeno- and deoxy-sugars. *J Chem Soc C* 1967:252.
- [113] Pross A, Sternhell S. Oxidation of hydrazones with iodine in the presence of base. *Aust J Chem* 1970;23:989.
- [114] Ford MC, Waters WA. Properties and reactions of free alkyl radicals in solution. Part II. Reactions with iodine, bromine, and sulphuryl chloride. *J Chem Soc* 1951:1851.

- [115] Eweiss NF, Katritzky AP, Nie P-L, Ramden CA. The conversion of amines into iodides. *Synthesis* 1977:634.
- [116] Lorenzo A, Molina P, Vilaplana MJ. Preparation of Benzyl Iodides from Benzylamines. *Synthesis* 1980:853.
- [117] Olah GA, Narang SC, Field LD, Fung AP. Synthetic methods and reactions. 113. Reactions of nitro- and nitrosoalkanes with iodotrimethylsilane. *J Org Chem* 1983;48:2766.
- [118] Taylor EP. Synthetic neuromuscular blocking agents. Part II. Bis(quaternary ammonium salts) derived from laudanosine. *J Chem Soc* 1952:142.
- [119] Daub GH, Castle RN. The synthesis of some substituted benzyl iodides. *J Org Chem* 1954;19:1571.
- [120] Stone H, Shechter H. 1,6-Diiodohexane. *Org Synth Coll* 1963;IV:323.
- [121] Olah GA, Welch J. Synthetic methods and reactions. XIII.1 preparation of alkyl halides from alcohols with alkali halides in polyhydrogen fluoride/pyridine solution. *Synthesis* 1974:653.
- [122] King HS. Methyl iodide. *Org Synth Coll* 1943;II:399.
- [123] Hartman WW, Byers JR, Dickey JB. n-Hexadecyl iodide. *Org Synth Coll* 1943;II:322.
- [124] Lauwers M, Regnier B, Van Eenoo M, Denis JN, Krief A. Diphosphorus tetraiodine (P₂I₄) a valuable reagent for regioselective synthesis of iodoalkanes from alcohols. *Tetrahedron Lett* 1979:1801.
- [125] Tipson RS, Clapp MA, Cratcher LH. The action of sodium iodide on some esters of p-toluenesulfonic acid. *J Org Chem* 1947;12:133.
- [126] House HO, Lord RC, Rao HS. The Synthesis of Spiropentane-d₈. *J Org Chem* 1956;21:1487.
- [127] Place P, Roumestant M-L, Gore J. Reaction of magnesium halides with sulfonates. *Bull Soc Chim Fr* 1976:169.
- [128] Martinez AG, Alvarez RM, Fraile AG, Subramanian LR, Hanack M. Herstellung von vinyl-iodiden durch umsetzung von vinyl-triflaten mit Magnesiumiodid. *Synthesis* 1986:222.
- [129] Coe GG, Landauer SR, Rydon HN. The organic chemistry of phosphorus. Part II. The action of triphenyl phosphite dihalides on alcohols: two further new methods for the preparation of alkyl halides. *J Chem Soc* 1954:2281.
- [130] Rydon HN. Alkyl iodides: neopentyl iodide and iodocyclohexane. *Org Synth Coll* 1988;VI:830.
- [131] Corey EJ, Anderson JE. Useful method for the conversion of alcohols to iodides. *J Org Chem* 1967;32:4160.
- [132] Haynes RK, Holden M. Formation of iodides and esters from alcohols and tributyl-diiodophosphorane and diiodotriphenylphosphorane. *Aust J Chem* 1982;35:517.
- [133] Mitsunobu O. The use of diethyl azodicarboxylate and triphenylphosphine in synthesis and transformation of natural products. *Synthesis* 1981:1.
- [134] Loibner H, Zbiral E. Reactions with organophosphorus compounds. XLI. New synthetic aspects of the triphenylphosphine-diethyl azodicarboxylate-hydroxy compound system. *Helv Chim Acta* 1976;59:2100.
- [135] Oshikawa T, Yamashita M. Conversion of alcohols into haloalkanes in the tertiary phosphine/methyl halide/4-methyl-1,2,4-triazolidine-3,5-dione (MTAD) system. *Bull Chem Soc Jpn* 1984;57:2675.

- [136] Jung ME, Ornstein PL. A new method for the efficient conversion of alcohols into iodides via treatment with trimethylsilyl iodide. *Tetrahedron Lett* 1977;2659.
- [137] (a) Olah GA, Narang SC, Gupta BGB, Malhotra R. Synthetic methods and reactions. 62. Transformations with chlorotrimethylsilane/sodium iodide, a convenient in situ iodotrimethylsilane reagent. *J Org Chem* 1979;44:1247. (b) Olah GA, Narang SC, Gupta BGB, Malhotra R. Hexamethyldisilane/iodine: convenient in situ generation of iodotrimethylsilane. *Angew Chem Int Ed* 1979;18:612.
- [138] Morita T, Yoshida S, Okamoto Y, Sakurai H. Chlorotrimethylsilane/sodium iodide: a new reagent for conversion of alcohols into iodides. *Synthesis* 1979;379.
- [139] Imamoto T, Matsumoto T, Kusumoto T, Yokoyama M. A convenient method for the preparation of alkyl iodides from alcohols. *Synthesis* 1983;460.
- [140] Stone H, Shechter H. 1,4-Diiodobutane. *Org Synth Coll* 1963;IV:321.
- [141] Cope AC, Burrows EP, Derieg ME, Moon S, Wirth W-D. Rimocidin. I. Carbon skeleton, partial structure, and absolute configuration at C-27. *J Am Chem Soc* 1965;87:5452.
- [142] Long LH, Freeguard GF. Low-temperature cleavage of ethers. *Nature* 1965;207:403.
- [143] Povlock TP. Cleavage of ethers by boron triiodide. *Tetrahedron Lett* 1967;4131.
- [144] Denis JN, Krief A. One pot synthesis of α -bromo and α -iodo ketones from epoxides. *Tetrahedron Lett* 1981;22:1429.
- [145] Obayashi M, Utimoto K, Nozaki H. Magnesium iodide induced rearrangement of α,β -epoxysilanes to β -ketosilanes as applied to the stereoselective synthesis of tetrahomo-terpenoid of codling moth. *Tetrahedron Lett* 1977;1807.
- [146] Aizpurua JM, Palomo C. Reductive halogenation of epoxides induced by halosilanes and 1,1,3,3-tetramethyldisiloxane (TMDS). *Tetrahedron Lett* 1984;25:3123.
- [147] Otsubo K, Inanaga J, Yamaguchi M. A highly stereoselective conversion of α,β -epoxy esters to α -hydroxy esters. An efficient route to optically active α -hydroxyesters. *Tetrahedron Lett* 1987;28:4435.
- [148] Kolbe M, Barth J. A convenient preparation of iodoalkyl esters from lactones. *Synth Commun* 1981;11:763.
- [149] Gresham TL, Jansen JE, Shaver FW. β -propiolactone. VIII. Reactions with organic and inorganic acids, acid chlorides and anhydrides. *J Am Chem Soc* 1950;72:72.
- [150] Alvarez E, Nunez MT, Martin VS. Mild and stereocontrolled synthesis of iodo- and bromohydrins by halogen-tetrakis(isopropoxy)titanium opening of epoxy alcohols. *J Org Chem* 1990;55:3429.
- [151] Wilson CV. The reaction of halogens with silver salts of carboxylic acids. *Org React* 1957;9:332.
- [152] Cristol S, Firth W Jr. Communications. A convenient synthesis of alkyl halides from carboxylic acids. *J Org Chem* 1961;26:280.
- [153] Uemura S, Tanaka S, Okano M, Hamana M. Decarboxylative ipso halogenation of mercury(II) pyridinecarboxylates. Facile formation of 3-iodo- and 3-bromopyridines. *J Org Chem* 1983;48:3297.
- [154] Barton DHR, Faro HP, Serebryakov EP, Woolsey NF. Photochemical transformations. Part XVII. Improved methods for the decarboxylation of acids. *J Chem Soc* 1965;2438.
- [155] Sheldon RA, Kochi JK. Oxidative decarboxylation of acids by lead tetraacetate. *Org React* 1972;279.

- [156] Concepcion JI, Francisco CG, Freire R, Hernandez R, Salazar JA. Iodosobenzene diacetate, an efficient reagent for the oxidative decarboxylation of carboxylic acids. *J Org Chem* 1986;51:402.
- [157] Singh R, Just G. An efficient synthesis of aromatic iodides from aromatic carboxylic acids. *Synth Commun* 1988;18:1327.
- [158] Moriarty RM, Khosrowshahi JS, Dalecki TM. Hypervalent iodine iodinate decarboxylation of cubyl and homocubyl carboxylic acids. *J Chem Soc Chem Commun* 1987:675.
- [159] (a) Ringold HJ, Stork G. Steroids. XCIII. Introduction of the cortical hormone side-chain. *J Am Chem Soc* 1958;80:250. (b) Halpern O, Djerassi C. Steroidal sapogenins. XXXVIII. synthesis of cortisone from botogenin. *J Am Chem Soc* 1959;81:439. (c) Rothman ES, Perlstein T, Wall ME. Steroidal sapogenins. LXIV. C-21 acetoxylation of 12-keto steroids. *J Org Chem* 1960;25:1966.
- [160] Djerassi C, Lenk C. α -Iodoketones (Part 2). Reaction of Enol Acetates with N-Iodosuccinimide. *J Am Chem Soc* 1953;75:3493.
- [161] Arazi OO, Corral RA, Bertorello HE. N-Iodohydantoins. II. Iodinations with 1,3-Diiodo-5,5-dimethylhydantoin. *J Org Chem* 1965;30:1101.
- [162] Cambie RC, Hayward RC, Jurlina JL, Rutledge PS, Woodgate PD. Reactions of enol acetates with thallium(I) acetate-iodine. *J Chem Soc Perkin Trans 1* 1978:126.
- [163] Rubottom GM, Mott RC. Reaction of enol silyl ethers with silver acetate-iodine. Synthesis of α -iodo carbonyl compounds. *J Org Chem* 1979;44:1731.
- [164] Jung ME, Mossman AB, Lyster MA. Direct synthesis of dibenzocyclooctadienes via double ortho Friedel-Crafts alkylation by the use of aldehyde-trimethylsilyl iodide adducts. *J Org Chem* 1978;43:3698.
- [165] Barton DHR, O'Brien RE, Strehl S. A new reaction of hydrazones. *J Chem Soc* 1962:470.
- [166] Neuman RC Jr, Holmes GD. Photochemistry of organic iodides. III. Photolytic formation of isomeric vinyl radicals from cis- and trans-vinyl iodides. *J Org Chem* 1968;33:4317.
- [167] Sherrod SA, Bergman RG. Synthesis and solvolysis of 1-cyclopropyl-1-iodoethylene. Generation of an unusually stable vinyl cation. *J Am Chem Soc* 1969;91:2115.
- [168] (a) Paquette LA, Schostarez H, Annis GD. Total synthesis of (+)-pentalenolactone E methyl ester. *J Am Chem Soc* 1981;103:6526. (b) Paquette LA, Annis GD, Schostarez H. An effective approach to stereocontrolled lactone annulation. Application to the total synthesis of pentalenolactone E methyl ester and a partial elaboration of quadron. *J Am Chem Soc* 1982;104:6646. (c) Hart PA, Tripp MP. Optical rotatory dispersion and circular dichroism of some optically active iodides. *J Chem Soc Chem Commun* 1969:174. (d) McKittrick BA, Scannell RT, Stevenson R. Natural benzofurans: synthesis of the arylbenzofuran constituents of *Sophora tomentosa*. *J Chem Soc Perkin Trans 1* 1982:3017. (e) Nakata M, Ikeyama Y, Takao H, Kinoshita M. Synthetic studies of rifamycins. II. Syntheses of methyl 2,4,6,7-tetra-deoxy-4-c-methyl-3-O-methyl- α -L-arabino-heptopyranoside-6-ulose and its derivatives utilizable in the construction of the rifamycin ansa chain portion. *Bull Chem Soc Jpn* 1980;53:3252. (f) Krubiner AM, Gottfried N, Oliveto EP. Synthesis of 17-deoxy-17 α - and 17 β -20-pregnynes and -20-pregnenes. *J Org Chem* 1969;34:3502.
- [169] Horiuchi CA, Satoh JY. A new synthesis of α -iodo carboxylic acids using iodine-copper salt. *Chem Lett* 1984:1509.

- [170] Rathke MW, Lindert A. The halogenation of lithium ester enolates. A convenient method for the preparation of alpha-iodo and alpha-bromo esters. *Tetrahedron Lett* 1971:3995.
- [171] Ziegler FE, Fowler KW, Rodgers WB, Wester RT. Ambient-temperature Ullman reaction: 4,5,4',5'-tetramethoxy-1,1'-biphenyl-2,2'-dicarboxaldehyde. *Org Synth* 1987;65:108.
- [172] Eaborn C, Njim AA, Walton DRM. 1,2-Dihydrobenzocyclobutene ('benzocyclobutene'): lithiation, and the preparation of some 3-substituted derivatives. *J Chem Soc Perkin Trans 1* 1972:2481.
- [173] Wilbur DS, Stone WE, Anderson KW. Regiospecific incorporation of bromine and iodine into phenols using (trimethylsilyl)phenol derivatives. *J Org Chem* 1983;48:1542.

HYPERVALENT IODINE

TOSHIFUMI DOHI¹ AND YASUYUKI KITA²

¹College of Pharmaceutical Sciences, Ritsumeikan University, Kusatsu, Shiga, Japan

²Emeritus Professor of Osaka University, Ritsumeikan University, Kusatsu, Shiga, Japan

7.1 INTRODUCTION

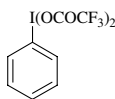
The first report of a hypervalent iodine compound in history was in 1886, when iodo-benzene dichloride (PhICl_2) was accidentally obtained by Willgerodt during his attempt at ring chlorination of iodobenzene by passing chlorine gas to the solution [1]. Hence, the discovery of the first hypervalent iodine compound (Willgerodt's reagent) is more than 100 years ago. Nowadays, hypervalent iodine reagents are receiving considerable attention as an oxidant due to their low toxicity, mild reactivity, ready availability, high stability, easy handling, and so on. Representative examples of the reagents that are used in synthesis are shown in Figure 7.1. A predominant use of these reagents is replacing the highly toxic heavy metal oxidizers, that is, lead(IV), mercury(II), and thallium(III) reagents, as useful alternatives. Extensive applications as stoichiometric oxidants were found to mediate a wide array of bond-forming reactions and other oxidative transformations. For example, phenyliodine(III) diacetate (PIDA) and phenyliodine(III) bis(trifluoroacetate) (PIFA)-induced oxidations of phenols and related reactions have been applied to many total syntheses of biologically important natural products and their pivotal intermediates. The pentavalent iodines, Dess–Martin periodinane (DMP) and its precursor, 2-iodoxybenzoic acid (IBX), are widely known as mild and highly selective reagents for the oxidation of alcohols. The details of synthetic versatility of these reagents have also been documented in several review articles by key contributors in this field [2–4].



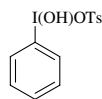
Dichloriodobenzene



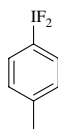
Phenyliodine(III) diacetate (PIDA)
or
diacetoxyiodobenzene (DIB)
or
iodosobenzene diacetate (IBD)



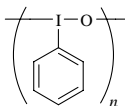
Phenyliodine(III) bis(trifluoroacetate) (PIFA)
or
bis (trifluoroacetoxy) iodobenzene (BTIB)



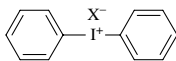
[Hydroxy(tosyloxy)iodo]benzene (HTIB)
(Koser's reagent)



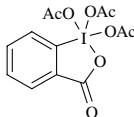
p-Iodotoluene difluoride



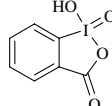
Iodosobenzene
or
iodosylbenzene



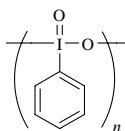
Diphenyliodonium salts
(X = halide, etc.)



Dess-Martin periodinane
(DMP)



o-Iodoxybenzoic acid
(IBX)



Iodoxybenzene
or
iodylbenzene

FIGURE 7.1 Representative hypervalent iodine reagents in organic synthesis and chemistry.

In addition, iodonium salts, typically in the diaryl forms, can be practically used as a photoacid generator (PAG) for industrial applications for initiating cationic radical polymerizations in photoimaging systems [5]. It is known that some iodonium salts possess antifungal and antimicrobial activities, and other miscellaneous biological properties have been found in recent years.

In this chapter, the fundamental theories regarding the structures and properties such as reactivities, applications, and recent progresses of hypervalent iodine compounds are briefly introduced for prospecting the future outlook.

7.2 STRUCTURES AND PROPERTIES

In a seminal *Angewandte Chemie* article in 1969 [6], Musher declared “hypervalency” for specific molecules involving atoms exceeding the number of their original valences in the traditional theory by utilizing more lone pairs for bonding. The hypervalent bonds of iodine were defined as a three-center four-electron (3c–4e) bond using a valence bond model from Pimentel and Rundle [7]. Later, Dykstra, Cahill, and Martin gave the theoretical orbital model of the hypervalent bonds [8]. Hence, trivalent iodine molecules (λ^3 -iodanes, IX_3 or ArIX_2 , Ar = aryl) take the T-shaped structure with the linear X–I–X system being a 3-center 4-electron bond with highest occupied molecular orbital (HOMO) at the orbitals of the hypervalent iodine ligands (X, Fig. 7.2), in which the iodine atom is thus highly electrophilic while the ligands are anionic; such highly polarized hypervalent bonds are weaker than regular covalent bonds, where the least electronegative one among the three ligands is attached to the iodine atom through a usual covalent bond (in case of ArIX_2 , the Ar group). On the other hand, pentavalent iodine molecules (λ^5 -iodanes, IX_5 , or ArIX_4) have two hypervalent iodine bonds, thus taking the square bipyramidal structures.

For classification of hypervalent (polyvalent) molecules, Martin and Arduengo introduced a very convenient nomenclature, which is called the Martin–Arduengo designation [9]. In this N –I– L designation (N is the number of formal valence shell electrons about iodine atom; L is the number of ligands), the iodine atoms in trivalent and pentavalent forms are generalized to 10–I–3 and 12–I–5 systems, respectively.

The crystal structure of PhICl_2 , the first discovered hypervalent iodine compound in history [1], was reported in 1953, which was later qualified by Chaloner et al. at the low-temperature measurement [10]. The molecule has the characteristic T-shape with the Cl–I–C group being almost linear and symmetrical (Fig. 7.3). The I–Cl

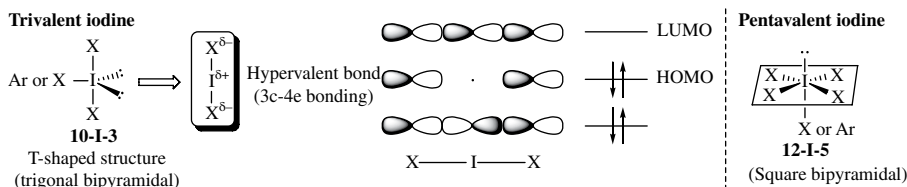


FIGURE 7.2 General structure and bonding of hypervalent iodine compounds.

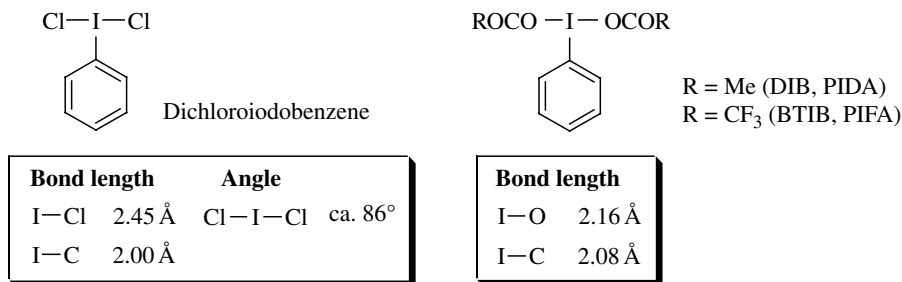


FIGURE 7.3 Bond length and angle of dichloriodobenzene and iodobenzene dicarboxylates.

distance is 2.45 Å, while the C—I bond length is 2.00 Å, which is typical in the case of a nonhypervalent covalent bond. In the solid state the molecules form an infinite zigzagged chain, in which one of the chlorine atoms interacts with the iodine of the next unit with an intermolecular I...Cl secondary bond distance of 3.40 Å.

In [bis(acyloxy)iodo]benzenes (PhI(OCOR)₂, Fig. 7.3), the iodine atoms similarly take a distorted T-shaped geometry with the three ligands [11]. For instance, the distances of two symmetrical I—O bonds of (diacetoxyiodo)benzene (R = Me, commonly abbreviated as DIB, or PIDA, iodosobenzene diacetate (IBD)) and [bis(trifluoroacetoxy)iodo]benzene (R = Me, BTIB or PIFA) are less influential in the carboxylate ligands of the acetate and trifluoroacetate (around 2.15 Å). (In this Section, we would like to use the abbreviations, PIDA and PIFA, respectively, for the compounds of PhI(OAc)₂ and PhI(OCOCF₃)₂.)

[Hydroxy(tosyloxy)iodo]benzene (HTIB), so-called Koser's reagent, has unsymmetrical two types of hypervalent iodine bonds as the almost collinear O—I—O segment (Fig. 7.4). The geometry at the iodine center is similarly planar T-shaped, a configuration observed with other typical trivalent organoiodine compounds. The structure of HTIB was determined in 1976 [12], and the single-crystal X-ray structural data showed the I—OH distance, 1.94 Å, and the I—OTs distance, 2.47 Å, to be quite longer than that of the former bond. The presence of very long I—OTs bond indicates the significant ionic character of this compound, which is in accordance with later reactivity studies.

The anhydrides of HTIB and relative [hydroxy(methanesulfonyloxy)]iodobenzene were prepared by drying their acetonitrile solutions. Crystallographic structures were obtained for the anhydrides, except that of HTIB. An almost linear alignment of iodine and two types of oxygen ligands in good agreement with hypervalent bonds was observed. In this case, the longer distance between the iodine and bridged oxygen (2.01 Å) compared to that in monomeric [hydroxy(methanesulfonyloxy)]iodobenzene (1.95 Å) influences the I—OMs distance to make it shorter (2.35 Å) [13]. This is rationalized by considering the *trans* influence between the two ligands in the hypervalent iodine bonds [14].

Resulting from the self-assembly in aqueous media, PIDA and its analogues also form oligomeric cationic species. PhI(OCOCF₃)OI(OCOCF₃)Ph was prepared from iodosobenzene ((PhIO)_n) or PhI(OCOCF₃)₂ (PIFA) by reacting with appropriate amounts of strong acids and bases [15]. The structures of μ -oxo bridged dimers,

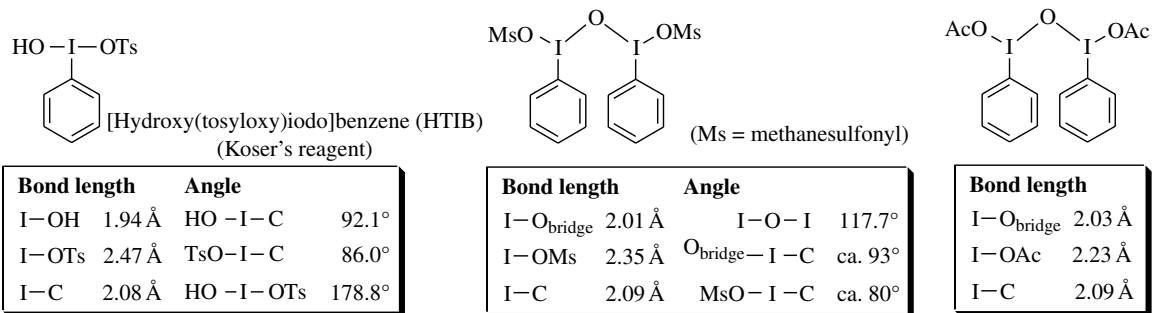


FIGURE 7.4 Structure of HTIB, and dimers of [hydroxy(methanesulfonyloxy)iodo]benzene and iodobenzene diacetate.

$\text{PhI}(\text{OAc})\text{OI}(\text{OAc})\text{Ph}$ and $\text{PhI}(\text{OCOCF}_3)\text{OI}(\text{OCOCF}_3)\text{Ph}$, were well-characterized by X-ray crystallographic analysis. These μ -oxo compounds possess the longer bonds between the iodine and acid ligands, for example, 2.23 Å of the I–OAc distance for $\text{PhI}(\text{OAc})\text{OI}(\text{OAc})\text{Ph}$ compared to 2.16 Å for that of PIDA itself. Recent investigations have revealed that the excellent oxidizing behavior of these μ -oxo bridged dimers was caused by the highly polarized structure and weak binding of the iodine and acid ligands over PIDA and PIFA, especially, in oxidations of phenolic compounds [16].

The crystal structure of a representative heterocyclic pentavalent iodine compound, 1-hydroxy-1,2-benziodoxol-3(1*H*)-one (IBX), was first reported in 1997 [17]. On the other hand, the fine structure of DMP, a related hypervalent iodine reagent very popular for synthetic chemists, was very recently determined more than 10 years later [18]. The proposed structures of these compounds were thus confirmed after their success in broad applications for organic synthesis (Fig. 7.5). These 12–I–5 molecules take the square bipyramidal structures, in which the cyclic structures of IBX and DMP are planar, with the exception of the exocyclic oxygens and acetoxy groups. The bond distance between the iodine and cyclic oxygen is significantly longer in IBX (2.26 Å) than in DMP (2.10 Å) due to the strong *trans* influence of the hydroxy group (I–OH: 1.93 Å) over the acetoxy groups (I–OAc: 2.06–2.11 Å). The observed bond angles are also in accordance with the distorted hypervalent iodine bonds with one conventional covalent bonding between the iodine and phenyl group.

The hypervalent iodine compounds having two carbon ligands are represented in diaryliodonium salts. The configuration of diphenyliodonium chloride ($\text{Ph}_2\text{I}^+\text{Cl}^-$) is similar to other trivalent organoiodine compounds, but has planar dimeric structure in the crystal state [19]. The two $\text{Ph}_2\text{I}^+\text{Cl}^-$ units link through the halogen bridges with mean bond lengths of I–Cl being 3.09 Å (Fig. 7.6), which is remarkably ionic and longer than the covalent bond of iodine chloride by about 0.77 Å. The unique bondings in $\text{Ph}_2\text{I}(\mu\text{-Cl})_2\text{IPh}_2$ dimer are explained as secondary bondings between the iodine atom of $\text{Ph}_2\text{I}^+\text{Cl}^-$ and Cl unit in the other molecule.

Similarly, the T-shaped structures of alkynyl(phenyl)iodonium salts, that is, (ethynyl)phenyliodonium trifluoromethanesulfonate (see Fig. 7.6) [20], and alkenyl(phenyl)iodonium salts, that is, (4-*tert*-butylcyclohexenyl)phenyliodonium tetrafluoroborate [21], are highly ionic. Interestingly, it was found during the characterization that the former compound has the unusual shortest carbon–carbon triple bond (1.15 Å) in the

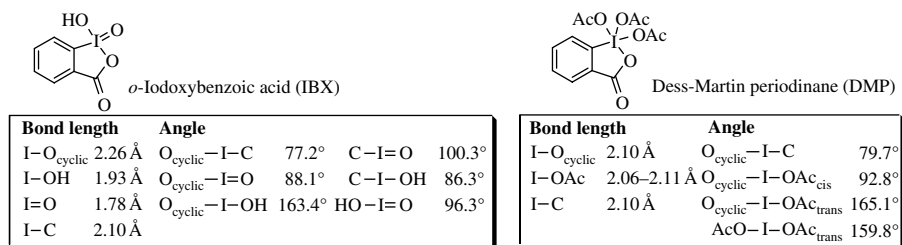


FIGURE 7.5 Structure of IBX and DMP.

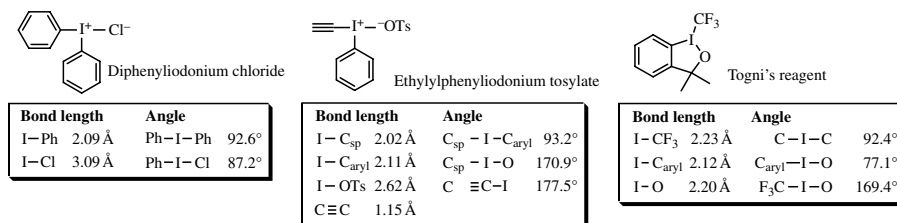


FIGURE 7.6 Structure of diaryliodonium salt, alkynyliodonium salt, and Togni's reagent.

crystal states, which is caused by the substitution of the extremely electron-deficient iodine atom [20].

It is known that five-membered cyclic hypervalent iodine(III) compounds are more stable than their acyclic forms having analogous ligands [22, 23]. For example, stable cyclic iodonanes having labile azido, cyano, and nitrate ligands were prepared in good yields by the ligand exchanges of acetoxy and chloro benziodoxoles with trimethylsilyl compounds or silver nitrate [23]. Later, Togni et al. reported in 2006 the first synthesis of trifluoromethyl benziodoxolone from the corresponding cyclic 1-chloro-1,3-dihydro-3,3-dimethyl-1,2-benziodoxole by a similar approach using trifluoromethyl trimethylsilane [24]. This reagent is particularly useful for electrophilic trifluoromethylation of many nucleophilic substrates, and the so-called Togni's reagent. The T-shaped geometry at the iodine typical for the class of hypervalent iodine compounds is seen with the bond angles that belong to the heterocyclic structure of other hypervalent iodine compounds, but the relatively long bond length between iodine and trifluoromethyl ligand (2.23 Å) compared to that in other organoiodine(I) compounds, which might account for the high electrophilic nature of the trifluoromethyl group. The distinctive feature of Togni's reagent is the considerably higher stability based on the heterocyclic structures than that of their acyclic analogues. This stabilization is usually explained by the bridging of the apical and the equatorial positions by the five-membered ring as well as the better overlap of the lone pair of electrons on the iodine atom with the π -orbitals of the benzene ring.

Iodosobenzene (PhIO) exists as polymeric zigzag forms on the basis of the network of the oxygen bridge between two hypervalent iodine atoms through the hypervalent bond and secondary interaction (Fig. 7.7) [25]. Hence, the two types of bond distances between iodines and oxygen are 2.04 and 2.37 Å, respectively, with the C-I-O bond angle of near 90°. Similarly, iminoiodanes have linear polymeric, asymmetrically bridged structure with the T-shaped geometry around the iodine centers. Indeed, characterization of *N*-tosyl iminophenylidane revealed the formation of the polymeric zigzag chain based on the iodine and nitrogen networks [26]. The polymers consist of monomeric PhINT units, bridged by secondary I...N interactions with a length of 2.48 Å. The extensive I...O and I...N secondary bondings thus make the solid-state polymers soluble only in coordinating solvents that can break the tight networks. The sulfonyliminoiodananes (PhINSO₂R) are used as the versatile nitrene source in many metal-catalyzed amination reactions, since the synthesis and utility of this new class of reagents based on the function of nitrene were demonstrated in the 1970s [27].

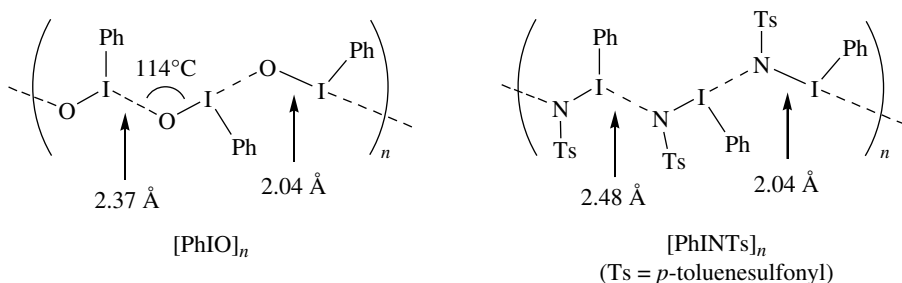


FIGURE 7.7 Oligomeric structures of PhIO and PhINTs.

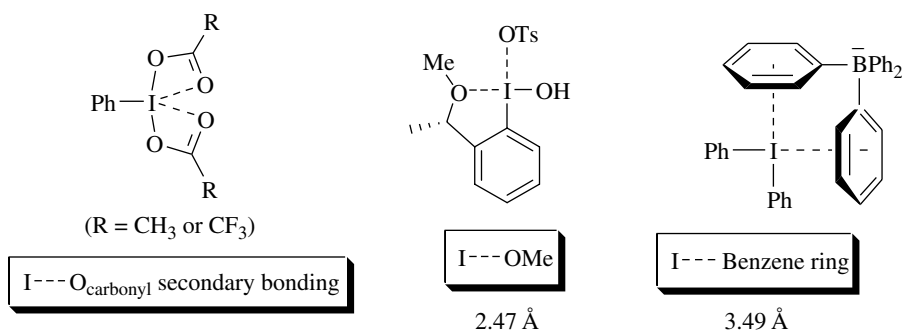


FIGURE 7.8 Secondary bonding in hypervalent iodine molecules at the iodine center.

In [bis(acyloxy)iodo]benzenes ($\text{PhI}(\text{OCOR})_2$, Fig. 7.3), the single-crystal X-ray structural data for these compounds indicate pentagonal planar coordination of iodine together with the primary T-shaped iodine(III) geometry with two weak secondary intramolecular $\text{I} \cdots \text{O}$ interactions with the carboxylate oxygens (Fig. 7.8, left) [11]. The crystal structures of (diacetoxyiodo)benzene and [bis(trifluoroacetoxy)iodo]benzene exhibit the arrangements of two intramolecular secondary contacts between the iodine atom and the Lewis base carbonyl oxygens. The secondary bondings are stronger in the more electronegative ligand, trifluoroacetate (2.81–2.85 Å), rather than the acetoxy groups (3.03–3.15 Å), suggesting the high electrophilicity of the iodine atom of the former [bis(trifluoroacetoxy)iodo]benzene. The presence of the secondary bondings between the iodine and carboxy groups was also confirmed by spectroscopic studies [28].

The secondary interaction of the iodine and oxygen atom was utilized for constructing the pseudocyclic chiral moiety around the iodine center in some electrophilic reagent aiming at asymmetric transformations, such as [hydroxy(tosyloxy)iodo]-[2-(1-methoxyethyl)benzene] (Fig. 7.8, center) [29]. The secondary bonding between the iodine atom and the methoxy group was confirmed (2.47 Å), whose value is apparently smaller than the sum of van der Waals radii. Tetraphenylborate anion (BPh_4^-) can act as a π -ligand toward the hypervalent iodine atom, as shown in the crystal structure of diphenyliodonium tetrafluoroborate (Fig. 7.8, right) [30]. The

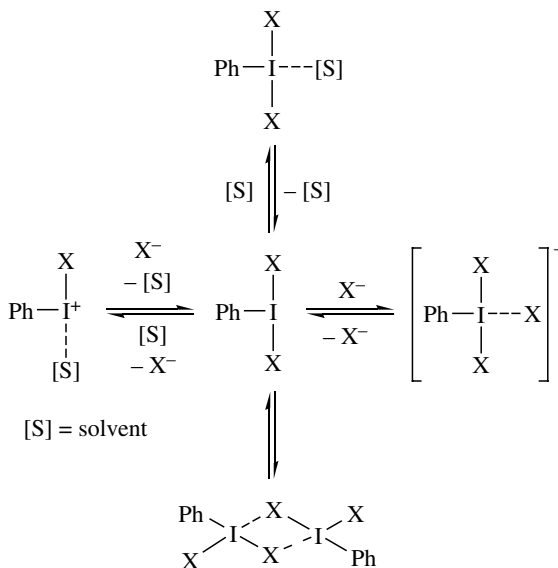


FIGURE 7.9 Equilibrium of PhIX_2 -type hypervalent iodine compound in solution.

phenyl groups of the borate anion coordinate to the iodine center at the interatomic distance of 3.49 Å.

Richter, Koser, and coworkers investigated the solution structure and nature of species in equilibrium in aqueous solutions of phenyliodine(III) organosulfonates [31]. Upon dissolution in water, HTIB ($\text{PhI}(\text{OH})\text{OTs}$) underwent ionization to give hydroxy(phenyl)iodonium cation, PhI^+OH (Fig. 7.9, center to left), which seems to be ligated with at least one solvent molecule, water, at an apical site of the iodine atom. The ion-pair dissociation equilibria were also observed during the photoinitiated cationic polymerizations [32]. The hydroxy(phenyl)iodonium, PhI^+OH , can combine with [oxo(aquo)iodo]benzene, $\text{PhI}^+(\text{H}_2\text{O})\text{O}^-$, a hydrated form of PhIO that is usually observed in the aqueous solution, producing the dimeric μ -oxodiiiodine cation, $\text{Ph}(\text{OH})\text{I}-\text{O}-\text{I}^+(\text{H}_2\text{O})\text{Ph}$, and dication, $\text{Ph}(\text{H}_2\text{O})\text{I}^+-\text{O}-\text{I}^+(\text{H}_2\text{O})\text{Ph}$. The coordination of solvent (Fig. 7.9, center to top), free ligand (center to right), and ligand in hypervalent iodine compound (center to bottom) can even occur in nondissociated hypervalent iodine atom. These equilibria also occur in any hypervalent iodine compounds, and, for example, association and dissociation of (*Z*)-(β -bromoalkenyl)(phenyl)iodonium bromides were observed in chloroform solution and vinyl- λ^3 -iodane dimers were detected [33]. The mechanistic aspects of the solvolysis of these iodonium salts were detailed by Okuyama and Ochiai, respectively [34].

In 1960, Berry proposed a mechanism for the rearrangement, in which D_{3h} geometries of complexes (for the case of five ligands) interconvert to others via a square-pyramidal C_{4v} transition state, while maintaining at least C_{2v} symmetry throughout the entire process. Molecular dynamics of hypervalent iodine compounds at the iodine centers are typically explained by the general guideline of the Berry pseudorotation

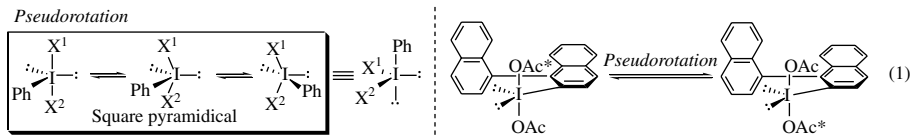


FIGURE 7.10 Pseudorotation of hypervalent iodine compounds at the iodine center.

(BPR) [35]. For the trigonal-bipyramidal structures (Fig. 7.10, left), the exchange of the apical and equatorial ligands concertedly occurs through the bond bending to form square pyramidal structure. The apical ligands, X^1 and X^2 , and equatorial phenyl group stereomutate via the repeated pseudorotation on the iodine center. In general, the pseudorotation rapidly occurs in equilibrium.

On the other hand, it was reported that some cyclic hypervalent iodine compounds are chemically and configurationally stable below 15°C , with the barrier to isomerization being over 15 kcal mol^{-1} [36]. Chiral hypervalent iodine compounds, acetoxiodo(III)binaphthyls, undergo degenerate isomerization of the acetoxyligands at the iodine (Fig. 7.10, Eq. 7.1) [37]. In the spectroscopic studies, the two acetoxyligands are nonequivalent at -10°C in ^1H nuclear magnetic resonance (NMR) and the signals for these groups appear at 1.52 and 2.0 ppm, respectively, as sharp singlets. These two signals coalesce at 34°C to one singlet at 1.73 ppm. The pseudorotation pathways on the iodine are responsible for the degenerate isomerization, and the stereomutation becomes fast on the NMR timescale at room temperature.

7.3 REACTIVITY

In most cases, the reactivities of hypervalent iodine reagents are typically explained by the two-electron-transfer processes. For instance, the oxidations with trivalent iodine compounds (λ^3 -iodanes) typically involve ligand exchange with substrates (Nu^1) at the iodine centers as an initial step and successive reductive elimination for releasing the iodobenzene (PhI) coproduct with attack of nucleophiles (Nu^2), yielding the product $\text{Nu}^1\text{--Nu}^2$ (Fig. 7.11) [38]. In the latter event, both mechanisms via the ligand coupling (LC) and substitution were suggested [39]. The hypervalent iodine(III) atoms possess great electrophilicities that are required for initial interactions with substrates and ligand exchange. The two X ligands serve as good leaving groups in not only the initial ligand exchange but also the last step for the reductive elimination.

The two types of mechanism, associative and dissociative paths, were generally considered during the ligand-exchange processes. For trivalent iodine compounds (Fig. 7.12, PhIX_2), the tetracoordinated species are involved ($[\text{PhIX}_2\text{Nu}]^-$), while the latter dissociative case generates charged iodonium ions ($[\text{PhI}^+\text{X}]$). For an example of tetracoordinated iodanes, the crystal and molecular structures of $[\text{Cl}_3\text{S}]^+[\text{ICl}_4]^-$ and $[\text{PhCH}_2\text{N}^+\text{Me}_3][\text{ICl}_4]^-$ were reported, in which the tetracoordinated anions shape square planar geometry [40]. It was also reported that the treatment of cyclic chloriodinanes with potassium hexafluorocumyl oxide gave the corresponding dialkoxy

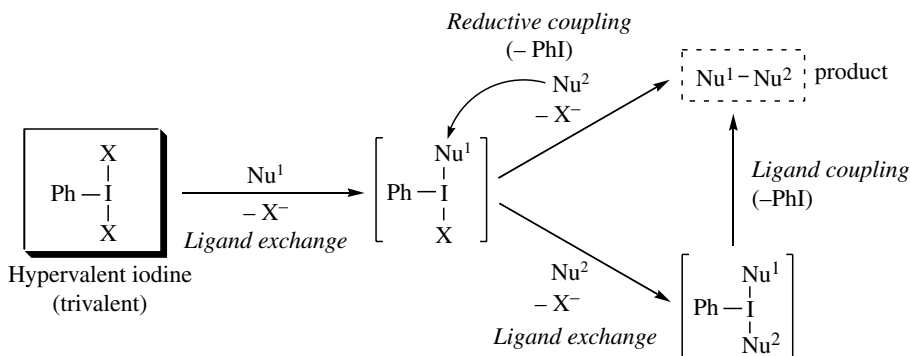


FIGURE 7.11 General reactivity of hypervalent iodine reagent with nucleophiles.

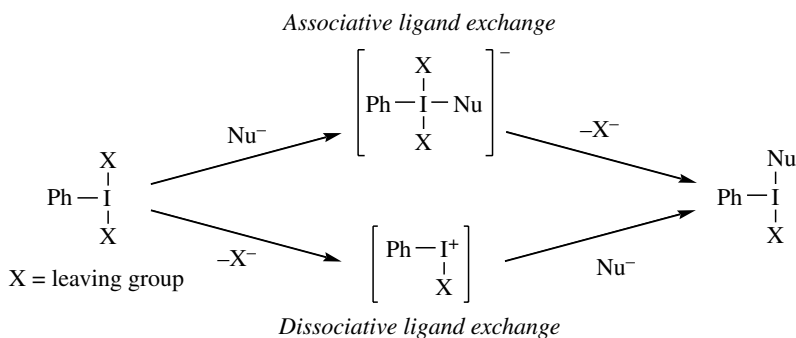


FIGURE 7.12 Two distinct ligand exchange pathways in the reaction of nucleophile.

species $[\text{Nu} = (\text{CF}_3)_2\text{CPhO}]$ [41]. The ligand exchange seems to rapidly occur on the NMR timescale with 0.08–0.10 M concentration in the solvent alcohol, $(\text{CF}_3)_2\text{CPhOH}$, suggesting an associative exchange mechanism. Similarly, it was believed that [methoxy(tosyloxy)iodo]benzene, an acyclic monoalkoxyiodinane, was readily hydrolyzed to HTIB in the presence of water via a tetracoordinated intermediate [42]. On the other hand, strong experimental proof supporting the dissociative path is not reported, but the iodonium ions, $[\text{PhI}^+\text{X}]$, might be present as stabilized solvated forms. Thereafter, the nucleophiles replace the solvent molecular, completing the ligand-exchange process.

The ligand exchange would generally occur for a wide range of nucleophilic molecules and atoms. The reaction of $\text{PhI}(\text{O}_2\text{CR})_2$ ($\text{R} = \text{Ph}$, 4-MeOC₆H₄, 4-O₂NC₆H₄, etc.) with lithium acetylides smoothly gave alkynylphenyliodonium carboxylates by the ligand exchanges [43]. The reversible ligand exchanges with alcohols were involved before the generation of oxygen-centered radicals [44] as well as during the oxidations using pentavalent iodine reagents, IBX and DMP [45]. The reaction of $\text{PhI}(\text{OCOCF}_3)_2$ with potassium phthalimide, a nitrogen nucleophile, gave λ^3 -iodane phthalimide [46]. The hypervalent iodine species with sulfur ligands, $[\text{PhI}(\text{SC}_6\text{F}_4\text{H})_2]$ and $[\text{PhI}(\text{SCN})_2]$, were in situ prepared from $\text{PhI}(\text{OAc})_2$ or PhICl_2 with 2,3,5,6-tetrafluorothiophenol and

trimethylsilyl isothiocyanate, respectively, for the disulfenylation and thiocyanation of alkynes and alkenes [47, 48]. [Hydroxy(tosyloxy)iodo]arenes ($\text{ArI}(\text{OH})\text{OTs}$) can yield diaryliodonium salts with introduction of second aromatic rings by ligand transfer from silylated, stannylated, and borylated aromatic compounds [49, 50]. Similarly, vinyl and alkynyliodonium salts were synthesized from vinyl and alkynylsilanes by the ligand exchanges upon treatment with indosobenzene [51]. A variety of functionalized alkynyliodonium salts were prepared in good yields via the iodonium-transfer process between alkynylstannanes and $\text{PhI}^+\text{CN F}_3\text{CSO}_3^-$ [52]. Hypervalent iodine compounds (ArIX_2) reacted with organolithium reagents (RLi) instantaneously even at -80°C , forming unstable all-carbon ligated hypervalent iodine species, ArIR_2 [53]. It was also reported in the same work that the ligand exchange even occurred between the two molecules of hypervalent iodine compounds, as shown in Figure 7.13, because of the facility of this process on the iodine center.

It was reported that treating *trans*-vicinal iodo trifluoroacetates with peracids gave the corresponding *cis*-hydroxy trifluoroacetates by an oxidative displacement reaction. *m*-Chloroperbenzoic acid (*m*CPBA) also induced the oxidations of alkyl iodides at room temperature, yielding alcohols and/or their derivatives, or olefins depending on the conditions and structure of substrates (Fig. 7.14) [54]. The reactions probably involve the initial formation of some labile alkyl- λ^3 -iodanes followed by rapid reductive elimination of the in situ formed hypervalent iodine group. This accounted for the excellent leaving ability of the iodanyl groups and their high tendency of converting into more stable monovalent iodine compounds.

Owing to the excellent leaving group ability of the aryl iodide moiety, diaryliodonium salts are much more reactive than the usual aryl halides. Similarly, the vinyliodonium salts are regarded as the highly activated alternative of vinyl iodides in substitution reactions. The high reactivities of aryliodonium salts in general formula, $\text{Ar}(\text{R})\text{I}^+\text{X}^-$, in these reactions are well expressed by the term “hypernucleofuge.” Surprisingly, it was determined that the leaving group ability of the iodobenzene moiety in [(4-*tert*-butylcyclohexenyl)phenyl]iodonium salt is about 10^6 times greater than that of the superleaving group, triflate, in 4-*tert*-butylcyclohexenyl triflate (Fig. 7.15) [55, 56]. Indeed, formation of cyclohexenyl carbocation by heterolysis during the solvolysis

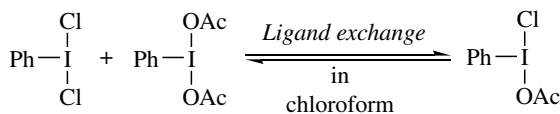


FIGURE 7.13 Ligand exchange between hypervalent iodine molecules.

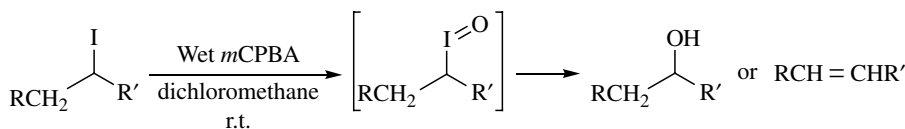


FIGURE 7.14 Early example of hypervalent iodine moiety as leaving group.

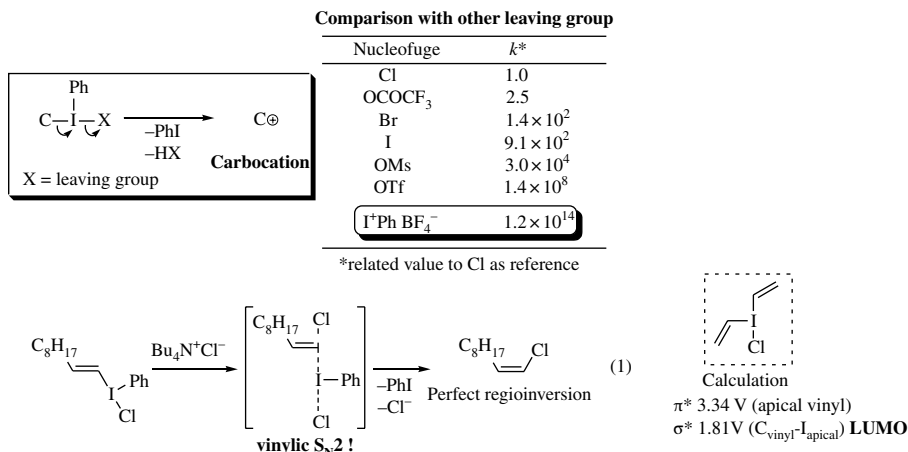


FIGURE 7.15 Relative index of leaving group ability of hypervalent iodine group versus others. (1) Unprecedented vinylic S_N2 reaction utilizing the hypernucleofuge.

of the tetrafluoroborate salts spontaneously proceeded at room temperature in alcohols. This came from the hypervalency of the iodine atom, since the onium salts with tetrahedral geometries showed only poor ability as leaving groups.

The detailed mechanistic investigations of the nucleophilic substitutions of alkenyliodonium salts were presented by Ochiai and Okuyama [34]. It is surprising to find that the excellent nucleofugality of the λ³-phenyliodonium group even caused the unprecedented S_N2-type nucleophilic substitutions at the vinylic carbons of the iodonium salts with exclusive stereoinversion, a hitherto unknown process depending on the structure of substrates, nature of nucleophiles, and reaction conditions (Fig. 7.15, Eq. 7.1) [57]. For example, the evidence that the substitution reaction proceeds via a concerted bimolecular S_N2 mechanism was presented when (*E*)-β-alkylvinylidonium tetrafluoroborates were treated with tetrabutylammonium halides (Bu₄N⁺X⁻, X = Cl, Br, I), which resulted in exclusive introduction of the halide groups with perfect regioinversion of the alkene geometry.

The nucleophilic substitution mechanisms at the vinylic carbons were further divided to involve in-plane nucleophilic attack on the σ* orbital of the iodine–vinyl carbon and out-of-plane attack on the π* orbital of the vinyl moiety. The in-plane nucleophilic vinylic substitutions were well-rationalized by the theoretical studies, and computational quantum chemistry calculations have suggested the overview of the actual mechanistic route [58]. In the ab initio MO calculations of chloro(divinyl)-λ³-iodane, the σ* orbital lies lower in energy than the π* orbital (1.81 vs. 3.34 eV). Hence, the LUMO in the iodonium salts lies in the σ* orbital, which is in marked contrast with the vinyl halides having π* LUMO. The presence of the low-lying σ* orbital is responsible for the unusual in-plane nucleophilic attack of the iodonium salts and excludes common reaction pathways in other organic molecules.

Strong bases would induce reductive α-elimination of λ³-iodanes to afford generation of carbenes (Fig. 7.16). Evidence for generation of alkylidenecarbenes was

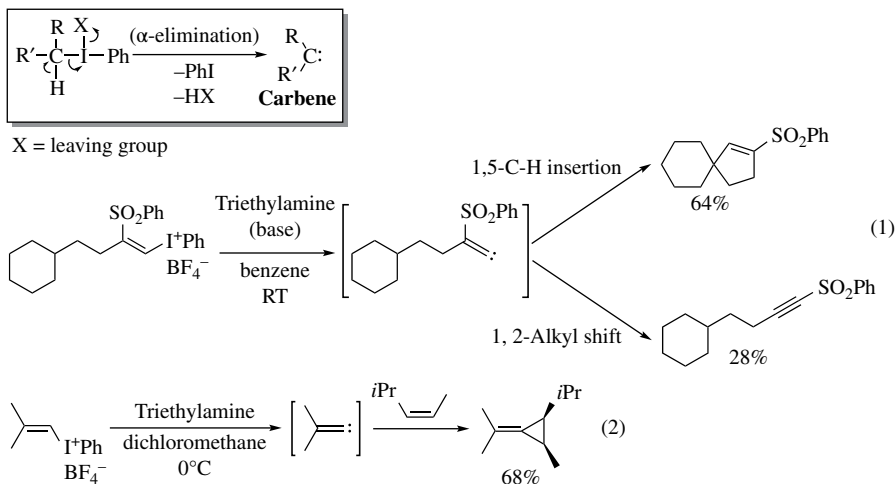
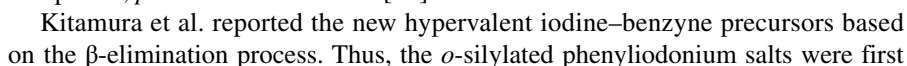
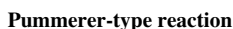


FIGURE 7.16 α -Elimination of hypervalent iodine group generating carbenes.

obtained in the deuterium experiment by treating 1-alkenylidonium salts with a base. The alkyne-forming reaction involved alkylidenecarbenes via reductive α -elimination followed by the 1,2-deuterium shift [59]. Depending on the structure and reaction conditions, the unsaturated carbenes would undergo typical reactivities of free carbenes, resulting in the 1,2-rearrangement to alkyne, intramolecular insertion of the carbon–hydrogen bond, and cyclopropanation by trapping with alkenes. For example, $[\beta$ -(phenylsulfonyl)alkylidene]carbenes generated from the (Z)- $[\beta$ -(phenylsulfonyl)alkenyl]iodonium tetrafluoroborates by base treatment predominantly underwent intramolecular 1,5-C–H insertions to yield 1-(phenylsulfonyl)cyclopentenones rather than the 1,2-migration leading to alkynes (Fig. 7.16, Eq. 7.1) [60]. The lack of regioselectivity for the intramolecular insertion of carbenes strongly suggests the involvement of a free alkylidenecarbene. 2-Methyl-1-propenylidene carbene, generated from (2-methylpropenyl)phenyliodonium tetrafluoroborate to *cis*- and *trans*-4-methyl-2-pentene, was perfectly stereospecific, indicating the generation of singlet carbene (Eq. 7.2) [61]. Furthermore, the small negative Hammett values for the cyclopropanation suggested that alkylidenecarbene is mildly electrophilic.

The alternative reductive β -elimination can occur in iodonanes binding to the carbon ligand as well as the heteroatomic ligand (Fig. 7.17). The β -*syn*-elimination process was earlier reported for the in situ generated λ^3 -iodanyl species in the conversion of some iodoalkanes to alkenes under oxidative conditions [62]. The *anti*-elimination process is also quite facile due to the high nucleofugality of the iodanyl group as supported in the difficulty of isolation of vinylidonium salts of corresponding Z-isomers [63].

The β -elimination process of a heteroatomic ligand is well-recognized as a key step in the oxidation of alcohols to carbonyl compounds in hypervalent iodine chemistry. Takaya et al. reported the first use of PhIO for the oxidation of activated alcohols such as benzyl alcohols under reflux conditions in dry dioxane (Fig. 7.17, Eq. 7.1) [64]. Needless to say, the well-known alcohol oxidations with pentavalent



introduced for the effective generation of benzyne utilizing the hypernucleofuge of the hypervalent iodine atom [74]. Benzyne can be generated from specific iodonium salts by the fluoride-triggered desilylative β -elimination upon treatment with tetrabutylammonium fluoride for the reactions with trapping agents under mild conditions (Fig. 7.18).

Surprisingly, the facile β -elimination of the hypervalent iodine atom might allow the rapid generation of even the highly strained alkynes, for example, norbornyne and cyclohexynes, from the corresponding cyclic alkenyliodonium salts [75].

Introduction of the oxygen functionalities to the α -carbon of enolizable carbonyl compounds is a famous process in hypervalent iodine chemistry effectively occurring by simple treatment with $\text{PhI}(\text{OAc})_2$ in acetic acid [76] as well as other hypervalent iodine reagents in suitable conditions [77] (see also Chapter 16). The α -iodanyl ketone intermediates produced during the reactions can participate in the associative $\text{S}_{\text{N}}2$ displacement of the iodanyl part by acetic acid, affording the α -acetoxy products with liberation of iodobenzene (Fig. 7.19, Eq. 7.1). The alternative $\text{S}_{\text{N}}1$ -like process to generate the α -acyl cation seems to be difficult and excluded by considering the high electron deficiency of the unstable cationic species.

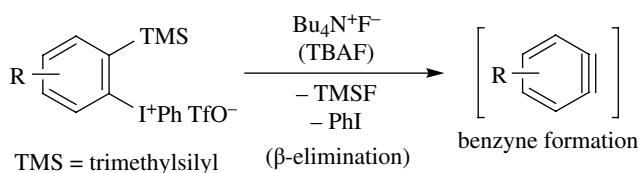


FIGURE 7.18 Facile formation of benzyne.

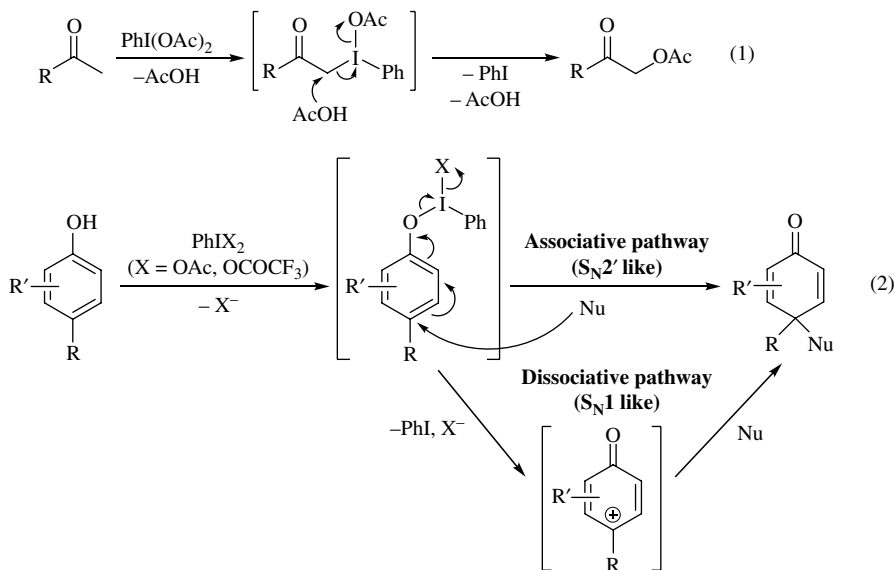


FIGURE 7.19 Reductive elimination pathways. (1) $\text{S}_{\text{N}}2$ displacement during α -acetoxylation (2) Ambient associative and dissociative eliminations in phenolic oxidations.

On the other hand, pathways would alter to dissociative that involve cationic intermediates for electron-rich substrates and cation-stabilizing molecules depending on the conditions, which was partially supported with several theoretical and experimental evidences [78]. The key intermediate, phenoxy- λ^3 -iodane species, in the phenolic oxidations using hypervalent iodine reagent would alternatively produce discrete phenoxenium ions by dissociation of iodobenzene from the intermediate (Eq. 7.2). Subsequent attack of the nucleophile delivers quinones and related dearomatized products. Nonetheless, the attack of a nucleophile on the intermediate in an associative manner with release of iodobenzene is still possible depending on the substrates and reaction conditions in favor of the S_N1 -like pathway.

In most cases, the reactivities of hypervalent iodine(III) reagents are typically explained by the two-electron-transfer processes. On the other hand, the same reagents are also known to act as selective and efficient single-electron-transfer (SET) oxidizing agents for electron-rich aromatic compounds if treated under specific reaction conditions [79, 80]. Kita et al. launched the first report of the SET-oxidizing ability of hypervalent iodine compounds in 1991 for the novel and direct nucleophilic substitution of *p*-substituted phenyl ethers (R = alkyl) with azide (N_3^-) using a hypervalent iodine(III) reagent, $PhI(OCOCF_3)_2$, in the highly polar, but low nucleophilic fluoroalcohol solvents, 1,1,1,3,3,3-hexafluoro-2-propanol (HFIP) or 2,2,2-trifluoroethanol (TFE) (Fig. 7.20) [79]. The phenyl ethers are generally inert to the iodine(III) reagents and would not react via the ligand exchange of the protected phenolic oxygen. The generation of aromatic cation radicals induced by the SET oxidation process through the charge-transfer (CT) complex of $PhI(OCOCF_3)_2$ and the phenyl ethers could be determined based on detailed UV and Electron Spin Resonance (ESR) spectroscopic studies. It was later clarified that the reactive intermediate was then effectively trapped by general nucleophiles, enabling the selective introductions of different kinds of nucleophiles (N_3^- , AcO^- , ArS^- [Ar = aryl], SCN^- , and β -dicarbonyl compounds, etc.), furnishing the oxidative aromatic substitution of a variety of *p*-substituted electron-rich phenyl ethers. This reactivity was applied in the synthetic courses of naturally occurring or nonnatural molecules having important and diverse biological actions (see the applications in the following section of this chapter and more details in Chapters 16 and 17). The umpolung of the aromatic rings was carried out without the use of any metal oxidant. That is the first case confirming the aromatic cation radical involvement during the hypervalent iodine-mediated oxidations,

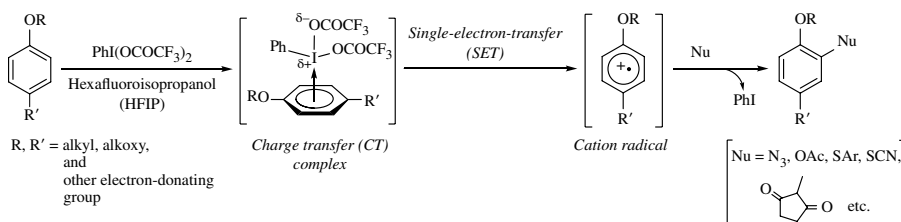


FIGURE 7.20 Unique SET oxidation ability of hypervalent iodine reagent toward phenyl ether rings.

and the organoiodine compounds, specifically $\text{PhI}(\text{OCOCF}_3)_2$, were determined to have an excellent SET oxidation ability toward electron-rich aromatic rings.

On the other hand, the side-chain activation of phenyl ethers having suitable functional tethers for initiating the oxidations is a powerful strategy in the synthesis of dearomatized spirocyclic compounds. The first side-chain activation report was the activation of the enamide tethers of the substituted phenols for spirocyclizations during the synthetic studies of natural products (see Section 7.4) [81]. For example, the cyclization of phenol ethers bearing alkyl aminoquinones proceeded using hypervalent iodine reagent via this type of activation mode, affording azacarbo-cyclic spirodienone compounds (Fig. 7.21).

The in situ formed amido- λ^3 -iodane species having a suitable cation stabilizing group, such as the methoxy group on the nitrogen at the amide groups, would release nitrenium intermediates. This was successfully applied by Kikugawa and Wardrop by the oxidative coupling of *N*-methoxyamides with aromatic rings (Fig. 7.22, Eq. 7.1) [82] and oxidative dearomatizing spiro-lactamizations [83].

Hofmann rearrangement with trivalent hypervalent iodine reagents in the presence of moisture transforms amides to the corresponding amines possessing one less carbon atom (Fig. 7.22, Eq. 7.2). The modern versions of the Hofmann rearrangement can proceed under mildly acidic or neutral conditions [84, 85]. This involves the concerted process of elimination of iodobenzene and migration of the amide carbon group. Likewise, Moriarty's group reported that the oxidation of styrene with PhIO in methanol can afford the phenyl-rearranged dimethyl acetal as a result of the similar concerted oxidative rearrangement [86].

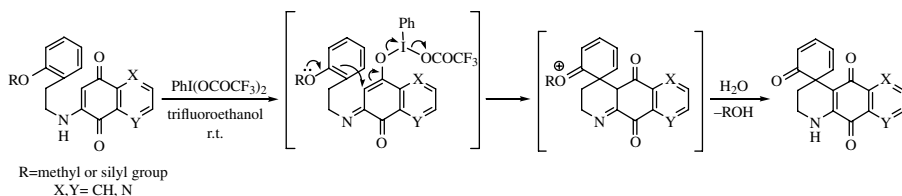


FIGURE 7.21 Alternative oxidation of phenyl ether compounds: side-chain activation.

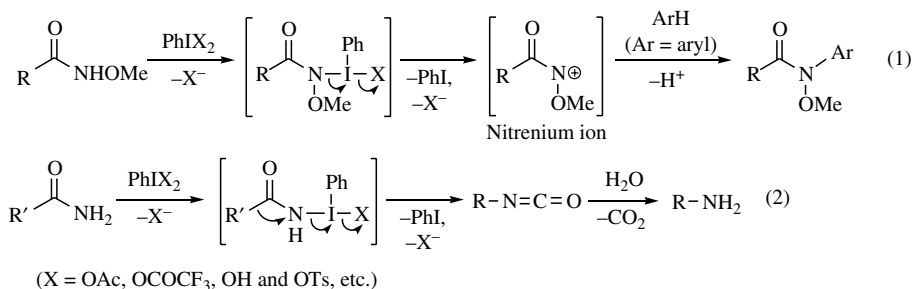


FIGURE 7.22 Dissociative and associative elimination pathways for amido- λ^3 -iodanes.

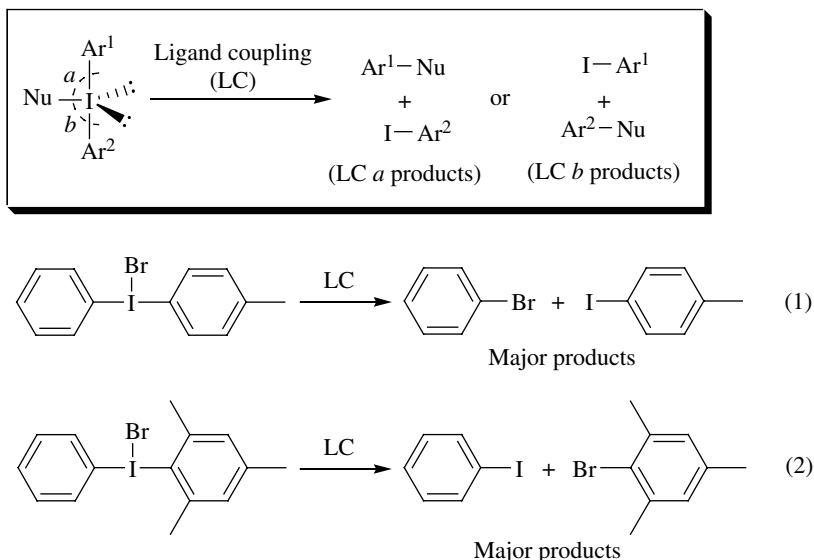


FIGURE 7.23 Ligand coupling at the hypervalent iodine center.

Regarding the oxidative bond-forming event using hypervalent iodine reagents, the introduction of nucleophiles toward substrates would possibly occur via the LC mechanism at the iodine center (Fig. 7.23) [87]. In general, the arylation of nucleophiles (Nu) with diaryliodonium salts ($\text{Ar}^1\text{I}^+\text{Ar}^2$) is assumed to involve the tricoordinated intermediate (Fig. 7.23, $\text{Ar}^1\text{Ar}^2\text{INu}$) before the LC steps [88]. Owing to the competition of the two possible LC pathways of Nu and Ar^1 (LC path *a*) or Nu and Ar^2 (LC path *b*) at the iodine atoms in the intermediates, a mixture of two types of biaryl products, Ar^1Nu and Ar^2Nu , were typically obtained in the unsymmetrical salts ($\text{Ar}^1 \neq \text{Ar}^2$). Early studies revealed that the products obtained from these two pathways were effected by both electronic and steric factors of the two differential aryl rings (Ar^1 , Ar^2), where the nucleophiles would preferentially be introduced to a relatively electron-deficient aryl ring and/or sterically congested *ipso* carbon atom [89]. The latter interesting phenomenon is the so-called *ortho* effect, and nucleophiles are preferentially installed at the more hindered carbon of the aromatic rings. Thus, thermal decomposition of phenyl(*p*-tolyl)bromide yielded bromobenzene and *p*-iodotoluene as major products from the preferred LC outcomes (see Eq. 7.1). Here, the reaction was in preference of the electronic factor. On the other hand, mesityl(phenyl)iodonium bromide allowed the biased production of bromomesitylene by the “*ortho* effect” over the electronic factor (Eq. 7.2). For theoretical prediction of the LC selectivities, Widdowson et al. hypothesized the equatorial deposition of the bulky group in the geometry of the tricoordinated diaryliodonium fluorides based on the knowledge from the *ab initio* MO calculations [90].

Usually, the LC mechanisms are believed to proceed via a concerted process with retention of configuration of the stereo- and regiocenters of the ligands. For example,

nucleophilic vinylic substitutions of the *Z*-isomer of alkenyl(phenyl)iodonium salts with tetrabutylammonium halides resulted in retention of the configuration of the alkenyl moiety, yielding vicinal (*Z*)-alkenyl halides in only a stereoselective manner [91].

Some hypervalent iodine compounds having a specific ligand, such as derived from organic peroxides, can induce thermal homolytic cleavage between the iodonium atom and the ligand to produce radical species, even at low temperature [92]. The homolytic cleavage of the putative and labile iodanyl azides were found to induce azidations at the benzylic positions and α -site of the heteroatoms, such as in *N,N*-dimethylanilines. The iodosylbenzene/trimethylsilyl azide reagent combination to induce direct *N*-alkyl azidation of dimethylanilines and $\text{PhI}(\text{OCOCF}_3)_2$ with trimethylsilyl azide for the benzylic azidation of *p*-alkylanisoles were independently reported by Magnus et al. [93] and Kita's group [94] (Fig. 7.24, Eq. 7.1). Similar radical processes also occurred with the thermal decomposition of $\text{PhI}(\text{OAc})_2$ in the presence of sodium azide, and this method aided the generation of carbon-centered radicals by hydrogen abstraction from the solvents of alcohols, ethers, and aldehydes.

The preparation, structural study, and chemistry of stable cyclic azidoiodinanes derived from benziodoxole were reported by Zhdankin's group [95]. The cyclic azidoiodinanes were revealed to initiate similar radical processes upon heating at 80–132°C, which are potentially useful reagents for direct azidation of organic substrates.

The detailed investigations for radical reactivities of the cyclic hypervalent (*tert*-butylperoxy)iodanes were provided by Ochiai et al. in the 1990s [96]. It was clarified that the *in situ* formed 1-(*tert*-butylperoxy)-1,2-benziodoxol-3(1*H*)-one would oxidize benzyl and allyl ethers to the esters at room temperature in the presence of alkali metal carbonates (Fig. 7.24, Eq. 7.2). The (*tert*-butylperoxy)iodane can generate the *tert*-butylperoxy radical and an iodine-centered radical, even at room temperature via rapid homolytic bond cleavage of the hypervalent iodine(III)–peroxy bond. The strong evidence of the hydrogen abstraction by these radical species was obtained by the detection and trapping of the generated carbon radicals with a stable nitroxyl radical agent, such as 2,2,6,6-tetramethylpiperidine 1-oxyl (TEMPO).

Suárez et al. have investigated for a long time the reactivities of alkoxy radicals generated by the homolytic decompositions of the iodine(III)–alkoxy bonds. The photolysis of hydroxy compounds in the combination of $\text{PhI}(\text{OAc})_2$ and molecular iodine led to the efficient generation of alkoxy radical derivatives, which relayed to carbon-centered radicals by intramolecular hydrogen abstraction of organic compounds, typically, carbohydrates, to finally produce the corresponding cyclic ethers in good yield [97]. The photolysis was also valuable in nitroamines, cyanoamines, and phosphoramidates for neutral aminyl radical generations for other synthetic applications [98]. In addition to these, some other types of radical processes are documented in greater detail in the following section (see Section 7.4) as well as in Chapters 16 and 17.

The benzylic oxidations and other C–H oxidations with IBX, a pentavalent iodine reagent, were proposed to involve a SET event from the substrates to the iodine atom [99]. The reaction mechanism of the oxidation processes was well-studied



FIGURE 7.24 Homolytic cleavage of hypervalent iodine bonds. (1) Radical azidation (2) Benzylic oxidation.

by Nicolaou's group, and the oxidation potentials and cyclization rates of a set of *N*-aryl-*N*-(phenylthio)amides were in good accord with the mechanism invoking SET from an anilide molecules to the iodine(V) atom of a solvent-activated IBX, followed by loss of a proton to produce carbon-centered radical species for the C–H oxidations.

One of the other important characteristics of hypervalent iodine atoms is the highly inductive electronic nature as a substituent [100]. The electron-deficient alkynyliodonium salts acted as a dienophile to readily undergo Diels–Alder-type cycloaddition at room temperature with a range of dienes, affording functionalized vinyliodonium adducts [51, 101]. The large positive Hammett substitution constants of hypervalent iodine atoms also allowed the unsaturated iodonium salts to act as a good Michael acceptor [102–104]. The fates of the additions, such as carbene generation and ylide formation, were highly dependent on the nature of the substrates, reaction conditions, and structure of the products, as described in the personal records and in a part of several reviews [105]. The α -vinyl protons of the vinyliodonium salts are quite acidic by taking advantage of the presence of electron-withdrawing iodyl groups, which is utilized for the formation of alkylidene–carbene iodonium ylides as well as the ylides of active methylene compounds [106, 107]. The fluoride-assisted elimination of the silyl group of α -silyl vinyliodonium salts can also occur to generate iodonium ylides [108].

The wide array of reactivities of hypervalent iodine compounds are quite miscellaneous. With the earlier-mentioned summarization, the more detailed discussions of the reactivities of hypervalent iodine reagents are thus referred to in several comprehensive publications [2, 3].

7.4 APPLICATION

7.4.1 Synthesis of Natural Products

Recently, hypervalent iodine reagents have received a great deal of attention in organic synthesis due to their low toxicities, ready availabilities, easy handlings, and reactivities similar to that of heavy metal reagents and anodic oxidations. A variety of available reactions for natural product syntheses have been developed based on the reactivities mentioned in the earlier section, and hypervalent iodine reagents are now extensively accepted for use in natural product syntheses as a mild, safe, and economical alternative to heavy metal reagents [109]. These reactions are expected to be utilized for pharmaceutical and agrochemical processes due to their safety and mild reaction conditions. In this section, the outline and aspects of hypervalent iodine-induced reactions that are used in the key reactions for the total syntheses of natural products are briefly illustrated for the purpose of update.

Pioneering studies on hypervalent iodine-induced reactions for total syntheses of several natural products were reported by Kishi et al. in the 1970s. By using the hypervalent iodine-induced oxidative cyclization of indole, the formal stereospecific total synthesis of sporidesmin A, a toxic metabolite of *Pithomyces chartarum*, was accomplished, albeit at low yields of the key oxidative cyclization of the tryptamine derivative mediated by hypervalent iodine reagent (Fig. 7.25) [110].

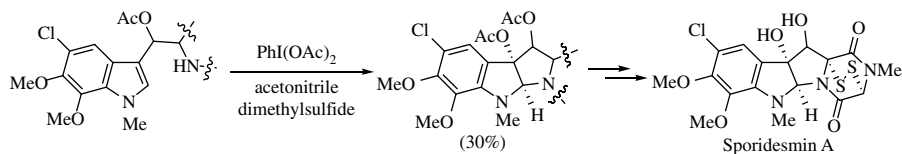


FIGURE 7.25 Early report of hypervalent iodine reagent in natural product synthesis.

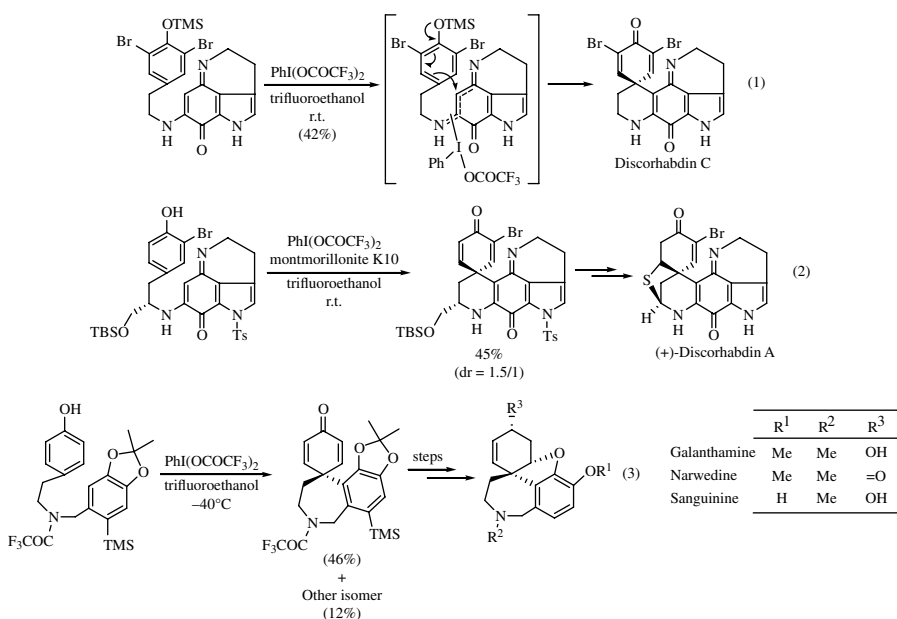


FIGURE 7.26 Synthesis of spirocyclic natural products utilizing hypervalent iodine-induced biomimetic phenolic oxidations.

Other early applications of hypervalent iodine reagents in natural products are the total syntheses of bioactive alkaloids, that is, salutaridine, (–)-codeine, and 6a-epipretazettine by Szanty’s and White’s groups in the early 1980s [111].

In 1987, Kita et al. first developed a general and high-yielding route to spiroacetones and quinone monoacetals by phenolic oxidations with hypervalent iodine reagents, specifically PIFA [112]. Based on their contributions, PIDA and PIFA have come to play particularly important roles in replicating the biomimetic phenolic oxidation processes under mild conditions for the total syntheses of biologically important natural products and their pivotal intermediates [113]. The research group accomplished the total synthesis of discorhabdin C, an antitumor marine alkaloid, via hypervalent iodine oxidation of the *O*-silylated phenol derivative to the azacarbocyclic spirodienone as a key step (Fig. 7.26, Eq. 7.1) [114]. Thus, the phenethylaminoindole was treated with $\text{Me}_3\text{SiOC(OMe)=CHMe}$ followed by the oxidative spirocyclization with PIFA in fluoroethanol to give the spiropyrroloquinolinedione natural product. The total synthesis of more complex sulfur-linked discorhabdin A

was later reported by the same group based on the diastereoselective oxidative spirocyclization of the phenolic precursors using the hypervalent iodine reagent (Eq. 7.2) [115]. A similar treatment of norbelladine derivatives using PIFA employed a mild and efficient method for preparing *Amaryllidaceae* alkaloids, galanthamine for the treatment of Alzheimer's disease as a selective acetylcholinesterase inhibitor as well as related alkaloids, such as narwedine, norgalanthamine, sanguinine, lycoramine, and maritidine (Eq. 7.3) [116].

One of the recent applications of phenolic oxidations in these few years includes the first asymmetric synthesis of the natural indole alkaloid (+)-decursivine [117]. The key step is the PIFA-mediated intramolecular oxidative [3 + 2] cycloaddition of 5-hydroxy tryptophan with a substituted cinnamamide in a highly diastereoselective manner (Fig. 7.27, Eq. 7.1). Using PIDA, highly efficient total syntheses of the 11-membered cyclic aspercyclide A and its analogues have been achieved by chemo- and regioselective intramolecular oxidative phenolic coupling from differently substituted diphenols (Eq. 7.2) [118]. In addition, oxidative 1,2- and 1,3-alkyl shifts of phenol derivatives mediated by a hypervalent iodine reagent were utilized for the rapid synthesis of several functionalized polycyclic systems as well as a formal synthesis of acetylaspidoalbidine, a hexacyclic alkaloid belonging to the *Aspidosperma* family [119].

As described in the previous section, the functionalizations of carbonyl compounds at the α -carbon represent one of the important transformations mediated by hypervalent iodine reagents established early on by Koser and Moriarty. A broad range of both carbon and heteroatom substituents can be introduced into the α -positions [120]. In particular, the α -oxygenated carbonyl compounds obtained are versatile intermediates in organic synthesis. One example in total synthesis is the

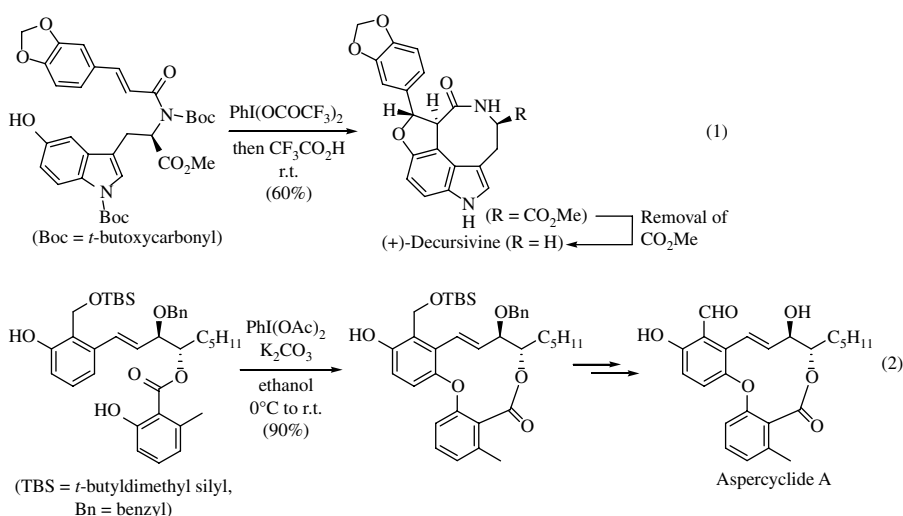


FIGURE 7.27 Total syntheses of decursivine and aspercyclide by hypervalent iodine-induced phenolic couplings.

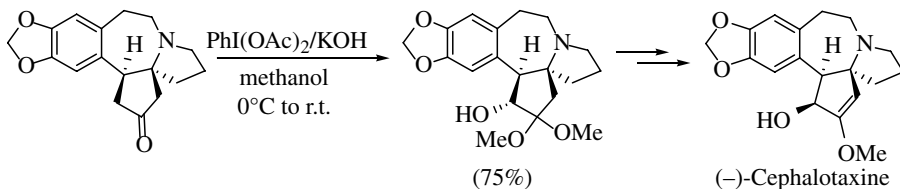


FIGURE 7.28 α -Hydroxylation of carbonyl moiety in cephalotaxine structure.

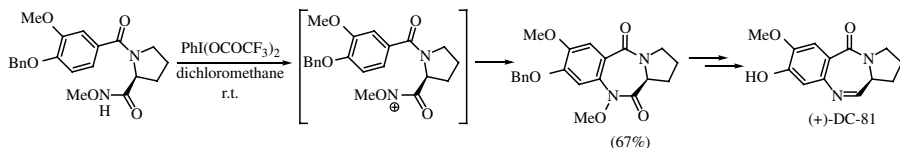


FIGURE 7.29 Oxidative aromatic C–H amidation for construction of DC-81 core structure.

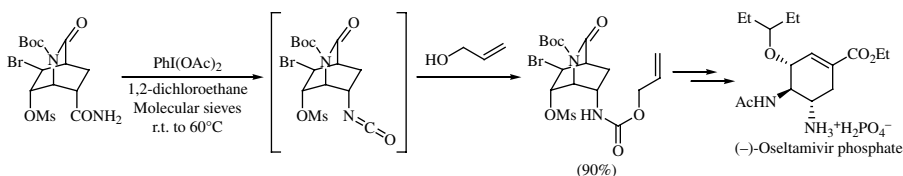


FIGURE 7.30 Hofmann rearrangement in application of aseltamivir synthesis.

late-stage introduction of the α -hydroxy group into the cephalotaxine structure, the parent member of a class of structurally unique antileukemia Cephalotaxus alkaloids (Fig. 7.28) [121].

Treatment of *N*-methoxyamides with PIFA generated electron-deficient nitrogen species, nitrenium ions, which can react intra- or intermolecularly with an aromatic group and other π -bonds (see Fig. 7.22, Eq. 7.1) [82, 83]. This was applied, for example, for synthetic access to the antitumor antibiotic DC-81 (Fig. 7.29) [122]. The key cyclization step embraced the generation of *N*-acylnitrenium intermediate and its successive intramolecular trapping by the aromatic ring. Hofmann-type rearrangement of primary amides using hypervalent iodine reagents (see Fig. 7.22, Eq. 7.2) [85] was used in several total syntheses, such as for the practical synthesis of the influenza drug (–)-oseltamivir phosphate (Fig. 7.30) [123].

The Pummerer-type reaction using hypervalent iodine reagent was utilized for the total synthesis of a sulfur-containing pyrroloiminoquinone alkaloid, (\pm)-makaluvamine F [124]. The reactions leading to the construction of the α -amino dihydrobenzothiophene part involve the efficient cyclization of the benzyl thioether followed by azidation at the α -position of the sulfur group of the dihydrobenzothiophene via the Pummerer-like mechanism (Fig. 7.31).

Feldman's group reported that the oxidative cyclization of a phenylthiolated dihydrooroidin derivative by hypervalent iodine reagent was triggered by the extended

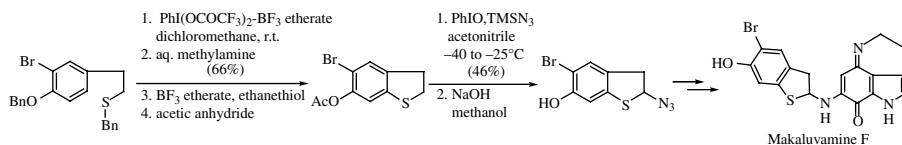


FIGURE 7.31 Oxidative aromatic C–H sulfenylation and aliphatic α -azidation during the course of makaluvamine synthesis.

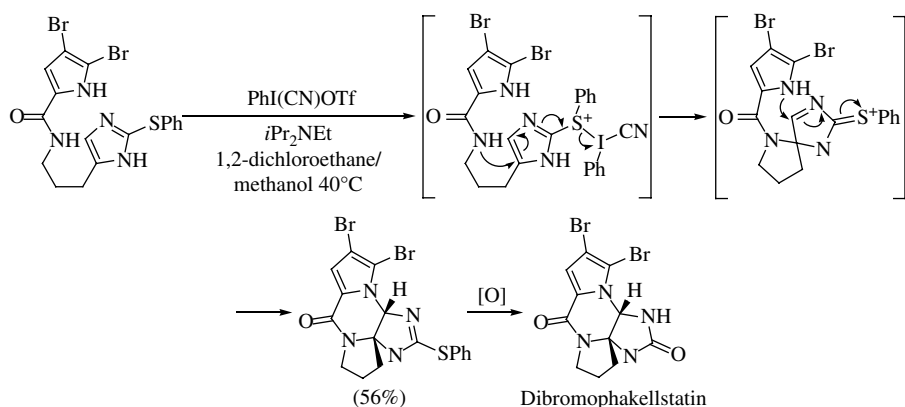


FIGURE 7.32 Synthesis of dibromophakellstatin core structure via Pummerer-like reaction.

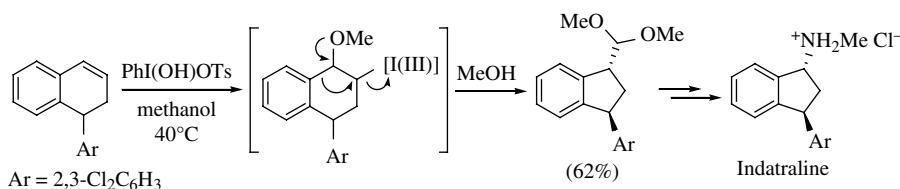


FIGURE 7.33 Ring contraction in indatraline synthesis.

additive Pummerer mechanism for the sunfenylated imidazole ring (Fig. 7.32) [125]. The effective transformation using $\text{PhI}(\text{CN})\text{OTf}$ served the biomimetic approach to the marine alkaloids, (\pm)-dibromophakellstatin and its family.

HTIB promotes ring contraction of 1,2-dihydronaphthalenes, which is an efficient method to regiospecifically construct *trans*-1,3-disubstituted indane ring systems [126]. The reaction proceeds via 1,2-alkoxy iodanylation of alkene unit followed by rearrangement (Fig. 7.33). The new approach for the total synthesis of (\pm)-indatraline featured this strategy as the key step.

The PIFA-mediated domino reaction of 2,3-epoxy-1-alcohols leading to the lactols involves ring opening of epoxide by water and the subsequent oxidative cleavage of the cyclic 1,2-diol intermediates (Fig. 7.34, Eq. 7.1) [127]. The bicyclic lactol structures were directly obtained in a single operation, and the reaction is applicable to the construction of an optically active compound, thus enabling the

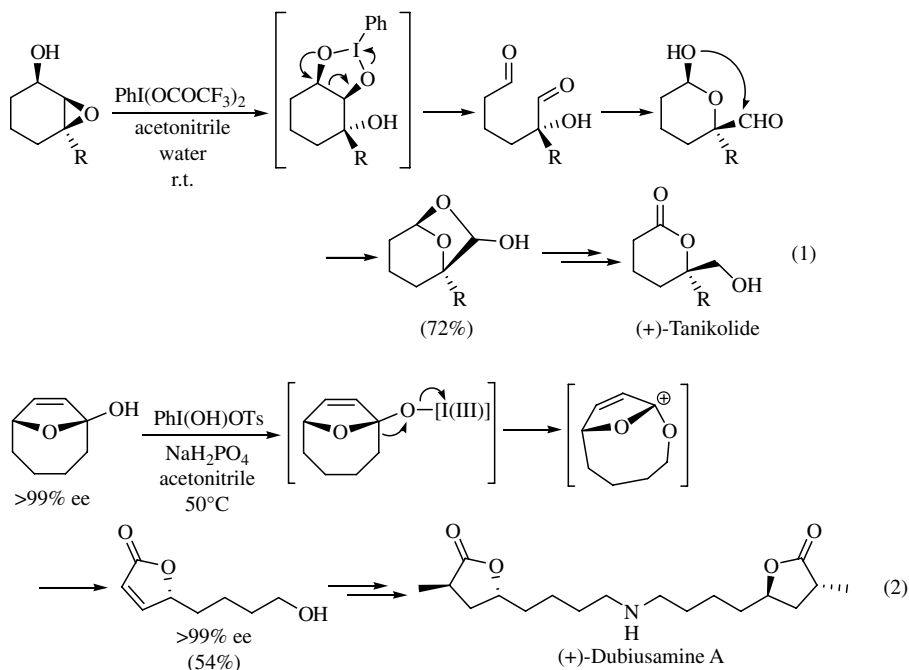


FIGURE 7.34 Application of oxidative cleavage reactions. (1) synthesis of tanikolide (2) dubiusamine A.

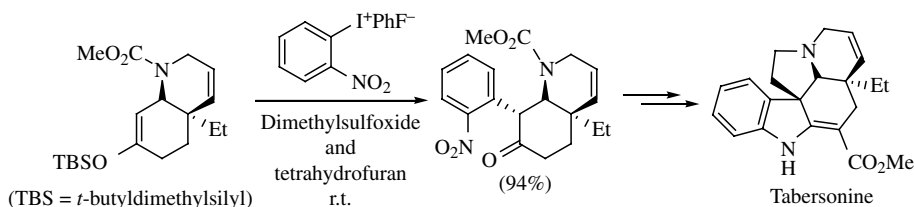


FIGURE 7.35 α-Arylation of carbonyl group for obtaining tabersonine intermediate.

efficient and concise asymmetric synthesis of (+)-tanikolide, an antifungal marine natural product.

Recently, a new oxidative fragmentation for the 9-oxabicyclo[4.2.1]non-7-en-1-ols was utilized for the concise construction of the 5-(4-hydroxybutyl)-2(5*H*)-furanone structures [128]. When using optically pure (–)-(*R*)-5-(4-hydroxybutyl)-2(5*H*)-furanone, the formal total synthesis of (+)-dubiusamine A was achieved on the basis of this strategy (Fig. 7.34, Eq. 7.2).

Total syntheses utilizing the typical reactivities of arylidonium salts were reported for the access to several natural products, especially those having biaryl ethers, α-aryl carbonyl moieties, and polycyclic nitrogen heterocycles [129]. In the stereocontrolled synthesis of (±)-tabersonine (Fig. 7.35), the silyl enol ether part

was arylated with an excellent yield by using (2-nitrophenyl)phenyliodonium salt as the reactive aryl source [130]. The more electron-deficient 2-nitrophenyl group was chemoselectively transferred from the iodonium salt in this aryl-transfer process.

Remarkably, the direct and highly selective asymmetric version of the α -arylations of prochiral ketones was effected by a combination of chiral lithium amide bases and diaryl iodonium salts [131]. The versatility of this asymmetric system was nicely demonstrated for the desymmetrization of the 4-substituted cyclohexanone toward the short synthesis of (–)-epibatidine (see Chapter 17).

Regarding the other types of iodonium salts, the high reactivities and unique characteristics of alkynyliodonium salts (see the previous sections), such as Michael acceptor and carbene-like reactivities, were utilized for the total synthesis of (–)-agelastatin A and B, pareitropone, (\pm)-lennoxamine, and (\pm)-magnofargesin [132]. The benzyne formation of the cyclohexenyliodonium salt was applied in the reaction with enolate to deliver the cyclobutanol product during the access to guanacastepenes, the biologically active diterpene natural products [133].

Hypervalent iodine(V) reagents, specifically DMP [1,1,1-tris(acetyloxy)-1,1-dihydro-1,2-benziodoxol-3-(1*H*)-one], are widely used for the oxidation of alcohol functionalities in complex molecules to carbonyl compounds during the late stages of natural product syntheses because of their mild reactivities in chemoselective and functional group-tolerable transformations as well as high-yielding processes under mild conditions [134]. Besides, recently IBX was found to be favorable in synthetic organic chemistry due to its less acidic nature, and it was sometimes advantageous as a rather efficient oxidant for some natural product syntheses [135].

As an early example involving IBX oxidation of alcohols in complex molecules, the total synthesis of the antifungal agent GM222712 via selective oxidation of the primary alcohol moiety of diol was reported [136]. Some time later, a report of the first total synthesis of (\pm)-strychnofoline including IBX alcohol oxidation for producing a labile aldehyde intermediate appeared [137]. The final step of the total synthesis of wailupemycin B relied on the chemoselective IBX oxidation of the 1,2-diol to the α -hydroxy ketone structure in the presence of the glycol [138]. Likewise, the selective oxidation of the triol to the corresponding 1,2-diketo compound was carried out using IBX during the total synthesis of tetrodotoxin, the puffer fish poison [139].

Furthermore, one of the other recent important contributions of IBX in total synthesis is the applications of the dehydrogenation of aliphatic ketones to α,β -unsaturated carbonyl moieties that were originally developed by Nicolaou's group in early twenty-first century (see also Chapter 16) [140]. The selective oxidations to the desired α,β -unsaturated carbonyl moieties in the late-stage synthesis of cortistatin molecules are the remarkable applications of this type of transformation [141]. The α,β -unsaturated moiety was preinstalled for the aliphatic ketone moiety in the complex intermediate by the dehydrogenation for the next-stage stereoselective introduction of the heteroatom functionalities into the central steroidal core (Fig. 7.36). Accordingly, the total syntheses of the highly selective antiproliferative natural products, cortistatins, were achieved in their naturally occurring enantiomeric forms.

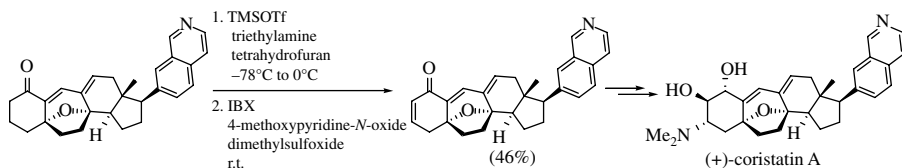


FIGURE 7.36 Utilization of carbonyl α,β -dehydrogenation for coristatin synthesis.

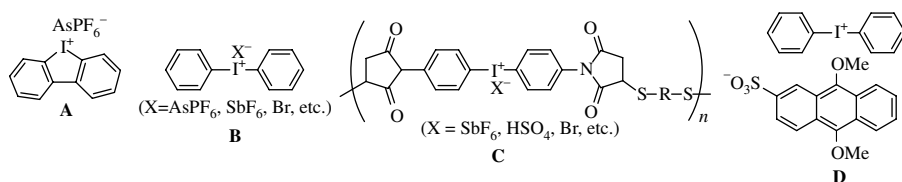


FIGURE 7.37 Photoacid generators based on hypervalent iodine compounds.

There are many further applications with hypervalent iodine reagents for syntheses of complex molecules. The more detailed summarizations of the applications of hypervalent iodine reagents in natural product syntheses are available in several review articles including ours [109].

7.4.2 The Photochemical Applications of Diaryliodonium Salts

The diaryliodonium salts of early discovered hypervalent iodine compounds have practical use as a new class of PAG in many types of cationic polymerizations [142–146]. The type A and B diphenyliodonium salts (Fig. 7.37) were first characterized to be an efficient photoinitiated acid generator via decomposition of some radical mechanisms for the cationic polymerization of olefins, lactones, epoxides, and other cyclic ethers. The true initiators in cationic polymerizations were believed to be the Brønsted acid, in this case, hydrogen halides [143]. The same research group also reported photosensitive polyimidothioether polymers containing the unit of diaryliodonium salts in the main chain (Fig. 7.37, type C) [144]. The photochemistry of diaryliodonium salts was later investigated in more detail by several other research groups, such as Dektar and Hacker [145]. It was concluded that direct photolysis of the salts favored heterolytic cleavage, yielding the phenyl cation and iodobenzene. Meanwhile, the sensitized photodecomposition in the type D salts led to homolytic cleavage to the phenyl radical and the iodobenzene radical cation [146]. The advances of molecular design in diaryliodonium salts in PAG applications are summarized in several recent reviews by contributors [5].

These diaryliodonium salt-based PAGs are promising especially in industrial applications as a metal-free alternative that can easily modulate solubility by tuning the organic parts. Recent efforts include the design of a new visible light-sensitive photoinitiator system utilization in frontal polymerizations, and covalent grafting of glassy carbon electrodes [147–149]. Besides these diaryliodonium salts, other trivalent iodine compounds, that is, HTIB, cyclic iodinanones, and periodonium salt were tested as PAGs in polymer films for photoresist formulations [150].

7.4.3 The Biological Properties of Iodonium Salts

It was reported that iodonium salts show some biological activities. A brief description of these specific biological activities was found in *Chemical Review* published in 1996 [3]. Due to the potent antifungal and antimicrobial activities of a wide range of iodonium salts including diaryl and other types of compounds, their potential applications as disinfectants as well as preservatives for diverse food materials are expected, as found in many numbers of such patent claims. The update of the recent reports on biological activity researches includes inhibition of flavoproteins, hydrogenase complex, hypoxic pulmonary vasoconstriction, potent antibacterial activities against ice nucleation active (INA), *Pseudomonas syringae* and oral and dental anaerobes, stimulation of glucose uptake in skeletal muscle cells through mitochondrial complex I inhibition and activation of AMP-activated protein kinase, sensitivity of a solubilized membrane enzyme, and others [151].

7.5 RECENT PROGRESS AND FEATURE OUTLOOK

Since the discovery of the first hypervalent organoiodine compound (Willgerodt's reagent) more than 100 years ago [1], hypervalent iodine reagents have become useful in many synthetic applications, but stoichiometric amounts have usually been employed and needed. Accordingly, catalytic utilization of hypervalent iodines is a highly desirable goal. Figure 7.38 illustrates the general catalytic cycle including the oxidations for hypervalent iodine compounds. The catalytic utilization of hypervalent iodine reagent would be possible if the released iodoarenes or iodine(III) species is successfully reoxidized in situ to iodine(III) or (V). The first trial for the catalyzation of the reagent was reported in the electrolytic *gem*-difluorination of dithioacetals [152]. Anodic oxidation of (*p*-methoxy)iodobenzene to the active trivalent iodine species took place efficiently at a positive potential of 1.9 V versus silver-silver chloride electrode (SSCE), while the cyclic dithioacetals did not cause any undesired oxidations under the electrolytic conditions due to their higher oxidation

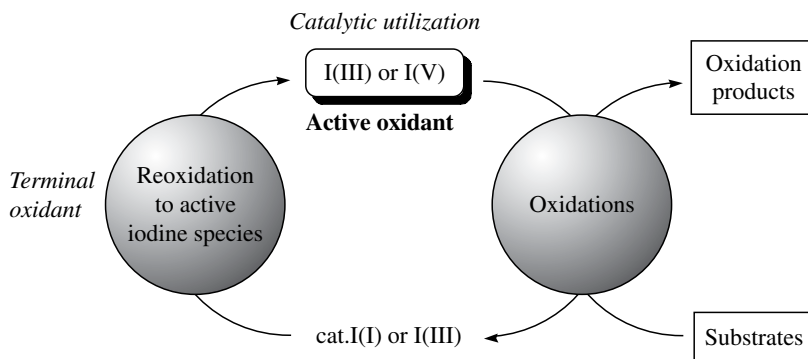


FIGURE 7.38 Catalytic utilization of hypervalent iodine reagent.

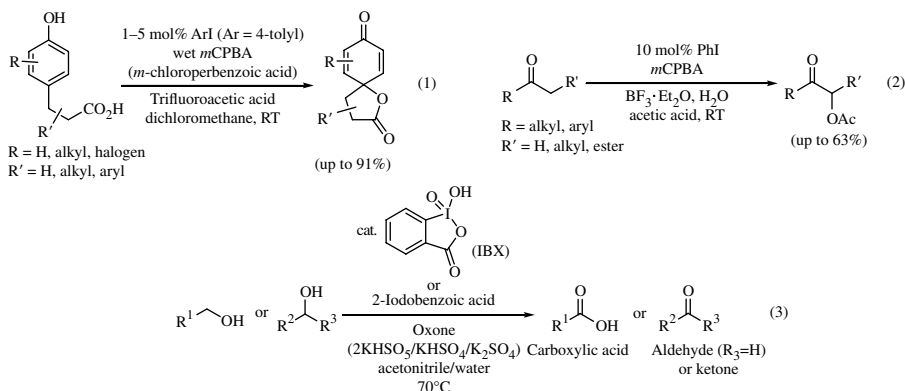


FIGURE 7.39 Pioneering researches in catalyzations.

potentials (over 1.9 V versus SSCE). However, the catalytic conditions based on the electrochemical reoxidations were problematic in the presence of a more oxidizable substrate due to the relatively high oxidation potential of iodobenzene.

Fortunately, hypervalent iodine reagents meet the criteria for being a new organocatalyst, based on the many reliable catalytic conditions reported in 2005 (Fig. 7.39) [153–155]. The catalytic strategy is now available for carrying out many representative types of both iodine(III)- and iodine(V)-induced oxidations together with suitable terminal oxidants, for example, *m*CPBA or Oxone®, the success of which are already summarized in several accounts and review articles [156]. Recently, the catalytic strategies have been expanding in other types of transformations along with optimization of the catalytic conditions, reoxidants, and iodine catalysts themselves [157–184]. In addition to the extension of α -oxygenations [158–162], Figure 7.40 includes the summary of the selected catalytic reports. The examples include the new iodine(III) catalytic system for the organocatalytic *syn*-diacetoxylation of alkenes (Eq. 7.1) [163], spirolactamization [164] by new dinuclear catalysts with a green oxidant, peracetic acid (Eq. 7.2) [165], oxidative aromatic substitution for cyclizations of aryl *N*-methoxy ethanesulfonamides (Eq. 7.3) [166], and related cyclizations [167] as well as its intermolecular version using the Kita's catalyst (Eq. 7.4) [168], first carbon–carbon bond-forming case in catalytic preparation of the core structure of the galanthamine type Amaryllidaceae alkaloids using a new reoxidation system (Eq. 7.5) [169], catalytic cyclizations of alkynes (Eq. 7.6) [170] and related cyclizations [171], the catalytic versions of hypervalent iodine-induced Hofmann rearrangements (Eq. 7.7) [172], the iodoarene-catalyzed oxidative cleavage of carbon–carbon unsaturated bonds (Eq. 7.8) [173]. For catalytic use of pentavalent iodine reagents, 2-iodobenzenesulfonic acid (IBS)-catalyzed efficient oxidation of alcohols [174], oxidative rearrangements of tertially allylic alcohols (Eq. 7.9) [175], ring expansions (Eq. 7.10), [176] and other catalytic reactions by the IBS catalyst [177, 178], oxidations to quinones using water-soluble iodoarene catalyst (Eq. 7.11) [179] were reported. Besides, some transition metals and organocatalysts work as a cocatalyst for a green and mild

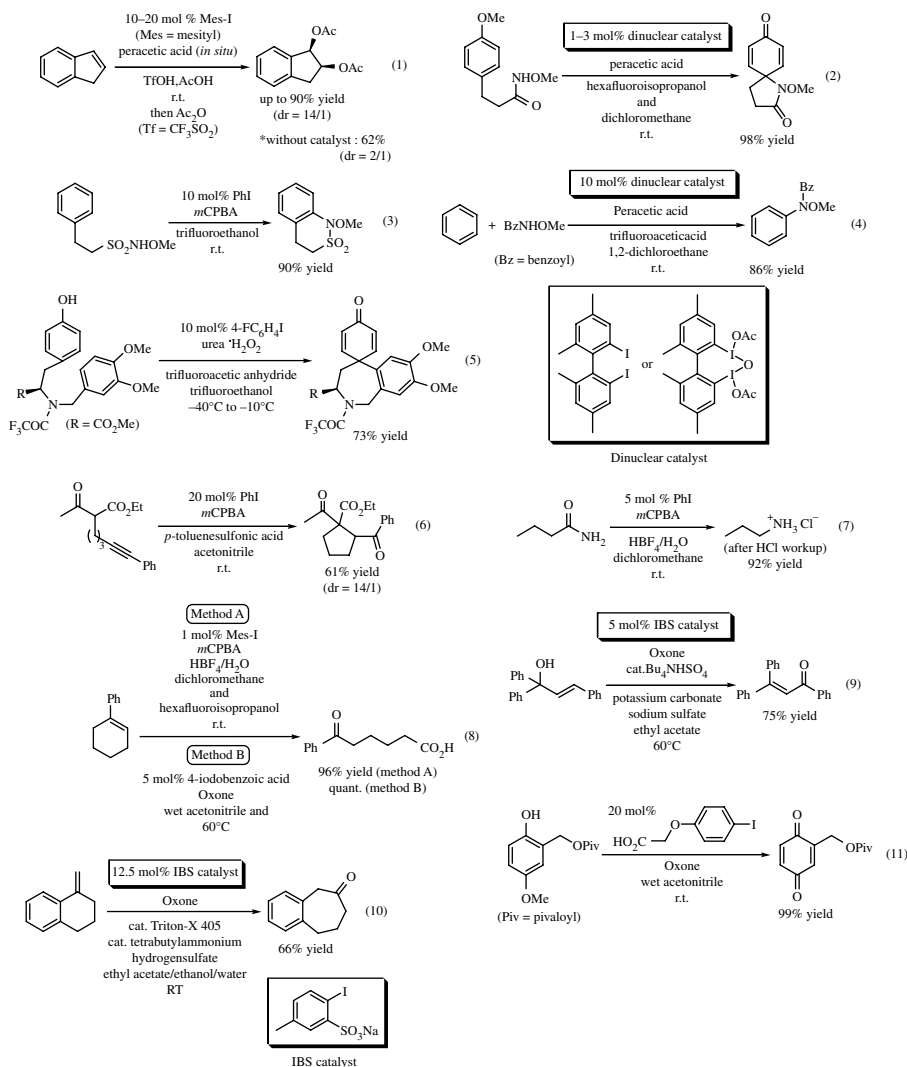


FIGURE 7.40 Selected examples of hypervalent iodine-catalyzed oxidative transformations of organic molecules.

catalytic generation of hypervalent iodine species in oxidations of alcohols and specific hydrocarbons [183, 184].

In spite of the significant advances with regard to hypervalent iodine reagents in organic synthesis, asymmetric induction by hypervalent iodine reagent control is still challenging [185]. Early reports of the designs of chiral hypervalent iodine compounds for asymmetric reactions are shown in Figure 7.41 [186–189]. Efforts have thus been devoted to the design of new chiral reagents with the aim of achieving

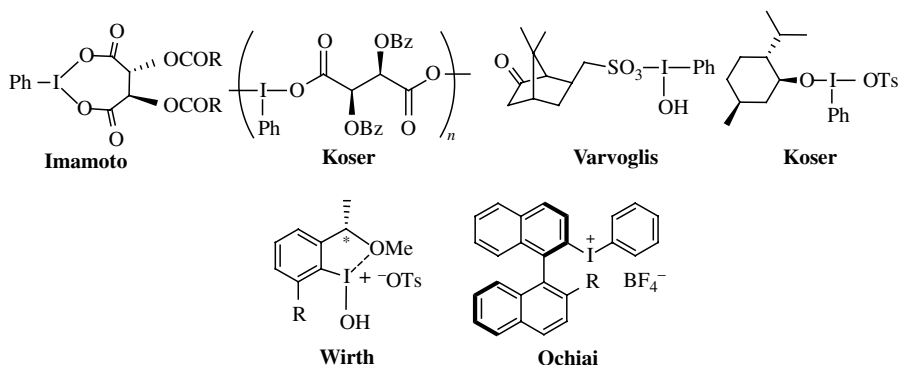


FIGURE 7.41 Chiral hypervalent iodine compounds examined in early studies.

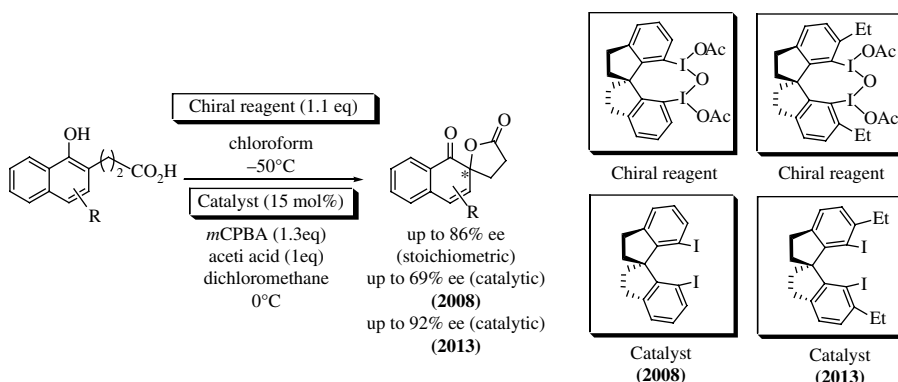


FIGURE 7.42 Catalytic asymmetric dearomatizing spirocyclization based on new chiral hypervalent iodine reagent.

asymmetric oxidations with high stereoselectivities [186–194], but no effective chiral hypervalent iodine compounds had ever been reported until very recently.

The breakthrough in asymmetric controls by hypervalent iodine reagents was reported by Kita et al., who established in 2008 the first protocol for asymmetric dearomatizing *ortho*-spirocyclization of naphthols bearing a carboxylic acid moiety as an intramolecular nucleophilic side chain by designing a novel chiral hypervalent iodine(III) compound based on the spirobiindane backbone (Fig. 7.42). Surprisingly, the reactions were found to proceed at unprecedented excellent levels for asymmetric inductions at that time under stoichiometric conditions (up to 86% ee value at -50°C) and even catalytic conditions with *m*CPBA (up to 69% ee at 0°C) [195]. This is a landmark event that established the chiral iodine compound as a new entrant for asymmetric organocatalysis. The results are noteworthy because the use of other chiral iodoarenes (as in Fig. 7.41) resulted in the formation of almost racemic spirocyclic lactones. The same research group demonstrated theoretical elucidation of the catalyst structure and synthesized a series of *ortho*-functionalized catalyst alternatives for

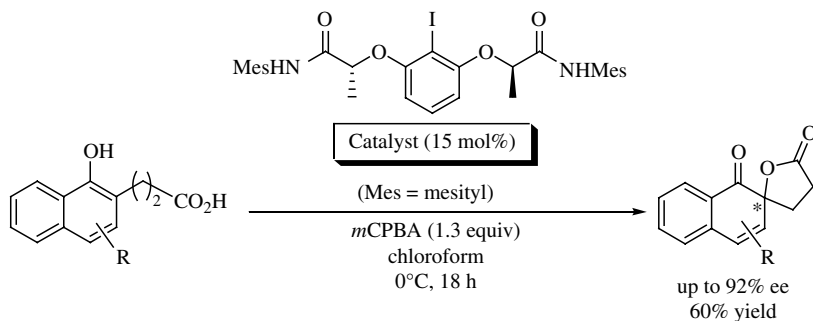


FIGURE 7.43 Ishihara's flexible chiral catalyst in second report.

improving the enantioselectivities up to 92% ee under the catalytic conditions, proving the reasonable transition-state model of the phenolic oxidations induced by hypervalent iodine reagents.

Since the report on the asymmetric dearomatization of naphthols, reports on several asymmetric phenolic oxidations as well as other transformations have appeared [196–203].

Recently, the dearomatizing reactions and catalytic systems by Kita were applied to further catalyst screening by others. Based on Fujita's chiral lactate-type iodoarene compounds [194], Ishihara's group discovered in 2010 a new *C*₂-symmetric hypervalent iodine catalyst *bearing the two chiral lactate groups* at the *ortho* positions of the iodoaryl ring in their evaluation of catalysts for the same reactions [196]. It is noteworthy that the new catalyst successfully provided the same spirocyclic product with up to 92% ee by 10–15 mol% loadings (Fig. 7.43).

The other recent advances in asymmetric oxidations using hypervalent iodine reagents includes the stoichiometric use of Ishihara's type catalysts for other asymmetric transformations, that is, oxidative *endo*-cyclizing lactonizations reported by Fujita et al. (Fig. 7.44, Eq. 7.1) [197], diamination of styrenes and other alkenes (Eq. 7.2) [198], intramolecular amino oxygenative cyclizations (Eq. 7.3) [199], and oxidative cyclizations to fluoroamines (Eq. 7.4) [200].

Regarding the trials of nonintramolecular catalytic asymmetric transformations, Quideau et al. reported the asymmetric oxidations of *ortho*-substituted-1-naphthols, where the asymmetric hydroxylative phenol dearomatizations were effected by a modified chiral iodobinaphthyl catalyst (Fig. 7.45) [201]. The subsequent epoxidation of *ortho*-quinols in a regio- and diastereo-selective fashion under the catalytic conditions with stoichiometric *m*CPBA provided the moderate optical activities of the observed products in enantioselectivities up to 50% ee value. The stoichiometric version involving similar dearomatization to *ortho*-quinols using chiral 2-(*o*-iodoxyphenyl)-oxazoline catalysts was also reported by Birman for a few substrates to provide the Diels–Alder-type *ortho*-quinol dimers with significant levels of asymmetric inductions up to 77% ee value [202].

In addition, it should be noted that the spirocyclic relatives of Kita's chiral iodoarene catalysts in Figure 7.42 have been recently reported by Volp and Harned for

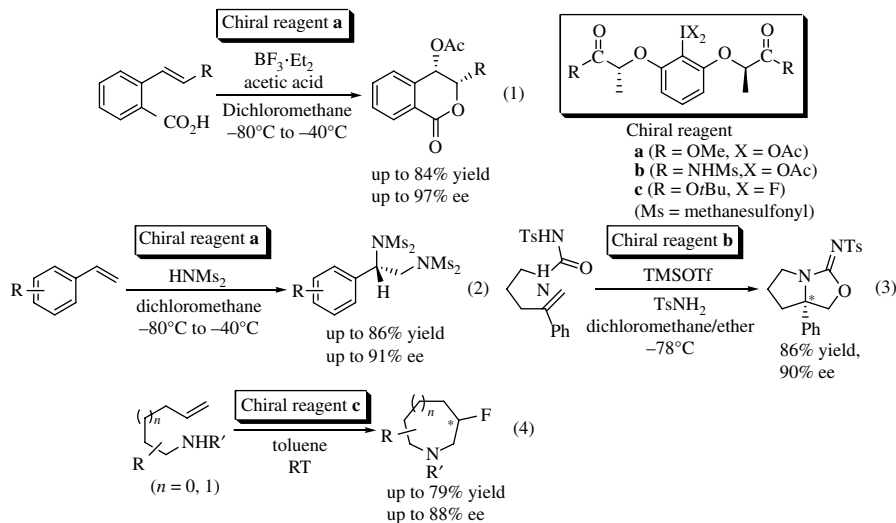


FIGURE 7.44 Application of Ishihara's chiral reagents in several types of hypervalent iodine-mediated transformations.

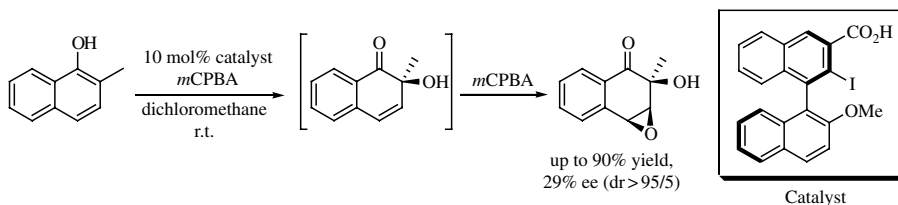


FIGURE 7.45 Dearomatizing asymmetric *ortho*-hydroxylation of phenols.

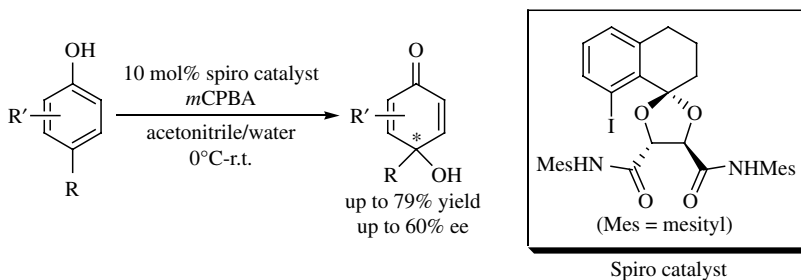


FIGURE 7.46 Dearomatizing asymmetric *para*-hydroxylation of phenols.

the corresponding *para*-quinol formation in an asymmetric manner (Fig. 7.46) [203]. Interestingly, the spirocyclic acetal catalyst with 2.2 equivalents of *m*CPBA as reoxidant can furnish the asymmetric hydroxylated center of *p*-quinols remote to the phenol-derived functionality, despite the low to moderate ee values.

An alternative role of hypervalent iodine reagents in asymmetric transformations is the cooperative use with asymmetric catalysts. Besides the chiral metal complexes, the recent combination of hypervalent iodine reagents with some chiral organocatalysts encourages extension of hypervalent iodine chemistry for effecting several asymmetric transformations in other areas [204].

In addition to these recent significant advances, the innovative research frontispieces of this area of oxidative cross-couplings that have made an appearance in the past few years should be noted. In particular, the biaryl-constructing cross-coupling strategies that can effectively utilize unfunctionalized C–H bonds have now opened new metal-free synthetic areas in organic synthesis [205]. The expected role of the hypervalent iodine reagent in the twentieth century was a simple replacement of the heavy metal oxidants, which goes beyond to alternatives to even metal catalysts as much as the unique reactivities and selectivities have been pioneered. With such contributions, hypervalent iodine chemistry will continue to make an impact in the twenty-first century [206].

REFERENCES

- [1] Willgerodt C. Über einige aromatische jodidchloride. *J Prakt Chem* 1886;33:154.
- [2] Varvoglis A. *Hypervalent Iodine in Organic Synthesis*. San Diego: Academic Press; 1997; Zhdankin VV, Stang PJ, Ochiai M. *Chemistry of Hypervalent Compounds*. In: Akiba K, editor. New York: Wiley-VCH; 1999; Wirth T, Ochiai M, Varvoglis A, Zhdankin VV, Koser GF, Tohma H, Kita Y. Hypervalent iodine chemistry—modern developments in organic synthesis. In: Wirth T, editor. *Topics on Current Chemistry*. Berlin: Springer-Verlag; 2003.
- [3] Examples of comprehensive reviews: (a) Stang PJ, Zhdankin VV. Organic polyvalent iodine compounds. *Chem Rev* 1996; 96:1123; (b) Zhdankin VV, Stang PJ. Recent developments in the chemistry of polyvalent iodine compounds. *Chem Rev* 2002;102:2523; (c) Zhdankin VV, Stang PJ. Chemistry of polyvalent iodine. *Chem Rev* 2008;108:5299; (d) Zhdankin VV. Hypervalent iodine(III) reagents in organic synthesis. *ARKIVOC* 2009:1; (e) Zhdankin VV. Organoiodine(V) reagents in organic synthesis. *J Org Chem* 2011;76:1185; (f) Yusubov MS, Zhdankin VV. Hypervalent iodine reagents and green chemistry. *Curr Org Synth* 2012;9:247.
- [4] (a) Varvoglis A. Polyvalent iodine compounds in organic synthesis. 1984:709; (b) Moriarty RM, Vaid RK, Koser GF. [Hydroxy(organosulfonyloxy)iido]arenes in organic synthesis. *Synlett* 1990:365; (c) Kita Y, Tohma H, Yakura T. Hypervalent iodine reagents in organic synthesis: development of novel reactions and their application to biologically active natural products. *Trends Org Chem* 1992;3:113; (d) Varvoglis A. Chemical transformations induced by hypervalent iodine reagents. *Tetrahedron* 1997;53:1179; (e) Kitamura T, Fujiwara Y. Recent progress in the use of hypervalent iodine reagents in organic synthesis. A Review. *Org Prep Proceed Int* 1997;29:409; (f) Wirth T, Hirt UH. Hypervalent iodine compounds. Recent advances in synthetic applications. *Synthesis* 1999:1271; (g) Tohma H, Kita Y. Hypervalent iodine reagents for the oxidation of alcohols and their application to complex molecule synthesis. *Adv Synth Catal* 2004;346:111; (h) Moriarty RM. Organohypervalent iodine: development, applications, and future directions. *J Org Chem* 2005;70:2893; (i) Wirth T. Hypervalent iodine chemistry in synthesis: scope and new directions. *Angew Chem Int Ed* 2005;44:3656.

- [5] For some recent reviews, see: (a) Crivello JV. Cationic polymerization - iodonium and sulfonium salt photoinitiators. *Adv Polym Sci* 1984;62:1; (b) Toba Y. The design of photoinitiator systems. *J Photopolym Sci Technol* 2003;16:115; (c) Crivello JV. Design and synthesis of photoacid generating systems. *J Photopolym Sci Technol* 2008;21:493.
- [6] Musher JJ. Chemistry of hypervalent molecules. *Angew Chem Int Ed Engl* 1969;8:54.
- [7] (a) Pimentel GC. The bonding of trihalide and bifluoride ions by the molecular-orbital method. *J Chem Phys* 1951;19:446; (b) Rundle RE. Implications of some recent structures for chemical valence theory. *Surv Prog Chem* 1963;1:81.
- [8] Cahill PA, Dykstra CE, Martin JC. The structure and stability of the 10-F-2 trifluoride ion, a compound of a hypervalent first row element. *J Am Chem Soc* 1985;107:6359.
- [9] Perkins CW, Martin JC, Arduengo AJ, Lau W, Alegria A, Kochi JK. An electrically neutral σ -sulfuranyl radical from the homolysis of a perester with neighboring sulfenyl sulfur: 9-S-3 species. *J Am Chem Soc* 1980;102:7753.
- [10] (a) Archer EM, van Schalkwyk TGD. The crystal structure of benzene iododichloride. *Acta Crystallogr* 1953;6:88; (b) Carey JV, Chaloner PA, Hitchcock PB, Neugebauer T, Seddon KR. Synthesis and decomposition of dichloriodoaranes. An improved low temperature x-ray structure of dichloriodobenzene and the structure of 1-chloro-2,3,5,6-tetrakis(chloromethyl)-4-methylbenzene. *J Chem Res (S)* 1996;358.
- [11] (a) Lee C-K, Mak TCW, Li W-K, Kirner JF. Iodobenzene diacetate. *Acta Crystallogr* 1977;B33:1620; (b) Alcock NW, Countryman RM, Esper s S, Sawyer JF. Secondary bonding. Part 5. The crystal and molecular structures of phenyliodine(III) diacetate and bis(dichloroacetate). *J Chem Soc, Dalton Trans* 1979:854; (c) Stergioudis GA, Kokkou SC, Bozopoulos AP, Rentzeperis PJ. Structure of bis(trifluoroacetato)(phenyl)iodine(III), C10H5F6IO4. *Acta Crystallogr* 1984;C40:877; (d) Alcock NW, Harrison WD, Howes C. Secondary bonding. Part 13. Aryltellurium(IV) and -iodine(III) acetates and trifluoroacetates. The crystal and molecular structures of bis(p-methoxyphenyl)tellurium diacetate, μ -oxobis[diphenyltrifluoroacetoxytellurium] hydrate, and [bis(trifluoroacetoxo)iodo]benzene. *J Chem Soc, Dalton Trans* 1984:1709.
- [12] Koser GF, Wettach RH, Troup JM, Frenz BA. Hypervalent organoiodine. Crystal structure of phenylhydroxytosyloxyiodine. *J Org Chem* 1976;41:3609.
- [13] Richter HW, Paul NM, Ray DG, Ray CA, Liable-Sands LM, Concolino T, Lam M, Rheingold AL, Koser GF, Golen JA. Anhydrides of real and hypothetical [hydroxy(R-O)iodo]benzenes. *Inorg Chem* 2010;49:5413.
- [14] (a) Ochiai M, Sueda T, Miyamoto K, Kiprof P, Zhdankin VV. Trans influence on hypervalent bonding of aryl λ 3-iodanes: their stabilities and isodesmic reactions of benzo-doxolones and benziodazolones. *Angew Chem Int Ed* 2006;45:8203; (b) Sajith PK, Suresh CH. Quantification of the trans influence in hypervalent iodine complexes. *Inorg Chem* 2012;51:967.
- [15] (a) Gallos J, Varvoglis A, Alcock NW. Oxo-bridged compounds of iodine(III): syntheses, structure, and properties of μ -oxobis[trifluoroacetato(phenyl)iodine]. *J Chem Soc, Perkin Trans 1* 1985:757; (b) Nemykin VN, Koposov AY, Netzel BC, Yusubov MS, Zhdankin VV. Self-assembly of hydroxy(phenyl)iodonium ions in acidic aqueous solution: preparation, and x-ray crystal structures of oligomeric phenyliodine(III) sulfates. *Inorg Chem* 2009;48:4908.
- [16] (a) Takenaga N, Uchiyama T, Kato D, Fujioka H, Dohi T, Kita Y. Efficient phenolic oxidations to construct ortho-spirolactone structures using oxo-bridged hypervalent iodine(III) compound. *Heterocycles* 2011;82:1327; (b) Dohi T, Uchiyama T, Yamashita D,

- Washimi N, Kita Y. Efficient phenolic oxidations using μ -oxo-bridged phenyliodine trifluoroacetate. *Tetrahedron Lett* 2011;52:2212; (c) Dohi T, Nakae T, Takenaga N, Uchiyama T, Fukushima K, Fujioka H, Kita Y. μ -oxo-bridged hypervalent iodine(III) compound as an extreme oxidant for aqueous oxidations. *Synthesis* 2012;44:1183.
- [17] Stevenson PJ, Treacy AB, Nieuwenhuyzen M. Preparation of dess-martin periodinane- the role of the morphology of 1-hydroxy-1,2-benziodoxol-3(1h)-one 1-oxide precursor. *J Chem Soc, Perkin Trans 2* 1997:589.
- [18] Schroeckeneder A, Stichnoth D, Mayer P, Trauner D. The crystal structure of the dess-martin periodinane. *Beilstein J Org Chem* 2012;8:1523.
- [19] Alcock NW, Countryman RM. Secondary bonding. Part 1. Crystal and molecular structures of diphenyliodonium chloride, bromide, and iodide. *J Chem Soc, Dalton Trans* 1977:217.
- [20] Stang PJ, Arif AM, Crittelle CM. Ethynyl(phenyl)iodonium triflate, [HC-CIPh][OSO₂CF₃], preparation, spectroscopic properties, formation mechanism, and X-Ray structure analysis. *Angew Chem, Int Ed* 1990;29:287.
- [21] Ochiai M, Sumi K, Takaoka Y, Kunishima M, Nagao Y, Shiro M, Fujita E. Reactions of vinylsilanes with lewis acid-activated iodosylbenzene: stereospecific syntheses of vinyl-iodonium tetrafluoroborates and their reactions as highly activated vinyl halides. *Tetrahedron* 1988;44:4095.
- [22] (a) Baker GP, Mann FG, Sheppard N, Tetlow AJ. The structure of o-iodosobenzoic acid and of certain derivatives. *J Chem Soc* 1965:3721; (b) Balthazor TM, Godar DE, Stults BR. Synthesis and structure of benziodazoles. *J Org Chem* 1979;44:1447; (c) Amey RL, Martin JC. Synthesis and reaction of substituted arylalkoxyiodinanes: formation of stable bromoarylalkoxy and aryldialkoxo heterocyclic derivatives of tricoordinate organoiodine(III). *J Org Chem* 1979;44:1779; (d) Ochiai M, Masaki Y, Shiro M. Synthesis and structure of 1-alkynyl-1,2-benziodoxol-3(1h)-ones. *J Org Chem* 1991;56:5511; (e) Ochiai M, Ito T, Masaki Y, Shiro M. A stable crystalline alkylperoxyiodinane: 1-(tert-butylperoxy)-1,2-benziodoxol-3(1h)-one. *J Am Chem Soc* 1992;114:6269; (f) Moss RA, Zhang H. A phosphorylated iodosobenzoate: the intermediate in the iodosobenzoate cleavage of a reactive phosphate. *J Am Chem Soc* 1994;116:4471; (g) Zhdankin VV, Kuehl CJ, Krasutsky AP, Fromanek MS, Bolz JT. Preparation and chemistry of stable azidoiodinanes: 1-azido-3,3-bis(trifluoromethyl)-3-(1h)-1,2-benziodoxole and 1-azido-1,2-benziodoxol-3-(1h)-one. *Tetrahedron Lett* 1994;35:9677.
- [23] Akai S, Okuno T, Takada T, Tohma H, Kita Y. Preparation of novel cyclic hypervalent iodine(III) compounds having azido, cyano, and nitrato ligands. *Heterocycles* 1996;42:47.
- [24] (a) Eisenberger P, Gischig S, Togni A. Novel 10-i-3 hypervalent iodine-based compounds for electrophilic trifluoromethylation. *Chem Eur J* 2006;12:2579; (b) Kieltisch I, Eisenberger P, Gischig S, Togni A. Mild electrophilic trifluoromethylation of carbon- and sulfur-centered nucleophiles by a hypervalent iodine(III)-CF₃ reagent. *Angew Chem, Int Ed* 2007;46:754; (c) Koller R, Stanek K, Stolz D, Aardoom R, Niedermann K, Togni A. Zinc-mediated formation of trifluoromethyl ethers from alcohols and hypervalent iodine trifluoromethylation reagents. *Angew Chem, Int Ed* 2009;48:4332.
- [25] Carmalt CJ, Crossley JG, Knight JG, Lightfoot P, Martin A, Muldowney MP, Norman NC, Orpen AG. An examination of the structures of iodosylbenzene (PhIO) and the related imido compound, PhINSO₂C₆H₄Me-4, by x-ray powder diffraction and EXAFS (extended x-ray absorption fine structure) spectroscopy. *J Chem Soc, Chem Commun* 1994:2367.

- [26] (a) Mishra AK, Olmstead MM, Ellison JJ, Power PP. Detailed structural characterization of the polyvalent iminoiodinanes ArINTs (Ar = C₆H₅ or 2, 4, 6-Me₃C₆H₂; Ts = SO₂C₆H₄-4-Me) and the aryldichloroiodinane 2, 4, 6-i-Pr₃C₆H₂ICl₂. *Inorg Chem* 1995;34:3210; (b) Boucher M, Macikenas D, Ren T, Protasiewicz JD. Secondary bonding as a force-dictating structure and solid-state aggregation of the primary nitrene sources (arylsulfonylimino)iiodoarenes (ArINSO₂Ar'). *J Am Chem Soc* 1997;119:9366.
- [27] Recent reviews: (a) Gephart RT, Warren TH. Copper-catalyzed sp³ C-H amination. *Organometallics* 2012;31:7728; (b) Roizen JL, Harvey ME, Du Bois J. Metal-catalyzed nitrogen-atom transfer methods for the oxidation of aliphatic C-H bonds. *Acc Chem Res* 2012;45:911; (c) Ramirez TA, Zhao B, Shi Y. Recent advances in transition metal-catalyzed sp³ C-H amination adjacent to double bonds and carbonyl groups. *Chem Soc Rev* 2012;41:931.
- [28] Bell R, Morgan KJ. Organic compounds of multivalent iodine. I. Infrared spectra. *J Chem Soc* 1960:1209.
- [29] Hirt UH, Spingler B, Wirth T. New chiral hypervalent iodine compounds in asymmetric synthesis. *J Org Chem* 1998;63:7674.
- [30] Knop O, Cameron TS, Bakshi PK, Linden A, Roe SP. Crystal chemistry of tetradial species. Part 5. Interaction between cation lone pairs and phenyl groups in tetraphenylborates: crystal structures of Me₃S⁺, Et₃S⁺, Me₃SO⁺, Ph₂I⁺, and 1-azoniaproPELLANE tetraphenylborates. *Can J Chem* 1994;72:1870.
- [31] Richter HW, Cherry BR, Zook TD, Koser GF. Characterization of species present in aqueous solutions of [hydroxy(mesyloxy)iodo]benzene and [hydroxy(tosyloxy)iodo]benzene. *J Am Chem Soc* 1997;119:9614.
- [32] Ledwith A, Al-Kass S, Sherrington DC, Bonner P. Ion-pair dissociation equilibria for iodonium and sulfonium salts useful in photoinitiated cationic polymerization. *Polymer* 1981;22:143.
- [33] (a) Okuyama T, Takino T, Sato K, Oshima K, Imamura S, Yamataka H, Asano T, Ochiai M. Vinylic SN₂ reaction of 1-decenyliodonium salt with halide ions. *Bull Chem Soc Jpn* 1998;71:243; (b) Ochiai M, Kida M, Sato K, Takino T, Goto S, Donkai N, Okuyama T. Association and dissociation of (z)-(β-bromoalkenyl)(phenyl)iodonium bromide in chloroform solution: detection of vinyl-λ₃-iodane dimer in solution. *Tetrahedron Lett* 1999;40:1559.
- [34] (a) Ochiai M. Nucleophilic vinylic substitutions of λ₃-vinyliodanes. *J Organomet Chem* 2000;611:494; (b) Okuyama T. Solvolysis of vinyl iodonium salts. New insights into vinyl cation intermediates. *Acc Chem Res* 2002;35:12.
- [35] (a) Berry RS. Correlation of rates of intramolecular tunneling processes, with application to some group V compounds. *J Chem Phys* 1960;32:933; (b) a recent summary: Moberg C. Stereomutation in trigonal-bipyramidal systems: a unified picture. *Angew Chem, Int Ed* 2011;50:10290.
- [36] Reich HJ, Cooperman CS. Structure and stereolability of triaryliodine (III) compounds. Degenerate isomerization of 5-phenyl-5h-dibenziodole. *J Am Chem Soc* 1973;95:5077.
- [37] Ochiai M, Takaoka Y, Masaki Y, Nagao Y, Shiro M. Synthesis of chiral hypervalent organoiodinanes, iodo(III)binaphthyls, and evidence for pseudorotation on iodine. *J Am Chem Soc* 1990;112:5677.
- [38] Moriarty RM, Prakash O. Hypervalent iodine in organic synthesis. *Acc Chem Res* 1986;19:244.

- [39] (a) Grushin VV. Carboranylhalonium ions: from striking reactivity to a unified mechanistic analysis of polar reactions of diarylhalonium compounds. *Acc Chem Res* 1992;25:529; (b) Ligand coupling reaction with heteroatomic compounds. In: Finet P, editor. *Tetrahedron Organic Chemistry Series*. Vol. 18. Oxford: Pergamon Press; 1998; (c) Ozanne-Beaudenon A, Quideau S. Regioselective hypervalent-iodine(III)-mediated dearomatizing phenylation of phenols through direct ligand coupling. *Angew Chem Int Ed* 2005;44:7065.
- [40] (a) Edwards AJ. Crystal structure of trichlorosulfonium(IV) tetrachloroiodate(III). *J Chem Soc, Dalton Trans* 1978:1723; (b) Kajigaeshi S, Kakinami T, Moriwaki M, Tanaka T, Fujisaki S. Halogenation using quaternary ammonium polyhalides. XV. An effective chlorinating agent benzyltrimethylammonium tetrachloroiodate, benzylic chlorination of alkylaromatic compounds. *Tetrahedron Lett* 1988;29:5783.
- [41] Amey RL, Martin JC. Synthesis and reaction of substituted arylalkoxyiodinanes: formation of stable bromoarylalkoxy and arylalkoxy heterocyclic derivatives of tricoordinate organoiodine(III). *J Org Chem* 1979;44:1779.
- [42] Koser GF, Wettach RH. Synthesis and characterization of [methoxy(tosyloxy)iodo]benzene, an acyclic monoalkoxyiodinane. *J Org Chem* 1980;45:4988.
- [43] Stang PJ, Boehschar M, Wingert H, Kitamura T. Acetylenic esters. Preparation and characterization of alkynyl carboxylates via polyvalent iodonium species. *J Am Chem Soc* 1988;110:3272.
- [44] Togo H, Muraki T, Hoshina Y, Yamaguchi K, Yokoyama M. Formation and synthetic use of oxygen-centered radicals with (diacetoxyiodo) arenes. *J Chem Soc, Perkin Trans 1* 1997:787. See also Refs. 97 and 98 by Suárez.
- [45] De Munari S, Frigerio M, Santagostino M. Hypervalent iodine oxidants: structure and kinetics of the reactive intermediates in the oxidation of alcohols and 1,2-diols by o-iodoxybenzoic acid and dess-martin periodinane. A comparative ¹H-NMR study. *J Org Chem* 1996;61:9272.
- [46] Hadjirapoglou L, Spyroudis S, Varvoglis A. Phenyliodine(III) bis[phthalimide]: a novel polyvalent iodine compound. *Synthesis* 1983:207.
- [47] Kita Y, Okuno T, Tohma H, Akai S. Preparation of bis(arylthio)iodobenzene and reaction with 1-alkynes. A novel route to 1,2-bis(arylthio)alkenes. *Tetrahedron Lett* 1994;35:2717.
- [48] (a) Kita Y, Okuno T, Egi M, Iio K, Takeda Y, Akai S. An effective p-thiocyanation of phenols using phenyliodine dichloride-lead(II) thiocyanate. *Synlett* 1994:1039; (b) Bruno M, Margarita R, Parlanti L, Piancatelli G, Trifoni M. Hypervalent iodine chemistry: novel and direct thiocyanation of alkenes using [bis(acetoxy)iodo]benzene/trimethylsilyl isothiocyanate reagent combination. Synthesis of 1,2-dithiocyanates. *Tetrahedron Lett* 1998;39:3847.
- [49] Koser GF, Wettach RH, Smith CS. New methodology in iodonium salt synthesis. Reactions of [hydroxy(tosyloxy)iodo]arenes with aryltrimethylsilanes. *J Org Chem* 1980;45:1543.
- [50] (a) Pike VW, Butt F, Shah A, Widdowson DA. Facile synthesis of substituted diaryliodonium tosylates by treatment of aryltributylstannanes with koser's reagent. *J Chem Soc, Perkin Trans 1* 1999:245; (b) Carroll MA, Pike VW, Widdowson DA. New synthesis of diaryliodonium sulfonates from arylboronic acids. *Tetrahedron Lett* 2000;41:5393.
- [51] (a) Ochiai M, Sumi K, Nagao Y, Fujita E. Vinyliodonium salts: their stereospecific synthesis and reactions as the activated vinyl halides. *Tetrahedron Lett* 1985;26:2351; (b)

- Ochiai M, Kunishima M, Sumi K, Nagao Y, Fujita E, Arimoto M, Yamaguchi H. Reaction of alkynyltrimethylsilanes with a hypervalent organoiodine compound: a new general synthesis of alkynyliodonium salts. *Tetrahedron Lett* 1985;26:4501.
- [52] Williamson BL, Stang PJ, Arif AM. Preparation, molecular structure, and diels-alder cycloaddition chemistry of β -functionalized alkynyl(phenyl)iodonium salts. *J Am Chem Soc* 1993;115:2590.
- [53] Barton DHR, Jaszberenyi JC, Lessmann K, Timar T. Hypervalent iodine in carbon-carbon bond forming reactions. A new reaction of hypervalent iodine compounds and organolithium reagents. *Tetrahedron* 1992;48:8881.
- [54] (a) Cambie RC, Lindsay BG, Rutledge PS, Woodgate PD. Oxidative displacement of iodine from vicinal iodocarboxylates and alkyl iodides. *J Chem Soc, Chem Commun* 1978:919; (b) Reich HJ, Peake SL. Hypervalent organoiodine chemistry. Syn elimination of alkyl iodoso compounds. *J Am Chem Soc* 1978;100:4888.
- [55] Okuyama T, Takino T, Sueda T, Ochiai M. Solvolysis of cyclohexenyliodonium salt, a new precursor for the vinyl cation: remarkable nucleofugality of the phenyliodonio group and evidence for internal return from an intimate ion-molecule pair. *J Am Chem Soc* 1995;117:3360.
- [56] Ochiai M. In: Akiba K, editor. *Chemistry of Hypervalent Compounds: Organic Synthesis Using Hypervalent Organiiodines*. New York: Wiley-VCH; 1999. p 359.
- [57] (a) Ochiai M, Oshima K, Masaki Y. Inversion of configuration in nucleophilic vinylic substitutions of (E)- β -alkylvinyliodonium tetrafluoroborates with halides. *J Am Chem Soc* 1991;113:7059; (b) Okuyama T, Takino T, Sato K, Ochiai M. In-plane vinylic S_N2 substitution and intramolecular β -elimination of β -alkylvinyl(chloro)- λ 3-iodanes. *J Am Chem Soc* 1998;120:2275.
- [58] (a) Lucchini V, Modena G, Pasquato L. S_N2 and AdN-E mechanisms in bimolecular nucleophilic substitutions at vinyl carbon. The relevance of the luno symmetry of the electrophile. *J Am Chem Soc* 1995;117:2297; (b) Okuyama T, Yamataka Y. A theoretical study on the reactivity of vinyl iodonium ions. *Can J Chem* 1999;77:577.
- [59] Ochiai M, Takaoka Y, Nagao Y. Hypervalent alkenyliodonium tetrafluoroborates. Evidence for generation of alkylidenecarbenes via base-induced α -elimination. *J Am Chem Soc* 1988;110:6565.
- [60] Ochiai M, Kunishima M, Tani S, Nagao Y. Generation of [β - (phenylsulfonyl) alkylidene]carbenes from hypervalent alkenyl- and alkynyliodonium tetrafluoroborates and synthesis of 1-(phenylsulfonyl) cyclopentenes. *J Am Chem Soc* 1991;113:3135.
- [61] Ochiai M, Sueda T, Uemura K, Masaki Y. Nature of alkylidenecarbenes generated from alkenylphenyliodonium tetrafluoroborates via base-induced α -elimination. *J Org Chem* 1995;60:2624.
- [62] Reich HJ, Peake SL. Hypervalent organoiodine chemistry. Syn elimination of alkyl iodoso compounds. *J Am Chem Soc* 1978;100:4888.
- [63] Ochiai M, Oshima K, Masaki Y. Stereoselective synthesis of highly labile (Z)- β -alkylvinylphenyliodonium perchlorates. *J Chem Soc. Chem Commun* 1991:869.
- [64] (a) Takaya T, Enyo H, Imoto E. Novel reactions of iodosobenzene with various organic compounds. *Bull Chem Soc Jpn* 1968;41:1032; (b) More recent report, see: Kida M, Sueda T, Goto S, Okuyama T, Ochiai M. Synthesis and nucleophilic substitution of allenyl(m-nitrophenyl)iodanes as a new propynyl cation-equivalent species: synthesis of propynyl ethers, esters, and amides. *Chem Commun* 1996:1933.

- [65] Dess DB, Martin JC. A useful 12-I-5 triacetoxyperiodinane (the dess-martin periodinane) for the selective oxidation of primary or secondary alcohols and a variety of related 12-I-5 species. *J Am Chem Soc* 1991;113:7277.
- [66] (a) Frigerio M, Santagostino M. A mild oxidizing reagent for alcohols and 1,2-diols: *o*-iodoxybenzoic acid (IBX) in DMSO. *Tetrahedron Lett* 1994;35:8019; (b) Munari S, Frigerio M, Santagostino M. Hypervalent iodine oxidants: structure and kinetics of the reactive intermediates in the oxidation of alcohols and 1,2-diols by *o*-iodoxybenzoic acid and dess-martin periodinane. A comparative ¹H-NMR study. *J Org Chem* 1996; 61:9272.
- [67] (a) Moriarty RM, Vaid RK, Duncan MP, Ochiai M, Inenaga M, Nagao Y. Hypervalent iodine oxidation of amines using iodosobenzene: synthesis of nitriles, ketones and lactams. *Tetrahedron Lett* 1988;29:6913; (b) Ochiai M, Inenaga M, Nagao Y, Moriarty RM, Vaid RK, Duncan MP. Oxidative decarboxylation of cyclic amino acids and dehydrogenation of cyclic secondary amines with iodosobenzene. *Tetrahedron Lett* 1988;29:6917.
- [68] (a) Nicolaou KC, Mathison CJN, Montagnon T. New reactions of IBX: oxidation of nitrogen- and sulfur-containing substrates to afford useful synthetic intermediates. *Angew Chem, Int Ed* 2003;42:4077; (b) Nicolaou KC, Mathison CJN, Montagnon T. *O*-iodoxybenzoic acid (ibx) as a viable reagent in the manipulation of nitrogen- and sulfur-containing substrates: scope, generality, and mechanism of IBX-mediated amine oxidations and dithiane deprotections. *J Am Chem Soc* 2004;126:5192.
- [69] Ngouansavanh T, Zhu J. IBX-mediated oxidative ugi-type multicomponent reactions: application to the N and C1 functionalization of tetrahydroisoquinoline. *Angew Chem, Int Ed* 2007;46:5775.
- [70] Scartozzi M, Grondin R, Leblanc Y. Synthesis of γ - and δ -lactams by an intramolecular ene reaction of azo compounds. *Tetrahedron Lett* 1992;33:5717.
- [71] But TYS, Toy PH. Organocatalytic mitsunobu reactions. *J Am Chem Soc* 2006;128:9636.
- [72] (a) Tamura Y, Yakura T, Shirouchi Y, Haruta J. Pummerer-type reaction of α -acyl sulfides using phenyl iodosyl bis(trifluoroacetate). *Chem Pharm Bull* 1986;34:1061; (b) Tohma H, Egi M, Ohtsubo M, Watanabe H, Takizawa S, Kita Y. A novel and direct α -azidation of cyclic sulfides using a hypervalent iodine(III) reagent. *Chem Commun* 1998:173.
- [73] (a) Greaney MF, Motherwell WB. Observations on the α -fluorination of α -phenylsulfanyl esters using (difluoroiodo)toluene. *Tetrahedron Lett* 2000;41:4463; (b) Greaney MF, Motherwell WB, Tocher DA. Studies on the additive fluoro-pummerer reaction of phenylsulfanylated lactams with difluoroiodotoluene. *Tetrahedron Lett* 2001;42:8523.
- [74] (a) Kitamura T, Todaka M, Shin-machi I, Fujiwara Y. A convenient and efficient synthesis of benzotriazoles and benzisoxazolines using a new hypervalent iodine-benzyne precursor. *Heterocyc Commun* 1998;4:205; (b) Kitamura T, Yamane M, Inoue K, Todaka M, Fukatsu N, Meng Z, Fujiwara Y. A new and efficient hypervalent iodine-benzyne precursor, (phenyl)[*o*-(trimethylsilyl)phenyl]iodonium triflate: generation, trapping reaction, and nature of benzyne. *J Am Chem Soc* 1999;121:11674.
- [75] (a) Laird DW, Gilbert JC. Norbornyne: a cycloalkyne reacting like a dicarbene. *J Am Chem Soc* 2001;123:6704; (b) Fujita M, Kim WH, Sakanishi Y, Fujiwara K, Hirayama S, Okuyama T, Ohki Y, Tatsumi K, Yoshioka Y. Elimination-addition mechanism for nucleophilic substitution reaction of cyclohexenyl iodonium salts and regioselectivity of nucleophilic addition to the cyclohexyne intermediate. *J Am Chem Soc* 2004;126:7548; (c) Okuyama T, Fujita M. Generation of cycloalkynes by hydro-iodonio-elimination of vinyl iodonium salts. *Acc Chem Res* 2005;38:679.

- [76] Mizukami F, Ando M, Tanaka T, Imamura J. The acetoxylation of p-substituted acetophenones and β -diketones with (diacetoxyiodo)benzene. *Bull Chem Soc Jpn* 1978;51:335.
- [77] (a) Moriarty RM, Hu H, Gupta SC. Direct α -hydroxylation of ketones using iodosobenzene. *Tetrahedron Lett* 1981;22:1283; (b) Koser GF, Relenyi AG, Kalos AN, Rebrovic L, Wettach RH. One-step α -tosyloxylation of ketones with [hydroxy(tosyloxy)iodo]benzene. *J Org Chem* 1982;47:2487.
- [78] (a) Moriarty RM, Prakash O. Oxidation of phenolic compounds with organohypervalent iodine reagents. *Org React* 2001;57:327; (b) Kürti L, Herczegh P, Visy J, Simonyi M, Antus S, Pelter A. New insights into the mechanism of phenolic oxidation with phenyliodonium(III) reagents. *J Chem Soc, Perkin Trans 1* 1999:379; (c) Pelter A, Ward RS. Two-electron phenolic oxidations using phenyliodonium dicarboxylates. *Tetrahedron* 2001;57:273. See also Ref. 109. (d) Hypervalent iodine oxidation of p-alkoxyphenols and related compounds: a general route to p-benzoquinone monoacetals and spiro lactones Tamura Y, Yakura T, Haruta J, Kita Y. *J Org Chem* 1987;52:3927.
- [79] (a) Kita Y, Tohma H, Inagaki M, Hatanaka K, Yakura T. A novel oxidative azidation of aromatic compounds with hypervalent iodine reagent, phenyliodine(III) bis(trifluoroacetate) (PIFA) and trimethylsilyl azide. *Tetrahedron Lett* 1991;32:4321; (b) Kita Y, Tohma H, Hatanaka K, Takada T, Fujita S, Mitoh S, Sakurai H, Oka S. Hypervalent iodine-induced nucleophilic substitution of para-substituted phenol ethers. Generation of cation radicals as reactive intermediates. *J Am Chem Soc* 1994;116:3684.
- [80] (a) Kita Y, Takada T, Tohma H. Hypervalent iodine reagents in organic synthesis: nucleophilic substitution of p-substituted phenol ethers. *Pure Appl Chem* 1996;68:627; (b) Dohi T, Ito M, Yamaoka N, Morimoto K, Fujioka H, Kita Y. Hypervalent iodine(III): selective and efficient single-electron-transfer (SET) oxidizing agent. *Tetrahedron* 2009;65:10797.
- [81] (a) Kita Y, Yakura T, Tohma H, Kikuchi K, Tamura Y. A synthetic approach to discorhabdin alkaloids: hypervalent iodine oxidation of p-substituted phenol derivatives to azacarbocyclic spirodienones. *Tetrahedron Lett* 1989;30:1119; (b) Kita Y, Takada T, Ibaraki M, Gyoten M, Mihara S, Fujita S, Tohma H. An intramolecular cyclization of phenol derivatives bearing aminoquinones using a hypervalent iodine reagent. *J Org Chem* 1996;61:223.
- [82] Kikugawa Y, Kawase M. An electrophilic aromatic substitution by N-methoxyamides via hypervalent iodine intermediates. *Chem Lett* 1990:581.
- [83] (a) Wardrop DJ, Basak A. N-methoxy-n-acylnitrenium ions: application to the formal synthesis of (-)-TAN1251A. *Org Lett* 2001;3:1053; (b) Wardrop DJ, Zhang W. N-methoxy-N-acylnitrenium ions: application to the formal synthesis of (\pm)-desmethyl-amino FR901483. *Org Lett* 2001;3:2353; (c) Miyazawa E, Sakamoto T, Kikugawa Y. Synthesis of spirodienones by intramolecular ipso-cyclization of N-Methoxy-(4-halogenophenyl)amides using [hydroxy(tosyloxy)iodo]benzene in trifluoroethanol. *J Org Chem* 2003;68:5429.
- [84] (a) Loudon GM, Radhakrishna AS, Almond MR, Blodgett JK, Boutin RH. Conversion of aliphatic amides into amines with [i,i-bis(trifluoroacetoxy)iodo]benzene. 1. Scope of the reaction. *J Org Chem* 1984;49:4272; (b) Boutin RH, Loudon GM. Conversion of aliphatic amides into amines with [i,i-bis(trifluoroacetoxy)iodo]benzene. 2. Kinetics and mechanism. *J Org Chem* 1984;49:4277.
- [85] Lazbin IM, Koser GF. N-phenyliodonio carboxamide tosylates: synthesis and hydrolysis to alkylammonium tosylates. *J Org Chem* 1987;52:476.

- [86] Moriarty RM, Khosrowshahi JS, Prakash O. Solvohyperiodination. A comparison with solvohallation. *Tetrahedron Lett* 1985;26:2961.
- [87] Oae S, Uchida Y. Ligand-coupling reactions of hypervalent species. *Acc Chem Res* 1991;24:202.
- [88] (a) Lancer KM, Wiegand GH. The ortho effect in the pyrolysis of iodonium halides. A case for a sterically controlled nucleophilic aromatic (SN) substitution reaction. *J Org Chem* 1976;41:3360; (b) Grushin VV. Cyclic diaryliodonium ions: old mysteries solved and new applications envisaged. *Chem Soc Rev* 2000;29:315.
- [89] For early reports, see: (a) Yamada Y, Okawara M. Steric effect in the nucleophilic attack of bromide anion on diaryl- and aryl-2-thienyliodonium ions. *Bull Chem Soc Jpn* 1972;45:1860; (b) Yamada Y, Kashima K, Okawara M. Substituent effect in the nucleophilic attack by the bromide ion on the p-tolyl-substituted phenyliodonium ions. *Bull Chem Soc Jpn* 1974;47:3179.
- [90] Martin-Santamaria S, Carroll MA, Carroll CM, Carter CD, Rzepa HS, Widdowson DA, Pike VW. Fluoridation of heteroaromatic iodonium salts: experimental evidence supporting theoretical prediction of the selectivity of the process. *Chem Commun* 2000:649.
- [91] (a) Ochiai M, Oshima K, Masaki Y. Synthesis of (Z)-1,2-Dihalo-1-alkenes by the reaction of (Z)-(β -Halovinyl) phenyliodonium salts with n-Bu₄NX or KX/CuX. Competitions between nucleophilic vinylic substitutions and aromatic substitutions. *Chem Lett* 1994:871; (b) Okuyama T, Takino T, Sato K, Ochiai M. Ligand coupling mechanism of nucleophilic vinylic substitution of iodonium salts with hypervalent 10-I-3 and 12-I-4 intermediates. *Chem Lett* 1997:955.
- [92] Milas NA, Plesnicar B. Organic peroxides. LXIII. Formation of di-tert-butyl polyoxides in the reaction of tert-butyl hydroperoxide with iodosobenzene and iodosobenzene diacetate in methylene chloride and in diethyl ether at -80 to +5.deg. *J Am Chem Soc* 1968;90:4450.
- [93] (a) Magnus P, Lacour J, Weber W. Direct N-Alkyl Azidonation of N,N-Dialkylarylamines with the iodosylbenzene/trimethylsilyl azide reagent combination. *J Am Chem Soc* 1993;115:9347; (b) Fontana F, Minisci F, Yan YM, Zhao L. A novel and mild source of carbon-centered radicals by iodosobenzene diacetate (IBDA) and sodium azide from alcohols, ethers, aldehydes, amides and alkyl iodides. *Tetrahedron Lett* 1993;34:2517.
- [94] Kita Y, Tohma H, Takada T, Mitoh S, Fujita S. A novel and direct alkyl azidation of p-alkylanisoles using phenyl iodine(III) bis(trifluoroacetate) (PIFA) and trimethylsilyl azide. *Gyoten M. Synlett* 1994:427.
- [95] Zhdankin VV, Krasutsky AP, Kuehl CJ, Simonsen AJ, Woodward JK, Mismash B, Bolz JT. Preparation, X-ray crystal structure, and chemistry of stable azidoiodinanes - derivatives of benziodoxole. *J Am Chem Soc* 1996;118:5192.
- [96] Ochiai M, Ito T, Takahashi H, Nakanishi A, Toyonari M, Sueda T, Goto S, Shiro M. Hypervalent (tert-butylperoxy)iodanes generate iodine-centered radicals at room temperature in solution: oxidation and deprotection of benzyl and allyl ethers, and evidence for generation of α -oxy carbon radicals. *J Am Chem Soc* 1996;118:7716.
- [97] (a) Concepción JI, Francisco CG, Hernández R, Salazar JA, Suárez E. Intramolecular hydrogen abstraction. Iodosobenzene diacetate, an efficient and convenient reagent for alkoxy radical generation. *Tetrahedron Lett* 1984;25:1953; (b) Martín A, Salazar JA, Suárez E. Synthesis of chiral spiroacetals from carbohydrates. *Tetrahedron Lett* 1995;36:4489; (c) Martín A, Pérez-Martín I, Suárez E. Intramolecular hydrogen

- abstraction promoted by amidyl radicals. Evidence for electronic factors in the nucleophilic cyclization of ambident amides to oxocarbenium ions. *Org Lett* 2005;7:2027.
- [98] de Armas P, Carrau R, Concepción JI, Francisco CG, Hernández R, Salazar JA, Suárez E. Synthesis of 1,4-epimine compounds. Iodosobenzene diacetate, an efficient reagent for neutral nitrogen radical generation. *Tetrahedron Lett* 1985;26:2493.
- [99] (a) Nicolaou KC, Baran PS, Zhong Y-L. Selective oxidation at carbon adjacent to aromatic systems with IBX. *J Am Chem Soc* 2001;123:3183; (b) Nicolaou KC, Baran PS, Zhong Y-L, Barluenga S, Hunt KW, Kranich R, Vega JA. Iodine(v) reagents in organic synthesis. Part 3. New routes to heterocyclic compounds via o-iodoxybenzoic acid-mediated cyclizations: generality, scope, and mechanism. *J Am Chem Soc* 2002;124:2233.
- [100] Mironova AA, Maletina II, Iksanova SV, Orda VV, Yagupol'skii LM. Electronic nature of substituents containing polyvalent iodine. *Zh Org Khim* 1989;25:306.
- [101] Murch P, Arif AM, Stang PJ. Regiochemistry of diels-alder reactions of diverse β -functionalized alkynyliodonium salts with unsymmetrical dienes. *J Org Chem* 1997;62:5959.
- [102] (a) Ochiai M, Kunishima M, Nagao Y, Fuji K, Shiro M, Fujita E. Tandem michael-carbene insertion reactions of alkynyliodonium salts. Extremely efficient cyclopentene annulations. *J Am Chem Soc* 1986;108:8281; (b) Ochiai M, Kunishima M, Tani S, Nagao Y. Generation of [β -(phenylsulfonyl)alkylidene]carbenes from hypervalent alkynyl- and alkynyliodonium tetrafluoroborates and synthesis of 1-(phenylsulfonyl)cyclopentenenes. *J Am Chem Soc* 1991;113:3135.
- [103] (a) Ochiai M, Kunishima M, Fuji K, Nagao Y. Alkynyliodonium tetrafluoroborates as a good michael acceptor for an azido group. A stereoselective synthesis of (Z)-(β -azidovinyl)iodonium salts. *J Org Chem* 1988;53:6144; (b) Ochiai M, Uemura K, Oshima K, Masaki Y, Kurishima M, Tani S. Michael type addition of halides to alkynyl(phenyl) iodonium tetrafluoroborates. Stereoselective synthesis of (z)- β -halovinyl(phenyl) iodonium halides. *Tetrahedron Lett* 1991;32:4753.
- [104] (a) Stang PJ, Surber BW. Alkynyl sulfonate esters. Preparation and characterization of acetylenic tosylates, $RC\equiv COTs$. *J Am Chem Soc* 1985;107:1452; (b) Stang PJ, Boehshar M, Lin J. Acetylenic esters. Preparation and characterization of hitherto unknown alkynyl carboxylate, $RC\equiv COCOR1$, and alkynyl phosphate, $RC\equiv COPO(OR1)2$, esters. *J Am Chem Soc* 1986;108:7832.
- [105] (a) Ochiai M. Reactivities, properties and structures. *Top Curr Chem* 2003;224:5; (b) Ochiai M, Kitagawa Y. Reaction of $\lambda3$ -vinyl iodanes: generation and alkylidene-transfer of monocarbonyl iodonium ylides. *J Synth Org Chem Jpn* 2000;58:1048.
- [106] Neilands O, Karele B. Iodonium derivatives of β -diketones. XVII. Aryliodonium derivatives isopropylidene malonate. *Zh Org Khim* 1971;7:1611.
- [107] Stang PJ, Wingert H, Arif AM. Crystal structure of a novel tricoordinate vinyliodinane species and evidence for an alkylidenecarbene-iodonium ylide. *J Am Chem Soc* 1987;109:7235.
- [108] Ochiai M, Kunishima M, Fuji K, Shiro M, Nagao Y. Synthesis and structural analysis of a vinyliodonium salt with an α -silyl substituent, and generation of an iodonium ylide from it. *J Chem Soc, Chem Commun* 1988:1076.
- [109] (a) Kita Y, Tohma H. Synthetic applications (total synthesis and natural product synthesis). *Top Curr Chem* 2003;224:209; (b) Silva LF, Jr, Olofsson B. Hypervalent iodine reagents in the total synthesis of natural products. *Nat Prod Rep* 2011;28:1722.
- [110] Kishi Y, Nakatsuka S, Fukuyama T, Havel M. Total synthesis of sporidesmin A. *J Am Chem Soc* 1973;95:6493.

- [111] (a) Szanty C, Blasko G, Barczai-Beke M. Studies aiming at the synthesis of morphine. II. Studies on phenolic coupling of N-norreticuline derivatives. *Tetrahedron Lett* 1980;21:3509; (b) White JD, Chong WKM, Thirring K. Phenolic oxidative coupling with hypervalent iodine. A synthesis of 6a-epipretazettine. *J Org Chem* 1983;48:2300; (c) White JD, Caravatti G, Kline TB, Edstrom E, Rice KC, Brossi A. Biomimetic total synthesis of (-)-codeine. *Tetrahedron* 1983;39:2393.
- [112] Tamura Y, Yakura T, Haruta J, Kita Y. Hypervalent iodine oxidation of p-alkoxyphenols and related compounds: a general route to p-benzoquinone monoacetals and spiro lactones. *J Org Chem* 1987;52:3927.
- [113] For recent reviews, see:(a) Harayama Y, Kita Y. Pyrroloiminoquinone alkaloids. Discorhabdins and makaluvamines. *Curr Org Chem* 2005;9:1567; (b) Ciufolini MA, Braun NA, Canesi S, Ousmer M, Chang J, Chai D. Oxidative amidation of phenols through the use of hypervalent iodine reagents. Development and applications. *Synthesis* 2007:3759; (c) Quideau S, Pouysegu L, Deffieux D. Oxidative dearomatization of phenols. Why, how and what for? *Synlett* 2008:467; (d) Pouysegu L, Deffieux D, Quideau S. Hypervalent iodine-mediated oxygenative phenol dearomatization reactions. *Tetrahedron* 2010;66:2235.
- [114] (a) Kita Y, Tohma H, Inagaki M, Hatanaka K, Kikuchi K, Yakura T. Hypervalent iodine oxidation of o-silylated phenol derivatives to azacarbocyclic spirodienones; synthetic approach to the anticancer marine alkaloid, discorhabdin C. *Tetrahedron Lett* 1991;32:2035; (b) Kita Y, Tohma H, Inagaki M, Hatanaka K, Yakura T. Total synthesis of discorhabdin C: a general aza spiro dienone formation from O-silylated phenol derivatives using a hypervalent iodine reagent. *J Am Chem Soc* 1992;114:2175.
- [115] (a) Tohma H, Harayama Y, Hashizume M, Iwata M, Egi M, Kita Y. Synthetic studies on the sulfur-cross-linked core of antitumor marine alkaloid, discorhabdins: total synthesis of discorhabdin A. *Angew Chem, Int Ed* 2002;41:348; (b) Tohma H, Harayama Y, Hashizume M, Iwata M, Kiyono Y, Egi M, Kita Y. The first total synthesis of discorhabdin A. *J Am Chem Soc* 2003;125:11235.
- [116] (a) Kita Y, Takada T, Gyoten M, Tohma H, Zenk MH, Eichhorn J. An oxidative intramolecular phenolic coupling reaction for the synthesis of amaryllidaceae alkaloids using a hypervalent iodine(III) reagent. *J Org Chem* 1996;61:5857; (b) Kita Y, Arisawa M, Gyoten M, Nakajima M, Hamada R, Tohma H, Takada T. Oxidative intramolecular phenolic coupling reaction induced by a hypervalent iodine(III) reagent: leading to galanthamine-type amaryllidaceae alkaloids. *J Org Chem* 1998;63:6625.
- [117] Sun D-Q, Zhao Q-W, Li C-Z. Total synthesis of (+)-decursivine. *Org Lett* 2011;13:5302.
- [118] Yoshino T, Sato I, Hirama M. Total synthesis of aspercyclides A and B via intramolecular oxidative diaryl ether formation. *Org Lett* 2012;14:4290.
- [119] Guerard KC, Guerinot A, Bouchard-Aubin C, Menard M-A, Lepage M, Beaulieu MA, Canesi S. Oxidative 1,2- and 1,3-alkyl shift processes: developments and applications in synthesis. *J Org Chem* 2012;77:2121.
- [120] (a) Moriarty RM, Prakash O. Oxidation of carbonyl compounds with organohypervalent iodine reagents. *Org React* 1999;54:273; (b) Merritt EA, Olofsson B. α -Functionalization of carbonyl compounds using hypervalent iodine reagents. *Synthesis* 2011:517.
- [121] Li WZ, Wang YQ. A novel and efficient total synthesis of cephalotaxine. *Org Lett* 2003;5:2931.
- [122] Correa A, Tellitu I, Dominguez E, Moreno I, SanMartin R. An efficient, pifa-mediated approach to benzo-, naphtho-, and heterocycle-fused pyrrolo[2,1-c][1,4]diazepines. An advantageous access to the antitumor antibiotic DC-81. *J Org Chem* 2005;70:2256.

- [123] Satoh N, Akiba T, Yokoshima S, Fukuyama T. A practical synthesis of (-)-oseltamivir. *Angew Chem, Int Ed* 2007;46:5734.
- [124] (a) Kita Y, Egi M, Tohma H. Total synthesis of sulfur-containing pyrroloiminoquinone marine product, (±)-makaluvamine F. Using hypervalent iodine(III)-induced reactions. *Chem Commun* 1999:143; (b) Kita Y, Egi M, Takada T, Tohma H. Development of novel reactions using hypervalent iodine(III) reagents. Total synthesis of sulfur-containing pyrroloiminoquinone marine product, (±)-makaluvamine F. *Synthesis* 1999:885.
- [125] (a) Feldman KS, Skoumbourdis AP. Extending pummerer reaction chemistry. Synthesis of (±)-dibromophakellstatin by oxidative cyclization of an imidazole derivative. *Org Lett* 2005;7:929; (b) Feldman KS, Skoumbourdis AP, Fodor MD. Extending pummerer reaction chemistry. Synthesis studies in the phakellin alkaloid area. *J Org Chem* 2007;72:8076.
- [126] (a) Silva LF, Jr. Hypervalent iodine-mediated ring contraction reactions. *Molecules* 2006;1:421; (b) Silva LF, Jr, Siqueira FA, Pedrozo EC, Vieira FYM, Doriguetto AC. Iodine(III)-promoted ring contraction of 1,2-dihydronaphthalenes: a diastereoselective total synthesis of (±)-indatraline. *Org Lett* 2007;9:1433.
- [127] (a) Fujioka H, Matsuda S, Horai M, Fujii E, Morishita M, Nishiguchi N, Hata K, Kita Y. Facile and efficient synthesis of lactols by a domino reaction of 2,3-epoxy alcohols with a hypervalent iodine(III) reagent and its application to the synthesis of lactones and the asymmetric synthesis of (+)-tanikolide. *Chem Eur J* 2007;13:5238; (b) Kita Y, Matsuda S, Fujii E, Horai M, Hata K, Fujioka H. Domino reaction of 2, 3-epoxy-1-alcohols and pifa in the presence of H₂O and the concise synthesis of (+)-tanikolide. *Angew Chem, Int Ed* 2005;44:5857.
- [128] Kawasumi M, Iwabuchi Y. Concise entry to chiral 5-(4-hydroxybutyl)-2(5h)-furanone via HTIB-mediated novel oxidative fragmentation: formal total synthesis of (+)-dubiusamine A. *Org Lett* 2013;15:1788.
- [129] Early examples:(a) Hickey DMB, Leeson PD, Novelli R, Shah VP, Burpitt BE, Crawford LP, Davies BJ, Mitchell MB, Pancholi KD, Tuddenham D, Lewis NJ, O'Farrel C. Synthesis of thyroid hormone analogs. Part 3. Iodonium salt approaches to SK & F L-94901. *J Chem Soc, Perkin Trans 1* 1988:3103; (b) de Sousa JDF, Rodrigues JAR, Abramovitch RA. Synthesis of cularine and sarcocapnine via enium ions and a new, highly diastereoselective reductive methylation. *J Am Chem Soc* 1994;116:9745; (c) Gao P, Portoghesi PS. Monophenylation of morphinan-6-ones with diphenyliodonium iodide. *J Org Chem* 1995;60:2276; (d) Gao P, Larson DL, Portoghesi PS. Synthesis of 7-arylmorphinans. Probing the "address" requirements for selectivity at opioid δ receptors. *J Med Chem* 1998;41:3091.
- [130] Kozmin SA, Rawal VH. A general strategy to aspidosperma alkaloids: efficient, stereo-controlled synthesis of tabersonine. *J Am Chem Soc* 1998;120:13523.
- [131] Aggarwal VK, Olofsson B. Enantioselective α-arylation of cyclohexanones with diaryl iodonium salts: application to the synthesis of (-)-epibatidine. *Angew Chem, Int Ed* 2005;44:5516.
- [132] (a) Feldman KS, Saunders JC, Wroblewski ML. Alkynyliodonium salts in organic synthesis. Development of a unified strategy for the syntheses of (-)-agelastatin A and (-)-agelastatin B. *J Org Chem* 2002;67:7096; (b) Feldman KS, Cutarelli TD, Di Florio R. Total synthesis of the tropoloisoquinoline alkaloid pareitropone via alkynyliodonium salt chemistry and related studies. *J Org Chem* 2002;67:8528; (c) Couty S, Liegault B, Meyer C, Cossy J. Synthesis of 3-(arylmethylene)isoindolin-1-ones from ynamides by heck-suzuki-miyaura domino reactions. Application to the synthesis of lennoxamine.

- Tetrahedron 2006;62:3882; (d) Wardrop DJ, Fritz J. Total synthesis of (\pm)-magnofargesin. *Org Lett* 2006;8:3659.
- [133] Gampe CM, Carreira EM. Total syntheses of guanacastepenes N and O. *Angew Chem, Int Ed* 2011;50:2962.
- [134] For an early review in natural product synthesis, see: Tohma H, Kita Y. Hypervalent iodine reagents for the oxidation of alcohols and their application to complex molecule synthesis. *Adv Synth Catal* 2004;346:111.
- [135] (a) Nicolaou KC, Chen JS, Edmonds DJ, Estrada AA. Recent advances in the chemistry and biology of naturally occurring antibiotics. *Angew Chem, Int Ed* 2009;48:660; (b) Satam V, Harad A, Rajule R, Pati H. 2-Iodoxybenzoic acid (IBX): an efficient hypervalent iodine reagent. *Tetrahedron* 2010;66:7659; (c) Duschek A, Kirsch SF. 2-iodoxybenzoic acid-A simple oxidant with a dazzling array of potential applications. *Angew Chem, Int Ed* 2011;50:1524.
- [136] Bueno JM, Coteron JM, Chiara JL, Fernández-Mayoralas A, Fiandor JM, Valle N. Stereoselective synthesis of the antifungal GM222712. *Tetrahedron Lett* 2000;41:4379.
- [137] Lerchner A, Carreira EM. First total synthesis of (\pm)-strychnofoline via a highly selective ring-expansion reaction. *J Am Chem Soc* 2002;124:14826.
- [138] Kirsch S, Bach T. Total synthesis of (+)-wailupemycin B. *Angew Chem, Int Ed* 2003;42:4685.
- [139] Ohyabu N, Nishikawa T, Isobe M. First asymmetric total synthesis of tetrodotoxin. *J Am Chem Soc* 2003;125:8798.
- [140] (a) Nicolaou KC, Montagnon T, Baran PS. Modulation of the reactivity profile of IBX by ligand complexation: ambient temperature dehydrogenation of aldehydes and ketones to α,β -unsaturated carbonyl compounds. *Angew Chem, Int Ed* 2002;41:993; (b) Nicolaou KC, Montagnon T, Baran PS, Zhong Y-L. Iodine(v) reagents in organic synthesis. Part 4. O-iodoxybenzoic acid as a chemospecific tool for single electron transfer-based oxidation processes. *J Am Chem Soc* 2002;124:2245.
- [141] (a) Nicolaou KC, Sun YP, Peng XS, Polet D, Chen DYK. Total synthesis of (+)-cortistatin A. *Angew Chem, Int Ed* 2008;47:7310; (b) Nicolaou KC, Peng XS, Sun YP, Polet D, Zou B, Lim CS, Chen DYK. Total synthesis and biological evaluation of cortistatins A and J and analogues thereof. *J Am Chem Soc* 2009;131:10587.
- [142] Bachofner HE, Beringer FM, Meites L. Diaryliodonium salts. V. The electroreduction of diphenyliodonium salts. *J Am Chem Soc* 1958;80:4269.
- [143] (a) Crivello JV, Lam JHW. New photoinitiators for cationic polymerization. *J Polym Sci Polym Symp* 1976;56:383; (b) Crivello JV, Lam JHW. Diaryliodonium salts. A new class of photoinitiators for cationic polymerization. *Macromolecules* 1977;10:1307.
- [144] Crivello JV, Lam JHW. Photosensitive polymers containing diaryliodonium salt groups in the main chain. *J Polym Sci Polym Symp* 1979;17:3845.
- [145] (a) Pappas SP, Pappas BC, Gatechair LR, Schnabel W. Photoinitiation of cationic polymerization. II. Laser flash photolysis of diphenyliodonium salts. *J Polym Sci, Polym Chem Ed* 1984;22:69; (b) Timpe HJ, Schikowsky V. Investigations on the photolysis of diaryliodonium salts. *J Prakt Chem* 1989;331:447; (c) Dektar JL, Hacker NP. Photochemistry of diaryliodonium salts. *J Org Chem* 1990;55:639.
- [146] (a) Naitoh K, Yamaoka T, Umehara A. Intra-ion-pair electron transfer mechanism for photolysis of diphenyliodonium salt sensitized by 9,10-dimethoxyanthracene-2-sulfo-

- nate counteranion. *Chem Lett* 1991;1869; (b) Naitoh K, Kanai K, Yamaoka T, Umehara A. A novel chemical amplification type positive resist using diphenyliodonium 9,10-dimethoxyanthracene-2-sulfonate as photoinitiator. *J Photopolym Sci Technol* 1991;4:411; (c) Naitoh K, Yamaoka T, Umehara A. Acid generation and deprotecting reaction by diphenyliodonium 9,10-dimethoxyanthracene-2-sulfonate in a novolak positive photoresist based on chemical amplification. *Polym Adv Technol* 1992;3:117.
- [147] (a) Tarumoto N, Miyagawa N, Takahara S, Yamaoka T. Diphenyliodonium salts with diazoxide group for a photo-acid generator. *J Photopolym Sci Technol* 2004;17:719; (b) Tarumoto N, Miyagawa N, Takahara S, Yamaoka T. Diphenyliodonium salts with pyranine conk as an environment-friendly photoacid generator and their applications to chemically amplified resists. *Polym J* 2005;37:545; (c) Tarumoto N, Miyagawa N, Takahara S, Yamaoka T. Visible-light-sensitive photo-acid generator incorporating food dye for use in chemically amplified resists. *J Photopolym Sci Technol* 2005;18:673.
- [148] (a) Crivello JV. Photoactivated cationic ring-opening frontal polymerization of oxetanes. *Polym Prepr Am Chem Soc Div Polym Chem* 2006;47:208; (b) Crivello JV. A new visible light sensitive photoinitiator system for the cationic polymerization of epoxides. *J Polym Sci Part A* 2009;47:866.
- [149] Vase KH, Holm AH, Norrman K, Pedersen SU, Daasbjerg K. Covalent grafting of glassy carbon electrodes with diaryliodonium salts: new aspects. *Langmuir* 2007;23:3786.
- [150] (a) Miyagawa N, Takahara S, Yamaoka T. Trivalent iodine compounds and periodonium salt as PAG. *J Photopolym Sci Technol* 2002;15:379; (b) Miyagawa N, Kishimoto Y. Direct and sensitized photolysis of cyclic iodine compounds as photo-acid generator. *J Photopol Sci Technol* 2011;24:369.
- [151] (a) Moulton P, Martin H, Ainger A, Cross A, Hoare C, Doel J, Harrison R, Eisenthal R, Hancock J. The inhibition of flavoproteins by phenoxaiodonium, a new iodonium analogue. *Eur J Pharmacol* 2000;401:115; (b) Magnani P, Doussiere J, Lissolo T. Diphenylene iodonium as an inhibitor for the hydrogenase complex of rhodobacter capsulatus. Evidence for two distinct electron donor sites. *Biochim Biophys Acta* 2000;1459:169; (c) Murphy TM, Vu H, Nguyen T, Woo CH. Diphenylene iodonium sensitivity of a solubilized membrane enzyme from rose cells. *Protoplasma* 2000;213:228; (d) Jones RD, Thompson JS, Morice AH. The NADPH oxidase inhibitors iodonium diphenyl and cadmium sulphate inhibit hypoxic pulmonary vasoconstriction in isolated rat pulmonary arteries. *Physiol Res* 2000;49:587; (e) Menkissoglu-Spiroudi U, Karamanoli K, Spyroudis S, Constantinidou H-IA. Hypervalent iodine compounds as potent antibacterial agents against ice nucleation active (INA) pseudomonas syringae. *J Agric Food Chem* 2001;49:3746; (f) Goldstein EJC, Citron DM, Warren Y, Merriam CV, Tyrrell K, Fernandez H, Radhakrishnan U, Stang PJ, Conrads G. In vitro activities of iodonium salts against oral and dental anaerobes. *Antimicrob Agent Chemother* 2004;48:2766; (g) Hutchinson DS, Csikasz RI, Yamamoto DL, Shabalina IG, Wikstroem P, Wilcke M, Bengtsson T. Diphenylene iodonium stimulates glucose uptake in skeletal muscle cells through mitochondrial complex I inhibition and activation of AMP-activated protein kinase. *Cell Signal* 2007;19:1610; (h) Doroshov JH, Juhasz A, Ge Y, Holbeck S, Lu J, Antony S, Wu Y, Jiang G, Roy K. Antiproliferative mechanisms of action of the flavin dehydrogenase inhibitors diphenylene iodonium and di-2-thienyliodonium based on molecular profiling of the NCI-60 human tumor cell panel. *Biochem Pharmacol* 2012;83:1195; (i) Doroshov JH, Gaur S, Markel S, Lu J, van

- Balgooy J, Synold TW, Xi B, Wu X, Juhasz A. Effects of iodonium-class flavin dehydrogenase inhibitors on growth, reactive oxygen production, cell cycle progression, nadph oxidase 1 levels, and gene expression in human colon cancer cells and xenografts. *Free Radic Biol Med* 2013;57:162
- [152] For early trials, see: (a) Fuchigami T, Fujita T. Electrolytic partial fluorination of organic compounds. 14. The first electrosynthesis of hypervalent iodobenzene difluoride derivatives and its application to indirect anodic gem-difluorination. *J Org Chem* 1994;59:7190; (b) Fujita T, Fuchigami T. Electrolytic partial fluorination of organic compounds. 20. Electrosynthesis of novel hypervalent iodobenzene chlorofluoride derivatives and its application to indirect anodic gem-difluorination. *Tetrahedron Lett* 1996;37:4725; (c) Hara S, Hatakeyama T, Chen S-Q, Ishii K, Yoshida M, Sawaguchi M, Fukuhara T, Yoneda N. Electrochemical fluorination of β -dicarbonyl compounds using p-iodotoluene difluoride as a mediator. *J Fluorine Chem* 1998;87:189
- [153] Dohi T, Maruyama A, Yoshimura M, Morimoto K, Tohma H, Kita Y. Versatile hypervalent-iodine(III)-catalyzed oxidations with m-chloroperbenzoic acid as a cooxidant. *Angew Chem Int Ed* 2005;44:6193.
- [154] Ochiai M, Takeuchi Y, Katayama T, Sueda T, Miyamoto K. Iodobenzene-catalyzed α -acetoxylation of ketones. In situ generation of hypervalent (diacyloxyiodo)benzenes using m-chloroperbenzoic acid. *J Am Chem Soc* 2005;127:12244.
- [155] Thottumkara AP, Bowsher MS, Vinod TK. In situ generation of o-iodoxybenzoic acid (IBX) and the catalytic use of it in oxidation reactions in the presence of oxone as a co-oxidant. *Org Lett* 2005;7:2933.
- [156] (a) Richardson RD, Wirth T. Hypervalent iodine goes catalytic. *Angew Chem, Int Ed* 2006;45:4402; (b) Ochiai M, Miyamoto K. Catalytic version of and reuse in hypervalent organo- λ 3- and - λ 5-iodane oxidation. *Eur J Org Chem* 2008:4229; (c) Dohi T, Kita Y. Hypervalent iodine reagents as a new entrance to organocatalysts. *Chem Commun* 2009:2073; (d) Yusubov MS, Zhdankin VV. Development of new recyclable reagents and catalytic systems based on hypervalent iodine compounds. *Mendeleev Commun* 2010;20:185.
- [157] Alternative reoxidants for the catalytic reactions in Refs. 153–155: (a) Schulze A, Giannis A. Oxidation of alcohols with catalytic amounts of IBX. *Synthesis* 2006:257; (b) Page PCB, Appleby LF, Buckley BR, Allin SM, McKenzie MJ. In situ generation of 2-iodoxybenzoic acid (IBX) in the presence of tetraphenylphosphonium monoperoxy-sulfate (TPPP) for the conversion of primary alcohols into the corresponding aldehydes. *Synlett* 2007:1565; (c) Sheng J, Li X, Tang M, Gao B, Huang G. An efficient method for the α -acetoxylation of ketones. *Synthesis* 2007:1165; (d) Minamitsuji Y, Kato D, Fujioka H, Dohi T, Kita Y. Organoiodine-catalyzed oxidative spirocyclization of phenols using peracetic acid as a green and economic terminal oxidant. *Aust J Chem* 2009;62:648.
- [158] (a) Yamamoto Y, Togo H. PhI-catalyzed α -tosyloxylation of ketones with m-chloroperbenzoic acid and p-toluenesulfonic acid. *Synlett* 2006:798; (b) Yamamoto Y, Kawano Y, Toy PH, Togo H. Phi- and polymer-supported phi-catalyzed oxidative conversion of ketones and alcohols to α -tosyloxyketones with m-chloroperbenzoic acid and p-toluenesulfonic acid. *Tetrahedron* 2007;63:4680; (c) Tanaka A, Togo H. 4-MeC₆H₄I-Mediated efficient α -tosyloxylation of ketones with oxone and p-toluenesulfonic acid in acetonitrile. *Synlett* 2009:3360.
- [159] Guilbault A-A, Legault CY. Drastic enhancement of activity in iodane-based α -tosyloxylation of ketones: iodine(III) does the hypervalent twist drastic enhancement of activity

- in iodane-based α -tosyloxylation of ketones: iodine(III) does the hypervalent twist. *ACS Catal* 2012;2:219.
- [160] Pu Y, Gao L, Liu H, Yan J. An effective catalytic α -phosphoryloxylation of ketones with iodobenzene. *Synthesis* 2012;44:99.
- [161] Uyanik M, Yasui T, Ishihara K. Hypervalent iodine-catalyzed oxylactonization of keto-carboxylic acids to ketolactones. *Bioorg Med Chem Lett* 2009;19:3848.
- [162] (a) Yan J, Wang H, Yang Z, He Y. An efficient catalytic sulfonyloxylation of alkenes using hypervalent iodine(III) reagent. *Synlett* 2009:2669; (b) Zhou Z-S, He X-H. A convenient phosphoryloxylation of pentenoic acids with catalytic hypervalent iodine(III) reagent. *Tetrahedron Lett* 2010;51:2480.
- [163] Zhong W, Liu S, Yang J, Meng X, Li Z. Metal-free, organocatalytic syn diacetoxylation of alkenes. *Org Lett* 2012;14:3336.
- [164] Dohi T, Maruyama A, Minamitsuji Y, Takenaga N, Kita Y. First hypervalent iodine(III) -catalyzed C-N bond forming reaction: catalytic spirocyclization of amides to n-fused spiroactams. *Chem Commun* 2007:1224.
- [165] Dohi T, Takenaga N, Fukushima K, Uchiyama T, Kato D, Motoo M, Fujioka H, Kita Y. Designer μ -oxo-bridged hypervalent iodine(III) organocatalysts for greener oxidations. *Chem Commun* 2010;46:7697.
- [166] (a) Moroda A, Togo H. Iodobenzene-catalyzed preparation of 3,4-dihydro-1h-2,1-benzothiazine 2,2-dioxides from 2-aryl-n-methoxyethanesulfonamides with m-chloroperoxybenzoic acid. *Synthesis* 2008:1257; (b) Yu Z, Ju X, Wang J, Yu W. Iodobenzene-mediated intramolecular oxidative coupling of substituted 4-hydroxyphenyl-n-phenylbenzamides for the synthesis of spirooxindoles. *Synthesis* 2011:860.
- [167] (a) Antonchick AP, Samanta R, Kulikov K, Lategahn J. Organocatalytic, oxidative, intramolecular C-H bond amination and metal-free cross-amination of unactivated arenes at ambient temperature. *Angew Chem Int Ed* 2011;50:8605; (b) Alla SK, Kumar RK, Sadhu P, Punniyamurthy T. Iodobenzene catalyzed C-H amination of N-substituted amines using m-chloroperbenzoic acid. *Org Lett* 2013;15:1334.
- [168] Samanta R, Bauer JO, Strohmman C, Antonchick AP. Organocatalytic, oxidative, intermolecular amination and hydrazination of simple arenes at ambient temperature. *Org Lett* 2012;14:5518.
- [169] Dohi T, Minamitsuji Y, Maruyama A, Hirose S, Kita Y. A New H_2O_2 /acid anhydride system for the iodoarene-catalyzed C-C bond-forming reactions of phenols. *Org Lett* 2008;10:3559.
- [170] Rodriguez A, Moran WJ. Iodobenzene-catalyzed intramolecular oxidative cyclization reactions of δ -alkynyl β -ketoesters. *Org Lett* 2011;13:2220.
- [171] Ngatimin M, Frey R, Levens A, Nakano Y, Kowalczyk M, Konstas K, Hutt OE, Lupton DW. Iodobenzene-catalyzed oxabicyclo[3.2.1]octane and [4.2.1]nonane synthesis via cascade C-O/C-C formation. *Org Lett* 2013;15:5858.
- [172] (a) Miyamoto K, Sakai Y, Goda S, Ochiai M. A catalytic version of hypervalent aryl- λ 3-iodane-induced hofmann rearrangement of primary carboxamides: iodobenzene as an organocatalyst and m-chloroperbenzoic acid as a terminal oxidant. *Chem Commun* 2012;48:982; (b) Zagulyaeva AA, Banek CT, Yusubov MS, Zhdankin VV. Hofmann rearrangement of carboxamides mediated by hypervalent iodine species generated in situ from iodobenzene and oxone: reaction scope and limitations. *Org Lett* 2010;12:4644; (c) Yoshimura A, Middleton KR, Luedtke MW, Zhu C, Zhdankin VV. Hypervalent

- iodine catalyzed hofmann rearrangement of carboxamides using oxone as terminal oxidant. *J Org Chem* 2012;77:11399; (d) Moriyama K, Ishida K, Togo H. Hofmann-type rearrangement of imides by in situ generation of imide-hypervalent iodines(III) from iodoarenes. *Org Lett* 2012;14:946.
- [173] (a) Miyamoto K, Sei Y, Yamaguchi K, Ochiai M. Iodomesitylene-catalyzed oxidative cleavage of carbon-carbon double and triple bonds using m-chloroperbenzoic acid as a terminal oxidant. *J Am Chem Soc* 2009;131:1382; (b) Thottumkara PP, Vinod TK. Oxidative cleavage of alkenes using an in situ generated iodonium ion with oxone as a terminal oxidant. *Org Lett* 2010;12:5640.
- [174] (a) Uyanik M, Akakura M, Ishihara K. 2-Iodoxybenzenesulfonic acid as an extremely active catalyst for the selective oxidation of alcohols to aldehydes, ketones, carboxylic acids, and enones with oxone. *J Am Chem Soc* 2009;131:251; (b) Koposov AY, Litvinov DN, Zhdankin VV, Ferguson MJ, McDonald R, Tykwinski RR. Preparation and reductive decomposition of 2-iodoxybenzenesulfonic acid. X-ray crystal structure of 1-hydroxy-1h-1,2,3-benziodoxathiole 3,3-dioxide. *Eur J Org Chem* 2006:4791; (c) Uyanik M, Ishihara K. 2-Iodoxybenzenesulfonic acid (IBS) catalyzed oxidation of alcohols. *Aldrichim Acta* 2010;43:83.
- [175] Uyanik M, Fukatsu R, Ishihara K. IBS-catalyzed oxidative rearrangement of tertiary allylic alcohols to enones with oxone. *Org Lett* 2009;11:3470.
- [176] Purohit VC, Allwein SP, Bakale RP. Catalytic oxidative 1,2-shift in 1,1'-disubstituted olefins using arene(iodo)sulfonic acid as the precatalyst and oxone as the oxidant *Org Lett* 2013;15:1650.
- [177] Uyanik M, Mutsuga T, Ishihara K. IBS-catalyzed regioselective oxidation of phenols to 1,2-quinones with oxone. *Molecules* 2012;17:8604.
- [178] Cui L-Q, Liu K, Zhang C. Effective oxidation of benzylic and alkane C-H bonds catalyzed by sodium o-iodobenzenesulfonate with oxone as a terminal oxidant under phase-transfer conditions. *Org Biomol Chem* 2011;9:2258.
- [179] (a) Yakura T, Konishi T. A novel catalytic hypervalent iodine oxidation of para-alkoxyphenols to para-quinones using 4-iodophenoxyacetic acid and oxone. *Synlett*. 2007:765; (b) Yakura T, Omoto M, Yamauchi Y, Tian Y, Ozono A. Hypervalent iodine oxidation of phenol derivatives using a catalytic amount of 4-iodophenoxyacetic acid and oxone as a co-oxidant. *Tetrahedron* 2010;66:5833.
- [180] Ngatimin M, Frey R, Andrews C, Lupton DW, Hutt OE. Iodobenzene catalysed synthesis of spirofurans and benzopyrans by oxidative cyclisation of vinylogous esters. *Chem Commun* 2011;47:11778.
- [181] Ojha LR, Kudugunti S, Maddukuri PP, Kommareddy A, Gunna MR, Dokuparthi P, Gottam HB, Botha KK, Parapati DR, Vinod TK. Benzylic carbon oxidation by an in situ formed o-iodoxybenzoic acid (IBX) derivative. *Synlett* 2009:117.
- [182] Xu Y, Yang Z, Hu J, Yan J. A new method for the benzylic oxidation of alkylarenes catalyzed by hypervalent iodine(III). *Synthesis* 2013;45:370.
- [183] Yusubov MS, Zagulyaeva AA, Zhdankin VV. Iodine(V)/ruthenium(III)-cocatalyzed oxidations: a highly efficient tandem catalytic system for the oxidation of alcohols and hydrocarbons with oxone. *Chem Eur J* 2009;15:11091.
- [184] Yakura T, Ozono A. Novel 2,2,6,6-tetramethylpiperidine 1-oxyl-iodobenzene hybrid catalyst for oxidation of primary alcohols to carboxylic acids. *Adv Synth Catal* 2011;353:855.

- [185] (a) Liang H, Ciufolini MA. Chiral hypervalent iodine reagents in asymmetric reactions. *Angew Chem, Int Ed* 2011;50:11849; (b) Ngatimin M, Lupton DW. The discovery of catalytic enantioselective polyvalent iodine mediated reactions. *Aust J Chem* 2010;63:653; (c) Parra A, Reboredo S. Chiral hypervalent iodine reagents: synthesis and reactivity. *Chem Eur J* 2013;19:17244; (d) Farid U, Wirth T. *Asymmetric Synthesis II: Stereoselective Synthesis with Hypervalent Iodine Reagents*. In: Christmann M, Bräse S, editors. Weinheim: Wiley-VCH; 2012. p 197.
- [186] Imamoto T, Koto H. Asymmetric oxidation of sulfides to sulfoxides with trivalent iodine reagents. *Chem Lett* 1986:967.
- [187] (a) Ray DG, Koser GF. Iodinanes with chiral ligands. Synthesis and structure of iodine(III) dibenzoyl tartrates. *J Org Chem* 1992;57:1607; (b) Hatzigrigoriou E, Varvoglis A, Bakola-Christianopoulou M. Preparation of [hydroxy((+)-10-camphor-sulfonyl)oxy]iodo]benzene and its reactivity toward carbonyl compounds. *J Org Chem* 1990;55:315; (c) Ray DG, Koser GF. Iodinanes with iodine(III)-bound homochiral alkoxy ligands: preparation and utility for the synthesis of alkoxysulfonium salts and chiral sulfoxides. *J Am Chem Soc* 1990;112:5672; (d) Ray DG, Koser GF. Facile synthetic entry into the 1,3-dihydro-3-methyl-3-phenyl-1,2-benziodoxole family of λ 3-iodanes. *Tetrahedron Lett* 1996;37:6453.
- [188] (a) Wirth T, Hirt UH. Chiral hypervalent iodine compounds. *Tetrahedron: Asymmetry* 1997;8:23; (b) Hirt UH, Spingler B, Wirth T. New chiral hypervalent iodine compounds in asymmetric synthesis. *J Org Chem* 1998;63:7674; (c) Hirt UH, Schuster MFH, French AN, Wiest OG, Wirth T. Chiral hypervalent organo-iodine(III) compounds. *Eur J Org Chem* 2001:1569.
- [189] Ochiai M, Kitagawa Y, Takayama N, Takaoka Y, Shiro M. Synthesis of chiral diaryliodonium salts, 1,1'-binaphthyl-2-yl(phenyl)iodonium tetrafluoroborates: asymmetric α -phenylation of β -keto ester enolates. *J Am Chem Soc* 1999;121:9233.
- [190] Ladziata U, Carlson J, Zhdankin VV. Synthesis and oxidative reactivity of new chiral hypervalent iodine(V) reagents based on (S)-proline. *Tetrahedron Lett* 2006;47:6301.
- [191] (a) Tohma H, Takizawa S, Watanabe H, Kita Y. Hypervalent iodine(III) oxidation catalyzed by quaternary ammonium salt in micellar systems. *Tetrahedron Lett* 1998;39:4547; (b) Tohma H, Takizawa S, Watanabe H, Fukuoka Y, Maegawa T, Kita Y. Hypervalent iodine(V)-induced asymmetric oxidation of sulfides to sulfoxides mediated by reversed micelles: novel nonmetallic catalytic system. *J Org Chem* 1999;64:3519; (c) Tohma H, Takizawa S, Morioka H, Maegawa T, Kita Y. Novel catalytic asymmetric sulfoxidation in water using the hypervalent iodine reagent iodoxybenzene. *Chem Pharm Bull* 2000;48:445.
- [192] (a) Altermann SM, Richardson RD, Page TK, Schmidt RK, Holland E, Mohammed U, Paradine SM, French AN, Richter C, Bahar AM, Witulski B, Wirth T. Catalytic enantioselective α -oxysulfonylation of ketones mediated by iodoarenes. *Eur J Org Chem* 2008:5315; (b) Altermann SM, Schafer S, Wirth T. New chiral hypervalent iodine(V) compounds as stoichiometric oxidants. *Tetrahedron* 2010;66:5902.
- [193] (a) Richardson RD, Page TK, Altermann S, Paradine SM, French AN, Wirth T. Enantioselective α -oxytosylation of ketones catalyzed by iodo arenes. *Synlett* 2007:538; For a recent work on this catalytic reaction, see: (b) Guilbault A-A, Basdevant B, Wanie V, Legault CY. Catalytic enantioselective α -tosyloxylation of ketones using iodoaryloxazoline catalysts: insights on the stereinduction process. *J Org Chem* 2012; 77:11283.

- [194] Chiral lactate groups were originally introduced by Fujita and co-workers as the ortho ring substituent for constructing a chiral environment around the iodine center: Fujita M, Okuno S, Lee HJ, Sugimura T, Okuyama T. Enantiodifferentiating tetrahydrofuran-ylation of but-3-enyl carboxylates using optically active hypervalent iodine(III) reagents via a 1,3-dioxan-2-yl cation intermediate. *Tetrahedron Lett* 2007;48:8691.
- [195] (a) Dohi T, Maruyama A, Takenaga N, Senami K, Minamitsuji Y, Fujioka H, Cammerer SB, Kita Y. A chiral hypervalent iodine(III) reagent for enantioselective dearomatization of phenols. *Angew Chem, Int Ed* 2008;47:3787; (b) Dohi T, Takenaga N, Nakae T, Toyoda Y, Yamasaki M, Shiro M, Fujioka H, Maruyama A, Kita Y. Asymmetric dearomatizing spirolactonization of naphthols catalyzed by spirobiindane-based chiral hypervalent iodine species. *J Am Chem Soc* 2013;135:4558.
- [196] (a) Uyanik M, Yasui T, Ishihara K. Enantioselective oxidative spirolactonization catalyzed by in situ generated chiral hypervalent iodine(III) species. *Angew Chem, Int Ed* 2010;49:2175; (b) Uyanik M, Yasui T, Ishihara K. Chiral hypervalent iodine-catalyzed enantioselective oxidative spirolactonization of 1-naphthol derivatives and one-pot diastereo-selective oxidation to epoxyspirolactones. *Tetrahedron* 2010;66:5841.
- [197] Stoichiometric use of Ishihara's catalyst for other reactions: (a) Fujita M, Yoshida Y, Miyata K, Wakisaka A, Sugimura T. Enantiodifferentiating endo-Selective Oxylactonization of ortho-Alk-1-enylbenzoate with a Lactate-Derived Aryl- λ -3-Iodane. *Angew Chem, Int Ed* 2010;49:7068; (b) Fujita M, Wakita M, Sugimura T. Enantioselective prevost and woodward reactions using chiral hypervalent iodine(III) : switch over of stereochemical course of an optically active 1,3-dioxolan-2-yl cation. *Chem Commun* 2011;47:3983.
- [198] Roben C, Souto JA, Gonzalez Y, Lishchynskyi A, Müniz K. Enantioselective metal-free diamination of styrenes. *Angew Chem, Int Ed* 2011;50:9478.
- [199] (a) Farid U, Wirth T. Highly stereoselective metal-free oxyaminations using chiral hypervalent iodine reagents. *Angew Chem, Int Ed* 2012;51:3462; The same research group has recently extend the asymmetric conditions to work in the stereoselective rearrangements of alkenes: (b) Farid U, Malmedy F, Claveau R, Albers L, Wirth T. Stereoselective rearrangements with chiral hypervalent iodine reagents. *Angew Chem, Int Ed* 2013;52:7018.
- [200] Kong W, Feige P, de Haro T, Nevado C. Regio- and enantioselective aminofluorination of alkenes. *Angew Chem, Int Ed* 2013;52:2469.
- [201] Quideau S, Lyvinec G, Marguerit M, Bathany K, Ozanne-Beaudenon A, Buffeteau T, Cavagnat D, Chénéde A. Asymmetric hydroxylative phenol dearomatization through in situ generation of iodonanes from chiral iodoarenes and m-CPBA. *Angew Chem, Int Ed* 2009;48:4605.
- [202] Boppisetti JK, Birman VB. Asymmetric oxidation of o-alkylphenols with chiral 2-(o-iodoxyphenyl)-oxazolines. *Org Lett* 2009;11:1221.
- [203] Volp KA, Harned AM. Chiral aryl iodide catalysts for the enantioselective synthesis of para-quinols. *Chem Commun* 2013;49:3001.
- [204] Fernandez Gonzalez D, Benfatti F, Waser J. Asymmetric organocatalysis meets hypervalent iodine chemistry for the α -functionalization of carbonyl compounds. *ChemCatChem* 2012;4:955.
- [205] Kita Y, Dohi T, Morimoto K. Hypervalent iodine induced metal-free C-H cross couplings to biaryls. *J Synth Org Chem, Jpn* 2011;69:1241.

- [206] Very recent reviews:(a) Dohi T, Kita Y. New site-selective organoradical based on hypervalent iodine reagent for controlled alkane sp^3 C-H oxidations. *ChemCatChem* 2014;6:76; (b) Singh FV, Wirth T. Oxidative Rearrangements with Hypervalent Iodine Reagents. *Synthesis* 2013;45:2499; (c) Brown M, Farid U, Wirth T. Hypervalent iodine reagents as powerful electrophiles. *Synlett* 2013;24:424; (d) Kajiyama D, Saitoh T, Nishiyama S. Application of electrochemically generated hypervalent iodine oxidant to natural products synthesis. *Electrochemistry* 2013;81:319; (e) Tellitu I, Dominguez E. The application of [bis(trifluoroacetoxy)iodo]benzene (PIFA) in the synthesis of nitrogen-containing heterocycles. *Synlett* 2012;23:2165; (f) Bernini R, Fabrizi G, Pouysegu L, Deffieux D, Quideau S. Synthesis of biologically active catecholic compounds via ortho-selective oxygenation of phenolic compounds using hypervalent iodine(V) reagents. *Curr Org Synth* 2012;9:650; (g) Yusubov MS, Zhdankin VV. Hypervalent iodine reagents and green chemistry. *Curr Org Synth* 2012;9:247.

IODINE AND HALOGEN BONDING

GIANCARLO TERRANEO, GIUSEPPE RESNATI,
AND PIERANGELO METRANGOLO

Laboratory of Nanostructured Fluorinated Materials (NFMLab), Department of Chemistry, Materials, and Chemical Engineering “Giulio Natta”, Politecnico di Milano, Milan, Italy

8.1 INTRODUCTION

The physical and chemical properties of molecular systems are heavily influenced by the intermolecular forces. The anomalous boiling behavior of water as well as all the complex recognition events occurring in biological systems and the solubility profiles of a given compound in different solvents are selected phenomena where the fine balance between different intermolecular forces play a major role. As a result, hydrogen bonding (HB), dipole–dipole interactions, ion–dipole interactions, and van der Waals forces are the basis for understanding phenomena related to chemical reactivity, catalysis, and biomolecular structure and function and are essential in any chemical, biological, and physical description [1].

Fluorine, chlorine, bromine, iodine, and astatine belong to the 17th group of the periodic table and are known as the halogens (X). The insertion of a halogen atom in a compound gives rise to halogenated systems. Halogen atoms are usually close to the molecular surface in organic derivatives, namely, they are conveniently positioned to be easily involved in intermolecular interactions and can affect, or even drive, recognition and self-assembly processes. Most of the noncovalent interactions given by halogen atoms in haloorganics belong to two main classes. In the first class the halogen atoms act as electron density donor sites toward electron-deficient partners as hydrogen atoms or metal cations. This interaction can be easily understood in terms of the high electronegativity of halogen atoms resulting in a high electron

density at their surface [2]. In the second class, halogen atoms act as electron density acceptor sites and attractively interact with electron donors. This latter interaction class is known as the halogen bond (XB) and has been widely observed in many different contexts even if it may seem conflicting with the high electronegativity of halogens [3].

In recent years, the halogen bond has evolved from a scientific curiosity to a chemical interaction frequently pursued when design and manipulation of aggregation processes are targeted. According to the International Union of Pure and Applied Chemistry (IUPAC) definition: A halogen bond occurs when there is evidence of a net attractive interaction between an electrophilic region associated with a halogen atom in a molecular entity and a nucleophilic region in another, or the same, molecular entity [4].

The electrophilic nature for halogen atom has long been considered as strangeness and the persistent biases resulting from the approximation that halogen atoms are neutral entities in dihalogens or fully negative elements in the halocarbons has long prevented electrophilic halogens from being considered responsible for the frequent formation of strong attractive interactions.

Recent theoretical studies have fully explained the electrophilic nature of halogen in terms of anisotropic distribution of the electron density around the atoms [5]. This anisotropy determines the formation of a region of positive, or less negative, electrostatic potential, the so-called σ hole [6], on the outermost surface of the halogen atom. In a halogen derivative $Y-X$ ($Y = C, N$, halogen atom, etc.) there is a depletion of electron density (σ hole) on the extension of the covalent bond formed by the halogen (Fig. 8.1) and the atomic radius along the covalent bond is smaller than in the perpendicular direction as an outcome of this anisotropic distribution of the electron density.

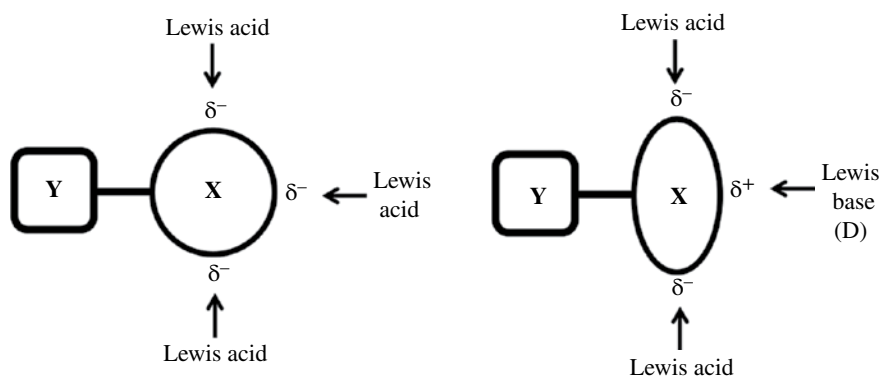


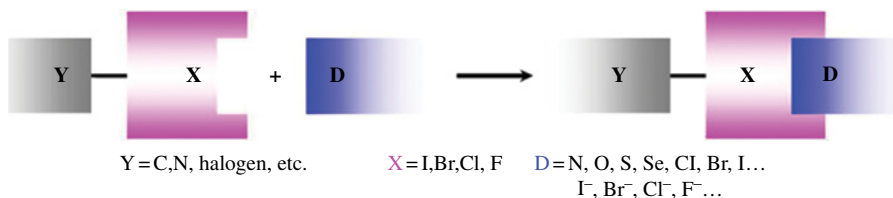
FIGURE 8.1 Schematic representation of the electron density distribution of covalently bound halogen atoms (X) and the resulting attractive interactions with Lewis acids and bases. Left: Traditional textbook description. Right: Description based on the anisotropic distribution of the electron density.

In general, halogen bonds can be depicted as follows:



where X is the electrophilic halogen atom (Lewis acid, XB donor), D is an electron density donor (Lewis base, XB acceptor), and Y is typically a carbon, nitrogen, or halogen atom (Scheme 8.1).

The depleted electron density on the extension of the Y–X bond increases on moving from F to I, namely, increases with the polarizability of the halogen atom [7]. Therefore the strength of the halogen bond donor increases in the order $Cl < Br < I$ [8], and fluorine atom can work as a halogen bond donor only when attached to particularly strong electron-withdrawing groups [9]. Importantly, the σ -hole region is surrounded, in all the halogen atoms, by an electroneutral ring and, further out, a negatively charged belt (Fig. 8.2).



SCHEME 8.1 General scheme for the formation of halogen bond.

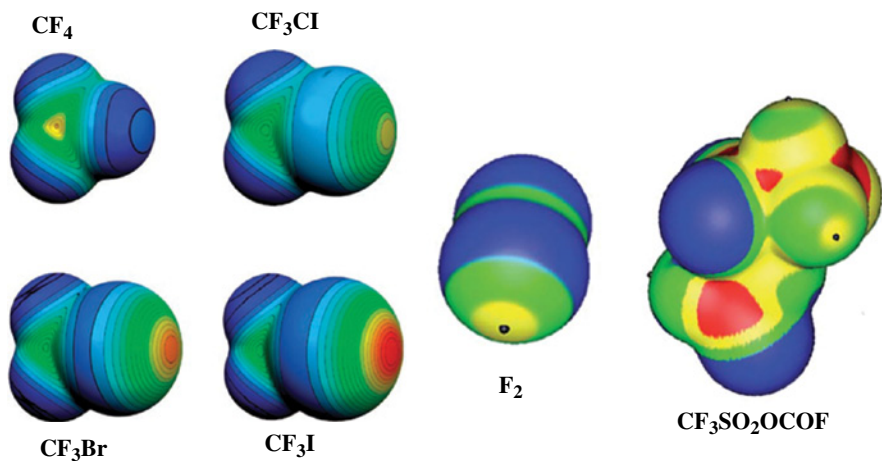


FIGURE 8.2 Left: The molecular electrostatic potential at the isodensity surface with 0.001 au: CF₄, CF₃Cl, CF₃Br, and CF₃I. Color ranges are as follows: Red, greater than 27 kcal mol⁻¹; yellow, between 20 and 14 kcal mol⁻¹; green, between 12 and 6 kcal mol⁻¹; blue, negative. Right: F₂ and CF₃SO₂OCOF (the CF₃ group is on top). Color ranges are as follows: Red, greater than 20 kcal mol⁻¹; yellow, between 20 and 9 kcal mol⁻¹; green, between 9 and 0 kcal mol⁻¹; blue, negative. For F₂ and CF₃SO₂OCOF the black hemispheres denote the positions of the most positive potentials associated with the fluorines. (See insert for color representation of the figure.)

The σ hole becomes more extended and more positive as the electron-withdrawing effect of the neighboring groups increases [10]. This feature allows for the careful tuning of the strength of the halogen bond by changing the Y residue [11].

According to this model, halogen atoms may act as amphiphilic sites. They function as Lewis bases when interacting with electron density acceptor sites through electron density donation from their nonbonding orbitals (negative belt), while they act as Lewis acids when accepting electron density into the σ hole from Lewis bases [12].

Halogen bond denotes any electron density donation to halogen atoms by neutral or anionic Lewis bases (e.g., N, O, S, P, halogens, π electrons). From a geometric point of view, the attractive nature of XB results in 35–10% shortening of the interatomic distance of participating atoms (D and X) below the sum of their van der Waals radii [13] and in an elongation of the Y–X covalent bond [14]. These evidences can be understood in term of charge-transfer interaction where the electrons in the n orbital of D are donated to the antibonding X–Y orbital.

The linear directionality of XB is a quite distinctive feature for this noncovalent interaction and the stronger the XB is, the closer to 180° the angle between the covalent and noncovalent bonds in the D \cdots X–Y system is [15]. Both the position of the region with positive electrostatic potential in the starting halogen derivative and the $n \rightarrow \sigma^*$ donation of electron density in the complex can be used to rationalize this directionality [16]. The XB interaction energies strongly depend on the nature of the involved XB donors and acceptors. They typically cover the range 5–30 kJ mol $^{-1}$ and, in special cases, they can be as high as 180–200 kJ mol $^{-1}$.

Iodine is a better halogen bonding donor than lighter halogens, namely, it affords stronger and more directional interactions. As for the other halogens, its electron density acceptor ability increases with the increased electron-withdrawing ability of the atom bound to it. The order X–I > C(sp)–I > C(sp 2)–I > C(sp 3)–I (X = halogen) is generally followed. Iodohalogen diatomic molecules and iodoheteroarenes [17] where the heteroaromatic ring is positively charged are particularly good halogen bond donors, but also iodoalkynes [18] and some iodoarenes [19] form fairly strong XB interactions.

I $_2$ has all the features to function as a very good halogen bond donor, the positive cap on any iodine atoms in I $_2$ being comparable to the σ hole on the iodine atom of an iodoperfluorocarbon or iodoethynyl derivative (Fig. 8.3) [20].

Iodoperfluorocarbons are frequently used halogen bonding donors and they have been extensively employed by P. Metrangolo and G. Resnati during the last 15 years to investigate some basic features of the interaction and to exploit them in applicatively useful systems [22]. Iodoalkynes are less conventional halogen bonding donors despite the fact that the triple bond effectively increases the electrophilic character of the iodine atom [23], and recent papers have proven the ability of the C \equiv C–I moiety to drive the formation of different halogen-bonded systems with interesting physical and chemical properties [24]. The exploitation of iodoperfluorocarbons and iodoalkynes as XB donors has been well-documented in recent reviews and will be not discussed in this chapter [25].

In this chapter we present a brief overview of selected halogen-bonded systems involving exclusively iodine molecule (I $_2$) as XB donor. Few examples with BrI and ClI XB donors will also be discussed with the aim to show how the XB strength can

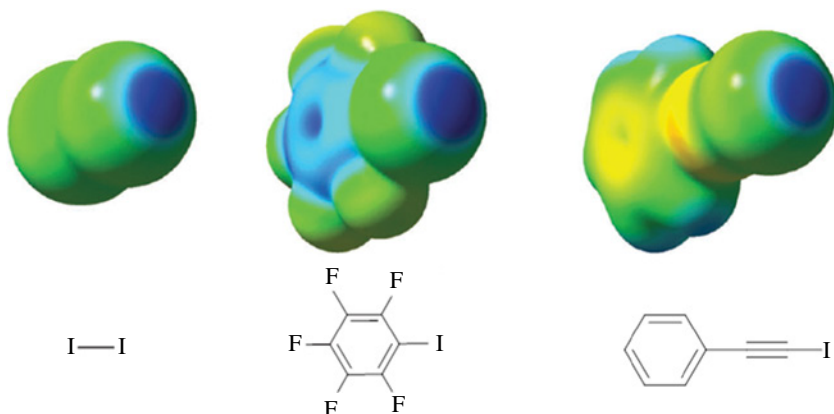


FIGURE 8.3 Molecular electrostatic potential surfaces of representative halogen bond donors. Red indicates negative charge density and blue positive charge density. The plots have been set to the same color scale for facilitating visual comparison. For interpretation of the references to color in this figure legend, the reader is referred to the web version of this chapter. Reproduced with permission from Ref. [21] © Royal Society of Chemistry.

be tuned by changing the electron-withdrawing ability of the atom bound to iodine. The halogen bonding acceptors selected here (D in Eq. 8.1) will cover different classes of organic neutral molecules having free electron lone pairs and π systems that could function as electron donor sites (D = N, O, P, S, As, Se, Te, π systems). A limited number of examples involving charged halogen bonding acceptors will be discussed too (D = I⁻, Cl⁻, or Br⁻).

Examples chosen will be selected in the liquid and solid state, and we will provide the information of the strength of halogen-bonded complexes in terms of both thermodynamic data and percentage reduction distance in a D \cdots I pair relative to the sum of the van der Waals radii of the involved atoms. The illustrated cases will span over a wide range of fields covering both fundamental and applied sciences, from supramolecular chemistry and crystal engineering to functional cocrystals.

This chapter covers only a part of the contributions that I₂ has given to supramolecular chemistry during the past few years. The chosen examples are good representatives of the future opportunities that I₂ could open in the field of self-assembly and materials sciences.

8.2 I₂ AS HALOGEN BONDING DONOR

8.2.1 Perspective

The history of the halogen bond involving iodine molecule dates back approximately 200 years ago when the I₂ \cdots NH₃ adduct, probably the first halogen-bonded system ever prepared, was synthesized in J. L. Gay-Lussac's laboratory by J. J. Colin [26], and he observed that the reaction between dry gaseous ammonia and dry iodine provided to the

Color of iodine in various solutions	
A. Violet Solutions	B. Brown Solutions
Hydrocarbons:	Iodides:
Hexane	Ethyl iodide
Benzene (thiophene free)	Amyl iodide
Toluene ¹	Cetyl iodide
<i>o</i> -Xylene ²	Phenyl iodide
<i>m</i> -Xylene	Potassium iodide { In water
<i>p</i> -Xylene	Hydrogen iodide { solutions
Halogen compounds:	Oxygen compounds.
Chloroform	Alcohols:
Ethylene chloride ³	Methyl alcohol
Ethylidene chloride	Ethyl alcohol
Tetrachlorethylene ⁴	<i>n</i> -Butyl alcohol
Carbon tetrachloride	Dimethylethyl carbinol
Isobutyl chloride ⁵	Heptyl alcohol
Amyl chloride	Ethers:
Chlorobenzene	Ethyl ether
Benzalchloride	Dimethyl acetal
Benzotrichloride	Anisol

FIGURE 8.4 Part of the table from Lachman's seminal paper published in 1903 reporting the different colors for several solvents upon addition of I_2 . Reproduced with permission from Ref. [30].

formation of a liquid a somewhat metallic luster. The characterization of the complex and the molecular understanding of the interaction between NH_3 and I_2 raised more than 50 years later when F. F. Guthrie obtained the same liquid in pure form after adding powdered iodine to aqueous ammonia and proposed the structure $NH_3 \cdots I_2$ [27].

Almost 100 years later the association constants (K_a) between I_2 (XB donors) and arenes (XB acceptors) provided by H. A. Benesi and J. H. Hildebrand [28], along with R. S. Mulliken's studies on the quantum mechanical nature of these interactions [29] set the fundamental information for all the experimental and theoretical studies that have been performed during the following years on halogen-bonded complexes.

The ability of I_2 to interact with a variety of Lewis bases was studied using different techniques both in solution and in the solid state. The observation that solutions of molecular iodine in different electron-donating solvents have different colors played a fundamental role in understanding the interaction of iodine molecule with systems having free lone pairs. Water or alcohols solutions of I_2 are brown, while when I_2 is dissolved in carbon tetrachloride, benzene, or other solvents of low basicity, red to violet solutions are obtained (Fig. 8.4) [30]. A. Lachman had proposed as early as 1903 the formation of "solvent $\cdots I_2$ " complexes in solution in order to explain the color variation and 40 years later the different reactivity of the I_2 molecule in different solvents was interpreted by J. Kleinberg and A. W. Davidson [31] in terms of the strength of solvent $\cdots I_2$ interaction.

8.2.2 UV-VIS Spectroscopy

The ultraviolet-visible (UV-VIS) spectroscopy provided important information on the strength of I_2 molecule as an XB donor. The interaction of I_2 with a solvent endowed with Lewis basic properties affects the UV-VIS spectrum of the

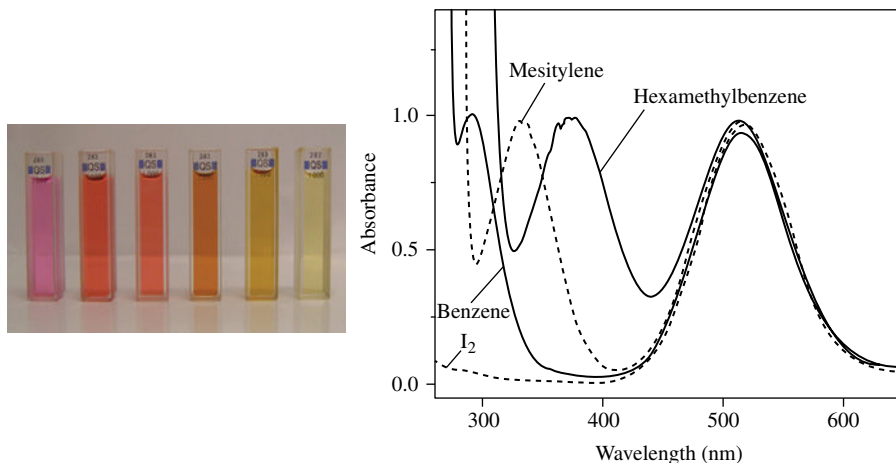


FIGURE 8.5 Left: The color of iodine solutions relates with the electron-donating ability of the employed solvents. From left to the right the characteristic colors of I₂ dissolved in hexane, toluene, dichloroethane, acetonitrile, methanol and pyridine [3d]. Right: Electronic spectra of CCl₄ solutions of I₂ before and after the addition of excess amount of benzene, mesitylene, and hexamethylbenzene ($\lambda_{\text{charge transfer}}^{\text{max}}$ 369 nm). A charge-transfer band appears upon cosolvent addition and its λ_{max} increases with the strength of the XB acceptors (benzene, 285 nm; mesitylene, 327 nm; hexamethylbenzene, 369 nm). Reproduced with permission from Ref. [32] © Royal Society of Chemistry. (See insert for color representation of the figure.)

system, which may vary significantly with respect to the starting “isolated” molecules (Fig. 8.5).

Two pronounced changes generally occur in the spectrum: A hypsochromic shift is observed in the visible region, while a new band appears in the UV region due to the charge-transfer phenomena between the XB acceptor and donor. Numerous studies using different XB acceptor solvents such as azines and azoles, ethers, carbonyl and sulfur derivatives, and π systems (Fig. 8.5) allowed to get detailed insights in the formation of halogen-bonded I₂⋯solvent complexes. Association constants derived from UV–VIS experiments have shown that polarizable Lewis bases are excellent XB acceptors toward I₂, and the obtained trend follows the hard–soft acid–base theory. XB acceptors possessing a lone pair form more stable adducts than systems possessing π electrons (Fig. 8.6). This may be related to the fact that a lone pair interacts more favorably with the σ hole of the XB donors than a π -electron system. The values of K_a of complexes involving diatomic molecules such as ICl and IBr with pyridine have shown how the XB strength tends to increase with the electronegativity of the atom bound to iodine, consistent with the general trend that the more positive the σ hole is, the stronger the halogen-bonded complex [33].

The huge number of K_a data from UV–VIS spectroscopy has also allowed to define an I₂ basicity scale ($\text{p}K_{\text{B-12}} = \log(K_a)$) [34]. This scale is analogous to the $\text{p}K_{\text{B-H}}$ scale commonly used to describe basicity toward protons. It is based on the use of I₂ as a reference Lewis acid and can be used to anticipate the solution behavior of I₂ [32].

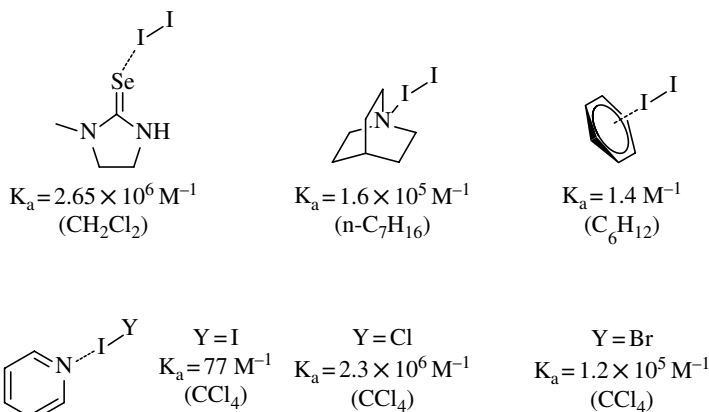


FIGURE 8.6 Association constants (K_a) for representative halogen-bonded complexes in organic solvents obtained through UV–VIS measurements. The used solvent is given in parenthesis [21].

Anions are generally good nucleophiles and might be expected to function as valuable XB acceptors. In the recent years this ability was confirmed with a great variety of XB donors [35]. The behavior of anionic species in the formation of halogen-bonded systems has been well-documented in recent papers and reviews [36]. In this section only few selected examples will be presented.

The formation of the triiodide anion I_3^- and analogous mixed trihalides Y I_2^- ($\text{Y} = \text{Br}, \text{Cl}, \text{F}$) can be easily rationalized in terms of XB. I^- , the electron donor, is the XB acceptor and attractively interacts with the σ hole of I_2 , the electron acceptor [37], which functions as the XB donor. The $n \rightarrow \sigma^*$ donation results in the formation of an XB on the extension of the covalent bond of molecular iodine. The experimental ΔH of the reaction $\text{I}_2 + \text{I}^- \rightarrow \text{I}_3^-$ is -17 kJ mol^{-1} in water (K^+ counterion) and -126 kJ mol^{-1} in the gas phase [38] while the computed gas-phase value (MP2/LANL2DZ level) is $139.0 \text{ kJ mol}^{-1}$ [39].

The formation of the I_3^- in solution was postulated in 1959 by E. E. Havinga and coworkers due to the increased solubility of the molecular iodine in water upon addition of iodide anion [40]. After that evidence, numerous studies were performed on polyiodide systems and for further information on this topic, see the dedicated chapter.

Also, polyiodides are well-documented in the literature [41] and they can be considered as halogen-bonded adducts when their geometry is in keeping with the directionality of the interaction. Some examples of polyhalide anions such as I_4^{2-} and I_7^{3-} and some mixed systems such as Cl_2I_2^- or Br_2I_2^- will be presented onward in the solid-state section.

8.2.3 IR Spectroscopy

Infrared (IR) spectroscopy is a valuable tool to study halogen-bonded complexes formed by I_2 . The frequency of the I–I stretching in the IR region is lowered upon XB adduct formation, and it is strongly correlated with the basicity of the XB acceptor;

the stronger the base the larger the shift [42]. The I–I stretching variation is related not only to the change of force constant of the I–I bond but also to the coupling of the I–I and I...D stretching bands, but, unfortunately, the two band usually overlap. This behavior has limited the use of IR spectroscopy for studying the formation of I₂...D halogen-bonded systems. The iodine frequency shift on XB complex formation could not be used to create an iodine scale as was the case for the UV–VIS method, the use of IR spectroscopy being limited to assessing the formation of new halogen-bonded systems.

I–Cl shows shift perturbations similar to those of I₂, but the low solubility of the compound in several solvents, its high reactivity, and easy ionization have restricted its use for establishing relative basicities of different derivatives.

8.2.4 Raman Spectroscopy

Raman spectroscopy can be considered a very reliable tool for identifying the iodine moiety in neutral I₂...D adducts and polyiodide species both in solution [43] and in the solid state [44]. The I–I stretching mode, at 180 cm^{−1} in solid I₂, moves on I–I...D adducts formation. Its position depends on the physical state of the system and in linear adducts the I–I stretching mode is typically observed in the region 140–210 cm^{−1}. The frequently observed lower-frequency shift is due to the lowered bond order, and consequent increases in the I–I distance, resulting from the charge transfer occurring on interaction formation. For example, the interaction of I₂ with different solvents causes an I–I frequency decrease related to the electron-donating ability of the solvent, the I–I stretching mode being at 167, 202, and 205 cm^{−1} in pyridine, ethanol, and benzene, respectively [45]. Cl–I...D complexes show a similar trend and a similar correlation between the changes of the vibration bands and the relative basicity of the D moiety [45].

P. Deplano and coworkers [46] analyzed a huge number of Raman spectra in the solid state for various I₂...D neutral adducts and polyiodide species starting from I₄^{2−} up to I₂₉^{3−}. The analyses allowed for the classification and the prediction of the possible vibrational mode for the I–I molecule in all the polyiodide systems. It was also possible to suggest that the formation of discrete units is highly unlikely.

G. Resnati *et al.* have recently demonstrated the unique ability of the diiodide of 1,6-bis(trimethylammonium)hexane (hexamethonium diiodide, HMET²⁺·2I[−]) to trap one I₂ molecule and to form the discrete I₄^{2−} dianion, which has a low stability as isolated species [47] (Fig. 8.7). Similarly, the triiodide of 2,2,9,9,16,16-hexamethyl-2,9,16-triazoniaheptadecane (HMTAHD³⁺), a structurally related tri-ammonium cation, traps two I₂ molecules and forms the discrete I₇^{3−} trianion [48]. The obtainment of these unusual polyiodides as isolated species is driven by a combination of two factors, the ability of I[−] to work as very efficient XB acceptors toward I₂ and the dimensional control provided by the size matching [49] of the intramolecular N⁺–N⁺ separation in the cation with the separation of the iodide anions in the halogen-bonded I...I₂...I[−] moiety, which are 8.9 and 9.7 Å in HMET²⁺ and I₄^{2−}, respectively. The discrete polyiodide systems were obtained both from solution and from the gas/solid reaction and either the bi- and the triammonium cations are able to reversely uptake and release I₂ by external stimulus demonstrating their dynamically porous character.

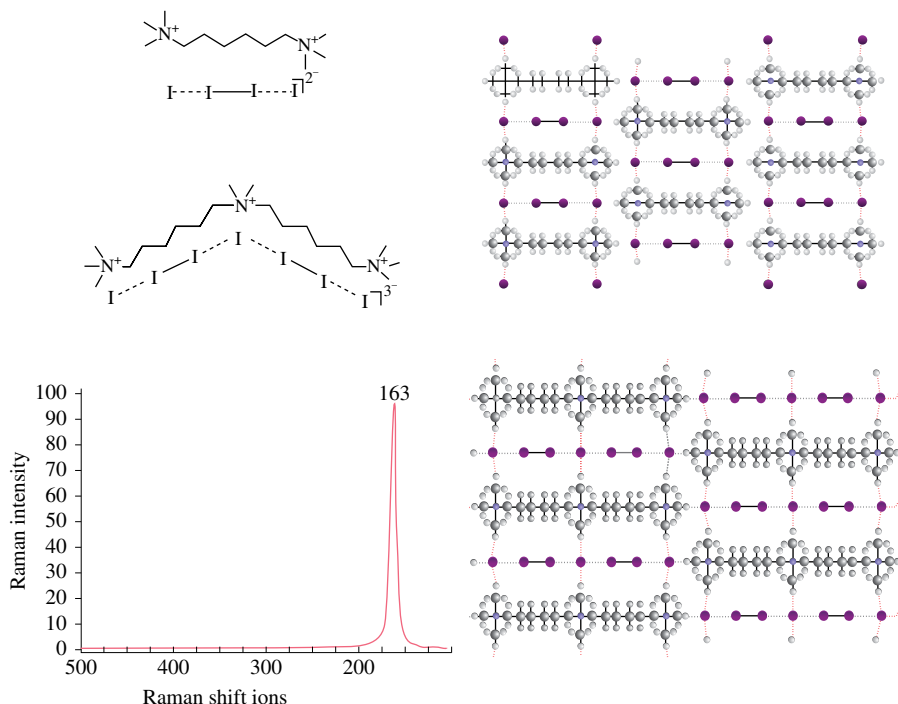


FIGURE 8.7 Top left: Molecular structures of the polyiodides $\text{HMET}^{2+} \cdot \text{I}_4^{2-}$ and $\text{HMTAHD}^{3+} \cdot \text{I}_7^{3-}$. Bottom left: Raman spectrum of $\text{HMTAHD}^{3+} \cdot \text{I}_7^{3-}$. Right: Ball-and-stick representation of the crystal packings of $\text{HMET}^{2+} \cdot \text{I}_4^{2-}$ (top) and $\text{HMTAHD}^{3+} \cdot \text{I}_7^{3-}$ (right) viewed along *c* crystallographic axis; XBs and $\text{I} \cdots \text{H}$ HBs are dashed lines, respectively; color code: Carbon, gray; nitrogen, blue; iodine, purple; hydrogen, white. For interpretation of the references to color in this figure legend, the reader is referred to the web version of this chapter.

The Raman spectra of $\text{HMET}^{2+} \cdot \text{I}_4^{2-}$ and $\text{HMTAHD}^{3+} \cdot \text{I}_7^{3-}$ show the vibrational $\text{I}-\text{I}$ mode at 161 and 163 cm^{-1} , respectively. The lower frequency, with respect to isolated I_2 , is nicely consistent with the charge transfer from the iodide anions to the iodine molecule(s) occurring on interaction formation.

8.2.5 Solid State and Crystal Structures

The design and construction of new crystalline materials with specific properties is a frontier research topic with remarkable applicative potential. Crystal engineering [50] has rapidly grown within this frame and has developed its basic guidelines dissecting the crystalline system into one or more cooperative supramolecular synthons [51]. Engineered multicomponent crystals (cocrystals) [52] have been developed and applied in a great variety of areas spanning from green chemistry to biomedical treatments and material sciences [53].

XB is playing an increasingly important role in crystal engineering and solid-state chemistry, and it is not surprising to find several examples where I_2 molecules have been used to construct new engineered cocrystals. In the following section a brief

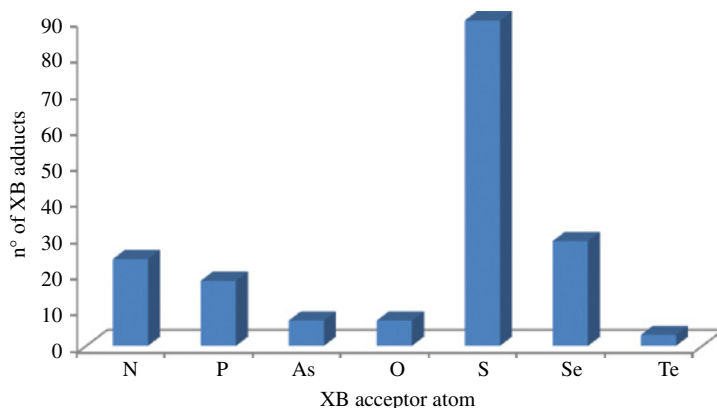


CHART 8.1 Histogram representing the distribution of halogen-bonded adducts formed by I₂ as a function of the XB acceptor atom. Search performed on CSD 5.34.

inventory of the recent I₂⋯D halogen-bonded system will be presented; the XB acceptors D will be either a neutral or an anionic systems. The percentage distance reduction in an I⋯D pair, in comparison with the sum of the van der Waals radii of the involved atoms, will be used as an indication of the strength of the XB. The neutral XB acceptors will be discussed first dividing them as in the groups of the periodic table, while the anionic XB acceptors will be presented later on.

A search in the Cambridge Structural Database (CSD 5.34) [54] was performed for systems containing halogen-bonded I₂ molecules, namely, for adducts with intermolecular I⋯D distances (D = N, O, P, S, As, Se, and Te) shorter than the sum of the van der Waals radii of involved atoms. Structures with no 3D atomic coordinates or with crystallographic disorder on the XB donors are not considered.

In CSD, 178 crystal structures have been found wherein one or more I₂ molecules are halogen-bonded to a lone pair–possessing atom D [55]. The distribution of the atoms that function as electron donors toward the σ hole in I₂ is summarized in Chart 8.1. Sulfur is the most common XB acceptor atom, followed by nitrogen and selenium while P, O, As, and Te atoms function as the acceptors in quite few structures.

8.2.5.1 XB Acceptors from the 15th Group

I₂ molecule strongly interacts with XB acceptors where the electron donor site is an sp³-nitrogen atom. 1,4-Diazabicyclo[2.2.2]octane (DABCO) is a very good neutral XB acceptor and on crystallization with equimolar amounts of I₂ a discrete, linear, and dimeric I₂⋯DABCO adduct [56] is formed wherein the donor:acceptor ratio is 1:1 as both the donor and the acceptor modules are monodentate, the I⋯N distance is as short as 2.366 Å (corresponding to a 33% reduction of N and I van der Waals radii), and a nonminor elongation of the I–I covalent distance is observed (2.8536 Å relative to 2.715 in pure and solid I₂). The use of different crystallization conditions affords discrete, linear, and trimeric I₂⋯DABCO⋯I₂ adducts where the I⋯N separation

is slightly longer and the I–I separation is slightly shorter than in the dimeric adduct (2.4213 and 2.8305 Å, respectively). Also, N-monoalkyl-substituted DABCO derivatives can coordinate iodine through the lone pair–possessing nitrogen when the non-nucleophilic PF_6^- moiety is used to avoid the possible competing binding of iodine by the anion (Fig. 8.8). The I...N distance is even longer than the trimeric adduct (2.519 Å, 28% reduction of van der Waals radii) indicating that the presence of a positive charge on DABCO consistently reduces the electron donor ability of the nitrogen atom and a weaker XB is formed.

The I_2 ...hexamethylenetetramine cocrystal is another nice example where an sp^3 -nitrogen atom functions as XB acceptor towards the I_2 molecule [57]. The iodine molecule bridges two hexamethylenetetramine molecules forming an infinite undulated supramolecular chain where donor and acceptor modules alternate (Fig. 8.9). The I...N distances are nonequivalent, $\text{I1}\cdots\text{N1}$ and $\text{I2}\cdots\text{N2}$ being 2.439 and 3.482 Å, which correspond to a 31 and 2% reduction of van der Waals distances, respectively. The formation of the strong $\text{I1}\cdots\text{N1}$ XB results in an enhancement of electron density

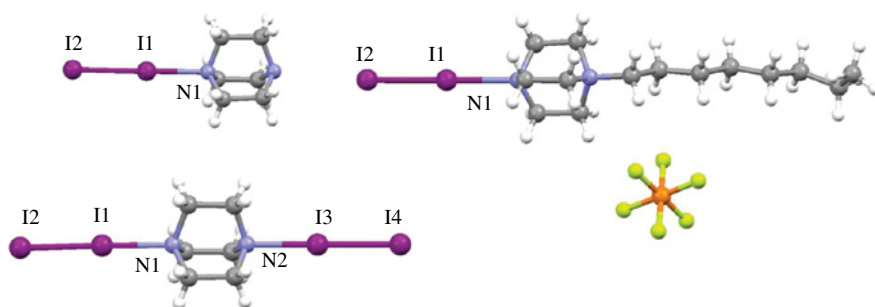


FIGURE 8.8 Ball-and-stick representation of the I_2 ...DABCO halogen-bonded cocrystals: Adduct with 1:1 ratio (top left), 1:2 ratio (bottom left), and I_2 ...*N*-octyl-DABCO $^+\text{PF}_6^-$ cocrystal (right). Due to their reduced length, XBs are represented by solid lines (similar to covalent bonds) [56]. Color code: fluorine, yellow; phosphorous, orange; other elements as in Figure 8.7. For interpretation of the references to color in this figure legend, the reader is referred to the web version of this chapter.

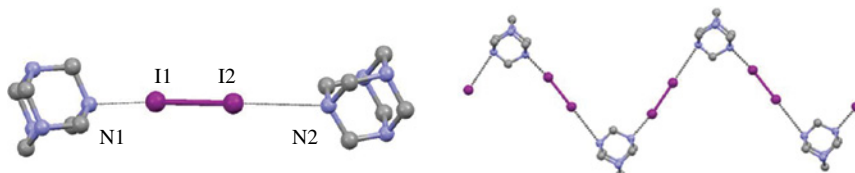


FIGURE 8.9 Ball-and-stick representation of the I_2 ...hexamethylenetetramine cocrystal. The asymmetric unit of the system is on the left and the infinite, halogen-bonded, and undulated chain is on the right. XBs are shown as black dotted lines. Color code as in Figure 8.7. For interpretation of the references to color in this figure legend, the reader is referred to the web version of this chapter.

on the I₂ moiety, the electron acceptor ability of I₂ is reduced, its interaction with N2 becomes weak, and the I₂⋯N2 separation is quite long.

I₂ forms strong halogen-bonded complexes also with sp²-hybridized nitrogen atoms. Pyridine and its derivatives can be considered typical representatives for this class of XB acceptors. The first crystal structure involving an I₂⋯N_{sp²} synthon was probably reported by O. Hassel in 1961 [58]. The iodine molecule interacted with 4-picoline to give discrete dimers with an I⋯N distance 2.322 Å long (33% reduction of van der Waals distances).

Cocrystallization of 1,2-bis(4-pyridyl)ethylene, a widely used module in XB crystal engineering [59], with I₂ gives an adduct with a 1:2 ratio between XB acceptor and donor [60]. The 1,2-bis(4-pyridyl)ethylene functions as a ditopic XB acceptor and the two nitrogen atoms are halogen-bonded to two distinct iodine molecules, which work as monodentate XB donors. The second iodine atom of each I₂ unit interacts with the iodine atom of a symmetry-related I₂ molecule through a type I halogen-halogen interaction [61]. The final supramolecular architecture is a quasi-linear infinite chain where the XB acceptor molecules are separated from each other by two I₂ units (Fig. 8.10). Distances are as follows: I1⋯N1 2.422 Å (29% reduction of van der Waals radii) and I2⋯I2_(-2-x, 1-y, -1-z) 3.885 Å. Type I halogen-halogen interactions are not stabilizing interactions and are generally caused by close packing requirements.

4-Cyanopyridine forms a cocrystal with I₂, and the crystal structure is highly educational from the XB point of view as I₂ molecules fully exploit their high versatility as supramolecular synthons (Fig. 8.11). The asymmetric unit is composed of two 4-cyanopyridine molecules and two I₂ molecules. As expected, the pyridine nitrogen atoms are halogen-bonded to one iodine atom of two different I₂ units (I1⋯N1 is 2.554 Å and I3⋯N3 is 2.543 Å, 30% reduction of van der Waals radii). These I1 and I3 atoms behave as amphoteric species after orthogonal directions: They function as “head on” XB donors with the N1 and N3 nitrogen atoms and as “side-on” XB acceptors with the closest iodine atoms, namely, I4 and I2, respectively. In other words, the negative belts of I1 and I3 point to the σ holes I4 and I3 (I4⋯I1 and I2⋯I3 distances are 3.921 and 3.885 Å, respectively). By interacting with each other through the σ hole⋯negative belt supramolecular synthon, I₂ molecules construct a ribbon wherein an iodine⋯iodine infinite chain is decorated by

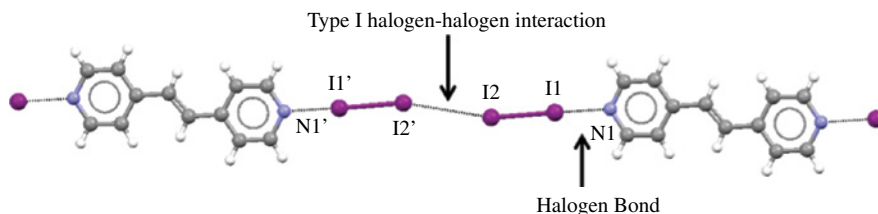


FIGURE 8.10 Ball-and-stick representation of the supramolecular chain formed by 1,2-bis(4-pyridyl)ethylene and I₂. XBs and type I halogen-halogen interactions are shown as black dotted lines and highlighted with arrows. Color code as in Figure 8.7. For interpretation of the references to color in this figure legend, the reader is referred to the web version of this chapter.

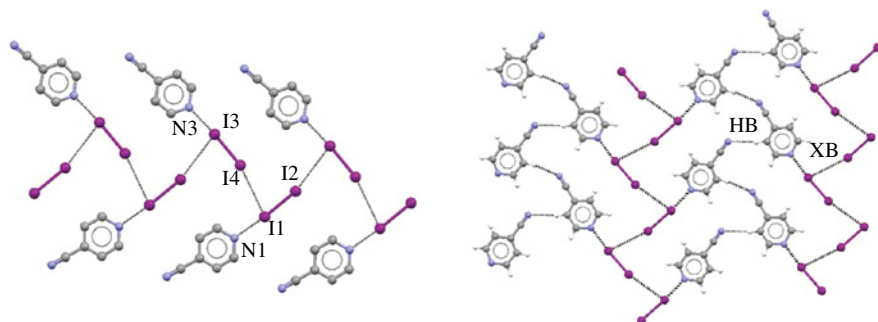


FIGURE 8.11 Ball-and-stick representation of halogen-bonded $I_2 \cdots 4$ -cyanopyridine cocrystal showing the ribbon of iodine...iodine chain decorated with cyanopyridine pendants (left) and the planar layer arrangement (right). XBs and HBs are shown as black dotted lines. Color code as in Figure 8.7. For interpretation of the references to color in this figure legend, the reader is referred to the web version of this chapter.

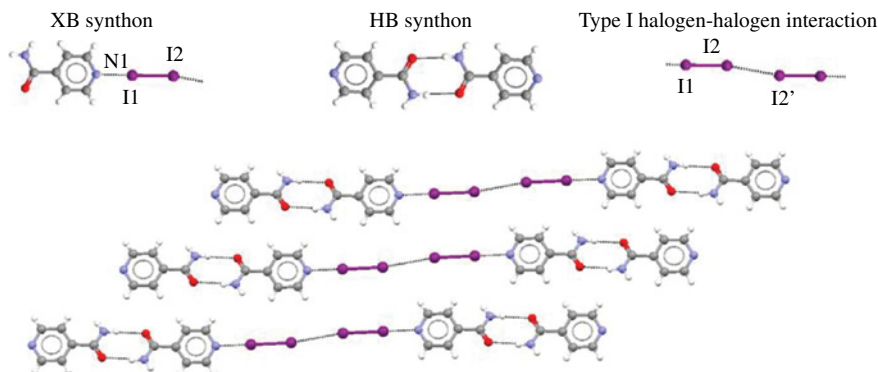


FIGURE 8.12 Top: Snapshots of the crystal packing representing the three interactions that are present in the $I_2 \cdots$ isonicotinamide complex. Bottom: Crystal packing showing the alternating arrangement between XB donors and acceptors couples. Color code: oxygen, red; other elements as in Figure 8.7. All the noncovalent interactions are shown as black dotted lines. For interpretation of the references to color in this figure legend, the reader is referred to the web version of this chapter.

4-cyanopyridine pendants bound via XBs. Notably, the cyano groups, which are Lewis bases and can work as XB acceptors [62], do not form any XB in this system. They work as HB acceptors and the attractive interactions with pyridine hydrogens connect the halogen-bonded ribbons into 2D planar layers (Fig. 8.11).

Also, the crystal packing of the $I_2 \cdots$ isonicotinamide adduct shows the concomitant presence of XB, type I halogen-halogen interactions, and HB (Fig. 8.12) [63]. Isonicotinamide has four potential electron donor sites: the oxygen atom, the pyridine and amide nitrogen atoms, and the extended π system. In the cocrystal with iodine, isonicotinamide dimers are formed thanks to the amide-amide pairing, a particularly

robust synthon in crystal engineering. Two pyridine nitrogen atoms are at the endings of linear and hydrogen-bonded dimers; they both work as XB acceptors and bind two I₂ molecules (I⋯N distance 2.442 Å, 32% reduction of van der Waals radii) after a quite linear geometry. Two tetrameric and rod-shaped adducts (assembled via HB and XB) further interact with each other thanks to type I halogen–halogen interactions (I₂⋯I₂_(-1-x, 1-y, 3-z) 3.631 Å), and fairly linear infinite chains are formed wherein isonicotinamide and diiodine couples alternate. In the overall crystal packing these chains are connected through π – π interactions involving pyridine rings.

Iodine can also work as a bidentate XB donor against N_{sp²} atoms, and this is typically the case for electron donors weaker than pyridine, as is the case with pyrazine and quinoxaline derivatives, which typically give rise to infinite supramolecular chains [64]. In some of these halogen-bonded chains the I⋯N distances are in the range of 2.992–2.941 Å corresponding to 15–17% reduction of van der Waals radii and the iodine atoms are involved in short contacts also with sulfur atoms present in the XB acceptor module, thus indicating once more the propensity of iodine to form numerous and diversified interactions.

Ten structures containing Cl–I molecule are reported in the CSD. 2-Chloroquinoline forms a dimer with ClI where the N⋯I distance is 2.432 Å (32% reduction of van der Waals radii). These dimers interact with each other to give infinite chains (Fig. 8.13, left) where the chlorine and iodine atoms of any ClI unit form a bifurcated HB with a quinoline proton [65]. An interesting structure was reported by A.I. Popov and coworkers in 1967 (Fig. 8.13, right) [66]. The iodine atom of ClI forms a nonsymmetric and bifurcated XB interaction with two adjacent nitrogen atoms of pentamethylenetetrazole. The I⋯N1 contact is as short as 2.347 Å (33% reduction of van der Waals radii) and the other contact is much longer (I⋯N2 is 3.347 Å, 2% reduction of van der Waals radii). This bonding pattern can also be interpreted as the entrance of the iodine σ hole on the nitrogen–nitrogen bond. No other interactions are present in the crystal lattice.

Only two structures have been found in CSD having BrI⋯N interaction [67]. In both cases only the iodine atom functions as an XB donor, and distances are in the range of 2.405–2.410 Å (32% reduction of van der Waals radii).

In general, the products R₃PnX₂, formed when dihalogens (X₂) react with trivalent organic derivatives of group 15 elements (R₃Pn, Pn = pnicogen atom, R = alkyl, aryl,

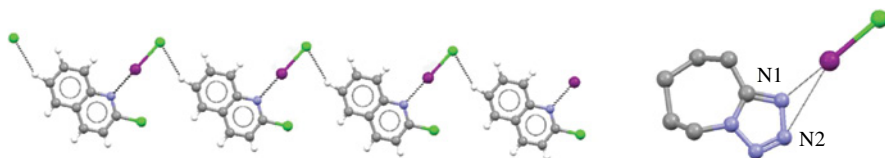


FIGURE 8.13 Left: Supramolecular infinite chain formed by XB and HB in ClI⋯2-chloroquinoline complex. Right: Halogen-bonded ClI⋯pentamethylenetetrazole dimer. Color code: chlorine, green; other elements as in Figure 8.7. XBs and HBs are pictured as black dotted lines. For interpretation of the references to color in this figure legend, the reader is referred to the web version of this chapter.

alkoxy, aryloxy, dialkylamino, etc.), can have remarkably different structures, which can encompass three main classes: (1) halogen-bonded adducts (also called charge-transfer or “spoke” adducts in the less recent literature), (2) ionic halide salts, and (3) molecular five-coordinate species adopting a trigonal bipyramidal geometry (Chart 8.2, left, mid, and right, respectively) [68]. The pnictogen atom in the first and second class of compounds has a tetrahedral geometry and the ionic halide salts can be considered the products formed by such strong XBs that X–Pn distances are as short as typical “covalent” bonds and the charge transfer from Pn to X is remarkable enough to allow for the heterolytic cleavage of the X–X covalent bonds. The nature of the pnictogen heavily influences the most common structure of the product R_3PnX_2 . No easily accessible d orbitals are present on nitrogen, which forms halogen-bonded adducts with great preference. Heavier pnictogens preferentially form ionic halide salts and molecular five-coordinate species, but here we will discuss only the halogen-bonded adducts.

N.A. Barnes and coworkers [68] have reported the formation (Fig. 8.14, left) of linear and extremely short I–I⋯P interactions spanning the range 2.451–2.513 Å (34–35% reduction of van der Waals radii). These short I⋯P distances correspond to extremely long I–I distances (3.081–3.257 Å). This feature indicates the high efficiency of the phosphorus to donate electron density and function as an extremely good XB acceptor unit. Different tritoly arsines have been reported to form short I–I⋯As interactions (Fig. 8.14, mid) [69]. The observed I⋯As distances (2.735 and 2.742 Å, 30% van der Waals radii reduction) correspond to a smaller percentage reduction of van der Waals distances with respect to the phosphorus complexes, but the As atom can also be considered a good XB acceptor for I_2 .

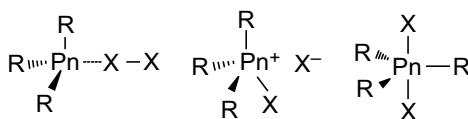


CHART 8.2 Main structural types of R_3PnX_2 adducts.

FIGURE 8.14 Asymmetric units for three halogen-bonded cocrystals having the I–I⋯P/As and Br–I⋯P contacts. The CSD codes and XB length are reported for each complex. Color code as in Figure 8.7. For interpretation of the references to color in this figure legend, the reader is referred to the web version of this chapter.

Only one halogen-bonded cocrystal involving BrI is reported. The XB acceptor is triphenylphosphine [70] and the observed I...P distance (2.461 Å, 35% reduction of van der Waals radii) is similar to analogous adducts involving I₂ (Fig. 8.14, right).

8.2.5.2 XB Acceptors from the 16th Group

Neutral and anionic oxygen atoms can behave as efficient XB acceptors [71]. C. Walbaum and coworkers [72] have reported the assembling of infinite supramolecular chains through the O...I...O synthon involving two molecules of dibenzo-24-crown-8. I...O distances are 2.932 Å long and correspond to 16% van der Waals radii

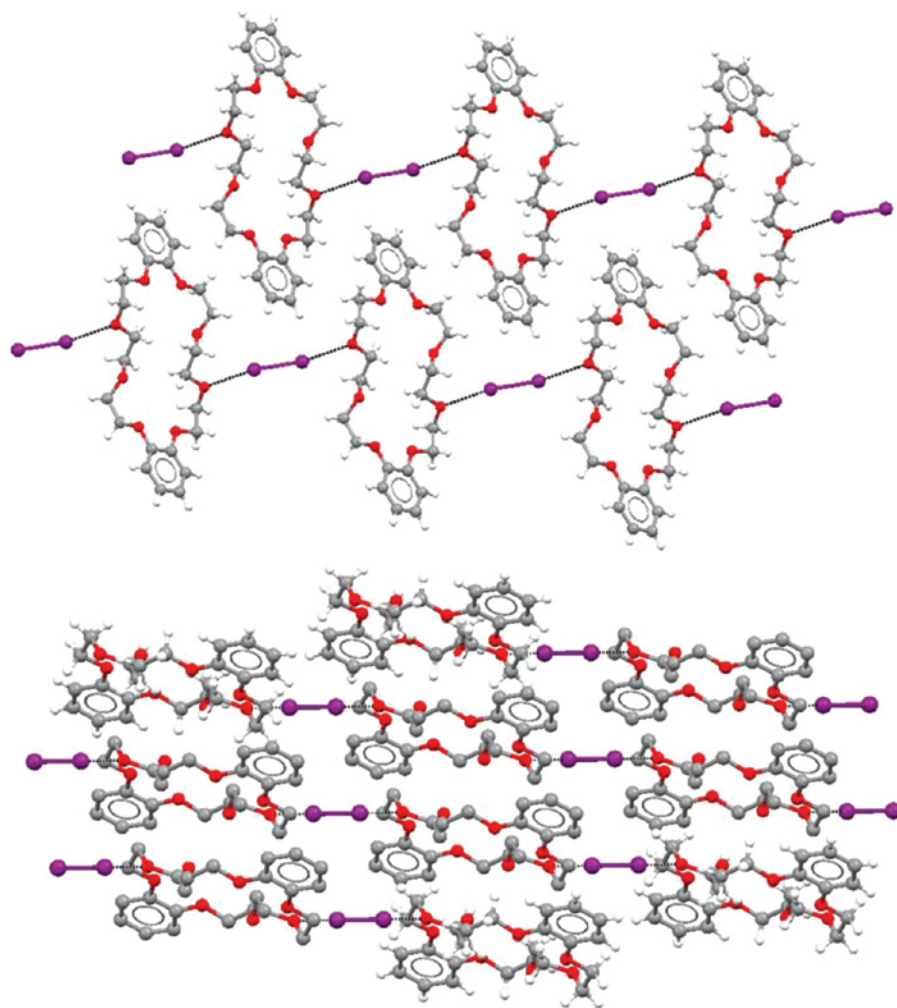


FIGURE 8.15 Views of I₂...dibenzo-24-crown-8 complex along the *a*-axis (top) and the *c*-axis (bottom). Color code as in Figure 8.12. XBs are shown as black dotted lines. For interpretation of the references to color in this figure legend, the reader is referred to the web version of this chapter.

reduction; the I–I \cdots O angles are 170°. The XB donors and acceptors form separate domains (Fig. 8.15), and no other noncovalent interactions stabilize the crystal packing. Three other interesting structures display the I–I \cdots O interaction. The shortest interaction distance is observed in the cocrystal between 1,4-dioxane and I₂ [73] (2.808 Å, 20% reduction of van der Waals radii), wherein both the XB donor and acceptor are ditopic and infinite chains are formed. A series of metal–organic frameworks based on cadmium have been used to trap I₂ from solution or in a gas–solid process. The molecular iodine is halogen-bonded with perchlorate, and the I \cdots O distances are in the range of 2.924–3.141 Å (11–16% van der Waals radii reduction) [74].

The I–I \cdots S synthon is the most abundant in CSD and here we discuss the most recent structures where it is present. In a dinuclear nickel complex reported by B. Buchner and coworkers [75], the I₂ molecule is coordinated to a sulfur atom bound to the metal center (Fig. 8.16, left) and the I \cdots S distance is very short (2.755 Å, 34% van der Waals radii reduction), similar to the I₂ \cdots DABCO complexes described earlier.

The S \cdots I–I \cdots S motif is found in the complex between I₂ and [Ru(dcbpy)₂(SCN)₂], the most widely used dye in dye-sensitized solar cells. In this structure, reported by M. Haukka et al. [76], one I₂ molecule bridges two sulfur atoms of two isothiocyanate units at two different metal complexes (I1 \cdots S2 2.954 Å and I4 \cdots S1 3.531 Å, 22 and 7% van der Waals radii reduction, respectively) (Fig. 8.16, right). Another I₂ molecule also forms two XBs, one with a sulfur atom and another with the π system of the dipyrindyl ligand (I2 \cdots S1 2.836 Å, 24% van der Waals radii reduction, and I3 \cdots π system 3.615 Å).

The thione units of differently functionalized five-membered heterocycles work as effective XB acceptors [77]. The I \cdots S distances are quite short (WURGEW: 2.545 Å, 33% van der Waals radii reduction; WURGIA: 2.615 Å, 31% reduction; WURGOG: 2.686 Å, 29% reduction) and result in nonminor elongation of the I–I distance relative to pure I₂ (Fig. 8.17).

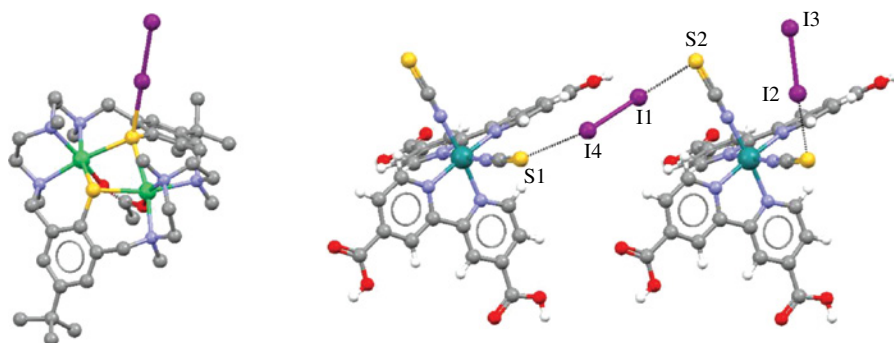


FIGURE 8.16 Halogen-bonded adducts assembled thanks to the I–I \cdots S synthon. Left: asymmetric unit of a dinuclear nickel complex; color code: sulfur, dark yellow; nickel, green; other colors as in Figure 8.7. Hydrogen atoms are omitted for clarity. Right: Dimer of two Ru(II)-centered metal complexes forming the S \cdots I–I \cdots S motif. Color code: ruthenium, emerald green; sulfur, dark yellow; oxygen, red; other colors as in Figure 8.7. For interpretation of the references to color in this figure legend, the reader is referred to the web version of this chapter.

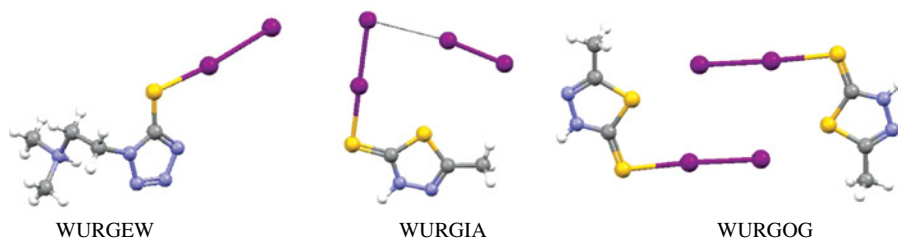


FIGURE 8.17 Asymmetric units for three halogen-bonded cocrystals having I–I···S contacts. I···S XBs are dark solid lines; I···I XBs are shown as black dotted lines. CSD codes are reported for each complex. Color code as in Figure 8.14. For interpretation of the references to color in this figure legend, the reader is referred to the web version of this chapter.

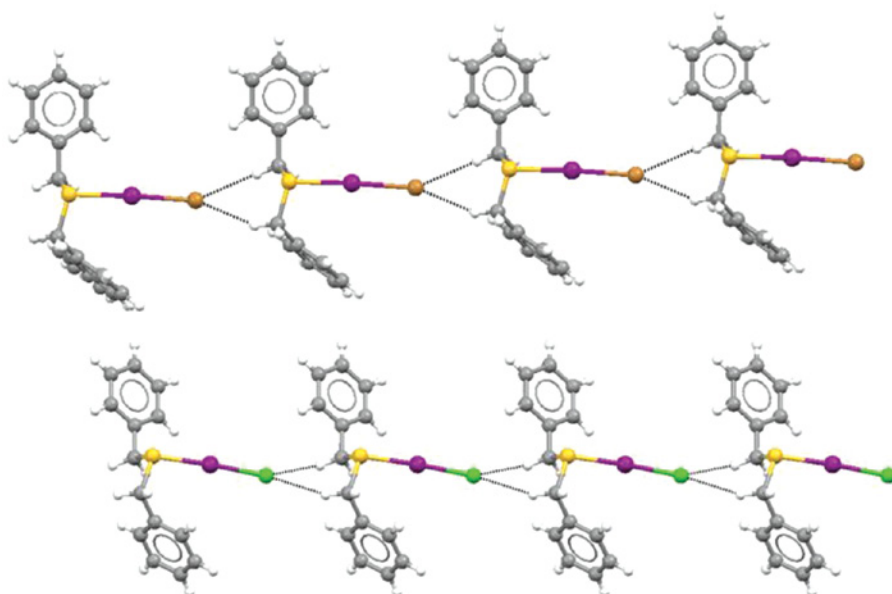


FIGURE 8.18 Hydrogen- and halogen-bonded polymers present in the crystal packing of BrI···dibenzylsulfide (top) and ClI···dibenzylsulfide (bottom) adducts. Color code as in Figures 8.13 and 8.14. XBs are shown as solid lines and HBs as black dotted lines. For interpretation of the references to color in this figure legend, the reader is referred to the web version of this chapter.

The ability of sulfur to work as a very good XB acceptor on interaction with iodine is confirmed by the adducts formed by Br–I and Cl–I. Good examples of Br–I···S and Cl–I···S synthons were reported by A.J.P. White et al. [78]. They described that the adducts formed by dibenzylsulfide with these interhalogens are quite similar. The iodine atoms are strongly halogen-bonded to the S atom, and the I···S distance is shorter in the Cl–I adduct (2.575 Å) than in the Br–I adduct (2.616 Å, 30% reduction of van der Waals radii), due to the higher electronegativity of Cl, compared

to Br that makes the σ hole on iodine in Cl–I more positive and thus more prone to interact with the electron donor. The bromine and chlorine atoms form weak and similar HBs with the benzylic protons of a nearby dibenzyl disulfide, and similar polymeric chains are formed where HB and XB interactions alternate along the chains (Fig. 8.18).

The behavior of dihalogens (X_2) with divalent organic derivatives of group 16 elements R_2Ch (Ch = chalcogen atom, R = alkyl, aryl, alkoxy, aryloxy, dialkylamino, etc.) recalls that described earlier for R_3Pn pnictogen derivatives. Halogen-bonded adducts (here too called charge-transfer or “spoke” adducts in the less recent literature) or oxidative addition products (having either a see-saw or a T shape) are formed depending on the nature of R , X , and Ch . The heavier the chalcogen, the less common the formation of halogen-bonded adducts, but various such systems have been described for selenium and even for tellurium. Some of those formed by diiodine are described here.

The formation of supramolecular adducts involving selenium as an XB acceptor has been known for a long time [15], and B. Muller et al. [79] recently reported very simple and elegant systems containing the $I_2 \cdots Se$ synthon. Dimethyldiselenide and I_2 form a 1:1 adduct (Fig. 8.19, left) where the $I \cdots Se$ distance is 2.849 Å (27% reduction of van der Waals radii). Under different preparation conditions, a 1:2 adduct is formed (Fig. 8.19, right) wherein the $I \cdots Se$ distance is longer (2.932 Å, 24% van der Waals radii reduction) than in the 1:1 complex, probably due to the other short contacts present in the two systems, namely, the overall crystal packing requirements.

1-Phenylselenenyl-8-phenylsulfenyl naphthalene allows for a direct comparison of the relative ability of selenium and sulfur atoms to function as XB acceptor sites on interaction with I_2 [80]. In the 1:2 adduct with iodine, one I_2 molecule shows a quite short $I \cdots Se$ contact (Fig. 8.20, left) (2.844 Å, 27% van der Waals radii reduction). The other I_2 molecule is not bound to sulfur but is pinned at either ends by two $I \cdots I$ XBs involving the second iodine atoms of two selenium-bound I_2 molecules ($I \cdots I$ distance 3.526 Å, $I1-I2 \cdots I3a_{(2-x, -y, 1-z)}$ 108.01°, $I2 \cdots I3a_{(1+x, -1+y, z)}$ 176.33°). Iodine shows a similar selenium for sulfur preference in the 1:1 adduct with an acenaphthene derivative bearing the phenylselenenyl and phenylsulfenyl

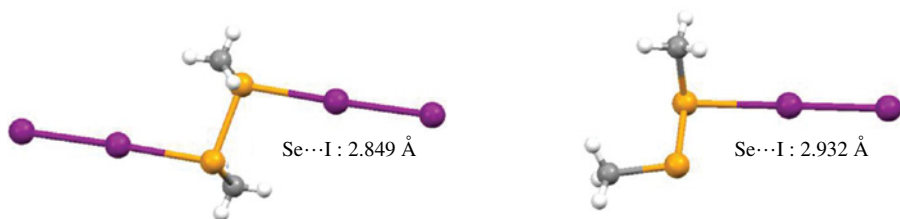


FIGURE 8.19 Unit cells for $I_2 \cdots 1,2$ -dimethyldiselenide adducts in 1:1 (left) and 1:2 ratio (right). The $I \cdots Se$ distances are reported. Color code: selenium, dark yellow; other colors as in Figure 8.7. For interpretation of the references to color in this figure legend, the reader is referred to the web version of this chapter.

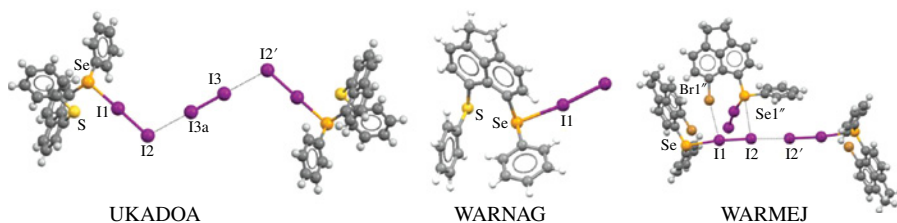


FIGURE 8.20 Left: 1:2 XB adduct between iodine and 1-phenylselenenyl-8-phenylsulfenylphthalene. Mid: Asymmetric units of 1:1 XB adduct (6-(phenylsulfanyl)-1,2-dihydroacenaphthylen-5-yl)(phenyl) selenide and I₂. Right: Network of noncovalent interactions between three 6-phenylselenenyl-5-bromoacenaphthene-I₂ halogen-bonded adducts. Color code as in Figures 8.17 and 8.18. CSD codes for any complex are reported. Competing XB acceptor sites are labeled with their atomic symbol. XB are shown as solid lines for I...Se contact and black dotted lines for I...I contact; other interactions are shown as black dotted lines. For interpretation of the references to color in this figure legend, the reader is referred to the web version of this chapter.

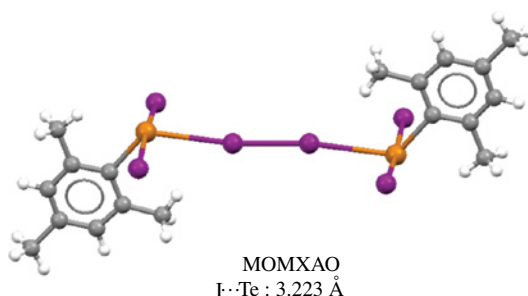


FIGURE 8.21 Dimers assembled by the Te...I...Te motif. Color code: tellurium, orange; other colors as in Figure 8.19. For interpretation of the references to color in this figure legend, the reader is referred to the web version of this chapter.

pendants in the peri positions (Fig. 8.20, mid) [81]. Iodine also interacts attractively with 6-phenylselenenyl-5-bromoacenaphthene (Fig. 8.20, right) wherein it forms a net of short contacts. As expected, the shortest interaction is the I...Se XB (I1...Se1 distance 2.956 Å), and the other short contacts I₂ is involved in are a type I iodide...iodine interaction (I2...I2' ^(2-x, 1-y, 2-z) distance 3.473 Å), I...Br XB (I1...Br1'' ^(x, 0.5-y, 0.5+z) distance 3.657 Å), and an I...Se chalcogen bond (I2...Se1'' ^(x, 0.5-y, 0.5+z) distance 3.875 Å).

Consistent with the greater reactivity of tellurium, relative to selenium and sulfur, and its tendency to preferentially form oxidative addition products, see-saw adducts, wherein tellurium is inserted in an iodine molecule, are formed when diiodine is reacted with 6-phenyltellurylacenaphthene derivatives bearing in position 5 a bromine, phenylselenenyl, or phenylsulfenyl residue [81].

Nevertheless, in five structures present in the CSD, tellurium atoms function as XB acceptors for molecular iodine and the I...Te distances are rather short (26–30%

reduction of van der Waals radii of the interacting elements) [82]. Interestingly, one structure [83] shows an XB-based $\text{Te}\cdots\text{I}\cdots\text{Te}$ motif (Fig. 8.21), which is similar to that involving N, O, or S atoms as an XB acceptor ($\text{I}\cdots\text{Te}$ distance 3.223 Å, 20% van der Waals radii reduction), and tellurium atoms show a see-saw geometry as an aromatic residue and two other iodine atoms are bound to tellurium.

8.2.5.3 π Systems as XB Acceptors

I_2 can form halogen-bonded and solid complexes with aromatic systems such as benzene and toluene or their derivatives. These adducts are similar to those formed in solution. In principle any systems possessing π electrons can work as XB acceptors toward I_2 , but they are less efficient than lone pair–possessing acceptors due to the minor localization of the electron density in π clouds compared to lone pairs.

This may account for the limited number of CSD structures having $\text{I}_2\cdots\pi$ contacts that satisfy the geometrical requirements of halogen-bonded complexes [84].

In 1986 S. Mitani reported [85] a crystal structure where diiodine is halogen-bonded to coranene, a polyaromatic formed by seven rings fused together. The coranene molecules stacking via π – π interactions forms columnar domains, which are inclined as the overlap of coranene units is not perfect and there is an offset of 46.5° between two adjacent molecules so that a part of the π system is free to attractively interact with the σ hole of iodine. The diiodine molecule sits quasi-orthogonal to one of the peripheral carbon–carbon bonds of the polyaromatic system; the shortest $\text{I}\cdots\text{C}$ distances are 3.204 and 3.404 Å. The $\text{I}_2\cdots\text{coranene}$ XB contacts form a corrugated chain where the XB donors and acceptors alternate and adjacent chains are connected by HBs between the negative belt of any iodine atom and one H atom of a nearby chain. The combined effect of XBs, HBs, and π – π interactions causes a net segregation between coranenes and I_2 molecules (Fig. 8.22).

D. R. M. Walton and coworkers [86] described a tricomponent complex where I_2 , fullerene- C_{60} , and toluene are present in a 1:1:1 ratio. Iodine acts as a bidentate XB donor and is sandwiched between a C_{60} and a toluene unit (Fig. 8.23, left), which are both disordered. One iodine atom of I_2 is halogen-bonded to a C_{60} surface and the other to toluene, the shortest $\text{I}\cdots\text{C}$ distances being close to 3.1 Å in both cases.

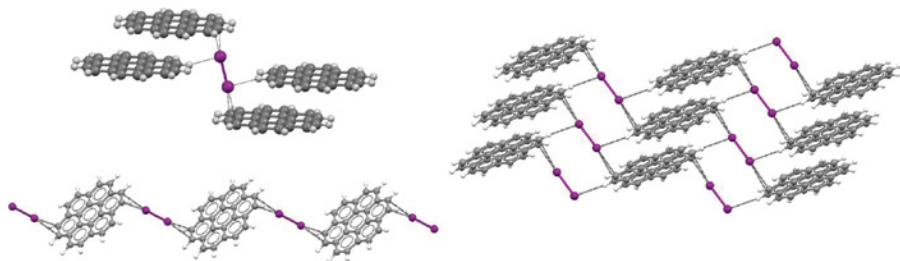


FIGURE 8.22 Diiodine–coranene adduct. Top left: one diiodine molecule, the two quasi-orthogonal coranene molecules bound via XB, and the two lateral coranene molecules bound via HB. Bottom left: a part of an infinite halogen-bonded chain. Right: crystal packing showing the segregation between coranene and I_2 molecules.

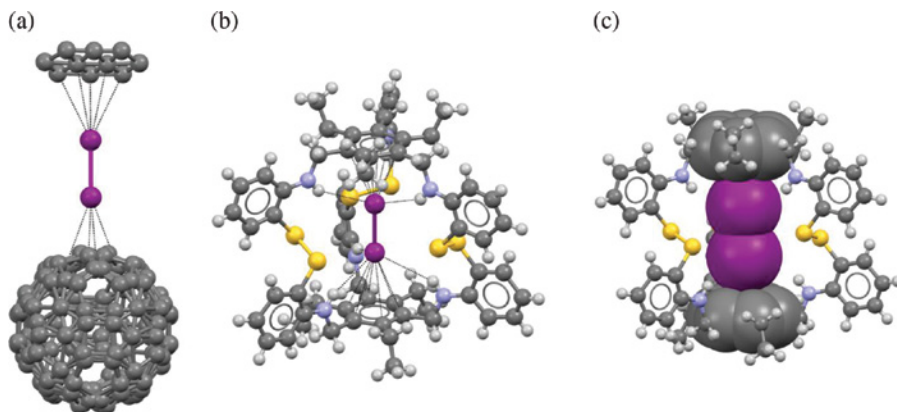


FIGURE 8.23 Left: C₆₀⋯I₂⋯toluene trimer. Mid: I₂ entrapped in the molecular cage, XBs and HBs are shown as black dotted lines. Right: Same view of Mid but the iodine and the aromatic ring are represented in a space-filling model to show the tight interaction between the two fragments. Color code as in Figure 8.19. For interpretation of the references to color in this figure legend, the reader is referred to the web version of this chapter.

In 2012 Y.-C. Horng et al. reported [87] the X-ray structure of an organic molecular container that was able to trap molecular I₂. The XB acceptor is a cylinder-shaped dimer formed by two tripodal trisulfide precursors connected by three dynamic disulfide bonds. The iodine molecule is trapped into the cavity formed by the tripodal trisulfide capsule and is located perpendicular to the benzene ring of the aromatic units ($\angle_{\text{I-Centroid-H}}$ is 89°). I₂ encapsulation can occur both in solution and in solid–gas reaction and is driven by a cooperative effect of XB (between its σ hole and the aromatic π systems) and HBs (between the negative belt of I₂ and NH groups). The distance for the I⋯benzene ring centroid XB is 3.128 Å, while the H⋯I contact is 3.124 Å (Fig. 8.23, mid and right).

8.2.5.4 XB Acceptors from the 17th Group

The use of anionic electron donors in XB-directed crystal engineering has received less attention than neutral electron donors. However, in two recent review papers [25], [35] we have shown the reliability and potential of anionic XB acceptors when the construction of new supramolecular assemblies with specific properties is pursued. The general ability of anions to work as effective XB acceptors is indicated by the diversity of the reported systems and the variety of associated functions, for example, transmembrane anion transport and organocatalysis [88].

While oxygen- and sulfur-centered anions can also function as XB acceptors, halide anions form a particularly numerous and diversified set of X-bonded supramolecular anions. It seems they are nicely tailored to function as XB acceptors as they succeed in interacting with XB donors as weak as iodomethane and other haloalkanes with no electron-withdrawing groups close to the electrophilic halogen [89]. These X-bonded adducts are particularly significant as they prove that haloalkanes

with a weak σ hole can also function as XB donors if challenged by particularly good acceptors.

As discussed earlier, I_3^- can be understood as the 1:1 halogen-bonded adduct between I_2 and I^- and is the simplest and best known halogen-bonded adduct. Diiodine forms many other polyiodides and mixed polyhalides with halide anions, and they have been discussed in a recent review published by P. H. Svensson *et al.* [41] They show quite different stoichiometries and geometries [90], and many of them correspond to those expected for halogen-bonded systems. In this section we focus on structures where the $\cdots X \cdots I \cdots X \cdots$ unit is present ($X = Cl, Br, \text{ and } I$) either as a discrete motif or as the component of more extended systems [91].

The halogen-bonded $\cdots I \cdots I \cdots I^-$ motif is formed when two iodide anions attractively interact with the iodine σ -holes, which are on the extension of the $I-I$ bond. The mean length of the $I \cdots I^-$ contacts in these motifs is 3.40 Å (18% reduction of van der Waals radii) and, consistent with the XB character, the I_2 unit linearly bridges two iodide anions (the mean value for the $I-I \cdots I^-$ angle being quite close to 180°).

In most of the CSD structures a symmetric, halogen-bonded, supramolecular anion is present and the two $I \cdots I^-$ distances are identical as the $\cdots I \cdots I \cdots I^-$ motif is on a crystallography symmetry element. When this is not the case, the two interaction distances are different. The hexane-1,6-diaminium diiodide \cdots iodine adduct (CSD code: UJOMAI) is a nonsymmetric adduct (Reiss, G.J., Private Communication, 2010) where the two $I \cdots I^-$ distances are 3.338 and 3.425 Å (20 and 17% van der Waals radii reduction). The difference in the interaction length can be understood in terms of a two step process for the formation of the I_4^{2-} species where the first I^- enters the positive σ hole of I_2 and forms a strong and short XB. Electrostatic interactions pin the second I^- close to the formed I_3^- and a weak and long XB develops with the σ hole of the triiodide anion.

In some crystal packings the I_4^{2-} structural unit gives rise to more extended polyiodides consistent with the general ability of an iodide anion to function as a polydentate XB acceptor. The stoichiometry and the structure of the formed polyiodide are the result of a subtle balance of several factors, among others the steric and electronic features of the anion and the anion neighborhood (e.g., the cation) [92], the stoichiometry of the reaction, and the conditions of crystal formation (e.g. the solvent(s) and its(their) polarity) [93]. A discrete [94] I_4^{2-} is reported in Fig. 8.24 along with honeycomb [95] and cubic [96] systems wherein the iodides of the I_4^{2-} are halogen-bonded to two and five other I_2 molecules, respectively.

The design and obtainment of polyiodides with a preestablished composition and crystalline structure is a challenging target, and the obtainment of the rare and poorly stable $\cdots I \cdots I \cdots I^-$ dianion as a discrete species is particularly difficult [97]. In 2010 we reported that when the diiodide salt of the 1,6-bis(trimethylammonium) hexane cation (hexamethonium, $HMET^{2+}$, cation) reacts with one equivalent of I_2 , a salt containing the discrete $\cdots I \cdots I \cdots I^-$ is produced [47]. Formation of the halogen-bonded $[I_4]^{2-}$ dianion is favored both by size matching of the interacting charged moieties (the N^+-N^+ and $I^- \cdots I^-$ separations in XB cocrystal are 8.9 and 9.7 Å, respectively) and by a network of $C-H \cdots I^-$ HBs, which drive an effective dimensional encapsulation of molecular iodine. The complex is formed both from solution and from gas–solid reaction, demonstrating the dynamically porous character of

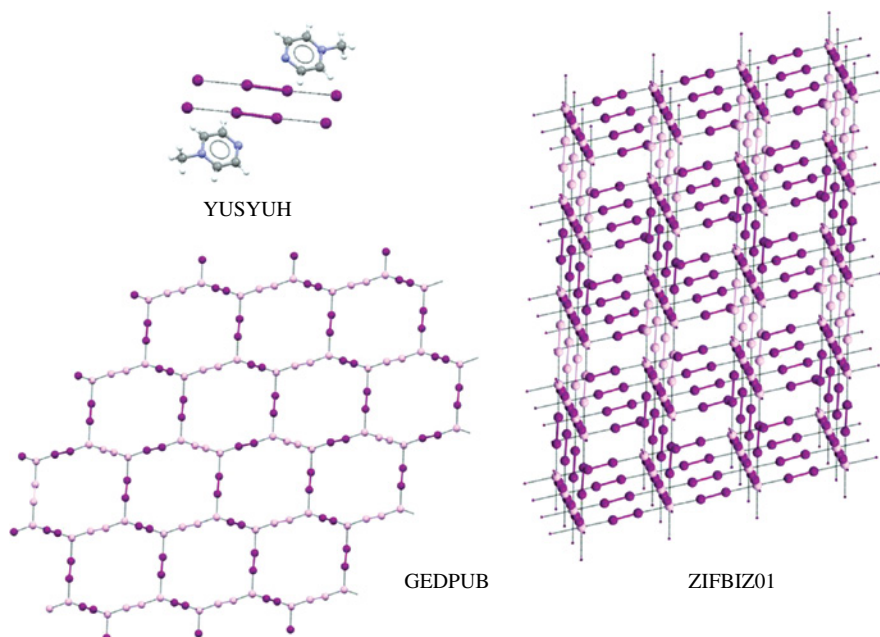
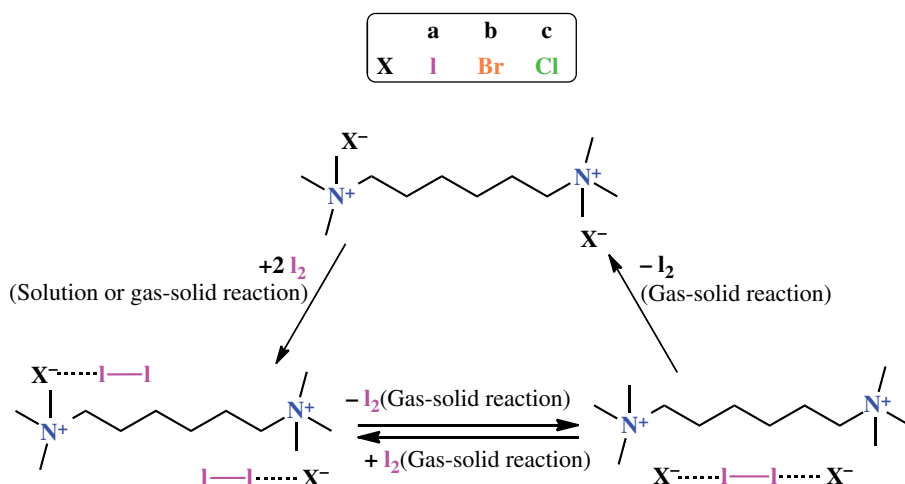


FIGURE 8.24 Top left: two discrete $\text{I}\cdots\text{I}\cdots\text{I}^-$ dianions present in the crystal of the 1-methylpyrazin-1-ium iodide $\cdots\text{I}_2$ adduct. Color code as in Figure 8.7. The honeycomb (bottom left) and cubic (right) nets formed when two and five iodine molecules (dark gray or pink in on line version) are halogen-bonded to either endings of the $\text{I}\cdots\text{I}\cdots\text{I}^-$ unit (light gray or pink in on line version). In the two latter structures, cations have been omitted for clarity. XBs are shown as black dotted lines. For interpretation of the references to color in this figure legend, the reader is referred to the web version of this chapter.



SCHEME 8.2 Synthesis of tetrahalide dianions via thermally induced deiodination reactions of the bis- $\text{I}\cdots\text{I}\cdots\text{X}^-$ -adducts and other interconversion reactions involving hexamethonium halides.

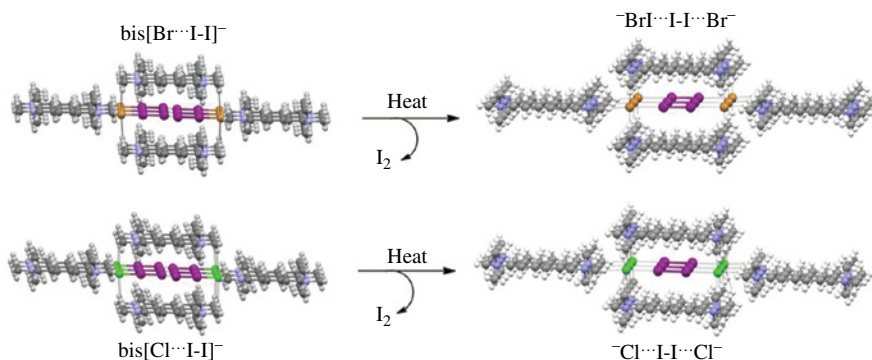


FIGURE 8.25 Ball-and-stick partial representation of a column of $[\text{Br I}_2]^-$ and $[\text{Cl I}_2]^-$ dimers and hydrogen-bonded HMET^{2+} cations (left) that form (upon heating and release of only one I_2 molecule) the poorly stable $[\text{Br}_2 \text{I}_2]^{2-}$ and $[\text{Cl}_2 \text{I}_2]^{2-}$ dianions (right), which are also hydrogen-bonded to HMET^{2+} cations.

bis(trimethylammonium)alkane diiodide salts. On reaction with two equivalents of I_2 , hexamethonium chloride, and bromide afford the corresponding mixed trihalides $\text{HMET}^{2+} \cdot 2\text{XI}_2^-$ ($\text{X} = \text{Cl}^-$, Br^-), which undergo thermally induced crystal-to-crystal elimination of one I_2 molecule, and the virtually unknown tetrahalides $[\text{Cl}_2 \text{I}_2]^{2-}$ and $[\text{Br}_2 \text{I}_2]^{2-}$ are obtained in quantitative yields (Scheme 8.2) [98]. Similarly, slow heating of $\text{HMET}^{2+} \cdot 2\text{I}_3^-$ affords $\text{HMET}^{2+} \cdot [\text{I}_4]^{2-}$ via elimination of one I_2 molecule. In the three tetrahalide dianions, the halide anions Cl^- , Br^- , and I^- double-pin a single I_2 molecule via short XBs and afford the tetrahalide units, which are selectively encaged by the HMET^{2+} dications as a consequence of size matching of the components and a network of cooperative HBs. The starting units in the $\text{HMET}^{2+} \cdot 2\text{XI}_2^-$ trihalides are preorganized to respond dynamically to heating and represent a functional structure that promotes the formation of the poorly stable tetrahalide species.

For instance, when microcrystalline hexamethonium bis-diiodobromide and bis-diiodochloride are slowly heated, new crystalline solids appear at ca. 100°C , and the reactions are complete at ca. 160°C . The new solids are stable at room temperature and in contact with air for over 1 week. Elemental analyses confirm that only one I_2 molecule is released, and structure solution from powder X-ray diffraction analyses proves that the $[\text{Br}_2 \text{I}_2]^{2-}$ and $[\text{Cl}_2 \text{I}_2]^{2-}$ tetrahalide anions are present as discrete species (Fig. 8.25). In all cases, the lighter halogen atoms occupy the outer positions of the dianions and hold the I_2 molecules at each end through short and linear $\text{I}-\text{I} \cdots \text{X}^-$ ($\text{X} = \text{Br}, \text{Cl}$) XBs.

The $\text{I}-\text{I} \cdots \text{X}^-$ distances are 3.398 and 3.171 Å ($\sim 15\%$ reduction in the sum of van der Waals radius of iodine and the Pauling ionic radius of the halide anion), and the $\text{I}-\text{I} \cdots \text{X}^-$ angles are 177.2° and 175.7° in $[\text{Br}_2 \text{I}_2]^{2-}$ and $[\text{Cl}_2 \text{I}_2]^{2-}$, respectively. Cation and anion size matching is quite good, and the N^+-N^+ and $\text{Br}^- \cdots \text{Br}^-$ separations are 8.74 and 9.481 Å, respectively. As expected, the mixed tetrahalides $[\text{I}_2 \text{X}_2]^{2-}$ are held in place by a network of $\text{X} \cdots \text{H}-\text{C}$ HBs.

REFERENCES

- [1] (a) Steed JW, Atwood LJ. *Supramolecular Chemistry*. 2nd ed. John Wiley & Son; 2009. (b) Lehn J-M. *Supramolecular Chemistry Concept and Perspectives*. New York: Wiley-VCH; 1995.
- [2] Clayden J, Greeves N, Warren S. *Organic Chemistry*. 2nd ed. Oxford; 2012.
- [3] (a) Metrangolo P, Neukirch H, Pilati T, Resnati G. Halogen bonding based recognition processes: A world parallel to hydrogen bonding. *Acc Chem Res* 2005;38:386–395. (b) Metrangolo P, Resnati G, Pilati T, Biella S. Halogen bonding in crystal engineering. *Struct Bonding* 2008;126:105–136. (c) Rissanen K. Halogen bonded supramolecular complexes and networks. *CrystEngComm* 2008;10:1107–1113. (d) Erdélyi M. Halogen bonding in solution. *Chem Soc Rev* 2012;41:3547–3557. (e) Troff RF, Mäkelä T, Topic F, Valkonen A, Raatikainen K, Rissanen K. Alternative motifs for halogen bonding. *Eur J Org Chem* 2013;1617–1637.
- [4] Desiraju GR, Ho PS, Kloo L, Legon AC, Marquardt R, Metrangolo P, Politzer P, Resnati G, Rissanen K. Definition of the halogen bond (IUPAC Recommendations 2013). *Pure Appl Chem* 2013;85:1711–1713.
- [5] (a) Awwadi FF, Willet RD, Peterson KA, Twamley B. The nature of halogen...halogen synthons: Crystallographic and theoretical studies. *Chem Eur J* 2006;12:8952–8960. (b) Karpfen A. In: Metrangolo P, Resnati G., editors. *Halogen Bonding Fundamentals and Applications*. Berlin: Springer; 2008. p 1–16.
- [6] Clark T, Hennemann M, Murray JS, Politzer P. Halogen bonding: The σ -hole. *J Mol Model* 2007;13:291–296.
- [7] Legon AC. Prereactive complexes of dihalogens XY with lewis bases B in the gas phase: A systematic case for the halogen analogue $B \cdots XY$ of the hydrogen bond $B \cdots HX$. *Angew Chem, Int Ed* 1999;38:2686–2714.
- [8] Metrangolo P, Pilati T, Resnati G. Halogen bonding and other noncovalent interactions involving halogens: A terminology issue. *CrystEngComm* 2006;8:946–947.
- [9] (a) Metrangolo P, Murray JS, Pilati T, Politzer P, Resnati G, Terraneo G. The fluorine atom as a halogen bond donor, viz. a positive site. *CrystEngComm* 2011;13:6593–6596. (b) Metrangolo P, Murray JS, Pilati T, Politzer P, Resnati G, Terraneo G. Fluorine-centered halogen bonding: A factor in recognition phenomena and reactivity. *Cryst Growth Des* 2011;11:4238–4246. (c) Chopra D, Guru Row TN. Role of organic fluorine in crystal engineering. *CrystEngComm* 2011;13:2175–2186.
- [10] Politzer P, Murray JS. Halogen bonding: An interim discussion. *ChemPhysChem* 2013;14:278–294.
- [11] Riley KE, Murray JS, Fanfrlík J, Řezáč J, Sola RJ, Concha MC, Ramos FM, Politzer P. Halogen bond tunability I: The effects of aromatic fluorine substitution on the strengths of halogen-bonding interactions involving chlorine, bromine, and iodine. *J Mol Model* 2011;17:3309–3318.
- [12] Zhang X, Zeng Y, Li X, Meng L, Zheng S. A computational study on the nature of the halogen bond between sulfides and dihalogen molecules. *Struct Chem* 2011; 22:567–576.
- [13] (a) Bondi A. van der Waals volumes and radii. *J Phys Chem* 1964;68:441–451. (b) Shannon RD. Revised effective ionic radii and systematic studies of interatomic distances in halides and chalcogenides. *Acta Crystallogr Sect A* 1976;32:751–767.

- [14] Legon AC. The halogen bond: An interim perspective. *Phys Chem Chem Phys* 2010;12:7736–7747.
- [15] (a) Bent HA. Structural chemistry of donor-acceptor interactions. *Chem Rev* 1968;68:587–648. (b) Shields ZP, Murray JS, Politzer P. Directional tendencies of halogen and hydrogen bonding. *Int J Quantum Chem* 2010;110:2823–2832.
- [16] Ananthavel SP, Manoharan M. A theoretical study on electron donor-acceptor complexes of Et₂O, Et₂S and Me₃N with interhalogens, I–X (X=Cl and Br). *Chem Phys* 2001;269:49–57.
- [17] (a) Raatikainen K, Cametti M, Rissanen K. The subtle balance of weak supramolecular interactions: The hierarchy of halogen and hydrogen bonds in haloanilinium and halopyridinium salts. *Beilstein J Org Chem* 2010; 6, 1–13. (b) Zordan F, Mínguez Espallargas G, Brammer L. Unexpected structural homologies involving hydrogen-bonded and halogen-bonded networks in halopyridinium halometallate salts. *CrystEngComm* 2006; 8:425–431. (c) Mínguez Espallargas G, Zordan F, Arroyo Marín L, Adams H, Shankland K, van de Streek J, Brammer L. Rational modification of the hierarchy of intermolecular interactions in molecular crystal structures by using tunable halogen bonds. *Chemistry* 2009;15:7554–7568.
- [18] (a) Sun A, Goroff NS, Lauher JW. Preparation of poly(diiododiacetylene), an ordered conjugated polymer of carbon and iodine. *Science* 2006;312:1030–1034. (b) Zou J-W, Jiang Y-J, Guo M, Hu G-X, Zhang B, Liu H-C, Yu Q-S. Ab Initio study of the complexes of halogen-containing molecules RX (X=Cl, Br, and I) and NH₃: Towards understanding the nature of halogen bonding and the electron-accepting propensities of covalently bonded halogen atoms. *Chem Eur J* 2005;11:740–751.
- [19] (a) Glaser R, Chen N, Wu H, Knotts N, Kaupp M. ¹³C NMR study of halogen bonding of haloarenes: Measurements of solvent effects and theoretical analysis. *J Am Chem Soc* 2004;7:4412–4419. (b) Raatikainen K, Rissanen K. Hierarchical halogen bonding induces polymorphism. *CrystEngComm* 2009;11:750–752. (c) Allen FH, Goud BS, Hoy VJ, Howard JAK, Desiraju GR. Molecular recognition via iodo...nitro and iodo...cyano interactions: Crystal structures of the 1:1 complexes of 1,4-diiodobenzene with 1,4-dinitrobenzene and 7,7,8,8-tetracyanoquinodimethane (TCNQ). *J Chem Soc Chem Commun* 1994;23:2729–2730.
- [20] Molecular electrostatic potential surfaces have been calculated at MP2/6-31+G(d,p)-LANL2DZdp from see Ref. 21.
- [21] Beale, T.M., Chudzynski, M.G., Sarwar, M.G., Taylor, M.S. Halogen bonding in solution: Thermodynamics and applications. *Chem Soc Rev* 2013, 42, 1667–1680.
- [22] (a) Priimagi A, Cavallo G, Forni A, Gorynsztejn-Leben M, Kaivola M, Metrangolo M, Milani R, Shishido A, Pilati T, Resnati G, Terraneo G. Halogen bonding versus hydrogen bonding in driving self-assembly and performance of light-responsive supramolecular polymers. *Adv Funct Mater* 2012;22:2572–2579. (b) Fox D, Metrangolo P, Pasini D, Pilati T, Resnati G, Terraneo G. Site-selective supramolecular synthesis of halogen-bonded cocrystals incorporating the photoactive azo group. *CrystEngComm* 2008; 10:1132–1136. (c) Nayak SN, Terraneo G, Forni A, Metrangolo M, Resnati G. C–Br...O supramolecular synthon: in situ cryocrystallography of low melting halogen-bonded complexes. *CrystEngComm* 2012;14:4259–4261. (d) Sgarbossa P, Bertani R, Di Noto V, Piga M, Giffin GA, Terraneo G, Pilati T, Metrangolo P, Resnati G. Interplay between structural and dielectric features of new low k hybrid organic-organometallic supramolecular ribbons. *Cryst Growth Des* 2012;12:297–305. (e) Bruce DW, Metrangolo P, Meyer F, Pilati T, Präsaug C, Resnati G, Terraneo G, Wainwright SG, Whitwood AC.

- Structure–function relationships in liquid-crystalline halogen-bonded complexes. *Chem Eur J* 2010;16:9511–9524. (f) Abate A, Biella S, Cavallo G, Meyer F, Neukirch H, Metrangolo P, Pilati T, Resnati G, Terraneo G. Halide anions driven self-assembly of haloperfluoroarenes: Formation of one-dimensional non-covalent copolymers. *J Fluorine Chem* 2010;130:1171–1177. (g) Gattuso G, Notti A, Pappalardo S, Parisi M, Pilati T, Resnati G, Terraneo G. Ion-pair separation via selective inclusion/segregation processes. *CrystEngComm* 2009;11:1204–1206. (h) Biella S, Gattuso G, Notti A, Metrangolo P, Pappalardo S, Parisi MF, Pilati T, Resnati G, Terraneo G. Halogen bonding-based anion coordination in calixarene/inorganic halide/diiodoperfluorocarbon assemblies. *Supramol Chem* 2009;21:149–156. (i) Cariatì E, Cavallo G, Forni A, Leem G, Metrangolo P, Meyer F, Resnati G, Righetto S, Terraneo G, Tordin E. Self-complementary nonlinear optical-phoretargeted to halogen bond-driven self-assembly of electro-optic materials. *Cryst Growth Des* 2011;11:5642–5648. (j) Cavallo G, Biella S, Lu J, Metrangolo P, Pilati T, Resnati G, Terraneo G. Halide anion-templated assembly of di- and triiodoperfluorobenzenes into 2D and 3D supramolecular networks. *J Fluorine Chem* 2010;131:1165–1172.
- [23] (a) Gao K, Goroff NS. Two new iodine-capped carbon rods. *J Am Chem Soc* 2000;122:9320–9321. (b) Perkins C, Libri S, Adams H, Brammer L. Diiodoacetylene: Compact, strong ditopic halogen bond donor. *CrystEngComm* 2012;14:3033–3038.
- [24] Baldrighi M, Cavallo G, Chierotti MR, Gobetto R, Metrangolo P, Pilati T, Resnati G, Terraneo G. Halogen bonding and pharmaceutical cocrystals: the case of a widely used preservative. *Mol Pharm* 2013;10:1760–1772.
- [25] (a) Metrangolo P, Meyer F, Pilati T, Resnati G, Terraneo G. Halogen bonding in supramolecular chemistry. *Angew Chem Int Ed* 2008;47:6114–6127. (b) Cavallo G, Metrangolo P, Pilati T, Resnati G, Sansotera M, Terraneo G. Halogen bonding: A general route in anion recognition and coordination. *Chem Soc Rev* 2010;39:3772–3783.
- [26] Colin M. Mémoires sur l’Iode. *Ann Chim* 1814;91:252–272.
- [27] Guthrie F. On the iodide of iodammonium. *J Chem Soc* 1863;16:239–244.
- [28] Benesi HA, Hildebrand JH. A spectrophotometric investigation of the interaction of iodine with aromatic hydrocarbons. *J Am Chem Soc* 1949;71:2703–2707.
- [29] Mulliken RS. Structures of complexes formed by halogen molecules with aromatic and with oxygenated solvents. *J Am Chem Soc* 1950;72:600–608.
- [30] Lachman A. A probable cause of the different colors of iodine solutions. *J Am Chem Soc* 1903;25:50–55.
- [31] Kleinberg J, Davidson AW. The nature of iodine solutions. *Chem Rev* 1948;42:601–609.
- [32] Rosokha, S.V., Kochi, J. *Halogen Bonding: Fundamentals and Applications*. Metrangolo, P, Resnati G., editors. Berlin: Springer, 2008, 136–160.
- [33] McKinney WJ, Popov AI. Chemistry of halogens and a polyhalides. XXX. Influence of solvent properties on the formation of pyridine-iodine charge-transfer complexes. *J Am Chem Soc* 1969;91:5215.
- [34] Laurence C, Gal J-F. *Lewis Basicity and Affinity Scales. Data and Measurement*. 1st ed. Chichester: John Wiley & Sons Ltd; 2010.
- [35] (a) Metrangolo P, Pilati T, Terraneo G, Biella S, Resnati G. Anion coordination and anion-templated assembly under halogen bonding control. *CrystEngComm* 2009; 11:1187–1196 and references therein. (b) Mele A, Metrangolo P, Neukirch H, Pilati T, Resnati G. A halogen-bonding-based heteroditopic receptor for alkali metal halides. *J Am*

- Chem Soc 2005;127:14972–14793. (c) Jentzsch AV, Emery D, Mareda J, Metrangolo P, Resnati G, Matile S. Ditopic ion transport systems: anion– π interactions and halogen bonds at work. *Angew Chem, Int Ed* 2011;50:11675–11678. (d) Dimitrijević E, Kvak O, Taylor MS. Measurements of weak halogen bond donor abilities with tridentate anion receptors. *Chem Commun* 2010;46:9025–9027.
- [36] (a) Cametti M, Raatikainen K, Metrangolo P, Pilati T, Terraneo G, Resnati G. 2-Iodoimidazolium receptor binds oxoanions via charge-assisted halogen bonding. *Org Biomol Chem* 2012;10:1329–1333. (b) Martí-Rujas J, Colombo L, Lü J, Dey A, Terraneo G, Metrangolo P, Pilati T, Resnati G. Hydrogen and halogen bonding drive the orthogonal self-assembly of an organic framework possessing 2D channels. *Chem Commun* 2012;48:8207–8209. (c) Kilah NL, Wise MD, Serpell CJ, Thompson AL, White NG, Christensen KE, Beer PD. Enhancement of anion recognition exhibited by a halogen-bonding rotaxane host system. *J Am Chem Soc* 2010;132:11893–11895. (d) Mele A, Metrangolo P, Neukirch H, Pilati T, Resnati G. A halogen-bonding-based heteroditopic receptor for alkali metal halides. *J Am Chem Soc* 2005, 127, 14972–14973. (e) Sarwar, M.G., Dragisic, B., Sagoo, S., Taylor, M. S. A tridentate halogen-bonding receptor for tight binding of halide anions. *Angew Chem Int Ed* 2010, 49, 1674–1677. (f) Creighton JA, Thomas KM. Raman spectroscopic studies of halide-ion complexes of carbon tetrahalides in solution. *J Chem Soc Dalton Trans* 1972, 2254–2257. (g) Lindeman SV, Hecht J, Kochi JK. The charge-transfer motif in crystal engineering. Self-assembly of acentric (diamondoid) networks from halide salts and carbon tetrabromide as electron-donor/acceptor synthons. *J Am Chem Soc* 2003;125:11597–11606. (h) Sarwar MG, Dragisic B, Dimitrijević E, Taylor MS. Halogen bonding between anions and iodoperfluoroorganics: Solution-phase thermodynamics and multidentate-receptor design. *Chem Eur J* 2013; 19:2050–2058.
- [37] Tebbe K-F. In A. L. Rheingold, editor. *Homoatomic Rings, Chains and Macromolecules of Main-Group Elements*. Amsterdam: Elsevier; 1977. p 551–606 and references therein.
- [38] Do K, Klein TP, Pommerening CA, Sunderlin LS. A new flowing afterglow-guided ion beam tandem mass spectrometer. Applications to the thermochemistry of polyiodide ions. *J Am Soc Mass Spectrom* 1997;8:688–696.
- [39] Albrecht M, Gossen V, Peters T, Hoffmann A, Raabe G, Valkonen A, Rissanen K. Anion– π interactions in salts with polyhalideanions: Trapping of I_4^{2-} . *Chem Eur J* 2010;16:12446–124503.
- [40] Havinga EE, Wiebenga EH. Interpretation of the structure of polyhalogen complexes by the mo-method. *Recl Trav Chim Pays-Bas* 1959;78:724–738.
- [41] (a) Küpper FC, Feiters MC, Olofsson B, Kaiho T, Yanagida S, Zimmermann MB, Carpenter LJ, Luther III GW, Lu Z, Jonsson M, Kloo L. Commemorating two centuries of iodine research: An interdisciplinary overview of current research. *Angew Chem Int Ed* 2011;50:11598–11620. (b) Yin Z, Wang QX, Zeng MH. Iodine release and recovery, influence of polyiodide anions on electrical conductivity and nonlinear optical activity in an interdigitated and interpenetrated bipillared-bilayer metal–organic framework. *J Am Chem Soc* 2012;134:4857–4863. (c) Svensson PH, Kloo L. Synthesis, structure, and bonding in polyiodide and metal iodide–iodine systems. *Chem Rev* 2003;103:1648–1684. (d) Heeger AJ. Semiconducting and metallic polymers: The fourth generation of polymeric materials. *Angew Chem, Int Ed Engl* 2001;40:2591–2611. (e) Rajpure KY, Bhosale CH. “(Photo)electrochemical investigations on spray deposited n-Sb₂S₃ thin film/polyiodide/C photoelectrochemical solar cells. *Mater Chem Phys* 2000; 63:263–269.

- [42] Yarwood Y, Person WB. Far-infrared intensity studies of iodine complexes. *J Am Chem Soc* 1968;90:594–600.
- [43] (a) Stammreich H, Forneris R, Tavares Y. High-resolution Raman spectroscopy in the red and near infrared—II: Vibrational frequencies and molecular interactions of halogens and diatomic interhalogens. *Spectrochim Acta* 1961;17:1173–1184. (b) Klaboe P. The Raman spectra of some iodine, bromine, and iodine monochloride charge-transfer complexes in solution. *J Am Chem Soc* 1967;89:3667–3676.
- [44] (a) Marks TJ. Rational synthesis of new unidimensional solid: Chemical and physical studies of mixed-valence polyiodides. *Ann NY Acad Sci* 1978;313:594–616. (b) Schramm CJ, Scaringe RP, Stojakovic DR, Hoffmann BM, Ibers JA, Marks TJ. Chemical, spectral, structural, and charge transport properties of the “molecular metals” produced by iodination of nickel phthalocyanine. *J Am Chem Soc* 1980;102:6702–6713. (c) Ferraro JR. Structural, conductivity and spectroscopic aspects of one-dimensional transition metal complexes. *Coord Chem Rev* 1982;43:205–232.
- [45] Ginn SGW, Wood JL. Intermolecular vibrations of charge transfer complexes. *Trans Faraday Soc* 1965:777–787.
- [46] Deplano P, Ferraro JR, Mercuri ML, Trogu EF. Structural and Raman spectroscopic studies as complementary tools in elucidating the nature of the bonding in polyiodides and in donor- I_2 adducts. *Coord Chem Rev* 1999;188:71–95.
- [47] Abate A, Brischetto M, Cavallo G, Lahtinen M, Metrangolo P, Pilati T, Radice S, Resnati G, Rissanen K, Terraneo G. Dimensional encapsulation of $-I\cdots I_2\cdots I-$ in an organic salt crystal matrix. *ChemCommun* 2010:2724–2726.
- [48] Lin J, Martí-Rujas J, Metrangolo P, Pilati T, Radice S, Resnati G, Terraneo G. Solution and solid state synthesis of the discrete polyiodide I_7^{3-} under modular cationtemplation. *Cryst Growth Des* 2012;12:5757–5762.
- [49] (a) Nelen MI, Eliseev AV. Electrostatic molecular recognition in rigid frameworks. *J Chem Soc Perkin Trans* 1997;2:1359–1364. (b) Hosseini MW, Lehn JM. Anion receptormolecules. Chain length dependent selective binding of organic and biological dicarboxylate anions by ditopic polyammonium macrocycles. *J Am Chem Soc* 1982;104:3525–3527.
- [50] (a) Desiraju GR *Crystal Engineering: The Design of Organic Solids*. Amsterdam: Elsevier; 1989. (b) Braga D, Grepioni F, Desiraju GR. Crystal engineering and organometallic architecture. *Chem Rev* 1998;98:1375–1405. (c) Gavezotti A. Are crystal structures predictable?. *Acc Chem Res* 1994;27:309–314. (d) Blake AJ, Champness NR, Hubberstey P, Li WS, Withersby MA, Schroder M. Inorganic crystal engineering using self-assembly of tailored building-blocks. *Coord Chem Rev* 1999;183:117–138. (e) Braga D, Desiraju GR, Miller J, Orpen AG, Price S. Innovation in crystal engineering. *CrystEngComm* 2002;4:500–509. (f) Desiraju GR. Crystal engineering: A holistic view. *Angew Chem, Int Ed* 2007;46:8342–8356.
- [51] (a) Desiraju GR Supramolecular synthons in crystal engineering – A new organic synthesis. *Angew Chem, Int Ed* 1995;34:2311–2327. (b) Desiraju GR. Designer crystals: Intermolecular interactions, network structures and supramolecular synthons. *Chem Commun* 1997;1475–1482.
- [52] (a) Kitaigorodsky AI. *Mixed Crystals, Solid State Sciences*. Volume 33. Berlin: Springer Verlag; 1984. (b) Desiraju GR. Crystal and co-crystal. *CrystEngComm* 2003;5:466–467. (c) Dunitz JD. Crystal and co-crystal: A second opinion. *CrystEngComm* 2003;5:506–506. (d) Aakeroy CB, Salmon DJ. Building co-crystals with molecular sense and supramolecular sensibility. *CrystEngComm* 2005;7:439–448. (e) Steurer W. What is a crystal? Introductory remarks to an ongoing discussion. *Z Kristallogr.* 2007;222:308–309.

- (f) Bond AD. What is a co-crystal?. *CrystEngComm* 2007;9:833–834. (g) Zukerman-Schpector J, Tiekink ERT. What is a co-crystal?. *Z Kristallogr* 2008;223:233–234. (h) Stanly GP. Diversity in single- and multiple-component crystals. The search for and prevalence of polymorphs and cocrystals. *Cryst Growth Des* 2007;7:1007–1026.
- [53] (a) Cheney M, Zaworotko MJ, Beaton S, Singer RD. Cocrystal controlled solid-state synthesis: A green chemistry experiment for undergraduate organic chemistry. *J Chem Educ* 2008;85:1649–1651. (b) Hirsch AKH, Alphey MS, Lauw S, Seet M, Barandun L, Eisenreich W, Rohdich F, Hunter WN, Bacher A, Diederich F. Inhibitors of the kinase IspE: Structure-activity relationships and co-crystal structure analysis. *Org Bio Chem* 2008;6:2719–2730. (c) Zaworotko MJ. Molecules to crystals, crystals to molecules ... and back again?. *Cryst Growth Des* 2007;7:4–9.
- [54] Allen FH. The Cambridge Structural Database: A quarter of a million crystal structures and rising. *Acta Cryst* 2002;B58:380–388.
- [55] The search has been performed on I₂ molecule (zero charge on both iodine atom) which interacts with N, O, P, S, As, Se and Te atoms as halogen bonding acceptors. The distance XB donor and acceptor has to be shorter than the sum of vdW radii. The contact between XB donor and acceptor has been set with the CSD keyword either “intermolecular contact” and “any bond type”. The angle I-I...D has been limited between 140° and 180°. Restrictions: 3D coordinates, no disordered structure and no errors.
- [56] Peuronen A, Valkonen A, Kortelainen M, Rissanen K, Lahtinen M. Halogen bonding based “catch and release”: Reversible solid state entrapment of elemental iodine with mono-alkylated DABCO salts. *Cryst Growth Des* 2012;12:4157–4169. CCDC code: HEKZEE.
- [57] Pritzkow H. Die kristallstrukturenzweieraddukte des hexamethylentetraminsmitjod. *Acta Crystallogr, Sect B Struct Crystallogr Cryst Chem* 1975;31:1589–1593. CCDC code: HXMTDI.
- [58] Hassel O, Romming C, Tufte T. Crystal structure of the 1:1 addition compound formed by 4-picoline and iodine. *Acta Chem Scand* 1961;15:967–974. CCDC code: PICOLI.
- [59] (a) Caronna T, Liantonio R, Logothetis TA, Metrangolo P, Pilati T, Resnati G. Halogen bonding and p...p stacking control reactivity in the solid state. *J Am Chem Soc* 2004; 126:4500–4501. (b) Bertani R, Chaux F, Gleira M, Metrangolo P, Milani R, Pilati T, Resnati G, Sansotera M, Venzo A. Supramolecular rods via halogen bonding-based self-assembly of fluorinated phosphazene nanopillars. *Inorg Chim Acta* 2007;360:1191–1199. (c), Bianchi R, Forni A, Pilati T. N...Br halogen bonding: 1D infinite chains through the self-assembly of dibromotetrafluorobenzenes with dipyrityl. *Chem-Eur J* 2003;9:1631–1638. (d) Forni A, Metrangolo P, Pilati T, Resnati G. Halogen bond distance as a function of temperature. *Cryst Growth Des* 2004;4:291–295. (e) Metrangolo P, Meyer F, Pilati T, Proserpio DM, Resnati G. Dendrimerictectons in halogen bonding-based crystal engineering. *Cryst Growth Des* 2008;8:654–659. (f) Lucassen ACB, Karton A, Leitun G, Shimon LJW, Martin JML, van der Boom M. Co-crystallization of sym-triiodo-trifluorobenzene with bipyridyldonors: Consistent formation of two instead of anticipated three N...I halogen bonds. *Cryst Growth Des* 2007;7:386–392.
- [60] Walsh RB, Padgett CW, Metrangolo P, Resnati G, Hanks TW, Pennington WT. Crystal engineering through halogen bonding: complexes of nitrogen heterocycles with organic iodides. *Cryst Growth Des* 2001;1:165–175. CSD code: QIHBOY.
- [61] Ramasubbu N, Parthasarathy R, Murray-Rust P. Angular preferences of intermolecular forces around halogen centers: Preferred directions of approach of electrophiles and nucleophiles around carbon-halogen bond. *J Am Chem Soc* 1986;108:4308–4314.

- [62] Selected examples: (a) Bond AD, Griffiths J, Rawson JM, Hulliger J. Inducing structural polarity using fluorinated organics: X-ray crystal structures of p- $\text{XC}_6\text{F}_4\text{CN}$ ($\text{X} = \text{Cl}, \text{Br}, \text{I}$). *Chem Commun* 2001;2488–2489. (b) Gleason WB, Britton D. Structure of 4-cyano-4'-iodobiphenyl at 297 and 183 K. *Cryst Struct Commun* 1978;7:365–370. (c) Metrangolo P, Pilati T, Resnati G, Stevenazzi A. Metric engineering of perfluorocarbon-hydrocarbon layered solids driven by the halogen bonding. *Chem Commun* 2004;1492–1493. (d) Yan D, Delori A, Lloyd GO, Friscic T, Day GM, Jones W, Lu J, Wei M, Evans DG, Duan X. A cocrystal strategy to tune the luminescent properties of stilbene-type organic solid-state materials. *Angew Chem Int Ed* 2011;50:12483–12486. (e) Desiraju R, Harlow RL. Cyano-halogen interactions and their role in the crystal structures of the 4-halobenzonitriles. *J Am Chem Soc* 1989;111:6757–6764.
- [63] Aakeroy CB, Desper J, Helfrich BA, Metrangolo P, Pilati T, Resnati G, Stevenazzi A. Combining halogen bonds and hydrogen bonds in the modular assembly of heteromeric infinite 1-D chains. *Chem Commun* 2007;4236–4238.
- [64] (a) Bailey RD, Drake GW, Grabarczyk M, Hanks TW, Hook LL, Pennington WT. Synthesis, structure and thermal decomposition of nitrogen-iodine charge-transfer complexes. *J Chem Soc Perkin Trans* 1997;2:2773–2780. (b) Isaia F, Aragoni MC, Arca M, Demartin F, Devillanova FA, Ennas G, Garau A, Lippolis V, Mancini A, Verani G. Molecular iodine stabilization in an extended $\text{N}\cdots\text{I}\cdots\text{N}$ assembly. *Eur J Inorg Chem* 2009;3667–3672. CSD CODE: IHISEY. (c) Tamilselvi A, Mugesh G. Interaction of heterocyclic thiols/thiones eliminated from cephalosporins with iodine and its biological implications. *Bioorg Med Chem Lett* 2010;20:3692–3697. CSD CODE: WURGAS.
- [65] Bernardinelli G, Gerdl R. 2-Chloroquinoline iodonochloride. *Acta Crystallogr Sect B Struct Crystallogr Cryst Chem* 1976;32:1906–1907. CSD CODE: CLQUIC.
- [66] Baenziger NC, Nelson AD, Tulinsky A, Bloor JH, Popov AI. Two independent determinations of the crystal and molecular structure of the iodine monochloride complex of pentamethylenetetrazole. *J Am Chem Soc* 1967;89:6463–6465. CSD CODE: PMTTIC and PMTTIC01.
- [67] (a) Soled S, Carpenter GB. The crystal structures of 2,2'-bipyridine-2ICl and 2,2'-bipyridine-2IBr. *Acta Crystallogr Sect B Struct Crystallogr Cryst Chem* 1974;30:910–914. CSD CODE: TAGNIZ. (b) Aragoni MC, Arca M, Devillanova FA, Hursthouse MB, Huth SL, Isaia F, Lippolis V, Mancini A, Ogilvie HR, Verani G. Reactions of pyridyl donors with halogens and interhalogens: An X-ray diffraction and FT-Raman investigation. *J Organomet Chem* 2005;690:1923–1927. CSD CODE: TASPEJ.
- [68] (a) Barnes NA, Flower KR, Fyyaz SA, Godfrey SM, McGown AT, Miles PJ, Pritchard RG, Warren JE. Can the solid state structures of the dihalogen adducts R_3EX_2 ($\text{E} = \text{P}, \text{As}$; $\text{R} = \text{alkyl}, \text{aryl}$; $\text{X} = \text{Br}, \text{I}$) with the molecular spoke geometry be considered good mimics of the gold(I) systems $[(\text{R}_3\text{E})\text{AuX}]$ ($\text{E} = \text{As}, \text{P}$; $\text{R} = \text{alkyl}, \text{aryl}$; $\text{X} = \text{Cl}, \text{Br}, \text{I}$)?. *CrystEngComm* 2010;12:784–794. CSD CODE: VUNVIK. (b) Barnes NA, Godfrey SM, Khan RZ, Pierce A, Pritchard RG. A structural and spectroscopic study of *tris*-aryl substituted R_3PI adducts. *Polyhedron* 2012;35:31–46. CSD CODE: RARWIS, RARWOY, RARWUE and RAWXOZ.
- [69] Barnes NA, Flower KR, Godfrey SM, Hurst PA, Khan RZ, Pritchard RG. Structural relationships between o-, m- and p-tolyl substituted R_3EI_2 ($\text{E} = \text{As}, \text{P}$) and $[(\text{R}_3\text{E})\text{AuX}]$ ($\text{E} = \text{As}, \text{P}$; $\text{X} = \text{Cl}, \text{Br}, \text{I}$). *CrystEngComm* 2010;12:4240–4251. CSD CODE: WAJTOS and WAJVAG.
- [70] Bricklebank N, Godfrey SM, McAuliffe CA, Pritchard RG. Tertiary phosphine adducts of mixed halogens, R_3PIBr ; synthesis and structure in the solid state and solution. *J Chem Soc Dalton Trans* 1993;2261–2270. CSD CODE: PESJOM.

- [71] (a) Reimann S, Bunesco A, Litschko R, Erfle S, Domke L, Bendrath F, Abilov ZA, Spannenberg A, Villinger A, Langer P. Formal [3+3] cyclocondensations of 1,3-bis(silyloxy)-1,3-butadienes with 1-chloro-1,1-difluoro-4,4-dimethoxybut-3-en-2-one and 1,1-difluoro-4,4-dimethoxybut-3-en-2-one. Regioselective synthesis of fluorinated salicylates and pyran-4-ones. *J Fluorine Chem* 2012;139:28–45. (b) Chu Q, Wang W, Huang Q, Yan C, Zhu S. Fluorine-containing donor-acceptor complexes: Crystallographic study of the interactions between electronegative atoms (N, O, S) and halogen atoms (I, Br). *New J Chem* 2003;27:1522–1527. (c) Higashiya S, Chung WJ, Lim DS, Ngo SC, Kelly IV WH, Toscano PJ, Welch JT. Synthesis of mono- and difluoroacetyltrialkylsilanes and the corresponding enol silyl ethers. *J Org Chem* 2004;69:6323–6328.
- [72] Walbaum C, Pantenburg I, Meyer G. Iodine molecules included in the structure of dibenzo-24-crown-8, (I₂)@ (db24c8). *Crystals* 2011;1:215–219. CSD CODE VAQKUV.
- [73] Bock H, Holl S. Crystallization and structure determination of σ -donor/acceptor complexes between 1,4-dioxane and the polyiodine molecules I₂, I₂C=Cl₂, (IC)₄S and (IC)₄NR (R = H, CH₃). *Z. Naturforsch B Chem Sci* 2001;56:111–112, CSD CODE: QOJKEF.
- [74] Liu Q-K, Ma J-P, Dong Y-B. Highly efficient iodine species enriching and guest-driven tunable luminescent properties based on a cadmium(II)-triazole MOF. *Chem Commun* 2011;47:7185–7187. CSD CODE: ITIWAK, ITIWIS, ITIWOY and ITIWUE.
- [75] Krupskaya Y, Alfonsov A, Parameswaran A, Kataev V, Klingeler R, Steinfeld G, Beyer N, Gressenbuch M, Kersting B, Buchner B. Interplay of magnetic exchange interactions and Ni-S-Ni bond angles in polynuclear nickel(II) complexes. *ChemPhysChem* 2010;11:1961–1970. CSD CODE: WAJZAK.
- [76] Tuikka M, Hirva P, Rissanen K, Korppi-Tommola J, Haukka M. Halogen bonding - a key step in charge recombination of the dye-sensitized solar cell. *Chem Commun* 2011, 47, 4499–4501. CSD CODE: EPISEC.
- [77] Ref. 64 CSD code: WURGEW.
- [78] Asseily GA, Davies RP, Rzepa HS, White AJP. A solid-state structural and theoretical study on the 1:1 addition compounds of thioethers with dihalogens and interhalogens I-X (X = I, Br, Cl). *New J Chem* 2005;29:315–319. CSD CODE: QAQTAE.
- [79] Mueller B, Takaluoma TT, Laitinen RS, Seppelt K. Syntheses and structures of two dimethyl diselenide–diiodine adducts and the first well characterized diorgano disulfide-nitrosonium adduct. *Eur J Inorg Chem* 2011;4970. CSD CODE: ICIYIE.
- [80] Knight FR, Fuller AL, Buhl M, Slawin AMZ, Woollins JD. Hypervalent adducts of chalcogen-containing peri-substituted naphthalenes; reactions of sulfur, selenium, and tellurium with dihalogens. *Inorg Chem* 2010;49:7577–7596. CSD CODE: UKADOA.
- [81] Knight FR, Arachchige KSA., Randall RAM, Buhl M, Slawin AMZ, Woollins JD. Exploring hypervalency and three-Centre, four-electron bonding interactions: Reactions of acenaphthene chalcogen donors and dihalogen acceptors. *Dalton Trans* 2012;41:3154–3165. CSD CODE: WARMEJ, WARMUZ and WARNAG.
- [82] (a) de Oliveira GM, Faoro E, Lang ES. New Aryltellurenyl iodides with uncommon valences: synthetic and structural characteristics of [R₂TeTeI₂R], [R₂TeTeR₂][Te₄I₁₄], and [RTe(I)I₂] (R=2,6-Dimethoxyphenyl). *Inorg Chem* 2009;48:4607–4609. (b) Faoro E, de Oliveira GM, Lang ES, Pereira CB. Synthesis and structural features of new aryltellurenyl iodides. *J Organomet Chem* 2010;695:1480–1486. (c) Faoro E, de Oliveira GM, Lang ES, Pereira CB. Rhodium-catalyzed regioselective arylation of phenylazoles and related compounds with arylboron reagents via C–H bond cleavage. *J Organomet Chem* 2011;696:2438–2444.

- [83] Faoro E, de Oliveira GM, Lang ES. Attainment of new Te^{II} and Te^{IV} iodides by unexpected removal of the mesityl group of $[\text{mesTeI}^2]^-$: Synthesis and structural features of $[\text{TeI}_4][\text{Co}(\text{en})_3] \cdot \text{I}$, $[\text{TeI}_6][\text{Co}(\text{en})_3] \cdot \text{I}$, $[\{\text{TeI}_6\}\{\text{Te}_2\text{I}_{10}\}][\text{Co}(\text{NH}_3)_6]_2 \cdot 21 \cdot 6\text{H}_2\text{O}$ and $[(\text{mesTeI}_2)_2(\mu\text{-I}_2)][\text{Co}(\text{bpy})_3] \cdot \text{I}_3 \cdot 2\text{CHCl}_3$ (mes = 2,4,6-trimethylphenyl; en = ethylenediamine; bpy = bipyridine). *Polyhedron* 2009;28:63–68. CSD CODE: MOMXAO.
- [84] The CSD search has been performed on I_2 molecule (zero charge on both iodine atoms and only one atom bound to each iodine atom) which interacts with aromatic systems. Restrictions: 3D coordinates, no disordered structure and no errors.
- [85] Mitani S. Crystal structure of coronene iodide. *Annu Rep Res R.I. Kyoto U* 1986;19:1–4. CSD CODE: DUPCIA10.
- [86] Birkett PR, Christides C, Hitchcock PB, Kroto HW, Prassides K, Taylor R, Walton DRM. Preparation and single crystal structure determination of the solvated intercalate $\text{C}_{60}\text{-I}_2$ -toluene. *J Chem Soc Perkin Trans 2* 1993;1407–1409. CSD CODE: LAVNIF.
- [87] Huang P-S, Kuo C-H, Hsieh C-C, Horng Y-C. Selective capture of volatile iodine using amorphous molecular organic solids. *Chem Commun* 2012;48:3227–3229. CSD CODE: MAVVAI.
- [88] (a) Jentzsch AV, Emery D, Mareda J, Metrangolo P, Resnati G, Matile S. Ditopic ion transport systems: Anion- π interactions and halogen bonds at work. *Angew Chem Int Ed* 2011;50:11675–11678. (b) Kniep F, Jungbauer SH, Zhang Q, Walter SM, Schindler S, Schnapperelle I, Herdtweck E, Huber SM. Organocatalysis by neutral multidentate halogen-bond donors. *Angew Chem Int Ed* 2013;52:7028–7032.
- [89] Fan M, Shevchenko IV, Voorhies RH, Eckert SF, Zhang H, Lattman M. Main-group-element calix[4]arenes: Variable coordination and conformational isomerism at phosphorus and silicon. *Inorg Chem* 2000;39:4704–4712.
- [90] Spandl J, Daniel C, Brudgam I, Hartl H. Synthesis and structural characterization of redox-active dodecamethoxoheptaohexavanadium cluster. *Angew Chem Int Ed* 2003;42:1163–1166.
- [91] The CSD search has been performed on I_2 molecule (zero charge on both iodine atoms and only one atom bound to each iodine atom) which interacts with iodide anion possessing one negative charge and zero atoms bound to it. Restrictions: 3D coordinates.
- [92] (a) Blake AJ, Gould RO, Li WS, Lippolis V, Parsons S, Radek C, Schröder M. Template assembly of polyiodide networks at complexed metal cations: Synthesis and structures of $[\text{Pd}_2\text{Cl}_2(\text{[18]aneN}_2\text{S}_6)] \cdot 1.5\text{I}_3(\text{I}_3)_2$ and $[\text{K}(\text{[15]aneO}_5)_2]\text{I}_9$. *Angew Chem Int Ed Engl* 1998;37:293–296. (b) Bailey RD, Hook LL, Pennington WT. Crystal engineering through charge transfer interactions; assisted formation of a layered coordination polymer (4-cyanopyridine)cadmium(II) iodide-diiodine. *Chem Commun* 1998;1181–1182. (c) Blake AJ, Gould RO, Parsons S, Radek C, Schröder M. Self-assembly of polyanions at a metal cation template: syntheses and structures of $[\{\text{Ag}(\text{[18]aneS}_6)\}_n\text{I}_n]$ and $[\text{Ag}(\text{[18]aneS}_6)]_3\text{I}_3$. *Angew Chem Int Ed Engl* 1995;34:2374–2376.
- [93] (a) Tebbe K-F. In Rheingold AL, editor. *Polyhalogen Cations and Polyhalide Anions. Homoatomic Rings, Chains and Macromolecules of Main-Group Elements*. Amsterdam: Elsevier; 1997. (b) Blake AJ, Devillanova FA, Gould RO, Li W-S, Lippolis V, Parsons S, Radek C, Schröder M. Template self-assembly of polyiodide networks. *Chem Soc Rev* 1998;27:195–205.
- [94] Nelyubina YV, Antipin MY, Dunin DS, Kotov VY, Lyssenko KA. Unexpected “amphoteric” character of the halogen bond: The charge density study of the co-crystal of N-methylpyrazine iodide with I_2 . *Chem Commun* 2010;46:5325–5327.

- [95] Dolder S, Liu S-X, Beurer E, Ouahab L, Decurtins S. Synthesis and characterization of a new pyrazine functionalized TTF derivative and crystal structure of its charge-transfer complex with iodine. *Polyhedron* 2006;25:1514–1518.
- [96] Blake AJ, Gould RO, Li W-S, Lippolis V, Parsons S, Radek C, Schroder M. Silver-thioether crown complexes as templates for the synthesis of extended polyiodide networks: Synthesis and X-ray crystal structures of $[\text{Ag}_2([15]\text{aneS}_3)_2]\text{I}_{12}$, $[\text{Ag}([18]\text{aneS}_6)]\text{I}_7$, $[\text{Ag}([18]\text{aneS}_6)]\text{I}_3$, and $[\text{Ag}([9]\text{aneS}_3)_2]\text{I}_5$. *Inorg Chem* 1998;37:5070–5077.
- [97] (a) Sedinkin SL, Rath NP, Bauer EB. Synthesis and structural characterization of new phosphinooxazoline complexes of iron. *J Organomet Chem* 2008;693:3081–3091. (b) Iyoda M, Hasegawa M, Kuwatani Y, Nishikawa H, Fukami K, Nagase S, Yamamoto G. Effects of molecular association in the radical-cations of 1,8-bis(ethylenedithiotetrathiafulvalenyl)naphthalene. *Chem Lett* 2001;1146–1147. (c) Spandl J, Daniel C, Brudgam I, Hartl H. Synthesis and structural characterization of redox-active dodecamethoxohepta-oxohexavanadium clusters. *Angew Chem Int Ed* 2003;42:1163–1166. (d) Kuwatani Y, Ogura E, Nishikawa H, Ikemoto I, Iyoda M. 4,5-Diodo-4',5'-Ethyleledioxytetrathiafulvalene and its metallic radical salts. *Chem Lett* 1997;817–818.
- [98] Martí-Rujas J, Meazza L, Lim GL, Terraneo G, Pilati T, Harris KDM, Metrangolo P, Resnati G. An adaptable and dynamically porous organic salt traps unique tetrahalide dianions. *Angew Chem Int Ed* 2013;52:13444–13448.

PART II

PRODUCTION OF IODINE

9

HISTORY OF IODINE

JAMES L. MARSHALL AND VIRGINIA R. MARSHALL

Department of Chemistry, University of North Texas, Denton, TX, USA

SUMMARY

Bernard Courtois (1777–1838) serendipitously discovered iodine in Paris while reacting varec (ashes of seaweed) with sulfuric acid. He was using varec as a source of potash (potassium carbonate), necessary in the manufacture of saltpeter (potassium nitrate) used in gunpowder.

9.1 HISTORY OF SALTPETER

The seventh-century Taoist alchemists in western China stumbled upon a concoction of honey, sulfur, and saltpeter that caused smoke, fire, sparks, and thunder—called *huo yao*, or “fire drug”—thought to be the elixir of life [1]. We know the incendiary mixture today as gunpowder [2]. By the mid-1200s the Chinese discovery had spread to the Western world [1]. Roger Bacon (1214–1294) of Oxford recognized it as a mixture of “saltpeter, sulfur, and charcoal” (preferably of hazelwood), with the saltpeter in excess [2]. The Battle of Crécy in northern France in 1346 at the beginning of the Hundred Years’ War may be marked as the formal introduction of gunpowder on the battlefield as “gonnes” were used beside the famous longbowmen [1]. In an attempt to understand the nature of gunpowder, Robert Boyle (1627–1691) studied gunpowder in vacuum, generated by pumps originally used in his gas law experiments. Boyle was puzzled by the behavior of gunpowder, which combusted in an evacuated jar just as it did in the

open atmosphere, when heated by the sun's rays concentrated by a magnifying glass [1]. Boyle did not understand that saltpeter (known today to be KNO_3) contained its own "air." Carl Wilhelm Scheele (1742–1786) got his first hint of the nature of this supporter of combustion when he observed sparks as saltpeter was heated with oil, and he went on to discover oxygen [3b]. Today we understand the basic reaction of gunpowder to be $2 \text{KNO}_3 + 3 \text{C} + \text{S} \rightarrow \text{K}_2\text{S} + \text{N}_2 + 3 \text{CO}_2$. The evolved gases expand and serve as the propellant in rockets and guns [1]. Saltpeter (meaning "salt-rock") is the most soluble of the nitrates and wicks up rapidly in soil; it was first observed in China where a climate of alternatively cold/hot wet/dry climates allowed it to form on soil surfaces [1]. In Medieval Europe on stable and barn stone walls, saltpeter grew in the form of "blooms" resembling cotton tufts. Recent analyses show such growths of saltpeter are surprisingly pure, often greater than 95% KNO_3 [4]. Saltpeter diggers—*Salpetergraber* in Germany or *Salpêtrier* in French (Bretcher U. Personal Communication. Consulting Engineer, Kuster and Hager, Uznach)—soon learned to excavate soil about stables, pigeon cotes, manure piles, or barnyards to collect the saltpeter therein. As the demand for saltpeter increased, the saltpeter plantation/refinery was born, called the nitrery (*Nitrière* in French, *Nitriary* in German) (Bretcher U. Personal Communication. Consulting Engineer, Kuster and Hager, Uznach) (Fig. 9.1). The manager of a nitrery would lay down a stratum of lime and cover it with manure, garbage, corpses, and any other organic material, including a periodic dowsing with the urine of "drinkers of wine or strong beer" [1]. The major qualification of a nitrery manager was his ability to tolerate the incredible stench of his enterprise. After a few months the saltpeter diggers unearthed copious amounts of saltpeter-rich soil. An aqueous washing of the soil was reacted with ashes, filtered, concentrated by boiling, and cooled to produce white crystals of saltpeter (Fig. 9.2). Today we understand the chemistry of the process. Ammonia released from organic material is oxidized to nitrates. The lime (CaO) keeps the pH 7–8 required by the nitrifying bacteria. The product, calcium nitrate ("lime saltpeter"), is useless because it is hygroscopic, and the resulting gunpowder absorbs moisture. Hence, the calcium nitrate is reacted with ashes (potash; potassium carbonate) to precipitate the calcium salts and leave a potassium nitrate solution: $\text{Ca}(\text{NO}_3)_2 (\text{aq}) + \text{K}_2\text{CO}_3 (\text{aq}) \rightarrow \text{CaCO}_3 (\text{s}) + 2\text{KNO}_3 (\text{aq})$ (Bretcher U. Personal Communication. Consulting Engineer, Kuster and Hager, Uznach) [4]. During the 1600s Great Britain found a cheap source of saltpeter—the East India Company could allow import of the commodity from India at one-quarter of the domestic cost [1].¹ France continued to produce its saltpeter from its home nitreries and itinerant saltpeter gatherers but by necessity had to purchase some of its supply from Holland at an exorbitant price. Louis XVI (1752–1793) established the Gunpowder Administration in 1775, and as manager he appointed Antoin-Laurent Lavoisier (1743–1794), who promptly increased saltpeter production and improved the gunpowder manufacture process [3a]. This self-sufficiency would be vital when Great Britain blockaded France during the French Revolutionary Wars (1792–1802) and the Napoléonic Wars (1803–1815).

¹Later, when Indian saltpeter became excessively expensive, Chilean saltpeter could be exploited. However, this South American commodity is mainly sodium nitrate, which is inferior because it is hygroscopic [1]. Bird and bat guano have also been rich sources of ammonia. With the development of the Haber process (the combination of nitrogen and hydrogen gas to form ammonia by Fritz Haber 1868–1934) in 1913 [8c], there was no further need for organic sources of ammonia for the munitions industry.



FIGURE 9.1 Saltpeter works as shown in a 1598 woodcut [10]. The rows of hills (C) were filled with manure, garbage, soil, blood, ash, and lime and were periodically soaked with urine. The nitrogenous compounds released ammonia, which were oxidized to nitrates. After a year or so the “ripened” saltpeter beds were processed in the “refinery,” the work shed (B) (see Fig. 9.2). The bucket (A) collected rainwater. A cord of wood (D) was used as fuel for the hearths in the shed. A saltpeter digger (E) would remove soil “ripe” for processing.

9.2 COURTOIS IN DIJON

Bernard Courtois was born in Dijon, France, the son of the wine merchant Jean-Baptiste Courtois (1748–ca. 1807). The Courtois home was directly across the street from the Académie de Dijon (Fig. 9.3), where the father won the position of chemistry demonstrator, hired by Louis-Bernard Guyton de Morveau (1737–1816), a lawyer and chemist who founded the chemistry department at Dijon Academy [5]. Guyton de Morveau is well-known as one of the authors of the modern system of chemical nomenclature in 1787 (the others being Lavoisier [3a], Claude-Louis Berthollet (1748–1822) [3c], and Antoine Fourcroy (1755–1809)) [5]. In 1780 Jean-Baptiste was



FIGURE 9.2 The refining of saltpeter in the shed (1556) [11]. The “ripened” soil was leached in vat (B); the filtered solution was drained through a plug (C) into a collection vat (D). This filtrate was concentrated on a hearth (A), then poured into crystallization buckets (E) with inserted copper sticks on which saltpeter crystallized as the solution cooled.

also assigned manager of the new Saint Médard Nitrary in Dijon (1.7 km east, on the outskirts of town) (Fig. 9.4), one of the government-sponsored plantations established to cope with the saltpeter shortage [5]. As a boy the precocious Bernard Courtois absorbed considerable chemical knowledge and laboratory experience at the Académie laboratory and at the nitrary.

9.3 COURTOIS IN PARIS

In 1798 Bernard Courtois became a laboratory assistant at the École Polytechnique, arranged by Morveau who had moved to Paris in 1791 to become a member of the Legislative Assembly and also a professor at l'École Polytechnique [5]. At this time the École Polytechnique was located in the Palais Bourbon, directly across the Seine from the Place de la Révolution, today la Place de la Concorde, where



FIGURE 9.3 Southward view on Rue Monge in Dijon, France (N47° 19.12 E05° 02.02). The Académie de Dijon is to the left (51 Rue Monge); Courtois' home (where Bernard Courtois was born, 78 Rue Monge) is the building with two chimneys on the right side, 50m away, immediately this side of the half-timbered house. The Académie was founded in 1725 and moved to this Rue Monge location in 1772. (At this time, the street was called Rue Ponternant.) Dijon is 250 km southeast of Paris.



FIGURE 9.4 This is what remains of the largest and oldest (1582) plantation/refinery in Dijon—the Raffinerie des argentieres (N 47° 19.01 E 05° 03.25), formerly in the country, but now a residential neighborhood with no hint of the original nitrery. In the early 1800s there were several nitreries in every city. Saint Médard (which Jean-Baptiste Courtois owned) was 600m north (N 47° 19.33 E 05° 03.36). *Inset:* Street sign expanded, “Street of the [saltpeter] refinery.”



FIGURE 9.5 This is the view northward on Rue Saint-Ambroise in northeast Paris (N 48° 51.76 E 02° 22.70). The home and salpêtrière of Bernard Courtois where he discovered iodine was on the left; the present address is 31 Saint-Ambroise (old address 9), now the site of modern apartments. The plantation measured roughly 100×100 m.

Lavoisier was guillotined in 1794 [3a]. At l'École Polytechnique, Bernard Courtois worked with Fourcroy and Thénard (the discoverer of hydrogen peroxide, 1777–1857), then with Armand Séguin (1767–1835) [6]. Séguin is perhaps best known for serving as the human guinea pig for Lavoisier's respiration studies; classic drawings by Mme. Lavoisier show him with the “gas masks” in Lavoisier's laboratory at la Petit Arsenal [3a]. In Séguin's laboratory Bernard worked with opium compounds and apparently isolated morphine, although this was not formally acknowledged [5]. Séguin delayed publication and was scooped in 1804 by Friedrich Wilhelm Adam Sertürner (1783–1841) of Paderborn, Germany, who gave the drug its modern name [5].

In 1804 Bernard terminated his studies at l'École Polytechnique, which was becoming militarized upon Napoléon's edict and was moved to its new site near the Panthéon [6]. Bernard now assisted his father, who had moved to Paris in 1802 to set up a nitrary and had settled on Rue Saint Marguerite (today Rue Trousseau) [5], about 1 km northeast of the Seine on the outskirts of town. Six years later Bernard assumed ownership of his own nitrary, another kilometer north on Rue Saint-Ambroise (Fig. 9.5), where he remained till 1810–1821 [5]. It was here that he discovered iodine.

9.4 DISCOVERY OF IODINE

Potash was scarce because of the Napoleonic Wars (1803–1815), and Bernard Courtois had resorted to varec imported from the Brittany and Normandy seacoasts [5]. One day in late 1811 while cleaning pots he accidentally discovered that concentrated sulfuric acid reacted with varec in an exothermic reaction to yield a violet cloud that condensed on a cold metallic or ceramic surface in the form of crystals with the color and luster of graphite [7a]. Courtois performed some research on the crystals, and discovered a fulminating powder when he reacted the dark crystals with ammonia—he had produced nitrogen triiodide [[5], 7a]. Not being a regular member of the scientific establishment, he could not immediately publish his findings. In May 1812 he shared his experiences with his colleagues Nicolas Clément (1779–1842) and Charles Bernard Désormes (1771–1862), two scientists from Dijon who had studied at l'École Polytechnique when Bernard was there. Unfortunately, they were slow in their analysis of the new substance and did not report it to the Académie for 18 months.

Sir Humphry Davy (1778–1829) of London embarked on a 2-year scientific tour of Europe in 1813, and because of his fame Napoléon granted him special permission to travel through France. While in Paris (October 15–December 23, 1813) Davy was given a sample of Courtois' "substance nouvelle," which he analyzed using the traveling laboratory chest he carried on all his journeys [6]. Joseph Louis Gay-Lussac (1778–1850), a member of the elite Société d'Arcueil [7b] who had formulated the law of combining volumes [7b], was motivated by this British intruder to initiate his own research. In a few weeks the two scientists had conducted detailed independent studies on this substance, which had previously been shelved for 1½ years.

In December 1813 there appeared [7] in *Annales de Chimie* (the prestigious journal of the Académie des Sciences) several back-to-back papers on "une substance nouvelle dans le Vareck" (a new substance from varec), which was called "l'iode" from the Greek word for "violet." These articles were authored by Courtois [7a], Gay-Lussac [7b], and Davy [7c] (Courtois' paper was read by Clément, since Courtois was not a member of the Académie; he was identified only as a lowly "salpêtrier from Paris" [7a]). Reflecting tensions between France and Great Britain, the (London) Royal Society delighted in noting (January 20, 1814) that [8b] "iodine was discovered about two years ago; but such is the deplorable state of scientific men in France, that no account of it was published till the arrival of our English philosopher there" [5].

One who reads these December papers of *Annales de Chimie* [7] can begin to appreciate the fascination and confusion of the chemists as they tried to comprehend this "substance nouvelle"—this was half a century before the periodic table and the concept of chemical families. Iodine was difficult to categorize: It was *very* strange because it had the physical appearance and the heavy weight of a *metal*, but it dissolved in ether [7a]. It behaved like oxygen or chlorine because it reacted with metals [7b, 7c]. In fact, because of its odor [7a], iodine was originally thought to contain chlorine [7b]. However, it was found to react with hydrogen gas to form not hydrochloric acid but a *new* acid (hydroiodic acid) [7b, 7c], proven by its reaction with lead and silver nitrate

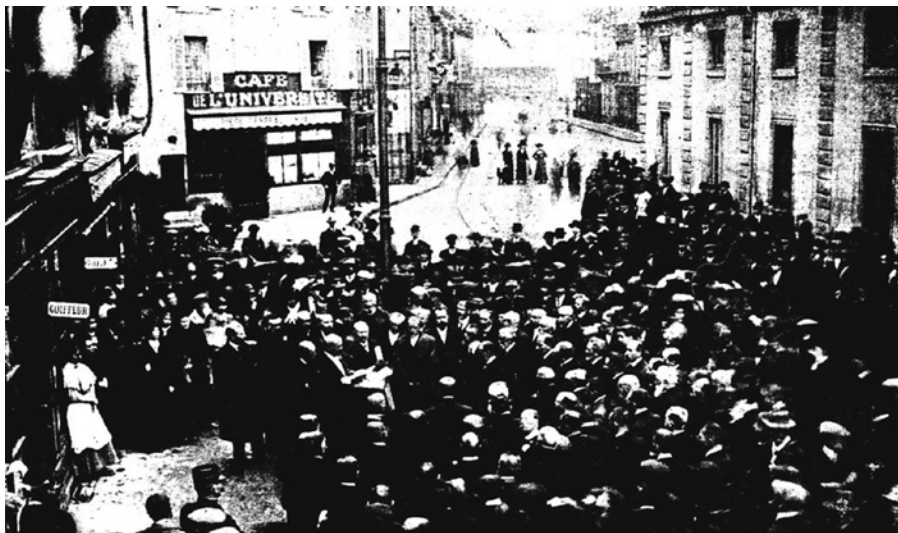


FIGURE 9.6 This photograph viewing northward on Rue Monge was taken on the 100th anniversary of the discovery of iodine (November 9, 1911) [5]. The Academy is to the right; the crowd is facing left toward the home of Courtois, where a plaque is being mounted.



FIGURE 9.7 Plaque on the Courtois home. Translation: “In this house was born on 8 February 1777 the pharmacist Bernard Courtois who discovered iodine in 1811.”

to form unknown *yellow* salts (instead of white) [7a]. Ultimately, it was decided that it must be a “corp nouveau” (a “new body”) [7c] because it could not be broken down chemically, even in the presence of red-hot carbon.

In these December papers and others that followed [8b], vigorous competition between Gay-Lussac and Davy developed into bitter contention about *who* should be credited with *what*. Duplicate claims were published, even with regard to who named the new element. Gay-Lussac said he should be credited for naming it “l’iode.” However, Davy maintained the correct name was *iodine*, in analogy to *chlorine*, which he had named in 1810 when he recognized its elemental nature [8a]. Previously, chlorine had been called “oxymuriatic acid,” believed to be a compound of HCl and oxygen [8b]. Fortunately, in spite of heated arguments about proper recognition, it was agreed that Courtois, who could easily have been lost in the shuffle, should be given credit for the initial discovery [7b, 7c].

In 1815 the Napoléonic Wars were over, and cheap Indian saltpeter became available [1]. Courtois turned his total attention to iodine and with the help of Clément and Désormes developed methods for extracting iodine from seaweed in quantity [5]. By 1820 the medicinal properties of iodine had become known and Courtois became a commercial manufacturer. In 1831 he was awarded the Montyon Prize by l’Académie for his contributions to medical science, but he never benefited financially from his discovery and died penniless [5].

On November 9, 1913, the scientific community commemorated in Dijon the 100th anniversary of the discovery of iodine by holding a banquet at the Dijon Académie and mounting a plaque on the old Rue Monge house (Figs. 9.6 and 9.7) [9]. No bust or portrait was prepared for the celebration, because no likeness of Courtois was known [9], just as for Smithson Tennant (the discoverer of osmium and iridium) [3d].²

²Careful research by French historians, including detailed interviews with descendants, has verified that no drawing, painting, or other likeness of Bernard Courtois has survived [9].

REFERENCES

- [1] Kelly J. *Gunpowder*. New York: Basic Books (Perseus Books Group); 2004.
- [2] Partington JR. *A History of Greek Fire and Gunpowder*. Baltimore: Johns Hopkins University Press; 1999.
- [3] Marshall JL, Marshall VR. Phlogiston and Lavoisier. The HEXAGON of Alpha Chi Sigma (a) 2005;96(1):4–7; (b) Carl Wilhelm Scheele. 2005;96(1):8–13; (c) The road to karlsruhe. 2006;97(4):50–55; (d) The platinum metals. 2009;100(1):8–13.
- [4] Bretcher U. Ulrich Bretscher’s Black Powder Page. Available at <http://www.musketeer.ch/blackpowder/saltpeter.html>. Accessed June 13, 2014.
- [5] Toraude LG. *Bernard Courtois et la Découverte de l’Iode*. Paris: Vigot Frères; 1921.
- [6] Swain PA. Bernard Courtois (1777-1838), famed for discovering iodine (1811) and his life in Paris from 1798. *Bull Hist Chem* 2005;30 (2):103–111.
- [7] (a) Courtois B. Découte d’une substance nouvelle dans le Vareck. *Ann Chim* 1813;88:304–310. (b) Gay-Lussac JL. Sur un nouvel acide formé avec la sustance

découverte par M. Courtois. Ann Chim 1813;88:311–318, Sur la combinaison de l'iode avec l'oxygene. Ann Chim 1813;88:319–321. (c) Davy H. Sur la nouvelle substance découverte par M. Courtois, dans le sel de Vareck. Ann Chim 1813;88:322–329.

- [8] Partington JR. *A History of Chemistry*. Volume IV. London: Macmillan; 1961.(a)p 51–57,(b)p 85–90,(c)p 636.
- [9] Guyotjeanin C. Revue d'Histoire de la Pharmacie 1995;42(2):117–123. Kindly furnished by Dr. Michel Pauty, Président de l'Académie des Sciences, Arts et Belles-Lettres de Dijon.
- [10] Guttman O. *Monumenta Pulveris Pyrii*. London: The Artists press; 1906.
- [11] Hoover HL, Hoover LH English translation of Agricola G. *De Re Metallica*. New York: Dover, 1950. London, 1912, edition.

10

PRODUCTION PROCESS IN THE PAST

TATSUO KAIHO

Nihon Tennen Gas Co., Ltd., Chiba, Japan

Iodine has been produced from seaweed in France, Ireland, Scotland, Norway, the U.S.S.R., and Japan. Seaweed was a major source of iodine for the world before 1959 and still remains a resource for this purpose in China [1].

The modern seaweed-based chemical industry started with the extraction of basic industrial chemicals such as soda (sodium carbonate), potash (a mixture of potassium salts, mostly potassium carbonate), and iodine. The soda and potash were used in making glass, pottery, and soap and for leather tanning. Potash was also important as an agricultural fertilizer. This industry developed in Normandy and Brittany in the late seventeenth century. Kelp production spread during the eighteenth century from Normandy and Brittany to the Channel Islands, to the Western Isles and the Orkneys of Scotland, to Ireland, Norway, and Sweden [2].

The seaweeds were dried on dunes and burned in pits or kilns to produce the ash called kelp. Seaweed kilns are trenches dug in the ground, between 5 and 10 m long and completely lined with flat stones, fixed together with clay. There are still plenty of seaweed kilns to be seen today along the coast of Roscoff, Pouldreuzic, and Plozévet in France (Fig. 10.1).

The seaweed is burnt in stone kilns, with care being taken to avoid reaching too high a temperature for if the ash is allowed to fuse, much iodine would be lost by volatilization. The product obtained after burning is known either as kelp or as varec. The kelp obtained by any of these methods is then lixiviated with water, which extracts the soluble salts, and the liquid is concentrated, when the less soluble salts, which are chiefly alkaline chlorides, sulfates, and carbonates, crystallize out and can be removed (Table 10.1). Sulfuric acid is now added to the liquid, and any alkaline



FIGURE 10.1 Remains of a seaweed kiln on the coast in Brittany.

TABLE 10.1 Major product yield from destructive distillation of *macrocystis*

Characteristics	Percentage	Characteristics	Percentage
Wet weight	100	Tar	2.1
Dry weight	12	Potash salts	3.0
Gas	2.3	Charcoal	1.2
Ammonia	3.3	Iodine	0.01

sulfides and sulfites present are decomposed, while iodides and bromides are converted into sulfates, and hydroiodic and hydrobromic acids are liberated and remain dissolved in the solution. The liquid is run into the iodine and gently warmed, with manganese dioxide in small quantities being added from time to time, when the iodine distills over and is collected (Fig. 10.2). Commercial iodine may be purified by mixing it with a little potassium iodide and then subliming the mixture; this removes any traces of bromine or chlorine [3, 4].



FIGURE 10.2 The monument of iodine discovery and buildings of the old iodine factory in Poulconq.

TABLE 10.2 Process of iodine production in the past

Method	Method	Reaction	References
Ash	Kelp burning	$2\text{NaI} + 3\text{H}_2\text{SO}_4 + \text{MnO}_2 \rightarrow \text{I}_2 + 2\text{NaHSO}_4 + \text{MnSO}_4 + 2\text{H}_2\text{O}$	
Precipitation	Copper	$2\text{NaI} + \text{Cl}_2 \rightarrow 2\text{NaCl} + \text{I}_2$ $2\text{NaI} + 2\text{CuSO}_4 + 2\text{FeSO}_4 \rightarrow 2\text{CuI} + \text{Na}_2\text{SO}_4 + \text{Fe}_2(\text{SO}_4)_3$	[6, 7]
	Silver	$2\text{CuI} + \text{O}_2 \rightarrow 2\text{CuO} + \text{I}_2$ $\text{NaI} + \text{AgNO}_3 \rightarrow \text{AgI} + \text{NaNO}_3$ $2\text{AgI} + \text{Fe} \rightarrow \text{FeI}_2 + 2\text{Ag}$	[5]
Adsorption	Activated C	$2\text{FeI}_2 + 3\text{Cl}_2 \rightarrow 2\text{FeCl}_2 + 2\text{I}_2$ $2\text{NaI} + 2\text{NaNO}_2 + 2\text{H}_2\text{SO}_4 \rightarrow \text{I}_2 + 2\text{NO} + 2\text{H}_2\text{O} + 2\text{Na}_2\text{SO}_4$	[8]
	Starch	$2\text{NaI} + \text{NaClO} + \text{H}_2\text{SO}_4 \rightarrow \text{I}_2 + \text{NaCl} + \text{Na}_2\text{SO}_4 + \text{H}_2\text{O}$	[9]

While iodine production at present mainly employs two processes—the air-blowout method and the ion-exchange resin method [1]—four other iodine recovery processes were used in the past, as shown in Table 10.2. Generally, they can be divided into two categories, viz. the precipitation method and the adsorption method.

In the first process, impurities, such as clay, sand, and oil, are removed by filtration from brine, and the solution is passed through a stream of sulfur dioxide and then through a number of containers holding bundles of copper wire. Passing the solution over bales of copper wire precipitates insoluble cuprous iodides. At intervals, the bales are agitated with water to separate the adhering iodide; the bales are then recycled. The cuprous iodide suspended in the water is filtered, dried, finely

ground, and sold. Iodine can be obtained from crude cuprous iodide by oxidation and sublimation.

In the second process, silver iodide is precipitated by the addition of a silver nitrate solution. The silver iodide is filtered and treated with scrap iron to form metallic silver and a solution of ferrous iodide. The silver is redissolved in nitric acid and recycled, and the solution is treated with chlorine to liberate the iodine.

The third process uses active carbon or charcoal on brines that have been acidified to pH 2 by sulfuric acid and then oxidized by sodium nitrite to liberate iodine. The brine solution, containing the free iodine, is treated directly with active charcoal. The iodine-saturated charcoal is then separated and washed. Iodine absorbed on active charcoal is recovered by the elution of sodium hydroxide or sodium carbonate. The combined eluents are acidified with sulfuric acid and then oxidized with sodium nitrite to form iodine precipitate. The treated charcoal is washed free from salts and may then be reused for adsorbing a further quantity of iodine.

The fourth process uses starch on brines that have been acidified to pH 2 by sulfuric acid and then oxidized by sodium nitrite to liberate iodine. The liberated iodine is treated with starch, which forms the well-known inclusion complex with iodine. When the starch is saturated with iodine, the iodine starch complex is separated in a centrifuge. Iodine is elutriated from starch with water followed by sodium bisulfite. The regenerated starch is returned to the absorption process. The iodine-rich elutriant is acidified and oxidized to precipitate iodine. The crude iodine is then separated in a centrifuge and purified with hot sulfuric acid or refined by sublimation.

The history of iodine production is summarized in Figs. 10.3 and 10.4.

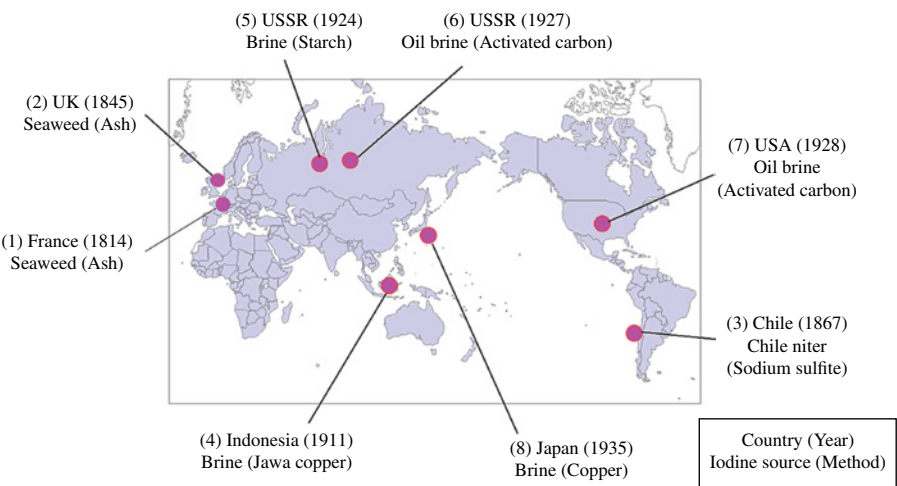


FIGURE 10.3 History of iodine production (1).

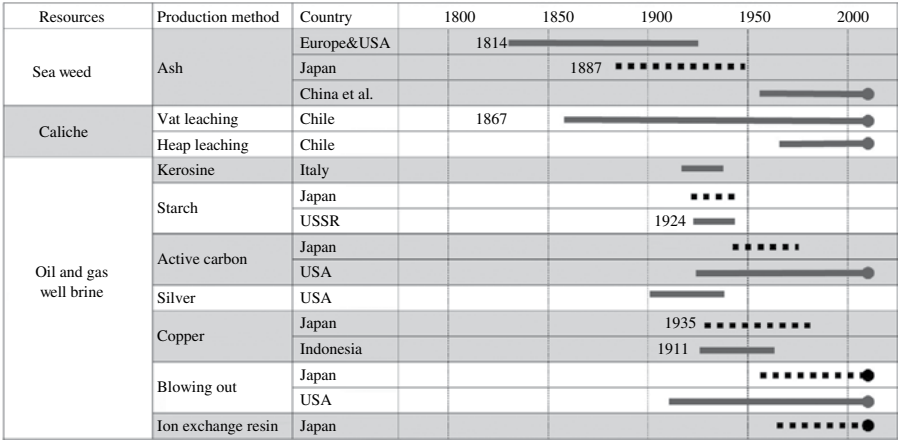


FIGURE 10.4 History of iodine production (2).

REFERENCES

[1] Lyday PA. *Iodine and Iodine Compounds*, Ullmann's Encyclopedia of Industrial Chemistry, Wiley-VCH, Weinheim; 2005.

[2] Lobban CS, Wynne MJ. *The Biology of Seaweeds*, University of California Press, Berkeley; 1982.

[3] Chapman VJ. *The Algae*, Macmillan, London; 1962.

[4] Holmyard EJ. *Elementary Chemistry*, 3rd edn, Arnold, London; 1937.

[5] (a) Kirk RE, Othmer DF. *Iodine and Iodine Compounds*, Kirk-Othmer Encyclopedia of Chemical Technology, vol. 13, 3rd edn, Wiley, New York; 1981. pp. 655–656. (b) Robertson GR. Ind Eng Chem 1934; 26(4): 376.

[6] Mellor JW. *Comprehensive Treatise on Inorganic and Theoretical Chemistry Supplement, II*, Longmans, Green, London; 1922. p. 822.

[7] Schantl E. An interesting occurrence of iodine. Chem Ztg, 56, 341–342.

[8] Manning PDV. Chem Met Eng 1934; 4: 568.

[9] Ishikawa T. Nippon Kagaku Zasshi 1942; 63: 164.

11

IODINE PRODUCTION FROM CALICHE

ARMIN LAUTERBACH

SQM, Santiago, Chile

11.1 INTRODUCTION

11.1.1 Occurrence of Iodine in Nature

No less than 99.6% of the earth's mass can be accounted for by 32 of the chemical elements [1]. The remaining of 0.4% is apportioned among 64 elements, all of which are present as traces. Iodine is one of these 64. Estimates of abundance of constituent elements in the lithosphere place iodine 46th on a restricted list of 59 elements (37 very rare elements are excluded) and 61st on a list in which 96 elements are included. Iodine is, indeed, one of the scarcest of nonmetallic elements in the total composition of the earth. Whenever and wherever it occurs, the quantities of iodine are generally exceedingly small and require very sophisticated chemical methods to detect them. Only a few substances characteristically contain iodine in relatively large quantities. These are seaweeds, sponges, and corals; the underground waters from certain deep oil-well and gas-well boring and mineral springs, and, the most impressive of all, the vast natural deposits of sodium nitrate ("caliche" ore) found in the northern part of Chile. Even in these, however, the proportion of iodine is small, rarely exceeding 1 part in 500.

11.1.2 Mineral Deposits

The mineral lautarite, $(\text{Ca}(\text{IO}_3)_2)$, and dietzeite, $(\text{Ca}(\text{IO}_3)_2\text{CaCrO}_4)$, are the two crystalline forms in which iodine naturally occurs in "caliche," the natural salt-peter

Chilean mineral. The only iodine obtained from minerals has been a by-product of the processing of nitrate ore in Chile. “Caliche” is the name for nitrate deposits occurring in the Atacama Desert, of Northern Chile and west of the Andes Mountains. The Atacama Desert is known as the driest of the world’s deserts, where measurable rainfall (1 mm or more) may be as infrequent as once every 5–29 years. Associated with the caliche deposits, with an area averaging 700 km in the north–south direction, by 30 km in an east–west direction, it can be estimated that the iodine reserves may total over 5 million tons. Features of the deposits that appear to defy rational explanation are the abundance of nitrate minerals, which are scarce in other saline complexes, and the presence of the other, less abundant minerals containing perchlorate, iodate, chromate, and dichromate, which do not exist in any other saline complexes. The first iodine recovery from caliche was in 1852, but the first iodine was exported to Europe in 1868, becoming the most important by-product of nitrate production in terms of value. Figure 11.1 shows a map indicating the location zone for caliche deposits in the Atacama Desert. The photographs of Figure 11.2 show a

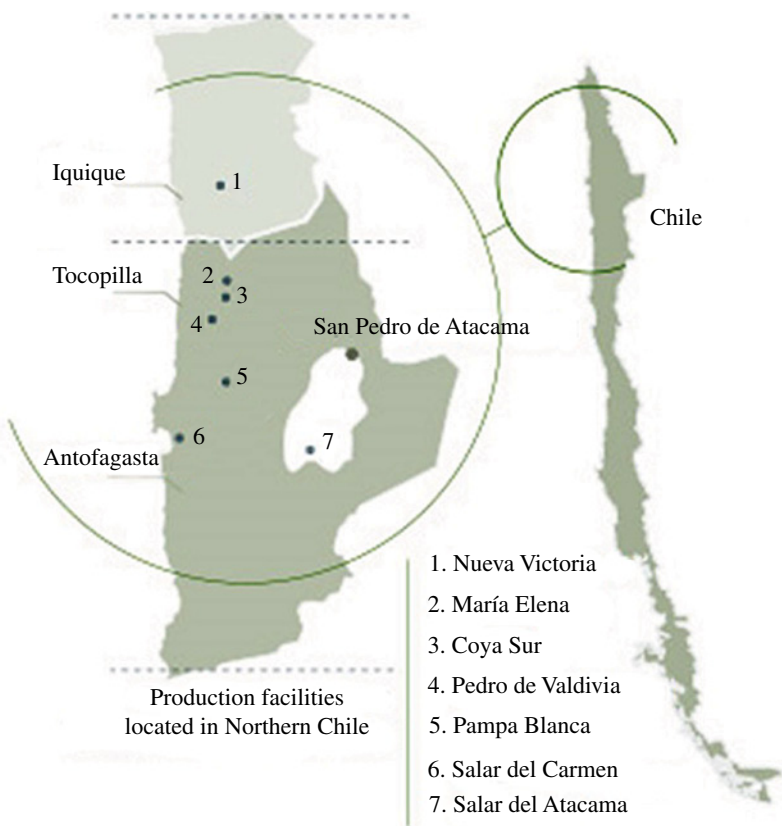


FIGURE 11.1 Location of iodine deposit.

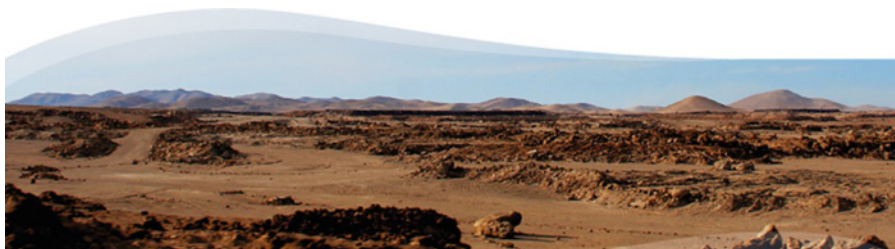


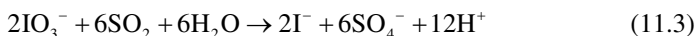
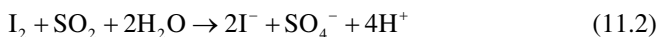
FIGURE 11.2 Atacama Desert. (*See insert for color representation of the figure.*)

typical scenery of the desert. Charles Darwin, who visited the Chilean nitrate deposits in 1835, speculated that they were formed at the margin of inland extension of the sea. Since that time many theories have been proposed about its origin. Although it is speculation, there are claims that the widespread saline materials of the Atacama Desert came from distant lands and, more probably, from local sources such as the nearby Pacific Ocean and the volcanic activity in the nearby Andean Highland during the late tertiary and quaternary period. The sources of exotic constituents—nitrates, iodate, perchlorate, and chromate—are less well-understood. Iodine is chiefly of oceanic origin, as iodine-rich organic material ejected in bubble spray and as gaseous iodine formed by photochemical oxidation of iodide at the ocean surface; iodine is formed by photochemical reactions in the troposphere at the ground level in the nitrate fields.

11.2 PRODUCTION TECHNOLOGY

11.2.1 Specific Characteristics of the Chilean Technology

In Chile, iodine is recovered from solutions containing iodate; therefore recovery is based on the reduction of iodate. Because of cost considerations the most convenient reducing agent has been SO_2 obtained by sulfur combustion. The process is based on the following reactions:



As, normally, the iodate concentration, expressed as I° , is greater than its solubility, reaction (11.1) would produce not only dissolved but also crystallized iodine inside the SO_2 absorption tower, and the inert gas left over after SO_2 absorption would

partially blow out some of the forming iodine. Therefore, the reaction inside the tower needs to be continued until the iodate is transformed completely into iodide, according to reaction (11.3), which corresponds to reaction (11.1) plus reaction (11.2). The process is normally carried out transforming into iodide 5/6 of the iodate inside the tower, and reacting the remaining 1/6 iodate with the 5/6 iodide exiting the tower according to reaction (11.4). As a result, elemental iodine is obtained, of which up to 0.4 g l^{-1} remains as solution and the excess crystallizes. Consequently, iodine is obtained indirectly according to reaction (11.1).

11.3 OBTAINING IODATE SOLUTIONS

Iodate solutions are obtained basically by three processes: heap leaching of caliche with low nitrate (<5%) and iodine content (over 500 ppm), heap leaching of high nitrate and high iodine content, and vat leaching.

11.3.1 Heap Leaching of Low Nitrate Grade Caliche

This process is shown in Figure 11.3, where it can be seen that the caliche heaps are leached in parallel. Fresh water is added for compensating the water in the purge and the evaporation losses. A purge, not shown, is required for avoiding an excessive increase in dissolved salts, which would harm the process, mainly because of unwanted crystallization of salts contained in the caliche, as sulfates, chlorides, and nitrates. The product of this process is a concentrated iodide solution of about 100 g l^{-1} , consisting basically of a mixture of iodic and sulfuric acid.

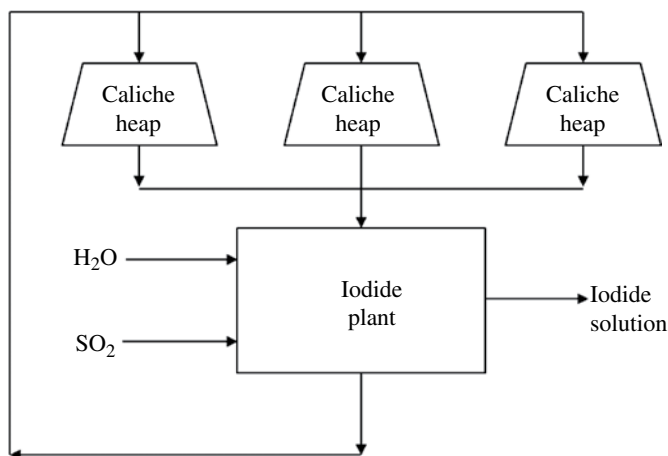


FIGURE 11.3 Heap leaching for iodine obtainment only.

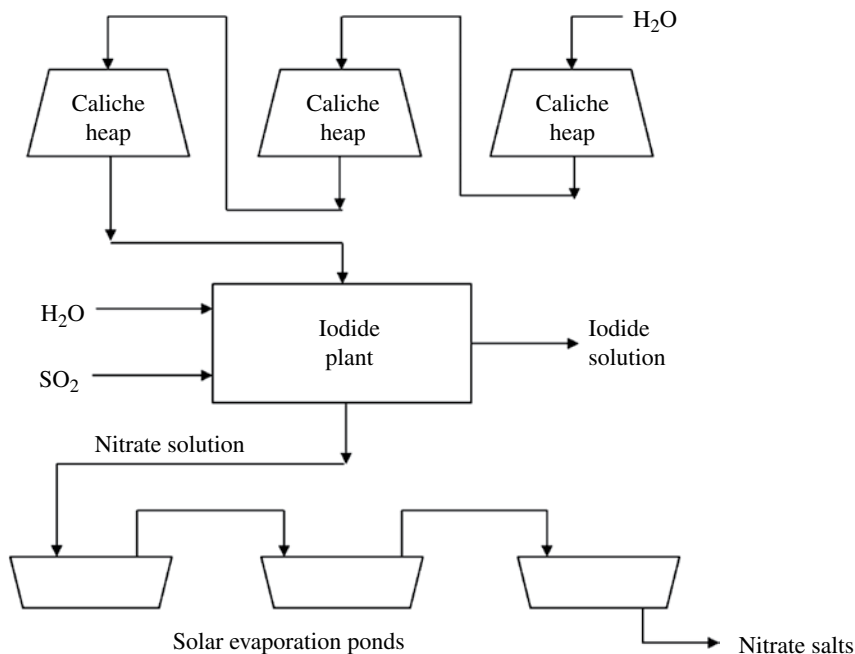


FIGURE 11.4 Heap leaching for obtaining iodine and sodium nitrate only.

11.3.2 Heap Leaching of High Nitrate, High Iodine Grade Caliche

As seen from Figure 11.4, in this case the heaps are arranged in series in order to increase the nitrate concentration, and consequently also the iodine concentration. Nitrate concentration needs to be as high as possible to minimize the solar evaporation pond surface requirements. Iodine concentration, on the other hand, reaches a value of about 1 g l^{-1} , which is a concentration exceeding in 0.6 g l^{-1} its saturation.

11.3.3 Vat Leaching

This process has been the traditional leaching process and is presently used only by SQM. The other Chilean iodine producers use only heap leaching. Vat leaching is explained in Figure 11.5. The vat solution is first submitted to a temperature drop to crystallize sodium nitrate. The mother liquor is then submitted to an iodine extraction process similar to that for heap leaching, but the end product is prilled or flaked iodine. Also, this plant uses the concentrated iodide solutions obtained from the heap leaching processes, which are oxidized to iodine by means of iodate contained in the mother liquor.

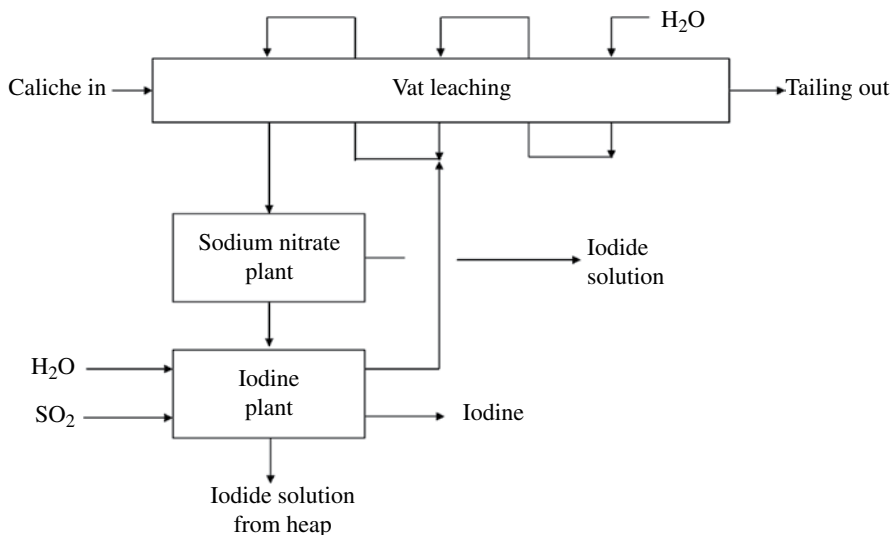


FIGURE 11.5 Vat leaching for sodium nitrate and iodine production.

11.4 DESCRIPTION OF THE IODINE EXTRACTION PROCESS

SQM is presently using two processes for iodine extraction from iodate-containing solutions: one treating heap leach solutions, similar to the process employed by other Chilean companies, and the other treating the mother liquor from the vats. The first process produces only concentrated iodide solutions, and the second obtains not only concentrated iodide but also the final product as prilled or flaked iodine.

11.4.1 Heap Leach Solutions

The process for treating heap leach solutions is described in Figure 11.6. As can be seen, the brine containing iodate is divided into two streams, with 5/6 passing through the SO₂ absorption tower and the remaining 1/6 reacting with the outgoing iodide. The obtained iodine, which may be in solution form or partially crystallized, is then submitted to a kerosene extraction process and afterward reduced to iodide with SO₂. If the concentration of iodine does not exceed its solubility, blowout instead of kerosene can be used, as other Chilean and all foreign Japanese and U.S. companies do.

The SO₂ flow operates in series: first 1/6 of the SO₂ is used for reducing the iodine of the kerosene to iodide, and the remaining 5/6 is injected in the absorption tower, where iodate is reduced to iodide.

11.4.2 Vat Solutions

Figure 11.7 shows this alternative. Here the mother liquor from the sodium nitrate crystallization plant, containing about 1.5 g l⁻¹ iodine as iodate, is decanted for

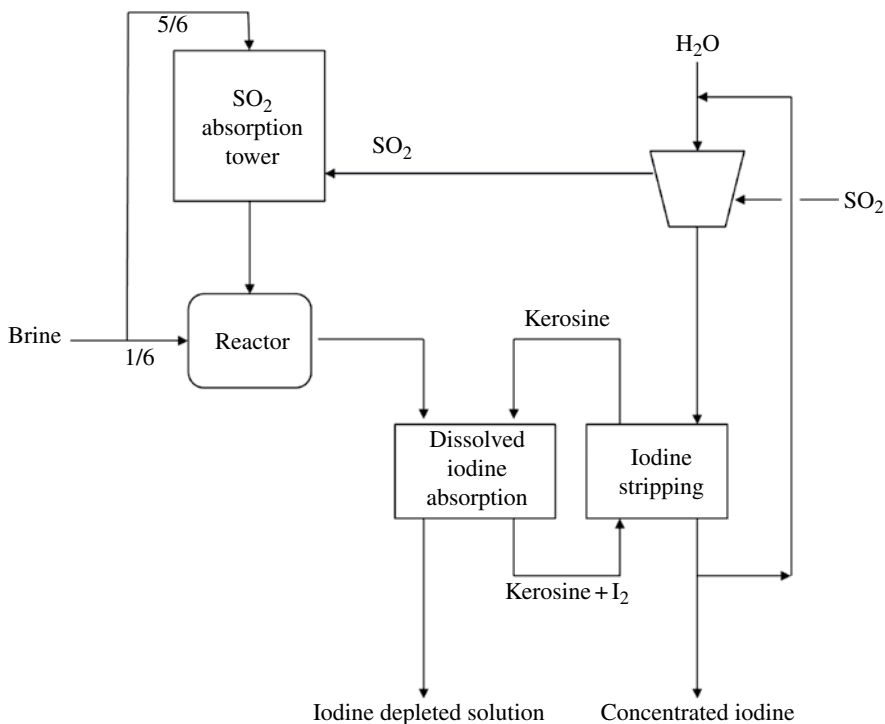


FIGURE 11.6 Treating of heap leach solutions.

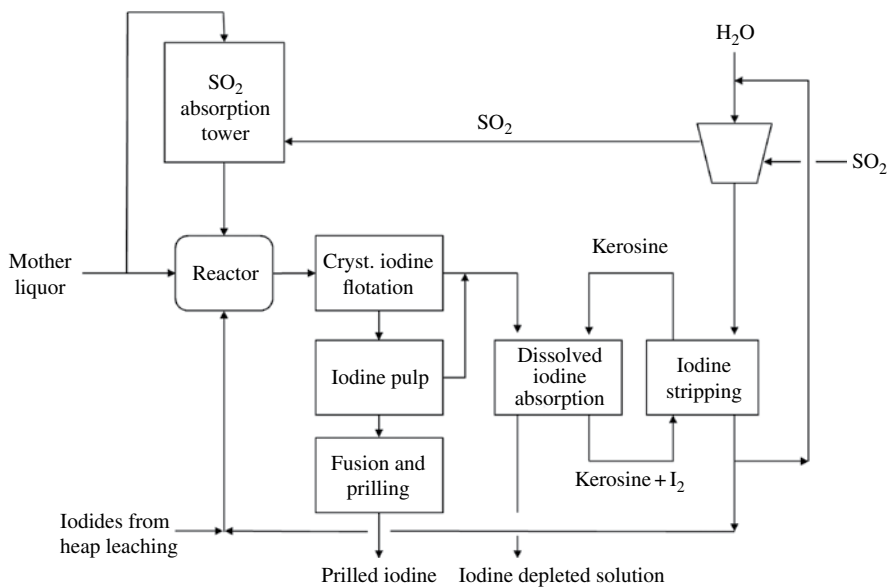


FIGURE 11.7 Treating of vat solution.

clarification and concentration homogenization. From there the solution is split. The larger fraction is fed into an absorption tower where it is contacted with SO_2 , obtained by sulfur combustion. In the absorption tower, iodate is reduced all the way to iodide. After leaving the absorption tower, the resulting iodide solution, together with the iodide solution coming from the kerosene extraction plant, and the iodide solution from different heap leaching plants are contacted with the smaller iodate fraction in the stoichiometric proportion of 5 mol iodide to 1 mole iodate, producing iodine.

Up to 0.4 g l^{-1} of the iodine stays in solution and the rest precipitates as crystallized iodine, which is removed by notation. This operation does not require a flotation agent due to the hydrophobic character of the crystallized element. From the notation cell a heavy pulp is obtained, which is introduced into a heat exchanger where it is heated under pressure up to 120°C , to melt the iodine that flows into the first reactor for settling. From there the melt flows into a second reactor for sulfuric acid drying and refining. The refined iodine is either naked or prilled and packed in 50 and 25-kg plastic-lined fiber drums.

The solution leaving the notation cell, containing about 0.4 g l^{-1} iodine, is sent to a kerosene solvent extraction process, or alternatively to a blowing-out process, to recover the dissolved product. After neutralization with soda ash to the initial incoming alkalinity, the solution is returned to the nitrate caliche leaching process. The iodine-charged kerosene is contacted with an acidic concentrated iodide solution containing SO_2 , which reduces the iodine to iodide. Chilean companies using blowout also obtain a concentrated iodide solution, which is submitted to hydrogen peroxide oxidation to obtain elemental iodine. The flaked product is obtained in the manner already described.

Until 1990, some flaked iodine and iodine-containing wastes were sublimed to obtain an especially high-grade product. This process was dropped from the current industrial processes in view of the quality improvements reached in current operations. Sublimed iodine is produced only in small quantities by specialized companies that offer this product for special minor applications requiring the highest purity.

REFERENCE

- [1] Lauterbach A, Uber G. *Iodine and Iodine Compounds*, *Kirk-Othmer Encyclopedia of Chemical Technology*. New York: John Wiley & Sons, Inc.; 2011. p 1–28.

12

IODINE PRODUCTION FROM OILFIELD BRINE

STANLEY T. KRUKOWSKI

Oklahoma Geological Survey, Mewbourne College of Earth and Energy, The University of Oklahoma, Norman, OK, USA

12.1 IODINE PRODUCTION IN THE UNITED STATES

12.1.1 Historical Background

The first iodine production in the United States occurred between 1917 and 1921. It was harvested from seaweed in California. After the seaweed was distilled to produce acetic acid, the residues were processed for potash fertilizers and iodine [1]. Between 1928 and 1932, the first commercial production of iodine in the United States was from brines in the state of Louisiana. A number of Louisiana oilfield brines had concentrations of about 35 ppm iodine [1]. Oilfield brines in parts of California contain 30–70 ppm iodine (Fig. 12.1) in the Monterey Formation (Miocene) and Repetto Formation (Pliocene); these were produced at various times between 1928 and 1966. In Michigan, natural brines containing 15–30 ppm iodine are present in the Sylvania Formation (Devonian) at a depth of about 1300 m. The Michigan brines were processed mainly for bromine, and the by-product iodine, by the Dow Chemical Company until the wells were plugged and abandoned in 1987.

All iodine production in the United States today comes from iodine-rich (300 ppm iodine) natural brines on the northern flank of the Anadarko Basin in northwestern Oklahoma (Fig. 12.2). Oklahoma iodine production began in 1977. At present three companies operate two major plants and one miniplant for the recovery of iodine.

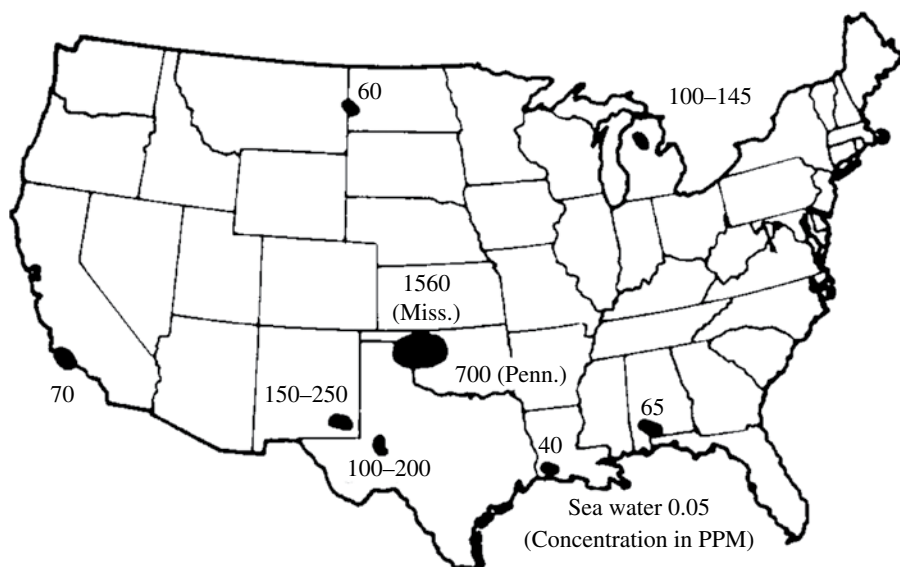


FIGURE 12.1 Areas of known iodine concentrations in the United States [2]. Exceptionally high iodine concentrations in northwest Oklahoma are in Mississippian (Miss.) and Pennsylvanian (Penn.) strata.

Total production last reported by the U.S. Geological Survey was in 2005, when the United States produced 1570 tonnes [4]. Oklahoma's first iodine operation was the Woodward Iodine Corporation. It opened early in 1977 as a joint venture between Amoco Production Company and Houston Chemicals, a subsidiary of Pittsburg Plate Glass Industries [2]. Asahi Glass Company of Japan purchased the company in 1984 [1], and then sold it in 1994 to Ise Chemical Industries Company Ltd. of Japan [5, 6]. Today, MIC Specialty Chemicals (a subsidiary of Mitsubishi International) exclusively distributes the iodine produced by Woodward [7]. Woodward Iodine Corporation operates 12 production wells in the Woodward Trench, just north of Woodward, and injects the waste brine back into the trench through four injection wells; three additional wells are operated as disposal wells. Brine production wells and injection wells are 2130–2290 m deep at Woodward.

A second iodine plant located near Vici in Oklahoma was started in late 1987 by IOCHEM Corporation of Japan. It is a subsidiary company of Toyota Tsusho America, Inc. A long-term contract with Schering AG of Germany today accounts for the majority of IOCHEM's production. IOCHEM also extracts iodine-rich brines in a southern extension of the Woodward Trench, operating nine production wells and four injection wells at depths of 3000–3183 m.

North American Brine Resources (NABR) operates the remaining iodine installation in Oklahoma at a miniplant near Dover, where oilfield brines, collected from many producing oil and gas wells of northwestern Oklahoma, are processed. The company also had a major operation in the Woodward Trench about 35 km north of Woodward, which included two production wells and three injection wells, about

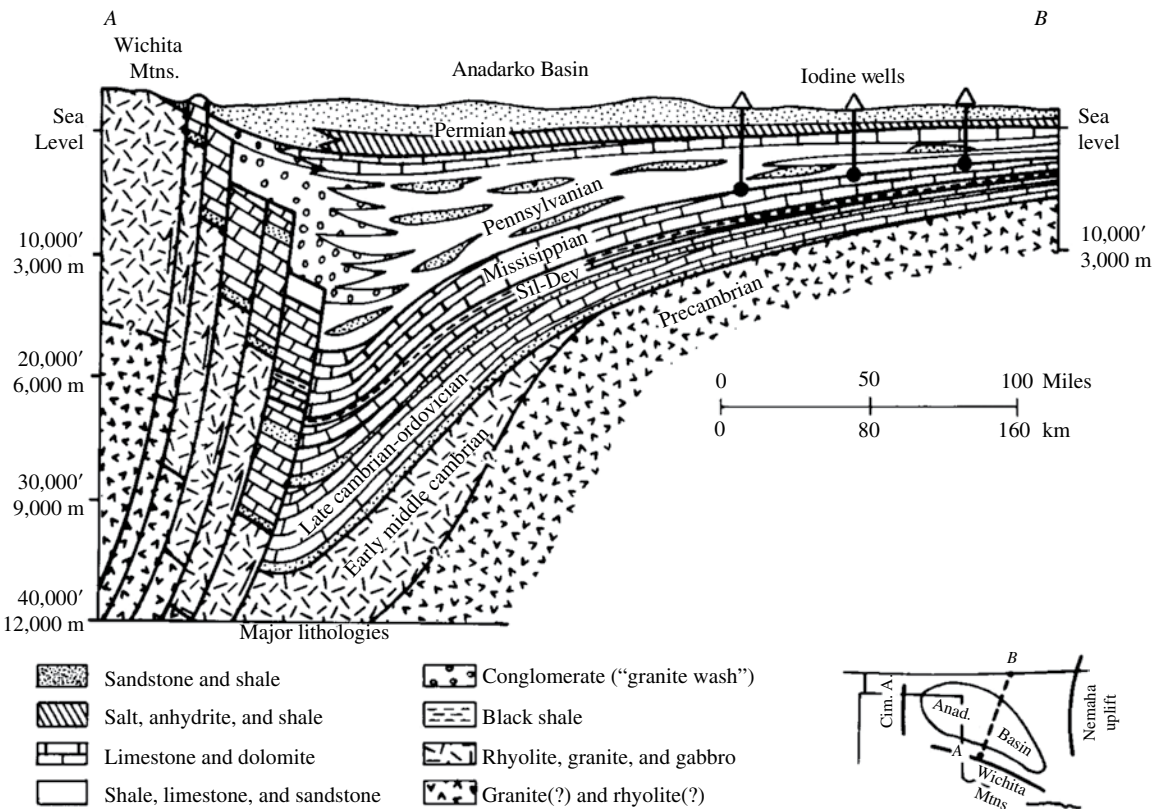


FIGURE 12.2 Generalized north-south structural cross section through the Anadarko Basin of western Oklahoma (modified from Johnson [3]). Iodine-rich brines are produced from basal Pennsylvanian sandstones on the northern flank of the basin.

1800 m deep; this facility began operations in 1989 and was recently dismantled [8]. NABR began operations in 1989 as a joint venture of Beard Oil Company (40% share) and two Japanese firms (Godoe USA, Inc., 50% share, and Inorgchem Development, Inc., 10% share) [9]. In 2003 NABR, as a joint venture between Mitsui & Company of Japan and the Beard Oil Company, was sold to a group of U.S. private investors and is now operated as a limited liability company [10].

Iofina, Inc., a newcomer to the North American iodine industry, is involved in exploring and producing both iodine and natural gas in Montana. The company has signed five third-party Iodine Extraction and Collection Agreements with two operators in California and one each in Oklahoma, Texas, and Wyoming since 2011. The Oklahoma plant, known as IO#2, began producing iodine in the fourth quarter of 2012.

12.1.2 Oilfield Brine Production

About 45% of the iodine currently consumed in the world comes from brines processed in Japan, the United States, the Commonwealth of Independent States (CIS; the former Soviet Union), and Indonesia [11]. The remainder (55%) is produced from desert evaporite deposits in Chile. These figures fluctuated a bit over the past few years, but remain relatively the same. In Japan, iodine is produced from brines associated with natural gas wells. The iodine content of Japanese subterranean brines ranges up to 150–160 ppm. Iodine production in the United States comes from deep-well brines associated with petroleum and natural gas fields. Iodine content in older iodine-producing rock formations (Mississippian–Pennsylvanian) in Oklahoma may range up to 1500 ppm, but typically the iodine content of produced brines is about 300 ppm. In the CIS, iodine production is associated with oil recovery mainly in Turkmenistan, Azerbaijan, and Russia, accounting for 97% of CIS's total production [11, 12]. Uzbekistan also produces minor amounts of iodine.

Iodine, with trace amounts of bromine, is also present in oilfield brines in Indonesia. These occur in Pliocene sandstones and diatomaceous marls in the Gujangan Anticline [13]; however, Indonesian iodine typically comes from brines not associated with oil and gas deposits [11].

12.1.3 Iodine Production in Oklahoma

All iodine production in the United States now comes from iodine-rich (300 ppm iodine) natural brines in the deep subsurface of the Anadarko Basin of northwestern Oklahoma (Fig. 12.2). Oklahoma's first iodine operation started operations early in 1977. After the discovery of the iodine-rich brines at Woodward, Oklahoma, a 12-year program was launched that analyzed brine samples collected by the Amoco Production Company [2]. Amoco noted the unusually high concentrations of iodine in the Woodward area; concentrations ran as high as 1560 ppm in Chesterian (Mississippian) limestones and 700 ppm in Morrowan (basal Pennsylvanian) sandstones. Morrowan sandstones in the area are as much as 100 m thick and are preserved as channel sands in a south-trending paleovalley (the Woodward Trench) that cuts into the Chesterian land surface (Fig. 12.3). Although iodine concentrations are

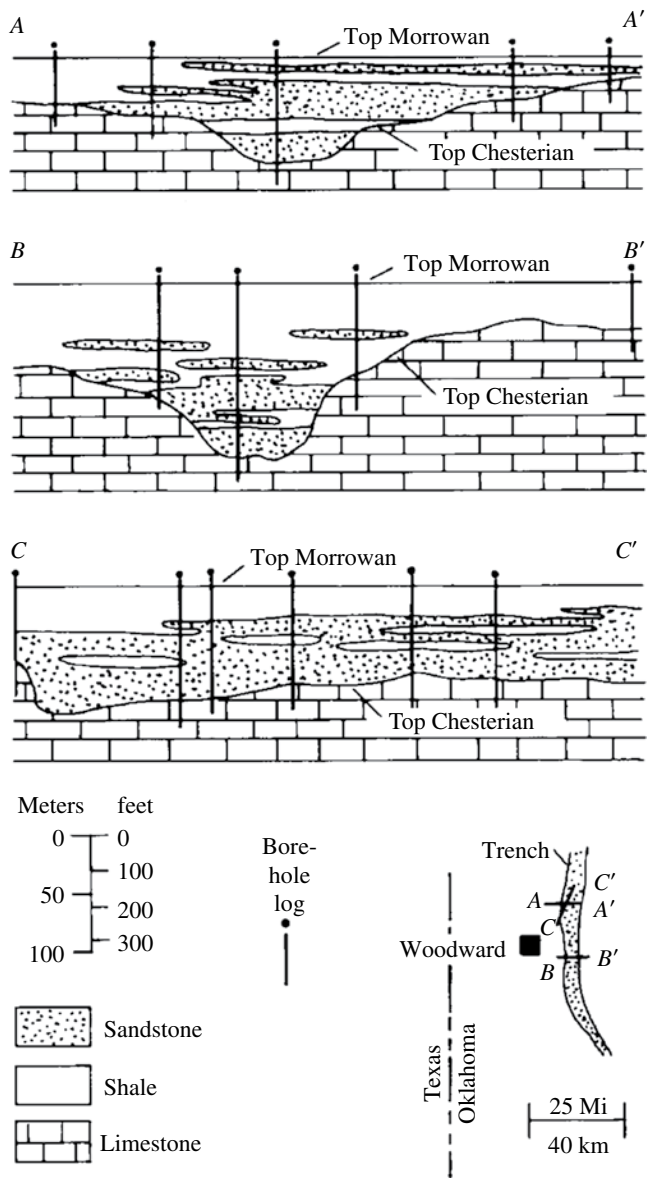


FIGURE 12.3 Cross sections showing iodine-bearing Morrowan channel sandstones preserved in the Woodward Trench that has been cut into Chesterian limestones (modified from Cotton [2] and Johnson [3]). Datum is top of Morrowan strata. Length of A–A' and B–B' is about 10km; length of C–C' is about 15km.

higher in Chesterian strata, the Chesterian limestones have low permeability and do not yield large volumes of water. Alternatively, the Morrowan sandstones in the trench have higher porosity (~14%) and higher permeability (about 20–40 md), yielding large volumes of brine that average about 300 ppm iodine. Production wells yield 5000–10,000 barrels (200,000–400,000 gal) of brine per day [6].

The Woodward Trench has an average width of 1.6 km; its known length is about 115 km [2]. Brine production wells and injection wells are 2130–2290 m deep toward the northern end of the Woodward Trench. In a southern extension of the Woodward Trench near Vici, Oklahoma, extraction of iodine-rich brines from Morrowan sandstones occurs at depths of 3000–3183 m. A miniplant near Dover, Oklahoma, serves as an oilfield brine injection/disposal site, collecting waste oilfield brines from a number of oil and gas producing wells in nearby parts of northwestern Oklahoma. Johnson and Gerber [6] reported that these oilfield brines contain concentrations of iodine in the range of 100–1000 ppm. The oilfield brines are processed in the miniplant, where iodine is extracted before the brines are injected into wells at the site for disposal.

The origin of iodine-rich brines associated with sediments of the northern flank of the Anadarko Basin has provided a challenge for oilfield scientists for many years. The high concentration of iodine in the Chester limestone (Mississippian) led to speculation that its source was limestone. Moran's [14] work with iodine isotope ratios indicated that the organic-rich Woodford Shale (Upper Devonian–Lower Mississippian) was the probable source rock for the high concentrations of iodine. The iodine-rich brines probably migrated from the Woodford Shale into several brine reservoirs in northwestern Oklahoma [6].

12.1.4 Technology

12.1.4.1 Exploration Techniques

Iodine production has historically been a by-product of either oil and natural gas production or nitrate fertilizer processing. Cotten [2] and Johnson and Gerber [6] describe how the Amoco Production Company approached the prospect of producing iodine from brines associated with oil and natural gas exploration drill holes in the Woodward Trench of northwest Oklahoma. Reports on the chemistry of subsurface water samples from these exploratory wells showed that a variety of potentially economic minerals were present. Feasibility studies indicated that iodine was the most favorable mineral for development, based on the fact that its concentrations were relatively high, and that the United States was almost entirely dependent on foreign imports for its supplies.

Scientists at the Amoco Research Center determined that 60,000 barrels per day of 300 ppm iodine-rich brine had to be produced over a 10-year period to be an economically viable project. Additional holes on 640-acre centers were drilled into the Morrow Formation (Pennsylvanian) in the trench, and their electric logs examined to determine the thickness of water-bearing sands with porosities greater than 10%. These criteria helped determine the concentration (grade) of iodine and the amount (reserves) of resources present. A joint venture by Pittsburgh Plate Glass Industries and Amoco Production Company brought the necessary expertise together to form

the Woodward Iodine Corporation. In 1977 Woodward Iodine began producing iodine from the Morrow subterranean brines.

Iodine geochemical data obtained from surface soil samples is used as an exploration tool in the petroleum industry [15–18]. Positive anomalies of trace iodine geochemistry have been used as an indirect indicator of hydrocarbon accumulation in the subsurface. Perhaps future study of this phenomenon will lead to exploration techniques in the search for subterranean iodine-rich brines.

12.1.4.2 Mining

Iodine produced from underground brines is pumped to the surface using electric submersible pumps and through a system of pipelines is transported to the processing facility. Natural gas either is flared off or is extracted from the brines in a gas separator in which the natural gas is physically separated from the brine. The iodine-rich brine is collected in storage tanks before entering the processing plant for iodine extraction. Corrosion-resistant pipe and storage tanks are necessary to contain fluids and vapors during transport and storage; in addition, calcium-scale inhibitors are introduced to prevent calcium carbonate-scale buildup from occurring on exposed metallic surfaces [19].

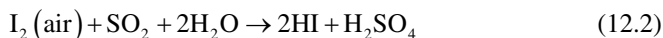
12.1.4.3 Production Process

The blowout process (also known as the air-stripping process) is the principal method for extracting iodine from brines. Initially the brine undergoes a process consisting of skimming and settling that removes impurities such as oil, clay, and other undesirable materials. Chlorine is then injected into the brine, where oxidation occurs:



The I_2 remains in solution and is extracted from the brine in a countercurrent air blowout process where free iodine is stripped from solution as it is exposed to large volumes of air [6, 11].

The iodine-depleted brine is discarded or injected into wells, returning the brine to the original underground formation; this also serves to maintain fluid pressures in the reservoir and helps prevent subsidence. The iodine-rich air leaves the stripping column and enters an absorption column where the vapor is submitted to a cocurrent desorption process. A reducing environment is maintained by adding sulfur dioxide (SO_2) and water. The iodine is reduced to iodide:



This hydriodic and sulfuric acid solution is maintained in an interim storage vessel. When chlorine gas is injected into this hydriodic acid solution, it undergoes oxidation and iodine crystallization:



Johnson and Gerber [6] identified the oxidized crystallizer liquor as a mixture of water, sulfuric acid, hydrochloric acid, and iodine crystals.

The next step separates the iodine crystals from this liquor. This is accomplished through batch filtration, followed by vacuum drying of the filter cake. Wet iodine filter cake is transferred to a fusion kettle. Sulfuric acid, coming into contact with the melted product, helps in controlling humidity (drying) and in removing impurities. The final step converts the fused iodine into a flake or prill product. These are then prepared for shipping [6, 11].

12.1.5 Regulatory and Environmental Considerations

12.1.5.1 Health and Safety

Iodine is relatively safe to handle because it is a crystalline solid at normal room temperature and pressure; it has a relatively low vapor pressure of 1 kPa at 25°C compared to other halogens (e.g., 700 kPa for chlorine). Personal protective equipment (PPE) is not necessary when handling properly packaged containers; however, chemically approved gloves, clothing, eyewear, and masks or respirators should be worn when solid iodine is not packaged properly [11].

An upper limit of 0.1 ppm iodine in air was set by the U.S. Occupational Safety and Health Administration (OSHA), because unprotected short-term exposure (up to 1 h) can be hazardous to lungs and eyes. Severe irritation to the eyes and respiratory track, which may lead to pulmonary edema, can occur when exposed to concentrations above 0.1 ppm over extended periods. Burns also may result if contact with the skin is prolonged. Chronic absorption of iodine results in iodism, a condition whose symptoms include insomnia, inflammation of eyes and nasal passages, bronchitis, tremors, diarrhea, and weight loss [11].

12.1.5.2 Land Use and Zoning

Permits for brine wells are similar for oil and natural gas wells, particularly if there is coproduction of these resources, or if injection wells are part of the iodine-extraction operation. In Oklahoma the Oklahoma Corporation Commission regulates and permits borehole drilling, maintenance, abandonment, and reclamation. Most iodine operations are located in remote areas, so industrial zoning is not a major concern. When it is necessary to abandon iodine-producing brine wells, the boreholes are plugged with concrete so that producing formations are sealed to prevent contamination of water aquifers, other rock units, and the soils where the drill pad was located.

12.1.5.3 Pollution Control and Other Environmental Considerations

In the production of iodine, special considerations for chemical reagents, such as chlorine, sulfur dioxide, ammonia, and sulfuric acid, must be taken into account and documented in risk management plans. This includes emissions from nonpoint sources (fugitive emissions), and single-point-source emissions. Fugitive emissions are those from leaking valves, corroded pipe, and others. Point-source emissions would be represented by equipment (such as natural gas compressors, boilers, and scrubbers) discharging noxious substances (usually as gases) into the environment.

The U.S. Environmental Protection Agency (EPA) requires risk communication be filed with appropriate governmental entities. The Superfund Amendments and Reauthorization Act of 1986 (SARA Title 3; also known as the Right to Know Act of 1986) sets forth guidelines for essential emergency planning for local communities. Potential chemical hazards are identified by the producer who files various risk communications annually with the local emergency committee, fire departments, the Oklahoma Department of Environmental Quality, and others. This notifies respective agencies of potential problems associated with hazardous materials used at the site.

In the United States, iodine is a federally regulated List II chemical under the Comprehensive Methamphetamine Act of 1996; so iodine producers are required to report to the U.S. Drug Enforcement Agency (DEA) and other enforcement authorities all iodine buyers and customers. Iodine is an essential ingredient in the manufacture of methamphetamines, which are commonly produced illegally (sold as “meth” or “speed”). These customs requirements call for iodine sellers to record all sales and to report detailed information about their customers. Producers maintain tight control over inventories and have increased security at warehouses and other storage facilities.

REFERENCES

- [1] Lyday PA. Crude iodine production. *Ind Miner* 1986;222:65–76.
- [2] Cotten HM. Iodine in northwestern Oklahoma, Johnson, K.S. & Russell, J.A. (editors.) *Proceedings of 13th Annual Forum on the Geology of Industrial Minerals*. Norman: Oklahoma Geological Survey Circular; 1978; Volume 79:89–94.
- [3] Johnson KS. Geologic evolution of the Anadarko Basin. In: Johnson KS, editor. *Anadarko Basin Symposium, 1988*. Volume 90, Norman: Oklahoma Geological Survey Circular; 1989. p 3–12.
- [4] Lyday PA. *Iodine, Mineral Commodity Summaries 2007*. Washington, DC: U.S. Geological Survey; 2007. p 80–81.
- [5] U.S. Geological Survey. *Iodine, Mineral Industry Surveys 1997 Annual Review*. Washington, DC: U.S. Geological Survey; 1998. p p11.
- [6] Johnson KS, Gerber WR. Iodine geology and extraction in northwestern Oklahoma. In: Johnson KS, editor. *Proceedings of the 34th Forum on the Geology of Industrial Minerals, 1998*. Volume 102, Norman: Oklahoma Geological Survey Circular; 1999. p 73–79.
- [7] Krukowski ST. Iodine. *Min Eng* 2013;65:74–78.
- [8] Krukowski ST. *Iodine*. *Min Eng* 2005;57:39–41.
- [9] Ohl JP, Arndt RH. The mineral industry of Oklahoma. *Minerals Yearbook, Volume 2, Area Reports: Domestic*. Washington, DC: U.S. Bureau of Mines; 1988. p 395–404.
- [10] Krukowski ST. Iodine. *Min Eng* 2004;56:27–28.
- [11] Lauterbach A, Ober G, Rios S, Basinger W, Shipp A. *Iodine, High Performance Chemistry*. Santiago: Sociedad Quimica y Minera de Chile S.A; 2001.
- [12] Lyday PA. *Iodine, Mineral Commodity Summaries 2004*. Washington, DC: U.S. Geological Survey; 2004. p 83–84.

- [13] Lyday PA. *Iodine, Mineral Facts and Problems, 1985 Edition*. Volume 675, Washington, DC: U.S. Department of the Interior, U.S. Bureau of Mines Bulletin; 1985. p 377–384.
- [14] Moran JE. Origin of iodine in the Anadarko Basin, Oklahoma. *Am Assoc Petrol Geol Bull* 1996;80:381–391.
- [15] Tedesco SA. *Surface Geochemistry in Petroleum Exploration*. New York: Chapman & Hill; 1994.
- [16] Tedesco SA, Goudge CK. How iodine surveys help locate southeast Colorado Morrow reservoirs. *Oil Gas J* 1994;92:86–89.
- [17] Tedesco SA, Andrew JA. Integration of seismic data, iodine geochemistry yields Lodgepole exploration model. *Oil Gas J* 1995;93:56–60.
- [18] Leaver JS, Thomasson MR. Case studies relating soil iodine geochemistry to subsequent drilling results. In: Schumacher D, LeSchack LA, editors. *Surface Exploration Case Histories: Applications of Geochemistry, Magnetism, and Remote Sensing*. Volume 11, American Association of Petroleum Geologists Studies in Geology No. 48 and Society of Exploration Geophysicists Geophysical References Series. Tulsa: American Association of Petroleum Geologists; 2002. p 41–57.
- [19] Hamon WW Jr. *Vice President, Personal Written Communication*. IOCHEM Corporation; 2002.

13

IODINE PRODUCTION FROM NATURAL GAS BRINE

NOBUYUKI KANEKO¹ AND TATSUO KAIHO²

¹*Institute for Geo-Resources and Environment, Geological Survey of Japan, AIST, Tsukuba, Ibaraki, Japan*

²*Nihon Tennen Gas Co., Ltd., Chiba, Japan*

13.1 NATURAL GAS BRINE

13.1.1 Introduction

Japan accounts for approximately 30% of global iodine production from natural gas brine. The brine found in pores of Neogene to Quaternary marine sediments is saturated to oversaturated with microbial methane. Natural gas is produced by degassing with depressurization of naturally emerging, pumped-up, or gas-lifted pore water. After the natural gas is extracted, the high concentrations of iodine in the brine in the form of I^- are refined. Japan's iodine production has remained at constant levels because the amount of water extracted for this purpose has to be maintained at constant levels to prevent land subsidence associated with pumping of water from unconsolidated formations.

Iodine production in Japan occurs at the Minami-Kanto gas field near Tokyo, the Niigata gas field, the Nakajo oil and gas field, both in Niigata Prefecture, and the Sadowara gas field in Miyazaki Prefecture (Fig. 13.1), all of which are brine-dissolved gas fields. Deep horizons of the Niigata and Nakajo fields also have structural accumulations of thermogenic hydrocarbons. Another potential gas field that is being developed is located in southern Okinawa-jima, the brine from which includes iodine at high concentrations.

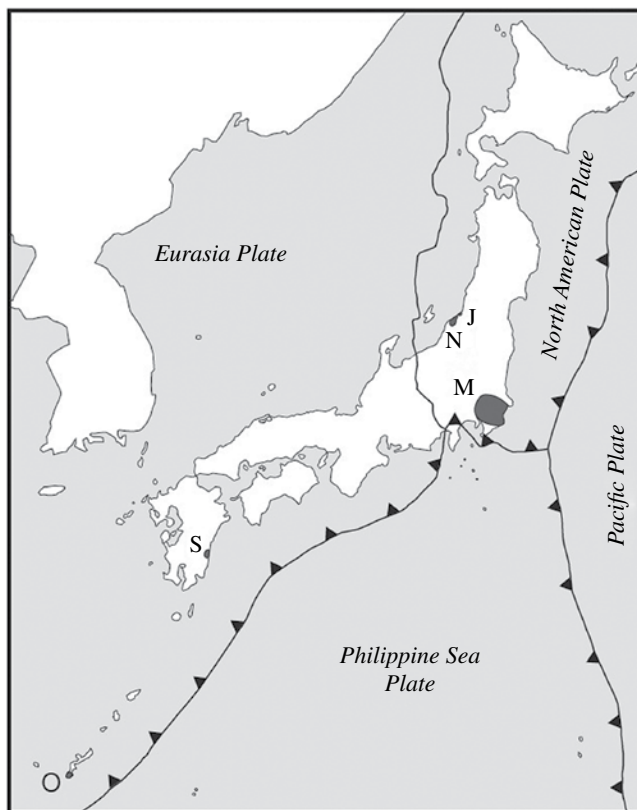


FIGURE 13.1 Active and potential iodine gas fields in Japan. M, Minami-Kanto; J, Nakajo; N, Niigata; S, Sadowara; O, Okinawa. Plate boundaries are also shown.

Unlike conventional gas deposits that accumulate in anticlines, these brine-dissolved gas deposits exist at shallow depths (<2000m) in synclinal areas of young sedimentary basins.

13.1.2 Iodine-Producing Fields in Japan

13.1.2.1 Minami-Kanto Gas Field

This field, which is located mainly in Chiba Prefecture near Tokyo, is responsible for approximately 90% of Japan's iodine production. The total volume of water that has been extracted for iodine production has been voluntarily controlled. The main reservoirs are the Pleistocene Kiwada, Otadai, and Umegase formations of the Kazusa group (Fig. 13.2), the sedimentary environment for which was bathyal marine. Turbidite sandstone is well-developed in the Otadai and Umegase formations, and the pores of the sandstone contain very high concentrations of iodine [1, 2].

The area offshore of the Kanto sedimentary basin is characterized by the juncture of the Pacific Plate, the Philippine Sea, and the North American Plates (Fig. 13.1).

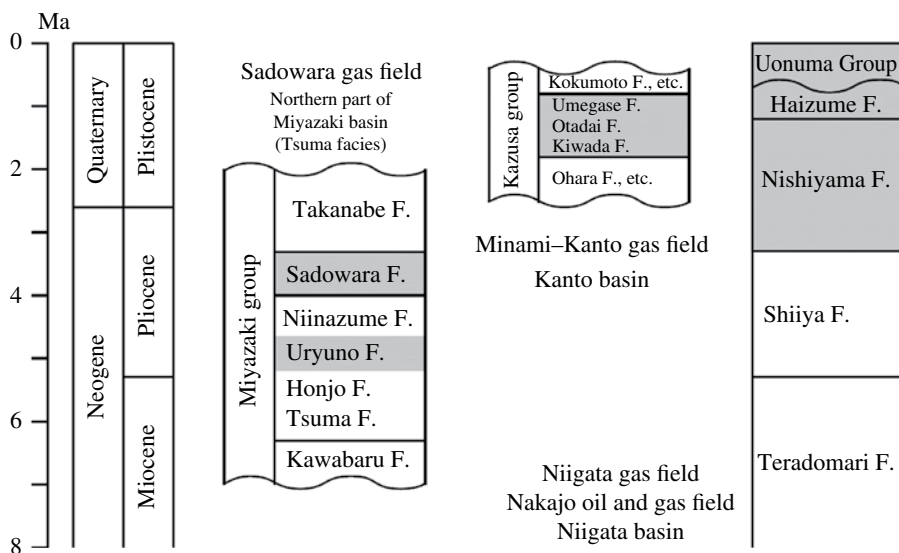


FIGURE 13.2 Geologic time and stratigraphy of iodine-producing sedimentary basins in Japan.

The Kazusa group filled a forearc basin of the subduction zone along the Sagami Trough between the Philippine Sea and the North American Plates. Overlapping of the forearc basin has attributed to subduction of the Pacific Plate [3, 4].

The area referred to as the Boso Peninsula is unusual in that the thick sediments that were successively deposited in a short time since the Pleistocene were subsequently uplifted and exposed. Consequently, the area is characterized by a low geothermal gradient of less than $2^{\circ}\text{C } 100\text{ m}^{-1}$.

13.1.2.2 Niigata Gas Field

This field is situated in the Niigata backarc basin. Its reservoirs consist of the shallow marine Haizume formation to the nonmarine Uonuma group of the Pleistocene age (Fig. 13.2). These formations overlay thickly deposited Neogene marine sediments since the opening of the Japan Sea. The Higashi-Niigata gas field, which is a part of the Niigata gas field, has been developed as a suburb of Niigata City. This gas field also produces thermogenic gas that has accumulated in the deeper horizons.

Development of this field has been terminated in urban areas because of the problem of land subsidence. However, in suburban areas, reinjection of water underground to compensate for the water that was extracted to produce methane and iodine has resulted in the iodine concentration of these reservoirs having decreased somewhat.

13.1.2.3 Nakajo Oil and Gas Field

The reservoir is in the Nishiyama formation, which is below the Haizume formation in the Niigata gas field (Fig. 13.2). Iodine is extracted from edge-water of submarine conventional gas accumulation reserved in stratigraphic traps of pinched-out

sandstones. The gas signature is methane-dominant and consists of a mixture of microbial and thermogenic gas. This field is also characterized by hydrocarbon accumulation in the deep horizons.

13.1.2.4 Sadowara Gas Field

The Philippine Sea Plate subducts beneath the Eurasian Plate in southwestern Japan. The Sadowara gas field developed in the Miyazaki sedimentary basin, which is the forearc basin associated with the juncture of the southwestern Japan and Ryukyu arcs (Fig. 13.1). The reservoir occurs within the weakly consolidated siltstone of the Uryuno and Sadowara formations, which are called the Tsuma facies of the Miyazaki group and distributed in the northern part of the basin (Fig. 13.2).

More detailed descriptions of the geological and geochemical characteristics of each gas field have been reported [5, 6].

13.2 CHARACTERISTICS OF BRINE

Beneath the surface of marine sediments, any dissolved oxygen in pore water is initially consumed through the action of microbes and the oxidation of organic matter, followed by subsequent utilization of any oxides and oxoacid ions. As a result, submarine brine is depleted in SO_4^{2-} , but rich in I^- and NH_4^+ . In such a reductive environment, methanogens can produce CH_4 from CO_2 , H_2 , and H^+ . The origin of hydrocarbons of the earlier-mentioned gas fields was reported [7–9]. The chemical composition of iodine-rich brine from Japanese gas fields and seawater is listed in Table 13.1 [10–14]. Brines from the Minami-Kanto gas field contain iodine at concentrations exceeding 100 ppm, as well as high levels of HCO_3^- and humic substances [15].

13.3 IODINE ACCUMULATION IN BRINE

Relatively little is known about the mechanisms by which iodine accumulates in interstitial brine. The iodine concentration of seawater is approximately 0.06 ppm, and it occurs as IO_3^- and I^- ; the latter is the only chemical state in submarine anoxic condition.

As iodine is a biophilic element, it is transported together with organic matter into sediments. It was previously considered that seaweeds, particularly members of the brown algae family, were the origin for iodine in brine. However, even though they concentrate iodine from seawater and move it from shallow to bathyal environments, seaweeds are easily consumed by benthic organisms and they are rarely preserved in sediments. In addition, microalgae also concentrate iodine [16], implying that they may be responsible for an increase of iodine in sediments. Since the sediments of iodine-producing basins are also generally rich in terrestrial organic matter, it may be possible that this organic matter is responsible for the adsorption of iodine from

TABLE 13.1 Selected chemical compositions of iodine-accumulated brine in Japan

	Nakajo		Niigata		Minami-Kanto		Sadowara	Okinawa	Seawater
	mg/kg	mg/l	mg/l	mg/l	mg/l	mg/l	mg/l	mg/l	mg/kg
Na ⁺	12,760		9,070	10,000	11,700	10,900	11,320	12,400	10,560
K ⁺	163		480	300	360	358	51	42	380
Ca ²⁺	317	800	310	190	210	262	610	577	400
Mg ²⁺	93	420	480	500	510	364	955	221	1,270
NH ₄ ⁺	178	120	150	120	280	198	56	63	
Cl ⁻	19,400	19,290	14,000	18,000–19,500	19,900	19,470	19,013	20,020	18,980
HCO ₃ ⁻	836	290 ^a	770	1000	1,280	710	196	194	140
I ⁻	85	67	40	110–130	110	93	80	110	0.06
Br ⁻	134	107	90	120	160	122	132	93	65
SO ₄ ²⁻	16			0	0	0		0.75	2650
pH		7.7		7.9	7.7	7.6	7.3	7.5	8.2
temp.(°C)	74	59.8					45.0	49.0	

^aTotal CO₂

seawater. Another idea is that marine organic matter contains iodine derived from fecal matter and that this iodine is released and transferred to refractory terrestrial organic matter in the bottom sediments.

Iodine concentrations in the pore water of marine subsurface sediments increase with depth. Egeberg and Dickens [17] reported that sediments from 730 m at Blake Ridge had iodine concentrations of 230 ppm and that this iodine diffuses to the surface. Uprising I^- changes to IO_3^- at the oxic/anoxic interface where it is reduced, binds with organic matter, and is transported to the deep sediments again. This recycling is considered to concentrate the iodine in subsurface sediments.

13.3.1 Radiometric Age of Iodine-129

The absolute age of brine has been determined using radiometric ^{129}I , which has a half-life of 15.7 million years. The minimum ages of iodine in brine, which have been calculated as 50 Ma for the Minami-Kanto field [15] and as 40–46 Ma for the Niigata and Nakajo fields [18], are considerably older than the ages of the host sediments. Based on what is known about the geology of these areas, it is difficult to explain how very large amounts of water have been displaced from such compacted old sediments. It therefore seems likely that iodine ages have been overestimated.

The brine was not deposited at the same time as the host sediments in general. The porosity of sediments has been shown to decrease from 60 to 70% at the surface to about 30% at a depth of 1000 m due to compaction with burial. Thus, the burial rate of pore water appears to be slower than that of solid sediments, which is why older pore water can generally be found in younger sediments. Like microbial methane, brine may receive iodine from the sinking thick sediments. The brine then accumulates the iodine over extended periods; in the case of the gas fields described earlier, these periods may span from about 2 million to 15 million years. Moreover, the effects of diffusion and recycling described earlier result in iodine ages that are considerably older than those of the host sediments.

13.4 PRESERVATION AND DESTRUCTION OF BRINE DEPOSITS

Although iodine is known to exist at high concentrations in submarine sediments, the commercial production of iodine from brine involves drilling on land.

As marine sediments have been exposed in terrestrial environments through basin evolution, these sediments have been exposed to meteoric water. The mixing of fossil seawater and meteoric water can be verified based on the concentration of chloride and the composition of hydrogen and oxygen isotopes of the water. Since meteoric water contains very little iodine and methane, any iodine and natural gas deposits in such exposed areas are destroyed. Thus, in order to preserve these iodine deposits, limiting the invasion of meteoric water into these areas is considered to be important.

As described earlier, the production of both iodine and methane from gas brine is restricted from the geologically young sediments near the seashore. Subduction of the Pacific Plate has moved the deposition center of the Kanto sedimentary basin into Tokyo Bay, preventing the invasion of meteoric ground water from the western to northern mountain areas, such as the Kanto and Ashio Mountains, and ensuring the preservation of the Minami–Kanto gas field.

13.5 PRODUCTION OF IODINE FROM NATURAL GAS BRINE

In Japan, iodine is produced from natural gas brine by a blowing-out process and an ion-exchange process.

13.5.1 Blowing-Out Method

This method takes advantage of the easy vaporization property of iodine and is suited to processing brine at high temperature. The brine is pumped from the wells (depth: 500–2000 m) to the brine pit to settle down and remove sand and impurities in the brine. The iodine-rich brine is acidified with hydrochloric acid or sulfuric acid, and the acidified brine is treated with an oxidizing agent, chlorine or sodium hypochlorite, to liberate iodine. The oxidized brine diffuses to the top of a blowing-out tower and the iodine vaporizes. This vapor is then drawn into an absorption tower where it comes into contact with an absorbing agent, sodium hydrogen sulfite, which absorbs, concentrates, and reduces iodine to iodide. Chlorine is added to the iodide solution to crystallize the iodine. The resulting iodine sludge is fed to a melting tank, where it is directly heated with steam to 120°C, to separate impurities. The molten iodine is transferred to the iodine storage tank for flaking. The flaker consists of two water-cooled cylindrical drums made of Hastelloy C, an alloy that is resistant to corrosion by iodine. The molten iodine flows into the trough formed by the drums, is crystallized in the cooled drum, and then removed by scraping. Iodine flakes are packed in fiber drums lined with plastic bags (Fig. 13.3 and 13.5a). An alternative refining process is the prilling process [19]. The molten iodine is introduced into a prilling tower through a perforated surface so as to form a plurality of molten streams, which transform into droplets, and then solidified to prills by a counter-current flow of cold air and atomized water. Prilled iodine is flowable and easy to handle (Fig. 13.5b).

13.5.2 Ion-Exchange Resin Method

Sand and impurities in the brine are removed by settling and filtering. An oxidizing agent, chlorine or sodium hypochlorite, is added and the brine is oxidized. The resultant brine is passed through a column packed with an anion-exchange resin that adsorbs the iodine, which is in the form of a polyiodide. The

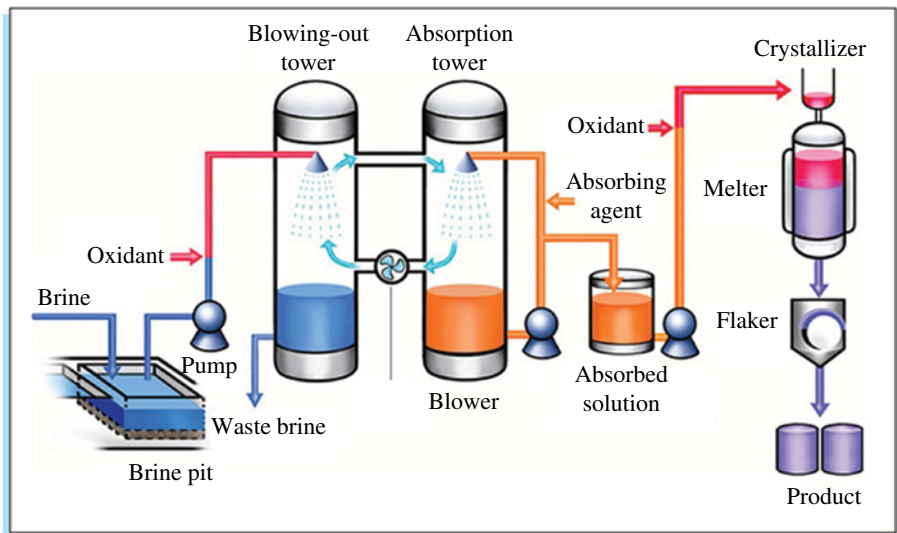


FIGURE 13.3 Blowing-out process of iodine. A view of Blowing-out and Absorption towers (bottom). (See insert for color representation of the figure.)

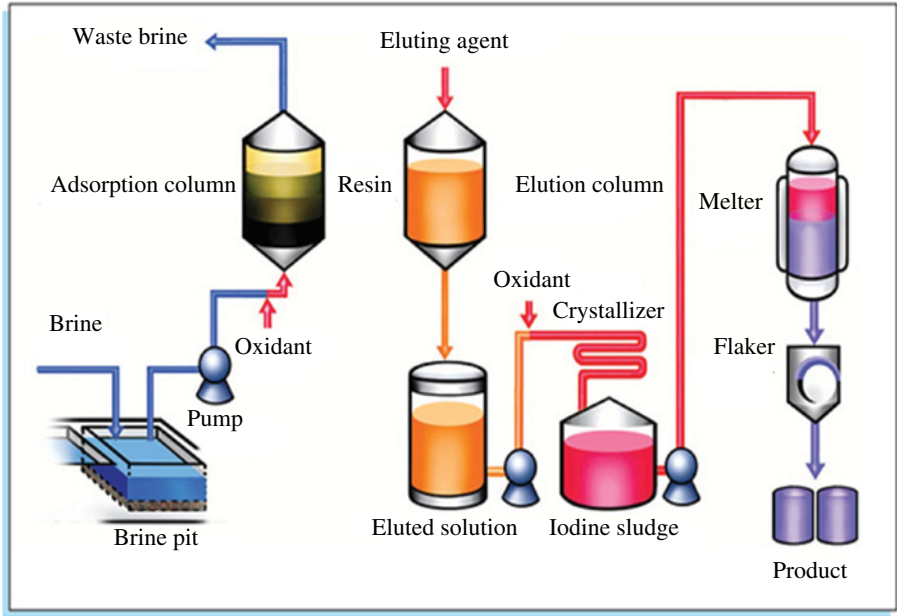


FIGURE 13.4 Ion-exchange Resin (IER) Process of iodine. A view of IER column (bottom).
(See insert for color representation of the figure.)

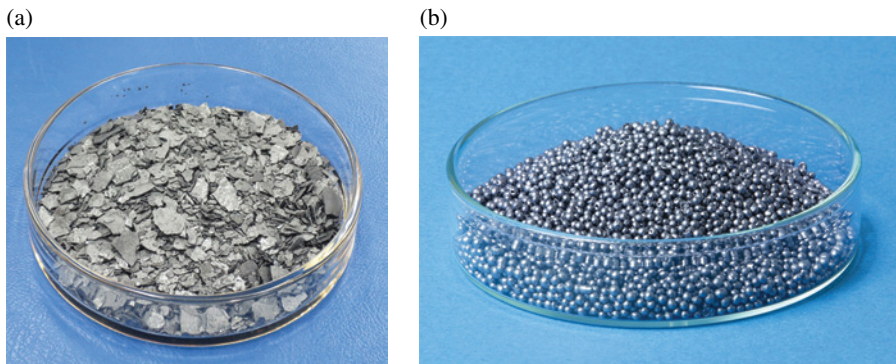


FIGURE 13.5 (a) Iodine product (flaked). Iodine flake is highly pure and low water content product. (b) Iodine product (prilled). Prilled iodine is easy to handle and dust free. (*See insert for color representation of the figure.*)

resin is then removed and transferred to an elution column where the polyiodide is eluted with a sulfite solution. Chlorine is added to the eluted solution and the iodine crystallized out. The refining process is similar to the blowing-out method (Fig. 13.4).

REFERENCES

- [1] Kunisue S, Mita I, Waki F. Relationship between subsurface geology and productivity of natural gas and iodine in the Mobara gas field, Boso Peninsula, central Japan. *J Jpn Assoc Petrol Technol* 2002;67:83.
- [2] Mita I, Waki F, Kunisue S. Control factors on gas-water ratio and iodine concentration around the Kujukuri district in Chiba prefecture, central Japan: special reference to the role of submarine-fan deposits and the faults in the Kazusa group. *J Jpn Assoc Petrol Technol* 2003;68:111.
- [3] Katsura Y. Depositional environments of the Plio-Pleistocene Kazusa group, Boso Peninsula [Dr. Thesis]: Tsukuba University; 1983.
- [4] Takahashi M. Tectonic boundary between Northeast and Southwest Japan arcs during Japan Sea opening. *J Geol Soc Jpn* 2006;112:14.
- [5] Fukuta O, Fujii N. Japanese iodine: production, geology, and geochemistry. *Ind Miner* 1982;175:101.
- [6] Fukuta O, Nagata S, Fujii N. Iodine from the Niigata dissolved dry gas producing area, Japan. *Ind Miner* 1982;180:69.
- [7] Kaneko N, Maekawa T, Igari S. Generation of archaeal methane and its accumulation mechanism into interstitial water. *J Jpn Assoc Petrol Technol* 2002;67:97.
- [8] Kato S, Waseda A, Iwano H. Petroleum geology of the Nanjo R-1 exploratory well, Okinawa Prefecture. *J Jpn Assoc Petrol Technol* 2011;76:244.
- [9] Kato S, Honda T, Omijya K. Geochemistry of natural gas and formation water from water-dissolved gas fields in Miyazaki Prefecture. *J Jpn Assoc Petrol Technol* 2012;77:86.

- [10] Japan Natural Gas Association. *Handbook of Natural Gas Dissolved in Water*. 1980.
- [11] Toho Earthtech, Inc. Production of iodine and its derivative. Available at <http://www.tohoearthtech.co.jp/business/iodine-manu/>. Accessed July 1, 2014.
- [12] Kanto Natural Gas Development Co., Ltd. Raw materials and characteristics. Available at <http://www.gasukai.co.jp/iodine/index3.html>. Accessed July 1, 2014.
- [13] Fukuta O. Natural gas associated with water and its deposits. *Chishitsu News*. 1979;296:6.
- [14] Mason B. *Principles of Geochemistry*. 3rd ed. New York: John Wiley & Sons; 1966.
- [15] Muramatsu Y, Fehn U, Yoshida S. Recycling of iodine in fore-arc areas: evidence from the iodine brines in Chiba, Japan. *Earth Planet Sci Lett* 2001;192:583.
- [16] Iwamoto K, Shiraiwa Y. Characterization of intracellular iodine accumulation by iodine-tolerant microalgae. *Proc Environ Sci* 2012;15:34.
- [17] Egeberg PK, Dickens GR. Thermodynamic and pore-water halogen constraints on gas hydrate distribution at ODP Site 997 (Blake Ridge). *Chem Geol* 1999;153:53.
- [18] Tomaru H, Lu Z, Fehn U, Muramatsu Y. Origin of hydrocarbons in the Green Tuff region of Japan: ¹²⁹I results from oil field brine and hot springs in the Akita and Niigata Basins. *Chem Geol* 2009;264:221.
- [19] Lauterbach A. Production of spherical shaped products of subliming substances. US Patent 5,437,691. Aug 1, 1995. New York: Chilean Nitrate Co.

14

RECYCLING OF IODINE

TATSUO KAIHO

Nihon Tennen Gas Co., Ltd., Chiba, Japan

14.1 INTRODUCTION

Iodine is used by a wide variety of industries. Around half, however, is used in applications directly related to human health, for example, X-ray contrast agents, biocides, and pharmaceuticals. Most of the remainder is used in industrial applications including optical polarizing film for liquid crystal displays (LCDs), catalysts, heat stabilizers, and the production of fluorine derivatives. The production of iodine is limited mainly to the two countries of Japan and Chile in South America, making iodine an extremely limited precious resource. Accordingly, recovery of expensive iodine from used iodine-containing materials or iodine compounds, and further, the manufacturing step of iodine-containing materials such as X-ray contrast agents and liquid crystal films, is very beneficial from the viewpoint of economy, natural environmental conservation, and the conservation of natural resources. Many iodine manufacturers have recently focused on collecting and recycling iodine from waste streams in view of sustainability. Iodine-containing materials discharged from production processes contain iodine in the form of an elemental substance or as various organic or inorganic compounds, and its state also varies, for example, waste liquid, oil, and sludge. The reproduction of iodine is made possible by utilizing proper treatment suited to each type of waste stream and iodine form (Tables 14.1 and 14.2).

The recycled iodine is then used to produce iodine and chemical derivatives. The following examples demonstrate the methods of recovering iodine from waste.

TABLE 14.1 Iodine waste stream and recovery process

Iodine waste streams	Pretreatment	Deiodination	Posttreatment and iodine recovery	Iodine production process
Iodine-mediated chemical reaction	Solid–liquid separation	High-temperature combustion	Mineralization Neutralization	Blowout process
X-ray contrast agents	Solvent recovery	Catalytic decomposition	Ion exchange	Ion-exchange resin process
Fluorine-containing polymer	Concentration	Multiple Decomposition	Concentration Precipitation	
Polarizing film	Separation of unreacted material		Membrane filtration (MF, UF, NF) Distillation Extraction Electrodialysis	

TABLE 14.2 Waste iodine form and recovery process

No.	Waste iodine	Iodine form	Method	Recovered iodine
1	X-ray contrast agent	ArI	Mineralization, Ion exchange	NaI
2	Polarizing film	KI	Nanofiltration Electrodialysis exchange	KI
3	Organic iodides	RI	Combustion	NaI
4	Inorganic iodides	MetI	Filtration, Ion exchange	NaI

14.2 IODINE WASTE FROM X-RAY CONTRAST AGENTS

The most modern contrast agents, that is, the nonionic ones, are usually 2,4,6-triiodo-1,3-benzenedicarboxylic acid derivatives [1], characterized by a strong bond of the iodine atoms to the aromatic ring. The strength of the iodine bond is, however, also affected by the structure of the concerned compound. Iodine, in fact, has to be recovered from effluents and waste streams for the production of 2,4,6-triiodo-1, 3-benzenedicarboxylic acid derivatives due to environmental reasons. The waste solution from the X-ray contrast agent production process [1] is mineralized using CuSO_4 at first. The solution is then alkalized with NaOH and heated for several hours. After mineralization, the solution is concentrated until the solution weight becomes half the initial weight. The resulting solution is filtered with a nano filtration membrane (Fig. 14.1) to obtain the iodides in the permeate while retaining copper. The recovery of iodine after mineralization is carried out by the oxidation of iodides to molecular

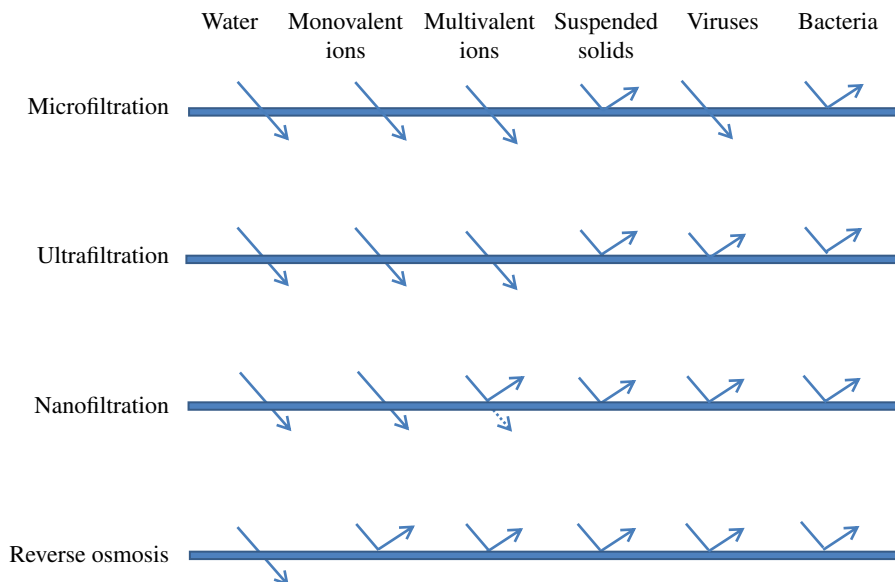


FIGURE 14.1 Membrane filtration. MF, micro filtration: 0.1–1 μm ; NF, nano filtration: 0.001–0.01 μm ; RO, reverse osmosis: 0.0001–0.001 μm ; UF, ultra filtration: 0.01–0.1 μm .

iodine according to known methods used for iodine production (see Chapter 13). The resulting retentate is percolated on a chelating resin, such as Amberlite IRC748,¹ for removing copper ion and is then discharged.

14.3 IODINE WASTE FROM POLARIZING FILMS

Commercial polarizing films have been produced from poly vinyl alcohol (PVA) and are usually prepared by soaking PVA films in I_2/KI solution with boric acid and by subsequent drawing to cause a high degree of uniaxial orientation. The PVA/I_2 complex film is used as optical polarizing film for high-quality LCDs. The waste fluid in polarizing film production contains iodine, potassium iodide, and boronic acids [2]. The waste fluid is neutralized or acidified to pH 7 or less and then subjected to electrodialysis to separate iodine as potassium iodide to reduce the total amount of iodine in the waste fluid. After the electrodialysis, the waste fluid is passed through a strongly basic anion-exchange resin to further reduce the total amount of iodine in the waste. Then, iodine is recovered from the electrodialysis eluent and the ion-exchange resin eluent. The recovery of iodine, from the electrodialysis eluent and the ion-exchange resin eluent, is carried out by oxidation of iodides to molecular iodine according to known methods used for iodine production (see Chapter 13, Fig. 14.2).

¹ AMBERLITE™ IRC748 is an iminodiacetic acid chelating cation-exchange resin with high selectivity for calcium, magnesium, copper (II), and strontium in chloralkali brines, for removing metals from solutions.

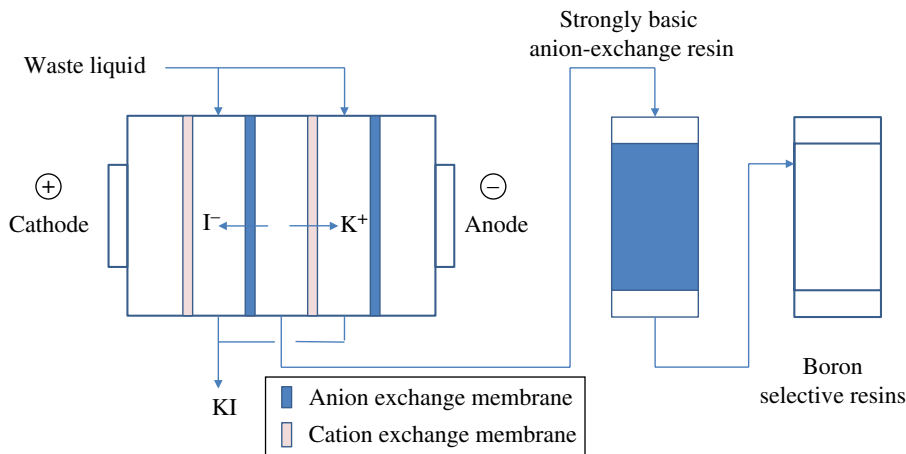


FIGURE 14.2 Electrodesialysis system and ion-exchange resin tower.

14.4 IODINE WASTE FROM THE INDUSTRY

Iodine and iodine compounds are often used as a catalyst in dehydrogenation, deprotection, or isomerization of organic substances. It is well-known that iodine, when absorbed into the human system, may cause various toxic symptoms, and iodine compounds, such as methyl iodide and ethyl iodide, which are usually generated during various chemical reactions in the presence of iodine, are poisonous to the human body. Therefore, at chemical plants that use iodine as a catalyst for reaction of organic substances, there exist problems that require immediate attention. Iodine should be recovered on an economical basis. Such recovery from plant waste will aid and control pollution problems. A conventional process for recovering iodine from waste material containing iodine or iodine compounds consists of burning waste material in a combustion chamber [3], thereby producing a combustion gas containing iodine, passing the combustion gas through a basic aqueous solution of sodium thiosulfate to react the iodine to produce sodium iodide, and recovering molecular iodine from iodide, which is carried out according to known methods used for iodine production (see Chapter 13, Fig. 14.3).

14.5 SUMMARY

The demand for iodine has grown significantly over the past 10 years. Most of this has come from optical polarizing films for LCDs. Medical needs have also been increasing in recent years in emerging economies such as China and India. However, a significant increase in the production of iodine cannot be expected, because of the land subsidence that is accompanying iodine mining in Japan. To achieve the new large-scale production of iodine in Chile, a pipeline has to be laid from the seashore to the inland desert where iodine ore is found, since the amount of groundwater taken

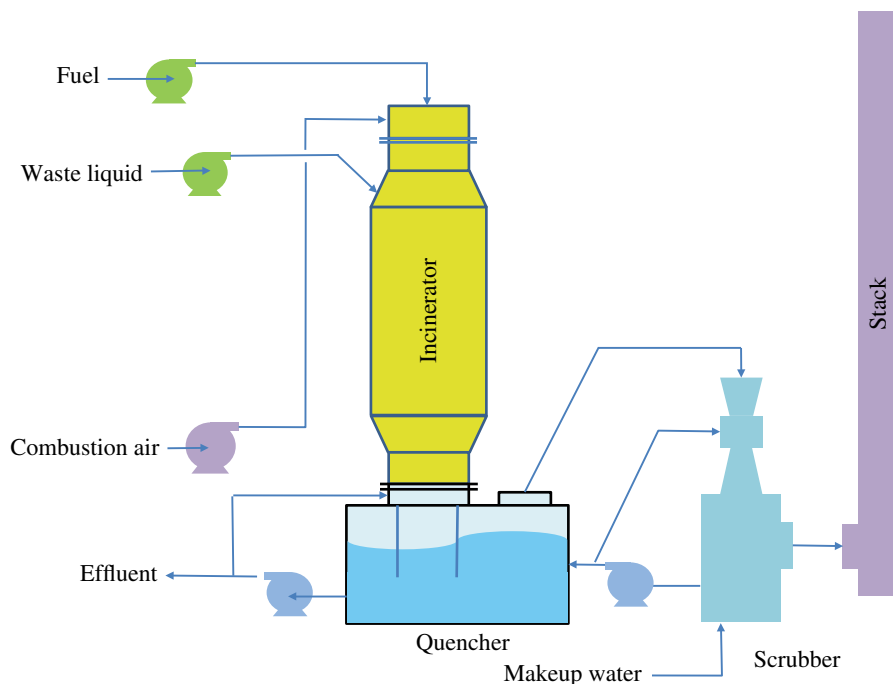


FIGURE 14.3 Incinerator to recover iodine.

is strictly restricted to preserve groundwater supplies. Therefore, it is very important that iodine manufacturers construct not only an efficient production system of iodine but also a system for recovering and recycling iodine from waste streams.

REFERENCES

- [1] Desantis N, Peretto I, Incandela S, Viscardi CF. Process for the recovery of copper from aqueous solutions containing iodinated organic compounds. US Patent 6,827,856. Dec 7, 2004. Milan: Bracco Imaging S.p.A.
- [2] Ezawa H, Otani Y. Method for recovering iodine from waste fluid in polarizing film production. JP Patent 2008-013379. Jan 24, 2008. Tokyo: Godo Shigen Sangyo Co. Ltd.
- [3] Shoji S, Hijihira H, Kanbe S. Method of recovering iodine. US Patent 7,736,617. Jun 15, 2010. Tokyo: Nippoh Chemicals Co. Ltd.

PART III

SYNTHESIS OF IODINE COMPOUNDS

15

IODINATING REAGENTS

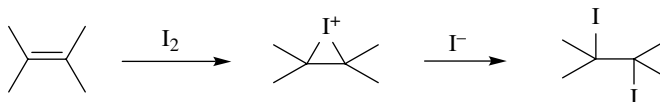
HARUHIKO TAGUCHI

Tokyo Chemical Industry Co., Ltd., Tokyo, Japan

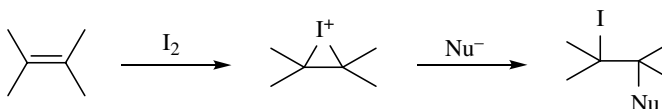
Iodinating reagents are one of the strong tools for the synthesis of organoiodine compounds, and a number of efficient reagents and their synthetic applications have been developed. Usually, iodinations can be performed by using electrophilic iodinating reagents and nucleophilic iodinating reagents. Radical species-mediated iodination reactions have also been reported. Iodine is a soft species with a large molecular size; it is easily polarizable and low in electronegativity. As such, iodinating reagents are used for the addition to unsaturated bonds such as in alkene, alkyne, aryl, heteroaryl compounds, for electrophilic substitution in metal carbanions, and for nucleophilic substitution from iodide ions such as metal iodides. In this chapter, the chemical character of iodinating reagents and their usages are described.

15.1 MOLECULAR IODINE

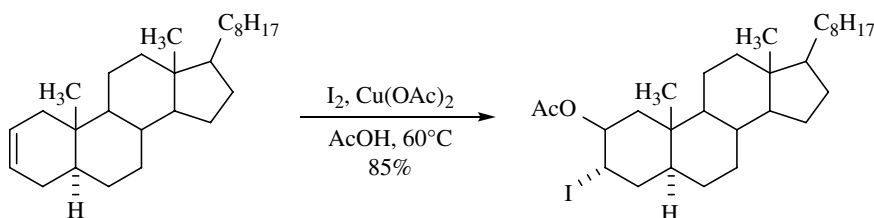
Molecular iodine is the most popular iodinating reagent and is widely used in organic synthesis [1]. Various synthetic applications have been reported and some additives efficiently enhance the reactivity of reaction substrates. Iodine is electrophilic and can react with various nucleophiles. In the reaction of iodine with alkene, three-membered iodonium ions are formed as an intermediate (Scheme 15.1). This chemical species has an electrophilic character, and 1,2-diiodidated compound is formed by the addition of iodide anion to it (Scheme 15.1) [1].



SCHEME 15.1



SCHEME 15.2



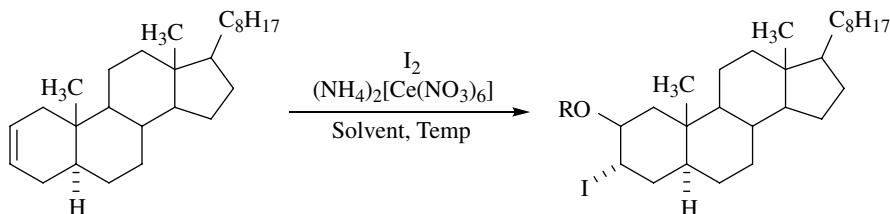
SCHEME 15.3

If other nucleophiles are present, nucleophiles are added instead of iodide ion (Scheme 15.2). In these reactions, some additives such as copper(II) salts [2, 3] or ammonium cerium(IV) nitrate (CAN) [4] are often used with alcohols [2, 4], or carboxylic acids [3], and amides to give corresponding vicinal iodoalkanes.

Examples are the acetoxy- and alkoxyiodination of 5- α -cholest-2-ene using molecular iodine and $Cu(OAc)_2$ [3] or CAN [4]. The *trans* addition to the olefin moiety occurs and the related steroidal *trans*-iodoacetate is given (Schemes 15.3 and 15.4).

The same reactions using CAN under various solvents are investigated (Scheme 15.4) [4]. Methanol, ethanol, and *tert*-butanol are used as a solvent, and when the reaction is in methanol, the corresponding steroidal iodomethoxide is formed (Table 15.1). While in ethanol, the reaction successfully proceeds, but the yield is slightly decreased compared with using methanol. When using *tert*-butanol, the nitrite ion is added to the steroidal olefin instead of *tert*-butanol to afford the nitrato-iodinated compound (Table 15.1). Acetic acid is used as a solvent; the result is similar to the reaction employing $Cu(OAc)_2$. In the reaction system using CAN, all the steroidal iodoalkoxides have *trans* configuration (Scheme 15.4).

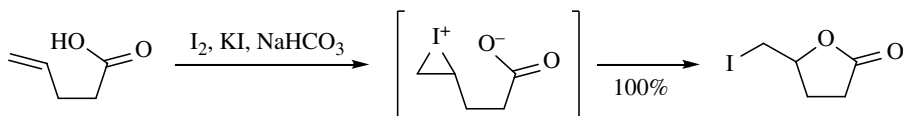
γ,δ - or δ,ϵ -Unsaturated carboxylic acids [5] and their amide derivatives [6] are cyclized under the presence of molecular iodine and a base. This iodolactonization process is performed by intramolecular nucleophilic attack from the carboxylic acid moiety to an iodonium ion generated by the action of iodine to a double bond of the unsaturated carboxylic acid (Scheme 15.5) [5].



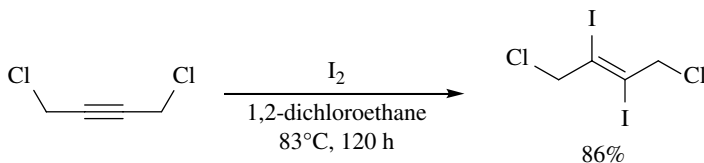
SCHEME 15.4

TABLE 15.1 Addition of iodoalkoxides to the steroidal olefin

Solvent	Temp (°C)	Yield (%)	Substituent (RO ⁻)
MeOH	50	70	MeO
EtOH	50	65	EtO
BuOH	reflux	45	NO ₂
AcOH	50	86	AcO



SCHEME 15.5

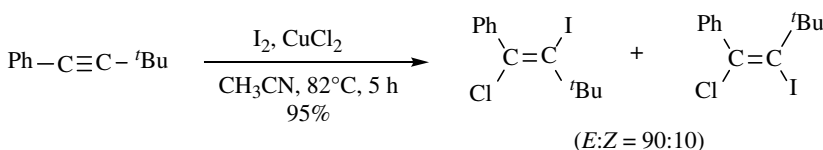


SCHEME 15.6

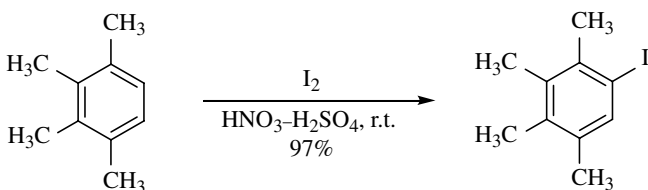
As with the reaction of alkenes, molecular iodine can add to alkynes to afford diiodides [7]. The reactivity of iodine to alkynes is lower compared to that of alkenes. To achieve the addition to them, this reaction requires high-temperature conditions and long reaction time (Scheme 15.6).

With the addition of iodine to alkylphenylacetylenes in the presence of CuCl_2 , iodo-chlorination proceeds and iodochlorinated alkenes are given with high *E* selectivity [8]. This addition is regiospecific and chlorine atom is introduced at the α -carbon of the phenyl group (Scheme 15.7).

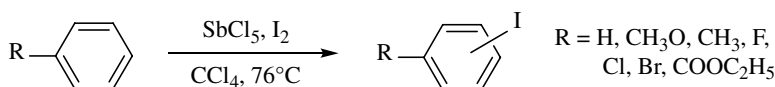
Generally, direct iodination of aromatic rings using molecular iodine needs the mixture of nitric acid and sulfuric acid as a solvent due to its mild electrophilic character [9]. This synthetic method, named the Tronov–Novikov method, is carried out at room temperature or reflux conditions and iodoaromatic compounds are



SCHEME 15.7



SCHEME 15.8



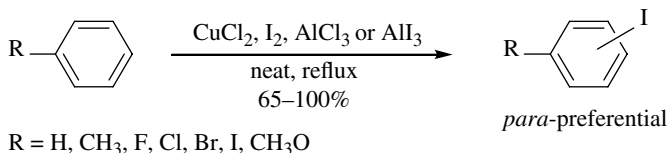
SCHEME 15.9

TABLE 15.2 Aromatic iodination using SbCl_5 and molecular iodine

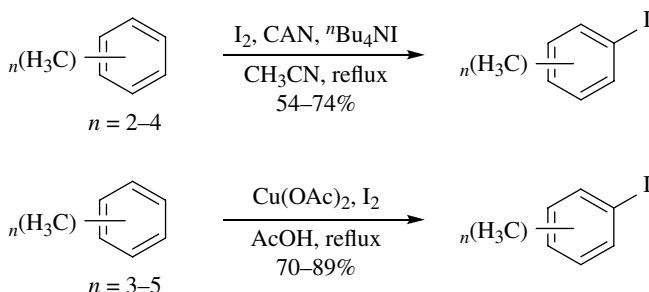
Substituent in R-Ph	Time (min)	Isomer distribution of R-PhI			Yield (%)
		<i>o</i> -	<i>m</i> -	<i>p</i> -	
H	30	—	—	—	84
CH_3	30	58	0	42	96
CH_3O	30	0	0	100	75
F	30	2	0	98	74
COOEt	300	0	100	0	48

obtained in moderate to excellent yields (Scheme 15.8). When reactions at high temperature or electron-rich aromatic rings are employed, diiodinated compounds are often obtained [9].

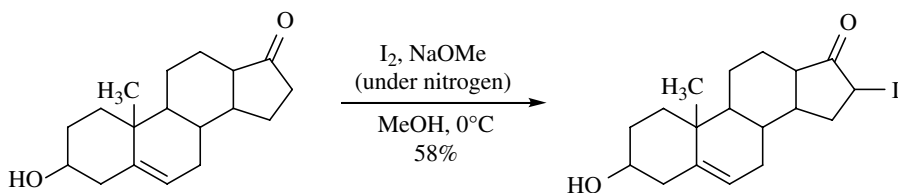
For iodination of aromatic rings, some additives are used as activators with molecular iodine to achieve electrophilic substitution reactions of an iodide ion to aromatic rings [10–14]. Equimolar mixtures of SbCl_5 [10] and iodine are used for aromatic iodination of certain aromatic rings, and the desired iodinated compounds are obtained with *para* regioselectivities preferentially except that ethyl benzoate and toluene are employed (Scheme 15.9 and Table 15.2). When using ethyl benzoate, which is an electron-poor aromatic ring, the iodination occurs at the *meta* position and the product yield is lower (Table 15.2).



SCHEME 15.10



SCHEME 15.11



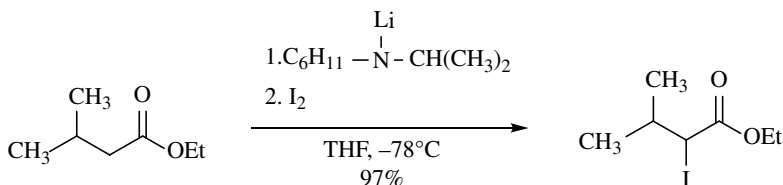
SCHEME 15.12

Copper(II) salts act to be activators for electron-rich aromatic rings; CuCl_2 is well used for this purpose [11, 12]. In this reaction system, polymethylbenzenes afford good results, whereas the reactivities to xylenes and toluene are not sufficient. To solve such a problem, some Lewis acids are used with CuCl_2 to enhance the reactivities of aromatic rings [12]. Benzene, toluene, and xylenes can react with molecular iodine in the presence of CuCl_2 and AlCl_3 or AlI_3 to give the corresponding iodinated compounds in good yield (Scheme 15.10).

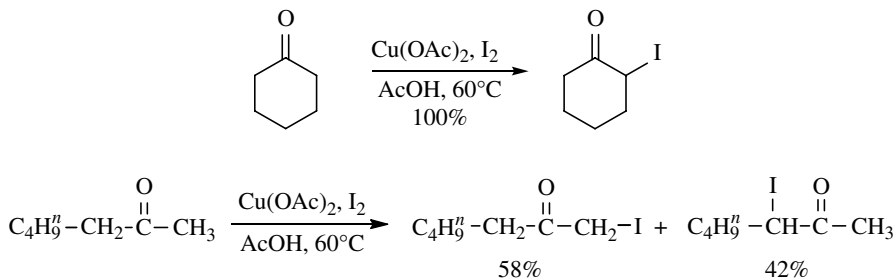
Polymethylbenzenes, which are strong electron-rich aromatic rings, are good electrophiles for iodination. Some efficient additives like CAN [13] and $\text{Cu}(\text{OAc})_2$ [14] are well used for their direct iodination reactions (Scheme 15.11).

Molecular iodine can also replace α -hydrogen of carbonyl compounds to iodine in the presence of a base (Scheme 15.12) [15]. Enolates prepared from ketones, aldehydes, or carboxylic acid derivatives under basic conditions react with molecular iodine to afford related α -iodinated carbonyl compounds [16].

When iodination of ketones such as methyl ketone derivatives, iodoform is obtained, which named Lieben iodoform reaction is a method for the detection of the methyl carbonyl group. On the other hand, when alkyl ketones except methyl



SCHEME 15.13



SCHEME 15.14

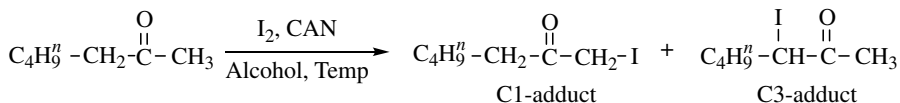
ketone are employed, α -iodination successfully proceeds to give the related α -iodinated ketones.

α -Iodinated esters are synthesized by the reaction of lithium enolates with molecular iodine [16]. Lithium *N*-isopropylcyclohexylamide is an effective base to prepare lithium enolates, and the iodination generally proceeds providing good yield (Scheme 15.13).

α -Iodination of carbonyl compounds with molecular iodine under acidic conditions is accomplished by using copper(II) salts [17] or CAN [18, 19]. The reaction involves Cu(OAc)_2 and molecular iodine in acetic acid, in which various ketones can be converted to related α -iodinated ketones [17]. When using symmetrical ketones, only a mono-iodinated product is formed (Scheme 15.14), while when asymmetrical ketones are employed, two iodinated products are formed (Scheme 15.14).

The CAN-assisted α -iodination of ketones is more regioselective (Scheme 15.15 and Table 15.3) [19]. Iodination of 2-heptanone in methanol at 25°C proceeds the C1 regioselectively, and 1-iodo-2-heptanone is obtained as the sole product. Even when the same reaction proceeds at 50°C , the C1 adduct is predominantly obtained. The regioselectivities of this reaction is dramatically varied by the choice of alcohol solvents and the reaction temperature (Table 15.3). The amount of C3 adduct is increased by using bulky solvents such as ethanol and propanol and high reaction temperatures (Table 15.3).

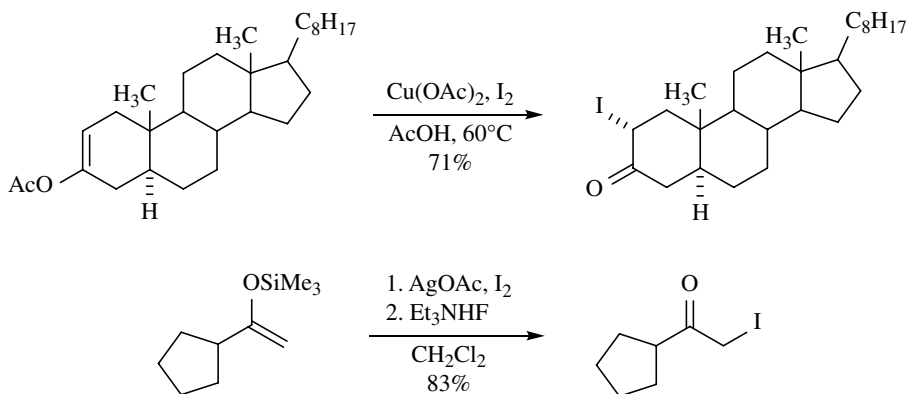
It is known that the cerium ion forms a cerium-alcohol complex in alcohol solvents, and it coordinates to a carbonyl group of ketones to enolize predominantly toward the C3 position; the attack of the iodide ion at the C3 position occurs thereafter [19]. However, due to the bulkiness of the alkoxy group, it is very difficult to attack the iodide ion at the C3 position. Therefore, it would seem that the iodide ion attacks the C1 position.



SCHEME 15.15

TABLE 15.3 Regioselectivities of α -iodination of ketones in alcohols

Solvent	Temp ($^{\circ}\text{C}$)	Yield (%)	Product ratio (C1 : C3)
MeOH	25	62	0 : 100
EtOH	25	51	21 : 79
n PrOH	25	47	8 : 92
MeOH	50	73	8 : 92
EtOH	50	88	64 : 36
n PrOH	50	95	71 : 29

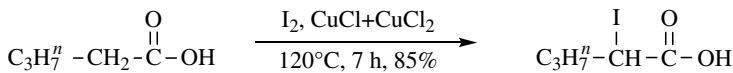


Enol acetate and enol silyl ethers of ketones are also α -iodinated with molecular iodine and some metal salts. There are certain cholestane derivatives whose enol acetates are iodinated in the presence of $\text{Cu}(\text{OAc})_2$ in acetic acid [17]. Similarly, enol silyl ethers of ketones are iodinated by molecular iodine with silver acetate [20] (Scheme 15.16).

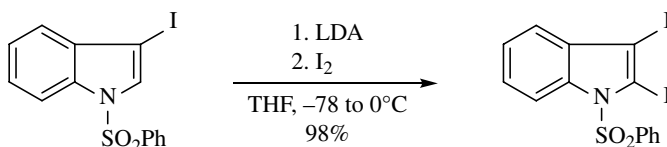
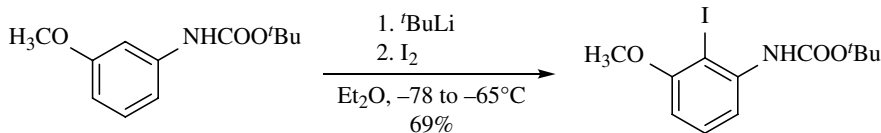
In these reactions, related enols are directly iodinated with retention of the configuration of their enol conformations. Thus, this synthetic method is useful to get designed α -iodinated ketones due to be able to introduce from related enol ketone derivatives.

The α -position of carboxylic acids can be substituted by an iodine atom by using molecular iodine with copper salts [21]. Various copper(II) salts can be used for this transformation; a mixture of CuCl and CuCl_2 is most effective in enhancing the reactivity of carboxylic acids (Scheme 15.17).

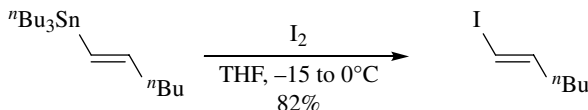
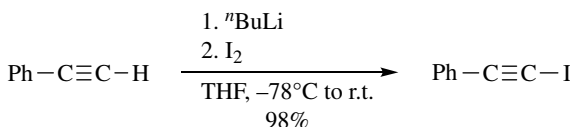
Molecular iodine is a soft electrophile and is conveniently used as a quenching reagent for metal carbanions [22]. Aryl [23] and heteroaryl [24] lithium compounds



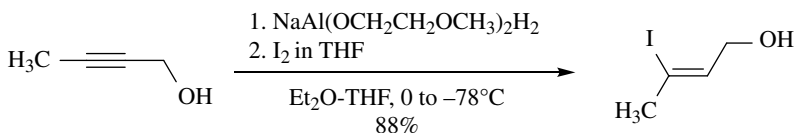
SCHEME 15.17



SCHEME 15.18



SCHEME 15.19

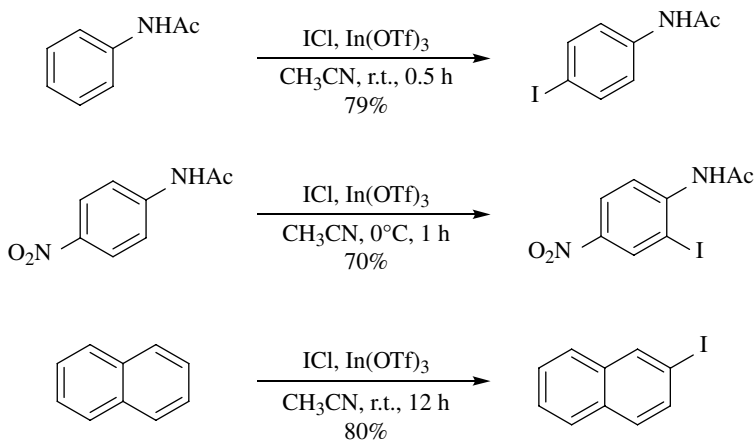


SCHEME 15.20

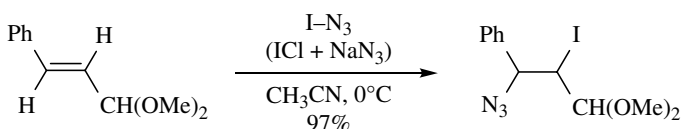
are good nucleophiles to molecular iodine, and it is easy to obtain iodinated compounds in moderate to good yields (Scheme 15.18).

Similarly, alkynyl [25] and alkenyl [26, 27] metal species are successfully quenched by iodine to produce the desired iodinated products. Vinylstannane [26], which is a versatile vinyl anion synthon, is directly transformed to a vinyl iodide by the action of molecular iodine (Scheme 15.19).

Cyclic alkenylaluminum intermediates are formed by the addition of sodium bis(2-methoxyethoxy)aluminum dihydride to propargyl alcohols, and the subsequent reaction with molecular iodine affords the (*Z*)- γ -iodoallylic alcohols regioselectively (Scheme 15.20).



SCHEME 15.21



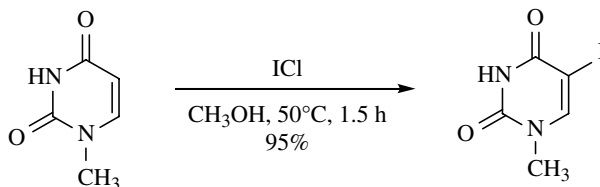
SCHEME 15.22

15.2 IODINE CHLORIDE

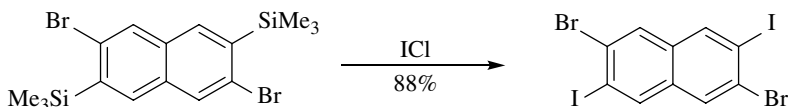
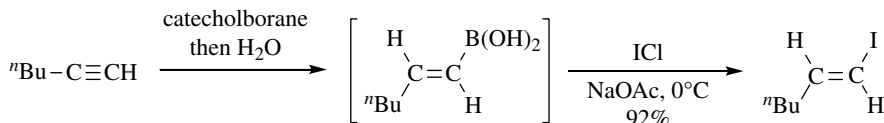
Iodine chloride is one of the interhalogens, and it is used for electrophilic iodinating reagents. Similar interhalogen compounds such as iodine bromide and iodine fluoride cannot be used as an iodinating reagent because of not being sufficiently electrophilic. The reactivity of iodine chloride is similar to molecular iodine. However, the electrophilicity of iodine chloride is higher than that of molecular iodine, which enables some iodination under milder reaction conditions. Direct aromatic iodination using iodine chloride proceeds smoothly by adding In(OTf)_3 as an activator at room temperature (Scheme 15.21) [28].

As mentioned in Chapter 15.1, direct iodination of aromatic rings with molecular iodine requires acidic and reflux conditions and is limited to only electron-rich aromatic rings. However, the method using ICl/In(OTf)_3 system is applicable to various aromatic rings and yields the desired iodoaromatic compounds under mild conditions and shorter reaction time even when electron-poor aromatic rings are employed (Scheme 15.21).

Iodine chloride is often used for the preparation of other iodinating reagents and iodine azide, which is prepared from iodine chloride and sodium azide [29]. The reaction of iodine azide with alkenes proceeds via the three-membered iodonium cation intermediate, and an azide ion is nucleophilically attacked from another side to the iodonium cation (Scheme 15.22).



SCHEME 15.23



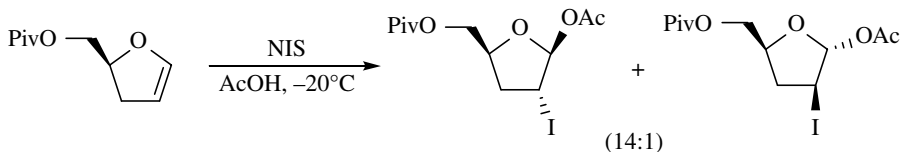
SCHEME 15.24

It is known that the C5-position of uracil is iodinated by various iodinated reagents. When using molecular iodine as an iodine donor, CAN [30] and Ag₂SO₄ [31] are often used for activation of the uracil base. However, iodine chloride directly introduces the iodine atom at the C5 position of uracil without any activator (Scheme 15.23) [32].

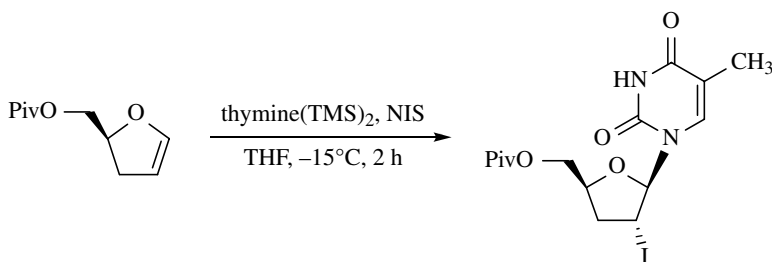
Iodine chloride cleaves a carbon–boron [33] and carbon–silyl [34] bond and inserts an iodine atom to form new iodine–carbon bonds. Vinylboronic acids, which are readily prepared via the hydroboration of terminal alkynes, are converted to the related vinyl iodide by iodine chloride (Scheme 15.24). Silyl groups of arylsilanes are directly replaced with an iodine atom by the action of iodine chloride (Scheme 15.24).

15.3 N-IODOSUCCINIMIDE

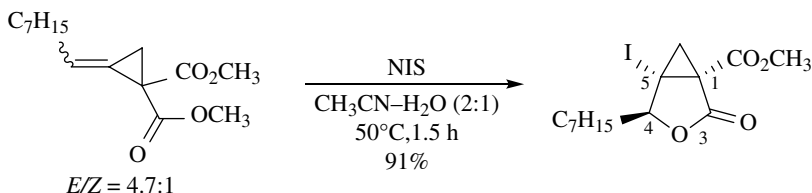
N-Iodosuccinimide (NIS) is an electrophilic iodinating reagent and is used to iodinate various substances similar to molecular iodine. The iodinating property of NIS is better than that of molecular iodine, and it is often chosen as an iodinating reagent instead of molecular iodine when its reactivity is insufficient. A number of iodination reactions using NIS have been reported and alkenes, hetero aromatic rings, and the α-position of ketones are successfully iodinated. Addition of acetic acid to a glycol in the presence of NIS regioselectively proceeds to produce a β-acetoxy-α-iodotetrahydrofuran derivative as a main isomer (Scheme 15.25) [35].



SCHEME 15.25



SCHEME 15.26

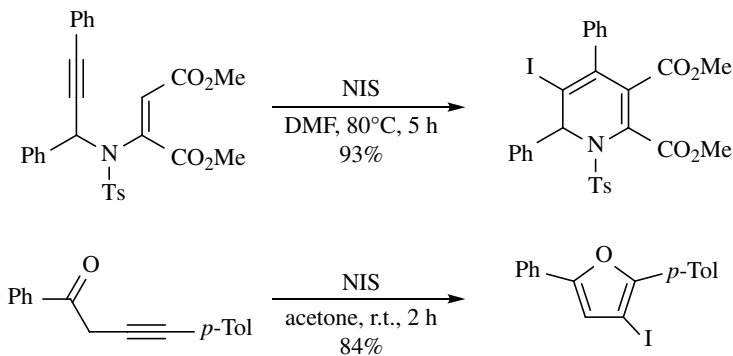


SCHEME 15.27

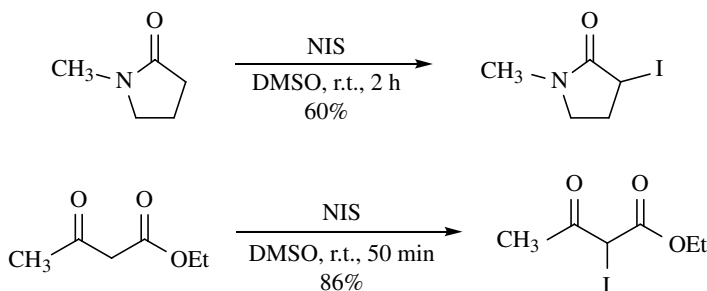
In this reaction, NIS is favored to approach from the β -face of the glycol due to its steric hindrance and the subsequent attack of the acetoxy ion occurs from the α -face, yielding the desired product with high stereoselectivity (Scheme 15.25). In the same manner, the 2',3'-deoxythymidine analogue is given by using a pyrimidine base (Scheme 15.26) [35].

Iodolactonization using NIS successfully cyclizes to produce the desired cyclic iodine compounds with stereospecificity [36, 37]. As in the case of molecular iodine, this reaction proceeds via formation of the three-membered iodonium ion as an intermediate. As shown Scheme 15.27, iodolactonization of alkyldenecyclopropyl esters with NIS affords the desired 4,5-*trans* adducts with high stereoselectivity regardless of the stereochemistry of the starting material (Scheme 15.27) [37].

Electrophilic iodocyclizations of 3-aza-1,5-enynes [38], β,γ -alkynylketones [39], and 3-silyloxy-1,5-enynes [40] are achieved by induction of NIS under metal-free conditions (Scheme 15.28). The plausible mechanism of these cyclizations is that the iodonium cation intermediates are generated by attack of the iodonium ion on the alkyne moiety and subsequent intramolecular nucleophilic substitutions lead to the corresponding cyclized compounds [38–40].



SCHEME 15.28



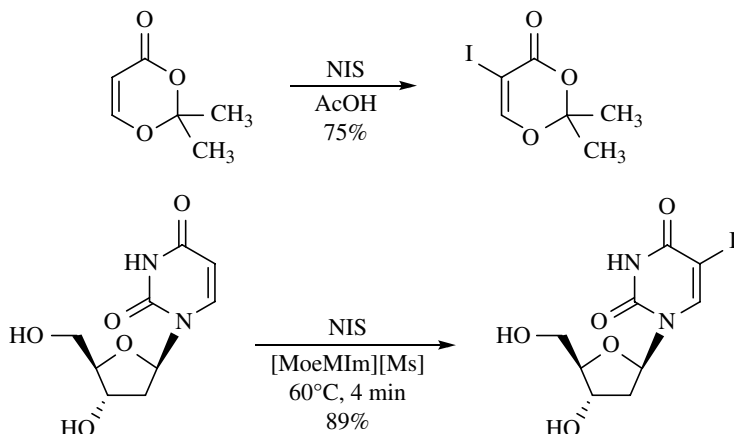
SCHEME 15.29

α-Iodination of ketones can be achieved using NIS under mild and catalyst-free conditions, with α-iodinated ketones being obtained in good to excellent yields [41]. Cyclic ketones and lactams are generally iodinated by NIS to afford α-iodinated cyclic ketones and lactones (Scheme 15.29). An active methylene proton of 1,3-dicarbonyl compounds such as 1,3-diketones, β-keto-esters, and malonic esters is directly replaced with an iodine atom (Scheme 15.29).

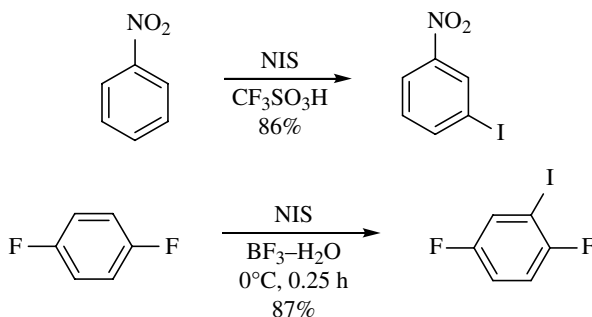
α-Iodoenones are obtained by the reaction of enones with NIS in an acetic acid solvent (Scheme 15.30) [42]. In addition, iodination at the C5 position of a pyrimidine base of nucleosides is performed by NIS in ionic liquids such as 1-methoxyethyl-3-methylimidazolium methanesulfonate ([MoeMIm][Ms]), and the 5-iodopyrimidine nucleosides are obtained in good yield (Scheme 15.30) [43].

NIS is dramatically activated by using triflic acid [44] or $\text{BF}_3 \cdot \text{H}_2\text{O}$ [45] and allowing the iodination of deactivated aromatic rings (Scheme 15.31). It is believed that a protosolvated iodine species is generated in situ and acts as a superelectrophilic iodonium ion.

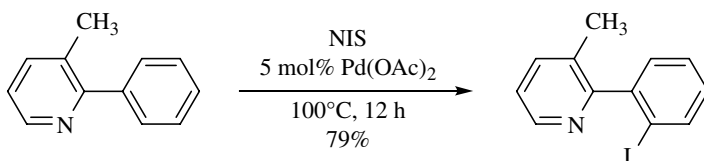
Iodination of aromatic compounds via C–H bond activation is achieved by using NIS as an oxidant [46, 47]. Pd complexes show good performance in activating the C–H bond and subsequent replacement with the C–I bond (Scheme 15.32) [46].



SCHEME 15.30



SCHEME 15.31



SCHEME 15.32

15.4 1,3-DIIODO-5,5-DIMETHYLHYDANTOIN

1,3-Diiodo-5,5-dimethylhydantoin (DIH) is a powerful electrophilic iodinating reagent and readily iodates various aromatic compounds under mild reaction conditions [48–50]. DIH is a pale yellow solid that does not sublime like molecular iodine, and has low toxicity. The reactivity of DIH is higher than that of NIS. In addition, DIH is atomic economical because both the iodine atoms in one molecule can be used for iodination. After iodination using DIH, dimethylhydantoin is formed

as a by-product, which can be easily removed by aqueous extraction. Anisole is rapidly iodinated by DIH at 20°C for 10 min, and the amount of DIH needed to complete the iodination is 0.5 equivalents (Scheme 15.33) [49].

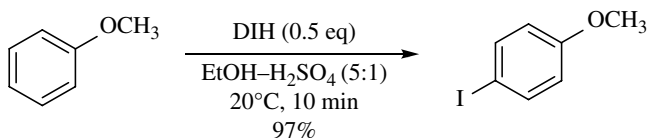
Enol acetates are iodinated by DIH under metal catalyst-free conditions, and the desired α -iodo ketones are obtained in good yield (Scheme 15.34) [50]. DIH is an efficient iodination reagent and various unreacted aromatic rings are easy to iodinate, whereas DIH has the disadvantage of limited solubility for aprotic solvents [48], and in some cases, it reacts with solvents [49, 50].

15.5 *N*-IODOSACCHARIN

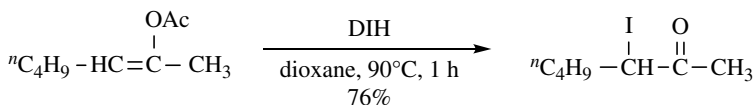
N-Iodosaccharin is a mild electrophilic iodinating reagent that is chemically stable and soluble in common polar organic solvents [51]. *N*-Iodosaccharin can convert various alkenes and activated aromatic rings into corresponding iodinated compounds (Scheme 15.35). In addition, *N*-iodosaccharin is an efficient reagent to synthesize benzyl and allyl iodides from the corresponding alcohols.

As shown in Scheme 15.35, *N*-iodosaccharin reacts with an aniline derivative to afford *p*-iodinated product with site selectively [51]. Moreover, *N*-iodosaccharin smoothly iodinate alkenes to afford the corresponding adducts of iodine in good yields (Scheme 15.36) [51]. It is noted that additions follow the Markovnikov rule with very high regioselectivity.

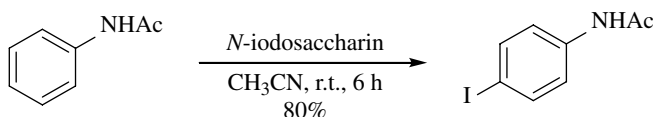
N-Iodosaccharin yields α -iodinated ketones by reacting with 1,3-dicarbonyl compounds or enol acetates (Scheme 15.37) [52]. This iodination proceeds under mild conditions without any additives, and the reaction is completed in a short time.



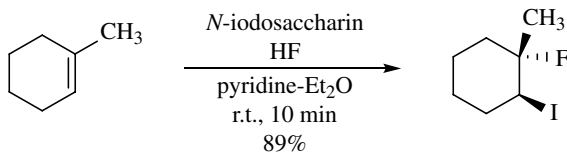
SCHEME 15.33



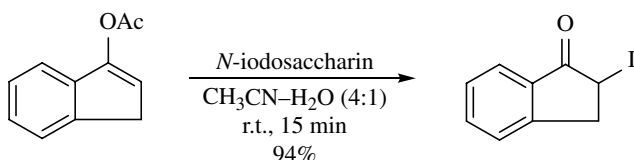
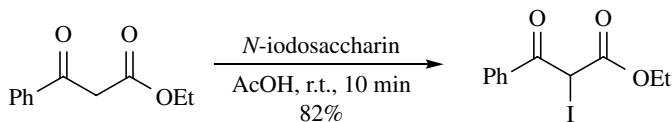
SCHEME 15.34



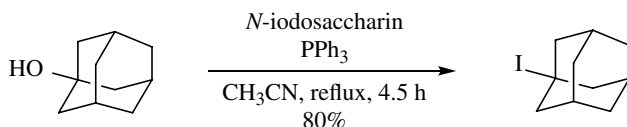
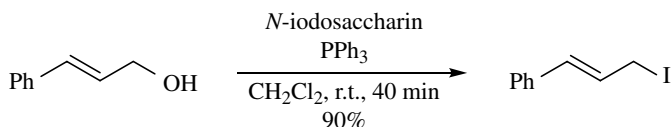
SCHEME 15.35



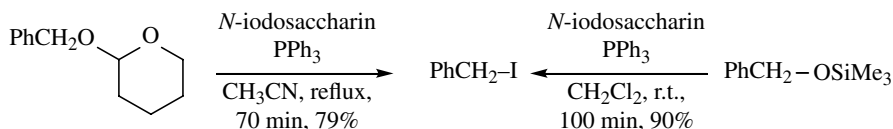
SCHEME 15.36



SCHEME 15.37



SCHEME 15.38



SCHEME 15.39

The most remarkable property of *N*-iodosaccharin is that various alcohols are directly iodinated in the presence of triphenylphosphine [53]. Thus, iodinations of allylic and benzylic alcohols are carried out, with good yields being obtained (Scheme 15.38). Furthermore, 1-adamantol is also iodinated in refluxing acetonitrile to produce 1-iodoadamantane (Scheme 15.38).

Some hydroxyl group-protected alcohols can be directly iodinated by the reaction with *N*-iodosaccharin (Scheme 15.39) [54]. This iodination is a convenient synthetic

method due to easily prepared iodinated compounds from alkoxysilanes or alkyl-oxytetrahydropyrans without deprotection (Scheme 15.39).

15.6 BIS(PYRIDINE)IODONIUM TETRAFLUOROBORATE

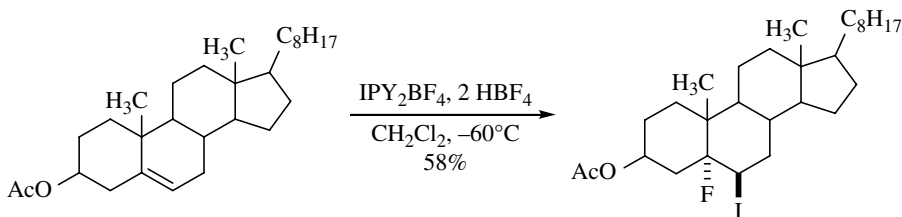
Bis(pyridine)iodonium tetrafluoroborate (IPy_2BF_4), often referred to as Barluenga's reagent, is a mild iodonium source and can be used as an electrophilic iodinating reagent [55]. IPy_2BF_4 is a chemically stable solid and is soluble in both organic and aqueous solvents. Due to these advantages, its reactivity has been widely studied, and a number of synthetic applications have been developed [55, 56]. IPy_2BF_4 reacts with unsaturated bonds such as alkenes [57], alkynes [58], and aromatic rings [59–61] to iodinate in a manner similar to other iodinating reagents. In the reaction of IPy_2BF_4 with alkenes in the presence of two equivalents of HBF_4 , vicinal fluoriodoalkanes are obtained with regioselectivity (Scheme 15.40) [57].

This reaction proceeds with the Markovnikov's rule for addition of electrophilic iodine to alkenes (Scheme 15.40). The acid HBF_4 is an essential additive to neutralize pyridine and liberates the iodonium source.

IPy_2BF_4 can also react with alkynes to afford 1,2-iodofunctionalized alkenes [58]. The regioselectivity of this reaction depends on the substituents of the alkynes and the nucleophilicity of the nucleophiles. In reactions using terminal alkynes, *anti*-addition products are obtained [58]. While using internal alkynes with stronger nucleophiles (I^-), *syn*-addition proceeds, and with weaker ones (CH_3COOH , HCOOH , Cl^- , pyridine), *anti*-addition products are given. Furthermore, a mixture of *syn*- and *anti*-adducts is produced by the reactions of borderline nucleophiles (Br^-) with internal alkynes or by using internal alkynes having a bulky group [58].

Monoiodination of aromatic rings is achieved by the reaction of IPy_2BF_4 with aromatic rings in the presence of HBF_4 [59, 60] or $\text{CF}_3\text{SO}_3\text{H}$ [59–61] with excellent regioselectivity. HBF_4 is suitable for activated aromatics, and $\text{CF}_3\text{SO}_3\text{H}$ is much more effective for iodinating deactivated aromatics (Scheme 15.41) [60].

The α -position of enamines is directly iodinated by the action of IPy_2BF_4 at room temperature [62]. Various enamines are generally used for α -iodination, and the desired α -iodoenamines are obtained in excellent yields even when tertiary enamines are employed (Scheme 15.42).

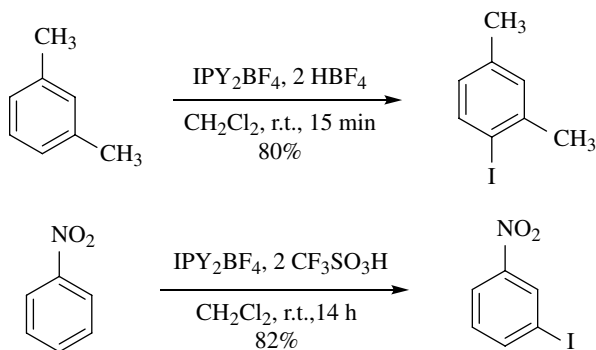


SCHEME 15.40

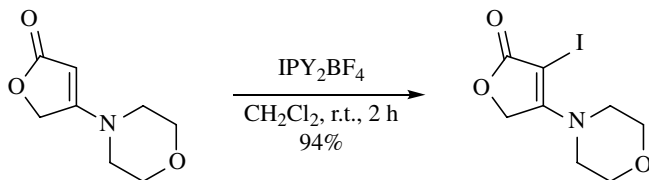
IPy_2BF_4 is an efficient reagent to perform heterocyclization under metal-free conditions [63–66]. Scheme 15.43 shows that some 2-alkynyl aromatics are successfully cyclized and the desired cyclic compounds are given [63, 65].

In some of the most remarkable results of this reaction, *N*-unprotected 2-alkynyl anilines are effectively cyclized to produce *N*-free 3-iodoindoles [63]. Easy access to isoquinolines is accomplished by using 2-alkynyl benzyl azides and IPy_2BF_4 under low temperature. NIS can also be used for this cyclization, but it needs to be carried out at 50°C to cyclize them [65].

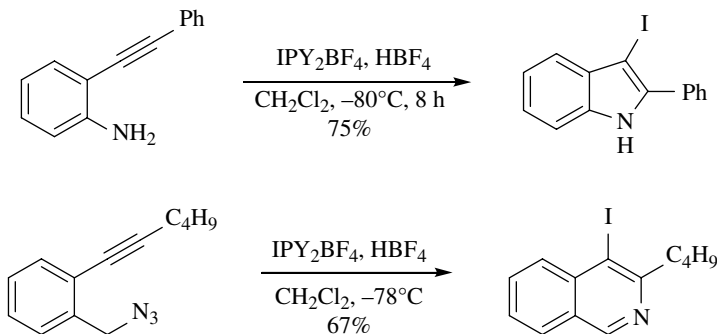
The carbon–silyl bond of vinylsilanes is easily replaced with the carbon–iodo bond by the action of IPy_2BF_4 in the presence of two equivalents of HBF_4 [67].



SCHEME 15.41



SCHEME 15.42



SCHEME 15.43

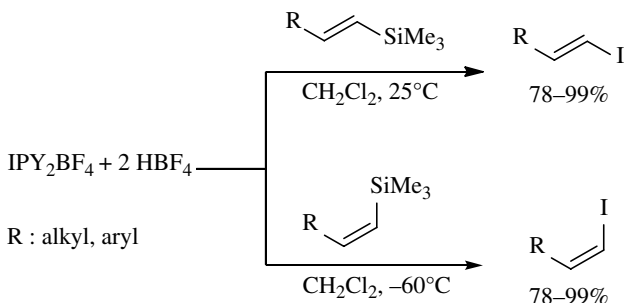
Transformation of *E*-vinylsilanes into the *E*-isomer of vinyl iodides is carried out at 25°C, while for the same transformation using *Z*-vinylsilanes, the reaction is carried out at -60°C to give the *Z*-isomer (Scheme 15.44) [56]. This reaction proceeds stereospecifically and affords the desired vinyl iodides with retention of configuration.

15.7 OTHERS

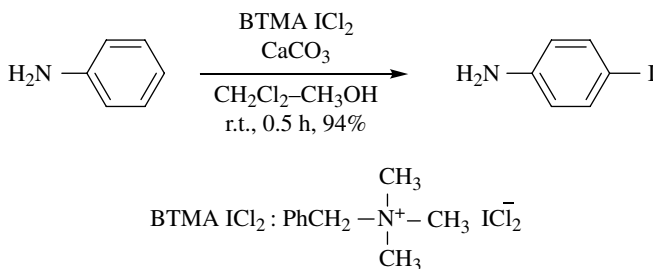
Other electrophilic iodinating reagents not mentioned earlier have been developed. Benzyltrimethylammonium dichloroiodate (BTMA ICl₂) [68] and pyridinium iodochloride (PyICl) [69] are used for iodination of aromatic rings. In addition, 1-chloro-2-iodoethane [70–72] has soft electrophilicity and is used as an efficient iodide donor to aromatic and thermally stable carbanions.

BTMA ICl₂ is a chemically stable solid having higher reactivity than molecular iodine, which effectively iodates phenols and aromatic amines in dichloromethane–methanol at room temperature (Scheme 15.45) [68]. Calcium carbonate powders are used for this transformation to remove the generated hydrogen chloride. It seems that methyl hypoiodite generated from BTMA ICl₂ and methanol acts as an active species [68].

PyICl can be prepared by mixing equivalent moles of pyridine with iodonemonochloride in acetic acid. PyICl is a pale yellow solid and can be handled safely [69]. PyICl is an efficient iodinating reagent to iodinate aromatic rings sim-



SCHEME 15.44



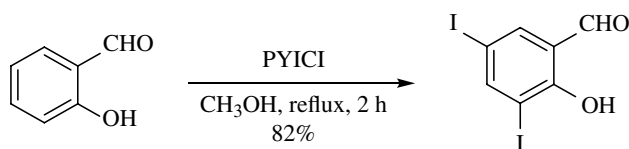
SCHEME 15.45

ilar to IPy_2BF_4 . IPy_2BF_4 requires some acids to neutralize excess pyridine and liberate the iodonium source. In contrast to IPy_2BF_4 , PyICl can be used immediately for iodination without any acids [69]. An example of one of the applications using PyICl as an iodinating reagent is that hydroxylated aromatic ketones and aldehydes are iodinated in methanol to afford the desired iodinated aromatic compounds in good yield (Scheme 15.46).

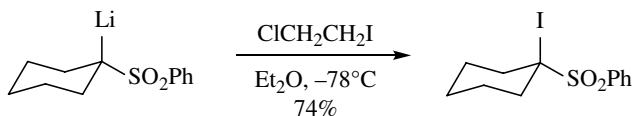
Aryl lithium and thermally stable lithium–carbanion species react with 1-chloro-2-iodoethane at low temperature to produce related iodinated compounds [70–72]. In this reaction, 1-chloro-2-iodoethane acts as a quencher to lithiated compounds similar to molecular iodine (Scheme 15.47) [70].

Some nucleophilic iodinating reagents are conveniently used in organic synthesis. Diphosphorustetraiodide (P_2I_4) [73] has been used for a long time and others such as trimethylsilyl iodide (TMSI) [74–76], diiodosilane (DIS) [75, 76], and methyltriphenoxyphosphonium iodide (MTPI) [77, 78] have the nucleophilic character and are efficiently used for the synthesis of iodinated compounds. Phosphorous chemistry–based nucleophilic iodination using PPh_3/I_2 /imidazole [79] and PPh_3/NIS [80] systems is one of the efficient methods for iodination of alcohols under mild conditions. Furthermore, *N,N*-dimethyl-*N*-(methylsulfanylmethylene)ammonium iodide is used as a mild nucleophilic iodide ion source [81].

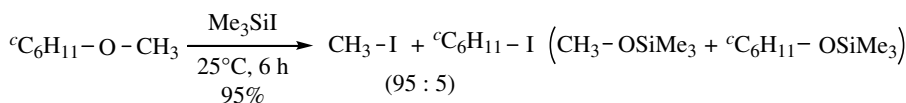
TMSI has both a hard Lewis acid moiety, which shows affinity to oxygen functionalities, and a soft nucleophilic iodide ion [74–76]. This remarkable chemical property enables it to cleave the carbon–oxygen bonds of ethers to afford the corresponding iodoalkanes. As an example, cyclohexyl methyl ether is cleaved by the action of TMSI on methyl iodide and cyclohexyl trimethylsilyl ether (Scheme 15.48) [74]. Only 5% of cyclohexyl iodide is observed.



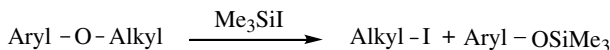
SCHEME 15.46



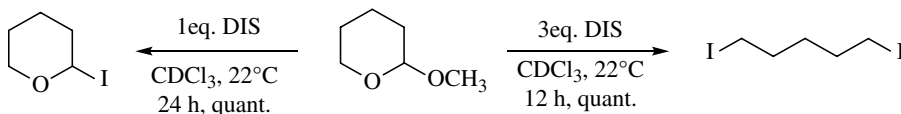
SCHEME 15.47



SCHEME 15.48



SCHEME 15.49



SCHEME 15.50

It is suggested that this reaction proceeds via coordination of oxygen to the silyl group with consequent nucleophilic attack of the iodide ion to cleave the carbon–oxygen bonds. Trityl, benzyl, and *tert*-butyl ethers are cleaved at a much faster rate than the other alkyl ethers such as methyl, ethyl, isopropyl, and cyclohexyl. When aryl alkyl ethers are employed, alkyl iodides are obtained as the sole product since iodide ion attacks only the alkyl groups (Scheme 15.49) [74].

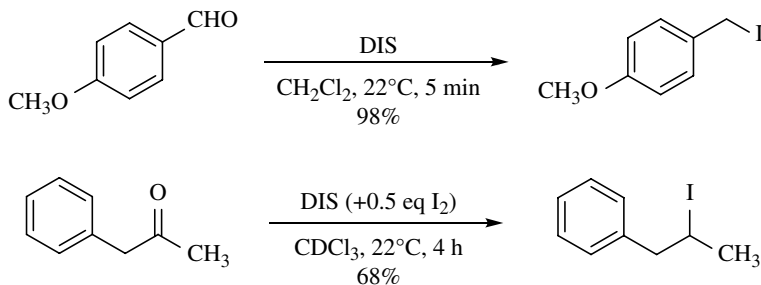
Diiodosilane (DIS) is a stronger Lewis acid than TMSI and is a good donor of iodide ions, which can be used for cleavage of the carbon–oxygen bonds of acetals whereupon reductive deoxygenation proceeds to afford iodoalkanes [75]. Furthermore, ketones and aldehydes are also reduced by DIS to produce primary and secondary iodoalkanes [75].

As shown in Scheme 15.50, when one equivalent of DIS is used, cleavage of the carbon–oxygen bond of 2-methoxytetrahydropyran occurs to replace the methoxy group with iodide. When three equivalents of DIS are used, reductive deoxygenation via cleavage of its carbon–oxygen bonds proceeds to produce 1,5-diiodopentane [75]. Reductive deoxygenation of aromatic acetals rapidly occurs within several minutes by using two equivalents of DIS, and the desired iodoalkanes are produced. However, reductive deoxygenation of aliphatic acetals requires a longer time (30 min to 24 h) to complete the reduction.

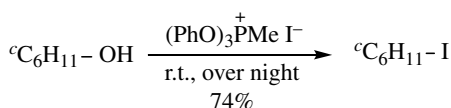
DIS effectively reduces aldehydes and ketones to produce the corresponding primary and secondary iodoalkanes [75]. Aromatic aldehydes are immediately reduced, while reductive iodination of aliphatic aldehydes and ketones takes more time compared with that of aromatic aldehydes (Scheme 15.51).

MTPI is a solid compound and stable in the absence of moisture [77, 78]. MTPI is effectively used for iodination of alcohols [77]. It is especially effective for iodinating the hydroxy groups of nucleosides [78]. The reaction of MTPI with cyclohexanol is carried out at room temperature without solvent, and iodocyclohexane is obtained in 74% yield (Scheme 15.52) [77].

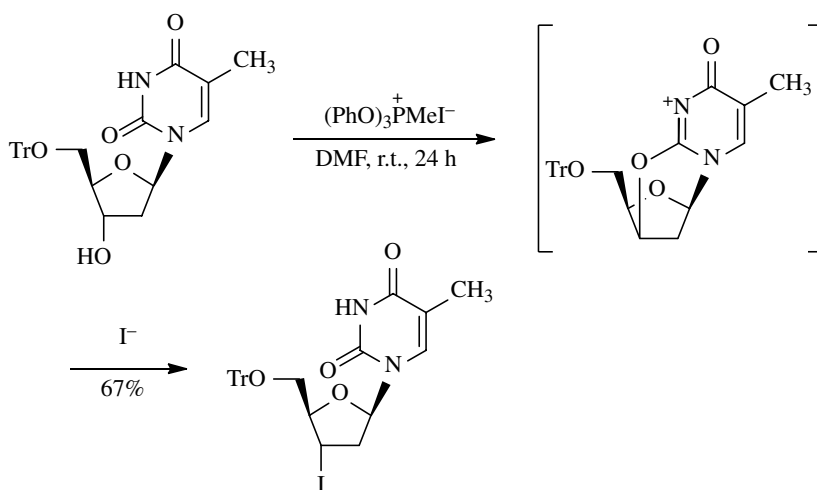
MTPI is prepared *in situ* from triphenylphosphite and methyl iodide. Otherwise, MTPI is commercially available and it can be used as an iodinating reagent without further purification. MTPI directly iodates the 3'-hydroxy groups of uridine and thymidine derivatives with α -selectivity [77]. For example, α -selective 3'-iodination of 5'-*O*-tritylthymidine is accomplished by using MTPI in DMF to produce 3'-iodo-5'-*O*-tritylthymidine in 67% yield (Scheme 15.53) [77].



SCHEME 15.51



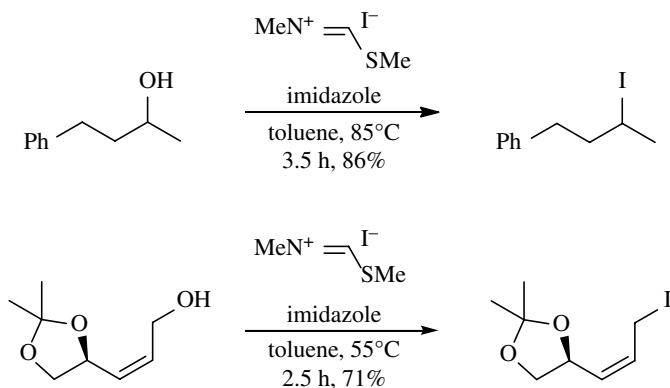
SCHEME 15.52



SCHEME 15.53

In this reaction, the $O^2,3'$ -anhydrothymidine derivative is formed as an intermediate by conjugation of the pyrimidine base with the $3'$ -hydroxy group. It is subsequently opened by the attack of an iodide ion from the α -face. When using thymidine and an excess of MTPI in DMF, a diiodination reaction proceeds, and the desired $3',5'$ -diiodothymidine is produced in 76% yield. Similar iodination of the thymidine derivative is performed by the PPh_3/I_2 system [82], but the yield of $3'$ -iodothymidine derivative is insufficient (47%).

N,N-Dimethyl-*N*-(methylsulfanylmethylene)ammonium iodide is an efficient nucleophilic iodinating reagent, and various alcohols are directly transformed into



SCHEME 15.54

iodoalkanes [81]. Primary and secondary alcohols are directly iodinated in good yield. In addition, allylic alcohols are successfully iodinated to afford the desired allylic iodides (Schemes 15.54).

One of the excellent characteristics of *N,N*-dimethyl-*N*-(methylsulfanylmethylene) ammonium iodide is that purification is easier since by-products of the reaction can be easily removed. Phosphorous-based iodinating reagents often make the formed crystalline phosphine oxides difficult to remove.

REFERENCES

- [1] Smith MB. *Encyclopedia of Reagents for Organic Synthesis, Iodine*. Chichester: John Wiley & Sons; 1995. p 2796.
- [2] Onoe A, Uemura S, Okano M. Alkoxythiocyanation and alkoxyiodination of olefins with copper(II) salts. *Bull Chem Soc Jpn* 1974;47:2818.
- [3] Horiuchi CA, Satoh JY. Syntheses of steroidal *trans*-iodo acetates. *Bull Chem Soc Jpn* 1987;60:426.
- [4] Horiuchi CA, Nishio Y, Gong D, Fujisaki T, Kiji S. A new alkoxyiodination and nitrate-iodination of olefins using iodine-cerium(IV) ammonium nitrate. *Chem Lett* 1991;20:607.
- [5] Wen R, Laronze J-Y, Lévy J. Methylene-indolines, indoleines and indoleniniums XVII. Rearrangement of de-ethyltabersonine in acetic acid. *Heterocycles* 1984;22:1061.
- [6] Knapp S, Rodriques KE, Levorse AT, Ornaf RM. *Tetrahedron Lett* 1985;26:1803.
- [7] Bridges AJ, Fischer JW. A simple preparation of several new 2,3- and 1,2,3-substituted buta-1,3-dienes from 1,4-dichlorobutene. *Tetrahedron Lett* 1983;24:445.
- [8] Uemura S, Onoe A, Okano M. Stereochemistry of chlorination and chloroiodination of alkylphenylacetylenes by CuCl_2 . *J Chem Soc Chem Commun* 1975:925.
- [9] Merkushev EB. Advances in the synthesis of iodoaromatic compounds. *Synthesis* 1988:923.
- [10] Uemura S, Onoe A, Okano M. Aromatic bromination and iodination with mixtures of antimony (V) chloride and halogens. *Bull Chem Soc Jpn* 1974;47:147.

- [11] Baird WC, Surridge JH. Halogenation with copper(II) halides. Synthesis of aryl iodides. *J Org Chem* 1970;35:3436.
- [12] Sugita T, Idei M, Ishibashi Y, Takegami Y. Aromatic iodination with aluminum and copper(II) chlorides and iodine. *Chem Lett* 1982;11:1481.
- [13] Sugiyama T. A mild and convenient procedure for conversion of aromatic compounds into their iodides using ammonium hexanitratocerate(IV). *Bull Chem Soc Jpn* 1981;54:2847.
- [14] Horiuchi CA, Satoh JY. A convenient procedure for iodination of electron-rich aromatic compounds using iodine-copper(II) acetate. *Bull Chem Soc Jpn* 1984;57:2691.
- [15] Freiberg LA. Mechanism of oxidation of enolizable nonmethyl ketones by base and iodine. The role of atmospheric oxygen. *J Am Chem Soc* 1967;89:5297.
- [16] Rathke MW, Lindert A. The halogenation of lithium ester enolates. A convenient method for the preparation of α -iodo and α -bromo esters. *Tetrahedron Lett* 1971;12:3995.
- [17] Horiuchi CA, Satoh JY. Novel α -iodination of ketones using iodine/copper(II) acetate. *Synthesis* 1981:312.
- [18] Horiuchi CA, Kiji S. A new α -iodination of ketones using iodine-cerium(IV) ammonium nitrate. *Chem Lett* 1988;17:31.
- [19] Horiuchi CA, Kiji S. A new α -iodination of ketones using iodine-ammonium cerium(IV) nitrate in alcohol or acetic acid. *Bull Chem Soc Jpn* 1997;70:421.
- [20] Rubottom GM, Mott RC. Reaction of enol silyl ethers with silver acetate-iodine. Synthesis of α -iodo carbonyl compounds. *J Org Chem* 1979;44:1731.
- [21] Horiuchi CA, Satoh JY. A new synthesis of α -iodo carboxylic acid using iodine-copper salt. *Chem Lett* 1984;13:1509.
- [22] Mongin F, Quéguiner G. Advances in the directed metallation of azines and diazines (pyridines, pyrimidines, pyrazines, pyridazines, quinolines, benzodiazines and carbolines). Part 1: Metallation of pyridines, quinolines and carbolines. *Tetrahedron* 2001;57:4059.
- [23] Lee W-I, Jung J-W, Sim J, An H, Suh Y-G. Microwave-assisted synthesis of 3-substituted indoles via intramolecular arene-alkene coupling of *o*-iodoanilino enamines. *Tetrahedron* 2013;69:7211.
- [24] Saulnier MG, Gribble GW. Generation and reactions of 3-lithio-1-(phenylsulfonyl) indole. *J Org Chem* 1982;47:757.
- [25] Usanov DL, Yamamoto H. Enantioselective alkynylation of aldehydes with 1-haloalkynes catalyzed by tethered bis(8-quinolinato) chromium complex. *J Am Chem Soc* 2011;133:1286.
- [26] Hoshi M, Hayatsu T, Okimoto M, Kodama S. Transfer of alk-1-enyl group from boron to tin: A highly stereoselective synthesis of (*E*)-alk-1-enyltributylstannanes. *Synlett* 2009:2945.
- [27] Zurwerra D, Gertsch J, Altmann K-H. Synthesis of (–)-dactylolide and 13-desmethylene-(–)-dactylolide and their effects on tubulin. *Org Lett* 2010;12:2302.
- [28] Johnsson R, Meijer A, Ellervik U. Mild and efficient direct aromatic iodination. *Tetrahedron* 2005;61:11657.
- [29] Padwa A, Blacklock T, Tremper A. 3-Phenyl-2*H*-azirine-2-carboxaldehyde. *Org Synth* 1977;57:83.
- [30] Asakura J-I, Robins MJ. Cerium(iv) catalyzed iodination at C5 of uracil nucleosides. *Tetrahedron Lett* 1988;29:2855.
- [31] Piao D, Basavapathruni A, Iyidogan P, Dai G, Hinz W, Ray AS, Murakami E, Feng JY, You F, Dutschman GE, Austin DJ, Parker KA, Anderson KS. Bifunctional inhibition of

- HIV-1 reverse transcriptase: A first step in designing a bifunctional triphosphate. *Bioorg Med Chem Lett* 2013;23:1511.
- [32] Robins MJ, Barr PJ, Giziewicz J. Nucleic acid related compounds. 38. Smooth and high-yield iodination and chlorination at C-5 of uracil bases and *p*-toluyl-protected nucleosides. *Can J Chem* 1982;60:554.
- [33] Kabalka GW, Gooch EE, Hsu HC. A convenient procedure for the syntheses of vinyl iodides via the reaction of iodine monochloride with vinylboronic acids. *Synth Commun* 1981;11:247.
- [34] Funk RL, Vollhardt KPC. Hexa-1,5-diyn-3-ol ethers as tetramethynyl synthons in cobalt-catalysed acetylene co-oligomerisations; a one-step synthesis of 2,3,6,7-tetrakis(trimethylsilyl)naphthalene. *J Chem Soc Chem Commun* 1976:833.
- [35] Kim CU, Misco PF. Facile, highly stereoselective synthesis of 2',3'-dideoxy- and 2',3'-didehydro-2',3'-dideoxy nucleosides via a furanoid glycal intermediate. *Tetrahedron Lett* 1992;33:5733.
- [36] Bongini A, Cardillo G, Orena M, Sandri S, Tomasini C. Factors affecting the regioselectivity of allylic imidate iodocyclization. *J Org Chem* 1986;51:4905.
- [37] Ma S, Lu L. An efficient stereoselective synthesis of 4,5-*trans*-1,5-*cis*-3-oxabicyclo[3.1.0]hexan-2-ones via the iodolactonization of alkylidenecyclopropyl esters. *J Org Chem* 2005;70:7629.
- [38] Xin X, Wang D, Wu F, Li X, Wan B. Cyclization and N-iodosuccinimide-induced electrophilic iodocyclization of 3-aza-1,5-enynes to synthesize 1,2-dihydropyridines and 3-iodo-1,2-dihydropyridines. *J Org Chem* 2013;78:4065.
- [39] Sniady A, Wheeler KA, Dembinski R. 5-*Endo-dig* electrophilic cyclization of 1,4-disubstituted but-3-yn-1-ones: Regiocontrolled synthesis of 2,5-disubstituted 3-bromo- and 3-iodofurans. *Org Lett* 2005;7:1769.
- [40] Huber F, Kirsch SF. NIS-Mediated electrophilic cyclization of 3-silyloxy-1,*n*-enynes. *J Org Chem* 2013;78:2780.
- [41] Sreedhar B, Reddy PS, Madhavi M. Rapid and catalyst-free α -halogenation of ketones using *N*-halosuccinamides in DMSO. *Synth Commun* 2007;37:4149.
- [42] Iwaoka T, Murohashi T, Katagiri N, Sato M, Kaneko C. Use of 1,3-dioxin-4-ones and related compounds in synthesis. Part 37. 5-Trifluoromethyl-1,3-dioxin-4-ones as versatile building blocks for trifluoromethylated aliphatic compounds. *J Chem Soc Perkin Trans* 1992;1:1393.
- [43] Kumar V, Yapp J, Muroyama A, Malhotra SV. Highly efficient method for C-5 halogenation of pyrimidine-based nucleosides in ionic liquids. *Synthesis* 2009:3957.
- [44] Olah GA, Wang Q, Sandford G, Prakash GKS. Iodination of deactivated aromatics with *N*-iodosuccinimide in trifluoromethanesulfonic acid (NIS- $\text{CF}_3\text{SO}_3\text{H}$) via in situ generated superelectrophilic iodine(I) trifluoromethanesulfonate. *J Org Chem* 1993;58:3194.
- [45] Prakash GKS, Mathew T, Hoole D, Esteves PM, Wang Q, Rasul G, Olah GA. *N*-Halosuccinimide/ $\text{BF}_3\text{-H}_2\text{O}$, efficient electrophilic halogenating systems for aromatics. *J Am Chem Soc* 2004;126:15770.
- [46] Kalyani D, Dick AR, Anani WQ, Sanford MS. A simple catalytic method for the regioselective halogenation of arenes. *Org Lett* 2006;8:2523.
- [47] Du B, Jiang X, Sun P. Palladium-catalyzed highly selective *ortho*-halogenation (I, Br, Cl) of aryl nitriles via sp^2 C-H bond activation using cyano as directing group. *J Org Chem* 2013;78:2786.

- [48] Virgil SC. *Encyclopedia of Reagents for Organic Synthesis*, 1,3-Diiodo-5,5-dimethylhydantoin. Chichester: John Wiley & Sons; 1995. p 1895.
- [49] Chaikovskii VK, Filimonov VD, Funk AA, Skorokhodov VI, Ogorodnikov VD. 1,3-Diiodo-5,5-dimethylhydantoin—An efficient reagent for iodination of aromatic compounds. *Russ J Org Chem* 2007;43:1291.
- [50] Orazi OO, Corral RA, Bertorello HE. *N*-Iodohydantoin. II. Iodinations with 1,3-diiodo-5,5-dimethylhydantoin. *J Org Chem* 1965;30:1101.
- [51] Dolenc D. *N*-Iodosaccharin - a new reagent for iodination of alkenes and activated aromatics. *Synlett* 2000:544.
- [52] Dolenc D. Iodination of enol acetates and 1,3-diones using *N*-iodosaccharin. *Synth Commun* 2003;33:2917.
- [53] Firouzbadi H, Iranpoor N, Ebrahimzadeh F. Facile conversion of alcohols into their bromides and iodides by *N*-bromo and *N*-iodosaccharins/triphenylphosphine under neutral conditions. *Tetrahedron Lett* 2006;47:1771.
- [54] Firouzbadi H, Iranpoor N, Ebrahimzadeh F. Direct conversion of trimethylsilyl and tetrahydropyranyl ethers into their bromides and iodides under neutral conditions using *N*-bromo and *N*-iodosaccharins in the presence of triphenylphosphine. *J Iran Chem Soc* 2008;5:400.
- [55] Chalker JM, Thompson AL, Davis BG. Safe and scalable preparation of Barluenga's reagent (bis(pyridine)iodonium(I) tetrafluoroborate). *Org Synth* 2010;87:288.
- [56] Barluenga J. Transferring iodine: more than a simple functional group exchange in organic synthesis. *Pure Appl Chem* 1999;71:431.
- [57] Barluenga J, Campos PJ, Gonzalez JM, Suarez JL, Asensio G. Regio- and stereoselective iodofluorination of alkenes with bis(pyridine)iodonium(I) tetrafluoroborate. *J Org Chem* 1991;56:2234.
- [58] Barluenga J, Rodríguez MA, Campos PJ. Electrophilic additions of positive iodine to alkynes through an iodonium mechanism. *J Org Chem* 1990;55:3104.
- [59] Barluenga J, González JM, García-Martín MA, Campos PJ, Asensio G. An expeditious and general aromatic iodination procedure. *J Chem Soc Chem Commun* 1992:1016.
- [60] Barluenga J, Gonzalez JM, García-Martín MA, Campos PJ, Asensio G. Acid-mediated reaction of bis(pyridine)iodonium(I) tetrafluoroborate with aromatic compounds. A selective and general iodination method. *J Org Chem* 1993;58:2058.
- [61] Barluenga J, González JM, García-Martín MA, Campos PJ. Polyiodination on benzene at room temperature a regioselective synthesis of derivatives. *Tetrahedron Lett* 1993; 34:3893.
- [62] Campos PJ, Arranz J, Rodríguez MA. α -Iodination of enaminones with bis(pyridine) iodonium(I) tetrafluoroborate. *Tetrahedron Lett* 1997;38:8397.
- [63] Barluenga J, Trincado M, Rubio E, González JM. IPy_2BF_4 -Promoted intramolecular addition of masked and unmasked anilines to alkynes: Direct assembly of 3-iodoindole cores. *Angew Chem Int Ed* 2003;42:2406.
- [64] Barluenga J, Vázquez-Villa H, Ballesteros A, González JM. Cyclization of carbonyl groups onto alkynes upon reaction with IPy_2BF_4 and their trapping with nucleophiles: A versatile trigger for assembling oxygen heterocycles. *J Am Chem Soc* 2003;125:9028.
- [65] Fischer D, Tomeba H, Pahadi NK, Patil NT, Yamamoto Y. Synthesis of 1,3,4-trisubstituted isoquinolines by iodine-mediated electrophilic cyclization of 2-alkynyl benzyl azides. *Angew Chem Int Ed* 2007;46:4764.

- [66] Crone B, Kirsch SF, Umland K-D. Electrophilic cyclization of 1,5-enynes. *Angew Chem Int Ed* 2010;49:4661.
- [67] Barluenga J, Alvarez-García LJ, González JM. IPy_2BF_4 is also a useful reagent for stereospecific iodine-silicon exchange in open chain trimethylsilylalkenes. *Tetrahedron Lett* 1995;36:2153.
- [68] Kajigaeshi S, Kakinami T, Yamasaki H, Fujisaki S, Okamoto T. Halogenation using quaternary ammonium polyhalides. VII. Iodination of aromatic amines by use of benzyltrimethylammonium dichloroiodate(1—). *Bull Chem Soc Jpn* 1988;61:600.
- [69] Khansole SV, Mokle SS, Sayyed MA, Vibhute YB. Pyridinium iodochloride: An efficient reagent for iodination of hydroxylated aromatic ketones and aldehydes. *J Chin Chem Soc* 2008;55:871.
- [70] Anderson MB, Lamothe M, Fuchs PL. Intramolecular acylation of an α -sulfonyl anion generated via halogen-metal exchange of an α -halosulfone bearing an unsymmetrical anhydride. *Tetrahedron Lett* 1991;32:4457.
- [71] Ronald RC, Lansinger JM, Lillie TS, Wheeler CJ. Total synthesis of frustulosin and aurocitrin. *J Org Chem* 1982;47:2541.
- [72] Nevill CR, Fuchs PL. Annulation reactions of *ortho*-chloromethyl aryl cuprates. *Synth Commun* 1990;20:761.
- [73] Lauwers M, Regnier B, Eenoo MV, Denis JN, Krief A. Diphosphorus tetraiodine (P_2I_4) a valuable reagent for regioselective synthesis of iodoalkanes from alcohols. *Tetrahedron Lett* 1979;20:1801.
- [74] Jung ME, Lyster MA. Quantitative dealkylation of alkyl ethers via treatment with trimethylsilyl iodide. A new method for ether hydrolysis. *J Org Chem* 1977;42:3761.
- [75] Keinan E, Perez D, Sahai M, Shvily R. Diiodosilane. 2. A multipurpose reagent for hydrolysis and reductive iodination of ketals, acetals, ketones, and aldehydes. *J Org Chem* 1990;55:2927.
- [76] Keinan E, Sahai M. Diiodosilane. 3. Direct synthesis of acyl iodides from carboxylic acids, esters, lactones, acyl chlorides and anhydrides. *J Org Chem* 1990;55:3922.
- [77] Rydon HN. Alkyl iodides: Neopentyl iodide and iodocyclohexane. *Org Synth* 1971;51:44.
- [78] Verheyden JPH, Moffatt JG. Halosugar nucleosides. II. Iodination of secondary hydroxyl groups of nucleosides with methyltriphenoxyposphonium iodide. *J Org Chem* 1970;35:2868.
- [79] Garegg PJ, Samuelsson B. Novel reagent system for converting a hydroxy-group into an iodo-group in carbohydrates with inversion of configuration. *J Chem Soc Chem Commun* 1979:978.
- [80] Hanessian S, Ponpipom MM, Lavalley P. Procedures for the direct replacement of primary hydroxyl groups in carbohydrates by halogen. *Carbohydr Res* 1972;24:45.
- [81] Ellwood AR, Porter MJ. Selective conversion of alcohols into alkyl iodides using a thioiminium salt. *J Org Chem* 2009;74:7982.
- [82] Verheyden JPH, Moffatt JG. Halo sugar nucleosides. III. Reactions for the chlorination and bromination of nucleoside hydroxyl groups. *J Org Chem* 1972;37:2289.

16

OXIDIZING AGENTS

TOSHIFUMI DOHI¹ AND YASUYUKI KITA²

¹ College of Pharmaceutical Sciences, Ritsumeikan University, Kusatsu, Shiga, Japan

² Emeritus Professor of Osaka University, Ritsumeikan University, Kusatsu, Shiga, Japan

The simplest iodine-based oxidant in organic synthesis is molecular iodine. Iodine can also constitute various inorganic compounds owing to its divertible oxidation states, some of which possess oxidizing abilities. For example, some oxides, such as iodine pentoxide (I_2O_5) and iodic acid (HIO_3) as well as the inorganic salt sodium periodate (NaIO_4), are preferably used as water-soluble oxidizing agents in aqueous synthesis. On the other hand, organic iodides having high-valent forms also act as an oxidant, and hypervalent iodine reagents show unique reactivities for many useful transformations.

In this chapter, we succinctly introduce these iodine-based oxidants dealing with brief information on their reactivity patterns.

16.1 MOLECULAR IODINE

Molecular iodine has powerful oxidation ability to oxidize various substrates. As a result, it was widely utilized as an economic oxidizing agent to induce many transformations, such as early oxidation of sulfides, [1] aromatic compounds, and various molecules containing oxygen functional groups, oxidative protection and deprotection of some functional groups, some carbon–carbon bond formation of heterocycles, in extensive studies [2]. In addition, a method for simple, efficient, and high-yield oxidation of alcohols with broad generality of substrates was recently established by combined use of molecular iodine and potassium carbonate [3]. Benzylic and aliphatic secondary alcohols were smoothly oxidized to the corresponding ketones with excess amount of molecular iodine and potassium carbonate under the refluxing

conditions in *t*-butyl alcohol solvent. For example, sterically hindered menthol and protected-D-ribofuranose were effectively converted to menthone and the D-ribofuranone in good yields (Fig. 16.1, Eq. 1). On the other hand, the oxidation of primary alcohols provided the corresponding esters via aldehydes under the same conditions in methanol (Eq. 2) as well as other alcohols. Similarly, oxidation of alcohols can occur under aqueous conditions in the presence of potassium iodide using the molecular iodine/potassium carbonate combination [4]. In this case, aldehydes were selectively obtained in excellent yields.

Molecular iodine also transforms aldehydes to nitriles in ammonia water [5]. Hence, the direct synthesis of nitriles from alcohols has become possible in a one-pot manner by conversion of alcohols to aldehydes followed by formation of nitriles. Thus, the treatment of aromatic and aliphatic alcohols with iodine in ammonia water was carried out to obtain the desired nitriles in high yields (Eq. 3) [6].

Dehydrogenation was also observed in the aromatization of Hantzsch 1,4-dihydropyridines [7]. It is possible to aromatize 4-alkyl- or aryl-substituted Hantzsch 1,4-dihydropyridines to the corresponding pyridines in high yields by treatment with molecular iodine in refluxing methanol (Eq. 4).

In addition, the molecular iodine/potassium carbonate in organic solvent and molecular iodine/potassium carbonate/potassium iodide system in water can oxidize the carbon–nitrogen bond of imidazolidines [8]. This enables the direct synthesis of

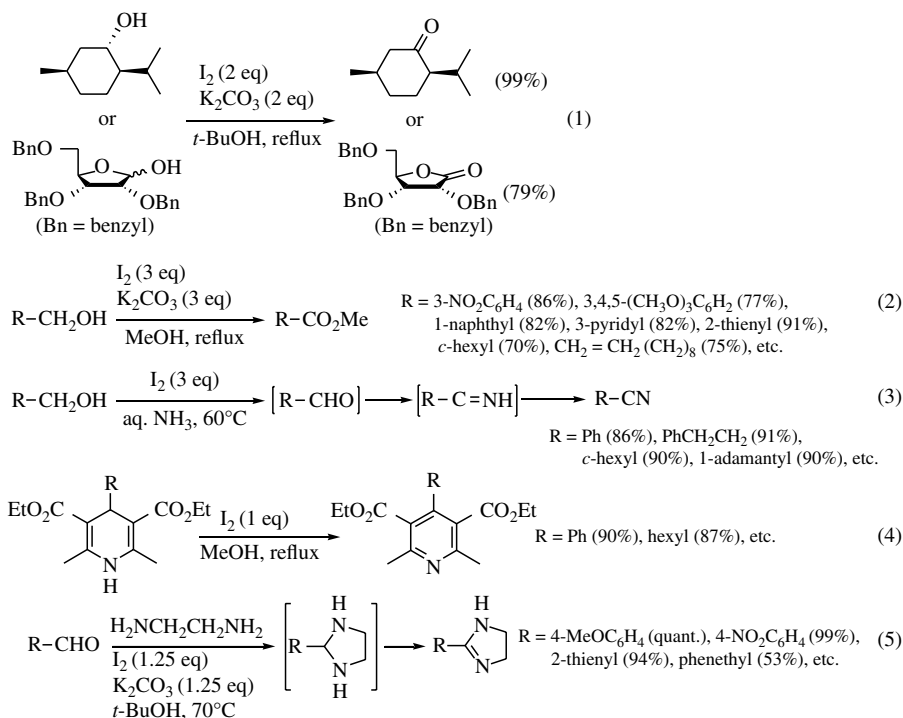


FIGURE 16.1 Dehydrogenative oxidations by molecular iodine.

2-imidazolines and benzimidazoles by dehydrogenation from aldehydes and ethylenediamines or phenylene diamines, respectively, via in situ formed imidazolidines (Eq. 5). In the latter case with potassium iodide, generation of potassium triiodide (KI_3) during the reactions was proposed as the active species for the oxidations.

16.2 INORGANIC IODINE COMPOUNDS

Among the iodine-containing inorganic oxidants, I_2O_5 , HIO_3 , and NaIO_4 are the commercially available compounds typically used in synthesis. Like other iodine-based oxidants, these inorganic compounds are stable microcrystalline solids in air at room temperature. Nicolaou and coworkers demonstrated that both I_2O_5 and HIO_3 can serve as mild and selective oxidizing agents for α,β -dehydrogenation of aldehydes and ketones in dimethyl sulfoxide (DMSO) (Fig. 16.2) [9]. For example, the dehydrogenation of 4-(1,1-dimethylethyl)cyclohexanone using HIO_3 in DMSO provides 4-(1,1-dimethylethyl)-2-cyclohexen-1-one with 95% yield (Eq. 1). As active species at 80°C , the monomeric and oligomeric complexes with DMSO were isolated and determined to involve I_2O_5 and HIO_3 into the efficient oxidations. Although this type of dehydrogenation can also proceed with other pentavalent 1-hydroxy-1,2-benziodoxol-3(1*H*)-one 1-oxides (IBX) (see Section 16.3.5), a remarkable difference to be noted is that alcohols do not react with HIO_3 and the aldehydes derived from the oxidation of primary alcohols were not detected at all during the dehydrogenation. This unique chemoselective issue permits the selective dehydrogenation of aldehydes and ketones in the presence of additional alcohols.

I_2O_5 and HIO_3 can promote aromatization of Hantzsch 1,4-dihydropyridines (see Section 16.1) and 1,3,5-trisubstituted pyrazolines in water [10]. These heterocyclic compounds were efficiently converted to the corresponding pyridines and pyrazoles by the treatment of these water-soluble inorganic oxidants. HIO_3 also effected oxidation of sulfides to sulfoxides and thiols to disulfides in an aqueous medium [11].

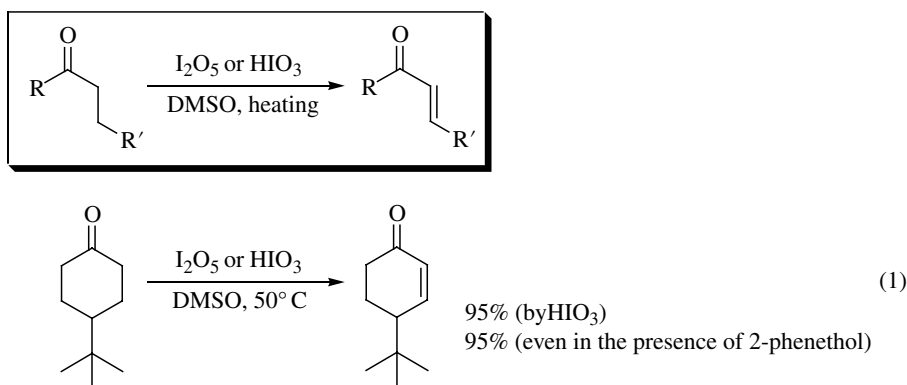


FIGURE 16.2 Dehydrogenation of carbonyl compounds to α,β -unsaturated compounds using inorganic iodine oxidants.

NaIO_4 demonstrates powerful oxidation abilities acting as a heptavalent inorganic iodine oxidant [12]. It is sometimes used as a stronger oxidant in the conversion of sulfides to sulfoxides at a lower temperature. Phenols and hydrazones can be oxidized into the corresponding quinones and ketones in an aqueous organic solvent. The most popular use of this reagent in organic synthesis is for the oxidative carbon–carbon bond cleavage of vicinal diols. Due to the high chemoselectivity over various other functional groups, the periodate cleavage was historically used for detection of 1,2-diol components in complex organic molecules in their structural assignment in old years.

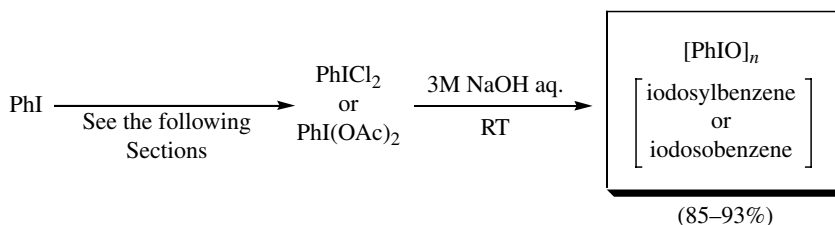
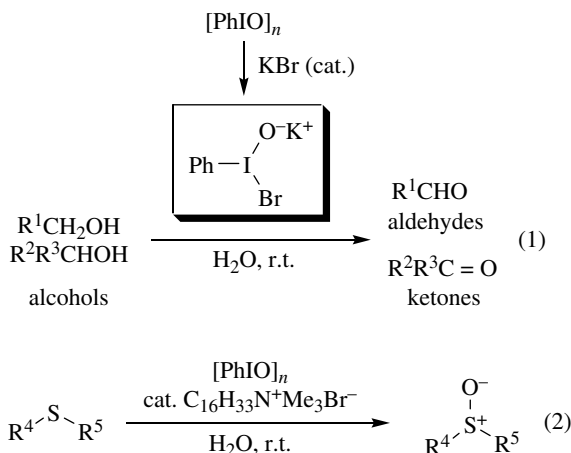
16.3 ORGANIC HYPERVALENT IODINE COMPOUNDS

With the increasing impetus for developing greener synthetic processes, hypervalent iodine reagent has recently received much attention in organic synthesis as an oxidant based on organic iodides by virtue of its safety and environmental friendliness. As documented in detail in several books and reviews [13], the synthetic versatility of these reagents has been expanding day by day. A number of trivalent and pentavalent iodine reagents, for example, iodobenzene diacetate, [bis(trifluoroacetoxy)iodo]benzene, [hydroxy(tosyloxy)iodo]benzene (Koser's reagent), iodosobenzene, Dess–Martin periodinane (DMP), and 2-iodoxybenzoic acid, are now commercially available, and they serve as a useful synthetic tool showing reactivities similar to that of a series of heavy metals, such as lead(IV)-, mercury(II)-, cadmium(IV)-, and thallium(III)-based agents. These facets inspired us to use the organo-oxidant in the synthesis of natural products and other complex molecules [14]. The recent successes in their catalytic uses further encourage the design of new organic iodine compounds, especially for asymmetric oxidations, for use as an oxidation organocatalyst, which looks promising with regard to new applications and developments in the future [15, 16]. From the next section on, general preparations for these hypervalent iodine compounds including their derivatives are described along with their typical reactivities in organic transformations.

16.3.1 Iodosylbenzene (Iodosobenzene)

Polymeric iodosylbenzene, $(\text{PhIO})_n$, is readily prepared upon treatment of iodobenzene diacetate (phenyliodine(III) diacetate, $\text{PhI}(\text{OAc})_2$) with strong alkaline aqueous solution (Fig. 16.3) [17]. Alternatively, it is obtained from iodobenzene dichloride. It is a yellowish amorphous powder stable in air and toward moisture at room temperature with light protection. Other iodosylarene derivatives having different aromatic moieties can be obtained in a similar way using corresponding aryl iodine diacetates and chlorides.

Iodosylbenzene is only slightly soluble in water due to its polymeric structure, and its insolubility in most organic solvents except for alcohols limits its applications in organic synthesis. Therefore, it is usually utilized for oxidations after suitable activations, such as by adding some Brønsted and Lewis acids (boron trifluoride, trimethylsilyl triflate, etc.), to decompose its polymeric network [18]. As an additive,

**FIGURE 16.3** Preparation of iodosylbenzene.**FIGURE 16.4** Oxidation of alcohols and sulfides by using iodosylbenzene with bromide salts.

inorganic and organic bromides, such as potassium bromide and cetyltrimethylammonium bromide, are also effective for the activation of iodosylbenzene. Iodosobenzene/potassium bromide was used for aqueous oxidations of various alcohols to aldehydes and ketones, and further carboxylic acids (Fig. 16.4, Eq. 1) [19]. It should be mentioned that iodosobenzene is inherently not so reactive as to effectively cause the alcohol oxidations, and electrospray ionization (ESI) mass spectrometric studies might reveal the participation of in situ formed reactive hypervalent iodine species, $[\text{PhIBrO}^-]$, for initiating the reactions. On the other hand, quaternary ammonium salts can alternatively catalyze the selective oxidation of sulfides to sulfoxides by iodosylbenzene (Eq. 2) [20]. The micellar and reverse micellar systems consisting of iodosobenzene and cetyltrimethylammonium bromide were proposed for the new activation modes.

Recently, a new idea to isolate and use monomeric iodosylbenzene species was suggested by Ochiai's research group, who prepared hydroxy(phenyl)iodonium ion, $\text{PhI}^+(\text{OH})\text{BF}_4^-$, as a complex with 18-crown-6 (18C6), by treatment of $(\text{PhIO})_n$ with tetrafluoroboric acid (HBF_4) in the presence of 18C6 (Fig. 16.5) [21]. The obtained prisms are stable enough to be suitable for characterization by X-ray structural analysis.

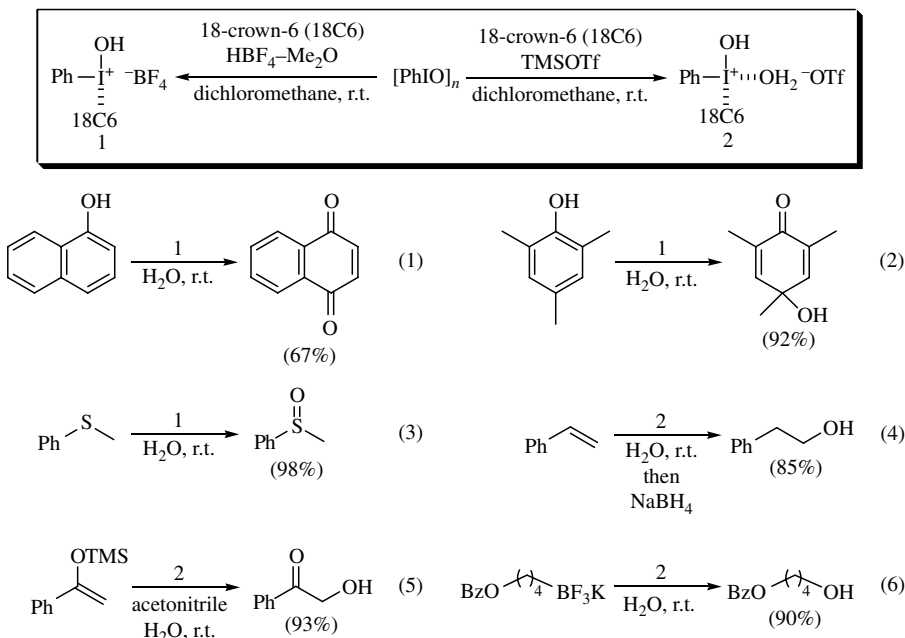


FIGURE 16.5 Oxidations using highly reactive iodosylbenzene monomer - 18C6 complexes.

The related complex, $\text{PhI}(\text{OH})\text{OTf} \cdot 18\text{C6} \cdot \text{H}_2\text{O}$, with a water molecule coordinated to the iodine(III) atom was also prepared. In these cases, the three adjacent oxygen atoms of 18C6 contact with the hypervalent iodine(III) atom and associate with the hydroxyl group through hydrogen bonding, thus strongly stabilizing the monomeric form. Without the need for any other activation, these monomeric iodosylbenzenes were highly reactive and served as versatile oxidants, especially in water, for oxidations toward a variety of functional groups, such as phenols (Eqs. 1 and 2), sulfides (Eq. 3), olefins (Eq. 4), silyl enol ethers (Eq. 5), and organoboron compound (Eq. 6).

Iodosylbenzene has been employed as the terminal oxidant in reactions using metal catalysts. Metalloporphyrins and related complexes catalyzed oxygenations of organic substrates, such as hydroxylation of hydrocarbons and epoxidation of alkenes, which frequently involved iodosylbenzene as an efficient source of oxygen [22]. Due to its mild reactivity, it also served as a proper oxidant for application in organocatalytic reactions, such as alcohol oxidations and asymmetric α -functionalization of carbonyl compounds, and therefore new exciting synthetic possibilities lie in this field [23].

16.3.2 Iodobenzene Diacetate (Phenyliodine(III) Diacetate)

Traditionally, iodobenzene diacetate (diacetoxiodobenzene, phenyliodine(III) diacetate) is prepared directly from iodobenzene by oxidation with peracetic acid (which is usually generated in situ from hydrogen peroxide and acetic anhydride) in

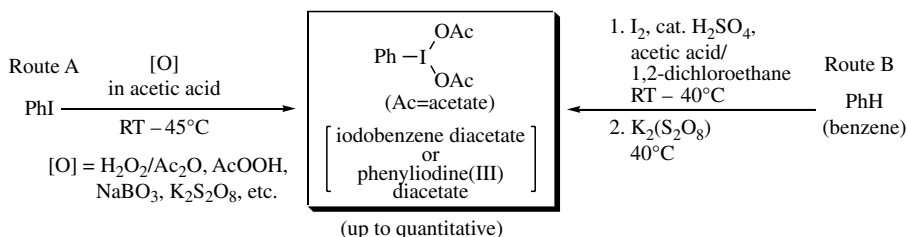


FIGURE 16.6 Preparation of iodobenzene diacetate.

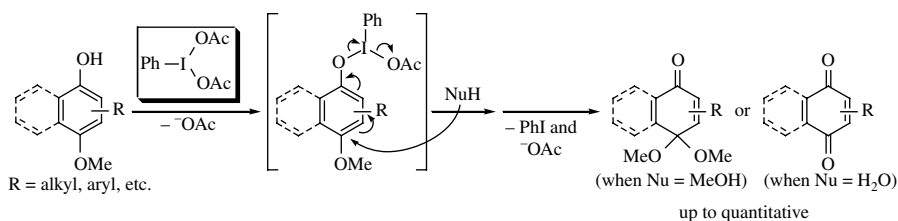


FIGURE 16.7 Phenolic oxidations using iodobenzene diacetate.

acetic acid solution (Fig. 16.6, route A) [24]. A general approach for the preparation of its derivatives typically includes this peracid oxidation toward various iodoarenes. These carboxylate-type hypervalent iodine compounds are generally colorless, stable microcrystalline solids compatible with usual storage for a long time period.

Alternative approaches employed appropriate inorganic oxidants, such as sodium perborate (NaBO_3), in acetic acid or acetic anhydride. The milder oxidation of iodoarenes with sodium perborate in acetic acid around 40°C is effective for the preparation of a diverse class of iodoarene diacetate compounds including heteroarenes [25]. During these preparations, it was revealed that addition of strong Brønsted acid, such as triflic acid, dramatically enhances the reaction rate, improving the yields and further expanding the substrate scope [26]. A more convenient straightforward procedure starting from aromatic compounds accompanying sequential ring iodination and formation of iodoarene diacetates was reported (route B), the reaction of which involves various arenes with molecular iodine, acetic acid, and potassium μ -peroxo-hexaoxodisulfate ($\text{K}_2\text{S}_2\text{O}_8$) in the presence of a small amount of concentrated sulfuric acid [27].

Regarding the reactivity of iodobenzene diacetate, an extreme number of reactions was reported in the literature. Particularly, this reagent is valuable for reproducing biomimetic oxidation processes of phenols under mild conditions. The phenolic oxidations, and most of other oxidations with hypervalent iodine reagents, involve exchange of the ligands by substrates at the iodine centers as the initial step (Fig. 16.7). The phenoxyiodine(III) intermediate as a result of the exchange by the phenolic oxygen then induces the rapid elimination of iodobenzene (PhI) with introduction of nucleophiles (NuH). As a result, in the presence of water, quinones were obtained in *para*-non-substituted and methoxy-substituted phenols, whereas

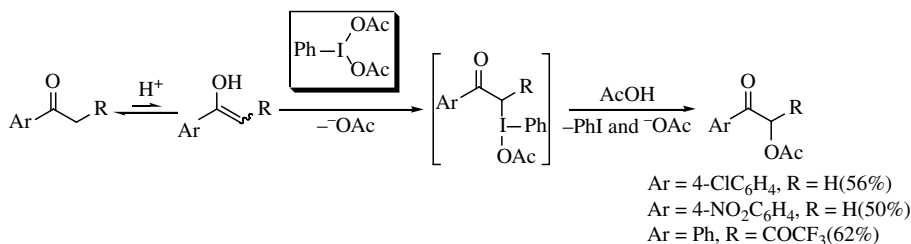


FIGURE 16.8 α -Acetoxylation of enolizable ketones using iodobenzene diacetate.

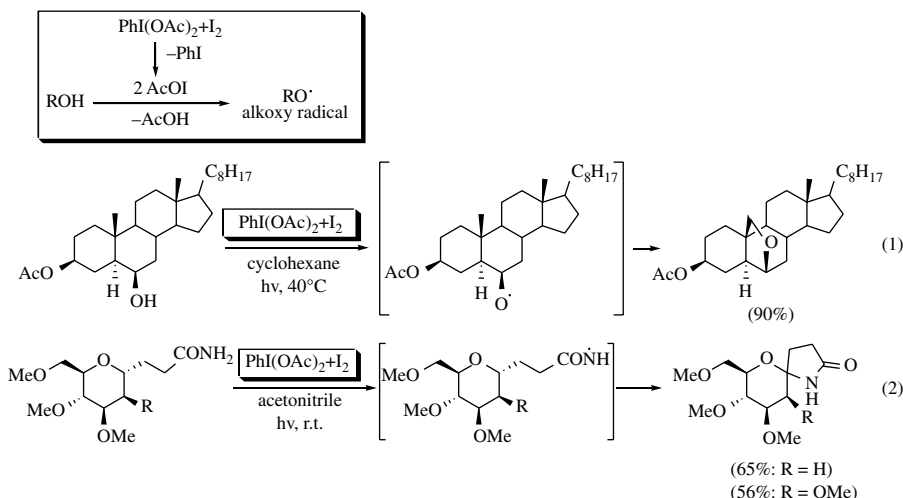


FIGURE 16.9 Hydroxy and amide-group directed radical C-H oxidations initiated by a combination of iodobenzene diacetate and molecular iodine.

monoacetals were produced in an alcohol solvent [28]. There are many contributions for the total syntheses of biologically important natural products and their pivotal intermediates using this type of reaction [29].

Introduction of an acetoxy group to the α -carbon of carbonyl compounds occurs using iodobenzene diacetate under suitable conditions. The reactions are applicable to various ketones and other enolizable carbonyl compounds [30]. In particular, aryl ketones and β -diketones are the suitable substrates to cause enolizations under weakly acidic conditions, such as provided by acetic acid, and α -acetoxylation proceeds smoothly providing high yields (Fig. 16.8). During the reactions, α -iodanyl ketones are produced as putative intermediates by ligand exchange between the acetoxy group and in situ generated enols at the iodine center. The α -iodanyl part is then replaced by an acetoxy group, leading to α -acetoxyated products.

It is well-known that hydrogen abstraction of alcohols occurs smoothly by the action of iodobenzene diacetate and molecular iodine under irradiation or upon heating, leading to the formation of corresponding alkoxy radicals (Fig. 16.9).

O-radical generation is generally explained by homolytic fragmentation of hypoiodous alcohols, where the real species for iodination of the alcohol groups is probably acetic acid iodyl ester (AcOI). Subsequent intramolecular hydrogen abstraction by alkoxy radicals is particularly useful for stereoselective synthesis of various polycyclic oxygen-containing ring systems. For example, the photolysis of cholestanediol acetate in the presence of $\text{PhI}(\text{OAc})_2\text{-I}_2$ in cyclohexane for 50 min at 40°C provides cyclized cholestane in 90% yield via intramolecular H abstraction of the steroid methyl by the alkoxy radical and oxidative recombination of the formed methyl radical with the hydroxy group (Eq. 1) [31]. Suárez and coworkers have thoroughly investigated this methodology for various useful transformations of carbohydrates.

The iodobenzene diacetate/molecular iodine combination is also an efficient system for generation of neutral nitrogen-centered radicals from various N–H groups. Similarly, a tandem intramolecular hydrogen abstraction/radical oxidation/nucleophilic cyclization furnishes the carbon–nitrogen bond at the cyclic ether to give a specific bicyclic spirolactam under irradiation with tungsten filament lamps at room temperature, indicating that the photo-induced amidyl radical derived from the carbohydrate is involved during the reaction (Eq. 2) [32].

16.3.3 [Bis(trifluoroacetoxy)iodo]benzene (Phenyliodine(III) Bis(trifluoroacetate))

[Bis(trifluoroacetoxy)iodo]benzene (phenyliodine(III) bis(trifluoroacetate)) is a colorless, stable microcrystal, which was originally prepared by ligand-exchange reactions of other hypervalent iodine compounds by treatment with trifluoroacetic acid. The replacement of the acetic acid ligands in diacetoxiodobenzene with stronger carboxylic acids can smoothly proceed at room temperature, which allows the simple production of [bis(trifluoroacetoxy)iodo]arenes by dissolving diacetoxiodoarenes in trifluoroacetic acid (Fig. 16.10, route A) [33]. In addition, a similar strategy for preparation of diacetoxo analogues (see Section 16.3.2) is applicable as the second general approach to obtain bis(trifluoroacetoxy) compounds (route B). Thus, iodoarenes can be directly oxidized to the corresponding [bis(trifluoroacetoxy)iodo]arenes by trifluorinated peracetic acid, generated from trifluoroacetic acid anhydride with sodium percarbonate, urea–hydrogen peroxide, and so on [34]. Recently, alternative methods to obtain a series of [bis(trifluoroacetoxy)iodo]arenes by oxidation of organic iodides using $\text{K}_2\text{S}_2\text{O}_8$ or Oxone® (a mixture of $2\times\text{KHSO}_5$,

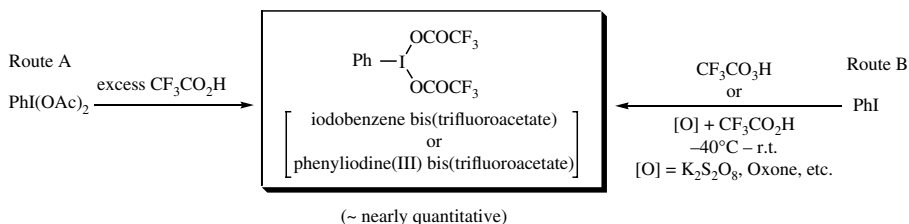


FIGURE 16.10 Preparation of iodobenzene bis(trifluoroacetate).

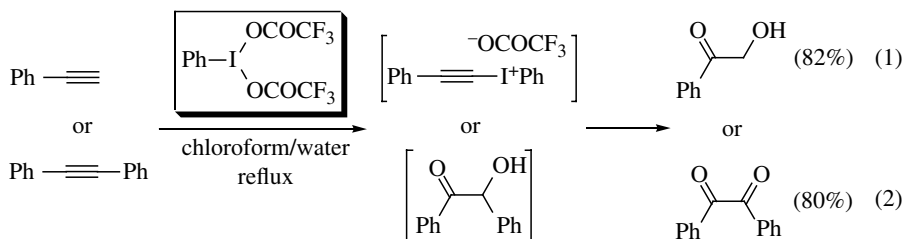


FIGURE 16.11 Direct oxidations of alkynes to α -hydroxyketones and 1,2-diketones.

KHSO_4 , and K_2SO_4) with trifluoroacetic acid were reported [35]. This versatile procedure is quite attractive for the preparation of the perfluoroalkane derivatives, $\text{C}_n\text{F}_{2n+1}\text{I}(\text{OCOCF}_3)_2$ ($n=4, 6, 8, 10, 12$).

In the literature, the possible high reactivity of [bis(trifluoroacetoxy)iodo]benzene was first estimated by Spyroudis and Varvoglis, who demonstrated the relatively high dehydrogenating ability of this reagent toward several classes of organic substrates [33]. Later, the enhanced reactivity was further proved in oxidations of alkyne functionalities [36, 37]. The oxidation of alkynes with [bis(trifluoroacetoxy)iodo]benzene enabled a short and efficient construction of the hydroxyacetone group (Fig. 16.11, Eq. 1). Thus, the treatment of ethynylcarbinols with the reagent in refluxing chloroform-containing water provided dihydroxyacetone products in moderate to good yields [36]. The reactions presumably involve the formation of alkyneiodonium salts at first and subsequent hydrolysis to dihydroxyacetones. Notably, the same transformation of ethynylcarbinols could provide satisfactory yields only by using toxic mercuric(II) oxide. The prominent results strongly encouraged the use of a hypervalent iodine reagent in environmentally benign processes as a metal-free alternative, replacing toxic heavy metal oxidizers based on lead(IV), mercury(II), and thallium(III).

Similarly, diketones were prepared from internal alkynes via α -hydroxyketones (Eq. 2) [37].

Hypervalent iodine(III) reagents are important for oxidative spiroannulation processes, and [bis(trifluoroacetoxy)iodo]benzene has been found to be one of the most effective oxidants for synthesizing dearomatized spirocyclic compounds from phenols. In nature, a variety of natural products bearing spirocyclic systems exist, and many of them are biosynthetically formed by oxidative spiroannulation processes. Similarly, *para*- and *ortho*-substituted phenol derivatives having nucleophilic side chains afford a variety of spirocyclohexadienones via formation of carbon–oxygen, carbon–nitrogen, and carbon–carbon bonds with promotion by hypervalent iodine reagents (Fig. 16.12). Kita and coworkers first demonstrated that the reaction becomes remarkably effective by using [bis(trifluoroacetoxy)iodo]benzene in highly polar, but low nucleophilic fluoroalcohol solvents, 1,1,1,3,3,3-hexafluoro-2-propanol (HFIP) and 2,2,2-trifluoroethanol (TFE) [38]. In this mechanism, the oxidation of phenols should proceed via the phenoxyiodine(III) intermediate by exchange of the carboxylate ligands with the phenolic oxygen at the iodine center

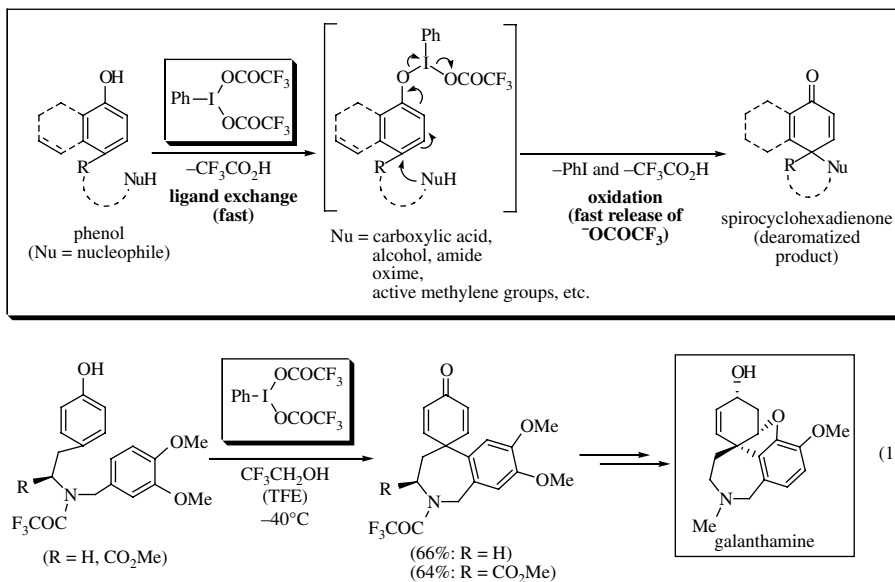


FIGURE 16.12 Dearomatizing oxidative spirocyclization of phenols and its application to natural product synthesis.

of the reagent. The cyclizations with introduction of internal nucleophiles (alcohols, amides, carboxylic acids, water, oximes, alkenes and alkynes or enamides, electron-rich aromatic rings, fluoride ion, etc.) then occurs due to the rapid elimination of iodobenzene (PhI) and trifluoroacetoxy anion, yielding the dearomatized cyclohexadienones bearing spiroannulated structures at the *para* or *ortho* positions of the original phenol group. Compared with diacetoxyiodobenzene, [bis(trifluoroacetoxy)iodo]benzene, because of the excellent trifluoroacetoxy leaving groups, facilitates both the steps, thus demonstrating high reactivity in the phenolic oxidations and dearomatizations.

In evaluating the high functional group availability and low toxicity of the reagent, the methods were widely used for total synthesis of natural products having important biological properties [29]. Thus, synthesis of maritidine, galanthamine, and discorhabdins was achieved by dearomatizing spirocyclizations using [bis(trifluoroacetoxy)iodo]benzene [38]. The effective spirocyclization of *para*-substituted phenols having the aromatic nucleophilic part accompanying carbon–carbon bond formation could produce the core structure of galanthamine-type Amaryllidaceae alkaloids and other five- to seven-membered spirodienones on a large scale (Fig. 16.12, Eq. 1). For example, this has practical applications for the production of galanthamine, a biologically active alkaloid and drug for Alzheimer's disease.

As mentioned, the reactivities of hypervalent iodine(III) reagents are normally explained by the two-electron-transfer processes in most cases. On the other hand, hypervalent iodine(III) reagents, especially [bis(trifluoroacetoxy)iodo]arenes, can

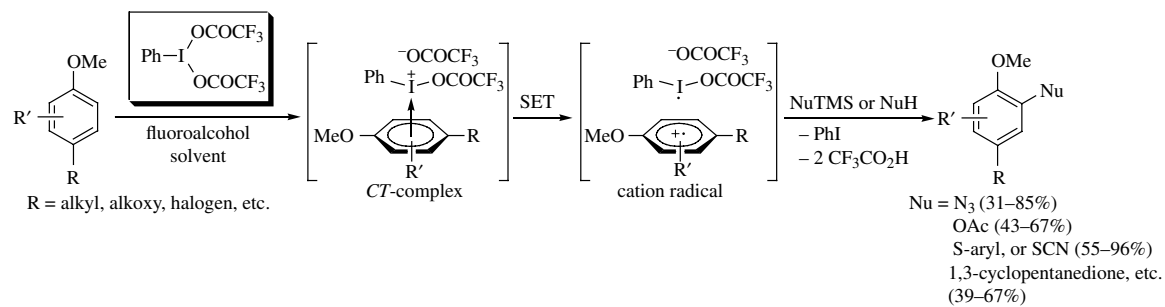


FIGURE 16.13 SET-induced oxidative coupling of phenyl ethers with various nucleophiles discovered by Kita's group.

act as selective and efficient single-electron-transfer (SET) oxidizing agents toward electron-rich aromatic compounds by suitable activation under specific conditions. The reaction based on the SET oxidation mechanism was first discovered in 1990 by Kita's group during aromatic substitution of *p*-substituted phenyl ethers by azide (N_3^-) using [bis(trifluoroacetoxy)iodo]benzene in the highly polar, but low nucleophilic HFIP (Fig. 16.13) [39]. Later, the same research group defined the SET oxidation ability of the hypervalent iodine reagent by confirming the generation of aromatic cation radicals through the charge-transfer (CT) complex with electron-rich aromatic compounds. Notably, the umpolung of the aromatic rings occurred without the use of any metal agent. Azide and other nucleophiles (AcO , ArS , [$\text{Ar} = \text{aryl}$], thiocyanate, and β -dicarbonyl compounds, etc.) were effectively introduced to the aromatic cation radicals at the selective *ortho* positions, producing various functionalized aromatic products as a result of the ring substitutions.

It should be emphasized that the SET reactivity of hypervalent iodine species highly depends on the employed reaction conditions and activators, and the use of fluoroalcohol as solvent is essential in order to induce SET oxidation as the reactions do not occur in other ordinary solvents. The fluoroalcohols exhibit high ionizing powers with low nucleophilicities, which effectively stabilizes in situ generated reactive aromatic cation radical species. Alternatively, the addition of appropriate Lewis acids enhances the SET oxidizing ability of the reagent by coordination to the iodine ligand. Typical examples include boron trifluoride etherate ($\text{BF}_3 \cdot \text{Et}_2\text{O}$) and trimethylsilyl triflate (TMSOTf). The polarized and more electron-deficient iodine center by these activations seems to favor π -complexation with aromatic rings. This strategy has significant advantages in controlling the reactivity of the oxidants and the reaction course. As a result, a wide array of reactivities based on the SET mechanism were found depending on the added Lewis acids for more extensive applications [40]. The most important elaboration is the oxidative biaryl coupling reactions, which furnish the new carbon–carbon bond directly from unfunctionalized aromatic compounds. This theme is separately dealt with in Chapter 17, which details couplings of iodo compounds along with recently discovered novel metal-free cross-coupling methods with hypervalent iodine reagent.

[Bis(trifluoroacetoxy)iodo]benzene can take dimeric and oligomeric structures through the oxygen bridge, depending on the conditions. The dimer μ -oxo-bis[trifluoroacetato(phenyl)iodine] [$(\text{PhI}(\text{OCOCF}_3))_2\text{O}$] was effectively prepared from iodosobenzene [$(\text{PhIO})_n$] and an equimolar molecular amount of trifluoroacetic acid (Fig. 16.14) [41]. Stable microcrystals of the dimer were compatible for X-ray crystallographic analysis, supporting the oxygen-bridged structure. As in the case of other trivalent hypervalent iodine compounds, storage of the μ -oxo dimer is possible for a long time period.

In the dimer, the strong *trans* influence of the bridged oxygen induces extension of the iodine(III)–trifluoroacetoxy bond lengths. Thus, the bonds are more polar and the iodine atoms more electrophilic, which means that the μ -oxo compound might become a promising candidate for potentially replacing well-used reagents in view of the reactivity because of possible smooth interactions with substrates. In accordance with this prediction, excellent oxidizing behavior of the μ -oxo dimer was demonstrated

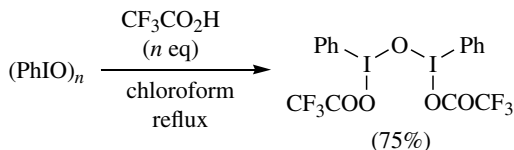


FIGURE 16.14 Preparation of μ -oxo [bis(trifluoroacetoxy)iodo]benzene dimer.

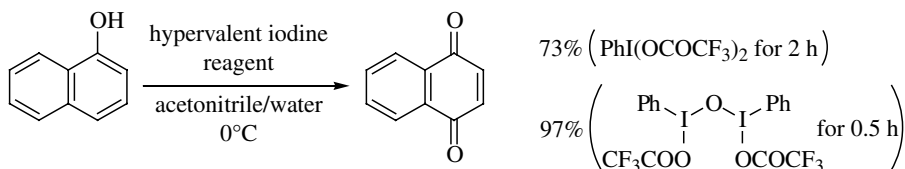


FIGURE 16.15 Efficient oxidation of phenols to quinones using μ -oxo hypervalent iodine dimer.

in a series of well-established phenolic oxidations [42]. The reactions sometimes resulted in better product yields compared to those using [bis(trifluoroacetoxy)iodo]benzene. Thus, the dimer in aqueous oxidation of 1-naphthol produced 1,4-naphthoquinone with 97% yield in 30 min, while the yield reached a maximum of 73% by the alternation to [bis(trifluoroacetoxy)iodo]benzene even after optimization (Fig. 16.15). These results clearly suggest that this dimer is one of the reasonable choices for the hypervalent iodine reagent for phenolic oxidations and in other transformations. Generally, the reactions are operative with known procedures without the need of any optimization.

16.3.4 [Hydroxy(tosyloxy)iodo]benzene and Its Derivatives

[Hydroxy(tosyloxy)iodo]benzene ($\text{PhI}(\text{OH})\text{OTs}$), which is accessible from iodobenzene diacetate by ligand exchange in the action of *p*-toluenesulfonic acid (*p*-TsOH) in water-containing solvent (Fig. 16.16, route A), was first discovered by O. Neiland and B. Carele in 1970, and the structure was later determined by Koser in 1976 by X-ray crystallographic analysis [43]. It is a slightly yellow-colored solid sufficiently stable for isolation. Of particular recent interest, their preparation focuses on more direct approaches from iodoarenes (route B) and even noniodiated aromatic compounds (route C). For example, one-pot conversion of iodoarenes to [hydroxy(tosyloxy)iodo]arenes at room temperature was established by treatment with *m*-chloroperbenzoic acid (*m*CPBA) including water and successively with *p*-TsOH or in the presence of the sulfonic acid [44]. A short-cut route from various aromatics was possible by avoiding preparation of iodoarene compounds, which involves an additional iodine source, that is, molecular iodine, in the presence of catalytic amount of triflic acid [45].

Due to the high polarity and electrophilic nature, organosulfonate and its derivatives were recognized early on as very reactive hypervalent iodine reagents in

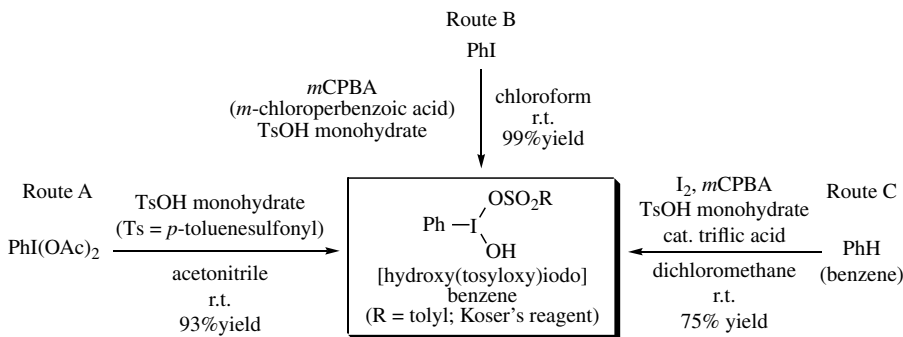


FIGURE 16.16 Preparation of [hydroxy(tosyloxy)iodo]benzene (HTIB).

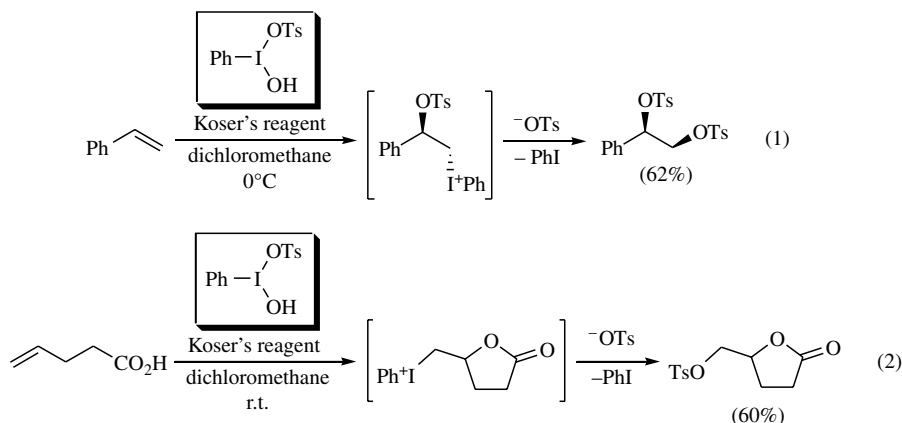


FIGURE 16.17 Tosyloxylation of alkenes utilizing HTIB.

oxidative transformations [46]. The excellent reactivity was initially reported for oxidations of alkenes, with rapid dioxxygenations yielding a variety of vicinal ditosyloxylation compounds (Fig. 16.17) [47]. The stereospecific *syn*-1,2-ditosyloxylation of styrenes occurred during the process, and the mechanism was thus explained as *anti*-addition of the electrophilic iodane to the carbon–carbon double bond and successive $\text{S}_{\text{N}}2$ -like introduction of the second sulfonyloxy group accompanying stereoinversion (Eq. 1). The intramolecular version of this reaction in appropriate alkenoic acids and alcohols extended its utility in ring construction for producing tosyloxylation lactones and cyclic ethers (Eq. 2) [48].

The α -functionalizations of ketones represent one of the useful reactions mediated by [hydroxy(organosulfonyloxy)iodo]benzenes established by Koser and Moriarty [49]. The results for typical substrates in α -tosyloxylation are shown in Fig. 16.18. Cyclic and acyclic active methylene compounds as well as enolizable aliphatic and aromatic ketones were easily converted to the corresponding α -tosyloxy carbonyl compounds with good yields by only treating with

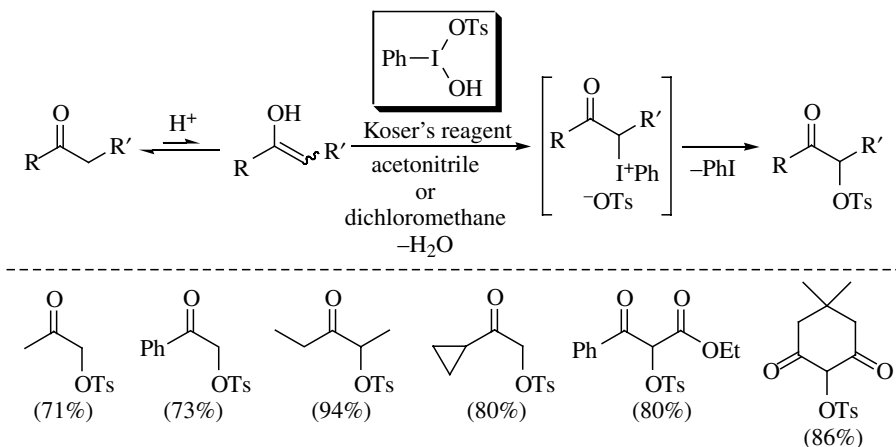


FIGURE 16.18 α -Tosyloxylation of ketones using HTIB.

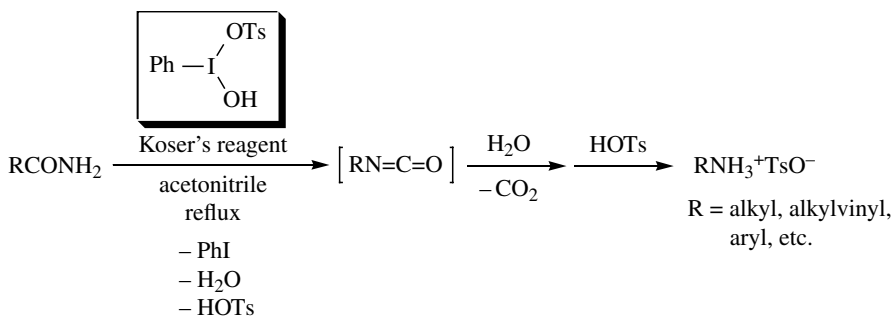
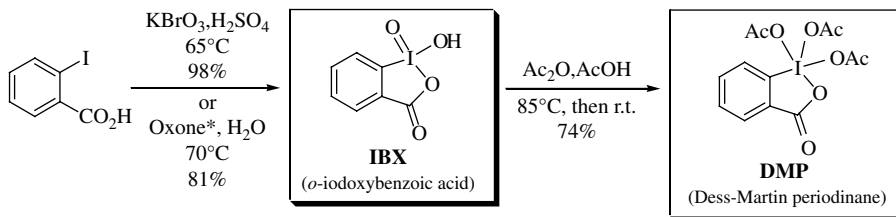


FIGURE 16.19 Hofmann-type rearrangement of primary amides using HTIB.

[hydroxy(tosyloxy)i]benzene in a refluxing solvent. Tertiary carbon would not react at all because of the steric disadvantage; otherwise the reaction preferentially occurred at the most enolizable site in carbonyl compounds. Consistent with the biased distribution of the internal enols under acidic conditions, the attempt to oxygenation of 2-butanone, hence, resulted in the reaction at the secondary carbon over primary one. The transformation was applicable for extended organosulfonates, that is, methane and chiral camphor sulfonate, and even phosphonates by applying the appropriate hydroxy(organosulfonyloxy) and (phosphoryloxy) iodanes [50].

[Hydroxy(organosulfonyloxy)i]benzenes are of importance in Hofmann-type rearrangement of amides (Fig. 16.19). In this method, notable improvements to convert long-chain aliphatic amides, which are unreactive under other Hofmann rearrangement conditions, to desired amines as sulfonate salts were possible [51]. Interestingly, a structurally unique cubane amine was synthesized by utilizing this method.



*potassium peroxymonosulfate
(as a mixture of $2\text{KHSO}_5/\text{KHSO}_4/\text{K}_2\text{SO}_4$)

FIGURE 16.20 Preparation of Dess-Martin periodinane (DMP) and its precursor, *o*-iodoxybenzoic acid (IBX).

16.3.5 Dess–Martin Periodinane and *o*-Iodoxybenzoic Acid

1,1,1-Tris(acetyloxy)-1,1-dihydro-1,2-benziodoxol-3(1*H*)-one, the very famous alcohol oxidizing agent, so-called Dess–Martin periodinane (DMP), can be obtained from 1-hydroxy-1,2-benziodoxole-3(1*H*)-one 1-oxide (IBX) on a 100 g scale by using acetic anhydride (Ac_2O) in the presence of 0.5% *p*-toluenesulfonic acid or by acetic anhydride (Ac_2O) in acetic acid solution (Fig. 16.20) [52]. On the other hand, IBX can be originally prepared by oxidation of 2-iodobenzoic acid with potassium bromate (KBrO_3) in an aqueous solution of sulfuric acid. (Caution: this method contaminates some explosive and toxic impurities to IBX and DMP.) Later, this preparative method was improved using Oxone® to obtain IBX with high purity [53]. These reagents are currently commercially available from many chemical suppliers on a small scale. Note that *these pentavalent iodine compounds are potentially explosive under excessive heating (around 200°C) or some impact*. It is a clear contrast to the fact that most trivalent hypervalent iodine compounds have melting points. In this light, stabilized IBX inclusive (SIBX), that is, a mixture of IBX with benzoic acid (22%) and isophthalic acid (29%), were introduced [54].

Both DMP and IBX are widely utilized for selective oxidation of alcohols to aldehydes and ketones in extensive substrates containing a different series of other functional groups, such as silyl ethers, allyl group, alkenes, alkynes, acetals, thioethers, thioketals, amines, amides, azide, pyridines and indoles, carbohydrates, polyhydroxy derivatives and polyethers, various nucleoside derivatives, selenides, tellurides, and phosphine oxides. In the oxidations, primary alcohols were selectively transformed to the corresponding aldehydes, while the formation of overoxidized carboxylic acids was not detected. These remarkable characteristics in chemo and product selectivities as well as their sufficient reactivities under mild and around neutral conditions make them attractive in the numerous stages of fine synthesis of natural products [55]. When carrying out IBX oxidation, DMSO should normally be used as a solvent due to its insolubility in most organic solvents.

As regards some other important reactions in organic synthesis, IBX can readily cause dehydrogenation of aldehydes and ketones to α,β -unsaturated carbonyl compounds [56]. IBX of suitable complexation with ligands, that is, 4-methoxypyridine *N*-oxide, is a remarkably effective oxidant for allowing the dehydrogenation of

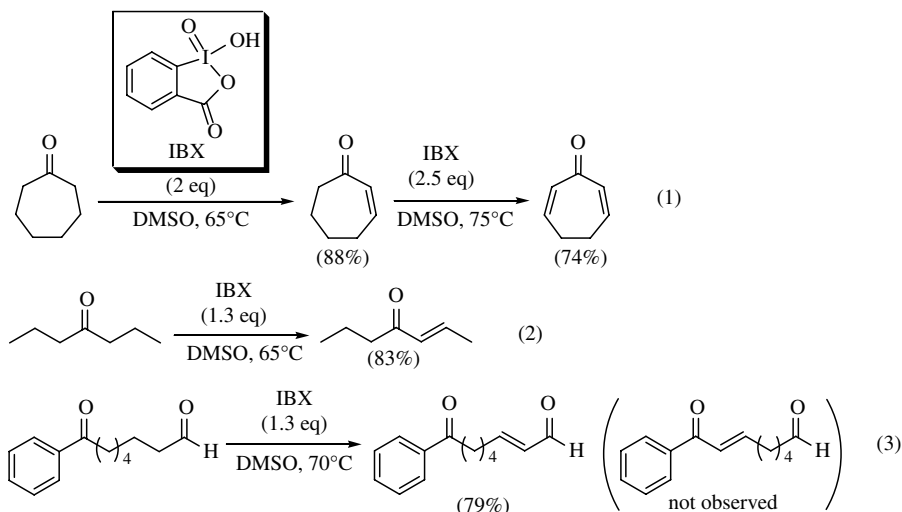


FIGURE 16.21 Selective α,β -dehydrogenation of carbonyl compounds.

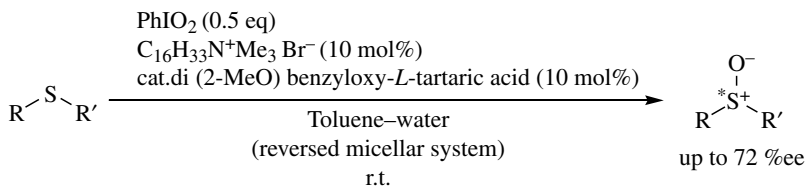
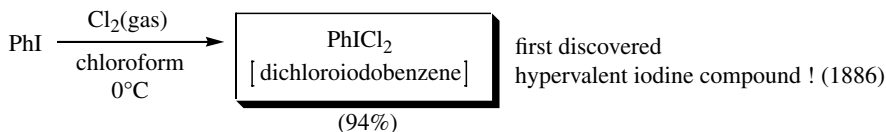
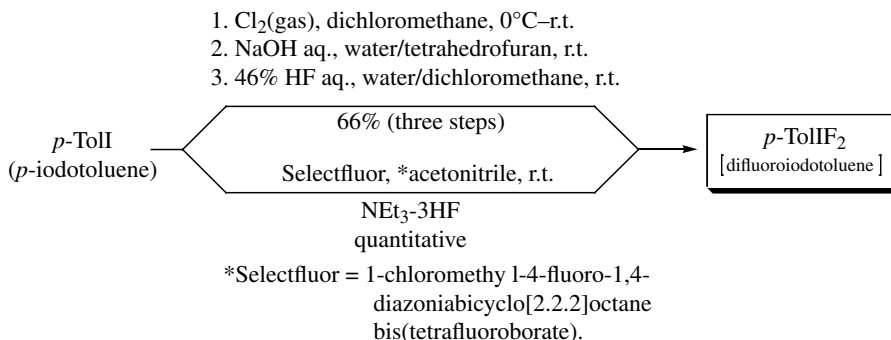


FIGURE 16.22 Asymmetric oxidation of sulfides to sulfoxides using iodylbenzene and chiral tartaric acid under micellar conditions.

carbonyl compounds even at room temperature. At elevated temperature over 60°C , IBX itself shows sufficient dehydrogenating ability (Fig. 16.21). Cyclic and acyclic ketones can be selectively oxidized to either mono- α,β -unsaturated or bis-unsaturated dienes depending on the amount of IBX and temperature (Eqs. 1 and 2). The dehydrogenations preferentially occur at the site of enolizable and sterically less-hindered aldehydes in the presence of ketone functionalities. For example, the dehydrogenation of the keto aldehyde, that is, η -oxo-benzeneoctanal, exclusively yielded α,β -unsaturated aldehyde by treatment with IBX (1.3 equivalents) in DMSO at 70°C as a result of selective reaction at the position of the aldehyde (Eq. 3). No α,β -conjugated ketone was observed during the reaction.

Among pentavalent iodine reagents, the noncyclic compound PhIO_2 (iodylbenzene; also named iodoxybenzene) has only limited applications due to its scarce solubility based on its polymeric structure and potential explosive nature at its soluble point upon heating. A rare example of its remarkable use in asymmetric reactions was reported regarding the aqueous systems in Fig. 16.4 [57]. In the presence of the chiral tartaric acids, the asymmetric oxidations of sulfides using PhIO_2 in the cationic reverse micellar systems afforded the corresponding chiral sulfoxides in good yields with up to 72% ee (Fig. 16.22). Several methods for the preparation of iodylarenes

**FIGURE 16.23** Preparation of dichloriodobenzene.**FIGURE 16.24** Preparation of difluoriodotoluene, a relatively stable difluoriodoarene compound.

from iodoarenes are present, which include a new procedure for the preparation of various iodylarenes from the corresponding iodoarenes using NaIO_4 as the oxidant in water with 30% volume of acetic acid [58].

16.3.6 Others

Iodobenzene dichloride (PhICl_2) was classically obtained directly from iodobenzene by passing chlorine gas through the organic solution containing it (Fig. 16.23) [59]. It is the first reported hypervalent iodine compound in history that was accidentally obtained by Willgerodt in 1886 during his attempt at ring chlorination of iodobenzene. In order to avoid the use of gaseous molecular chlorine, the recent new preparative methods for this type of compounds consist of more convenient procedures, such as using sodium perborate in aqueous hydrochloric acid, 30% hydrogen peroxide in a mixture of aqueous hydrochloric acid and fluoroalcohol, and one-pot preparation from aromatic compounds based on the sequential treatment of elemental iodine/ NaIO_4 in an acetic acid–acetic anhydride–sulfuric acid mixture followed by excess concentrated hydrochloric acid (aqueous) [60]. Generally, these dichlorides are sensitive to light and heat, gradually decomposing even at room temperature. In synthesis, they not only serve as a source of various chlorinations, but also cause several oxidative transformations.

As a related analogue bearing other halogen ligand, difluoriodoarenes were prepared as a fluorinating agent by an old approach involving replacement of the chloride ligands with fluorides using aqueous hydrofluoric acid in the presence of mercuric oxide (HgO) or a modified procedure without the use of HgO via iodosylarenes (Fig 16.24) [61, 62]. Recently, a more convenient method consisting of direct

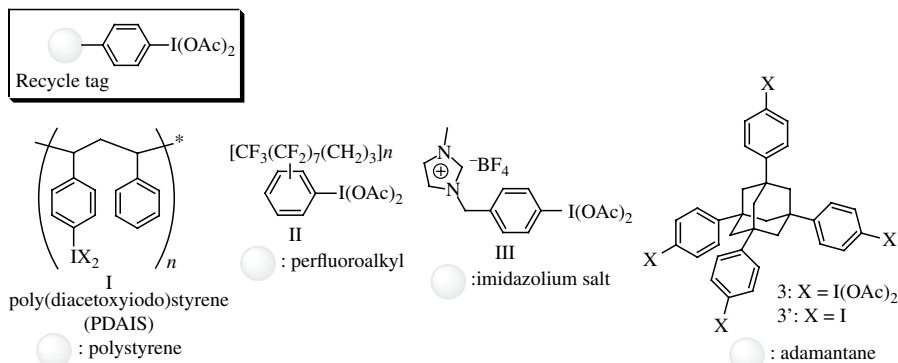


FIGURE 16.25 Representative examples of recyclable hypervalent iodine(III) compounds.

fluorination of iodoarenes by Selectfluor™ (1-chloromethyl-4-fluoro-1,4-diazoniabicyclo[2.2.2]octane bis(tetrafluoroborate)) was reported [63]. Like other dihalides, the difluorides are not stable compounds and are highly sensitive to moisture, and thus are commonly freshly prepared in solution form.

In general, tri and pentavalent hypervalent iodine reagents can oxidize substrates, by compensation of more stable monovalent iodine formation as the driving force. Despite their environmentally benign characteristics, a general problem in chemical reactions emerged from the coproduction of stoichiometric amounts of iodoarenes. Therefore, several types of recyclable hypervalent iodine reagents have been produced to facilitate the separation of the iodine coproduct from the reaction mixture as well as the reuse of the reagents (Fig. 16.25) [64]. For example, attaching the reagent to an insoluble polymer support, such as polystyrene, is a promising way for its recovery and recycling. Accordingly, the type I polymer-supported hypervalent iodine reagents poly(diacetoxyiodo)styrene (PDAIS) and poly[bis(trifluoroacetoxyiodo)]styrene (PBTIS), incorporating the hypervalent iodine moieties in their polymer backbones, were independently introduced into hypervalent iodine chemistry by Togo et al. and Ley et al., [65] which were successfully used in many oxidative transformations as an recyclable alternative.

Despite the utility and versatility of these polymer-supported reagents, one significant drawback is the lower reactivity than in the case of the corresponding monomeric forms, for example, PDAIS versus iodobenzene diacetate, owing to low solubility in various solvents and steric hindrance of the reactive sites by the polymer chains. In addition, the degradative loss of polystyrene resin is sometimes associated with benzylic oxidation of the polystyrene chain after repeated use. With recent progress in fluorous chemistry and the use of ionic liquid mediums, therefore, the preparation and use of hypervalent iodine compounds bearing type II fluorous tags and ionic supports, such as type III imidazolium salt, as recyclable reagents were reported [66, 67]. These tagged reagents were useful in many cases, but sometimes showed significant changes in reactivity, being different from conventional hypervalent iodine reagents.

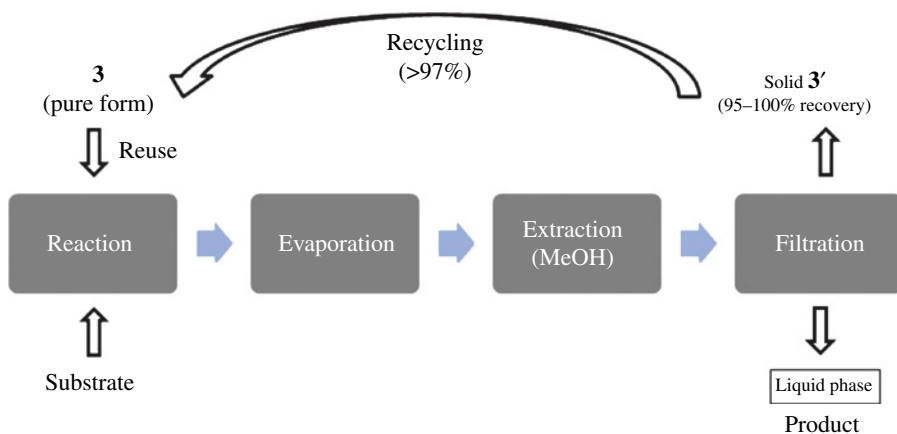


FIGURE 16.26 A schematic recycle diagram for adamantane-based recyclable hypervalent iodine reagent.

As a structurally new recyclable hypervalent iodine reagent, 1,3,5,7-tetrakis[4-(diacetoxyiodo)phenyl]adamantane (**3**), which has a reactivity very similar to that of conventional iodobenzene diacetate, was developed [68]. In combination with the high solubility in organic solvents, the high reactivity comes from the tetrahedral structure, in which reactive sites do not interfere with each other. A comparison of many reactions demonstrated that the reactivity is almost equal to those of conventionally used reagents. Adamantane **3** is thermally stable (mp [decomp.] 195–196°C) and is not sensitive to air and moisture.

The recovery was easily performed by precipitation by taking advantage of the insolubility of the reduced form **3'**, produced after the reactions in methanol (Fig. 16.26). The operation usually started with the removal of the used solvent. Methanol was added to the resulting oily mixture to extract the oxidation product, while the reagent **3'** simultaneously precipitated as a powder. The heterogeneous solution was then filtered, and the solid on the filter was washed several times with small amounts of methanol to quantitatively recover iodide **3'**. This operation facilitated the product purification steps; the product in the filtrate could be purified by short column chromatography. The recovered adamantane reagent **3'** was reactivated to the hypervalent iodine state **3** by *m*CPBA. Typically, the overall efficiency of the recycling (use → recovery → reactivation) was more than 90% with regard to molecular yield. Importantly, no degradation of the molecules was observed for the adamantane reagent **3** during the oxidations and in the reoxidation step even after repeated use, due to the absence of oxidation-sensitive benzylic proton, and thus repeated use was possible.

Derivatives of these recyclable hypervalent iodine reagents having other ligands were also reported. Other various recyclable reagents, especially derived from penta-valent iodine reagents, were systematically reported by Zhdankin and other research groups [69, 70]. Very recently, a recyclable reagent with magnetic nanoparticle

support has been suggested, and the new reagent demonstrated sufficient reactivities as well as simple recycling basis of attraction of magnetic force with the assistance of an external magnet [71].

REFERENCES

- [1] Gensch KH, Pitman IH, Higuchi T. *J Am Chem Soc* 1968;90:2096;Doi JT, Musker WK, deLeeuw DL, Hirschon AS. *J Org Chem* 1981;46:1239.
- [2] Togo H, Iida S. *Synlett* 2006;2159;Jereb M, Vrazic D, Zupan M. *Tetrahedron* 2011;67:1355;Veisi H. *Curr Org Chem* 2011;15:2438.
- [3] Mori N, Togo H. *Synlett* 2004;880;Mori N, Togo H. *Tetrahedron* 2005;61:5915.
- [4] Gogoi P, Konwar D. *Org Biomol Chem* 2005;3:3473.
- [5] Misono A, Osa T, Koda S *Bull Chem Soc Jpn* 1966;39:854;Talukdar S, Hsu J-L, Chou T-C, Fang J-M. *Tetrahedron Lett* 2001;42:1103.
- [6] Mori N, Togo H. *Synlett* 2005:1456.
- [7] Yadav JS, Subba RBV, Sabitha G, Kiran KRGS. *Synthesis* 2000:1532.
- [8] Ishihara M, Togo H *Synlett* 2006;227;Gogoi P, Konwar D. *Tetrahedron Lett* 2006;47:79.
- [9] Nicolaou KC, Montagnon T, Baran PS. *Angew Chem Int Ed* 2002;41:1386.
- [10] Chai L, Zhao Y, Sheng Q, Liu Z-Q. *Tetrahedron Lett* 2006;47:9283.
- [11] Shirini F, Zolfigol MA, Lakouraj MM, Azadbar MR. *Russ J Org Chem* 2001;37:1340.
- [12] House HO. *Modern Synthetic Reactions*. 2nd ed. California: W. A. Benjamin Inc.; 1972. p 353.
- [13] Varvoglis A. *Hypervalent Iodine in Organic Synthesis*. San Diego: Academic Press; 1997;Zhdankin VV, Stang PJ, Ochiai M. In: Akiba K, editor, *Chemistry of Hypervalent Compounds*. New York: Wiley-VCH; 1999;Stang PJ, Zhdankin VV. *Chem Rev* 1996;96:1123;Kitamura T, Fujiwara Y. *Org Prep Proced Int* 1997;29:409;Zhdankin VV, Stang PJ. *Chem Rev* 2002;102:2523;Zhdankin VV, Stang PJ. *Chem Rev* 2008;108:5299;Zhdankin VV. *ARKIVOC* 2009;i:1;Zhdankin VV. *J Org Chem* 2011;76:1185;Yusubov MS, Zhdankin VV. *Curr Org Synth* 2012;9:247.
- [14] Wirth T, Ochiai M, Varvoglis A, Zhdankin VV, Koser GF, Tohma H, Kita Y. In: Wirth T, editor. *Hypervalent Iodine Chemistry—Modern Developments in Organic Synthesis*. Berlin: Springer-Verlag; 2003;Silva LF Jr., Olofsson B. *Nat Prod Rep* 2011;28:1722.
- [15] For reviews and accounts, see: Richardson RD, Wirth T *Angew Chem Int Ed* 2006;45:4402;Ochiai M, Miyamoto K. *Eur J Org Chem* 2008;4429;Dohi T, Kita Y. *Chem Commun* 2009;2073.
- [16] For a review and highlight, see: Liang H, Ciufolini MA. *Angew Chem Int Ed* 2011;50:11849;Ngatimin M, Lupton DW. *Aust J Chem* 2010;63:653.
- [17] Lucas HJ, Kennedy ER, Formo MW. *Org Synth* 1955;II:483;Saltzman H, Sharefkin JG. *Org Synth* 1973;V:658.
- [18] Zefirov NS, Zhdankin VV, Dan'kov YV, Sorokin VD, Semerikov VN, Koz'min AA, Caple R, Berglund B. *Tetrahedron Lett* 1986;27:3971;Moriarty RM, Epa WR, Awasthi AK. *Tetrahedron Lett* 1989;30:667.
- [19] Tohma H, Takizawa S., Maegawa T, Kita Y. *Angew Chem Int Ed* 2000;39:1306;Tohma H, Takizawa S, Maegawa T., Kita Y. *Adv Synth Catal* 2002;344:328;Tohma H, Maegawa T, Kita Y. *Synlett* 2003;723.

- [20] Tohma H, Maegawa T, Kita Y. *ARKIVOC* 2003;vi:62;Tohma H, Takizawa S, Watanabe H, Kita Y. *Tetrahedron Lett* 1998;39:4547.
- [21] Ochiai M, Miyamoto K, Shiro M, Ozawa T, Yamaguchi K. *J Am Chem Soc* 2003;125:13006;Ochiai M, Miyamoto K, Yokota Y., Suefuji T, Shiro M. *Angew Chem Int Ed* 2005;44:75.
- [22] Groves JT, Nemo TE. *J Am Chem Soc* 1983;105:5786;Collman JP, Lee VJ, Zhang X, Ibers JA, Brauman JI *J Am Chem Soc* 1993;115:3835;Irie R, Noda K, Ito Y, Katsuki T. *Tetrahedron Lett* 1991;32:1055;McGarrigle EM, Gilheany DG. *Chem Rev* 2005;105:1563.
- [23] A recent account: Fernandez Gonzalez D, Benfatti F, Waser J. *ChemCatChem* 2012;4:955.
- [24] Sharefkin JG, Saltzman H. *Org Synth* 1963;43:62.
- [25] McKillop A, Kemp D. *Tetrahedron* 1989;45:3299.
- [26] Hossain M, Kitamura T. *J Org Chem* 2005;70:6984.
- [27] Hossain M, Kitamura T. *Bull Chem Soc Jpn* 2007;80:2213.
- [28] Moriarty RM, Prakash O. *Org React* 2001;57:327;Lewis N, Wallbank P. *Synthesis* 1987;1103;Tamura Y, Yakura T, Haruta J, Kita Y. *J Org Chem* 1987;52:3927;Pelter A, Elgendy S. *Tetrahedron Lett* 1988;29: 677.
- [29] Tohma H, Kita Y. *Top Curr Chem* 2003;224:209;Ciufolini MA, Braun NA, Canesi S, Ousmer M, Chang J, Chai D. *Synthesis* 2007;3759;Quideau S, Pouységu L, Deffieux D. *Synlett* 2008;467;Pouységu L, Deffieux D, Quideau S. *Tetrahedron* 2010;66:2235.
- [30] Mizukami F, Ando M, Tanaka T, Imamura J. *Bull Chem Soc Jpn* 1978;51:335;Moriarty RM, Prakash O. *Org React* 1999;54:273.
- [31] Concepción JI, Francisco CG, Hernández R, Salazar JA, Suárez E. *Tetrahedron Lett* 1984;25:1953;Martín A, Salazar JA, Suárez E. *Tetrahedron Lett* 1995;36:4489.
- [32] de Armas P, Carrau R, Concepción JI, Francisco CG, Hernández R, Suárez E. *Tetrahedron Lett* 1985;26:2493;Martín A, Pérez-Martín I, Suárez E. *Org Lett* 2005;7:2027.
- [33] Spyroudis S, Varvoglis A. *Synthesis* 1975:445.
- [34] Zhdankin VV, Scheuller MC, Stang PJ. *Tetrahedron Lett* 1993;34:6853;Kazmierczak P, Skulski L. *Molecules* 2002;7:810;Page TK, Wirth T. *Synthesis* 2006;3153.
- [35] Hossain M, Kitamura T. *Bull Chem Soc Jpn* 2006;79:142;Zagulyaeva AA, Yusubov MS, Zhdankin VV. *J Org Chem* 2010;75:2119.
- [36] Tamura Y, Yakura T, Haruta J, Kita Y. *Tetrahedron Lett* 1985;26:3837;Kita Y, Yakura T, Terashi H, Haruta J, Tamura Y. *Chem Pharm Bull* 1989;37:891;Haruta J, Nishi K, Matsuda S, Akai S, Tamura Y, Kita Y. *J Org Chem* 1990;55:4583.
- [37] Vasileva VP, Khalfina IL, Karpitskaya LG, Merkushev EB. *Zh Org Khim* 1987;23:2225.
- [38] Tamura Y, Yakura T, Haruta J, Kita Y. *J Org Chem* 1987;52:3927;Kita Y, Tohma H, Inagaki M, Hatanaka K, Yakura T. *J Am Chem Soc* 1992;114:2175;Kita Y, Takada T, Gyoten M, Tohma H, Zenk MH; Eichhorn J. *J Org Chem* 1996;61:5857;Kita Y, Arisawa M, Gyoten M, Nakajima M, Hamada R, Tohma H, Takada T. *J Org Chem* 1998;63:6625.
- [39] Kita Y, Tohma H, Hatanaka K, Takada T, Fujita S, Mitoh S, Sakurai H, Oka S *J Am Chem Soc* 1994;116:3684;Kita Y, Tohma H, Inagaki M, Hatanaka K, Yakura T. *Tetrahedron Lett* 1991;32:4321.
- [40] A recent account: Dohi T, Ito M, Yamaoka N, Morimoto K, Fujioka H, Kita Y. *Tetrahedron* 2009;65:10797.

- [41] Gallos J, Varvoglis A, Alcock NW. *J Chem Soc Perkin Trans* 1985;1:757.
- [42] Takenaga N, Uchiyama T, Kato D, Fujioka H, Dohi T, Kita Y. *Heterocycles* 2011;82:1327;Dohi T, Uchiyama T, Yamashita D, Washimi N, Kita Y. *Tetrahedron Lett* 2011;52:2212;Dohi T, Nakae T, Takenaga N, Uchiyama T, Fukushima K, Fujioka H, Kita Y. *Synthesis* 2012;44:1183.
- [43] Neiland O, Carele B. *J Org Chem USSR* 1970;6:797;Koser GF, Wettach RH, Troup JM, Frenz BA. *J Org Chem* 1976;41:3609.
- [44] Yamamoto Y, Togo H. *Synlett* 2005:2486.
- [45] Merritt EA, Carneiro VMT, Silva LF Jr, Olofsson B. *J Org Chem* 2010;75:7416.
- [46] Koser GF. *Aldrichim Acta* 2001;34:89.
- [47] Rebrovic L, Koser GF. *J Org Chem* 1984;49:2462.
- [48] Shah M, Taschner MJ, Koser GF, Rach NL. *Tetrahedron Lett* 1986;27:4557;Kim H-J, Schlecht MF. *Tetrahedron Lett* 1987;28:5229.
- [49] Koser GF, Relenyi AG, Kalos AN, Rebrovic L, Wettach RH. *J Org Chem* 1982;47:2487;Moriarty RM, Vaid RK, Koser GF. *Synlett* 1990;365.
- [50] Lodaya JS, Koser GF. *J Org Chem* 1988;53:210;Hatzigrigoriou E, Varvoglis A, Bakola-Christianopoulou M. *J Org Chem* 1990;55:315;Moriarty RM, Condeiu C, Tao A, Prakash O. *Tetrahedron Lett* 1997;38:2401.
- [51] Vasudevan A, Koser GF. *J Org Chem* 1988;53:5158;Moriarty RM, Khosrowshahi JS, Awasthi AK, Penmasta R. *Synth Commun* 1988;18:1179.
- [52] Dess DB, Martin JC. *J Org Chem* 1983;48:4155;Dess DB, Martin JC. *J Am Chem Soc* 1991;113:777;Ireland RE, Liu L. *J Org Chem* 1993;58:2899.
- [53] Frigerio M, Santagostino M. *Tetrahedron Lett* 1994;35:8019;Frigerio M, Santagostino M, Sputore S. *J Org Chem* 1999;64:4537.
- [54] Ozanne A, Pouységu L, Depernet D, François B, Quideau S. *Org Lett* 2003;5:2903.
- [55] Reviews: Tohma H, Kita Y. *Adv Synth Catal* 2004;346:111;Nicolaou KC, Chen JS, Edmonds DJ, Estrada AA. *Angew Chem Int Ed* 2009;48:660;Satam V., Harad A., Rajule R, Pati H. *Tetrahedron* 2010;66:7659;Duschek A, Kirsch SF. *Angew Chem Int Ed* 2011;50:1524.
- [56] Nicolaou KC, Montagnon T, Baran PS. *Angew Chem Int Ed* 2002;41:993;Nicolaou KC, Montagnon T, Baran PS, Zhong Y-L. *J Am Chem Soc* 2002;124:2245.
- [57] Tohma H, Takizawa S, Watanabe H, Fukuoka Y, Maegawa T, Kita Y. *J Org Chem* 1999;64:3519;Tohma H, Takizawa S, Morioka H, Maegawa T, Kita Y. *Chem Pharm Bull* 2000;48:445.
- [58] Sharefkin JG, Saltzman H. *Org Synth* 1963;43:65;Kraszkiewicz L, Skulski L. *ARKIVOC* 2003;vi:120.
- [59] Willgerodt C. *J Prakt Chem* 1886;33:154;Lucas HG, Kennedy ER. *Org Synth* 1955;3:482.
- [60] Koyuncu D, McKillop A, McLaren L. *J Chem Res (S)* 1990;21;Podgorsek A, Iskra J. *Molecules* 2010;15:2857;Lulinski P, Obeid N, Skulski L. *Bull Chem Soc Jpn* 2001;74:2433.
- [61] Garvey BS Jr., Halley LF, Allen CFH. *J Am Chem Soc* 1937;59:1827;Sawaguchi M, Ayuba S, Hara S. *Synthesis* 2002;1802.
- [62] Hara S. Fluorination using hypervalent halogen fluorides. In: Laali KK, editor. *Advances in Organic Synthesis*. Hilversum: Bentham Science LTD; 2006. p 49.
- [63] Ye C, Twamley B, Shreeve JM. *Org Lett* 2005;7:3961.

- [64] Togo H, Sakuratani K. *Synlett* 2002;1966;Yusubov MS, Zhdankin VV. *Mendeleev Commun* 2010;20:185.
- [65] Togo H, Nogami G, Yokoyama M. *Synlett* 1998;534;Ley SV, Thomas AW, Finch H. *J Chem Soc Perkin Trans 1* 1999; 669.
- [66] Rocaboy C, Gladysz JA. *Chem-Eur J* 2003;9:88;Podgorsek A, Jurisch M, Stavber S, Zupan M, Iskra J, Gladysz JA. *J Org Chem* 2009;74:3133.
- [67] Qian W, Jin E, Bao W, Zhang Y. *Angew Chem Int Ed* 2005;44:952;Handy ST, Okello M. *J Org Chem* 2005;70:2874.
- [68] Tohma H, Maruyama A, Maeda A, Maegawa T, Dohi T, Shiro M, Morita T, Kita Y. *Angew Chem Int Ed* 2004;43:3595;Dohi T, Fukushima K, Kamitanaka T, Morimoto K, Takenaga N, Kita Y. *Green Chem* 2012;14:1493.
- [69] Mülbaier M, Giannis A. *Angew Chem Int Ed* 2001;40:4393;Sorg G, Mengel A, Jung G, Rademann J. *Angew Chem Int Ed* 2001;40:4395.
- [70] Yusubov MS, Drygunova LA, Zhdankin VV. *Synthesis* 2004;2289;Ladziata U, Willging J, Zhdankin VV. *Org Lett* 2006;8:167; See also ref. 64 of the Zhdankin's review.
- [71] Zhu C, Wei Y. *Adv Synth Catal* 2012;354:313.

REACTION OF IODO COMPOUNDS

TOSHIFUMI DOHI¹ AND YASUYUKI KITA²

¹College of Pharmaceutical Sciences, Ritsumeikan University, Kusatsu, Shiga, Japan

²Emeritus Professor of Osaka University, Ritsumeikan University, Kusatsu, Shiga, Japan

17.1 COUPLING REACTIONS WITH ORGANIC IODIDES

Due to the large atomic size of iodine, the carbon–iodine bonds in organic iodides have the longest length in comparison with other halogen bonds, that is, bromides, chlorides, and fluorides. This makes the bond energy and strength the lowest and markedly the weakest among the series of organic halides. As a result, organic iodides were favorably used as an excellent precursor for generating highly reactive carbon species, such as carbocations, anions, radicals, and carbenes, in organic reactions. For example, tertiary alkyl iodides can rapidly produce corresponding carbocations by the action of appropriate Lewis acids. Some aryl iodides would cause halogen–metal exchange, producing aryl anion species at low temperature. Dissociation to organic radicals by a radical initiator, such as 2,2'-azobisisobutyronitrile (AIBN), should readily occur for many alkyl iodides. Carbenoid formation from diiodomethane with an activated zinc–copper couple during the cyclopropanation of alkenes happens, which led to the historical discovery of the Simmons–Smith reaction in 1958.

In the long-time applications of organic iodides, alkyl iodides are traditionally known as the representative substrates in substitution and elimination reactions toward nucleophiles and bases. Meanwhile, sp^2 -aryl and -vinyl as well as sp^3 -alkynyl iodides have an important and special role in the modern organic synthesis, especially in metal-catalyzed coupling. In these couplings, the iodides are usually more reactive than related bromides and chlorides [1]. The formation of carbon–carbon

bonds in the coupling reactions using these organic iodides thus results in a pivotal synthetic class for constructing complex molecules and has received continuous interest from the scientific community.

In the following sections, we briefly introduce the specific role of the organic iodides during the coupling reactions, especially focusing on carbon–carbon bond-forming reactions to biaryls and the new design of the iodine-containing organic molecules.

17.1.1 Reductive Coupling

Most organic chemists say that the one of the most impressive reports in the early history of application of organic iodides is the Ullmann coupling reported more than a century ago [2]. By promotion of stoichiometric copper(0) metal, biaryls, the homocoupling products, were formed from two molecules of aryl iodides at high temperatures over 200°C in the typical case (Fig. 17.1). As the umpolung of the aromatic rings should formally occur during the reactions by the reductant, copper metal, this is classified as a reductive coupling. In these classical Ullmann-type reactions, the iodides are most reactive, with bromides and chlorides generally requiring much harsher conditions to couple each other.

Together with the investigations of the detailed reaction mechanism for each substrate case, further advances and efforts in the past few decades were mainly directed toward the catalytic use of copper and alternative metals, the stereocontrol of the coupling products by substrate and reagent controls, and the establishment of milder reaction systems using more reactive and soluble organometallic complexes, such as copper 2-thiophene carboxylate (CuTC, commercially available), for lowering the reaction temperature and expanding the scope of substrates [3]. However, most cases still limited their utility only in the homocouplings except for the intramolecular examples.

17.1.2 Metal-Catalyzed Cross-Coupling

Transition metal–catalyzed cross-couplings of organometallic reagents with organic halides, especially iodides, have emerged as a prominent area of research in synthetic chemistry. The cross-coupling reactions with various types of organometallic reagents have become important tools to create new carbon–carbon bonds in the synthetic molecules, which now encompass a range of aryl, alkynyl, and alkenyl substrates. Among them, Heck, Negishi, and Suzuki received the Nobel Prize in

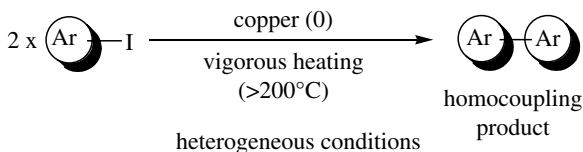


FIGURE 17.1 Classical Ullmann-type reductive coupling of aryl iodides.

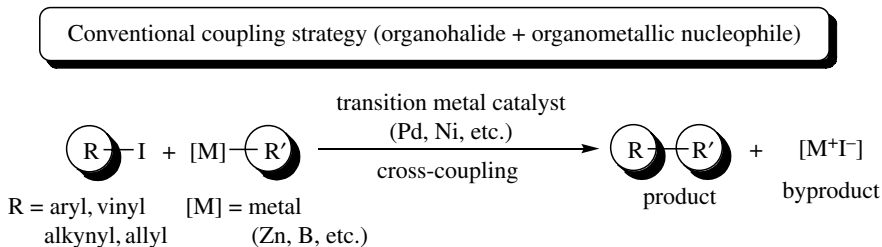


FIGURE 17.2 Transition metal-catalyzed cross-couplings between organohalides and organometallic reagents.

Chemistry for their pioneering contributions and applications in palladium-catalyzed cross-coupling reactions in the year 2010.

The well-known cross-coupling strategies using organometallic compounds (e.g., [M] = [Zn]; Negishi, [B]; Suzuki-Miyaura, [Sn]; Stille) employ organic halides in the presence of transition metal catalysts, such as palladium complexes (Fig. 17.2). These methods thus require stoichiometric amounts of the activated organometallic substrates, the preparation of which includes several synthetic steps. In addition, the use of organometallic substrates produces large amounts of metallic salts as wastes and by-products during the preparation and after the cross-coupling reactions. These aspects derived from the organometallic starting materials are not ideal and efficient with regard to environmental concerns and from a practical point of view.

In theory, a more direct approach in cross-couplings is the alternative use of carbon–hydrogen bonds instead of the organometallic molecules. Inspired by the aim of green sustainable chemistry, much effort has been dedicated to the development of the direct cross-couplings of carbon–hydrogen bonds in the past few decades (Fig. 17.3). Actually, direct C–H cross-couplings of aromatic compounds and organic iodides (Eq. 2) can proceed utilizing the defined transition metal catalysts under refined conditions, improving the atom economy, cost, and overall synthetic steps by avoiding the preparation of the substrates compared to the original routes (Eq. 1). In some cases, organic iodides played a critical role for developing the C–H cross-couplings during the reactions; otherwise, other halides (bromides and chlorides) did not work so well as the coupling partners and their use sometimes failed in the less efficient coupling reactions [4].

These cross-couplings can provide powerful tools for the construction of complex molecules in organic synthesis, and thus the development of a novel coupling method has been intensively studied by synthetic chemists. Accordingly, the classical coupling methods as well as the recent progress on palladium(II)-catalyzed C–H activations/C–C cross-couplings have been of continuous interest and have been frequently summarized in many reviews [5]. In the following sections, we therefore describe recent significant advances in the area of metal-catalyzed cross-couplings, in which diaryliodonium salts specifically play an indispensable role as the coupling partner.

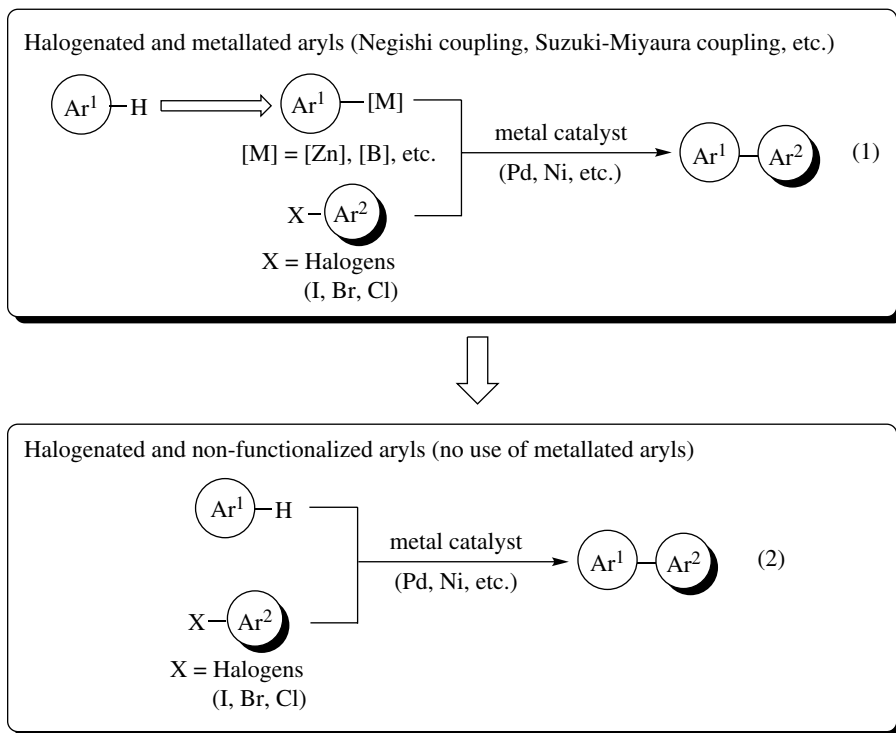


FIGURE 17.3 Recent advances in cross-coupling: From organometallic reagents to C-H bonds of organic molecules.

17.1.2.1 Iodonium Salts in Advances of Cross-Coupling

In the conventional and classical cross-couplings with organoiodides and organometallic compounds mentioned earlier, palladium and nickel salts typically worked as excellent metal catalysts, while cross-couplings using copper-based complexes were known to require stoichiometric amounts of the metals [6]. As an early study for copper-catalyzed alternatives, cross- and carbonylative-couplings of organostannanes and -boranes with diaryliodonium salts were first demonstrated in 1996 by Kang's research group (Fig. 17.4). The catalytic coupling in copper was also found to be applicable in Sonogashira-type cross-coupling of acetylenes and diaryliodonium salts [7].

Utilizing the high reactivity of diaryliodonium salts in copper-catalyzed processes, Gaunt has developed a new site-selective Cu(II)-catalyzed C-H bond functionalization process that can selectively arylate indoles at either the C3 or C2 positions in which the regioselectivity could be varied by altering the nature of the substituent on the indole nitrogen [8]. It is proposed that the site for arylation arises through a migration of copper from the C3 to the C2 carbon of indoles controlled by the nature of the substitution group on the nitrogen during the proposed Cu(I)/Cu(III) catalytic cycle. Later, this study led to breakthrough for unprecedented *meta*-selective arylation of

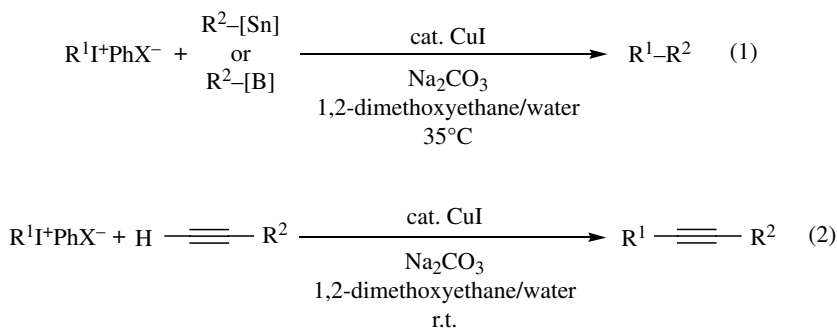


FIGURE 17.4 Early reports for copper-catalyzed cross-couplings utilizing diaryliodonium salts.

anilides and arylcarbonyl compounds by the same group (Fig. 17.5, Eq. 1). A possible rationalization of the novel selectivity was discussed by considering the formation of highly electrophilic Cu(III)–aryl species activating anilides and arylcarbonyl rings sufficiently to permit an *anti*–oxy-cupration of the carbonyl group across the *ortho* and *meta* positions on the arene rings. This dearomatizing process is likely to produce the Cu(III)–aryl species at the *meta* position, and successive reductive elimination would deliver the observed *meta* products. In addition, a method for the *meta*-selective arylation of a versatile series of α -aryl carbonyl compounds has thus been developed with diaryliodonium salts.

The regioselectivity of this transformation can be further controlled by the choice of directing groups on the aromatic ring. In fact, phenol derivatives and other electron-rich aromatic compounds caused selective arylation at the *para* position (Fig. 17.5, Eq. 2) [9]. In contrast to *meta* arylation, the electronic factor of the electron-donating groups governed the *para* selectivity (so, the authors call this transformation a copper-catalyzed Friedel–Crafts–type strategy). As such, by utilizing the nature of the directing group and the nature of the substituent, the catalytic systems were successfully employed in the control of the *meta* and *para* site-selective arylations of arenes using diaryliodonium salts.

Recently, this powerful copper-catalyzed direct arylation using iodonium salts has been applied to cyclic nonaromatic enamides [10]. As an example of trifluoromethylation, indoles and allylsilane derivatives reacted with Togni's reagent (1-trifluoromethyl-1,2-benziodoxol-3-(1*H*)-one) in the presence of a copper catalyst for successful installation of trifluoromethyl group into these structures [11]. Iodonium salts and Togni's reagent belong to a similar group of hypervalent iodine compounds with two carbon ligands (see Chapter 7). Similarly, for diaryliodonium salts, the radical character of the trifluoromethylation reaction was experimentally proven for Togni's reagent.

Asymmetric arylations of silyl enol ethers are successful using chiral copper catalysts in combination with diaryliodonium salts, which have been simultaneously reported by Gaunt and MacMillan in the same academic journal (Fig. 17.6) [12, 13]. The former group has developed the asymmetric transformation for obtaining optically active arylated carbonyl compounds involving the coupling of *N*-acyloxazolidinones

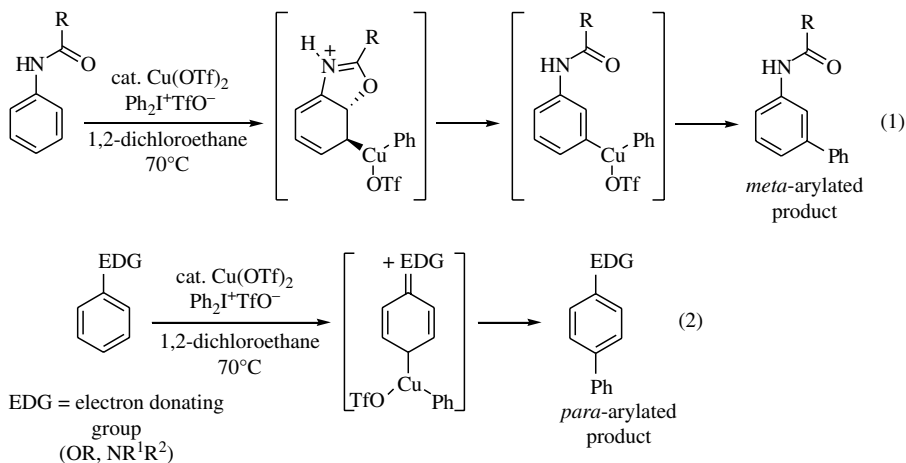


FIGURE 17.5 Recent pioneering studies using diaryliodonium salts: Copper-catalyzed *meta*- and *para*-arylations.

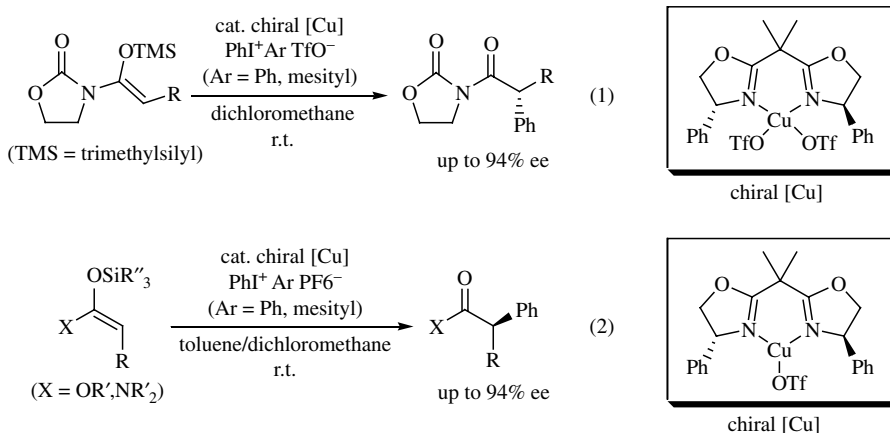


FIGURE 17.6 Asymmetric α -arylation of carbonyl compounds by using chiral copper catalysts and silyl enol ethers.

with diaryliodonium salts in the presence of a chiral copper(II) complex derived from a commercially available bisoxazoline ligand (Eq. 1) [12]. MacMillan's group has also established the enantioselective α -arylation of silyl enol ethers of both lactones and *N*-acyl oxazolidones using a combination of diaryliodonium salts and copper catalysis (Eq. 2) [13]. Employing a readily available copper iodide–PhBox catalyst, good to excellent yields and generally excellent enantioselectivities were observed in the obtained products. In these transformations, aryl mesityl iodonium salts were applicable for the selective aryl transfer over the mesityl group, thus avoiding preparation of the symmetrical diaryliodonium salts that are sometimes difficult to synthesize. These mild catalytic conditions are thought to provide a new route to the enantioselective construction of enolizable α -carbonyl benzylic stereocenters without racemization.

Although catalytic reactions involving low-valent palladiums (Pd(0) and Pd(II)) as catalytic intermediates are ubiquitous and extremely utilized in synthesis (Fig. 17.3), the unique reactivities of higher-valent palladium species in catalysis had not been recognized until recently. Systematic investigations in this decade now support the generation of hypothesized higher-valent palladium(IV) species, and it has been determined that hypervalent iodine compounds specifically have excellent oxidizing abilities to convert palladium species to the corresponding higher state of palladium(IV). A comprehensive and seminal review of the applications and mechanistic aspects of hypervalent iodine reagents in catalytic processes involving high-valent palladium(IV) species were summarized in several articles [14].

The involvement of palladium(IV) species was emphatically proposed by Sanford, one of the important contributors in this field, in 2004 in the first catalytic C–H acetoxylation of sp^2 as well as sp^3 carbons directed by the metal-coordinating chelating group for C–H activation [15]. As an extension of this chemistry, it was reasoned that diaryliodonium salts were applied as the two-electron oxidant to perform a catalytic C–H arylation reaction of aromatic and heteroaromatic rings involving the palladium(II)/(IV) process, enabling transfer of aryl groups from the iodonium salts at a C–H bond proximal to a nitrogen directing group (Fig. 17.7) [16]. The C2 arylated products were exclusively formed by the reaction of indoles, and thereby the palladium-catalyzed method in indoles is complementary to the C3-selective arylation using a copper catalyst (vide supra) [8]. In the same year, that is, 2005, Daugulis and Zaitsev reported diphenyliodonium salt as one example for Pd(II)-catalyzed C(sp^2)–H arylation of anilides [17]. The palladium-catalyzed C–H activation/arylation methods using diaryliodonium salts have also been applied to *ortho* arylation of phenol-derived aryl pivalates acting as an oxygen directing group [18].

Another type of transformation involving the generation of high-valent palladium species by a hypervalent iodine reagent is the oxidative diamination of alkenes employing a palladium(II) catalyst [19]. According to Müniz, internal alkenes carrying sulfonamide groups (Fig. 17.8) undergo clean deamination under the catalysis of palladium(II) in combination with a hypervalent iodine reagent, $\text{PhI}(\text{OAc})_2$. The reaction consists of two mechanistically different C–N bond formation events; it is initiated by *anti*-aminopalladation of alkenes followed by reductive substitution accompanying inversion of the stereochemistry at a secondary carbon attached to high-valent palladium(IV) generated in situ. The overall process thus usually provided *cis*-diamination products with complete selectivity in both the steps.

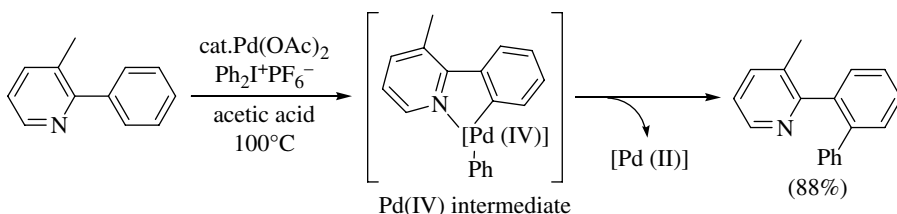


FIGURE 17.7 Directed C–H arylation using diaryliodonium salts involving palladium(IV) species.

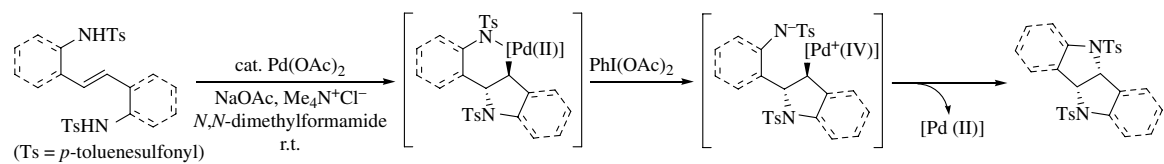


FIGURE 17.8 Alkene diamination involving palladium(IV) species in the presence of hypervalent iodine oxidant.

17.1.3 Oxidative Homo- and Cross-Couplings

17.1.3.1 Iodine-Based Coupling Initiator

Molecular iodine is known to oxidize carbanions to effectively produce carbon-centered radicals. Some two generated radicals would dimerize or couple with each other, leading to homocoupling products and cyclic compounds in inter- and intra-molecular fashion, respectively. The oxidative C–C bond-forming strategy was, for example, applied to the iodine-induced oxidative dimerizations of stabilized enolates of ketones and carboxylic acid [20]. Another variant of this radical coupling is based on the oxidation of stabilized benzyl carbanions [21]. Dimerization of oxidizable electron-rich indoles via electrophilic 3-iodo-3*H*-indol-1-iums intermediates was successfully triggered by treatment with molecular iodine at room temperature, but the example of C–C bond formation using molecular iodine is still rare [22]. Very recently, catalytic iodine with oxygen or *tert*-butyl hydroperoxide system as terminal oxidants was reported for the first time for the oxidative C–C bond formation for the C–H bonds neighboring the nitrogen atom in tetrahydroisoquinones [23]. This new oxidative coupling methodology is compatible with effective incorporation of a large number of nucleophiles, including enols and active methylene compounds, into tetrahydroisoquinones (Fig. 17.9), at room temperature. It was explained that this catalyst system regenerates molecular iodine, whilst in situ generated hypoiodides and further oxidized active iodine species postulated by other research groups [24, 25]

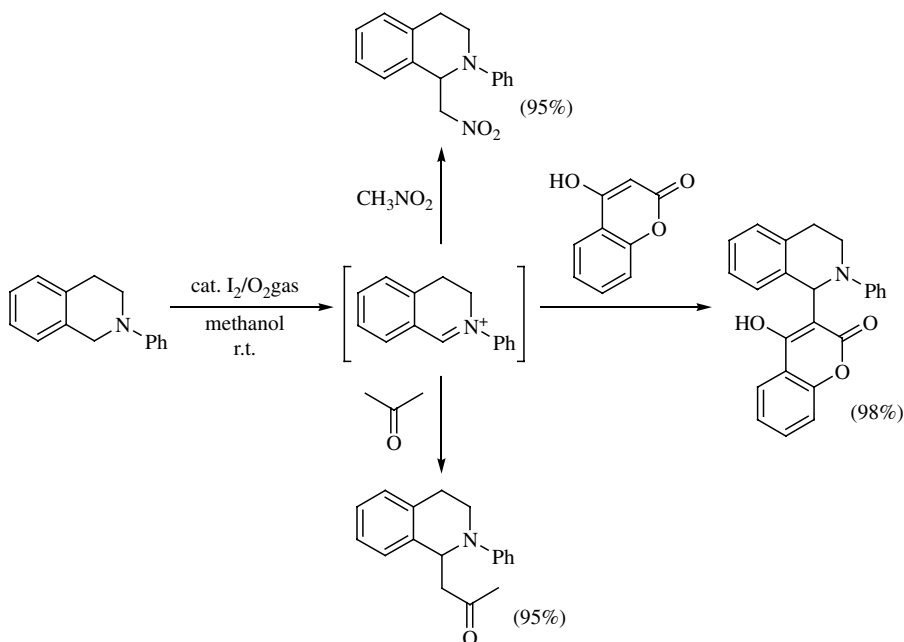


FIGURE 17.9 Oxidative coupling of reactive sp^3 C–H bond of tetrahydroisoquinolines with a series of carbon nucleophiles.

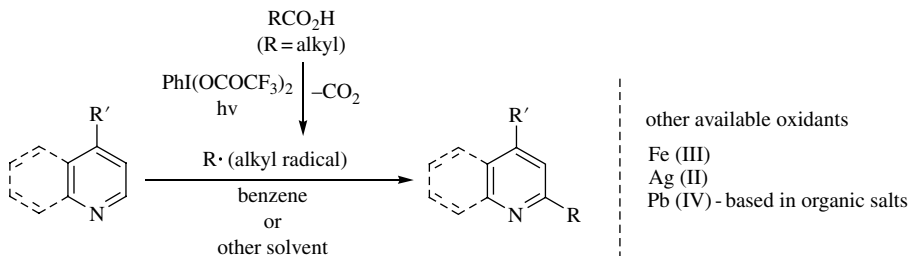


FIGURE 17.10 Decarboxylative coupling of alkyl radicals to specific aromatic rings by means of degradation of hypervalent iodine compounds.

during the catalytic reactions of inorganic and organic salts of iodide (I^-) in the presence of peroxides or other oxidants in other oxygenations thus cannot be perfectly excluded. Despite these recent developments, general success in the use of molecular iodine and/or hypoiodides as coupling initiators in C–C bond-forming couplings is very limited.

The rare examples for the couplings of two carbon atoms in C–H groups mediated by molecular iodine and similar low-valent iodine species would imply the difficulty of using monovalent iodines for C–H activations in an expanding range of C–C bond formations. Besides, it was sometimes insufficient for oxidations of less reactive molecules stable under oxidative conditions, though the mild oxidation power of these monovalent iodines is very useful in some situations for performing selective chemical transformations of oxidizable functionalities in complex substrates. Thus, higher-valent iodine species, especially hypervalent iodine reagents, possibly become a new tool in coupling reactions for C–C couplings of less reactive substrates. Apart from the oxidative coupling between C–H bonds, the use of hypervalent iodine reagents instead of other metal oxidants was reported in decarboxylative C–C couplings toward heteroaromatic compounds involving the generation of alkyl radicals [26]. The alkyl radicals were thus formed by radical decarboxylative pathways from carboxylic acids and the oxidant under irradiation of ultraviolet (UV) or upon heating, which can be trapped by π -deficient *N*-heteroaromatics, such as quinolones and pyridines (Fig. 17.10).

In theory, the attractive merit of the oxidative coupling strategy, which is superior to other coupling methods, is the use of two folds of C–H bonds in each coupling molecule. The conventional first-generation couplings by the catalysis of transition metals employ organic halides and organometallic compounds as an electrophile and nucleophile, respectively, for the formation of carbon–carbon bonds [5], thus requiring prefunctionalization of the coupling substrates (Fig. 17.11, for example, of coupling of arenes). Meanwhile, oxidative coupling is a straightforward and direct route that can reduce the synthetic step by avoiding the preparation of substrates. In addition, this strategy includes less waste material generation regarding the metal salts. However, early studies employing heavy metal oxidants revealed that effective coupling by the oxidative method was frequently troublesome because the formed coupling products, typically, would be further oxidized and would tend to produce oligomers and undesired by-products derived from uncontrolled oxidations.

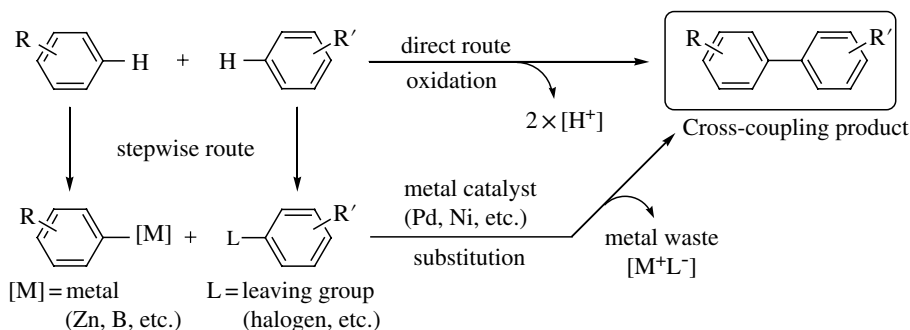


FIGURE 17.11 General cross-coupling routes to biaryls.

A pioneering metal-free example of oxidative coupling was first presented by Kita and coworkers in the 1990s using hypervalent iodine reagents, specifically, phenyliodine bis(trifluoroacetate) (PIFA), for electron-rich aromatic compounds, phenyl ethers. It was surprising that under known conditions the reaction of hypervalent iodine reagents with phenyl ethers would normally give diaryliodonium salts by dehydrative condensation. The unprecedented oxidative coupling thus seemed to involve a new reactivity of hypervalent iodine reagent. Indeed, the unique single-electron-transfer (SET) ability of PIFA by specific activation with additive and solvent for affording the corresponding aromatic cation radicals of phenyl ethers was the key role for initiating this type of coupling identified by the same research group [27]. The intramolecular couplings leading to cyclic biaryls via formation of aromatic cation radicals effectively proceeded by the treatment of PIFA with two equivalents of Lewis acids, such as boron trifluoride and trimethylsilyl trifluoromethanesulfonate (TMSOTf) (Fig. 17.12, Eq. 1). The biaryl synthetic method utilizing the oxygen-, sulfur-, and silicon-tethered templates could provide a practical route for multisubstituted biaryls (Eq. 2) [28]. The formed dibenzoheterocyclic structures can be cleaved by general procedures to give the symmetrical or unsymmetrical biaryls. The same research group continuously extended the SET strategy to the intermolecular variant for achieving homocoupling of electron-rich aromatic compounds (phenyl ethers and their sugar hybrid, and alkyl arenes) [29] and a few other heteroaromatic compounds [30]. During these studies, Domínguez and coworkers also expanded this chemistry to the syntheses of benzo[c]phenanthridine system and heterobiaryl compounds [31].

Despite their being ideal with regard to the green chemistry aspect, the oxidative method in intermolecular C–H couplings suffered because of the undesired formation of homodimers. In contrast, when the reactions of naphthalene and mesitylene or pentamethylbenzene (Fig. 17.13, Eq. 1) were examined using hypervalent iodine coupling conditions, the unexpected cross-coupling event occurred exclusively, which was also discovered by Kita and coworkers [32]. The oxidative cross-biaryl coupling between aromatic hydrocarbons was quite difficult because the reactivity of these substrates toward oxidant is too similar to discriminate one of these molecules selectively for activation. Even the novel method using a palladium catalyst with

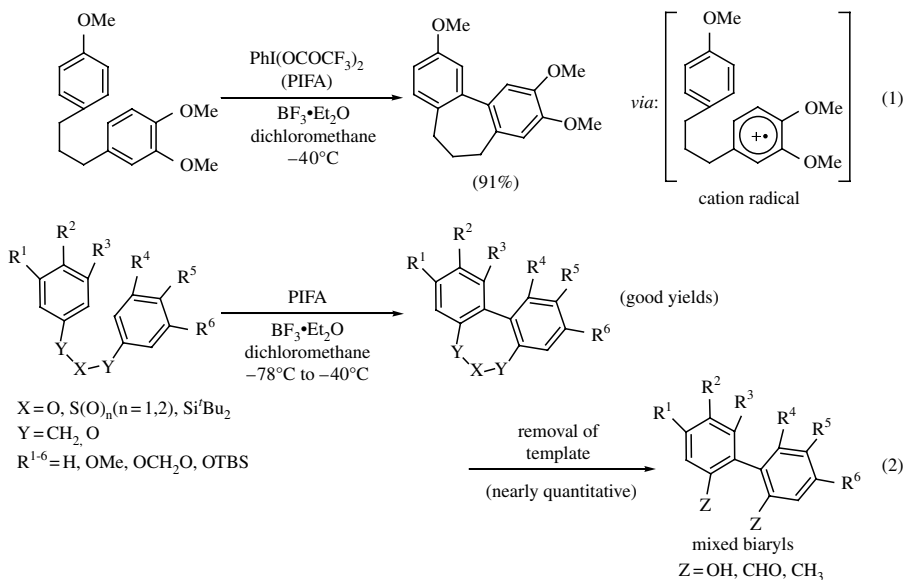
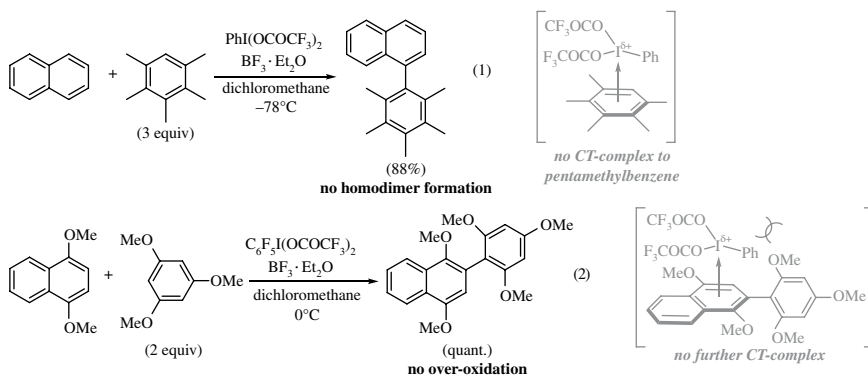


FIGURE 17.12 Hypervalent iodine-induced intramolecular biaryl couplings via SET oxidation process.

potassium persulfate in the presence of trifluoroacetic acid [33] was not successful, resulting in the major formation of a homocoupling product of mesitylene; the reaction of naphthalene with mesitylene produced a large amount of mesitylene dimer together with low yield formation of the desired mixed biaryl of naphthalene and mesitylene. Also, typical heavy metal oxidants (i.e., V(V) -, Mn(III) -, Mo(V) -, Fe(III) -, Tl(III) -, and Pb(IV) -based oxidants), nitric acid-based oxidants, and anodic oxidations were previously tested for several types of intermolecular cross-couplings, but all failed with regard to selective access to mixed biaryl compounds. The facts clearly suggest that the use of a hypervalent iodine reagent is indispensable for selective cross-couplings and efficient reactions.

Like the typical SET oxidation mechanism using a hypervalent iodine reagent through the charge-transfer complex (see Fig. 17.12), selective cross-coupling is hypothesized by the generation of a naphthalene cation radical. Subsequent in situ trapping of the cation radical by the existing mesitylene and the further one-electron oxidation and deprotonation furnish the aryl-aryl bond to give the mixed biaryl. The fast and selective SET event of naphthalene over mesitylene should occur for the realization of the cross-coupling; otherwise, homodimer formation would potentially occur. This can be experimentally expected by the measured oxidation potential of the aromatic compounds (naphthalene: $[E^{\text{ox}}] = 1.64 \text{ V}$, mesitylene: $[E^{\text{ox}}] = 1.83 \text{ V}$, respectively); however, the high selectivity toward naphthalene in the SET activation by PIFA cannot be determined simply by the oxidation potential. For example, the successful coupling of naphthalene ($[E^{\text{ox}}] = 1.64 \text{ V}$) and pentamethylbenzene ($[E^{\text{ox}}] = 1.58 \text{ V}$) cannot be explained only by the oxidation potentials. The unusual chemoselectivity



Mechanism

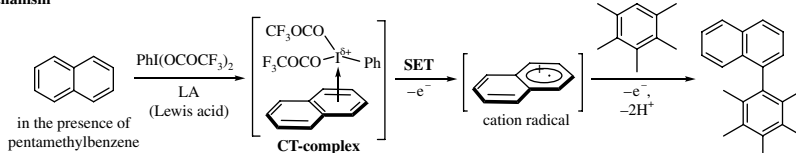


FIGURE 17.13 Oxidative cross-biaryl couplings via selective formation of aromatic cation radicals by hypervalent iodine SET oxidations.

probably indicated that PIFA would not form the C–T complex with the multiply substituted aromatic compounds by the steric factor.

By exploiting the SET oxidizing ability of hypervalent iodine reagents, very difficult intermolecular cross-coupling of highly oxygenated aromatic compounds was also accomplished by defining an oxidant (Fig. 17.13, Eq. 2) [34]. In this case, the use of a perfluorinated alternative ($C_6F_5I(OCOCF_3)_2$, FPIFA) was important to expel homocoupling, and PIFA caused cross-coupling along with approximately 10% formation of the undesired homodimer of methoxybenzene. Overoxidation of the formed biaryl that is sensitive to oxidation can be ruled out, which is rationalized by considering the steric repulsion in the C–T complex formation. Apparently, the methoxybenzene ring located perpendicular in the biaryl product sterically hampers the complexation with FPIFA.

The SET-induced cross-coupling strategy was also extended by another research group to the direct C3 arylation of *N*-acetylindoles with anisoles [35]. An application of the naphthalene–mesitylene cross-coupling in Fig. 17.13 appeared for direct four-component assembly en route to linear oligonaphthoarene molecules with a binaphthyl core [36]. The method represents an attractive straightforward alternative to the multistep syntheses based on the traditional metal-catalyzed cross-couplings.

The intermolecular oxidative coupling of phenols is extremely difficult due to the sensitivity of the remaining phenol functionality in the coupling products. Indeed, the rate of coupling is compatible with that of the activation of phenol starting materials (Fig. 17.14, k_1 versus k_2), causing the competitive overoxidation of the phenol coupling products. Therefore, enhancing the rate k_1 of the ligand exchange process of phenols at the hypervalent iodine atom is essential to realize

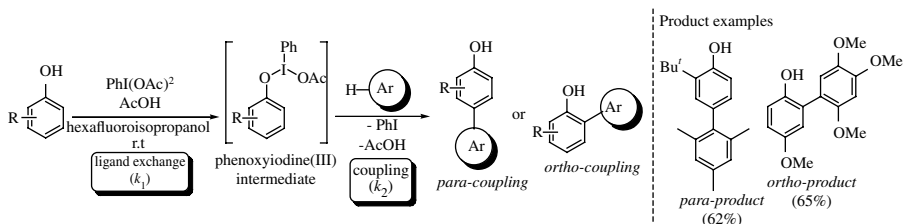


FIGURE 17.14 Oxidative cross-biaryl couplings of phenols using hypervalent iodine reagent.

efficient phenol cross-coupling. Recently, addition of acetic acid has been found to remarkably affect the enhancement of the coupling yield in the phenol oxidative cross-couplings [37]. As the phenol rapidly interacts with the activated iodine reagent with the aid of acetic acid, homocoupling of the phenols and overoxidation of the coupling products are suppressed. The reaction generally involves the generation of a phenoxenium cation by the two-electron oxidation of phenols via the phenoxyiodine(III) intermediate, which then reacts preferentially at the *para* over the *ortho* positions with another coupling partner. On the other hand, the formation of an aromatic cation radical in Fig. 17.13 for phenols renders the product biased to undesired homocoupling. Therefore, the controllable two-electron oxidizing ability of the hypervalent iodine reagent by addition of acetic acid is highly important for the successful cross-coupling of phenols. The reaction is applicable for direct synthesis of hexahydroxytriphenylene, a discotic liquid crystal, by the oxidative tricyclization of catechol.

It is known that the oxidations of *p*-methoxy-substituted phenols and *N*-protected anilines with PIFA and other hypervalent iodine reagents in the presence of electron-rich styrene derivatives results in the formation of *trans*-dihydrobenzofurans and indoles, the formal [3+2] coupling products at the phenolic oxygen or aniline nitrogen, and their *ortho* aromatic carbon, albeit in low yields [38]. With respect to the protocols of the reported phenolic oxidations with hypervalent iodine reagents in fluoroalcohols (see Chapters 7 and 16), a unique oxidative coupling utilizing similar cycloadducts of suitably *N*-protected anilines and phenols with aromatic compounds as an intermediate has recently been suggested by Canesi's research group (Fig. 17.15) [39]. In contrast to the results in Fig. 17.14 [37], this coupling is useful for the coupling of phenols at the *ortho* positions in good yields. During this coupling, dearomatized formal [3+2] cycloadducts are first formed from the phenols or anilines containing a sulfonyl group after trapping of the in situ generated phenoxenium ions and related *N*-analogues by another aromatic partner. The presence of substituents (R in Fig. 17.15) on the 4-position of the aromatic ring directs the course of the reaction site exclusively at the *ortho* positions. By subsequent treatment with an acid, the isolatable tricyclic intermediates can then in situ readily collapse into the finally observed cross-coupling biaryls with aromatization as the driving force. Thus, formal cross-coupling via the cycloadducts differs from the earlier-mentioned coupling examples with regard to the reaction mechanism.

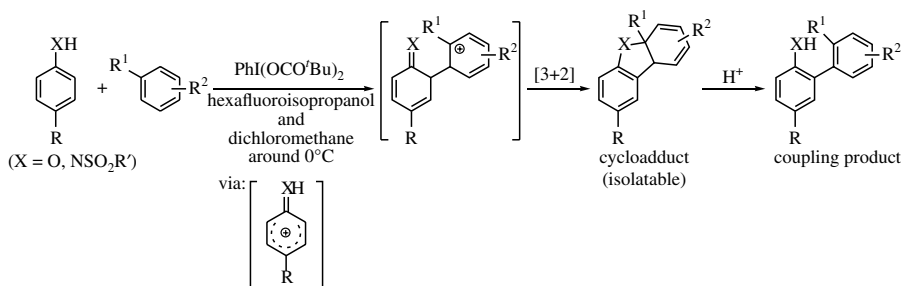


FIGURE 17.15 An alternative new coupling via [3 + 2] cycloadducts of phenols and anilides with aromatics.

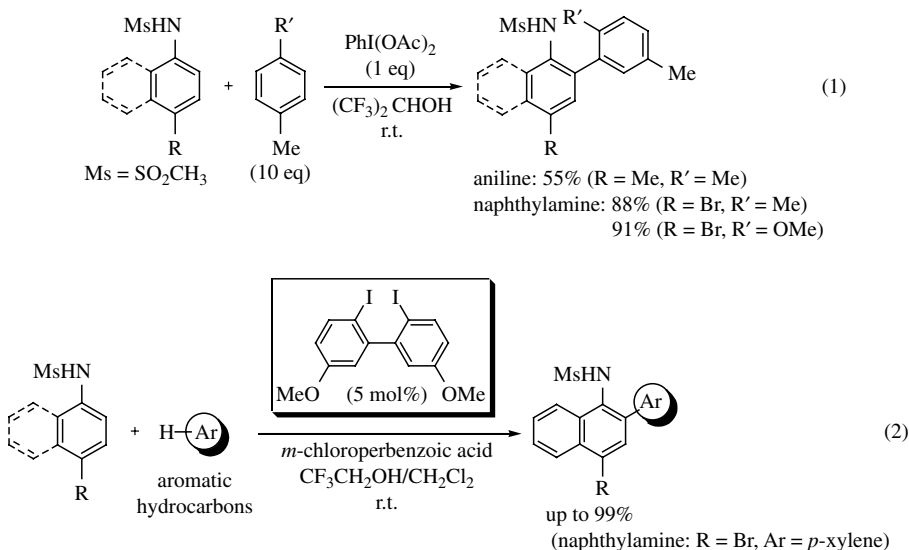


FIGURE 17.16 Oxidative biaryl couplings of *N*-arylsulfonamides with aromatic hydrocarbons. (1) stoichiometric method; (2) *in situ* catalytic strategy utilizing 2,2'-diiodobiphenyl designer catalyst.

Kita and coworkers have reported the direct formations of biaryl compounds by similar oxidative coupling of *N*-alkylsulfonyl anilides and a variety of aromatic compounds, specifically, nonactivated aromatic hydrocarbons [40]. Under stoichiometric hypervalent iodine conditions, suitably protected anilides can typically couple with aromatic nucleophiles at the *ortho*-carbons of the nitrogen group (Fig. 17.16, Eq. 1). By selecting the alkylsulfonyl groups, the *C*-selective reactions occur over the reported facile *N*-arylation processes for typical aniline substrates [41], probably through the stabilization of the positively charged aromatic ring at the *ortho* positions by possible σ -donation of the sulfonyl oxygens. Thus, the role of the substituent attached to the nitrogen atom is very important both in controlling the selectivity and

in suppressing undesired overoxidations, and the moderate steric size of methanesulfonyl group generally provides good results. The cycloadducts observed in Fig. 17.15 were not detected under catalytic conditions.

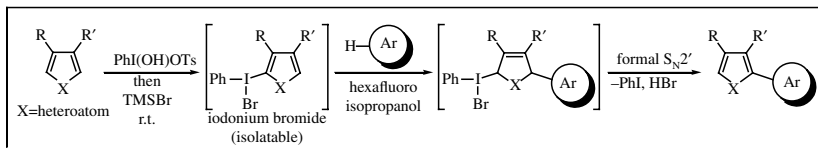
In this work, notably, the same research group has further extended the reaction system to the catalytic version (Fig. 17.16, Eq. 2). This is the first report of the C–H/C–H' oxidative cross-biaryl coupling under the organocatalysis in the intermolecular manner. Success depends on the designation of the specific 2,2'-diiodobiphenyl catalysts that produce in situ highly reactive hypervalent iodine species, and these catalysts can afford the same biaryl products, while other monomeric organoiodine compounds examined in the study failed to significantly decrease the product yields (e.g., 10 mol% iodobenzene; up to 38% yield for the coupling of 4-bromo-*N*-methanesulfonyl-1-naphthylamine and *p*-xylene). In future, it is expected that such catalyst-controlled methods will become important for developing greener synthetic methods using hypervalent iodine-based cross-coupling strategies.

17.1.4 Metal Catalyst–Free Carbon–Carbon Bond-Forming Cross-Coupling Involving Hypervalent Iodine Oxidants And Species as Carbon Sources

17.1.4.1 Reactions Involving Reactive Organoiodonium Intermediate

Before the establishment of transition metal chemistry in the cross-couplings, the reactions of diaryliodonium salts for arylation of several types of organometallic reagents, such as Grignard reagent and organolithium compounds, were investigated, especially by Beringer's group [41]. The sole use of these salts in metal catalyst–free processes was, however, usually unsatisfactory in terms of product yields; hence a transition metal catalyst was highly desirable for improving the yield and reaction scope [42]. Much later, the reaction of allyltrimethylsilane with a few aromatic compounds was reported using hypervalent iodine reagent for allylation of aromatic rings; it was suggested that the reaction involves a reactive allyl iodine intermediate [43]. At almost the same time, C–C bond formations in the reactions of Lewis acid–activated hypervalent iodine reagent (PhIO and tetrafluoroboric acid combination)–silyl enol ether adduct with electron-rich alkenes and other π -nucleophiles were also demonstrated [43]. In this case, the reactive α -ketomethyl arylidonium intermediate was generated at the first step by a low-temperature reaction of silyl enol ethers and the reagent. The successive treatment with π -nucleophiles at elevated temperature afforded α -ketomethylated coupling products in a few cases.

In spite of these examples of metal catalyst–free cross-couplings in the 1980s, they drew only limited interest from organic chemists due to narrow applicability of the substrates and coupling combinations. In 2009, Kita and coworkers reported a metal-free oxidative cross-coupling reaction based on the new activation of heteroaromatic diaryliodonium(III) salts (Fig. 17.17) [44]. In this novel coupling, the iodonium salts were first in situ prepared effectively in a fluoroalcohol solvent by treatment of heteroaromatic compounds (thiophenes and pyrroles) with [hydroxy(tosyloxy)iodo]benzene (HTIB, Koser's reagent, Ts = *p*-toluenesulfonyl) at room temperature [45]. The sequential cross-coupling was triggered by bromotrimethylsilane (TMSBr), and thus the cross-coupled biaryls were produced upon addition of other nucleophilic aromatic



Example of Coupling Products (no homo-coupling occurred)

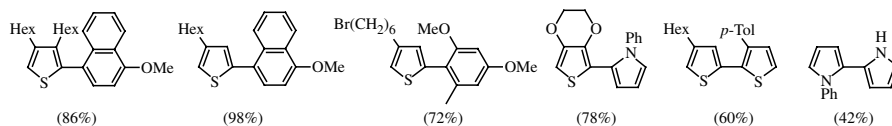


FIGURE 17.17 Diaryliodonium salt strategy for couplings of heteroaromatics.

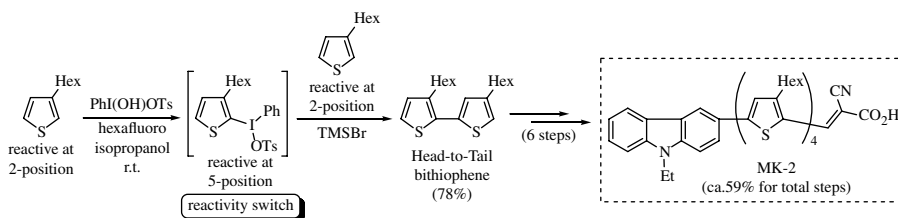


FIGURE 17.18 Unique coupling selectivity: head-to-tail (H-T) thiophene dimer formation and its application for the efficient synthesis of a photovoltaic dye molecule, MK-2.

coupling partners followed by TMSBr to the solution of diaryliodonium salts. No reaction would occur in the absence of TMSBr. Among the series of diaryliodonium salts having different counterions, only iodonium bromides [46] can work as a cross-coupling initiator, even with the action of other Lewis and Brønsted acids, and thus they were determined as the key reaction intermediates. The iodonium bromides would be generated by facile ligand exchange of tosylate by the silyl bromide. Interestingly, the reaction proceeded in a manner to remote arylation of the iodonium functionalities. The highly polar and less nucleophilic protic solvent, hexafluoroisopropanol [47], seems to assist the formal S_N2' hydroarylation with the arenes.

Regarding the substrate scope, the treatment of various electron-rich heteroaromatic compounds with nucleophilic aromatic partners under cross-coupling conditions produced the corresponding mixed heteroaromatic biaryls in very good yields as the sole coupling product. Formation of homodimer was not observed in every case. During the transformations, the reactions would proceed selectively at the α -carbon of the heteroaromatic rings.

A variety of unsymmetrical dimers of 3-alkyl and alkoxy thiophenes can be prepared by this method via iodonium salts without the formation of other regioisomers [48]. For example, the desired H-T-linked thiophene dimer was obtained in a perfect regio (over 99% selectivity) from 3-hexylthiophene with the standard procedure that uses HTIB and TMSBr (Fig. 17.18). The 3-alkyl thiophenes are inherently reactive at the most electron-rich 2-position of the thiophene ring, rapidly yielding the corresponding thienyliodonium(III) salts by the dehydrative condensation with HTIB

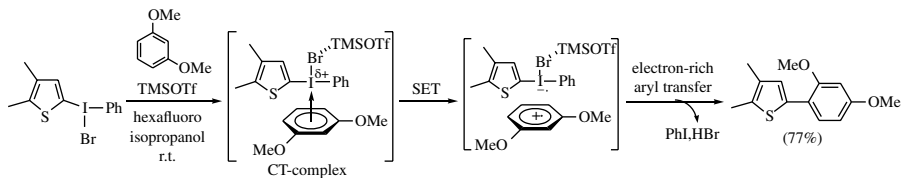


FIGURE 17.19 Alternative cross-coupling of heteroaryliodonium salts based on SET oxidation process.

[45] during the transformation. Interestingly, the formed salts, on the other hand, can exclusively react with external aromatic nucleophiles by suitable activations at the alternative α -position of the thiophene ring remote to the iodonium functionality. As a result, the two-thiophene connection can selectively occur at the 5-position of the thiophene ring of the iodonium salts and the inherently reactive 2-position of the 3-alkylthiophenes. This type of oxidative coupling is quite unique for hypervalent iodine reagents, as other oxidative coupling methods that use metal-based oxidants would typically produce symmetric homodimers as the major product. In general, electron-rich mixed heteroaromatic biaryls are promising synthetic precursors in many scientific fields. Therefore, this selectivity switching, a concept for modulating the reactivity of the heteroaromatic compounds based on the involvement of iodonium salts, has been further applied to concise syntheses of several useful artificial molecules utilizing organic materials, such as the efficient photovoltaic donor–acceptor oligothiophene dye, MK-2, which has dramatically improved yields compared to known approaches.

A unique coupling strategy in hybridizing the earlier-discussed two mechanistically different couplings has been pioneered by utilizing SET oxidation ability of in situ formed diaryliodonium intermediates [49]. The SET oxidizing coupling strategy is operative using heteroaryliodonium bromides with the activation of TMSOTf under metal-free conditions (Fig. 17.19). The iodonium substrates themselves are inactive toward any aromatic compound, and the added Lewis acid plays a key role for inducing the SET oxidation process, which was confirmed by spectroscopic studies. Enhancing the electrophilicity of the iodine atom of the salts through coordination of the Lewis acid to the bromo atom seems to facilitate the initial interaction to form the C–T complex of the salts and aromatic rings. The electron-rich heteroaryl ring transfers to the generated aromatic cation radical in preference to the less electron-rich phenyl group of iodonium salts, finalizing *ipso* substitution to yield heteroaromatic biaryl products. The *ipso* selectivity is a clear contrast to the non-SET coupling described in Fig. 17.17.

The reactivities of diaryliodonium salts such as arylating agents under acidic conditions have rarely been reported to date, since these salts scarcely react to organic molecules except under basic conditions, using a catalyst or at high temperature (see the next part on the reactions of iodonium salts with other nucleophiles). The results in Fig. 17.19 were thus the first and only examples revealing the unprecedented SET oxidation ability of iodonium salts, while the SET oxidation ability of hypervalent iodine reagents having one carbon group (i.e., phenyliodine(III) bis(trifluoroacetate) (PIFA)) has now become popular [27].

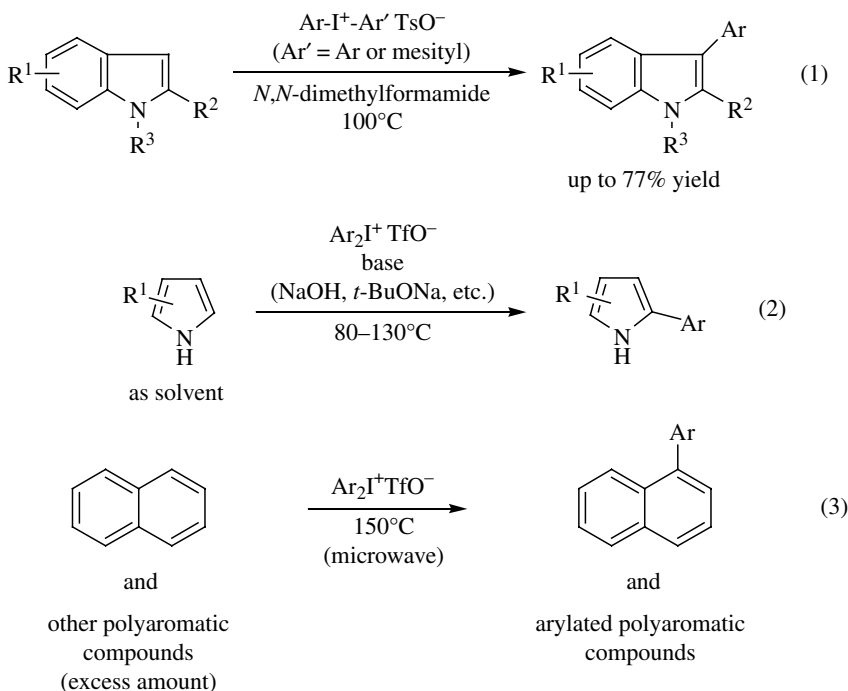


FIGURE 17.20 Other metal-free oxidative couplings using diaryliodonium salts.

To summarize, these new couplings based on the diaryliodonium intermediates have been discovered during the challenges associated with uncovering the new reactivities of the σ -aryl hypervalent iodine compounds. These new metal catalyst-free oxidative couplings via the diaryliodonium intermediates were tolerant of a wide range of substrates [50]. The use of recyclable alternatives to the hypervalent iodine reagents was possible and could improve the reactions to be more practical [51].

The research field of metal-free couplings using hypervalent iodine reagents is further expanding by using diaryliodonium salts [52]. It has been revealed that indoles and pyrroles can be arylated at high temperature at the β -positions, producing biaryls in moderate yields even in the absence of metal catalysts (Fig. 17.20, Eq. 1). In addition, base-promoted arylation of arenes and *N*-heteroarenes with diaryliodonium salts has been described (Eq. 2). More recently, naphthalene and other polyaromatic compounds with diaryliodonium salts has been reacted under microwave irradiation at 150°C for base-, metal-, and solvent-free C–H arylation (Eq. 3).

17.1.4.2 Reactions of Iodonium Salts with Other Nucleophiles

Along with the synthetic advances for their preparation (see Chapter 16), diaryliodonium salts have been used in organic synthesis as versatile arylating agents and for other applications [42]. These compounds are generally stable to air and moisture, and in recent years, some research groups have successfully developed convenient

synthetic routes from unfunctionalized arenes with hypervalent iodine reagents or iodoarenes in combination with appropriate oxidants [53]. By utilizing the excellent nature of the hypervalent iodine compounds as a leaving group that would form a more stable monovalent iodine state, it was revealed in early reports that the iodonium salts can react with anionic nucleophiles under basic conditions for use in nucleophilic substitutions with organometallic reagents and heteroatomic anions [41], metal enolates [54], and its analogues [55], in the absence of any catalyst. With recent further optimizations and elucidations for these early studies aiming at producing more valuable transformations, the iodonium salts in anionic metal-free nucleophilic couplings seems to have gained increasing importance in organic chemistry. In this section, we briefly describe several recent developments regarding this subject.

The enantioselective introduction of electrophiles to the α -carbon of carbonyl groups has remained a challenging topic in organic synthesis, having been widely investigated by many researchers. In 1999, Ochiai and coworkers reported the asymmetric α -phenylation of cyclic β -keto esters using chiral diaryliodonium salts based on the 1,1'-binaphthalene structure under basic conditions [56]. Although the selectivity was low (up to 53% ee with 37% yield of the product) and applicability was limited to only few substrates (Fig. 17.21, Eq. 1), this is the first report describing the utilization of optically active diaryliodonium salts in an asymmetric reaction.

As the second example of asymmetric α -arylation of ketones using typical iodonium salts, Aggarwal and Olofsson suggested the utilization of chiral lithium amide as a counterbase for generating chiral enolates [57]. The method involves Simpkins' base (chiral α -methyl benzylamine base) [58] to desymmetrize 4-substituted cyclohexanones by asymmetric enolization followed by nucleophilic coupling with the diaryliodonium salts, producing α -aryl cyclic ketones with high enantioselectivities (Fig. 17.21, Eq. 2). Fortunately, the new reaction was successfully applied during a concise synthesis of the alkaloid, (-)-epibatidine.

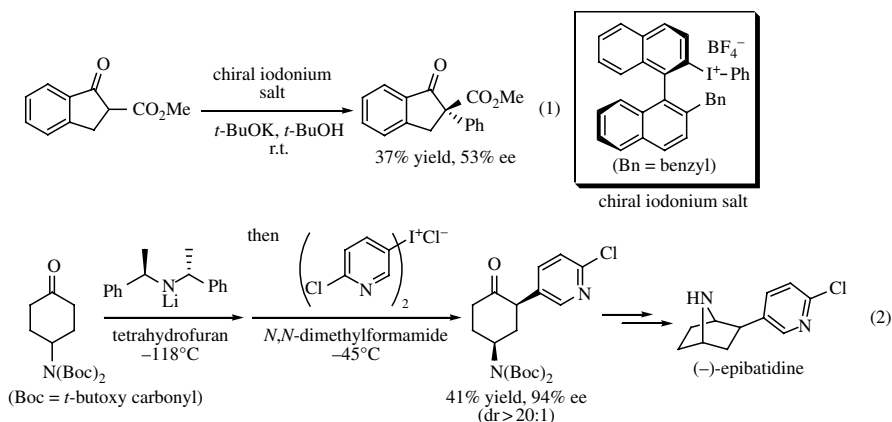


FIGURE 17.21 Asymmetric direct α -arylation of carbonyl compounds using chiral diaryliodonium salt (Eq. 1) or chiral base (Eq. 2).

To date, only these two types of metal-free asymmetric α -arylations where the asymmetric induction is controlled by the chiral iodonium salt or the chiral lithium base have been described in the literature.

Ozanne-Beaudenon and Quideau reported some phenoxides as an alternative carbon nucleophile toward diaryliodonium salts [59]. Usual O-arylation event for diaryliodonium salts [41] did not occur, but their report somewhat accompanied unprecedented dearomatization of specific phenols and naphthols along with the C-arylation based on the ambident nature of the used phenoxides, giving arylated cyclohexa-2,4-dienone derivatives (Fig. 17.22).

In recent years, Olofsson's research group has mainly been contributing to significant improvements to the classically reported nucleophilic substitutions for the diaryliodonium salts by further optimizing the reaction conditions. The optimizations regarding the base, solvent, temperature, and reaction time have defined the reliable conditions as the use of potassium *tert*-butoxide in tetrahydrofuran for the O-arylation of phenols and of the same base in refluxing toluene for the carboxylic acids, which enables very efficient and practical metal-free O-arylations of a broad scope of phenols and carboxylic acids under mild conditions (Fig. 17.23, Eqs. 1 and 2) [60].

These arylations are applicable to sulfonic acids, which provide O-arylated sulfonate esters. On the other hand, a metal-free S-arylation salts forming diaryl sulfones occurred for arylsulfonic acid salts using diaryliodonium salts (Fig. 17.23, Eq. 3) [61].

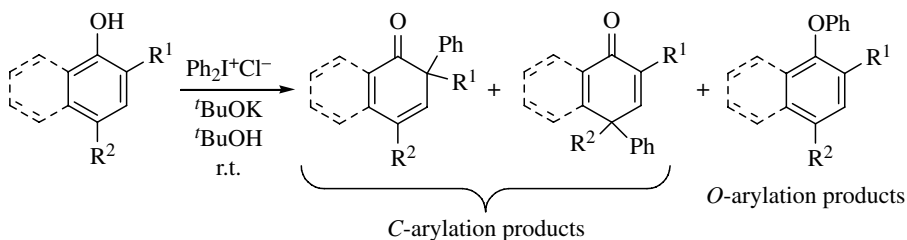


FIGURE 17.22 Dearomatizing C-arylation of phenols and naphthols using diaryliodonium salts as an arylating agent.

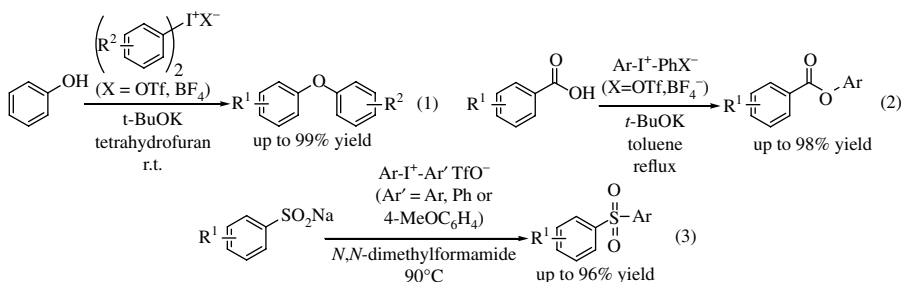


FIGURE 17.23 Efficient metal catalyst-free arylations of heteroatoms utilizing diaryliodonium salts.

Nucleophilic amination and fluorination of diaryliodonium salts are also possible by employing suitably *N*-protected amines and appropriate fluoride salts as nucleophiles for the metal-free *N*-arylation [62] and synthesis of aryl fluorides [63], respectively.

In addition, the aqueous reaction of sodium tetraphenylborate and diaryliodonium salts was reported under microwave irradiations for the Suzuki-type biaryl couplings [64]. However, these couplings proceeded even with the monovalent iodoarenes in the presence of the inorganic salt albeit with low yields [65]. Because of the lack of detailed investigations, there is confusion about whether the mechanistic aspects of the reactions really belong to a “metal catalyst-free” coupling or whether they would work “without adding extra transition metal catalyst” by only relying on the homeopathic quantities of the palladium metal contaminant.

REFERENCES

- [1] For the statements in recent summarizations, see: Ley SV, Thomas AW. *Angew Chem Int Ed* 2003;42:5400; Rudolph A, Lautens M. *Angew Chem Int Ed* 2009;48:2656; Chen X, Engle KM, Wang D-H, Yu J-Q. *Angew Chem Int Ed* 2009;48:5094.
- [2] Ullmann F, Bielecki J. *Chem Ber* 1901;34:2174; Ullmann F. *Ber Dtsch Chem Ges* 1904;37:853.
- [3] Recent reviews: Hassan J, Sevignon M, Gozzi C, Schulz E, Lemaire M. *Chem Rev* 2002;102:1359; Evano G, Blanchardi N, Toumi M. *Chem Rev* 2008;108:3054; Monnier F, Taillefer M. *Angew Chem Int Ed* 2008;47:3096; Monnier F, Taillefer M. *Angew Chem Int Ed* 2009;48:6954; Sperotto E, van Klink GPM, van Koten G, de Vries JG. *Dalton Trans* 2010;39:10338.
- [4] Alberico D, Scott ME, Lautens M. *Chem Rev* 2007;107:174; Seregin IY, Gevorgyan V. *Chem Soc Rev* 2007;36:1173; Lyons TW, Sanford MS. *Chem Rev* 2010;110:1147.
- [5] Shimizu M, Hiyama T. *Cross Coupling; Science of Synthesis, Stereoselective Synthesis*, De Vries JG, Molander GA, Evans PA, editors. Stuttgart, Germany: Georg Thieme Verlag; 2011;3:567; *Metal-Catalyzed Cross-Coupling Reactions*, De Meijere A, Diederich F, editors. Weinheim: Wiley-VCH Verlag GmbH & Co. KGaA; 2004; Negishi E. *Handbook of Organopalladium Chemistry for Organic Synthesis*. Volume 1. Hoboken: John Wiley & Sons, Inc.; 2002. p 673; Chen X, Engle KM, Wang D-H, Yu J-Q. *Angew Chem Int Ed* 2009;48:5094; Suzuki A. *Angew Chem Int Ed* 2011;50:6722 (Nobel Lecture); Negishi E. *Angew Chem Int Ed* 2011;50:6738 (Nobel Lecture).
- [6] Piers, E., Romero MA. *J Am Chem Soc* 1996;118:1215; Allred GD, Liebeskind LS. *J Am Chem Soc* 1996;118:2748; Falck JR, Bhatt RK, Ye J. *J Am Chem Soc* 1996;117:5973.
- [7] Kang S-K, Yamaguchi T, Kim T-H, Ho P-S. *J Org Chem* 1996;61:9082; Kang S-K, Yoon S-K, Kim Y-M. *Org Lett* 2001;3:2697.
- [8] Phipps RJ, Grimster NP, Gaunt MJ. *J Am Chem Soc* 2008;130:8172; Phipps RJ, Gaunt MJ. *Science* 2009;323:1593; Duong HA, Gilligan RE, Cooke ML, Phipps RJ, Gaunt, MJ. *Angew Chem Int Ed* 2011;50:463.
- [9] Ciana C-L, Phipps RJ, Brandt JR, Meyer F-M, Gaunt MJ. *Angew Chem Int Ed* 2011;50:458.
- [10] Gigant N, Chausset-Boissarie L, Belhomme M-C, Poisson T, Pannecoucke X, Gillaizeau I. *Org Lett* 2013;15:278.

- [11] Shimizu R, Egami H, Nagi T, Chae J, Hamashima Y, Sodeoka M. *Tetrahedron Lett* 2010;51:5947; Shimizu R, Egami H, Hamashima Y, Sodeoka M. *Angew Chem Int Ed* 2012;51:4577.
- [12] Bigot A, Williamson AE, Gaunt MJ. *J Am Chem Soc* 2011;133:13778.
- [13] Harvey JS, Simonovich SP, Jamison CR, MacMillan DW. *J Am Chem Soc* 2011;133:13782.
- [14] Deprez NR, Sanford MS. *Inorg Chem* 2007;46:1924; Hickman AJ, Sanford MS. *Nature* 2012;484:177; Müniz K. *Angew Chem Int Ed* 2009;48:9412; Sehnal P, Taylor RJ, Fairlamb IJS. *Chem Rev* 2010;110:824; Xu L, Li B, Yang Z, Shi Z. *Chem Soc Rev* 2010;39:712.
- [15] Dick AR, Hull KL, Sanford MS. *J Am Chem Soc* 2004;126:2300; Desai LV, Hull KL, Sanford MS. *J Am Chem Soc* 2004;126:9542.
- [16] Kalyani D, Deprez NR, Desai LV, Sanford MS. *J Am Chem Soc* 2005;27:7330; Deprez NR, Kalyani D, Krause A, Sanford MS. *J Am Chem Soc* 2006;128:4972; Deprez NR, Sanford MS. *J Am Chem Soc* 2009;131:11234.
- [17] Daugulis O, Zaitsev VG. *Angew Chem Int Ed* 2005;44:4046.
- [18] Xiao B, Fu Y, Xu J, Gong T-J, Dai J-J, Yi J, Liu L. *J Am Chem Soc* 2010;132:468.
- [19] Müniz K. *J Am Chem Soc* 2007;129:14542.
- [20] Saegusa T, Ito Y, Koniohe T, Harada T. *J Am Chem Soc* 1977;99:1487; Babler JH, Sarussi SJ. *J Org Chem* 1987;52:3462; Porter NA, Jill JH, Rosenstein IJ, McPhail AT. *Tetrahedron Lett* 1993;34:4457; Langer T, Illich M, Helmchen G. *Tetrahedron Lett* 1995;36:4409.
- [21] For an example, see: Yeh H, Yeh S, Chen C. *Chem Commun* 2003:2632.
- [22] Li Y-X, Ji K-G, Wang H-X, Ali S, Liang Y-M. *J Org Chem* 2011;76:744.
- [23] Dhineshkumar J, Lamani M, Alagiri K, Prabhu KR. *Org Lett* 2013;15:1092.
- [24] Kirihaara M, Asai Y, Ogawa S, Noguchi T, Hatano A, Hirai Y. *Synthesis* 2007:3286.
- [25] Uyanik M, Ishihara K. *ChemCatChem* 2012;4:177.
- [26] Minisci F, Vismara E, Fontana F, Claudia M, Barbosa N. *Tetrahedron Lett* 1989;30:4569; Togo H, Aoki M, Yokoyama M. *Tetrahedron Lett* 1991;32:6559; Togo H, Aoki M, Kuramochi T, Yokoyama M. *J Chem Soc Perkin Trans 1* 1993:2417.
- [27] Kita Y, Tohma H, Hatanaka K, Takada T, Fujita S, Mitoh S, Sakurai H, Oka S. *J Am Chem Soc* 1994;116:3684; Kita Y, Tohma H, Inagaki M, Hatanaka K, Yakura Y. *Tetrahedron Lett* 1991;32:4321; Kita Y, Takada T, Tohma H. *Pure Appl Chem* 1996;68:627.
- [28] Kita Y, Gyoten M, Ohtsubo M, Tohma H, Takada T. *Chem Commun* 1996;1481; Takada T, Arisawa M., Gyoten M, Hamada R, Tohma H, Kita Y. *J Org Chem* 1998;63:7698; Hamamoto H, Anilkumar G, Tohma H, Kita Y. *Chem-Eur J* 2002;8:5377.
- [29] Arisawa M, Utsumi S, Nakajima M, Ramesh NG, Tohma H, Kita Y. *Chem Commun* 1996, 469; Tohma H, Morioka H, Takizawa S, Arisawa M, Kita Y. *Tetrahedron* 2001;57:345; Tohma H, Iwata M, Maegawa T, Kita Y. *Tetrahedron Lett* 2002;43:9241.
- [30] Tohma H, Iwata M, Maegawa T, Kiyono Y, Maruyama A, Kita Y. *Org Biomol Chem* 2003;1:1647; Dohi T, Morimoto K, Kiyono Y, Maruyama A, Tohma H, Kita Y. *Chem Commun* 2005:2930; Dohi T, Morimoto K, Maruyama A, Kita Y. *Org Lett* 2006;8:2007; Dohi T, Morimoto K, Ito M, Kita Y. *Synthesis* 2007, 2913.
- [31] Moreno I, Tellitu I, Etayo J, SanMartin R, Domínguezm E. *Tetrahedron* 2001;57:5403; Moreno I, Tellitu I, San Martin R, Domínguezm E. *Synlett* 2001:1161.
- [32] Dohi T, Ito M, Morimoto K, Iwata M, Kita Y. *Angew Chem Int Ed* 2008;47:1301.

- [33] Stuart DR, Fagnou K. *Science* 2007;316:1172; Rong Y, Li R, Lu W. *Organometallics* 2007;26:4376.
- [34] Dohi T, Ito M, Itani I, Yamaoka N, Morimoto K, Fujioka H, Kita Y. *Org Lett* 2011;13:6208.
- [35] Gu Y, Wang D. *Tetrahedron Lett* 2010;51:2004.
- [36] Faggi E, Sebastian RM, Pleixats R, Vallribera A, Shafir A, Rodriguez-Gimeno A, Ramirez de Arellano C. *J Am Chem Soc* 2010;132:17980.
- [37] Morimoto K, Sakamoto K, Ohnishi Y, Miyamoto T, Ito M, Dohi T, Kita Y. *Chem-Eur J* 2013;19:8726; Morimoto K, Dohi T, Kita Y. *Eur J Org Chem* 2013:1659.
- [38] Wang, S., Gates, B.D., Swenton, J.S. *J Org Chem* 1991;56:1979; Tohma H, Watanabe H, Takizawa S, Maegawa T, Kita Y. *Heterocycles* 1999;51:1785.
- [39] Jean A, Cantat J, Bérard D, Bouchu D, Canesi S. *Org Lett* 2007;9:2553; Jacquemot G, Menard M-A, L'Homme C, Canesi S. *Chem Sci* 2013;4:1287.
- [40] Ito M, Kubo H, Itani I, Morimoto K, Dohi T, Kita Y. *J Am Chem Soc* 2013;135:14078.
- [41] Beringer FM, Brierley A, Drexler M, Gindler EM, Lumpkin CC. *J Am Chem Soc* 1953;75:2708; Beringer FM, Dehn JW, Jr., Winicov M. *J Am Chem Soc* 1960;82:2948.
- [42] For reviews, see: Merritt EA, Olofsson B. *Angew Chem Int Ed* 2009;48:9052; Yusubov MS, Maskaev AV, Zhdankin VV. *ARKIVOC* 2011;1:370; Stang PJ. *J Org Chem* 2003;68:2997.
- [43] Lee K, Kim DY, Oh DY. *Tetrahedron Lett* 1988;29:667. Zhdankin VV, Tykwinski R, Caple R, Berglund B, Kozmin AS, Zefirov NS. *Tetrahedron Lett* 1988;29:3703; Zhdankin VV, Mullikin M, Tykwinski R, Berglund B, Caple R, Zefirov NS, Kozmin AS. *J Org Chem* 1989;54:2605.
- [44] Kita Y, Morimoto K, Ito M, Ogawa C, Goto A, Dohi T. *J Am Chem Soc* 2009;131:1668.
- [45] Dohi T, Ito M, Morimoto K, Minamitsuji Y, Takenaga N, Kita Y. *Chem Commun* 2007:4152; Ito M, Ogawa C, Yamaoka N, Fujioka H, Dohi T, Kita Y. *Molecules* 2010;15:1918; Dohi T, Yamaoka N, Itani I, Kita Y. *Aust J Chem* 2011;64:529; Dohi T, Yamaoka N, Kita Y. *Tetrahedron* 2010;66:5775.
- [46] Tohma H, Maegawa T, Takizawa S, Kita Y. *Adv Synth Catal* 2002;344:328; Dohi T, Takenaga N, Goto A, Maruyama A., Kita Y. *Org Lett* 2007;9:3129; Dohi T, Takenaga N, Goto A, Fujioka H, Kita Y. *J Org Chem* 2008;73:7365.
- [47] Ebersson L, Hartshorn MP, Persson O, Radner F. *Chem Commun* 1996:2105; Bégué J-P, Bonnetdelpon D, Crousse B. *Synlett* 2004, 18; Dohi T, Yamaoka N, Kita Y. *Tetrahedron* 2010;66:5775.
- [48] Morimoto K, Yamaoka N, Ogawa C, Nakae T, Fujioka H, Dohi T, Kita Y. *Org Lett* 2010;12:3804; Morimoto K, Nakae T, Yamaoka N, Dohi T, Kita Y. *Eur J Org Chem* 2011:6326; Dohi T, Yamaoka N, Nakamura S, Sumida K, Morimoto K, Kita Y. *Chem-Eur J* 2013;19:2067.
- [49] Dohi T, Ito M, Yamaoka N, Morimoto K, Fujioka H, Kita Y. *Angew Chem Int Ed* 2010;49:3334.
- [50] Kita Y, Dohi T, Morimoto K. *J Synth Org Chem Jpn* 2011;69:1241.
- [51] Dohi T, Morimoto K, Ogawa C, Fujioka H, Kita Y. *Chem Pharm Bull* 2009;57:710; Dohi T, Kita Y. *Chem Commun* 2009, 2073; Dohi T. *Chem Pharm Bull* 2010;58:135.
- [52] Ackermann L, Dell'Acqua M, Fenner S, Vicente R, Sandmann R. *Org Lett* 2011;13:2358; Wen J, Zhang R-Y, Chen S-Y, Zhang J, Yu X-Q. *J Org Chem* 2012;77:766; Castro S, Fernandez JJ, Vicente R, Fananas FJ, Rodriguez F. *Chem Commun* 2012;48:9089.

- [53] For recent advances, see: Hossain MD, Kitamura T. *Tetrahedron* 2006;62:6955; Hossain MD, Ikegami Y, Kitamura T. *J Org Chem* 2006;71:9903; Kraszkiewicz L, Skulski L. *Synthesis* 2008;2373; Bielawski M, Zhu M, Olofsson B. *Adv Synth Catal* 2007;349:2610; Bielawski M, Aili D, Olofsson B. *J Org Chem* 2008;73:4602; Jalalian N, Olofsson B. *Tetrahedron* 2010;66:5793; Merritt EA, Carneiro VMT, Silva LF, Jr., Olofsson B. *J Org Chem* 2010;75:7416; Ito M, Itani I, Toyoda Y, Morimoto K, Dohi T, Kita Y. *Angew Chem Int Ed* 2012;51, 12555.
- [54] Beringer FM, Forgione PS, Yudis MD. *Tetrahedron* 1960;8:49; Beringer FM, Galton SA, Huang SJ. *J Am Chem Soc* 1962;84:2819.
- [55] Chen K, Koser GF. *J Org Chem* 1991;56:5764; Iwama T, Birman VB, Kozmin SA, Rawal VH. *Org Lett* 1999;1:673; Gao P, Portoghese PS. *J Org Chem* 1995;60:2276.
- [56] Ochiai M, Kitagawa Y, Takayama N, Takaoka Y, Shiro M. *J Am Chem Soc* 1999;121:9233.
- [57] Aggarwal VK, Olofsson B. *Angew Chem Int Ed* 2005;44:5516.
- [58] Simpkins NS. *Pure Appl Chem* 1996;68:691; Cox PJ, Simpkins NS. *Tetrahedron: Asymmetr* 1991;2:1.
- [59] Ozanne-Beaudenon A, Quideau S. *Angew Chem Int Ed* 2005;44:7065.
- [60] Jalalian N, Ishikawa EE, Silva LF, Jr., Olofsson B. *Org Lett* 2011;13:1552; Petersen TB, Khan R, Olofsson B. *Org Lett* 2011;13:3462; Jalalian N, Petersen TB, Olofsson B. *Chem-Eur J* 2012;18:14140.
- [61] Umierski N, Manolikakes G. *Org Lett* 2013;15:188.
- [62] Carroll MA, Wood RA. *Tetrahedron* 2007;63:11349.
- [63] Martin-Santamaria S, Carroll MA, Carroll CM, Carter CD, Rzepa HS, Widdowson DA, Pike VW. *Chem Commun* 2000, 649; Carroll MA, Nairne J, Smith G, Widdowson DA. *J Fluorine Chem* 2007;128:127; Ross TL, Ermert J., Hocke C, Coenen HH. *J Am Chem Soc* 2007;129:8018; Wang B, Qin L, Neumann KD, Uppaluri S, Cerny RL, Di Magno SG. *Org Lett* 2010;12:3352; Graskemper JW, Wang B., Qin L, Neumann KD, DiMagno, SG. *Org Lett* 2011;13:3158.
- [64] Yan J, Zhu M, Zhou Z. *Eur J Org Chem* 2006:2060; Yan J, Hu W, Zhou W. *Synth Commun* 2006;36:2097; Yan J, Hu W, Rao G. *Synthesis* 2006:943.
- [65] For the related reports, see: Leadbeater NE, Marco M. *Angew Chem Int Ed* 2003;42:1403; Leadbeater NE, Marco M. *J Org Chem* 2003;68:5660; Arvela RK, Leadbeater, NE, Sangi MS, Williams VA, Granados P, Singer RD. *J Org Chem* 2005;70:161.

18

METAL IODIDES–MEDIATED REACTION

MAKOTO SHIMIZU¹, IWAO HACHIYA¹, AND JUNJI INANAGA²

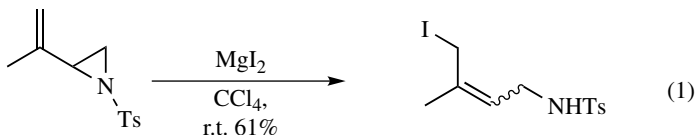
¹*Department of Chemistry for Materials, Mie University, Tsu, Mie, Japan*

²*Institute for Molecular Chemistry and Engineering, Kyushu University, Fukuoka, Japan*

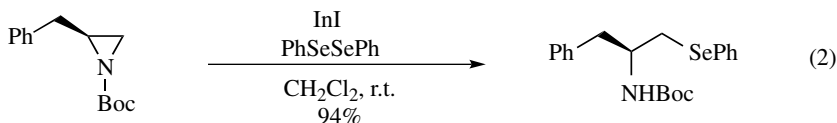
18.1 METAL IODIDES–MEDIATED REACTION

Recently a number of reactions have been published regarding the use of metal halides in organic synthesis. Among them, metal chlorides and bromides are most frequently used for many organic transformations, whereas an increasing number of papers have appeared using metal iodides in this particular decade, and they are most conveniently categorized as follows:

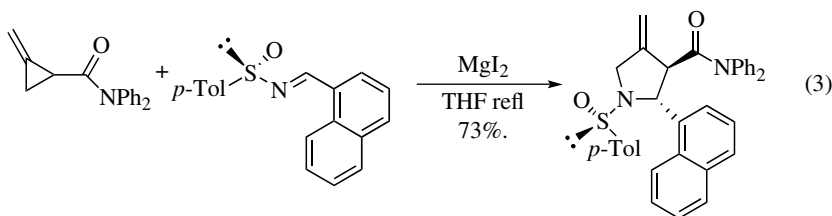
1. As sources of an iodide ion: Examples of MgI_2 -, InI_3 -, SmI_2 -, and TiI_4 -mediated iodinations/organic transformations are representative (Eq. 1) [1].



2. As sources of metal ions (involving low-valent metals): InI -, SmI_2 -, and TiI_4 -mediated reductive transformations represent typical examples (Eq. 2) [2].



3. As promoters for chemoselective reactions (involving use as Lewis acids): For example, relatively mild Lewis acidity of metal iodides as compared with their chloro and bromo counterparts offers specific transformations (Eq. 3) [3].



In this chapter, among metal iodides recently introduced in the literature, particular attention is given to characteristic features of SmI₂ and TiI₄, and their use in synthetic organic chemistry is discussed in detail.

18.1.1 Introduction

Titanium(IV) iodide [4] is a rare molecular binary metal iodide, consisting of isolated molecules of tetrahedral Ti(IV) centers. TiI₄ can be distilled without decomposition at 1 atm (bp 377°C). It is also conveniently purified by sublimation (180°C/0.8 mmHg). The compound is a close relative to TiCl₄. The difference in melting point between TiCl₄ (mp -24°C) and TiI₄ (mp 150°C) is comparable to the difference between the melting points of CCl₄ (mp -23°C) and Cl₄ (mp 168°C), reflecting the stronger intermolecular van der Waals bonding in the iodides. Regarding the use of titanium halides in organic synthesis, although titanium tetrachloride is frequently used in Mukaiyama aldol-type reaction and pinacol coupling reaction via low-valent species, titanium iodide is rarely used for such reactions. Recent studies show that titanium tetraiodide is an excellent reagent for the reductive formation of enolate species from α-halo carbonyl or imino compounds, and the subsequent reactions with carbonyl compounds give aldol products in good yields. Regarding chemoselective reductions using titanium tetraiodide, α-dicarbonyl or α-imino carbonyl compounds were chemoselectively reduced with TiI₄ to give α-hydroxy or amino ketones, respectively. Subsequent reactions with aldehydes or imines realize the selective formation of 1,2-diol or diamine derivatives. Pinacol coupling of aromatic and unsaturated aldehydes was efficiently promoted by titanium tetraiodide in propionitrile to give the 1,2-diol derivatives with high selectivities in high yields. Chemoselective deoxygenation of sulfoxides was also carried out successfully to give sulfides in good to excellent yields. In this chapter the following three types of reactions are discussed.

1. Use as Lewis acid
2. Iodination reaction
3. Reduction

18.1.2 Use as Lewis Acid

Titanium(IV) iodide promotes Mukaiyama aldol- and Mannich-type reactions. This type of reaction can be modified using TiI_4 as catalyst. In this case, good diastereoselectivity is obtained using a chiral ketene silyl acetal (Eq. 1) [5]. For example, in the presence of a catalytic amount of TiI_4 , the reaction gives an antiprodukt with high diastereoselectivity (Eq. 2) [6]. Also, 1,4- and 1,2-double nucleophilic addition of ketene silyl acetals proceeds with α,β -unsaturated aldimines in the presence of titanium(IV) iodide. This kind of reaction can be effected by other Lewis acids such as titanium chloride, titanium bromide, and aluminum chloride (Eq. 3) [7]. Nazarov reaction can also be conducted with TiI_4 to give a cyclopentanone derivative in moderate yield (Fig. 18.1). This reaction involves the reduction of an initially formed α -iodinated ketene, which is discussed later (Eq. 4) [8].

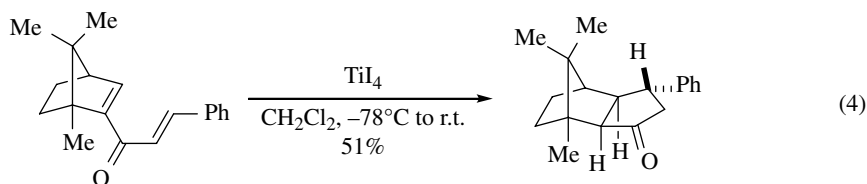
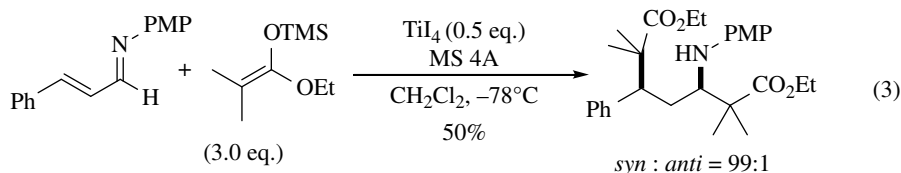
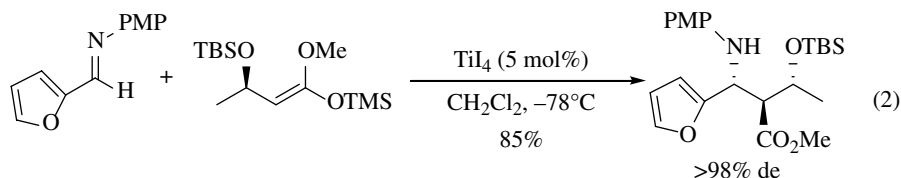
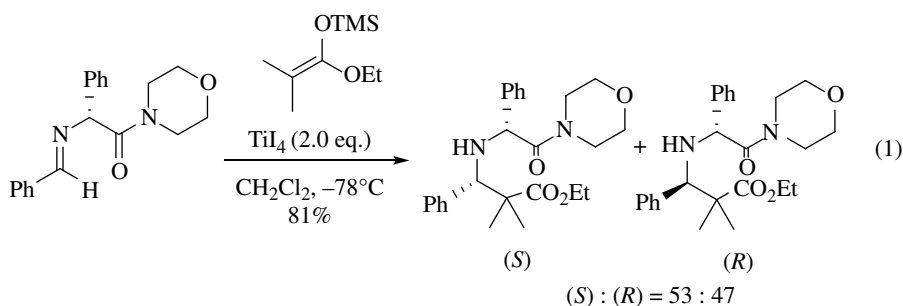


FIGURE 18.1 Lewis acid.

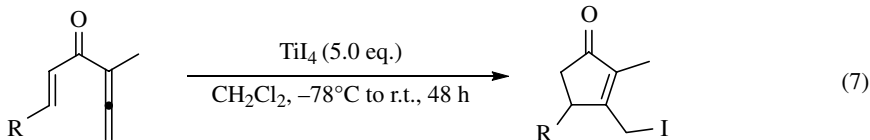
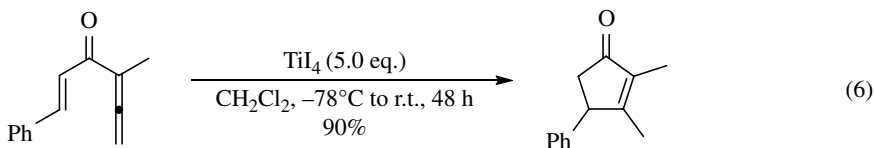
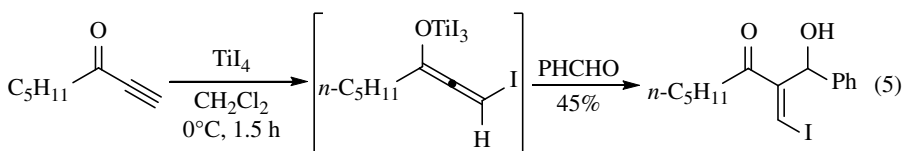
18.1.3 Iodination

Titanium iodide is a good iodination reagent for olefins and acetylenes. When alkynyl ketone is treated with titanium iodide, the iodotitanation reaction proceeds to give iodo allenolate, which in turn adds to aldehyde to afford α -iodovinylidene- β -hydroxyketone. This kind of reaction is reported using titanium bromide and chloride as a halogenation reagent to give the corresponding bromide and chloride, respectively (Eq. 5) [9a]. In a similar manner, allenyl vinyl ketones undergo interesting cyclization reactions to give cyclopentenones (Eqs. 6-7) [9b] (Fig. 18.2).

Simple olefins are also iodinated with titanium iodide to give iodoalkanes in moderate to good yields (Eq. 8). Phenyl acetylene gives α -iodostyrene, whereas 2,2-diiodoalkanes are major products from 1-alkynes when they are treated with titanium (IV) iodide (Eqs. 9 and 10) [10a]. In the presence of acetals, the reaction gives intriguing C–C bond forming products (Eqs. 11 and 12) [10a, 10b] (Fig. 18.3).

When a suitable vinyl ketone is used, an intramolecular Prins cyclization takes place to give an iodo alcohol in moderate yield (Eq. 13) [11]. Aza-Prins-type reaction also proceeds with activated imines to give 1,3-iodoamines in good yield (Eq. 14) [12]. 2-Iodopyridines are conveniently prepared via an attack of iodide anion onto the cyano group followed by cyclization (Eq. 15) [13] (Fig. 18.4).

Cyclopropanes can be used for good acceptors of iodine. For example, spiro[2.5]cycloocta-4,7-dien-6-one undergoes ring-opening iodination reaction to give aromatized iodoethylphenol (Eq. 16) [14]. Titanium(IV) iodide reacts with diethyl azodicarboxylate (DEAD) to generate iodine. This reaction is used for the ring-opening diiodination of *gem*-aryl- disubstituted methylenecyclopropanes (Eq. 17) [15]. Other examples involving the iodination of sulfonates with TiI_4 are also known [16] (Fig. 18.5).



R = Me (28%)
R = 4-MeOC₆H₄ (27%)
R = 4-CF₃C₆H₄ (14%)

FIGURE 18.2 Iodotitanation reagent 1.

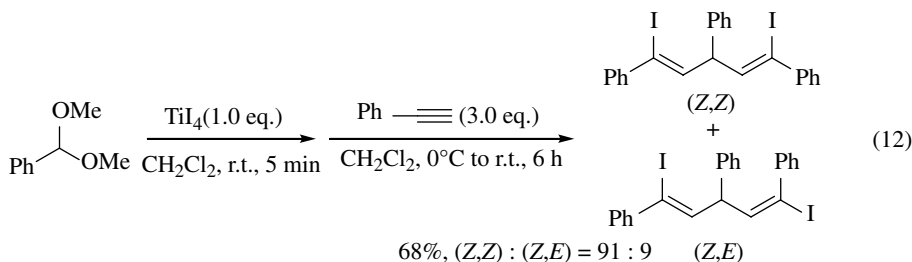
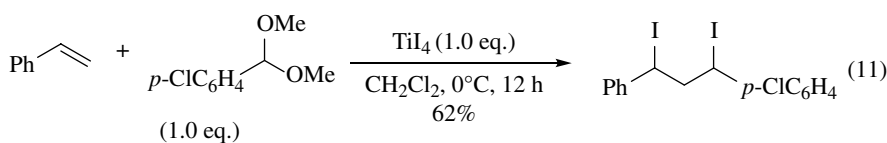
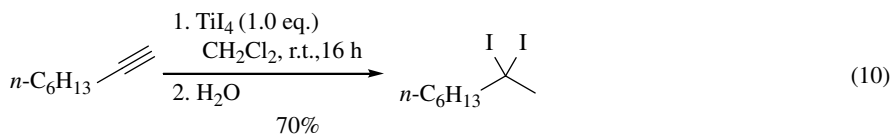
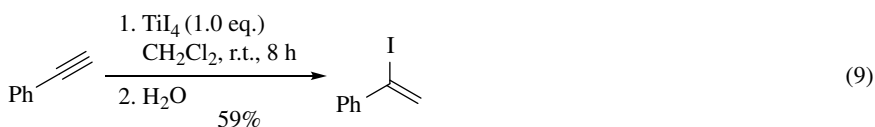
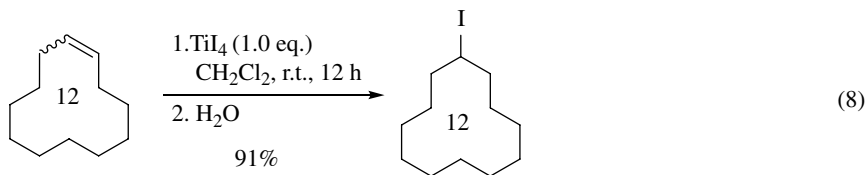


FIGURE 18.3 Iodotitanation reagent 2.

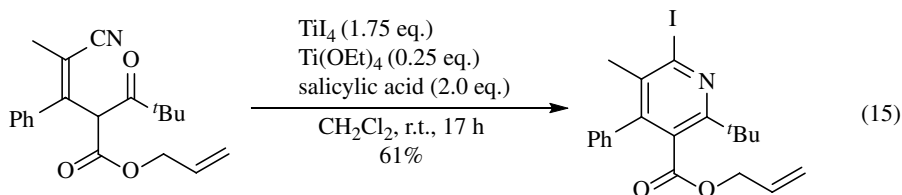
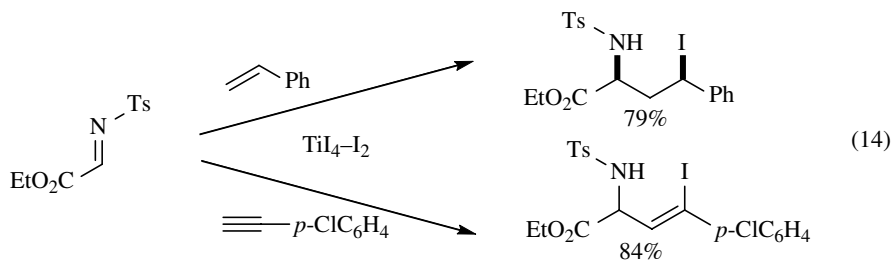
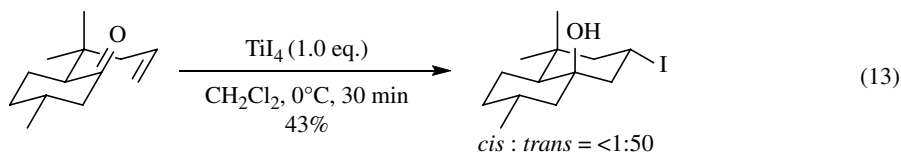
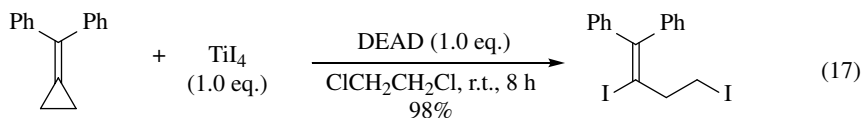
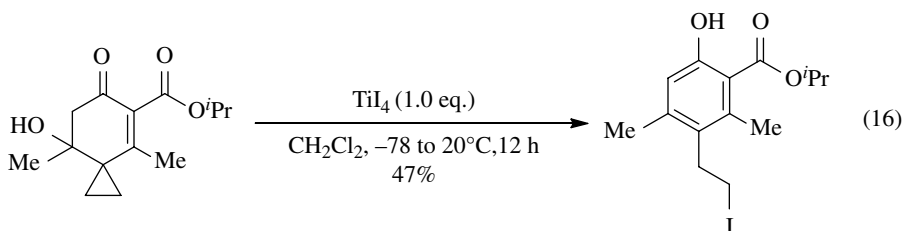


FIGURE 18.4 Iodotitanation reagent 3.



DEAD = diethyl azodicarboxylate

FIGURE 18.5 Iodotitanation reagent 4.

18.1.4 Reduction

α -Diketones are readily reduced with titanium(IV) iodide to give α -hydroxy ketones. The use of acetonitrile as solvent is crucial for the specific reduction (Eqs. 18-20) [17a] (Fig. 18.6).

Imino ketones can also be used for this type of reduction. In this case, chemoselective reduction is possible at the imino moiety (Eq. 21) [17b]. When aldehyde or imine is present in this type of reduction, reductive aldol or Mannich-type reaction also takes place to give α -amino- β -hydroxyketones [18] or α,β -diaminocarbonyl compounds (Eqs. 22-23) [19]. For the synthesis of α -hydroxy- β -aminoesters, reductive Mannich-type reaction may be carried out using α -allyloxy- α -trimethylsiloxy acetate as substrate with imines (Eq. 24) [20] (Fig. 18.7).

First discovered by Reformatsky in 1887, the reaction of α -halocarbonyl compounds and aldehydes in the presence of zinc is the first example of a large member of now commonly used carbon-carbon bond forming reactions. Recently, the combined use of TiCl_4 and R_4NI was reported to be a good tool for aldol reaction of α -haloketones. AlI_3 and CeI_3 also effect the Reformatsky-type reaction. Generation of enolate or aza-enolate can be conducted using simple α -halo ketones and oximes with titanium(IV) iodide as reducing agent (Eq. 25). Using α -iodo ketones aldol reaction proceeds with *syn*-selectivity [21a]. α -Tosyloxy ketones are also good substrates for this reductive aldol reaction [21b]. The enolates and aza-enolates thus generated undergo aldol and Mannich-type reactions with aldehydes, enals, and imines (Eqs. 26-28) [22] (Fig. 18.8).

Reductive ring opening of *N*-tosylaziridines is readily carried out with titanium(IV) iodide to form the titanium enolates, which in turn are subjected to addition reaction with aldehydes and imines to give aldol or Mannich-type products in good yields (Eq. 29) [23a]. Although the reaction does not proceed well with ketone derivatives, use of oxime ether effects the desired addition in a diastereoselective manner (Eq. 30) [23b]. Azetidine-3-ones can be used for a similar reductive aldol reaction to give amino hydroxyl ketones in good yields; in certain cases a combined use of TiI_4 and InCl_3 or TiCl_4 gives better results (Eqs. 31 and 32) [23c, 23d] (Fig. 18.9).

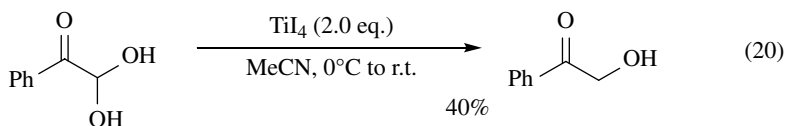
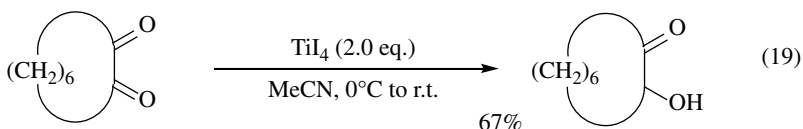
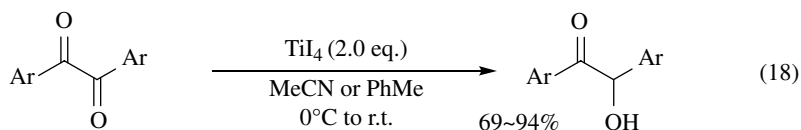


FIGURE 18.6 Reducing reagent.

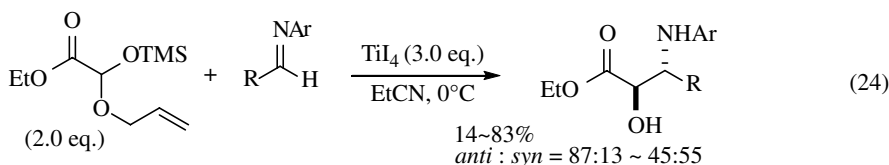
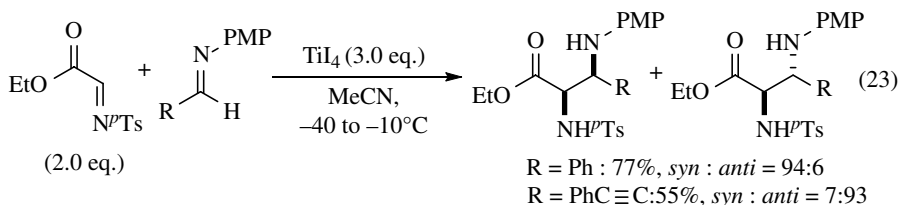
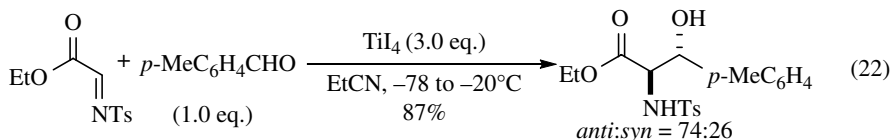
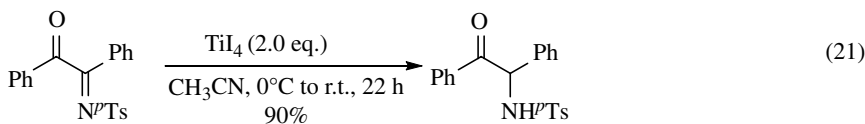


FIGURE 18.7 Reducing reagent and subsequent C-C bond formations 1.

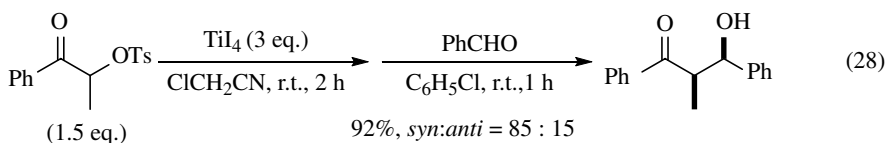
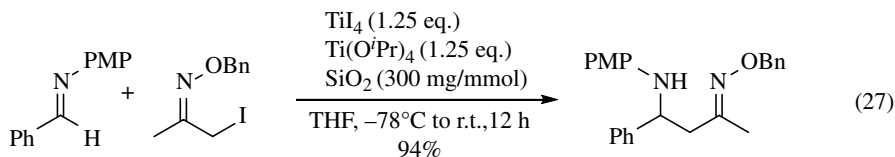
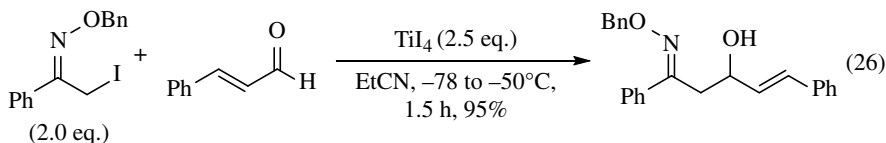
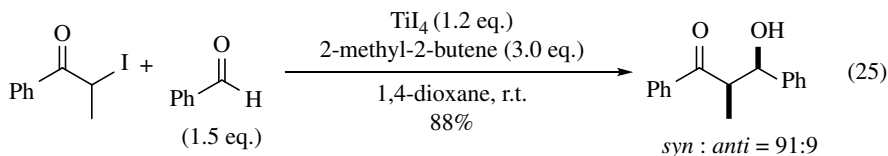


FIGURE 18.8 Reducing reagent and subsequent C-C bond formations 2.

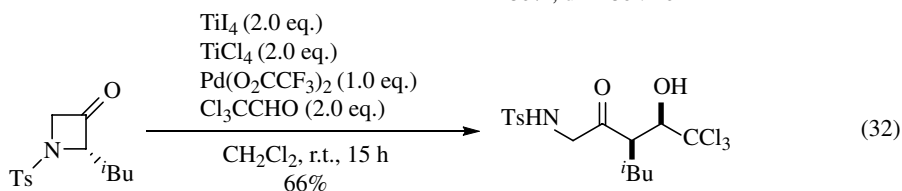
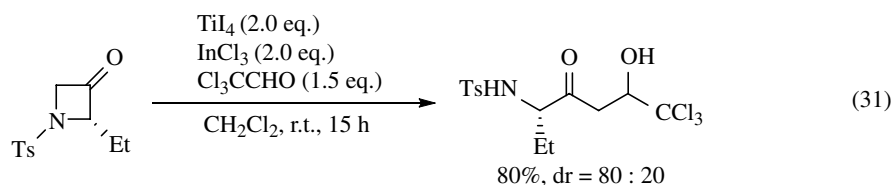
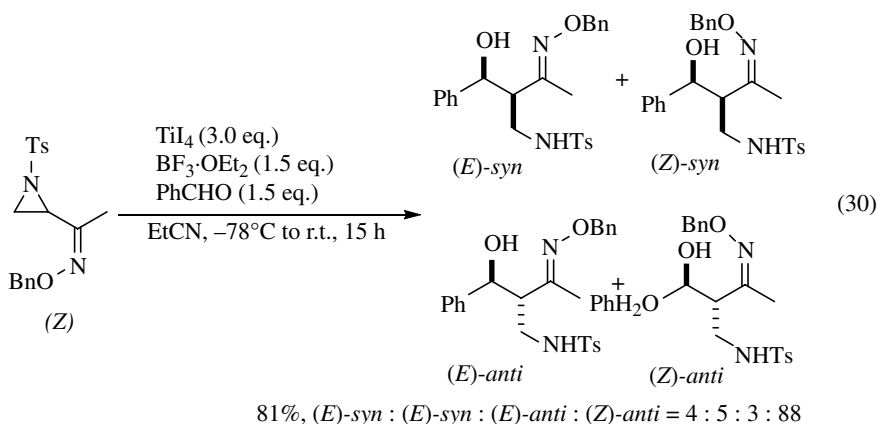
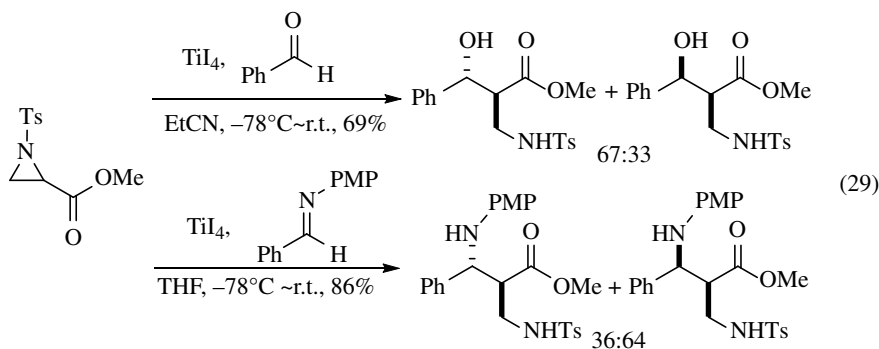


FIGURE 18.9 Reducing reagent and subsequent C-C bond formations 3.

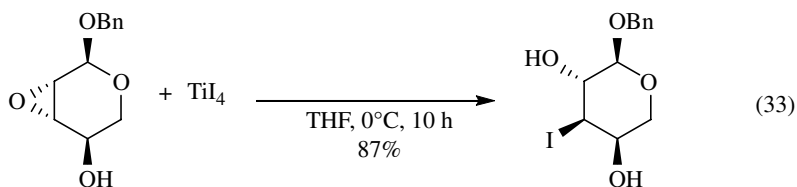


FIGURE 18.10 Iodination reagent.

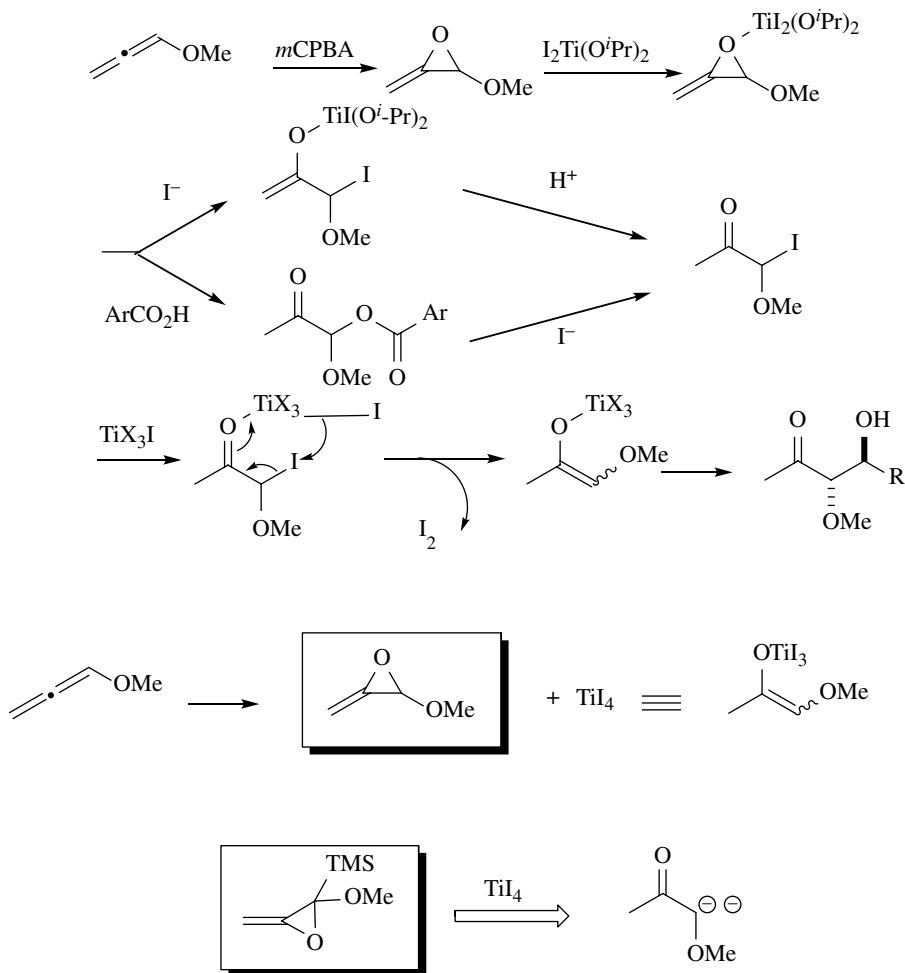


FIGURE 18.11 Reaction with methoxyallene oxide (reaction pathways).

Related to this ring opening, titanium(IV) iodide is also a good reagent for the ring-opening iodination of epoxide to give iodohydrins (Eq. 33) [24] (Fig. 18.10).

More intrinsic reactions are observed starting from alkoxyallenes. When methoxyallene is treated with *m*-chloroperbenzoic acid (*m*-CPBA), the reaction gives methoxyallene oxide, which in turn is treated with titanium(IV) iodide/titanium(IV) isopropoxide and an acetal successively in the presence of salicylic acid to afford a *syn*-aldol adduct derived from the enolate of methoxyacetone (Eq. 34) [25]. The reaction mechanism of this reaction can be explained in terms of ring-opening iodination of epoxide followed by enolate formation via reduction of α -iodomethoxyacetone with iodide anion. When aldehydes are used as acceptors, use of a 1:1 mixture of TiI_4 – $\text{Ti}(\text{O}^i\text{Pr})_4$ gives *anti*-aldol products (Eq. 35). Starting with methoxytrimethylsilyllallene, the same reaction gives dehydrated α,β -unsaturated ketones (Eq. 36) [26]. Ethoxyallene may be used for the Michael addition reaction of the alkoxyacetone enolate generated in a similar fashion (Eq. 37) [27] (Figs. 18.11, 18.12, and 18.13).

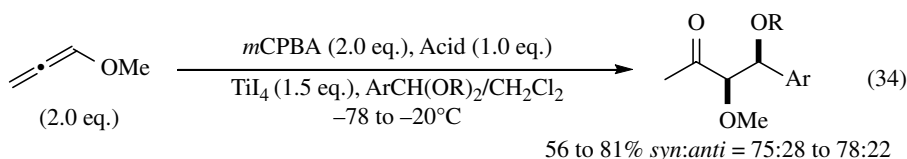


FIGURE 18.12 Reaction with methoxyallene oxide.

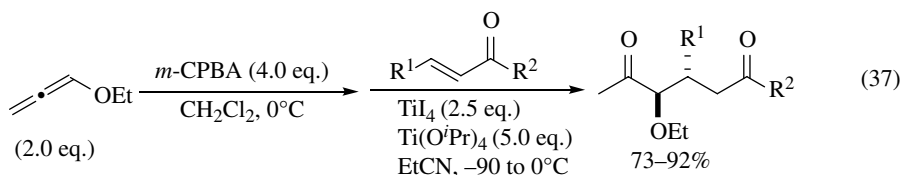
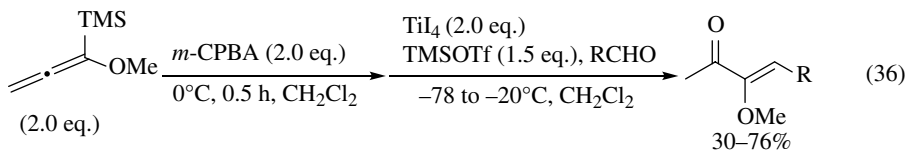
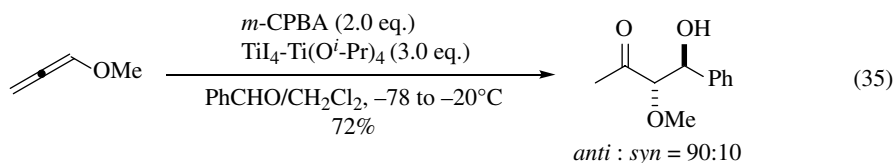


FIGURE 18.13 Reaction with alkoxyallene oxides.

Sulfoxides are reduced readily with titanium(IV) iodide to give sulfides in good yields. This reaction tolerates the presence of ketones, ethers, esters, amides, and olefins (Eq. 38) [28] (Fig. 18.14).

Aldehydes undergo simple pinacol coupling reaction with titanium(IV) iodide to give 1,2-diols with high *DL* selectivity (Eq. 39) [29]. β -Bromoaldehydes are excellent substrates for this type of coupling reaction, although analogous bromine-free enals do not always undergo efficient homo-coupling reaction (Eq. 40). The coupling products can be transformed into saturated derivatives by simple hydrogenation (Eqs. 41 and 42) [30a] (Figs. 18.15, 18.16, and 18.17).

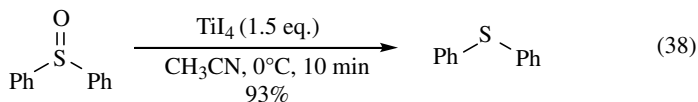


FIGURE 18.14 Reduction of sulfoxides.

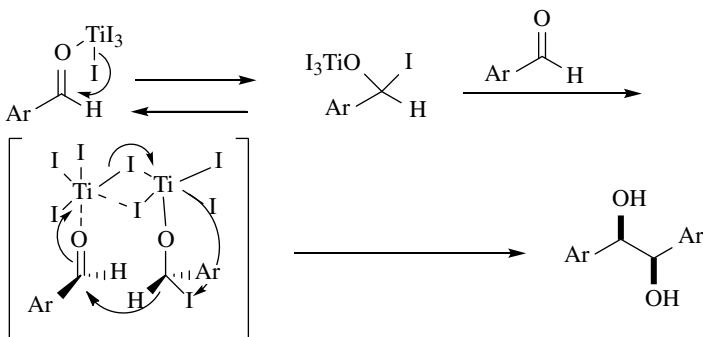
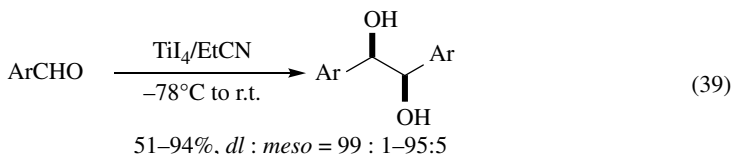


FIGURE 18.15 Pinacol coupling of aromatic aldehydes.

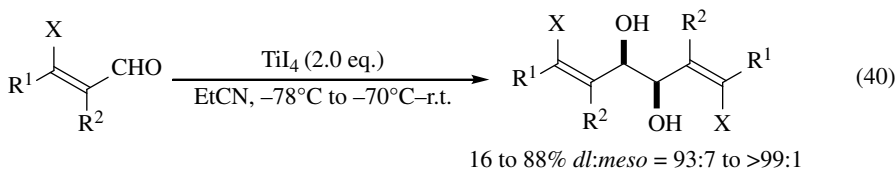


FIGURE 18.16 Pinacol coupling of halogenated unsaturated aldehydes.

(*Z*)-3-Iodo-3-trimethyl-silylpropenal is an excellent substrate for the DL-selective pinacol coupling under the influence of TiI_4 . The trimethyliodo-vinyl moiety of the coupling product is in turn efficiently utilized for the C–C bond forming reactions via the Suzuki coupling reaction (Eq. 43) [30b] (Fig. 18.18).

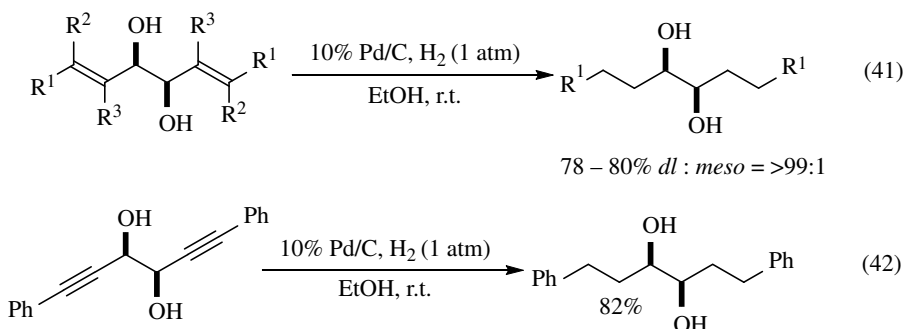


FIGURE 18.17 Subsequent reduction.

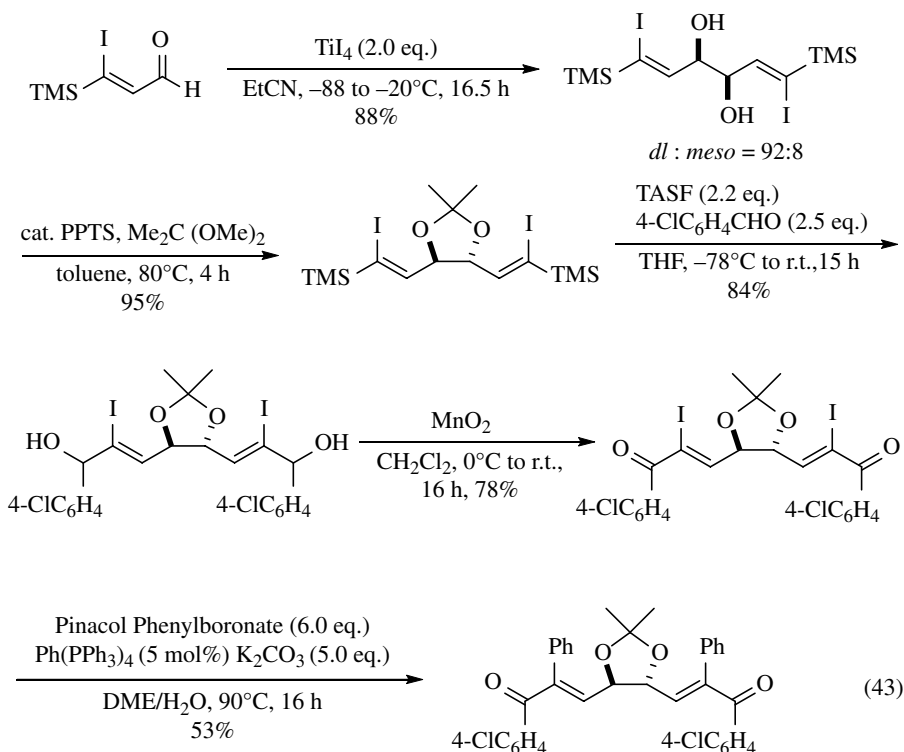


FIGURE 18.18 Application of the pinacol coupling products.

This type of coupling reaction may be extended to a crossed version, when saturated aldehyde is used in propionitrile, and the reaction gives an intriguing α -hydroxy imine (Eq. 44) [31] (Fig. 18.19).

Related reactions using titanium(IV) chloride/tetraalkylammonium iodide have been extensively investigated and many intriguing C–C bond forming reactions have already been reported [32]. Titanium(IV) iodide is reduced with LAH, Cu, or Zn to give low-valent species that can be used for the reduction of fluorotrichloromethane (Eq. 45) [33], pinacol coupling reaction (Eq. 46) [34], and Reformatsky-type reactions (Eq. 47) [35] (Fig. 18.20).

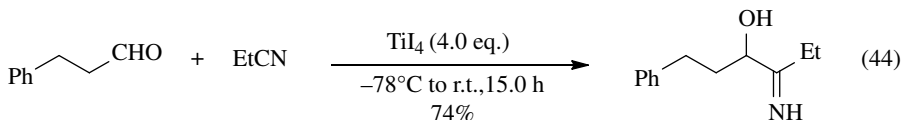


FIGURE 18.19 Reductive C–C bond formation of nitriles.

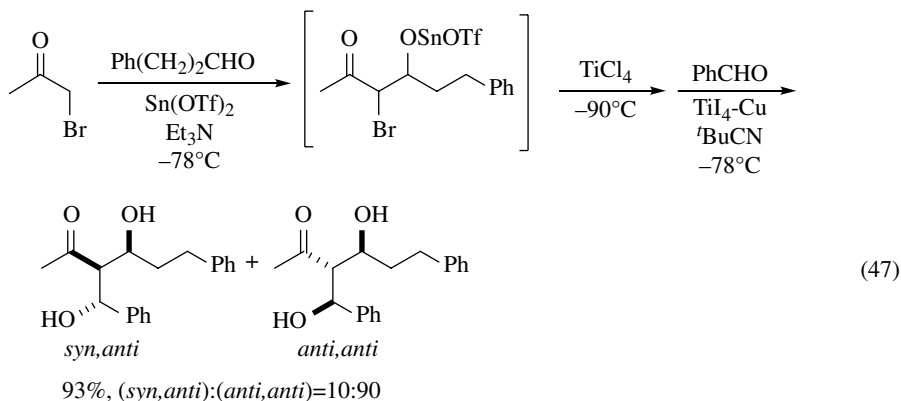
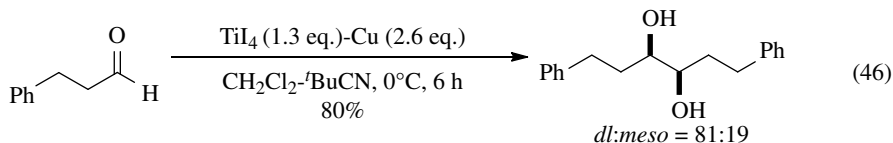
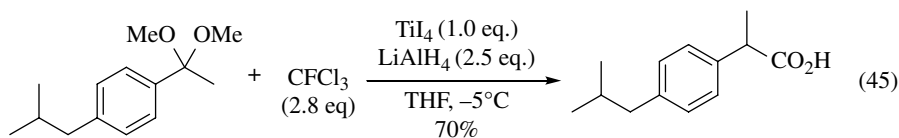


FIGURE 18.20 Other examples of titanium iodides.

18.1.5 Conclusion

The ability of iodide anion to reduce various substrates has been utilized in many organic transformations. The combination of a “soft” iodide anion with relatively “hard” metal titanium has not attracted much attention in synthetic organic chemistry so far. As described earlier, the use of titanium tetraiodide may broaden its characteristic features to induce C–C bond forming reactions as a Lewis acid, to iodinate unsaturated bonds, and to reduce substrates in a chemoselective manner, leading to specific transformations of organic molecules.

18.2 METAL IODIDE-MEDIATED REACTION (SmI_2)

18.2.1 Introduction

Samarium(II) iodide (SmI_2) is a green solid with a melting point of 520°C , where the samarium atom has a coordination number of seven in a capped octahedral configuration [36]. It can be formed by heating samarium powder with iodine under argon at 860°C or by high-temperature decomposition of SmI_3 , the more stable solid [37]. SmI_2 is commercially available as a powder or a tetrahydrofuran (THF) solution, and it can also be conveniently prepared from samarium powder and 1,2-diiodoethane, diiodomethane, or iodine in oxygen-free aprotic organic solvents like THF, tetrahydropyran, or acetonitrile (Fig. 18.21) [38].

The redox potential of the $\text{SmI}_2\text{--SmI}_2^+$ couple in THF has been reported to be -1.41 V (versus Ag/AgNO_3), and it can be increased by the addition of coordinating solvents such as hexamethylphosphoric triamide (HMPA) and water, or lithium salts like LiBr [39]. For example, in the presence of four equivalents of HMPA, the reduction potential of SmI_2 in THF is increased to -1.79 V [38c, 39b].

SmI_2 has played an ever-increasing role as one of the most attractive one-electron reducing agents in organic synthesis [38]. The emerging utility of SmI_2 resides not only in its ability to reduce a variety of functional groups, but also in its capacity to promote a number of important carbon–carbon bond forming reactions that proceed through either single-electron or successive two-electron processes. In addition, the stereochemical course of these reactions can often be highly controlled on the coordination sphere of the samarium ion. In this section, a brief overview of SmI_2 -promoted organic reactions will be provided by classifying them into two main categories: (1) simple reduction of functional groups and unsaturated bonds, and (2) carbon–carbon bond formation via reductive coupling process.

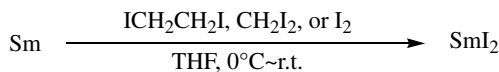


FIGURE 18.21 Preparation of SmI_2 as a THF solution.

18.2.2 Reduction of Functional Groups and Unsaturated Bonds

Organic halides ($R-X$; $X = I, Br, Cl$) and sulfonates ($R-OSO_2R'$) can be reduced to the corresponding hydrocarbons ($R-H$) with the aid of SmI_2 . It has been revealed that the reduction of aliphatic halides proceeds through a successive two-electron transfer–protonation path, whereas aromatic halides undergo one-electron reduction followed by hydrogen atom abstraction (Fig. 18.22) [39a].

The SmI_2 -promoted reduction of α,β -epoxy ketones is a convenient way to get β -hydroxy ketones, which are sometimes difficult to obtain by a traditional aldol reaction (Fig. 18.23) [40].

Regioselective reduction of conjugated esters in the presence of isolated C–C double bonds and reduction of certain type of aromatic rings are also possible (Fig. 18.24) [41, 42].

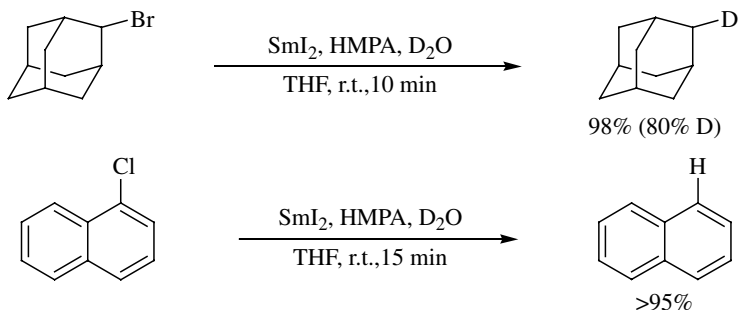


FIGURE 18.22 Reduction of aliphatic and aromatic halides.

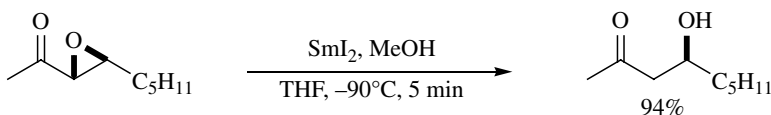


FIGURE 18.23 Reduction of an α,β -epoxy ketone.

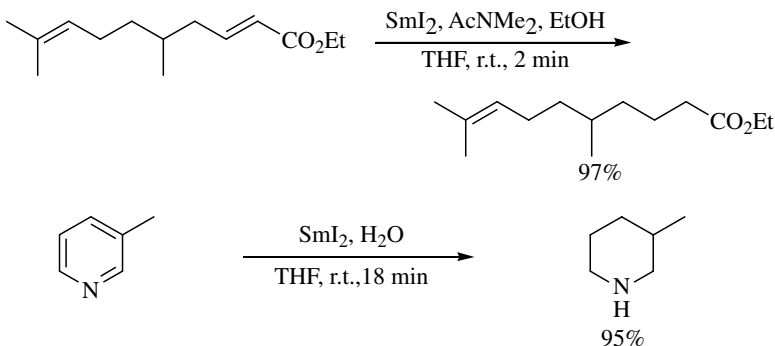


FIGURE 18.24 Reduction of carbon–carbon double bonds.

18.2.3 Reductive Carbon–Carbon Bond Forming Reaction

SmI_2 nicely promotes the pinacol coupling reaction of carbonyl compounds to give the corresponding 1,2-diols in good yields. This protocol has been successfully applied to the synthesis of a complex natural product, grayanotoxin III (Fig. 18.25) [43].

Conjugated esters and amides are rapidly hydrodimerized at room temperature with the use of a SmI_2 /THF/HPMA system in the presence of a proton source. A perfect stereoselection has been realized in the reaction of *N,N*-dibenzyl crotonamide (Fig. 18.26) [44].

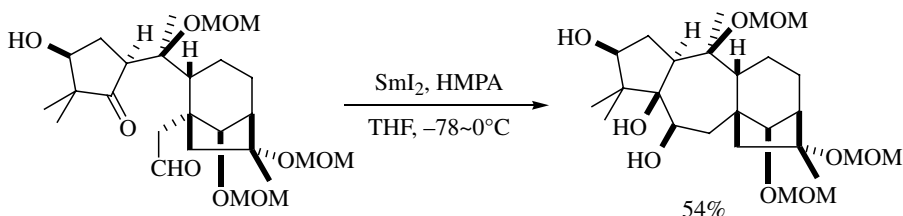


FIGURE 18.25 Pinacol-type coupling reaction.

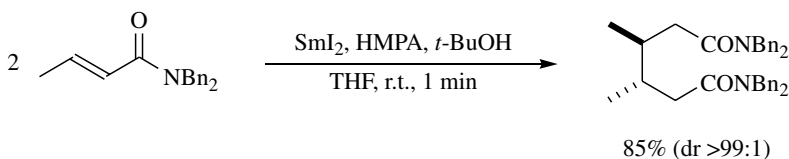


FIGURE 18.26 Hydrodimerization of crotonamide.

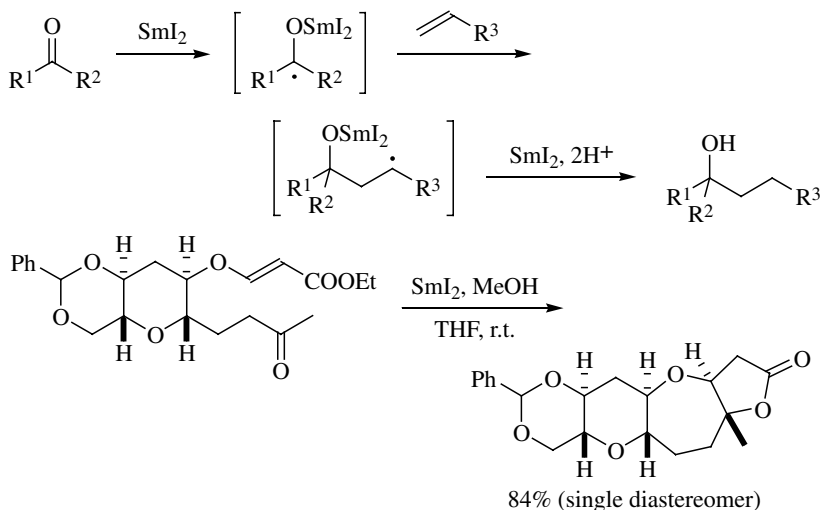


FIGURE 18.27 Carbonyl-olefin coupling reaction.

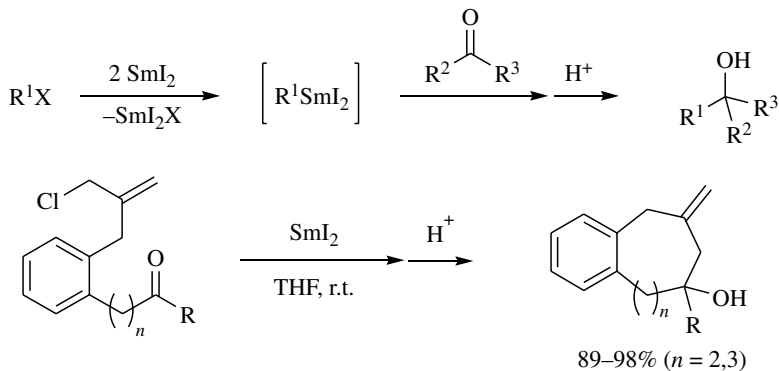


FIGURE 18.28 Barbier-type reaction.

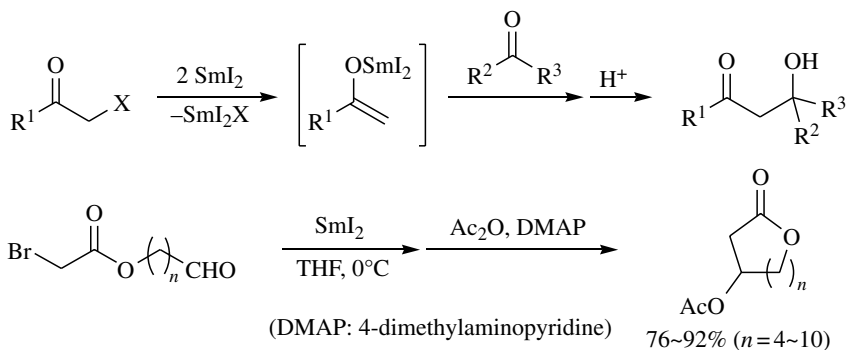


FIGURE 18.29 Reformatsky-type reaction.

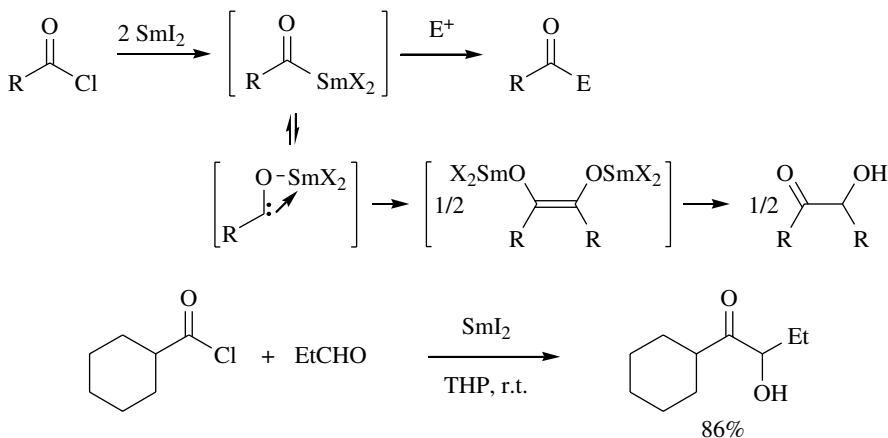


FIGURE 18.30 Reaction of acyl chloride.

Aldehydes and ketones easily accept one electron from SmI_2 to give the corresponding ketyls (anion radicals), which may attack electron-deficient C–C double bonds, and the resulting new radical species further undergoes one-electron reduction followed by protonation to afford the corresponding alcohols. This protocol has been effectively utilized for the stereoselective synthesis of polycyclic polyether natural products (Fig. 18.27) [45].

SmI_2 is highly effective for Barbier-type reactions [46]. The protocol is sometimes superior to the conventional one using magnesium metal. Thus, very efficient eight- and nine-membered ring cyclization has been achieved by using SmI_2 (Fig. 18.28) [47].

The SmI_2 -promoted Reformatsky-type reaction also takes place very easily. Application of this protocol to intramolecular reactions has enabled the construction of so-called medium rings in significantly high yields (Fig. 18.29) [48].

The SmI_2 -promoted successive two-electron reduction of acid chlorides produces the corresponding acyl samarium species that is in equilibrium with a cabenoid species, which undergoes either dimerization or a coupling reaction with electrophiles to give various types of α -ketols (Fig. 18.30) [49].

REFERENCES

- [1] (a) Arena G, Chen CC, Leonori D, Aggarwal VK. Concise synthesis of (+)-allo-kainic acid via MgI_2 -mediated tandem aziridine ring opening-formal [3 + 2] cycloaddition. *Org Lett* 2013;15:4250–4253. (b) Yadav JS, Subba Reddy BV, Mahesh Kumar G. Indium trihalide mediated regioselective ring opening of aziridines: a facile synthesis of 2-haloamines. *Synlett* 2001;15:1417–1418. (c) Wang Y, Lam HW. Stereoselective formation of alkenyl halides via magnesium halide promoted ring opening of bis-activated cyclopropenes. *J Org Chem* 2009;74:1353–1355.
- [2] Braga AL, Schneider PH, Paixao MW, Deobald AM, Peppe C, Bottega DP. Chiral selenoamines from indium selenolates. A straightforward synthesis of selenocysteine derivatives. *J Org Chem* 2006;71:4305–4307.
- [3] Scott ME, Lautens M. Synthesis of highly functionalized pyrrolidines via a selective iodide-mediated ring expansion of methylenecyclopropyl amides. *J Org Chem* 2008;73:8154–8162.
- [4] (a) Blumenthal WB, Smith H. Titanium tetraiodide. *Ind & Eng Chem* 1950;42:249–251. (b) Lowry RN, Fay RC, Chamberland BL. Titanium(IV) iodide. *Inorg Synth* 1967;X:1–6. (c) Tornqvist EGM, Libby WF. Crystal structure, solubility, and electronic spectrum of titanium tetraiodide. *Inorg Chem* 1979;18:1792–1796. (d) Jongen L, Gloger T, Beekhuizen J, Meyer G. Divalent titanium: The halides ATiX_3 (A = K, Rb, Cs; X = Cl, Br, I). *Z Anorg Allg Chem* 2005;631:582–586.
- [5] Shimizu M, Kume K, Fujisawa T. Switchover of the diastereoselectivity induced by a simple selection of titanium(IV) halides in the addition reaction of silyl ketene acetals to a chiral imine. *Tetrahedron Lett* 1995;36:5227–5230.
- [6] Shimizu M, Kume K, Fujisawa T. A catalytic amount of titanium tetrahalide as promoter for the addition reaction of silyl ketene acetals to imines. *Chem Lett* 1996;25:545–546.
- [7] Shimizu M, Morita A, Kaga T. Double nucleophilic addition to α, β -unsaturated aldimines induced by titanium tetrahalides. *Tetrahedron Lett* 1999;40:8401–8405.

- [8] White TD, West FG. Halide trapping of the Nazarov intermediate in strained polycyclic systems: a new interrupted Nazarov reaction. *Tetrahedron Lett* 2005;46:5629–5632.
- [9] (a)Taniguchi M, Hino T, Kishi Y. Aldol reaction of allenolates generated via 1,4-addition of iodideanionoritsequivalentto α,β -acetylenicketones. *Tetrahedron Lett* 1986;27:4767–4770.(b) Marx VM, Cameron TS, Burnell DJ. Formation of halogenated cyclopent-2-enone derivatives by interrupted Nazarov cyclizations. *Tetrahedron Lett* 2009;50:7213–7216.
- [10] (a)Shimizu M, Toyoda T, Baba T. An intriguing hydroiodination of alkenes and alkynes with titanium tetraiodide. *Synlett* 2005;16:2516–2518.(b)Shimizu M, Okura K, Arai T, Hachiya I. Titanium tetraiodide-promoted tandem Prins reaction of alkynes with acetals: synthesis of (Z,Z)-1,5-diiodo-1,3,5-triarylpenta-1,4-dienes. *Chem Lett* 2010;39:1052–1054.
- [11] Miles RB, Davis CE, Coates RM. Syn- and anti-selective Prins cyclizations of δ,ϵ -unsaturated ketones to 1,3-halohydrins with Lewis acids. *J Org Chem* 2006;71:1493–1501.
- [12] Shimizu M, Baba T, Toudou S, Hachiya I. Aza-Prins reaction promoted by titanium tetraiodide and iodine. *Chem Lett* 2007;36:12–13.
- [13] Hachiya I, Minami Y, Shimizu M. Titanium tetraiodide induced cyclization of 2-(2-cyanoalk-1-enyl)- β -keto esters into 2-iodopyridines. *Heterocycles* 2009;79:365–371.
- [14] (a)Bose G, Langer P. Synthesis and reactivity of 1-hydroxyspiro[2.5]cyclooct-4-en-3-ones. *Tetrahedron Lett* 2004;45:3861–3863.(b)Bose G, Bracht K, Bednarski PJ, Lalk M, Langer P. Synthesis, reactions and structure-activity relationships of 1-hydroxyspiro[2.5]cyclooct-4-en-3-ones: illudin analogs with in vitro cytotoxic activity. *Bioorg Med Chem* 2006;14:4694–4703.
- [15] Shao L-X, Zhao L-J, Shi M. Dihalogenation of gem-aryl-disubstituted methylenecyclopropanes by DEAD, DIAD/TiX₄ or free halogen. *Eur J Org Chem* 2004;4894–4909.
- [16] Lepore SD, Mondal D, Li SY, Bhunia AK. Stereoretentive halogenations and azidations with titanium(IV) enabled by chelating leaving groups. *Angew Chem Int Ed* 2008;47:7511–7514.
- [17] (a)Hayakawa R, Sahara T, Shimizu M. Reduction of 1,2-diketones with titanium tetraiodide: a simple approach to α -hydroxy ketones. *Tetrahedron Lett* 2000;41:7939–7942.(b)Shimizu M, Sahara T, Hayakawa R. Chemoselective reduction of α -imino carbonyl compounds to α -amino carbonyl compounds with titanium tetraiodide. *Chem Lett* 2001;30:792–793.
- [18] Shimizu M, Takeuchi Y, Sahara T. Reductive aldol reaction of α -imino esters promoted by titanium tetraiodide: selective synthesis of α -amino- β -hydroxy esters. *Chem Lett* 2001;30:1196–1197.
- [19] Shimizu M, Inayoshi K, Sahara T. Diastereoselective reductive imino-aldol reaction of α -imino esters promoted by titanium tetraiodide: Synthesis of α,β -diamino esters. *Org Biomol Chem* 2005;3:2237–2238.
- [20] Shimizu M, Sahara T. Use of α -allyloxy- α -trimethylsiloxyacetate for reductive imino aldol reaction promoted by titanium tetraiodide: a rapid access to β -amino- α -hydroxy esters. *Chem Lett* 2002;31:888–889.
- [21] (a)Shimizu M, Kobayashi F, Hayakawa R. Reformatsky-type reaction of α -haloketones promoted by titanium tetraiodide. *Tetrahedron* 2001;57:9591–9595.(b)Hachiya I, Inagaki T, Ishihara Y, Shimizu M. Titanium tetraiodide-promoted reductive enolate formation of α -tosyloxy ketone derivatives and aldol reaction with aldehydes. *Bull Chem Soc Jpn* 2011;84:419–421.

- [22] (a) Shimizu M, Toyoda T. Aza-Reformatsky-type reaction of α -iodomethyl ketone O-alkyl oximes promoted by titanium tetraiodide. *Org Biomol Chem* 2004;2:2891–2892. (b) Shimizu M, Tanaka M, Itoh T, Hachiya I. Remarkable effects of additives to facilitate aza-Mannich type reaction: a rapid access to β -amino ketone O-alkyl oximes. *Synlett* 2006;17:687–1690.
- [23] (a) Shimizu M, Kurokawa H, Nishiura S, Hachiya I. Titanium tetraiodide mediated reductive opening of aziridines, leading to the aldol and Mannich-type reactions. *Heterocycles* 2006;70:57–64. (b) Shimizu M, Nishiura S, Hachiya I. Titanium tetraiodide promoted reductive opening of 2-(1-benzoyloxyiminoethyl)aziridines, leading to aza-aldol reaction. *Heterocycles* 2007;74:177–183. (c) Hata S, Fukuda D, Hachiya I, Shimizu M. Reductive aldol and Mannich-type reactions of azetidin-3-ones promoted by titanium tetraiodide. *Chem Asian J* 2010;5:473–477. (d) Hata S, Fukuda D, Hachiya I, Shimizu M. Regioselective ring-opening reaction of 2-mono-substituted azetidin-3-ones promoted by the combined use of titanium tetraiodide and its chloro or bromo counterpart. *Heterocycles* 2012;84:301–307.
- [24] Shah STA, Abdel-Jalil RJ, Khan KM, Heinrich AM, Richter M, Voelter W. Regioselective conversion of anhydro sugars into halohydrins and X-ray study. *Z Naturforsch B Chem Sci* 2004;59:337–340.
- [25] Hayakawa R, Shimizu M. Novel carbon-carbon bond formation reaction of methoxyallene oxide promoted by TiI_4 . *Org Lett* 2000;2:4079–4081.
- [26] Hayakawa R, Makino H, Shimizu M. Use of 1-methoxy-1-(trimethylsilyl)allene oxide and titanium tetraiodide as a dianion synthon of methoxyacetone. *Chem Lett* 2001;30:756–757.
- [27] Shimizu M, Itohara S. Use of alkoxyallene oxide and titanium tetraiodide/titanium tetraisopropoxide for the conjugate addition reaction of alkoxyacetone enolate. *Lett Org Chem* 2005;2:648–651.
- [28] Shimizu M, Shibuya K, Hayakawa R. Chemoselective deoxygenation of sulfoxides with titanium tetraiodide. *Synlett* 2000;11:1437–1438.
- [29] Hayakawa R, Shimizu M. Titanium(IV) iodide promoted pinacol coupling. *Chem Lett* 2000;29:724–725.
- [30] (a) Shimizu M, Goto H, Hayakawa R. Pinacol coupling reaction of β -halo- α,β -unsaturated aldehydes promoted by TiI_4 . *Org Lett* 2002;4:4097–4099. (b) Shimizu M, Okimura H, Manabe N, Hachiya I. 3-Iodo-3-trimethylsilylpropenal as a useful unit for pinacol coupling and subsequent functional group transformations. *Chem Lett* 2008;37:28–29.
- [31] Shimizu M, Goto H. Reductive coupling of aldehydes with nitriles promoted by titanium tetraiodide. *Lett Org Chem* 2004;1:346–348.
- [32] (a) Yachi K, Maeda K, Shinokubo H, Oshima K. Stereospecific conversion of iodohydrin derivatives into alkenes by means of an allylsilane-titanium tetrachloride system and its application to stereoretentive deoxygenation of epoxides. *Tetrahedron Lett* 1997;38:5161–5164. (b) Maeda K, Shinokubo H, Oshima K. Enolate formation from α -iodo aldehydes and α -iodo ketones by means of allylsilane-titanium tetrachloride and its application to an aldol reaction. *J Org Chem* 1998;63:4558–4560. (c) Yachi K, Shinokubo H, Oshima K. Reaction of titanate-type aldehyde enolate with ketones to provide 3-hydroxy aldehydes. *J Am Chem Soc* 1999;121:9465–9466. (d) Inoue A, Kitagawa K, Shinokubo H, Oshima K. Simple and efficient TiCl_4 -mediated synthesis of biaryls via arylmagnesium compounds. *Tetrahedron* 2000;56:9601–9605. (e) Tsuritani T, Ito S, Shinokubo H, Oshima K. TiCl_4 - $n\text{-Bu}_4\text{NI}$ as a reducing reagent: pinacol coupling and

- enolate formation from α -haloketones. *J Org Chem* 2000;65:5066–5068.(f) Han Z, Uehira S, Shinokubo H, Oshima K. TiCl_4 - $n\text{-Bu}_4\text{NX}$ ($X = \text{I}, \text{Br}, \text{and Cl}$) combination-induced coupling of α,β -unsaturated ketones with aldehydes. *J Org Chem* 2001;66:7854–7857.(g) Han Z, Uehira S, Tsuritani T, Shinokubo H, Oshima K. Enolate formation from cyclopropyl ketones via iodide-induced ring opening and its use for stereoselective aldol reaction. *Tetrahedron* 2001;57:987–995.(h) Tsuritani T, Shinokubo H, Oshima K. Coupling of vinylcyclopropanes with aldehydes induced by a $\text{TiCl}_4/n\text{-Bu}_4\text{NI}$ combination: synthesis of conjugated dienols. *Synlett* 2002;13:978–980.(i) Yagi K, Tsuritani T, Shinokubo H, Oshima K. Intramolecular tandem Michael-type addition/aldol cyclization induced by $\text{TiCl}_4\text{-R}_4\text{NX}$ combinations. *Org Lett* 2002;4:3111–3114.
- [33] García M, del Campo C, Llama EF, Sinisterra JV. Synthesis of α,α -disubstituted acetic acids using low-valent titanium. *J Chem Soc Perkin Trans* 1995;1:1771–1773.
- [34] (a) Mukaiyama T, Yoshimura N, Igarashi K. Diastereoselective pinacol coupling reaction of aliphatic and aromatic aldehydes promoted by low valent titanium iodide in situ formed by titanium(IV) iodide and copper. *Chem Lett* 2000;29:838–839.(b) Mukaiyama T, Yoshimura N, Igarashi K, Kagayama A. Efficient diastereoselective pinacol coupling reaction of aliphatic and aromatic aldehydes by using newly utilized low valent titanium bromide and iodide species. *Tetrahedron* 2001;57:2499–2506.(c) Yoshimura N, Igarashi K, Funasaka S, Mukaiyama T. Synthesis of vicinal bis(alkylthio) derivatives by reductive coupling of dithioacetals derived from aromatic aldehydes with low valent titanium iodide species. *Chem Lett* 2001;30:640–641.(d) Yoshimura N, Mukaiyama T. An efficient method for the preparation of vicinal tertiary diamines by reductive coupling of aminoacetals mediated by low valent titanium iodide species. *Chem Lett* 2001;30:1334–1335.
- [35] Arai H, Shiina I, Mukaiyama T. A convenient method for the preparation of unsymmetrical bis-aldols by way of sequential two aldol reactions. *Chem Lett* 2001;30:118–119.
- [36] Greenwood NN, Earnshaw A. *Chemistry of the Elements*. 2nd ed. Oxford: Butterworth-Heinemann; 1997. Chapter 30 The Lanthanide Elements ($Z = 58\text{--}71$); p 1227–1249.
- [37] (a) Jantsch G, Skalla N. Zur Kenntnis der Halogenide der seltenen Erden. IV. Über Samarium(II) jodid und den thermischen Abbau des Samarium(III) jodids. *Zeitschrift für anorganische und Allgemeine Chemie* 1930;193:391–405.(b) Wataya K. Production of anhydrous samarium diiodide. JP patent 3,305,184 (B2). 2002 July 22.
- [38] (a) Girard P, Namy JL, Kagan HB. Divalent lanthanide derivatives in organic synthesis. 1. Mild preparation of samarium iodide and ytterbium iodide and their use as reducing or coupling agents. *J Am Chem Soc* 1980;102:2693–2698.(b) Krief A, Laval AM. Coupling of organic halides with carbonyl compounds promoted by SmI_2 , the Kagan reagent. *Chem Rev* 1999;99:745–778.(c) Procter DJ, Flowers RA II, Skrydstrup T. *Organic Synthesis using Samarium Diiodide: A Practical Guide*, Chapter 2 The Reagent and the Effect of Additives. Cambridge: RSC Publishing; 2009. p 5–19.
- [39] (a) Inanaga J, Ishikawa M, Yamaguchi M. A mild and convenient method for the reduction of organic halides by using a SmI_2 -THF solution in the presence of hexamethylphosphoric triamide (HMPA). *Chem Lett* 1987;16:1485–1486.(b) Shabangi M, Flowers RA II. Electrochemical investigation of the reducing power of SmI_2 in THF and the effect of HMPA cosolvent. *Tetrahedron Lett* 1997;38:1137–1140.(c) Knettle BW, Flowers RA II. Influence of HMPA on reducing power and reactivity of SmBr_2 . *Org Lett* 2001;3:2321–2324.(d) Dahlen A, Hilmersson G. Samarium(II) iodide mediated reductions—influence of various additives. *Eur J Inorg Chem* 2004;2004:3393–3403.(e) Szostak M, Spain M, Parmar D, Procter DJ. Selective reductive transformations using samarium diiodide-water. *Chem Commun* 2012;48:330–346.

- [40] Molander G, Hahn G. Lanthanides in organic synthesis. 4. Reduction of α,β -epoxy ketones with samarium diiodide. A route to chiral and nonracemic aldols. *J Org Chem* 1986;51:2596–2599.
- [41] Inanaga J, Sakai S, Handa Y, Yamaguchi M, Yokoyama Y. Selective conjugate reduction of α,β -unsaturated esters and amides via SmI_2 -promoted electron transfer process. *Chem Lett* 1991;20:2117–2118.
- [42] Kamochi Y, Kubo T. The novel reduction of pyridine derivatives with samarium diiodide. *Heterocycles* 1993;36:2383–2396.
- [43] Kan T, Hosokawa S, Nara S, Oikawa M, Ito S, Matsuda F, Shirahama H. Total synthesis of (-)-grayanotoxin III. *J Org Chem* 1994;59:5532–5534.
- [44] Inanaga J, Handa Y, Tabuchi T, Otsubo K, Yamaguchi M, Hanamoto T. A facile reductive dimerization of conjugated acid derivatives with samarium diiodide. *Tetrahedron Lett* 1991;32:6557–6558.
- [45] (a)Carroll GL, Little RD. Inter- and intramolecular reductive coupling reactions: An approach to the phorbol skeleton. *Org Lett* 2000;2:2873–2876.(b)Suzuki K, Nakata T. Convergent synthesis of the ABCDEF-ring system of yessotoxin and adriatoxin. *Org Lett* 2002;4:3943–3946.
- [46] Miller RS, Sealy JM, Shabangi M, Kuhlman ML, Fuchs JR, Flowers RA II. Reactions of SmI_2 with alkyl halides and ketones: inner-sphere vs outer-sphere electron transfer in reactions of Sm(II) reductants. *J Am Chem Soc* 2000;122:7718–7722.
- [47] Tamiya H, Goto K, Matsuda F. Efficient medium-ring cyclization under non-high-dilution conditions using SmI_2 . *Org Lett* 2004;6:545–547.
- [48] Tabuchi T, Kawamura K, Inanaga J, Yamaguchi M. Preparation of medium- and large-ring lactones. SmI_2 -induced cyclization of ω -(α -bromoacyloxy) aldehydes. *Tetrahedron Lett* 1986;27:3889–3890.
- [49] Namy JL, Colomb M, Kagan HB. Samarium diiodide in tetrahydropyran: preparation and some reactions in organic chemistry. *Tetrahedron Lett* 1994;35:1723–1726.

PART IV

BIOLOGICAL APPLICATION OF IODINE

19

IODINATED X-RAY CONTRAST AGENTS

WERNER KRAUSE

Bayer Healthcare Pharmaceuticals, Berlin, Germany

19.1 HISTORICAL ASPECTS

Soon after W. C. Roentgen's discovery of X-rays in 1895, it became obvious that elements with high atomic numbers Z can be used as contrast enhancing agents since the X-ray absorption coefficient μ is proportional to Z^4 according to $\mu = \rho Z^4 / AE^3$ with ρ = density, A = atomic mass, and E = X-ray energy. Early examples include sodium iodide ($Z=53$ for iodine) and strontium bromide ($Z=38$ for Sr and 35 for Br). They combined excellent water solubility with high X-ray absorption coefficients. However, toxicity rapidly ended their use. Nevertheless, iodine remained on the screening list and today all extracellular (unspecific) X-ray contrast agents contain iodine as the contrast-providing element. The more iodine atoms are present per molecule, the higher is the efficacy. Currently used nonionic monomeric or dimeric extracellular X-ray contrast agents typically contain three (monomers) or six iodine atoms (dimers), which is equivalent to approximately 49% of iodine per molecule compared to 85% for sodium iodide.

Iodine has retained its dominating role as a contrast-providing element for a number of reasons, above all for its high absorption coefficient, its "easy" chemistry, and its relative inertness. The caveat to the latter point is, however, that even in covalent organic bonds iodine is "toxic" and needs to be shielded from any interactions with the organism by covering it up with as many hydrophilic groups as possible so that it practically becomes "invisible" to the body. The only objective of extracellular contrast agents used for CT, angiography, or urography is to absorb

X-rays and nothing else, that is, no interaction whatsoever with the organism should occur. The tricky task of the synthetic chemist therefore is to come up with structures that make the contrast agent highly hydrophilic without losing the high iodine content. Other factors that determine the tolerability of extracellular X-ray contrast agents are the viscosity and osmolality of the pharmaceutical preparations, which are—as is the case for hydrophilicity—determined by the chemical structures of the agents. The historical development of contrast agents and their classification are illustrated in Figures 19.1, 19.2, and 19.3.

The situation is different for targeted X-ray contrast agents, for example, for imaging specific tissues or organs such as the bile duct or the liver. Here, the molecules do need partial structures that interact with the organism and direct them to their targets. Alternatively, carriers may be used, such as liposomes or polymers, which either transport the agent to the liver, spleen, or lymph nodes or simply prolong their circulation in the blood for extended imaging periods.

19.2 EXTRACELLULAR (UNSPECIFIC) CONTRAST AGENTS

19.2.1 Chemical Synthesis

The structures of all currently used extracellular or unspecific X-ray contrast agents are based on the triiodobenzene ring with iodine atoms in positions 1, 3, and 5, which constitutes the most stable and versatile basic structure. Nontargeted (extracellular)

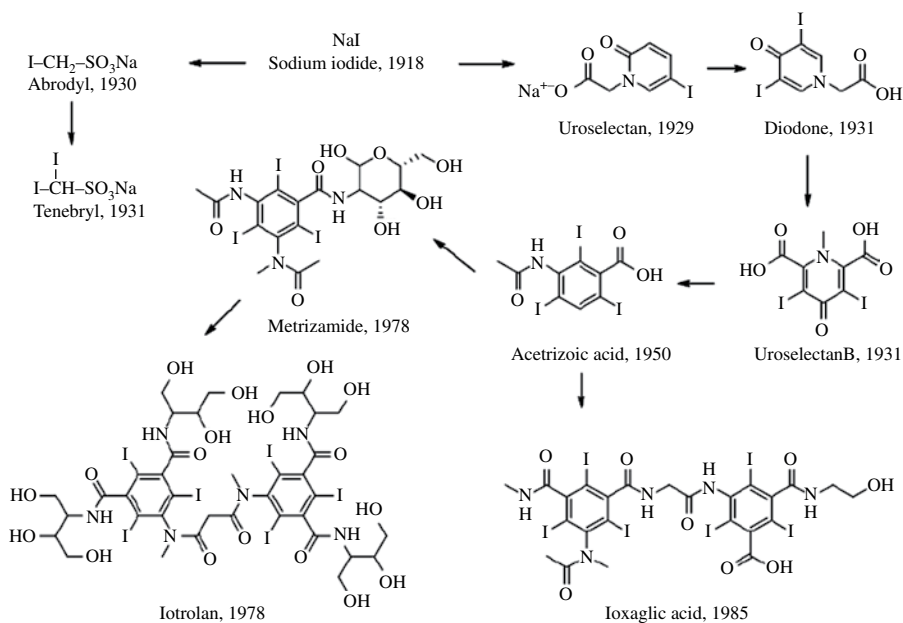


FIGURE 19.1 Historical development of iodinated X-ray contrast agents.

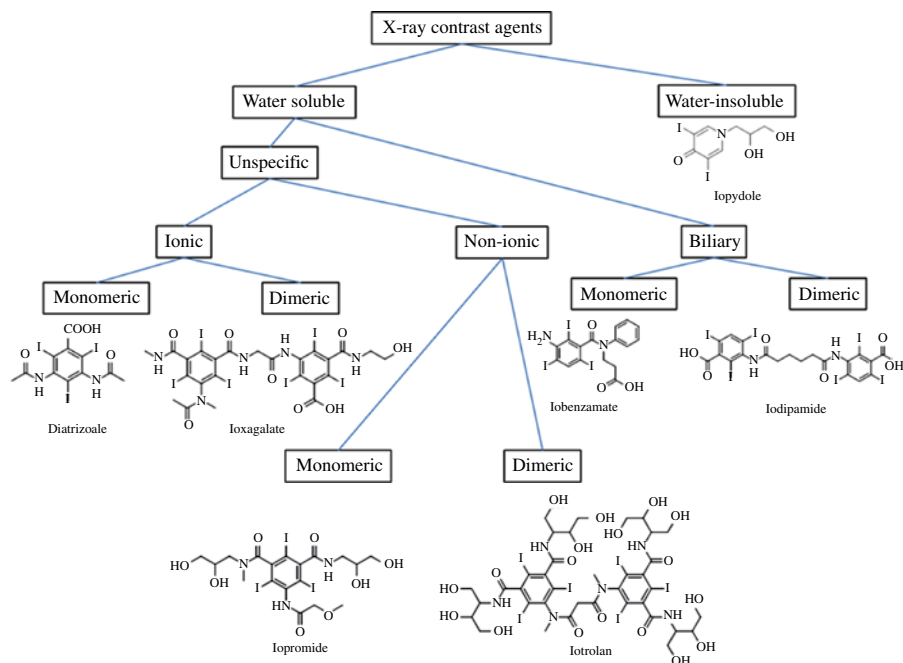


FIGURE 19.2 Classification of iodinated X-ray contrast agents.

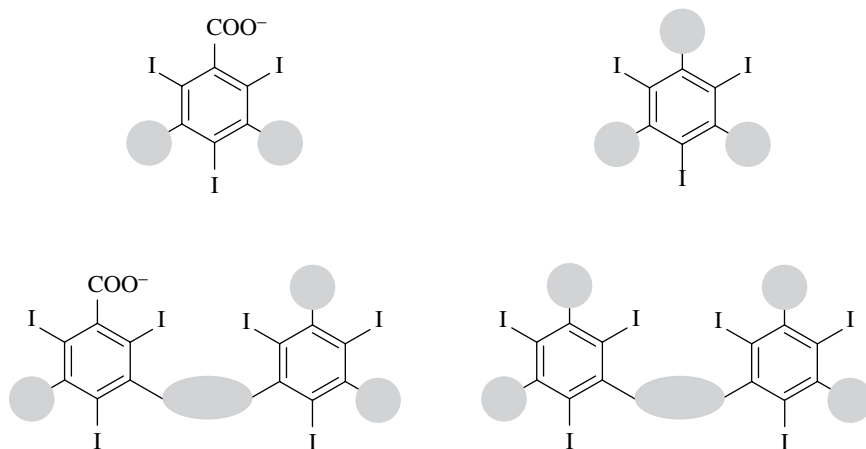
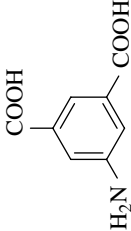
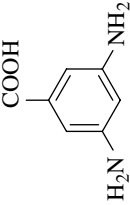
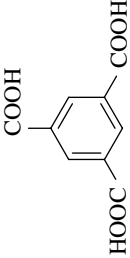
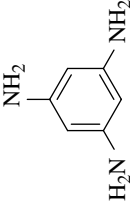
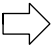



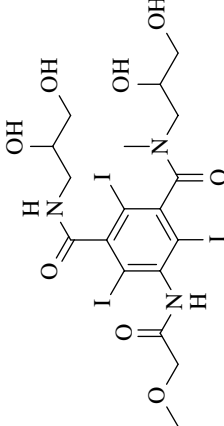
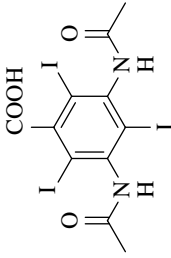
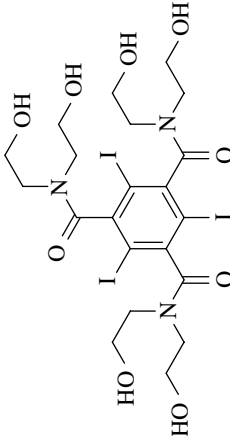


FIGURE 19.3 The four different types of iodinated extracellular contrast agents. The gray bubbles represent hydrophilic substituents. Top left: ionic monomer, top right: nonionic monomer, bottom left: ionic dimer, bottom right: nonionic dimer.

and targeted (biliary) agents differ by the number of additional substituents. In the first case, all remaining positions (2, 4, and 6) are filled with hydrophilic groups. In bile duct-specific agents, based on the triiodobenzene ring, only two of the remaining positions are substituted.

TABLE 19.1 Basic molecular templates for the synthesis of iodinated monomeric X-ray contrast agents

			
Aminoisophthalic acid	Diaminobenzoic acid	Trimesic acid	Triaminobenzene
			
			Not verified
Iopromide	Diatrizoic acid	Iosimid (not approved)	

As illustrated in Table 19.1, four types of substitution patterns of triiodobenzenes are possible for extracellular contrast agents, originating from diaminobenzoic acid, aminophthalic acid, trimesic acid, or from triaminobenzene. Due to poor stability (triamino type) or high cost of goods (tricarboxyl type), the last two basic structures have not been achieved or are not used.

Table 19.2 provides an overview of extracellular contrast agents that have been approved by the Food and Drug Administration (FDA). The ionic agents are based on either diaminobenzoic acid or aminoisophthalic acid. All nonionic compounds are exclusively based on the aminoisophthalic acid building block and differ by their hydrophilic side chains. Water solubility of these compounds is in the range of 1 g ml^{-1} . However, in order to achieve iodine concentrations up to 400 mg ml^{-1} , some commercially used preparations are oversaturated solutions. Therefore particular caution has to be applied in their production process to avoid precipitation via tiny amounts of seeding crystals.

The synthesis of iodinated extracellular X-ray contrast agents starts with the introduction of iodine into the basic molecule, which is performed via substitution, followed by derivatization of the carboxyl and amino groups. Basically, iodination uses the I^+ intermediate, which is generated from aqueous Cl-I . Replacement of hydrogen by iodine on an aromatic ring system needs activation via neighboring electronegative groups such as amino groups. If the activation is insufficient, only two of the possible three positions will be iodinated, which is the case for bile duct-specific contrast agents. Triiodinated compounds are less water soluble than their precursors and precipitate, facilitating purification. Acylation of the amino group(s) provides the final product. Acylated amino groups have an increased electronegativity and thereby strengthen the stability of the carbon-iodine bonds. The synthesis of the ionic monomer diatrizoic acid is illustrated in Figure 19.4. The acid is transformed into either the sodium or the meglumine salt or mixtures thereof. It is used for intravenous injection (imaging of the vascular system) or for oral administration (imaging of the gastrointestinal tract). However, due to its high osmolality, it has largely been replaced by nonionic monomers or dimers.

Nonionic monomers require a much more sophisticated route of synthesis due to the increased solubility of intermediates. Additional purification steps such as extraction, chromatography, and recrystallization have a significant impact on the cost of goods. The synthesis of unsymmetrical structures such as for iopromide, with different substituents at the two carboxamides, makes the synthesis even more intricate. Figure 19.4 illustrates the route to the symmetrical iopamidol.

Triiodinated aromatic contrast agents are normally very stable to degradation. However, minor contaminants in the formulation, such as copper ions and glucose, could lead to deiodination [1]. In the organism, intravascular contrast agents are not metabolized but excreted unchanged via glomerular filtration in the kidney.

Improvements of the triiodobenzene moieties aim at further reducing the viscosity of dimeric compounds. Iosimenol (viscosity of 7.7 mPas at $350 \text{ mg iodine per ml}$) and ioforminol (GE-145, 10.2 mPas) are currently in clinical development [2, 3].

A number of approaches include structures moving beyond triiodobenzenes. Wharton et al. synthesized C_{60} fullerenes linked to a dimeric hydrophilic triiodobenzene moiety [4]. The fullerene was subsequently derivatized with four

TABLE 19.2 Chemical structures and characteristics of iodinated contrast agents, approved by the FDA (osmolality and viscosity data taken from package inserts and ACR manual on contrast media, version 8, 2012)

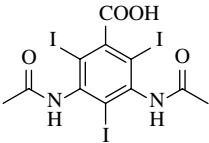
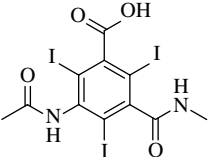
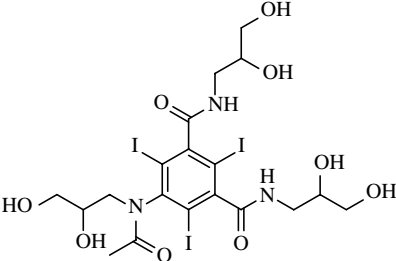
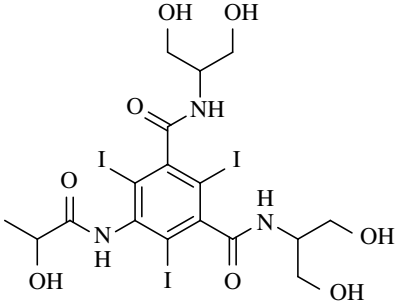
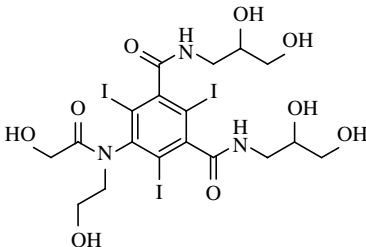
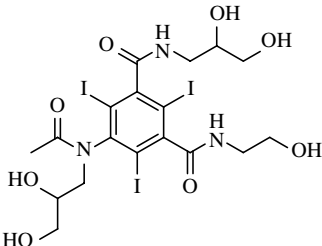
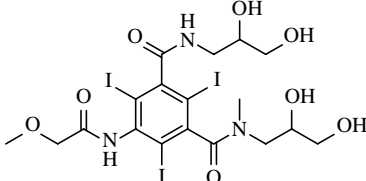
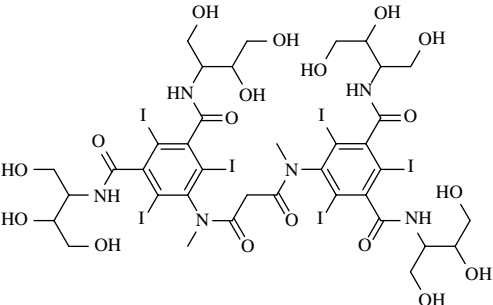
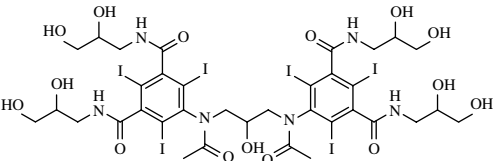
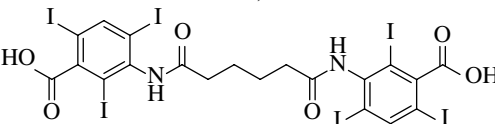
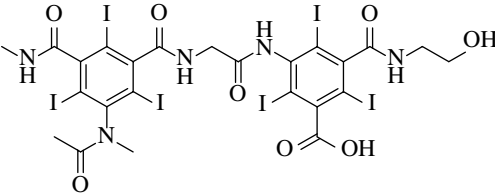
Subtype	Structure	Iodine concentration	Osmolality	Viscosity at 37°C
Compound (trade name)	Year of FDA approval	mg ml ⁻¹	mmOsm	kg ⁻¹ cps
Ionic, monomeric, extracellular				
		85	349	1.5
		141	556	1.5
		370 (IV)	1551	10.5
		370 (GIT)	1940	8.4
Diatrizoic acid (MD-76, MD-Gastroview, Cystografin, 1955)				
		141	600	1.5
		202	1000	2
		282	1400	4
Iothalamic acid (Conray, 1962)				
Nonionic, monomeric, extracellular				
		140	322	1.5
		180	408	2.0
		240	520	3.4
		300	672	6.3
		350	844	10.4
Iohexol (Omnipaque, 1985)				
		200	413	2.0
		250	524	3.0
		300	616	4.7
		370	796	9.4
Iopamidol (Isovue, 1985)				

TABLE 19.2 (Cont'd)

Subtype	Structure	Iodine concentration	Osmolality	Viscosity at 37°C
Compound (trade name)	Year of FDA approval	mg ml ⁻¹	mmOsm	kg ⁻¹ cps
		160	355	1.9
		240	502	3.0
		300	651	5.5
		320	702	5.8
		350	792	9.0
Ioversol (Optiray, 1988)				
		300	610	5.1
		350	721	8.1
Ioxilan (Oxilan, 1995)				
		150	328	1.5
		240	483	2.8
		300	607	4.9
		370	774	10.0
Iopromide (Ultravist, 1995)				
Ionic, dimeric, extracellular				
		320	600	7.5
Ioxaglic acid (Hexabrix, 1985)				

(Continued)

TABLE 19.2 (Cont'd)

Subtype	Structure	Iodine concentration	Osmolality	Viscosity at 37°C
Compound (trade name) Year of FDA approval		mg ml ⁻¹	mmOsm	kg ⁻¹ cps
Nonionic, dimeric, extracellular				
		240	270	3.9
Iotrolan (Osmovist, 1989, discontinued)				
		270 320	290 290	6.3 11.8
Iodixanol (Visipaque, 1996)				
Ionic, dimeric, biliary				
		257	664	5.6
Iodipamide (Cholografin, 1954)				

additional hydrophilic substituents resulting in good water solubility of 460 mg ml⁻¹. The downside of this approach is the reduced iodine content of 24% compared to 49% for the classical contrast agents.

Wilbur and Palmer described the synthesis of iodinated boranes, for example, [Ph₃PMe]₂B₁₀I₉CO₂H, as an alternative to triiodobenzenes [5, 6]. The compounds exhibit a high iodine content, that is, 62% for the mentioned example. Srivastava described carboranes with up to 11 iodine atoms per molecule [7]. These compounds have not reached the stage of clinical testing.

19.2.2 Analytics

Since extracellular iodinated contrast agents are stable and not degraded or metabolized, their concentrations in formulations or in biological material, such as blood or urine, can be determined via the measurement of iodine concentrations. A suitable

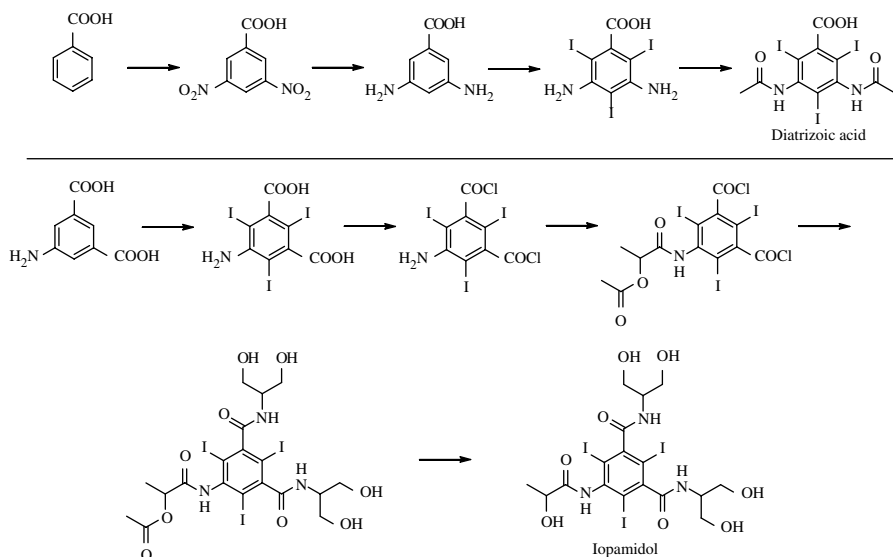


FIGURE 19.4 Synthesis of the ionic monomer, diatrizoic acid (top), and of the nonionic monomer, iopamidol (bottom).

method with high precision and accuracy is X-ray fluorescence spectrometry using a ^{241}Am source by which undiluted samples can be measured [8].

If unchanged drugs need to be quantified, which is the case whenever degradation should occur, such as in environmental samples from sewers and groundwater, specific methods have to be utilized consisting of appropriate separation techniques and identification of the drugs and/or their degradation products. Examples include high-performance liquid chromatography/mass spectrometry (HPLC/MS) [9], high-performance liquid chromatography/ultraviolet detection (HPLC/UV) [10], and the use of radiolabelled contrast agents [11].

An interesting field is the stereoisomerism of contrast agents carrying polyhydroxycarbon side chains with several asymmetric carbon atoms resulting in quite a number of enantiomers and diastereoisomers. Additional asymmetric centers are formed by steric hindrance leading to rotamers. For iotrolan, 19 isomers could be separated by high-resolution HPLC [12]. Results on the isomerism of iodixanol were published by Priebe et al. [13].

19.2.3 Physicochemical Characteristics

The pharmacological and toxicological characteristics of extracellular X-ray contrast agents are determined by the hydrophilicity of the compound and by the osmolality and viscosity of the formulation.

A measure for the hydrophilicity is the partition coefficient, which is determined in either n-butanol or n-octanol/water. In the system n-butanol/water, nonionic

monomers typically show partition coefficients of 0.03–0.15, nonionic dimers of 0.005 (iotrolan), which means that the latter are much more hydrophilic than the former. For comparison, the partition coefficients of biliary contrast agents with one free position on the aromatic ring are greater than 5. Allergy-like reactions to contrast agents have been attributed to insufficient hydrophilicity.

The osmolality of contrast agent formulations depends on the number of molecules or ions in the solution and on the temperature [14]. Measurements are performed by commercially available osmometers at predefined temperatures. At iodine concentrations of 300 mg ml⁻¹, high-osmolar contrast agents exhibit osmolalities around 1500 mOsm kg⁻¹. Examples are ionic monomeric agents such as diatrizoate. Low-osmolar compounds (nonionic monomers) fall into the range of 600–700 mOsm kg⁻¹. Nonionic dimers (iotrolan, iodoxanol) are isotonic to blood with an osmolality of 300 mOsm kg⁻¹. There is a strong dependence of osmolality on the concentration of the contrast agent. For iopromide solutions with 150, 240, 300, and 370 mg iodine per ml the respective osmolalities are 328, 483, 607, and 774 mOsm kg⁻¹. In addition to electric charge, the osmolality of a contrast agent determines the pain a patient is suffering during injection. Osmolalities of 1500 mOsm kg⁻¹ elicit strong pain, whereas injection of nonionic isotonic agents is painless. High osmolality is also accountable for side effects such as cardiovascular reactions (increase of heart rate and blood pressure) and diuresis. Osmolalities of different agents are summarized in Table 19.2.

Iodinated contrast agents, and in particular nonionic dimers, form aggregates in solution via hydrogen bridges resulting in a lower osmolality of the formulation compared to theoretical values [15]. Hypersensitivity reactions observed after contrast injection have been attributed to these aggregates [16].

Viscosity is another important factor that determines the characteristics of contrast agents. Since CT requires very rapid injections (≥ 20 ml sec⁻¹), viscosity might become the rate-limiting factor. Viscosity depends on the concentration and the temperature of the formulation and—at iodine concentrations of 300 mg ml⁻¹—is in the range of 5–10 mPas for nonionic monomers and greater than 15 mPas for nonionic dimers. For iopromide solutions with 150, 240, 300, and 370 mg iodine per ml the respective viscosities are 1.5, 2.8, 4.9, and 10.0 mPas. Further details are provided in Table 19.2.

19.2.4 Pharmacokinetics

The pharmacokinetics of all extracellular (unspecific) contrast agents is practically identical. After intravenous bolus injection, the blood levels of iodine (representative of the contrast agent) decline in two phases. The first phase (distribution phase) has a half-life of 3–10 min and the second phase (elimination phase) of 1–2 h. Due to their high hydrophilicity, protein binding is low (<5%) and passage of membranes is minimal. Accordingly, contrast agents do not cross the blood–brain barrier and are transferred through the blood–placenta barrier only to a very limited amount. Likewise, they are not excreted into breast milk and are not absorbed after oral

administration. Their volume of distribution is practically identical to the extracellular space volume (0.21 kg^{-1}).

The elimination of contrast agents is rapid and proceeds mainly via glomerular filtration in the kidneys. Accordingly, the half-life is prolonged up to 10 h in cases of renal impairment.

19.2.5 Diagnostic Imaging

Diagnostic imaging using X-rays and iodine as contrast enhancer is a modality with very low sensitivity. For plain X-ray imaging (radiography = taking one image, fluoroscopy = continuous imaging), an iodine concentration of 15 mg ml^{-1} is required to provide sufficient contrast, which explains the huge doses of contrast agents that are normally used. Methods with increased sensitivity are digital subtraction angiography (DSA, 10 mg ml^{-1} needed), and, in particular, CT (1 mg ml^{-1}). For comparison, magnetic resonance imaging (MRI) requires concentrations of the contrast-giving elements (Gd, Mn, Fe) of $1\text{--}10\text{ }\mu\text{g ml}^{-1}$, nuclear medicine of $1\text{ ng ml}^{-1}\text{--}100\text{ }\mu\text{g ml}^{-1}$ ($^{99\text{m}}\text{Tc}$, ^{111}In), and positron emission tomography (PET) of less than 1 pg ml^{-1} (^{18}F).

In the most efficient CT modality, the X-ray source rotates around the patient with the detector opposite to the source. The image sections of the body or of the organ of interest are fed into a computer and reconstructed either two-dimensionally (conventional CT) or three-dimensionally (helical CT). Examples are provided in Figure 19.5. Time as the fourth dimension of images provides additional valuable information. For the reconstruction of the images, each pixel is assigned a density value in Hounsfield Units (HU), which is determined by the absorption of X-rays by the target tissue. Water, by definition, has a value of 0 HU and air of -1000 HU. All tissues range from -500 to -900 HU (lungs) to the densest tissue, bones, with $40\text{--}1000$

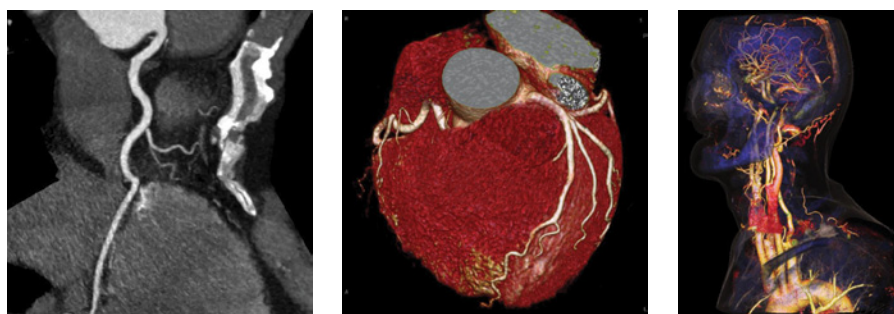


FIGURE 19.5 CT images. Left: Coronary CTA, slice thickness 0.6 mm , two-dimensional rendering. Middle: Coronary CTA, slice thickness 0.6 mm , three-dimensional rendering. Right: Carotid artery, slice thickness 0.75 mm , three-dimensional rendering. Courtesy of Siemens AG (collection of MIP, VRT images) and Friedrich-Alexander University Erlangen-Nuremberg, Institute of Medical Physics, Erlangen, Germany. (See insert for color representation of the figure.)

HU. Other examples include fat with -80 to -120 HU and muscles with 40 – 50 HU. In order to differentiate two targets in a specific area of interest, a difference in density of 30 HU is needed. In other words, if iodinated contrast agents are of benefit, they need to increase the density by 30 HU, which is equivalent to an iodine concentration at the target of 1 mg ml^{-1} .

As an example, liver imaging using CT with the objective of detecting liver lesions such as tumors will be described in more detail. Normal liver tissue has a density of 50 – 70 HU. Liver metastases have densities of 40 – 50 HU and are therefore difficult to detect. Other lesions may even have the same density as normal liver tissue. Intravenous injection of 100 – 150 ml of a contrast agent increases the difference in density between normal and tumor tissue to more than 30 HU due to differences in vascular density, for example, making the lesions clearly visible, either by increasing their density over that of normal tissue or by increasing the density of normal tissue and leaving that of the metastases unaffected. However, due to the pharmacokinetics of the contrast agent, this effect lasts for only 20 – 30 sec during the arterial phase of distribution and for the same time interval during the portal venous phase. Modern CT machines are normally fast enough to cope with this problem. However, if this time window is missed or more time is required, for example, for a biopsy, another injection of contrast agent is needed, which is not recommended due to the cumulative side effects of the agents, in particular on the kidneys.

Other X-ray imaging techniques are named after the target organ/tissue they are examining, such as arteriography for the inspection of arteries, myelography for the spinal cord, urography for renal and urinary system imaging, colonoscopy for the gut, lymphography for the lymphatic system, and cholegraphy for the biliary duct.

19.2.6 Safety and Tolerability

Iodinated contrast agents are among the most tolerable compounds used in medicine, in particular taking into consideration that they are administered in extremely high doses. For example, in CT a typical dose is 100 – 150 ml of an agent with a concentration of 300 mg iodine per ml (equivalent to approximately 600 mg contrast agent per ml) resulting in a total dose of 30 – 45 g of iodine or 60 – 90 g of contrast agent. In specific applications, up to 200 g may be reached.

Side effects can be classified according to their severity (mild, moderate, severe), their onset (immediate, delayed/late), their mechanism (related to charge, osmolality, allergy-like), their route of administration (risk: intrathecal > intraarterial > intravenous), or their target (risk: head > heart > periphery).

Minor side effects include nausea and vomiting, urticaria, pruritus, and local pain (normally after i.v. injection). Moderate effects are severe vomiting, extensive urticaria, bronchospasm, and edema. Severe reactions include syncope, convulsion, hypotension, shock, and pulmonary edema. The incidence of side effects is 5 – 12% for high-osmolar agents, which are rarely used any more, and below 1% for low-osmolar agents [17]. Severe, life-threatening contrast reactions are very rare and occur unpredictably and immediately or within the first 20 min after contrast media injection in 0.01 – 0.02% of patients. The mortality after intravascular injection is very

low (1:170,000) [18]. Other reports indicate two fatalities per million [19]. Risk factors include allergy, asthma, dehydration, and renal insufficiency. Appropriate premedication may reduce the incidence of side effects.

Effects of contrast agents on hemodynamics include reduction of blood pressure and contractility and increase of left ventricular end-diastolic pressure. In particular ionic compounds affect blood coagulation and platelet activity.

Renal side effects cover a wide range from small changes in creatinine clearance up to renal failure and the need for subsequent hemodialysis [20]. The incidence of clinically significant renal effects in patients with normal kidney function is extremely low. Risk factors include preexisting renal impairment (serum creatinine $\geq 2.0 \text{ mg dl}^{-1}$), diabetes, and dehydration [21]. Sufficient hydration of the patient prior to contrast injection is an important measure to reduce the risk of renal side effects.

Allergy-like adverse events can occur either early (up to 20 min) or delayed (30 min up to 1 week). They are believed to be independent of dose and concentration [22]. Delayed reactions are most commonly of cutaneous nature. Their incidence has been published as 0.5–14% [23].

19.2.7 Environmental Aspects

Due to their high chemical and metabolic stability, extracellular contrast agents are excreted unchanged and finally end up in the sewage system contributing to the bio-burden of absorbable organic halogen (AOX). Their high hydrophilicity prevents them from being filtered from the sewage. Microbiological transformation is normally slow and only attacks the hydrophilic side chains and does not affect the triiodinated core [24]. In effluents of sewage treatment plants, concentrations of 15 g l^{-1} were found for iopamidol, one of the widely used contrast agents. As a consequence, measurable concentrations can be detected in lakes and rivers (0.49 g l^{-1}) and in the groundwater (2.4 g l^{-1}) [25]. However, ecotoxicological investigations resulted in a ratio of predicted environmental concentration to the predicted no-effect concentration of 0.0002 indicating that there are no environmental risks [26].

In the river Rhine, concentrations continuously increase from the Upper Rhine to the estuary. In Basel, the average concentrations of most iodine-based radiocontrast agents are below $0.1 \mu\text{g l}^{-1}$. On the Lower Rhine and in the Rhine Delta, concentrations are mostly around 0.2 – $0.5 \mu\text{g l}^{-1}$. The highest concentrations registered in the Rhine were about $1.3 \mu\text{g l}^{-1}$. Partly, concentrations are even higher in the tributaries reaching concentrations up to 10 – $30 \mu\text{g l}^{-1}$.

19.3 TARGETED CONTRAST AGENTS

Due to their pharmacokinetics, extracellular contrast agents are best suited for imaging of all targets that are easily accessible via the extracellular space, that is, via perfusion of tissues and organs, and via their route of excretion, that is, the kidneys. Accordingly, the gall bladder and in particular the bile duct cannot be imaged, and dedicated contrast agents had to be developed.

19.3.1 Biliary Contrast Agents

Biliary contrast agents are used for imaging the bile duct and gall bladder (cholangiography). They are either slowly infused intravenously or injected into the liver or the bile duct. Some compounds can be given orally. The prerequisites for contrast agents suitable for biliary imaging are reduced hydrophilicity (increased lipophilicity) compared to extracellular agents and, very importantly, negative charge. Only with these attributes are the compounds able to pass membranes and can be taken up by the hepatocytes and transported into the bile duct.

Reduction of hydrophilicity can be achieved starting from triiodobenzene derivatives by omitting one of the hydrophilic substituents on the benzene ring and by reducing the hydrophilicity of one or more of the side chains by, for example, replacing hydroxyl groups by less hydrophilic moieties such as ether groups. The compounds can be monomeric for oral use (iopanoate) or dimeric for injection (iodipamide, see Table 19.2). In parallel with the reduction of hydrophilicity, water solubility of these agents is lower so that formulations contain less iodine (50 mg ml^{-1}) than those of extracellular agents (up to 400 mg ml^{-1}).

Further consequences of the reduced hydrophilicity are increased, saturable protein binding (70–95%), uptake by hepatocytes in the liver, metabolism, excretion via the biliary tract (65–90% of the dose), and less tolerability compared to extracellular compounds such as a high incidence of allergic reactions or renal and hepatic toxicity.

Unfortunately, the concentration in the liver is not high enough to allow for liver imaging due to saturation of the involved transport mechanisms.

19.3.2 Liver-Specific Agents

The search for liver-specific contrast agents has been triggered by the pharmacokinetic characteristics of extracellular agents. Following bolus injection of iopromide, maximal iodine concentration and therefore maximal enhancement is observed in the liver after approximately 60 s, which declines rapidly with a half-life of 50 s [27]. Accordingly, the time window for optimal imaging is very short.

For liver targeting, two different approaches have been followed, hepatocyte-directed agents and targeting of the reticuloendothelial system (RES) via the Kupffer cells.

19.3.2.1 Hepatocyte-Specific Contrast Agents

Approximately 70% of liver cells are hepatocytes and therefore constitute the primary target in the search for liver contrast agents. Accordingly, the efforts in the development of liver-specific agents concentrated first on this cell type.

The most obvious approach in the search for liver-specific agents was the modification of triiodinated biliary contrast agents to achieve higher concentrations in the liver. The target was to reach iodine concentrations of 1 mg iodine per gram of liver tissue or higher. However, up to now, this goal could only be verified in animal models but not in humans.

Further, iodinated fatty acids and iodinated triglycerides have been investigated in the search for liver-specific contrast agents. Intraiodol is an iodinated Intralipid, a nutritional product prepared from soybean and egg yolk [28], which was formulated in an emulsion with an iodine concentration of 50 mg ml⁻¹. A variety of modifications of the preparations were made but the necessary enhancement of liver tissue of 30 HU could not be achieved. Iodinated triglycerides of various structures either alone or incorporated into lipid emulsions that were supposed to make use of the endogenous pathway of hepatic lipid metabolism have been synthesized by some groups [29]. Another approach described in the literature was the coupling of triiodobenzene moieties to steroids such as cholesterol, which were supposed to act as carriers [30].

However, none of the described efforts has been successful so far.

19.3.2.2 *RES-Specific Liver Contrast Agents*

The RES includes macrophages in the blood and lymph nodes and Kupffer cells in the liver. The latter represent approximately 10% of liver cells. The main task of the RES is to eliminate foreign particles via phagocytosis. Accordingly, contrast agents that are intended to use this approach need to be particles. However, in parallel to phagocytosis, mediators are released resulting in adverse events such as reduction in blood pressure and fever, which is one of the major limitations of this approach.

The first particulate contrast agent was thorium dioxide, which was extremely effective, well-tolerated on a short-term basis but very toxic in the long run leading mainly to cancer [31]. Colloidal iodine was also effective but not sufficiently tolerated [32].

The first RES-specific iodinated lipids were emulsions of iodine-containing poppy seed oil (AG 52-315, AG 60-99, EOE-13), which were very effective but not very well-tolerated resulting in headache, fever, and chills [33]. A modified version, Lipiodol or Ethiodol, has long been in use for the detection or, in combination with cytotoxic agents, the treatment of hepatocellular carcinoma following injection into the hepatic artery. However, in addition to side effects, Lipiodol exhibits a very long residence time in the liver and is cleared only after months, which is not acceptable for a diagnostic agent.

Another approach was the modification of intravascular triiodobenzene contrast agents into pro-drugs, which are less water soluble and form particles that can be taken up by macrophages and transported into the liver where they are degraded into the original intravascular contrast agents and subsequently excreted via the kidneys [34]. Modified compounds included iothalamate [35], metrizoic acid [36], and others [37]. All were very effective but limited in use due to side effects.

Liposomes are particles that are formed by lipids with polar head groups and one or more nonpolar chains (Figure 19.6). Examples for suitable lipids include soy phosphatidylcholine (PC), distearoyl phosphatidylcholine (DSPC), and dipalmitoylphosphatidylcholine (DPPC). Added cholesterol functions as a stabilizer. Four different types of liposomes have been described: small unilamellar (SUV, single membrane), large unilamellar (LUV, single membrane), multilamellar (MLV, more than one membrane), and multivesicular (liposome in liposome) particles.

Liposomes are able to carry contrast agents either within their center (hydrophilic compounds) or within their vesicle wall (lipophilic compounds). Their preparation is

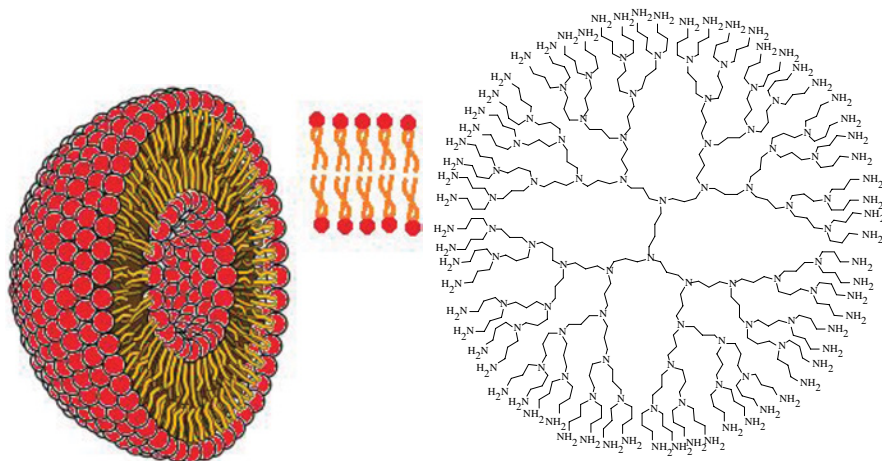


FIGURE 19.6 Left: Structure of a liposome and of the underlying lipid bilayer. Right: Basic structure of a polypropylenimine (PAMAM) dendrimer with a 1,4-diaminobutane core. The amino groups in the outer shell can be derivatized with triiodobenzoic acid moieties.

relatively simple and reproducible and has been described extensively in the literature. Nearly all available iodinated X-ray contrast agents meanwhile have been encapsulated into liposomes. Depending on the size of the liposomes, the particles either are taken up by the RES (large liposomes, ~400 nm) and lead to very effective liver and spleen imaging or circulate in the blood (“blood-pool agents”) for a long time and allow for long and extensive imaging of the vascular system (small particles <100 nm) or—following leakage out of the blood vessels—for the detection of vascularized tumors. Alternatively, the surface of the liposomes can be modified, for example, by pegylation [38], to further prolong circulation times or by the attachment of, for example, ICAM-1 monoclonal antibodies, which are supposed to direct the liposomes to atherosclerotic plaques [39].

However, due to the side effects observed in clinical trials (fever, allergy-like reactions), iodine-containing liposomes have not yet been approved by regulatory authorities.

19.3.3 Polymeric Iodinated Contrast Agents

Research into polymeric contrast agents was triggered by the objective of reducing the osmotic pressure on the one hand and of increasing the size to an extent that the molecules are big enough to stay in the intravascular space and are suitable as blood-pool agents on the other hand. Another possible use included water-insoluble polymers as carriers for contrast agents of the gastrointestinal tract or for radiopaque bone cement.

A variety of natural or synthetic polymers were used to which triiodobenzenes were linked, such as polypeptides (albumin, polylysine, polyaspartate, etc.), polyacrylates, polysaccharides (dextran), and others.

A polymeric contrast agent using iodinated building blocks has been described by Torchilin [40]. In water, the polymer formed micelles of 80-nm diameter at an iodine concentration of 20 mg ml⁻¹ leading to prolonged enhancement of the liver and spleen in animal models.

Pepiöl et al. described the synthesis of copolymers of methyl-methacrylate and 4-iodobenzoyl-oxo-ethylmethacrylate for use as radiopaque bone cement [41]. However, the iodine content was relatively low. For improvement, they added a tetra-iodinated closo-carborane (8,9,10,12-I₄-1,2-closo-C₂B₁₀H₈) as a contrast enhancer.

Other examples include copolymerization of glycidyl methacrylate and 2-methacryloyloxyethyl-triiodobenzoate as described by Aviv [42] or of triiodobenzoyl polylysine and methoxypoly(ethylene glycol).

Dendrimers are another class of polymers that have been used as building blocks and that are able to carry substituents such as triiodobenzenes at their surface. The divergent synthesis of dendrimers starts from a core such as ammonia (leading to three primary branches), 1,4-diaminobutane (leading to four primary branches), or any other amino-substituted molecule, which are grown via alkylation leading to—for example—polypropylenimines (PAMAM), polyamidoamines (POPAM), or polylysines. Triiodobenzenes can be coupled to free amino groups on the outer shell of the dendrimer leading to a total number of $3 \times 2^{n-1}$ iodinated substituents if ammonia is used as core, with $n = 1, 2, 3$, etc., being the number of generations, and $2 \times 2^{n-1}$ substituents for 1,4-diaminobutane [43]. An example of an unsubstituted PAMAM dendrimer is provided in Figure 19.6.

19.3.4 Other Targets

Trialkyl-triiodobenzenes, for example 1,3,5-tri-*n*-hexyl-2,4,6-triiodobenzene, have been synthesized for imaging of the gastrointestinal tract [44]. Oil/water emulsions are orally administered and lead to coating of the gut mucosa, so far only in animal models. Diiodo-aminobenzene rings with phosphonate groups, linked to small peptides via the amino group, have been described; no imaging data are provided, however [45].

Calcium-seeking contrast agents for bone damage detection have been based on dimeric triiodobenzenes with eight carboxyl groups as chelators for calcium [46]. Cationic dimers with four ammonium groups have been described as cartilage-seeking agents for the evaluation of osteoarthritis [47].

19.4 SUMMARY AND CONCLUSIONS

Iodinated contrast agents have been and will remain in the next future an indispensable part of diagnostic imaging procedures, in particular for use in conjunction with CT. Despite the success of competing technologies such as MRI or ultrasound, X-ray imaging and above all CT constitute a backbone of medical diagnosis. The number of annual CT scans in the United States alone is estimated at 70 million. Approximately half of these procedures include the use of contrast agents. Triiodobenzene derivatives

are among the best tolerated substances used in medicine so that the very high doses administered to patients do not pose problems if appropriately used. As a consequence, improvements are not easy to achieve.

What is clearly needed is targeted contrast agents that are able to extend the scope of the currently available extracellular compounds to organ- or disease-specific applications. Good progress has been made with liposomes and with polymers. However, the way to go is still very long until a stage similar in performance to the unspecific, extracellular agents has been reached.

Although research is now extending its focus into noniodine areas, such as using Gd, Dy, Au, Bi, PT, or Pd-containing compounds for CT imaging [48–50], none of these approaches has achieved regulatory approval so far and currently it is not foreseeable when that goal will be achieved.

REFERENCES

- [1] Chellquist E, Wheeler S, Strasters J, Wolfe H, Storflor HJ. The effect of glucose and copper on the stability of diatrizoic acid. *Pharm Sci Technol* 1999;53:247.
- [2] Riefke B, Gonzalez L, Carretero J, Gonzalez C, Jimenez I, Alguacil LF, Boehle F, Martin F, Martin JL. The effect of glucose and copper on the stability of diatrizoic acid. *Acad Radiol* 2002;9 (Suppl 1):S178.
- [3] Wistrand LG, Rogstad A, Hagelin G, Roed L, Oulie I, Gram A, Evan P, Rasmussen H, Grant D, Iveson P, Newton B, Thaning M. GE-145, a new low-osmolar dimeric radiographic contrast medium. *Acta Radiol* 2010;51 (9):1014.
- [4] Wharton T, Wilson LJ. Highly-iodinated fullerene as a contrast agent for x-ray imaging. *Bioorg Med Chem* 2002;10 (11):3545.
- [5] Wilbur DS. Iodinated borane cage molecules as x-ray contrast media. U.S. Patent 5,489,673 A. 1993 Aug 16. To University of Washington, Seattle.
- [6] Palmer AM. Iodinated polyhedral boranes for cancer detection [Ph.D. Thesis]. Columbus: Ohio State University; 2011.
- [7] Srivastava RR, Hamlin DK, Wilbur DS. Synthesis of highly iodinated icosahedral mono- and dicarbon carboranes. *J Org Chem* 1996;61:9041.
- [8] Krause W, Miklantz H, Kollenkirchen U, Heimann G. Physicochemical parameters of x-ray contrast media. *Invest Radiol* 1994;29:72.
- [9] Jacobsen PB, Larsen A, Konarboland R, Skotland T. Biotransformation of nonionic x-ray contrast agents in vivo and in vitro. *Drug Metab Dispos* 1999;27:1205.
- [10] Arbughi T, Bertani F, Celeste R, Grotti A, Tirone P. High-performance liquid chromatographic assay of the X-ray contrast agent iopipерidol in plasma and urine of rats and humans. *J Chromatogr* 1999;B729:323.
- [11] Rode U, Müller R. Transformation of the ionic X-ray contrast agent diatrizoate and related triiodinated benzoates by *Trametes versicolor*. *Appl Environ Microbiol* 1998;64:3114.
- [12] Krause W, Schneider PW. Chemistry of X-ray contrast agents. *Top Curr Chem* 2002; 222:107.
- [13] Priebe H, Dugstad H, Heglund IF, Sande R, Tonseth CP. Synthesis, analysis, and toxicity of three compounds formed during the analysis of iodixanol. *Acta Chem Scand* 1995;49:737.

- [14] Miklantz H, Fichte F, Wegscheider K. Osmolality of nonionic contrast media. In: Taenzer V, Wende S, editors. *Recent Developments in Nonionic Contrast Media*. Stuttgart: Georg Thieme Verlag; 1989. p 16.
- [15] Pietre D, Felder E. Development, chemistry, and physical properties of iopamidol and its analogues. *Invest Radiol* 1980;15 (Suppl):S301.
- [16] Speck U, Boehle F, Krause W, Martin JL, Miklantz H, Schuhmann-Giampieri G. Delayed hypersensitivity to X-ray CM: possible mechanisms and models. *J Acad Radiol* 1997;5 (1):S162.
- [17] *Manual on Contrast Media*. Reston: American College of Radiology; 2012, Version 8.
- [18] Katayama H, Yamaguchi K, Kozuka T, Takashima T, Seez P, Matsuura K. Adverse reactions to ionic and nonionic contrast media. A report from the Japanese Committee on the Safety of Contrast Media. *Radiology* 1990;175 (3):621.
- [19] Lasser EC, Lyon SG, Berry CC. Reports on contrast media reactions: analysis of data from reports to the U.S. Food and Drug Administration. *Radiology* 1997;203:605.
- [20] Hesley G, Hartman R. Review of common and uncommon contrast media reactions. *Appl Radiol* 2008;37 (4):20.
- [21] Rich MW, Crecelius CA. Incidence, risk factors, and clinical course of acute renal insufficiency after cardiac catheterization in patients 70 years of age or older. A prospective study. *Arch Intern Med* 1990;150 (6):1237.
- [22] Bush WH, Swanson DP. Acute reactions to intravascular contrast media: types, risk factors, recognition, and specific treatment. *Am J Roentgenol* 1991;157:1153.
- [23] Loh S, Bagheri S, Katzberg RW, Fung MA, Li CS. Delayed adverse reaction to contrast-enhanced CT: a prospective single-center study comparison to control group without enhancement. *Radiology* 2010;255:764.
- [24] Kormos JL, Schulz M, Ternes TA. Occurrence of iodinated x-ray contrast media and their biotransformation products in the urban water cycle. *Environ Sci Technol* 2011;45 (20):8723.
- [25] Ternes TA, Hirsch R. Occurrence and behavior of x-ray contrast media in sewage facilities and the aquatic environment. *Environ Sci Technol* 2000;34 (13):2741.
- [26] Steger-Hartmann T, Laenge R, Schweinfurth H, Tschampel M, Rehmann I. Investigations into the environmental fate and effects of iopromide (ultravist), a widely used iodinated x-ray contrast medium. *Water Res* 2002;36 (1):266.
- [27] Krause W, Groell R, Kern R, Baumgartner C, Rienmueller R. Application of pharmacokinetics to electron-beam tomography of the abdomen. *Acad Radiol* 1999;6 (8):487.
- [28] Wretling A. Development of fat emulsions. *J Parent Ent Nutr* 1981;5:230.
- [29] Weichert JP, Lee FT, Chosy SG, Longino MA, Kuhlman JE, Heise DM, Levenson GE. Combined hepatocyte-selective and blood-pool contrast agents for the CT detection of experimental liver tumors in rabbits. *Radiology* 2000;216:71.
- [30] Longino MA, Weichert JP, Schwendner SW, Szabo SM, Counsell RE, Glazer GM. Biodistribution of a new lipid-soluble CT contrast agent. Evaluation of cholesteryl iopanoate in the rabbit. *Invest Radiol* 1983;18:275.
- [31] MacMahon E, Murphy AS, Bates MI. Endothelial-cell sarcoma of liver following thorotrast injections. *Am J Pathol* 1947;23 (4):585.
- [32] Olsson O. On hepatosplenography with Jodsol. *Acta Radiol* 1941;22:749.
- [33] Miller DL, Simmons JT, Chang R. Hepatic metastasis detection: comparison of three CT contrast enhancement methods. *Radiology* 1987;165:785.

- [34] Lin Y. Hepatic metastasis detection: comparison of three CT contrast enhancement methods. U.S. Patent 4,396,598. 1983 Jan 11. To Mallinckrodt, Inc.
- [35] Hansen PE, Holtermann H, Wille K. X-ray contrast agents. EP0108638. 1984 July 16. To Nyegaard.
- [36] Hansen PE, Holtermann H, Wille K. X-ray contrast agents. U.S. Patent 5,349,085. 1994 Sept 20. To Nycomed Imaging AS.
- [37] Illig CR. Nanoparticulate diagnostic mixed carbamic anhydrides as X-ray contrast agents for blood pool and lymphatic system imaging. U.S. Patent 5,472,683. 1995 Mar 9. To Eastman Kodak Company.
- [38] Sachse A, Leike JU, Schneider T, Wagner SE, Roessling G, Krause W, Brandl M. Biodistribution and computed tomography blood-pool imaging properties of polyethylene glycol-coated iopromide-carrying liposomes. *Invest Radiol* 1997;32:44.
- [39] Danila D, Partha R, Elrod DB, Lackey M, Casscells SW, Conyers JL. Antibody-labeled liposomes for CT imaging of atherosclerotic plaques: in vitro investigation of an anti-ICAM antibody-labeled liposome containing iohexol for molecular imaging of atherosclerotic plaques via computed tomography. *Tex Heart Inst J* 2009;36:393.
- [40] Torchilin VP, Frank-Kamenetsky MD, Wolf GL. CT visualization of blood pool in rats by using long-circulating, iodine-containing micelles. *Acad Radiol* 1999;6:61.
- [41] Pepiol A, Teixidor F, Saralidze K, van der Marel C, Willems P, Voss L, Knetsch MLW, Vinas C, Koole LH. Development of a highly radiopaque vertebroplasty cement using tetraiodinated o-carborane as a contrast additive. *Biomaterials* 2011;32:6389.
- [42] Aviv H, Bartling S, Kiesling F, Margel S. Radiopaque iodinated copolymeric nanoparticles for X-ray imaging applications. *Biomaterials* 2009;30:5610.
- [43] Krause W, Hackmann-Schlichter N, Maier FK, Müller R. Dendrimers in diagnostics. *Top Curr Chem* 2000;210:261.
- [44] Estep KG, Josef KA, Bacon ER, Illig CR, Toner JL, Mishra D, Blazak WF, Miller DM, Johnson DK, Allen JM, Spencer A, Wilson SA. 1,3,5-Trialkyl-2,4,6-triiodobenzenes: novel X-ray contrast agents for gastrointestinal imaging. *J Med Chem* 2000;43:1940.
- [45] Shalem H, Shatzmiller S, Feit BA. Synthesis of model compounds for potential contrast agents containing phosphonate and peptide moieties. *J Chem Soc Perkin Trans* 2000; 1:2831.
- [46] Parkesh R, Gowin W, Lee TC, Gunnlaugsson T. Synthesis and evaluation of potential CT (computer tomography) contrast agents for bone structure and microdamage analysis. *Org Biomol Chem* 2006;4:3611.
- [47] Stewart RC, Bansal PN, Entezari V, Lusic H, Nazarian RM, Snyder BD, Grinstaff MW. Contrast-enhanced CT with a high-affinity cationic contrast agent for imaging ex vivo bovine, intact ex vivo rabbit, and in vivo rabbit cartilage. *Radiology* 2013;266 (1):141.
- [48] Krause W. Liver-specific X-ray contrast agents. *Top Curr Chem* 2002;221:173.
- [49] Krause W, Handreke K, Schuhmann-Giampieri G, Rupp K. Efficacy of the iodine-free computed tomography liver contrast agent, Dy-EOB-DTPA, in comparison with a conventional iodinated agent in normal and in tumor-bearing rabbits. *Invest Radiol* 2002; 37:241.
- [50] Schumann H, Wassermann BC, Schutte S, Velder J, Aksu Y, Krause W, Raduechel B. Synthesis and characterization of water-soluble tin-based metallodendrimers. *Organometallica* 2003;22:2034.

20

IODINE AS DISINFECTANT*

WALDEMAR GOTTARDI

Department of Hygiene, Microbiology and Social Medicine, Division of Hygiene and Medical Microbiology, Innsbruck Medical University, Innsbruck, Austria

20.1 HISTORICAL SURVEY

As far as is known, the first use of iodine in medical practice was as a remedy for bronchocele [1]. Soon afterward, Lugol [2] treated scrofuloderma (tuberculous lesions of the skin) with an iodine/iodide solution bearing his name, which is in use till now (as Strong Iodine Solution *United States Pharmacopeia* [USP] XXIII). The first specific reference to the use of iodine in wounds was made in 1839 [3, 4]. Iodine was officially recognized by the Pharmacopoeia of the United States in 1830, specifically as *tinctura iodini* (tincture of iodine). The first fundamental papers with a scientific basis about the degerming efficiency of iodine were published from 1874 to 1881 by Davaine [5]. In 1874, he found iodine to be one of the most efficacious antiseptics, a notion that is still valid 140 years later. On the basis of Davaine's experiences, Koch experimented with the disinfecting effect of iodine against anthrax spores. His results are contained in a comprehensive paper entitled "Desinfektion" [6]. In the meantime, the literature about the use of iodine as a disinfectant has expanded markedly. Clinicians and microbiologists described a great number of experimental data and clinical applications, which can be found in numerous surveys [7–14].

*This contribution is a modification by the author (W.G.) of the section "Iodine and iodine compounds," 5th edition, in Block SS, editor: "Disinfection, Sterilization, and Preservation," Lippincott Williams & Wilkins, Philadelphia 2001.

Despite the successes that have been achieved with iodine, it was ascertained early on that it also possesses properties unsuitable for practical applications. Goebel [15] referred to the fact that iodine has an unpleasant odor; in addition, it stains the skin with an intense yellow-brownish color, causes blue stains in the laundry in the presence of starch, and combines with iron and other metals. Furthermore, its solutions are not stable (under certain circumstances); it irritates animal tissue, and it is a poison. The adverse side effects of iodine, its painfulness on open wounds, and the possibility of allergic reactions have in the past 100 years led to the development of a great many iodine-based preparations with the aim of avoiding these incompatibilities without a significant loss of germicidal efficiency. In this connection, the iodophors finally approached this goal to a great extent.

20.2 CHEMISTRY

Elemental iodine dissolves in water and other polar solvents forming a brown solution, which is in contrast to polar solvents (CCl_4 , benzene, hydrocarbons) where it presents a violet color. Whereas in violet solutions, iodine is present as I_2 molecules (as in the gas phase), the brown color is explained by the formation of a compound between iodine and the solvent molecule (charge-transfer complexes). Its solubility in water is very poor (334 ppm at 20°C) but can be increased by the addition of alkali iodides, causing the formation of well-soluble alkali tri- and polyiodides (see Eqs. 20.3, 20.5, and 20.6). Another way to increase solubility is by adding polymeric compounds, which are able to form soluble complexes with iodine, the so-called iodophors.

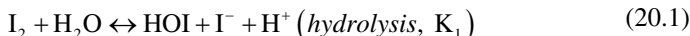
20.2.1 Kinds of Disinfecting Iodine Solutions

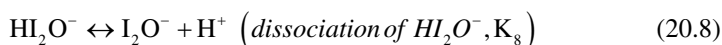
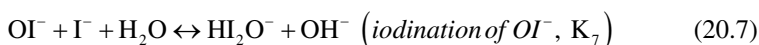
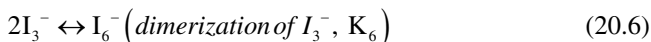
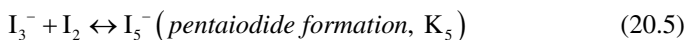
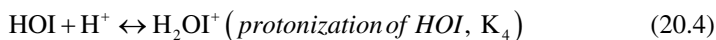
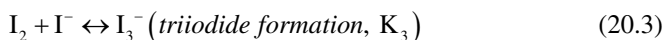
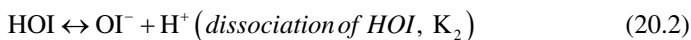
Disinfectants on an iodine basis can be divided into three main groups according to the solvent and substances interfering (by complexing) with iodine species: (i) pure aqueous solutions, (ii) alcoholic solutions, and (iii) iodophoric preparations. All of them contain iodides whose concentrations influence to a great extent their chemical and microbicidal properties.

A reliable understanding of the processes coming about at disinfection, which comprises killing of microorganisms but also interactions with the material to be disinfected (e.g., innate surfaces, living tissue, body fluids), is essentially based on knowledge of the species occurring in the particular solvent, their equilibrium concentrations, and their individual reactivities.

20.2.1.1 Aqueous Solution

For the system iodine/water, nine different equilibria (Eqs. 20.1–20.9) are specified [16], which produce at least 10 new iodine species: I^- , I_2 , I_3^- , I_5^- , I_6^{2-} , HOI , OI^- , HI_2O^- , I_2O^{2-} , H_2OI^+ , and IO_3^- .





As can be seen, it deals with a system of appreciable complexity with several associated equilibria governed mainly by H^+ and I^- ions, which implies that pH and additional iodide are influencing equilibrium concentrations. Another important feature is the reaction rate: While reactions Equations (20.1–20.8) are judged to run almost instantaneously, disproportionation to iodate (Eq. 20.9) proceeds rather slow with a rate influenced very much by pH and additional iodide, as can be easily deduced from the rate law (Eq. 20.10) [17].

$$d[\text{IO}_3^-] / dt \approx 4 \times 10^{-38} [\text{I}_2]^3 / [\text{I}^-]^3 [\text{H}^+]^4 \quad (20.10)$$

The brackets in Equation 20.10 refer to the equilibrium concentrations of the bracketed species. Because the reactions (Eqs. 20.1–20.9) are well-studied with important contributions published since the early 1980s that focus on the fate of radioiodine species that emerge in the course of nuclear accidents [16], a calculation represents the easiest way to approach the equilibrium concentrations, whereas experimentally it would require immense labor, quite apart from the fact that for some species no analytical methods are available [18].

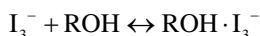
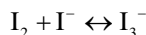
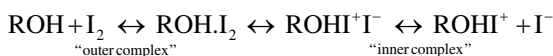
Several investigations into the equilibrium concentrations of aqueous iodine solutions have been done; they differ mainly with regard to the equilibria considered and the regulating parameter, pH, and additional iodide. One study investigated all the immediately established equilibria (Eqs. 20.1–20.8) and both the regulating parameters [18].

It dealt with fresh iodine solutions not altered by disproportionation (iodate formation) and provided results about the equilibrium concentrations of the species I^- , I_2 , I_3^- , I_5^- , I_6^{2-} , HOI , OI^- , HI_2O^- , IO_2^- , and H_2OI^+ . Its results for selected variations of total iodine and iodide, Lugol's solution and its dilutions, and the rates of iodate formation are the basis for most of the following conclusions:

- Additional iodide and pH have a very great influence (several powers of 10) on the individual equilibrium concentrations, and consequently conditions can be indicated in which the number of species of importance is drastically reduced. In the most common case, iodine in the presence of additional iodide at $\text{pH} \leq 6$, only I^- , I_2 , and I_3^- play a role.
- In such a system the analysis is fairly simple because HOI and all species derived from it (OI^- , HI_2O^- , I_2O^{2-} , H_2OI^+) and the higher polyiodides can be neglected without any noticeable loss of precision. In other words, in this case only the triiodide equilibrium (Eq. 20.3) is relevant, and it is not influenced by pH. This has two consequences: (i) the distribution of the three species is the same at pH 6 or less; and (ii) a sufficiently precise evaluation can be based on the sole determination of $[\text{I}_2]$ (e.g., potentiometrically [19] or by dialysis [20]) and $[\text{I}^-]$ (iodide electrode), while triiodide is calculated from both. However, there also exist methods that allow a measurement of these species in a single operation [21, 22], which, however, is not applicable to iodophoric preparations.
- An exception are systems with very high iodide *and* iodine concentration where equilibria 20.5 and 20.6 are of importance, which, however, are independent of pH, too. In the high-leveled Lugol's solution, for example, the species I_5^- and I_6^{2-} make up 8.2% of the oxidation capacity and should not be neglected.
- In absence of additional iodide, at pH 8–9 and high dilution [$\text{c}(\text{I}_2) \leq 10^{-5} \text{ M}$], on the other hand, HOI amounts to over 90% of the oxidation capacity. Absence of iodide is obligatory, too, for the presence of the iodine cation H_2OI^+ [23], however, in an extremely acid milieu that is without any relevance for practice (see later).
- The poor solubility of elemental iodine in water (338.3 ppm, 25°C, pH 5) can be increased by addition of iodide. This feature was first used by Lugol [2] to whom we owe the well-known disinfecting solution bearing his name. Lugol's solution is a highly concentrated iodine formulation with 5% iodine (0.197 mol l^{-1}) and 10% KI ($0.6024 \text{ mol l}^{-1}$) and the following calculated equilibrium concentrations: $6.129 \times 10^{-4} \text{ M}$ (155.6 ppm) free molecular iodine, 0.406 M ($51,650 \text{ ppm}$) iodide, 0.1803 M ($68,640 \text{ ppm}$) triiodide, $9.95 \times 10^{-4} \text{ M}$ (631 ppm) pentaio-dide, and $7.03 \times 10^{-3} \text{ M}$ (5350 ppm) hexaiodide. Lugol's solution, with a three-fold molar excess of iodide, is completely soluble at any dilution. This applies to all iodine/iodide ratios at least down to a twofold excess. Less iodide would cause a gap of solubility of free molecular iodine.
- The problem of stability can be reduced to the rate of iodate formation (Eq. 20.9). Calculations based on this rate law (Eq. 20.10) reveal that at pH less than 6, the formation of iodate can be excluded; above pH 7, however, it has to be taken into account. The presence of iodide shifts the range of stability to higher pH values, for example, Lugol's solution, which is stable up to pH 8.5 [17]. See also Section 20.2.2 later.

20.2.1.2 Alcoholic Solution

Iodine equilibrates with alcohols by undergoing “outer” and “inner” complexes, which finally results in the formation of triiodide, a reaction that is accomplished after approximately 24 h [24]:

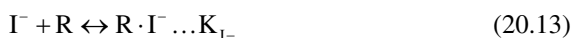


Therefore, as in the aqueous system, we have several oxidizing iodine species: I_2 , $\text{ROH} \cdot \text{I}_2$, ROHI^+ , I_3^- , and $\text{ROH} \cdot \text{I}_3^-$. Calculations concerning their distribution, however, even if possible, are of no use in a bactericidal context in a solvent that is itself a strong disinfectant.

20.2.1.3 Solutions of Iodophors

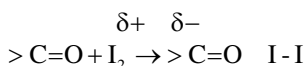
Iodophors are polymeric organic molecules (alcohols, amides, sugars) capable of complexing iodine species, resulting in reduced equilibrium concentrations of the species compared with pure aqueous solutions with the same total iodine and total iodide concentrations.

Because iodophoric preparations always contain appreciable iodide, the relevant species that must be considered are restricted to I^- , I_2 , and I_3^- , for which the (simplified) complexing reactions Equations (20.11–20.13) can be written as follows:



R = structural regions of the iodophor molecule capable of forming complexes.

As far as the chemistry of aqueous disinfectant solutions containing iodophors is understood today, both electronic and steric effects are responsible for these interactions [25]. Thus, taking as an analogy the known interactions with oxygen compounds of low molecular weight, such as amides, esters, ketones, and ether [26, 27], it can be assumed that between molecular iodine and the iodophor molecules, which without exception contain such functional oxygen-containing groups (e.g., povidone contains a carbonyl oxygen of the amide function in the pyrrolidinone ring), donor–acceptor complexes are formed (see also Eq. 20.11), with iodine playing the part of the acceptor:



Furthermore, the iodophors, especially in high concentrations, because of the spatial arrangement of the dissolved polymer molecules with near regions of helix-like structure [20], are clearly able to surround the iodine species in the manner of clathrates and withdraw it from equilibrium (Eqs. 20.11–20.13). This interaction

must be of importance for the iodide ion and particularly for the large-mass triiodide ion. However, because no quantitative data (mass law constants) are available, an exact calculation for iodophoric preparations is not feasible. Nevertheless, qualitative investigations of the interactions with the iodophoric molecule polyvinyl-pyrrolidone (Gottardi, unpublished) reveal that K_{I^-} is much less than K_{I_2} and $K_{I_{3-}}$. With regard to the normal conditions of use, that is, the presence of appreciable iodide and pH less than 7, this has the following consequences [18]:

1. HOI and the species derived from (OI^- , HI_2O^- , I_2O^{2-} , and H_2OI^+) can be neglected.
2. Since the reactions Equations (20.11–20.30) reduce the equilibrium concentrations of I_2 , I_3^- , and to a certain degree also I^- , the species I_5^- and I_6^{2-} can be ignored as well.

Therefore, in iodophoric preparations only the triiodide equilibrium (Eq. 20.3) and the interactions of the iodophoric molecules with I_2 , I_3^- , and I^- are important, all of which are independent of the pH. Because HOI is virtually not present, stability problems concern only interactions with oxidable components (e.g., impurities of the iodophoric matrix) but not the disproportionation to iodate.

20.2.1.4 Influence of Temperature

Though not usually considered, temperature should not be overlooked. In a study dealing with 10 different povidone–iodine preparations the results concerning the relative alteration of free iodine with temperature fitted to an exponential function of the form

$$\Delta\% [I_2]_{\Delta t} = 100 \left[10^{(0.023 \pm 0.0026)\Delta t} - 1 \right]$$

which is valid from 10 to 40°C [28]. Following this equation, $[I_2]$ increases about 5.4 and 100% if the temperature rises about 1.0 and 13.1°C. This increase of $[I_2]$ must be considered in the application of povidone–iodine preparations as disinfectants or antiseptics on living tissues. Because of their higher temperature (30–36°C), the employed povidone–iodine preparations exhibit a significantly higher $[I_2]$ than they do at room temperature ($\Delta t = 10\text{--}16^\circ\text{C}$: $\Delta\% [I_2] = 70\text{--}130\%$). Therefore, a significantly higher degerming efficiency can also be expected compared with that obtained in *in vitro* experiments, which usually are conducted at room temperature.

20.2.1.5 Atypical Behavior of Iodophors at Dilution

If 10% povidone–iodine is diluted, the concentration of free molecular iodine unexpectedly increases and passes through a maximum approximately in the 0.1% solution.

As can be seen in Figure 20.1, the concentration of free iodine in a 10% povidone–iodine solution comes to approximately 2.0 mg and $8 \times 10^{-6} \text{ M l}^{-1}$ and rises in a 1:100 dilution nearly tenfold. On further dilution, after passing the maximum ($[I_2] \approx 10^{-4} \text{ M l}^{-1}$) the free iodine behaves increasingly “normally”—that is, it decreases—and

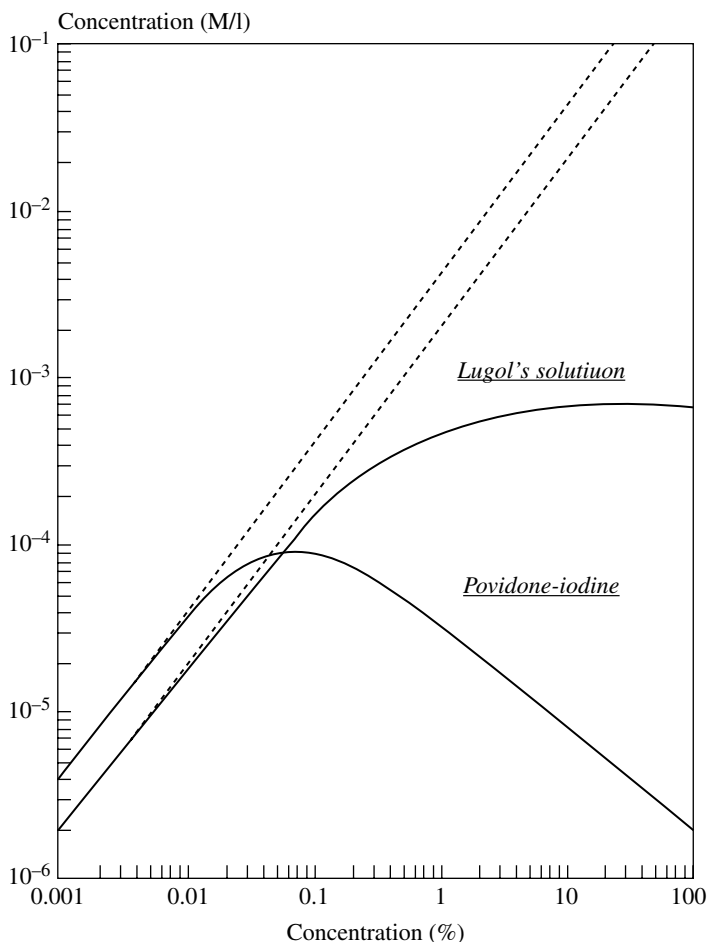


FIGURE 20.1 Total available (---; dashed lines) and free molecular. (—) iodine in aqueous povidone–iodine (determined potentiometrically [19]) and in Lugol's solution (calculated after [29]). Reproduced with permission from Ref. [29].

below 0.01% the povidone–iodine solution can be regarded as a simple aqueous solution of iodine.

Because $[I_2]$ depends not only on the concentration of povidone–iodine, but on total iodine (in general 1%) and total iodide (iodine/iodide ratio; see Pinter et al.) [30], and the presence of iodine complexing pharmaceutical additives, it undergoes considerable variations. Figure 20.1 shows the typical course of $[I_2]$ of a pure aqueous povidone–iodine at dilution. The ordinate of the maximum (and to a lesser degree also its abscissa), therefore, is not a constant for different iodophors and preparations containing iodophors. It also shows the behavior of Lugol's solution on dilution, which explains the drastic reduction of free iodine caused by the complexing properties of the povidone molecules.

20.2.2 Individual Reactivities of Iodine Species

Much labor was devoted to clear up these questions. Some answers are widely accepted:

- Iodide (I^-) as a nonoxidizing species has no degerming activity.
- This is true for iodate (IO_3^-) as well, which acts as an oxidant only at an acidic pH, as HIO_3 (<pH 4).
- Free¹ iodine (I_2) is the only species with a proved correlation between equilibrium concentration and bactericidal activity. Its solvated forms, $I_2 \cdot H_2O$ or $I_2 \cdot ROH$, are thought to be the real microbicidal agents in aqueous and alcoholic solution.
- Triiodide (I_3^-) probably has no degerming activity, which was deduced from the negative effect increasing iodide concentration has on the inactivation of polio virus [31]. On the other hand, triiodide represents the reservoir of oxidation capacity in noniodophoric preparations (Lugol's solution). It is the main species responsible for staining of tissue [32].
- Hypoiodous acid (HOI) is thought to contribute to bactericidal action, which is a plausible analogy with the Cl_2/H_2O system where HOCl is the real active species. Although [33] claimed differing behaviors of I_2 and HOI against certain germs, reports on the bactericidal properties of HOI and on attempts to establish a difference between I_2 and HOI should be treated cautiously [18]. Although it is possible to manipulate an aqueous iodine solution to exhibit more than 90% of the oxidation capacity as HOI (pH \approx 8.5, no additional iodide), such systems in general have no practical importance, mainly because of stability problems (see later). On the other hand, given a similar reactivity of I_2 and HOI in high diluted systems [$c(I_2) \leq 10^{-5} M$] without additional iodide (as is usual in drinking water disinfection), and in the pH range of 3–9, a more or less constant bactericidal activity of iodine in aqueous solution can generally be expected [34].
- Iodine cation (H_2OI^+) is thought to be a very potent iodinating agent. Many publications assign some relevance to this species as being responsible for disinfection, which can be traced back to a comprehensive and very often cited study dealing with the halogens in disinfection [31]. However, exact calculations [18] show that the iodine cation has some importance, if at all, only under *very acidic* conditions (pH < 1) and in the *total absence* of additional iodide where it amounts at the most to only $\approx 0.3\%$ of total iodine at high dilution. Under practical conditions, that is, in the presence of iodide (to regulate the concentration of free molecular iodine and improving stability), however, *the iodine cation is virtually absent* and therefore of no importance. For example, a solution with $c(I_2) = 0.001$ and $c(I^-) = 0.01 \text{ mol l}^{-1}$ generates $[I_2] = 1.31 \times 10^{-4} \text{ mol l}^{-1}$ or 33.3 ppm at pH < 8. The concentration of the iodine cation, however, comes to $[H_2OI^+] = 2.15 \times 10^{-13} \text{ mol l}^{-1}$, which is *about 9 powers of 10 less than $[I_2]$* . Even if we attribute a higher reactivity to the iodine cation, which is thought to play an important role in certain organic substitutions, this can hardly explain any real contribution to the disinfecting process.

¹ The term "free" serves to distinguish from complex bound I_2 as it is discussed in iodophoric preparations and refers to the solvated forms $I_2 \cdot H_2O$ and $I_2 \cdot ROH$.

20.2.2.1 Virtual Impossibility of Discriminating Microbicidal Activities of I_2 and HOI

A frequently quoted issue is the contribution of free molecular iodine, I_2 , and HOI to disinfection processes and the differences in their bactericidal power [31]. As set forth earlier, a solution containing predominantly I_2 needs a pH <5 and absence of iodide, while in the case of HOI it is pH \approx 8.4. A comparison of the killing effect of I_2 and HOI presupposes that the susceptibility of bacteria for the interaction with these iodine species is the same in both pH ranges, which is a coarse simplification. Therefore, a definite differentiation is probably not feasible, an assertion that applies to other iodine species as well.

20.2.3 Stability of Iodine-Based Disinfectants

Iodine and other disinfectants based on halogens in the oxidation states 0 or +1, as far as they are not present as pure substances (i.e., without a solvent), can gradually lose a part of their degerming properties during storage. This is due to (i) substitutions of covalent hydrogen, for example, O–H, N–H, CH (stemming from the solvent, iodo-phoric molecules, and pharmaceutical additives), (ii) additions to olefinic double bonds (I_2 , HOI), and (iii) the disproportionation of the hypohalous acid to halate in aqueous preparations (Eq. 20.9), which has no degerming properties (see earlier). Although substitutions, which in the case of iodine are thought to be fewer than with chlorine and bromine, and additions can be avoided by an appropriate composition, the equilibria 20.1 through 20.8 are established in any case if water is present, and iodate formation (Eq. 20.9) can begin.

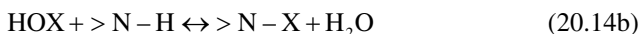
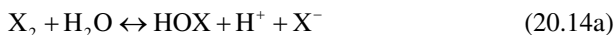
On the basis of calculated equilibrium concentrations, reaction times, and initial rates of iodate formation, the following conclusions have been drawn concerning the stability of iodine-containing disinfecting solutions [17, 18, 34]:

1. Below pH 6, a decrease of disinfecting effectiveness due to the formation of iodate can be excluded.
2. Above pH 7, the formation of iodate, whose extent largely depends on the pH value as well as on the iodide concentration, must be regarded carefully. Raising the pH value lowers the stability (iodate formation increases), whereas raising the iodide concentration improves the stability (iodate formation is reduced).
3. Because of the stabilizing effect of the iodide ion, provided that its concentration is high enough, the opposite effect of the pH value can be overcompensated. As a result, iodine-based preparations can also exhibit sufficient stability for practice in the weak alkaline range (e.g., Lugol's solution, pH <9).
4. In highly diluted iodine solutions ($<10^{-5} \text{ M l}^{-1}$, or 2.54 mg l^{-1}), which are present in disinfections of potable water or swimming-pool water, only a slow iodate formation can be expected even in the absence of additional iodide and pH \leq 8. In accordance with this, in disinfection plants on an iodine basis, no significant iodate amounts have been detected [35].
5. Because iodate formation can be avoided at pH \leq 6, iodine preparations are kept at a pH of 5–6 by appropriate buffers (generally on a citrate and phosphate

basis). Stability problems arising from very slow substitution reactions at the organic matrix of iodophors ($\text{C-H} + \text{I}_2 \rightarrow \text{C-I} + \text{H}^+ + \text{I}^-$) are governed by the addition of a small amount of iodate (as NaIO_3 or KIO_3), which by slow comproportionation (reverse of Eq. 20.9) regenerates consumed iodine.

20.2.3.1 Absence of N-Iodo Compounds in Aqueous Solution

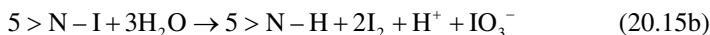
The well-known equilibria of halogen with N-H compounds:



lead to numerous N-chloro compounds, which play an important role in chlorine-based disinfection practice; this however, is not the case with iodine.² Although N-iodo compounds can be synthesized in a nonaqueous system [37, 38], in contact with water they immediately hydrolyze.



HOI immediately begins to disproportionate according to Eq. 20.9; iodide and protons develop, and a comproportionation reaction (reverse of reaction Eq. 20.1) also takes place, forming molecular iodine. Within minutes, the reaction settles, the ratio of the resulting products, I_2 and IO_3^- , complying with the stoichiometry of Equation (20.15b) [39].



Because the reactions Equations (20.15a and 20.15b) are far on the right side, practically no N-iodo compound is present. N-iodo compounds are virtually without any relevance for disinfection.

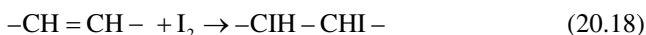
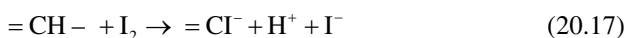
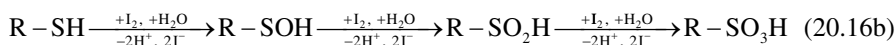
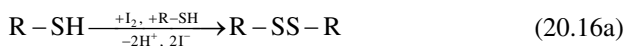
20.2.4 Reaction with Proteinaceous Material: Bacterial Kill and Consumption Effects

Halogens react not only with living microorganisms but also with their environment, that is, dead bacteria, dissolved proteins, and amino acids. Compared with chlorine, the chemism is substantially simpler because iodine does not react with amino functions under conditions prevailing at disinfection in practice. The main targets are therefore aromatic C-H functions, sulfur-containing amino acids (cysteine, methionine), and unsaturated fatty acids.

The interaction with S-H compounds runs in two directions, the oxidation to disulfides (Eq. 20.16a), on the one hand, and to sulfur-oxygen acids, that is, sulfenic,

² This assertion complies with the pH range relevant for disinfection (pH 4-8) and not with alkaline conditions at 0°C where N-iodo alkyl amines can be synthesized even in aqueous solution [35].

sulfinic, and sulfonic acids (Eq. 20.16b), on the other hand. Because these reactions run with similar speed, the portion of the diverse products is mainly governed by the mode of mixing. Equation 20.17 describes the substitution at activated aromatic compounds, for example, the amino acids tyrosine, histidine, and the nucleosides cytosine and uracil, while Equation 20.18 refers to the addition of I_2 to the olefinic function of unsaturated fatty acids.



20.2.4.1 Iodine's Mode of Action as a Microbicide

Iodine, mainly in its molecular form, can penetrate the cell wall of microorganisms rapidly [33], which can be deemed as its fundamental feature. Although the exact details about the killing of a living cell by the I_2 molecule (or one of the reaction products occurring in aqueous solution; see Eqs. 20.1–20.9) are not known, it is plausible that microbial kill by iodine is based on the reactions outlined in Equation 20.16–20.18, which could have the following consequences:

1. Oxidation of the S–H group [31] of the amino acid cysteine results in loss of the ability to connect protein chains by disulfide (–S–S–) bridges, an important factor in the synthesis of proteins.
2. Iodination of the phenolic and imidazolic group of the amino acids tyrosine and histidine, which easily form monoiodo or diiodo derivatives, and iodination of the pyrimidine derivatives cytosine and uracil could increase the bulk of the molecules, leading to a form of steric hindrance in hydrogen bonds.
3. Addition of iodine to unsaturated fatty acids (Eq. 20.18) is supposed to lead to a change in the physical properties of the lipids and to cause membrane immobilization [40].

Annotation: Of these points the first might be the most important, because of both the ubiquitous SH groups and the very fast and irreversible reaction with iodine (see also Section 20.3.2.1).

20.2.4.2 Effect of Iodine-Consuming (Reducing) Material

With in vitro experiments using peptone solutions, it was shown that iodine reacts with proteins at least three times slower than chlorine and nearly four times slower than bromine [41]. Hence, in disinfection under conditions occurring in practice, that

is, in the presence of dissolved proteins (blood, serum, sputum), iodine is much more efficient than chlorine (and bromine) because the share of the employed halogen concentration that is available for the actual degerming reaction is considerably greater. The comparatively low reactivity with proteins (no N-iodo compounds), which is sufficient, however, to achieve high killing rates, is one of the reasons for the excellent degerming properties of iodine.

However, there is a minor drawback with iodine, which can be deduced from Equations (20.16–20.18): consumption effects are always connected with the formation of iodide. Thus, by the reactions Equations (20.16–20.18) not only is the reservoir of available iodine (oxidation capacity) diminished, but the triiodide equilibrium (Eq. 20.3) is shifted to the right. This means that the bactericidal power (which is a function of $[I_2]$) is diminished to a higher degree than would be estimated on the basis of the loss of total iodine. This disadvantage is avoided with formulations that are able to reoxidize the formed iodide, such as “enzyme-based iodine” [32, 42].

20.3 PREPARATIONS CONTAINING OR RELEASING FREE IODINE

20.3.1 Solutions of Iodine and Iodide

To this group belongs a great variety of preparations containing elemental iodine and potassium (or sodium) iodide in water, ethyl alcohol, and glycerol, or in mixtures of these solvents. They rank with the oldest disinfectants and have survived nearly 200 years owing to their efficacy, economy, and stability. The following are official preparations according to USP XXIII: (i) Iodine Topical Solution, an aqueous solution containing 2.0% iodine and 2.4% sodium iodide; (ii) Strong Iodine Solution (Lugol's Solution), an aqueous solution containing 5% iodine and 10% potassium iodide; (iii) Iodine Tincture containing 2.0% iodine and 2.4% sodium iodide in aqueous ethanol (1:1); and (iv) Strong Iodine Tincture containing 7% iodine and 5% potassium iodide in 95% ethanol. Because all of these preparations contain large amounts of iodide ($0.16\text{--}0.6\text{ mol l}^{-1}$), the triiodide equilibrium (Eq. 20.3) mainly becomes important. As a result, these solutions virtually contain chiefly molecular iodine, iodide, and triiodide and are therefore very stable because there is no HOI present (see earlier). Because of their high content of free molecular iodine (e.g., Lugol's solution: $[I_2] = 155.6\text{ ppm}$), they are powerful disinfectants with the disadvantage of staining and a toxic potential, which should not be underestimated (see Section 20.5).

20.3.2 Preparations Containing Organic Complexing Agents

Besides preparations with complexing agents of low molecular weight, such as tetra-glycine hydroperiodide [13], or the inclusion compound iodine–maltosylcyclodextrin [43], this group includes the important “iodophors,” whose name generally indicates the combination of iodine with a carrier (as these complexing agents are usually called) of high molecular weight. In aqueous solution, iodophors form the

same iodine species as do the pure aqueous iodine solutions (see earlier). However, the polymer carriers, because of their complexing properties, partly reduce the equilibrium concentrations of the iodine species and give the iodophor preparations properties that make them superior in some respects to solutions containing only iodine and iodide.

20.3.2.1 Iodophors

An iodophor is a complex of iodine with a carrier that has at least three functions: (i) to increase the solubility of iodine, (ii) to provide a sustained-release reservoir of the halogen, and (ii) to reduce the equilibrium concentration of free molecular iodine. The carriers are neutral polymers, such as polyvinyl pyrrolidinone, polyether glycols, polyvinyl alcohols, polyacrylic acid, polyamides, polyoxyalkylenes, and polysaccharides.

In the solid state iodophors form crystalline powders of a deep brown to black color that usually do not smell of iodine, indicating a tight bonding with the carrier molecules. Their solubility in water is good but depends on the chain length of the polymeric molecules and varies in the case of povidone–iodine between 5% (type 90/04, average molecular weight near 1,000,000) and more than 20% (type 17/12, average molecular weight near 10,000). The best-known iodophor is povidone–iodine, a compound of 1-vinyl-2-pyrrolidinone polymer with iodine, which according to USP XXIII contains not less than 9.0% and not more than 12.0% available iodine. On the basis of spectroscopic investigations [44], it was found that povidone–iodine (in the solid state) is an adduct not with molecular iodine (I_2) but with hydrotriiodic acid (HI_3), where the proton is fixed via a short hydrogen bond between two carbonyl groups of two pyrrolidinone rings and the triiodide anion is bound ionically to this cation.

A completely different situation occurs in solution where this structure no longer exists and equilibria between I_2 , I^- , I_3^- , and the polymeric organic molecules are established (Eqs. 20.11–20.13). The high amount of carrier molecules ($\sim 90\text{ g l}^{-1}$) results in the content of free molecular iodine being greatly reduced in such preparations (10% aqueous solution of povidone–iodine: $c(I_2) \approx c(I^-) \approx 0.04\text{ M l}^{-1}$, $[I_2] \approx 1 \times 10^{-5}\text{ M l}^{-1}$ or 2.54 ppm), in comparison with pure aqueous solutions with the same total iodine and total iodide content (aqueous iodine solution: $c(I_2) = c(I^-) = 0.04\text{ M l}^{-1}$, pH 5: $[I_2] = 5.77 \times 10^{-3}\text{ M l}^{-1}$ or 1466 ppm³). The high content of free iodide (which varies between 10^{-3} and 10^{-1} M l^{-1} , according to the preparation) also means that HOI can be disregarded, and only I_2 is responsible for disinfection (see earlier).

20.3.2.2 Relevance of Free Molecular Iodine to the Efficiency of Iodophor Preparations

The real bactericidal agent is free molecular iodine, because it is this species alone for which a correlation between concentration and bactericidal activity has been proved, and not for the total iodine or iodophor concentration [25, 30, 32, 45].

³ This is a hypothetical value because the solubility of molecular iodine lies at 334 ppm (25°C) and an aqueous solution of this composition will contain undissolved iodine.

However, the various commercial preparations differ in the amount and kind of pharmaceutical additives, such as detergents and back fattening agents, all of which usually have iodine complexing properties, as well as in the ratio of total iodine to total iodide [30]. This results in a significant difference in the concentration of free molecular iodine, in spite of the fact that the actual iodophor concentration or the concentration of the total (titratable) iodine might be the same.

These circumstances justify the necessity to be informed about free iodine for which three different methods have been described: extraction with a nonpolar solvent, for example, heptane [46], dialysis [20], and potentiometrically [19]. The latter was the basis for an essentially improved version, which has been proven to be the most favorable approach concerning equipment, labor, and precision.⁴ Free iodine is the yardstick for bactericidal potency (killing rate), whereas the total iodine, which follows from the specification or simply can be assayed by titration, points to the disinfection capacity. The latter comprises *all* oxidizing iodine species and therefore should not be confused with free molecular iodine, which except in highly diluted solutions (see Fig. 20.1) amounts to only a small fraction of the total available (i.e., titratable) iodine. For aqueous preparations, the determination of free iodine is a reliable and simple means to make predictions of the bactericidal properties [47] and, as already pointed out, should be specified by the manufacturer.

In view of the fact that free iodine is also a measure for irritation, it is a severe default on the part of the authorities not to insist on specifying the “free iodine” as an integral parameter for iodine, and particularly for iodophoric preparations.

20.3.2.3 Forms of Application

According to USP XXIII, the following application forms of povidone–iodine are approved: Povidone–Iodine Topical Solution, Povidone–Iodine Cleansing Solution, Povidone–Iodine Ointment, and Povidone–Iodine Topical Aerosol Solution. Concerning the available iodine, they have to contain not less than 85% and not more than 120% of the labeled amount. In general, povidone–iodine preparations contain 1–10% povidone–iodine, which is equivalent to 0.1–1.0% of available iodine. They may contain a small amount of alcohol (Topical and Cleansing Solution); the cleansing solutions contain one or more surface-active agents. The aerosol solution, however, is a povidone–iodine solution under nitrogen in a pressurized container.

20.3.2.4 Influence of Iodine Consumption on the Efficacy of Povidone–Iodine Preparations

Because iodophoric preparations are mainly used as medical antiseptics, the influence of iodine-consuming body fluids is a very important feature with regard to bactericidal capacity and rate. Mainly in the presence of blood, which is characterized by S–H functions, the reservoir of available iodine is substantially diminished and, because of the formed iodide (Eqs. 20.16a–20.17), the triiodide equilibrium (Eq. 20.3) is shifted to the right. Both effects decrease the proportion of free molecular iodine (see earlier).

⁴ The monograph “Convenient procedure for measuring the free iodine in antiseptic preparations” can be acquired from the author (waldemar.gottardi@i-med.ac.at).

On the other hand, when povidone–iodine preparations are contaminated with liquid substrata, the dilution effect (see earlier) causes an increase in the equilibrium concentration of free molecular iodine. The extent to which this effect compensates for the other two depends on the content of reducing substances. Thus, with whole blood, a large decrease in the concentration of free molecular iodine occurs, whereas in the presence of plasma (exudates) this concentration actually remains unchanged if the ratio is not too high [48].

Quantitative investigations into consumption of iodine (and also other oxidizing substances) with blood are distinguished by a poor reproducibility, which can be attributed to the different reactions of iodine with SH groups (Eqs. 20.16a and 20.16b). It is important to note that in practice no substantial decrease of the bactericidal efficacy of 10% povidone–iodine preparations is likely to occur with body fluids having a composition similar to plasma (volume substrate/volume povidone–iodine 10% ≤ 0.6). However, contamination by greater than 25% full blood should be avoided.

20.3.2.5 Iodophoric Preparations and the Term “Active Agent”

In the search for the ideal disinfectant (i.e., the impossible combination of immediate bacterial kill with complete lack of unwanted side reactions) a lot of work was done by microbiologists comparing preparations based on differing chemistries or killing mechanism (e.g., chlorine, iodine, aldehydes, peroxides, chlorhexidine, quats).

The results of such studies are generally presented in terms such as, for example, “0.25% chlorhexidine and 0.025% benzalkonium chloride was more (or less) effective than 10% povidone iodine.”

Such a formulation implies that povidone–iodine is an active agent; however, this is not the case. The basic requirement to designate a substance as an active agent is (i) a defined molecule, and (ii) a positive correlation between the concentration of these defined molecules and bactericidal activity. Both criteria are not fulfilled with povidone–iodine.

Concerning the nature of povidone–iodine, with regard to disinfection the following points have been made [49]:

1. Although in the solid state povidone–iodine forms a crystalline powder with a delineated structure in which iodine is present in the form of discrete HI_3 units (see Fig. 20.2), it is not a uniform compound because the polymeric carrier

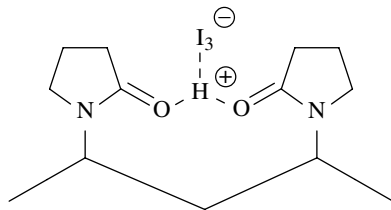


FIGURE 20.2 Structure of solid povidone–iodine [44].

molecules show a molecular weight distribution. In aqueous solution, however, HI_3 molecules are no longer there but an equilibrium exists between I^- , I_2 , I_3^- , which are more or less complexed by the organic carrier molecules.

2. Povidone–iodine preparations with 10% povidone–iodine and 1% titratable iodine can easily be adjusted to contain a range of 0.1 more than 20 ppm free molecular iodine (I_2). Indeed, in a comparison of 10 commercially available preparations, a range of 0.2–10 ppm free molecular iodine was found [50].
3. Because of a possible range in $[\text{I}_2]$ of two powers of magnitude, preparations specified to contain 10% povidone–iodine will exhibit remarkable variations in bactericidal activity.
4. Because there is no direct and positive correlation between bactericidal activity and the concentration of povidone–iodine (dose action relation), it follows that povidone–iodine cannot be regarded as an *active agent* (like chlorohexidine) but a *pharmaceutic base material*.
5. As long as free molecular iodine (as the most important species) is not specified (see earlier), both quantitative killing results (log reductions) and evaluation of toxicity relate only to the *batch number X* of the *preparation Y* of the *manufacturer Z* and do not contribute to solve basic issues of iodine and disinfection.

Although they have been published [49], these assertions are not accepted (obviously because they are not read or understood); this also applies to the previously stated necessity to specify for iodine-based preparations, in addition to total (titratable) iodine, at least the free molecular iodine, which provides information about toxic effects as well as microbicidal activity.

20.3.3 Solid Iodine–based Microbicidal Compositions

To this group belong resins containing quaternary ammonium groups loaded with triiodide and higher polyiodide ions (e.g., pentaiodide). In contrast to the “classical” disinfectants, which contain antimicrobial agents that are dispersed in a liquid (or gas) phase, these resins rank among the “nonclassical chemical disinfectants” (NCCD), which consist of active moieties attached to, associated with, or stored (or a combination thereof) in a solid phase [51]. Their mode of action is explained either by direct, physical contact with their surface or by slowly releasing a disinfecting agent (in this case iodine) into the bulk phase being disinfected. Because the residuals of total iodine washed out by the water flowing through the resin are very low, the resins seem to be ideally suited for application in point-of-use water purification units [52].

20.3.4 Preparations Producing Iodine In Situ

Preparations of this kind do not contain elemental iodine, but rather iodide (NaI or KI), and produce the former by an oxidation process ($2\text{I}^- \rightarrow \text{I}_2 + 2\text{e}^-$), which can be performed either chemically or by electrical current. In the first case it generally deals with stable dry powder concentrates, which start to produce iodine only when they come in contact with water. Examples of oxidants that were used to produce iodine in

situ are chloramine-T, 1,3-dichloro-5,5-dimethyl hydantoin [53], and NH_2Cl [54]. A recent development uses calcium peroxide as an oxidant and horseradish peroxidase as a catalyst [32]. The great advantage of this concept called “enzyme-based iodine (EBI)” is, on the one hand, the combination of a relative high concentration of free molecular iodine (15 ppm) with a comparatively very low concentration of total iodine (≈ 30 ppm). This is in contrast, for example, to iodophoric preparations where the ratio is not 1:2 but $\approx 1:1000$. On the other hand, the EBI system is able to reoxidize reduced iodine, which results in a constant level of active iodine during its use-life. This outstanding feature was demonstrated at repeated cycles of endoscope processing [42].

The production of iodine by anodic oxidation of an aqueous iodide solution is another feasibility to supply a diluted disinfecting solution in situ in large volumes recommended for municipal drinking water supplies, cooling towers, and swimming pools [55]. In a closed disinfecting system, electric current can be used to reoxidize consumed (reduced) iodine for which a potentiometric steering is possible (Gottardi, unpublished data).

20.3.5 Synopsis of Composition and Active Iodine Forms in Disinfectant Solutions

Table 20.1 gives a synopsis of the different preparations containing and applications using iodine. Besides the total concentration of iodine and iodide, the presumable active species and their calculated, measured, or estimated equilibrium concentrations are shown. Furthermore, a tentative description of the conditions in alcoholic solutions is given. In contrast to pure alcoholic solutions (containing only iodine and an alcohol), where iodine predominately occurs in the solvated molecular form, $\text{I}_2\cdot\text{ROH}$ (besides some triiodide; see Section 20.2.1.2), alcoholic preparations used in practice (Tincture and Strong Tincture of Iodine, USP XXIII) also contain iodide and water, with the result that the equilibria 20.1 through 20.8 are established, too. However, because of the iodide content, no HOI is present, and only the solvated iodine molecules $\text{I}_2\cdot\text{ROH}$ and $\text{I}_2\cdot\text{H}_2\text{O}$ – apart from the alcohol itself – appear to be responsible for disinfection. A differentiation between the two forms according to relative reactivity should turn out in favor of the hydrate complex because of the greater stability of the I_2 –alcohol–solvate complex (inductive effect of the alkyl group increases the electron-donating properties of the oxygen).

HOI as a virtual contributor to the microbicidal process is to be expected only in iodine/water systems of high dilution and very low iodide concentration, as is the case with disinfection of drinking and swimming-pool water on an iodine basis.

20.4 ORGANIC IODINE COMPOUNDS

Compounds of this class contain iodine bound to a carbon atom and they differ from the previously described disinfectants in that they contain no free iodine and are not oxidizing. Iodoform (triiodomethane), probably the oldest pharmaceutically used iodine compound, forms yellow crystals with a characteristic anesthetic odor. It came

TABLE 20.1 Composition and active iodine form in disinfectant solutions containing iodine

Components	Solvent	Examples	Total iodine content (total iodide content)	Iodine form mainly responsible for microbiocidal effect (concentration proportion of the total iodine concentration)
I ₂	Ethanol H ₂ O	Solution of iodine in alcohol Drinking water, swimming- pool iodination	1% 10 ⁻⁵ to 10 ⁻⁶ M l ⁻¹	I ₂ ·ROH I ₂ -aq, HOI ([I ₂] + [HOI]): 0.25–2.5 ppm; 98–100%)
I ₂ , I ⁻ I ₂ , I ⁻	H ₂ O H ₂ O	Lugol's solution EBI 30–40 ppm (110–130 ppm)	5% (10% KI)	I ₂ -aq (155.6 ppm; 0.31%) I ₂ -aq (15 ppm; ~50%)
I ₂ , I ⁻ , polym, org-complexing agents, additives	Ethanol/H ₂ O H ₂ O	Iodine tincture Mucosal disinfectant and washing concentrates based on iodophores	2% (2.4% NaI) 0.5–1.0% (iodide content vary greatly depending on the preparation (0.05%)	I ₂ ·ROH, I ₂ -aq I ₂ -aq (0.2–10 ppm, 0.003–0.1%)
I ₂ , I ⁻ , polym, org-complexing agents, additives	Propanol/H ₂ O	Skin disinfectants(sprays)		I ₂ ·ROH, I ₂ -aq

into extensive use as a dusting powder, especially as a local anti-infective agent to promote granulation and diminish infections of open wounds [13]. Because of its toxicity (it may cause sleeplessness, hallucinations, and spasms), it has been replaced by other preparations, especially those containing iodophors, and it is no longer specified in the USP.

A special application still in use is filling of cavities in dentistry and oral surgery with triiodomethane containing pastes or gauzes coated therewith. Particularly, a calcium hydroxide-iodoform mixture was considered suitable as a root-filling material [56]. Filling of large cavities, however, should be avoided as O'Connor et al. [57] reported on a severe iodoform toxicity with bismuth-iodoform-paraffin paste after a total maxillectomy. Concerning the bactericidal mechanism, iodoform was supposed to produce elemental iodine and formaldehyde in connection with water [12]. This assertion seems to be doubtful as it was impossible to detect any free iodine in an aqueous slurry of CHI_3 at 37°C and pH 7 with a method that is sensitive down to $2.5 \times 10^{-8} \text{ M l}^{-1}$ [58].

Iodine derivatives of quinoline exhibit protozoacide and metazoacide properties and have shown excellent results in prophylactic and therapeutic use [13]. Iodoquinol (USP XXIII, 5,7-diiodo-8-quinolinol) and Clioquinol (USP XXIII, 5-chloro-7-iodo-8-quinolinol) are the best-known active substances of this type and serve as the basis for creams, ointments, powders, and tablets. To this class of compounds belong also the iodine-containing X-ray contrast media. Examples are Iocetamic Acid, Iopanoic Acid, and Iothalamic Acid (all USP XXIII). They contain a benzene ring system with three iodine atoms in the meta-position and are used as such but also in the form of their derivatives. The radioactive compounds Iodohippurate Sodium I 123 and I 131 (USP XXIII) are used for nuclear medical purposes. Of historical interest are the *iodonium compounds* with the general formula $[\text{R}_2\text{I}^+]\text{X}^-$, where R is an organic radical and X^- an inorganic or organic anion, for example, diphenyliodonium chloride. The structure resembles the onium compounds (e.g., quaternary ammonium), and the active part of these compounds is iodine in the oxidation state +3 [59].

20.5 TOXICITY

Toxicity comprises all unwanted side reactions which can be classified as primary effects like *irritation* and *staining*, and secondary effects that are the biological consequences of *incorporation*. In discussing these features, it is necessary to take into account (i) the composition of the preparation, that is, the equilibrium concentrations of the iodine species I_2 , I^- , and I_3^- , (ii) their specific contribution to toxic effects, (iii) the nature of the tissue coming in contact with the iodine system, and (iv) the mode and time of application.

- *Irritation* is a result of iodinating or oxidizing reactions for which chiefly free molecular iodine is responsible. Because these reactions are the same that cause bacterial kill, in general a positive correlation between both features can be expected. However, the surprisingly low toxicity of the enzyme-based low-level iodine disinfecting system [42] reveals that a high concentration of free molecular iodine

(15 ppm) is well-tolerated if total iodine (triiodide) is very low (30–40 ppm).

- *Staining* is mainly caused by the triiodide ion and only to a minor degree to free molecular iodine [32]. The deep brownish color on skin is often misinterpreted as a kind of burn.
- For *incorporation* effects two routes are possible: diffusion through the treated tissue and uptake as drinking water. In the first case, uncharged molecular iodine plays the main role because it is able to diffuse through the skin. For the ionic species like I^- and I_3^- , however, the intact skin acts as a barrier [60]. The triiodide ion, therefore, is retained in the outer layers of the horny skin where it causes staining that cannot be removed by washing. However, because of the equilibrium $I_3^- \leftrightarrow I_2 + I^-$, as long as staining is visible molecular iodine is formed, which diffuses in deeper regions of the skin where it is reduced provoking an increase of serum iodide. On the other hand, there is also a diffusion out of the skin causing a remanent bactericidal action (see later). Therefore, staining, though caused by the charged species I_3^- , also gives rise to a real incorporation and should be deemed as a sign of toxicity. The contribution of iodide to incorporation is confined to ingestion (iodinated drinking water, iodide-containing foodstuffs) and resorption at the disinfection of mucous tissues.

Although the symptoms are clear in irritation and staining, the secondary effects (based on incorporation) have diverse manifestations: elevated iodide levels in urine and serum, and deviations (usually an increase) in serum levels of parameters connected with thyroid function, T_4 (thyroxine or tetraiodothyronine), T_3 (triiodothyronine), and thyrotropin (thyroid-stimulating hormone [TSH]).

20.5.1 Topical Antiseptic Preparations

20.5.1.1 Iodine Tincture

High doses of free iodine, such as in the form of iodine tincture, are highly toxic if they enter body cavities and cause swelling and bleeding of mucous membranes. Consumption of 30 g of iodine tincture can be fatal [61]. As an antidote for such accidents, 10–20 g sodium thiosulfate (reduction of iodine to iodide) or starch (formation of inclusion compounds) orally is recommended [62].

20.5.1.2 Lugol's Solution

The high concentration of free iodine ($[I_2] = 155.6 \text{ ppm}$) proves that it is a powerfully disinfecting but also rather toxic solution, with strong staining properties grounded on the high triiodide concentration (0.18 mol l^{-1}). It should be used only externally on very small areas where it can be recommended in emergency, for example, at injuries by contaminated hypodermic needles.

20.5.1.3 Enzyme-Based Iodine

Toxicity tests including oral toxicity, primary dermal irritation, acute inhalation, ocular toxicity, acute dermal irritation, and sensitization assays in test animals (rat, rabbit, and guinea pig) showed no evidence of toxicity for EBI except a slight irritation at the

unwashed rabbit eye and at the primary dermal test [42]. The authors attribute the low toxicity on external and internal surfaces of living animals to the low level of total iodine (i.e., triiodide) in the germicide.

20.5.1.4 Povidone–Iodine

Povidone–iodine preparations were introduced in the 1960s with the aim to prevent primary toxic effects, which is founded on their low concentration of free molecular iodine. Their low toxic potential was inferred from the increase in serum iodide with their use, which is less than with iodine tincture or Lugol's solution [12]. Since the carrier polyvinyl pyrrolidinone was used as a blood substitute, toxicity can be deemed as a secondary problem. The good tolerableness becomes apparent in the successful application in healing burned skin, whereas iodine resorption remains in any case a drawback. Hunt et al. [63] found that the amount of absorbed iodine was directly related to the size of the burn. Kuhn et al. [64] also state that on treating burns with a povidone–iodine preparation, plasma iodine (i.e., iodide) sharply increased from 6.4 ± 0.4 to $20.7 \pm 4.7 \mu\text{g } 100 \text{ ml}^{-1}$; however, the authors also state that the thyroid function does not seem to be modified by plasma iodine overload. Glöbel et al. [65] investigated iodine uptake after use of povidone–iodine preparations (Betaisodona) as a mouth antiseptic, vaginal gel, and liquid soap in subjects with normal thyroid function. By measuring serum iodide, T_3 , T_4 , TSH, and urinary iodide excretion (as an index of thyroid function), the authors observed an increase in iodine supply of up to 2 mg daily, but in no case the developing of hyperthyroidism or hypothyroidism. Because the test conditions were drastic (e.g., hands and forearms were washed 10 times for 2½ min with povidone–iodine liquid soap within 5 h), one would tend to think that povidone–iodine preparations are nontoxic at least in healthy adults.

In contrast, application of topical iodinated antiseptics in neonates (in-term and preterm) caused, besides notably increased urinary iodide excretion, significant high levels of TSH, which was interpreted in terms of a transient thyroid dysfunction [66, 67]. In a large-scale study at an obstetric ward it was found that the iodine overload of the mothers, caused by skin disinfection prior to delivery using an iodophor preparation, induces a transient impairment of thyroid function of the infants, especially if breastfed. Because this situation is detrimental to screening for congenital hypothyroidism, iodophor preparations are not recommended in obstetrics [68]. All three author groups recommend exercising caution in the use of iodine-containing antiseptics in neonates and the preferable use of noniodinated substances with similar antibacterial efficacy.

However, in a prospective, controlled study it was found that transient hypothyroidism is not a common sequela of routine skin cleansing with povidone–iodine in premature newborn infants in North America, an iodine-sufficient area [69]. This result differs from the foregoing studies that were performed in Europe, which is generally accepted as a iodine-deficient area.

The irritation potential of povidone–iodine solutions was investigated by comparing subjective and objective assessment techniques with three similar formulations (all containing 10% povidone–iodine and variable amounts of potassium iodate: 0, 0.03, and 0.225%), which were applied for 1–8 h to the skin [70]. The methods used,

subjective assessment of erythema, objective measurement of skin color (erythema meter), and laser Doppler blood-flow measurements, showed consistent results indicating a steady increase in cutaneous irritation, which in one case (the preparation with highest level of potassium iodate) was essentially elevated. However, since these experiments were conducted with the povidone–iodine specimen occluded using aluminum chambers, the results should not be transferred to the normal condition where the povidone–iodine solution dries on the skin forming a protective film with very reduced free iodine.

That povidone–iodine can also evoke fatal consequences if misapplied was shown in a case report on surgical debridement of a hip wound where a patient died 10h following a continuous postoperative wound irrigation with Betadine. Toxic manifestations of systemic iodine absorption appeared to cause the demise [71].

Concerning toxicity of topical preparations, the following generalizations can be made:

1. Because the stratum corneum of intact skin is an effective barrier against electrolytes [60], it is penetrated by iodine in the form of molecular iodine and not of iodide or triiodide.
2. In body cavities (e.g., during treatment of mucous membranes, perineal wash) that are not protected by a stratum corneum, however, the incorporation of iodide and triiodide also becomes important because iodine preparations always contain these species.
3. Depending on the chemical nature of the tissue—dry skin with a lower, or surfaces of body cavities with a higher reducing potential—the penetrating iodine will be reduced more or less fast to iodide.
4. The degree of irritation and the amount of total iodine absorbed by the body mainly depend on:
 - a. The composition of the applied solution with regard to the concentrations of the main iodine species, I_2 , I_3^- , and I^- .
 - b. The time of application
 - c. The treated area.
 - d. The nature of the treated area (horny skin, mucosa).
 - e. The physical condition (intact skin, open wounds).

Long-term applications (irrigation) on open wounds with concentrated formulations (e.g., undiluted povidone–iodine preparations) should be avoided.

5. As long as it is not reduced (i.e. staining is visible), free iodine present in the skin diffuses not only into deeper regions but also back (out of the skin), resulting in a certain period of residual bactericidal activity on the skin surface (see later). The reduced portion, however, remains for some time in the body and gives rise to an increase in the level of serum iodide.
6. The incorporated iodine in the form of iodide and organic bound iodine (which comes to ~75% of the total resorbed iodine) leaves the body by urinary excretion with a biologic half-life of approximately 2 days [65]. This finding also

suggests that the frequency of treatments (e.g., in case of burned skin) be taken into account because it can provoke an unexpected accumulation.

7. If the mode of application of an iodine preparation leads one to expect a measurable increase of serum iodide, the change to another disinfectant is indicated in case of neonates and persons with disturbed thyroid functions.

20.5.2 Ingestion of Iodinated Drinking Water

Although it has limited use in terrestrial fields, elemental iodine is considered to be an appropriate water drinking disinfectant on extended space flights because it does not present other hazards (like chlorine gas or ozone) that are unacceptable in a confined space [72]. In view of the known potential risks associated with elevated intakes of iodine—in particular, congenital goiter—the effects of iodine and iodide on thyroid function in humans were investigated [73]. The experiments failed to confirm the differential effect of I_2 on maintenance of serum T_4 concentrations relative to the effect of I^- that was observed in prior experiments in rats [74]. However, based on the elevations in TSH, the authors have expressed some concern over the potential impacts of chronic consumption of I_2 in drinking water.

20.6 PRACTICAL APPLICATIONS

20.6.1 Human Medicine

The most important application of iodine in human medicine is in the disinfection of skin, which has been in use since the mid-nineteenth century [10]. In addition to prophylaxis (e.g., preoperative preparation of the skin, surgical disinfection of hands, disinfection of the perineum), iodine preparations are also used for therapeutic purposes, for example, the treatment of infected and burned skin. The oldest account in this regard dates back to 1829: “Mémoire sur l’emploi de l’iode dans les maladies scrofuleuses” [2].

The high-level aqueous and alcoholic iodine preparations used up to the 1960s have been replaced, to a great extent, by the iodophors because of fewer unwanted side reactions (see Section 20.3.2.1). Among the investigated iodophors, povidone–iodine is usually considered the compound of choice [12]. However, the initial enthusiasm for this compound was curtailed by the observation of intrinsic bacterial contamination of a 10% povidone–iodine preparation (Pharmadine) by *Pseudomonas cepacia*, leading to an outbreak of pseudobacteremia in a hospital [75]. Another surprising feature was the increased bactericidal activity of dilute povidone–iodine preparations [45]. These events initiated a thorough study of the physico-chemical fundamentals of povidone–iodine [20, 19] and the articulation of the importance of galenics in the microbicidal efficacy of povidone–iodine solutions [30]. Attempts were also made to replace the povidone carrier by other macromolecules that might be still more harmless than povidone, which after all has been used as a blood substitute. In this connection polymers built up of sugar molecules (e.g., polydextrose) are

of great interest. An interesting member of this group is cadexomer iodine, which, when formulated as a topical wound dressing, adsorbs exudate and particulate matter from the surface of granulating wounds and, as the dressing becomes moist, releases iodine. The product thus has the dual effect of cleansing the wound and exerting a bactericidal action [76].

When rigid aseptic precautions are required and no painful irritations are expected, however, iodine tincture is used as the strongest disinfectant based on iodine. A detailed review of the use of iodine in human medicine is given by Knolle [12], and a good historical account and information on aqueous solutions of iodine and tincture is given by Reddish [7].

Iodine has also been used for the disinfection of medical equipment, such as catgut, catheters, knife blades, ampules, plastic items, rubber goods, brushes, multiple-dose vials, and thermometers [13]. It should be mentioned, however, that disinfection with iodine is not appropriate for every sort of material. Many metal surfaces, in particular, are not resistant to oxidation and can be altered. Furthermore, some plastics absorb elemental iodine causing a brownish staining, which fades very slowly if at all.

20.6.2 Veterinary Medicine

Disinfection of cow's udder before and after milking with iodine is a widely adopted application, which started in 1985 when it was found that dipping teats in 0.1, 1, and 2.5% tinctures of iodine markedly reduced the numbers of staphylococci that were recovered from milking machine liners [77]. Today it is performed using iodophoric preparations with 0.25–1.0% available iodine. This treatment is well-tolerated and reduces the incidence of intramammary infections caused by *Streptococcus* and *Staphylococcus* pathogens common around dairies [78, 79]. With regard to the possible contamination of milk with iodine, however, contamination would seem to be less likely with a preparation containing low concentrations of total iodine. An example is the animal drug IodoZyme™, an EBI powder concentrate that produces on dissolution 500 ppm total iodine with 150 ppm I₂ [80]. The manufacturer claims that it is as effective as conventional 0.5% iodine teat dip (based on povidone–iodine), but contains only 1/10th of total iodine compared to the latter.

20.6.3 Disinfection of Water

20.6.3.1 Drinking Water

The first known field use for iodine in water treatment was in World War I by Vergnoux [53], who reported rapid sterilization of water for troops. Since that time several studies have been made [53] showing that iodination is suitable for the disinfection of drinking water, especially in emergency situations. Of considerable importance is the work of Chang and Morris [81], which led to the development of tetraglycine hydroperiodide tablets (Globaline), which have been successfully used to disinfect small or individual water supplies in the U.S. Army. This method of water purification (addition of iodine tablets or calcium hypochlorite to the water, followed by a 25- or 30-min disinfectant contact period, respectively, before drinking) is still

in use in the U.S. Army. The Travelers Medical and Vaccination Center [82] claims that chemical disinfection using iodine ("Potable Aqua" tablets) is more reliable for water purification than chlorine or silver. Since the killing effect of iodine depends on the temperature, they recommend the following standing times: 60, 30, and 15 min at 5, 15, and 30°C (one iodine tablet for 1 l of water).

The use of iodine involves some health risks because the chemicals carrying out the disinfection are not removed in these procedures [83]. On the other hand, it was demonstrated in two prison water systems that iodine in doses up to 1.0 ppm is sufficient for disinfection, does not produce any discernible color, taste, or odor, and has no adverse effect upon general health or thyroid function. Thomas et al. [84] reported a 15-year pilot project in which they observed no instances of ill effect caused by the use of iodine for water disinfection. The authors found that iodination is an effective and economic means of water purification, of particular advantage in rural and underdeveloped countries. More recently, the iodine resins have been successfully used as a basis for purifier units that, as long as they are not exhausted, work very well, bringing about a kill of 4 logs. For emergency and for travelers, "pocket purifiers" have been developed whose performance was officially approved through registration by the U.S. Environmental Protection Agency [85]. A description and discussion of iodine-containing ion-exchange resins for point-of-use water including a new resin type providing a more consistent and more controllable level of iodine was given by Osterhoudt [52]. For the disinfection of the drinking water supplies aboard a spacecraft, iodine was chosen because of its low risk potential (compared to ozone or chlorine). For the Skylab mission it was furnished by a 30 g l⁻¹ stock solution containing KI and I₂ in a 2:1 molar ratio, while for the Space Shuttle program a new device for the controlled release of I₂, termed the Microbial Check Valve (MCV), was introduced, which is a canister containing an iodinated strong base ion-exchange resin packed with polyiodide anions (I₃⁻, I₅⁻, I₇⁻) [72].

20.6.3.2 *Swimming-Pool Water*

Compared with chlorine, the use of iodine has the advantage that it virtually does not react with ammonia or other nitrogenous compounds and therefore produces no compounds that are likely to contribute to swimmers' discomfort in the form of eye irritation or obnoxious odors [86]. The use of iodine in swimming-pool disinfection has the following advantages [87]: (i) approximately one-third saving on chemical cost, (ii) no disagreeable odor or taste, (iii) no irritation of the mucous membranes, (iv) good disinfection of swimming-pool waters, (v) no danger in storage or use, because the material is in crystalline form, (vi) the residual is stable and does not fluctuate quickly, (vii) pH is stable after balance is reached, and (viii) swimmers' comfort is enhanced.

On the other hand, iodine is a notoriously poor algicide, and the control of algal growth requires additional measures. Probably the most serious flaw in the use of iodine is the difficulty in controlling the color of the pool water, mainly in the presence of a large amount of iodide, which generates a yellowish-brown color (produced by I₃⁻ ions). The problem of color control plus the inability of iodine to control algae all but eliminate it from use by the swimming-pool industry [53]. During the last years no important contributions concerning this topic have been made.

20.6.3.3 Wastewater

Only a few contributions deal with the use of iodine in the disinfection of waters that, in contrast to drinking and swimming-pool water, do not come in direct contact with man, for example, wastewater and industrial waters. Because these waters in general are highly charged with dissolved nitrogenous substances (proteins and their hydrolysis products), the use of iodine, which does not react with nitrogen compounds, should confer great advantages because of low iodine consumption.

For applications that range in technical dimensions, however, the question of costs also has to be considered, and because iodine is nearly three times as expensive as chlorine per mole, the advantages and disadvantages of iodine must be weighed carefully. In a study about disinfection with a mixture of I^- and NH_2Cl that generates elemental iodine, Kinman and Layton [54] found that this system offers considerable potential for use in water disinfection for potable waters, industrial waters, and waters that must be discharged to shellfish areas. Investigating alternatives to wastewater disinfection in pilot plant studies, Budde et al. [88] compared the disinfectants chlorine, ozone, and iodine and found that for the same level of fecal coliform destruction, iodine was the most expensive under all conditions studied. Nevertheless, innovations were presented during the past few years maintaining the use of iodine in this field. Besides an electrolytic approach [50], a method using solid iodine as source was published [89]. In both cases the resulting diluted iodine solution is recommended for disinfection of cooling tower waters, sewage, and wastewater.

The suitability of iodine for the food processing industry, particularly as iodinated ice for fish and fish products preservation, is also claimed [89].

20.6.4 Disinfection of Air

Since Lombardo [90] first advocated the use of iodine as an aerial disinfectant, experiments on the disinfection of air have been carried out, mainly during World War II. Plesch [91] recommended the aerial disinfection of air-raid shelters with iodine vapors as a prophylactic measure against influenza. White et al. [92] reported iodine to be effective as an aerial disinfectant at concentrations much below its saturation vapor pressure, and Raymond [93] found a “relatively tolerable” concentration of 0.1 mg ft^{-3} (3.5 mg m^{-3}) to be sufficient for a rapid kill of freshly sprayed salivary organisms. However, iodine vapors pose dangers to the respiratory organs, which has been demonstrated by the fact that the maximum allowed concentration of iodine comes to 1.0 mg M^{-3} (threshold limit value) [94], which is less than one-third of the concentration recommended by Raymond [93]. In spite of this drawback, iodine-based procedures were proposed (mainly in the Far East) with the aim to disinfect air by iodine-containing wall coatings [95], ceramics loaded with iodine [96], and vaporizing solutions containing iodine among other constituents [97, 98].

20.7 RESIDUAL EFFECTS OF IODINE PREPARATIONS

The aforementioned back diffusion of the not-reduced portion of the absorbed iodine, which takes place much slower than the uptake, interestingly, has been recognized relatively late [99]. By means of a photometric method, this iodine flux ($[dim] = \text{mass/area/time}$) has been ascertained on the skin after application of Lugol's solution and povidone-iodine preparations with various concentrations of free iodine. The most important findings are the following: the intensity of the iodine flux depends on the amount of iodine absorbed by the skin, which increases with the concentration of free iodine of the applied solution and the time of application. Applying Lugol's solution (155.6 ppm free iodine) for only 1 min, the flux could be detected for approximately 24 h (range: $50\text{--}0.005 \mu\text{g I}_2 \text{ cm}^{-2} \cdot \text{min}^{-1}$), whereas after application of a povidone-iodine preparation (10 ppm free iodine) for 3–5 min the flux was detectable $\frac{1}{2}$ to 1 h (range: $0.2\text{--}0.005 \text{ mg I}_2 \text{ cm}^{-2} \cdot \text{A min}$). The latter result suggests that even the application of iodophor preparations could give rise to a persistent (residual) microbicidal action. This has been proven by comparing the surviving colony-forming units (CFUs) of *Micrococcus luteus* (applied to the skin by artificial contamination) on normal skin as well as on skin that has been treated for 5 min with a povidone-iodine preparation (10 ppm free iodine) immediately before contamination. A logarithmic reduction rate of 0.4 was found, a result that confirmed the bactericidal action of the iodine diffusing out of the skin. As long as iodine diffuses out of the skin, an active disinfection from the inner regions of the skin takes place, and an effective action on the residential pathogens can be expected, a feature that seems to be unique in the field of skin disinfection.

In this regard, Hartmann [100] found by a special method that the reduction of the total resident flora was significantly higher using povidone-iodine than it was with isopropanol. This is in contrast to the usual findings, mainly in testing preparations for surgical hand scrub, which exhibit in general a better degerming activity of alcohols [101].

20.8 RANGE OF ACTION

Iodine is an excellent and prompt effective microbicide with a broad range of action that includes almost all of the important health-related microorganisms, such as enteric bacteria, enteric viruses, bacterial viruses, and protozoan cysts [102]. Mycobacteria and the spores of bacilli and clostridia can also be killed by iodine [103]. Furthermore, iodine also exhibits a fungicidal and trichomonacidal activity [12]. As is expected, varying amounts of iodine are necessary to achieve complete disinfection of the different classes of organisms. Within the same class, however, the published data on the disinfecting effect of iodine correspond only to a small extent. In particular, the published killing times of spores [103] and viruses [12] are widely disparate. One reason for this might be the nonuniform sensitivity

of microorganisms to iodine, which applies not only to the type of organism but also to the growth conditions.

Pyle and McFeters [104] demonstrated that bacterial isolates (predominantly *Pseudomonas* sp.) from water systems disinfected by iodine showed differences (which did not always have the same sign, however) of up to 4 logs decrease in CFUs after contact with iodine (1 mg l^{-1} , pH 7, 1 min) depending on whether they were grown in brain heart infusion or after cultivation in phosphate buffer. A similar result was attained with *Legionella pneumophila*, which also showed a differing susceptibility to iodine with cultures grown in well water, on rich agar media, or attached to stainless steel (biofilm). Water cultures of legionellae associated with stainless-steel surfaces were 135 times more resistant to iodination than were unattached legionellae, and they were 210,000 times more resistant to iodination than were agar-grown cultures [105]. Both studies indicate that growth conditions can dramatically affect the susceptibility to iodine (and other disinfectants) and must be considered when evaluating the efficacy of a disinfecting agent.

As mentioned by Hoehn [101], comparison of previously published references concerning effectiveness in disinfection processes for different microorganisms are difficult because of the myriad different environmental conditions under which experiments are conducted (e.g., pH value, temperature, concentration and type of iodine preparation, time of exposure to the disinfectant, and amount and type of dissolved organic and inorganic substances). Another problem is the fact that, in general, most of these conditions are not described in detail, and an exact comparison of the germicidal effectiveness of iodine against different organisms, as well as a comparison with the other halogens, is therefore practically impossible. In spite of these difficulties, some authors have tried to summarize the disinfecting properties of iodine and the other halogens by reviewing the literature and analyzing the existing data. The most important conclusions are as follows:

- A standard destruction (i.e., a 99.999% kill in 10 min at 25°C) of enteric bacteria, amoebic cysts, and enteric viruses requires I_2 residuals of 0.2, 3.5, and 14.6 ppm, respectively [33].
- On a weight basis, iodine can inactivate viruses more completely over a wide range of water quality than other halogens [31].
- In the presence of organic and inorganic nitrogenous substances, iodine is the cysticide of choice because it does not produce side reactions that interfere with its disinfecting properties [31].
- Iodine requires the smallest dosage (in mg per liter) compared to chlorine or bromine to “break any water” to provide a free residual [31].
- I_2 is two to 3 times as cysticidal and 6 times as sporocidal as HOI, whereas HOI is at least 40 times as virucidal as I_2 . This behavior is explained on the one hand by the higher diffusibility of molecular iodine through the cell walls of cysts and spores and on the other hand by the higher oxidizing power of HOI [33].

TABLE 20.2 Practical application of iodine as a disinfectant: concentration, exposure time, disinfective result

Scope of application	Concentration	Condition	Exposure time	Disinfective result	References
Drinking water	8 ppm	—	10 min	“Kill of water-borne pathogens”	[109]
	3–4 ppm	25°C	12 min	“Reduces 10 bacterial/ml to less than 10° bacterial/ml”	[81]
Drinking water in emergency	3–4 ppm	3°C	22 min		
	5–6 ppm	20–25°C	10 min	“Excellent disinfectant for water supplies under emergency conditions”	
	5–6 ppm	Near 0°C	20 min	“Water safe for drinking”	[110]
	5 drops I ₂ tincture to a quart of water	Clear water	30 min		
	10 drops I ₂ tincture to a quart of water	Cloudy water	30 min	“Water of virtual potable quality”	[112]
	4.0–8.0 mg/l ⁻¹	Turbid water of low quality	30 min		
Swimming-pool water	0.2 (0.1) ppm	—		“Provides water of satisfactory quality”	[111]
	0.2 ppm			“Maintains the water at a satisfactory bacteriological quality”	[112]
General germicidal action	1:20,000	Absence of organic matter	1 min	“Most bacteria are killed”	[113]
	1:20,000		15 min	“Wet spores are killed”	[113]
Disinfection of skin	1:200,000		15 min	“Will destroy all vegetative forms of bacteria”	[113]
	1% tincture	—	90 s	“Will kill 90% of the bacteria”	[113]
	5% tincture	—	60 s	“Will kill 90% of the bacteria”	[113]
	7% tincture	—	15 s	“Will kill 90% of the bacteria”	[113]
	1% aqueous I ₂ solution	Skin of hands	20 min	“Inactivation of rhinovirus”	[114]
	2% aqueous I ₂ solution	Skin of hands	3 min	“Inactivation of rhinovirus”	[114]

Annotation: Based on actual understanding, HOI has no importance at conditions of disinfection in practice [18].

- For some microorganisms, iodine resistance also has been ascertained (e.g., *Pseudomonas alcaligenes* and *Alcaligenes faecalis*), which can account for the bulk of the microbial flora in iodinated swimming pools [106]. Other studies, however, show that iodine does not induce resistance in isolates of *Pseudomonas*, *Klebsiella*, *Enterobacteria*, *Escherichia coli*, and other species [107, 108].
- Because disinfection is a chemical reaction, the influence of temperature on reaction speed—as a rule of thumb lowering the temperature about 10°C halves the speed—must be considered for microbicidal events in such a way that either the contact time or the concentration of the disinfectant have to be increased if cold water has to be treated. The lack of efficiency at low temperatures was demonstrated by Regunathan and Beauman [84], who showed that some iodine preparations designated to purify canteen water worked well against *Giardia* at 20°C but not at 3°C if used according to the instructions.
- With regard to culture conditions, iodine (1500×) exhibits greater difference in CM×t values (concentration in molarity multiplied by time in minutes to achieve 99% decrease in viability) than chlorine (68×) against water-cultured and agar-grown *Legionellae*. Iodine was 50 times more effective than chlorine when used with agar-grown cultures but was only twice as effective when tested against water-grown *Legionellae* cultures [104].

A survey of concentration, exposure time, and disinfective results in practical applications of iodine is given in Table 20.2.

REFERENCES

- [1] Halliday A. Observations on the use of the different preparations of iodine as a remedy for bronchocele, and in the treatment of scrofula. *Lond Med Repos* 1821;16:199.
- [2] Lugol JGA. *Memoire sur l'emploi de l'iode dans les maladies scrofuleuses*. Paris 1829 (Cited in Horn, 1972).
- [3] Davies J. *Selections in Pathology and Surgery*. Part II. London: Longmans, Orme, Brown, Green & Longmans; 1839.
- [4] Boinet AA. *Iodothérapie*. 2nd ed. Paris: Masson; 1865.
- [5] Vallin E. *Traité des désinfectants et de la désinfection*. Paris: Masson; 1882.
- [6] Koch R. Über desinfektion. In: *Mitteilungen aus dem Kaiserlichen Gesundheitsamte*. 1st ed. Berlin: Struck, ed; 1881. p 234.
- [7] Reddish GF. *Antiseptics, Disinfectants, Fungicides, and Chemical and Physical Sterilization*. 2nd ed. Philadelphia: Lea & Febiger; 1957. p 223–225.
- [8] Sykes G. *Disinfection and Sterilization*. 2nd ed. London: Chapman & Hall; 1972.
- [9] Bolek S, Boleva V, Schwotzer H. Halogene und Halogenverbindungen. In: Horn H, Privora M, Weuffen W, editors. *Handbuch der Desinfektion and Sterilisation*. Volume I, Berlin: Verlag Volk und Gesundheit; 1972. p 132.

- [10] Horn H, Privora M, Weuffen W. In: Weuffen W, editor. *Handbuch der Desinfektion und Sterilisation*. Volume I, Chapter 7: Halogene und Halogenverbindungen Berlin: VEB Verlag Volk und Gesundheit; 1972.
- [11] Horn H, Privora M, Weuffen W. In: Weuffen W, editor. *Handbuch der Desinfektion und Sterilisation*. Volume III, Berlin: VEB Verlag Volk und Gesundheit; 1974.
- [12] Knolle P. Alt und aktuell—Keime und Jod. *Hosp Hyg* 1975;67:389–402.
- [13] Gershenfeld L. Iodine. In: Block SS, editor. *Disinfection, Sterilization and Preservation*. 2nd ed. Philadelphia: Lea & Febiger; 1977.
- [14] Gottardi W. Iodine and iodine compounds. In: Block SS, editor. *Disinfection, Sterilization, and Preservation*. 5th ed. Chapter 8. Philadelphia: Lippincott Williams & Wilkins; 2001. p. 159–183.
- [15] Goebel W. On the disinfecting properties of Lugol's solutions. *Zentralbl Bakt* 1906;42:86–176.
- [16] Clough PN, Starke HC. A review of the aqueous chemistry and partitioning of inorganic iodine under LWR severe accident conditions. *Eur Appl Res Rept-Nucl Sci Technol* 1985;6 (4):631–776.
- [17] Gottardi W. The formation of iodate as a reason for the decrease of efficiency of iodine containing disinfectants. *Zentralbl Bakt Hyg, I Abt Orig B* 1981;172:498–507.
- [18] Gottardi W. Iodine and disinfection: theoretical study on mode of action, efficiency, stability, and analytical aspects in the aqueous system. *Arch Pharm Pharm Med Chem* 1999;332 (5):151–157.
- [19] Gottardi W. Potentiometric evaluation of the equilibrium concentrations of free and complex bound iodine in aqueous solutions of Polyvinylpyrrolidone-iodine (Povidone-iodine). *Fresenius Z Anal Chem* 1983;314:582–585.
- [20] Horn D, Ditter W. Physikalisch-chemische Grundlagen der mikrobiziden Wirkung wässriger POVIDONE-Iod-Lösungen. In: Hierholzer G, Gortz G, editors. *POVIDONE-Iod in der Operativen Medizin*. Berlin: Springer; 1984.
- [21] Gottardi W. Determination of the equilibrium concentrations of the components halogen, halide, hypohalite, and/or hypohalous acids in aqueous solutions. *Ger Offen DE* 1996;4:440,872.
- [22] Gottardi W. Redox-potentiometric/titrimetric analysis of aqueous iodine solutions. *Fresenius J Anal Chem* 1998;362:263–269.
- [23] Bell RP, Gelles E. The halogen cations in aqueous solution. *J Chem Soc* 1951; 73:2734.
- [24] Bhattacharjee B, Varshney A, Bhat SN. Kinetics of transformation of outer charge-transfer complexes to inner complexes. *J Ind Chem Soc* 1983;LX:842–844.
- [25] Gottardi W. The influence of the chemical behavior of iodine on the germicidal action of disinfectant solutions containing iodine. *J Hosp Infect* 1985;6 (Suppl):1–11.
- [26] Yamada H, Kozima K. The molecular complexes between iodine and various oxygen-containing organic compounds. *J Am Chem Soc* 1960;82:1543.
- [27] Schmulbach CD, Drago RS. Molecular addition compounds of iodine III. *J Am Chem Soc* 1960;82:4484.
- [28] Gottardi W, Koller W. The concentration of free iodine in aqueous povidone-iodine containing systems and its variation with temperature. *Monatsch Chem* 1986;117:1011–1020.
- [29] Gottardi W. Redoxpotential and germicidal action of aqueous halogen solutions. *Zentralbl Bakt Hyg I Abt Orig B* 1980;170:422–430.

- [30] Pinter E, Rackur H, Schubert R. Die Bedeutung der Galenik für die mikrobizide Wirksamkeit von Polyvidon-Iod-Lösungen. *Pharm Ind* 1983;46:3–8.
- [31] Krusé WC, Asce M, Hsu Y, Griffith AC, Stringer R. Halogen action on bacteria, viruses and protozoan. Proceedings on National Specialty Conference on Disinfection. Amherst: ASCE; 1970. p. 113–137.
- [32] Hickey J, Panicucci R, Duan Y, Dinehart K, Murphy J, Kessler J, Gottardi W. Control of the amount of free molecular iodine in iodine germicides. *J Pharm Pharm* 1997;49: 1195–1199.
- [33] Chang SL. Modern concept of disinfection. *Proc ASCE, J Sanit Eng Div* 1971;97:689.
- [34] Gottardi W. Aqueous iodine solutions as disinfectants: composition, stability, comparison with chlorine and bromine solutions. *Zentralbl Bakt Hyg, I Abt Ori B* 1978;167:206–215.
- [35] Black AP, Kinman RN, Smith JJ. Iodine for the disinfection of water. *J Am Water Works Assoc* 1968;60:69–83.
- [36] Jander J, Knuth K, Renz W. Studies on nitrogen iodine compounds. VI. Preparation and infrared studies on N-iodomethylamines. *Z Anorg Allg Chem* 1972;392:143–158.
- [37] Gottardi W. Diiodamine: acyl derivatives. *Monatsh Chem* 1974;105:611–620.
- [38] Gottardi W. The reaction of N-bromo-compounds with iodine: a convenient synthesis of N-iodo compounds. *Monatsh Chem* 1975;106:1019–1025.
- [39] Gottardi W. On the usability of N-iodo-compounds as disinfectants. *Zentralbl Bakt Hyg, I Abt Orig B* 1978;167:216–223.
- [40] Apostolov K. The effects of iodine on the biological activities of myxoviruses. *J Hyg* 1980;84:381–388.
- [41] Gottardi W. On the reaction of chlorine, bromine, iodine and some N-chloro and N-bromo compounds with peptone in aqueous solution. *Zentralbl Bakt Hyg, I Abt Orig B* 1976;162:384–388.
- [42] Duan Y, Dinehart K, Hickey J, Panicucci R, Kessler J, Gottardi W. Properties of an enzyme-based low level iodine disinfectant. *J Hosp Infect* 1999;43 (3):219–229.
- [43] Kawakami M, Sakamoto M, Kumazawa T. Mouthwashes containing iodine-maltosyleyclodextrin inclusion compound as a microbicide with high water-solubility. *Japan Patent* 297473. CA; 1986, 109(16), 134972w.
- [44] Schenck HU, Simak P, Haedicke E. Structure of polyvinylpyrrolidinone-iodine (povidone-iodine). *J Pharm Sci* 1979;68:1505–1509.
- [45] Berkelmann RL, Holland BW, Anderson RL. Increased bactericidal activity of dilute preparations of povidone-iodine solutions. *J Clin Microbiol* 1982;15:635.
- [46] Pollack W, Iny O. A physicochemical study of PVP-I solutions leading to the reformulation of 'Betadine' preparation (5% PVP-I). *J Hosp Infect* 1985;6 (Suppl A):25–30.
- [47] Gottardi W, Puritscher M. Degerming experiments with aqueous Povidone-iodine containing disinfecting solutions: influence of the concentration of free iodine on the bactericidal reaction against *Staphylococcus aureus*. *Zentralbl Bakt Hyg B* 1986;182: 372–380.
- [48] Gottardi W, Koller W. The influence of the consumption on the efficacy of Povidone-iodine preparations. *Hyg Med* 1987;12:150–154.
- [49] Gottardi W. Povidone-iodine: bactericidal agent or pharmaceutical base material. Reflections on the term active agent in disinfecting systems containing halogens. *Hyg Med* 1991;16:346–351.

- [50] Gottardi W, Koller W. The concentration of free iodine in aqueous povidone-iodine containing systems and its variation with temperature. *Monatsch Chem* 1986;117: 1011–1020.
- [51] Kril MB, Fitzpatrick TW, Janauer GE. Toward a protocol for testing solid microbial compositions. *Proceedings of the 3rd Conference on Progress in Chemical Disinfection*. Binghamton; 1986.
- [52] Osterhoudt LE. Iodinated resin and its use in water disinfection. *Spec Publ—R Soc Chem* 1997;196(Progress in Ion Exchange):227–234.
- [53] White GC. *Handbook of Chlorination*. New York: Van Nostrand Reinhold; 1972.
- [54] Kinman RN, Layton RF. New method for water disinfection. *J Am Water Works Assoc* 1976;68:298–302.
- [55] Sampson RL, Sampson AH. Electrolytic process and apparatus for the controlled oxidation of inorganic and organic species in aqueous solutions. US Patent 5,419,816; 1995.
- [56] Kubota K, Golden BE, Penugonda B. Root canal filling materials for primary teeth: a review of the literature. *ASDC J Dent Child* 1992;59 (3):225–227.
- [57] O'Connor AF, Freeland AP, Heal DJ, Rossouw DS. Iodoform toxicity following the use of B.I.P.P. *J Laryngol Otol* 1977;91 (10):903–907.
- [58] Gottardi W. Die potentiometrische Bestimmung von Jod und jod-freisetzenden Oxidationsmitteln. *Mikrochim Acta* 1982;I:371–386.
- [59] Gershenfeld L, Witlin B. Iodonium compounds and their antibacterial activity. *Am J Pharm* 1948;12:158–169.
- [60] Goldsmith LA. *Biochemistry and Physiologie of the Skin*. Oxford: Oxford University Press; 1983.
- [61] Yamada H, Kozima K. The molecular complexes between iodine and various oxygen-containing organic compounds. *J Am Chem Soc* 1967;82:1543.
- [62] Kuschinsky G, Lüllmann H. *Kurzes Lehrbuch der Pharmakologie und Toxikologie*. 10th ed. Stuttgart-New York: Georg Thieme; 1984.
- [63] Hunt JL, Sato R, Heck EL, Baxter CR. A critical evaluation of povidone-iodine absorption in thermally injured patients. *J Trauma* 1980;20:127–129.
- [64] Kuhn JM, Wasserman D, Vallee G, Izhembart M, Menard JF, Bricaire H, Luton JP. Thyroid function of burned patients: effect of iodine therapy. *Rev Med Intern* 1987;8 (1):21–26.
- [65] Glöbel B, Glöbel H, Anders C. Resorption von Iod aus PVP-Iod-Preparation nach Anwendung beim Menschen. *Dtsch Med Wochenschr* 1984;109:1401–1404.
- [66] Vilain E, Bompard Y, Laplanche S, De Kermadec S, Aufrant C. Application breve d'antiseptique iode en soins intensifs neonatals: consequences sur la fonction thyroïdienne. *Arch Pediatr* 1994;1 (9):795–800.
- [67] Linder N, Davidovich N, Reichman B, Kuint J, Lubin D, Meyerovitch J, Sela BA, Dolfin Z, Sack J. Topical iodine-containing antiseptics and subclinical hypothyroidism in preterm infants. *J Pediatr* 1997;131 (3):434–439.
- [68] Chanoine JP, Boulvain M, Bourdoux P, Pardou A, Van-Thi HV, Delange F. Increased recall rate at screening for congenital hypothyroidism in breast fed infants born to iodine overloaded mothers. *Arch Dis Child* 1988;63 (10):1207–1210.
- [69] Brown RS, Bloomfield S, Bednarek FJ, Mitchell ML, Braverman LE. Routine skin cleansing with povidone-iodine is not a common cause of transient neonatal hypothyroidism in North America: a prospective controlled study. *Thyroid* 1997;7 (3):395–400.

- [70] Dykes PJ, Marks R. Evaluation of the irritancy potential of povidone-iodine solutions: comparison of subjective and objective assessment techniques. *Clin Exp Dermatol* 1992;17 (4):246–249.
- [71] D'Auria J, Lipson S, Garfield JM. Fatal iodine toxicity following surgical debridement of a hip wound: case report. *J Trauma (US)* 1990;30 (3):353–355.
- [72] Atwater JE, Sauer RL, Schultz JR. Numerical simulation of iodine speciation in relation to water disinfection aboard manned spacecraft I. Equilibria. *J Environ Sci Health* 1996;A31 (8):1965–1979.
- [73] Robison LM, Sylvester PW, Birkenfeld P, Lang JP, Bull RJ. Comparison of the effect of iodine and iodide on thyroid function in humans. *J Toxicol Environ Health Part A* 1998;55:93–106.
- [74] Thrall KD, Sauer RL, Bull RJ. Evidence of thyroxine formation following iodine administration in Sprague-Dawley rats. *J Toxicol Environ Health* 1992;37 (4):535–548.
- [75] Craven DE, Moody B, Connolly BS, Kollisch NR, Stottmeier KD, McCabe WR. Pseudobacteremia caused by povidone-iodine solution contaminated with *Pseudomonas cepacia*. *N Engl J Med* 1981;305:621–623.
- [76] Anna D, Anna F, Robert SK. Antiseptics on wounds: an area of controversy. *Wounds* 2003;159 (5):149–166.
- [77] Newbould FHS, Barnum DA. Effect of dipping cow's teats in a germicide after milking on the number of micrococci on the tea-cup liners. *J Milk Food Technol* 1958;21:348.
- [78] Boddie RL, Nickerson SC. Evaluation of two iodophor teat germicides: activity against *Staphylococcus aureus* and *Streptococcus agalactiae*. *J Dairy Sci* 1846–1850; 1997;80(8).
- [79] Boddie RL, Nickerson SC, Adkinson RW. Efficacies of teat germicides containing 0.5% chlorhexidine and 1% iodine during experimental challenge with *Staphylococcus aureus* and *Streptococcus agalactiae*. *J Dairy Sci* 1997;80 (11):2809–2814.
- [80] West Agro, Inc. Iodozyme. Leaflet 1995;5/44–1042/2. Kansas City: West Agro, Inc. 1995.
- [81] Chang SL, Morris JC. Elemental iodine as a disinfectant for drinking water. *Ind Eng Chem* 1953;45:1009.
- [82] Travelers Medical and Vaccination Center. 1999. Drinking and eating safely. Available at <http://www.tnvc.com.au/info3.html>. Accessed July 10, 2014.
- [83] Schaub AS. Preventive medicine considerations for army individual soldier water purification. Proceedings of the 3rd Conference on Progress in Chemical Disinfection. Binghampton; 1986.
- [84] Thomas WC Jr, Malagodi MH, Oates TW, McCourt JP. Effects of an iodinated water supply. *Trans Am Clin Climatol Assoc (USA)* 1978;90:153–162.
- [85] Regunathan P, Beauman WH. A comparison of point-of-use disinfection methods. Proceedings of the 3rd Conference on Progress in Chemical Disinfection. Binghampton; 1986.
- [86] Black AP. Swimming pool disinfection with iodine. *Water Sewage Works* 1961;108:286.
- [87] Putnam EV. Iodine vs chlorine treatment of swimming pools. *Parks Recreations* 1961;44:162.
- [88] Budde PE, Nehm P, Boyle WC. Alternatives to wastewater disinfection. *J Water Pollut Control Fed (USA)* 1977;49:2144–2156.
- [89] Harvey WA, Mullins TF, MacDonald DJ. Method of disinfecting water and food stuff preservation with iodine species. Patent WO 9855404; 1998.

- [90] Lombardo F. Vapori di soluzione iodoiodurata come profilassi e terapia della influenza. *Riforma Med* 1926;42:1011–1012.
- [91] Plesch J. Methods of air disinfection. *Br Med J* 1941;1:798.
- [92] White LJ, Baker AH, Twort CC. Aerial disinfection. *Nature* 1944;153:141–142.
- [93] Raymond WF. Iodine as an aerial disinfectant. *J Hyg* 1946;44:359–361.
- [94] Lewis RJ, Sweet DV, editors. *Regulations, Recommendations and Assessments Extracted From the Registry of Toxic Effects of Chemical Substances*. Cincinnati: U.S. Department of Health and Human Services, National Institute for Safety and Health; 1986.
- [95] Suzuki K. Antimicrobial wall coatings containing iodinated anion exchange resins. Patent JP 10317529; 1998.
- [96] Okubo T. Device for deodorization of air in closed space using ceramics loaded with disinfectant. Patent JP 09070427; 1997.
- [97] Na F, Fan S. Method and apparatus for air disinfection and deodorization. Patent CN 1091319; 1994.
- [98] Huang D, Zhu X. Indoor air disinfectants and their manufacture. Patent CN 1069414; 1993.
- [99] Gottardi W. The uptake and release of molecular iodine by the skin: chemical and bactericidal evidence of residual effects caused by povidone-iodine preparations. *J Hosp Infect* 1995;29:9–18.
- [100] Hartmann AA. A comparison of povidone-iodine and 60% n-propanol on the resident flora using a new test method. *J Hosp Infect* 1985;6 (Suppl A):73–78.
- [101] Rotter M. Procedures for hand hygiene in German-speaking countries. *Zentralbl Hyg Umweltmed* 1996;199 (2-4):334–349.
- [102] Hoehn RC. Comparative disinfection methods. *J Am Water Works Assoc* 1976;68: 302–308.
- [103] Wallhäusser KH. *Sterilisation, Desinfektion. Konservierung*. Stuttgart: Georg Thieme; 1978.
- [104] Pyle BH, McFeters GA. Iodine sensitivity of bacteria isolated from iodinated water systems. *Can J Microbiol* 1989;35:520–523.
- [105] Cargill KL, Pyle BH, Sauer RL, McFeters GA. Effects of culture conditions and biofilm formation on the iodine susceptibility of *Legionella pneumophila*. *Can J Microbiol* 1992;38 (5):423–429.
- [106] Favero MS, Drake CH. Factors influencing the occurrence of high numbers of iodine-resistant bacteria in iodinated swimming pools. *Appl Microbiol* 1966;14:627–635.
- [107] Hingst V, Klippel KM, Sonntag HG. Investigations concerning the epidemiology of microbicidal resistance to biocides. *Zbl Hyg* 1995;197:232–251.
- [108] Reimer K, Schreier H, Erdos G, König B, König W, Fleischer W. Molecular effects of a microbicidal substance on relevant microorganisms: electron microscopic and biochemical study on povidone-iodine. *Zentralbl Hyg Umweltmed* 1998;200:423–434.
- [109] Committee of Medical Research. *Advances in Military Medicine*. Volume 11, Boston: Little, Brown; 1948. p 527.
- [110] United States Public Health Service. *The Ship's Medicine Chest and First Aid at Sea*. Misc. Publ. No. 9, Washington: U.S. Public Health Service; 1940. p 27.
- [111] Black AP, Lackey JB, Lackey EW. Effectiveness of iodine for the disinfection of swimming pool water. *Am J Publ Health* 1959;49:1060–1068.

- [112] United States Public Health Service. Safe drinking water in emergency. Publ. No. 387, Health Information Series No. 74, Washington, DC: U.S. Public Health Service; 1964.
- [113] Gilman AG, Goodman LS, Gilman A. *The Pharmacological Basis of Therapeutics*. 6th ed. New York: Macmillan; 1980.
- [114] Carter CH, Hendley JO, Mika LA. Rhinovirus inactivation by aqueous iodine in vitro and on skin. *Proc Soc Exp Biol Med* 1980;165:380.

21

SYNTHETIC THYROID HORMONE

STEVEN E. ROKITA

Department of Chemistry, Johns Hopkins University, Baltimore, MD, USA

21.1 INTRODUCTION

Iodide is a micronutrient required for humans and other mammals solely to produce thyroxine (T₄) and triiodothyronine (T₃) (Fig. 21.1). These amino acids are collectively described as thyroid hormones (THs) based on their origins in the thyroid. T₄ distribution through the circulatory system is widespread but requires carrier proteins such as thyroxine-binding globulin, transthyretin, and albumin to overcome its poor solubility [1]. THs are essential during early development and throughout life. Iodide deficiency, insufficient thyroid function, or poor response to THs in young children can lead to physical and mental impairment that in its severest form causes cretinism [2, 3]. THs additionally affect the basal rate of metabolism, heart rate, and other basic processes throughout the body to maintain a healthy homeostasis.

21.2 THYROID HORMONE BIOSYNTHESIS

The relative simplicity of T₄ and T₃ belies their complex and energy intense formation. First, iodide must be selectively concentrated in the thyroid by transport from the circulatory system into follicular cells of the thyroid by means of a sodium iodide symporter (Fig. 21.1) [4]. Iodide is then passed into the thyroid colloid where

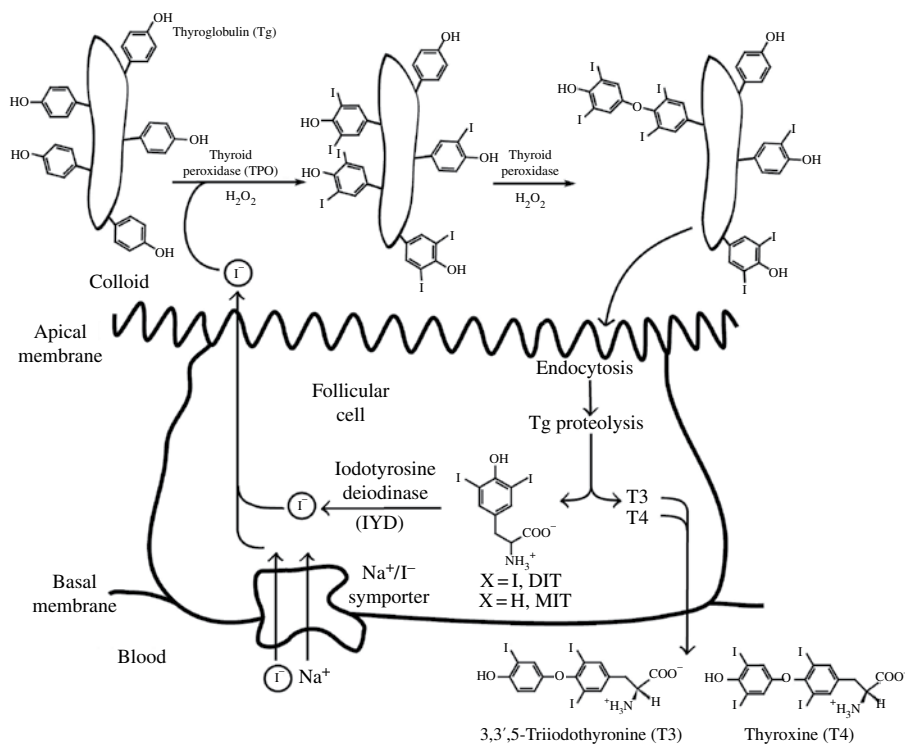


FIGURE 21.1 From iodide uptake to thyroxine release by the thyroid.

it is oxidized by thyroid peroxidase (TPO) and hydrogen peroxide for iodination of tyrosyl residues on the surface of thyroglobulin (Tg), a dimeric protein with identical subunits of high molecular weight (ca. 330,000 Da) [5]. Further oxidation of thyroglobulin by TPO and hydrogen peroxide couples adjacent iodinated tyrosyl residues together to form the ether-containing thyronine core. A dehydroalanine residue was long considered to be the remaining product of this coupling although a more recent study suggests formation of an aminomalonic semialdehyde residue [6]. Before the hormones can be released into circulation, the modified thyroglobulin must reenter follicular cells by endocytosis and undergo extensive proteolysis. Although each thyroglobulin polypeptide contains over 100 tyrosine residues, only about one of these is converted to T4. T3 is formed even less frequently [7]. The majority of iodination produces two biologically inactive products: mono- and diiodotyrosine (MIT and DIT, respectively). If these by-products persist, valuable iodide equivalents can be lost. To prevent this, the enzyme iodotyrosine deiodinase (IYD) acts in the thyroid to recycle the iodide by reductive deiodination of MIT and DIT [8]. The importance of dietary iodide and the consequences of its deficiency is discussed in more detail in the following section (Chapter 22).

21.3 THYROID HORMONE METABOLISM

The tetraiodinated T4 is considered a prohormone and exhibits only about 10% of the cellular activity expressed by its triiodinated analog T3. Thus, TH response can be independently controlled within each peripheral target through selective deiodination. This and equivalent transformations are catalyzed by the enzyme iodothyronine deiodinase. Despite the similarities between the reactions promoted by this deiodinase and IYD, their structures and catalytic strategies differ considerably. IYD is a member of the nitro-FMN reductase structural superfamily and relies on an active site flavin mononucleotide for catalysis [8, 9]. Its physiological substrates are MIT and DIT, but it also supports reductive dehalogenation of the equivalent bromo- and chloro-tyrosine [10]. Fluorotyrosine remains inert but still binds to IYD with relatively high affinity. Its K_d is only one order of magnitude higher than those of the other halogenated tyrosines.

Three isozymes of iodothyronine deiodinase (D1, D2, and D3) are variably expressed in different organs, but all belong to the thioredoxin superfamily, and all contain an active site selenocysteine that is essential for catalysis [11]. The substrate preference and selectivity of deiodination differ among the deiodinases [12, 13]. The isozyme D1 catalyzes deiodination of both rings to enhance TH activity by converting T4 to T3 or to suppress activity by forming the inactive isomer rT3 (Fig. 21.2). This isozyme additionally deiodinates a variety of further metabolites of THs. In contrast, the isozyme D2 is primarily considered an activator and predominantly converts T4 to T3. Isozyme D3 acts as its complement by promoting deiodination of T4 and T3 to the inactive derivatives rT3 and T2 (Fig. 21.2). Peripheral organs control their response to circulating THs by differentially expressing these isozymes. For example, D1 and D2 are both expressed in the thyroid and other tissues, whereas D3 is primarily expressed in the skin, placenta, and central nervous system. The presence of D1 and D2 in the thyroid suggests that the native ratio of T4/T3 secreted from the thyroid is not based solely on their levels derived directly from thyroglobulin oxidation. Serum contains an average ratio of T4/T3 at about 16 for normal individuals, but this ratio decreases to about 13 for

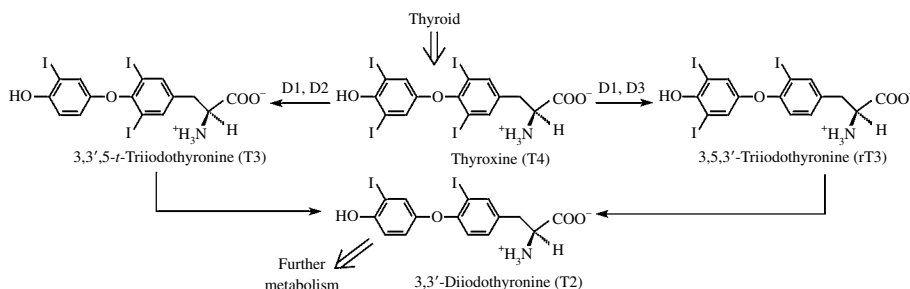


FIGURE 21.2 Deiodination of thyroid hormones.

patients suffering from hypothyroidism and increases to about 20 for patients suffering from hyperthyroidisms [14]. Overall, 80% of the circulating T3 derives from T4 [3].

21.4 THYROID DISEASE

Any defects that affect the proper concentration, balance, or influence of THs have the potential to cause thyroid disease and goiter (swelling of the thyroid). Reduced formation of THs causes hypothyroidism and most commonly results from either insufficient dietary iodide or an autoimmune response to TPO or, on occasion, thyroglobulin (Hashimoto's thyroiditis). At least diet can be amended easily, and many countries supplement table salt with either sodium or potassium iodate to prevent the dietary deficiency. Congenital defects are another source of hypothyroidism. Common symptoms of hypothyroidism include fluid retention, weight gain, fatigue, and lethargy, and treatments typically rely on thyroid replacement therapy. In contrast, hyperthyroidism is the result of excessive THs and causes a variety of complementary symptoms including weight loss, hyperactivity, anxiety, and trembling muscles. If TH production cannot be controlled by antithyroid drugs such as methimazole or propylthiouracil, then the thyroid is often destroyed by ^{131}I radiation or removed surgically. This then similarly requires daily thyroid replacement therapy.

The molecular basis of congenital thyroid disease is quite diverse since numerous processes contribute to thyroid function. Proper levels of T3 cannot be maintained without coordination of the deiodinases D1, D2, and D3. Either mutation or misregulation of these enzymes can result in hypo- or hyperthyroidism. Defects have also been identified upstream of T3 formation [15]. Synthesis of its precursor T4 depends on the precise coordination of a number of proteins including the iodide sodium symporter, thyroglobulin, the peroxidase TPO, the enzymes responsible for generating hydrogen peroxide, and the iodide salvage enzyme IYD (Fig. 21.1). Diminished activity of any one of these has the potential to seriously disrupt thyroid function. Advances in DNA sequencing have provided a variety of details on the genetic basis of thyroid disease and can often pinpoint the exact defect. Recently, mutations affecting IYD activity were identified in a series of patients with decreased ability to release iodide from MIT and DIT [16, 17]. The mutant proteins were additionally expressed *in vitro* and characterized chemically and physically to provide insights into their physiological consequences. Their properties were further rationalized once crystal structures for IYD and its complexes with MIT and DIT were solved [9, 18].

Mutations affecting the protein machinery responsible for TH synthesis and degradation are not the only causes of thyroid disease. Problems can also arise from misregulation of these processes caused by loss of sensitivity to thyroid stimulating hormone. This hormone is produced by the pituitary, which in turn is controlled by thyrotropin-releasing hormone from the hypothalamus [19]. Alternatively, distribution of TH can be compromised by defective carrier proteins within the

circulatory system since over 99% of TH in plasma is protein bound [3]. Inability to respond to physiological concentrations of TH represents yet another cause of thyroid disease. This may occur if cell surface receptors for TH are not maintained at the necessary levels or cannot bind its ligand with sufficient affinity. Disorders can additionally result from defects in the intracellular signal transduction pathway or the nuclear receptors that affect transcription of numerous genes [20]. Finally, all the systems describe earlier are subject to disruption by exposure to certain xenobiotics [21].

21.5 HORMONE REPLACEMENT THERAPY

Patients suffering from hypothyroidism due to low activity of the thyroid typically respond very well to TH supplements administered on a daily basis. TH is also used to suppress thyroid stimulation when treating thyroid cancer [3]. Most commonly, the sodium salt of the natural L-isomer of T4 (levothyroxine) is prescribed and sold by various manufacturers under names such as Synthroid®, Levothroid®, Levo-T®, Unithroid®, and others. Previously, thyroid extracts (mainly porcine) were used for replacement therapy, but the ratio of T4 and T3 was often variable and, depending on the source, not equivalent to that maintained in humans. Benefits of combining synthetic T4 and T3 have been debated in the literature and public forums, but recent studies indicate that such therapy offers no advantages over supplements of T4 alone [22]. T4 is readily bound to its plasma carrier proteins and has a half-life of about 6–8 days although this is shorter in hyperthyroidism and longer in hypothyroidism [3]. T3 has a weaker affinity for these same binding proteins and is much more quickly metabolized. Its half-life is only about 1 day. TH is subject to conjugation of its phenolic oxygen with either sulfate or glucuronate in addition to the deiodination described earlier. Oxidative decarboxylation and deamination *in vivo* also generate tetra- and triiodothyroacetate (Fig. 21.3).

21.6 SYNTHETIC PREPARATION OF T4

A short review on the history and synthesis of T4 was recently published and provides a concise synopsis of the literature [23]. Of course, many preparations and formulations of commercial levothyroxine are likely proprietary and not available to the public. Certainly, formulation is very important for a compound with such poor solubility as T4 in water at neutral pH. T4 was originally synthesized in its racemic

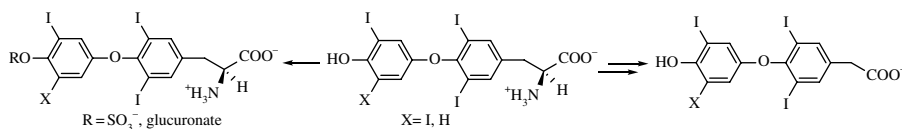


FIGURE 21.3 Metabolism of TH by processes other than deiodination.

form to confirm the structure of the iodine-containing hormone isolated from thyroids [24]. Later, L-tyrosine was used as a starting material to produce the natural L-T4 [25]. This began with nitration of L-tyrosine followed by a coupling with 4-methoxyphenol (Fig. 21.4). Reduction of the nitro groups allowed for iodination of the tyrosine ring through the Sandemeyer reaction. After demethylation of the phenolic oxygen, the two remaining iodines were added by standard electrophilic aromatic substitution. Final deprotection of the α -amino acid yielded the desired L-T4 in about 25%.

Recently, 3,5-diiodo-L-tyrosine has been coupled in yields as high as 94% with a diiodophenol derivative designed to generate L-T4 directly without need of protecting group chemistry (Fig. 21.5) [26]. A copper-catalyzed coupling of 4-methoxyphenylboronic acid to a protected L-tyrosine has also been used to generate the same diiodo derivative used in Figure 21.4 (Fig. 21.6) [27]. Both chemical and optical purity of L-T4 along with shelf-life stability are crucial for its pharmaceutical use.

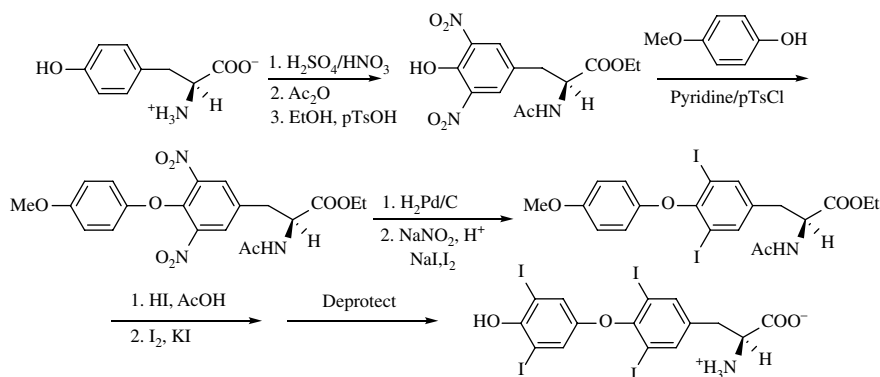


FIGURE 21.4 The first synthetic protocol for generating L-T4.

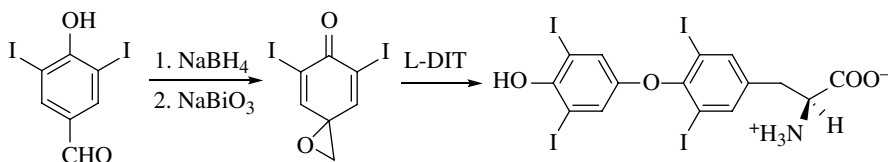


FIGURE 21.5 Synthesis of L-T4 without need of protecting groups.

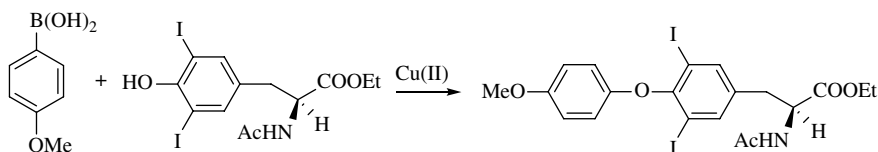


FIGURE 21.6 Formation of the phenyl ether linkage of L-T4 by coupling with phenylboronic acid.

readily to the active L-T3. Still, methyl substitution does not sustain high activity under any circumstances as illustrated by L-Me₃, an analogue of T3. The enhanced activity of DL-MB-T3 may derive from its ability to mimic the greater activity of T3 over that of T4. This derivative may also be resistant to degradation by the deiodinase D3 responsible for deactivation of TH. Another study evaluated 47 analogues of T3 that differed only in their substituent at the 3' position (R, Fig. 21.8) [31]. Biological activity of these analogues ranged over four orders of magnitude and demonstrated the importance of hydrophobicity but not volume at this position. These and related investigations affirm the importance, but not requirement, of the iodo group for biological activity. Speculation on the role of the iodo substituents continues today although one special contribution has been identified from the crystal structure of the complex formed between transthyretin and 3,3'-diiodothyronine [32]. A direct interaction between the side chain hydroxyl of Ser117 and an iodo group is evident and suggests formation of a halogen bond with similar stability as that of a hydrogen bond [33]. Such interactions are not universal for recognition of TH and its derivatives, however. No halogen bonding is apparent in the cocrystals of IYD containing its oxidized flavin cofactor and either MIT or DIT [9, 18].

T3 analogues can additionally be tailored to compensate for specific mutations affecting response to TH. This offers a more elegant although perhaps less practical strategy for overcoming the low affinity of a TH receptor as compared to simply increasing TH concentration through supplementation. This concept was first reduced to practice when a T3 analogue was developed to bind preferentially to a TH nuclear receptor containing a His to Ala mutation. Such receptors were unresponsive to TH but responsive to an analogue illustrated in Fig. 21.9a [34]. In a complementary strategy, other analogues have been designed as selective inhibitors of the nuclear receptor, and the compound illustrated in Figure 21.9b was the first of its type to suppress the effect of T3 in cell culture and whole animals [35]. Synthetic derivatives of TH may therefore serve many strategies well beyond hormone replacement therapy for alleviating thyroid disease.

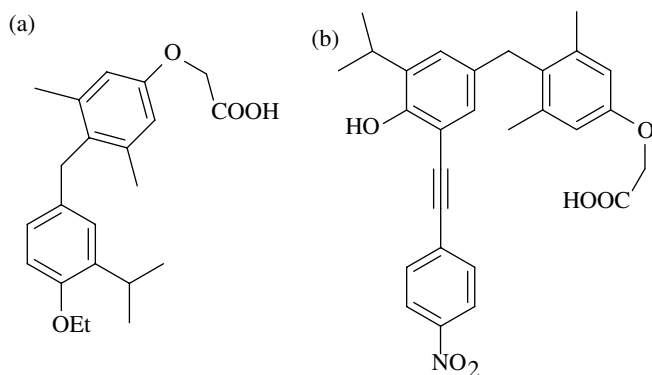


FIGURE 21.9 (a) A T3 analogue with high affinity for a mutant TH nuclear receptor and (b) an alternative analogue for selective suppression of signaling by a nuclear receptor subtype.

REFERENCES

- [1] Hoffenberg R, Ramsden DB. The transport of thyroid hormones. *Clin Sci* 1983;65:337–342.
- [2] Burrows GN, Oppenheimer JH, Volpé R. *Thyroid Function and Disease*. Philadelphia: Saunders; 1989.
- [3] Farwell AP, Braverman LF. Thyroid and antithyroid drugs. In: Hardman JG, Limbird LE, editors. *Goodman & Gilman's The Pharmacological Basis of Therapeutics*. New York: McGraw-Hill; 2001. p 1563–1596.
- [4] Dohán O, de la Vieja A, Paroder V, Riedel C, Artani M, Reed M, Ginter CS, Carrasco N. The sodium/iodide symporter (NIS); characterization, regulation and medical significance. *Endocr Rev* 2003;24:48–77.
- [5] Nunez J, Pommier J. Formation of thyroid hormones. *Vitam Horm* 1982;39:175–229.
- [6] Ma Y-A, Sih CJ, Harms A. Enzymatic mechanism of thyroxine biosynthesis. Identification of the “lost three-carbon fragment”. *J Am Chem Soc* 1999;121:8967–8968.
- [7] DeGroot LJ, Laarse PR, Refetoff S, Stanbury JB. *The Thyroid and Its Diseases*. New York: Wiley & Sons; 1984.
- [8] Rokita SE, Adler JM, McTamney PM, Watson JA. Efficient use and recycling of the micronutrient iodide in mammals. *Biochimie* 2010;92:1227–1235.
- [9] Thomas S, McTamney PM, Adler JM, LaRonde-LeBlanc N, Rokita SE. Crystal structure of iodotyrosine deiodinase, a novel flavoprotein responsible for iodide salvage in thyroid glands. *J Biol Chem* 2009;284:19659–19667.
- [10] McTamney PM, Rokita SE. A mammalian reductive deiodinase has broad power to dehalogenate chlorinated and brominated substrates. *J Am Chem Soc* 2009;131:14212–14213.
- [11] Callebaut I, Curcio-Morelli C, Mornon J-P, Gereben B, Buettner C, Huang S, Castro B, Fonseca TL, Harney JW, Larsen PR, Bianco AC. The iodothyronine selenodeiodinases are thioredoxin-fold family proteins containing a glycoside hydrolase clan GH-A-like structure. *J Biol Chem* 2003;278:36887–36896.
- [12] Bianco AC, Salvatore D, Gereben B, Berry MJ, Larsen PR. Biochemistry, cellular and molecular biology and physiological roles of the iodothyronine selenodeiodinases. *Endocr Rev* 2002;23:38–89.
- [13] St. Germain DL, Galton VA, Hernandez A. Defining the roles of the iodothyronine deiodinases: current concepts and challenges. *Endocrinology* 2009;150:1097–1107.
- [14] Mortoglou A, Candiloros H. The serum triiodothyronine to thyroxine (T3/T4) ratio in various thyroid disorders and after levothyroxine replacement therapy. *Hormone* 2004;3:120–126.
- [15] Lever EG, Medeiros-Neto GA, DeGroot LJ. Inherited disorders of thyroid metabolism. *Endocr Rev* 1983;4:213–239.
- [16] Moreno JC, Klootwijk W, van Toor H, Pinto G, D'Alessandro M, Lèger A, Goudie D, Polak M, Gruters A, Visser TJ. Mutations in the iodotyrosine deiodinase gene and hypothyroidism. *N Engl J Med* 2008;358:1811–1818.
- [17] Afink G, Kulik W, Overmars H, Veenboer T, van Cruchten A, Craen M, Ris-Stalpers C. Molecular characterization of iodotyrosine dehalogenase deficiency in patients with hypothyroidism. *J Clin Endocrinol Metab* 2008;93:4894–4901.
- [18] Buss JM, McTamney PM, Rokita SE. Expression of a soluble form of iodotyrosine deiodinase for active site characterization by engineering the native membrane protein from *Mus musculus*. *Protein Sci* 2011;21:351–361.

- [19] Zoeller RT, Tan SW, Tyl RW. General background on the hypothalamic-pituitary-thyroid (HPT) axis. *Crit Rev Toxicol* 2007;37:11–53.
- [20] Liu Y-Y, Brent GA. Thyroid hormone crosstalk with nuclear receptor signaling in metabolic regulation. *Trends Endocr Met* 2009;21:166–173.
- [21] Tan SW, Zoeller RT. Integrating basic research on thyroid hormone action into screening and testing programs for thyroid disruptors. *Crit Rev Toxicol* 2007;37:5–10.
- [22] Wiersinga WM. Do we need still more trials on T4 and T3 combination therapy in hypothyroidism? *Eur J Endo* 2009;161:955–959.
- [23] Chemburkar SR, Deming KC, Reddy RE. Chemistry of thyroxine: an historical perspective and recent progress on its synthesis. *Tetrahedron* 2010;66:1955–1962.
- [24] Harington CR, Barger G XXIII. Chemistry of thyroxine. III. Constitution and synthesis of thyroxine. *Biochem J* 1927;21:169–183.
- [25] Chalmers JR, Dickson GT, Elks J, Hems BA. The synthesis of thyroxine and related substances. part V. A synthesis of L-thyroxine from L-tyrosine? *J Chem Soc* 1949:3424–3433.
- [26] Salamonczyk GM, Oxa VB, Sih CJ. A concise synthesis of thyroxine (T4) and 3,5,3'-triiodo-L-thyronine (T3). *Tetrahedron Lett* 1997;38:6965–6968.
- [27] Evans DA, Katz JL, West TR. Synthesis of diaryl ethers through the copper-promoted arylation of phenols with arylboronic acids. An expedient synthesis of thyroxine. *Tetrahedron Lett* 1998;39:2937–2940.
- [28] Toussaint B, Schimmel H, Klein CL, Wierowski M, Emonsa HJ. Towards the certification of the purity of calibrant reference materials for thyroid hormones: A chicken and egg dilemma. *J Chromatogr A* 2007;1156:236–248.
- [29] Neu V, Bielow C, Gostomski I, Wintringer R, Braun R, Reinert K, Schneider P, Stuppner H, Huber CG. Rapid and comprehensive impurity profiling of synthetic thyroxine by ultrahigh-performance liquid chromatography–high-resolution mass spectrometry. *Anal Chem* 2013;85:3309–3317.
- [30] Jorgensen EC, Murray WJ. Thyroxine analogs. 22. Thyromimetic activity of halogen-free derivatives of 3,5-dimethyl-L-thyronine. *J Med Chem* 1974;17:434–439.
- [31] Leeson PD, Ellis D, Emmett JC, Shah VP, Showell GA, Underwood AH. Thyroid hormone analogues. Synthesis of 3'-substituted 3,5-diiodo-L-thyronines and quantitative structure-activity studies of in vitro and in vivo thyromimetic activities in rat liver and heart. *J Med Chem* 1988;31:37–54.
- [32] Wojtczak A, Luft J, Cody V. Mechanism of molecular recognition: structural aspects of 3,3-diiodo-L-thyronine binding to Human serum transthyretin. *J Biol Chem* 1992;267:353–357.
- [33] Auffinger P, Hays FA, Westhof E, Ho PS. Halogen bonds in biological molecules. *Proc Natl Acad Sci U S A* 2004;101:16789–16794.
- [34] Hassan AQ, Koh JT. A functionally orthogonal ligand-receptor pair created by targeting the allosteric mechanism of the thyroid hormone receptor. *J Am Chem Soc* 2006;128:8868–8874.
- [35] Nguyen N-H, Apriletti JW, Baxter JD, Scanlan TS. Hammett analysis of selective thyroid hormone receptor modulators reveals structural and electronic requirements for hormone antagonists. *J Am Chem Soc* 2005;127:4599–4608.

IODINE DEFICIENCY DISORDERS AND THEIR CORRECTION USING IODIZED SALT AND/OR IODINE SUPPLEMENTS

MICHAEL B. ZIMMERMANN

*Laboratory for Human Nutrition, Department of Health Science and Technology,
Swiss Federal Institute of Technology (ETH) Zürich, Zurich, Switzerland*

ECOLOGY AND DIETARY SOURCES, ABSORPTION, METABOLISM AND EXCRETION

Iodine (as iodide) is widely but unevenly distributed in the earth's environment. In many regions, leaching from glaciation, flooding, and erosion have depleted surface soils of iodide, and most iodide is found in the oceans. The concentration of iodide in sea water is $\approx 50 \mu\text{g l}^{-1}$. Iodide ions in seawater are oxidized to elemental iodine, which volatilizes into the atmosphere and is returned to the soil by rain, completing the cycle [1]. However, iodine cycling in many regions is slow and incomplete, leaving soils and drinking water iodine depleted. Crops grown in these soils are low in iodine, and humans and animals consuming food grown in these soils become iodine deficient. Iodine-deficient soils are common in mountainous areas and areas of frequent flooding. Iodine deficiency in populations residing in these areas persist until iodine enters the food chain through addition of iodine to foods (e.g., iodization of salt) or dietary diversification introduces foods produced outside the iodine-deficient area. The native iodine content of most foods and beverages is low. In

general, commonly consumed foods provide 3–80 µg per serving [2, 3]. Foods of marine origin have higher iodine content because marine plants and animals concentrate iodine from seawater. Iodine in organic form occurs in high amounts in certain seaweeds. Major dietary sources of iodine are iodized salt, bread (made with iodized salt), marine fish, and milk and milk products [2, 3]. Iodophors used for cleaning milk cans and teats can increase the native iodine content of dairy products. Iodine content in foods is also influenced by iodine-containing compounds used in irrigation, fertilizers, and livestock feed. Iodine is ingested in several chemical forms. Iodide is rapidly and nearly completely absorbed in the stomach and duodenum. Iodate, widely used in salt iodization, is reduced in the gut and absorbed as iodide. In healthy adults, the absorption of iodide is greater than 90% [4]. Iodine deficiency is the main cause of endemic goiter (see later), but other dietary substances that interfere with thyroid metabolism can aggravate the effect, and they are termed goitrogens [5]. They are found in cassava, millet, sweet potato, beans, and crucifera vegetables (e.g., cabbage). Most of these substances do not have a major clinical effect unless there is coexisting iodine deficiency. Deficiencies of selenium, iron, and vitamin A can also exacerbate the effects of iodine deficiency [6]. The body of a healthy adult contains 15–20 mg of iodine, of which 70–80% is in the thyroid. In chronic iodine deficiency, the iodine content of the thyroid may fall to less than 20 µg. In iodine-sufficient areas, the adult thyroid traps 50–60 µg of iodine per day to balance losses and maintain thyroid hormone synthesis. A sodium iodide symporter (NIS) in the basolateral membrane transfers iodide into the thyroid at a concentration gradient 20–50 times that of plasma [7]. Iodine comprises 65 and 59% of the weights of T₄ and T₃, respectively. In target tissues, such as liver, kidney, heart, muscle, pituitary, and the developing brain, T₄ is deiodinated to T₃. T₃ is the main physiologically active form of thyroid hormone. The thyroid hormone regulates a variety of physiologic processes, including reproductive function, growth, and development. More than 90% of ingested iodine is ultimately excreted in the urine, with only small amounts appearing in the feces.

22.1 EFFECTS OF DEFICIENCY

Iodine deficiency has multiple adverse effects on growth and development in animals and humans. These are collectively termed iodine deficiency disorders (IDD) (Table 22.1) and are one of the most important and common human diseases [8]. They result from inadequate thyroid hormone production due to lack of sufficient iodine. Thyroid enlargement (goiter) is the classic sign of iodine deficiency (Figure 22.1). It is a physiologic adaptation to chronic iodine deficiency. As iodine intake falls, secretion of TSH increases in an effort to maximize uptake of available iodine, and TSH stimulates thyroid hypertrophy and hyperplasia. Initially, goiters are characterized by diffuse, homogeneous enlargement, but over time, thyroid follicles may fuse and become encapsulated, a condition termed nodular goiter. Large goiters may be cosmetically unattractive, can obstruct the trachea and esophagus, and may damage the recurrent laryngeal nerves and cause hoarseness. Although goiter is the

most visible effect of iodine deficiency, the most serious adverse effect is damage to reproduction. Severe iodine deficiency during pregnancy is associated with a greater incidence of stillbirths, abortions, and congenital abnormalities. Iodine prophylaxis with iodized oil in pregnant women in areas of severe deficiency reduces fetal and perinatal mortality [9]. The fetal brain is particularly vulnerable to iodine deficiency. Normal levels of thyroid hormones are required for neuronal migration and myelination of the central nervous system [10]. The most severe form of neurological damage from fetal hypothyroidism is termed cretinism (Figure 22.2). It is characterized by gross mental retardation along with varying degrees of short stature, deaf mutism, and spasticity [11]. Two distinct types have been described. The more common, neurologic cretinism has specific neurologic deficits that include spastic quadriplegia with sparing of the distal extremities. The myxedematous form is seen most frequently in Central Africa and has the predominant finding of profound hypothyroidism, with thyroid atrophy and fibrosis. Up to 10% of populations with severe iodine deficiency may be cretinous. Although new cases of cretinism are now rare, iodine deficiency still affects many countries (see later) and can impair cognitive development. A meta-analysis of 18 studies concluded that moderate to severe iodine deficiency reduces mean IQ scores by 13.5 points [12]. Iodine deficiency is thus considered one of the most common causes of preventable mental retardation worldwide. Even in areas of mild to moderate iodine deficiency, cognitive impairment in school-age children is at least partially reversible by administration of iodine [13, 14]. Overall, iodine deficiency produces subtle but widespread adverse effects in a population, including decreased educability, apathy, and reduced work productivity, resulting in impaired social and economic development.

TABLE 22.1 Iodine deficiency disorders, by age group

Age groups	Health consequences of iodine deficiency
All ages	Goiter Increased susceptibility of the thyroid gland to nuclear radiation
Fetus	Abortion Stillbirth Congenital anomalies Perinatal mortality
Neonate	Infant mortality Endemic cretinism
Child and adolescent	Impaired mental function Delayed physical development
Adults	Impaired mental function Reduced work productivity Toxic nodular goiter, iodine-induced hyperthyroidism Hypothyroidism in moderate to severe iodine deficiency



FIGURE 22.1 Large nodular goiter in a 14-year-old boy in an area of severe iodine deficiency in northern Morocco.



FIGURE 22.2 Neurological cretinism. This photograph of a 9-year-old girl from Western China demonstrates the three characteristic features: severe mental deficiency together with squint, deaf mutism, and motor spasticity of the arms and legs.

22.2 REQUIREMENTS AND PREVALENCE OF IODINE DEFICIENCY WORLDWIDE

The U.S. Food and Nutrition Board of the National Academy of Sciences has set an Adequate Intake (AI) for iodine in infancy and a Recommended Dietary Allowance (RDA) for children, adults, and pregnant and lactating women [4] (Table 22.2). The World Health Organization (WHO) has established recommended nutrient intakes for iodine [8] (Table 22.2).

Several methods are available for assessment of iodine nutrition [11]. The most commonly used are measurement of thyroid size and concentration of UI [8]. Additional indicators include newborn TSH, and blood concentrations of thyroglobulin, thyroxine (T4), or triiodothyronine (T3). UI is a sensitive indicator of recent iodine intake (days) and serum thyroglobulin shows an intermediate response (weeks to months), whereas changes in the goiter rate reflect long-term iodine nutrition (months to years).

Until 1990, only a few countries, including Switzerland, some of the Scandinavian countries, Australia, the United States, and Canada, were completely iodine sufficient. Since then, globally, the number of households using iodized salt has risen from less than 20% to greater than 70%, dramatically reducing iodine deficiency [8]. This effort has been achieved by a coalition of international organizations, including the WHO, the International Council for the Control of Iodine Deficiency Disorders (ICCIDD), the Global Alliance for Improved Nutrition (GAIN), the Micronutrient Initiative, and the United Nations Children’s Fund (UNICEF), working closely with national IDD control committees and the salt industry; this informal partnership was established after the World Summit for Children in 1990.

The two most commonly used approaches to assessing iodine nutrition on the population level are estimation of the household penetration of adequately iodized

TABLE 22.2 Recommendations for iodine intake (µg day⁻¹) by age or population group

Age or population group	U.S. Institute of Medicine [4]		Age or population group	World Health Organization [8]
	EAR	AI or RDA		RNI
Infants 0–12 months	–	110–130	Children 0–5 years	90
Children 1–8 years	65	90	Children 6–12 years	120
Children 9–13 years	73	120		
Adults ≥14 years	95	150	Adults >12 years	150
Pregnancy	160	220	Pregnancy	250
Lactation	200	290	Lactation	250

AI, Adequate Intake; EAR, Estimated Average Requirement; RDA, Recommended Daily Allowance; RNI, Recommended Nutrient Intake.

salt (HHIS) and measurement of urinary iodine concentrations (UICs) [8]. UIC surveys are usually done in school-age children, because they are a convenient population, easy to reach through school-based surveys and usually representative of the general population. Therefore, the WHO recommends the use of UICs from 6- to 12-year-old children in nationally representative surveys, expressed as the median in $\mu\text{g l}^{-1}$, to classify a population's iodine status [8] (Table 22.3). More countries are beginning to carry out studies in high-risk population groups, that is, women of reproductive age, pregnant women, and younger children; however, data is limited and the majority of countries still conduct routine iodine monitoring in children. Nationally representative UIC surveys are available for 117 countries, and for 33 countries, subnational surveys are available. There are no UIC data available for 43 countries, but the majority of these have small populations. Available UIC data now cover 97.4% of the world's population of school aged children (SAC) (6 to 12 year-olds). Figure 22.3 shows countries classified by iodine nutrition according to degree of public health importance based on the median UIC. Iodine intake is inadequate in 32 countries, adequate in 71, more than adequate in 36, and excessive in 11. Of the 32 countries with iodine deficiency, 9 are classified as moderately deficient, 23 as mildly deficient, and none as severely deficient. Based on the current estimates, the iodine intake of 30.0%, or 246.2 million of SAC worldwide, is insufficient (Table 22.4). Over one-half of the children with low intakes are in two regions: 78 million children in Southeast Asia and 58 million children in Africa. The smallest proportions with low intakes are in the Americas (13.7%) and the Western Pacific (19.8%), while the greatest proportions of children with inadequate iodine intake are in European (43.9%) and the African (39.5%) regions. Inferring from the proportion of SAC to the general population, 1.92 billion people globally have inadequate iodine intakes. Data on household coverage with iodized salt is available for 128 out of 196 UNICEF member states, most of which are low-income countries. Out of 128 countries with data, 37 countries have salt iodization coverage that meets the international goal of at least 90% of households consuming adequately iodized salt. Fifty-two countries have coverage rates of between 50 and 89%, and 39 countries have coverage rates of less than 50%. The world map in Figure 22.4 shows countries classified by their household coverage rates. Overall, approximately 70% of households worldwide have access to iodized salt. Those with the greatest access are living in the WHO regions of the Western Pacific and the Americas, and those with the least access are residing in the Eastern Mediterranean region.

22.3 PROPHYLAXIS AND TREATMENT

There are two methods commonly used to correct iodine deficiency in a population: iodized oil and iodized salt. In nearly all regions affected by iodine deficiency, the most effective way to control iodine deficiency is through salt iodization [11]. All salt for human consumption, including salt used in the food industry, should be continuously iodized. In Switzerland, previously affected by endemic goiter and cretinism, a monitored national program, in place for over half a century, has effectively eliminated

TABLE 22.3 Epidemiological criteria from the World Health Organization for assessment of iodine nutrition in a population based on median or range of urinary iodine concentrations [8]

	Iodine intake	Iodine nutrition
School-aged children		
<20 µg l ⁻¹	Insufficient	Severe iodine deficiency
20–49 µg l ⁻¹	Insufficient	Moderate iodine deficiency
50–99 µg l ⁻¹	Insufficient	Mild iodine deficiency
100–199 µg l ⁻¹	Adequate	Optimum
200–299 µg l ⁻¹	More than adequate	Risk of iodine-induced hyperthyroidism in susceptible groups
>300 µg l ⁻¹	Excessive	Risk of adverse health consequences (iodine-induced hyperthyroidism, autoimmune thyroid disease)
Pregnant women		
<150 µg l ⁻¹	Insufficient	
150–249 µg l ⁻¹	Adequate	
250–499 µg l ⁻¹	More than adequate	
≥500 µg l ^a	Excessive	
Lactating women^b		
<100 µg l ⁻¹	Insufficient	
≥100 µg l ⁻¹	Adequate	
Children <2 years of age		
<100 µg l ⁻¹	Insufficient	
≥100 µg l ⁻¹	Adequate	

^aThe term excessive means in excess of the amount needed to prevent and control iodine deficiency.

^bIn lactating women, the numbers for median urinary iodine are lower than the iodine requirements, because of the iodine excreted in breast milk.

iodine deficiency. Iodine can be added to salt in the form of potassium iodide (KI) or potassium iodate (KIO₃). Because KIO₃ has higher stability in the presence of salt impurities, humidity, and porous packaging, it is the recommended form [8]. Iodine is usually added at a level of 20–40 mg iodine kg⁻¹ salt, depending on the local salt intake. But in industrialized countries, because about 90% of salt consumption is from purchased processed foods, if only household salt is iodized it will not supply adequate iodine. Thus, it is critical that the food industry use iodized salt. The current push to reduce salt consumption to prevent chronic diseases and the policy of salt iodization to eliminate iodine deficiency do not conflict: iodization methods can fortify salt to provide recommended iodine intakes even if per capita salt intakes are reduced to less than 5 g day⁻¹. Worldwide, sustainability of iodized salt programs has become a major focus. These programs are fragile and require a long-term commitment from national governments, donors, consumers, and the salt industry. In some regions, iodization of salt may not be practical for control of iodine deficiency, at least in the short term. This may occur in remote areas where communications are poor or where there are numerous

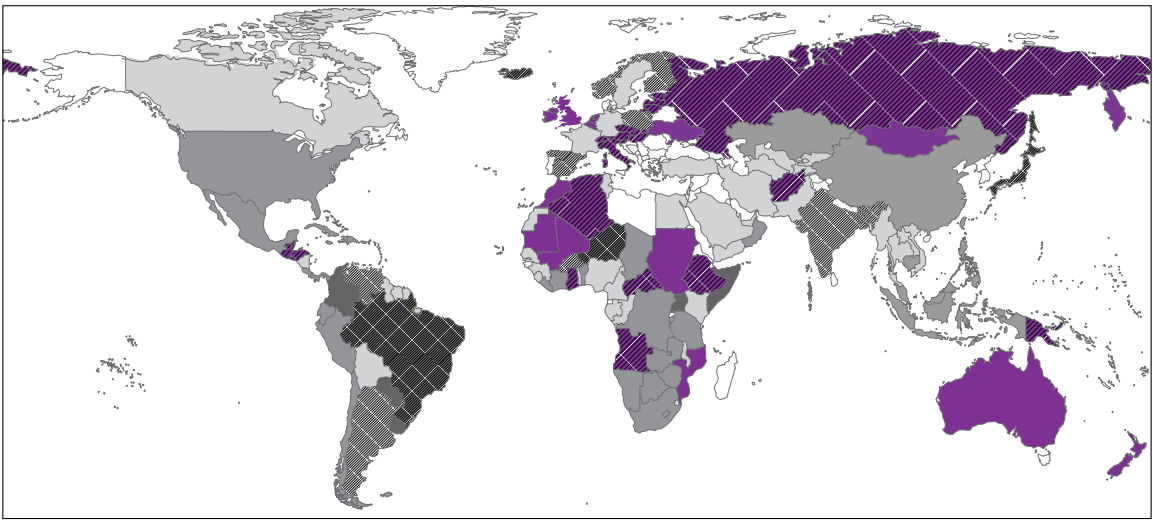


FIGURE 22.3 By country, national iodine status based on the median urinary iodine concentration (data from <http://www.iccid.org/>).

TABLE 22.4 Number of countries, proportion of population, and number of individuals with insufficient iodine intake in school-age children and in the general population, by who region, 2012

WHO region ^a	Insufficient iodine intake (urinary iodine concentration <100 µg l ⁻¹)				
	Children 6 to 12-year-olds			General population	
	Countries (<i>n</i>)	Proportion (%)	Total <i>n</i> (millions)	Proportion (%)	Total <i>n</i> (millions)
Africa	10	39.5	58.1	40.1	322.2
Americas	2	13.7	14.6	13.7	125.7
Eastern Mediterranean	4	38.6	30.7	37.4	199.2
Europe	11	43.9	30.5	44.2	393.1
South-East Asia	0	31.9	78.4	31.7	565.3
Western Pacific	5	19.8	33.9	17.9	319.4
Global total	32	29.8	246.2	28.7	1924.9

^aBased on the 193 WHO member states and United Nations population estimates in the year 2010.

very small-scale salt producers. In these areas, other options for correction of iodine deficiency should be considered, such as iodized oil [11]. Iodized oil is a long-lasting, “depot” form of iodine supplementation, prepared by esterification of the unsaturated fatty acids in seed or vegetable oils, and addition of iodine to the double bonds. It can be given orally or by intramuscular injection. The intramuscular route has a longer duration of action (up to 2 years), but oral administration is more common because it is simpler. Iodized oil is recommended for populations with moderate to severe iodine deficiency that do not have access to iodized salt, and may be targeted to women of childbearing age, pregnant women, and children. The recommended dose is 400mg iodine year⁻¹ for women and 200mg iodine year⁻¹ for children 7–24 months of age [8]. Iodine can also be given as KI or KIO₃ as drops or tablets, and iodine supplements (≈150µg day⁻¹) are often recommended for pregnant and lactating women residing in areas of mild to moderate iodine deficiency [9].

SUMMARY

Iodine is an essential component of hormones produced by the thyroid gland. Thyroid hormones, and therefore iodine, are essential for mammalian life. Optimal dietary iodine intake for healthy adults is 150–250µg day⁻¹. In regions where iodine in soils and drinking water is low, humans and animals may become iodine deficient. Iodine deficiency has multiple adverse effects in humans due to inadequate thyroid hormone production that are termed the iodine deficiency disorders (IDD). Iodine deficiency during pregnancy and infancy may impair growth and neurodevelopment of the offspring and increase infant mortality. Deficiency during childhood reduces somatic growth and cognitive and motor function. Assessment methods include urinary iodine

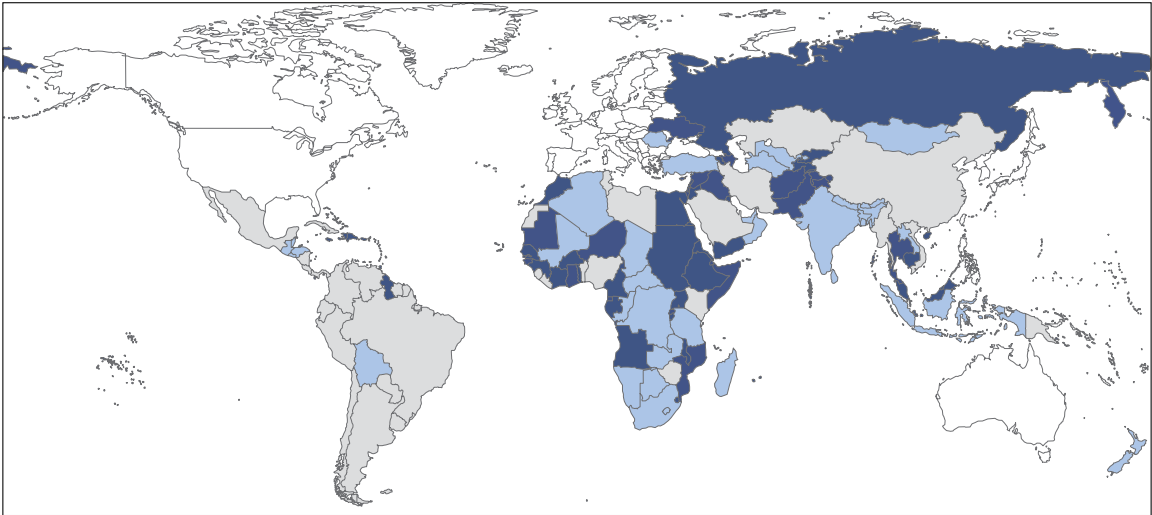


FIGURE 22.4 Coverage of households with adequately iodized salt (data from <http://www.iccid.org/>).

concentration (UIC), goiter, newborn thyrotropin (TSH), and blood thyroglobulin. In most countries, the best strategy to control iodine deficiency in populations is iodization of salt, one of the most cost-effective ways to contribute to economic and social development.

REFERENCES

- [1] Goldschmidt VM. *Geochemistry*. Oxford: Clarendon Press; 1954. xi. p. 11–27.
- [2] Pearce EN, Pino S, He X, Bazrafshan HR, Lee SL, Braverman LE. Sources of dietary iodine: bread, cows' milk, and infant formula in the Boston area. *Clin Endocrinol Metab* 2004;89 (7):3421–3424.
- [3] Haldimann M, Alt A, Blanc A, Blondeau K. Iodine content of food groups. *J Food Compos Anal* 2005;18 (6):461–471.
- [4] Institute of Medicine AoS. *Dietary Reference Intakes for Vitamin A, Vitamin K, Arsenic, Boron, Chromium, Copper, Iodine, Iron, Manganese, Molybdenum, Nickel, Silicon, Vanadium and Zinc*. Washington, DC: National Academy Press; 2001. p 258–289.
- [5] Gaitan E. Goitrogens in food and water. *Annu Rev Nutr* 1990;10:21–39.
- [6] Zimmermann MB, Kohrle J. The impact of iron and selenium deficiencies on iodine and thyroid metabolism: biochemistry and relevance to public health. *Thyroid* 2002;12 (10):867–878.
- [7] Eskandari S, Loo DD, Dai G, Levy O, Wright EM, Carrasco N. Thyroid Na⁺/I⁻ symporter. Mechanism, stoichiometry, and specificity. *J Biol Chem* 1997;272 (43):27230–27238.
- [8] World Health Organization, UNCSF, International Council for Control of Iodine Deficiency Disorders. *Assessment of Iodine Deficiency Disorders and Monitoring their Elimination: A Guide for Programme Managers*. 3rd ed. Geneva: World Health Organization; 2007.
- [9] Zimmermann MB. Iodine deficiency in pregnancy and the effects of maternal iodine supplementation on the offspring: a review. *Am J Clin Nutr* 2009;89 (2):668S–672S.
- [10] Auso E, Lavado-Autric R, Cuevas E, Del Rey FE, Morreale De Escobar G, Berbel P. Iodine deficiency in pregnancy and the effects of maternal iodine supplementation on the offspring: a review. *Endocrinology* 2004;145 (9):4037–4047.
- [11] Zimmermann MB, Jooste PL, Pandav CS. Iodine-deficiency disorders. *Lancet* 2008;372 (9645):1251–1262.
- [12] Bleichrodt N, Shrestha RM, West CE, Hautvast JG, van de Vijver FJ, Born MP. The benefits of adequate iodine intake. *Nutr Rev* 1996;54 (4 Pt 2):S72–S78.
- [13] Zimmermann MB, Connolly K, Bozo M, Bridson J, Rohner F, Grimci L. Iodine supplementation improves cognition in iodine-deficient schoolchildren in Albania: a randomized, controlled, double-blind study. *Am J Clin Nutr* 2006;83 (1):108–114.
- [14] Gordon RC, Rose MC, Skeaff SA, Gray AR, Morgan KM, Ruffman T. Iodine supplementation improves cognition in mildly iodine-deficient children. *Am J Clin Nutr* 2009;90 (5):1264–1271.

23

PHARMACEUTICALS: THERAPEUTIC AGENTS

TATSUO KAIHO

Nihon Tennen Gas Co., Ltd., Chiba, Japan

23.1 INTRODUCTION

Halogens have played an important role in the development of pharmaceuticals for several decades. The effectiveness of many complex molecules is significantly enhanced by the presence of a halogen atom. A significant number of drugs and drug candidates in clinical development have halogen substituents. Insertion of halogen atoms on lead compounds was predominantly performed to exploit their steric effects, through the ability of these bulk atoms to occupy the full binding site of molecular targets. According to the analysis by M. Z. Hernandez et al. [1], the majority of halogenated drugs contain fluorine, followed by chlorine, while those with bromine are rare (Fig. 23.1). Only a few iodine-containing drugs are known such as the thyroid hormone thyroxine (see Chapter 22), an anti-herpesvirus, anti-viral drug, idoxuridine (IDU), and a class III antiarrhythmic agent, amiodarone (Fig. 23.2). Since C–I bonds are highly polarizable, the iodinated compounds are relatively unstable.

On the other hand, iodinated contrast media for X-rays (see Chapter 19) categorized as diagnostic drugs are very stable compared to the iodinated therapeutic agents.

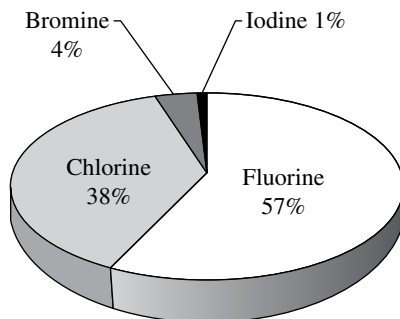


FIGURE 23.1 Halogenated drugs.

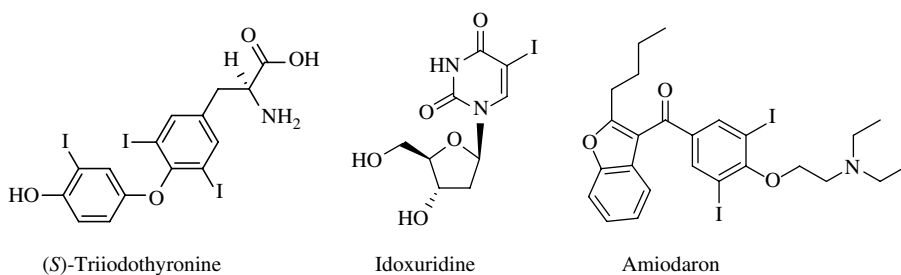
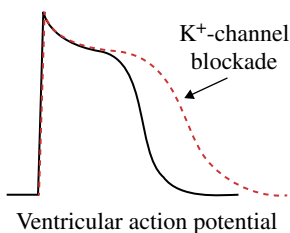
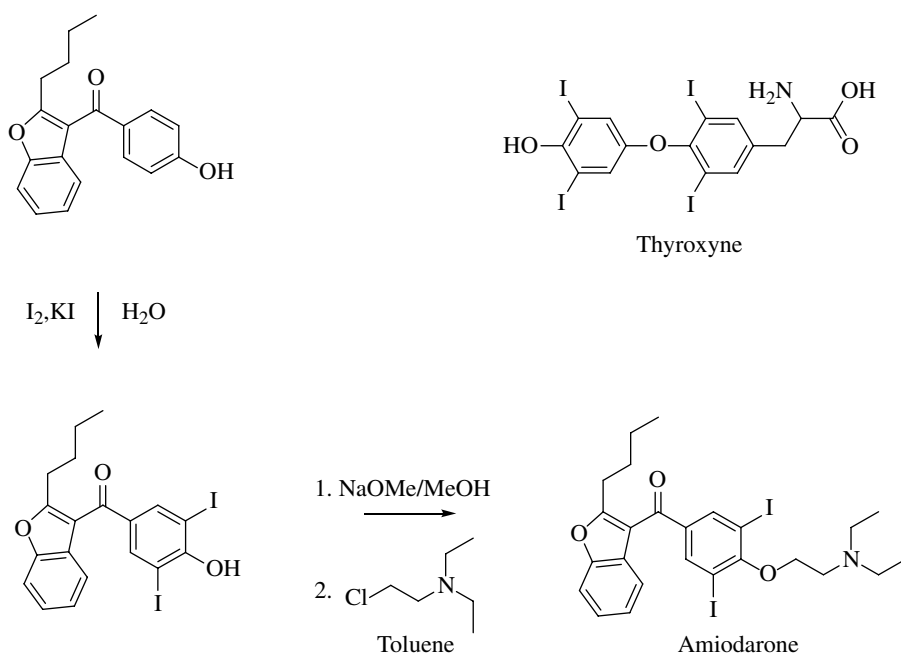


FIGURE 23.2 Iodine containing drugs.

23.2 ANTIARRHYTHMIC AGENT: AMIODARONE

Amiodarone was synthesized in 1961 by Tondeur and Binon in the Labaz Laboratories in Belgium [2]. Structural features of the drug include its high iodine content and its resemblance to thyroxine (T4). It was originally introduced in 1962 in the clinic for treatment of angina pectoris, but later the drug was found to be very efficacious in the treatment of cardiac arrhythmias ranging from paroxysmal atrial fibrillation to life-threatening ventricular tachyarrhythmias [3]. Amiodarone is categorized as a class III antiarrhythmic agent, and prolongs phase III (Fig. 23.3) of the cardiac action potential, the repolarization phase in which there is normally decreased calcium permeability and increased potassium permeability [4]. However, the use of amiodarone is associated with several side effects, including photosensitivity, corneal microdeposits, pulmonary toxicity, hepatotoxicity, peripheral neuropathy, hyperthyroidism, and hypothyroidism. Amiodarone is a benzofuran derivative containing two atoms of iodine per molecule (Fig. 23.4). Hence, a normal daily maintenance dose of amiodarone (200–400 mg) generates about 6–12 mg of iodine per day. This results in an iodine load that far exceeds the World Health Organization's recommended optimal iodine intake of 0.15–0.3 mg/day. In patients treated with amiodarone, urinary and plasma levels of inorganic iodide are found to increase up to 40-fold, whereas thyroidal iodide uptake and clearance decrease significantly [5, 6]. Therefore amiodarone is only used in life-threatening arrhythmia due to its fatal side effects and severe allergic reactions. Patients who are allergic to iodine or amiodarone should not use this drug.

Delayed repolarization by amiodarone

**FIGURE 23.3** Class III antiarrhythmic agent prolongs phase III of the cardiac action potential.**FIGURE 23.4** Synthesis of amiodarone.

23.3 EYE DROPS: IDOXURIDINE

IDU is an anti-herpesvirus antiviral agent. It was synthesized by William Prusoff in 1959 [7]. IDU is a structural analogue of thymidine, one of the four building blocks of DNA. It is a thymidine analogue, synthesized through iodination in the 5 position of deoxyuridine, and similar enough to be incorporated into viral DNA during replication. However, the iodine atom blocks base pairing. Its similarity to thymidine also facilitates its phosphorylation by the herpesvirus-induced enzyme, thymidine kinase. The resulting 5'-monophosphate is further enzymatically phosphorylated, yielding the triphosphate that is subsequently incorporated into herpes DNA as well as cellular DNA of infected cell leading to miscoding and the synthesis of

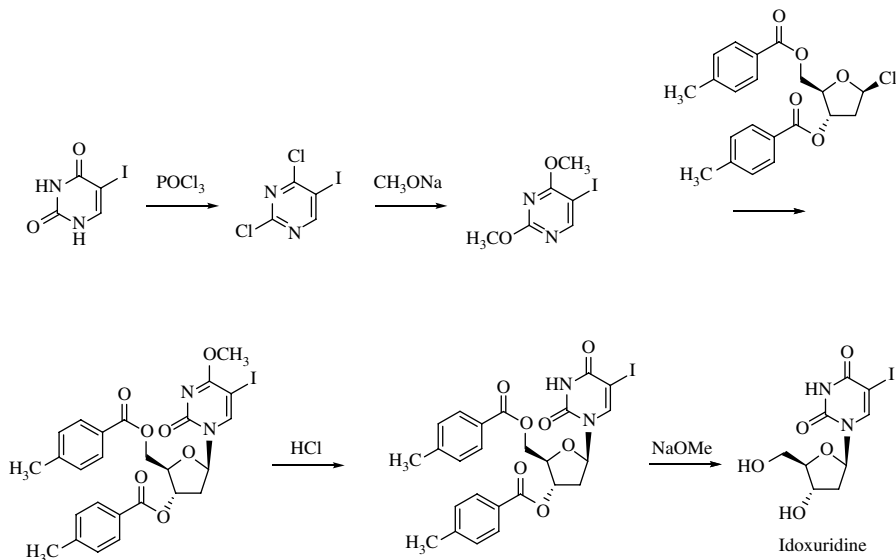


FIGURE 23.5 Synthesis of idoxuridine (1).

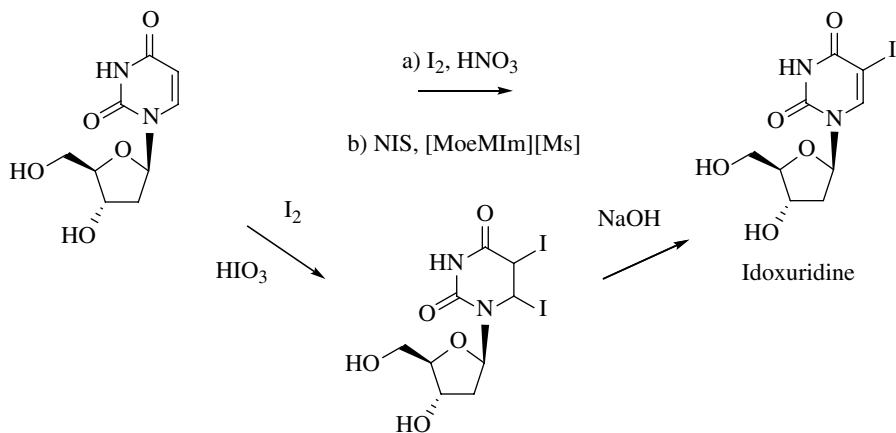


FIGURE 23.6 Synthesis of idoxuridine (2).

defective proteins. IDU is today a clinically used anti-herpes drug [8] even though its use is somewhat restricted due to its high general cell toxicity. IDU is mainly used topically to treat herpes simplex keratitis [9]. Preparation of IDU is as follows. IDU can be obtained by several related ways: (i) The reaction of 5-iodouracil with refluxing POCl_3 and dimethylaniline gives 2,4-dichloro-5-iodopyrimidine, which, by reaction with NaOCH_3 in refluxing methanol, is converted into 2,4-dimethoxy-5-iodopyrimidine. Reaction with 2-deoxy-3,6-di-*O*-*p*-toluoyl-D-ribofuranosyl chloride in acetonitrile then yields the ribofuranosyl pyridone, which is

demethylated with acetic anhydride–dry HCl to afford 2'-deoxy-5-iodo-3',6'-di-*O*-*p*-toluoyluridine. Finally, this compound is hydrolyzed with NaOCH₃ in methanol (Fig. 23.5) [10, 11]. (ii) Alternatively, 2'-deoxyuridine is iodinated with iodine, iodic acid, acetic anhydride, CCl₄ and water to give 2'-deoxy-5,6-diiodo-5,6-dihydrouridine, which is then treated with NaOH to eliminate HI. (iii) 2'-Deoxyuridine can also be iodinated directly with a) iodine and nitric acid in refluxing chloroform [12] or b) N-iodosuccinimide (NIS) in 1-methoxyethyl-3-methylimidazolium methanesulfonate (see Scheme 15.30) [13] (Fig. 23.6).

REFERENCES

- [1] Hernandez MZ, Cavalcanti SMT, Moreira DRM, de Azevedo WF Jr, Leite ACL. Halogen atoms in the modern medicinal chemistry: hints for the drug design. *Curr Drug Targets* 2010;11 (3):303–314.
- [2] Deltour G, Binon F, Tondeur R, Goldenberg C, Henaux F, Sion R, Deray E, Charlier R. Studies in the benzofuran series. VI. Coronary-dilating activity of alkylated and aminoalkylated derivatives of 3-benzoylbenzofuran. *Arch Int Pharmacodyn Thé* 1962;139:247–54.
- [3] Wiersinga WM. Pharmacotherapeutics of the thyroid gland. In: Weetman AP, Grossmann A, editors. *Amiodarone and the Thyroid, Handbook of Experimental Pharmacology*. Volume 128, Berlin/Heidelberg: Springer Verlag; 1997. p 225–287.
- [4] Singh BN, Vaughan Williams EM, Br J. The effect of amiodarone, a new anti-anginal drug, on cardiac muscle. *Pharmacol* 1970;39 (4):657–67.
- [5] Loh KC. Amiodarone-induced thyroid disorders: a clinical review. *Postgrad Med J* 2000;76:133–140.
- [6] Rao RH, McCreedy VR, Spathis GS. Iodine kinetic studies during amiodarone treatment. *J Clin Endocrinol Metab* 1986;62:563–568.
- [7] Prusoff WH. Synthesis and biological activities of iododeoxyuridine, an analog of thymidine. *Biochim Biophys Acta* 1959;32 (1):295–296.
- [8] Maxwell E, Am J. Treatment of herpes keratitis with 5-iodo-2-deoxyuridine (IDU): a clinical evaluation of 1500 cases. *Ophthalmol* 1963;56:571–573.
- [9] Gilman AG, Rall TW, Nies AS, Taylor P, editors. *Goodman and Gilman's the Pharmacological Basis of Therapeutics*. 8th ed. New York: McGraw-Hill; 1990.
- [10] Chang PK, Welch AD. Iodination of 2'-deoxycytidine and related substances. *J Med Chem* 1963;6:428–430.
- [11] Amiard G, Torelli V. Process for the preparation of 5-iodo-2-desoxy-uridine France Patent 1336866. September 6, 1963. Paris: Roussel Uclaf.
- [12] Trivedi MA. A rapid method for the synthesis of 5-iodo-2'-deoxyuridine (IUDR) and optimisation of the parameters. *J Label Compd Radiopharm* 1993;33 (7):607–612.
- [13] Kumar V, Yapp J, Muroyama A, Malhotra SV. Highly efficient method for C-5 halogenation of pyrimidine-based nucleosides in ionic liquids. *Synthesis* 2009:3957–62.

AGROCHEMICALS AND ANTHELMINTICS

PETER JESCHKE¹ AND TATSUO KAIHO²

¹*Bayer CropScience AG, Monheim am Rhein, Germany*

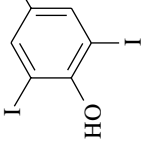
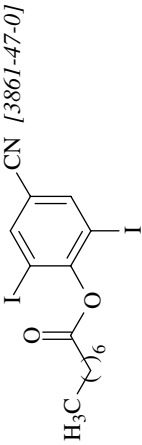
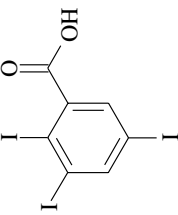
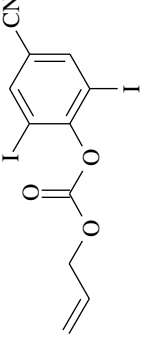
²*Nihon Tennen Gas Co., Ltd., Chiba, Japan*

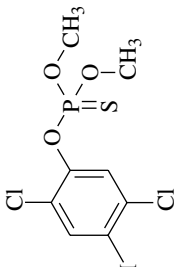
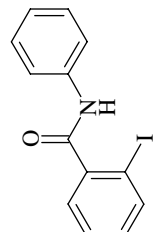
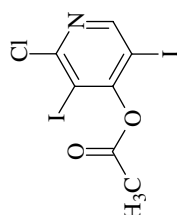
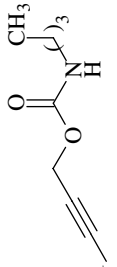
24.1 INTRODUCTION

In the past 33 years a significant increase of halogenated active ingredients in the field of modern crop protection research and development was observed. Interestingly, there has been a remarkable rise in the number of commercial products containing “mixed” halogens, for example, one or more further halogen atoms. A survey of new active ingredients (the total number up to August 2013 was 169) used as agrochemicals (insecticides/acaricides, fungicides, and herbicides), provisionally approved by International Organization for Standardization (ISO) during the past 15 years (1998–2013, see <http://www.alanwood.de>), shows that around 78% of these are halogen-substituted (Br, I < Cl/F, Cl < F). Today, a number of these halogenated-modified compounds are among the best-selling agrochemicals [1–3]. Generally, iodine-containing compounds are in the minority and some of them are “mixed” with other halogens like bromine or chlorine. Typical iodine-containing compounds, in use for a long time (cf. herbicides **1**, **2**, and **4**; fungicide **6**; PGR **3**; discontinued **5** and **7**) [4–10] or to date (e.g., fungicides for wood protection **8**, **9** and the mildewcide **10**) [11–13] as agrochemicals, are summarized in Table 24.1.

(1*R*,2*R*,5*R*)-(–)-Celarure B1 (**11**) [14], a male attractant for the Mediterranean fruit fly (*Ceratitis capitata*), is significantly more attractive than trimedlure (TML) [15], the current standard male attractant used in detection programs. Synthesizing racemic **11** instead of its specific stereoselective enantiomer would likely be more

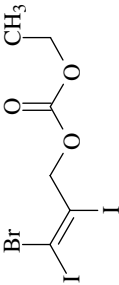
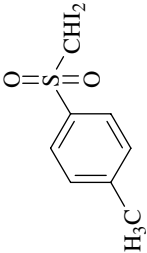
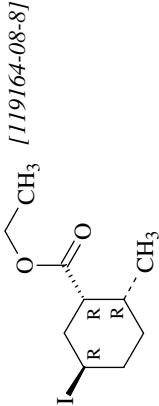
TABLE 24.1 Iodine-substituted compounds used as agrochemicals

Compound no.	Common name, trade name	Chemical structure [CAS RN]	Applications (comments)	Selected references
1	Ioxynil, Centrol®	 [1689-83-4]	Herbicide	Fletcher and Smith [4]
2	Ioxynil octanoate, Hawk®	 [3861-47-0]	Herbicide	Simmonds [5]
3	Triiodobenzoic acid, "TIBA"	 [88-82-4]	Plant Growth Regulator (PGR)	Irving [6]
4	Iodobomil	 [25671-45-8]	Herbicide	Ost et al. [7]

5	Iodofenphos, Nuvan [®]	 [18181-70-9]	Insecticide, Acaricide, Ectoparasiticide (discontinued)	Haddow and Marks [8]
6	Benodanil, Apache [®]	 [15310-01-7]	Fungicide	Frost and Hampel [9]
7	Clidionate	 [69148-12-5]	Herbicide (discontinued)	Schroeder et al. [10]
8	Iodocarb, "TPBC" Acticide [®]	 [55406-53-6]	Fungicide (wood protection)	Hansen [11]

(Continued)

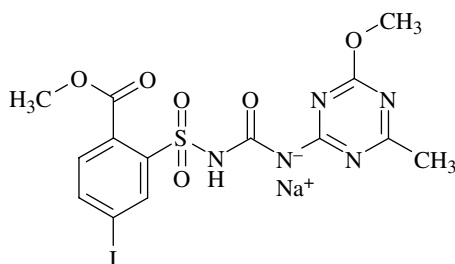
TABLE 24.1 (Cont'd)

Compound no.	Common name, trade name	Chemical structure [CAS RN]	Applications (comments)	Selected references
9	EBIP	 [77352-88-6]	Fungicide, Termiticide (wood protection)	Morisawa et al. [12]
10	DMTS	 [20018-09-1]	Fungicide, Antimicrobial (Mildewicide)	Littel et al. [13]
11	(-)-Ceralure B1	 [119164-08-8]	Insect attractant	Jang et al. [14]
12	Yokafume	CH ₃ -I [74-88-4]	Insecticide Acaricide Rodenticide Soil sterilant Fungicide	Ruzo [16]

cost-effective to produce and might also be useful as control as well as for detection of this pest.

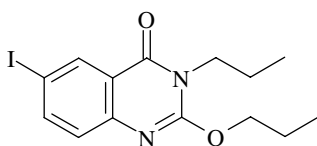
Methyl iodide (**12**) is active as a soil fumigant working by vapor action on soil-borne diseases, nematodes, insects, and weed seeds. It is under development as a replacement for methyl bromide [16] and for use in strawberries, tomatoes, peppers, turf, nursery crops, and field-grown ornamentals. The application is by incorporation in soil, by injecting irrigation water through subsurface/buried drip tubing prior to planting alone or in combination with other fumigants, at 134–263 kg ha⁻¹.

Halogens have very different reactivity, and in case of iodine it usually requires some form of activation (see Chapter 15) for introducing iodine to active ingredients. Outstanding progress has been made especially in synthetic methods for particular iodine-substituted key intermediates that were previously prohibitively expensive. Introduction of a carbon–iodine bond in agrochemicals can lead to diverse effects. The iodo-containing compounds can reflect (i) moderate chemical and biological stability, (ii) good hydrophobicity or lipophilicity, which increases



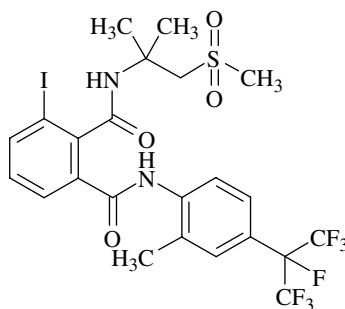
Iodsulfuron-methyl-sodium (**13**)

(Hussar®, Bayer CropScience, 1999)



Proquinazid (**14**)

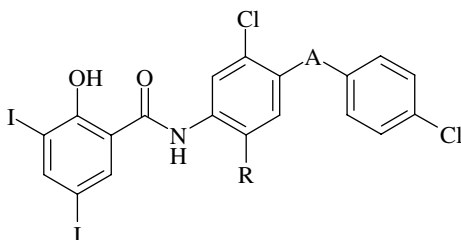
(Talius®, DuPont, 2005)



Flubendiamide (**15**)

(Belt®, Nihon Nohyaku Co., Ltd./
Bayer CropScience, 2006)

FIGURE 24.1 Modern iodine-containing agrochemicals (**13**)–(**15**).



Closantel (**16**); A = CHCN, R = CH₃

Rafoxanide (**17**); A = O, R = H

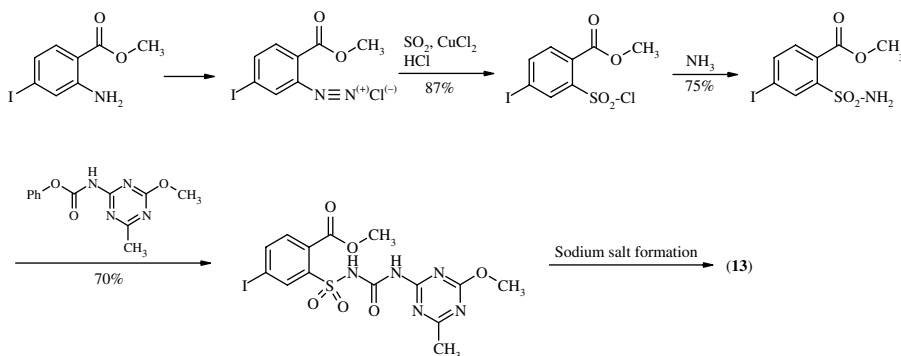
FIGURE 24.2 Iodine-containing anthelmintics closantel (**16**) and rafoxanide (**17**).

biological membrane permeability, (iii) high bulkiness, and (iv) halogen bonding interactions.

Three modern iodine-containing agrochemicals, including iodosulfuron-methyl-sodium (**13**; herbicide; CAS RN [1444550-36-7]), proquinazid (**14**, fungicide; CAS RN [189278-12-4]), flubendiamide (**15**, insecticide; CAS RN [272451-65-7]) (see Fig. 24.1), as well as the well-known anthelmintics closantel (**16**; CAS RN [57808-65-8]) and rafoxanide (**17**; CAS RN [22662-39-1]) (see Fig. 24.2) used as endo- and ectoparasiticides are described in detail here.

24.2 HERBICIDES

Because of their unique mode of action, herbicidal sulfonylureas have been developed and commercialized worldwide in over 80 countries, for use with all major agronomic crops [17]. In the biosynthetic pathway of the branched-chain amino acids valine (Val), leucine (Leu), and isoleucine (Ile), they interfere with a key enzyme acetohydroxyacid synthase (AHAS; EC 2.2.2.1) required for plant cell growth, which is also referred to as acetolactate synthase (ALS) [18]. When introduced in 1999, iodosulfuron-methyl-sodium (methyl 4-iodo-2-(4-methoxy-6-methyl-1,3,5-triazin-2-ylcarbamoyl)benzoate, sodium salt (**13**) (see Fig. 24.1)) was the first “safened” sulfonylurea herbicide available commercially [19], and has been marketed by Bayer CropScience as a broad-spectrum pre- and postemergent herbicide active on a wide range of broadleaf and some grass weeds on cereals and maize. In combination with mefenpyr-diethyl (1-(2,4-dichlorophenyl)-4,5-dihydro-5-methyl-1*H*-pyrazole-3,5-dicarboxylic acid diethyl ester) as cereal safener, the results demonstrated that the safener acted via specific catalytic enhancement of herbicide degradation in cereals, but not in target weeds such as the wild oat [20]. In cereals, (**13**) is available commercially under the trade name Hussar®, as a straight product in a 1:3 ratio with mefenpyr-diethyl as safener. Its introduction provided the farmer with a single, innovative, and easy one-pass solution, which saved both time and costs.



SCHEME 24.1 Synthetic pathway of iodosulfuron-methyl-sodium (**13**).

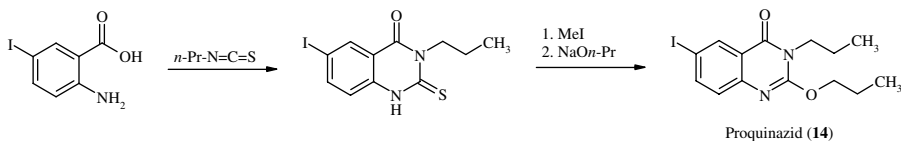
Starting with the commercially available 2-amino-4-iodobenzoic acid methyl ester, the 2-(methoxycarbonyl)-5-iodobenzene sulfonamide can be synthesized via diazotization, treatment with sulfur dioxide/ Cu(II) chloride under acidic conditions, and amide formation. Subsequent coupling with 4-methoxy-6-methyl-1,3,5-triazin-2-ylcarbamic acid phenyl ester leads to iodosulfuron-methyl, which is sold as sodium salt (**13**) (Scheme 24.1).

At a rate of 2.5–10.0 g a.i. ha^{-1} , (**13**) controls more than 50 different broadleaf weed species, including some very competitive weeds that cause a substantial reduction in cereal productivity such as common cleavers (*Gallium aparine*), common chamomile (*Matricaria chamomilla*), chickweed (*Stellaria media*), radish (*Raphanus* ssp.), creeping thistle (*Cirsium arvense*), and dead nettle (*Lamium* ssp.) [17]. It was found that though the application of (**13**) at the lower end of the suggested use rate is usually sufficient to control broadleaf weeds, a higher rate is needed for consistent grass weed control. Major grass weeds controlled with 7.5–10.0 g a.i. ha^{-1} dose rate applied at the three-leaf stage up to the end of tillering are redtop (*Agrostis gigantea*), bentgrass (*Apera spica-venti*), ryegrasses (*Lolium multiflorum*), *Lolium perenne*, *Lolium persicum*, and *Lolium rigidum*, canarygrasses *Phalaris brachystachys*, *Phalaris canariensis*, and *Phalaris paradoxa*, meadow grasses *Poa annua*, and *Poa trivialis*.

24.3 FUNGICIDES

Proquinazid (6-iodo-2-propoxy-3-propyl-4(3*H*)-quinazolinone) (**14**), the first non-systemic fungicide belonging to the quinazolin-4-one class, was launched in 2005 as a potent preventative powdery mildewicide for cereal and the grapevine markets. In addition, (**14**) could successfully be registered as grapevine fungicide Talendo® in Hungary and Austria in 2005. DuPont has since gained more registrations in key countries [21].

Proquinazid (**14**) can be prepared starting from commercially available 5-iodoanthranilic acid (Scheme 24.2).



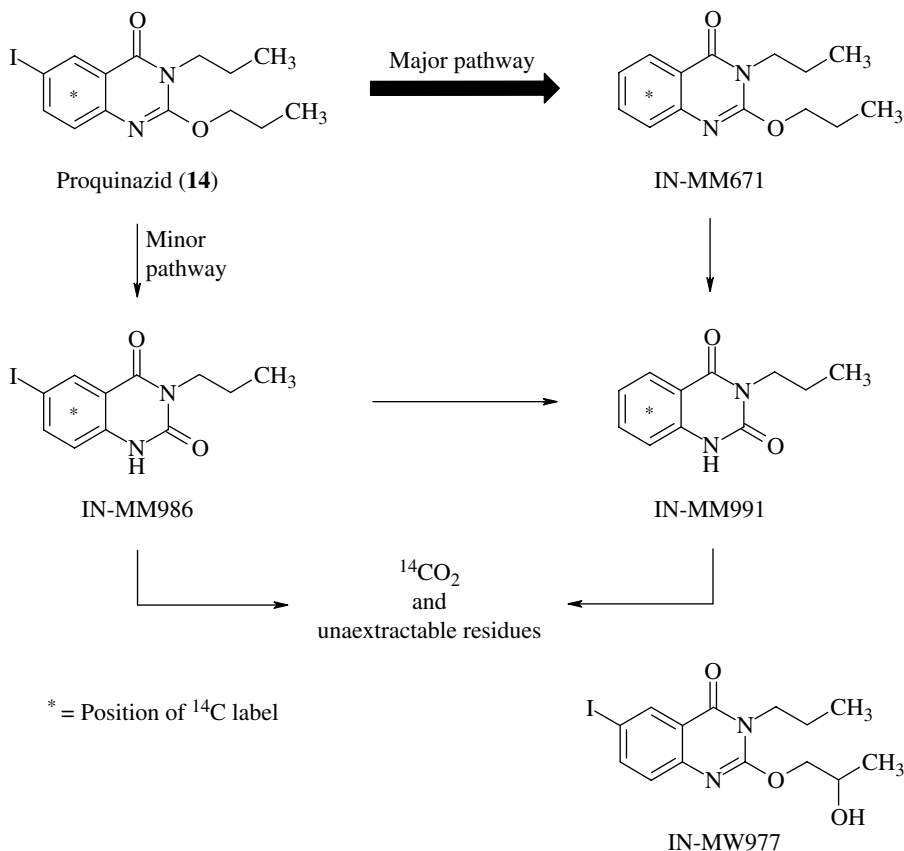
SCHEME 24.2 Synthesis of proquinazid (**14**).

Cyclization with *n*-propyl isothiocyanate leads to 2,3-dihydro-6-iodo-3-propyl-2-thioxo-4(1*H*)-quinazolinone. The subsequent introduction of a *n*-propoxy substituent via a methylation displacement sequence concludes the synthesis [22].

None of the other halogenated analogs (including disubstituted derivatives) were more potent than the *mono*-iodo-substituted proquinazid (**14**) (ranking of halogen atoms: Cl < Br < I; wheat powdery mildew (*Blumeria graminis*) EC₉₀ = <0.5) in advanced tests [21]. In July 2010, **14** was moved by the Fungicide Resistance Action Committee (FRAC) from “Unknown Mode of Action” to the E1 class (“signal transduction”) as a result of findings in powdery mildew of grapevine (*Erysiphe necator*) that this new mildewicide showed characteristics similar to those of the protectant fungicide quinoxyfen (Quintec®). However, the exact molecular target is unknown and is considered to be distinct from that of quinoxyfen [23, 24]. Proquinazid (**14**) exhibits a long residual activity, acts in a preventive manner, and does not show any significant curative activity against powdery mildew pathogens. It is locally systemic and allows for the protection of untreated leaves or neighboring plants by distribution of the active ingredient via the vapor phase. Morphologically, the active ingredient inhibits spore germination and affects the signal transduction pathway involved in the appressorium differentiation phase of the infection process. Talius® (for use in cereals, 200 g l⁻¹, EC) controls powdery mildew infections on cereal at approximately 40 g a.i. ha⁻¹ and provides an excellent residual activity of up to 6 weeks from a single application. Proquinazid (**14**) enhances yield quality and can be applied twice in a season, but for resistance management reasons it should be mixed with a broad-spectrum fungicide or a powdery mildewicide with a different mode of action [22]. Talendo (for use in grapes, fruits, and vegetables, 200 g l⁻¹, EC) is recommended for the control of powdery mildew (*Uncinula necator*) in grapes, at a rate of approximately 50 g a.i. ha⁻¹. It also helps in delivering undamaged, perfectly shaped grapes and reduces the threat of secondary infection with other fungi as gray mould (*Botrytis cinera*).

Aerobic degradation studies of (**14**) in the soils at 20°C are shown in Scheme 24.3.

The main metabolic pathway of **14** in the soil is its deiodination forming 2-propoxy-3-propylquinazolin-4(3*H*)-one (IN-MM671), which is subsequently dealkylated to 3-propylquinazoline-2,4(1*H*,3*H*)-dione (IN-MM991). Metabolism of rats predominantly comprises phenyl ring hydroxylation and hydroxylation at the *n*-propyl and *n*-propoxy side chains, as well as hydrolysis of some side chains. Major excretory metabolites include conjugates of these metabolites. Finally, it is to be noted that the end points for **14** were also considered applicable to 2-[(2*RS*)-2-hydroxypropyl]oxy]-6-iodo-3-propylquinazolin-4(3*H*)-one (IN-MW977) as a metabolite (see Scheme 24.3), which consists of two optical hydroxyl isomers that



SCHEME 24.3 Degradation pathway of proquinazid (**14**).

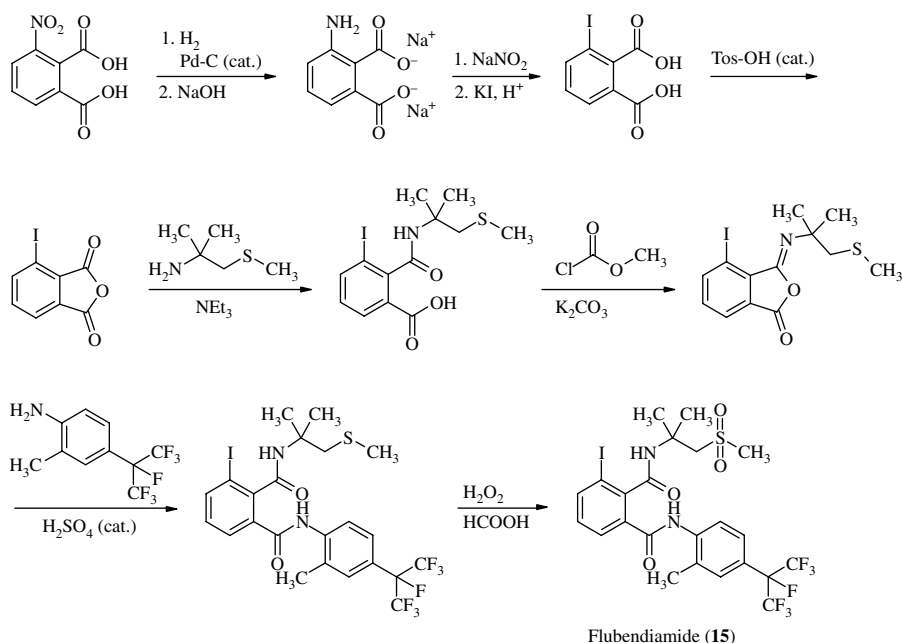
are not analytically distinguishable (EFSA, 2009). This metabolite is included in the residue definition for risk assessment [25].

24.4 INSECTICIDES

Flubendiamide (*N*²-[1,1-dimethyl-2-(methylsulfonyl)ethyl]-3-iodo-*N*¹-[2-methyl-4-[1,2,2,2-tetrafluoro-1-(trifluoromethyl)ethyl]phenyl]-1,2-benzenedicarboxamide) (**15**) is the first insecticide belonging to a new chemical class named 1,2-benzendicarboxamides or phthalic acid diamides [26]. Nihon Nohyaku Co. discovered **15** in 1998, and the global development was accelerated by a collaboration with Bayer CropScience since 2001. Flubendiamide (**15**) was registered in Japan in 2007 under the trade name of Phoenix[®] and as Takumi[®] in other countries. It is the first synthetic compound to possess insecticidal activity via ryanodine receptor (RyR) modulation [27]. With EC₅₀ values between 0.004 and 0.58 mg l⁻¹, **15** provides a very high,

selective broad-spectrum activity against all important lepidopterous pests such as diamondback moth (*Plutella xylostella*), tobacco caterpillar (*Spodoptera litura*), or cotton bollworm (*Helicoverpa amigera*), including known resistant species [26, 28, 29]. Excellent results were achieved in cotton, soybean, corn, rice, vegetables, top fruits, grapes, and orchard crops in many countries of the world. In addition to the excellent field performance, its selectivity between lepidopterous pests and beneficial arthropods indicates that **15** is compatible with Integrated Pest Management (IPM) programs [30]. Three characteristics make the molecule quite unique: an iodine atom at the 3-position of the phthalic acid moiety (ranking of halogen atoms: $F < Cl < Br < I$), an aliphatic alkylsulfonylalkyl amide group, and a heptafluoro-*iso*-propyl group in the anilide moiety. The bulky and moderate lipophilic iodine atom at the 3-position of the phthalic acid aryl moiety leads to a considerable increase in insecticidal activity of **15** and reduces its phytotoxicity to crops. The starting compound, 3-nitro-phthalic acid, is hydrogenated to yield the corresponding 3-amino-phthalic acid sodium salt, which is transformed into 3-iodo-phthalic anhydride by the well-known Sandmeyer reaction followed by acid treatment (see Scheme 24.4).

The desired phthalamic acid derivative was obtained regioselectively by reaction with the alkylamine. Phthalamic acid was cyclized to isoimide, which was reacted with the heptafluoro-*iso*-propylaniline to afford the diamide. However, this route was not suitable as a practical manufacturing process. Therefore, the alternative route that matches green chemistry was investigated to resolve the problems of low productivity and wastewater discharges (see Scheme 24.5).

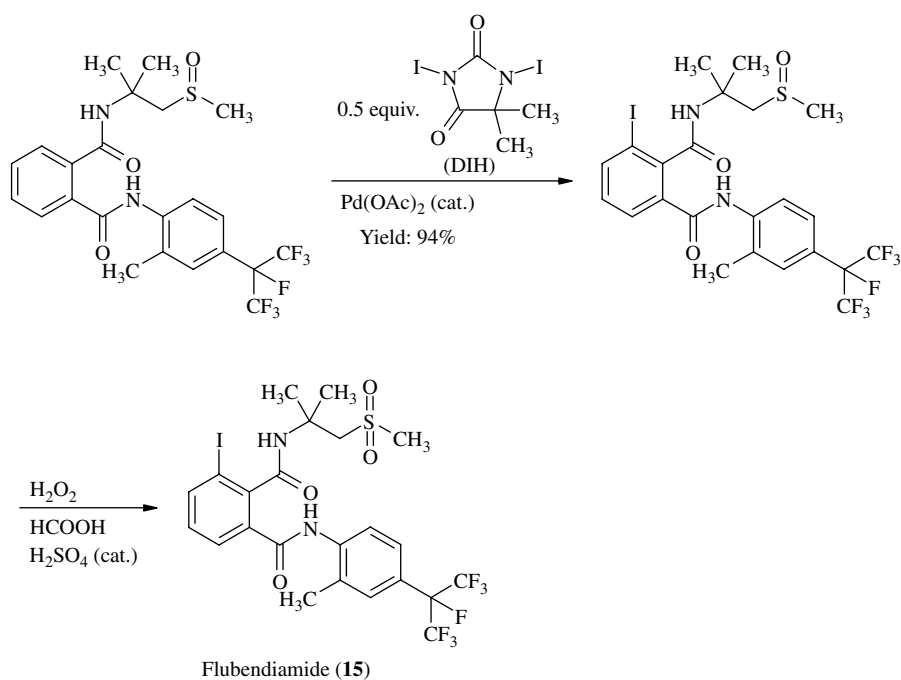


SCHEME 24.4 Synthesis of flubendiamide (**15**).

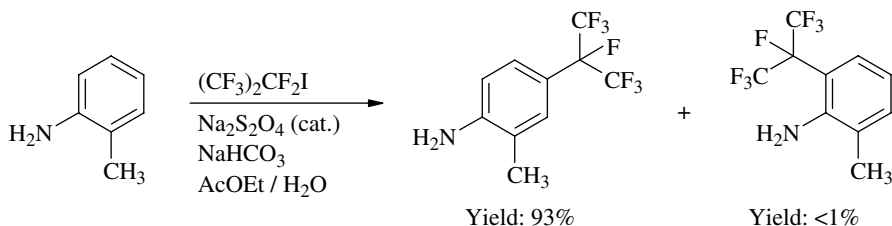
The diamide is iodinated with the efficient iodine donor 1,3-iodo-5,5-dimethylhydantoin (DIH; similar reactivity to *N*-iodosuccinimide (NIS) by a palladium-catalyzed reaction and followed by the oxidation with hydrogen peroxide to give **15**. This novel palladium-catalyzed iodination reaction demonstrates a very high regioselectivity and excellent yield [31].

The heptafluoro-*iso*-propylaniline can be synthesized by the reaction of *ortho*-toluidine with heptafluoro-*iso*-propyliodide under radical reaction conditions [32] (Scheme 24.6).

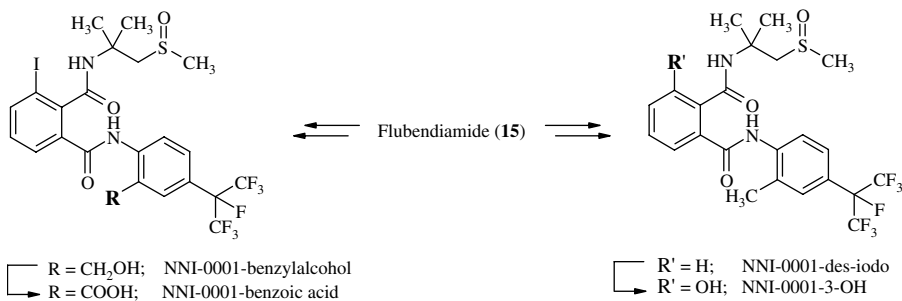
The regioselectivity (*para* versus *ortho*) of this reaction is also quite high. Flubendiamide (**15**) has demonstrated a broad-spectrum activity against all lepidop-



SCHEME 24.5 Palladium-catalyzed regioselective iodination [26].



SCHEME 24.6 Synthesis of heptafluoro-*iso*-propylaniline by radical coupling [26].



SCHEME 24.7 Proposed metabolic pathway of flubendiamide (**15**) in plants [35].

terous pests, but proved inactive against other insect orders such as Coleoptera, Hemiptera, and Acarina. With regard to different larval stages of lepidopterous pests, **15** is most effective against the first instar larvae, followed by the third and fifth instar larvae. Furthermore, it was shown that **15** induces RyR-sensitive cytosolic Ca²⁺ transients that are independent of extracellular Ca²⁺ concentration in isolated neurons from the tobacco budworm (*Heliothis virescens*), as well as transfected Chinese hamster ovary (CHO) cells expressing the RyR from the fruit fly (*Drosophila melanogaster*) [33]. Binding studies on microsomal membranes from tobacco budworm (*H. virescens*) flight muscle revealed that **15** interacts with a site distinct from the ryanodine binding site, and disrupts the Ca²⁺ regulation of ryanodine binding by an allosteric mechanism [34]. This novel insecticide mode of action seems to be restricted to insect RyR: **15** was completely inactive on all three mammalian RyR subtypes, which likely explains the excellent toxicological profile of this promising substance class. Based on its unique symptoms and novel mode of action, **15** cannot be expected to demonstrate any cross-resistance with conventional insecticides.

According to the metabolism studies of **15** in plants (cabbage, tomato, apple), the NNI-0001-benzylalcohol and NNI-0001-benzoic acid were formed by stepwise oxidation (via benzaldehyde) of the *ortho*-methyl group at the aniline ring (Scheme 24.7).

On the other hand, NNI-0001-des-iodo and NNI-0001-3-OH were formed by desiodination of **15** followed by hydroxylation at the phthalic acid ring [35].

Flubendiamide (**15**) poses minimal risk to freshwater or marine/estuarine organisms (fish, invertebrates, plants). No acute toxicity to honey bees has been observed, and no adverse effect on the adult mortality, flight intensity, behavior, and hive condition were observed in the semifield test [36].

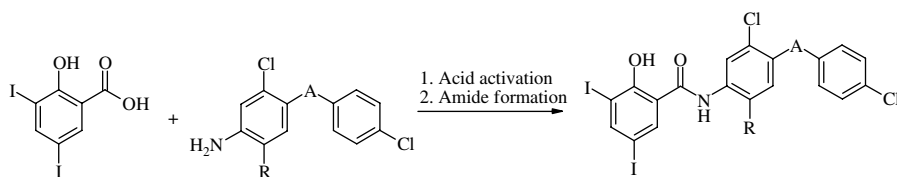
24.5 ANTHELMINTICS

Halogenated sylicylanilides, like the iodine-containing closantel (*N*-[5-chloro-4-[(4-chlorophenyl)cyanomethyl]-2-methylphenyl]-2-hydroxy-3,5-diiodo-benzamide) (**16**, Flukiver®, Janssen, [CAS RN: 57808-65-8]) and rfoxanide (*N*-[3-chloro-4-[(4-chlorophenoxy)phenyl]-2-hydroxy-3,5-diiodo-benzamide) (**17**, Ranox®, Pfizer, [CAS

RN: 22662-39-1]) (Fig. 24.2), are important anthelmintics (endo- and ectoparasitocides) that are most widely used in the control of pathogenic nematodes (*Heamonchus* spp.) and liver fluke (*Fasciola* spp.) infestation in sheep and cattle, and sheep botflies (*Oestrus ovis*) in sheep in many parts of the world [37].

Both anthelmintics, **16** and **17**, can easily be prepared by coupling of activated 3,5-diiodo-2-hydroxy-benzoic acid (e.g., via acid chloride formation with PCl_3) with the corresponding anilines [38] (Scheme 24.8).

Improved fasciolicidal activity of **16** and **17** has been achieved by incorporation of a *para*-chloro-phenyl-A ($\text{A}=\text{O}$, CHCN) chain in the aniline moiety of the anilide [39]. In both anthelmintics the active pharmacophore is a 3,5-diiodosalicyloyl moiety [40]. The primary action of salicylanilides such as **16** and **17** is the inhibition of electron transport-associated oxidative phosphorylation, which was first confirmed in vitro in the sheep liver fluke (*Fasciola hepatica*), the giant roundworm (*Ascaris lumbricoides*), and finally in vivo as well [41, 42]. Furthermore, it has been suggested that salicylanilides like rafoxanide (**17**) diminish ATP synthesis, resulting in increased internal intermediate pools in the pathway. Therefore, as an independent effect, the further metabolism of succinate is inhibited [37]. Closantel (**16**) was shown to have in vitro and in vivo effects on both the mobility and ultrastructure of the liver fluke (*F. hepatica*) [43]. It induces rapid spastic paralysis of the fluke, severe sloughing of the integument, swelling of the basal infoldings, mitochondrial deformation, and a reduced output of secretory products, especially in the tegumental and gastrodermal cells [37]. The spastic paralysis seen with **16** is similar to that observed with **17** and other salicylanilides [44]. Halogenated salicylanilides are extensively plasma-bound and poorly distributed to tissues. The ratio of closantel (**16**) in the plasma relative to that in the lung and kidney tissue is 6–7, 9–12 for the heart and liver, 30 for muscle, and about 100 for fat. A plasma to liver concentration ratio of 17.5 for **17** and a plasma to bile ratio of >50 and 35%, respectively, for **15** and **16** have been described [45]. Furthermore, extensive binding to plasma albumin (>97%) has been reported for both **16** and **17** [46]. Salicylanilides are poorly metabolized and are excreted mainly unchanged. In contrast to **17** [46], a reductive *mono*-deiodation was observed as the main metabolic pathway for **16** in sheep, cattle, and goats, resulting in the formation of its 3- and 5-*mono*-iodo isomers [47]. Because of steric hindrances by the *ortho*-methyl substituent in **16**, **17** is metabolized to 3,5-diiodosalicylic acid by amide cleavage via hydrolysis and is found in blood, milk, and muscle of cattle. However, the metabolic dehalogenation of both iodine atoms has not been observed [46].



SCHEME 24.8 Synthesis of salicylanilides.

Closantel (**16**) and rafoxanide (**17**) are highly effective against both immature and mature stages of nematodes in sheep and cattle. For example, a single injection of 5 mg a.i. kg⁻¹ completely cleared adult *Capillaria bovis* infection in cattle [48]. Because of their effectiveness against a wide range of hepatic and intestinal trematodes in a variety of animals, they are the most important drugs used for the treatment and control of fascioliasis in ruminants. Closantel (**16**) given orally at 15 and 20 mg a.i. kg⁻¹ is highly effective in reducing 8-week-old *Fascioloides magna* infestation in sheep [49]. Although salicylanilides such as **16** and **17** are primarily effective against helminthes, they show activity against numerous insects such as a range of Oestridae and arthropods like ticks in different animals as well.

24.6 SUMMARY

In the search for an “optimal product” in modern crop protection and animal health in terms of efficacy, environmental safety, user friendliness, and economic viability, the substitution of active ingredients with halogen atoms or halogen-containing substituents is an important tool [2]. Despite few examples, it has been shown that the introduction of iodine atoms into a molecule can influence the biological efficacy, depending on their mode of action, the physico-chemical properties or the target interaction of the compound. In the past few years, the technical availability of active ingredients containing iodine has been improved by an increase in access to new intermediates.

REFERENCES

- [1] Jeschke P. The unique role of halogen substituents in the design of modern agrochemicals. *Pest Manag Sci* 2010;66:10.
- [2] Jeschke P. The unique role of halogen substituents in the design of modern crop protection compounds. In: Jeschke P, Krämer W, Schirmer U, Witschel M, editors. *Modern Methods in Crop Protection Research*. Weinheim: Wiley-VCH Verlag GmbH; 2012. p 73.
- [3] Herrera-Rodriguez LN, Khan F, Robins KT, Meyer HP. Perspectives on biotechnological halogenation Part I: Halogenated products and enzymatic halogenation. *Chemistry Today* 2011;29:31.
- [4] Fletcher WW, Smith JE. The growth of bacteria, fungi, and algae in the presence of 3,5-dihalogeno-4-hydroxybenzonitriles with comparative data for substituted aryloxyalkanecarboxylic acids. *Proceedings of the British Weed Control Conference 7th*; August 2nd–4th, 1964; Glasgow; p 20. Volume 1, England: British Crop Protection Council.
- [5] Simmonds MJ. Experiments on weed control with hydroxybenzonitrile formulations in salad and bulb onions. *Proceedings of the British Weed Control Conference 9th*; November 18th–21st, 1968; Volume 1, England: British Crop Protection Council; 1968, 344.
- [6] Irving RM. *Okla Agr Exp Sta Tech Bull* 1968;T–128:15.
- [7] Ost W, Thomas K, Jerchel D, Linden G. Esters of halogenated p-hydroxybenzonitrile. *Ger Offen DE* 1919571, Oct. 30, 1969, to Boehringer, C. H., Sohn.

- [8] Haddow BC, Marks TG. Iodofenphos- broad review of a promising new insecticide. Proceedings of the British Insecticide and Fungicide Conference 5th, Volume 2, England: British Crop Protection Council; 1970; p 531.
- [9] Frost AJP, Hampel M. The development of benodanil for the control of cereal rust diseases. Proceedings of the European and Mediterranean Cereal Rusts Conference 4th; Interlaken: Swiss Fed. Res. Stn. Agron. Zurich, Switzerland; 1976; p 99.
- [10] Schroeder L, Thomas K, Linden G, Lust S. Pyridine derivatives. *Ger Offen* DE 2719904, Nov. 9, 1978, to Celamerck G.m.b.H. und Co. K.-G., Germany.
- [11] Hansen J. IPBC—a new fungicide for wood protection. *Mod Paint Coating* 1984;74:50, 52, 55, 90.
- [12] Morisawa Y, Kataoka M, Nagahori H, Sakamoto T, Nakata Y, Konishi K, Aiba T, Mizuno T, Ono S, Koichi N. Synthesis and antifungal activity of trihaloallyl and trihaloacryl derivatives. *Holzforschung* 1984;38:225.
- [13] Little KJ, Reid DS, Pohlmann JL, Leseiko OM. *A Profile of Diiodomethyl-p-Tolylsulfone. A Widely Used Antimicrobial*. Volume 133, Weinheim: Wiley-VCH Verlag GmbH Weinheim; 1996. Biodeterioration and Biodegradation; p 433.
- [14] Jang EB, Khirmian A, Holler TC, Casana-Giner V, Lux S, Carvalho LA. Field response of Mediterranean fruit fly (Diptera: Tephritidae) to ceralure B1: evaluations of enantiomeric B1 ratios on fly captures. *J Econ Entomol* 2005;98:1139.
- [15] Sonnet PE, Guss PL, Tumlinson JH, McGovern TP, Cunningham RT. Asymmetric synthesis of selected insect pheromones. *Synthesis and Chemistry of Agrochemicals*, ACS Symposium Series 355 (Synthetic Pyrethroids), Amer. Chem. Soc., Washington, D. C. 355; 1987. p 388.
- [16] Ruza LO. Physical, chemical and environmental properties of selected chemical alternatives for the pre-plant use of methyl bromide as soil fumigant. *Pest Manag Sci* 2006;62:99.
- [17] Ort O. Newer sulfonylureas. In: Jeschke P, Krämer W, Schirmer U, Witschel M, editors. *Modern Methods in Crop Protection Research*. Weinheim: Wiley-VCH Verlag GmbH; 2012. p 50.
- [18] Gutteridge S, Thompson ME. Acetohydroxyacid synthase inhibitors (AHAS/ALS): biochemistry of the target and resistance. In: Jeschke P, Krämer W, Schirmer U, Witschel M, editors. *Modern Methods in Crop Protection Research*. Weinheim: Wiley-VCH Verlag GmbH; 2012. p 29.
- [19] Hacker E., Bieringer H., Willms L., Ort O., Koecher H., Kehne H. Iodosulfuron plus mefenpyr-diethyl - a new foliar herbicide for weed control in cereals. *Proceedings of the Brighton Crop Protection Conference, Weeds*. November 15th–18th, 1999, Brighton, UK Volume 1; 1999, p 15.
- [20] Rosinger C, Bartsch K, Schulte W. Safeners for herbicides. In: Jeschke P, Krämer W, Schirmer U, Witschel M, editors. *Modern Methods in Crop Protection Research*. Weinheim: Wiley-VCH Verlag GmbH; 2012. p 371.
- [21] Selby TP, Sternberg CG, Bereznak JF, Coats RA, Marshall EA. The discovery of proquinazid: a new and potent powdery mildew control agent. In: Lyga JW, Theodoridis G, editors. *Synthesis and Chemistry of Agrochemicals VII*. Washington, DC: Oxford University Press; 2007. p 209.
- [22] Dietz J. Recently introduced powdery mildew fungicides. In: Jeschke P, Krämer W, Schirmer U, Witschel M, editors. *Modern Methods in Crop Protection Research*. Weinheim: Wiley-VCH Verlag GmbH; 2012. p 887.

- [23] Genet JL, Jaworska G. Baseline sensitivity to proquinazid in *Blumeria graminis* f. sp. *tritici* and *Erysiphe necator* and cross-resistance with other fungicides. *Pest Manag Sci* 2009;65:878.
- [24] Gilbert SR, Cool HJ, Fraaije BA, Bailey AM, Lucas JA. Impact of proquinazid on appressorial development of the barley powdery mildew fungus *Blumeria graminis* f.sp. *hordei*. *Pestic Biochem Physiol* 2009;94:127.
- [25] European Food Safety Authority. Reasoned opinion on the modification of the existing MRLs for proquinazid in tomatoes, aubergines and cucurbits with edible peel. *EFSA J* 2012;10:2896.
- [26] Hamaguchi H, Hirooka T. Flubendiamide. In: Jeschke P, Krämer W, Schirmer U, Witschel M, editors. *Modern Methods in Crop Protection Research*. Weinheim: Wiley-VCH Verlag GmbH; 2012. p 1396.
- [27] Tohnishi M, Nakao H, Furuya T, Seo A, Kodama H, Tsubata K, Fujioka S, Kodama H, Hirooka T, Nishimatsu T. Flubendiamide, a novel insecticide highly active against lepidopterous insect pests. *J Pestic Sci* 2005;30:354.
- [28] Hirooka T, Nishimatsu T, Kodama H, Reckmann U, Nauen R. The biological profile of flubendiamide, a new benzenedicarboxamide insecticide. *Pflanzenschutz-Nachrichten Bayer* 2007;60:183.
- [29] Kato K, Kiyonaka S, Sawaguchi Y, Tohnishi M, Masaki T, Yasokawa N, Mizuno Y, Mori E, Inoue K, Hamachi I, Takeshima H, Mori Y. Molecular characterization of flubendiamide sensitivity in the lepidopterous ryanodine receptor Ca^{2+} release channel. *Biochemistry* 2009;48:10342.
- [30] Nauen R, Konanz S, Hirooka T, Nishimatsu T, Kodama H. Flubendiamide: a unique tool in resistance management tactics for pest lepidoptera difficult to control. *Pflanzenschutz-Nachrichten Bayer* 2007;60:247.
- [31] Tonishi M, Nishimatsu T, Motoba K, Hirooka T, Seo A. Development of a novel insecticide, flubendiamide. *J Pestic Sci* 2010;35:490.
- [32] Ohnishi M, Yoshiura A, Kohno E, Tsubata K. A process for producing perfluoroalkylaniline derivatives. *Eur Pat Appl* EP 1006102, Jun. 7, 2000, to Nihon Nohyaku Co., Ltd. Japan.
- [33] Ebbinghaus-Kintscher U, Luemmen P, Lobitz N, Schulte T, Funke C, Fischer R, Masaki T, Yasokawa N, Tohnishi M. Phthalic acid diamides activate ryanodine-sensitive Ca^{2+} release channels in insects. *Cell Calcium* 2006;39:21.
- [34] Ebbinghaus-Kintscher U, Lümmer P, Raming K, Masaki T, Yasokawa N. Flubendiamide, the first insecticide with a novel mode of action on insect ryanodine receptors. *Pflanzenschutz-Nachrichten Bayer* 2007;60:117.
- [35] Justus K, Motoba K, Reiner H. Metabolism of flubendiamide in animals and plants. *Pflanzenschutz-Nachrichten Bayer* 2007;60:141.
- [36] Hall T. Ecological effects assessment of flubendiamide. *Pflanzenschutz-Nachrichten Bayer* 2007;60:167.
- [37] Swan GE. The pharmacology of halogenated salicylanilides and their anthelmintic use in animals. *J S Afr Vet Assoc* 1999;70:61.
- [38] Burke MH. Manufacture of a salicylanilide derivative. *S African Pat.* ZA 9007235, Jul. 31, 1991, to Chanelle Chemicals Ltd., Ire.
- [39] Brown GR, Chesterson GJ, Coles GC. Potentiation of fasciolicidal agents by benzoyl side chains, synthesis of benzoylsalicylanilides. *J Med Chem* 1985;28:143.

- [40] Srivastava RP, Sharma S. Synthesis of 2,5-disubstituted benzimidazoles, 1,3,4-thiadiazoles and 3,5-diiodosalicylanilides as structural congeners of rafoxanide and closantel. *Pharmazie* 1990;45:34.
- [41] Cornish RA, Behm CA, Butler RW, Bryant C. The in vivo effects of rafoxanide on the energy metabolism of *Fasciola hepatica*. *Int J Parasitol* 1977;7:217.
- [42] Van den Bossche H, Verhoeven H, Vanparijs O, Lauwers H, Thienpont D. Closantel, a new antiparasitic hydrogen ionophore. *Arch Int Physiol Biochem* 1979;87:851.
- [43] Suke PJ, Fairweather I. The effect of the hydrogen ionophore closantel upon the pharmacology and ultrastructure of the adult liver fluke *Fasciola hepatica*. *Parasitol Res* 1990;76:241.
- [44] Fairweather I, Holmes SD, Treadgold LT. *Fasciola hepatica*: motility response to fasciolicides in vitro. *Exp Parasitol* 1984;57:209.
- [45] Mohamed-Ali NAK, Bogan JA. The pharmacodynamics of the flukicidal salicylanilides rafoxanide, closantel and oxyclozanide. *J Vet Pharmacol Therapeut* 1987;10:127.
- [46] Dedek W, Grahl R, Schwarz H, Ludwig P. Metabolism, residues, and excretion of the anthelmintic ¹³¹I-rafoxanide in blood, milk, meat, and urine of the lactating cow. *Arch Exp Veterinärmedizin* 1978;32:951.
- [47] Short CR. Consideration of sheep as a minor species: comparison of drug metabolism and disposition with other domestic ruminants. *Vet Hum Toxicol* 1994;36:24.
- [48] Guerrero J. Closantel: a review of its antiparasitic activity. *Prev Vet Med* 1984;2:317.
- [49] Stromberg BE, Schlotthauer JC, Conboy GA. The efficacy of closantel against *Fascioloides magna* in sheep. *J Parasitol* 1984;46:2527.

PART V

INDUSTRIAL APPLICATION OF IODINE

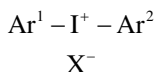
DIARYLIODONIUM SALT PHOTOACID GENERATORS

JAMES V. CRIVELLO

*Department of Chemistry and Chemical Biology, Rensselaer Polytechnic Institute,
Troy, New York, NY, USA*

25.1 INTRODUCTION

Diaryliodonium salts (**I**) are a class of stable, crystalline compounds that are readily prepared, purified, and characterized by conventional organic chemical methods and techniques. While these compounds have been known for well over 125 years, during much of this time they were viewed only as curiosities [1]. However, in the past 25–30 years, the discovery that diaryliodonium salts can serve as latent sources of a wide variety of protonic acids [2–5] that can be released under photolytic conditions has made these compounds the objects of considerable academic and industrial research and has led to their rapid commercialization and widespread use in many practical applications. It is the purpose of this chapter to present a brief overview of the technical aspects of diaryliodonium salt chemistry with an emphasis on their current and potential future areas of use. Accordingly, after a short discussion of the most important structural and chemical characteristics of diaryliodonium salts, the remainder of this chapter is divided into individual sections corresponding to the different application areas for these compounds as photoacid generators.



A diaryliodonium cation consists of two substituted or unsubstituted aromatic moieties bound together by bonds to a central, positively charged iodine atom. Since the iodine atom is formally in the +3 oxidation state, diaryliodonium salts can be considered to belong to the general class of hypervalent iodine compounds. The aromatic moieties (Ar^1 and Ar^2) may be the same or different consisting of benzene, naphthylene, or other aromatic, polynuclear aromatic, or heteroaromatic groups that may be further modified by a wide assortment and number of electron-donating and electron-withdrawing substituents. In all cases, the diaryliodonium cation ($\text{Ar}^1\text{--I}^+\text{--Ar}^2$) is balanced by an association with a negatively charged anion (X^-). Consequently, diaryliodonium salts are ionic species, and this characteristic has a large impact on many of their properties, in particular, on their solubility. The potential wide variations in the structural complexity of diaryliodonium salts provides for considerable freedom in the design of the chemical, spectroscopic, and physical properties of diaryliodonium salts and allows them to be tailored for use in specific applications.

To further elaborate on this important point, as noted before, a diaryliodonium salt may be considered to be composed of two components, namely, the cation, $\text{Ar}^1\text{--I}^+\text{--Ar}^2$ and the anion X^- . The structures of both of these components can be manipulated independent of one another, and both serve very different functions in the overall behavior of diaryliodonium salts as latent photoacid generators. The cation bears the chromophors responsible for the spectral absorption characteristics and resultant photochemistry of the diaryliodonium salt. The structure of the cation also determines the thermal stability and redox properties of the diaryliodonium salt. On the other hand, the anion is the ultimate source of the protonic acid that is generated and it is the major determinant of the strength and other chemical and physical properties of an acid that is generated. For each application, the structures of both the cation and the anion of a diaryliodonium salt acid generator must be carefully tailored and optimized for that specific use. In keeping with the already stated focus of this chapter, preparative methods for the synthesis of diaryliodonium salts will not be discussed here. Methods for the synthesis of diaryliodonium salts have been described in several previous review articles [6, 8]. The reader is directed to those general sources and to the references therein for further information regarding the preparation of these compounds.

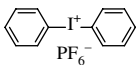
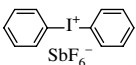
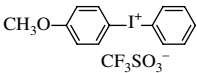
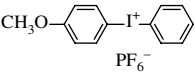
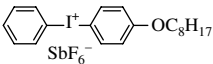
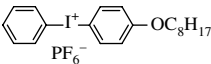
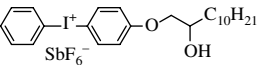
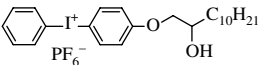
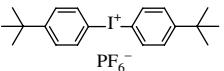
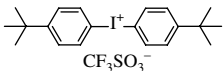
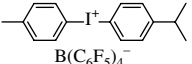
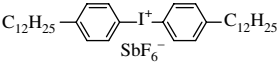
Shown in Table 25.1 are the structures of some representative, commercially available diaryliodonium salts. A large number of additional diaryliodonium salts have been prepared and characterized in the laboratory of the author of this chapter.

Diaryliodonium salt photoacid generators can be purchased from their suppliers in their solid, crystalline forms or conveniently dissolved in nonreactive liquid carriers of low volatility such as propylene carbonate, gamma-butyrolactone, or epsilon-caprolactone.

25.2 PHOTOINDUCED ACID GENERATION

The photosensitivity of diaryliodonium salts was noted rather soon after their discovery in 1984 as a new class of compounds [9]. As a result of detailed mechanistic studies [10–12], the mechanism of photolysis has been elucidated and is

TABLE 25.1 Structures of some commercially available diaryliodonium salt acid generators

 <p>Diphenyliodonium hexafluorophosphate (A)</p>	 <p>Diphenyliodonium hexafluoroantimonate (A)</p>
 <p>(4-methoxyphenyl)phenyliodonium trifluoromethylsulfonate (H)</p>	 <p>(4-methoxyphenyl)phenyliodonium hexafluorophosphate (H)</p>
 <p>(4-<i>n</i>-octyloxyphenyl)phenyliodonium hexafluoroantimonate (H)(C)</p>	 <p>(4-<i>n</i>-octyloxyphenyl)phenyliodonium hexafluorophosphate (H)</p>
 <p>(4{2-hydroxy-1-dodecyloxyphenyl}phenyl)iodonium hexafluoroantimonate (P)</p>	 <p>(4{2-hydroxy-1-dodecyloxyphenyl}phenyl)iodonium hexafluorophosphate (P)</p>
 <p>bis(4-<i>t</i>-butylphenyl)iodonium hexafluorophosphate (H)</p>	 <p>bis(4-<i>t</i>-butylphenyl)iodonium trifluoromethylsulfonate (H)</p>
 <p>4-isopropylphenyl-4'-methylphenyliodonium tetrakis(pentafluorophenyl)borate (R)</p>	 <p>bis(4-dodecylphenyl)iodonium hexafluoroantimonate (M)</p>

Commercial supplier: H, Hampford Research; R, Rhone Poulenc; P, Polysset Co.; A, Aldrich Chemical; M, Momentive Performance Materials; C, Cytec.

presented in Figure 25.1. In brief, the ultraviolet (UV) irradiation of a diaryliodonium salt causes its electronic excitation to the respective excited singlet and triplet states and the subsequent cleavage of a carbon–iodine bond by both homolytic and heterolytic pathways. The photolysis produces highly reactive radical, radical–cation, and cationic species. The subsequent interaction of these species with proton donors derived from the solvent, monomer, polymer, or adventitious impurities present ultimately results in the formation of protons that combine with the anion present to form a Brønsted acid, HX. The quantum yields for this process are high and of the order of 0.7 [13, 14].

Diaryliodonium salts containing substituted and unsubstituted phenyl groups typically absorb strongly in the region 220–300 nm, which makes them well-suited for use with short wavelength UV radiation. Considerable efforts have been made to extend the range of the sensitivity of diaryliodonium salts to longer wavelengths through the use of photosensitizers (PSs). The chief purpose of these efforts is to allow diaryliodonium salt photoacid generators to be used with long UV wavelength emitting light sources such as light emitting diodes (LEDs) and lasers and with visible light sources such as halogen lamps and, ultimately, sunlight. Many medical, dental, graphic arts, and three-dimensional (3D) imaging applications employ these light sources. It is also worth noting that while conventional mercury and xenon arc lamps emit at short UV wavelengths, most of their energy is emitted at wavelengths from 300 to 550 nm. This means that a large portion of the irradiation energy from these sources is usually wasted since it cannot be absorbed by the

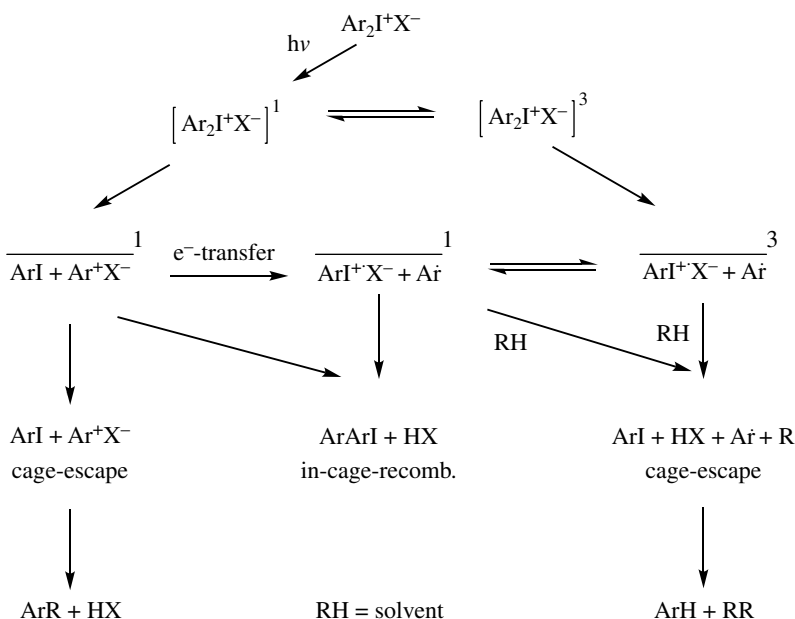


FIGURE 25.1 Mechanism of the photolysis of diaryliodonium salts.

photoinitiators. The use of photosensitizers with these conventional UV sources can greatly improve the response of a UV curable system by capturing more of the available light.

The use of electron-transfer PSs has been shown to be the most practical way in which the spectral broadening of the wavelength range of sensitivity of diaryliodonium salts may be achieved [15, 17]. Through the choice of an appropriate PS, it is now possible to carry out visible light photolysis of diaryliodonium salts at visible wavelengths using ambient sunlight. Electron-transfer photosensitization involves a photoinduced redox reaction as shown in Figure 25.2 in which a photoexcited compound (PS) transfers an electron (i.e., is oxidized) usually via the initial formation of an exciplex with the iodonium salt. Since the reduction potentials of diaryliodonium salts are low and of the order of -5 kcal mol^{-1} , this latter process is very facile and exothermic. The cation radical $[\text{PS}^+]$ derived from the PS subsequently reacts with the substrate or undergoes a series of further reactions to generate a Brønsted acid. The other product, a diaryliodine free radical, $\text{Ar}_2\dot{\text{I}}$, is unstable and undergoes irreversible decomposition to form an aryl radical and an aryl iodide.

Polynuclear aromatic hydrocarbons and certain acridine dyes were the first electron-transfer PSs to be developed. In recent years, the range of electron-transfer PSs for diaryliodonium salts has been greatly expanded. Included in Table 25.2 are a number of representative classes of electron-transfer PSs along with an approximate wavelength range in which they can be used. Through the application of electron-transfer PSs, the spectral sensitivity of diaryliodonium salts has been broadened to include the entire UV as well as the visible region of the spectrum.

Related to the earlier-discussed electron-transfer photosensitization and shown in Figure 25.3 is the proposed mechanism of the so-called radical promoted photosensitization [29–34]. In this latter process, carbon-centered radicals **II** and **III** are generated by the efficient photolysis of typical free radical photoinitiators, which are spontaneously oxidized at room temperature by a diaryliodonium salt to their corresponding carbocations. In Figure 25.3, the photolysis of 2,2-dimethoxy-2-phenylacetophenone is shown, which produces the readily oxidizable dimethoxyphenylmethyl free radical (**III**). The dimethoxybenzyl carbocation (**IV**) can interact directly with a monomer (Eq. 25.7) or further react with protogens to form protonic

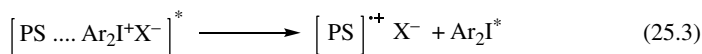
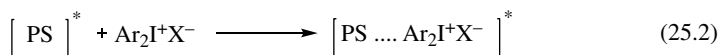
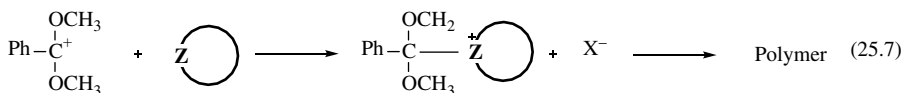
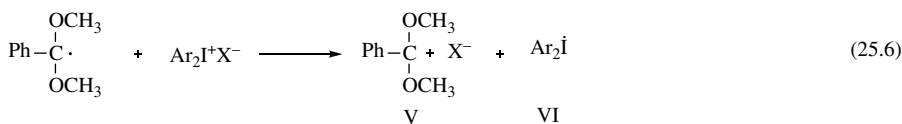
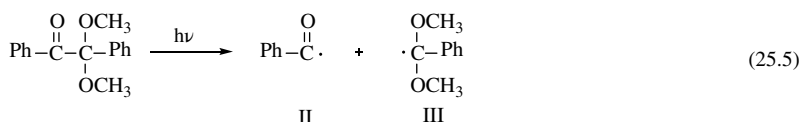


FIGURE 25.2 Proposed mechanism for the electron-transfer photosensitization of diaryliodonium salts.

TABLE 25.2 Classes of electron-transfer photosensitizers for diaryliodonium salts

Photosensitizer	Absorption range (nm)	References
Acridine dyes	413–539	[29]
Anthracenes	250–375	[16]
Alkoxyanthracenes	250–403	[30]
Perylene and pyrene	390–439	[31]
Carbazoles	250–340	[32, 33]
Phenothiazines	253–330	[34]
Benzophenothiazines	330–400	[35]
Thioxanthenes	380–420	[36, 37]
Quinoxalines	330–550	[38]
Curcumin	420–500	[39]

**FIGURE 25.3** Proposed mechanism for the free radical–promoted photosensitization of diaryliodonium salts.

acids. If a free radical photoinitiator having a long wavelength absorption is selected, the resulting diaryliodonium salt decomposition can be viewed as having been effectively “photosensitized” by this process.

25.3 PHOTOINITIATED CATIONIC POLYMERIZATIONS

The first applications of diaryliodonium salt photoacid generating systems were in the area of photoinitiated cationic polymerizations, and this field still remains a highly active area of research and increasing industrial commercialization. Cationic photopolymerization is a very versatile process in terms of the large number of types of monomers that can be employed. Thus, the cationic polymerization of alkenes, vinyl ethers, vinyl heterocyclic compounds, epoxides, oxetanes, and other cyclic

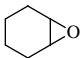
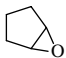

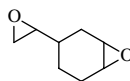
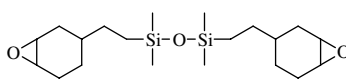
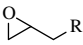
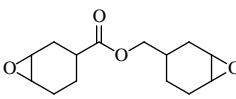
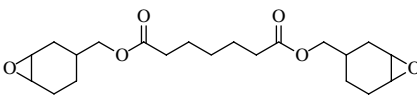
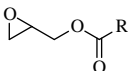
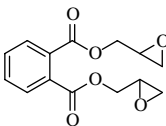
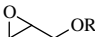
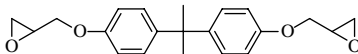
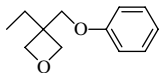
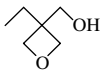
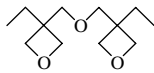
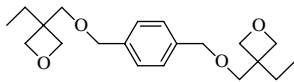
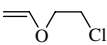
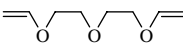
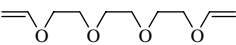

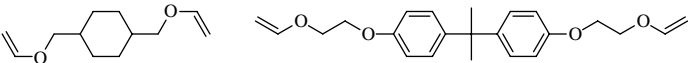
ethers, aziridines, oxazolines, lactones, spiroorthoesters, spiroorthocarbonates, lactams, and cyclic siloxanes are among the many different classes of monomers that can be employed [35–39]. While it is possible to carry out the cationic photopolymerization of monofunctional monomers to prepare linear polymers, it is not practical to do so. Instead, all current industrial applications of photopolymerizations are based on crosslinking or network-forming polymerizations employing multifunctional monomers or mixtures of mono- and multifunctional monomers. Such photopolymerizations are encompassed within the general technological term “UV curing.” Most efforts in the field of cationic UV curing to date have been focused on multifunctional epoxides, oxetanes, and vinyl ethers as monomers. The main factors in this decision are the high reactivity of these monomers and their commercial availability. Within these three classes of monomers, mono- and multifunctional epoxide monomers have received the most attention. The photopolymerization of epoxide monomers generally gives polymers with excellent mechanical properties, good adhesion to metals, glass, and plastics, and also excellent chemical resistance. UV curing of epoxide monomers is best suited to applications in which thin layers on flat or nearly flat substrates are polymerized or “cured” by exposure to UV light. Very often, the curing process involves very short exposure times ranging from fractions of seconds to seconds.

Epoxides are a broad class of monomers whose reactivity in cationic photopolymerization varies widely. In recent years, it has been shown that the primary factors that determine the reactivity of epoxide monomers are the ring strain, inhibition factors and whether the monomer bears functional groups that can competitively interact either with the initiating protonic acid or with the propagating oxonium ion center [40]. In Table 25.3 are shown the structures of a number of epoxide monomers and a subjective designation of the order of their reactivities as high, medium, and low. In practice, it is usual to use a combination of several such monomers to provide the properties and photopolymerization rates necessary to meet the requirements of a specific application. Also included in Table 25.3 are the structures of some commercially available oxetane and vinyl ether monomers that can be employed for use in applications involving photoinitiated cationic polymerization.

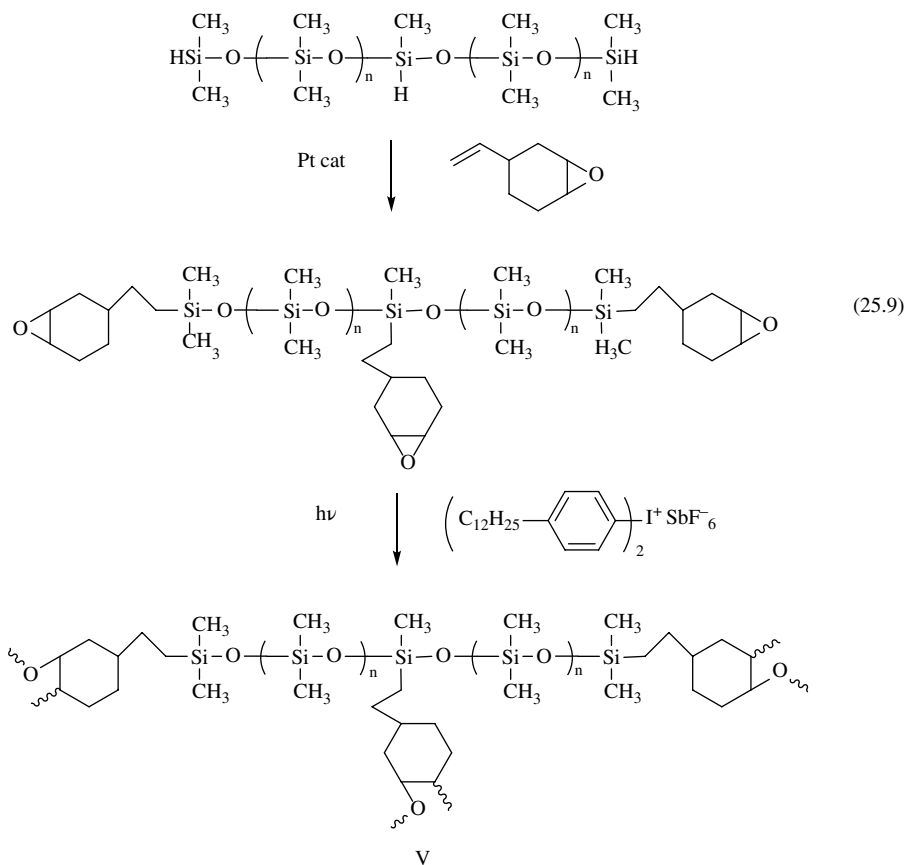
Diaryliodonium salts that are useful as photoinitiators for cationic polymerizations are limited to those that produce very strong protonic acids on photolysis. This means that diaryliodonium salts, which possess anions that on photolysis generate superacids such as HPF_6 , HAsF_6 , HBF_4 , HSbF_6 , and $\text{HB}(\text{C}_6\text{F}_5)_4$, having Hammett acidity values of $H^\circ = -15$ or lower, are of primary interest [41]. On the other hand, while strong mineral and organic acids such as H_2SO_4 , H_3PO_4 , $\text{C}_6\text{H}_5\text{SO}_3\text{H}$, and $\text{CF}_3\text{SO}_3\text{H}$ with H° values of -12 to -14 may induce the cationic polymerizations of certain monomers, the rates of those polymerizations are generally not sufficiently high enough to be of commercial interest.

The major commercial applications of photoinitiated cationic polymerization lie in UV curable coatings for metals, glass, and plastics, structural and pressure-sensitive adhesives, and printing inks. In addition, a wide assortment of specialty applications, too numerous to list here, are also served by this technology. UV-curable cationic systems are replacing traditional thermally cured solvent-based

TABLE 25.3 Structures of epoxide, oxetane, and vinyl ether monomers used in photoinitiated cationic polymerization

Epoxide monomers				
High reactivity				
				
Medium reactivity				
				
Low reactivity				
				
Oxetane monomers				
				
Vinyl ethers				
				
				

technology in many of these applications. The main factors driving the adoption of photoinitiated cationic polymerization technology come from the high rates of polymerization that can be achieved with such systems under ambient air conditions together with the environmental benefits that derive from the very low energy requirements and lack of the use of volatile organic solvents. A good example of the power of this technology is UV-curable epoxy–silicone release agents [42, 43]. The relevant chemistry is depicted in Equation (25.9). Silicone resins bearing terminal and pendant epoxy groups are readily synthesized by the platinum-catalyzed hydrosilylation of 4-vinyl-1,2-epoxycyclohexane with an appropriate Si–H functional silicone oligomer. UV-induced photopolymerization of the resulting epoxy-functional silicone is carried out using bis(4-dodecylphenyl)iodonium hexafluoroantimonate as a photoinitiator. Crosslinked epoxy–silicone release coatings (**V**) are applied and UV-cured reel-to-reel at speeds of 300–600 m min^{−1} using a reverse roll coater and two medium-pressure mercury arc lamps as the light source. The floor space required for this process is approximately 20–30 m. This system replaces a solvent-based release coating that originally required a 150-m natural gas-fired

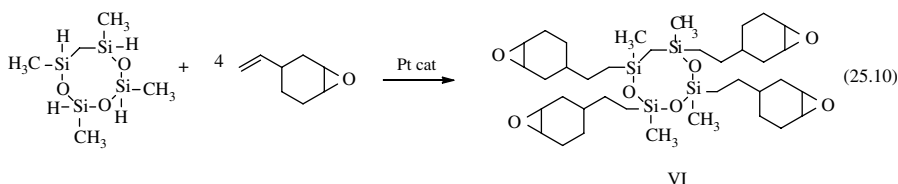


oven for cure. In Figure 25.4 are shown several commercial examples of cationically cured silicone paper release coatings applied to a variety of label applications.

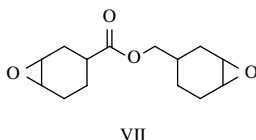
In a related development, work begun in this laboratory in the late 1980s and early 1990s led to the development of a new class of highly reactive, linear, branched, and cyclic epoxy functional silicon-containing monomers [44, 45]. These monomers can be readily prepared in high yields by the platinum-catalyzed hydrosilation of Si–H functional silanes and silicones with epoxides containing vinyl double bonds such as 4-vinyl-1,2-epoxycyclohexane or allyl glycidyl ether. A simple example of this reaction is shown in equation 10 for the preparation of the cyclic tetrafunctional epoxy monomer, **VI**. The company 3M ESPE has commercialized this monomer under the trade name Silorane™ as a photocurable dental composite [46]. UV cures of the dental composites are accomplished with a visible light–responsive initiator system consisting of a diaryliodonium salt together with camphoroquinone as a PS. As dental composites, these UV-curable systems provide excellent hardness and chemical resistance together with low volume shrinkage.



FIGURE 25.4 Examples of UV-cured silicone-epoxy paper release coatings applied on label stock backings.



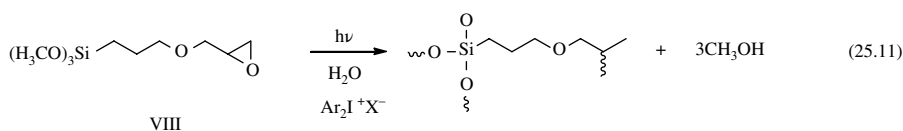
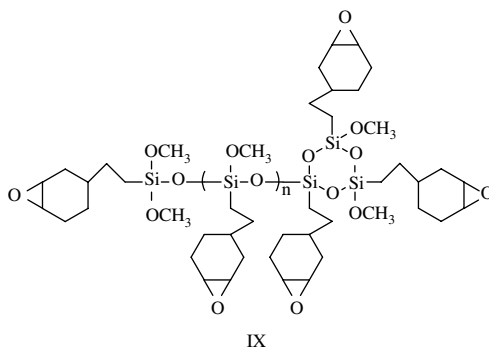
In a different application, a major can manufacturing company, the Coors Brewing Co., replaced its entire exterior thermally cured over print coating and printed graphics with UV-curable cationic epoxy-based offset systems and achieved a production rate of 4 billion cans year⁻¹ [47]. As with many coating and printing ink applications, the UV-curable formulations in this case are based on the biscycloaliphatic epoxy monomer, **VII**, shown here as the main component.



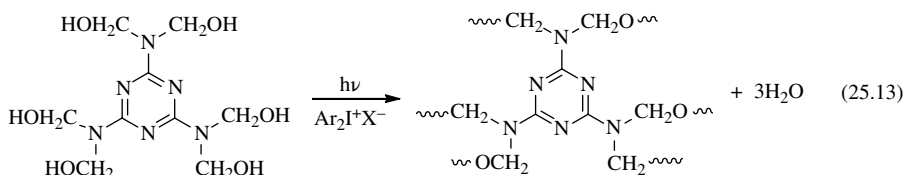
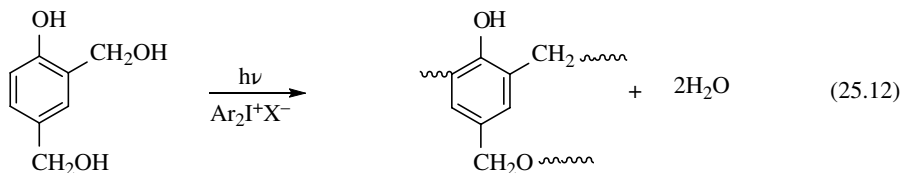
25.4 PHOTOINITIATED CONDENSATION POLYMERIZATIONS

A number of condensation polymerizations are acid-catalyzed and can be conveniently carried out using diaryliodonium salts as photoacid generators. For example, the condensation of alkoxy silanes can be performed under UV

irradiation conditions in the presence of added water or moisture provided by the atmosphere. These sol–gel-type polymerizations give modified silicate materials that are of special interest for hard, abrasion-, and scratch-resistant coatings for plastics. Some application areas include UV-curable coatings for eyeglass lenses and for poly(carbonate) automobile headlamp covers. Photocurable hybrid systems that combine cationically curable epoxy resins along with sol–gel silicones have also been developed [48–50]. These coatings are based on glycidoxypropyltrialkoxysilanes (**VIII**), and they are also of increasing interest for abrasion-resistant coatings, the formation of microlenses, optical fiber adhesives, and electronic and LED encapsulants. Lastly, the synthesis of highly reactive epoxy functional silicone resins with structure **IX** have been reported by first carrying out a conventional sol–gel reaction on a monomer bearing both alkoxyisilane and epoxy groups [51]. Irradiation of these highly reactive oligomeric resins in the presence of a diaryliodonium salt cationic photoinitiator yields crosslinked, glassy polymers with exceptional hardness, low coefficient of expansion, and thermal stability.



The photoinduced acid-catalyzed condensation polymerizations of phenol formaldehyde, urea formaldehyde, and hexamethylolmelamine resins have been reported to take place in the presence of diaryliodonium salt photoacid generators [52]. These resins have found some uses as UV-curable adhesives, composites, and additives to other UV-curable resins. They have also been employed in photoimaging as will be discussed in the next section. The UV cures of these systems (Eqs. 25.12 and 25.13) are comparatively slow and, in general, a thermal postcure is required to complete the condensation reaction.



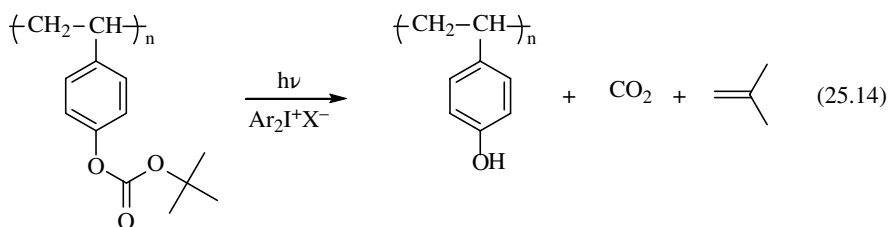
25.5 IMAGING USING DIARYLIODONIUM PHOTOACID GENERATORS

A broad area of applications that makes use of the unique photosensitivity properties of diaryliodonium salts as photoacid generators is imaging. This field can be further broken down according to the various different imaging technologies in which these compounds are currently employed.

25.5.1 High-Performance Positive Photoresists

In the mid-1970s, high-performance photolithography used to define features within microelectronic integrated circuits had reached a crossroad [53, 54]. Several factors contributed to the technological crisis that resulted. First, to produce smaller features than were available at the time using 405-nm UV irradiation, it became necessary to work at the shorter 365-nm Hg line and even at lower wavelengths. However, the available energy at those wavelengths from conventional arc lamp light sources is relatively low. This necessitated the use of more sensitive photoresists. The negative-working photoresists of that time did not possess sufficient photosensitivity to meet this requirement. In addition, due to growing environmental restrictions, it was no longer possible to use the organic solvent-based development protocols required to process those negative resists. As an alternative, positive-working photoresists employing photoacid generators such as diaryliodonium salts were developed by workers at IBM [55, 56]. The first version of the photolithographic resins that were developed is shown in Equation (25.14). The chemistry used was termed “chemical amplification” and involves the photoacid-catalyzed deblocking reaction of poly(4-*t*-butoxycarbonyloxystyrene) (**X**). The products of this deblocking reaction are carbon dioxide, isobutene, and poly(4-hydroxystyrene) (**XI**). Carbon dioxide and isobutene are gases, while poly(4-hydroxystyrene) can be dissolved in aqueous basic solutions of tetra-*n*-butylammonium hydroxide. Since

under imagewise exposure, the polymer is rendered base-soluble and selectively removed in the irradiated zones, it is a positive photoresist. Many generations of this chemistry have been developed and optimized over the course of the past 25–30 years. The present high-performance lithographic photoresists, which allow imaging of features in the 15- to 32-nm wavelength range, still rely on this same basic photoacid deblocking chemistry. The diaryliodonium salts used in such photolithographic systems have also undergone considerable development and optimization for this demanding application. The cation of the diaryliodonium salt must be designed to be soluble in the photoresist polymer. This can be a significant challenge since many advanced photoresist polymers are now based on fluorine-containing monomers and the inherent solubility of ionic species such as diaryliodonium salts in such materials is low. To overcome this problem, diaryliodonium salts are fitted with various fluorinated and nonfluorinated substituents on the aromatic rings. The requirements with respect to the acid strength are considerably lower for the deblocking chemistry shown in Equation (25.14) than for cationic photopolymerizations. Alkyl sulfonic acids and perfluoroalkylsulfonic acids (H° values -12 to -14) are sufficiently strong to efficiently carry out the deblocking chemistry. In most cases, diaryliodonium salts bearing long chain perfluoroalkanesulfonate anions are used since the resulting acids are soluble in the photoresist and have both a low volatility and low diffusion rates in the photopolymer. The combination of these properties contributes to good resolution and edge control in the final developed photoresist. At the present time, triarylsulfonium salt photoacid generators have largely displaced diaryliodonium salts from this application due to their higher thermal stability.



The importance of this contribution for development in high-performance micro-lithography cannot be overstated. It is safe to say that it is highly unlikely that modern microelectronic technology would be possible without both the discovery of photoacid generators such as diaryliodonium salts and their implementation in positive photoresists such as poly(*t*-butoxycarbonyloxystyrene).

25.5.2 High-Performance Negative Photoresists

High-performance negative-working photoresists are obtained when oligomers or polymers bearing cationically polymerizable functional groups are exposed in an imagewise fashion to UV irradiation in the presence of a diaryliodonium salt

25.5.3 Three-Dimensional Imaging Applications For Photoacid Generators

Three-dimensional imaging has become an area of very rapid growth for the use of diaryliodonium salt photoacid generators [57, 58]. There are several different technologies for the production of solid objects that are classified under various names including “3D imaging,” “rapid prototyping,” or the more recent but less accurate term “additive manufacturing.” Only three of these technologies will be discussed in this chapter. They are stereolithography, digital imaging, and 3D inkjet printing. All three technologies employ CAD–CAM engineering design to create a 3D computer image of an object that is to be translated into a corresponding 3D solid plastic object. Similarly, all three technologies rely on the layer-by-layer deposition and the photopolymerization of a “photopolymer” consisting of liquid reactive monomers and/or oligomers together with a photoinitiator to create the solid object. Finally, all three technologies utilize diaryliodonium salts as cationic photoinitiators and epoxy monomers and oligomers in the imaging process. Epoxide resins and cationic photoinitiators are used primarily because their low inherent volume shrinkage on photopolymerization allows the construction of 3D solid objects with high fidelity and low distortion. The excellent mechanical properties, solvent and thermal resistance, and good photoresponse are additional benefits that the cationic cure of epoxy photopolymers brings to these applications. Since the chemistry involved in 3D imaging is essentially the same as utilized in photoinitiated cationic polymerizations, in general, the same considerations as discussed previously with respect to the structure of cation and anion of the diaryliodonium salt are applied here as well.

Stereolithography is the first and oldest of the 3D imaging technologies. As practiced by 3D Systems, Inc., the computer generated CAD–CAM image is cut by the computer into thin slices and each slice is written onto the surface of a liquid photopolymer contained in a bath using a highly focused laser beam. The first image is written onto a movable stage submerged just below the surface of the liquid photopolymer and after it is written, the stage is lowered into the bath by an increment equal to the thickness of the next layer to be written. The photopolymer flows over the first layer, and the second layer is written. This process is repeated until the entire solid object is written. Then the stage is raised out of the bath revealing the entire solid plastic object. Stereolithography is capable of producing a wide range of highly complex 3D objects with fine detail and functionality. Using this technique, the models shown in Figure 25.6 were produced by photoinitiated cationic polymerization using epoxy–silicone monomers with diaryliodonium salt photoinitiators.

Digital imaging, invented by EnvisionTec, Inc., resembles stereolithography in some of its elements. In this method, the image of an entire layer is projected through a window and onto a thin layer of photopolymer in contact with the stage. Then the stage is moved incrementally and fresh photopolymer allowed to flow into the space between the window and the first image. The image of the next layer is projected through the window, and the process is repeated until the entire solid object is generated. In Figure 25.7 is shown a prototype tissue scaffold that was produced using the digital imaging technique.

In 3D inkjet printing, the photopolymer is deposited onto the surface of a movable stage using an inkjet printhead. Each printed layer is hardened with UV light, and then the next layer is printed on the top of the first one and so on. This simple process is



FIGURE 25.6 Stereolithographic models produced using epoxy-silicone monomers.

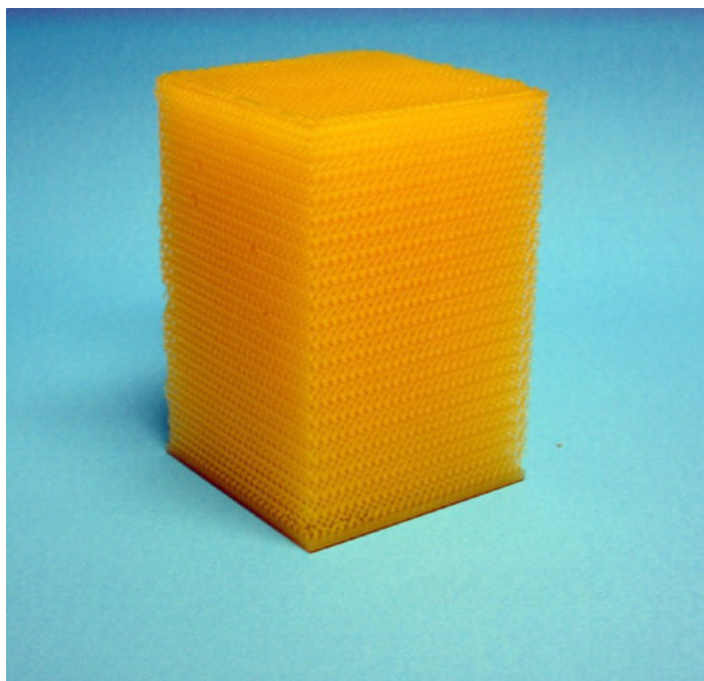


FIGURE 25.7 Tissue scaffold produced using digital imaging.

surprisingly versatile and remarkably precise in generating solid objects with a high degree of fidelity. Moreover, with the simultaneous use of several printheads, solid objects composed of several different materials can be constructed. A leader in 3D inkjet printing is the Objet Division of the Stratasys Corporation. Some typical examples of 3D printed objects that were constructed using diaryliodonium salts are shown in Figure 25.8.

Three-dimensional imaging was initially developed to provide a rapid and low-cost means for the fabrication of engineering models and prototypes. At the present

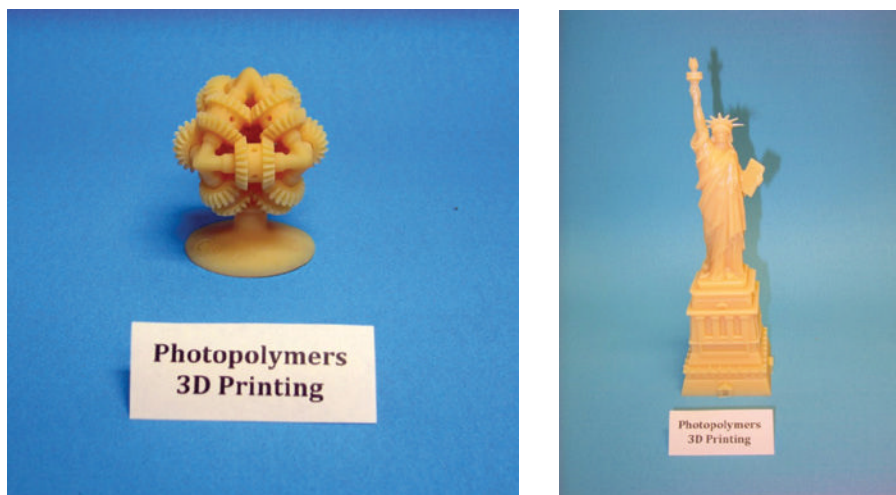


FIGURE 25.8 Examples of 3D printed objects.

time, this is still the one of the major applications for the use of the technology. Rapid prototyping using 3D imaging has revolutionized engineering design in the aerospace, automotive, and machine parts industries by significantly shortening the development time by rapidly providing accurate working models. In the meantime, the range of applications of 3D imaging has expanded rapidly and enormously and the list of new areas for the use of this technology continues to grow. Only a few other representative examples will be discussed here. Digital imaging has made a very large impact in the way in which molds for investment casting are fabricated. This, in turn, has allowed for the design and rapid fabrication of custom metal machine parts including gears, dental implants, watch parts, fasteners, and jewelry. In a very different application, stereolithography is being employed by Align Technology, Inc., for the fabrication of personalized orthodontic retainers used to straighten and correct teeth position and alignment. Three-dimensional inkjet printing as practiced by Objet-Stratasys provides low-cost equipment for the production of manufacturing models for appliances, toys, complex automobile parts, manufacturing equipment, dental aligners, and architectural models to name a few applications.

25.6 SUMMARY

Diaryliodonium salt photoacid generators are latent, highly photosensitive sources of strong protonic acids. These photoacid generators are available as well-characterized solid, crystalline compounds from a number of commercial sources. They are used as efficient photoinitiators in cationic epoxide ring-opening crosslinking polymerizations and are employed widely for use in UV-curable coatings for metals, glass, and plastics. They also find major uses as pressure-sensitive adhesives, structural adhesives, and in printing inks as well as in many other applications. A rapidly growing area for the use of diaryliodonium salts in photopolymerizations is their use in 3D imaging

technology. Diaryliodonium salt photoacid generators have played a major role in the development of high-performance positive photoresists for the commercial production of integrated circuits and will continue to do so far into the future.

REFERENCES

- [1] Banks DF. Organic polyvalent iodine compounds. *Chem Rev* 1965;66:243–264.
- [2] Crivello JV, Lam JHW. Photosensitized cationic polymerizations using dialkylphenacyl-sulfonium and dialkyl(4-hydroxyphenyl)sulfonium salt photoinitiators. *J Polym Sci Symp* 1976;56:383–393.
- [3] Crivello JV, Lam JHW. Diaryliodonium salts. A new class of photoinitiators for cationic polymerization. *Macromolecules* 1977;10:1307–1315.
- [4] Crivello JV. Photoinitiated cationic polymerization. In: Pappas SP, editor. *UV Curing: Science and Technology*. Stamford: Technology Marketing Corp.; 1978. p 24–77.
- [5] Crivello JV. Photo and thermal catalysts for cationic polymerization. In: Brunelle DJ, editor. *Ring-Opening Polymerization*. Munich: Hanser; 1993. p 157–196.
- [6] Sandin RB. Organic compounds of polyvalent iodine. *Chem Rev* 1943;32:249–276.
- [7] Olah GA. *Halonium Ions*. New York: Wiley; 1975. p 55–88.
- [8] Koser GF. The chemistry of the functional groups, suppl. D. In: Patai S, Rappoport Z, editors. *The Chemistry of Halides, Pseudo-halides and Azides*. New York: Wiley; 1983. p 1265–1351.
- [9] Hartmann C, Meyer V. Ueber eine neue Klasse jodhaltiger, stickstofffreier organischer Basen. *Chem Ber* 1894;27:426–432.
- [10] Dektar JL, Hacker NP. Photochemistry of diaryliodonium salts. *J Org Chem* 1990;55:639–647; Comparison of the photochemistry of diarylchloronium, diarylbromonium, and diaryliodonium salts. *J Org Chem* 1991;56:1838–1844.
- [11] De Voe RJ, Sahyun MRV, Serpone M, Sharma DK. Transient intermediates in the photolysis of iodonium cations. *Can J Chem* 1987;65:2342–2349.
- [12] Timpe HJ, Schikowsky VJ. Investigations on photolysis of diaryliodonium salts. *J Prakt Chem* 1989;331:447–452.
- [13] Pappas SP, Gatechair LR. Photoinitiation of cationic polymerization. III. Photosensitization of diphenyliodonium and triphenylsulfonium salts. *Proceedings of Society of Photographic Sciences and Engineering*. New York: Wiley; 1982. p. 46–50.
- [14] Baumann H, Timpe HJ, Böttcher H. Initiatorsysteme fuer kationische Photopolymerisationen. *Z Chim* 1983;23 (3):102–104.
- [15] Crivello JV, Lam JHW, Volante CN. Photoinitiated cationic polymerization using diaryliodonium salts. *ACS Ctg Plast Prepr* 1977;37 (2):4–5.
- [16] Crivello JV. The discovery and development of onium salt cationic photoinitiators. *J Polym Sci, Part A: Polym Chem* 1999;37 (23):4241–4254.
- [17] Gatechair LR, Pappas SP. Photoinitiation of cationic polymerization. IV. Direct and sensitized photolysis of aryl iodonium and sulfonium salts. *Proc Org Ctg Appl Polym Sci Div* 1982;46:707–708.
- [18] Crivello JV, Lam JHW. Dye sensitized photoinitiated cationic polymerization. *J Polym Chem Part A Polym Chem* 1978;16:2441–2451.

- [19] Crivello JV, Jang M. Anthracene electron-transfer photosensitizers for onium salt induced cationic photopolymerizations. *J Photochem Photobiol A Chem* 2003;159:173–188.
- [20] DeVoe RJ, Sahyun MRV, Schmidt E. Electron transfer sensitized photolysis of onium salts. *Can J Chem* 1988;66 (2):319–324.
- [21] Crivello JV. Photosensitization of onium salt initiated cationic photopolymerization by carbazole monomers, polymers and oligomers. *Photoinitiated Polymerization. ACS Symp Ser* 2003;847:219–229.
- [22] Hua Y, Crivello JV. Development of Polymeric Photosensitizers for Photoinitiated Cationic Polymerization. *J Polym Chem Part A Polym Chem* 2000;38:3697–3709.
- [23] Gomurashvili Z, Crivello JV. Phenothiazine photosensitizers for onium salt photoinitiated cationic polymerization. *J Polym Chem Part A Polym Chem* 2001;39:1187–1197.
- [24] Crivello JV. A new visible light sensitive photoinitiator system for the cationic polymerization of epoxides. *J Polym Sci Part A Polym Chem* 2008;46 (11):3820–3829.
- [25] Manivannan G, Fouassier JP. Primary processes in the photosensitized polymerization of cationic monomers. *J Polym Sci Part A Polym Chem* 1991;29:1113–1124.
- [26] Fouassier JP, Burr D, Crivello JV. Time-resolved laser spectroscopy of the sensitized photolysis of iodonium salts. *J Photochem Photobiol A Chem* 1989;49:317–324.
- [27] Bulut U, Gunbas GE, Toppare L. A quinoxaline derivative as a long wavelength photosensitizer for diaryliodonium salts. *J Polym Sci Part A Polym Chem* 2010;48:209–213.
- [28] Crivello JV, Bulut U. Curcumin: A naturally occurring long-wavelength photosensitizer for diaryliodonium salts. *J Polym Sci Part A Polym Chem* 2005;43:5217–5231.
- [29] Ledwith A. Possibilities for promoting cationic polymerization by common sources of free radicals. *Polymer* 1978;19:1217–1220.
- [30] Yagci Y, Borbely J, Schnabel W. On the mechanism of acylphosphine oxide promoted cationic polymerization. *Eur Polym J* 1989;25 (2):129–131.
- [31] Klemm E, Flammersheim H-J, Martin R, Hörhold H-H. Stepwise epoxide/methacrylate photopolymerization with diaryl iodonium salt photoinitiators. *Angew Makromol Chem* 1985;135:131–138.
- [32] Crivello JV, Liu S. Photoinitiated cationic polymerization of epoxy alcohol monomers. *Chem Mater* 1998;10 (11):3724–3731.
- [33] Mowers WA, Crivello JV, Rajaraman S. Free radical acceleration of photoinitiated cationic polymerization by a hybrid system. *RadTech Report* 2000 March/April;14:34–41.
- [34] Hua Y, Crivello JV. Synergistic free radical effects in photoinitiated cationic polymerization. *Photoinitiated Polymerization*. In: Belfield KD, Crivello JV, editors. *ACS Symposium Series* 847; Washington, DC: ACS; 2003. p. 178–201.
- [35] Gandini A, Cheradame H. *Cationic Polymerization, Advances in Polymer Science* 34/35. New York: Springer Verlag; 1980.
- [36] Goethals EJ, editor. *Cationic Polymerization and Related Processes*. New York: Academic Press; 1984.
- [37] Kennedy JP. *Cationic Polymerization of Olefins: A Critical Inventory*. New York: Wiley-Interscience; 1975.
- [38] Penczek S, Kubisa P, Matyjaszewski K. *Cationic Ring-Opening Polymerization of Heterocyclic Monomers; Advances in Polymer Science*. Volume 37, Berlin: Springer-Verlag; 1980.
- [39] Penczek S, Kubisa P, Matyjaszewski K. *Cationic Ring-Opening Polymerization Part II: Synthetic Applications; Advances in Polymer Science*. Volume 68/69, Berlin: Springer-Verlag; 1985.

- [40] Crivello JV. Structure-Reactivity Relationships of Epoxide Monomers in Photoinitiated Cationic Polymerization (Chapter 27). In: Fouassier JP, Allonas X, editors. *Basics and Applications of Photopolymerization Reactions*. Volume 2, Kerala: Research Signpost; 2010. p 101–117.
- [41] Olah GA, Surya Prakash GK, Sommer J. *Superacids*. New York: Wiley; 1985.
- [42] Eckberg RP, LaRochelle RW. Ultraviolet curable epoxy silicone coating compositions. U.S. Patent 4,279,717. July 21, 1981. To G.E. Corp.
- [43] Eckberg RP. Ultraviolet curable epoxy silicone coating compositions. U.S. Patent 4,977,198. December 11, 1990. To G.E. Corp.
- [44] Crivello JV, Lee JL. New epoxy-functional silicone monomers for cationic UV curing. Proceedings of Radtech '90 North America Conference, Chicago. March 25, 1990. p. 432.
- [45] Crivello JV, Lee JL. The synthesis, characterization, and photoinitiated cationic polymerization of silicon-containing epoxy resins. *J Polym Sci, Part A: Polym Chem* 1990;28:479–503.
- [46] Weinmann W, Thalacker C, Guggenberger R. Siloranes in dental composites. *Dental Mater* 2005;1:66–74.
- [47] Donhowe E, Brady R. Cationic UV curing technology and metal packaging. *RadTech Rept* 1993;7 (2):18–23.
- [48] Crivello JV, Mao Z. Preparation and cationic photopolymerization of organic–inorganic hybrid matrixes. *Chem Mater* 1997;9 (7):1562–1569.
- [49] Versace DL, Belon C, Croutxe-Barghorn C. Concomitant organic–inorganic UV-curing catalyzed by photoacids. *Macromolecules* 2008;41 (20):7390–7398.
- [50] Sangermano M, Voit B, Sordo F, Eichhorn KJ, Rizza G. High refractive index transparent coatings obtained via UV/thermal dual-cure process. *Polymer* 2008;48 (8):2018–2022.
- [51] Crivello JV, Mao Z. Cationic photopolymerization of organic-inorganic hybrid matrices. *Chem Mater* 1997;9 (7):1554–1561.
- [52] Crivello JV. UV curable composition of a thermosetting condensation resin and group VIA onium salt. U.S. Patent 1,102,687. 1978 Jul 25. To G.E. Corp.
- [53] Bowden MJ. Introduction to microlithography” In: Thompson LF, Willson CG, Frechet JMJ, editors. *ACS Symp. Ser. 266*. Washington, D.C.: American Chemical Society; 1984. p. 39–124.
- [54] Willson CG. Organic resist materials. In: Thompson LF, Willson CG, Bowden MJ. *ACS Symp. Ser. 219*. Washington, DC: American Chemical Society; 1983. p. 87–160.
- [55] Ito H, Willson CG, Frechet JMJ. Positive- and negative-working resist compositions with acid generating photoinitiator and polymer with acid labile groups pendant from polymer backbone. SPE Regional Technical Conference, November 1982. New York: Ellenville; 1982.
- [56] Frechet JMJ, Eichler E, Ito H, Willson CG. Poly(p-tert-butoxycarbonyloxystyrene): a convenient precursor to p-hydroxystyrene resins. *Polymer* 1983;24 (8):995–1000.
- [57] Jacobs PF. *Stereolithography and Other RP&M Technologies*. New York: American Society of Mechanical Engineers; 1995.
- [58] Jacobs PF. *Rapid Prototyping and Manufacturing, Fundamentals of Stereolithography*. Dearborn: Society of Manufacturing Engineers; 1992.

POLARIZING FILMS

BART KAHR¹ AND KEVIN M. KNOWLES²

¹*Department of Chemistry and Molecular Design Institute, New York University,
New York, NY, USA*

²*Department of Materials Science and Metallurgy, University of Cambridge,
Cambridge, UK*

26.1 INTRODUCTION

By the middle of the nineteenth century, the British Empire had expanded across the globe and into many tropical places burdened by malaria. The toxicology of the anti-malarial drug quinine was studied widely in the interest of urgent national priorities. While investigating the effects of quinine in dogs, the toxicologist Dr. William Bird Herapath and his assistant accidentally mixed tincture of iodine with the urine of a dog that had ingested large quantities of quinine. Instantly, metallic crystallites precipitated from the urine. These iodine-rich crystals would transform the science and practice of optics because ultimately they could be fashioned into large-aperture, linear polarizers of visible light.

Electromagnetic radiation consists of sets of transverse electromagnetic waves in which the electric and magnetic field vectors **E** and **H** are mutually perpendicular and lie in a plane normal to the wave vector **k** defining the direction in which the light propagates [1]. Visible light—that detected by the human eye—has a wavelength between 400 and 700 nm [2]. Wavelengths just shorter than 400 nm fall in the ultra-violet part of the spectrum of electromagnetic radiation, while wavelengths slightly longer than 700 nm fall within the infrared part of this spectrum [2]. Light in which **E** oscillates in one plane as it propagates is said to be plane-polarized or linearly polarized. Incoherent light, such as sunlight, consists of a series of light waves whose electric and magnetic field vectors fluctuate continuously and at random; it is

unpolarized. For many applications in science and engineering, there is a need to select the polarization of light from a particular light source so that it is plane-polarized. This is a key requirement for the identifications of minerals and rocks from thin sections with a petrological microscope [3], and it is necessary for the use of liquid crystals in displays [2].

Optical accessories that select a particular polarization of light are known as polarizers. One of the first devices for producing plane-polarized light was the Nicol prism invented by the Scottish geologist William Nicol, details of which he reported in the October–December 1828 issue of the *Edinburgh New Philosophical Journal* [4]. The Nicol prism makes use of the phenomenon of double refraction first described in calcite by Rasmus Bartholin (Erasmus Bartholinus) in 1669 [1, 5, 6]. Double refraction is a consequence of light propagation in anisotropic media [1, 3, 7, 8]. In an anisotropic crystal, plane-polarized light wave entering a crystal at a general angle is split into two waves whose electric field vectors are polarized at right angles to one another. These vectors are aligned with the refractivity extrema in the plane of the crystal perpendicular to the wave vector in the medium. To make a Nicol prism, a pair of optical quality calcite (CaCO_3) rhombohedra, about three times as long as wide, are shaped, and glued together with Canada balsam [4, 7–9] so as to make a parallelepiped. The crystals are arranged so that light traveling with one of the polarization modes of the first crystal is reflected at the interface between the crystals. The specific orientations of the crystalline components of the Nicol prism and the refractive index of the Canada balsam relative to the refractivity extrema seen by the two waves within the crystal into which the light is shone together ensure that unpolarized light entering the prism and traveling parallel to its length exits the device as plane-polarized light [4, 7, 8].

In some anisotropic crystals, noticeable absorption of one or both of these waves can occur at specific wavelengths. This is the phenomenon of linear dichroism. In the trigonal mineral tourmaline, the absorption of one of these two waves is particularly strong, so that tourmaline is able to polarize light by selective absorption, albeit somewhat inefficiently [1, 8]. This differential absorption is a consequence of the dissymmetry of the environments of the light-absorbing transition metals in tourmaline [10–12]. A tourmaline polarizer is a so-called dichroic filter. If two transparent thin sections of tourmaline are cut so that their c -axes lie parallel to the plane of the thin section and are perpendicular to one another, light passed through one of the thin sections is then almost completely absorbed by the other, so that very little light passes through the pair. In the nineteenth century, such “crossed polars” were fashioned as tourmaline tongs [13], which held anisotropic samples between the arms.

High-quality mineral polarizers such as tourmaline and calcite-based Nicol prisms have been superseded by other methods of producing polarized light, most notably through the use of polarizing polymer films. As Edwin Land, inventor of the polarizing sheet, noted in his 1951 review [14], iodine played a pivotal part in the development of these films. Today, while both iodine and iodine-free polarized films are widely available, it is still the case that those incorporating iodine are regarded as being superior in terms of transmittance and polarization efficiency for the visible

part of the electromagnetic spectrum [15]. Iodine has played an outstanding role in the production of polarized light.

26.2 IODINE AND THE DEVELOPMENT OF POLARIZED FILM

The origin of the commercial polarizing film is found in Herapath's 1852 paper in *Philosophical Magazine* [16]. Herapath showed that brilliant emerald green plates could precipitate from warm, concentrated acetic acid solutions of disulfates of a variety of alkaloids such as quinine, $C_{20}H_{24}N_2O_2$, and cinchonine, $C_{19}H_{22}N_2O$, to which elemental iodine was then added. Herapath used tourmaline thin sections as well as a Nicol prism to demonstrate the remarkable polarizing effect of these new crystalline compounds. As shown in Figure 26.1, where the crystals cross at 90° with respect to one another, Herapath noted that no light was transmitted. The pair, he said, "was black as midnight." Herapath was able to show that his synthetic crystals were at least five times more effective than the best tourmaline crystals in transmitting a polarized ray of light. He also showed that only iodine, sulfuric acid, and quinine were required to synthesize these crystals, conjecturing that he had produced

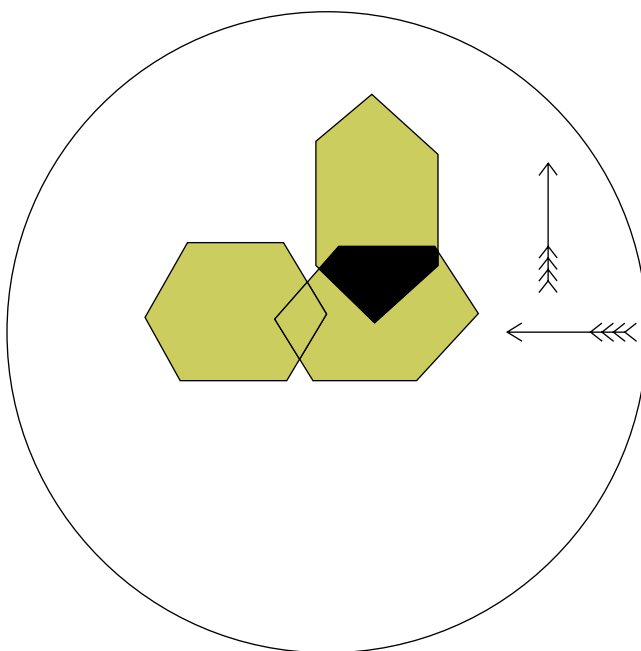


FIGURE 26.1 Overlapping hexagonal-shaped crystals of herapathite crystals viewed in transmitted, unpolarized white light [16]. *Arrows* denote the orientation of the absorbing direction in the crystals. Extinction is apparent when crystals overlap and their long axes are orthogonal to one another. Courtesy of Taylor and Francis and *Philosophical Magazine*. (See insert for color representation of the figure.)

an iodide of the disulfate of quinine. The Austrian mineralogist Haidinger proposed the name herapathite in 1853 as shorthand for Herapath's multicomponent compound [17–19]. That same year, Herapath also adopted this name and promoted herapathite crystals as “artificial tourmalines,” having succeeded in growing thin plates of herapathite 1.5 cm^2 [20]. Herapath claimed in this 1853 paper that “there is no doubt tourmaline and Nichol's [sic] prisms will be soon superseded by these new crystals,” because of the cost of the mineral polarizers in comparison with Herapath's perception of the cost of herapathite: “there is not the least doubt that before long these splendid and useful crystals will be offered for sale by opticians at as many shillings as tourmaline now cost pounds,” he concluded [20]. Had this been achievable, it would surely have been a boon, given the acute shortage of Iceland spar calcite that would develop later in the nineteenth century through overmining of the Helgustaðir quarry in the Eastern fjords of Iceland, from which almost all large, clear prisms of optical calcite were obtained at that time [21]. Haidinger [22] and Valentin [23] also expressed their keen interest in replacing tourmaline and calcite polarizers by herapathite plates. Unfortunately, however, Herapath's expectation was hard to realize because of the difficulty in growing sufficiently large single herapathite crystals [14].

Some two decades after Herapath's work, Jörgensen deduced that the chemical formula of herapathite was $4(\text{C}_{20}\text{H}_{24}\text{N}_2\text{O}_2)$, $3(\text{H}_2\text{SO}_4)$, 2HI , I_4 , $6(\text{H}_2\text{O})$. His 1869 doctoral thesis on polyiodides of alkaloids was followed by a series of papers showing that herapathite was one of a family dichroic polyiodide salts that could be prepared from alkaloids and other organic bases including quinidine, cinchonidine, and even aniline and toluidene [24–27]. In the 1930s, West showed that herapathite has an orthorhombic crystal structure with an unusually large unit cell: $a=15.15\text{ \AA}$, $b=19.24\text{ \AA}$, and $c=33.30\text{ \AA}$ [28]. However, it has only been in recent years that the crystal structure of herapathite has been determined: Kahr et al. showed that herapathite crystallizes in the space group $P2_12_1$ [29]. The room temperature structure gave cell parameters of $a=15.2471(3)\text{ \AA}$, $b=18.8854(4)\text{ \AA}$, and $c=36.1826(9)\text{ \AA}$. These values resemble those reported by West, but are significantly different. This is easily understood given the complexity of the formula unit. The herapathite recently analyzed contains an acetic acid molecule in addition to the components identified by Jörgensen. It is quite likely that there are several distinct solvates/salts with slightly varying composition that have traditionally fallen under the name “herapathite.” In the refined crystal structure, iodine is wholly in the form of triiodide anions lying roughly parallel to b , the absorbing axis. A view of the crystal structure is shown in Figure 26.2, in which there are three I_3^- anions aligned within a channel created by five protonated quinines. The sulfate counterions and included solvent have been removed for clarity. The large optical anisotropy found in herapathite has recently been shown by density functional theory to arise from transitions between the molecular levels of the I_3^- chains [30].

Despite the difficulties in growing large single crystals of herapathite in the nineteenth century, Ferdinand Bernauer succeeded in the 1930s in preparing sheets of herapathite crystals up to 1 dm^2 for commercial applications such as microscope polarizers [19, 31–37]. Bernauer's polarizers were manufactured in Jena by the German photographic firm Zeiss under the trade name Bernotar or Herotar (Fig. 26.3).

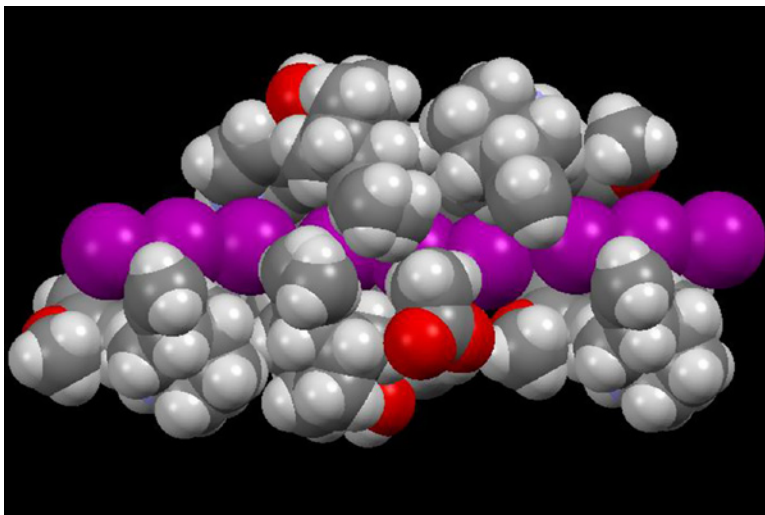


FIGURE 26.2 Three purple triiodide ions lined up along the b -axis (horizontal) within a channel created by five quinine molecules in herapathite. Molecules of solvation (water and acetic acid) as well as sulfate counterions have been removed for clarity. (See insert for color representation of the figure.)



FIGURE 26.3 Examples of Herotar and Bernotar filters from 1936 and 1937. Note the recognition of Prof. Bernauer in the instructions (“Gebrauchsanweisung”) as the inventor of these photographic filters. Courtesy of Volkmar Kleinfeldt. (See insert for color representation of the figure.)

In these polarizers, the herapathite single crystals were sandwiched between plates of glass. The most practical use of herapathite, and the first really large-aperture linear polarizer, arose as a consequence of Edwin Land's reading Sir David Brewster's 1858 book on kaleidoscopes, in which herapathite was acknowledged as the best polarizer for the eyepiece of a kaleidoscope [38]. Land left Harvard College in 1926 after his freshman year, moved to New York City, and subsequently invented polycrystalline herapathite polarizers consisting of nanocrystals aligned within polymer sheets [14]. At first, Land aligned ground herapathite particles in a solution of nitrocellulose lacquer with a 10,000 gauss (1 tesla) magnetic field. He obtained strong dichroism in this way, demonstrating the principle. This was to lead ultimately to the 1933 U.S. patent 1,918,848 describing the first production of a colloidal mass of herapathite crystals extruded into a sheet and dried to produce "a polarizing body comprising a set suspending medium having herapathite particles dispersed and immovably embedded therein with their polarizing axes oriented to be in substantial parallelism, the set suspension being adapted to retain its polarizing properties independent of external support" [39].

Land's invention was soon marketed as "Polaroid" which could be fabricated into very large sheets. In his 1938 article reviewing these new inexpensive polarizers, Grabau from Land's research laboratories in Boston stated that "sheets (of Polaroid) thirty inches wide have long been on public display" [40] (e.g., see Figure 26.4). He noted that while the usefulness of Polaroid sheets was limited to visible light, its degree of polarization within this range was impressive, greater than 99.6% for light of wavelengths between 480 and 680 nm. Grabau went on to describe the use of Polaroid to eliminate glare in sunglasses and photographic filters, for petrographic microscopy, and in photoelastic testing, as well as for use in three-dimensional (3D) glasses.

Despite the evident success of herapathite films, later termed the *J* polarizer by Land [14], it was apparent that there were innumerable chemistries that could be harnessed for making sheet polarizers. The *J* polarizer was imperfect because it scattered light in part. Work in the Land–Wheelwright Laboratories, renamed the Polaroid Corporation in 1937, produced a number of modifications to the *J* polarizer [14]. The members of the family of polarizers described by Land in U.S. patent 2,237,567 granted in 1941 are based on staining or dyeing sheets of stretched polyvinyl alcohol, PVA [41]. The preferred method described in this patent was that of absorbing iodine into a previously stretched and cooled sheet of PVA. The resulting material was termed the *H* polarizer by Land [14], and it quickly replaced the *J* polarizer as "Polaroid." Uniaxial stretching of the PVA sheet produced a preferred alignment of PVA molecules along the direction of elongation. Iodine molecules absorbed into the PVA film align preferentially with this direction causing it to be the one along which light from an unpolarized light source is absorbed [14]. Subsequent work on the structure of the PVA–iodine system has produced a picture consistent with a partially crystalline arrangement of PVA molecules with PVA–iodine complexes formed in the amorphous PVA regions [42–44]. Two other non-iodine-based methods of producing polarized sheet material referred to in Land's 1941 patent are the use of dyes and the staining of PVA through the reduction of dissolved metallic salts, that is, through the impregnation into the PVA sheet of nanoscopic

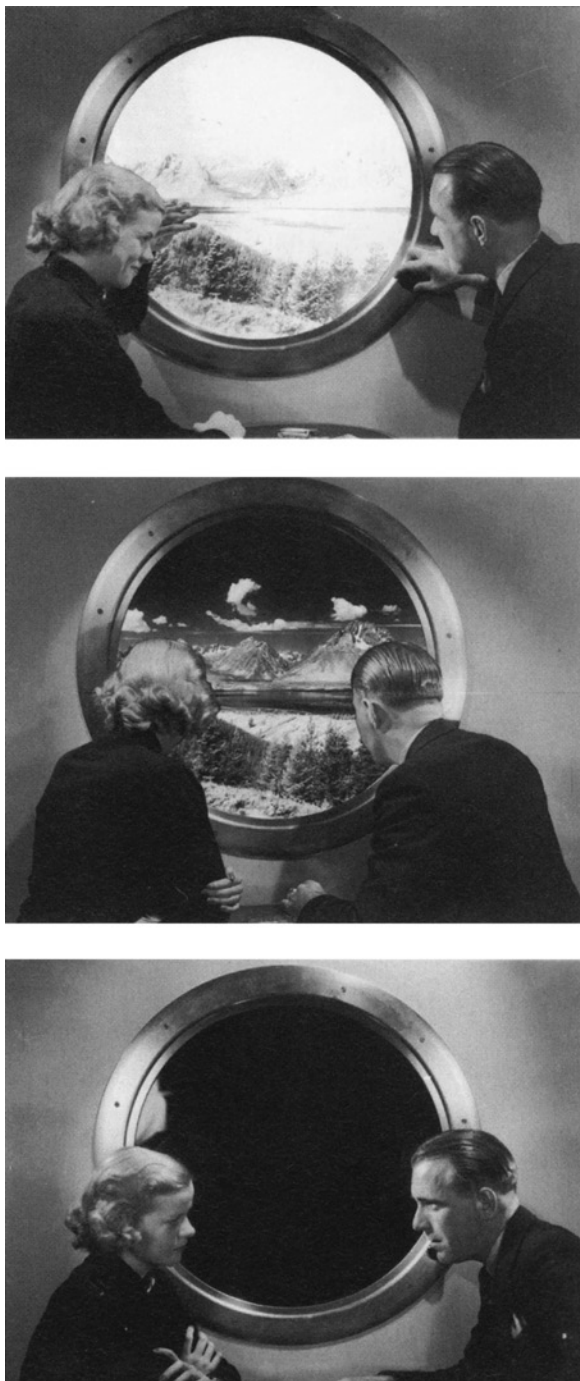


FIGURE 26.4 Rotating *H*-sheet train windows, Los Angeles. Polaroid Archives, Harvard University.

metallic needles. Remarkably, these methods of producing polarizing films specified in Land's 1941 patent are still found in contemporary commercial polarizers. Later generations of Polaroid had improved resistance to heat and moisture. This was achieved by immersion in a solution of concentrated boric acid, as specified in U.S. patent Re. 23,297 [45]. The boric acid acted as a crosslinking agent in the PVA film, causing it to have a higher glass transition temperature and a reduced tendency to crystallize [46]. Intriguingly, following the invention of the *H* polarizer, Zeiss continued to market polarizing camera filters 5 cm in diameter under the name Bernotar. On dismantling a Bernotar camera filter made in the late 1940s, one of us (BK) found that Zeiss was then using polymer sheets as the polarizing material, as opposed to large herapathite single crystals.

26.3 MODERN POLARIZING FILMS

Iodine is no longer critical to the preparation of polarizers, of which there are now innumerable types depending on the wavelengths of interest and the applications. These are reviewed authoritatively by Bennett [47]. Today, calcite polarizing prisms tend to be of the Glan-type named after Paul Glan [48]. These prisms have the optical axes of the calcite in the entrance and exit planes in order to maximize the refractivity difference between the two rays in the birefringent components. Wire-grid polarizers transmit the *E* field orthogonal to closely spaced parallel wires, whereas the orthogonal component is dissipated. Such materials have recently been reinvented as so-called plasmonic polarizers, sometimes integrated with solid-state laser gain media. The phenomena of diffraction, interference, scattering, and nonnormal reflection and transmission have all been exploited to fashion practical light polarizers. The central role of iodine is waning. At the same time, the promise of plastic electronics has inspired an enormous effort in the synthesis of single molecular crystal films [49]. As these crystal growth techniques are refined, perhaps it may become possible one day to realize the dream of growing enormous plates of herapathite, large enough to cover car windscreens.

REFERENCES

- [1] Lipson SG, Lipson H. *Optical Physics*. Cambridge: Cambridge University Press; 1969.
- [2] Tilley RJD. *Colour and Optical Properties of Materials*. Chichester: John Wiley and Sons; 2000.
- [3] Battey MH. *Mineralogy for Students*. 2nd ed. London: Longman; 1981.
- [4] Nicol W. On a method of so far increasing the divergency of the two rays in calcareous-spar, that only one image may be seen at a time. *Edinburgh New Philos J* 1828;6:83.
- [5] Bartholinus E. *Experimenta Crystalli Islandici Disdiaclastici quibus mira et infolita Refractio detegitur*. Copenhagen: Danielis Paulli; 1669.
- [6] Kahr B, Claborn K. The lives of Malus and his bicentennial law. *ChemPhysChem* 2008;9:43.

- [7] Gay P. *An Introduction to Crystal Optics*. London: Longmans; 1967.
- [8] Dana ES, Ford WE. *A Textbook of Mineralogy*. 4th ed. New York: John Wiley and Sons; 1932.
- [9] Mills AA. Canada balsam. *Ann Sci* 1991;48:173.
- [10] Faye GH, Manning PG, Nickel EH. The polarized optical absorption spectra of tourmaline, cordierite, chloritoid and vivianite: Ferrous-ferric electronic interaction as a source of pleochroism. *Am Miner* 1968;53:1174.
- [11] Wilkins RWT, Farrell EF, Naiman CS. The crystal field spectra and dichroism of tourmaline. *J Phys Chem Solids* 1969;30:43.
- [12] Townsend MG. On the dichroism of tourmaline. *J Phys Chem Solids* 1970;31:2481.
- [13] Calas G. Tourmaline research: Unlocking Ali Baba's cave. *Elements* 2011;7:291.
- [14] Land E. Some aspects of the development of sheet polarizers. *J Opt Soc Am* 1951;41:957.
- [15] Chang JB, Yuk SB, Park JS, Kim JP. Dichroic and spectral properties of anthraquinone-based azo dyes for PVA polarizing film. *Dye Pigm* 2011;92:737.
- [16] Herapath WB. On the optical properties of a newly-discovered salt of quinine, which crystalline substance possesses the power of polarizing a ray of light, like tourmaline, and at certain angles of rotation of depolarizing it, like selenite. *Philos Mag Series 4* 1852;3:161.
- [17] Haidinger W. Ueber die von Hrn. Dr. Herapath und Hrn. Prof. Stokes in optischer Beziehung untersuchte Jod-Chinin-Verbindung. *Ann Phys Chem* 1853;165:250.
- [18] Haidinger W. On the iodo-quinine compound, investigated in its optical relations by Dr. Herapath and Professor Stokes. *Philos Mag Series 4* 1853;6:284.
- [19] Knowles KM. Herapathite – the first man-made polarizer. *Philos Mag Lett* 2009;89:745.
- [20] Herapath WB. On the manufacture of large available crystals of sulphate of iodo-quinine (herapathite) for optical purposes as artificial tourmalines. *Philos Mag Series 4* 1853;6:346.
- [21] Kristjánsson L. *Iceland Spar and its Influence on the Development of Science and Technology in the Period 1780–1930*. 3rd ed. Reykjavik: University of Iceland; 2010.
- [22] Haidinger W. Herapathit-Zangen, geschenkt von Herrn Professor v. Nörrenberg. *Sitzungsber Akad Wiss Wien* 1855;15:82.
- [23] Valentin G. *Die Untersuchung der Pflanzen- und der Thiergewebe in polarisirtem Lichte*. Leipzig: W. Engelmann; 1861.
- [24] Jörgensen SM. Ueber den sogenannten Herapathit und ähnliche Acidperjodide. *J Prakt Chem* 1876;14:213.
- [25] Jörgensen SM. Ueber den sogenannten Herapathit und ähnliche Acidperjodide. *J Prakt Chem* 1876;14:356.
- [26] Jörgensen SM. Ueber den sogenannten Herapathit und ähnliche Acidperjodide. *J Prakt Chem* 1877;15:65.
- [27] Jörgensen SM. Ueber den sogenannten Herapathit und ähnliche Acidperjodide. *J Prakt Chem* 1877;15:418.
- [28] West CD. Crystallography of herapathite. *Am Miner* 1937;22:731.
- [29] Kahr B, Freudenthal J, Phillips S, Kaminsky W. Herapathite. *Science* 2009;324:1407.
- [30] Liang L, Rulis P, Kahr B, Ching WY. Theoretical study of the large linear dichroism of herapathite. *Phys Rev B* 2009;80:art. No. 235132.
- [31] Bernauer F. Ein neuer Weg zur Herstellung von Polarisatoren. *Fortschr Miner* 1930;14:227.
- [32] Bernauer F. Polarisationsvorrichtung. German Patent 547,429. 1932 Mar, 10.
- [33] Bernauer F. Neue Wege zur Herstellung von Polarisatoren. *Fortschr Miner* 1935;19:22.

- [34] Rösch S. Einige Eigenschaften und Anwendungen dichroitischer Flächenpolarisatoren. Fortschr Miner 1937;21:89.
- [35] Haase M. Neue Polarisationsfilter unter Verwendung dichroitischer Kristalle. Z. Techn Physik 1937;18:69.
- [36] Honty L. A multiplication method for the measurement of the absorption of light in thin layers. Časopis pro pěstování matematiky a fysiky 1937;66:152.
- [37] Schumann H, Piller H. Über die Verwendungsmöglichkeit moderner Polarisationsfilter in mineralogischen Mikroskopen. Neues Jahrb Miner Monatshefte 1950, Jahrgang 1950, 1.
- [38] Brewster D. *The Kaleidoscope, its History, Theory and Construction with its Application to the Fine and Useful Arts*. 2nd ed. London: John Murray; 1858. p 122.
- [39] Land EH, Friedman JS. Polarizing refracting bodies. U.S. Patent 1,918,848. 1933 Jul, 18. To Norwich Research Inc.
- [40] Grabau M. Polarized light enters the world of everyday life. J Appl Phys 1938;9:215.
- [41] Land EH. Light polarizer and process for manufacturing the same. U.S. Patent 2,237,567. 1941 Apr, 8. To Polaroid Corporation.
- [42] Haisa M, Itami H. X-ray diffraction study of the polyvinyl alcohol-iodine system. J Phys Chem 1957;61:817.
- [43] Miyasaka K. PVA-Iodine complexes: Formation, structure, and properties. In: Zachmann H-G, editor. *Structure in Polymers with Special Properties*. New York: Springer; 1993. p 91.
- [44] Miyazaki T, Katayama S, Funai E, Tsuji Y, Sakurai S. Role of adsorbed iodine into poly(vinyl alcohol) films drawn in KI/I₂ solution. Polymer 2005;46:7436.
- [45] Hyman M, West CD. Sheetlike light-polarizing complex of iodine and a polyvinyl compound with protective surface boric acid-polyvinyl compound complex. U.S. Patent Re. 23,297. 1950 Nov 28. To Polaroid Corporation.
- [46] Miyazaki T, Takeda Y, Akane S, Itou T, Hoshiko A, En K. Role of boric acid for a poly (vinyl alcohol) film as a cross-linking agent: Melting behaviors of the films with boric acid. Polymer 2010;51:5539.
- [47] Bennett JM. Polarizers, in *Handbook of Optics: Volume I - Geometrical and Physical Optics, Polarized Light, Components and Instruments*, Third Ed. In: Bass M, editor. New York: McGraw-Hill; 2010, Chapter 13.
- [48] Glan P. Ueber einen Polarisator. Carl's Repertorium für Experimental-Physik 1880; 16:570.
- [49] Forrest SR. The path to ubiquitous and low-cost organic electronic appliances on plastic. Nature 2004;428:911.

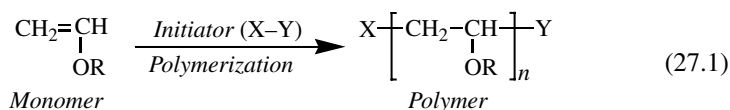
IODINE IN POLYMER SYNTHESIS: AN IMPORTANT ELEMENT FOR PRECISION POLYMERIZATIONS

MITSUO SAWAMOTO

*Department of Polymer Chemistry, Graduate School of Engineering,
Kyoto University, Kyoto, Japan*

27.1 INTRODUCTION

Iodine and its compounds play critical, indispensable, and versatile roles in polymerization and polymer synthesis, perhaps much more important than generally perceived. In chain-growth or addition polymerization of alkenes or vinyl monomers (Eq. 27.1), for example, it indeed dates back to the late nineteenth century that a mixture of molecular iodine and styrene was found to give a viscous solution, particularly under visible light, which is now understood as a cationic polymerization of styrene where iodine is an initiator. Iodine and alkyl iodides are also well-known chain-transfer agents in radical polymerization to reduce, or more positively, adjust polymer molecular weights. In organometallic chemistry, a variety of metal iodides and metal–iodide complexes often catalyze interesting polymerizations by varying mechanisms.



The versatility of iodine and iodides in part stems from the fact that carbon–iodine and iodine–iodine bonds can be cleaved both heterolytically (or ionically) and

homolytically (or radically). As substituents, more specifically, iodine are characterized as (i) weakly electron-withdrawing, (ii) soft or readily polarizable, and (iii) resonance-inducing, and thereby they acts as a Lewis acid (electron acceptor), a good leaving group, and a radical acceptor, among others, depending on monomers and reaction conditions. Because of these dual or multiple characters, *cationic* and *radical* polymerizations are where molecular iodine, alkyl iodide, iodide salts, and metal–iodide complexes find widespread usages and critical functions, including those as *initiators*, *catalysts*, *end-capping agents*, and *chain-transfer agents*, as summarized in Figure 27.1.

In addition to these characteristics and roles, however, the importance of iodine in polymer synthesis has increasingly been recognized in the last two decades when a number of *precision* and *living* polymerizations have extensively been developed around the world. As discussed in the following sections, the roles of iodine and iodine compounds in these precision polymerizations are not only to initiate or affect but to control the reactions as well, and in not a few cases, iodine compounds are so critically important and essential that some of precision polymerizations would not be possible without them.

Iodine: Versatile
An important element in precision polymerizations

- Iodine: mildly electron-withdrawing
resonance-inducing (soft / polarizable)
- ⇒ Good leaving group–initiator (Cationic / Radical)
- ⇒ Good ligand–catalyst (Lewis acid / Metal complex)

● Functions in polymerization

Function	Cationic polymerization	Radical polymerization
Initiator	$(R-I) \xrightarrow{MX_n} R^+ + ^-I-MX_n$	$(R-I) \xrightarrow{ML_n} R^\bullet + I-ML_n$
Catalyst	$R-I \xrightarrow{(MX_n)} R^+ + ^-I-MX_n$ (MX_n : I_2 , ZnI_2 , etc.)	$R-I \xrightarrow{(ML_n)} R^\bullet + I-ML_n$ (ML_n : $FeCpI(CO)_2$, etc.)
End-capping	$P^+ \xrightarrow{(R_4N^+I^-)} P-I$ (Dormant)	$P^\bullet \xrightarrow{(I_2)} P-I$ (Dormant)
Chain transfer		$P^\bullet \xrightarrow{(R-I)} P-I + R^\bullet$ (Dormant)

FIGURE 27.1 Iodine: important and versatile in cationic and radical polymerizations.

This chapter is an updated overview focused on the versatile functions of iodine and its compounds in precision and living polymerizations. Comprehensive reviews are available for both living cationic and living radical polymerizations, along with original papers [1–4]. In particular, Ref. [3] includes reviews published by the author and his coworkers to cover recent advancements up to 2012.

27.2 LIVING POLYMERIZATION AND PRECISION POLYMERIZATION

Chain-growth (addition) polymerization primarily consists of initiation (intermediate formation from an initiator), propagation (chain growth), chain transfer, and termination. While the first two are responsible for generation and formation of polymers, the latter two are major chain-breaking side reactions that reduce polymer molecular weight and deteriorate the primary architecture of the resulting macromolecules. This is why conventional addition polymerizations, however useful and efficient in polymer production they might be, often fail to give precisely controlled and well-defined polymers.

Living polymerization is defined as a chain-growth polymerization free from chain-transfer, termination, and other chain-breaking reactions (Fig. 27.2). Thanks to the absence of these side reactions, the growing species (reaction intermediates) remain active throughout the polymerization, thereby enabling precision control of

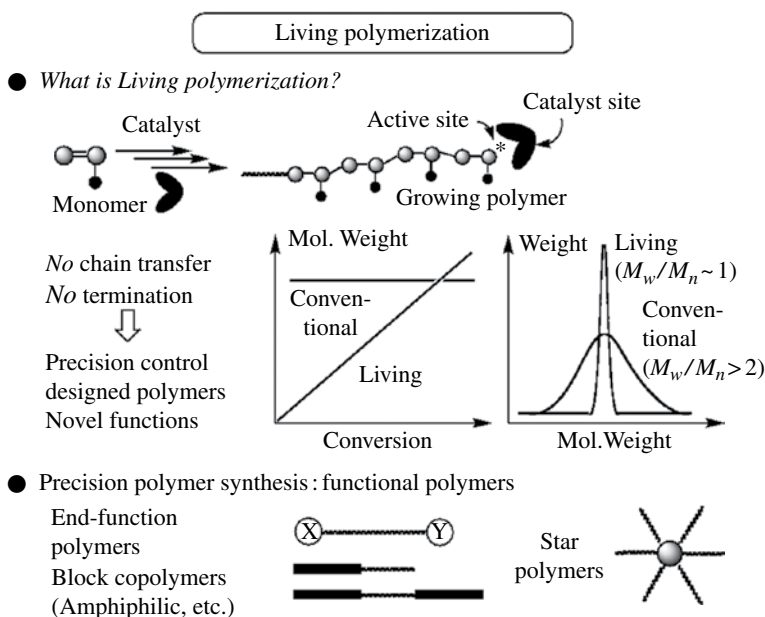


FIGURE 27.2 Living polymerization: definition and features.

molecular weights (directly proportional to monomer conversion) and architectures of resulting polymers. Given increasing demands on advanced new polymeric materials, living polymerization is considered among the best methods to synthesize as-designed, well-defined, and tailor-made polymers. In a more general context, living polymerization and related reactions are known as *precision* polymerization.

27.3 IODINE IN LIVING CATIONIC POLYMERIZATION CATIONIC POLYMERIZATION: PROBLEMS IN CONTROL

Cationic polymerization of alkene monomers is a chain-growth reaction mediated by a carbocationic intermediate, and mechanistically similar to electrophilic addition in organic chemistry (Fig. 27.3). More than 100 monomers with electron-donating substituents, typically isobutene and vinyl ethers, can be polymerized by this mechanism, and some processes (butyl rubber production from isobutene) are commercially important.

Cationic vinyl polymerization, however, is quite prone to chain transfer, due to the highly reactive but unstable carbocationic growing species where the β -protons of the active site are acidic and thereby susceptible to nucleophilic attack by monomers and counteranions, and thus the process has been considered to be beyond precision control required for living polymerization.

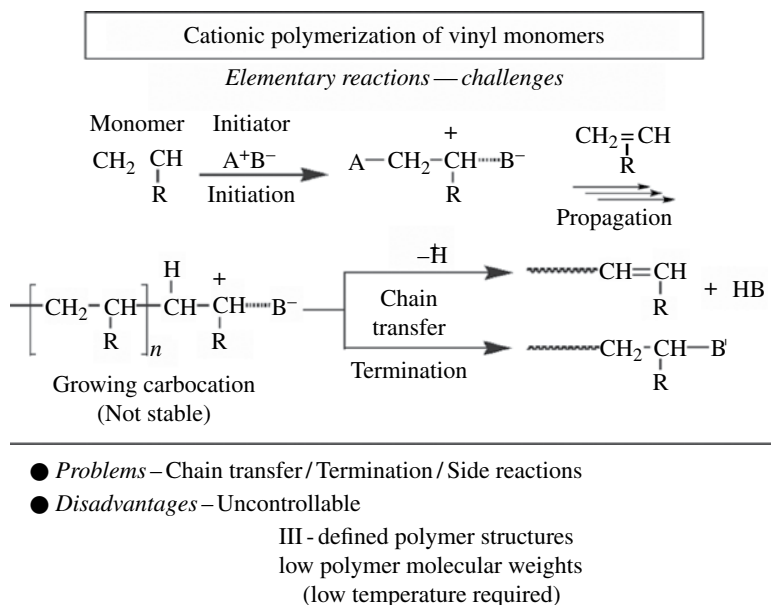


FIGURE 27.3 Cationic polymerization of vinyl monomers: mechanism and problems.

27.4 LIVING CATIONIC POLYMERIZATION

Despite such general perception for a more than a century, in 1984 Higashimura and the author reported the first example of living cationic polymerization for vinyl monomers (Fig. 27.4). Therein, critical are combinations of hydrogen iodide or alkyl iodide as an *initiator* and molecular iodine or zinc iodide as a mild Lewis acid or a *catalyst*, and the initiator–catalyst pairs are often known as *initiating systems*.

Obviously, in the mechanism, iodine compounds are essential in attaining living cationic polymerization, and their roles are multiple, acting as *initiator*, *catalyst*, and *end-capping agent*, depending on where iodine is located (Fig. 27.5). Thus, the carbon–iodine bond in the initiator is ionically cleaved by the catalyst, to induce carbocation formation and its propagation. Different from those in conventional (nonliving) cationic polymerization, the iodine-assisted generation of the growing carbocations is reversible, that is, while reacting with electron-rich monomers, they sooner or later recombine (become end-capped) with the iodine in the counteranion, thus regenerating a terminal with a carbon–iodine bond. This covalent terminal therefore functions as “dormant” species, which is critical in controlling cationic propagation, particularly in suppressing chain transfer via proton elimination (cf., Fig. 27.3). In some cases, addition of alkylammonium iodide enhances the formation of dormant ends in polar media, thus leading to another living cationic process.

Subsequent extensive studies have led to a variety of initiating systems (Fig. 27.6) to be applicable to nearly all of cationically polymerizable vinyl monomers, some of

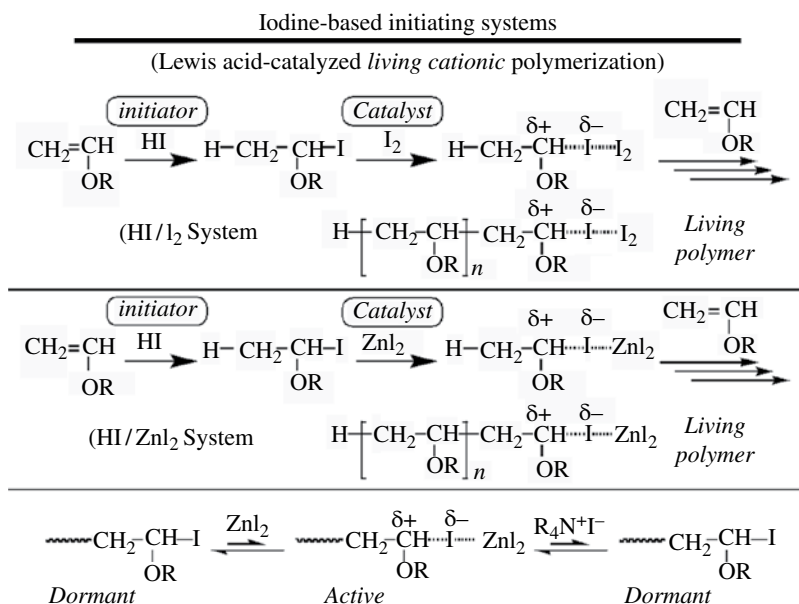


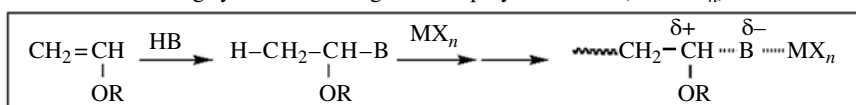
FIGURE 27.4 Living cationic polymerization with iodine-based initiating systems: note that iodine is present in both the initiator and the catalyst, playing a critical role.

● Functions in *cationic* polymerization

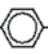
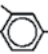

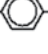
Function	General	Typical examples
Initiator	$\text{(R-I)} \xrightarrow{\text{MX}_n} \text{R}^+ + ^-\text{I-MX}_n$	(R-I) Alkyl iodine $\text{CH}_3 \text{ CH I}$ OR HI
Catalyst	$\text{R-I} \xrightarrow{\text{MX}_n} \text{R}^+ + ^-\text{I-MX}_n$ $(\text{ML}_n: \text{I}_2, \text{ZnI}_2, \text{etc.})$	$\text{(MX}_n)$ Lewis acid I_2
End-capping	$\text{P}^+ \xrightarrow{\text{R}_4\text{N}^+\text{I}^-} \text{P-I}$ (Dormant)	$\text{(R}_4\text{N}^+\text{I}^-)$ Iodide salt $n\text{Bu}_4\text{N}^+\text{I}^-$

FIGURE 27.5 Iodine in living cationic polymerization: multiple functions.

Initiating systems for living cationic polymerization (HB/MX_n)



● Protonic acids (HB):

HX	RCO ₂ H	R-  -CO ₂ H	$\begin{array}{c} \text{O} \\ \\ \text{R}^1-\text{P}-\text{OH} \\ \\ \text{R}^2 \end{array}$	RSO ₃ H
HCl HBr (HI)	CF ₃ CO ₂ H CHCl ₂ CO ₂ H CH ₂ Cl ₂ CO ₂ H CH ₃ CO ₂ H	O ₂ N-  -CO ₂ H O ₂ N-  -CO ₂ H Cl-  -CO ₂ H	$\begin{array}{c} \text{O} \\ \\ \text{PhO}-\text{P}-\text{OH} \\ \\ \text{PhO} \end{array}$ $\begin{array}{c} \text{O} \\ \\ \text{Ph}-\text{P}-\text{OH} \\ \\ \text{Ph} \end{array}$ $\begin{array}{c} \text{O} \\ \\ \text{Ph}-\text{P}-\text{OH} \\ \\ \text{H} \end{array}$	CH ₃ SO ₃ H

● Lewis acids (MX_n): $\text{(ZnI}_2)$, ZnBr₂, ZnCl₂; $\text{(SnI}_2)$, SnCl₂; $\text{(I}_2)$;
ZnI(acac)₂, Al(acac)₃, Fe(acac)₃

FIGURE 27.6 Initiating systems for living cationic polymerization; note that iodine compounds (enclosed in the figure) are often employed.

which carry functional and polar pendent substituents (Fig. 27.7). With these, living cationic polymerization is also very effective in *precision polymer synthesis*, that is, the synthesis of polymers with well-defined molecular weights, architectures, and functions, including block polymers, amphiphilic polymers, polymers with pendent functions, end-functionalized polymers, star-shaped macromolecules, among many others, some of which are finding industrial applications.

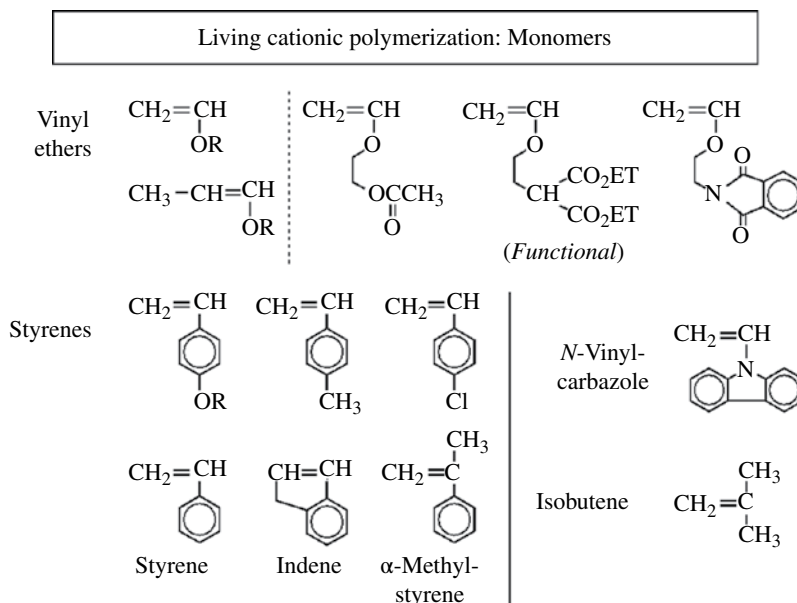


FIGURE 27.7 Monomers for living cationic polymerization, leading to a variety of precision polymers of well-designed functions.

27.5 IODINE IN LIVING RADICAL POLYMERIZATION

27.5.1 Radical Polymerization: Problems in Control

Azo, peroxide, and related radical-generating compounds initiate a chain-growth polymerization of vinyl monomers via carbon-radical intermediates, generally coined as *radical polymerization* (Fig. 27.8). Feasible under relatively mild conditions and even in water (emulsion and dispersion), this is among the most important addition polymerizations, rivaling coordination counterparts for α -olefins (ethylene, propylene, etc.), that have widely been employed for commercial mass-scale production of polymeric materials.

Despite these advantages and extensive industrialization, radical polymerization inherently involves serious side reactions, most important of which are radical recombination and disproportionation, or collectively bimolecular termination (Fig. 27.8). Thus, similar to cationic analogs, radical polymerization has also been considered to be beyond precision reaction control, though the reasons for the problems are different (chain transfer for cationic versus termination for radical).

27.5.2 Living Radical Polymerization: Metal-Catalyzed Systems

In 1995, however, the author and his group developed another living process: Living radical polymerization mediated by binary initiating systems consisting of an alkyl halide (initiator) and a transition metal complex (catalyst) (Fig. 27.9). The metal

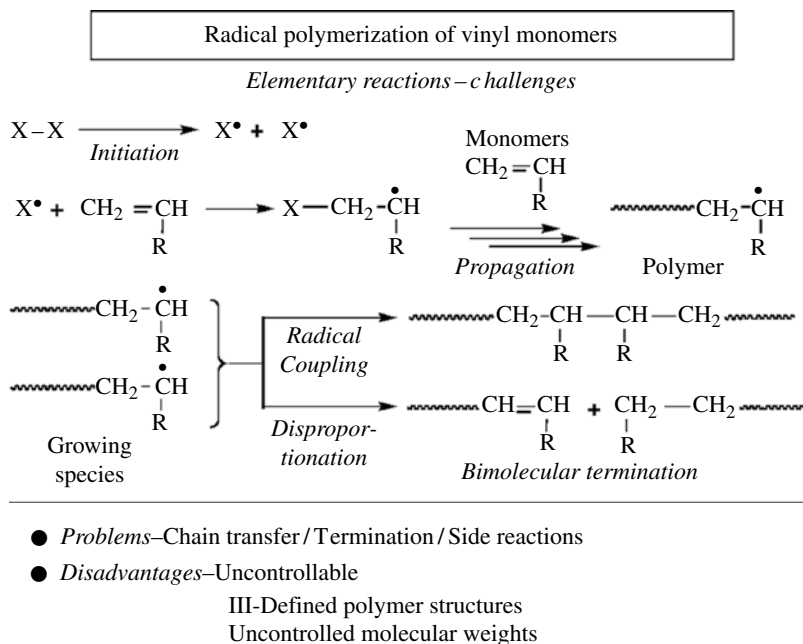


FIGURE 27.8 Radical polymerization of vinyl monomers: mechanism and problems.

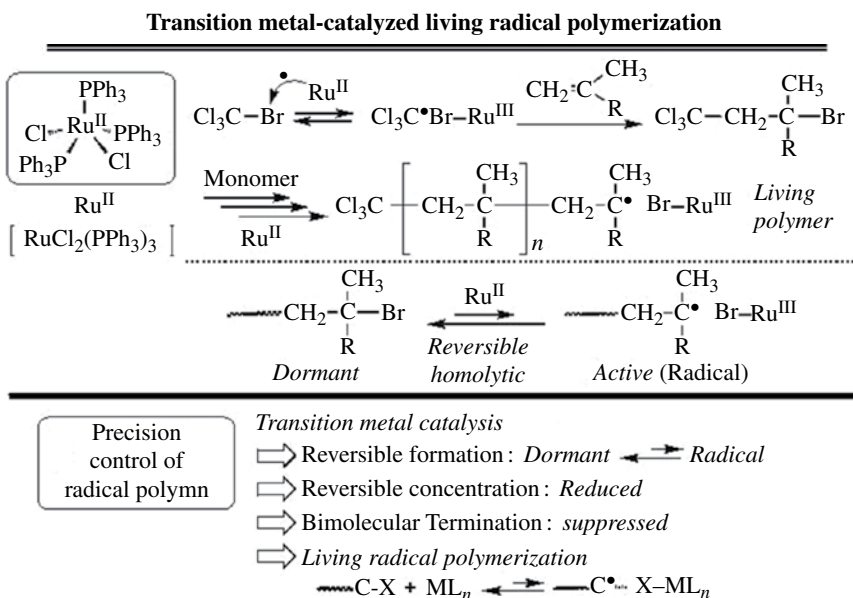


FIGURE 27.9 Living radical polymerization with transition metal catalysts: a general mechanism for precision control.

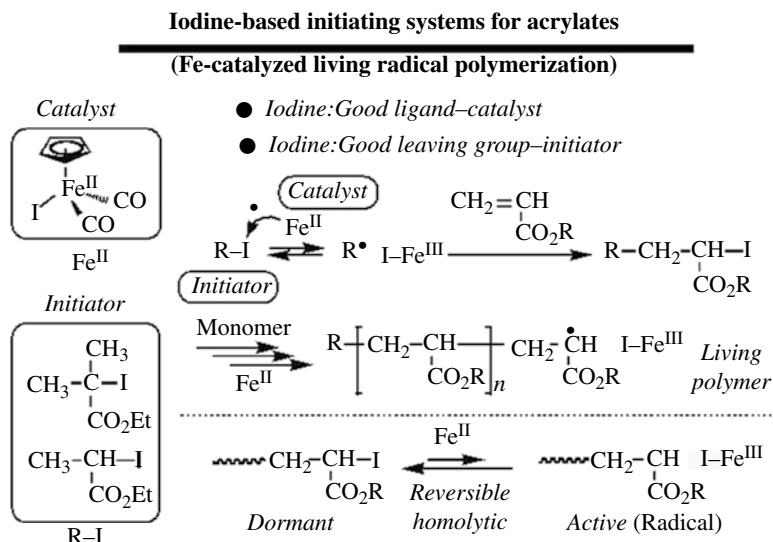


FIGURE 27.10 Iodine in transition metal–catalyzed living radical polymerization: initiators and catalysts for acrylates.

catalyst homolytically but reversibly cleaves the carbon–halogen bond in the initiator and dormant growing ends to induce radical formation and its growth.

Herein, iodine also plays a key role as a readily polarizable leaving group in the initiator as well as resonance-inducing ligand in the metal complex catalyst and is particularly useful for acrylates (Fig. 27.10). Thus, the carbon–iodine bonds in alkyl and perfluoroalkyl iodides and in the growing ends are also efficient chain-transfer agents for radicals, and they also facilitate the formation of dormant species from growing radicals, thus realizing living (or iodine-transfer) radical polymerizations of vinyl acetate and tetrafluoroethylene. Figure 27.11 summarizes such versatile functions of iodine in living and precision radical polymerization; see also Figure 27.5 for comparison with the iodine’s roles in living cationic polymerization.

As with the cationic counterparts, extensive and worldwide research has led to a wide variety of living radical polymerization with transition metal catalysts (Refs. [3e] and [3f]). This includes systematic search of initiators and metal catalysts (Fig. 27.12), as well as reaction mechanisms, and once again iodine has turned out to be uniquely versatile as ingredients in initiators (iodides), catalysts (metal complexes), and end-capping agents (or chain-transfer agents) for effective generation of dormant species (cf., Fig. 27.11).

Further, the scope of monomers to be applicable to these precision polymerizations is expanding to include most radically polymerizable alkenes (methacrylates, acrylates, acrylamides, styrene, etc.) (Fig. 27.13). Importantly, precision or living radical polymerizations of some important monomers are possible *only* with iodine compounds as initiators; such monomers include acrylates and vinyl acetate, along with ethylene/acrylate for copolymerization. Note that these monomers generally

● Functions in *radical* polymerization

Function	General	Typical examples
Initiator	$\text{R-I} \xrightarrow{\text{ML}_n} \text{R}^\bullet + \text{I-ML}_n$	R-I Alkyl iodine $\text{CH}_3\text{-CH-I}$ CO_2R
Catalyst	$\text{R-I} \xrightarrow{\text{ML}_n} \text{R}^\bullet + \text{I-ML}_n$ (ML_n : FeCpl(CO)_2 , etc.)	MX_n Metal complex FeCpl(CO)_2 , etc.)
End-capping	$\text{P}^\bullet \xrightarrow{\text{I}_2} \text{P-I}$ (Dormant)	I_2 Molecular iodine
Chain transfer	$\text{P}^\bullet \xrightarrow{\text{R-I}} \text{P-I} + \text{R}^\bullet$ (Dormant)	R-I Alkyl iodine $\text{CH}_3\text{-CH-I}$ $\text{C}_3\text{F}_7\text{-I}$ OCOR ($\text{R}_\text{F}\text{-I}$)

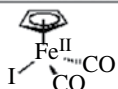
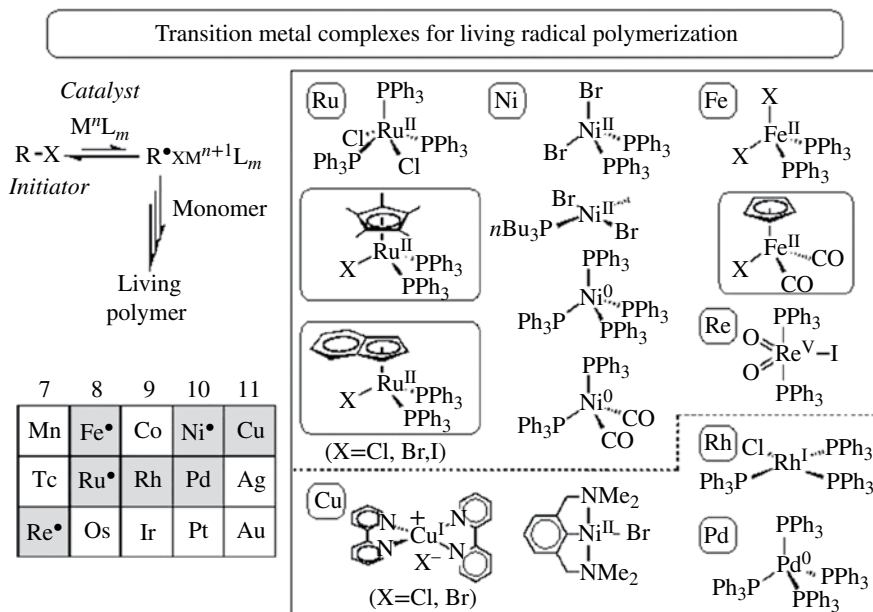
FeCpl(CO)_2 : 

FIGURE 27.11 Iodine in living radical polymerization: multiple functions in relation to transition metal catalysts as well as chain-transfer agents.



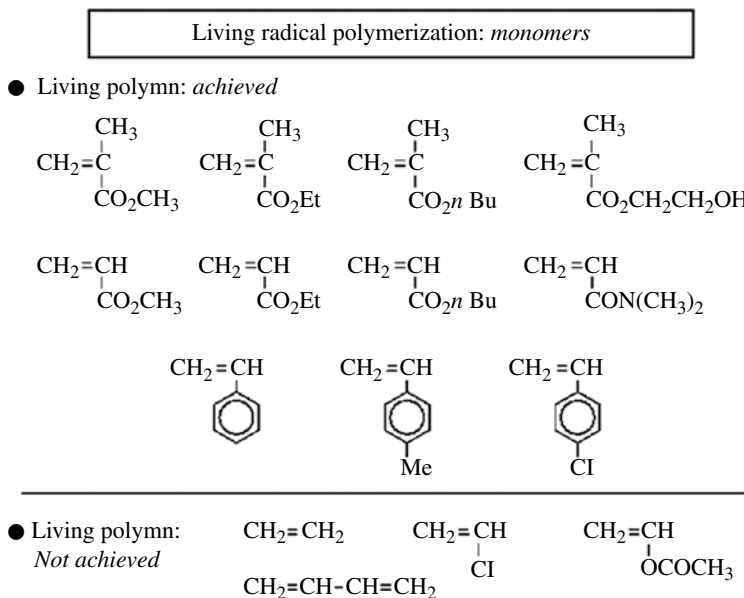


FIGURE 27.13 Monomers for transition metal-catalyzed living radical polymerization. Note some of them carry unprotected polar functions that are often excluded for use in ionic living polymerizations and coordination polymerizations.

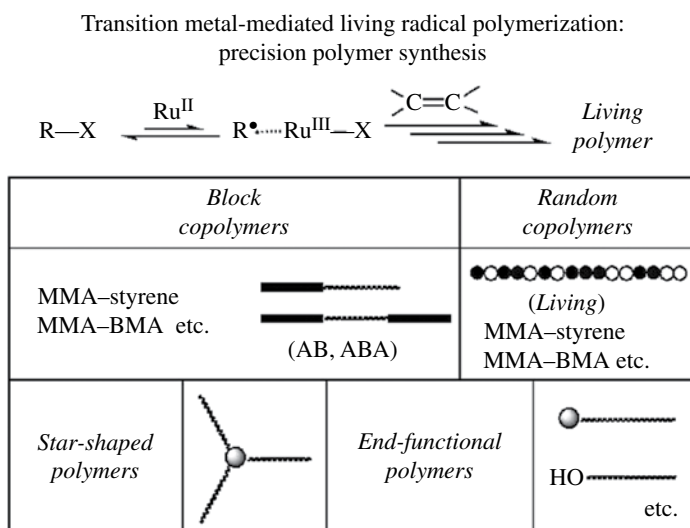


FIGURE 27.14 Precision functional polymers and related polymeric materials by transition metal-catalyzed living radical polymerization.

involve less stable growing radicals that, in turn, form dormant species with homolytically less dissociable carbon–halogen covalent terminals, particularly with chlorine and bromine, and thus a carbon–iodine terminal is essential.

Equally important, recent extensive developments have inspired “precision polymer synthesis” by living cationic and living radical polymerizations (the latter employed far more frequently), particularly with the use of monomers with functional pendent groups, and a vast variety of functional polymers have been synthesized (Fig. 27.14). Given far more general importance in radical polymerization, extensive research and development is under way in industry as well as in academia, and iodine and iodine compounds will certainly play a critical role in these developments.

REFERENCES

- [1] (a) Sawamoto M. Modern cationic vinyl polymerization. *Prog Polym Sci* 1991;16: 111–172. (b) Higashimura T, Sawamoto M. Living Cationic Polymerization - a Review. *Kobunshi Ronbunshu* 1989;46:189–201.
- [2] (a) Miyamoto M, Sawamoto M, Higashimura T. Living Polymerization of Isobutyl Vinyl Ether with the Hydrogen Iodide Iodine Initiating System. *Macromolecules* 1984;17:265–268. (b) Miyamoto M, Sawamoto M, Higashimura T. Synthesis of Monodisperse Living Poly(vinyl Ethers) and Block Copolymers by the Hydrogen Iodide Iodine Initiating System. *Macromolecules* 1984;17:2228–2230.
- [3] (a) Sawamoto M, Kamigaito M. Living radical polymerization with transition metal complexes. *Kobunshi Ronbunshu* 1997;54:875–885. (b) Kamigaito M, Ando T, Sawamoto M. Metal-catalyzed living radical polymerization. *Chem Rev* 2001;101:3689–3745. (c) Ando T, Kamigaito M, Sawamoto M. Recent development of transition metal-catalyzed living radical polymerization - Design and development of the metal complexes. *Kobunshi Ronbunshu* 2002;59:199–211. (d) Kamigaito M, Ando T, Sawamoto M. Metal-catalyzed living radical polymerization: Discovery and developments. *Chem Rec* 2004;4:159–175. (e) Ouchi M, Terashima T, Sawamoto MM. Precision control of radical polymerization via transition metal catalysis: From dormant species to designed catalysts for precision functional polymers. *Acc Chem Res* 2008;41:1120–1132. (f) Ouchi M, Terashima T, Sawamoto M. Transition Metal-Catalyzed Living Radical Polymerization: Toward Perfection in Catalysis and Precision Polymer Synthesis. *Chem Rev* 2009;109:4963–5050. (g) Ouchi M, Sawamoto M. Living Radical Polymerization with Active Catalysts Promotion of Catalytic Cycle via Dynamic Transformation of the Metal Complex. *Kobunshi Ronbunshu* 2011; 68:289–306.
- [4] (a) Kato M, Kamigaito M, Sawamoto M, Higashimura T. Polymerization of Methyl-Methacrylate with the Carbon-Tetrachloride Dichlorotris(Triphenylphosphine)Ruthenium(II) Methylaluminum Bis(2,6-Di-Tert-Butylphenoxide) Initiating System - Possibility of Living Radical Polymerization. *Macromolecules* 1995;28:1721–1723. (b) Ando T, Kato M, Kamigaito M, Sawamoto M. Living radical polymerization of methyl methacrylate with ruthenium complex: Formation of polymers with controlled molecular weights and very narrow distributions. *Macromolecules* 1996;29:1070–1072.

IODINE IN DYE-SENSITIZED SOLAR CELLS

LARS KLOO

KTH Royal Institute of Technology, Stockholm, Sweden

28.1 BACKGROUND

Since the pioneering work by Honda and Fujishima in the 1960s, the photoelectrochemical cell attracted an increasing level of research interest [1]. The 1960s–1980s offered several important advances, not the least because of the work by the groups of H. Gerischer (MPI Berlin) [2], R. Memming (University of Hamburg) [3], M. Grätzel (École Polytechnique Fédérale de Lausanne, EPFL) and others aiming at a dye-sensitized solar cell (DSSC) [4]. Step-by-step suitable combinations of materials were identified, and in 1991 the *Nature* paper by Grätzel and O'Regan marked a dramatic improvement by incorporating a nanostructured semiconductor substrate to the DSSC [4]. The consequence in terms of a large increase in effective surface for the adsorption of the sensitizing dye molecules generated a large leap from conversion efficiencies below 1% to efficiencies above 7%. By this groundbreaking paper, although initially met with some distrust, the whole research field was converted from an academic research field into that of an emerging solar cell technology with the potential to take up the challenge from established solar cell technologies.

A DSSC is in principle conceptually very simple (see Fig. 28.1); it consists of only three components: two electrodes, of which at least one is photosensitive, and an electrolyte. The analogy to other electrochemical cells, such as a battery, a fuel cell, or even the pioneering water-splitting cells by Honda and Fujishima, is obvious [1].

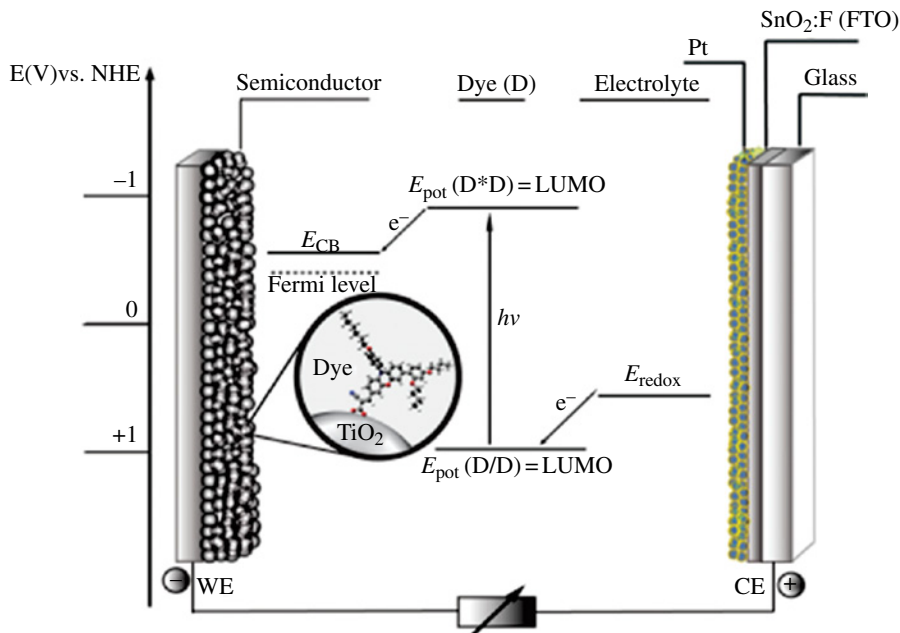


FIGURE 28.1 A schematic view of the DSSC device highlighting the role of the sensitizing dye. The figure is taken from Ref. [5].

The overall function of a DSSC is schematically shown in Figure 28.1 and can be described as follows [6]: The dye molecules absorb light and as a consequence the photon energy is transferred to an electron, resulting in a dye-excited state. Since the dye molecules are attached to a nanostructured, wide bandgap semiconductor substrate it is injected into the conduction band of the semiconductor. In this type of cells, the semiconductor is typically denoted as of n type and the mesoporous film is a few micrometers thick. The film thickness is controlled depending on semiconductor material, sensitizing dye, and electrolyte system used. The electron concentration gradient in the mesoporous film causes diffusion of the energy-rich electrons to the back contact of the transparent and conducting glass substrate. The energy-rich electrons can then be used or their energy stored. The less energy-rich electrons are led back to the counterelectrode, typically made of an inert conducting material, transferring the electron back to the electrolyte system. In the final step, closing the electron transport cycle, the redox-active electrolyte transports the electron back to the oxidized dye molecules, and through regeneration (reduction) the dye molecules are ready to absorb light again in a regenerative system. It is as redox-active electrolyte agents that iodine has come to play an important role.

In the 1991 *Nature* paper, the state-of-the-art materials used involved a working electrode consisting of 10–20 nm sintered TiO_2 particles sensitized by metal–organic dyes based on Ru, a counterelectrode consisting a platinized Fluorine-doped tin

oxide (FTO) substrate and a redox-active electrolyte based on an organic solvent and I^-/I_3^- as the redox system. Remarkably, in spite of about 20 years of intense research, this combination of materials has only very recently been challenged in terms of both conversion efficiency and long-term stability. This fact highlights the complexity of the conceptually simple DSSC devices.

Focusing on the I^-/I_3^- redox system, it was far from an obvious choice. Initial attempts included quinones, hexacyanoferrates, and in particular bromide [7]. However, in combination with the Ru-based dyes used, iodide was singled out as an efficient agent for the central dye regeneration process. In a regenerative solar cell process, the resulting oxidized species from the dye reduction is triiodide, thus forming an I^-/I_3^- redox system. Of course, adding iodine to the electrolyte system from the start allows control of energy levels and central processes in the DSSC device.

In the following, the role and state of knowledge regarding the iodine-based redox systems will be handled at/in the three components of the DSSC separately; at the photoelectrode, at the counterelectrode, and finally in the electrolyte. In this context, it should be noted that essentially all information communicated refers to n-type DSSC devices, and that similar descriptions regarding the role of iodine can also be made for p-type DSSCs [8].

28.2 IODINE AT THE PHOTOELECTRODE

28.2.1 Regeneration of the Sensitizing Dye

Regeneration of the oxidized dye at the photoelectrode is a central process in the DSSC. In this aspect, other redox systems have been found to regenerate (reduce) the dye molecules at a higher rate than the iodide ion of the I^-/I_3^- system. However, as will be discussed later, a successfully working redox system must also fulfill other requirements in order to qualify as a plausible redox system for DSSCs.

In the regeneration step, the concept of overpotential is often discussed. By overpotential is normally meant the difference between the energy of the sensitizing dye HOMO (highest occupied molecular orbital) and the energy (potential) of the redox system in the electrolyte. Thermodynamically, it is often found that an overpotential (also sometimes referred to as “driving force”) must exist for the electron transfer from the reduced form of the electrolyte redox system to the oxidized sensitizing dye to take place at a reasonable rate. An optimal overpotential for reduction of the sensitizing dyes is typically found to be in the range of 0.25 V [9]. However, for the I^-/I_3^- system to regenerate a sensitizing dye at sufficiently high rates, an overpotential in the range of 0.5 V is noted. Only rather recently could Boschloo and Hagfeldt show that this seemingly unnecessarily high overpotential could be traced to the two-electron character of the I^-/I_3^- system [10]. Of course, the Nernst equation shows that the overpotential can be massaged a bit through the concentrations and relative concentrations of the iodide ions and iodine, although other factors again come into play limiting the degrees of freedom

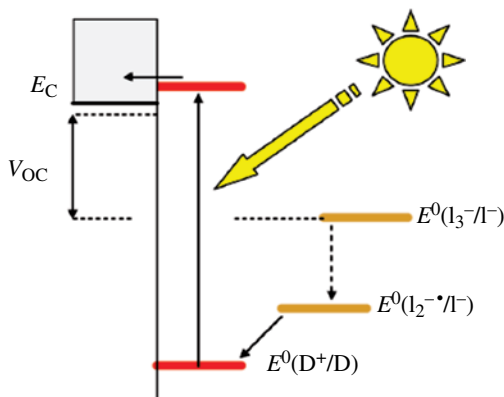


FIGURE 28.2 The two-step mechanism of sensitizing dye molecule regeneration of the iodide/triiodide redox mediator. The figure is taken from Ref. [10].

(see the later section on the electrolyte). In fact, the reduction process can be divided into two steps, into two linked redox systems—the I^-/I_3^- and the I^-/I_2^- systems—where the overpotential of the latter is only 0.2–0.3 V. The loss of another 0.2–0.3 V thus represents an intrinsic property of the redox system as a whole and is thus difficult to circumvent (Fig. 28.2). This insight has recently triggered an intense search for alternative and one-electron redox systems.

The mechanism of regeneration has been extensively studied by a selection of experimental techniques. In a recent review by Meyer and coworkers it is stated that although I_2^- is clearly formed (Eq. 28.1) with a subsequent disproportionation to give I_3^- (Eq. 28.2), it is not experimentally verified that I_2^- is formed directly through a concerted interaction of the oxidized dye molecule with two iodide ions [11].



However, theoretically, different plausible mechanisms of dye reduction have been studied and suggest a concerted reaction of two iodide ions initiating the electron transfer to the oxidized dye resulting in the I–I bond formation in an I_2^- radical anion. In studies involving metal–organic dye models the reaction may take place via an outer-sphere or an inner-sphere mechanism, although the former, which is enhanced by ligand interactions, is slightly favored (Fig. 28.3) [12]. Also, indirect support for an outer-sphere reaction is gained from the very similar process noted for models based on organic dye molecules [13]. Subsequent and more advanced studies involving also *ab initio* molecular dynamics offer support to the two-step mechanism proposed.

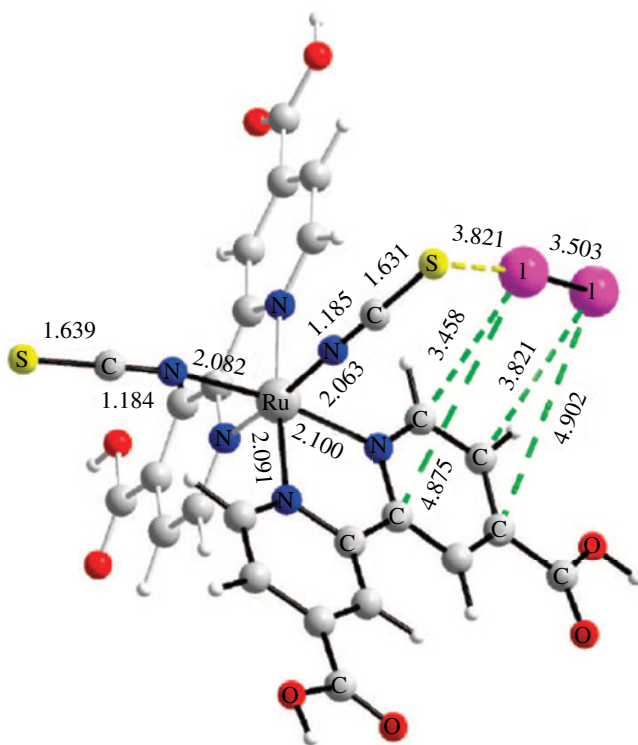


FIGURE 28.3 Outer-sphere binding of I_2^- in a N3 dye model. The figure is taken from Ref. [12]. (See insert for color representation of the figure.)

28.2.2 Recombination Loss Reactions

The electrons injected into the semiconductor substrate by the photoexcited dye molecules move toward the back contact by a diffusion mechanism. However, not all energy-rich electrons reach the back contact to allow their energy to be harvested. There are several loss mechanisms; some are inherent in the nanostructured, semiconductor material, some involve the trivial reduction of adsorbed and oxidized dye molecules, and others involve backdonation to the redox-active electrolyte, solid, or liquid. In the case of DSSCs based on a liquid, iodide/triiodide-based electrolyte, the most likely target of loss recombination is to an oxidized component of the redox system. In this case, either the triiodide ions or iodine molecules dissolve in the electrolyte. Since the triiodide ion and iodine are involved in a labile equilibrium (Eq. 28.3),



It is not obvious which of the two is the main target of reduction. Equilibrium (Eq. 28.3) is also affected by the polarity of the electrolyte solvent and the relative amounts

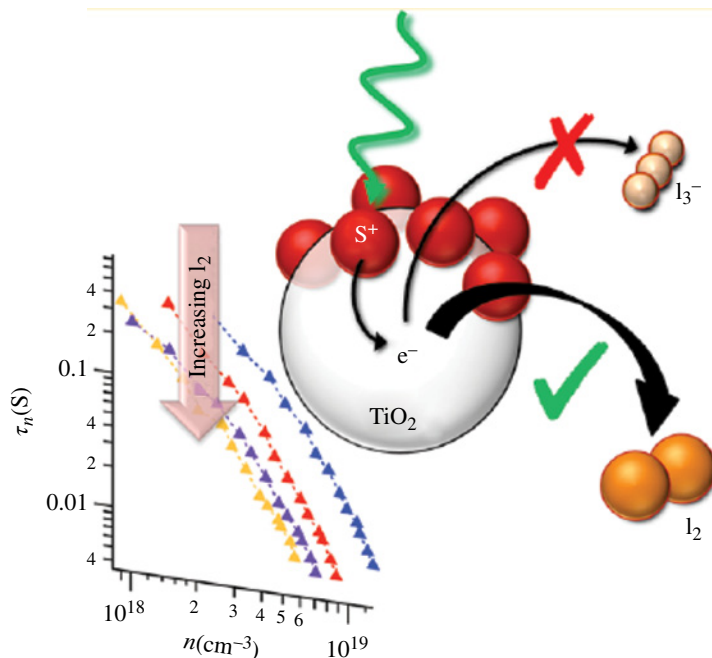


FIGURE 28.4 A schematic view of the recombination loss reaction to I_3^- . The figure is taken from Ref. [14].

of iodide salt and iodine added to the electrolyte. Typically, a rather polar organic solvent or an ionic liquid is used as solvent in liquid-based DSSCs. This means that the equilibrium constant of (Eq. 28.3) favors the triiodide state. This tendency is furthermore enhanced by the considerably higher concentration of iodide than iodine in the electrolyte. The reason for the choice of a high iodide concentration is to promote an efficient regeneration/reduction of the dye molecules, and the reason for a comparably low (but sufficiently high) iodine concentration is to allow efficient reduction of iodine/triiodide at the counterelectrode and at the same time reduce recombination losses at the working (photo)electrode [6].

Recombination losses may occur either directly from the semiconductor substrate surface or via the adsorbed dye molecules. Which mechanism dominates is highly dependent on the contents of the electrolyte, as well as the type of dye and the degree of dye coverage.

Since equilibrium (Eq. 28.3) is strongly shifted toward the triiodide ion, it is tempting to assume that recombination losses predominantly take place through the reduction of triiodide ions. However, O'Regan and coworkers recently showed that instead iodine molecules are the likely victims of recombination loss reactions; see Figure 28.4 [14].

However, it should be noted that one of the major reasons for the success of the iodide/triiodide redox system in DSSC electrolytes is the very favorable balance between the, on the one hand, efficient and fast dye regeneration reaction, and, on the

other hand, the very sluggish recombination loss reaction. The reason is most likely that the former in its initial step works as a one-electron transfer (fast) and the other essentially is a two-electron transfer (slow). In the search for alternative redox systems, thus two-electron systems have long been the target. Only very recently has a combination of designed dye molecules and one-electron redox systems challenged the champion iodine-based redox system.

28.3 IODINE AT THE COUNTERELECTRODE

Many different counterelectrode materials may be used in DSSC devices, such as conducting metal oxides, carbon materials, and metals. In the initial DSSC devices it was noted that the charge-transfer resistance at the counterelectrode, representing the reduction of iodine/triiodide, was a problem significantly hampering the overall DSSC performance. The deposition of Pt nanoparticles on an FTO surface, however, significantly reduced this problem [15]. It is thought that the catalytic function of the platinum nanoparticles reduce the charge-transfer reaction through a mechanism involving iodine molecule adsorption to the metal surface with a subsequent I–I bond splitting process in combination with the reduction to iodide ions. Of course, this makes the platinized FTO electrode highly adapted for the iodide/triiodide redox couple and may thus be far from optimal for alternative redox systems [16]. One such example is organic thiolate/disulphide systems, where the platinized FTO counterelectrodes work very poorly and other materials are preferably used instead [17].

28.4 IODINE IN THE ELECTROLYTE

In the initial search for suitable DSSC redox systems, in particular those that were compatible with the Ru-based metal–organic dyes used, iodide appeared as a main candidate [4]. The DSSC device is conceptually quite simple, but the optimization of the device as a whole is a delicate matter involving several intimate and delicately dependent processes, in particular at the electrode surfaces. In the combination of materials in the early days of DSSC, iodide (salts) as dye reducing agent stood out as an optimal choice. Of course, in a regenerative DSSC device, iodine/triiodide is formed automatically from the oxidation of iodide (regeneration process of the dye molecules) without specific addition. In optimization of the devices, it was found that addition of iodine was favorable up to specific concentrations, depending on which solvent was used [18]. The solvents offering the highest conversion efficiencies are typically low-viscous polar organic solvents, such as nitriles or carbonates [19]. Optimized concentrations of iodide salts and iodine are typically in the range of 1 M or more for the iodide salts and about 50 mM of iodine. Several different iodide salts have been investigated, and typically iodide is added as a mixture of salts, an organic salt as the bulk (to allow high solubilities), and an inorganic salt of a small highly

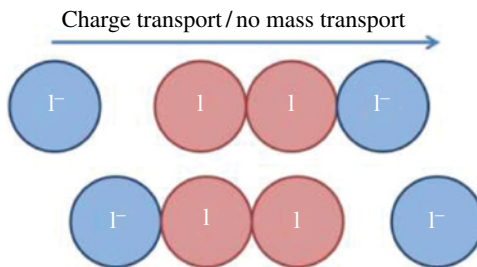


FIGURE 28.5 A illustration of the Grotthuss mechanism of conductivity in a polyiodides type of material.

polarizing cation, such as lithium or magnesium (to inflict shifts in the semiconductor substrate conduction band energy).

Another class of electrolyte solvents is ionic liquids. The use of ionic liquids reduces the volatility problem of typical organic solvents, and they also offer better chemical and electrochemical stability [20]. However, one major drawback of ionic liquids as solvents is the intrinsic relatively high viscosity. A high viscosity is commonly associated with low ion and molecule mobility, which of course will affect the charge and mass transport in ionic–liquid-based DSSCs. The viscosity problem was noted at an early stage, and several strategies have been employed to reduce the problem. In all systems so far, though, an optimized iodide/triiodide redox system involves a higher concentration of iodine in order to reduce the electrolyte charge and mass-transport limitation typically four to five times (about 0.2 M) higher than in a low-viscous organic solvent. Spectroscopic studies show that chemical availability also affects the necessity for a higher iodine concentration in ionic–liquid electrolytes [21]. Typical diffusion constants of the rate-limiting triiodide ion in low-viscous organic solvents are about $10^{-6} \text{ cm}^2 \text{ s}^{-1}$, whereas in reasonably low-viscous ionic liquids they are about an order of magnitude lower.

The higher concentrations of iodine used in ionic–liquid-based DSSC devices open up for another mechanism of charge transport, a Grotthuss or relay mechanism [22]. Such a mechanism has been proposed to explain the ability of water to conduct electricity, through “hopping” protons. Polyiodides are known to function in a similar way, thus allowing for charge transport without a net mass transport through the exchange of iodide ions (Fig. 28.5). Excess charge transport has been interpreted in this way, although recent work based on advanced isotope labeling instead suggests that the boost in conductivity is caused by ion-pair dissociation [23].

An interesting but not very extensively studied and related type of system is the liquid-crystal electrolyte. Such electrolytes are essentially ionic liquids with either a long-chain functionality added to the salt cation or a similar functionality introduced by a solvent additive. In such systems, it has been proposed that enhanced conductivity can be attributed to a Grotthuss mechanism in liquid-crystal channels (Fig. 28.6) [25].

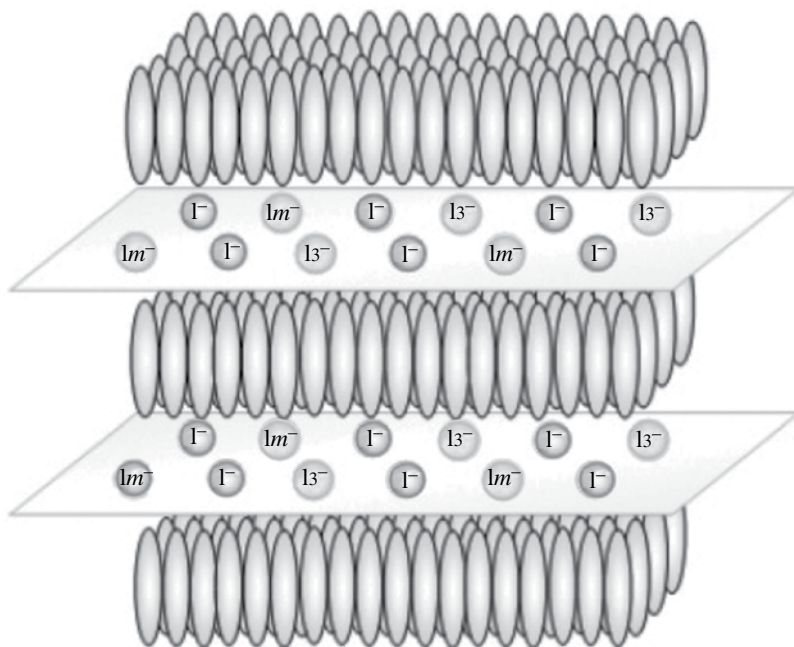


FIGURE 28.6 The channels promoting a Grotthuss type of conduction mechanism proposed to form in liquid-crystal-based electrolytes. The figure is taken from Ref. [24].

28.5 CHALLENGES WITH THE IODINE-BASED REDOX SYSTEM

Although having constituted the best working redox systems since the very early days of DSSCs, the iodide/triiodide system is far from perfect. Several challenges (or problems) with the iodine-based system have been identified. Some examples are given here:

- **Evaporation.** Even though the volatility of iodine is notably reduced by the excess iodide present in the electrolyte solvents, lack of long-term stability can in several cases be traced to a loss of iodine.
- **Photosensitivity.** Triiodide (and higher polyiodides) ions absorb light at shorter wavelengths. This both reduces conversion efficiencies through shadowing of the sensitizing dye and also gives rise to unwanted photoinitiated side reactions. Such side reactions will with time lead to a degradation of DSSC performance.
- **Corrosivity.** Triiodide/iodine is quite corrosive toward many materials, in particular to those that can be oxidized involving rather noble metals, such as silver. Since silver metal is a preferred material for DSSC contacts, it represents a significant practical problem.
- **Photovoltage.** The large overpotential previously mentioned prevents high photovoltages, which in turn effectively limits the maximum conversion efficiencies that can be extracted from an iodine-based DSSC.

These challenges have triggered a search for alternatives. The known alternatives can roughly be divided into two different categories: alternative two-electron systems and alternative one-electron systems [16].

Right from the start, iodide was not the only halide to be used in DSSCs. Bromide, with its oxidized companion—the tribromide ion—represents an alternative. Consequently, many other combinations of halides or pseudohalides have also been tested in DSSCs. Many of them have been outcompeted by the iodide/triiodide systems because of lack of chemical stability or less appropriate redox potentials. Recently, results from several different sulfur-based systems have been reported [17, 26]. These systems mimic the iodide/triiodide system in the sense that they involve the formation of a S–S bond upon dye regeneration. So far, none of the sulfur-based alternatives have been able to challenge the iodide/triiodide system in terms of performance, albeit they have reduced some of the drawbacks noted earlier. Lack of sufficient solubility and limitations in mobility have been noted as the main causes. Nevertheless, recent studies on iodine/sulfur tandem systems show promising results [27].

One-electron systems were also under the magnifying glass from the start of DSSC studies. Here, two major drawbacks could be identified. First, in a one-electron system the unwanted recombination loss reaction turned out to be competing in rate with the desired dye regeneration reaction, thus resulting in low overall conversion efficiencies. Second, most one-electron systems studied so far involved either comparably large metal complexes or organic molecules; all of which show low ion mobilities and consequently severe mass-transport limitations at higher irradiation levels. A solution to the first problem was recently offered through the combination of a $\text{Co}^{\text{II}}/\text{Co}^{\text{III}}$ redox system and a designed organic dye with long-chain functionalities (thought to block/retard the recombination loss reaction) [28]. This advance has opened for considerably higher DSSC photovoltages and so far the highest conversion efficiencies recorded for a liquid-based DSSC [29].

28.6 CONCLUSIONS AND OUTLOOK

For about 20 years the iodide/triiodide redox system ruled the field of DSSC devices in terms of stability and conversion efficiency. However, since the redox system is not without drawbacks, recent alternatives have made the future of the iodide/triiodide redox system in DSSC devices less prominent.

REFERENCES

- [1] Fujishima A, Honda K. Electrochemical properties of water at a semiconductor electrode. *Nature* 1972;238:37–38.
- [2] Gerischer H. Electrochemical photo and solar cells—principles and experiments. *Electroanal Chem Interfac Electrochem* 1975;58:263–274.
- [3] Memming R. *Semiconductor Electrochemistry*. Weinheim: Wiley-VCH; 2001.

- [4] (a) Desilvestro J, Grätzel M, Kavan L, Moser J. Highly efficient sensitization of titanium oxide. *J Am Chem Soc* 1985;107:2988–2990. (b) O'Regan B, Grätzel M. A low-cost, high-efficiency solar cell based on dye-sensitized colloidal TiO₂ films. *Nature* 1991;353:738–740.
- [5] Karlsson KM. Design, synthesis and properties of organic sensitizers for dye-sensitized solar cells [Thesis]. Stockholm: KTH Royal Institute of Technology; 2011.
- [6] Hagfeldt A, Boschloo G, Sun L, Kloo L, Pettersson H. Dye-sensitized solar cells. *Chem Rev* 2010;110:6595–6663.
- [7] (a) Vrachnou E, Vlachopoulos VN, Grätzel M. Efficient visible light sensitization of TiO₂ by surface complexation with Fe(CN)₆(4–). *J Chem Soc Chem Commun* 1987;868–870. (b) Vlachopoulos N, Liska P, Augustynski J, Grätzel M. Very efficient visible light energy harvesting and conversion by spectral sensitization of high surface area polycrystalline titanium oxide films. *J Am Chem Soc* 1988;110:1216–1220.
- [8] Gibson EA, Pleux LL, Fortage JRM, Pellegrin Y, Blart E, Odobel F, Hagfeldt A, Boschloo G. Role of the triiodide/iodide redox couple in dye regeneration in p-type dye-sensitized solar cells. *Langmuir* 2012;28:6485–6493.
- [9] Yum J-H, Baranoff E, Kessler F, Moehl T, Ahmad S, Bessho T, Marchioro A, Ghadiri E, Moser J-E, Yi C, Nazeeruddin MK, Grätzel M. A cobalt complex redox shuttle for dye-sensitized solar cells with high open-circuit potentials. *Nat Commun* 2013;6:31.
- [10] Boschloo G, Hagfeldt A. Characteristics of the iodide/triiodide redox mediator in dye-sensitized solar cells. *Acc Chem Res* 2009;42:1819–1826.
- [11] Rowley JG, Farnum BH, Ardo S, Meyer GJ. Iodide chemistry in dye-sensitized solar cells: making and breaking I–I bonds for solar energy conversion. *J Phys Chem Lett* 2010;1:3132–3140.
- [12] Privalov T, Boschloo G, Hagfeldt A, Svensson PH, Kloo L. A study of the interactions between I(–)/I₃(–) redox mediators and organometallic sensitizing dyes in solar cells. *J Phys Chem C* 2009;113:783–790.
- [13] Nyhlen J, Boschloo G, Hagfeldt A, Kloo L, Privalov T. Regeneration of oxidized organic photo-sensitizers in grtzel solar cells: quantum-chemical portrait of a general mechanism. *ChemPhysChem* 2010;11:1858–1862.
- [14] Richards CE, Anderson AY, Martiniani S, Law C, O'Regan BC. The mechanism of iodine reduction by TiO₂ electrons and the kinetics of recombination in dye-sensitized solar cells. *J Phys Chem Lett* 2012;3:1980–1984.
- [15] Papageorgiou N, Maier WF, Grätzel M. An iodine/triiodide reduction electrocatalyst for aqueous and organic media. *J Electrochem Soc* 1997;144:876–884.
- [16] Cong J, Yang X, Kloo L, Sun L. Iodine/iodide-free redox shuttles for liquid electrolyte-based dye-sensitized solar cells. *Energy Environ Sci* 2012;5:9180–9194.
- [17] Tian H, Yu Z, Hagfeldt A, Kloo L, Sun L. Organic redox couples and organic counter electrode for efficient organic dye-sensitized solar cells. *J Am Chem Soc* 2011;133:9413–9422.
- [18] Grätzel M. Solar energy conversion by dye-sensitized photovoltaic cells. *Inorg Chem* 2005;44:6841–6851.
- [19] Yu Z, Vlachopoulos N, Gorlov M, Kloo L. Liquid electrolytes for dye-sensitized solar cells. *Dalton Trans* 2011;40:10289–10303.
- [20] Gorlov M, Kloo L. Ionic liquid electrolytes for dye-sensitized solar cells. *Dalton Trans* 2008:2655–2666.

- [21] Yu Z, Gorlov M, Nissfolk J, Boschloo G, Kloo L. Investigation of iodine concentration effects in electrolytes for dye-sensitized solar cells. *J Phys Chem C* 2010;114:10612–10620.
- [22] Grotthuss CJDD. Sur la décomposition de l'eau et des corps qu'elle tient en dissolution à l'aide de l'électricité galvanique. *Ann Chim* 1806;58:54–74.
- [23] Call F, Stolwijk NA. Impact of I₂ additions on iodide transport in polymer electrolytes for dye-sensitized solar cells: reduced pair formation versus a grotthuss-like mechanism. *J Phys Chem Lett* 2010;1:2088–2093.
- [24] Kloo L. Catenated compounds—group 17—polyhalides. In: Reedijk J, Poepelmeier K, editors. *Comprehensive Inorganic Chemistry II*. Volume 1, Oxford: Elsevier; 2013. p 233–249.
- [25] (a) Yamanaka N, Kawano R, Kubo W, Kitamura T, Wada Y, Watanabe M, Yanagida S. Ionic liquid crystal as a hole transport layer of dye-sensitized solar cells. *Chem Commun* 2005;740–742. (b) Kawano R, Nazeeruddin MK, Sato A, Grätzel M, Watanabe M. Amphiphilic ruthenium dye as an ideal sensitizer in conversion of light to electricity using ionic liquid crystal electrolyte. *Electrochem Commun* 2007;9:1134–1138.
- [26] (a) Li D, Li H, Luo Y, Li K, Meng Q, Armand M, Chen L. Non-corrosive, non-absorbing organic redox couple for dye-sensitized solar cells. *Adv Funct Mater* 2010;20:3358–3365. (b) Wang M, Chamberland N, Breau L, Moser J-E, Humphry-Baker R, Marsan BT, Zakeeruddin SM, Grätzel M. An organic redox electrolyte to rival triiodide/iodide in dye-sensitized solar cells. *Nat Chem* 2010;2:385–389.
- [27] Cong J, Yang X, Hao Y, Kloo L, Sun L. A highly efficient colourless sulfur/iodide-based hybrid electrolyte for dye-sensitized solar cells. *RSC Adv* 2012;2:3625–3629.
- [28] Feldt SM, Gibson EA, Gabrielsson E, Sun L, Boschloo G, Hagfeldt A. Design of organic dyes and cobalt polypyridine redox mediators for high-efficiency dye-sensitized solar cells. *J Am Chem Soc* 2010;132:16714–16724.
- [29] Yella A, Lee H-W, Tsao HN, Yi C, Chandiran AK, Nazeeruddin MK, Diau EW-G, Yeh C-Y, Zakeeruddin SM, Grätzel M. Porphyrin-sensitized solar cells with cobalt (II/III)–based redox electrolyte exceed 12 percent efficiency. *Science* 2011;334:629–634.

29

FLUORINATED REPELLENTS

TOYOMICHI SHIMADA

Asahi Glass Co., Ltd., Tokyo, Japan

29.1 OVERVIEW OF FLUORINATED REPELLENTS

29.1.1 Iodine and Fluorinated Repellents

Fluorochemicals are widely used in modern life, especially those possessing perfluoroalkyl groups and low surface tension. They are used as oil and water repellents for clothes, shoes, and umbrellas; oil- and grease-resistant agents for fast-food packaging and paper trays; and antifouling agents for carpeting. In this chapter, these compounds will be collectively called fluorinated repellents.

Chemicals containing the perfluoroalkyl group are also used as fire extinguishing agents, leveling agents for floor polishing, and emulsifiers. Excellent reviews on these applications are already present in the literature [1, 2]; therefore, they will not be discussed in this chapter. The treatment of smartphones and tablet screens with perfluoropolyethers to impart an anti-fingerprint feature will also not be discussed; this is because iodine is not typically used to produce those chemicals.

Iodine and chemicals containing iodine are used as the main raw materials for the synthesis of fluorinated repellents. Perfluoroalkyl iodide is the most widely used compound for the synthesis.



The manufacturing process is as follows.



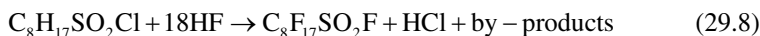
The last reaction is a telomerization reaction. A compound, called a telogen, reacts with ethylenically unsaturated compounds, taxogens, to generate compounds called telomers [3, 4].

Various compounds used in repellents can be synthesized from the telomers. In the following formulas, Rf indicates $\text{CF}_3\text{CF}_2(\text{CF}_2\text{CF}_2)_n$.



These chemicals are converted to the fluorinated epoxy compounds, urethanes, and esters, and used in a variety of applications.

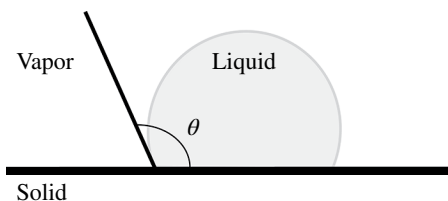
In addition to telomerization, another method called electrochemical fluorination [5] is also used to manufacture chemicals containing perfluoroalkyl groups, but iodine is not used in these processes. The typical reactions are presented here:



29.1.2 Repellency

The degree of repellency of a solid surface to a liquid droplet is measured by the angle θ formed between the solid surface and the tangent at a point on the three-phase boundary, as shown in Figure 29.1. This angle is called the static contact angle. The repellency of the solid surface increases with an increase in the contact angle.

The Zisman theory defines the surface tension of a solid surface as being equal to that of the liquid having the highest surface tension that can completely wet the solid surface; this is called the critical surface tension, γ_c . After acquiring the contact angles for a series of probe liquids, the critical surface tension of the surface is derived. This is done by first plotting the cosine of each contact angle against the known surface tension of the probe liquid, and then these plots are extrapolated to zero degrees [6].

**FIGURE 29.1** Static contact angle θ .**TABLE 29.1** Critical surface tensions of repellent surfaces

Surface	Surface functional group	γ_c /mNm ⁻¹	Ref.
Perfluorolauric acid	-CF ₃	6	[7]
Polytetrafluoroethylene	-CF ₂ -	18	[8]
Octadecylamine	-CH ₃	22	[9]
Paraffin wax	-CH ₃ , -CH ₂ -	23	[9]
Polyethylene	-CH ₂ -	31	[9]
Poly (dimethyl siloxane)	-Si(CH ₃) ₂ -O-	24	[9]

TABLE 29.2 Surface tensions of liquids

Liquid	γ_l /mNm ⁻¹ (20° C)
n-Octane	21.62
n-Hexadecane	27.47
Methanol	22.70
Ethanol	22.10
2-Propanol	23.00
Water	72.80

The ability of a solid surface to repel a liquid droplet can be estimated by comparing the critical surface tension of the solid with the surface tension of the liquid. If the former is smaller than the latter, the solid can repel the liquid. Tables 29.1 and 29.2 show data for critical surface tension and surface tension, respectively. The tables make it clear that chemicals with perfluoroalkyl groups can repel oils and alcohols, and paraffin wax and silicone, which are used as water repellents, cannot repel those liquids.

29.1.3 Fluorinated Repellents

The 3M company released the first fluorinated repellent, synthesized using electrochemical fluorination, in 1956. Later, DuPont released the repellents, synthesized by telomerization, and several other companies brought their telomerization products to market. Many companies do not conduct fluorination; they modify fluorinated chemicals purchased from companies having access to fluorination techniques.

29.1.4 Oil and Water Repellents for Clothing

Fluorinated repellents find the largest application in clothing. There is a wide range of uses of these repellents in weatherproof coatings on clothes, shoes, and accessories in sports and outdoor activities. The repellents can also be used as antifouling coatings for suits, ties, and bags. The coatings have been applied to natural fibers like cotton and wool, synthetic fibers like polyesters and polyamides, and natural/synthetic leather.

Oil and water repellency and durability are the major requirements for application of these repellents in the clothing industry. Several techniques are defined by industry organizations to test these requirements. The most widely used tests for water repellency are spray tests. In this test, water is sprayed on a piece of tilted fabric treated with repellents, and the degree of water penetration is rated [10]. To test for oil repellency, several hydrocarbon liquids with different surface tensions are placed on the treated fabric. The fabric is then rated based on the lowest surface tension liquid that cannot penetrate the fabric [11].

Durability tests are usually defined as pretreatment processes for characteristics like colorfastness. There are durability tests for abrasion [12], repeated home laundering [13], and dry cleaning [14]. The oil and water repellency tests are carried out after durability tests.

Repellent finishing comprises three steps. First, the treatment bath, composed of 2–3% fluorinated repellents and a small amount of penetrating and antistatic agents, is prepared. Second, a roll of cloth is dipped in the bath and then squeezed to remove the water. Third, the roll of cloth is dried and cured at 120–180°C for a few minutes.

Fluorinated repellents are usually aqueous emulsions, but in some cases, these are solutions composed of organic solvents and fluoropolymers. Solution-type repellents are easier to dry than emulsion-type repellents and can form repellent coatings without curing. These agents are used in cleaners and are supplied to consumers in spray cans for imparting repellency to umbrellas, shoes, and bags. The aqueous emulsions of repellents are prepared by polymerizing fluoromonomers and other monomers in the presence of emulsifiers. Cationic emulsifiers are typically used. In those cases, the emulsion particles are positively charged and the fiber surface is negatively charged so the particles can be uniformly distributed on the fibers to make a uniform coating.

Typical examples of repellent polymers are the copolymer of a fluorinated acrylate, an inexpensive, long alkyl acrylate that can impart water repellency, and a chlorinated monomer, like vinyl chloride or vinylidene chloride, which improves durability by strengthening adhesion to fibers.

29.1.5 Oil- and Grease-Resistant Agents for Paper and Paperboard

Fluorinated repellents are used for a variety of applications in food packaging industries. The repellents work as barriers to water, oil, and grease and impart durability to paper and paperboard used for pet food and fast food packaging.

Oil- and grease-resistant properties are measured using several kinds of oils and greases with different surface tensions. Like the oil repellency tests for clothing, oils are placed on the treated paper, and the test piece is rated based on the oil/grease with the lowest surface tension that cannot wet the test piece.

There are two methods for applying oil- and grease-resistant agents during the manufacture of paper: size press application and wet-end application. In the former method, the agent penetrates the surface of the paper. In the latter method, the fluorinated agent is mixed with the paper pulp and the paper is formed from the mixture. In the latter case, the agent is required to concentrate on the surface of the paper during the drying process. Copolymers of fluorinated monomers and other monomers [15, 16] and derivatives of perfluoropolyethers [17, 18], manufactured without iodine, are used for these purposes.

29.1.6 Stain- and Soil-Resistant Agents for Carpeting

Large quantities of fluorinated repellents are used in carpeting to keep it clean. Oil and water repellency make accidental spills easier to remove, and dry soil resistance prevents soiling from shoes. These are important for maintaining carpets and rugs.

Foam application is common in this field. The repellent emulsions are applied with foaming agents and other additives. Spray application was common in the past, but it is no longer recommended in order to avoid inhalation of the treating chemicals.

Fluorinated urethanes are often used because they are effective for dry soil resistance. The chemicals are synthesized from fluorinated alcohols and isocyanates in an organic solvent. Emulsifiers are then added, and the solvent is stripped off and replaced with water.

29.2 PFOA ISSUES

Perfluorooctanoic acid (PFOA) is a synthetic chemical substance. PFOA is often used in emulsion polymerization of fluoropolymers because of its excellent performance as an emulsifier. Conventional fluorinated repellents often unintentionally contain trace amounts of PFOA and precursors that can decompose into PFOA. PFOA is persistent in the environment. It is also bioaccumulative and has the tendency to stay in the body once it is absorbed. It is widely used and has persistent and bioaccumulative characteristics; therefore, it is closely scrutinized by government regulation agencies and scientists.

Perfluoroalkanoic acids (PFAAs), perfluoroalkanoic acids with longer perfluorinated alkyl groups than PFOA, like perfluorodecanoic acid, and their precursors are thought to be stable and bioaccumulative as well.

In 2006, the U.S. Environmental Protection Agency invited the eight major manufacturers of fluorinated resins and repellents (Arkema, Asahi, BASF Corporation, Clariant, Daikin, 3M/Dyneon, DuPont, and Solvay Solexis) to participate in a voluntary initiative called the 2010/15 PFOA Stewardship Program. The program had two goals; these included (i) commitment to reduce facility emissions and product

content of PFOA, PFAAs, and their precursors by 95% by 2010, based on a baseline from the year 2000; (ii) commitment to work toward the elimination of the chemicals by 2015.

29.3 ALTERNATIVE TECHNOLOGIES

To overcome PFOA issues, a variety of alternative technologies and products have been developed. In this chapter, the correlation between the repellent characteristics of fluoropolymer coatings and the chemical and higher-order structures of perfluoroalkyl groups will be reviewed, followed by a description of some alternative technologies.

29.3.1 Correlation between Repellency and Perfluoroalkyl Chain Length

The copolymers of perfluoroalkylethyl acrylate have been commonly used as repellents. In most cases, the carbon number of the perfluoroalkyl group, or the fluorinated carbon number, is equal to or greater than eight because the length is suitable for repellency.

Research on the homopolymers of perfluoroalkylethyl acrylates with different fluorinated carbon numbers has been conducted. The researchers studied the higher-order structures in the polymer films using wide-angle X-ray diffraction (WAXD) and differential scanning calorimetry (DSC) measurements, and the repellent characteristics based on contact angle measurements [19–21].

The WAXD measurements indicated that the perfluoroalkyl groups aggregate and form a hexagonal packing structure when the fluorinated carbon number is eight, as shown in Figure 29.2. This structure has almost the same spacing, 0.5 nm, as that of polytetrafluoroethylene crystal, and it also forms a lamellar structure, with a spacing of 3.4 nm, composed of bilayers of the monomer unit. Meanwhile, when the number of the fluorinated carbon is equal to or less than six, higher-order structures are not observed.

The DSC measurements show that when the fluorinated carbon number of the perfluoroalkyl group is eight, the polymer has a melting temperature well above room temperature. This behavior is different from that of the compounds with a fluorinated carbon number of six or less.

To evaluate the roughness and chemical heterogeneity of surfaces, dynamic contact angles are more suitable than the previously mentioned static contact angles. There are two kinds of dynamic contact angles, advancing contact angles θ_a and receding contact angles θ_r ; these are measured using droplets on a sample stage that can be tilted, as shown in Figure 29.3. The receding contact angles for water droplets have a high correlation to ratings in the water spray tests used to simulate rain.

The receding contact angles of the fluorinated acrylate films are quite large when the fluorinated carbon number is equal to or greater than eight, whereas the angles are small when the carbon number is six or less.

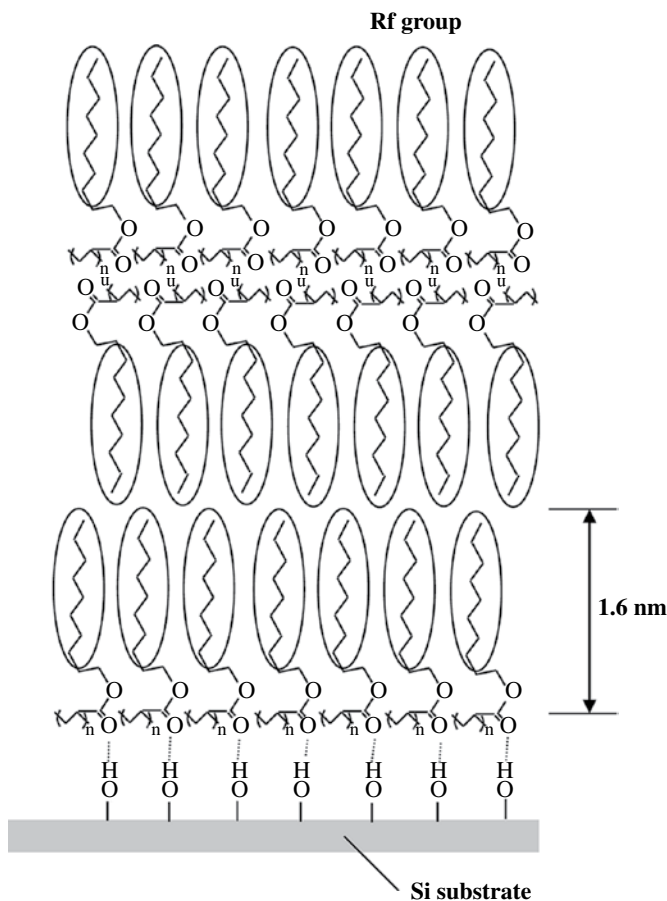


FIGURE 29.2 Structural model of the perfluorooctylethyl acrylate homopolymer film. Reprinted with permission from Ref. [21]. © 2008, American Chemical Society.

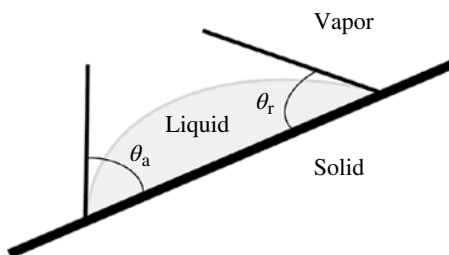


FIGURE 29.3 Advancing angle θ_a and receding contact angle θ_r .

Based on the WAXD, DSC measurements, and receding contact angle experiments, it was inferred that a higher-order structure, that is, the packing of perfluoroalkyl groups, is important for water repellency. This might be a basic concept to develop new chemicals, other than PFOAs, suitable to act as repellents.

29.3.2 Alternative Technologies to PFOA

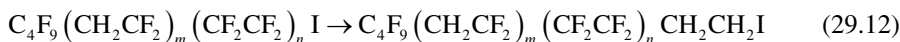
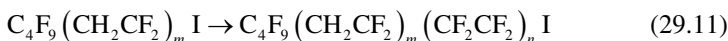
The major manufacturers of fluorinated repellents have initiated research and development on alternative technologies and products. Many new products have been released in almost all of the application fields. However, there are currently no new products for high-end applications such as clothing for military use. Therefore, further research is still needed.

In all of the following examples, the carbon number of the perfluoroalkyl group is equal to or less than six.

29.3.3 New Fluorinated Alkyl Acrylates

Research has been conducted to obtain new fluorinated alkyl acrylates or fluoroalkyl acrylates that aggregate to form higher-order structures with the packing of perfluoroalkyl groups because they can exhibit strong water repellency.

The introduction of a methylene unit between fluoromethylene units was investigated. This makes the fluoroalkyl groups biodegradable. The fluoroalkyl groups were synthesized by reaction of perfluoroethyl iodide and vinylidene fluoride and followed by tetrafluoroethylene and ethylene.



Among the acrylate polymers, the $\text{CH}_2=\text{CHCO}_2\text{CH}_2\text{CH}_2(\text{CF}_2\text{CF}_2)_2\text{CF}_2\text{CH}_2\text{C}_4\text{F}_9$ polymer had a melting temperature of 77.4°C above room temperature and a high receding contact angle of 105° [22, 23].

Other fluoroalkyl groups were synthesized from perfluoroalkyl iodide using $\text{CF}(\text{CF}_3)=\text{CH}_2$ followed by ethylene [24]; vinyl chloride, vinylidene chloride, or 1',2',2'-trifluorostyrene followed by ethylene [25], or vinylidene fluoride followed by propylene [26].

Fluoroalkyl acrylates with one or more phenylene units between the perfluoroalkyl group at one end and the acryloyl group at the other end were prepared. The polyacrylates made from these monomers exhibited good oil and water repellency [27–30].

29.3.4 New Fluorinated Monomers Other than Acrylates

A polymer shows good repellency if the main chain is rigid and can maintain a conformation having the pendent fluoroalkyl group at the outermost surface of the film. This can occur even if its conformation is not identical to hexagonal packing and it does not possess a melting temperature. Product development using monomers/polymers with rigid main chains has been conducted.

Among these, the most important fluorinated monomer is perfluorohexylethyl methacrylate. Its homopolymer has a glass transition temperature above room temperature [31], so it shows good water and oil repellency. Additionally, the simple structure of the methacrylate makes it cost-effective. Because of these properties, a number of methacrylate-based products are currently available.

Perfluorobutylethyl 2-chloroacrylate might be another example of this concept [32].

REFERENCES

- [1] Kissa E. *Fluorinated Surfactants and Repellents*. 2nd ed. New York: Marcel Dekker Inc.; 2001.
- [2] Zaggia A, Ameduri B. Recent advances on synthesis of potentially non-bioaccumulable fluorinated surfactants. *Curr Opin Colloid Interf Sci* 2012;17:188.
- [3] Haszeldine RN. The reactions of fluorocarbon radicals. Part I. The reaction of iodotrifluoromethane with ethylene and tetrafluoroethylene. *J Chem Soc* 1949:2856.
- [4] Blanchard WA, Rhode JC. Process for preparing perfluoroalkyl iodides U.S. Patent 3,226,449. 1965 to DuPont.
- [5] Gramstad T, Haszeldine RN. Perfluoroalkyl derivatives of sulphur. Part VI. Perfluoroalkanesulphonic acids $\text{CF}_3(\text{CF}_2)_n\text{SO}_3\text{H}$ ($n = 1-7$). *J Chem Soc* 1957;2640.
- [6] Zisman WA. *Contact Angle, Wettability, and Adhesion*. Washington, DC: American Chemical Society; 1964. p 1.
- [7] Hare EF, Shafrin EG, Zisman WA. Properties of films of adsorbed fluorinated acids. *J Phys Chem* 1954;58:236.
- [8] Fox HW, Zisman WA. The spreading of liquids on low energy surfaces. I. Polytetrafluoroethylene. *J Colloid Sci* 1950;5:514.
- [9] Owens DK. Estimation of the surface free energy of polymers. *J Appl Polym Sci* 1969;13:1741.
- [10] AATCC Committee RA63 Technical Manual. Volume 85, 2010. p 67.
- [11] AATCC Committee RA56 Technical Manual. Volume 85, 2010. p 183.
- [12] AATCC Committee RA29 Technical Manual. Volume 85, 2010. p 186.
- [13] AATCC Committee RA61 Technical Manual. Volume 85, 2010. p 195.
- [14] AATCC Committee RA43 Technical Manual. Volume 85, 2010. p 212.
- [15] Maekawa T, Sugimoto S, Shimada M, Kaneko K, Naruse H, Nakajima Y. Waterproofing/oilproofing agent composition PCT Int. Appl. WO 05/90,423. 2005 to Asahi Glass.
- [16] Kawana J, Sugimoto S. Water-resistant/oil-resistant agent composition, article treated with the composition, and processes for production of the composition and the article. PCT Int. Appl. WO 11/59,039. 2011 to Asahi Glass.

- [17] Maccone P, D'Aprile F, Visca M. Aqueous compositions of perfluoropolyether phosphates and use thereof to confer oleo-repellence to paper. U.S. Patent 7,141,140. 2006 to Solvay Solexis.
- [18] Russo A, Tonelli C, Visca M. (Per) fluoropolyether carboxylic acids and use thereof for the oleo-repellent paper sizing. U.S. Patent 7,252,740. 2007 to Solvay Solexis.
- [19] Maekawa T, Kamata S, Matsuo M. The relationship between structures and dynamic surface properties of perfluoroalkyl containing polymers. *J Fluorine Chem* 1991;54:84.
- [20] Honda K, Morita M, Otsuka H, Takahara A. Molecular aggregation structure and surface properties of poly(fluoroalkyl acrylate) thin films. *Macromolecules* 2005;38:5699.
- [21] Matsunaga M, Suzuki T, Yamamoto K, Hasegawa T. Molecular structure analysis in a dip-coated thin film of poly(2-perfluorooctylethyl acrylate) by infrared multiple-angle incidence resolution spectrometry. *Macromolecules* 2008;41:5780.
- [22] Sato K. Chapter 20 (The chapter title is written in Japanese. The title is not given in English by the publisher, so it is not available). In: Sawada H, editor. *Current Research Trends of Fluoropolymers*. Tokyo: CMC Publishing Co. Ltd.; 2013. p 195.
- [23] Kurihara S, Murata S, Sato K, Horiuti M, Mouri S, Abe H, Jin JS. Fluorine-containing polymer and surface-modifying agent containing the same as active ingredient. U.S. Patent 8,501,888. 2013 to Unimatec.
- [24] Kubota K, Miki J. Fluorine-containing composition and application thereof. PCT Int. App. WO 13/58,335. 2013 to Daikin.
- [25] Kubota K, Miki J. Fluorine-containing composition and surface treatment agent. PCT Int. App. WO 13/58,336. 2013 to Daikin.
- [26] Miki J, Kubota K, Mohara K. Fluorine-containing composition and fluorine-containing polymer. PCT Int. App. WO 13/58,337. 2013 to Daikin.
- [27] Hoshino T. Fluorinated compound and fluorinated polymer. PCT Int. App. WO 11/52,783. 2011 to Asahi Glass.
- [28] Hoshino T. Fluorinated compound and fluorinated polymer. PCT Int. App. WO 11/52,784. 2011 to Asahi Glass.
- [29] Hoshino T. Fluorine-containing compound, fluorine-containing polymer and fluorine-containing copolymer. PCT Int. App. WO 11/52,786. 2011 to Asahi Glass.
- [30] Hoshino T. Fluorine-containing compound and fluorine-containing polymer. PCT Int. App. WO 11/125,892. 2011 to Asahi Glass.
- [31] Morita M, Ishikawa T, Yamashita T, Kanemura T, Yamamoto I. Lyophobic and development properties of fluorine lyophobic resist. *Kobunshi Ronbunshu* 2009;66:102.
- [32] Yamamoto I, Masuto T. Surface-treating agent comprising fluoropolymer. PCT Int. App. WO 04/96,939. 2004 to Daikin.

ETCHING GAS

SEIJI SAMUKAWA

Tohoku University, Sendai, Japan

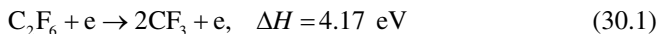
30.1 HIGH-PERFORMANCE SILICON DIOXIDE ETCHING

Generally, SiO_2 etching is performed using fluorocarbon gases to deposit a fluoropolymer on the underlying silicon. This deposit enhances the etching selectivity of SiO_2 over those of Si and SiN. CF_2 radicals are commonly used as the main gas precursor for polymer deposition. CF_3^+ ions are the dominant etchant for SiO_2 film because the etching yield of CF_3^+ for Si and SiO_2 is larger than that of CF^+ , CF_2^+ , and C_2F_4^+ [1–3]. CF_3^+ ions are efficiently generated from CF_3 radicals because of their lower ionization thresholds ($\text{CF}_3 + e \rightarrow \text{CF}_3^+$: 10.3 eV). Plasmas made from gases with a lower molecular weight (CF_4 , CHF_3 , and C_2F_6) result in a smaller amount of CF_2 and CF_3 radical generation, as well as a larger amount of F atoms, because of the higher degree of dissociation by high-energy electrons. As a result, a lesser degree of polymerization reduces etching selectivity. Conversely, gases with a higher molecular weight (C_3F_8 , C_4F_8) result in more polymerization with a larger number of CF_2 radicals, because the number of high-energy electrons is relatively reduced by the large cross sections of the electron collisions in momentum transfer and vibrational excitation at around 5 eV [4]. However, smaller amounts of ions (CF_3^+ ion) have also been observed in these plasmas. In particular, in high-aspect contact holes of less than 0.25 mm, the polymer deposition rate is higher than the SiO_2 etching rate. This condition causes aspect-ratio-dependent etching and etching stop. It is thus very difficult to control the balance between radical flux (CF_2 radicals) and ion flux (CF_3^+ ions) during SiO_2 contact etching in fluorocarbon plasma using conventional gas chemistry. Although Ar dilution (over 80%) of C_4F_8 is widely used to improve the

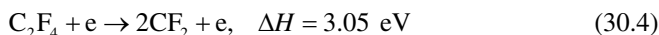
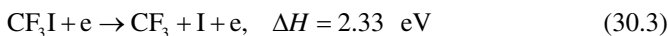
control of polymerization in higher-aspect contact holes, this method has problems, such as a decreased etching rate and lower etching selectivity. To solve these problems, it is necessary to generate selected radicals in fluorocarbon plasmas.

We report a new method for selective radical generation for high-performance sub-0.1 μm SiO_2 patterning, using CF_3I and C_2F_4 in an Ultra High Frequency (UHF) plasma [5]. This plasma mainly dissociates the weak C–I and C=C bonds in CF_3I and C_2F_4 , because the mean electron energy is low ($\sim 2\text{--}3\text{ eV}$). Therefore, CF_3 (CF_3^+) and CF_2 radicals are efficiently generated by using CF_3I and C_2F_4 in an UHF plasma. The flux of CF_2 and CF_3 radicals can be controlled by changing the ratio of these gases in the plasma. By applying UHF (500 MHz) power to high-density plasma, non-Maxwellian Electron Energy Distribution Functions (EEDFs) can be produced [6]. Schematic illustrations of typical EEDFs in the UHF plasma are shown in Figure 30.1. The UHF plasma appears to exhibit a bi-Maxwellian EEDF. The majority of the electrons (i.e., bulk electrons) are relatively cold and can be represented by a Maxwellian distribution with a relatively low electron temperature. The high-energy tail of the distribution is enhanced, and this enhancement can be described through a presence of the second (much less populated) pool of electrons with higher (with respect to bulk electrons) electron temperature. These high-energy electrons can achieve a sufficient level of ionization to produce a higher-density plasma ($>10^{11}\text{ cm}^{-3}$).

The lowest energy channels for generation of CF_3 and CF_2 radicals from the conventional C_2F_6 and C_4F_8 sources that do not involve complicated, unlikely bond rearrangements (for CF_2 formation from C_4F_8) are



where ΔH represents the thermodynamic heat of reaction (also the bond strength for these reactions, and those shown later) and C_3F_6 is a diradical species. With the new compounds explored here, CF_3 and CF_2 can be formed by the reactions:



Because the peak electron density is at an energy of about $2\text{--}3\text{ eV}$ (electron temperature T_e : $2\text{--}3\text{ eV}$) in the UHF fluorocarbon gas plasma, the C–I bond of about 2.33 eV and a C=C bond of about 3.05 eV are efficiently dissociated in CF_3I and C_2F_4 in reactions 30.3 and 30.4, whereas the rupturing of C–F bonds (5.45 eV) and the formation of CF_3 and CF_2 by reactions 30.1 and 30.2 require energies above the peak electron energy in the UHF plasma. In fact, the reported threshold for CF_2 formation from electron impact dissociation of C_4F_8 is quite high (10.5 eV) [7]. The UHF plasma and new source gases (CF_3I and C_2F_4) are thus an ideal combination for selective generation of CF_2 and CF_3 radicals in the plasma.

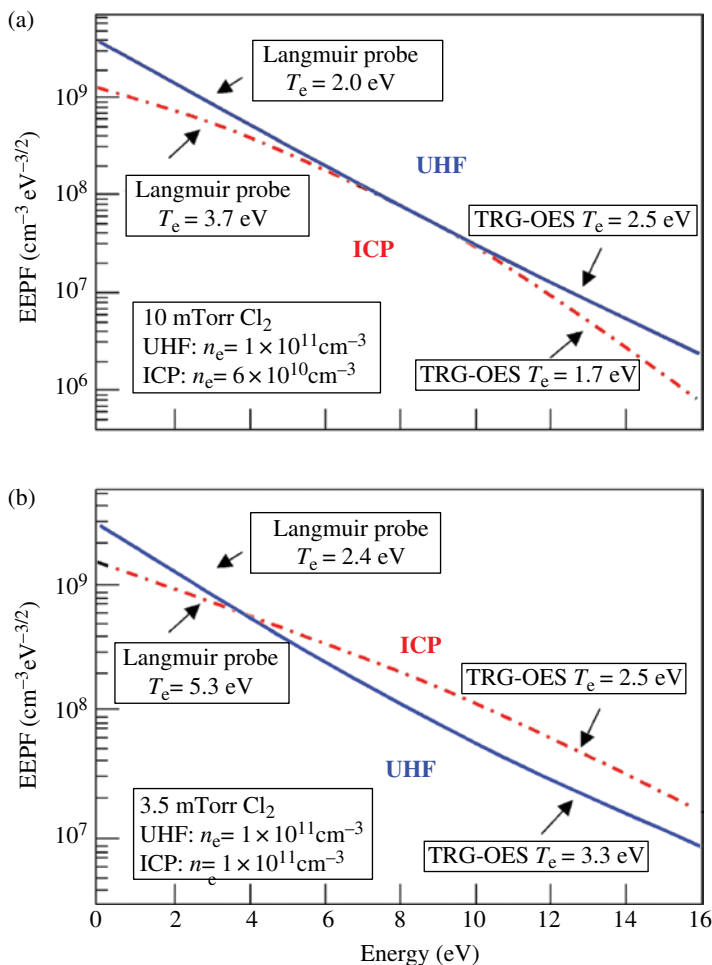


FIGURE 30.1 A qualitative picture of the EEPFs estimated from a combination of Langmuir probe and trace rare gas optical emission spectroscopy measurements of electron temperature at (a) 10 mTorr; and (b) 3.5 mTorr for the ICP and UHF plasma.

In this experiment, infrared diode laser absorption spectroscopy (IR-LAS) [8–10] and OES were used to measure the density of CF , CF_2 , and CF_3 radicals, as well as F atoms. The IR-LAS laser beam passed through the plasma region 16 times during the radical measurements. The CF , CF_2 , and CF_3 radical densities were measured 3 cm above the substrate. The absorption lines used were 1308.5 cm^{-1} for the CF radicals, 1132.7 cm^{-1} for the CF_2 radicals and 1262.1 cm^{-1} for the CF_3 radicals. We used the optical emission intensities for CF (202.4 nm), CF_2 (251.9 nm), and F (703.7 nm). The relative amounts of ion species, such as CF_3^+ and Ar^+ ions, were measured with a mass spectrometer. The plasma density and electron temperature in these UHF

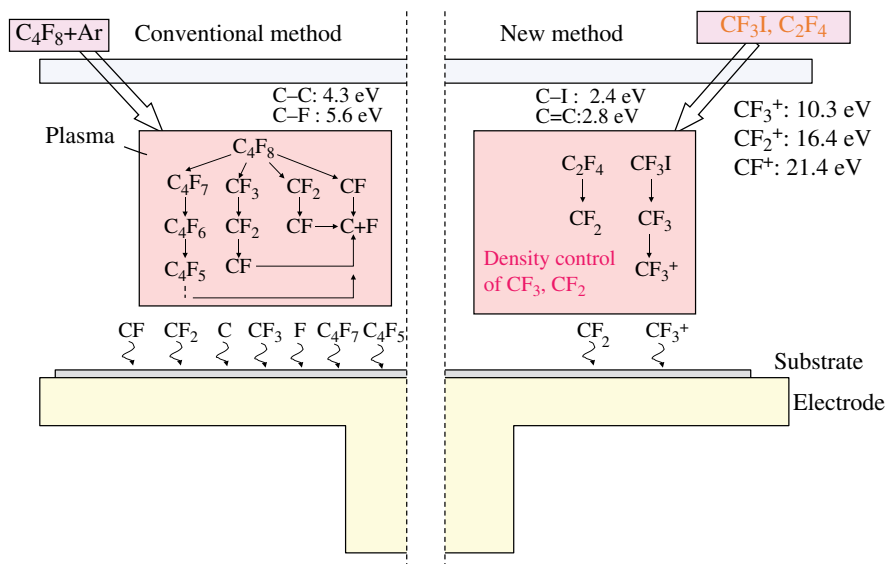


FIGURE 30.2 Concept of the new radical injection method. The CF_2 and CF_3 radicals are selectively generated from CF_3I and C_2F_4 gases in the plasma.

plasmas were measured with a Langmuir probe (Irie Co., Japan) located at the center of the UHF plasma reactor at the same height at which the OES and IR-LAS measurements were performed. To keep the tip surface clean, the probe tips (with an area of 0.0942 cm^2) and the reactor walls were heated to over 100°C . The reproducibility of the measurements was confirmed by repeating the measurements several times.

Six-inch diameter substrates were used on a 20-cm diameter electrode. The radio frequency (rf) bias (1 MHz) on the substrate was fixed at 500 W (1.6 W cm^{-2}) when the SiO_2 etching was done. The gas flow rate was 100 sccm, the pressure was 5 mTorr, and the UHF power was 1 kW. The polymer deposition rate on the silicon substrate was measured without rf bias voltage. The measured radical densities in the CF_3I and C_2F_4 plasmas show that they are efficient sources of CF_3 (CF_3^+) and CF_2 radicals when compared with conventional C_4F_8 and C_2F_6 plasmas (Figs. 30.2 and 30.3). This is easily understood from the differences in the bond strengths of reactions.

We found that the density ratios of CF_2 and CF_3 could be independently controlled by changing the gas flow ratio of the CF_3I and C_2F_4 mixture (Fig. 30.4), and that the polymer deposition rate can be accurately controlled by changing the density of CF_2 radicals (Fig. 30.5). Since polymer deposition occurred when using only the CF_2 radicals, the higher molecular weight radicals can be eliminated in the CF_3I/C_2F_4 mixture plasma. We also found that the CF_3I (more than 60%)/ C_2F_4 mixture plasma had a high plasma density of over $1 \times 10^{11} \text{ cm}^{-3}$ while maintaining a lower electron temperature (Fig. 30.6). This suggests that the addition of CF_3I contributed to the increase in the ion density because of the lower ionization thresholds of I^+ (9 eV) and CF_3^+ (10 eV) ions from CF_3I compared to the threshold of Ar^+ ions (16 eV) in C_4F_8/Ar

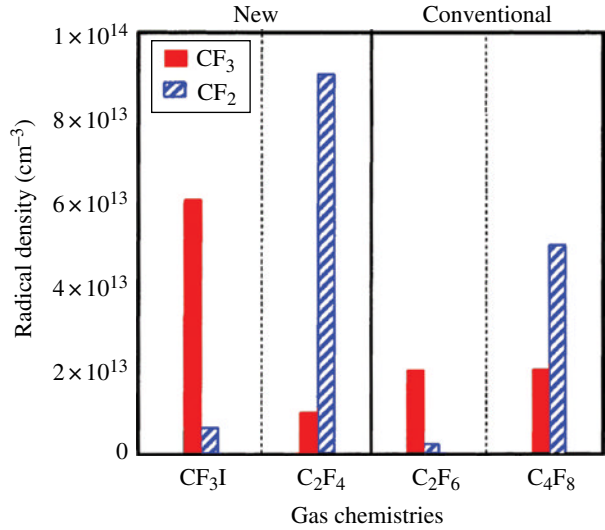


FIGURE 30.3 Line-averaged CF_3 and CF_2 radical densities in CF_3I , C_2F_4 , C_2F_6 , and C_4F_8 UHF plasmas under the same discharge condition. CF_3I and C_2F_4 were good sources of CF_3 and CF_2 radicals, respectively. Bias power: 500 W, flow rate: 100 sccm.

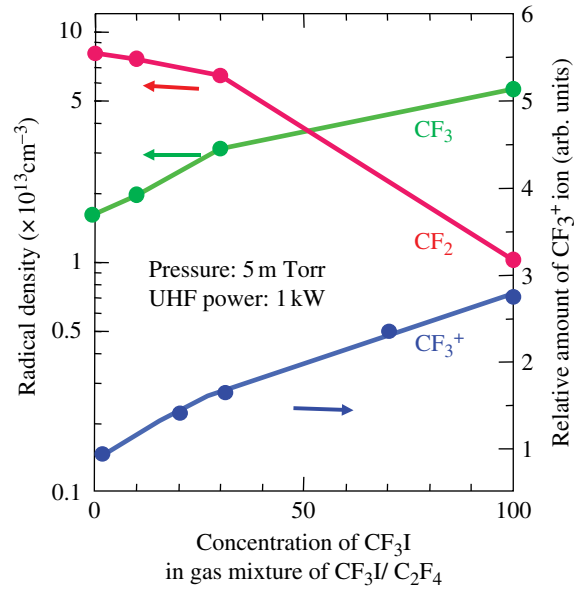


FIGURE 30.4 Density ratios of CF_2 and CF_3 by changing the gas flow ratio of the CF_3I and C_2F_4 mixture in the UHF plasma.

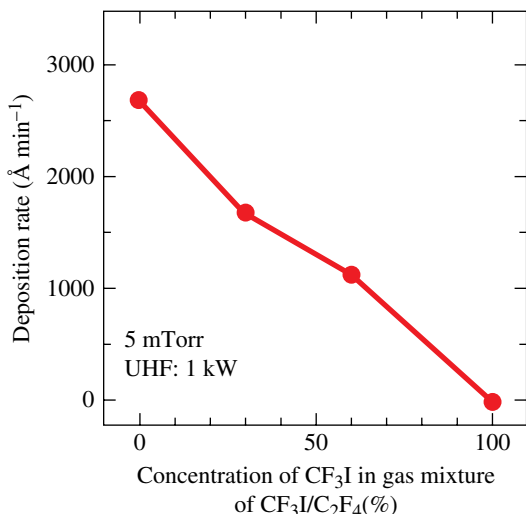


FIGURE 30.5 The polymer deposition rate on the Si substrate as a function of the gas flow ratio of the CF₃I and C₂F₄ mixture in the UHF plasma.

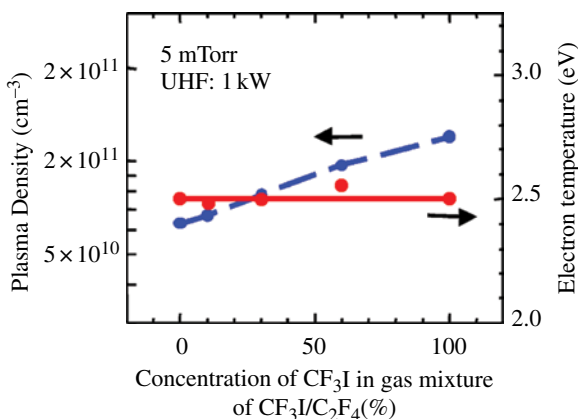


FIGURE 30.6 The plasma density and electron temperature as a function of the gas flow ratio of the CF₃I and C₂F₄ mixture in the UHF plasma.

plasma. In this plasma, high-energy electrons of the EEDF are considered to be reduced. These results also suggest that high-density (more than 10^{11} cm^{-3}) CF₃⁺ ions and CF₂ radicals were generated in the CF₃I and C₂F₄ gas mixture.

We investigated the etching characteristics of both C₂F₄/CF₃I and C₄F₈/Ar gas plasmas. The etching selectivity of SiO₂ to the underlying Si greatly improved when the C₂F₄ gas flow rate was increased in the C₂F₄/CF₃I plasma. A selectivity of over 20 for a bare sample was achieved when the gas mixture contained 80% C₂F₄ (Fig. 30.7). Under this condition, the thermal SiO₂ etching rate was 4000–5000 Å min⁻¹, which is

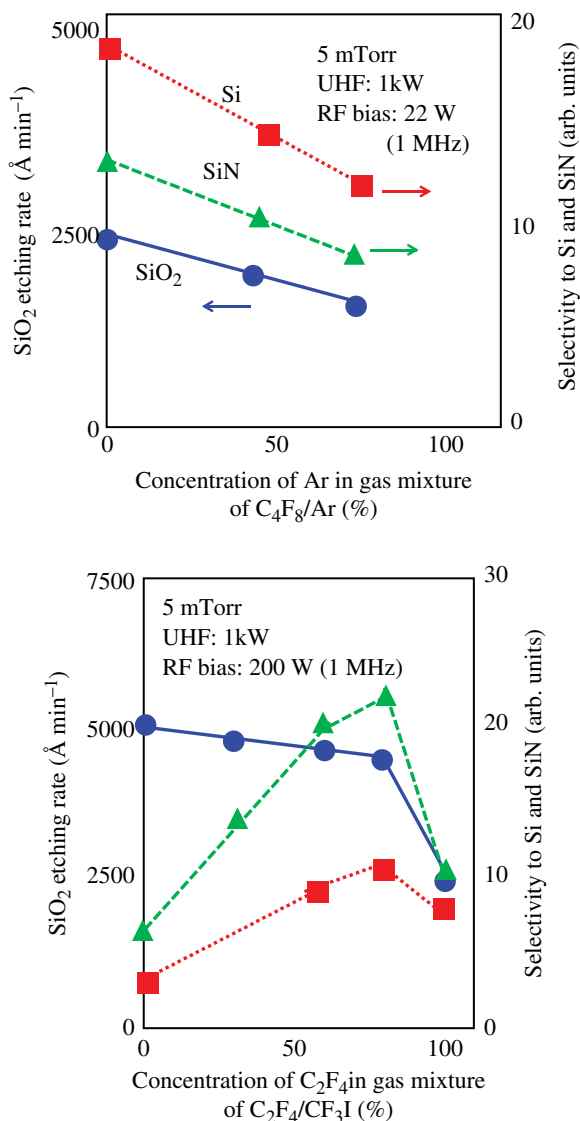


FIGURE 30.7 SiO_2 etching rate and etching selectivity to Si (poly-Si) and SiN in the $\text{CF}_3\text{I}/\text{C}_2\text{F}_4$ gas mixture and $\text{C}_4\text{F}_8/\text{Ar}$ gas mixture when rf bias of 200 W was supplied on the substrate. The sample was a bare wafer.

about twice that with conventional Ar (80%)/ C_4F_8 gas. We believe that the high etching rate and the high selectivity were due to the balance between CF_3^+ for the SiO_2 etchant and CF_2 for the polymerization. A highly anisotropic etched profile of a 0.05- μm -diameter contact hole with a sidewall angle of more than 88° was achieved while maintaining a high etching rate Boron Phosphor Silicate Glass (BPSG):

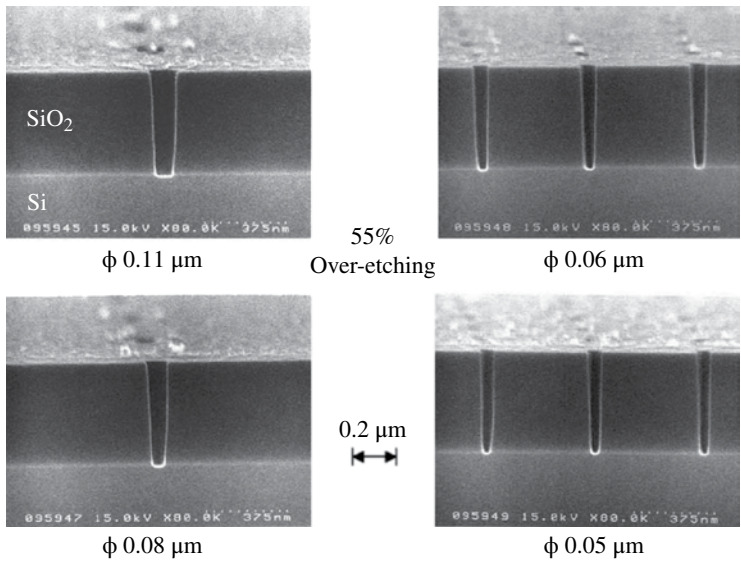


FIGURE 30.8 A contact hole etching profile from 0.11 to 0.05 μm in the $\text{CF}_3\text{I}/\text{C}_2\text{F}_4$ plasma. Source power: 1 kW, bias power: 500 W, pressure: 5 mTorr, flow rates: 100 sccm.

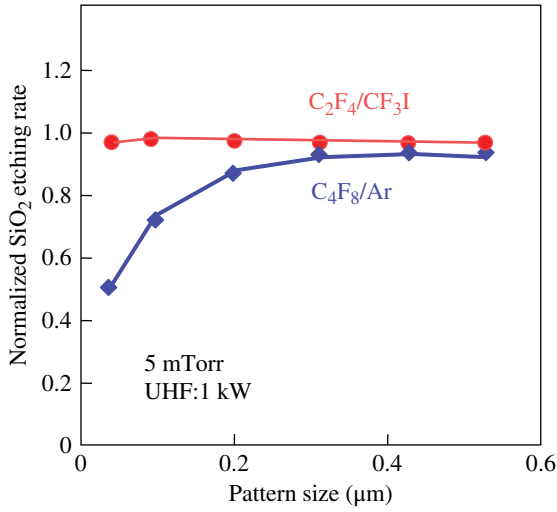


FIGURE 30.9 Pattern dependence of the etching rate at the pattern width between 0.05 and 0.5 μm in the photoresist-masked BPSG film using $\text{C}_2\text{F}_4/\text{CF}_3\text{I}$ and $\text{C}_4\text{F}_8/\text{Ar}$ plasmas.

$7000 \text{ \AA min}^{-1}$), and a high selectivity (>50) to the underlying Si in the $\text{C}_2\text{F}_4/\text{CF}_3\text{I}$ plasma (Fig. 30.8) [11]. Etching profiles were virtually the same as those for contact holes of more than 0.1- μm diameter. We measured the change in etching rates for hole diameters between 0.05 and 0.5 μm in a photoresist-masked BPSG film using both $\text{C}_2\text{F}_4/\text{CF}_3\text{I}$ and $\text{C}_4\text{F}_8/\text{Ar}$ plasmas (Fig. 30.9) [11]. The etching rates were normalized at

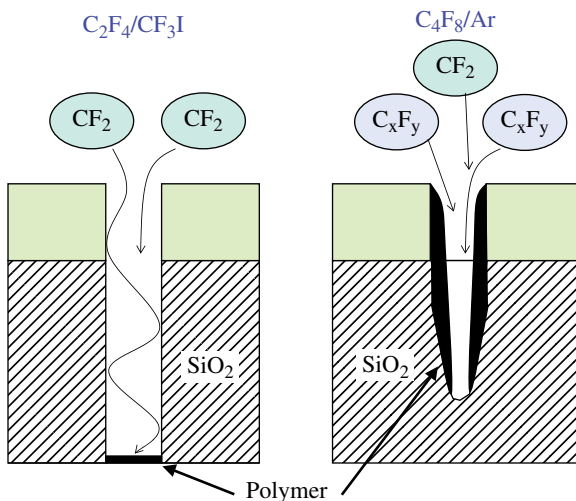


FIGURE 30.10 Polymer deposition mechanism in CF_3I/C_2F_4 gas mixture plasma and C_4F_8/Ar gas mixture plasma.

a contact hole of 0.5 μm . With the new chemistry, the pattern dependence of the SiO₂ etching rate is almost eliminated due to the optimum balance between polymerization and etching and by the suppression of higher molecular weight radicals. One possible mechanism for eliminating the etching stop in the new chemistry is depicted in Figure 30.10 [11]. The higher molecular weight radicals (C_xF_y) are preferentially formed in C_4F_8 plasmas. These species are more likely to form a thick film on both SiO₂ and Si, narrowing the width of the etched feature, depleting etchants from the bottoms of the features, and eventually stopping the etching of the SiO₂. CF_2 , on the other hand, will be less likely to stick to the sides of etched features [8, 9]. The selective generation of CF_2 radicals and CF_3 ions is thus advantageous for achieving a microloading-free, etching-stop-free, high etching rate and high etching selectivity at the same time.

30.2 ENVIRONMENTALLY HARMONIZED CF3I PLASMA FOR LOW-DAMAGE AND HIGHLY SELECTIVE LOW-*k* ETCHING

As the feature size of ultralarge-scale integrated circuits (ULSIs) becomes smaller, the resistance–capacitance (RC) delay time of their interconnects restricts the circuit performance. In an effort to reduce the RC delay, the conventional aluminum/SiO₂ interconnects have been replaced with copper (Cu)/low dielectric (low-*k*) film interconnects [12]. Since Cu film cannot be etched easily by plasma, owing to the low volatility of Cu compounds, precise etching technology for low-*k* films must be developed. Moreover, as a way of reducing the dielectric constant, introducing pores into low-*k* film (porous low-*k* film) has been investigated [13, 14]. Many kinds of low-*k* films have been proposed; however, SiOCH film is the most widely accepted.

This is due to such factors as easy transfer from the SiO_2 process, high thermal stability, and high Young's modulus [15]. As pores are introduced, damage by ultraviolet (UV) photon irradiation from the plasma during the SiOCH film etching becomes a serious problem. It was reported that UV irradiation removes the methyl groups (CH_3) from porous SiOCH low- k film, resulting in an increase in the dielectric constant [16–18]. To solve these problems, the effects of UV irradiation on low- k film during low- k etching processes must be monitored and controlled.

On the other hand, since most of these conventional gases have high global warming potential (CF_4 : 6500 and C_4F_8 : 8700), from the viewpoint of protecting the global environment, significantly reducing their emissions is strongly urged [19, 20]. Samukawa et al. previously proposed a new environmentally harmonized gas chemistry using CF_3I and C_2F_4 gases to replace these conventional gases because they have low global warming potential (<1.0) [21, 5, 22, 11]. CF_3I and C_2F_4 generate CF_3 and CF_2 radicals selectively because the binding energies of C–I (2.4 eV) and C=C (2.8 eV) are much smaller than that of C–F (5.6 eV). By controlling the flow rates of CF_3I and C_2F_4 , in a previous study, we achieved highly selective SiO_2 contact hole etching at a high rate [11]. Moreover, we also developed a technique for pulse-time modulation of an etching plasma [23]. Pulse-time-modulated plasma generates many negative ions and reduces charge buildup damage and UV irradiation damage. In this process, the input power is turned on and off at a rate of 10–100 μs . There is no UV irradiation during the pulse-off time. In addition, we also reported that the negative ions in the pulsed plasma play a beneficial role in the etching [24–28].

In the present study, we investigated low-damage porous SiOCH low- k etching by CF_3I plasma (as compared with CF_4 plasma). In addition, we investigated the effect of pulsed CF_3I plasma [28] for increasing the performance of porous SiOCH low- k etching.

30.3 EXPERIMENTAL

A schematic diagram of the experimental setup to generate inductively coupled plasma (ICP) as a plasma source (i) for low- k etching and (ii) for UV spectroscopy is shown in Figure 30.11. A one-turn antenna was driven by a 13.56-MHz rf, which generated a plasma with high density of more than 10^{11} cm^{-3} . The diameter of the chamber was 400 mm, and the plasma uniformity was about 10% on a 6-in. wafer. A rf bias of 1 MHz was applied to accelerate the ions toward the substrate during low- k etching (Fig. 30.11a). The typical pressure, gas flow, source power, and bias power were 20 mTorr, 30 sccm, 500 W (continuous wave [cw]), and 50 W, respectively. The UV spectrum, low- k etching characteristics, and low- k damage in the CF_3I plasmas were evaluated. As compared with CF_3I plasma, we also evaluated the CF_4 plasma because the CF_4 gas has a molecular structure similar to the CF_3I gas and it is widely used for low line-edge-roughness (LER) low- k etching processes.

UV spectra were measured by a vacuum UV spectrometer (Acton research VM 502), located at the bottom of the chamber, through a pinhole that was 80 mm deep

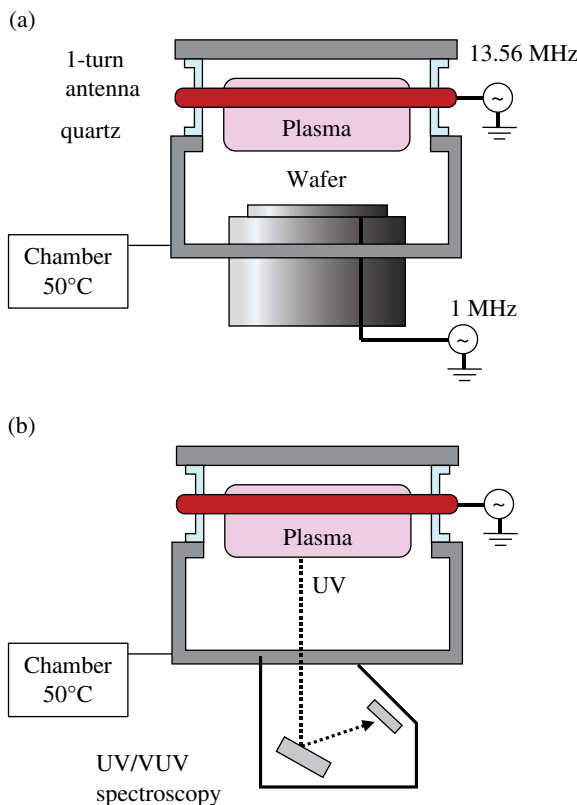


FIGURE 30.11 Schematic diagram of experimental setup to generate inductively coupled plasma (a) for low- k etching and (b) for UV spectroscopy measurement.

and 1 mm in diameter (Fig. 30.11b). The UV intensities in the wavelength range from 200 to 400 nm were measured, and the measurement step was 1 nm. To observe the UV damage, the UV-induced current in UV sensors and charge-pumping current in metal–nitride oxide semiconductor field-effect transistors (MNOSFETs) were evaluated (Fig. 30.12). The induced currents in the SiO_2 and SiOCH sensors (Fig. 30.12a, b) were measured by applying voltage to the electrode when the UV light with higher energy than the bandgap was irradiated [29–31]. This is because an electron–hole pair is generated by UV irradiation [32]. A rigid chemical vapor–deposited (CVD) SiOCH film was deposited as a low- k film; it had almost the same composition as the porous low- k film evaluated in this chapter. To evaluate the effects of UV on the electrical characteristics of MNOSFETs, we measured the charge-pumping current of the metal–nitride oxide semiconductor (MNOS) samples (as in Fig. 30.12c). After UV irradiation of the MNOS samples for 5 min, we measured the charge-pumping current, which corresponds to the interface-state density between Si and SiO_2 [33]. We used 200-nm-thick blanket wafers of porous CVD SiOCH ($k=2.5$) as samples for evaluating low- k etching. To evaluate trench etching, we prepared patterned samples

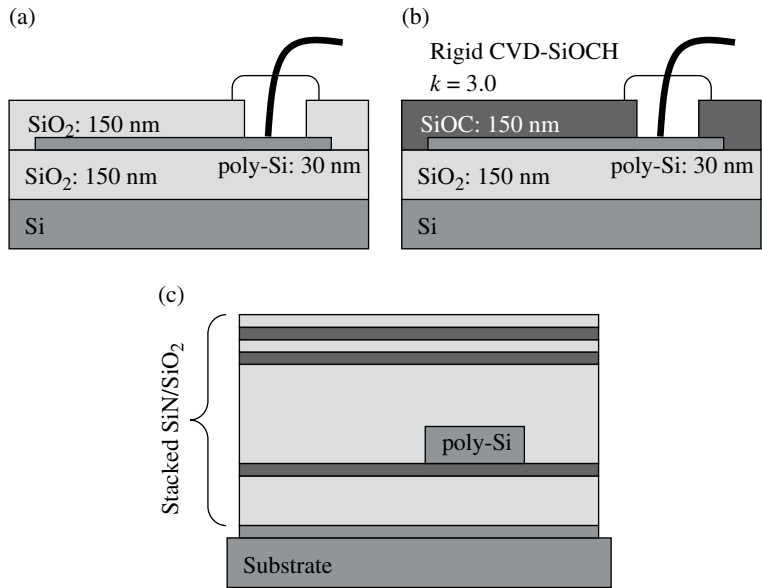


FIGURE 30.12 Schematic cross section of (a) SiO₂ UV sensor, (b) SiOCH UV sensor, and (c) MNOSFET.

where an antireflective film (ARC) and low- k cap film were etched beforehand using a conventional etching technique. The thickness of the low- k film in the patterned sample was 100 nm. The blanket wafers were also used to evaluate the low- k damage after etching. We evaluated the dielectric constant using a mercury (Hg) probe, and analyzed the film by X-ray photoelectron spectroscopy (XPS) and Fourier transform infrared (FTIR) spectrometry. We also evaluated the species desorption by thermal desorption spectrometry (TDS).

30.4 RESULTS AND DISCUSSION

30.4.1 UV Spectrum in CF₃I and CF₄ Plasmas

Figure 30.13 plots the UV spectrum in the case of the CF₃I and CF₄ plasmas as a function of source power. Although the CF₃I plasma had several sharp peaks, such as at 206 nm, the UV intensities between 250 and 400 nm are much smaller than those in the case of CF₄ plasma. We presume this is because CF₃I plasma has few high molecular weight radicals, such as C_{*x*}F_{*y*} [21, 22]. As the source power was increased, in the CF₃I plasma case, the UV intensities between 250 and 400 nm did not change significantly in contrast to those in the CF₄ case. This result also reveals that the CF₃I plasma did not generate a large amount of high molecular weight fluorocarbons.

Figure 30.14 shows the UV spectrum in CF₃I and CF₄ pulsed plasmas. The pulse-on time was fixed at 50 μs. In the case of CF₃I, the UV intensities were almost eliminated

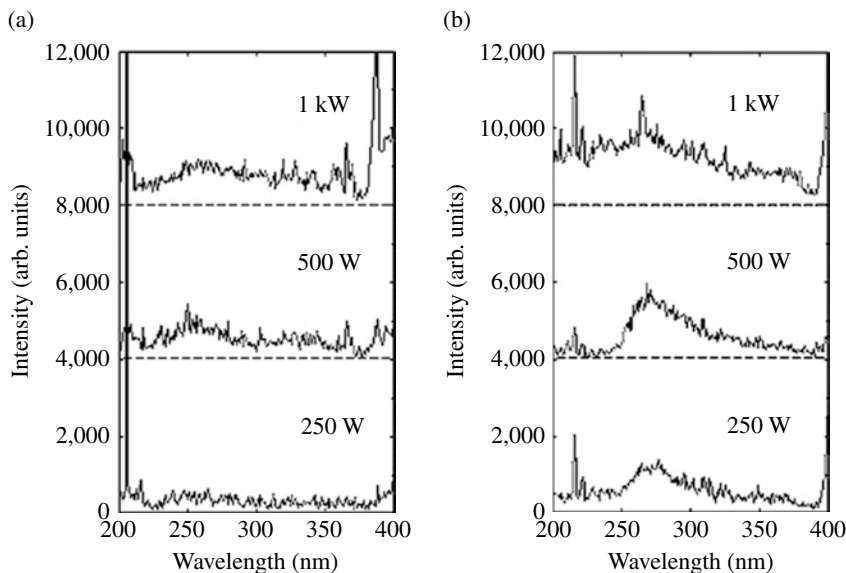


FIGURE 30.13 UV spectrum of plasmas as a function of ICP power: (a) CF_3I and (b) CF_4 . Conditions: 20 mTorr, gas flow: 30 sccm, continuous source power (13.56 MHz), no bias power, and substrate temperature: 20°C.

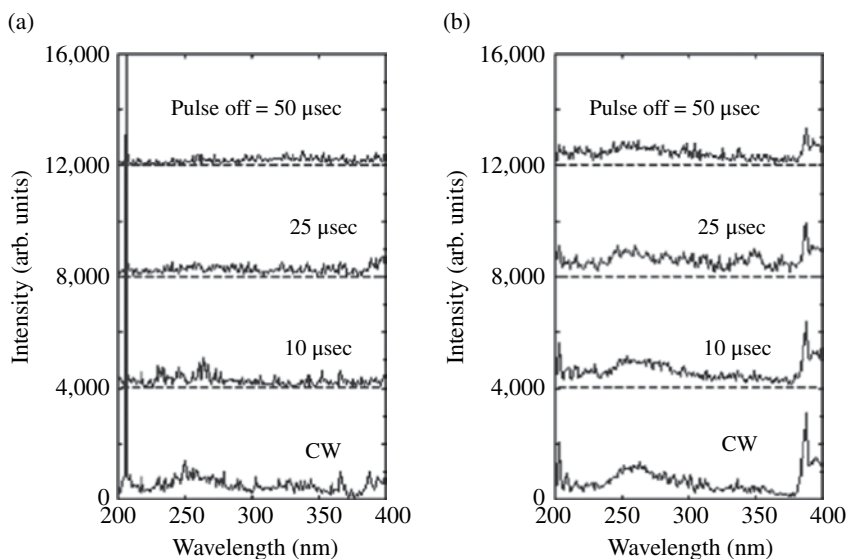


FIGURE 30.14 UV spectrum as a function of pulse-off time: (a) CF_3I plasma and (b) CF_4 plasma. Conditions: 20 mTorr, gas flow: 30 sccm, continuous/pulsed source power (peak power=500 W/13.56 MHz, pulse-on time=50 μs), no bias power, and substrate temperature: 20°C.

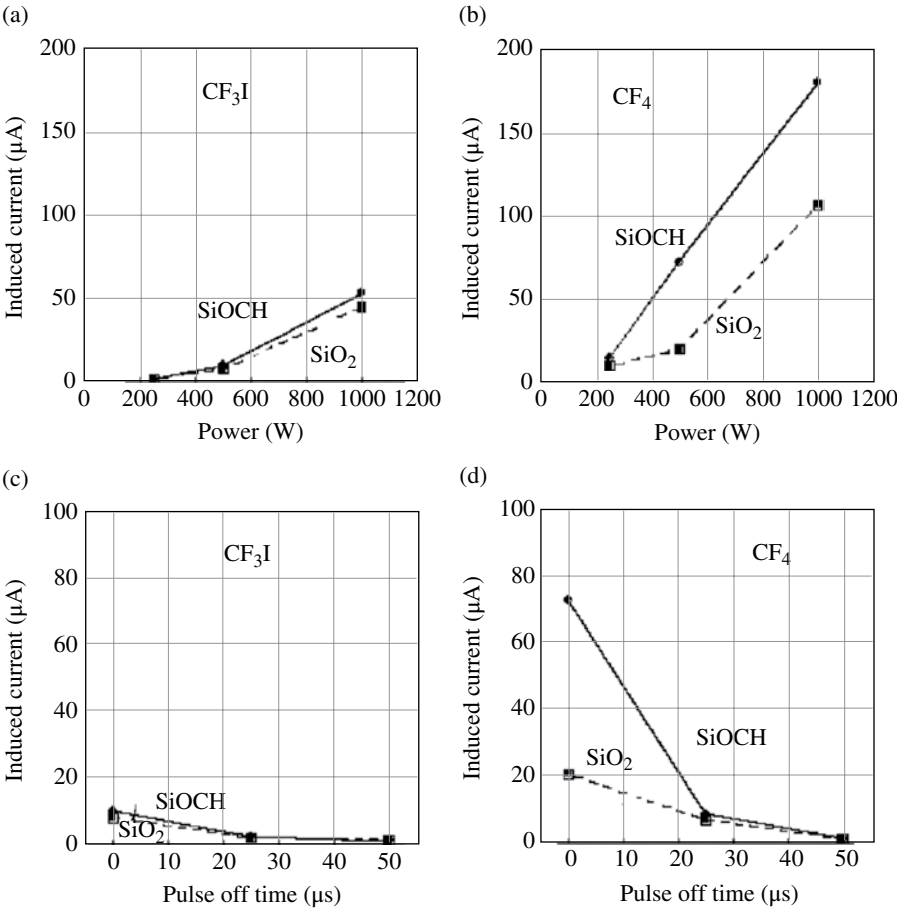


FIGURE 30.15 Induced currents of UV sensors (a) in CF_3I plasma on ICP power, (b) in CF_4 plasma on ICP power (both pulse-on and -off times were 50 μs), (c) in CF_3I plasma on pulse-off time, and (d) in CF_4 plasma on pulse-off time (the peak source power and pulse-on time were 500 W and 50 μs, respectively). Other conditions: 20 mTorr, gas flow: 30 sccm, pulsed source power (13.56 MHz), no bias power, and substrate temperature: 20°C.

as the pulse-off time increased, while the UV intensities in the CF_4 case were observed even at the pulse-off time of 50 μs. It is clear from these results that the UV intensity of the CF_3I plasma is lower in the wavelength region between 250 and 400 nm than that of CF_4 plasma. Using the UV sensors we developed, we evaluated the UV-induced current in low- k film when the UV was irradiated. Figure 30.15 plots the induced current as a function of source power and pulse-off time. In all evaluations, the induced current by CF_4 plasma is larger than that by CF_3I plasma. The binding energy between Si and CH_3 in $SiOCH$ film was estimated to be 3–4 eV [34]. This indicates that UV irradiation in the wavelength range of 300–400 nm can break this bond. Accordingly, we can speculate that there would be much less UV damage by CF_3I plasma than by CF_4 plasma

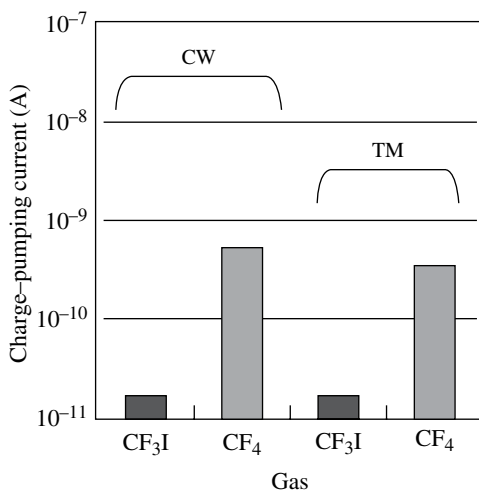


FIGURE 30.16 Charge-pumping currents after exposure to CF₃I and CF₄ plasma. During pulse time modulationTM operation, pulse-on and -off times were both 50 μ s. Other conditions: 20 mTorr, gas flow: 30 sccm, source power of 500 W (13.56 MHz), no bias power, substrate temperature: 20°C, and 5 min.

because the UV intensities between wavelengths of 300 and 400 nm are lower. In addition, to show the effects of UV irradiation on the electrical characteristics of a MNOSFET, we evaluated the charge-pumping current of the plasma-exposed sample [35]. The evaluation result suggests that the interface states of this MNOSFET are generated by UV exposure at a wavelength between 250 and 400 nm, corresponding to the bandgap of a SiN film. The charge-pumping current in CF₄ plasma was much larger than that in the CF₃I plasma (Fig. 30.16). This is because the UV intensity between 250 and 400 nm in the CF₄ plasma is larger than that in the CF₃I one. The pulse operation reduced the UV irradiation damage that occurs with both gas plasmas; however, the charge-pumping current in pulsed CF₃I plasma was much lower than that in CF₄ pulsed plasma. Accordingly, it is concluded that the damage in Metal Oxide semiconductor (MOS) devices due to low-*k* etching is reduced by using CF₃I plasma.

30.4.2 Etching Characteristics of Porous Low-*k* Film in CF₃I Plasma

Figure 30.17 shows the etching characteristics as a function of the rf bias power in the CF₃I and CF₄ plasmas. In the case of CF₃I plasma, the porous SiOCH etching selectivity to the photoresist is much higher than that in the case of CF₄ plasma. We can speculate that this is because the UV irradiation and the generation of F radicals in CF₄ enhanced resist etching (CF₃I plasma can generate fewer F radicals [36]). Figure 30.18 shows the etching characteristics as a function of pulse-off time in the cases of CF₃I and CF₄ pulsed plasmas. In the case of the CF₄ plasma, the SiOCH etching rate drastically decreased as the pulse-off time increased, while the SiOCH etching rate in CF₃I plasma case significantly increased. At a pulse-off time of 50 μ s,

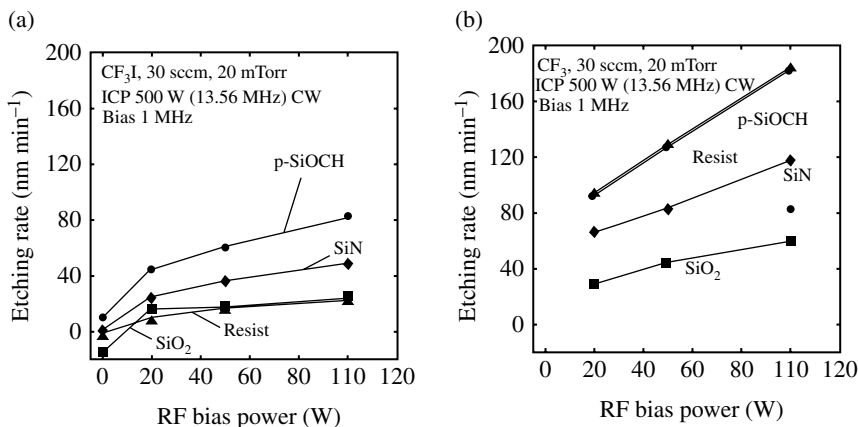


FIGURE 30.17 Etching characteristics as a function of bias power: (a) CF₃I plasma and (b) CF₄ plasma. Blanket wafers were used.

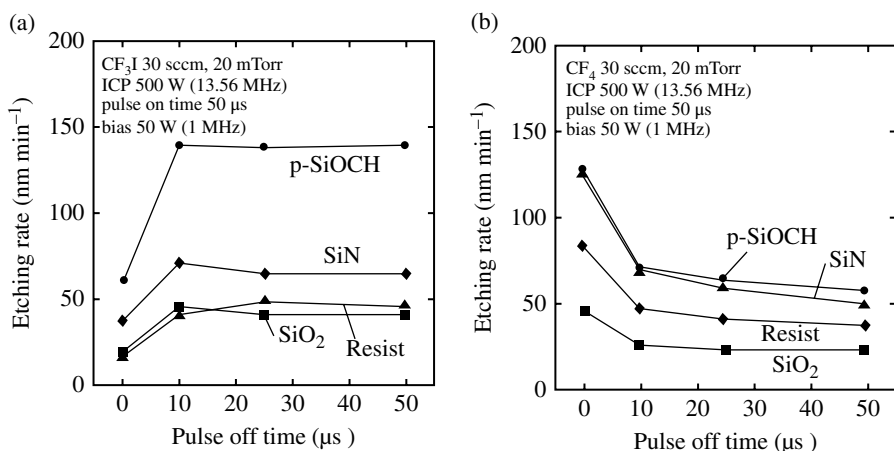


FIGURE 30.18 Etching characteristics as a function of pulse-off time: (a) CF₃I plasma and (b) CF₄ plasma. Blanket wafers were used.

the SiOCH etching rate was about 2.3 times higher than that in the case of the continuous wave CF₃I plasma. We previously reported that the etching rates for Si, Au, PtMn, NiFe, and SiO₂ in the case of a pulsed plasma increased because a large amount of negative ions can be injected into the substrate during the pulse-off time [24–28]. We can speculate that the low-*k* etching rate also increases due to the injected negative ions. We also reported previously that pulsed CF₃I plasma generates a large amount of negative ions by dissociative attachment even when the pulse-off time is less than 30 μs [28]. F⁻ and I⁻ negative ions are generated through dissociative attachment in the pulsed CF₃I plasma and their densities are about the same as the positive ions [28, 37]. On the contrary, the number of negative ions in CF₄ pulsed plasma is small because the attachment cross section is small [38, 39]. Accordingly,

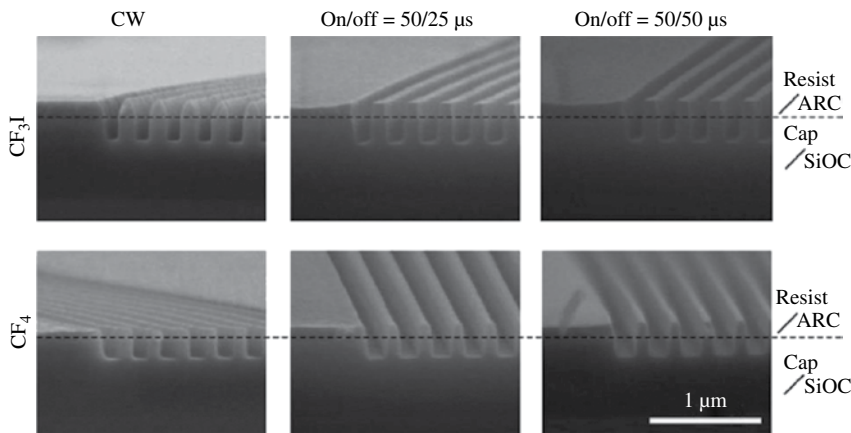


FIGURE 30.19 Trench profiles of porous low- k films etched by CF_3I and CF_4 plasma. Conditions: 20 mTorr, gas flow: 30 sccm, continuous/pulsed source power (peak power = 500 W/13.56 MHz, pulse-on time = 50 μs), bias power: 50 W (1 MHz), and substrate temperature: 20°C.

we conclude that high rate and highly selective low- k etching can be achieved with the CF_3I pulsed plasma.

Figure 30.19 shows low- k etching profiles as a function of pulse-off time. The trench widths in the case of the CF_4 plasma are much larger because the etching selectivity to photoresist was insufficient. Since the etching selectivity to the photoresist in the CF_3I plasma case is very large, well-controlled trench patterns were achieved; in particular, the etching profiles were drastically improved.

30.4.3 Evaluation of Low- k Damage during CF_3I Plasma Etching

The UV intensity of the CF_3I plasma in the wavelength range between 250 and 400 nm is lower than that of the CF_4 plasma, as shown in Figure 30.13. Since the UV wavelength, which corresponds to the binding energy between Si and CH_3 , is about 300–400 nm, CF_3I plasma can reduce the amount of CH_3 that is removed from a SiOCH film.

To observe the low- k damage that occurs in CF_3I plasma etching, we evaluated the dielectric constant after etching with CF_3I and CF_4 plasmas. We used a blanket porous SiOCH wafer, and etched to a depth of 50 nm into the wafer (residual thickness: 150 nm). Figure 30.20 plots the dielectric constants as a function of the pulse-off time. The dielectric constant of low- k film exposed to CF_3I cw plasma was about 0.1 smaller than that in the case of the CF_4 cw plasma. The dielectric constant of low- k film exposed to the pulsed CF_3I plasma with a pulse-off time of 50 μs was almost the same as that of the nonexposed samples.

To clarify how the dielectric constant increases due to plasma exposure, we analyzed a plasma-exposed film by FTIR, TDS, and XPS. We used a blanket porous SiOCH wafer and etched it to a depth of 50 nm (residual thickness: 150 nm). Figure 30.21 shows the Si- CH_3 peak intensity of FTIR as a function of the pulse-off time. The sample after CF_3I plasma etching had a larger number of methyl groups

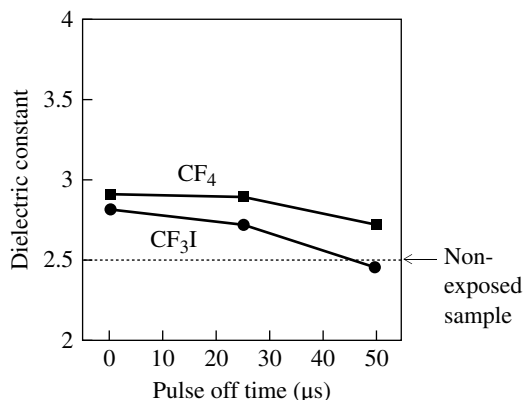


FIGURE 30.20 Dielectric constants of porous low- k films after exposure to CF_3I and CF_4 plasma as a function of pulse-off time. Blanket wafers were used. Conditions: 20 mTorr, gas flow: 30 sccm, continuous/pulsed source power (peak power = 500 W/13.56 MHz, pulse-on time = 50 μs), bias power: 50 W (1 MHz), and substrate temperature: 20°C.

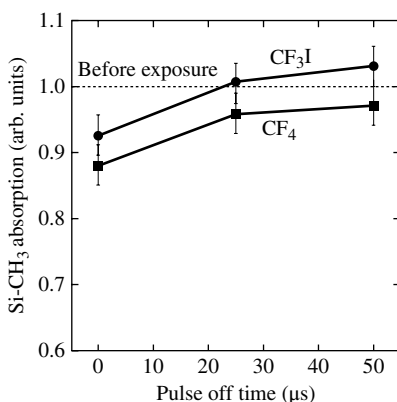


FIGURE 30.21 Si-CH₃ peak intensities of porous low- k film in FTIR analysis. These samples were etched by CF_3I and CF_4 plasmas. Blanket wafers were used. Conditions: 20 mTorr, gas flow: 30 sccm, continuous/pulsed source power (peak power = 500 W/13.56 MHz, pulse-on time = 50 μs), bias power: 50 W (1 MHz), and substrate temperature: 20°C.

than that after CF_4 plasma etching. In both gases, the Si-CH₃ peak intensities increased as the pulse-off time increased. With a pulse-off time in the CF_3I plasma of 50 μs, the Si-CH₃ peak intensity was almost the same as in the case of the nonexposed sample. This result corresponds to that for the dielectric constant, as indicated in Figure 30.20. It can thus be concluded from Figures 30.20 and 30.21 that the increases in the dielectric constant are due to the removal of methyl groups. Figure 30.22 shows the intensities of mass spectrometry during TDS analysis. The

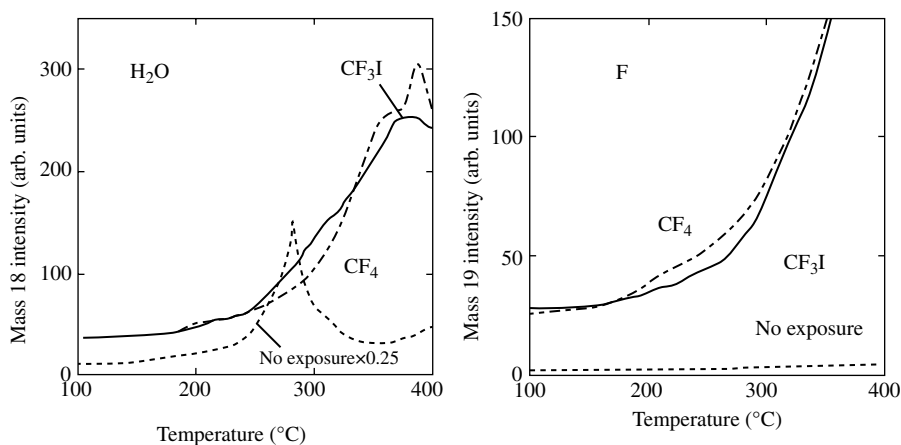


FIGURE 30.22 Peak intensities of mass spectrometry as a function of stage temperature in TDS analysis. Blanket wafers were evaluated just after etching. Conditions: 20 mTorr, gas flow: 30 sccm, continuous source power (power = 500 W/13.56 MHz), bias power: 50 W (1 MHz), and substrate temperature: 20 °C.

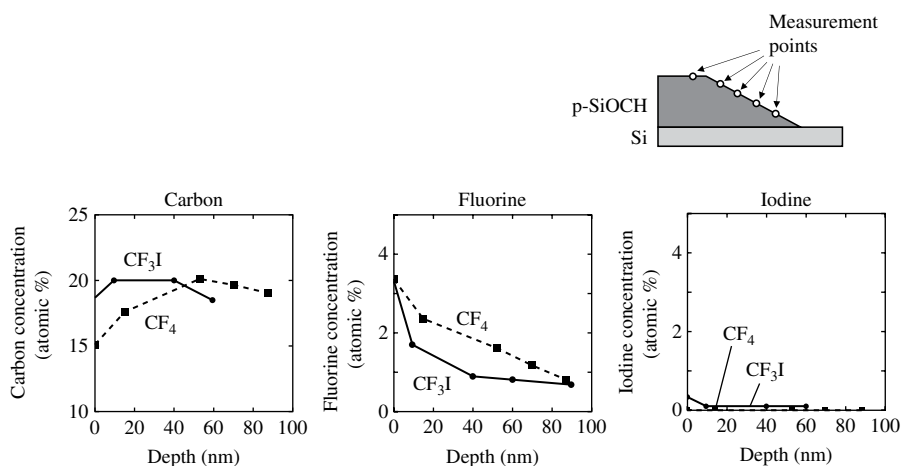


FIGURE 30.23 Carbon, fluorine, and iodine concentrations of low- k film just etched by CF_3I and CF_4 plasmas. Blanket wafers were used. Conditions: 20 mTorr, gas flow: 30 sccm, continuous source power (power = 500 W/13.56 MHz), bias power: 50 W (1 MHz), and substrate temperature: 20 °C.

stage temperature increases at a rate of $60^\circ\text{C min}^{-1}$. Since this analysis was done just after etching, the H_2O (mass = 18) mass spectra in the cases of CF_3I and CF_4 plasma exposures show little difference. However, fluorine atoms (mass = 19) were desorbed from the CF_4 plasma-exposed samples at a stage temperature of over 150°C . This indicates that the samples exposed to CF_4 plasma had a larger amount of fluorine than those exposed to CF_3I plasma. Figure 30.23 shows the film composition after

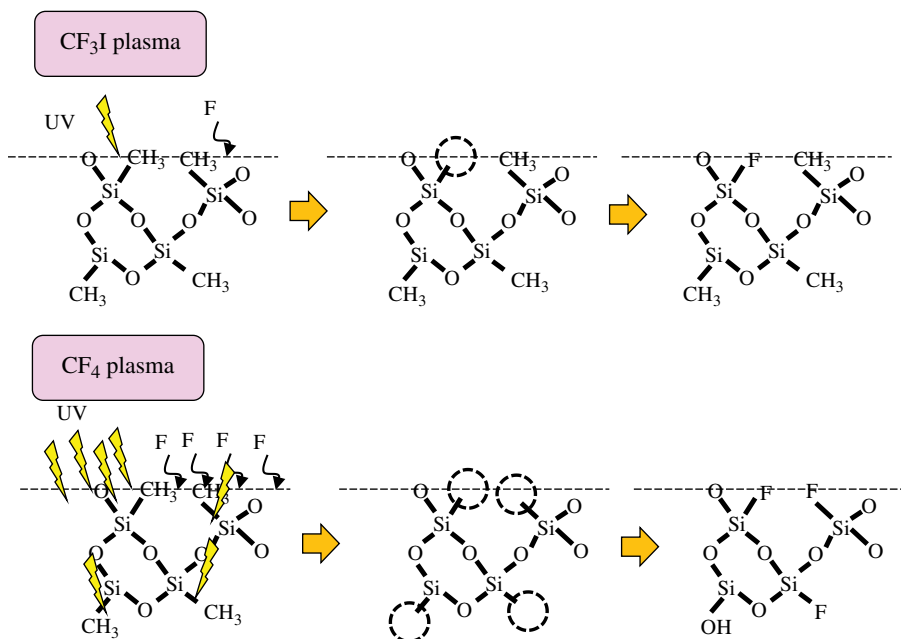


FIGURE 30.24 UV damage of SiOCH porous low- k film by CF₃I and CF₄ plasma irradiations.

CF₃I and CF₄ plasma etching as a function of the distance from the surface (depth). The samples were cut diagonally. The carbon concentration in the CF₃I case is almost constant from the surface to the bulk. However, in the CF₄ plasma-exposed sample, the carbon concentration from the surface to the 60-nm depth was smaller than that in the bulk. The fluorine concentration in the CF₄ plasma was higher than that in the CF₃I plasma. This indicates that the fluorine in the CF₄ plasma was able to easily attach to Si dangling bonds where the methyl groups had been removed. In addition, since no iodine signal in the low- k bulk is seen, we confirmed that the effect of iodine on etching characteristics was very small [36].

Accordingly, we can speculate on the mechanisms causing the differences in CF₃I and CF₄ etching, as depicted in Figure 30.24. In the CF₄ plasma, a larger number of methyl groups are removed from the porous SiOCH by UV irradiation with an energy of 3–4 eV. Fluorine or H₂O is absorbed in dangling bonds of Si. As a result, the dielectric constant increases. However, we can assume that the methyl groups are sustained in the CF₃I plasma because this plasma produces less UV irradiation.

30.5 SUMMARY

Low-damage and highly selective low- k etching could be achieved by using an environmentally harmonized gas chemistry (CF₃I) plasma. This is because the CF₃I plasma could reduce generating UV photons and F radicals. The etching rate for

low- k film is drastically increased by the pulsed CF_3I plasma. It is concluded from these results that CF_3I gas plasma has a higher potential as the gas chemistry for practical low- k etching.

REFERENCES

- [1] Tachi S, Miyake K, Tokuyama T. Chemical and physical sputtering in F^+ ion beam etching of Si. *Jpn J Appl Phys* 1982;21:141.
- [2] Sakai T, Hayashi H, Abe J, Horioka K, Okano H. Proceedings of 15 Dry Process Symposium. Institute of Electrical Engineers of Japan; 1993. p. 193.
- [3] Tatsumi T, Hayashi H, Morishita S, Noda S, Okigawa M, Itabashi N, Hikosaka Y, Inoue M. Mechanism of radical control in capacitive RF plasma for ULSI processing. *Jpn J Appl Phys* 1998;37:2394.
- [4] Itoh H, Miyachi T, Kawaguchi M, Nakao Y, H Tagashira H. Electron transport coefficients in SF_6 and $\text{c-C}_4\text{F}_8$ mixtures. *J Phys D* 1991;24:277.
- [5] Samukawa S, Mukai T, Tsuda K. New radical control method for high-performance dielectric etching with nonperfluorocompound gas chemistries in ultrahigh-frequency plasma. *J Vac Sci Technol A* 1999;17:2551.
- [6] Malyshev MV, Donnelly VM, Samukawa S. Ultrahigh frequency versus inductively coupled chlorine plasmas: Comparisons of Cl and Cl_2 concentrations and electron temperatures measured by trace rare gases optical emission spectroscopy. *J Appl Phys* 1998;84:1222.
- [7] Taoyoda H, Iio M, Sugai H. Cross section measurements for electron-impact dissociation of C_4F_8 into neutral and ionic radicals. *Jpn J Appl Phys* 1997;36:3730.
- [8] Takahashi K, Hori M, Maruyama K, Kishimoto S, Goto T. Measurements of the CF , CF_2 and CF_3 radicals in a CHF_3 electron cyclotron resonance plasma. *Jpn J Appl Phys* 1993;32:L694.
- [9] Takahashi K, Hori M, Goto T. Control of fluorocarbon radicals by on-off modulated electron cyclotron resonance plasma. *Jpn J Appl Phys* 1993;32:L1088.
- [10] Miyata K, Takahashi K, Kishimoto S, Hori M, Goto T. CF_x ($X=1-3$) radical measurements in ECR etching plasma employing C_4F_8 gas by infrared diode laser absorption spectroscopy. *Jpn J Appl Phys* 1995;34:L444.
- [11] Samukawa S, Mukai T. High-performance silicon dioxide etching for less than 0.1- μm -high-aspect contact holes. *J Vac Sci Technol B* 2000;18:166.
- [12] Zielinski EM, Russell SW, List RS, Wilson AM, Jin C, Newton KJ, Lu JP, Hurd T, Hsu WY, Cordasco V, Gopikanth M, Korthuis V, Lee W, Cerny G, Russell NM, Smith PB, O'Brien S, Havemann RH. Damascene integration of copper and ultra-low- k xerogel for high performance interconnects. *Tech Dig Int Electron Devices Meet*; 1997. p. 936.
- [13] Changming J, Wetzel J. Characterization and integration of porous extra low to (XLK) dielectrics. Proceedings of the 2000 International Interconnect Technology Conference; 2000 (unpublished).
- [14] Brown AS. *IEEE Spectrum* 2003;40:36.
- [15] Hoofman RJOM, Verheijden GJAM, Michelon J, Iacopi F, Travaly Y, Baklanov MR. Tokei Zs. Beyer GP. Challenges in the implementation of low- k dielectrics in the back-end of line. *Microelectron Eng* 2005;80:337.

- [16] Furusawa T, Miura N, Matsumoto M, Goto K, Hashii S, Fujiwara Y, Yoshikawa K, Yonekura K, Asano Y, Ichiki T, Kawanabe N, Matsuzawa T, Matsuura M. UV-hardened high modulus CVD-ULK material for 45 nm node Cu/low- k interconnects with homogeneous dielectric structures. Proceedings of the 2005 International Interconnect Technology Conference; 2005 (unpublished).
- [17] Ohtake H, Inoue N, Ozaki T, Samukawa S, Soda E, Inukai K. Highly selective low-damage processes using advanced neutral beams for porous low- k films. *J Vac Sci Technol B* 2005;23:210.
- [18] Yonekura K, Sakamori S, Goto K, Matsuura M, Fujiwara N, Yoneda M. Investigation of ash damage to ultralow- k inorganic materials. *J Vac Sci Technol B* 2004;22:548.
- [19] Misra A, Sees J, Hall L, Levy RA, Zaitsev VB, Aryusook K, Ravindranath C, Sigal V, Kesari S, Rufin D. Plasma etching of dielectric films using the non-global-warming gas CF_3I . *Mater Lett* 1998;34:415.
- [20] Krishnan N, Smati R, Raoux S, Dornfeld D. Alternatives to reduce perfluorinated compound (PFC) emissions from semiconductor dielectric etch processes. Proceedings of the 2003 IEEE International Symposium on Electronics and the Environment; 2003 (unpublished).
- [21] Samukawa S, Tsuda K. New radical-control method for SiO_2 etching with non-perfluorocompound gas chemistries. *Jpn J Appl Phys Part 2* 1998;37:L1095.
- [22] Samukawa S, Mukai T. Differences in radical generation due to chemical bonding of gas molecules in a high-density fluorocarbon plasma: Effects of the $\text{C}=\text{C}$ bond in fluorocarbon gases. *J Vac Sci Technol A* 1999;17:2463.
- [23] Samukawa S, Ohtake H, Mieno T. Pulse-time-modulated electron cyclotron resonance plasma discharge for high selective, highly anisotropic, and charge-free etching. *J Vac Sci Technol A* 1996;14:3049.
- [24] Ohtake H, Samukawa S, Oikawa H, Nashimoto Y. Enhancement of reactivity in Au etching by pulse-time-modulated Cl_2 plasma. *Jpn J Appl Phys Part 1* 1998;37:2311.
- [25] Samukawa S, Kumagai S, Shiroya T. Highly anisotropic and corrosionless PtMn etching using pulse-time-modulated chlorine plasma. *Jpn J Appl Phys Part 2* 2003;42:L1272.
- [26] Mukai T, Hada H, Tahara S, Yoda H, Samukawa S. High-performance and damage-free magnetic film etching using pulse-time-modulated Cl_2 plasma. *Jpn J Appl Phys Part 1* 2006;45:5542.
- [27] Mukai T, Ohshima N, Hada H, Samukawa S. Reactive and anisotropic etching of magnetic tunnel junction films using pulse-time-modulated plasma. *J Vac Sci Technol A* 2007;25:432.
- [28] Ohtake H, Samukawa S. Charging-damage-free and precise dielectric etching in pulsed $\text{C}_2\text{F}_4/\text{CF}_3\text{I}$ plasma. *J Vac Sci Technol B* 2002;20:1026.
- [29] Samukawa S, Ishikawa Y, Kumagai S, Okigawa M. On-wafer monitoring of vacuum-ultraviolet radiation damage in high-density plasma processes. *Jpn J Appl Phys Part 2* 2001;40:L1346.
- [30] Okigawa M, Ishikawa Y, Samukawa S. On-wafer monitoring of plasma-induced electrical current in silicon dioxide to predict plasma radiation damage. *J Vac Sci Technol B* 2005;23:173.
- [31] Ishikawa Y, Katoh Y, Okigawa M, Samukawa S. Prediction of ultraviolet-induced damage during plasma processes in dielectric films using on-wafer monitoring techniques. *J Vac Sci Technol A* 2005;23:1509.

- [32] Yunogami T, Mizutani T, Suzuki K, Nishimatsu S. Radiation damage in SiO_2/Si induced by VUV photons. *Jpn J Appl Phys Part 1* 1989;28:2172.
- [33] Okigawa M, Ishikawa Y, Samukawa S. Plasma-radiation-induced interface states in metal-nitride-oxide-silicon structure of charge-coupled device image sensor and their reduction using pulse-time-modulated plasma. *Jpn J Appl Phys Part 1* 2003;42:2444.
- [34] Worsley MA, Bent SF, Gates SM, Fuller NCM, Volksen W, Steen M, Dalton T. Effect of plasma interactions with low- k films as a function of porosity, plasma chemistry, and temperature. *J Vac Sci Technol B* 2005;23:395.
- [35] Geseneken G, Maes HE, Beltran N, Keersmaecker RF. DE IEEE Electron Device Lett 1984;31:42.
- [36] Fracassi F, d'Agostino R. Evaluation of trifluoroiodomethane as SiO_2 etchant for global warming reduction. *J Vac Sci Technol B* 1998;16:1867.
- [37] Marienfeld S, Fabrikant II, Braun M, Ruf M-W, Hotop H. High resolution low-energy electron attachment to CF_3I . *J Phys B* 2006;39:105.
- [38] Segawa S, Kurihara M, Nakano N, Makabe T. Dependence of driving frequency on capacitively coupled plasma in CF_4 . *Jpn J Appl Phys Part 1* 1999;38:4416.
- [39] Itoh H, Miyachi T, Kawaguchi M, Nakano Y, Tagashira H. Electron transport coefficients in SF_6 and $\text{c-C}_4\text{F}_8$ mixtures. *J Phys D* 1991;24:277.

OTHER INDUSTRIAL APPLICATIONS

TATSUO KAIHO

Nihon Tennen Gas Co., Ltd., Chiba, Japan

31.1 CATALYST

Acetic acid is an important industrial commodity chemical with a world demand of about 6.5 million tons per year and many industrial rises. The preferred industrial method for its manufacture is by the carbonylation of methanol, and this accounts for approximately 70% of the total world acetic acid manufacturing capacity [1]. The carbonylation of methanol, catalyzed by rhodium carbonyl iodide complex *cis*-[Rh(CO)₂I₂]⁻, was invented by Monsanto in the 1960s and was the leading technology for 25 years. In 1996, a new, more efficient process for the carbonylation of methanol, the so-called Cativa process, was developed by BP Chemicals, using an iridium catalyst instead of a rhodium catalyst. The process is based on an iridium carbonyl iodide catalyst, such as the [Ir(CO)₂I₂]⁻ (**1**). The Cativa and Monsanto processes are sufficiently similar that they can use the same chemical plant. The switch from rhodium to iridium also allows the use of less water in the reaction mixture. This change reduces the number of drying columns necessary, decreases formation of by-products, such as propionic acid, and suppresses the water gas shift reaction. The catalytic cycle for the Cativa process, shown in Figure 31.1, begins with the reaction of methyl iodide with the square planar active catalyst species (**1**) to form the octahedral iridium(III) species (**2**), the facial isomer of [Ir(CO)₂(CH₃)I₃]⁻. This oxidative addition reaction involves the formal insertion of the iridium (I) center into the carbon–iodine bond of methyl iodide. After ligand exchange (iodide for carbon monoxide), the migratory insertion of carbon monoxide into the iridium–carbon

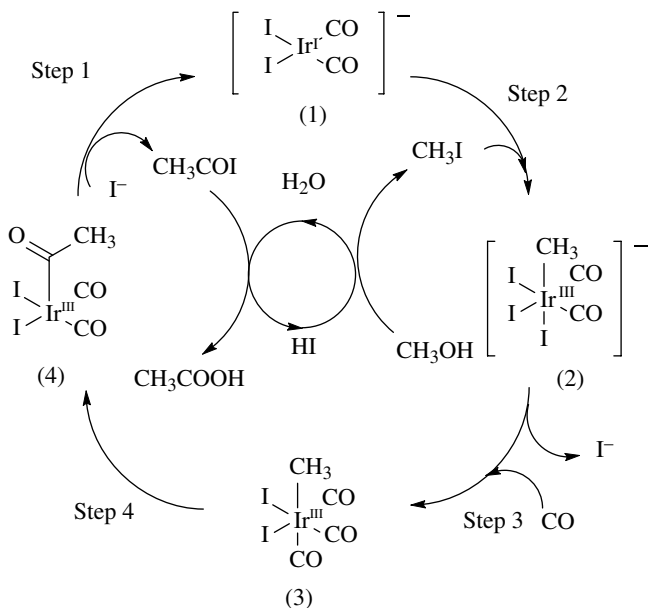


FIGURE 31.1 Reaction of Cativa process.

bond, step (3) to (4), results in the formation of a square pyramidal species with a bound acetyl ligand. The active catalyst species (1) is regenerated by the reductive elimination of acetyl iodide from (4), a deinsertion reaction [2]. The acetyl iodide is hydrolyzed to produce the acetic acid product, in the process generating hydroiodic acid, which is in turn used to convert the starting material (methanol) to the methyl iodide used in the first step. In both processes, iodo compounds (CH_3I , CH_3COI) play a very important role. Initial studies by Monsanto had shown iridium to be less active than rhodium for the carbonylation of methanol. Subsequent research, however, showed that the iridium catalyst could be promoted by ruthenium, and this combination leads to a catalyst that is superior to the rhodium-based systems. The greater stability of $[\text{MeIr}(\text{CO})_2\text{I}_3]^-$ compared with $[\text{MeRh}(\text{CO})_2\text{I}_3]^-$ accounts for the very different characters of the reactions catalyzed by the two metals. It is suggested that the broad features of the Rh/Ir reactivities can be rationalized since the M–C bond to a 5d metal (Ir) is generally stronger than that to the corresponding 4d metal (Rh); thus if metal–ligand bond making plays a key role in a step, then the 5d metal is more likely to react faster (e.g., in the oxidative addition), but if a metal–ligand bond-weakening or -breaking step plays a key role in a process (e.g., in the migration), it is likely that the 4d metal will be faster (Fig. 31.2).

31.2 STABILIZER

Polyamides or nylons are the first engineering plastics and still represent the biggest and most important class of these types of material. Polyamide production began with the synthesis of poly (hexamethylene adipamide), the original “polyamide”



FIGURE 31.2 The manufacture of acetic acid using the Cativa process 1, the reactor 2, distillation column to remove methanol, water, and carbon monoxide. Propionic acid is removed on further distillation. By kind permission of BP.

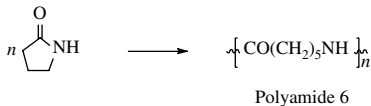
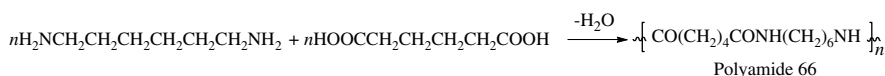


FIGURE 31.3 Synthesis of Polyamide 66 and Polyamide 6.

that was conducted by Wallace H. Carothers in DuPont Laboratory in 1935 (Fig. 31.3).

This invention resulted in the first patent for the production of synthetic polyamides in 1937 and the subsequent commercial production of Polyamide 66 for toothbrush filaments by DuPont in 1938 [3]. In 1941, DuPont introduced the first moldable polyamide grades. The other commercially important polypolyamide, Polyamide 6, based on caprolactam was first produced at the IG Farbenindustrie in Germany by P. Schlack in 1938 [4]. Polyamides are a versatile family of thermoplastics that have a broad range of properties ranging from relative flexibility to significant stiffness, strength, and toughness. Major properties such as resistance to chemicals, toughness, thermal stability, good appearance, and good process ability are key considerations that make polyamides suitable for engineering plastics. Polyamide 6 and Polyamide 66 continue to be the most popular types among commercial products, still accounting for 90% of the nylon used in the global market [5]. According to industrial statistics, the global consumption of Polyamide 6 and Polyamide 66 in the world was estimated at around 6.8 million tons in 2011 [6]. One of the major applications of nylon fibers is the manufacturing of tires, where heat resistance of the polymer is essential [7]. For example, the tires of a light vehicle while driving could reach a temperature near 120°C. Potassium

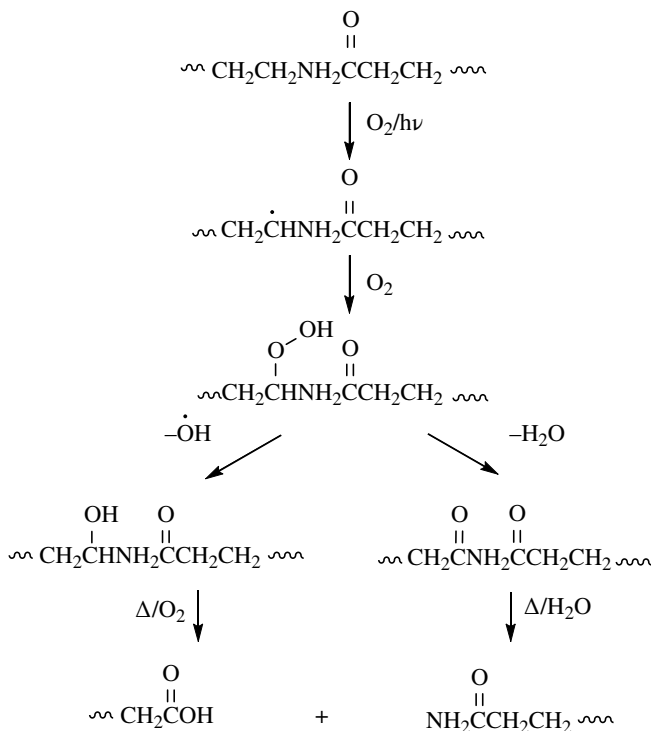
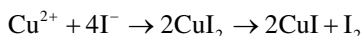


FIGURE 31.4 Degradation of polyamide by O_2 and light.

and cuprous iodides are used as heat-stabilizing agents in the manufacture of Polyamide 6 and Polyamide 66. The iodide and cuprous ions inserted within the nylon polymer net prevent the cracking of the chemical chain, keeping the properties of the material on heavy-duty conditions (Fig. 31.4). On average, the use of potassium and cuprous iodides allows stabilization up to 170°C , while with other combinations it could be 25°C less [8]. Aromatic amines are classical stabilizers for long-term thermal stability (LTTS) applications, but lead to discoloration in polyamides. Phenolic antioxidants also help to stabilize aliphatic polyamides by improving initial color after polycondensation. These antioxidants may be added to the condensation mass preferably prior to termination of the condensation reaction. At elevated aging temperatures, for example, above 150°C , the copper/iodide stabilizer systems show best performance, but at low aging temperatures, the phenolic antioxidant is more effective. The mechanism of stabilization with copper/halogen compounds is still subject to investigation. In the case of the stabilization of polyamides with Cu ions, it has suggested by G. Scott that the antioxidant effect is catalytic. Cu^{2+} oxidizes an alkyl radical to a carbonium ion, and the Cu^+ formed in this reaction reduces alkylperoxy radicals [9]. It is also described that I^- can reduce Cu^{2+} according to the following reaction:



However, according to the experiments using model compounds (see Fig. 31.5) by K. Jannssen et al. [10], the mechanism postulated here (radical scavenging) cannot in itself be responsible for the stabilization of aliphatic polyamides. The mechanism of stabilization is probably based on the decomposition of hydroperoxides. KI is responsible for the decomposition of hydroperoxides into nonradical products, whereas the metal salt catalyzes this decomposition reaction by complexation of metal salt onto an amide and/or hydroperoxide group. It is confirmed that the combination of metal salts with KI results in a synergistic mixture. Consequently, the most effective stabilizers against the long-term thermooxidative degradation for aliphatic polyamides are synergetic combinations of metal (mainly Cu and Mn) and halogen (mainly Br and I) salts [10] (Tables 31.1 and 31.2).

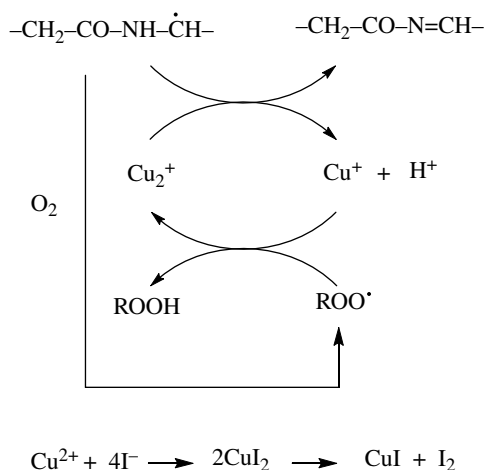


FIGURE 31.5 Stabilization mechanism of polyamide.

TABLE 31.1 Comparison of different polymer stabilizer systems

AO system	Advantages	Disadvantages
Cu/I	Very effective at low concentrations. Good contribution to LTTS at aging temperature above 150°C.	Dispersability in substrate is critical. Leaching in contact with water/water/solvent. May cause discoloration.
Aromatic amines	Good contribution to LTTS.	Need high concentration.
Phenols	Good contribution to LTTS at aging temperature below 150°C. Good color performance. Can be added during condensation. No negative interaction with other polymers in lents.	Discoloration.

TABLE 31.2 Effects of stabilizer systems on LTTS at different temperatures

Stabilizer	Oven aging, time to 50 retained elongation, hours at			
	100°C	120°C	150°C	165°C
None	480	24	6	3
0.003% Cu/0.14% I	5520	624	324	44
0.5% AO-7	6840	600	36	15

Polyamide 6; 1 mm injected molded dumbbells Circulating air oven.

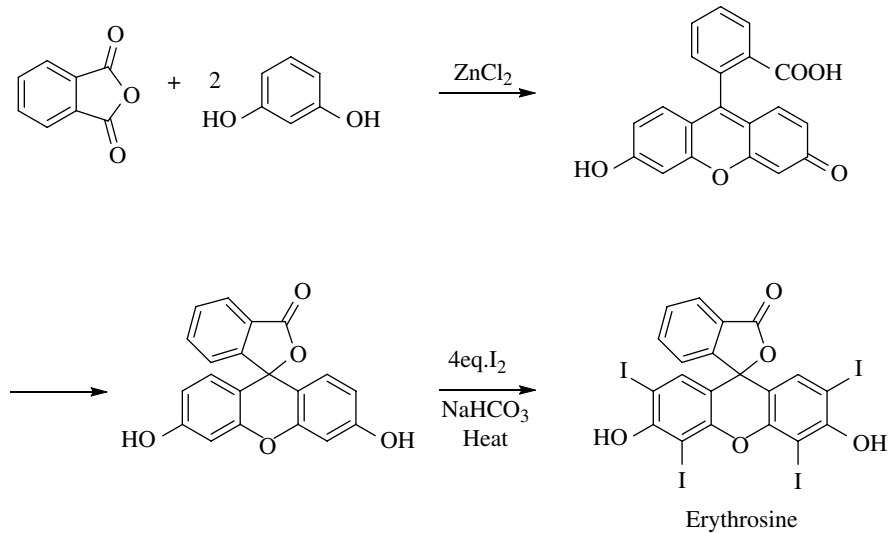


FIGURE 31.6 Synthesis of erythrosine.

31.3 COLORANT

Erythrosine can be manufactured by iodination of fluorescein, the condensation product of resorcinol and phthalic anhydride [11, 12].

Erythrosine is used as a food coloring, in printing inks, as a biological stain, a dental plaque disclosing agent, and a radiopaque medium (Fig. 31.6). Erythrosine is commonly used in sweets such as some candies and popsicles, and even more widely used in cake-decorating gels. In 1990 erythrosine was partially banned by the Food and Drug Administration (FDA) for known health risks, specifically thyroid cancer. However, a series of toxicology tests combined with a review of other reported studies concluded that erythrosine is nonmutagenic [13]. Erythrosine can be used in colored food in the United States without any restriction [14]. The ADI¹ for erythrosine was determined by JEFCA² to be 0.1 mg kg⁻¹ body weight based on erythrosine’s NOEL³

¹ ADI (acceptable daily intake) is used widely to describe “safe” levels of intake.
² Joint FAO/WHO Expert Committee on Food Additives (JECFA).
³ The no observable effect level (NOEL) is the dose (mg kg⁻¹) at which there is no adverse effect.

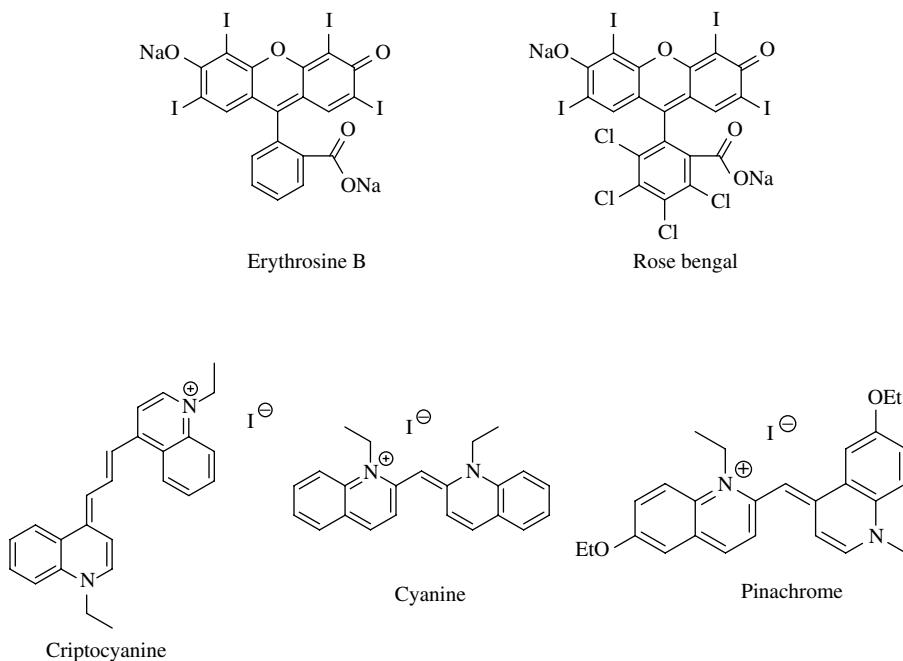


FIGURE 31.7 Other dyes contain iodine.



FIGURE 31.8 Iodine containing dyes: Erythrosine B (left), Rose Bengal, cyanine, Criptocyanine (right). (See insert for color representation of the figure.)

for thyroid and pituitary glands [15]. Some other dyes contain iodine, including Erythrosine B and Rose Bengal and blues from the cyanine group like Criptocyanine, cyanine, and pinachrome (see Figs. 31.7 and 31.8). Those are used in printer inks, photographic sensitizers, and some textile dyes.

REFERENCES

- [1] Jones JH. The Cativa™ process for the manufacture of acetic acid. *Platinum Metals Rev* 2000;44 (3):94–105.
- [2] Sunley GJ, Watson DJ. High productivity methanol carbonylation catalysis using iridium—the Cativa™ process for the manufacture of acetic acid. *Catal Today* 2000;58 (4):293–307.
- [3] Carrothers WH. Linear polyamides and their production. US Patent 2,130,523. 1938. To E.I. DuPont de Nemours and Co.
- [4] Schlack P. Preparation of polyamides. German Patent 748,253 (1938). US Patent 2,241,321. 1941.
- [5] Nexant Inc. Process Evaluation/Research Planning Report Nylon 6 and Nylon 6,6 PERP07/08S6, White Plains, NY. January 2009.
- [6] MacDonald B. *World PA6 & PA66 Supply/Demand Report 2011 by PCI Nylon*. Bad Homburg: PCI Nylon GmbH; 2011.
- [7] Lauterbach A, Ober G, Rios S, Basinger, W, Shipp A. Iodine, SQM Company brochure 2001.
- [8] Zweifel H, Ralph MD, Schiller M. *Plastic Additive Handbook*. 6th ed. Germany: Hanser Fachbuchverlag; 2009. p 80.
- [9] Scott G. In: Scott G, editor. *Atmospheric Oxidation & Antioxidants*. Volume 2, Amsterdam: Elsevier Science Publishers; 1993. p 141–218.
- [10] Janssen K, Gijsman P, Tummers D. Mechanistic aspects of the stabilization of polyamides by combinations of metal and halogen salts. *Polym Degrad Stabil* 1995;49 (1):127–133.
- [11] Baeyer A. *Ber. Deut. Chem. Ges.* 1871;4:555.
- [12] Vogel AI. *Textbook of Practical Organic Chemistry*. Longmans, London; 1956. p. 186.
- [13] Lin GHY, Brusick DJ. Mutagenicity studies on FD&C Red No.3. *Mutagenesis* 1986;1 (4):253–259.
- [14] Title 21 of the Code of Federal Regulations, Section 74.303.
- [15] EFSA Journal 2011;9(1)1854.

PART VI

BIOINORGANIC CHEMISTRY AND ENVIRONMENTAL CHEMISTRY OF IODINE

IODINE BIOINORGANIC CHEMISTRY: PHYSIOLOGY, STRUCTURES, AND MECHANISMS

FRITHJOF C. KÜPPER¹ AND PETER M.H. KRONECK²

¹*Oceanlab, University of Aberdeen, Newburgh, UK*

²*Department of Biology, University of Konstanz, Konstanz, Germany*

32.1 INTRODUCTION

The element iodine, $^{127}_{53}\text{I}$, like fluorine, chlorine, and bromine, belongs to group 17 of the periodic table. This group of elements is also called the halogens, with iodine being less abundant both in the Earth's crust and in seawater than the lighter elements of the halogens. The basic inorganic chemistry of the halogens is surprisingly well-understood, partly because much of the chemistry of halogens is that of singly bonded atoms or singly charged anions [1–4]. Since the discovery of iodine the question of its occurrence and distribution in nature has attracted the interest of numerous researchers [5]. The known iodine minerals seem to be formed and exist only in the upper layers of the Earth's crust, and only in deposits of organic origin. These minerals are, however, relatively rare. Most likely, the iodine content was enriched by organisms capable of accumulating iodine, and through the decay of these organisms it was withdrawn from the organic circulation. Another interesting feature relates to the observation that iodine solutions may be either violet or brown, the color depending upon the solvent. This variation of color with solvent has intrigued many chemists and has been the subject of numerous intensive investigations on solutions of iodine [6].

The predominant chemical forms of iodine are iodide (I^- , formal oxidation state –1), iodate (IO_3^- , –5), and organic iodine compounds (R-I). In the biogeochemical cycling of iodine, microorganisms, together with marine algae and phytoplankton, play crucial

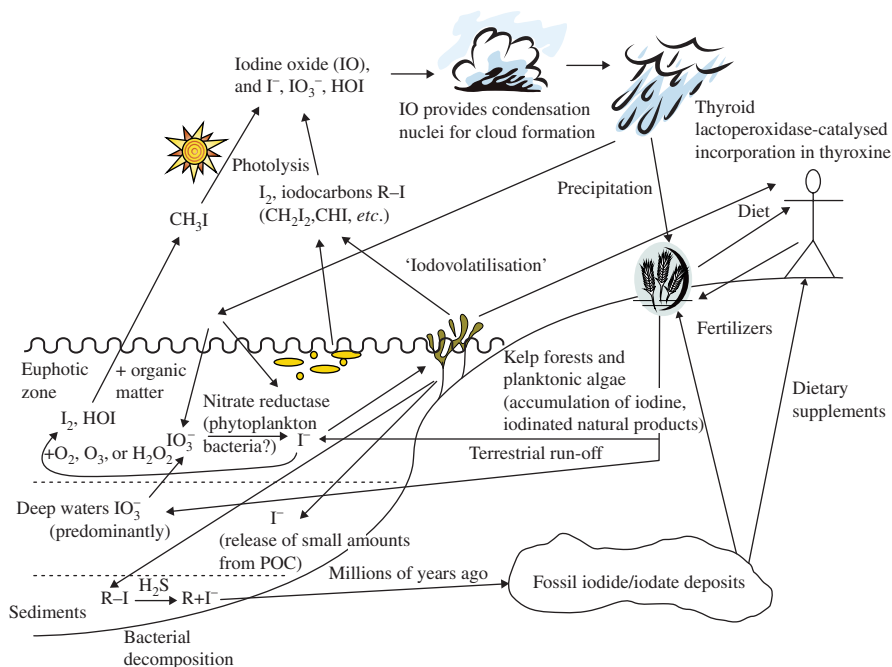


FIGURE 32.1 Schematic representation of the biogeochemical cycle of iodine. The primary source of the condensable iodine vapors is thought to be molecular iodine (I_2). Photolysis or other processes lead to the formation of I^\cdot radicals and iodine oxides, impacting the ozone layer. Iodine is deposited on land or back into the sea by rainfall or aerosols. From Ref. [9]. Permission from ICUR.

roles via the production and remineralization of R-I and via the redox chemistry of mainly I^- and IO_3^- [7, 8] (Fig. 32.1).

Notably, halogen substituents frequently add structural features to organic compounds that account for their potency and selectivity. These molecules carrying carbon–halogen bonds constitute a diverse group of natural products that display a wide range of biological activities, including anticancer and antibiotic properties. Many times, synthetic methods of introducing halogens into complex molecules prove to be difficult. Nature, however, has evolved a sophisticated toolbox for halogenating specific substrates fulfilling the requirements of both regio- and stereoselectivity. Over 4000 organohalogens have been naturally described with the majority isolated from marine organisms [10–14]. Several enzymatic strategies for the incorporation of halogen atoms into organic substrates are known. Halogenation is common amongst marine algal natural products and was largely thought to derive primarily from vanadium-dependent haloperoxidases (V-HPO). Note that the catalogue of known halogenating enzymes has expanded from the familiar HPOs to include oxygen-dependent enzymes and fluorinases. Structural characterization has provided a basis toward a mechanistic understanding of the specificity and chemistry of these enzymes.

Halogenating enzymes can be divided into the hydrogen peroxide (H_2O_2)-requiring HPOs (heme- or vanadium-dependent), the oxygen-dependent halogenases (flavin- or non-heme iron-dependent), and the nucleophilic halogenases. For all classes of halogenating enzymes, structural information has become available in recent years and has proven critical for our understanding of the mechanism [15–19].

Clearly, reactions involving the transformation of both inorganic and organic halogen compounds including those of iodine have a profound influence on the properties of the biosphere and continue to affect our daily life. Because of its global importance, research on the biogeochemistry of iodine and its compounds has become an important issue as documented by numerous publications in biology, chemistry, and the environmental sciences. In view of the complexity of the topic, two comprehensive reviews are recommended for further reading [5, 20].

In this chapter, the manifold roles of iodine, a prominent member of the halogen element family, will be discussed. Emphasis is laid on bioinorganic aspects of iodine compounds including the transformation of hypoiodite by vanadium-dependent enzymes. The structure and function of these enzymes will be highlighted.

32.2 BASIC CHEMISTRY OF IODINE AND ITS COMPOUNDS

32.2.1 General Properties

In the ground state, the gaseous iodine atom has two electrons in the outer s orbital and five electrons in the outer p orbitals ([Kr] $4d^{10}5s^25p^5$ electron configuration). The ^{127}I isotope (natural abundance 100%; atomic mass 126.904473 ma/u) has a magnetic moment $\mu/\mu_N = 2.81328$ and a nuclear spin $I = 5/2$. Thus, nuclear magnetic and electron paramagnetic resonance spectroscopies (NMR, EPR) can be applied as structural tools. Note that ^{127}I is a quadrupolar nucleus, which makes its observation by NMR spectroscopy difficult. However, in a highly symmetrical environment, for example, in the $[\text{IF}_6]^+$ cation, narrow linewidths and perfectly well-resolved hyperfine splittings can be observed in the ^{127}I NMR spectrum [21]. Iodine is never found in nature as a free element. Iodine occurs as iodide (I^-) in seawater and is taken up by seaweed, from which it has traditionally been extracted (Section 32.3). Chilean nitrate deposits contain up to 0.3% calcium iodate, $\text{Ca}(\text{IO}_3)_2$, also called *Lautarite* after the type locality Oficina Lautaro, Antofagasta, Chile [22]. It acts as an oxidant, and can thus be added to lotions and ointments as an antiseptic and deodorant. Diiodine (I_2) is a bluish-black, lustrous solid that turns into a bluish-violet gas with an irritating odor at ambient temperatures. The observed colors of the halogens arise from an electronic transition from the highest occupied π^* molecular orbital (HOMO) to the lowest unoccupied π^* molecular orbital (LUMO). The HOMO–LUMO energy gap decreases in the order $\text{F}_2 > \text{Cl}_2 > \text{Br}_2 > \text{I}_2$, leading to a progressive shift in the absorption maximum from the near-ultraviolet (UV) to the red region of the visible spectrum. Iodine forms compounds with most elements, but it is less reactive than the other halogens, which displace it from iodides. I_2 shows some metallic-like properties; it dissolves readily in organic solvents such as chloroform (CHCl_3), carbon

tetrachloride (CCl_4), or carbon disulfide (CS_2) forming purple solutions. Diiodine is much more soluble in aqueous iodide solutions than in water. At low concentrations of I_2 , the complex anion $[\text{I}_3]^-$ is formed. Iodine compounds are important in organic chemistry and very useful in medicine and photography. Lack of iodine is the cause of goiter (Derbyshire neck). The intense blue color with starch solution is characteristic of the free element.

32.2.2 Acid–Base and Redox Chemistry

Iodine shares typical characteristics of the halogens, such as the relatively high electronegativity value of 2.7 (Pauling scale), which compares to 4.0 (F), 3.2 (Cl), and 3.0 (Br). Consequently, it forms iodides with many elements, and it can undergo radical reactions. Although none of the halogens has been shown to form a discrete and stable cation X^+ , complexed or solvated I^+ does exist, for example $[\text{I}(\text{py})_2]^+$ in the salt $[\text{I}(\text{py})_2]^+ [\text{I}_3]^- \times 2\text{I}_2$ [23]. Notably, halonium ions are well-established since the 1930s, in which formally positively charged halogens are attached to two carbon atoms through three-center bonds. They are known to be a great source for unique pathways in the synthetic chemistry of organochlorides, bromides, and iodides. Mechanistic studies of these ions allowed significant insights into the origins of stereoselectivity in addition and displacement reactions. Iodonium ions, such as $[\text{I}(\text{Phe})_2]^+$, are quite stable, often isolable, and synthetically useful as reagents. Bromonium and chloronium ions are only occasionally isolable, but, nonetheless, well-documented. Most recently, it was demonstrated that fluorine can react through halonium ion pathways, and strong evidence was provided for the transient generation of a fluoronium ion in solution [24].

The standard reduction potential E° ($\text{X}_2/2\text{X}^-$) for $\text{X}=\text{I}$ is +0.54 V compared to +2.87 V (F), +1.36 V (Cl) and 1.09 V (Br). The first ionization energy, IE_1 , of I is 1008 kJ mol $^{-1}$, compared to 1681 kJ mol $^{-1}$ (F), 1251 kJ mol $^{-1}$ (Cl), and 1140 kJ mol $^{-1}$ (Br). The values of E° indicate the decrease in oxidizing power within the series $\text{F}_2 > \text{Cl}_2 > \text{Br}_2 > \text{I}_2$. Iodine is known in compounds with formal oxidation states ranging from -1 to $+7$. The high positive oxidation states are mainly observed in compounds with the very electronegative elements oxygen and fluorine. However, since the polarizability of iodine is quite high, the chemical bonds formed with the more electropositive elements in the periodic table tend to contain a fair degree of covalency. Among the halogens, iodine is more easily oxidized and more easily converted to stable salts containing the element in the $+1$ oxidation state. I_2 is not reactive toward dioxygen (O_2) or dinitrogen (N_2), but it does react with ozone (O_3) to form the unstable yellow oxide I_4O_9 , the nature of which is perhaps $\text{I}(\text{IO}_3)_3$. However, a stable oxide, I_2O_5 , can be prepared as a white, hygroscopic solid by the dehydration of iodic acid (HIO_3). In water, I_2 disproportionates into iodide anion and the hypoiodite anion, OI^- , the anion of hypoiodous acid, HIO (pK_a 10.64). Hereby, the position of the equilibrium depends upon the pH of the solution (Eq. 32.1).

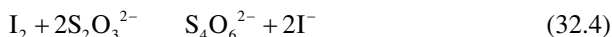


In general, hypohalous acids, HOX, are obtained in aqueous solution by the reaction of X_2 with Hg(II)O (Eq. 32.2).

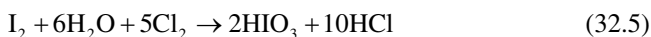


The chemical oxidation of H_2O_2 to O_2 by IOH or I_2 /HOI has been known for a long time [25]. The mixture of I^- and H_2O_2 represents a pseudo autocatalyzed redox system whose equilibrium depends strongly on pH conditions, with the degradation of H_2O_2 lowest around pH 5–7. The triiodide anion, I_3^- , is the result of complex formation between I_2 and I^- (Eq. 32.3) [26]. The equilibrium constant of I_3^- formation is quite small ($K_{eq} = 830 M^{-1}$) and I_2/I^- complexation is weak in diluted solutions.

Iodine rapidly oxidizes thiosulfate, $S_2O_3^{2-}$, to tetrathionate, $S_4O_6^{2-}$, a classical reaction in inorganic titrimetric analysis (Eq. 32.4). In contrast, both Cl_2 and Br_2 react slowly with this sulfur compound and oxidize it to sulfate, SO_4^{2-} .



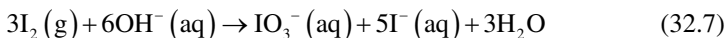
The transformation of thiosulfate by different oxidizing agents including iodine exhibits complex reaction kinetics. Besides the major product, sulfate, many sulfur-containing intermediates (mainly polythionates $S_xO_6^{2-}$ with a considerably long half-life) are produced. In the case of the reaction between pentathionate, $S_5O_6^{2-}$, and I_2 , the formation of a stable $S_5O_6I^-$ was postulated to explain the inhibitory effect by the iodide anion. The main outcome of these detailed kinetic investigations indicates that the oxidation of polythionates eventually leading to sulfate starts with an initiating equilibrium (a formal I^+ transfer to the inner sulfur of the sulfur chain to produce $S_xO_6I^-$) in which the iodide ion is also involved [27]. Iodine reacts with the other members of the halogen element family under a variety of experimental conditions to form several interhalogen compounds, such as the colorless gases pentafluoride iodine (V) fluoride (IF_5 /coordination number 5/coordination geometry square-based pyramidal) and heptafluoride iodine(VII) fluoride (IF_7 /7/pentagonal bipyramidal), the low melting solid iodine(I) bromide (IBr), or the yellow solid iodine (III) chloride, actually I_2Cl_6 . The most stable of the diatomic interhalogens are ClF and ICl, while IBr dissociates to some extent into its elements, and BrCl is substantially dissociated. In the presence of water, I_2 reacts with Cl_2 to form HIO₃ (Eq. 32.5).



This acid is also produced in the reaction of I_2 with hot concentrated nitric acid, which is reduced to nitric oxide gas (NO) (Eq. 32.6)



In hot alkali solution, I_2 produces iodate, IO_3^- (Eq. 32.7).



In addition to HOI and HIO_3 , several periodic acids are known, the most prominent examples are periodic acid, HIO_4 ($\text{p}K_{\text{a}}$ 1.64), and orthoperiodic acid, H_5IO_6 ($\text{p}K_{\text{a}}$ 3.3).

32.2.3 Coordination Chemistry

Although listed as a rather weak coordinating ligand, the iodide anion forms many interesting and structurally well-characterized metal complexes. Probably the most widespread class of metal complexes involving anionic ligands ($\text{M}^{n+} \leftarrow \text{IX}^-$) is that of the complexes of the halide ions fluoride, chloride, bromide, and iodide. The stabilities of halide complexes span an enormous range—from the alkali metal ions, whose formation of halide complexes in aqueous solution can barely be detected, to extremely stable complexes, such as the tetraiodidomercurate, $[\text{Hg(II)I}_4]^{2-}$, or tetrachloridothallate, $[\text{Tl(III)Cl}_4]^-$, the extent of whose dissociation is extremely small. The stabilities of halide complexes reflect a pattern by which metal ions (and ligands) can be divided into two general classes, as class A (*hard*) and class B (*soft*), respectively [28–31]. For hard (class A) metal ions, such as Li^+ , Mg^{2+} , Cr^{3+} , Co^{3+} , Fe^{3+} , or Cu^{2+} , the order of increasing stability of the halide complexes in aqueous solution is iodides < bromides < chlorides < fluorides. Conversely, for the soft (class B) metal ions, which include Cu^+ , Ag^+ , Pd^{2+} , Pt^{2+} , Hg^{2+} , and Tl^{3+} , the order of increasing stability of the halide complexes is fluorides < chlorides < bromides < iodides. Thus, F^- , Cl^- , H_2O , NH_3 , OH^- , and CH_3COO^- belong to the class of hard ligands, whereas I^- , CO , $\text{P}(\text{C}_6\text{H}_5)_3$, C_2H_4 , and RSH/RS^- are regarded as soft ligands. In contrast to hard metal ions, the soft metal ions also tend to form more stable complexes with (soft) sulfur-containing ligands than with (hard) oxygen-containing ligands. There is roughly a 20-kcal difference between the free energies of formation of HCl and HI favoring the reaction $[\text{MCl}_6]^{+m-6} + \text{HI} \rightleftharpoons [\text{MI}_6]^{+m-6} + \text{HCl}$. Even with metals showing pronounced class A group behavior, this equilibrium may be well to the right. Furthermore, if the conversion of solid salts from chlorides to bromides or iodides is carried out with liquid HBr or HI, the much higher volatility of HCl further promotes the conversion, which allows the spectroscopic characterization of the extremely weak hexaiodido complexes of trivalent lanthanides (Sm, Eu, Tm, and Yb) as triphenylphosphonium or pyridinium salts. By the same procedure, salts of iodo complexes of several d group metal ions, which are strongly oxidizing toward the iodide ion, were prepared as $[\text{Ti(IV)I}_6]^{2-}$, $[\text{Fe(III)I}_4]^-$ and $[\text{Au(III)I}_4]^-$. An attempt to prepare $[\text{Cu(II)I}_4]^{2-}$ was unsuccessful [32, 33]. On the other hand, a bis(μ -iodido)dicopper(I) complex (supported by *N*-(3,5-di-*tert*-butyl-2-hydroxybenzyl)-*N,N*-di-(2-pyridylmethyl)amine) could be crystallized and characterized, as expected from the class A/class B pattern [34]. Fe(III) iodide and iodo Fe(III) complexes were compounds not very familiar to inorganic chemists in the past. In one of the principal monographs on inorganic photochemistry it was stated that “complexes between Fe(III) and strongly reducing ligands (e.g., I^-) are so black that they cannot exist” [35]. The main reason for such a statement and general belief derive from the known reducing effect of the anion I^- towards the cation Fe^{3+} expressed by means of the standard electrode potential values $E^\circ(\text{FeIII/FeII}) = 0.77\text{ V}$, and $E^\circ(\text{I}_2/\text{I}^-) = 0.54\text{ V}$. One method to overcome the thermodynamic barrier and

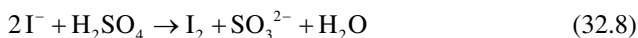
stabilize the Fe(III)-I⁻ bond was documented for [FeI(S₂CNEt₂)₂] in 1967, followed by iron(III) iodido complexes with Schiff base ligands, namely [Fe(salen)I], and finally, by applying low-temperature photochemical synthesis, pure FeI₃ was also prepared as recently reviewed [36].

In simple Crystal Field Theory (CFT), placing ligands as point charges around the metal ion in an octahedral ligand field, one of the factors governing the magnitude of the crystal field splitting energy, Δ_o (10dq), is the nature of the bound ligands. For a metal ion, the field strength increases according to the *spectrochemical series*, with weak to strong field ligands: I⁻ < Br⁻ < SCN⁻ < Cl⁻ < N₃⁻ < F⁻ < OH⁻ < O²⁻ < NCS⁻ < NO₂⁻ < CN⁻, CO. Here CO and CN⁻ are strong field ligands and I⁻ is the weakest. Note that CFT helps to explain thermodynamic properties, reactivity, color (e.g. black PtCl₆²⁻ vs yellow PtI₆²⁻) and magnetism of metal complexes. However, as model for chemical bonding, it is not fully realistic as both ionic and covalent forces are important in metal bonding. When discussing the reactivity of metal complexes, a ligand L1 can labilize another ligand L2 situated 180° from L1 in substitution reactions. This is called the *trans effect* which has been studied extensively for square planar Pt(II) complexes, such as *cis*- and *trans*-Pt(II)(NH₃)₂Cl₂. In the *trans*-influencing series of ligands, I⁻ takes an intermediate position between CN⁻ (strong effect) and H₂O (weak effect), but is more effective than Br⁻ and Cl⁻. Briefly, two factors contribute to the *trans effect*, a thermodynamic effect (strong σ donation of L1 into the metal orbital dx²-y² lengthens the metal-L2 bond) and a kinetic effect (ligands with good π acceptor capacity can stabilize a 5-coordinate transition state) [37, 38].

32.3 IODINE IN SEaweEDS AND MICROBES

32.3.1 Discovery and Early Studies of Iodine in Seaweed Ashes

Knowledge of the beneficial, goiter-preventing effects of seaweeds—undoubtedly due to their iodine content—goes back to Chinese emperor Shen-Nung (around 3000 BC). It was not until the time of Hippocrates, the forefather of modern medicine, that this knowledge reached Europe [39]. Still, the element responsible for these pharmacological effects remained elusive until the nineteenth century. Under pressure of the blockade of ports by the British Royal Navy, de facto shutting down the import of raw materials for gunpowder, French chemists were looking for novel sources for potassium nitrate. In this context, Bernard Courtois extracted the ashes of seaweeds, particularly abundant on the coasts of Normandy and Brittany, with concentrated sulfuric acid resulting in the formation of a blue-violet vapor (Eq. 32.8).



Nicolas Clément presented the findings on Courtois' behalf to the Imperial Institute of France, which led to the original publication in the *Annales de Chimie* [40]. This publication already used the name *iode* for the new substance, “due to the beautiful violet color of its vapor” (from the Greek *ιώδης*, i.e., *violet*). Shortly afterward, Joseph L. Gay-Lussac presented his results about the compounds that this novel

element formed with other elements [41, 42]. The eminent British chemist Sir Humphry Davy corresponded with his French peers and was given free passage to France where he received a sample of the new substance from André M. Ampère. Initially, Davy believed that it was merely a compound of chlorine but came to the conclusion that it was an element in its own right [43]. Despite the scientific fame of the discovery and the rising commercial interest in iodine, Courtois failed to capitalize on his discoveries and died in poverty aged only 62 [44]. Iodine production from seaweeds became a major economic activity in the coastal regions of Europe, in particular in parts of Brittany, Normandy, Ireland, and Scotland, and it features in many historic and travel accounts of these places (e.g., [45]).

32.3.2 Iodine Uptake, Accumulation, and Metabolic Function in Marine Algae

It is not entirely surprising that iodine as a novel element was discovered in the ashes of *Laminaria* and related brown algae, since they are the strongest iodine accumulators among all living systems [46, 47]. Even though iodine had been discovered in seaweed ashes, it was not until the late nineteenth century that algal iodine metabolism received any research interest. Exemplary for this period are the studies of Eschle [48], investigating the iodine content of *Fucus vesiculosus* and *Laminaria digitata*. Golenkin reported as early as 1894 the release of free iodine by the red alga *Bonnemaisonia asparagoides*—detected by a blue stain of starch in paper [49]. Several decades passed until this was more widely accepted by the community, in particular by the studies of Sauvageau [50] on red algae and of Kylin [51] and Dangeard [52] in the 1920s. The latter, obviously working in competition, were the first to report the emission of molecular iodine (I_2) from kelp (*L. digitata*) surfaces, termed “iodovolatilization.” The rise of nuclear physics and the availability of radioisotopes enabled studies of the uptake mechanism of iodine in brown algae, notably those of Tong and Chaikoff on the Pacific kelp *Nereocystis luetkeana* [53], of Bailey and Kelly on *Ascophyllum nodosum* [54], and of Shaw on *Laminaria* [55, 56].

More recently, it became clear that vanadium haloperoxidases, an intact cell wall, and low levels of hydrogen peroxide are required for sustained iodine uptake—protoplasts (i.e., algal cells, from which the cell wall has been enzymatically removed) do not take up iodine [47]. Only the macroscopic *Laminaria* sporophytes take up significant levels of iodine—the haploid, filamentous gametophytes do not. The former have high levels of haloperoxidases—the latter do not. However, iodine uptake can be induced in gametophytes upon addition of exogenous H_2O_2 and haloperoxidase. Subsequently, iodoperoxidases were purified from *Laminaria*, a novel subclass of the vanadium haloperoxidases, [57, 58] which may explain the selectivity for iodide uptake in *Laminaria* [47]. Iodine is accumulated in the apoplast of cortical *Laminaria* tissues [59]. *Laminaria* [46] and other seaweeds [60] show a marked seasonality of their iodine content, which is typically higher during the colder seasons and also (within the same species) increased at higher latitudes [46, 61]. It is tempting to hypothesize that in both cases this is likely due to reduced oxidative stress under cooler conditions in winter or at higher latitudes. Interestingly,

while the selectivity of the uptake mechanism for iodide is well-established, a recent study highlighted the capacity of *Laminaria* to decrease iodate concentrations in surrounding seawater, the metabolic pathways and mechanistic details of which remain unknown [62].

In the past, *in vivo* speciation studies of iodine in seaweeds (e.g., [63]) were limited by the necessity for an extraction step involving breaking up algal tissues and cells, thus potentially leading to extraction artifacts. The development of *in situ* K-edge X-ray absorption spectroscopy for both iodine and bromine changed that, enabling an unprecedented *in vivo* detection of both elements [9]. Using this approach, the biological significance of iodine accumulation in kelps was elucidated recently. X-ray absorption spectroscopy showed that the accumulated form is iodide, which is contained in a largely organic (rather than hydrated) environment, and which serves as a simple inorganic antioxidant, protecting the apoplast (cell wall space) of the cortical cell layers [64], analogous to the hypothesis proposed by Venturi [65] for animal systems. Upon oxidative stress, such as an oxidative burst [66–69], it undergoes a transition to a more hydrated form. Concomitantly, a strong efflux of accumulated iodide occurs. This constitutes the description of the first inorganic and of the chemically simplest antioxidant known from a living system [64]. Indeed, the reaction of iodide with the major reactive oxygen species is both thermodynamically and kinetically favorable. With the involvement of vanadium haloperoxidase and in the absence of organic cosubstrates, iodide effectively degrades H_2O_2 (halide-assisted disproportionation of hydrogen peroxide). A more recent study [70] underlined the uniqueness and importance of the iodide antioxidant system for *Laminaria*, while at the same time pointing out that the function of bromide is likely to be complementary to the iodide antioxidant system for detoxifying superoxide. This work also coined the term *iodide switch* for describing the preferential accumulation and targeted release of iodide upon oxidative stress, in comparison to bromide. While most of the iodine present in brown seaweeds is in the form of iodide, minor amounts are bound to organic molecules—in particular proteins as highlighted by a study on *Sargassum* [71].

Iodine accumulation in seaweeds—in particular in kelp species—has environmental significance, in particular also when it comes to iodine radioisotopes. Seaweeds have been found to accumulate ^{129}I originating either from nuclear weapons tests or from nuclear fuel reprocessing [72], and a time series study using seaweeds traced ^{129}I from the nuclear fuel reprocessing plants at La Hague and Sellafield along European and Arctic coasts [73]. A comprehensive review on ^{129}I speciation in biological samples including algae was published recently [74]. Most recently, *Macrocystis pyrifera* off the California coast contained detectable levels of ^{131}I from the Fukushima disaster in Japan in 2011 [75] and a green microalga, *Parachlorella* sp. *binos*, isolated near the Fukushima disaster site, was found to be a strong accumulator of radioactive iodine, strontium, and cesium, highlighting its potential for nuclear bioremediation [76].

Nevertheless, major open questions remain regarding the accumulation of iodide in kelp. So far, it is not clear how iodide is fixed in the apoplast, nor how its mobilization from this storage occurs during oxidative stress—both aspects arguably have

some bioengineering potential. The recent completion of the first brown algal genome [77] should help to provide new insights in this regard. However, the efflux of iodide during oxidative stress may be rather widespread in seaweeds: Besides *Laminaria*, this mechanism has been observed in both brown and red algae [62, 78]. It should also be highlighted that the biosynthetic pathways of iodinated halocarbons in marine algae [79] remain largely unknown to this date.

In comparison to seaweeds (macroalgae), much less is known about iodine metabolism in microalgae. Many microalgae exhibit high iodine tolerance and/or positive growth responses—and the haptophyte *Emiliania huxleyi* shows an approximately 10-fold accumulation of iodine compared to seawater [80]. Consistent with this and similar to *Laminaria*, a recent study on the haptophyte *Isochrysis* [81] found that iodide uptake requires peroxidase-mediated oxidation. Cold water diatom cultures were observed to reduce iodate to iodide, potentially providing a biotic explanation for the iodide maximum observed in surface ocean waters [82]. Indeed and consistent with this, off the western Antarctic peninsula, iodide concentrations increase and iodate concentrations decrease during the summer phytoplankton maximum [83]. However, iodate reduction may not be a uniform activity for all phytoplankton. Iodate reduction by *Isochrysis galbana* is relatively insensitive to deactivation of nitrate reductase activity [84], and phytoplankton blooms in mesocosm experiments in Antarctica resulted in the observation of fairly constant iodate and total iodine concentrations [85]. The latter two studies raise the question whether phytoplankton are really responsible (or the only players) for iodate reduction in seawater.

32.3.3 Atmospheric Impact

The first findings hinting at an atmospheric impact of molecular iodine emissions from seaweeds go back to Golenkin [49] in the late nineteenth century, and then especially Sauvageau [50], Kylin [51], and Dangeard [52] (see earlier). Another roughly half century passed until kelps were recognized as major emitters of iodocarbons [86]. This pioneering work triggered substantial research on algae as iodo- and halocarbon emitters in general (see Chapter 31). In the late 1990s, large-scale scientific field campaigns in western Ireland, a region with a large abundance of kelp, reported production rates of halocarbons [79] and discovered high levels of iodine oxides above kelp beds [87]. Shortly afterward, kelp iodine emissions were recognized as the cause for aerosol formation in the marine boundary layer [88], even though this work assumed that the biogenic precursor of these was chiefly diiodomethane (CH_2I_2), overlooking the much higher emissions of molecular iodine. Indeed, the millimolar iodide levels on the *Laminaria* surface exposed at low tide effectively scavenge atmospheric ozone, leading to the release of I_2 at rates up to about five orders of magnitude higher than the combined iodocarbon emissions. These studies [64, 89] unambiguously clarify the biochemical origin of particle-forming iodine oxides: Molecular iodine is photolyzed and further oxidized by ozone in the marine boundary layer, producing hygroscopic iodine oxides. The latter form ultrafine particles, leading to aerosol formation—establishing a unique link between a biological antioxidant and climatic processes. Since then, the atmospheric processes

investigating the link between molecular iodine, iodine oxides, and aerosol formation have been studied in considerable detail [90]. Also, other recent studies have investigated the release of I_2 more closely in *L. digitata* [91–95], but also in *A. nodosum* and several other brown and red algal species [95–97]. Such investigations were much facilitated by the development of novel techniques [[98] for review], such as vacuum UV resonance fluorescence for the detection of I_2 [96], a coupled diffusion denuder system combined with gas chromatography/mass spectrometry for the separation and quantification of molecular iodine and the activated iodine compounds iodine monochloride and hypiodous acid [99, 100], and time-of-flight aerosol mass spectrometry [101]. The latter enabled in situ measurements of molecular iodine in the marine boundary layer, which established the link to macroalgae and the implications for O_3 , IO, OIO, and NO_x [102], and subsequent particle formation [102] more clearly. Molecular iodine emission from *Laminaria* occurs in a remarkable, oscillatory time dependence of short, strong bursts with a complex time signature [91]. In a comparison of seven seaweed species, the kelps *Laminaria digitata* and *L. hyperborea* were the most potent emitters of I_2 , which was also observed—albeit at lower rates—from *Saccharina latissima* and *A. nodosum*, but not from *Fucus* species [95]. A more recent study [103], however, showed that mixing ratios above *A. nodosum* and *F. vesiculosus* beds increase with exposure time—after 6 h exposure to ambient air the mixing ratios were one order of magnitude higher than those initially present, in strong contrast with the emission characteristics of *L. digitata*, where most I_2 was emitted within the first half hour of exposure.

After exposure to air, intense I_2 emission is detectable from all thallus parts in *L. digitata*, but declines continuously over the next 180 min and is not affected by the light regime [94]. Molecular iodine release was investigated in a close simulation of tidal exposure in chamber experiments using a novel detection technique, incoherent broadband cavity-enhanced absorption spectroscopy (IBBCEAS), which showed that I_2 emission (at highly variable rates) occurs in four distinct stages: (1) moderate emissions from partially submerged samples; (2) a strong release by fully emerged samples; (3) slowing or stopping of I_2 release; and (4) later pulses of I_2 evident in some samples [92]. In similar chamber experiments, the link to particle formation was investigated more closely, confirming a linear relationship between particle concentration and I_2 emission and also that particle production from I_2 is more than a factor of 10 higher than that produced from CH_2I_2 for the same mixing ratios [93].

A recent study in Ireland [104] supports the hypothesis that human iodine intake in coastal regions is indeed dependent on seaweed abundance rather than proximity to the sea, underlining the critical importance of the molecular iodine release from algae for atmospheric processes and human health.

There is an interesting link between the type of halocarbons that are emitted and the physiological state of *Laminaria*: In the unstressed steady state, brominated compounds are predominantly released, whereas after induction of an oxidative burst, an endogenous defense reaction by oligoguluronates (an oligomeric degradation product of the major brown algal cell wall carbohydrate, alginate), there is a marked shift to iodinated compounds—in particular, compounds with multiple iodinations [70, 89]. This is likely due to the mobilization of iodide from its store due to the up to

millimolar levels of hydrogen peroxide occurring during the oxidative burst. Since iodide is the preferred substrate of vanadium haloperoxidases, this altered physiological situation will result in an increased incorporation of iodine in carbon skeletons e.g. due to the haloform reaction and, thus, an increased emission of halo-carbons with several iodine atoms.

As for iodine metabolism in general, much less is known about the atmospheric impact of iodine emissions from microalgae compared to macroalgae. It was recently suggested that Antarctic ice algae accumulate I^- , followed by I_2 release and particle formation [105]; however the same study highlighted significant, remaining gaps in understanding and highlighted the possibility of an unidentified iodine source. The very widespread marine cyanobacterium *Prochlorococcus marinus* is an important iodomethane producer, while another cyanobacterium, *Synechococcus*, is not [106]. Among members of three important microalgal lineages, the prymnesiophyte *Emiliania huxleyi*, the prasinophyte *Tetraselmis* sp., and the diatom *Thalassiosira pseudonana*, no increase in iodocarbon emission upon light stress was observed [107]. However, biogenic marine aggregates—including diatom mucilage and phyto-detritus—were found to be hotspots of iodocarbon production [108].

32.3.4 Iodine Transformations by Microbes

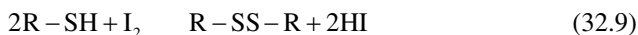
While algae have received most of the research interest by biochemists outside iodine accumulation in the thyroid, much of the role of microbes in global iodine cycling remains rather underexplored. The microbial contribution to the global iodine cycle was reviewed in 2008 [109]. Iodide oxidation linked to the formation of free iodine was first observed by a marine bacterium, *Pseudomonas iodooxidans*, in a marine aquarium where the process was blamed for fish fatalities [110]. Iodide-oxidizing bacteria occur in low abundance in seawater (from which they can be enriched by adding higher iodide concentrations) and in much higher abundance in iodide-rich brines accompanying natural gas deposits [111]. In particular, the latter include α -Proteobacteria that can oxidize I^- to I_2 , which are stimulated in their growth by both I^- and I_2 and which may have a competitive advantage over other microbes by suppressing the latter using I_2 [112]. Iodide oxidation in such α -Proteobacteria is mediated by a novel multicopper oxidase [8]. Most recently, it was found that laccase also oxidizes iodide to molecular iodine or hypoiodous acid, both of which are easily incorporated into natural soil organic matter [113]. Bacterial nitrate reductase activity has been implicated in the reduction of iodate in seawater [114] and a marine *Pseudomonas* sp. was found to be capable of dissimilatory iodate reduction under anaerobic growth conditions [115]. More recently, an iodate-reducing, anaerobic *Pseudomonas* sp. was isolated from marine sediments [115]. However, anaerobic microorganisms, in contrast to aerobic microorganisms, neither enhance nor repress the mobility of iodine [116]. A wide range of bacteria in terrestrial and marine environments are capable of methylating iodide [117, 118], and microbes have been implicated in iodine sorption in soils [119]. Iodine-accumulating bacteria were isolated from marine sediments with the uptake mechanism reminiscent of that described from brown algae [120, 121].

32.3.5 Iodinated Natural Products

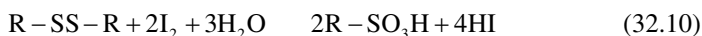
Not much is known about organic iodine metabolites and natural products other than the thyroid hormones. A recent review [122] mentions just over 110 iodine-containing natural products known to science, most of which originate from marine organisms. This low number of iodinated natural products is likely due to the low stability of the carbon–iodine bond (especially in comparison to C–Br and C–Cl, respectively), but probably also to some extent due to the still rather low research effort focusing on groups of organisms that are likely to harbor such compounds.

32.3.6 Iodine and Proteins

Studies on the iodination of proteins date way back to the nineteenth century [123], as the result of the widely held belief that it would be possible to imitate the activity of the naturally occurring protein thyroglobulin by introducing iodine into other proteins. Iodination of proteins has been investigated for several reasons: (i) to obtain thyroactive iodinated proteins and to study their mode of action, (ii) to determine active sites in enzymes and hormones, (iii) to alter proteins by introducing heavy atoms in known positions for crystallographic studies on the structure of proteins, (iv) to determine side chains (Cys, Met, Ser, Tyr, Trp) involved in interactions with other reagents and responsible for characteristic titration phenomena, and finally (v) to modify the antigenicity of proteins [124]. Iodine, in the presence of iodide at pH 3–5, can act as a reasonable oxidant for sulfhydryl groups (R–SH, R=cysteiny) to form a disulfide bond (Eq. 32.9).



The disulfide moiety can be oxidatively cleaved by iodine to cysteic acid, RSO_3H (Eq. 32.10).



Early on, halide anions including iodide were used as valuable spectroscopic probes and perturbing agents for mononuclear type 2 and dinuclear type 3 copper sites in proteins and enzymes, such as Cu, Zn superoxide dismutase (type 2 Cu), tyrosinase, and hemocyanin (type 3 Cu) [125–130]. A recent prominent example is the tetranuclear copper center (Cu₄Z) of bacterial nitrous oxide reductase (N₂OR), which reduces the greenhouse gas nitrous oxide (N₂O) to dinitrogen and water as final step of bacterial denitrification, an important branch of the biogeochemical nitrogen cycle (Eq. 32.11) [131].



Cu₄Z turned out to be the first reported biological example of an inorganic sulfide ion as part of a novel copper cluster. In the first crystal structures published, the Cu₄Z site consisted of four copper ions arranged in a μ_4 -sulfido bridged copper cluster solely coordinated by histidine residues (Fig. 32.2).

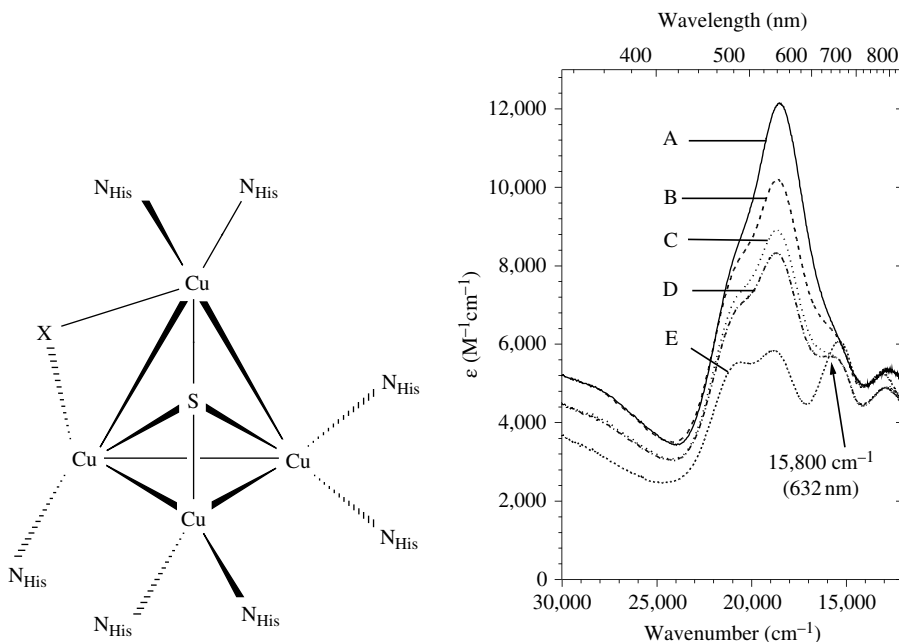


FIGURE 32.2 Left: Structure of CuZ in N_2OR . When prepared under the strict exclusion of dioxygen, the so-called purple form of N_2OR will be obtained, with X being sulfide (S^{2-}) versus X being OH^-/H_2O when prepared under oxidic conditions [132]. Right: Spectrophotometric titration of N_2OR from *Pseudomonas stutzeri* with inhibitor KI under anoxic conditions (A) enzyme $18\ \mu M$, in phosphate buffer, pH 7.0; (B) plus one equivalent KI/6 h reaction time (C) 2 equivalents. KI/10 h (D) three equivalents KI/16 h (E) ≈ 200 equivalents KI/36 h [133].

There was strong evidence from spectroscopic experiments (UV/Vis, EPR) that N_2OR formed stable adducts with Br^- and I^- [134]. N_2OR , in contrast to type 2 copper proteins, did not react with a large excess of F^- ; however, Cl^- , Br^- and I^- had increasingly strong effects on the UV/Vis and EPR spectra of purple N_2OR from *P. stutzeri* as illustrated for the reaction with iodide [133]. Dialysis against the strong oxidant $[Fe(cp)_2]PF_6$ did not remove the band with the absorption maximum centered at 632 nm (Fig. 32.2). Upon exposure of N_2OR from *Achromobacter cycloclastes* to sodium iodide this blue species could be crystallized. Structure determination of this adduct revealed that the inhibitor iodide was bound at the CuZ site bridging two Cu ions of the catalytic cluster providing evidence for this being the catalytic edge in nitrous oxide reductase (ligand X) (Figs. 32.2 and 32.3) [135].

32.4 VANADIUM HALOPEROXIDASES

32.4.1 Vanadium in Biological Systems

The biological function of vanadium is well-established and its biological chemistry has gained considerable interest [136–143]. Vanadium is the second most abundant transition metal in seawater ($\approx 35\ nM$) [144] and universally distributed in

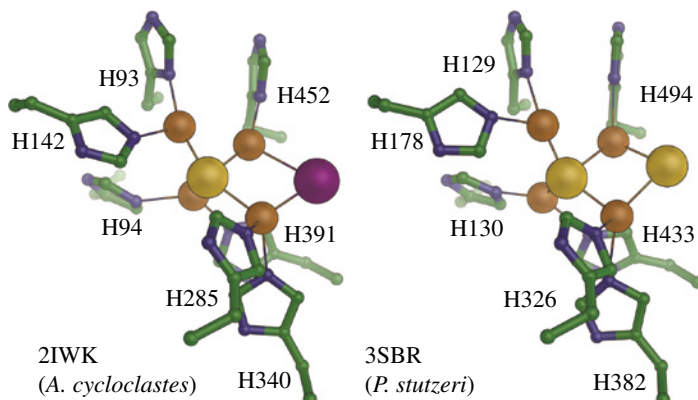


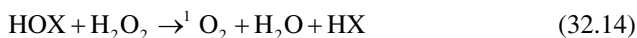
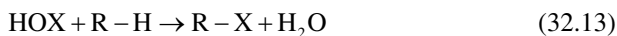
FIGURE 32.3 Structures of the CuZ–iodide adduct (N₂OR *Achromobacter cycloclastes*; PDB code 2IWK) and the native CuZ site (N₂OR *Pseudomonas stutzeri*; PDB code 3SBR). The addition of the soft ligand iodide yielded a bridging conformation that closely mimics the binding of S²⁻ in the purple N₂OR from *P. stutzeri*. Iodide in purple, sulfide in yellow. Adapted from Ref. [135] © Elsevier. (See insert for color representation of the figure.)

the soil [145]. Extraterrestrial vanadium compounds were shown to contain the metal in low oxidation states (V(II) and V(III)), reflecting anoxic environments during genesis. Pyroxenes were found in meteorites, which are typical V(II) containing minerals. The atmospheres of hot Jupiter-type exoplanets, as well as the atmospheres of early M-type stars, contain vanadium(II)oxide, which is also likely a constituent in interstellar clouds. The relevance of these findings for the generation of complex organic molecules out of simple ones under primordial conditions has been discussed recently in light of the catalytic potential of vanadium nitrides and vanadium oxides [141]. Furthermore, it has been known for a long time that ascidians accumulate high levels of vanadium in their blood cells. Recently, vanadium(IV) binding proteins (vanabins), from the vanadium-rich ascidian *Ascidia sydneiensis samea* have been characterized. The deduced amino acid sequences of the vanabins were highly conserved. Most strikingly, the sequences were rich in cysteine residues and the intervals between the cysteines were highly regular. Note that metallothioneins, which bind metal ions such as Zn, Cu, or Cd, are also rich in cysteines; however, the repetitive pattern of cysteine residues differs between metallothioneins and vanabins. Binding of vanadium(IV) to these vanabins was inhibited by the addition of copper(II) ions. The first structure of a vanabin protein was solved by NMR spectroscopy, which revealed a novel bow-shaped conformation, with four R-helices connected by nine disulfide bonds. Furthermore, it appeared that vanadyl cations (VO₂⁺) were coordinated by nitrogen atoms derived from lysine, arginine, or histidine, as suggested by the EPR results. Recently, vanabin2 was shown to act as a specific vanadium(V) reductase. This specificity may account for the specificity of vanadium accumulation in ascidians [146–151]. Amavadin is a vanadium(IV) complex that occurs, at least, in the fungus *Amanita muscaria*. Its biological role has not yet been elucidated; however, its characterization and reactivity have disclosed catalase- and peroxidase-type

activity, the latter toward thiols (including biological ones) and hydrocarbons [136]. Vanadium constitutes an inherent part of important enzymatic active sites; the most prominent examples are V-HPO and vanadium nitrogenase [152]. For both types of V-dependent enzymes there exist functional analogues in nature that are either more widely spread or more efficient, for example, the heme-dependent haloperoxidases and the conventional Mo-dependent nitrogenases, respectively. One might ask how these enzyme systems evolved, and in particular, whether the vanadium-containing enzymes known today are retained functional analogues that withstood evolutionary forces. The widespread physiological effects of vanadium are mainly attributed to the similarity of the vanadate (V) ions (VO_4^{3-}) and phosphate ions (PO_4^{3-}). Note that, depending on pH, there also exist important differences between these two anions with regard to charge, redox, and coordination properties [152, 153]. With one electron ($3d^1$ electron configuration) the V(IV), $S=1/2$ state can be easily accessed by EPR spectroscopy [154]. Because of the strong coupling to the ^{51}V nucleus (nuclear spin $I=7/2$), a characteristic splitting of the EPR signal into eight lines can be observed [149, 155]. Most recently, the application of ^{51}V solid-state NMR spectroscopy was introduced as a direct and sensitive reporter of the vanadium site in V-CPO. ^{51}V is a half-integer quadrupolar nucleus with high natural abundance (99.8%) and relatively high gyromagnetic ratio (Larmor frequency of 157.6 MHz at 14.1 T). The dominant anisotropic quadrupolar and chemical shielding interactions are directly observed in the solid-state NMR spectra and bear a wealth of information about the geometric and electronic structure of the vanadium site [156].

32.4.2 Discovery and General Properties of V-HPO

V-HPO are enzymes isolated primarily from marine algae, although they have also been purified from other organisms [139, 140, 157]. These enzymes catalyze the two-electron oxidation of halide ions (X^-) to the corresponding HOX. HOX can further react with a broad range of acceptors to form a diversity of halogenated compounds (Eqs. 32.12 and 32.13) [158]. When a nucleophilic acceptor is absent, a reaction may also occur between HOX and H_2O_2 producing singlet oxygen, $^1\text{O}_2$ (Eq. 32.14).



Historically, the haloperoxidases are named after the most electronegative halide they can oxidize. V-dependent chloroperoxidases (V-CPO) catalyze the oxidation of Cl^- , Br^- and I^- , vanadium bromoperoxidase (V-BPO) catalyzes only the oxidation of Br^- and I^- , and vanadium iodoperoxidases (V-IPO) are specific for iodide [139]. Notably, V-CPO had a much higher rate in the oxidation of bromide ($k_{\text{cat}} \approx 250 \text{ s}^{-1}$)

than in the oxidation of chloride ($k_{\text{cat}} \approx 20 \text{ s}^{-1}$) [159]. The brown seaweeds of the genus *Laminaria* are known as the most efficient iodine accumulators among all living species (Section 32.3.2). The V-IPOs found in these seaweed species play a major role in the production of I_2 and R-I compounds and in the accumulation of I^- . Recently, two different haloperoxidases, one specific for the oxidation of I^- iodide and the second that can oxidize both I^- and Br^- , were obtained from the brown alga *L. digitata*. The iodoperoxidase activity was significantly more efficient than the bromoperoxidase fraction in the oxidation of iodide. The two enzymes differed markedly in their molecular masses, trypsin digestion profiles, and immunological characteristics [7, 57, 58].

32.4.3 Three-Dimensional Structures of V-HPO

The first crystallized and one of the best-characterized V-HPO, thanks to the pioneering work of Dutch researcher Ron Wever, is the fungal V-CPO purified from *Curvularia inaequalis* [159, 160] (Fig. 32.4). Its X-ray structure (2.1 Å; PDB code 1IDQ), in complex with azide (N_3^-), reveals that the small ligand N_3^- coordinates directly to the vanadium center. In addition, three nonprotein oxygen ligands and one histidine nitrogen are bound. In the native state, vanadium is bound as hydrogen vanadate(V) in a trigonal bipyramidal geometry, with the metal coordinated to three

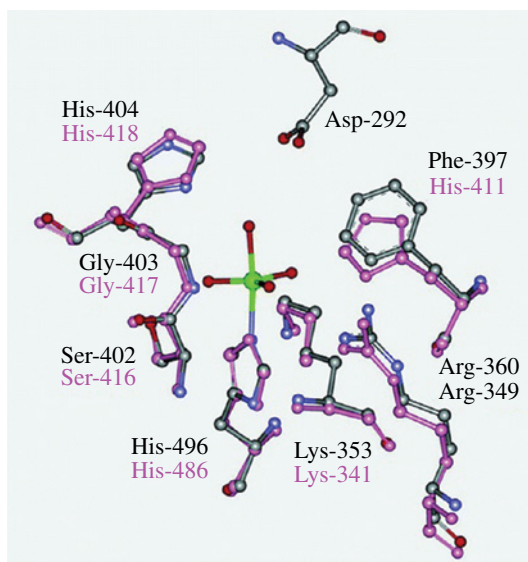


FIGURE 32.4 Active sites of V-CPO from *C. inaequalis* (black) and V-BPO from *A. nodosum* (white) have been superimposed to demonstrate the similar geometries. Active site residue labels correspond to V-CPO (top) and V-BPO (bottom). The vanadate geometry consists of an axial hydroxo group *trans* to His-496/His-486 and three equatorial oxo ligands (green/red). Below pH 8.0, protonation of one of the oxo groups may occur (PDB codes 1IDQ and 1QI9). Adapted from Ref. [156] © American Chemical Society.

oxygen atoms in the equatorial plane, and HO^- (from water) and one histidine nitrogen ($\text{N}\epsilon 2$) at the apical positions. The linkage between the metal and the histidine nitrogen was first assigned as a direct coordinating bond and later as a covalent bond. The hydrogen vanadate (HOVO_3^{2-}) is stabilized into a hydrogen bonding network, involving six highly conserved key residues, one apical histidine, two arginines, a lysine, a glycine, and a serine (Fig. 32.5). Kinetic and structural studies of single-site variants of V-CPO from *C. inaequalis* document the importance of these residues in binding vanadate, but also the rigidity of the active site, resulting from a large number of hydrogen bonding interactions. Notably, the only V-HPO presenting a substitution among these six residues (the serine is replaced by an alanine) is the V-IPO from *L. digitata*, although its three-dimensional structure has not been solved yet [57]. The homodimeric V-BPO from the brown alga *A. nodosum* (2.0\AA ;

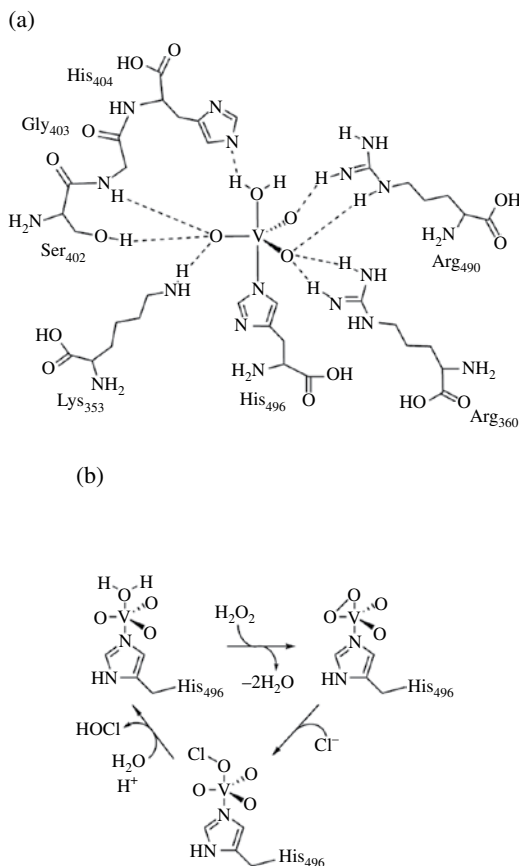


FIGURE 32.5 (a) Network of hydrogen bonds at the active site of native V-CPO from *C. inaequalis*; hydrogen bonds are drawn as dashed lines. (b) Proposed catalytic scheme of V-CPO. Adapted from Ref. [161].

PDB code 1QI9) has a nearly all-helical structure, with two four-helix bundles and only three small β -sheets. The holoenzyme contains trigonal bipyramidally coordinated vanadium atoms at its two active centers [162]. Despite the low sequence and overall structural similarity between V-BPO (*A. nodosum*) and V-CPO (*C. inaequalis*), the vanadium active sites are highly conserved on the N-terminal side of an α -helix and include the catalytic histidine residue (His418^{V-BPO}/His404^{V-CPO}). The V-BPO structure contains, in addition, a second histidine near the active site (His411^{V-BPO}), which might influence the redox potential of the catalytically active $\text{VO}_2\text{-O}_2$ species by protonation/deprotonation reactions (Fig. 32.4). The amino acids lining the first and the second hydrogen bonding spheres for the vanadium active site are highly conserved with one exception: a Phe residue in chloroperoxidases is invariably substituted by a His residue in bromoperoxidases. The structure of a V-BPO from the red algae *Corallina officinalis* (2.3 Å, PDB code 1QHB) showed a dodecameric architecture, with each subunit made up of 595 amino acid residues [163]. A cavity is formed by the N terminus of each subunit in the center of the dodecamer. Otherwise, the subunit fold and dimer organization of the enzyme were similar to those of the V-BPO dimer from the brown algae *A. nodosum*, with which it shares 33% sequence identity. The different oligomeric states of the two algal enzymes reflect separate mechanisms of adaptation to harsh environmental conditions and/or to chemically active substrates and products. The residues involved in vanadate binding were conserved between the two bromoperoxidases and the V-CPO from *C. inaequalis* (Fig. 32.4). However, most of the other residues forming the active site cavity are different in the three enzymes, which reflects differences in the substrate specificity and stereoselectivity of the reaction. Studies with a series of V-CPO variants suggest that the electrostatic potential distribution changes are detrimental to the chlorinating activity, yet their crystal structures reveal intact or nearly intact conformation of the active site. Thus, a delicate balance of multiple interactions between the active site residues has been proposed to be responsible for the activity of the V-CPOs [156]. The V-BPO from the macroalga *Corallina pilulifera* was reported to have a significant thermostability and stability toward organic solvents. The structural analysis of the recombinant enzyme (2.2 Å, PDB code 1UP8) revealed the presence of one Ca^{2+} ion per subunit, which significantly increased the enzyme stability. The remarkably high stability of the enzyme in the presence of organic solvents makes this V-BPO a useful biocatalyst [164].

An interesting observation resulted from a trapped phosphate intermediate in the crystal structure (1.5 Å, PDB code 3BB0) of vanadium-free apochloroperoxidase from *C. inaequalis* which catalyzes a dephosphorylation reaction [165]. Since the chloroperoxidase is functionally and evolutionary related to several acid phosphatases including human glucose-6-phosphatase and a group of membrane-bound lipid phosphatases, the structure may help to understand the mechanism of action of these enzymes as well. The trapped intermediate is bound to the active site as metaphosphate, PO_3^- , with its phosphorus atom covalently attached to the nitrogen atom of His496. An apical water molecule is within hydrogen bonding distance to the phosphorus atom, and it is in a perfect position for a nucleophilic attack on the metaphosphate–histidine intermediate to form the inorganic phosphate.

32.4.4 Catalytic Cycle of V-HPO

Vanadium haloperoxidases catalyze the oxidation of halide anions, Cl^- , Br^- and I^- , by hydrogen peroxide (Eq. 32.12). Earlier, Pecoraro and coworkers suggested that the V-HPOs may actually be peroxidases and that the well-known halogenation reactions may simply reflect the abundance of chloride in the marine environment [166]. The potentials for the oxidation of I^- , Br^- , and Cl^- span a range of 0.53–1.36 V (versus NHE), and the potentials for the oxidation of the pseudohalide anions, such as CN^- , OCN^- , or SCN^- , fall within or below this range, suggesting that the vanadium haloperoxidases may also catalyze the transformation of these compounds. Indeed, cyanide ($E^\circ = +0.375$ V) acts as an inhibitor of V-bromoperoxidase isolated from the marine alga *A. nodosum* through preferential oxidation of CN^- . Similarly, thiocyanate ($E^\circ = +0.77$ V) was reported to inhibit bromide peroxidation through preferential oxidation of thiocyanate over bromide. ^{13}C NMR studies of the oxidation of KC^{13}CN by H_2O_2 catalyzed by V-BPO showed the formation of several oxidized thiocyanate species, including the putative (unstable) dithiocyanate ether, hypothiocyanate, thiooxime, and bicarbonate [167, 168]. Bromine K-edge EXAFS experiments on samples containing bromide and V-BPO were carried out, with biomimetic vanadium complexes carrying Br-V, Br-C(aliphatic) and Br-C(aromatic) bonds as reference. From these studies [167, 168], it initially appeared that bromide did not coordinate to the vanadium center of the peroxidase, but bound covalently to carbon, with an active site serine as a possible candidate. However, more recent evidence by a combination of EXAFS and electrospray ionization quadrupole time of flight tandem mass spectrometry (ESI-Q-TOF MS/MS) of tryptic digests [169] provided an important correction to the iodinated Tyr and reactive brominated Ser residues that were proposed in earlier crystallographic [162] and spectroscopic [167, 168] studies, respectively. This study [169] found that native *Anv*BPO contains Br in the surface Tyr residues 447 (frequently dibrominated) and 398 (rarely monobrominated). These brominated Tyr residues are not likely to be reactive intermediates in the catalytic cycle of *Anv*BPO due to their location at the surface and the nature of the Br–Tyr bond. I XAS reveals I incorporation to a lower extent, which is not detectable by MS/MS.

In this series of experiments, two oxovanadium complexes, $[\text{VO}(\text{H}_2\text{O})_2(\text{sal-L-Leu})]$ and $[\text{VO}(\text{H}_2\text{O})_2(5\text{-Br-sal-Gly})]$, had been structurally characterized [168]. These complexes contained the water ligands in *cis* and *trans* positions to the oxo group, at V–OH₂ distances ranging from 2.008 to 2.228 Å, and were used to model the apical electron density feature observed in the structures of fungal and algal V-HPOs. Steady-state kinetic experiments suggested a mechanism in which hydrogen peroxide first binds the vanadate active site, followed by halide oxidation (Fig. 32.5) [170, 171]. The *C. inaequalis* V-CPO and the *A. nodosum* V-BPO were used to get deeper insights into the catalytic mechanism of vanadium-dependent peroxidases. The high conservation of the residues at the catalytic vanadium site and results from phylogenetic analyses strongly suggest that all V-HPOs share the same mechanism of action. The first step of the catalytic cycle involved the coordination of hydrogen peroxide by bound hydrogen vanadate, producing a

square-based pyramidal peroxovanadium complex, from which the X-ray structure of V-CPO has been resolved [172]. The propensity of vanadium(V) to coordinate peroxides is well-established, as illustrated by the classic spot test for vanadate, which is the formation of the red oxoperoxovanadium(V). Note that peroxovanadates are remarkably stable, which has permitted their structural characterization. Although the interaction between H_2O_2 and the bound hydrogen vanadate is widely accepted for V-HPOs, the subsequent steps of the catalytic cycle have not been fully elucidated. The halide substrate appears not to be directly coordinated by the peroxovanadium intermediate according to X-ray absorption spectroscopy for *A. nodosum* V-BPO, which led to the proposal of a halide fixation site in the vicinity of the active site [173]. Recently, such a fixation site could be identified in the crystal structure of V-BPO from the red algae *C. pilulifera* and a selected variant (Arg397Trp). Crystallographic studies in the presence of potassium bromide (cocrystallization or soaking experiments) revealed a specific halogen binding site involving residue Arg397 and other surrounding amino acids. All of the data sets obtained from the crystals where bromide had been introduced showed a consistent anomalous peak at approximately 3.6 Å from the oxygen of the vanadate. This is consistent with a previous proposal for the position of the bromide in the related *Ascophyllum bromoperoxidase* enzyme as determined by X-ray absorption spectroscopy experiments. The bromide anion appears to be bound to one of the terminal nitrogen atoms of Arg397 at a distance of 3 Å. The remaining residues in the environment of the bromide ion are mainly hydrophobic. A similar hydrophobic binding pocket has previously been observed in other protein structures where halogen is bound [174]. The presence of bromide in the active site is associated with the displacement of Leu337 with formation of the hydrophobic pocket. The environment of the active site could have additional changes upon binding of peroxide; however, no peroxo complex of the enzyme has been crystallized [175]. The peroxovanadium complex converts X^- to a halogen intermediate, X_2 or XOH . Note that both X_2 and XOH are in spontaneous equilibrium (Eq. 32.1), and both can account for the halogenation/oxygen insertion properties of the V-HPO/ $\text{H}_2\text{O}_2/\text{X}^-$ system. Most likely XOH is initially produced by a two-electron oxidation of X^- [176].

Structural and biochemical researches have focused on residues to the vicinity of the active site in V-CPO, V-BPO, and V-IPO, which could explain the origin of halide selectivity. As the halide is not directly bound to the vanadate, the neighboring amino-acids, which were thought to play a crucial role in substrate selectivity, were exchanged by site-directed mutagenesis. In *C. inaequalis* V-CPO, the serine residue hydrogen bonded to the vanadate cofactor has been changed to alanine [177]. This mutation led to a putative active site similar to the one proposed for *L. digitata* V-IPO [57] and significantly decreased the reactivity toward chloride, but had only minor effects on bromination kinetic parameters. Currently it is argued that halogen specificity depends on several factors, especially on the hydrogen bonding network in the active site and the redox state and the distribution of charges of vanadate center (Fig. 32.5). As discussed earlier, the redox potentials of $\text{X}_2/2\text{X}^-$ and XOH/X^- vary significantly, and they decrease in the same order, that is, $\text{Cl} > \text{Br} > \text{I}$. Thus, if the

peroxovanadium center of V-IPO has a low enough redox potential, Br⁻ and Cl⁻ oxidation will be chemically unfavorable. Differences in amino acid residues at the active site and in stabilization of the peroxovanadium intermediate will influence the redox potential, a condition that is crucial for halide discrimination [7].

32.5 CONCLUDING REMARKS AND FUTURE DIRECTIONS

In 2011, the scientific community celebrated the discovery of the novel chemical element iodine, ¹²⁷₅₃I, a member of the group 17 of the periodic table [5]. As it turned out, iodine, like the other halogens, had and still has a significant impact on numerous aspects of life on Earth. Notably, iodine plays a key role in thyroid function, with major implications for human health. Despite the paramount importance of iodine as a constituent of thyroid hormones and, thus, for the basic functioning of mammalian physiology, the number of iodine-containing natural products is lower compared to its relatives within the group of halogens, bromine and chlorine. Iodine has a rich bioinorganic chemistry because of its wide range of oxidation states, specifically the iodide anion serves as a valuable complexing agent for many transition metals including vanadium. In several respects, iodine is unique as an essential bioelement. It has the largest ion radius (213 pm as iodide) and the highest atomic mass of any ecologically and phylogenetically widespread biological element (126.9 Da). However, note that several microorganisms, mostly hyperthermophiles, employ with tungsten (atomic number 74, 183.84 Da) an even heavier element for redox catalysis [178–180]. Most important, iodine has a rich environmental chemistry. In view of its global importance, research on the biogeochemical cycle of this element has become a major issue and has attracted the interest of biologists, chemists, and ecologists. Surprisingly, iodide is both the chemically simplest and first inorganic antioxidant that has been demonstrated to be operative in a living system, with tremendous implications for atmospheric processes [64]. Clearly, the exploration of the environmental impact of iodine and its compounds will require interdisciplinary efforts including the application of advanced physical techniques.

ACKNOWLEDGMENTS

Funding from the U.K. Natural Environment Research Council (NERC) through the SOLAS and Oceans 2025 (WP4.5) programs and the MASTS pooling initiative (Marine Alliance for Science and Technology for Scotland, funded by the Scottish Funding Council and contributing institutions; grant reference HR09011) to FCK and from the Deutsche Forschungsgemeinschaft (Germany) to PMHK is gratefully acknowledged. FCK would also like to extend special thanks to Alison Butler (University of California, Santa Barbara) for her support and useful discussions. Furthermore, the authors are grateful for support from the European Community in the framework of the Access to Research Infrastructure Action of the Improving Human Potential Program to the EMBL Hamburg Outstation.

ABBREVIATIONS

EPR, electron paramagnetic resonance; EXAFS, extended X-ray absorption fine structure; NMR, nuclear magnetic resonance; N₂OR, nitrous oxide reductase; V-HPO, vanadium haloperoxidase; V-CPO, vanadium-chloroperoxidase; V-BPO, vanadium-bromoperoxidase; V-IPO, vanadium-iodoperoxidase

REFERENCES

- [1] Greenwood NN, Earnshaw A. *Chemistry of the Elements*. 2nd ed. Oxford: Butterworth-Heinemann; 1997.
- [2] Hollemann AF, Wiberg E. *Lehrbuch der Anorganischen Chemie*. Berlin: Walter de Gruyter; 1985.
- [3] Housecroft E, Sharpe AG. *Inorganic Chemistry*. 3rd ed. Essex: Pearson; 2008.
- [4] webelements.com/iodine. Available at <http://www.webelements.com/iodine>. Accessed June 17, 2014.
- [5] Küpper FC, Feiters MC, Olofsson B, Kaiho T, Yanagida S, Zimmermann MB, Carpenter LJ, Luther GW III, Lu Z, Jonsson M, Kloo L. Commemorating two centuries of iodine research: an interdisciplinary overview of current research. *Angew Chem Int Ed* 2011;50:11598–11620.
- [6] Kleinberg J, Davidson AW. The nature of iodine solutions. *Chem Rev* 1948;42: 601–609.
- [7] Leblanc C, Colin C, Cosse A, Delage L, La Barre S, Morin P, Fiévet B, Voiseux C, Ambroise Y, Verhaeghe E, Amouroux D, Donard O, Tessier E, Potin P. Iodine transfers in the coastal marine environment: the key role of brown algae and of their vanadium-dependent haloperoxidases. *Biochimie* 2006;88 (11):1773–1785.
- [8] Suzuki M, Eda Y, Ohsawa S, Kanesaki Y, Yoshikawa H, Tanaka K, Muramatsu Y, Yoshikawa J, Sato I, Fujii T, Amachi S. Iodide oxidation by a novel multicopper oxidase from the Alphaproteobacterium Strain Q-1. *Appl Environ Microbiol* 2012;78 (11): 3941–3949.
- [9] Feiters MC, Küpper FC, Meyer-Klaucke W. X-ray absorption spectroscopic studies on model compounds for biological iodine and bromine. *J Synchrotr Rad* 2005;12: 85–93.
- [10] Wagner C, König GM. Mechanisms of halogenation of marine secondary metabolites. In: Fattorusso E, Gerwick WH, Tagliatalata-Scafati O, editors. *Handbook of Marine Natural Products*. Dordrecht: Springer Science+Business Media B.V; 2012. p 977–1024.
- [11] Lane AL, Moore BS. A sea of biosynthesis: marine natural products meet the molecular age. *Nat Prod Rep* 2011;28 (2):411–428.
- [12] van Pee KH, Dong CJ, Flecks S, Naismith J, Patallo EP, Wage T. *Biological Halogenation has Moved Far Beyond Haloperoxidases*. Volume 59, San Diego: Elsevier Academic Press Inc; 2006. *Advances in Applied Microbiology*; p 127–157.
- [13] Gribble GW. Natural organohalogens: a new frontier for medicinal agents? *J Chem Educ* 2004;81 (10):1441–1449.
- [14] Gribble GW. Natural organohalogens—many more than you think. *J Chem Educ* 1994;71 (11):907–911.

- [15] La Barre S, Potin P, Leblanc C, Delage L. The halogenated metabolism of brown algae (Phaeophyta), its biological importance and its environmental significance. *Mar Drugs* 2010;8 (4):988–1010.
- [16] Butler A, Sandy M. Mechanistic considerations of halogenating enzymes. *Nature* 2009;460 (7257):848–854.
- [17] Blasiak LC, Drennan CL. Structural perspective on enzymatic halogenation. *Acc Chem Res* 2009;42 (1):147–155.
- [18] Neumann CS, Fujimori DG, Walsh CT. Halogenation strategies in natural product biosynthesis. *Chem Biol* 2008;15 (2):99–109.
- [19] Fujimori DG, Walsh CT. What's new in enzymatic halogenations. *Curr Opin Chem Biol* 2007;11 (5):553–560.
- [20] McFiggans G, Bale CSE, Ball SM, Beames JM, Bloss WJ, Carpenter LJ, Dunk R, Hornsby K, Jones CE, Lee JD, Jones RL, Langridge JM, LeCrane J-P, Shillings AJL, Leblanc C, Potin P, Thomas F, Von Glasow R. Iodine-mediated coastal particle formation: an overview of the Reactive Halogens in the Marine Boundary Layer (RHAMBLe) Roscoff coastal study. *Atmos Chem Phys* 2010;10 (6):2975–2999.
- [21] Lehmann JF, Schrobilgen GJ, Christe KO, Kornath A, Suontamo RJ. X-ray crystal structures of XF_6 Sb_2F_{11} ($\text{X} = \text{Cl}, \text{Br}, \text{I}$); $\text{Cl-35}, \text{Cl-37}, \text{Br-79}, \text{Br-81}$, and I-127 NMR studies and electronic structure calculations of the XF_6^+ cations. *Inorg Chem* 2004;43 (22):6905–6921.
- [22] Mindat.org. Lautarite. Available at <http://www.mindat.org/min-2346.html>. Accessed June 17, 2014.
- [23] Hassel O, Hope H. Structure of the solid compound formed by addition of two molecules of iodine to one molecule of pyridine. *Acta Chem Scand* 1961;15:407–416.
- [24] Struble MD, Scerba MT, Siegler M, Lectka T. Evidence for a symmetrical fluoronium Ion in solution. *Science* 2013;340 (6128):57–60.
- [25] Liebhaf's HA, Wu LS. Reactions involving hydrogen peroxide, iodine, and iodate ion. 5. Introduction to oscillatory decomposition of hydrogen peroxide. *J Am Chem Soc* 1974;96 (23):7180–7187.
- [26] Eigen M, Kustin K. The kinetics of halogen hydrolysis. *J Am Chem Soc* 1962;84: 1355–1361.
- [27] Xu L, Cseko G, Kegl T, Horvath AK. General pathway of sulfur-chain breakage of polythionates by iodine confirmed by the kinetics and mechanism of the pentathionate-iodine reaction. *Inorg Chem* 2012;51 (14):7837–7843.
- [28] Pearson RG. Absolute electronegativity and hardness: application to inorganic chemistry. *Inorg Chem* 1988;27 (4):734–740.
- [29] Pearson RG. Hard and soft acids and bases, HSAB, part II: underlying theories. *J Chem Educ* 1968;45 (10):643.
- [30] Pearson RG. Crystal field theory and substitution reactions of metal ions. *J Chem Educ* 1961;38 (4):164.
- [31] Ahrland S, Chatt J, Davies NR. The relative affinities of ligand atoms for acceptor molecules and ions. *Quart Rev Chem Soc* 1958;12:265–276.
- [32] Ryan JL. Weak or unstable iodo complexes. II. Iodo complexes of titanium(IV), iron(III), and gold(III). *Inorg Chem* 1969;8 (10):2058–2062.
- [33] Ryan JL. Weak or unstable iodo complexes. I. Hexaiodo complexes of the lanthanides. *Inorg Chem* 1969;8 (10):2053–2058.

- [34] Pavlova SV, To HL, Chan ESH, Li HW, Mak TCW, Lee HK, Chan SI. Synthesis, structure and dioxygen reactivity of a bis(mu-iodo)dicopper(I) complex supported by the N-(3,5-di-tert-butyl-2-hydroxybenzyl)-N,N-di-(2-pyridylmethyl) amine ligand. *Dalton Trans* 2006;18:2232–2243.
- [35] Balzani V, Carassiti V. *Photochemistry of Coordination Compounds*. New York: Academic Press; 1970. p 161.
- [36] Sima J, Brezova V. Photochemistry of iodo iron(III) complexes. *Coord Chem Rev* 2002;229 (1–2):27–35.
- [37] Marusak RA, Doan K, Cummings SD. *Integrated Approach to Coordination Chemistry*. Hoboken, New Jersey, USA: Wiley & Sons, Inc.; 2007.
- [38] Tobe ML, Burgess J. *Inorganic Reaction Mechanisms*. Harlow: Addison Wesley Longman; 1999.
- [39] McDowell LR. *Iodine. Minerals in Animal and Human Nutrition*. San Diego, CA: Academic Press; 1992. p 305–323.
- [40] Courtois B. Découverte d'une substance nouvelle dans le Vareck. *Ann Chim (Paris)* 1813;88:304–310.
- [41] Gay-Lussac J-L. Sur la combinaison de l'iode avec l'oxygène. *Ann Chim (Paris)* 1813;88: 319–321.
- [42] Gay-Lussac L-J. Sur un nouvel acide formé avec la substance découverte par M. Courtois. *Ann Chim (Paris)* 1813;88:311–318.
- [43] Davy H. Some experiments and observations on a new substance which becomes a violet coloured gas by heat. *Phil Trans Roy Soc Lond* 1814;104:74–93.
- [44] Wisniak J. Bernard courtois—the discoverer of iodine. *Educ Quim* 2002;13 (3):206–213.
- [45] Synge JM. *The Aran Islands*. London: George Allen & Unwin Ltd.; 1907.
- [46] Ar Gall E, Küpper FC, Kloareg B. A survey of iodine contents in *Laminaria digitata*. *Bot Mar* 2004;47:30–37.
- [47] Küpper FC, Schweigert N, Ar Gall E, Legendre JM, Vilter H, Kloareg B. Iodine uptake in *Laminariales* involves extracellular, haloperoxidase-mediated oxidation of iodide. *Planta* 1998;207:163–171.
- [48] Eschle NN. Ueber den Jodgehalt einiger Algenarten. *Z Phys Chem* 1897;23:30–37.
- [49] Golenkin M. Algologische Notizen; 1. Das Vorkommen von freiem Iod bei *Bonnemaisonia asparagoides*. *Bull Soc Imp Nat Moscou* 1894;8.
- [50] Sauvageau C. Sur quelques algues floridées renfermant de l'iode à l'état libre. *Bulletin de la Station Biologique d'Arcachon* 1925;22:3–43.
- [51] Kylin H. Über das Vorkommen von Jodiden, Bromiden und Jodidoxydasen bei Meeresalgen. *Hoppe-Seyler's Z Physiol Chem* 1929;186:50–84.
- [52] Dangeard P. Sur le dégagement de l'iode chez les algues marines. *Comptes Rendus Hebdomadaires des Séances de l'Académie des Sciences* 1928;186:892–894.
- [53] Tong W, Chaikoff IL. Metabolism of ^{131}I by the marine alga, *Nereocystis luetkeana*. *J Biol Chem* 1955;215:473–484.
- [54] Bailly NA, Kelly S. Iodine exchange in *Ascomyllum*. *Biol Bull Woods Hole* 1955;109:13–20.
- [55] Shaw T. The mechanism of iodine accumulation by the brown sea weed *Laminaria digitata*. The uptake of ^{131}I . *Proc Roy Soc Lond B* 1959;150:356–371.

- [56] Shaw TI. The mechanism of iodine accumulation by the brown sea weed *Laminaria digitata*. Respiration and iodide uptake. *Proc Roy Soc Lond B* 1960;152:109–117.
- [57] Colin C, Leblanc C, Michel G, Wagner E, Leize-Wagner E, van Dorsselaer A, Potin P. Vanadium-dependent iodoperoxidases in *Laminaria digitata*, a novel biochemical function diverging from brown algal bromoperoxidases. *J Biol Inorg Chem* 2005;10:156–166.
- [58] Colin C, Leblanc C, Wagner E, Delage L, Leize-Wagner E, Van Dorsselaer A, Kloareg B, Potin P. The brown algal kelp *Laminaria digitata* features distinct bromoperoxidase and iodoperoxidase activities. *J Biol Chem* 2003;278:23545–23552.
- [59] Verhaeghe EF, Fraysse A, Guerquin-Kern J-L, Wu T-D, Devès G, Mioskowski C, Leblanc C, Ortega R, Ambroise Y, Potin P. Microchemical imaging of iodine distribution in the brown alga *Laminaria digitata* suggests a new mechanism for its accumulation. *J Biol Inorg Chem* 2008;13:257–269.
- [60] Hou XL, Yan XJ. Study on the concentration and seasonal variation of inorganic elements in 35 species of marine algae. *Sci Total Environ* 1998;222 (3):141–156.
- [61] Saenko GN, Kravtsova YY, Ivanenko VV, Sheludko SI. Concentration of iodine and bromine by plants in the seas of Japan and Okhotsk. *Mar Biol* 1978;47:243–250.
- [62] Truesdale VW. The biogeochemical effect of seaweeds upon close-to natural concentrations of dissolved iodate and iodide in seawater—preliminary study with *Laminaria digitata* and *Fucus serratus*. *Estuar Coast Shelf Sci* 2008;78 (1):155–165.
- [63] Hou XL, Chai CF, Qian QF, Yan XJ, Fan X. Determination of chemical species of iodine in some seaweeds. *Sci Total Environ* 1997;204 (3):215–221.
- [64] Küpper FC, Carpenter LJ, McFiggans GB, Palmer CJ, Waite TJ, Boneberg EM, Woitsch S, Weiller M, Abela R, Grolimund D, Potin P, Butler A, Luther GW III, Kroneck PM, Meyer-Klaucke W, Feiters MC. Iodide accumulation provides kelp with an inorganic antioxidant impacting atmospheric chemistry. *Proc Natl Acad Sci U S A* 2008;105 (19):6954–6958.
- [65] Venturi S, Venturi M. Iodide, thyroid and stomach carcinogenesis: evolutionary story of a primitive antioxidant? *Eur J Endocrinol* 1999;140 (4):371–372.
- [66] Küpper FC, Gaquerel E, Boneberg E-M, Morath S, Salaün J-P, Potin P. Early events in the perception of lipopolysaccharides in the brown alga *Laminaria digitata* include an oxidative burst and activation of fatty acid oxidation cascades. *J Exp Bot* 2006;57: 1991–1999.
- [67] Küpper FC, Gaquerel E, Cosse A, Adas F, Peters AF, Müller DG, Kloareg B, Salaün JP, Potin P. Free fatty acids and methyl jasmonate trigger defense reactions in *Laminaria digitata*. *Plant and Cell Physiology* 2009;50 (4):789–800.
- [68] Küpper FC, Kloareg B, Guern J, Potin P. Oligoguluronates elicit an oxidative burst in the brown algal kelp *Laminaria digitata*. *Plant Physiol* 2001;125:278–291.
- [69] Küpper FC, Müller DG, Peters AF, Kloareg B, Potin P. Oligoalginatate recognition and oxidative burst play a key role in natural and induced resistance of the sporophytes of *Laminariales*. *J Chem Ecol* 2002;28:2057–2081.
- [70] Küpper FC, Carpenter LJ, Leblanc C, Toyama C, Uchida Y, Verhaeghe E, Malin G, Luther GW III, Kroneck PM, Kloareg B, Meyer-Klaucke W, Muramatsu Y, Megson IL, Potin P, Feiters MC. Speciation studies and antioxidant properties of bromine in *Laminaria digitata* reinforce the significance of iodine accumulation for kelps. *J Exp Bot* 2013;64 (10):2653–2664.
- [71] Hou XL, Yan XJ, Chai CF. Chemical species of iodine in some seaweeds II. Iodine-bound biological macromolecules. *J Radioanal Nucl Chem* 2000;245 (3):461–467.

- [72] Hou XL, Dahlggaard H, Nielsen SP, Ding W. Iodine-129 in human thyroids and seaweed in China. *Sci Total Environ* 2000;246 (2–3):285–291.
- [73] Hou XL, Dahlggaard H, Nielsen SP. Iodine-129 time series in Danish, Norwegian and northwest Greenland coast and the Baltic Sea by seaweed. *Estuar Coast Shelf Sci* 2000;51 (5):571–584.
- [74] Hou XL, Hansen V, Aldahan A, Possnert G, Lind OC, Lujanienė G. A review on speciation of iodine-129 in the environmental and biological samples. *Anal Chim Acta* 2009;632 (2):181–196.
- [75] Manley SL, Lowe CG. Canopy-forming kelps as California's coastal dosimeter: I-131 from damaged Japanese reactor measured in *Macrocystis pyrifera*. *Environ Sci Technol* 2012;46 (7):3731–3736.
- [76] Shimura H, Itoh K, Sugiyama A, Ichijo S, Ichijo M, Furuya F, Nakamura Y, Kitahara K, Kobayashi K, Yukawa Y, Kobayashi T. Absorption of radionuclides from the Fukushima nuclear accident by a novel algal strain. *PLoS One* 2012;7 (9):e44200.
- [77] Cock JM, Sterck L, Rouzé P, Scornet D, Allen AE, Amoutzias G, Anthouard V, Artiguenave F, Aury JM, Badger JH, Beszteri B, Billiau K, Bonnet E, Bothwell JH, Bowler C, Boyen C, Brownlee C, Carrano CJ, Charrier B, Cho GY, Coelho SM, Collén J, Corre E, Da Silva C, Delage L, Delaroque N, Dittami SM, Doulbeau S, Elias M, Farnham G, Gachon CM, Gschloessl B, Heesch S, Jabbari K, Jubin C, Kawai H, Kimura K, Kloareg B, Küpper FC, Lang D, Le Bail A, Leblanc C, Lerouge P, Lohr M, Lopez PJ, Martens C, Maumus F, Michel G, Miranda-Saavedra D, Morales J, Moreau H, Motomura T, Nagasato C, Napoli CA, Nelson DR, Nyvall-Collén P, Peters AF, Pommier C, Potin P, Poulain J, Quesneville H, Read B, Rensing SA, Ritter A, Rousvoal S, Samanta M, Samson G, Schroeder DC, Séguens B, Strittmatter M, Tonon T, Tregear JW, Valentin K, von Dassow P, Yamagishi T, Van de Peer Y, Wincker P. The *Ectocarpus* genome and the independent evolution of multicellularity in the brown algae. *Nature* 2010;465:617–621.
- [78] Chance R, Baker AR, Küpper FC, Hughes C, Kloareg B, Malin G. Release and transformations of inorganic iodine by marine macroalgae. *Estuar Coast Shelf Sci* 2009;82:406–414.
- [79] Carpenter LJ, Malin G, Küpper FC, Liss PS. Novel biogenic iodine-containing trihalomethanes and other short-lived halocarbons in the coastal East Atlantic. *Global Biogeochem Cy* 2000;14:1191–1204.
- [80] Iwamoto K, Shiraiwa Y. Characterization of intracellular iodine accumulation by iodine-tolerant microalgae. In: Watanabe MM, Kaya K, editors. *Innovative Researches on Algal Biomass*. Amsterdam: Elsevier Science Bv; 2012. p 34–42.
- [81] van Bergeijk SA, Hernandez Javier L. Uptake of iodide in the marine haptophyte *Isochrysis* sp. (T.ISO) driven by iodide oxidation. *J Phycol* 2013;49:640–647.
- [82] Chance R, Malin G, Jickells T, Baker AR. Reduction of iodate to iodide by cold water diatom cultures. *Mar Chem* 2007;105 (1–2):169–180.
- [83] Chance R, Weston K, Baker AR, Hughes C, Malin G, Carpenter L, Meredith MP, Clarke A, Jickells TD, Mann P, Rossetti H. Seasonal and interannual variation of dissolved iodine speciation at a coastal Antarctic site. *Mar Chem* 2010;118 (3–4):171–181.
- [84] Waite TJ, Truesdale VW. Iodate reduction by *Isochrysis galbana* is relatively insensitive to de-activation of nitrate reductase activity—are phytoplankton really responsible for iodate reduction in seawater? *Mar Chem* 2003;81 (3–4):137–148.
- [85] Truesdale VW, Kennedy H, Agusti S, Waite TJ. On the relative constancy of iodate and total-iodine concentrations accompanying phytoplankton blooms initiated in mesocosm experiments in Antarctica. *Limnol Oceanogr* 2003;48 (4):1569–1574.

- [86] Lovelock J. Natural halocarbons in the air and in the sea. *Nature* 1975;256:193–194.
- [87] Alicke B, Hebestreit K, Stutz J, Platt U. Iodine oxide in the marine boundary layer. *Nature* 1999;397:572–573.
- [88] O'Dowd CD, Jimenez JL, Bahreini R, Flagan RC, Seinfeld JH, Hämeri K, Pirjola L, Kulmala M, Jennings SG, Hoffmann T. Marine aerosol formation from biogenic iodine emissions. *Nature*. 2002;417:632–636.
- [89] Palmer CJ, Anders TL, Carpenter LJ, Küpper FC, McFiggans GB. Iodine and halo-carbon response of *Laminaria digitata* to oxidative stress and links to atmospheric new particle production. *Environ Chem* 2005;2:282–290.
- [90] Huang RJ, Seitz K, Neary T, O'Dowd CD, Platt U, Hoffmann T. Observations of high concentrations of I-2 and IO in coastal air supporting iodine-oxide driven coastal new particle formation. *Geophys Res Lett* 2010;37:L03803.
- [91] Dixneuf S, Ruth AA, Vaughan S, Varma RM, Orphal J. The time dependence of molecular iodine emission from *Laminaria digitata*. *Atmos Chem Phys* 2009;9 (3):823–829.
- [92] Ashu-Ayem ER, Nitschke U, Monahan C, Chen J, Darby SB, Smith PD, Dowd CDO, Stengel DB, Venables DS. Coastal iodine emissions. 1. Release of I-2 by *Laminaria digitata* in chamber experiments. *Environ Sci Technol* 2012;46 (19):10413–10421.
- [93] Monahan C, Ashu-Ayem ER, Nitschke U, Darby SB, Smith PD, Stengel DB, Venables DS, Dowd CDO. Coastal iodine emissions: part 2. Chamber experiments of particle formation from *Laminaria digitata*-derived and laboratory-generated I-2. *Environ Sci Technol* 2012;46 (19):10422–10428.
- [94] Nitschke U, Ruth AA, Dixneuf S, Stengel DB. Molecular iodine emission rates and photosynthetic performance of different thallus parts of *Laminaria digitata* (Phaeophyceae) during emersion. *Planta* 2011;233 (4):737–748.
- [95] Ball SM, Hollingsworth AM, Humbles J, Leblanc C, Potin P, McFiggans G. Spectroscopic studies of molecular iodine emitted into the gas phase by seaweed. *Atmos Chem Phys* 2010;10 (13):6237–6254.
- [96] Bale CSE, Ingham T, Commane R, Heard DE, Bloss WJ. Novel measurements of atmospheric iodine species by resonance fluorescence. *J Atmos Chem* 2008;60 (1):51–70.
- [97] Kundel M, Thorenz UR, Petersen JH, Huang RJ, Bings NH, Hoffmann T. Application of mass spectrometric techniques for the trace analysis of short-lived iodine-containing volatiles emitted by seaweed. *Anal Bioanal Chem* 2012;402 (10):3345–3357.
- [98] Hoffmann T, Huang RJ, Kalberer M. Atmospheric analytical chemistry. *Anal Chem* 2011;83 (12):4649–4664.
- [99] Huang RJ, Hoffmann T. Development of a coupled diffusion denuder system combined with gas chromatography/mass spectrometry for the separation and quantification of molecular iodine and the activated iodine compounds iodine monochloride and hypoiodous acid in the marine atmosphere. *Anal Chem* 2009;81 (5):1777–1783.
- [100] Huang RJ, Hou XL, Hoffmann T. Extensive evaluation of a diffusion denuder technique for the quantification of atmospheric stable and radioactive molecular iodine. *Environ Sci Technol* 2010;44 (13):5061–6.
- [101] Kundel M, Huang RJ, Thorenz UR, Bosle J, Mann MJD, Ries M, Hoffmann T. Application of time-of-flight aerosol mass spectrometry for the online measurement of gaseous molecular iodine. *Anal Chem* 2012;84 (3):1439–1445.
- [102] Huang RJ, Seitz K, Buxmann J, Poehler D, Hornsby KE, Carpenter LJ, Platt U, Hoffmann T. In situ measurements of molecular iodine in the marine boundary layer: the

- link to macroalgae and the implications for O-3, IO, OIO and NO_x. *Atmos Chem Phys* 2010;10 (10):4823–4833.
- [103] Huang RJ, Thorenz UR, Kundel M, Venables DS, Ceburnis D, Ho KF, Nitschke U, Stengel DB. The seaweeds *Fucus vesiculosus* and *Ascophyllum nodosum* are significant contributors to coastal iodine emissions. *Atmos Chem Phys*. 2013;13:5255–5264.
- [104] Smyth PPA, Burns R, Huang RJ, Hoffman T, Mullan K, Graham U, Seitz K, Platt U, O'Dowd C. Does iodine gas released from seaweed contribute to dietary iodine intake? *Environ Geochem Health* 2011;33 (4):389–397.
- [105] Atkinson HM, Huang RJ, Chance R, Roscoe HK, Hughes C, Davison B, Schonhardt A, Mahajan AS, Saiz-Lopez A. Iodine emissions from the sea ice of the Weddell Sea. *Atmos Chem Phys* 2012;12 (22):11229–11244.
- [106] Hughes C, Franklin DJ, Malin G. Iodomethane production by two important marine cyanobacteria: *Prochlorococcus marinus* (CCMP 2389) and *Synechococcus* sp. (CCMP 2370). *Mar Chem* 2011;125 (1–4):19–25.
- [107] Hughes C, Malin G, Nightingale PD, Liss PS. The effect of light stress on the release of volatile iodocarbons by three species of marine microalgae. *Limnol Oceanogr* 2006;51 (6):2849–54.
- [108] Hughes C, Malin G, Turley CM, Keely BJ, Nightingale PD. The production of volatile iodocarbons by biogenic marine aggregates. *Limnology and Oceanography* 2008;53 (2):867–872.
- [109] Amachi S. Microbial contribution to global iodine cycling: volatilization, accumulation, reduction, oxidation, and sorption of iodine. *Microb Environ* 2008;23 (4):269–276.
- [110] Gozlan RS, Margalith P. Iodide oxidation by *Pseudomonas* iodooxidans. *J Appl Bacteriol* 1974;37 (4):493–499.
- [111] Amachi S, Muramatsu Y, Akiyama Y, Miyazaki K, Yoshiki S, Hanada S, Kamagata Y, Ban-nai T, Shinoyama H, Fujii T. Isolation of iodide-oxidizing bacteria from iodide-rich natural gas brines and seawaters. *Microb Ecol* 2005;49:547–557.
- [112] Arakawa Y, Akiyama Y, Furukawa H, Suda W, Amachi S. Growth stimulation of iodide-oxidizing alpha-proteobacteria in iodide-rich environments. *Microb Ecol* 2012;63 (3):522–531.
- [113] Seki M, Oikawa J, Taguchi T, Ohnuki T, Muramatsu Y, Sakamoto K, Amachi S. Laccase-catalyzed oxidation of iodide and formation of organically bound iodine in soils. *Environ Sci Technol* 2013;47 (1):390–397.
- [114] Tsunogai S, Sase T. Formation of iodide-iodine in the ocean. *Deep-Sea Res* 1969;16: 489–496.
- [115] Amachi S, Kawaguchi N, Muramatsu Y, Tsuchiya S, Watanabe Y, Shinoyama H, Fujii T. Dissimilatory iodate reduction by marine *Pseudomonas* sp. strain SCT. *Appl Environ Microbiol* 2007;73 (18):5725–5730.
- [116] Amachi S, Minami K, Miyasaka I, Fukunaga S. Ability of anaerobic microorganisms to associate with iodine: I-125 tracer experiments using laboratory strains and enriched microbial communities from subsurface formation water. *Chemosphere* 2010;79 (4):349–354.
- [117] Amachi S, Kamagata Y, Kanagawa T, Muramatsu Y. Bacteria mediate methylation of iodine in marine and terrestrial environments. *Appl Environ Microbiol* 2001;67 (6): 2718–2722.
- [118] Amachi S, Kasahara M, Hanada S, Kamagata Y, Shinoyama H, Fujii T, Muramatsu Y. Microbial participation in iodine volatilization from soils. *Environ Sci Technol* 2003;37 (17):3885–3890.

- [119] Muramatsu Y, Yoshida S. Effects of microorganisms on the fate of iodine in the soil environment. *Geomicrobiol J* 1999;16 (1):85–93.
- [120] Amachi S, Kimura K, Muramatsu Y, Shinoyama H, Fujii T. Hydrogen peroxide-dependent uptake of iodine by marine Flavobacteriaceae bacterium strain C-21. *Appl Environ Microbiol* 2007;73 (23):7536–7541.
- [121] Amachi S, Mishima Y, Shinoyama H, Muramatsu Y, Fujii T. Active transport and accumulation of iodide by newly isolated marine bacteria. *Appl Environ Microbiol* 2005;71 (2):741–745.
- [122] Dembitsky V. Biogenic iodine and iodine-containing metabolites. *Nat Prod Commun* 2006;1 (2):139–175.
- [123] Baumann E. Ueber das normale Vorkommen von Jod im Thierkörper. (I. Mittheilung). *Z Phys Chem* 1895–1896;21:319–330.
- [124] Ramachandran LK. Protein-iodine interaction. *Chem Rev* 1956;56:199–218.
- [125] Tepper A, Bubacco L, Canters GW. Structural basis and mechanism of the inhibition of the type-3 copper protein tyrosinase from *Streptomyces antibioticus* by halide ions. *J Biol Chem* 2002;277 (34):30436–30444.
- [126] Solomon EI, Penfield KW, Wilcox DE. Active-sites in copper proteins an electronic-structure overview. *Struct Bonding*. 1983;53:2–57.
- [127] Valentine JS, Pantoliano MW. Protein-metal ion interactions in cuprozinc protein (Superoxide dismutase)—a major intracellular repository for copper and zinc in the eukaryotic cell. In: Spiro TG, editor. *Copper Proteins*. New York, Chichester, Brisbane, Toronto, Singapore: Wiley & Sons; 1981. p 291–358.
- [128] Solomon EI. Binuclear copper active site—hemocyanin, tyrosinase and type 3 copper oxidases. In: Spiro TG, editor. *Copper Proteins*. New York, Chichester, Brisbane, Toronto, Singapore: Wiley & Sons; 1981. p 41–108.
- [129] Cass AEG, Hill HAO, Hasemann V, Johansen JT. H-1 nuclear magnetic-resonance spectroscopy of yeast copper-zinc superoxidase-dismutase—structural homology with the bovine enzyme. *Carlsberg Res Commun* 1978;43 (6):439–449.
- [130] Rigo A, Stevanato R, Viglino P, Rotilio G. Competitive inhibition of Cu, Zn superoxide-dismutase by monovalent anions. *Biochem Biophys Res Commun* 1977;79 (3):776–783.
- [131] Zumft WG, Kroneck PMH. Respiratory transformation of nitrous oxide (N(2)O) to dinitrogen by Bacteria and Archaea. In: Poole RK, editor. *Advances in Microbial Physiology*. Volume 52, London: Academic Press Ltd-Elsevier Science Ltd; 2007. p 107–227.
- [132] Wust A, Schneider L, Pomowski A, Zumft WG, Kroneck PMH, Einsle O. Nature's way of handling a greenhouse gas: the copper-sulfur cluster of purple nitrous oxide reductase. *Biol Chem* 2012;393 (10):1067–1077.
- [133] Neese F. *Electronic structure and spectroscopy of novel copper chromophores in biology*. Konstanz: Universität Konstanz; 1997.
- [134] Dooley DM, Alvarez ML, Rosenzweig AC, Hollis RS, Zumft WG. Exogenous ligand binding to *Pseudomonas stutzeri* nitrous oxide reductase. *Inorg Chim Acta* 1996;242 (1–2):239–244.
- [135] Paraskevopoulos K, Antonyuk SV, Sawers RG, Eady RR, Hasnain SS. Insight into catalysis of nitrous oxide reductase from high-resolution structures of resting and inhibitor-bound enzyme from *Achromobacter cycloclastes*. *J Mol Biol* 2006;362 (1):55–65.

- [136] Da Silva JAL, Fraústo da Silva JJR, Pombeiro AJL. Amavadin, a vanadium natural complex: its role and applications. *Coord Chem Rev* 2013;257 (15–16):2388–2400.
- [137] Rehder D. *Bioinorganic Vanadium Chemistry*. Chichester: John Wiley & Sons; 2008.
- [138] Kustin K, Pessoa JC, Crans DC. *Vanadium the Versatile Metal*. Washington: American Chemical Society; 2007.
- [139] Wever R, van der Horst MA. The role of vanadium haloperoxidases in the formation of volatile brominated compounds and their impact on the environment. *Dalton Trans* 2013;42:11778–11786.
- [140] Wever R. Structure and function of vanadium haloperoxidases. In: Michibata H, editor. *Vanadium—Biochemical and Molecular Biological Approaches*. Dordrecht, Heidelberg, London, New York: Springer; 2012. p 95–126.
- [141] Rehder D. A possible role for extraterrestrial vanadium in the encounter of life. *Coord Chem Rev* 2011;255 (19–20):2227–2231.
- [142] Plass W. Vanadium haloperoxidases as supramolecular hosts: synthetic and computational models. *Pure Appl Chem* 2009;81 (7):1229–1239.
- [143] Rehder D. The coordination chemistry of vanadium as related to its biological functions. *Coord Chem Rev* 1999;182:297–322.
- [144] Butler A. Acquisition and utilization of transition metal ions by marine organisms. *Science* 1998;281 (5374):207–210.
- [145] Lagerkvist BJ, Oskarsson A. Vanadium. In: Nordberg GF, Fowler BA, Nordberg M, Friberg L, editors. *Handbook on the Toxicology of Metals*. 3rd ed. San Diego: Academic Press; 2007. p 905–924.
- [146] Kitayama H, Yamamoto S, Michibata H, Ueki T. Metal ion selectivity of the vanadium(v)-reductase Vanabin2. *Dalton Trans* 2013;42:11921–11925.
- [147] Ueki T, Michibata H. Molecular mechanism of the transport and reduction pathway of vanadium in ascidians. *Coord Chem Rev* 2011;255 (19–20):2249–2257.
- [148] Ueki T, Kawakami N, Toshishige M, Matsuo K, Gekko K, Michibata H. Characterization of vanadium-binding sites of the vanadium-binding protein Vanabin2 by site-directed mutagenesis. *Biochim Biophys Acta-Gen Subj* 2009;1790 (10):1327–1333.
- [149] Hamada T, Asanuma M, Ueki T, Hayashi F, Kobayashi N, Yokoyama S, Michibata H, Hirota H. Solution structure of vanabin2, a vanadium(IV)-binding protein from the vanadium-rich ascidian *Ascidia sydneiensis samea*. *J Am Chem Soc* 2005;127 (12):4216–4222.
- [150] Fukui K, Ueki T, Ohya H, Michibata H. Vanadium-binding protein in a vanadium-rich ascidian *Ascidia sydneiensis samea*: CW and pulsed EPR studies. *J Am Chem Soc* 2003;125 (21):6352–6353.
- [151] Ueki T, Adachi T, Kawano S, Aoshima M, Yamaguchi N, Kanamori K, Michibata H. Vanadium-binding proteins (vanabins) from a vanadium-rich ascidian *Ascidia sydneiensis samea*. *Biochim Biophys Acta Gene Struct Expr* 2003;1626 (1–3):43–50.
- [152] Crans DC, Smee JJ, Gaidamauskas E, Yang LQ. The chemistry and biochemistry of vanadium and the biological activities exerted by vanadium compounds. *Chem Rev* 2004;104 (2):849–902.
- [153] Plass W. Phosphate and vanadate in biological systems: chemical relatives or more? *Angew Chem Int Ed* 1999;38 (7):909–912.
- [154] Chasteen ND. Vanadyl(IV) electron-nuclear double resonance/electron spin-echo envelope modulation spin probes. *Meth Enzymol* 1993;227:232–244.

- [155] De Boer E, Boon K, Wever R. EPR studies on conformational states and metal ion exchange properties of vanadium bromoperoxidase. *Biochemistry* 1988;27 (5):1629–1635.
- [156] Pooransingh-Margolis N, Renirie R, Hasan Z, Wever R, Vega AJ, Polenova T. V-51 solid-state magic angle spinning NMR spectroscopy of vanadium chloroperoxidase. *J Am Chem Soc* 2006;128 (15):5190–208.
- [157] Butler A, Walker JV. Marine haloperoxidases. *Chem Rev* 1993;93 (5):1937–1944.
- [158] Martinez JS, Carroll GL, Tschirret-Guth RA, Altenhoff G, Little RD, Butler A. On the regiospecificity of vanadium bromoperoxidase. *J Am Chem Soc* 2001;123 (14):3289–3294.
- [159] Wever R, Hemrika W. Vanadium haloperoxidases. In: Messerschmidt A, Hubert R, Poulos T, Wieghardt K, editors. *Handbook of Metalloproteins*. Chichester: John Wiley & Sons; 2001. p 1417–1428.
- [160] Messerschmidt A, Wever R. X-ray structure of a vanadium-containing enzyme: chloroperoxidase from the fungus *Curvularia inaequalis*. *Proc Natl Acad Sci U S A* 1996;93 (1):392–396.
- [161] Winter JM, Moore BS. Exploring the chemistry and biology of vanadium-dependent haloperoxidases. *J Biol Chem* 2009;284 (28):18577–18581.
- [162] Weyand M, Hecht HJ, Kiess M, Liaud MF, Vilter H, Schomburg D. X-ray structure determination of a vanadium-dependent haloperoxidase from *Ascophyllum nodosum* at 2.0 angstrom resolution. *J Mol Biol* 1999;293 (3):595–611.
- [163] Isupov MN, Dalby AR, Brindley AA, Izumi Y, Tanabe T, Murshudov GN, Littlechild JA. Crystal structure of dodecameric vanadium-dependent bromoperoxidase from the red algae *Corallina officinalis*. *J Mol Biol* 2000;299 (4):1035–1049.
- [164] Garcia-Rodriguez E, Ohshiro T, Aibara T, Izumi Y, Littlechild J. Enhancing effect of calcium and vanadium ions on thermal stability of bromoperoxidase from *Corallina pilulifera*. *J Biol Inorg Chem* 2005;10 (3):275–282.
- [165] de Macedo-Ribeiro S, Renirie R, Wever R, Messerschmidt A. Crystal structure of a trapped phosphate intermediate in vanadium apochloroperoxidase catalyzing a dephosphorylation reaction. *Biochemistry* 2008;47 (3):929–934.
- [166] Sleboznick C, Hamstra BJ, Pecoraro VL. Modeling the biological chemistry of vanadium: structural and reactivity studies elucidating biological function. In: Hill HAO, Sadler PJ, Thomson AJ, editors. *Metal Sites in Proteins and Models: Phosphatases, Lewis Acids and Vanadium*. Berlin: Springer-Verlag Berlin; 1997. p 51–108.
- [167] Dau H, Dittmer J, Eppele M, Hanss J, Kiss E, Rehder D, Schulzke C, Vilter H. Bromine K-edge EXAFS studies of bromide binding to bromoperoxidase from *Ascophyllum nodosum*. *FEBS Lett* 1999;457:237–240.
- [168] Rehder D, Schulzke C, Dau H, Meinke C, Hanss J, Eppele M. Water and bromide in the active center of vanadate-dependent haloperoxidases. *J Inorg Biochem* 2000;80 (1–2):115–121.
- [169] Feiters MC, Leblanc C, Küpper FC, Meyer-Klaucke W, Michel G, Potin P. Bromine is an endogenous component of a vanadium bromoperoxidase. *J Am Chem Soc* 2005;127 (44):15340–15341.
- [170] Butler A, Carter JN, Simpson MT. Vanadium in proteins and enzymes. In: Bertini I, Sigel A, Sigel H, editors. *Handbook on Metalloproteins*. New York: Marcel Dekker; 2001.
- [171] Butler A, Carter-Franklin JN. The role of vanadium bromoperoxidase in the biosynthesis of halogenated marine natural products. *Nat Prod Rep* 2004;21 (1):180–188.

- [172] Messerschmidt A, Prade L, Wever R. Implications for the catalytic mechanism of the vanadium-containing enzyme chloroperoxidase from the fungus *Curvularia inaequalis* by X-ray structures of the native and peroxide form. *Biol Chem* 1997;378 (3–4):309–315.
- [173] Christmann U, Dau H, Haumann M, Kiss E, Liebisch P, Rehder D, Santoni G, Schulzke C. Substrate binding to vanadate-dependent bromoperoxidase from *Ascophyllum nodosum*: a vanadium K-edge XAS approach. *Dalton Trans* 2004;16:2534–2540.
- [174] Dauter Z, Dauter M. Entering a new phase: using solvent halide ions in protein structure determination. *Structure* 2001;9 (2):R21–R26.
- [175] Littlechild J, Rodriguez EG, Isupov M. Vanadium containing bromoperoxidase—insights into the enzymatic mechanism using X-ray crystallography. *J Inorg Biochem* 2009;103 (4):617–621.
- [176] Soedjak HS, Walker JV, Butler A. Inhibition and inactivation of vanadium bromoperoxidase by the substrate hydrogen peroxide and further mechanistic studies. *Biochemistry* 1995;34 (39):12689–12696.
- [177] Tanaka N, Hasan Z, Wever R. Kinetic characterization of active site mutants Ser402Ala and Phe397His of vanadium chloroperoxidase from the fungus *Curvularia inaequalis*. *Inorg Chim Acta* 2003;356:288–296.
- [178] Hille R. Molybdenum and tungsten in biology. *Trends BiochemSci* 2002;27 (7):360–367.
- [179] Johnson MK, Rees DC, Adams MWW. Tungstoenzymes. *Chem Rev* 1996;96 (7):2817–2839.
- [180] Kletzin A, Adams MWW. Tungsten in biological systems. *Fems Microbiol Rev* 1996;18 (1):5–63.

ATMOSPHERIC CHEMISTRY OF IODINE

LUCY J. CARPENTER

Wolfson Atmospheric Chemistry Laboratories, University of York, Heslington, York, UK

The ubiquitous presence of iodine in marine air and aerosol particles has been known since the early 1970s [1, 2]. Photooxidation of gaseous iodine species in air to soluble inorganic products allows a significant fraction of emitted iodine to partition to the aerosol phase, which is eventually removed by wet or dry deposition to the land or ocean. In fact, marine aerosol particles are generally enriched in iodine by two to three orders of magnitude compared to concentrations in seawater [3, 4]. Thus sea salt aerosol is a net sink of gaseous iodine (in contrast, it represents the main source of chlorine and bromine in the marine boundary layer), though it plays an important role in recycling gas-phase iodine. The cycle provides a vital route for terrestrial uptake of iodine, an essential component of mammalian health.

Of the few Tg year^{-1} of iodine believed to be emitted to the atmosphere, it is clear that the majority comes from the ocean. Anthropogenic release of atmospheric iodine is believed to be negligible, although methyl iodide (CH_3I) has been licensed as a pesticide in some countries as a replacement for the stratospheric ozone-destroying methyl bromide (CH_3Br). There is a small contribution to the CH_3I burden from natural land sources [5].

There are numerous biological pathways for production of volatile iodine compounds by marine ecosystems. These include methylation of iodine by marine microalgae (phytoplankton) [6] and by a wide variety of aerobic marine bacteria [7, 8], production of polyiodinated organic compounds from phytoplankton-containing haloperoxidase enzymes [9], and production from natural marine aggregates comprising a host of materials including phytoplankton and bacteria [10]. As a

consequence of these reactions, a large variety of volatile organic iodine compounds (VOIC) are emitted from marine algae and ecosystems [9, 11, 12]. Enhanced emissions have been found when algae are subject to high illumination [9, 12, 13]. In contrast, Hughes *et al.*, [14] found no effect of high light stress on iodocarbon release by three species of marine phytoplankton.

There is also evidence that nonbiological iodine sources are significant in the global inventory of iodine. CH_3I can be produced from sunlit irradiation of seawater [15, 5]. The suggested mechanism is photochemical generation of methyl and iodine radicals from, respectively, dissolved organic matter (DOM) and iodide present in the surface waters. Measurements in the North and tropical Atlantic have confirmed that surface saturation anomalies of CH_3I are correlated with light intensity and that the photochemical source of CH_3I is abiotic and suggest that this route can support at least half of the average sea-to-air flux [16, 17].

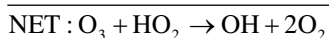
CH_3I is the most abundant organic iodine compound in the atmosphere [18], yet recent data suggest that other, more reactive oceanic organic iodine compounds such as CH_2ICl and CH_2I_2 also play a significant role. Both biological [19] and photochemical [20, 21] routes have been suggested for these dihalomethanes, in addition to production by macroalgae [22]. Dihalomethanes are estimated to contribute as much iodine globally as CH_3I and potentially two to four times the flux of I atoms from CH_3I in the lowest 200 m of the atmosphere due to their shorter atmospheric lifetimes [23]. Despite this, it seems that the additional presence of such compounds is not sufficient to explain the abundance of reactive iodine oxide (IO) radicals in the marine boundary layer. An additional source of iodine, some two to four times greater than that provided by iodine-containing mono- and dihalogenated alkanes, is required to reconcile models with observations [23–25]. An additional abiotic contribution to the atmospheric iodine budget could be the reaction of atmospheric O_3 deposited at the sea surface with iodide to evolve I_2 and HOI [26, 27]. Recent work suggests that this could be an efficient mechanism for iodine emission from the open ocean [28]. Table 33.1 compares atmospheric lifetimes of the most important iodine source gases.

Early model calculations of atmospheric iodine indicated that it was sufficiently abundant in the lower atmosphere to destroy significant quantities of ozone [34]. Tropospheric ozone is a greenhouse gas and at elevated concentrations a threat to human health and plant growth. Atmospheric iodine also perturbs the concentration ratios of NO_2/NO and OH/HO_2 [34], which are central to atmospheric oxidation

TABLE 33.1 Atmospheric lifetimes of volatile iodine source gases

Iodine species	Atmospheric lifetime in the lower troposphere	References
CH_3I	5–11 days	[5]; Ko and Poulet 2006; [29, 30]
CH_2ICl	0.1 days	[31, 30]
CH_2I_2	2–10 min	[32, 30]
I_2	~10 s	[33]

processes. A key species in these chemical cycles is the IO radical. IO was suggested to arise predominantly from photodissociation of CH_3I to I atoms followed by rapid reaction with O_3 (R1), leading to catalytic cycles for O_3 loss [34]:



Despite significant additions and revisions to the atmospheric mechanisms and kinetics of iodine photochemistry and indeed to the strength and nature of iodine source gases, the major features of these early predictions have been borne out, as discussed later.

Observational evidence for the presence of IO was first reported at the coastal site of Mace Head, Ireland [35], and since then numerous studies have indicated that IO is ubiquitous in the lower atmosphere of kelp-rich coastlines, with reported levels up to approximately 50 parts per trillion by volume (pptv) [36, 37]. However, it has become clear that such coastal regions offer a unique iodine-rich environment through direct emissions of very reactive molecular iodine (I_2) from seaweed [33, 38, 39], which in the atmosphere breaks down rapidly by either photolysis or, at night, reaction with nitrate radicals [33], to give rise to I radicals and thus IO (reaction R1). It was long established that seaweeds, particularly kelps, emit VOIC (e.g., [40–42, 12]). More recently it has been shown that the inorganic iodide efflux leading to I_2 formation after an oxidative burst is some three orders of magnitude higher than organic iodine emissions [43]. Volatilization of I_2 from kelps exposed to air appear to explain the observations ([44, 45] and references therein) of coastal “bursts” of iodine-containing ultrafine aerosol particles at low tide during the day. Iodine oxide particles (IOPs) are thought to arise *via* the recombination reactions of IO and OIO (formed from the IO self-reaction and IO+BrO cross-reactions) to form higher oxides (R4a, R5, R6) followed by condensation of further species such as sulfuric acid [46–48] (Fig. 33.1).



Evidence of the ability of these IOPs to grow to the point of becoming cloud condensation nuclei (CCN) has been demonstrated by McFiggans et al. [49] who observed daytime low tide formation of ultrafine particles of IO at low tide near

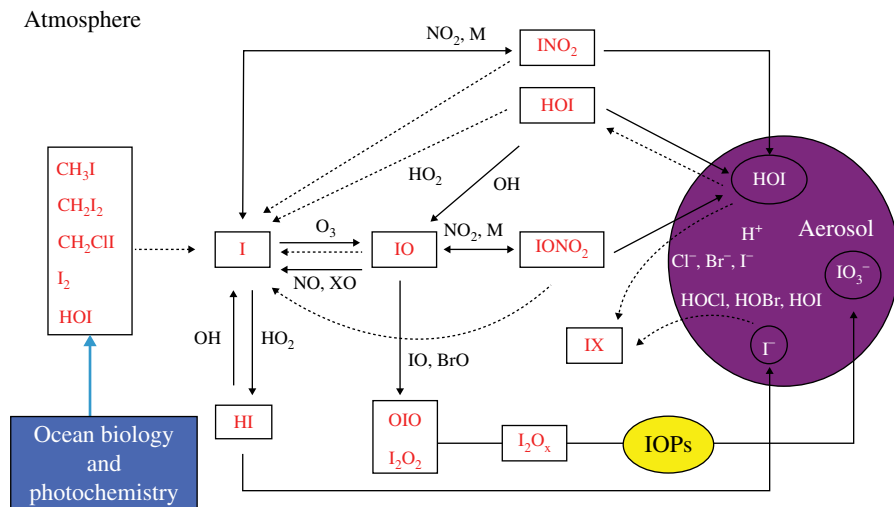


FIGURE 33.1 Simplified schematic of iodine photochemistry in the atmosphere. Lines represent photolysis, dotted lines illustrate phase equilibration from aerosol, X and Y are halogen atoms, and “IOPs” refers to iodine oxide particles.

Roscoff, France, with frequent associated increases in particle size to several tens of nanometer diameter, such that they would act as CCN at reasonable coastal supersaturations. It remains an open question as to whether the lower levels of iodine observed over the open ocean (see discussion later) are sufficient to form IOPs that survive long enough to grow through condensation and impact marine CCN.

Although strong links between iodine, new particles, and particle growth have now been established, the chemistry of the particle-forming higher oxides of iodine is poorly understood, in particular the branching of the IO self reaction and the fate of OIO [50, 51]: these reactions also impinge on the impact of iodine on gas-phase atmospheric chemistry. For comprehensive reviews on experimental data for reactions of iodine, the reader is referred to the 2003 special issue of *Chemical Reviews* on Atmospheric Chemistry ([52]), the “Halogens in the Troposphere” white paper (HiT) [53], and a second review of iodine in *Chemical Reviews* [54].

Measurements of IO have recently become available over the open ocean and/or in land-based locations representative of the open ocean environment, as shown in Table 33.2.

Typical maximum mixing ratios of 0.5–3 pptv IO in the lower troposphere suggest a global role for iodine chemistry. Indeed, it has been shown that observed ozone depletion in the tropical marine boundary layer cannot be explained in the absence of reactive halogen compounds [57]. The presence of reactive iodine species can activate the release of bromine and chlorine *via* heterogeneous reactions on sea-salt aerosol [61], and the combined presence of halogens in the marine environment acts synergistically to catalyze O_3 destruction, for example, via the cross-reaction of IO with BrO [62]. These reactions occur in addition to (R1–R3) and other O_3 -depleting

TABLE 33.2 Observations of IO in the troposphere over the open ocean using long-path (LP) and multi-axis (MAX) differential optical absorption spectroscopy (DOAS)

Location	Technique	Maximum mixing ratio ($\pm 2\sigma$)/ppt	References
Marine boundary layer, ship-based			
Western Pacific (2009)	MAX-DOAS	2.2 ± 0.5	[25]
Eastern Pacific (2010)	MAX-DOAS	0.9^a	[55]
Marine boundary layer, land-based			
Tenerife, Spain (1997)	LP-DOAS	3 ± 0.3	[56]
Cape Verde (2006–2007)	LP-DOAS	3.1 ± 0.4	[57]; [24]
Cape Verde (2010)	MAX-DOAS	1.5 ± 0.6	[58]
Marine boundary layer, aircraft			
Tropical Pacific (2010)	MAX-DOAS	0.5 ± 0.1	[59]
Free troposphere, land-based			
Tenerife, Spain (1997)	MAX-DOAS	0.4 ± 0.2	[60]
Free troposphere, aircraft			
Tropical Pacific (2010)	MAX-DOAS	0.1 ± 0.06	[59]

^aMaximum daily mean.

cycles including the self-reaction of IO (and in more polluted environments, the photolysis of iodine nitrate, IONO_2). The result is calculated to be a approximately 40% increase in photochemical O_3 destruction rates in the tropical marine boundary layer (compared to a hypothetical situation without halogens), with iodine responsible for about 2/3 of the halogen-related loss [57, 24].

Multi-axis (MAX) differential optical absorption spectroscopy (MAX-DOAS) measurements suggest IO mixing ratios of between 0.2 and 0.4 pptv in the north Atlantic free troposphere between 1 and 10 km [60] and approximately 0.1 pptv in the Pacific troposphere between 2 and 10 km [59], respectively. Such low levels of IO are challenging to retrieve accurately, but indicate that most of the IO vertical column is above the marine boundary layer ($\sim 10\times$ shallower than the overlying free troposphere). This is surprising since the majority of sources are very short-lived (Table 33.1) and could have implications for our understanding of iodine sources and/or the Ix ($\text{I} + \text{IO}$) lifetime with respect to irreversible uptake of reactive iodine to aerosol surfaces. Over the tropical tropospheric ozone column, Saiz-Lopez et al. [63] calculate an annually averaged depletion due to bromine and iodine of around 10% ozone, with largest effects in the middle to upper troposphere. Such ozone depletion is calculated to contribute about -0.10 W m^{-2} to the radiative flux at the tropical tropopause, which is significant for climate.

As discussed previously, the presence of iodine can also result in increased OH levels (e.g., through reactions (R2) and (R3)), which in turn affect the lifetime of methane with further implications for climate. Box models predict an instantaneous increase in surface (OH) of approximately 10% in the low- NO_x open ocean environment [57, 64]; however,

the integrated effects of halogens may actually have the opposite effect since formation of halogen nitrates accelerates the oxidation of NO_x ($\text{NO} + \text{NO}_2$). Keene et al. [65] calculated that the consequent lower NO_x concentrations coupled with direct reactions involving halogens yielded lower steady-state mixing ratios of OH and lower midday ratios of $\text{OH}:\text{HO}_2$ under a variety of NO_x regimes.

A surprising recent discovery is that significant quantities of IO are present in geographically diverse polar regions, even those remote from ocean sources, as observed from ground-based observations in both the Arctic and the Antarctic [66–69] and satellite observations of atmospheric columns of IO over Antarctica [70, 71]. Several pptv of IO was observed in the Antarctic spring and summer [67], and up to 3 pptv near Hudson Bay in the sub-Arctic during spring [69]. Complete destruction of O_3 by bromine chemistry during so-called “ozone-depletion events” (ODEs) is a regular feature of the polar lower troposphere in spring [72]. Due to strong chemical coupling with BrO, and the high abundance of bromine in the polar environment [73], even a few pptv of IO can amplify O_3 destruction [74, 69]. The presence of iodine is also suggested to enhance the oxidation of gaseous elemental mercury (Hg^0) to reactive gaseous mercury (Hg^{II}) [75, 67], which subsequently deposits to the snow pack, potentially leading to bioaccumulation of soluble and toxic forms of mercury.

As to polar iodine sources, recent Antarctic measurements suggest very high IO concentrations are present in snow interstitial air [68]. The initial source of iodine is postulated to be volatile organic compounds produced in the marginal ice zone (MIZ) and deposited to the snow pack during transport inland [68]. On the other hand, the observations of Mahajan et al. [69] indicate that the source of IO is the direct emission of iodine-containing compounds from leads formed in the ice. The occurrence of polynyas, open leads, and the MIZ is likely to increase as the Arctic sea ice continues to thin and retreat, which could enhance the rate of iodine flux to the polar atmosphere.

REFERENCES

- [1] Lovelock JE, Maggs RJ, Wade RJ. Halogenated hydrocarbons in and over the Atlantic. *Nature* 1973;241:194–196.
- [2] Moyers JL, Duce RA. Gaseous and particulate iodine in the marine atmosphere. *J Geophys Res* 1972;77:5229–5238.
- [3] Sturges WT, Barrie LA. Chlorine, bromine and iodine in Arctic aerosols. *Atmos Environ* 1988;22 (6):1179–1194.
- [4] Baker AR. Inorganic iodine speciation in tropical Atlantic aerosol. *Geophys Res Lett* 2004;31(23):L23S02. doi: 10.1029/2004GL020144.
- [5] Bell N, Hsu L, Jacob DJ, Schultz MG, Blake DR, Butler JH, King DB, Lobert JM, Maier-Reimer E. Methyl iodide: atmospheric budget and use as a tracer of marine convection in global models. *J Geophys Res* 2002;107 (D17):4340.
- [6] Itoh N, Tsujita M, Ando T, Hisatomi G, Higashi T. Formation and emission of monohalomethanes from marine algae. *Phytochemistry* 1997;45 (1):67–73.
- [7] Amachi S, Kamagata Y, Kanagawa T, Muramatsu Y. Bacteria mediate methylation of iodine in marine and terrestrial environments. *Appl Environ Microbiol* 2001;67:2718–2722.

- [8] Amachi S. Microbial contribution to global iodine cycling: volatilization, accumulation, reduction, oxidation, and sorption of iodine. *Microb Environ* 2008;23 (4):269–276.
- [9] Moore RM, Webb M, Tokarczyk R, Wever R. Bromoperoxidase and iodoperoxide enzymes and production of halogenated methanes in marine diatom cultures. *J Geophys Res* 1996;101:20899–20908.
- [10] Hughes C, Malin G, Turley CM, Keely BJ, Nightingale PD, Liss PS. The production of volatile iodocarbons by biogenic marine aggregates. *Limnol Oceanogr* 2008;53:867–872.
- [11] Laturnus F, Giese B, Wiencke C, Adams FC. Low-molecular-weight organoiodine and organobromine compounds released by polar macroalgae—the influence of abiotic factors. *Fres J Anal Chem* 2000;368 (2–3):297–302.
- [12] Carpenter LJ, Malin G, Liss PS, Kupper FC. Novel biogenic iodine-containing trihalo-methanes and other short-lived halocarbons in the coastal east Atlantic. *Global Biogeochem Cycles* 2000;14:1191–1204.
- [13] Laturnus F, Svensson T, Wiencke C, Öberg G. Ultraviolet radiation affects emission of ozone-depleting substances by marine macroalgae: results from a laboratory incubation study. *Environ Sci Technol* 2004;38:6605–6609.
- [14] Hughes C, Malin G, Nightingale P, Liss PS. The effect of light stress on the release of volatile iodocarbons by three species of marine phytoplankton. *Limnol Oceanogr* 2006;51:2849–2854.
- [15] Moore RM, Zafiriou OC. Photochemical production of methyl iodide in seawater. *J Geophys Res* 1994;99:16415–16420.
- [16] Happell JD, Wallace DWR. Methyl iodide in the Greenland/Norwegian Seas and the tropical Atlantic Ocean: evidence for photochemical production. *Geophys Res Lett* 1996;23:2105–2108.
- [17] Richter U, Wallace DWR. Production of methyl iodide in the tropical Atlantic Ocean. *Geophys Res Lett* 2004;31 (23):L23S03.
- [18] Carpenter LJ. Iodine in the marine boundary layer. *Chem Rev* 2003;103 (12):4953–4962.
- [19] Kurihara MK, Kimura M, Iwamoto Y, Narita Y, Ookai A, Eum Y-J, Tsuda A, Suzuki K, Tani Y, Yokouchi Y, Uematsu M, Hashimoto S. Distributions of short-lived iodocarbons and biogenic trace gases in the open ocean and atmosphere in the western North Pacific. *Mar Chem* 2010;118:156–170.
- [20] Carpenter LJ, Hopkins JR, Jones CE, Lewis AC, Parthipan R, Wevill DJ, Poissant L, Pilote M, Constant P. Abiotic source of CH₂I₂ and other reactive organic halogens in the sub-Arctic atmosphere? *Environ Sci Tech* 2005;39:8812–8816.
- [21] Martino M, Mills GP, Woeltjen J, Liss PS. A new source of volatile organoiodine compounds in surface seawater. *Geophys Res Lett* 2009;36:L01609.
- [22] Carpenter LJ, Sturges WT, Penkett SA, Liss PS, Alicke B, Hebestreit K, Platt U. Short-lived alkyl iodides and bromides at Mace Head, Ireland: links to biogenic sources and halogen oxide production. *J Geophys Res* 1999;104 (D1):1679–1689.
- [23] Jones CE, Hornsby KE, Sommariva R, Dunk RM, von Glasow R, McFiggans G, Carpenter LJ. Quantifying the contribution of marine organic gases to atmospheric iodine. *Geophys Res Lett* 2010;37:L18804. DOI: 10.1029/2010GL043990.
- [24] Mahajan AS, Plane JMC, Oetjen H, Mendes L, Saunders RW, Saiz-Lopez A, Jones CE, Carpenter LJ, McFiggans GB. Measurement and modelling of reactive halogen species over the tropical Atlantic Ocean. *Atmos Chem Phys* 2010a;10:4611–4624.

- [25] Großmann K, Frieß U, Peters E, Wittrock F, Lampel J, Yilmaz S, Tschritter J, Sommariva R, von Glasow R, Quack B, Krueger K, Pfeilsticker K, Platt U. Iodine monoxide in the Western Pacific marine boundary layer. *Atmos Chem Phys* 2013;13:3363–3378.
- [26] Garland JA, Elzerman AW, Penkett SA. The mechanism for dry deposition of ozone to seawater surfaces. *J Geophys Res* 1980;85:7488–7492.
- [27] Garland JA, Curtis H. Emission of iodine from the sea surface in the presence of ozone. *J Geophys Res* 1981;86:3183–3186.
- [28] Carpenter LJ, MacDonald SM, Shaw MD, Kumar R, Saunders RW, Parthipan R, Wilson J, Plane JMC. Atmospheric iodine levels influenced by sea surface emissions of inorganic iodine. *Nat Geosci* 2013;6:108–111. DOI: 10.1038/NGEO1687.
- [29] Youn D, Patten KO, Wuebbles DJ, Lee H, So C-W. Potential impact of iodinated replacement compounds CF₃I and CH₃I on atmospheric ozone: a three-dimensional modeling study. *Atmos Chem Phys* 2010;10:10129–10144. DOI: 10.5194/acp-10-10129-2010.
- [30] Ordóñez C, Lamarque J-F, Tilmes S, Kinnison DE, Atlas EL, Blake DR, Sousa Santos G, Brasseur G, Saiz-Lopez A. Bromine and iodine chemistry in a global chemistry-climate model: description and evaluation of very short-lived oceanic sources. *Atmos Chem Phys* 2012;12:1423–1447. DOI: 10.5194/acp-12-1423-2012.
- [31] Rattigan OV, Shallcross DE, Cox RA. UV absorption cross-sections and atmospheric photolysis rates for CF₃I, CH₃I, CH₂ICI and C₂H₅I. *J Chem Soc Faraday Trans* 1997; 93:2839.
- [32] Mössinger J, Shallcross DE, Cox RA. UV-VIS absorption cross-sections and atmospheric lifetimes of CH₂Br₂, CH₂I₂ and CH₂BrI. *J Chem Soc Faraday Trans* 1998;94:1391–1396.
- [33] Saiz-Lopez, A., and J. M. C. Plane (2004), Novel iodine chemistry in the marine boundary layer, *Geophys Res Lett*, 31, L04112
- [34] Chameides WL, Davis DD. Iodine: its possible role in tropospheric photochemistry. *J Geophys Res-Atm* 1980;85:7383–7398.
- [35] Alicke B, Hebestreit K, Stutz J, Platt U. Iodine oxide in the marine boundary layer. *Nature* 1999;397:572–573.
- [36] Wada R, Beames J, Orr-Ewing A. Measurement of IO radical concentrations in the marine boundary layer using a cavity ring-down spectrometer. *J Atmos Chem* 2007;58:69–87.
- [37] Whalley L, Furneaux K, Gravestock T, Atkinson H, Bale C, Ingham T, Bloss W, Heard D. Detection of iodine monoxide radicals in the marine boundary layer using laser induced fluorescence spectroscopy. *J Atmos Chem* 2007;58:19–39.
- [38] Palmer CJ et al. Iodine and halocarbon response of laminaria digitata to oxidative stress and links to atmospheric new particle production. *Environ Chem* 2005;2:282–290.
- [39] Dixneuf S, Ruth AA, Vaughan S, Varma RM, Orphal J. The time dependence of molecular iodine emission from Laminaria digitata. *Atmos Chem Phys* 2009;9:823–829.
- [40] Gschwend PM, McFarlane JK, Newman KA. Volatile halogenated organic compounds released to seawater from temperate marine macroalgae. *Science* 1985;227:1023–1035.
- [41] Manley SL, Dastoor MN. Methyl halide (CH₃X) production from the giant-kelp, *Macrocystis*, and estimates of global CH₃X production by kelp. *Limnol Oceanogr* 1987;32:709–715.
- [42] Nightingale PD, Malin G, Liss PS. Production of chloroform and other low-molecular-weight halocarbons by some species of macroalgae. *Limnol Oceanogr* 1995;40:680–689.
- [43] Küpper FC, Carpenter LJ, McFiggans GB, Palmer CJ, Waite TJ, Boneberg EM, Woitsch S, Weiller M, Abela R, Grolimund D, Potin P, Butler A, Luther GW 3rd, Kroneck PM,

- Meyer-Klaucke W, Feiters MC. Iodide accumulation provides kelp with an inorganic antioxidant impacting atmospheric chemistry. *Proc Natl Acad Sci U S A* 2008;105(19):6954–6958.
- [44] O'Dowd C, McFiggans G, Creasey DJ, Pirjola L, Hoell C, Smith MH, Allan BJ, Plane JMC, Heard DE, Lee JD, Pilling MJ, Kulmala M. On the photochemical production of new particles in the coastal boundary layer. *Geophys Res Lett* 1999;26:1707–1710.
- [45] O'Dowd CD, H'ameri K, M'akel'a JM, Pirjola L, Kulmala M, Jennings SG, Berresheim H, Hansson H-C, de Leeuw G, Kunz GJ, Allen AG, Hewitt CN, Jackson A, Viisanen Y, Hoffmann T. A dedicated study of new particle formation and fate in the coastal environment (PARFORCE): overview of objectives and achievements. *J Geophys Res* 2002;107:1–16. DOI: 10.1029/2001JD000555.
- [46] Burkholder JB, Curtius J, Ravishankara AR, Lovejoy ER. Laboratory studies of the homogeneous nucleation of iodine oxides. *Atmos Chem Phys* 2004;4:19–34.
- [47] Saunders RW, Plane JMC. Formation pathways and composition of iodine oxide ultra-fine particles. *Environ Chem* 2005;2:299–303.
- [48] Saunders RW, Plane JMC. Fractal growth modelling of I₂O₅ nanoparticles. *J Aerosol Sci* 2006;37:1737–1749.
- [49] McFiggans G, Bale CSE, Ball SM, Beames JM, Bloss WJ, Carpenter LJ, Dorsey J, Dunk R, Flynn MJ, Furneaux KL, Gallagher MW, Heard DE, Hollingsworth AM, Hornsby K, Ingham T, Jones CE, Jones RL, Kramer LJ, Langridge JM, Leblanc C, LeCrane JP, Lee JD, Leigh RJ, Longley I, Mahajan AS, Monks PS, Oetjen H, Orr-Ewing AJ, Plane JMC, Potin P, Shillings AJL, Thomas F, von Glasow R, Wada R, Whalley LK, Whitehead JD. Iodine-mediated coastal particle formation: an overview of the Reactive Halogens in the Marine Boundary Layer (RHaMBLe) Roscoff coastal study. *Atmos Chem Phys* 2010;10:2975–2999.
- [50] Gomez Martin JC, Ashworth SH, Mahajan AS, Plane JMC. Photochemistry of OIO: laboratory study and atmospheric implications. *Geophys Res Lett* 2009;36:Article Number: L09802.
- [51] Kaltsoyannis N, Plane JMC. Quantum chemical calculations on a selection of iodine-containing species (IO, OIO, IONO₂, (IO)₂, I₂O₃, I₂O₄ and I₂O₅) of importance in the atmosphere. *Phys Chem Chem Phys* 2008;10:1723–1733.
- [52] Rossi MJ. Heterogeneous reactions on salts. *Chem Rev* 2003;103:4823–4882.
- [53] von Glasow R, Platt U. Halogens in the troposphere—HitT, paper presented at EGU general assembly. Vienna: Geophysical Research Abs; 2005.
- [54] Saiz-Lopez A, Plane JMC, Baker A, Carpenter LJ, von Glasow R, Gomez-Martin JC, McFiggans G, Saunders RW. Atmospheric chemistry of iodine. *Chem Rev* 2012a;112(3):1773–1804.
- [55] Mahajan AS, Gomez Martin JC, Hay TD, Royer S-J, Yvon-Lewis S, Liu Y, Hu L, Prados-Roman C, Ordóñez C, Plane JMC, Saiz-Lopez A. Latitudinal distribution of reactive iodine in the Eastern Pacific and its link to open ocean sources. *Atmos Chem Phys* 2012;12:11609–11617.
- [56] Allan BJ, McFiggans G, Plane JMC, Coe H. Observations of iodine monoxide in the remote marine boundary layer. *J Geophys Res-Atm* 2000;105:14363–14369.
- [57] Read KA, Mahajan AS, Carpenter LJ, Evans MJ, Faria BV, Heard DE, Hopkins JR, Lee JD, Moller SJ, Lewis AC, Mendes L, McQuaid JB, Oetjen H, Saiz-Lopez A, Pilling MJ, Plane JM. Extensive halogen-mediated ozone destruction over the tropical Atlantic Ocean. *Nature* 2008;453:1232–1235.

- [58] Carpenter LJ, Fleming ZL, Read KA, Lee JD, Moller SJ, Hopkins J, Purvis R, Lewis AC, Müller K, Heinold B, Herrmann H, Wadinga Fomba K, van Pinxteren D, Müller C, Tegen I, Wiedensohler A, Müller T, Niedermeier N, Achterberg EP, Patey MD, Kozlova EA, Heimann M, Heard DE, Plane JMC, Mahajan A, Oetjen H, Ingham T, Stone D, Whalley L, Evans M, Pilling MJ, Leigh RJ, Monks PS, Karunaharan A, Vaughan S, Tschritter J, Pöhler D, Frieß U, Holla R, Mendes ML, Lopez H, Faria B, Manning AJ, Wallace DWR. Seasonal characteristics of tropical marine boundary layer air measured at the Cape Verde Atmospheric Observatory. *J Atmos Chem* 2010;67:87–140.
- [59] Dix B, Baidara S, Bresch JF, Hall SR, Schmidt KS, Wang S, Volkamer R. Detection of iodine monoxide in the tropical free troposphere. *Proc Natl Acad Sci U S A* 2013;110:2035–2040.
- [60] Puentedura O, Gil M, Saiz-Lopez A, Hay T, Navarro-Comas M, Gomez-Pelaez A, Cuevas E, Iglesias J, Gomez L. Iodine monoxide in the north subtropical free troposphere. *Atmos Chem Phys* 2012;12:4909–4921.
- [61] Vogt R, Sander R, Glasow RV, Crutzen PJ. Iodine chemistry and its role in halogen activation and ozone loss in the marine boundary layer: a model study. *J Atmos Chem* 1999;32:375–395.
- [62] Sander SP, Ravishankara AR, Golden DM, Kolb CE, Kurylo MJ, Molina MJ, Moortgat GK, Finlayson-Pitts BJ, Wine PH, Huie RE, Orkin VL. *Chemical Kinetics and Photochemical Data for Use in Atmospheric Studies, Evaluation Number 15*. Pasadena, CA: Jet Propulsion Laboratory; 2006.
- [63] Saiz-Lopez A, Lamarque JF, Kinnison DE, Tilmes S, Ordóñez C, Orlando JJ, Conley AJ, Plane JMC, Mahajan AS, Santos GS, Atlas EL, Blake DR, Sander SP, Schaubler S, Thompson AM, Brasseur G. Estimating the climate significance of halogen-driven ozone loss. *Atmos Chem Phys* 2012b;12:3939–3949.
- [64] Whalley LK, Furneaux KL, Goddard A, Lee JD, Mahajan A, Oetjen H, Read KA, Kaaden N, Carpenter LJ, Lewis AC, Plane JMC, Saltzman ES, Wiedensohler A, Heard DE. The chemistry of OH and HO₂ radicals in the boundary layer over the tropical Atlantic Ocean. *Atmos Chem Phys* 2010;10:1555–1576.
- [65] Keene WC, Long MS, Pszenny AAP, Sander R, Maben JR, Wall AJ, O'Halloran TL, Kerkweg A, Fischer EV, Schrems O. Latitudinal variation in the multiphase chemical processing of inorganic halogens and related species over the eastern North and South Atlantic Oceans. *Atmos Chem Phys* 2009;9:7361–7385.
- [66] Frieß U, Wagner T, Pundt I, Pfeilsticker K, Platt U. Spectroscopic measurements of tropospheric iodine oxide at neumayer station, Antarctica. *Geophys Res Lett* 2001;28:1941–1944.
- [67] Saiz-Lopez A, Mahajan AS, Salmon RA, Bauguitte SJB, Jones AE, Roscoe HK, Plane JMC. Boundary layer halogens in coastal Antarctica. *Science* 2007a;317:348–351.
- [68] Frieß U, Deutschmann T, Gilfedder BS, Weller R, Platt U. Iodine monoxide in the Antarctic snowpack. *Atmos Chem Phys* 2010;10:2439–2456.
- [69] Mahajan AS, Shaw M, Oetjen H, Hornsby KE, Carpenter LJ, Kaleschke L, Tian-Kunze X, Lee JD, Moller SJ, Edwards P, Commane R, Ingham T, Heard DE, Plane JMC. Evidence of reactive iodine chemistry in the Arctic boundary layer. *J Geophys Res* 2010b;115:D20303. DOI: 10.1029/2009JD013665.
- [70] Saiz-Lopez A, Chance K, Liu X, Kurosu TP, Sander SP. First observations of iodine oxide from space. *Geophys Res Lett* 2007b;34:L12812.

- [71] Schönhardt A, Richter A, Wittrock F, Kirk H, Oetjen H, Roscoe HK, Burrows JP. Observations of iodine monoxide columns from satellite. *Atmos Chem Phys* 2008;8: 637–653.
- [72] Oltmans SJ, Schnell RC, Sheridan PJ, Peterson RE, Li SM, Winchester JW, Tans PP, Sturges WT, Kahl JD, Barrie LA. Seasonal surface ozone and filterable bromine relationship in the high Arctic. *Atmos Environ* 1989;23:2431–2441.
- [73] Simpson WR, von Glasow R, Riedel K, Anderson P, Ariya P, Bottenheim J, Burrows J, Carpenter LJ, Frieß U, Goodsite ME, Heard D, Hutterli M, Jacobi H-W, Kaleschke L, Neff B, Plane J, Platt U, Richter A, Roscoe H, Sander R, Shepson P, Sodeau J, Steffen A, Wagner T, Wolff E. Halogens and their role in polar boundary-layer ozone depletion. *Atmos Chem Phys* 2007;7:4375–4418.
- [74] Sander R, Vogt R, Harris GW, Crutzen PJ. Modeling the chemistry of ozone, halogen compounds and hydrocarbons in the arctic troposphere during spring. *Tellus* 1997;49B: 522–532.
- [75] Calvert JG, Lindberg SE. The potential influence of iodine-containing compounds on the chemistry of the troposphere in the polar spring. II. Mercury depletion. *Atmos Environ* 2004;38:5105–5116.

PART VII

RADIOISOTOPE OF IODINE

34

RADIOACTIVE IODINE

YOSHIFUMI SHIRAKAMI

Research Centre Nihon Medi-Physics, Co., Ltd., Sodegaura, Chiba, Japan

34.1 INTRODUCTION

On March 11, 2011, a massive earthquake (magnitude 9.0) occurred off the Pacific coast of the Tohoku region in Japan. About an hour later, an unimaginably powerful tsunami, with waves reaching heights of more than 10 m, swept the Pacific coast. The tsunami struck all four reactors of the Fukushima Dai-ichi Nuclear Power Station complex, which was located near the coastline, leading to a loss of control. As a result, huge amounts of radioactive iodine, primarily iodine-131 [^{131}I], and radioactive cesium, primarily cesium-137 [^{137}Cs], were released into the air and sea causing serious radioactive contamination. In the past, with major nuclear power plant accidents occurring in Three Mile Island in the United States in 1979 and Chernobyl in Ukraine (the former Soviet Union) in 1986, and recently with the Fukushima disaster, the world is once again reminded of the real dangers of contamination with radioactive materials, including radioactive iodine.

Radioactive iodine is associated with such risks, but can also be of great benefit when used for medical purposes. Radioactive iodine has been used in the field of medicine (nuclear medicine), as diagnostic and therapeutic radiopharmaceuticals and therapeutic medical devices, throughout the world. Diagnostic radiopharmaceuticals include iodine-123 [^{123}I] and compounds labeled with radionuclides such as technetium-99m [$^{99\text{m}}\text{Tc}$] and fluorine-18 [^{18}F]. These agents are administered orally or intravenously to perform imaging of localized radiation from radionuclides (gamma- and X-rays) from the outside of the body using a radiation detector (e.g., single photon emission computed tomography [SPECT] camera and positron



FIGURE 34.1 Clinical application of radioisotopes: Outline of nuclear medicine procedure. Step 1: Administration of a diagnostic radiopharmaceutical into the patient's body (left). Step 2: Obtain images of the internal distribution of radioactivity using a SPECT or PET camera (center). Step 3: Diagnosis by the doctor of the patient's condition based on the image (right).

emission tomography [PET] camera), and to diagnose a patient's condition based on abnormalities in the internal distribution of radioactivity (Fig. 34.1).

Therapeutic radiopharmaceuticals include compounds labeled with radioactive iodine isotopes such as iodine-125 [^{125}I] and iodine-131 [^{131}I], and compounds labeled with radionuclides such as strontium-89 [^{89}Sr] and yttrium-90 [^{90}Y]. Therapeutic radiopharmaceuticals are administered orally or intravenously to the body to treat lesions with internal radiation from localized radionuclides emitting alpha- and beta-particles, or gamma- and X-rays. As a medical device, iodine-125 seeds (iodine-125 on a silver compound sealed in a titanium capsule) have been used for internal radiation treatment of prostate cancer.

As a historical lesson, radioactive contamination containing radioactive iodine from the Fukushima Dai-ichi Nuclear Power Station accident will be discussed, followed by a description of the application of radioactive iodine to medicine as the focus of the chapter.

34.2 NUCLEAR POWER PLANT ACCIDENT AND RADIOACTIVE IODINE

In the Fukushima Dai-ichi Nuclear Power Station accident in 2011, a steam explosion occurred in reactor No. 4 on March 15, 4 days after the day of the earthquake and tsunami (March 11), which released large amounts of radioactive gases into the air. Most of the radioactive gases released from the plant were radioactive iodine-131 and radioactive cesium-137. Small amounts of radioactive cesium-134 (half-life: 2.07 years), radioactive krypton-85 (half-life: 10.76 years), and radioactive plutonium-239 (half-life: 24,100 years, mainly present in soil) were also detected. Several steam explosions also took place a few times before and after the aforementioned explosion, releasing radioactive gases into the atmosphere and likely contaminating the sea. Because large amounts of radioactive iodine-131, which is highly volatile, had accumulated in the reactors during operation as a result of nuclear fission, it was released into the atmosphere when the explosion occurred, forming radioactive plumes. Radioactive cesium-137 is also assumed to have been released into the atmosphere with radioactive iodine in the

TABLE 34.1 Estimation of the total amount of radioactivity released into the atmosphere after the nuclear power plant accident^a

Radionuclide	Fukushima accident	Chernobyl accident
Iodine-131 (a)	130,000TBq	1,800,000TBq
Cesium-137	11,000TBq	85,000TBq
Convert into iodine-131 ^a (b)	440,000TBq	3,400,000TBq
Total ^b (a)+(b)	570,000TBq	5,200,000TBq

^aData from the Nuclear Safety Commission of Japan (August 24, 2011).
^bFor convenience, the total amount of radioactivity was calculated by correcting the effect of each radionuclide on the human body based on the radioactivity of iodine-131. The sum of the radioactivity of iodine-131 (a) and the radioactivity of cesium-137 multiplied by 40 (b) is the total amount of radioactivity ((a)+(b)).

form of oxide and hydroxide particles. Radioactive plumes mainly spread to inland areas under the influence of weather and geographic conditions.

Radioactive iodine in the atmosphere descended to the ground with rain and flowed into rivers contaminating drinking water and milk. It also hit mountains, descended to the ground at the feet of the mountains, and adhered to farm crops, causing radioactive contamination of vegetables and tea leaves. Radioactive contamination was also observed in the Kanto region including Tokyo, Kanagawa, and Chiba, more than 200km away from the site of the accident in Fukushima. Radioactive contamination concentrated in some places due to wind direction, terrain, and rainfall, creating localized hot spots.

The total amount of radioactivity released in the environment from the Fukushima Dai-ichi Nuclear Power Station is estimated to be 570,000TBq (Table 34.1). Looking at individual radionuclides, the largest amount of radioactivity was from iodine-131 (130,000TBq), which was at least 10-fold more than the cesium-137 (11,000TBq), which ranked second. The total amount of radioactivity from the Fukushima Dai-ichi Nuclear Power Station is estimated to be approximately 1/10 of that from the Chernobyl accident. It is of note that radioactive iodine was the primary nuclide from which a largest amount of radiation was released in both accidents. Radioactive iodine is known to be easily incorporated into the body through respiration and can accumulate in high concentrations in the thyroid (see Section 34.6). The Chernobyl accident has shown that, if infants inhale radioactive iodine, they are at high risk for developing thyroid cancer. It is also known that the risk of exposure to radioactive iodine can be reduced substantially by using iodine preparations (e.g., potassium iodide tablets or syrup) as prophylaxis. If the anticipated iodine-131 radiation dose in infants is not less than 50mSv, administration of iodine preparations is recommended. However, it is extremely difficult to predict the risk of exposure to radioactive iodine-131 in an accident that may occur abruptly.

After the Fukushima accident, on March 12 and 13, the Nuclear Safety Commission of Japan proposed that the government instruct residents living near the plant to take iodine preparations; however, the Commission was unable to reach anyone in the disaster area due to the confusion and none of the residents were able to take iodine preparations. It was discovered later that the radiation exposure did not require

prophylaxis with iodine preparations. However, it would have been difficult to prove that the levels of radiation exposure to all infants were less than 50 mSv, and it would have been even more difficult to predict the risk of exposure in advance. Adults older than 40 years are at extremely low risk of developing thyroid cancer and therefore need not receive prophylaxis with the iodine preparations. After the Chernobyl accident, psychological damage to more than 1 million people posed a greater threat than radiation exposure. It is said that most damage was caused by harmful rumors. Therefore, good judgment should be used to determine whether to use iodine preparations, which may also serve as a tranquilizer, taking into consideration adverse reactions to these products, and the appropriate provision of instructions.

A nuclear power plant accident should not occur again. However, if an accident does occur and if radioactive iodine is released, appropriate measures should be taken immediately after the accident, and a preventative system including prior distribution of iodine preparations should be established. Fortunately, the half-life of radioactive iodine-131 is short (8.03 days); and, in fact, the release of radioactive iodine into the atmosphere in Fukushima was settled quickly, with the level of contamination of drinking water and milk returning to normal in approximately 1 month (4 half-lives). The half-life of cesium-137, which was also released into the atmosphere, conversely is much longer (30.1 years) and the effect of cesium-137 is anticipated to be prolonged for decades or hundreds of years.

34.3 PROPERTIES OF RADIOACTIVE IODINE

The four representative radioactive iodine isotopes are iodine-123 [¹²³I], iodine-124 [¹²⁴I], iodine-125 [¹²⁵I], and iodine-131 [¹³¹I] (Table 34.2). Iodine-125 and iodine-131 are by-products of nuclear reactors, and application of these isotopes to healthcare started immediately after reactors were made practical in the 1950s. Iodine-125 has a relatively long half-life (59.4 days) and emits a weak X-ray (27.5 keV). In the 1950s,

TABLE 34.2 Physical properties and medical uses of representative radioactive iodine isotopes

Isotope	Half-life	Decay mode (intensity)	Gamma- or X-ray energy (intensity)	Use	Production reaction
¹²³ I	13.3 h	EC (100%)	159 keV (87%)	Diagnosis	¹²⁴ Xe(p,2n) ¹²³ Cs → ¹²³ Xe → ¹²³ I
¹²⁴ I	4.2d	EC (78%) β ⁺ (22%) 1550 keV	511 keV (50%)	Diagnosis	¹²⁴ Te(p,2n) ¹²⁴ I
¹²⁵ I	59.4d	EC (100%)	27.5 keV (139%) 35 keV (7%)	RIA Therapy	¹²⁵ Xe(n,γ) ¹²⁵ Xe(EC) → ¹²⁵ I
¹³¹ I	8.03d	β ⁻ (100%), 608 keV	364 keV (83%) 637 keV (7%)	Diagnosis, Therapy	²³⁵ U fission product ¹³⁰ Te(n,γ) ¹³¹ Te(β ⁻) → ¹³¹ I

EC, electron capture; β⁺, positron emitter; β⁻, beta particle emitter; RIA, radioimmunoassay

Rosalyn S Yalow et al. developed the radioimmunoassay (RIA) using protein labeled with iodine-125, and were awarded the 1977 Nobel Prize in Physiology or Medicine for the development. At the time, the RIA was the most sensitive biochemical method and was widely used for the analysis of hormones that were present in trace amounts in vivo and for immune reaction assay using antigen–antibody interactions until recently. After 2000, the enzyme-linked immunosorbent assay (ELISA), which is more simple and rapid without the need for radioactivity, has replaced the RIA, thereby ending its use. Currently, iodine-125 is most frequently used for internal radiation therapy (brachytherapy) in the form of implantable medical devices in which it is enclosed.

Iodine-131 (half-life: 8.03 days, beta-decay) is a unique radioactive iodine isotope that is used for both diagnosis and therapy. It is easily created as a fission product of uranium-235 or by neutron bombardment of tellurium-130 in a reactor. Iodine-131 was the first radioactive iodine isotope used for imaging, but has been replaced by iodine-123 in the development of recent diagnostic agents because of its high-energy gamma-ray radiation (364 and 637 keV). Iodine-131, however, is useful as a therapeutic radiopharmaceutical because it emits both gamma-rays and beta particles. Sodium iodide [^{131}I] has been used for 60 years in the treatment of thyroid hyperfunction. Its principal beta emissions have an energy of 608 keV and have a range of 0.5–2 mm in human tissues. More recently, Iodine Tositumomab [^{131}I] has been approved in the United States in 2004 as the world's first pharmaceutical for radioimmunotherapy. Iodine Tositumomab [^{131}I] is a monoclonal antibody (MoAbs) drug labeled with iodine-131. The radionuclide iodine-131 is suitable for radioimmunotherapy because its half-life (8.03 days) is similar to the biological half-life of MoAbs in vivo.

Iodine-123 is one of the most commonly used radionuclides along with technetium-99m (half-life: 6.02 h, gamma-ray energy: 140 keV) as a radioactive diagnostic agent for SPECT because its half-life (13.3 h) and gamma-ray energy (159 keV) are suitable for SPECT imaging. Iodine-123 is obtained in a cyclotron via the nuclear reaction of ^{124}Xe (p, 2n) ^{123}I with high yields. Xenon-124, a starting material of this nuclear reaction, is one of the stable xenon isotopes that accounts for only 0.095% of natural xenon gas. In the 1980s, enriched xenon-124 gas (isotopic ratio: $\geq 95\%$) became available, which permitted the development of radiopharmaceuticals using iodine-123.

Because iodine-124 is a positron (β^+)-emitting radionuclide, it can be used in PET, which can provide higher-resolution images than SPECT. Iodine-124 is useful in investigating the pharmacokinetics of MoAbs with slow biological processes because of its relatively long half-life (4.2 days), although its positron emission rate (22%) is low. The medical use of iodine-124, however, is limited to research purposes because the exposure dose may be increased by its long half-life.

Radioactive elements that are suitable for nuclear medicine are limited by the decay mode, emitted gamma- or X-ray energy, gamma- or X-ray emission rate, and half-life. In addition to the radioactive iodine isotopes listed earlier, metallic elements such as gallium-67 [^{67}Ga], gallium-68 [^{68}Ga], strontium-89 [^{89}Sr], yttrium-90 [^{90}Y], technetium-99m [$^{99\text{m}}\text{Tc}$], indium-111 [^{111}In], and radium-223 [^{223}Ra] are commonly used. None of these elements are essential for the human body, as all are compounds foreign to the body. Of the halogen elements, fluorine, chloride, and iodine with the exception of bromine are essential elements or essential trace elements. Fluorine-18

[^{18}F] is one of the optimum nuclides for PET (β^+ decay, half-life: 110 min). PET was implemented rapidly after the late 1990s due to advances in the performance of PET cameras and the establishment of the fluorine-18 labeling technique. At present, there are only a few commercially available PET imaging agents representative of fluorine-18-fluorodeoxyglucose [^{18}F], which is indicated for the diagnosis of tumors; however, next-generation fluorine-18-labeled radiopharmaceuticals are now under development. Unfortunately, there are no radioactive chlorine or bromine isotopes that have physical properties suitable for nuclear medicine.

As previously described, (i) iodine can be safely administered to humans as a drug because it is an essential trace element for the human body, (ii) radioisotopes suitable for both SPECT (iodine-123) and PET (iodine-124) are available, and (iii) radioisotopes suitable for internal radiotherapy (iodine-125 and iodine-131) are available, showing that iodine is one of the elements that largely contribute to nuclear medicine. More than 15 products (pharmaceuticals and medical devices) labeled with or containing radioactive iodine are now commercially available worldwide, and new pharmaceuticals and medical devices using radioactive iodine are still being developed.

Commercial use of iodine-123-labeled radiopharmaceuticals started in the 1980s in Japan and Europe. Japan has the largest number of iodine-123-labeled products on its market because the half-life of iodine-123 (13.3 h) is suitable for nationwide delivery. Another reason is that there are no nuclear reactors dedicated for medical purposes in Japan, and iodine-123 can be produced in a cyclotron, which has been developed domestically. Conversely in the United States, commercial use of iodine-123 was delayed because of difficulty in delivering products with short half-lives throughout the large country, despite many iodine-123 radiopharmaceuticals having been discovered in the country. In the 2010s, Iobenguane [^{123}I] and Ioflupane [^{123}I] were finally launched in the United States for the following reasons: (i) radioactive iodine-labeled products were essential to more appropriately satisfy various medical needs, (ii) no alternative radionuclides were available, and (iii) a distribution system that covers all areas of the United States has been established, enabling delivery of products with short half-lives such as iodine-123 radiopharmaceuticals. Commercial use of iodine-131-labeled radiopharmaceuticals has long been the most successful in the United States partly because of its long half-life (8.03 days).

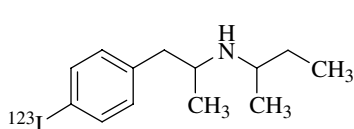
Radiation exposure of subjects is unavoidable in examinations using diagnostic radiopharmaceuticals. When an iodine-123-labeled radiopharmaceutical is administered intravenously at a standard dose (111–222 MBq), the internal radiation dose (effective dose) ranges from 0.5 to 2.2 mSv. The average annual natural radiation dose is 2.4 mSv (around the world), and the radiation dose per X-ray examination or computed tomography (CT) scan ranges from several to 10 mSv. That is, the radiation dose per radionuclide imaging is equivalent to or lower than that of the annual natural radiation dose or radiation dose per CT scan, suggesting that the health risk of radionuclide imaging is considerably low. To avoid unnecessary exposure, however, radionuclide imaging should be performed only when the benefit of diagnosis is considered to outweigh the risk of exposure. When a therapeutic radiopharmaceutical is to be used, the radiation dose to the lesion is naturally far higher (up to 1000 times) than the radiation dose for diagnosis, and

the treatment should also be performed only when the benefit of treatment is considered to outweigh the risk of exposure.

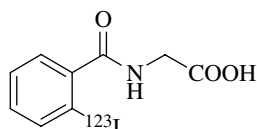
34.4 PHARMACEUTICALS AND MEDICAL DEVICES CONTAINING RADIOACTIVE IODINE

Sodium iodide [^{123}I] is the simplest, inorganic radiopharmaceutical containing radioactive iodine. Iodine is one of the essential trace elements, although its total amount in the human body (adult weighing 70 kg) is only 10–30 mg. Iodine, a chemical element that exists as iodide ions, is ingested via beverages and foods and localized mainly to the thyroid glands. Iodine and radioactive iodine ingested in the form of inorganic ions are eventually used for the synthesis of thyroid hormones, thyroxine, and triiodothyronine. Iodine is also known to be distributed in the brain, heart, mammary gland, and so on, in trace amounts, but there is uncertainty about its function.

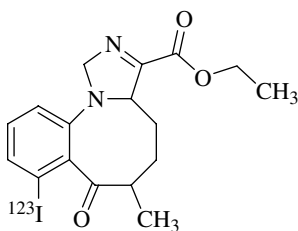
Figure 34.2 shows the chemical structures of representative organic radiopharmaceuticals containing radioactive iodine. What the compounds in Figure 34.2



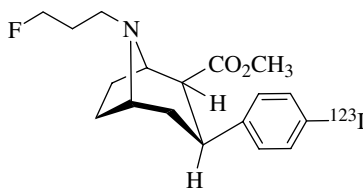
Iofetamine [^{123}I]
(Diagnosis of cerebrum blood flow disorders)



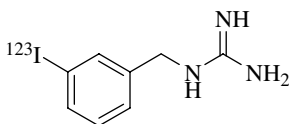
Iodhippurate [^{123}I]
(Diagnosis of kidney dysfunction)



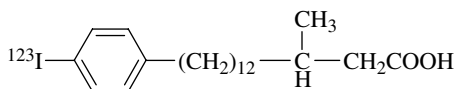
Iomazenil [^{123}I]
(Diagnosis of epilepsy)



Ioflupane [^{123}I]
(Diagnosis of Parkinson's disease)



Iobenguane [^{123}I]
(Diagnosis of heart failure)



BMIPP [^{123}I]
(Diagnosis of fatty acid metabolism
in myocardium)

FIGURE 34.2 Chemical structures and indications of pharmaceuticals containing radioactive iodine.

have in common is that they are labeled with radioactive iodine on the benzene ring. Pharmaceuticals labeled with radioactive iodine are often designed by imitating physiological compounds and known pharmaceuticals. For example, Iomazenil [^{123}I] is an analogue of the benzodiazepine receptor (BZR) antagonist flumazenil in which fluorine is replaced with iodine-123 on the benzene ring, beta-methyl-p-iodophenylpentadecanoic acid (BMIPP) [^{123}I] is an analogue of long-chain fatty acids represented by palmitic acid in which the iodine-123-labeled phenyl group is substituted at the omega end of the aliphatic side chain. There are several nonradioactive pharmaceuticals with iodine substitution such as anti-hyperthyroidism agents and CT contrast agents, but pharmaceuticals with substitution of halogen elements such as fluorine, chlorine, and bromine are more common, because iodine atoms are larger than those of other elements, which makes it slightly difficult to substitute for elements in physiological compounds without changing their original properties.

Of aliphatic carbon-halogen (C-X) bonds, the carbon-iodine (C-I) bond is weakest, unstable in vivo, and susceptible to enzymatic cleavage. In rare cases, free iodide ions in the body cause allergic reactions in patients with hypersensitivity to iodine, even in trace amounts. Iodine substitution of a pharmaceutical usually takes place on the benzene ring, where the C-I bond is stable. The optimum position of iodine substitution, that is, *ortho*, *meta*, or *para*, is determined by taking into account the lipid solubility, bioactivity, pharmacokinetics, and in vivo stability of each compound. For example, in the case of Iobenguane [^{123}I], iodine was easily eliminated from the drug in vivo when radioactive iodine substitution took place at the *ortho* or *para* position, whereas it was stable in vivo when the substitution took place at the *meta* position and, as a consequence, *m*-iodobenzylguanidine was selected for clinical application. In the case of BMIPP [^{123}I], the *para* position of the benzene ring was selected as the optimum labeling position at which myocardial cells recognize BMIPP [^{123}I] as fatty acid.

Radioactive iodine is also useful in labeling plasma proteins and MoAbs. Iodinated human serum albumin [^{131}I] for the measurement of circulating blood volume and Iodine Tositumomab [^{131}I] for the treatment of follicular lymphoma have been used in clinical practice. Radioactive iodine is substituted to a tyrosine residue (*meta* position on the benzene ring) in protein in the presence of oxidizing agents such as iodo-gen and *N*-chlorosuccinic acid.

In the field of medical devices, iodine-125 seeds (iodine-125 on a silver compound sealed in a titanium capsule measuring 5 mm in length and 1 mm in diameter) are commercially available for radiation therapy of prostate cancer. Usually, 60–80 iodine-125 seeds are implanted into the prostate of patients with prostate cancer using a special needle (permanent implantation). Low-energy-X-rays (27.5 keV) emitted by iodine-125 seeds are delivered to cancer cells. The X-rays travel only a short distance and do not affect surrounding normal tissues. Because this therapy, known as brachytherapy, does not require a laparotomy, patients can leave the hospital in 2 or 3 days and return to work shortly thereafter. Fewer adverse reactions and maintenance of sexual function are also major advantages of the brachytherapy.

34.5 LABELING REACTION OF PHARMACEUTICALS LABELED WITH RADIOACTIVE IODINE

The expiration dates of iodine-123-labeled pharmaceuticals are within 48 h of production because the half-life of iodine-123 is only 13.3 h. Therefore, iodine-123-labeled pharmaceuticals are manufactured at plants, delivered to hospitals the next morning, and used for patients' examinations in the morning of the same day. In other words, iodine-123-labeled pharmaceuticals are manufactured every day, and therefore the corresponding manufacturing methods should be as simple as possible.

Figure 34.3 shows an example of a radioactive iodine labeling reaction by the iodine-iodine isotope-exchange reaction. By this method, a compound having the benzene ring on which nonradioactive iodine has been substituted beforehand is labeled with radioactive iodine via the nucleophilic aromatic substitution through the addition of radioactive iodide ions to the compound in the presence of a copper ion catalyst (Fig. 34.3, top). In the case of Iofetamine [^{123}I], the desired compound can be obtained with a yield of about 90% by adding sodium iodide [^{123}I] using copper sulfate as a catalyst and allowing it to react at 200°C for 60 min (Fig. 34.3, bottom). This method is applicable only to thermostable products because it requires a relatively high temperature and sufficient reaction time. Because the method uses 1–10 mg of Iofetamine substituted by nonradioactive iodine as raw material, the nonradioactive iodine compound remains in the product after the reaction. (The raw material is chemically identical to the compound labeled with radioactive iodine and therefore cannot be separated.) Thus, it is difficult to obtain a radioactive iodine compound with high specific activity.

For this reason, a radioactive iodine substitution reaction using a precursor substituted by a leaving group (X) that would allow labeling under milder conditions was developed as shown in Figure 34.4 [1]. This method is used to add radioactive iodide ion [$^{123}\text{I}^-$] to a compound having the benzene ring substituted by X as the leaving group, allowing hydrated radioactive iodine cations [$^{123}\text{I}^+$] to form using an oxidizing agent, and labeling the compound with radioactive iodine via the electrophilic aromatic substitution reaction (Fig. 34.4, top). In the case of Ioflupane [^{123}I], the desired compound can be obtained by adding radioactive sodium iodide [^{123}I] to the trimethylstannyl-substituted

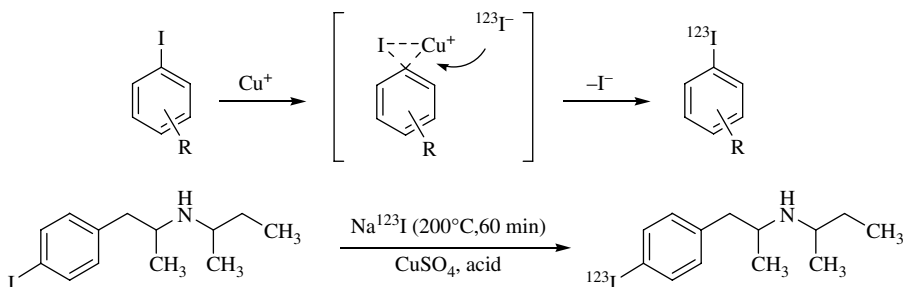


FIGURE 34.3 Nucleophilic aromatic substitution of radioactive iodine *via* the iodine-iodine isotope exchange reaction (top). Example of Iofetamine [^{123}I] labeling (bottom).

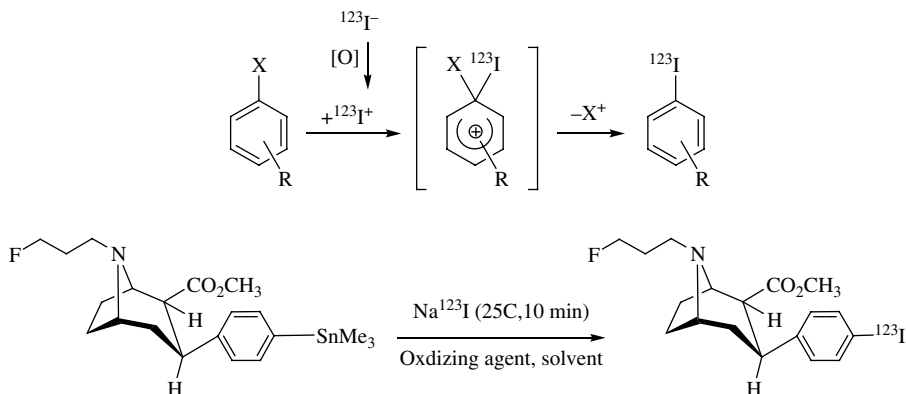


FIGURE 34.4 Electrophilic aromatic substitution reaction of radioactive iodine using a leaving group X substituted precursor (top). Example of Ioflupane [^{123}I] labeling (bottom).

precursor in the presence of an oxidizing agent and allowing it to react at room temperature for 10 min (Fig. 34.4, bottom). The amount of precursor used in this reaction is only a few micrograms. Theoretically, a carrier-free, high-specific-activity product can be obtained because the precursor does not contain iodine. If the number of molecules in the body to be targeted by the radiopharmaceutical is very small (e.g., transporters and receptors in the central nervous system), the dose of radiopharmaceutical administered to the body is preferably as low as possible. More recently, a labeling technique using trialkylstannyl precursor has been commonly used.

34.6 SODIUM IODIDE [^{123}I , ^{131}I]

Sodium iodide [^{123}I] capsule and sodium iodide [^{131}I] capsule are the simplest inorganic pharmaceuticals made from radioactive iodine. Both are used for the diagnosis of thyroid dysfunction and thyroid tumors. Sodium iodide [^{131}I] is also useful in treating hyperthyroidism (Graves' disease and thyroid tumors), by utilizing emitted internal beta radiation. Sodium iodide [^{123}I] is usually administered orally to adults at doses of 3.7–7.4 MBq, and imaging is performed 3–24 h after administration. When sodium iodide [^{131}I] is used for diagnosis, it is usually administered orally to adults at doses of 0.185–3.7 MBq. When sodium iodide [^{131}I] is used for treatment, it is administered orally in multiple doses, up to 7.4 GBq per dose, which is greater than 1000 times the comparable diagnostic dose.

Sodium iodide [^{123}I] and sodium iodide [^{131}I] are available in capsules containing adsorbing excipients such as sucrose. When administered orally to humans, radioactive iodide ions in the stomach gradually move into the blood and accumulate mainly in the thyroid glands. Within 24 h after administration, 10–40% of the radioactive materials have accumulated in the normal thyroid glands and are synthesized into thyroid hormones such as thyroxine and triiodothyronine. The thyroid uptake of radioactive iodine, on the other hand, may be greater than 70% in

patients with hyperthyroidism. The human thyroid glands are small organs located in the throat region, which weighs 15–20 g (<5 cm in length), and makes up only 1/3500 of body weight if the standard weight for adults is 70 kg. Nonetheless, radioactive iodine specifically accumulates in the thyroid glands, where it is enriched about 100 times. Radioactive iodine is rarely found in organs other than the thyroid, and the remaining radioactivity is excreted in the urine. Thus, radioactive iodide ions efficiently accumulate only in the thyroid glands, the target organ, and are rarely found in other organs, making them suitable for the diagnosis and treatment of thyroid glands.

With the exception of radioactive iodide ion, only a few radiopharmaceuticals specifically accumulate in a single organ in high concentrations. Radioactive fluoride ions (^{18}F , positron-emitting radionuclide, half-life: 110 min) are one such example. When sodium fluoride [^{18}F] is administered intravenously to the human body, more than 60% of radioactive fluorine accumulates in the bones within 1 h of administration. Bones make up about 10% of body weight, which means that radioactive fluorine accumulates in the bones at concentrations that are about six times that in other tissues. Because radioactive fluorine accumulates in bone metastases of tumors in especially high concentrations, it is used to detect bone metastases.

Most of radiopharmaceuticals are administered intravenously. Why then is radioactive sodium iodide the only one administered orally? If orally administered radioactive iodide ions move into the blood via the stomach, it seems more effective to directly inject radioactive iodide ions into the vein, to deliver radioactive iodine to the thyroid glands. When sodium iodide [^{123}I] was administered intravenously to rats, the thyroid uptake was only 0.15% at 1 h after administration, peaked at 0.80% at 15 h after administration, and then decreased with time. These results showed that the oral route was far more effective in allowing the uptake of radioactive iodine by the thyroid glands than the intravenous route. It remains to be seen why the thyroid uptake varies depending on the route of administration. Possible causes include the involvement of some carrier in the transportation of radioactive iodine in the blood or a mechanism of thyroid uptake, and the influence of the rate at which iodine is taken up by the thyroid gland. As described in 32.2, the majority of radioactive materials released from nuclear power plant accidents are radioactive iodine (primarily ^{131}I), and radioactive iodine descends to the ground as inorganic compounds, adhering to food (vegetables, tea leaves, and fruits) and contaminating drinking water and milk. As described earlier, if radioactive iodine is inhaled or taken orally, it accumulates in the thyroid glands in extremely high concentrations. In the event of a nuclear power plant accident, the use of the iodine preparations as prophylaxis against radiation exposure is one of the most important issues for discussion.

34.7 IOFETAMINE [^{123}I]

Iofetamine [^{123}I] (^{123}I -*N*-isopropyl-4-iodoamphetamine), a diagnostic imaging agent (injection) for ischemic brain diseases, was developed by R. M. Baldwin, H. S. Winchell, T. H. Lin, et al., of Medi-Physics, Inc. (the United States), in 1978 [2].

At that time, it was already known that amines were one of the major classes of neurotransmitters in the brain and certain iodinated amines were taken up by the brain. Winchell et al. then synthesized about 40 different iodine-123-labeled aniline, benzyl, and phenethylamine derivatives, with the aim of developing agents for diagnostic imaging of the brain. They investigated the biodistribution of these compounds intravenously injected into rats and succeeded in discovering Iofetamine [^{123}I], an amine compound with the highest brain uptake and brain/blood ratio [3]. The brain uptake ($\% \text{ g}^{-1}$, percentage of radioactivity in the brain relative to the total injected dose divided by the brain weight g) of Iofetamine [^{123}I] in rats was $1.57\% \text{ g}^{-1}$ at 5 min after administration and $2.14\% \text{ g}^{-1}$ at 60 min after administration, and the brain/blood ratio (ratio of the amount of radioactivity to each organ or tissue per unit weight) was 12.6 at 5 min after administration and 20.7 at 60 min after administration. In the human body, Iofetamine [^{123}I] began to accumulate in the brain immediately after administration. It gradually increased to reach 8.5% at 1.5 h after administration, and then slowly decreased [4]. In the human body, the uptake of radioactivity by the lungs was highest, with 48% accumulation within 1 min of administration followed by a rapid decrease, suggesting the presence of nonspecific amine receptors in the lungs.

Ischemic brain diseases that can be effectively diagnosed using Iofetamine [^{123}I] include cerebral infarction (acute and chronic), transient ischemic attack (TIA), cerebral artery occlusion/stenosis, intracranial hemorrhage, subarachnoid hemorrhage, moyamoya disease, and cerebral arteriovenous malformation. The brain is an organ with good blood flow; blood flow in the brain per unit time accounts for about 10% of blood flow all over the body. The average cerebral blood flow in healthy subjects determined using Iofetamine [^{123}I] was $47.2 \pm 5.4 \text{ ml}/100 \text{ g} \cdot \text{min}$ [5]. Because Iofetamine [^{123}I] accumulates in the brain in proportion to local blood flow in the brain, images of cerebral blood flow (scintigram) can be taken with a gamma camera or SPECT camera 15–30 min after intravenous administration of Iofetamine [^{123}I] ($111\text{--}222 \text{ MBq}$, 1–2 ml). Namely, in cases of ischemic brain diseases such as cerebral infarction, defects occur in brain areas wherein blood flow is decreased or blocked, making it possible to identify ischemic lesions and surrounding areas. In addition to nuclear medicine, X-ray, CT, and magnetic resonance imaging (MRI) are well-known brain imaging and diagnostic procedures. With high spatial resolution (resolution of 1 mm), X-ray, CT, and MRI can take images of subtle changes in the brain structure associated with pathologic conditions. X-ray and CT are advantageous in terms of the detection of cerebral hemorrhage, and MRI is advantageous in terms of the detection of brain tumors. Radionuclide imaging can assist in the visualization of vital structures and organs reflecting their activities at the cellular level, although it has lower spatial resolution than the other methods. That is to say, it is effective in detecting the early stages of impaired cerebral blood flow (before a change in the morphology occurs) that cannot be visualized by X-ray, CT, or MRI, and detecting lesions responsible for neurologic symptoms that cannot be explained by X-ray, CT, or MRI.

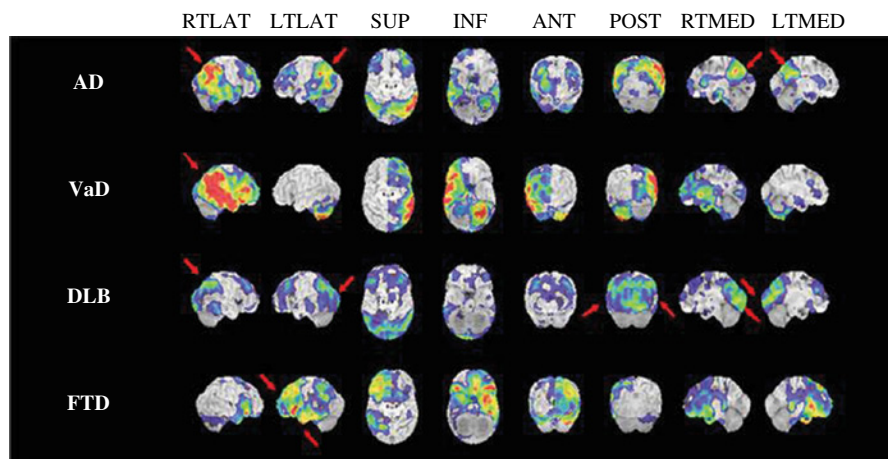


FIGURE 34.5 Cerebral blood flow maps of Iofetamine [^{123}I] in dementia patients by disease subtype. The distribution of blood flow is seen on each cross-section of the brain. White areas represent normal blood flow and red-yellow areas represent reduced blood flow. AD, Alzheimer's disease; ANT, anterior view; DLB, dementia with lewy bodies; FTD, frontotemporal dementia; INF, inferior view; LTLAT, left lateral view; LTMED, left medial view; POST, posterior view; RTLAT, right lateral view; RTMED, right medial view; SUP, superior view; VaD, vascular dementia. (See insert for color representation of the figure.)

The mechanism of Iofetamine [^{123}I] uptake by the brain is not precisely known. However, it is thought to first pass through the blood–brain barrier (BBB) and bind to the relative, nonspecific, high-volume amine receptor localized in the gray matter of the brain.

In 1985, Iofetamine [^{123}I] was approved for the first time in the world in Japan for the indication of regional cerebral blood flow scintigraphy. Unfortunately, its clinical use is extremely limited in Europe and the United States. Conversely, in Japan, where cerebrovascular disorder is always one of the most common causes of death, imaging with Iofetamine [^{123}I] has been widely used. As the analysis of the cerebral blood flow profile of Iofetamine [^{123}I] progressed, the regional cerebral blood flow maps of patients with dementia such as Alzheimer's disease (AD) were found to have distinctive profiles corresponding to each underlying cause (Fig. 34.5). Dementia has some subtypes that include vascular dementia (VaD), dementia with lewy bodies (DLB), frontotemporal dementia (FTD), and AD, which accounts for the largest percentage of dementia cases. In AD patients, blood flow is reduced symmetrically in the posterior cingulate gyrus. In VaD patients, a reduction in blood flow caused by underlying diseases such as cerebral infarction is observed, often only in one cerebral hemisphere (asymmetrical). In DLB patients, a reduction in blood flow appears in the occipital lobe. In FTD patients, a reduction in blood flow appears in the frontal and temporal lobe. With the rapid increase in the number of dementia patients in recent years, the use of Iofetamine [^{123}I] is substantially increasing to differentiate the subtypes of dementia.

34.8 IOFLUPANE [^{123}I]

Ioflupane [^{123}I] (ethyl-5,6-dihydro-7-iodo- ^{123}I -5-methyl-6-oxo-4*H*-imidazo[1,5-*a*][1,4]benzo-diazepine-3-carboxylate) is a phenyltropane radioactive diagnostic imaging agent (injection) developed by Neumeyer et al. of Research Biochemicals Internationals in the United States in 1992 [6]. Ioflupane [^{123}I] is a cocaine analogue that has a high affinity ($K_i=0.6\text{ nM}$) for the human dopamine transporter (DAT) [7]. A different cocaine analogue in which iodine was added to the benzene ring failed to produce an acceptable image for the DAT because of inferior DAT affinity and specificity as compared with cocaine, whereas Ioflupane [^{123}I] was found to have a much higher affinity for the DAT ($K_i=3.50\pm0.39\text{ nM}$, rats) than cocaine ($K_i=510\pm110\text{ nM}$, rats), indicating that its properties are ideal for DAT imaging. The DAT is a membrane protein that is intensely expressed in the substantia nigra of the brain to reuptake dopamine released from nigrostriatal dopamine nerve terminals. The expression of the striatal DAT is known to decrease in patients with Parkinson's disease. When brain images are taken with a SPECT camera 3–6 h after intravenous administration of Ioflupane [^{123}I] in healthy subjects, two striata that are symmetrically located deep in the brain, near its center, are visualized as two “comma-like” images (Fig. 34.6), because Ioflupane [^{123}I] binds tightly to the intensely expressed DAT in the striata. Comparatively, in patients with Parkinson's disease, neurons are destroyed with the progression of the disease, decreasing the expression of DAT in the striata. When Ioflupane [^{123}I] is administered, the radioactivity accumulation in the striata gradually decreases from the tail of the “comma” with the progression of the disease, and only the caudate nucleus is visualized in the shape of a “full-stop.” When the disease

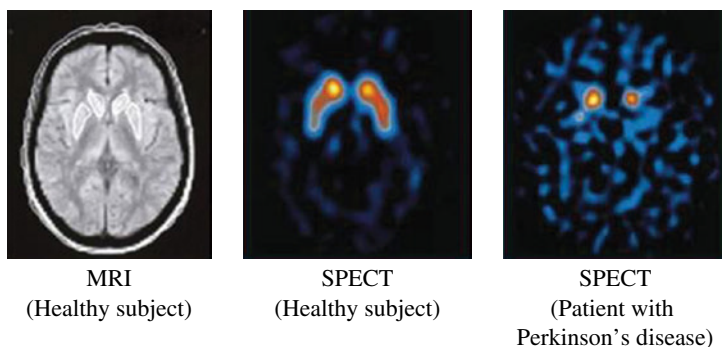


FIGURE 34.6 MRI and SPECT images of the human brain obtained with Ioflupane [^{123}I] (cross-section of the brain). Left: MRI image of the brain in a healthy subject, in which the striata are visualized as two white “comma-like” images that are symmetrically located near the center of the brain. Middle: SPECT image of the brain in a healthy subject, in which the striata are visualized as two red-yellow “comma-like” images as with MRI. Right: SPECT image of the brain of a Parkinson's disease patient, in which the radioactivity accumulation in the putamen (bottom part) of the striata disappears, and only the caudate nucleus (upper part) is visualized in the shape of a “full-stop.” When the disease further progresses, the radioactivity accumulation in the caudate nucleus also disappears. (*See insert for color representation of the figure.*)

progresses further, the caudate nucleus eventually disappears. In patients with Parkinson's disease, DAT density at the onset of symptoms decreases to less than half of that in healthy subjects, suggesting that DAT density begins to decrease long before symptoms develop. Therefore, early diagnosis through imaging with Ioflupane [^{123}I] and early intervention are preferable to halt disease progression.

More recently, Ioflupane [^{123}I] has also been found to be useful in the diagnosis of DLB. A decrease in DAT density is also observed in patients with DLB, and images obtained with Ioflupane [^{123}I] have proved that Parkinson's disease and DLB belong to the same group of diseases. As described earlier, dementia has some subtypes including DLB, AD, VaD, and FTD, and these subtypes require different treatment. If patients with DLB receive treatment for AD (e.g., psychotropic drugs), their symptoms may worsen. Therefore, the differential diagnosis of dementia is crucial.

In 2000, Ioflupane [^{123}I] was approved for the first time in the world in Europe as a diagnostic imaging agent for Parkinson's disease, and in 2006, an additional indication of DLB was approved. In 2011, Ioflupane [^{123}I] was approved in the United States as a diagnostic imaging agent for Parkinson's disease. In Japan, Ioflupane [^{123}I] was finally approved for the diagnosis of Parkinson's disease and DLB in 2013. So far, it has been approved in 34 countries.

34.9 BMIPP [^{123}I]

BMIPP [^{123}I] (15-(4-iodophenyl)-3(*R,S*)-methylpentadecanoic acid [^{123}I]) is an imaging agent (injection) for myocardial fatty acid metabolism that was developed by F. F. Knapp, K. R. Ambrose, M. M. Goodman, et al., of Oak Ridge National Laboratory in the United States in 1986 [8]. Fatty acid is a representative energy source, along with glucose and amino acids. From the 1970s, various radio isotope-labeled fatty acid probes, including palmitate [^{11}C], a naturally occurring fatty acid labeled with carbon-11, were developed and administered to humans to elucidate the fatty acid metabolism in the body. When palmitate [^{11}C] was administered intravenously, it rapidly accumulated in the myocardium, was gradually excreted, and disappeared about 60 min after injection. This fact and the corresponding images have documented that the heart mainly uses fatty acid as its energy source. However, the kinetics of palmitate [^{11}C] were too fast to image heart diseases. This is the point when BMIPP [^{123}I] appeared. BMIPP [^{123}I] has a methyl group at the beta-position (3-position) of the aliphatic side chain and a 4-iodophenyl group at the omega-position (15-position). Naturally occurring fatty acid is taken up in the myocardium and carbon chains are removed from the carboxylic end two at a time sequentially by enzymatic beta-oxidation in mitochondria. BMIPP [^{123}I], however, cannot undergo beta-oxidation due to steric hindrance of the methyl group at the beta-position (Fig. 34.7). If it undergoes beta-oxidation, 3-OH-BMIPP was thought to be formed, but this possibility was ruled out in an experiment using a rat perfusion heart. Intravenously administered BMIPP [^{123}I] that has bound to plasma albumin in the blood is transported and taken up in the myocardium via the long-chain fatty acid transporter (CD36) expressed on the surface of myocardial cells. BMIPP [^{123}I] is

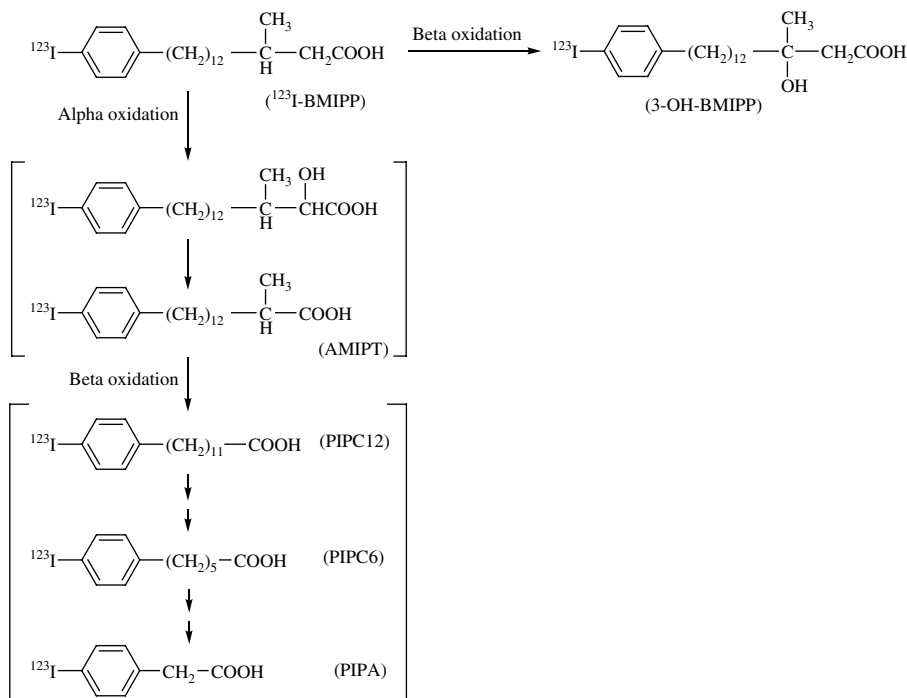


FIGURE 34.7 Fatty acid metabolic pathway of BMIPP [^{123}I] in the myocardium of rats. BMIPP cannot undergo beta-oxidation due to steric hindrance of the methyl group at the beta-position (3-position) of the aliphatic side chain. Therefore, it undergoes alpha-oxidation first (AMIPT formation), undergoes beta-oxidation 6 times, and then produces the end metabolite PIPA. (If it undergoes beta-oxidation first, 3-OH-BMIPP should be formed, but it was not detected in the metabolites.)

stored in the fatty acid pool in myocardial cells and then gradually undergoes alpha-oxidation (removal of a single carbon atom) to produce alpha-methyl-p-iodophenyltetradecanoic acid (AMIPT). It has been found that AMIPT then undergoes beta-oxidation six times and produces the end metabolite 4-iodophenyl acetic acid (PIPA). That is, BMIPP [^{123}I] images the myocardial fatty acid metabolism as an image of temporary metabolic trapping [9].

BMIPP [^{123}I] was approved in Japan in 1992 for the diagnosis of myocardial fatty acid metabolism. Unfortunately, it has not been approved in the United States and Europe, where its development has been discontinued.

34.10 IOBENGUANE [^{123}I]

Iobenguane [^{131}I] (3-iodo-benzylguanidine [^{131}I], or mIBG [^{131}I]), was developed by Wieland et al., in 1980 [10]. It was originally developed as a diagnostic imaging agent for the adrenal medulla by imitating the anti-hypertensive adrenergic blocking drug

guanethidine. The compound's isomers were synthesized by labeling with radioactive iodine at the 2-, 3-, and 4-positions on the benzene ring, and intravenously administering the compound to dogs. All of these isomers specifically accumulated in the adrenal glands as expected; in particular, the adrenal uptake of isomers labeled at the 3- and 4-positions was markedly high. Because the isomer labeled at the 4-position caused accumulation of iodide ion [^{131}I] (metabolic product) in the thyroid glands, the isomer labeled at the 3-position was chosen as the final clinical candidate. Iobenguane [^{131}I] also accumulated in relatively high concentrations in the myocardium, because it is rich in sympathetic nerves. Kline et al., then succeeded in visualizing the distribution of sympathetic nerves in the human myocardium by intravenously administering Iobenguane [^{123}I] wherein the radioactive iodine isotope was substituted with iodine-123, an isotope more suitable for SPECT [11].

In Japan, Iobenguane [^{123}I] was approved for the diagnosis of heart diseases in 1992, approved for the diagnosis of neuroblastomas as an additional indication in 2009, and approved for the diagnosis of pheochromocytomas as an additional indication in 2011. In European countries including the United Kingdom, France, and Germany, it was approved for the same indications as in Japan in the 1990s. In the United States, it was approved for the detection of primary and metastatic pheochromocytomas and neuroblastomas in 2008, and approved for cardiac risk evaluation in heart failure patients as an additional indication in 2013.

34.11 IOMAZENIL [^{123}I]

Diazepam, a benzodiazepine antianxiety drug, was developed in the 1960s and commonly used as a hypnotic drug. As a result, diazepam abuse and dependence became a social issue. In 1981, Hunkeler et al., of F. Hoffmann-La Roche Ltd (Switzerland) developed flumazenil, a BZR antagonist [12]. Flumazenil binds to the central BZRs, preventing the action of benzodiazepines. The drug was found to reverse the effects of benzodiazepines without exerting its own pharmacological effects. Iomazenil [^{123}I] (Ro16-015, 4-ethyl-5,6-dihydro)-7-iodo-5-methyl-oxo-4*H*-imidazo[1,5*a*][1, 4]benzodiazepine-3-carboxylate) is an analogue of flumazenil and is a BZR imaging agent (injection) developed by Beer et al., of the Paul Scherrer Institute (Switzerland) in cooperation with Hunkeler [13]. When Iomazenil [^{123}I] is administered intravenously to humans at a dose of 111–167 MBq, it rapidly accumulates in the brain. The whole brain uptake of radioactivity peaked at 12% at 10–20 min after administration, then gradually decreased to 7% over 3 h. With renal elimination being the primary route, 93% of the administered Iomazenil [^{123}I] was excreted in the urine within 24 h after administration. Iomazenil [^{123}I] accumulates in the cerebral cortex and cerebellum of healthy subjects, where the central BZRs are distributed densely. The central BZRs are known to decrease at the epileptic focus. About one-third of patients with epilepsy are refractory to medical treatment. Surgical intervention is beneficial for patients with intractable epilepsy. To determine the extent of resection, the epileptic focus must be located accurately. Because Iomazenil [^{123}I] can image epileptic foci as defects during a seizure-free interval, it is useful to determine the extent of resection.

In Japan, Iomazenil [^{123}I] was approved for the detection of epileptic foci in 2004. In Europe, it was marketed in several countries including Switzerland in the 1990s, but is no longer commercially available now. In the United States, it has not been approved. In Europe and the United States, fludeoxyglucose [^{18}F] is marketed for the same indication.

34.12 IODINE [^{131}I] TOSITUMOMAB

Since the development of MoAbs, radioisotope-labeled MoAbs have been expected to be a powerful diagnostic (radioimmunoimaging) and treatment (radioimmunotherapy) tool for cancer, and many studies have been conducted. Although many promising results have been obtained in animal experiments, the outcomes of clinical trials have mostly been disappointing. Meanwhile, Iodine [^{131}I] Tositumomab is one of the few successful examples of radioimmunotherapy. Kaminski et al., of the University of Michigan studied anti-B1 MoAb, which is specific for CD20 (phosphoprotein) expressed on the surface of human B cells. First, they administered unlabeled anti-B1 MoAb 685 mg to 28 patients with B cell lymphoma for whom chemotherapy had failed. After 1 week, iodine-131-labeled anti-B1 MoAb, that is, Iodine [^{131}I] Tositumomab, was administered to the patients at a dose of 1.26–5.96 GBq (34–161 mCi). As a result, complete remission was observed in 14 patients and partial remission was observed in 8 patients [14]. The treatment of these patients was successful for the following two reasons: (1) they studied lymphocytes that were known to be radiosensitive, and (2) they blocked nonspecific antibody binding sites in the body by administering unlabeled anti-B1 MoAb as pretreatment to increase the tumor uptake of radiolabeled anti-B1 MoAb. The progression-free survival rate was 56% at 5 years and the overall survival rate was 83% in the clinical study of Iodine [^{131}I] Tositumomab conducted [15]. In order to succeed in the field of radioimmunotherapy, the careful design of treatment protocols similar to that by Kaminski et al. is considered essential.

In 2004, Iodine [^{131}I] Tositumomab was approved for the treatment of non-Hodgkin's lymphoma in the United States. It has also been approved in Canada, but has not yet been approved in Europe or Japan. In Europe and Japan, Yttrium [^{90}Y] Ibritumomab tiuxetan, an antibody drug with the same indication, has been marketed.

34.13 SUMMARY AND FUTURE PERSPECTIVE

Radioactive iodine is used in radioactive iodine-labeled pharmaceuticals, both inorganic and organic compounds, and is of great benefit in the field of nuclear medicine, for both diagnosis and treatment. Radioactive iodine has advantages over other elements in that both a radioisotope suitable for SPECT (iodine-123) and a radioisotope suitable for PET (iodine-124) are available, which makes it unique. Iodine is one of the essential trace elements and is present as an iodide ion or thyroid hormone in the

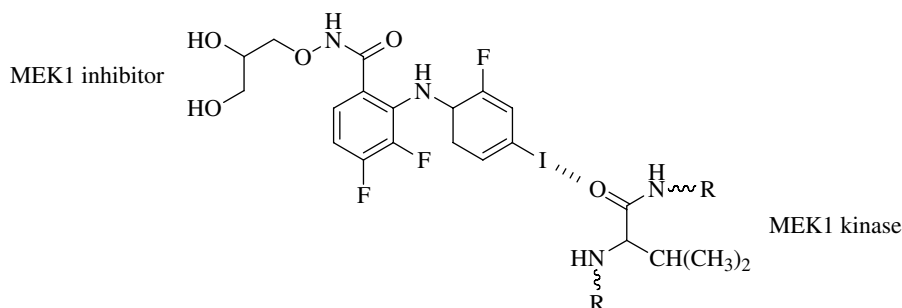


FIGURE 34.8 Halogen bonding between a MEK1 inhibitor and a MEK1 kinase.

body. However, most pharmaceuticals labeled with radioactive iodine are artificial organic compounds synthesized by imitating physiological compounds or known pharmaceuticals. That is, radioactive iodine has been used as a mere labeling tool or radioactive source, and the importance of its chemical properties and physiological significance are not realized. Likewise, the use of iodine is limited to the control of steric hindrance and lipophilic property in nonradioactive pharmaceuticals. Possibly because of this, there have been no pharmaceuticals containing a stable iodine isotope for more than 20 years since the development of several iodine contrast media.

Recently, the substitution of halogen in compounds has been shown to interact with carbonyl groups and hydroxyl groups like hydrogen bonding. A drug containing a stable iodine isotope has been developed using this “halogen bonding,” and a clinical study is under way [16]. Halogen bonding plays a role in the interaction between halogens in the molecules of drugs and carbonyl groups in the pockets of target enzymes, and a halogen bonding directly exerts an enzyme inhibitory effect (Fig. 34.8). Among the halogen elements, iodine is known to form the strongest halogen bonding. In the near future it is hoped that new pharmaceuticals containing radioactive iodine will be developed using radioactive iodine as the point of action of halogen bonding.

REFERENCES

- [1] Tonnesen GL, Hanson RN, Seitz DE. Position-specific radioiodination utilizing an aryltri-butylstannyl intermediate. Synthesis of 125I-iodotamoxifen. *Int J Appl Radiat Isot* 1981;32:171.
- [2] Baldwin RM, Lin TH, Winchell HS. Amines useful as brain imaging agents. U.S. Patent 4,360,511. Jun 19, 1980.
- [3] Winchell HS, Baldwin RM, Lin TH. Development of 123I-labeled amines for brain studies: localization of 123I iodophenylalkyl amines in rat brain. *J Nucl Med* 1980;21:940.
- [4] Seki H. A study on regional cerebral blood flow measurement by N-isopropyl-p-[123I] iodoamphetamine. *J Japen Med Soc* 1986;95:279.
- [5] Kuhl DE, Barrio J, Huang SC, Selin C, Ackermann RF, Lear JL, Wu JL, Lin TH, Phelps ME. Quantifying local cerebral blood flow by N-isopropyl-p-[123I] iodo-amphetamine (IMP) tomography. *J Nucl Med* 1982;23:196.

- [6] Neumeyer JL, Milius RA, Innis RB. Iodinated neuroprobe for mapping monoamine reuptake sites. US Patent 5,310,912. Feb 25, 1992.
- [7] Neumeyer JL, Wang S, Gao Y, Milius RA, Kula NS, Campbell A, Baldessarini RJ, Baldwin RM, Zea-Ponce Y, Innis RB. N- ω -fluoroalkyl analogs of (1R)-2 β -carbomethoxy-3 β -(4-iodophenyl)-tropane (β -CIT: Radiotracers for positron emission tomography and single photon emission computed tomography imaging of dopamine transporters. *J Med Chem* 1994;37:1558.
- [8] Knapp FF, Ambrose KR, Goodman MM. New radioiodinated methyl-branched fatty acids for cardiac studies. *Eur J Nucl Med* 1986;12:S39.
- [9] Yamamichi Y, Kusuoka H, Morishita K, Shirakami Y, Kurami M, Okano K, Itoh O, Nishimura T. Metabolism of iodine-123-BMIPP in perfused rat hearts. *J Nucl Med* 1995;36:1043.
- [10] Wieland DM, Wu JL, Brown LE, Mangner TJ, Swanson DP, Beierwaltes WH. Radiolabeled adrenergic neuro-blocking agents: adrenomedullary imaging with ¹³¹I iodobenzylguanidine. *J Nucl Med* 1980;21:349.
- [11] Kline RC, Swanson DP, Wieland DM, Thrall JH, Gross MD, Pitt GB, Beierwaltes WH. Myocardial imaging in man with ¹²³I meta-iodobenzylguanidine. *J Nucl Med* 1981;22:129.
- [12] Hunkeler W, Mohler H, Pieri L, Polc P, Bonetti EP, Cumin R, Schaffner R, Haefely W. Selective antagonists of benzodiazepines. *Nature* 1981;290:514.
- [13] Beer HF, Blauenstein PA, Hasler PH, Delaloye B, Riccabona G, Bangerl I, Hunkeler W, Bonetti EP, Pieri L, Richards JG, Schubiger PA. In vitro and in vivo evaluation of iodine-123-Ro-0154: a new imaging agent for SPECT investigations of benzo-diazepine receptors. *J Nucl Med* 1990;31:1007.
- [14] Kaminski MS, Zasadny KR, Francis IR, Fenner MC, Ross CW, Milik AW, Estes J, Tuck M, Regan D, Fisher S, Glenn SD, Wahl RL. Iodine-131-anti B1 Radioimmunotherapy for B-cell lymphoma. *J Clin Oncol* 1996;14:1974.
- [15] Schaefer NG, Huang P, Buchanan JW, Wahl RL. Radioimmunotherapy in non-Hodgkin lymphoma: opinions of nuclear medicine physicians and radiation oncologists. *J Nucl Med* 2011;52:830.
- [16] Roughley SD, Jordan AM. The medicinal chemist's toolbox: an analysis of reactions used in the pursuit of drug candidates. *J Med Chem* 2011;54:3451.

INDEX

- absorbable organic halogen (AOX) 367
absorbing agent 237
absorption tower 237
acaricide 441
acceptable daily intake (ADI) 552
acetic acid 547–9
acetoxyhydroxyacid synthase (AHAS;
EC 2.2.2.1) 444
acetrizic acid 356
active carbon 201, 211
addition polymerization 491
adrenal medulla 620
adsorption column 239
AgI 58
agrochemicals 439
air-stripping process 227
alcohol oxidation 116, 130, 281
aliphatic halides 344
alkene deamination 310
alkoxy radical 284
alkyl iodide 489, 490, 493
alkyl radical 312
alkynylidonium salt 130
allyl iodide (allylic iodide) 264
A-arylation 130
A-arylation of carbonyl compounds 308
A-azidation 117
 α -acetoxylation 118, 284
 α -diketone 335
 α -elimination 115
 α -fluorination 117
 α -hydroxy imine 342
 α -hydroxy ketone 335
 α -iodinated ester 256
 α -iodinated ketone (α -iodo ketone) 256,
257, 262, 264
 α -iodination 256, 257
 α -iodo ketone 335
 α -iodoenone 262
alpha-oxidation 620
 α -oxygenation 133
alternative two-electron systems 510
Alzheimer's disease (AD) 617
Amberlite 245
amiodarone 434
ammonia 59
amoco production company 222, 224, 226
Anadarko Basin 221, 223, 224, 226

- anionic XB acceptors 181
anthelmintics 439
antiarrhythmic agent 434
antiseptics 375, 380, 388, 395
antiviral drug 433
- bacterial viruses 401
Barbier-type reaction 346
Barluenga's reagent 266
benodanil 441
benzene 9, 11
benzodiazepine receptor (BZR) 612, 621
benzyltrimethylammonium
 dichloroiodate 268
benzyne 118
bernauer 482
bernotar 482
berry pseudorotation 111
 β -elimination 116
beta-oxidation 619, 620
biaryl 304
biaryl coupling 313
biliary contrast agent 364, 368
biogeochemical cycling 557
biological property 132
bis(pyridine)iodonium
 tetrafluoroborate 266
1,2-bis(4-pyridyl)ethylene 171
[bis(trifluoroacetoxy)iodo]benzene
 (BTIB) 106, 285
block 17 11
blood-pool agent 370
blowing-out method 237
blowing-out process 237, 238
blowout 244
blowout process 227
BMIPP [^{123}I] 620
boiling point 11
bond dissociation energy 13
Bonnemaïsonia 564
Boron phosphor silicate glass 529
Boso Peninsula 233
brachytherapy 609, 612
[Br₂I₂]² 184
brine 210, 221, 222, 224, 226–8
 chemical composition 234, 235
 natural gas brine 231, 237
Brittany 207
broadleaf weeds 445
- bromide 55, 60
bromine 12, 221
bromoperoxidase 572, 573, 575–7, 579
bromotrimethylsilane 318
BTMA ICl₂ 268
Butan-2-ol 11
- cadexomer iodine 398
caliche 213, 214, 216–18
Cambridge Structural Database (CSD 5.34) 169
capacitively coupled contactless
 conductivity detection (C4D) 34
carbene 115
carbon disulfide 11
carbon tetrachloride 11
carbonyl-olefin coupling reaction 345
cardiac action potential 434
C-arylation 323
catalyst 493, 495–8, 547
catalytic utilization 132
cation radical 288
cationic polymerization 464, 489, 492
cativa process 547–9
caudate nucleus 618
cerebral blood flow 617
certified reference materials (CRMs) 45
cetyltrimethylammonium chloride
 (CTAC) 28
C-H activation 309
chain-transfer 497, 498
chalcogen atom 178
charcoal 208
charge-transfer (CT) complex 10, 119,
 289, 314
C-H cross-coupling 305
CH₂I₂, 592, 594
CH₃I 594
CH₂ICl 592, 594
Chile 210, 559
China 210
chiral hypervalent iodine 134
chiral iodonium salt 322
chloride 60
chlorination 295
chlorine 9, 12, 210
chloroform 11
chloroperoxidase 572, 575, 579
cholangiography 368
cholegraphy 366

- cleavage-iodination 89
[Cl₂I₂]² 184
CII 2-chloroquinoline 173
CII pentamethylenetetrazole 173
Clioquinol (5-chloro-7-iodo-8-quinolinol) 393
closantel 450
cloud condensation nuclei (CCN) 593
cloud formation 558
cocrystals 168
colonoscopy 366
colorant 552
combustion 244
commercially available diaryliodonium salts 461
compaction 236
computed tomography (CT) 365
concentration 244
conductivity detection 33
copper (I) iodide 57
copper wire 209
copper-catalyzed process 306
coranene 180
coupling 316
coupling reaction 303
courtois 197, 199–201, 203, 204, 563, 564
covalent radius 10, 13
cretinism 423, 424, 426
criptocyanine 553
critical point 10
critical pressure 11
critical surface tension 515
critical temperature 11
cross-coupling 304
cross-resistance 450
crown ether 26
crystal engineering 168
crystal field theory 563
crystallizer 238, 239
C-selectivereactions 317
CuI 57
cuprous iodides 550
cyanine 553
4-cyanopyridine 171
cyclic iodine 109
cyclization-rearrangement 84
dearomatization 287
decarboxylation-iodination 90
decarboxylative coupling 312
decomposition 244
dehydrative condensation 319
dehydrogenation 117, 130, 246, 278
deiodination 244, 359
dementia with lewy body (DLB) 617
dendrimer 370, 371
density 11
deposits of organic origin 557
deprotection 246
Dess-Martin periodinane (DMP) 108, 293
(diacetoxyiodo)benzene (DIB) 106
diaryliodonium salts 131, 459
diastereoselectivity 331
diatrizoate 364
diatrizoic acid 358–60, 363
1,4-Diazabicyclo[2.2.2]octane 169
dibenzo-24-crown-8, 175
dichloriodobenzene 295
dichroism 484
didodecyldimethylammonium bromide (DDAB) 28
dielectric constant 11
dietzeite 213
differential optical absorption spectroscopy (DOAS) 595
difluoriodotoluene 295
digital imaging 473, 475
digital subtraction angiography 365
DIH *See* 1,3-diiodo-5,5-dimethylhydantoin (DIH)
2,2'-diiodobiphenyl catalyst 318
1,3-diiodo-5,5-dimethylhydantoin (DIH) 263
diiodotyrosine (DIT) 412–14
Dijon 199–201, 203
dimethyldiselenide 178
diodone 356
1,2-diol 330, 340, 345
1,4-dioxane 176
diphosphorustetraiodide 269
direct current (DC) amperometry 34
discovery 203–5
disinfectant 375, 376, 379, 380, 383, 386, 389–92, 397, 398, 402–4
dissociative ligand exchange 113
dissociative pathway 118

- distillation 244
dopamine transporter (DAT) 618
drinking water 391, 392, 394, 397–9, 403
DSSC counterelectrode 507
dual IC 47
dyes 484, 553
dye-sensitized solar cells 501
dynamic contact angles 518
dynamic viscosity 11
- efflux 565, 566
electrical resistivity 11
electrodialysis 244, 245
electron affinity 13
electron configuration 13
electron energy distribution functions 524
electron gain enthalpy 13
electronegativity 13
electronic configuration 13
electrophilic iodinating reagent 259, 260, 263, 264, 266, 268
electrospray ionization tandem mass spectrometry (ESI-MS) 36
eluent 26
eluting agent 239
elution column 239
Emiliana 566, 568
enantioselective α -arylation 308
enteric bacteria 401, 402
enteric viruses 401
entropy 11
environment 227, 228
environmentally harmonized gas chemistry 532
enzyme-based iodine (EBI) 391, 392, 394, 398
epilepsy 611, 621
epoxides 464
epoxy-silicone 466
EPR 559, 570–572
erythrosine B 553
etching rate 528
etching selectivity 523
ethanol 11
ethers 11
Ethiodol 369
ethyl acetate 11
extended X-ray absorption fine structure (EXAFS) 19, 576
extracellular contrast agent 355, 357, 359, 367
extraction 244
eye drops 435
- fatty acid metabolism 619
flaked 220
flaker 238, 239
flakes 237
flubendiamide 447
fluoride 60
fluorinated repellents 513
Fluorination 296
fluorine 12, 13
fluorine-doped tin oxide (FTO) 502
fluoroalcohol solvent 119, 288, 318
fluorocarbon gases 523
fluoropolymer 523
fluoroscopy 365
Food and Drug Administration (FDA) 552
food processing industry 400
fossil seawater 236
Fourier transform infrared spectrometer 534
France 210
frontotemporal dementia (FTD) 617
Fujita's chiral lactate-type iodoarene 136
Fukushima 565
fullerene-C60, 180
Functionalization of carbonyl compounds 126
- gaseous phase 11
Gay-Lussac 203, 205
Glan 486
global warming potential 532
glomerular filtration 359, 365
goiter 422–6, 431, 560, 563
Grotthuss mechanism of conductivity 508
- Haidinger 482
Halocarbons 566–8
halogen 12
halogen bond (XB) 159, 160
halogen bonding 623
halogen bonding acceptor 161
halogen bonding donor 161
halogenases 559

- halogenation 558
halogen-iodine exchange 83
haloperoxidase 564, 565, 568, 570, 572, 573, 576, 591
Hastelloy C 237
heap leaching 213, 216–18, 220
heat of fusion 10
heat of vaporization 10
heat-stabilizing agents 550
heptafluoro-iso-propylaniline 449
Herapath 479, 482
herapathite 482–4, 486
herbicides 444
Herotar 482, 483
hexamethylenetetramine 170
hexane 11
hexane-1,6-diaminium diiodide 182
HI 56
high capacity 41
higher-order structures 518
higher-valent palladium 309
highest occupied molecular orbital (homo) 11
high-osmolar agents 366
Hofmann rearrangement 120, 127, 292
HOI *see* Hypoiodous acid (HOI)
homocoupling 314
HOMO-LUMO 559
homolytic cleavage 122
homolytic fragmentation 285
Hounsfield Unit 365
H-sheet 485
humic substances 234
1-hydroxy-1,2-benziodoxol-3(1H)-one (IBX) 108, 293
hydration energy 13
hydriodic acid 56, 57
hydrodimerization 345
hydrogen abstraction 284
hydrogen iodide 56, 79, 86
hydrophilicity 356, 363, 364, 367
[hydroxy(tosyloxy)iodo]benzene (HTIB) 106, 291
hypernucleofuge 114
hyperthyroidism 414, 415
hypervalency 105
hypervalent bond 105
hypervalent iodine compounds 460
hypervalent iodine reagent 280
hypoiodous acid (HOI) 79, 382, 592–4
hypothyroidism 414, 415, 423, 434
 ^{127}I 559
 I_2 592, 594
 I_2 encapsulation 181
 I_2 NH_3 163
 I_2 π contact 180
 I_2 Se synthon 178
 I_2 Te synthon 179
 I_4^{2-} 182
IBBCEAS 567
IBr 59, 561
 IBr_3 , 59
ice algae 568
Iceland spar 482
ICl 60
 ICl_3 , 59
idoxuridine 434
IDU 433
IF 59
 IF_3 59
 IF_5 59
 IF_7 59
I-IAs interaction 174
I-I O synthon 175
I-I P interaction 174
I-I S synthon 176
imino ketones 335
Iminoiodane 109
inductively coupled plasma 532
inductively coupled plasma mass spectrometry (ICP-MS) 16, 36
industrial applications 547
inert element 55
Infrared diode laser absorption spectroscopy 525
Infrared (IR) spectroscopy 18
 I-I stretching 167
initiating system 493–5, 497
initiator 493
Inkjet printing 474
inorganic iodide 55
Inorganic iodine 279
insecticides 447
integrated pest management (IPM) 448
interhalogen compound 56
interhalogens 56, 59
intermolecular forces 159

- Intraiodol 369
- I₂O₅ 59
- IO radical 592, 593
- iobenguane [123I] 610–612, 620
- IOCHEM 222
- iodate 214–18, 220, 557–9, 561, 565, 566, 568
- iodic acid 560
- iodic anhydride 59
- iodide 55, 215–20, 557, 559–62, 564–71, 573, 578
- iodinating reagent 251
- iodination 338, 339
 - alcohols 86–9
 - aliphatic hydrocarbons 76
 - alkenes 78–80
 - alkyl halides 85, 86
 - alkynes 81, 82
 - aromatic hydrocarbons 78
 - aryl halides 83
 - carbonyl compounds 91
 - carboxylic acid 90
 - ethers 89
 - organometallics 92
 - organonitrogen compounds 85
 - sulfonic acid esters 87
- iodination of protein 569
- iodine
 - agrochemicals 5
 - biological activity 4
 - discovery 2
 - industrial application 3
 - isotopes 5
 - pharmaceuticals 4
 - physicochemical properties 2
 - production 2
 - recycle 3
 - synthesis 3
- iodine 55
- iodine cation (H₂O I⁺) 378, 382
- iodine chloride 259
- iodine containing wall 400
- iodine deficiency 421
- iodine deficiency disorders (IDD) 422, 425
- iodine heptafluoride 60
- iodine-123 [¹²³I] 605, 608
- iodine-124 [¹²⁴I] 608
- iodine-125 [¹²⁵I] 606, 608
- iodine-125 seed 606, 612
- iodine-129, 236
- iodine-131 [¹³¹I] 606, 608
- iodine [131I] tositumomab 622
- iodine in polymer synthesis 490
- iodine intake 422, 425–7, 429
- iodine (molecular, I₂) 557–9, 563–8
- iodine monobromide 60
- iodine monochloride 60
- iodine monofluoride 60
- iodine nutrition 425–7
- iodine oxide particles (IOPs) 593
- Iodine oxides 558, 566, 567
- iodine pentafluoride 60
- iodine pentoxide 59
- iodine resins 399
- iodine stripping 219
- iodine supplements 421, 429
- iodine teat dip 398
- iodine tincture 386, 392, 394, 395, 398
- iodine tribromide 60
- iodine trichloride 59
- iodine trifluoride 59
- iodine-based redox system 509
- iodine-interhalogen compounds 78
- iodinium ylide 124
- iodipamide 362, 368
- iodism 228
- iodixanol 362–4
- iodized oil 423, 426, 429
- iodized salt 427, 429
- iodoalkanes 332
- iodoalkynes 162
- iodoallylic alcohol 258
- iodobenzene diacetate 282
- iodobenzene dichloride 103, 295
- 2-iodobenzenesulfonic acid (IBS) 133
- iodoform (triiodomethane) 391, 393
- iodohippurate [123I] 611
- iodolactonization 252, 261
- iodomethylation 84
- iodonium bromide 319
- iodonium ion 560
- iodonium salt 108, 306
- iodoperoxidase 564, 572, 573, 579
- iodophors 376, 379–81, 384, 386, 387, 393, 397
- iodopyridine 332
- iodoquinol (5,7-diiodo-8-quinolinol) 393

- iodosobenzene 109, 280
iodosulfuron-methyl-sodium 443
iodosylbenzene 280
iodothyronine deiodinase (D1, D2, D3) 413
iodotitanation 332
iodotrimethylsilane 89
iodotyrosine (MIT) 412–14
iodotyrosine deiodinase (IYD) 412–14, 418
iodoxybenzene 294
iodoxylbenzene monomer 282
iodylbenzene 294
iofetamine [¹²³I] 611, 613, 615
Iofina, Inc. 224
ioflupane [¹²³I] 611, 613, 614, 618
ioforminol 359
iohexol 360
iomazenil [123I] 611, 612, 621
ion chromatography (IC) 25
ion exchange 244
ion exchange resin 244
ion exchanger 26
ion selective electrodes (ISEs) 17
ion-exchange capacity 31
ion-exchange process 237
ion-exchange resin method 237
ionic radius 13
ionic-liquid electrolytes 508
ionization energies 13
ionization enthalpy 10
iopamidol 360, 363, 367
iopanoate 368
iopromide 358, 359, 361, 364, 368
iosimenol 359
iosimid 358
iothalamate 369
iotrolan 356, 357, 362–4
ioversol 361
ioxaglic acid 356
ioxilan 361
ioxynil 440
Ipso substitution 320
IPy2BF₄ 266
Ireland 207, 564, 566, 567
iridium carbonyl iodide 547
Ishihara's chiral catalyst 137
isochrysis 566
isomerization 246
Isonicotinamide 172
IUPAC 36
J polarizer 484
Japan 210, 211, 222, 224, 237, 565
Jawa 210
Karnovsky fixative 43
Kazusa group 232, 233
Kelp 209
kerosene extraction 218, 220
ketones 10
KI *See* potassium iodide
kiln 207
kinematic viscosity 11
Kita's catalyst 133
Kita's spirobiindane catalyst 136
La Hague 565
labeling 613, 614, 621
Laminaria 564–7, 573
land 484
lautarite 213, 559
lead iodide 55
lead(II) nitrate 55
LEDs 462
lepidopterous pests 448
Levo-T 415
Levothroid 415
levothyroxine 415
Lewis acid 330, 331
ligand coupling 112, 121
ligand exchange 112, 319
limestone 224–6
limit of detection (LOD) 35
Lipidol 369
liposomes 369
liquid phase 11
liver-specific X-ray contrast agent 368
living cationic polymerization 492
living polymerization 491
living radical polymerization 491, 495–500
long-term thermal stability (LTTS) 550
low capacity 41
low dielectric (low-k) film 531
lowest unoccupied molecular orbital (LUMO) 11
low-osmolar agents 366
low-valent metal 329

- Lugol's solution 377, 378, 381–3, 386,
392, 394, 395, 401
Lymphography 366
- Macrocystis 565
Mannich reaction 331, 335
marine sediment 231, 233, 234, 236
Martin-Arduengo designation 105
matrix elimination 37
m-Chloroperbenzoic acid (mCPBA) 133
melter 238, 239
melting point 13
membrane filtration 245
meta arylation 307
metabolism 446
metal-free 138, 313
metal iodide 329
methamphetamine 229
methanol 548
methoxyallene 338
methyl iodide 443, 548, 591
metrizamide 356
metrizoic acid 369
MF 244
micellar systems 281, 294
michael acceptor 124
micro filtration 245
microbial methane 231, 236
microbicidal activities 383
microorganisms 557, 568, 578
microwave-induced combustion (MIC) 42
mildewcide 442
Minami-Kanto gas field 231, 232, 234, 237
mineral deposits 213
mineralization 244
mixed mode 29
MNOSFET 537
mobile phases 30
molar heat capacity 10
molecular iodine 9, 245, 251, 277, 311
monoliths 28
Monomers 464
Monsanto processe 547
Monterey Formation 221
Morrow Formation 226
 μ -Oxo compound 108
 μ -oxo hypervalent iodine 290
Mukaiyama aldol 331
myelography 366
- NaI 57
Nakajo oil and gas field 231, 233
nano filtration 245
naphthalene 58
natural gas 226–8
natural saltpeter 213
Nazarov reaction 331
negative ion 538
negative photoresists 471
nematodes 452
Nereocystis 564
neutralization 244
new fluorinated alkyl acrylates 520
NF 244, 245
 NI_3 , 59
Nicol prism 481
Niigata gas field 231, 233
N-iodosaccharin 264
N-iodosuccinimide 260
NIS 260
niter 210
nitrate 213, 220, 226
nitrenium 120, 127
nitrogen centered radicals 285
nitrogen triiodide 59
nitrous oxide (N_2O) reductase (N_2OR)
569, 570
NMR 559, 571, 572, 576
no observable effect level (NOEL)
552, 553
nonmetallic element 9
nonsupressed IC 33
Normandy 207
North American Brine Resources 222
Norway 207
nuclear medicine 610, 616, 622
nuclear power plant 606–8, 615
nucleophilic coupling 322
nucleophilic iodinating reagent 269, 271
nucleophilic substitution 115
- O-arylation 323
ODS columns 28
oil and water repellency 516
Oilfield 221, 222, 224, 226
o-iodoxybenzoic acid (IBX) 293
Oklahoma 221, 222, 224, 226, 228, 229
organic iodide 303
organocatalysis 318

- organocatalyst 133
ortho effect 121
osmolality 356, 359, 360, 363, 364
oxidant 238, 239
oxidation of alcohol 277, 293
oxidation potential 314
oxidation states 13
oxidative cleavage 129
oxidative coupling 311
oxidative cycloaddition 126
oxidative fragmentation 129
Oxone® 133, 293
ozone 591, 592, 594
ozone depletion events (ODEs) 596
- Parachlorella* 565
Paris 200–203
Parkinson's disease 611, 618, 619
partition coefficient 363, 364
pauling 13
perfluoroalkyl iodide 497, 513
periodic acid 562
periodic table 13
personal protective equipment 228
petroleum 224, 227
PFOA 517
pharmaceuticals 433
pharmacokinetics 364, 366, 367
phenol coupling 315
phenolic antioxidant 550
phenolic oxidation 125, 283
phenoxenium ion 119
phenyliodine(III) bis(trifluoroacetate) (PIFA) 106, , 285, 313
phenyliodine(III) diacetate (PIDA) 106, 282
pH/flow gradient 28
phosphorous triiodides 87
photoacid generator (PAG) 131, 459
photochemical 592, 595
photoelectrode 503
photographic sensitizers 553
photosensitivity 460
photosensitization 463
photosensitizers 462
physical properties 13
phytoplankton 591, 592
 P_2I_4 , 269
pinachrome 553
pinacol coupling reaction 340
Pittsburgh Plate Glass Industries 226
plant growth regulator (PGR) 440
pulse-time modulated plasma 532
pnictogen atom 173, 174
polar 596
polarizability 161
polarized light 480, 481
polaroid 484, 485
pollution 228
poly (hexamethylene adipamide) 548
polyacrylic acid 387
polyamide(s) 6, 66, 387, 549
polyether glycols 387
polyiodide(s) 18, 237, 240, 376, 378, 390, 399
polymeric structure 280, 294
polymerization 523
polymer-supported reagent 296
polyoxyalkylenes 387
polysaccharides 387
polyvinyl alcohols 387, 484
polyvinyl pyrrolidinone 382, 387, 395
porous SiOCH 537
positive photoresists 471
positron emission tomography (PET) 605–6, 609, 610
potash 208
potassium carbonate 207
potassium iodide 9, 57, 607
Poulconq, 209
povidone-iodine 380, 381, 387–90
precipitation 244
precision polymer synthesis 491, 494, 499
precision polymerization 491
pregnancy 423, 425
prilled 217–19
prilled iodine 237, 240
prilling 219
prilling tower 237
prills 237
prins cyclization 332
printer inks 553
prochlorococcus 568
production process in the past 207
proquinazid 445
protonic acids 459
protozoan cysts 401
pseudomonas iodooxidans 568

- pulsed amperometric detection (PAD) 34
pummerer-type reaction 127
PyICl 268
pyridine 10, 171
pyridinium iodochloride 268
- quantum yields 462
quinine 481–3, 486
quinone 283
- radical 122
radical polymerization 489, 490, 495, 496, 498
radioactive iodine 605–15, 621
radiography 365
radioimmunotherapy 609, 622
radiopharmaceuticals 610, 611, 615
rafoxanide 450
Raman spectroscopy 18
 1,6-bis(trimethylammonium)hexane 167, 182
 dynamically porous 167
 I-I stretching 167
recombination loss reaction 505
recyclable reagent 296
recycling 243
reducing ability 14
reduction 339–44, 347
reduction potential 13
reductive coupling 304
reductive elimination 114
reductive environment 234
Reformatsky-type reaction 342
refractive index 10
regioselective iodination 449
release coatings 466
reoxidant 133
Repetto Formation 221
resin 239
resistance-capacitance delay 531
retention 27
reverse osmosis (RO) 245
rhodium carbonyl iodide 547
ring contraction 128
ring opening 128
ring substitution 289
RO See reverse osmosis (RO)
rodenticide 442
Rose Bengal 553
Ru-based dyes 503
ryanodine receptor (RyR) 447
- Sadowara gas field 231, 234
safener 444
salicylanilides 451
saltpeter 197
saltpeter refinery 201
samarium(II) iodide (SmI_2) 343
Sandell-Kolthoff reaction 16, 44
sandstones 224, 226
Sargassum 565
S-arylation 323
schoeniger combustion 44
Scotland 207
seawater samples 26
seaweed 207, 221, 593
secondary bonding 110
secondary ion mass spectrometry (SIMS) 43
SelectfluorTM 296
Selective arylation 307
self-elution 37
Sellafield 565
separation mode 25
 σ -aryl hypervalent iodine 321
 σ hole 160
signal transduction 446
silver 209, 210
silver iodide 58
silver(I) nitrate 58
single photon emission computed tomography (SPECT) 605, 606, 609, 610, 616, 618, 621
Single-electron-transfer (SET) 119, 122, 288, 313
SiO₂ etching 523
soda 207
sodium bisulfite 210
sodium carbonate 210
sodium iodide 12, 57, 355, 356
sodium iodide [¹²³I] 614
sodium iodide [¹³¹I] 614
sodium nitrate plant 218
solar evaporation 217
sol-gel reaction 469
solid phase 10
solubility of iodine 11
Soluble organically bound iodine (SOI) 42

- solvent I_2 interaction 164
speciation analysis 36
specific heat 11
spiroannulation 286
spirocyclic compound 286
spirocyclization 120, 135, 287
spirolactone 125
stabilizer 548
standard atomic weight 10
starch 210
static contact angle 514
stereolithography 473, 475
striata 618
structures of epoxide 466
sublimation 210
sulfoxides 340
sulfur combustion 215, 220
sulfur dioxide 209
sulfuric acid 210
super electrophilic iodonium ion 262
suppressed IC 33
supramolecular synthon 168
suppressors 34
surfactant 29
swimming pool water 399
Synechococcus 568
Synthroid 415
- telomerization 514
terminal oxidant 282
tetrahydronaphthalene 56
1,3,5,7-tetrakis[4-(diacetoxyiodo)phenyl]
adamantine 297
tetramethyl ammonium hydroxide
(TMAH) 46
Tetraselmis.sp., 568
textile dyes 553
Thalassiosira 568
therapeutic agents 433
thermal conductivity 10
thermal desorption spectroscopy 534
thermooxidative degradation 551
three-center four-electron (3c-4e)
bond 105
three-membered iodonium ion 251, 261
thyroglobulin (Tg) 43, 412, 413
thyroid 411–15, 418, 422, 423, 425
thyroid peroxidase (TPO) 412
thyroxine (T4) 411–13
- TiO₂, 506
titanium(IV) iodide 331
TMSI 269, 270
Togni's reagent 109
toluene 10
tosyloxylation 291
trans influence 106
transitoin metal catalysts 496
trematodes 452
triiodide 377, 378, 380, 382, 386–8, 390,
391, 394–6, 482, 561
triiodide anion 9
triiodide/iodide-based electrolyte 506
triiodothyronine (T3) 411–13
trimethylsilyl iodide 269
trimethylstannyl-substituted precursor 613
triple point 10
Tronov-Novikov method 253
T-shaped structure 105
turbidite sandstone 232
two-dimensional IC (2D IC) 47
two-step mechanism 504
- UF. *See* ultra filtration (UF)
Ullmann coupling 304
ultra filtration (UF) 244, 245
Ultra High Frequency (UHF) plasma 524
ultralarge-scale integrated circuits 531
Unithroid 415
unsymmetrical dimers 319
uptake 564–6, 568
urinary iodine 426, 427
urography 366
Uroselectan 356
U.S.S.R., 207
UV curable coatings 465, 469
UV detection 35
UV irradiation 462
UV spectrum 534
UV/Vis 570
(UV-VIS) spectroscopy
halogen-bonded I_2 solvent
complexes 165
 I_2 basicity scale 165
mixed trihalides YI2 166
- van der Waals radius 10
vanadium 558, 559, 564, 565, 568,
570–578

- vanadium-dependent haloperoxidases
 (V-HPO) 558, 572–4, 576
- vapor density 11
- vapor pressure 10
- vaporization 237
- varec 207
- vat leaching 217, 218
- ventricular action potential 435
- veterinary medicine 398
- vinyl iodide 258, 260, 268
- vinylidene S_N2 , 115
- viscosity 356, 359, 360, 363, 364

- waste 244
- waste brine 222, 238, 239
- wastewater 400
- water 11
- water solubility 359, 362, 368
- wells 237
- Willgerodt's reagent 103

- Woodford Shale 226
- Woodward Iodine Corporation
 222, 227
- Woodward Trench 222, 224, 226
- working electrode 502
- wound dressing 398

- XB interaction energies 162
- X-ray absorption 19
- X-ray absorption coefficient 355
- X-ray absorption near-edge fine structure
 (XANES) 19
- X-ray absorption spectroscopy 577
- X-ray contrast agents 355
- X-ray fluorescence analysis (XRF) 43
- X-ray fluorescence spectrometry 363
- X-ray photoelectron spectroscopy 534
- X-ray structure 573, 577

- Zeiss 482

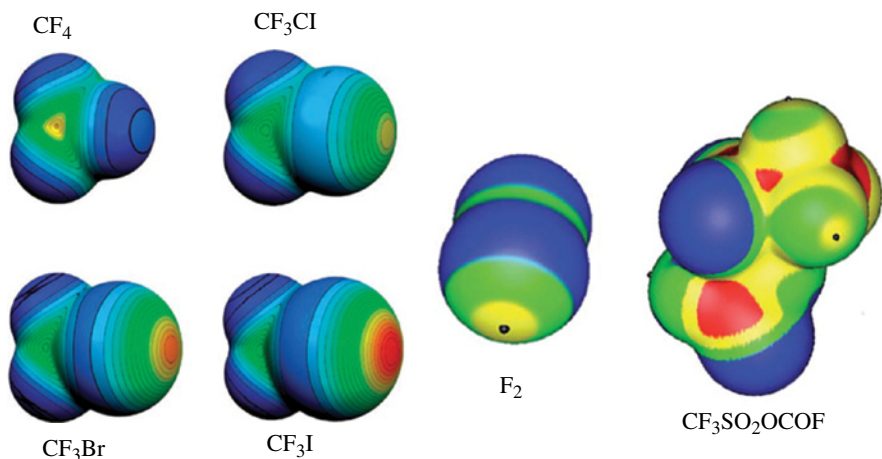


FIGURE 8.2 Left: The molecular electrostatic potential at the isodensity surface with 0.001 au: CF_4 , CF_3Cl , CF_3Br , and CF_3I . Color ranges are as follows: Red, greater than 27 kcal mol⁻¹; yellow, between 20 and 14 kcal mol⁻¹; green, between 12 and 6 kcal mol⁻¹; blue, negative. Right: F_2 and $\text{CF}_3\text{SO}_2\text{OCOF}$ (the CF_3 group is on top). Color ranges are as follows: Red, greater than 20 kcal mol⁻¹; yellow, between 20 and 9 kcal mol⁻¹; green, between 9 and 0 kcal mol⁻¹; blue, negative. For F_2 and $\text{CF}_3\text{SO}_2\text{OCOF}$ the black hemispheres denote the positions of the most positive potentials associated with the fluorines.

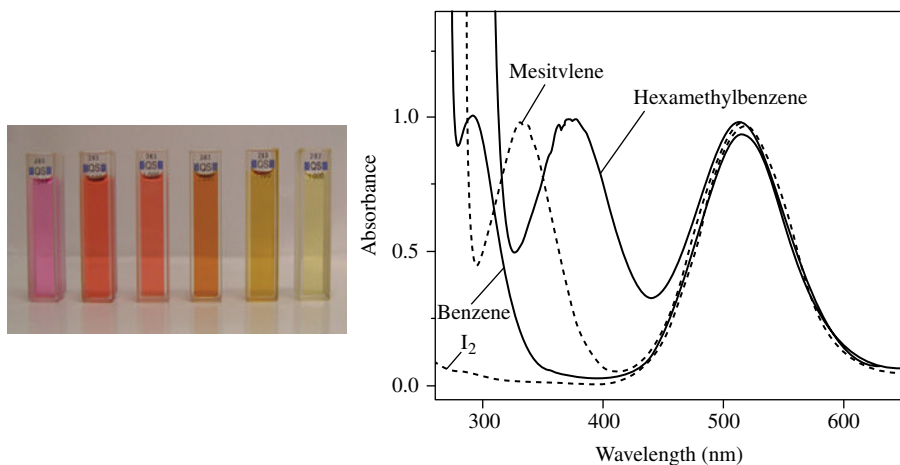


FIGURE 8.5 Left: The color of iodine solutions relates with the electron-donating ability of the employed solvents. From left to the right the characteristic colors of I_2 dissolved in hexane, toluene, dichloroethane, acetonitrile, methanol and pyridine. Right: Electronic spectra of CCl_4 solutions of I_2 before and after the addition of excess amount of benzene, mesitylene, and hexamethylbenzene ($\lambda_{\text{charge transfer}}^{\text{max}}$ 369 nm). A charge-transfer band appears upon cosolvent addition and its $\lambda_{\text{max}}^{\text{charge transfer}}$ increases with the strength of the XB acceptors (benzene, 285 nm; mesitylene, 327 nm; hexamethylbenzene, 369 nm). Reproduced with permission from Ref. [32] © Royal Society of Chemistry..

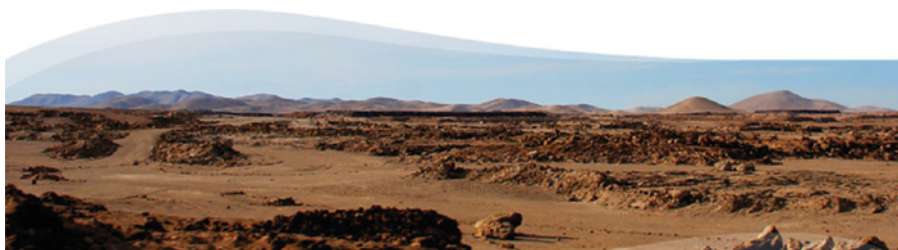


FIGURE 11.2 Atacama Desert.

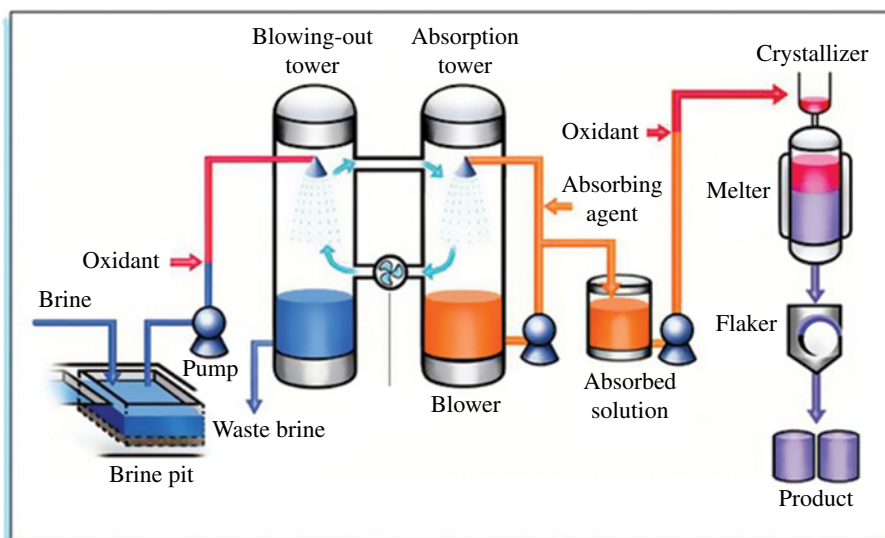


FIGURE 13.3 Blowing-out process of iodine. A view of Blowing-out and Absorption towers (bottom).

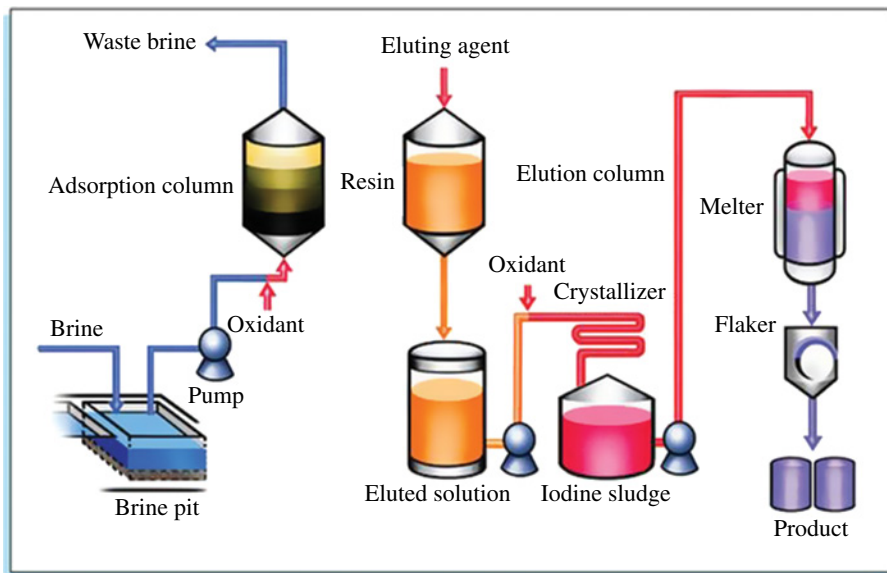
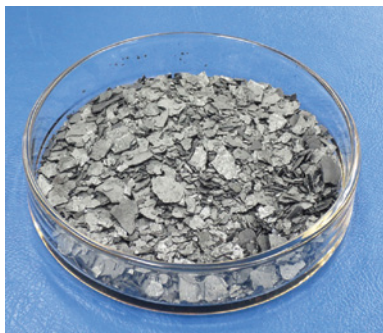


FIGURE 13.4 Ion-exchange Resin (IER) Process of iodine. A view of IER column (bottom).

(a)



(b)



FIGURE 13.5 (a) Iodine product (flaked). Iodine flake is highly pure and low water content product. (b) Iodine product (prilled). Prilled iodine is easy to handle and dust free.

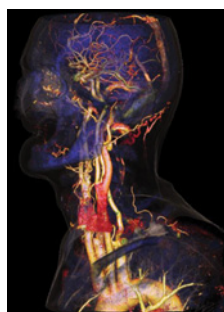
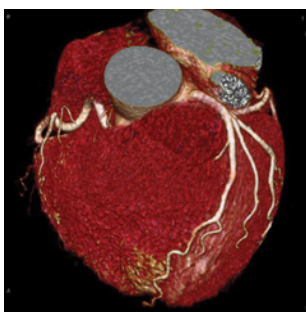


FIGURE 19.5 CT images. Left: Coronary CTA, slice thickness 0.6 mm, two-dimensional rendering. Middle: Coronary CTA, slice thickness 0.6 mm, three-dimensional rendering. Right: Carotid artery, slice thickness 0.75 mm, three-dimensional rendering. Courtesy of Siemens AG (collection of MIP, VRT images) and Friedrich-Alexander University Erlangen-Nuremberg, Institute of Medical Physics, Erlangen, Germany.

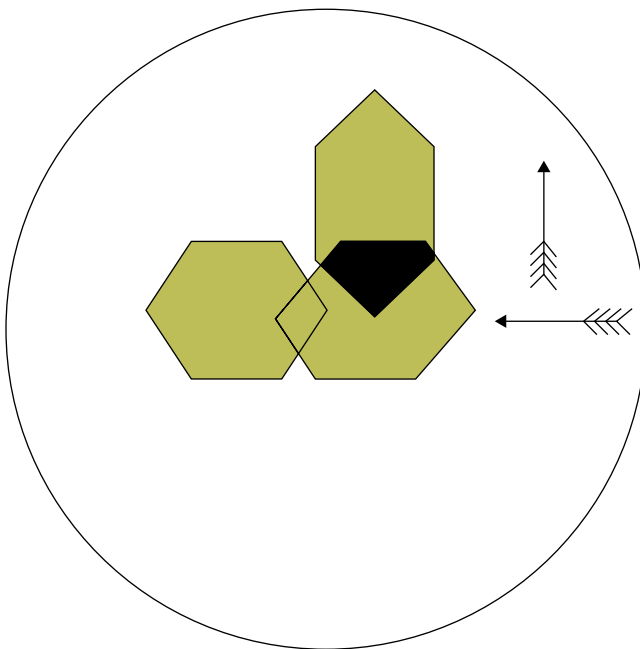


FIGURE 26.1 Overlapping hexagonal-shaped crystals of herapathite crystals viewed in transmitted, unpolarized white light (Ref. [16]). *Arrows* denote the orientation of the absorbing direction in the crystals. Extinction is apparent when crystals overlap and their long axes are orthogonal to one another. Courtesy Taylor and Francis and *Philosophical Magazine*.

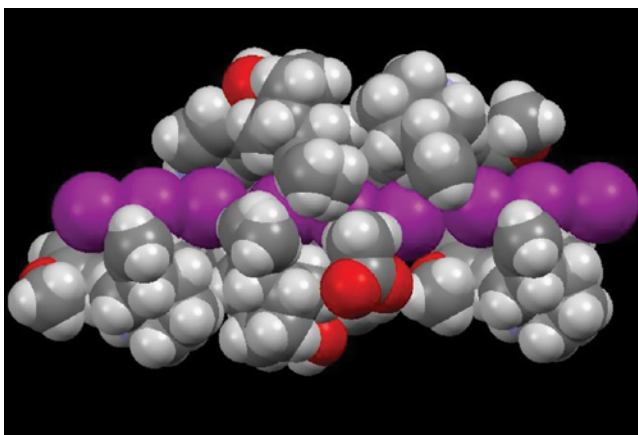


FIGURE 26.2 Three purple triiodide ions lined up along the b -axis (horizontal) within a channel created by five quinine molecules in herapathite. Molecules of solvation (water and acetic acid) as well as sulfate counterions have been removed for clarity.



FIGURE 26.3 Examples of Herotar and Bernotar filters from 1936 and 1937. Note the recognition of Prof. Bernauer in the instructions (“Gebrauchsanweisung”) as the inventor of these photographic filters. Courtesy of Volkmar Kleinfeldt.

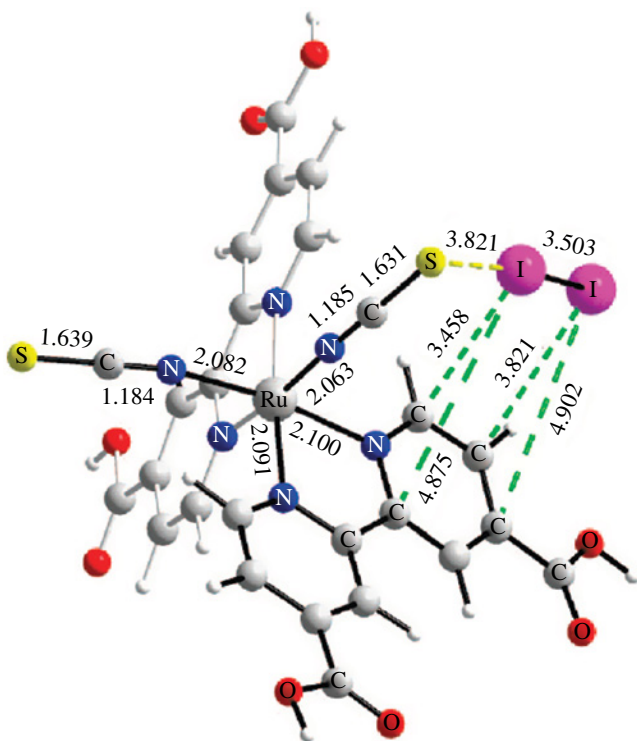


FIGURE 28.3 Outer-sphere binding of I_2 – in a N3 dye model. The figure is taken from Ref. [12].



FIGURE 31.8 Iodine containing dyes: Erythrosine B (left), Rose Bengal, cyanine, Cryptosyanine (right).

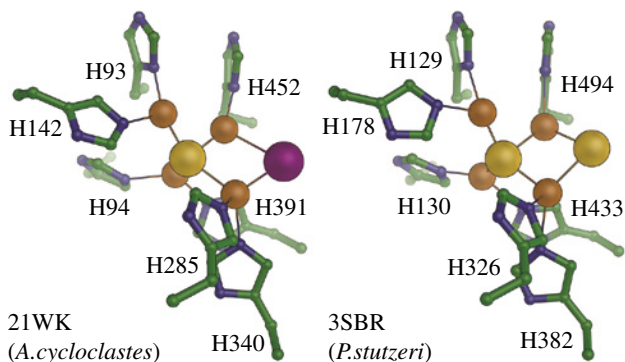


FIGURE 32.3 Structures of the CuZ-iodide adduct (N_2OR *Achromobacter cycloclastes*; PDB code 21WK) and the native CuZ site (N_2OR *Pseudomonas stutzeri*; PDB code 3SBR). The addition of the soft ligand iodide yielded a bridging conformation that closely mimics the binding of S^{2-} in the purple N_2OR from *P. stutzeri*. Iodine in purple, sulfide in yellow. Adapted from Ref. [135] © Elsevier.

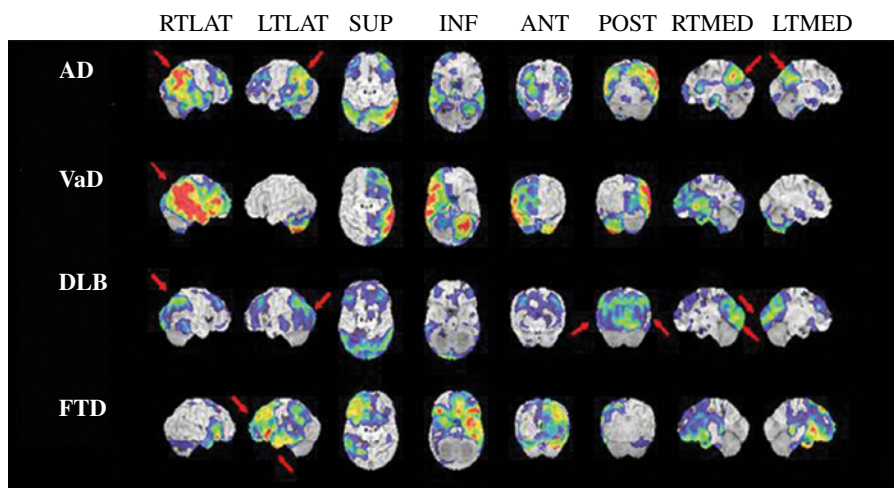


FIGURE 34.5 Cerebral blood flow maps of Iofetamine [^{123}I] in dementia patients by disease subtype. The distribution of blood flow is seen on each cross-section of the brain. White areas represent normal blood flow and red-yellow areas represent reduced blood flow. AD, Alzheimer's disease; ANT, anterior view; DLB, dementia with lewy bodies; FTD, frontotemporal dementia; INF, inferior view; LTLAT, left lateral view; LTMED, left medial view; POST, posterior view; RTLAT, right lateral view; RTMED, right medial view; SUP, superior view; VaD, vascular dementia.

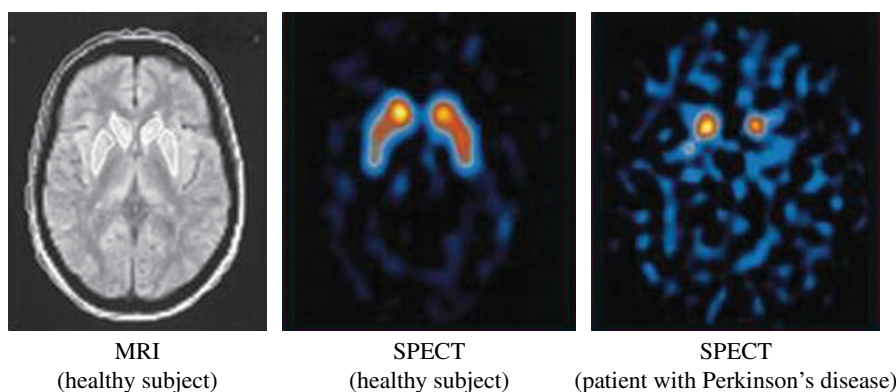


FIGURE 34.6 MRI and SPECT images of the human brain obtained with Ioflupane [^{123}I] (cross-section of the brain). Left: MRI image of the brain in a healthy subject, in which the striata are visualized as two white “comma-like” images that are symmetrically located near the center of the brain. Middle: SPECT image of the brain in a healthy subject, in which the striata are visualized as two red-yellow “comma-like” images as with MRI. Right: SPECT image of the brain of a Parkinson's disease patient, in which the radioactivity accumulation in the putamen (bottom part) of the striata disappears, and only the caudate nucleus (upper part) is visualized in the shape of a “full-stop.” When the disease further progresses, the radioactivity accumulation in the caudate nucleus also disappears.

WILEY END USER LICENSE AGREEMENT

Go to www.wiley.com/go/eula to access Wiley's ebook EULA.